

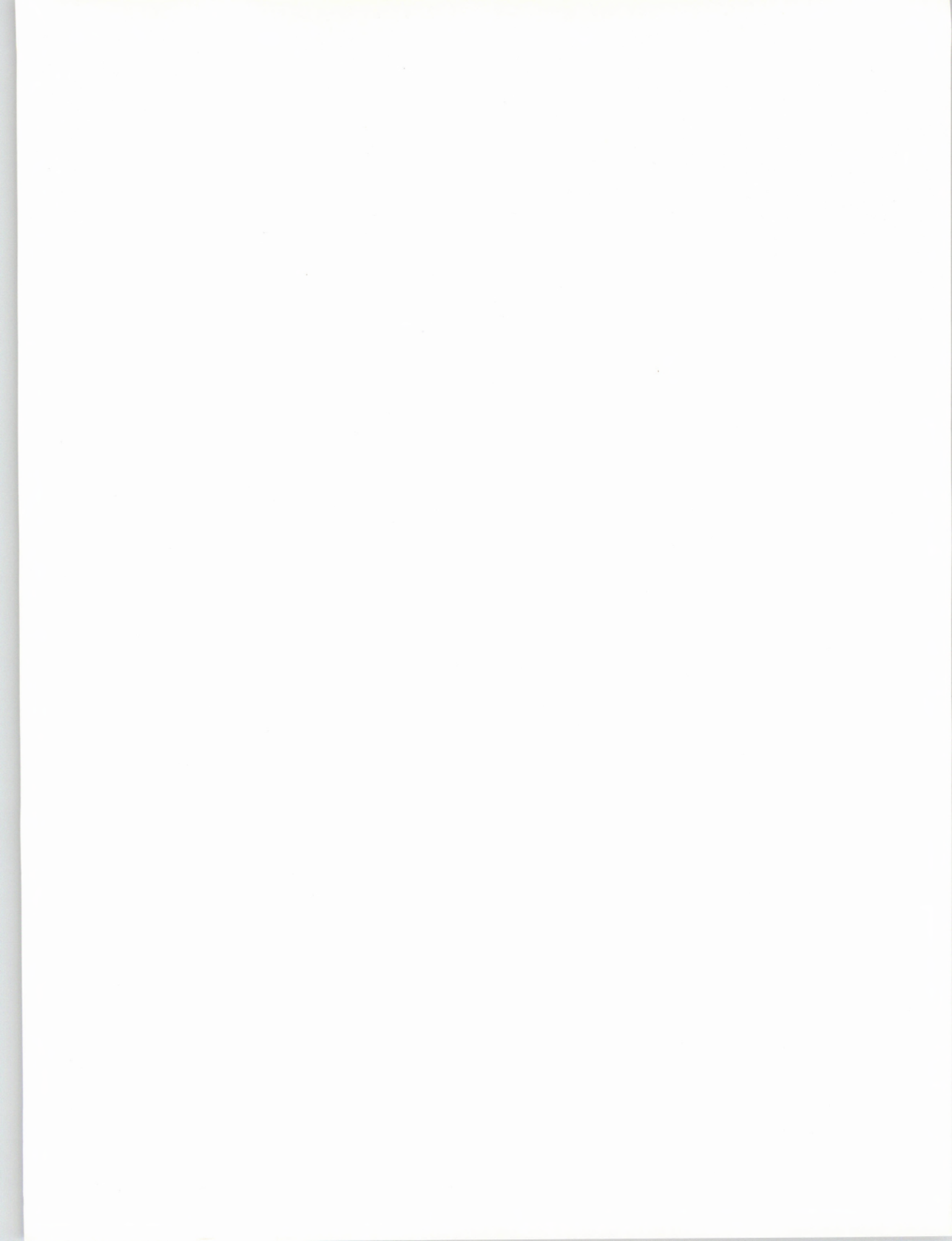
REVISTA PORTUGUESA DE QUÍMICA



RPTQAT 27(1/2)1-426(1985)
ISSN 0035-0419



Este número é inteiramente dedicado à publicação dos resumos das conferências e comunicações a apresentar na 2.^a Conferência Internacional sobre Química Bioinorgânica que terá lugar no Algarve, Portugal, de 15 a 19 de Abril de 1985



Rev. Port. Quím., 27, N.º 1/2
Pp. 1-426 — Lisboa, 1985

REVISTA PORTUGUESA DE QUÍMICA

Propriedade e edição da
SOCIEDADE PORTUGUESA DE QUÍMICA
em continuação da
REVISTA DE QUÍMICA PURA E APLICADA
fundada em 1905 por
Ferreira da Silva.
Subsidiada pelo
INSTITUTO NACIONAL DE INVESTIGAÇÃO CIENTÍFICA

Director	A. HERCULANO DE CARVALHO	
Editores	M.A.V. RIBEIRO DA SILVA Departamento de Química, Faculdade de Ciências Universidade do Porto — 4000 PORTO	A.J.C. VARANDAS Departamento de Química, Faculdade de Ciências e Tecnologia Universidade de Coimbra — 3000 COIMBRA
Editores convidados para este número da Revista	A.B.V.P. AGUIAR L.F. VILAS-BOAS	
Comissão redactorial	LUÍS ALCÁCER ALBERTO AMARAL J.M. PEIXOTO CABRAL JOÃO OLIVEIRA CABRAL JORGE C.G. CALADO R.A. GUEDES DE CARVALHO FERNANDA MADALENA A. COSTA A. ROMÃO DIAS JOSÉ TEIXEIRA DIAS SEBASTIÃO J. FORMOSINHO BERNARDO HEROLD JOSÉ SIMÕES REDINHA JOAQUIM J.B. ROMERO MANUEL ALVES DA SILVA J.J.R. FRAÚSTO DA SILVA CÉSAR A.N. VIANA ANTÓNIO V. XAVIER	

Os artigos publicados são de exclusiva responsabilidade dos seus autores

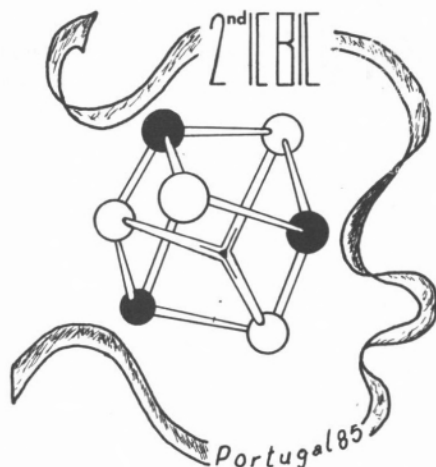
Administração
Fotocomposição, montagem,
impressão e acabamento
Capa

Av. da República, 37, 4.º — 1000 Lisboa
PROENÇA — Coop. Op. Artes Gráficas, CRL,
Rua D. Carlos de Mascarenhas, 39-51 B — 1000 Lisboa
Luís Filipe de Abreu

Publicação trimestral.

Portugal — Número avulso: 500\$00. Assinatura (quatro números): 1600\$00.
Outros países — Número avulso: U.S.\$12. Assinatura (quatro números): U.S.\$40

This issue of *Rev. Port. Quím.* is entirely dedicated to the publication of the abstracts of the lectures and communications to be presented at the 2nd International Conference on Bioinorganic Chemistry (April 15-19, 1985, Algarve, Portugal).



2ND INTERNATIONAL CONFERENCE ON BIOINORGANIC CHEMISTRY

International Organizing Committee:

I. BERTINI
(University of Florence)
H.B. GRAY
(Caltech, Pasadena)
B.G. MALMSTRÖM
(University of Göteborg)
J. REEDIJK
(State University of Leiden)
H. SIGEL
(University of Basel)
A.V. XAVIER
(New University of Lisbon)

National Organizing Committee:

A.B.V.P. AGUIAR
(Instituto Superior Técnico, Lisbon)
J.J.R. FRAÚSTO DA SILVA
(Instituto Superior Técnico, Lisbon)
I. MOURA
(New University of Lisbon)
J.J.G. MOURA
(New University of Lisbon)
L.F. VILAS-BOAS
(Instituto Superior Técnico, Lisbon)
A.V. XAVIER
(New University of Lisbon)

General Secretary:

A.V. XAVIER
(New University of Lisbon)

Conference Secretary:

MARGARIDA MARTINEZ

índice

PLENARY LECTURES

I. BERTINI	1	RELAXATION PHENOMENA IN NMR OF PARAMAGNETIC SPECIES
STURE FORSÉN	2	THE DOMAIN STRUCTURE OF CALMODULIN: SOME RECENT BIOPHYSICAL STUDIES
JEAN-MARIE LEHN	4	DESIGN OF CORECEPTOR MOLECULES FOR POLYNUCLEAR AND PHOTOACTIVE METAL ION COMPLEXES
ECKARD MÜNCK	5	STRUCTURE AND MAGNETISM OF IRON-SULFUR CLUSTERS IN PROTEINS
BERT L. VALLEE	6	CONCURRENT CRYOKINETIC AND CRYOSPECTROSCOPIC CHARACTERIZATION OF INTERMEDIATES IN METALLOENZYME ACTION
HARRY B. GRAY	8	ELECTRON TRANSFER AT FIXED DISTANCES IN METALLOPROTEINS
H. ALLEN O. HILL	9	THE ELECTROCHEMISTRY OF REDOX PROTEINS
PHILIP AISEN	10	THE BINUCLEAR IRON CENTER OF UTEROFERRIN
DAVID DOLPHIN	11	METALLOPORPHYRINS IN BIOCHEMISTRY

SESSION LECTURES

JAMES A. IBERS	14	CARBON MONOXIDE AND DIOXYGEN BINDING BY IRON(II) PORPHYRINS
W.E. BLUMBERG	15	METAL EPR TRUTH DIAGRAMS REVISITED 15 YEARS LATER
F. ANN WALKER V.L. BALKE J.T. WEST	15	THE EFFECT OF HYDROGEN-BONDING OF AMIDES ON THE STABILITY OF AXIAL LIGAND COMPLEXES OF METALLOPORPHYRINS
G.R. MOORE	17	THE INFLUENCE OF ELECTROSTATIC INTERACTIONS BETWEEN BURIED GROUPS ON THE STRUCTURE AND PROPERTIES OF GLOBULAR PROTEINS
HITOSHI OHTAKI	18	STRUCTURES OF GLYGINATO COMPLEXES OF BIOCHEMICALLY IMPORTANT DIVALENT TRANSITION-METAL IONS IN SOLUTION
H. KOZŁOWSKI G. FORMICKA-KOZŁOWSKA L.D. PETTIT I. STEEL	19	CAN COPPER(II) IONS ACTIVATE BIOLOGICALLY SMALL PEPTIDE MOLECULES?
KENNETH D. KARLIN YILMA GULTNEH RICHARD W. CRUSE JON C. HAYES JON ZUBIETA	20	DIOXYGEN BINDING AND ACTIVATION IN DINUCLEAR COPPER COMPLEX SYSTEMS
S. MARTIN NELSON	21	DI-COPPER COMPLEXES OF MACROCYCLIC LIGANDS AS MODELS FOR TYPE 3 COPPER PROTEINS
B.H. HUYNH L. KANG D.V. DERVARTANIAN H.D. PECK JR. J. LEGALL	23	A COMPARISON STUDY OF SULFITE REDUCTASE FROM SULFATE-REDUCING BACTERIA: A MÖSSBAUER INVESTIGATION
A.X. TRAUTWEIN	24	NEW ASPECTS OF MÖSSBAUER SPECTROSCOPY
A. SIMOPOULOS A. KOSTIKAS V. PAPAETHYMIU D. COUCOUVANIS M. KANATZIDIS	25	ELECTRONIC AND MAGNETIC PROPERTIES OF SYNTHETIC ANALOGS FOR THE M AND P CLUSTERS OF NITROGENASE
JACQUES MEYER JEAN-MARC MOULIS MARC LUTZ	26	RESONANCE RAMAN SPECTROSCOPY OF IRON-SULFUR PROTEINS
GIL NAVON HADASSAH SHINAR WOLFGANG KLAUI	27	AN ORGANOMETALLIC LITHIUM IONOPHORE
K.R.K. EASWARAN	28	IONOPHORE-METAL INTERACTIONS

PETER J. SADLER	30	GOLD DRUGS
ROBERT F. PASTERNAK JUDITH HEMPEL	31	SOLUTION KINETICS OF A GOLD(I) BIOLOGICALLY ACTIVE COMPLEX
JOSEPH E. COLEMAN PETER GETTINS	33	ALKALINE PHOSPHATASE: AN ENZYME WITH MULTIPLE CATALYTIC METAL IONS AT EACH ACTIVE CENTER: ^{31}P AND ^{113}Cd NMR IN SOLUTION CORRELATED WITH THE CRYSTAL STRUCTURE
SVEN LINDSKOG	35	THE STRUCTURAL BASIS OF KINETIC DIFFERENCES BETWEEN CARBONIC ANHYDRASE ISOENZYMES
C. LUCHINAT	36	A COMPARISON OF SOME pH-DEPENDENT PROPERTIES OF ZINC ENZYMES
MARVIN W. MAKINEN GREGG B. WELLS MOON B. YIM	37	MAGNETIC RESONANCE SPECTROSCOPY OF OXYGEN-17 TO PROBE THE ACTION OF METALLOENZYMES: LIVER ALCOHOL DEHYDROGENASE
MICHAEL ZEPPEZAUER	38	STRUCTURAL MODULATIONS OF THE CATALYTIC METAL BINDING SITE IN LIVER ALCOHOL DEHYDROGENASE DUE TO LOCAL AND GLOBAL CHANGES OF PROTEIN CONFORMATION DURING THE CATALYTIC CYCLE
DAVID F. BLAIR STEPHAN N. WITT SUNNEY I. CHAN	39	THE MECHANISM OF DIOXYGEN REDUCTION BY CYTOCHROME <i>c</i> OXIDASE
J.A. FEE T. YOSHIDA B. ZIMMERMAN D. KUILA W.R. RANGER	40	PROGRESS IN THE CHARACTERIZATION OF <i>THERMUS</i> RESPIRATORY PROTEINS
JOANN SANDERS-LOEHR	41	OXYGEN BINDING TO THE BINUCLEAR CENTER OF HEMERYTHRIN
W.G.J. HOL A. VOLBEDA	42	THE STRUCTURE OF THE COPPER-CONTAINING OXYGEN-TRANSPORTING HEMOCYANINS FROM ARTHROPODS
A.J. THOMSON C.P. BARRETT J. PETERSON C. GREENWOOD	44	OPTICAL DETECTION OF PARAMAGNETIC RESONANCE BY MAGNETIC CIRCULAR DICHROISM. APPLICATIONS TO METALLOPROTEINS
I. PECHT O. FARVER A. LICHT	45	ELECTRON TRANSFER PATHWAYS IN BLUE COPPER PROTEINS
K. LERCH	46	THE BINUCLEAR COPPER CENTER AND THE REACTION MECHANISM OF TYROSINASE
PETER M.H. KRONECK WOLFGANG JAKOB	47	ASCORBATE OXIDASE: FURTHER INVESTIGATIONS OF ITS STRUCTURE AND CATALYTIC PROPERTIES
B. MONDOVI A. FINAZZI AGRÒ G. ROTILIO S. SABATINI	48	REDOX TITRATIONS AND REVERSIBLE REMOVAL OF COPPER FROM BOVINE PLASMA AMINE OXIDASE
JAMES F. RIORDAN	50	ELECTRONIC ABSORPTION SPECTROSCOPY OF COBALT ANGIOTENSIN CONVERTING ENZYME
KATSUMI NIKI MITSUMASA FURUKAWA YOSHIKI KAWASAKI CHARLOTTE HINNEN	51	ELECTROCHEMICAL AND SPECTROELECTROCHEMICAL BEHAVIOR OF <i>c</i> -TYPE CYTOCHROMES AT ELECTRODE INTERFACE IN THE PRESENCE OF ELECTRON PROMOTERS
BORIS P. ATAÑASOV	52	ON THE MECHANISM OF ELECTRON TRANSFER BETWEEN MYOGLOBIN AND CYTOCHROME <i>c</i>
JACK PEISACH	53	ELECTRON SPIN ECHO SPECTROSCOPY AND THE STUDY OF METALLOPROTEINS
BRIAN M. HOFFMAN	54	ENDOR OF IRON SULFUR CENTERS
L.C. SIEKER R.E. STENKAMP L.H. JENSEN J. LEGALL	54	STRUCTURE OF A SMALL RUBREDOXIN: TENTATIVE ASSIGNMENT OF AMINO ACID SEQUENCE AND THREE DIMENSIONAL STRUCTURE OF THE RUBREDOXIN FROM <i>DESULFOVIBRIO</i> <i>DESULFURICANS</i> (STRAIN 27774)
P.J. STEPHENS T.V. MORGAN F. DEVLIN C.D. STOUT B.K. BURGESS	56	NOVEL REDOX CHEMISTRY OF <i>AZOTOBACTER</i> <i>VINELANDII</i> FERREDOXIN I

BHARAT B. KAUL CAROL J. HINSHAW JACK T. SPENCE JOHN H. ENEMARK SHANNATH L. MERBS	58	MODELS FOR THE MOLYBDENUM CENTERS OF THE MOLYBDENUM HYDROXYLASES
LUIGI G. MARZILLI NEVENKA BRESCIANI-PAHOR LUCIO RANDACCIO ENNIO ZANGRANDO JENNY P. GLUSKER	59	STRUCTURAL AND ^1H AND ^{31}P NMR SPECTROSCOPIC STUDIES OF B_{12} COMPOUNDS: A NEW CRYSTALLINE FORM OF VITAMIN B_{12}
SEYMOUR H. KOENIG RODNEY D. BROWN, III LOKESH BHATTACHARYYA C. FRED BREWER	60	COMPARATIVE PROTON AND DEUTERON NMR STUDIES OF Ca^{2+} - Mn^{2+} - CONCAVALIN A, PEA, AND LENTIL LECTINS: EVIDENCE FOR A COMMON SITE OF EXCHANGING WATER MOLECULES
ANDREA SCOZZAFAVA	61	THERMODYNAMIC AND STRUCTURAL PROPERTIES OF THE METAL BINDING SITES OF THE TRANSFERRINS

MINISYMPOSIA

1. Ni-Biochemistry

J.J.G. MOURA M. TEIXEIRA I. MOURA A.V. XAVIER J. LEGALL	63	<i>DESULFOVIBRIO GIGAS</i> HYDROGENASE; CATALYTIC CYCLE AND ACTIVATION PROCESS
S.P.J. ALBRACHT J.W. VAN DER ZWAAN R.D. FONTIJN E.C. SLATER	66	HYDROGENASE FROM <i>CHROMATIUM VINOSUM</i> : THE REDOX STATES OF NICKEL AND THE IRON-SULPHUR CLUSTER DURING CATALYSIS
ROBERT A. SCOTT MELVIN CZECHOWSKI DANIEL V. DERVARTANIAN JEAN LEGALL HARRY D. PECK JR. ISABEL MOURA	67	NICKEL X-RAY ABSORPTION SPECTROSCOPY OF <i>DESULFOVIBRIO GIGAS</i> HYDROGENASE
DANIEL V. DERVARTANIAN HANS J. KRUGER H.D. PECK JR. J. LEGALL	70	THE REACTIVITY OF THE NICKEL-CONTAINING HYDROGENASE FROM <i>DESULFOVIBRIO GIGAS</i> WITH OXYGEN, DEUTERIUM AND CARBON MONOXIDE
J.R. LANCASTER, JR. K. GILLIES K.R. ROGERS	73	BIOENERGETIC ROLE OF NICKEL-CONTAINING PROTEINS IN METHANOGENS

2. Mo-Biochemistry

R.C. BRAY G.N. GEORGE	76	THE NATURE OF THE <i>VERY RAPID</i> INTERMEDIATE IN XANTHINE OXIDASE TURNOVER
JOHN H. ENEMARK W.E. CLELAND JR. DAVID COLLISON FRANK E. MABBS	76	APPROACHES TO THE MOLYBDENUM CENTERS OF «OXO-TYPE» ENZYMES
C. DAVID GARNER JOHN R. NICHOLSON STUART K. HAGYARD JOHN CHARNOCK COLIN F. MILLS	78	COPPER-MOLYBDENUM SULPHUR CLUSTERS AND RELEVANCE TO MOLYBDENUM-INDUCED COPPER-DEFICIENCY IN RUMINANTS
EDWARD I. STIEFEL	80	MOLYBDENUM-SULFUR STRUCTURAL, REDOX AND REACTION CHEMISTRY
BARBARA K. BURGESS JUDITH F. RUBINSON JAMES L. CORBIN MICHAEL J. DILWORTH	81	AZIDE REDUCTION BY <i>AZOTOBACTER VINELANDII</i> NITROGENASE
R.N.F. THORNELEY D.J. LOWE	82	HYDROGEN AND NITROGEN INTERACTIONS AT THE ACTIVE SITE OF NITROGENASE

3. Nucleic Acid Metal Ion Interactions

R. BRUCE MARTIN	84	METAL ION BINDING TO NUCLEOSIDES AND NUCLEOTIDES
JEAN-CLAUDE CHOTTARD	85	PLATINUM OLIGONUCLEOTIDE MODELS OF PLATINUM-DNA INTERACTIONS

JAN REEDIJK	86	REACTIONS OF PLATINUM COMPOUNDS WITH NUCLEIC ACIDS AND OLIGONUCLEOTIDES
STEPHEN J. LIPPARD	87	THE BINDING OF PLATINUM COMPLEXES TO DNA
G.L. EICHHORN P. CLARK Y.A. SHIN J.J. BUTZOW J.M. RIFKIND R.P. PILLAI P.P. CHUKNYISKI D. WAYSBORT	88	THE INFLUENCE OF METAL ION-NUCLEIC ACID INTERACTIONS ON GENETIC INFORMATION TRANSFER (G.I.T.)
E.L. ANDRONIKASHVILI M. KHARATISHVILI N. ESIPOVA	90	INFLUENCE OF METAL IONS ON THE COOPERATIVITY OF DNA-PROTEIN INTERACTIONS
4. Uptake, Essentiality and Toxicity of the Chemical Elements		
J.J.R. FRAÚSTO DA SILVA	92	AN INTRODUCTION TO THE MINISYMPOSIUM
M.E. FARAGO	94	METAL IONS AND PLANTS
LOIS A. EGUCHI PAUL SALTMAN	95	THE AEROBIC REDUCTION OF Fe(III) COMPLEXES BY HEMOGLOBIN AND MYOGLOBIN
EDITH M. CARLISLE	97	SILICON ESSENTIALITY AND FUNCTION
N.D. CHASTEEN E.M. LORD C.E. HOLLOWAY H.J. THOMPSON	98	CHARACTERIZATION OF THE BIOCOMPLEXES OF VANADIUM METABOLISM IN THE RAT
EVERT NIEBOER	99	PHYSICO-CHEMICAL, METABOLIC AND MOLECULAR ASPECTS OF NICKEL CARCINOGENESIS
R.J. SHAMBERGER	100	SELENIUM BIOCHEMISTRY
5. Models of Iron Binding Sites in Biology		
JOHN T. GROVES THOMAS J. MCMURRY	102	SYNTHETIC ANALOGS OF OXIDIZED HEME PROTEINS. PREPARATION AND CHARACTERIZATION OF IRON(IV) PORPHYRINS
JOHN R. LINDSAY SMITH DAVID N. MORTIMER	103	TETRA(4-N-METHYLPYRIDYL)PORPHYRINATOIRON(III) PENTACATION, A POLAR CATALYST FOR MODEL SYSTEMS FOR CYTOCHROME P450 MONO-OXYGENASES
D. MANSUY	104	HEME MODEL STUDIES ON OLEFIN OXIDATION BY CYTOCHROME P-450
CHRISTOPHER A. REED GERALD E. WUENSCHLE PETER D. W. BOYD JOHN R. TATE SUSAN RASMUSSEN	106	DERIVATIZED PORPHYRINS AS MODELS FOR H-BONDED OXYHEMOGLOBIN AND CYTOCHROME OXIDASE
T.G. TRAYLOR JAMES MARSTERS LARRIE DEARDURFF	107	GEMINATE RECOMBINATION IN THE PHOTOLYTIC DISSOCIATION OF NO AND CO FROM HEMES AND HEME PROTEINS
M. SCHAPPACHER R. WEISS R. MONTIEL-MONTOYA A. TRAUTWEIN A. TABARD	108	FORMATION OF IRON(IV) OXO DERIVATIVES VIA REDUCTION OF FERROUS PORPHYRIN DIOXYGEN ADDUCTS AND REACTION WITH CARBON DIOXIDE
B.A. AVERILL K.S. BOSE P.E. LAMBERTY J.E. KOVACS G.L. LILLEY X. WU N.C. JAIN M.E. ROGERS E. SINN	109	SYNTHETIC APPROACHES TO THE METAL CENTERS OF NITROGENASE
D. COUCOUVANIS M. KANATZIDIS A. SALIFOGLU W.R. DUNHAM W.R. HAGEN	110	THE REACTIONS, STRUCTURAL CHARACTERIZATION AND ELECTRONIC PROPERTIES OF THE NEW METASTABLE $[\text{Fe}_6\text{S}_6\text{L}_6]^{3-}$ AND $[\text{Fe}_6\text{S}_6\text{L}_6]^{2-}$ COMPLEXES

LAWRENCE QUE JR.	112	IRON(III)-CATALYZED OXYGENATION OF CATECHOLS
KENNETH N. RAYMOND DAVID J. ECKER LARRY D. LOOMIS BERTHOLD MATZANKE	113	STRUCTURE, RECOGNITION AND TRANSPORT OF FERRIC ENTEROBACTIN IN <i>E. COLI</i>
DONALD T. SAWYER HIROSHI SUGIMOTO	115	ACTIVATION OF HYDROPEROXIDES BY $Fe^{II}(MeCN)_4(ClO_4)_2$ AND $Fe^{III}Cl_3$ IN ACETONITRILE; MODEL SYSTEMS FOR THE ACTIVE SITES OF PEROXIDASES, CATALASE, AND MONOOXYGENASES
K. WIEGHARDT K. POHL U. BOSSEK	116	SYNTHESES OF IRON MODEL COMPOUNDS WITH MACROCYCLIC N-DONOR LIGANDS

6. Proteins of Iron Storage and Transport

E.C. THEIL	117	FERRITIN: A GENERAL VIEW OF THE PROTEIN, IRON CORE, AND THE IRON-PROTEIN INTERFACE
R.R. CRICHTON	118	PRIMARY STRUCTURE STUDIES ON APOFERRITINS: IRON UPTAKE AND RELEASE
P.M. HARRISON G.C. FORD D.W. RICE J.M.A. SMITH A. TREFFRY J.L. WHITE	119	THE THREE-DIMENSIONAL STRUCTURE OF APOFERRITIN: A FRAMEWORK CONTROLLING FERRITIN'S IRON STORAGE AND RELEASE
N. DENNIS CHASTEEN CARL P. THOMPSON DONNA M. MARTIN	121	THE EFFECT OF HISTIDINE MODIFICATION ON THE IRON BINDING CENTERS OF HUMAN SERUM TRANSFERRIN
PHILIP AISEN	122	TRANSFERRIN AND IRON TRANSPORT
J. WEBB K.S. KIM V. TALBOT D. J. MACEY S. MANN J.V. BANNISTER R.J.P. WILLIAMS T.G. ST. PIERRE D.P.E. DICKSON R. FRANKEL	123	COMPARATIVE CHEMICAL AND BIOLOGICAL STUDIES OF INVERTEBRATE FERRITINS

7. Kinetics in Bioinorganic Chemistry

H. BRIAN DUNFORD ANNE-MARIE LAMBEIR CORNELIA BOHNE WILHELM BAADER	125	STEADY STATE AND BURST KINETIC STUDIES ON PEROXIDASES
M. BRUNORI A. COLOSIMO C. SILVESTRINI M.G. TORDI	126	KINETIC STUDIES OF THE REACTION OF PSEUDOMONAS CYTOCHROME OXIDASE (<i>c-d_p</i>)
J.D. SINCLAIR-DAY A.G. SYKES	126	BINDING SITES FOR INORGANIC REDOX PARTNERS ON [2Fe-2S] AND [4Fe-4S] FERREDOXINS
Z. BRADIĆ K. TSUKAHARA P.C. WILKINS R.G. WILKINS	128	REDUCTION BY RADICALS OF METMYOGLOBIN, METHEMERYTHRIN AND DERIVATIVES
ARTHUR E. MARTELL CARL J. RALEIGH	129	KINETICS AND REACTION PATHWAYS FOR THE AUTOXIDATION OF COBALT POLYAMINE COMPLEXES

ROUND TABLES

1. Metals on Medicine

KENNETH H. FALCHUK	131	CLINICAL DISORDERS OF ZINC METABOLISM AND THEIR TREATMENT
WARREN E.C. WACKER HENRY K. OLIVER	132	MAGNESIUM DEFICIENCY STATES
KARL H. BEYER JR.	133	FROM THEORY TO THERAPY: HOW TO MAKE A NEW DRUG OUT OF A NEW IDEA
N.J. BIRCH	134	LITHIUM IN MEDICINE
I.R. JUDSON A.H. CALVERT	135	CLINICAL APPLICATIONS OF PLATINUM METAL COMPLEXES

2. Environmental Bioinorganic Chemistry

J.M. WOOD	137	ENVIRONMENTAL ASPECTS OF NICKEL TRANSPORT AND NICKEL TOXICITY IN SELECTED ALGAL SPECIES
KURT J. IRGOLIC	138	ARSENIC IN THE ENVIRONMENT
MICHAEL R. HOFFMANN	139	KINETICS AND MECHANISM OF PHOTO-ASSISTED REACTIONS ON IRON OXIDE SURFACES
FRANÇOIS M.M. MOREL	140	IRON UPTAKE AND PHYTOPLANKTON GROWTH
J.E. CROSS D. READ G.L. SMITH D.R. WILLIAMS	141	PLUTONIUM SPECIATION FROM DISPOSAL VAULT INTO MAN

3. Biological Mineralization

R.J.P. WILLIAMS	143	BIO-MINERALS
J. WEBB T.G. ST. PIERRE D.P.E. DICKSON S. MANN C.C. PERRY R.J.P. WILLIAMS G. GRIME F. WATT	143	MÖSSBAUER AND PIXE STUDIES OF IRON BIOMINERALS

4. Electron Transfer Processes

C.M. GROENEVELD G.W. CANTERS	145	THE pH DEPENDENCE OF THE ELECTRON SELF EXCHANGE RATE OF AZURIN FROM <i>PSEUDOMONAS AERUGINOSA</i> AS STUDIED BY NMR
B. REINHAMMAR	146	ELECTRON TRANSFER AND PROTONATION STEPS IN THE REDUCTION OF DIOXYGEN TO WATER BY LACCASE
JOHN H. DAWSON MAUREEN K. GENO ELISABETH T. KINTNER	147	INTRAMOLECULAR ELECTRON TRANSFER BETWEEN TWO METALS BRIDGED BY SATURATED LIGANDS
R. WEVER A.C.F. GORREN R. BOELEN	148	ELECTRON TRANSFER REACTIONS IN CYTOCHROME <i>c</i> OXIDASE
A.V. XAVIER H. SANTOS J.J.G. MOURA I. MOURA J. LEGALL	149	MECHANISM AND REGULATION FOR A COUPLED TWO-ELECTRON TRANSFER IN A TETRAHAEM CYTOCHROME

POSTER SESSIONS

1. Metalloproteins

DEAN E. WILCOX ARTURO G. PORRAS MARK D. ALLENDORF LUNG-SHAN KAU DARLENE J. SPIRA EDWARD I. SOLOMON	151	STRUCTURE/FUNCTION CORRELATIONS OF THE COUPLED BINUCLEAR COPPER ACTIVE SITE
JUDITH M. NOCEK DONALD M. KURTZ JR. J. TIMOTHY SAGE PETER DEBRUNNER	153	A NITRIC OXIDE ADDUCT OF THE BINUCLEAR IRON CENTER IN DEOXYHEMERYTHRIN FROM <i>PHASCOLOPSIS GOULDII</i> . ANALOGUE OF A PUTATIVE INTERMEDIATE IN THE OXYGENATION REACTION
C.L. COYLE W.G. ZUMFT W. JAKOB P.M.H. KRONECK	154	CHARACTERIZATION OF A NOVEL COPPER ENZYME: BACTERIAL NITROUS OXIDE REDUCTASE
DUARTE MOTA DE FREITAS JOAN SELVERSTONE VALENTINE	156	ANION BINDING SITES OF REDUCED BOVINE COPPER-ZINC SUPEROXIDE DISMUTASE: A Cl-35 AND HIGH-RESOLUTION H-1 NMR STUDY
K. CICHUTEK H. WITZEL F. PARAK	157	IRON A AND IRON B IN PURPLE BOVINE SPLEEN ACID PHOSPHATASE
M. SAHLIN A. EHRENBERG A. GRÄSLUND B.-M. SJÖBERG	157	PARAMAGNETIC ¹ H NMR SPECTRA OF RIBONUCLEOTIDE REDUCTASE FROM <i>ESCHERICHIA COLI</i>

MICHAEL J. MARONEY A. LAWRENCE ROE LAWRENCE QUE JR. JUDITH C. NOCEK GUDRUN S. LUKAT DONALD M. KURTZ JR.	158	NMR AND EXAFS STUDIES OF HEMERYTHRIN COMPLEXES
ANDREW K. SHIEMKE JOANN SANDERS-LOEHR THOMAS M. LOEHR	159	RESONANCE RAMAN STUDY OF THE HYDROXIDE ADDUCT OF HEMERYTHRIN
J.M.A. SMITH G.C. FORD J.L. WHITE P.M. HARRISON	161	PRELIMINARY STRUCTURAL STUDIES ON BACTERIOFERRITIN
MORTEN J. BJERRUM ERIK LÅRSEN	162	MANGANESE CONTAINING SUPEROXIDE DISMUTASE. STRUCTURAL AND SPECTROSCOPIC INVESTIGATIONS
ROBERT W. HENKENS KATHLEEN H. GROOVER RITA A. SHEFFEY TAFFY J. WILLIAMS	162	ACTIVE SITE FORMATION IN THE LAST STAGES OF FOLDING OF CARBONIC ANHYDRASE
L. BANCI I. BERTINI F. BRIGANTI C. LUCHINAT	164	WATER PROTON RELAXATION PROPERTIES OF MANGANESE(II) PROTEINS: A NEW THEORETICAL FRAMEWORK
C. FRED BREWER LOKESH BHATTACHARYYA RODNEY D. BROWN, III SEYMOUR H. KOENIG	165	EXTENDED SITE BINDING INTERACTIONS BETWEEN CONCAVALIN A AND GLYCOPEPTIDES AND OLIGOSACCHARIDES
JONAS ÅNGSTRÖM JACQUES BAUDIER	166	EFFECTS OF Ca^{2+} AND Zn^{2+} ON THE 1NMR PROPERTIES OF BOVINE S100b
OU YAOHUA ZHANG YUN WEI YUEWANG ZHOU XIN	167	FT-IR STUDIES OF THE ACTIVE SITES IN AMINOACYLASE
R. WEVER H. PLAT E. DE BOER	169	BROMOPEROXIDASES FROM SEAWEED: A NOVEL CLASS OF ENZYMES CONTAINING VANADIUM?
VINCENT L. PECORARO GERBEN ZYLSTRA RONALD H. OLSEN	170	ISOLATION OF THE DNA SEQUENCE CODING FOR <i>PSEUDOMONAS AERUGINOSA</i> AZURIN
SERGIO PAULO SEVERO DE SOUZA DINIZ	171	THE EFFECT OF MOLYBDENUM ON NITROGEN FIXING ORGANISMS
RICHARD C. REEM JAMES W. WHITTAKER EDWARD I. SOLOMON	172	SPECTROSCOPIC STUDIES OF NONHEME IRON ACTIVE SITES
B. BARATA I. MOURA A.V. XAVIER J.J.G. MOURA J. LIANG B.H. HUYNH J. LEGALL	174	EPR AND MÖSSBAUER STUDIES ON <i>DESULFOVIBRIO GIGAS</i> Mo(Fe-S) PROTEIN
A.R. LINO A.V. XAVIER I. MOURA J. LEGALL L.G. LJUNGDAHL	175	COBALT CONTAINING B_{12} COFACTORS FROM METHANOGENIC BACTERIA — SPECTROSCOPIC CHARACTERIZATION
TINY VAN HOUWELINGEN G.W. CANTERS J.A. DUINE J. FRANK, JZN. G. STOBELAAR	177	A BLUE COPPER PROTEIN FROM <i>THIOBACILLUS VERSUTUS</i>
M.C. FEITERS C.M. GROENEVELD G.W. CANTERS S.S. HASNAIN	178	EXAFS STUDIES ON OXIDIZED AND REDUCED AZURIN AT HIGH AND LOW pH

K.K. RAO D.O. HALL P. CUENDET M. GRÄTZEL	180	WATER PHOTOLYSIS USING SEMICONDUCTOR-BOUND HYDROGENASES
VÍCTOR M. FERNÁNDEZ CLAUDE HATCHIKIAN DAULAT PATIL RICHARD CAMMACK	180	EPR SPECTRA OF THE NICKEL CENTRE AND IRON-SULPHUR CLUSTERS DURING ACTIVATION AND DEACTIVATION OF <i>DESULFOVIBRIO GIGAS</i> HYDROGENASE
MICHAEL K. JOHNSON ISABEL C. ZAMBRANO MELVIN H. CZECHOWSKI HARRY D. PECK JR. DANIEL V. DERVARTANIAN JEAN LEGALL	182	LOW TEMPERATURE MAGNETIC CIRCULAR DICHROISM SPECTROSCOPY AS A PROBE FOR THE OPTICAL TRANSITIONS OF PARAMAGNETIC NICKEL IN HYDROGENASE
MICHAEL K. JOHNSON JOYCE E. MORNINGSTAR DEBORAH E. BENNETT BRIAN A.C. ACKRELL EDNA B. KEARNEY	183	SPECTROSCOPIC EVIDENCE FOR [2Fe-2S], [3Fe-xS], AND [4Fe-4S] CLUSTERS IN RECONSTITUTIVELY ACTIVE MAMMALIAN SUCCINATE DEHYDROGENASE
K. NAGAYAMA	184	REDOX STATE STUDIES OF TWO IRON-SULFUR CENTERS IN 7Fe FERREDOXINS BY PROTON MAGNETIC RESONANCE
E. BILL A.X. TRAUTWEIN H. WINKLER F.-H. BERNHARDT	185	NITROSYL-BINDING TO THE MONONUCLEAR NON-HEME IRON OF PUTIDAMONOXIN: A MODEL FOR THE CORRESPONDING PEROXO COMPLEX
A.X. TRAUTWEIN E. BILL R. BLÄS S. LAUER H. WINKLER A. KOSTIKAS	186	EXPERIMENTAL AND THEORETICAL ELECTRONIC STRUCTURE STUDIES OF IRON SULFUR AND IRON MOLYBDENUM SULFUR COMPOUNDS VIA MÖSSBAUER SPECTROSCOPY AND MOLECULAR ORBITAL THEORY
JACQUES GAILLARD PIERRETTE AURIC JEAN-MARC MOULIS JACQUES MEYER	188	EVIDENCE FOR HIGH MULTIPLICITY SPIN STATES IN THE 2 [4Fe-4Se] ⁺ FERREDOXIN FROM <i>CLOSTRIDIUM PASTEURIANUM</i>
J. LAMPREIA I. MOURA A. XAVIER J.J.G. MOURA H.D. PECK JR. J. LEGALL	189	EPR STUDIES ON ADENYLYL SULFATE (APS) REDUCTASE — A FLAVIN, IRON-SULFUR CONTAINING PROTEIN
PAUL A. LINDAHL WILLIAM H. ORME-JOHNSON THOMAS A. KENT EDMUND P. DAY ECKARD MÜNCK	191	A [4Fe-4S] CLUSTER WITH SPIN S=3/2: STUDIES OF THE NITROGENASE Fe-PROTEIN FROM <i>A. VINELANDII</i> IN THE PRESENCE OF 0.4 M UREA
M. TEIXEIRA I. MOURA A.V. XAVIER J.J.G. MOURA G. FAUQUE B. PICKRIL J. LEGALL	194	NICKEL-IRON-SULFUR-SELENIUM CONTAINING HYDROGENASES ISOLATED FROM <i>DESULFOVIBRIO BACULATUS</i> STRAIN 9974
M. CZECHOWSKI G. FAUQUE Y. BERLIER P.A. LESPINAT J. LEGALL	196	PURIFICATION OF AN HYDROGENASE FROM AN HALOPHILIC SULFATE REDUCING BACTERIUM: <i>DESULFOVIBRIO SALEXIGENS</i> STRAIN BRITISH GUIANA
G. CHOTTARD J.P. MAHY P. BATTIONI D. MANSUY	198	A RESONANCE RAMAN STUDY OF THE MYOGLOBIN COMPLEXES FORMED BY REACTION WITH MONOSUBSTITUTED HYDRAZINES
JAN MINTOROVITCH JAMES D. SATTERLEE	199	THE INFLUENCE OF DISTAL AMINO ACIDS UPON LIGAND BINDING AS DETERMINED FROM CYANIDE ION BINDING TO SPERM WHALE MET-MYOGLOBIN AND THE MONOMER FRACTION <i>GLYCERA DIBRANCHIATA</i> MET-HEMOGLOBINS
J.T.J. LECOMTE S.D. EMERSON G.N. LA MAR	200	ASSIGNMENT OF PROTEIN RESONANCES IN THE PROTON NMR SPECTRUM OF METCYANOMYOGLOBIN
A.W. ADDISON J.J. STAPHANOS (STEPHANOS)	201	NITROSYLIRON(III) HEMOGLOBIN: AUTOREDUCTION AND SPECTROSCOPY

LAURA A. ANDERSSON V. RENGANATHAN ANDREW A. CHIU THOMAS M. LOEHR MICHAEL H. GOLD	203	SPECTRAL CHARACTERIZATION OF DIARYLPROPANE OXYGENASE, A NOVEL PEROXIDE-DEPENDENT, LIGNIN-DEGRADING HEME ENZYME
JOHN H. DAWSON MASANORI SONO KIM SMITH EBLE LOWELL P. HAGER	205	SPECTROSCOPIC PROPERTIES OF CHLOROPEROXIDASE COMPOUNDS II AND III — POSSIBLE STRUCTURAL MODELS FOR ANALOGOUS CYTOCHROME P-450 DERIVATIVES
RICHARD J. KASSNER MICHAEL G. KYKTA	206	ANION BINDING TO A CYTOCHROME <i>c</i> '
CARLOS O. AREAN GEOFFREY R. MOORE GLYN WILLIAMS ROBERT J.P. WILLIAMS	208	SELECTIVITY OF THE INTERACTION BETWEEN CYTOCHROME <i>c</i> AND TRANSITION METAL ION COMPLEXES OF EDTA AND RELATED LIGANDS
I. MOURA A.V. XAVIER J.J.G. MOURA M.Y. LIU G. PAI H.D. PECK JR. J. LEGALL W.J. PAYNE	210	NMR STUDIES OF A MONOHEME CYTOCHROME FROM <i>WOLINELLA SUCCINOGENES</i> , A NITRATE RESPIRING ORGANISM
I. MOURA A.V. XAVIER J.J.G. MOURA G. FAUQUE J. LEGALL G.R. MOORE B.H. HUYNH	212	STRUCTURAL HOMOLOGY OF TETRAHEME CYTOCHROME <i>c</i> ₃
A.R. LINO J.J.G. MOURA A.V. XAVIER I. MOURA G. FAUQUE J. LEGALL	215	CHARACTERIZATION OF TWO LOW-SPIN BACTERIAL SIROHEME PROTEINS

2. Mechanims of Metalloprotein Action

A. FERRI C. BARTOCCI A. MALDOTTI V. CARASSITI	216	MET-80 INVOLVEMENT IN PHOTOREDOX PROCESSES OF CYTOCHROME <i>c</i>
HAROLD M. GOFF D.V. BEHERE ENRIQUE GONZALEZ-VERGARA	217	THE HEME ENVIRONMENT OF PEROXIDASES: ¹⁵ N NMR OF BOUND C ¹⁵ N ⁻
JAMES D. SATTERLEE JAMES E. ERMAN	218	ELEMENTS OF THE PROPOSED PEROXIDASE MECHANISM ELUCIDATED FROM NMR AND IR STUDIES OF CYTOCHROME <i>c</i> PEROXIDASE FORMS
DAVID MYERS GRAHAM PALMER	220	MCD STUDIES ON THE HEME AND TRYPTOPHAN COMPONENTS OF CYTOCHROME <i>c</i> PEROXIDASE
ELKA V. ELENKOVA MASANORI SONO JOHN H. DAWSON ANN M. ENGLISH	220	MAGNETIC CIRCULAR DICHROISM STUDIES OF CYTOCHROME <i>c</i> PEROXIDASE AND ITS LIGAND COMPLEXES
JAMES TERNER CATHERINE M. RECZEK ANDREW J. SITTER	222	OBSERVATION OF THE Fe ^{IV} =O STRUCTURES OF HORSE RADISH PEROXIDASE COMPOUND II AND FERRYL MYOGLOBIN BY RESONANCE RAMAN SPECTROSCOPY
WALTHER R. ELLIS DAVID F. BLAIR HSIN WANG HARRY B. GRAY SUNNEY I. CHAN	224	THIN-LAYER SPECTROELECTROCHEMISTRY OF THE CYT <i>a</i> AND CYT <i>a</i> ₃ SITES IN BEEF HEART CYTOCHROME <i>c</i> OXIDASE
DAVID BICKAR A.L. LEHNINGER	225	DIFFERENTIATION OF THE ALLOSTERIC AND REDOX PROPERTIES OF CYTOCHROME <i>c</i>
STEPHEN L. MAYO JUDITH L. CAMPBELL JOHN H. RICHARDS HARRY B. GRAY	227	THE USE OF «NON-PERTURBATIVE» SITE-DIRECTED MUTAGENESIS FOR THE STUDY OF ELECTRON TRANSFER MECHANISMS IN METALLOPROTEINS

ALISON BUTLER MICHAEL ALBIN HARRY B. GRAY	228	Cu(II)-LADH: A MULTI-SITE REDOX SYSTEM
MICHAEL P. DOYLE SURENDRA N. MAHAPATRO	229	ELECTRON TRANSFER BETWEEN HEMOGLOBIN AND ARENEDIAZONIUM SALTS
MARY AYROVAINEEN HARRY B. GRAY	230	INTRAMOLECULAR ELECTRON TRANSFER IN Ru(NH ₃) ₅ -MODIFIED CYTOCHROMES <i>c</i>
ANDREW W. AXUP ROBERT J. CRUTCHLEY HARRY B. GRAY	231	INTRAMOLECULAR ELECTRON TRANSFER BETWEEN METAL REDOX SITES IN RUTHENIUM-MODIFIED MYOGLOBINS
FRASER A. ARMSTRONG H. ALLEN O. HILL B. NIGEL OLIVER	232	TOWARDS THE DESIGN OF ELECTROCHEMICAL INTERFACES WHICH PERMIT RAPID AND SPECIFIC HETEROGENEOUS ELECTRON TRANSFER TO REDOX ENZYMES
LARS-GUNNAR FRANZÉN ÖRJAN HANSSON LARS-ERIK ANDRÉASSON	233	EPR STUDIES ON THE FUNCTION OF THE 16, 24 AND 33 kDa SUBUNITS ON THE PHOTOSYSTEM II DONOR SIDE
PIERRE SÉTIF H. BOTTIN T. VÄNNGÅRD P. MATHIS	234	ABSORPTION AND EPR STUDIES OF PHOTOSYSTEM I PHOTOCHEMISTRY
DAVID F. BLAIR JEFF GELLES SUNNEY I. CHAN	235	PROTON PUMPING BY CYTOCHROME <i>c</i> OXIDASE: THE IMPORTANCE AND MECHANISMS OF ELECTRON GATING
STEPHAN N. WITT DAVID F. BLAIR JOEL E. MORGAN SUNNEY I. CHAN	236	REACTIONS OF CYTOCHROME <i>c</i> OXIDASE WITH CARBON MONOXIDE
ANN M. ENGLISH TUN-CHEONG CHEUNG JACK A. KORNBLATT	237	ELECTRON TRANSFER BETWEEN FERROCYTOCHROME <i>c</i> PEROXIDASE (CCP ^{II}) AND FERRICYTOCHROME <i>c</i> (C ^{III}): IONIC STRENGTH EFFECTS
PETER JENSEN MICHAEL T. WILSON ROLAND AASA BO G. MALMSTRÖM	238	CYANIDE-INHIBITION STUDIES ON CYTOCHROME <i>c</i> OXIDASE USING RAPID-FREEZE/EPR
LOUISE KARLE HANSON	239	REDOX PATHWAYS IN <i>c</i> -TYPE CYTOCHROMES. POSSIBLE ROLE OF THE BRIDGING SULFUR
GERALD T. BABCOCK GRAHAM PALMER JOHN M. JEAN LEAH N. JOHNSTON WILLIAM H. WOODRUFF	240	TIME-RESOLVED RESONANCE RAMAN STUDY OF THE OXIDATION OF CYTOCHROME OXIDASE BY DIOXYGEN
PER-ERIC THÖRNSTRÖM BASSAM SOUSSI LARS ARVIDSSON BO G. MALMSTRÖM	243	STEADY-STATE KINETICS OF CYTOCHROME <i>c</i> OXIDASE IN PHOSPHOLIPID VESICLES: THE EFFECTS OF pH, IONIC STRENGTH AND D ₂ O
G.D. ARMSTRONG T. RAMASAMI A.G. SYKES	244	ACTIVE SITE CHEMISTRY OF OCTAMERIC AND MONOMERIC HEMERYTHRIN FROM <i>THEMISTE ZOSTERICOLA</i>
J.D. SINCLAIR-DAY A.G. SYKES	245	ACID DISSOCIATION CONSTANTS FOR THREE PLASTOCYANINS
M.E. SANDER H. WITZEL	247	CARBOXYPEPTIDASE A, EVIDENCE FOR AN ANHYDRIDE INTERMEDIATE
JUNZO HIROSE MASAHIDE NOJI YOSHINORI KIDANI RALPH G. WILKINS	247	THE INTERACTION OF ZINC IONS WITH ARSANILAZOTYROSINE-248-CARBOXYPEPTIDASE A
P. GRUNWALD	248	KINETIC SALT EFFECT OF ALKALINE EARTH CHLORIDES ON THE UREASE CATALYZED UREA HYDROLYSIS
P. GRUNWALD	249	DEPENDENCE OF THE UREASE CATALYZED UREA HYDROLYSIS ON SUBSTRATE CONCENTRATION AND TEMPERATURE IN THE PRESENCE OF ALKALINE EARTH HALIDES
M. STEPHENSON	250	PROTEIN INTERACTION WITH THE COPPER(II)/ASCORBIC ACID/OXYGEN SYSTEM: EVIDENCE FOR A NON-SITE SPECIFIC REACTION

DAVID K. LAVALLEE DEBASISH KUILA	251	REACTIVITY PATTERNS IN THE NUCLEOPHILIC DEALKYLATION OF <i>N</i> -SUBSTITUTED METALLOPORPHYRINS
CECILIA FORSMAN LENA TIBELL INGVAR SIMONSSON SVEN LINDSKOG	253	INHIBITION OF HUMAN CARBONIC ANHYDRASE II BY SOME ORGANIC COMPOUNDS
GEROLAMO DEVOTO ENRICO SANJUST GIOVANNI FLORIS	254	INHIBITORY ACTIVITY OF Cu(II), Co(II) AND Ni(II) COMPLEXES WITH 1,4-BIS(3-AMINOPROPYL)PIPERAZINE AND 3,3'-DIAMINO-N-METHYLDIPROPYLAMINE TOWARD LENTIL SEEDLINGS DIAMINEOXIDASE
R.C. BRAY G.N. GEORGE F.F. MORPETH D.H. BOXER	255	THE NATURE OF THE HIGH-pH/LOW-pH TRANSITION IN SULPHITE OXIDASE AND IN NITRATE REDUCTASE
3. Metal Substituted Metalloproteins		
CHRISTIAN SARTORIUS MICHAEL ZEPPEZAUER MICHAEL F. DUNN	256	DETECTION AND CHARACTERIZATION OF INTERMEDIATES IN THE REACTION CATALYZED BY Co(II)-SUBSTITUTED HORSE LIVER ALCOHOL DEHYDROGENASE
I. BERTINI G. LANINI C. LUCHINAT C. HAAS W. MARET M. ZEPPEZAUER	257	¹ H NMR INVESTIGATION OF INHIBITOR BINDING TO COBALT(II) SUBSTITUTED LIVER ALCOHOL DEHYDROGENASE (LADH)
I. BERTINI G. LANINI C. LUCHINAT M.S. VIEZZOLI M. POLSINELLI E. GALLORI F. PAOLETTI	258	¹ H NMR SPECTRA OF ACTIVE SITE RESIDUES IN COBALT(II) ALKALINE PHOSPHATASE
I. BERTINI C. LUCHINAT L. MESSORI R. MONNANNI A. SCOZZAFAVA	259	CD AND ¹ H NMR STUDIES ON COBALT(II) SUBSTITUTED OVOTRANSFERRIN-OXALATE COMPLEXES
J. LORÖSCH U. QUOTSCHALLA W. HAASE	260	MAGNETIC AND EPR INVESTIGATIONS ON Co(II)-HEMOCYANIN: A MODEL FOR DEOXY-HEMOCYANIN
W. MARET C. HAAS M. ZEPPEZAUER H. DIETRICH R. MONTIEL-MONTOYA E. BILL A.X. TRAUTWEIN	261	Fe(II)- AND Fe(III)-SUBSTITUTED HORSE LIVER ALCOHOL DEHYDROGENASE
C. SYVERTSEN R. GAUSTAD T. LJONES	262	Cu ²⁺ BINDING TO DOPAMINE β-MONOOXYGENASE
STEFAN DAHLIN BENGT REINHAMMAR JONAS ÅNGSTRÖM	263	NMR STUDIES OF Ni(II)- AND Co(II)-SUBSTITUTED STELLACYANIN
PETER P. CHUKNYISKI JOSEPH M. RIFKIND KENNETH ALSTON	264	CONFORMATION AND TEMPERATURE DEPENDENT SPECTRAL CHANGES IN NICKEL HEMOGLOBIN
NICOLAY GENOV MARIA SHOPOVA RAINA BOTEVA	266	STUDIES ON THE LANTHANIDE COMPLEXES OF SUBTILISINS
4. Models for Metalloproteins		
H. TSAI W.V. SWEENEY C.L. COYLE	268	TRANSPORT OF HYDROGEN IONS BY A 4Fe-4S MODEL COMPOUND IN A DIRECTIONAL ELECTRON TRANSPORT SYSTEM
MICHELLE MILLAR TIMOTHY O'SULLIVAN	269	SYNTHESIS AND STUDY OF AN ANALOG FOR THE [Fe ₄ S ₄] ³⁺ CENTER OF OXIDIZED HIGH POTENTIAL IRON-SULFUR PROTEINS
J. GLOUX P. GLOUX B. LAMOTTE G. RIUS	270	ESR IN SINGLE CRYSTALS OF 4 IRON 4 SULFUR SYNTHETIC CUBANES: A NEW WAY FOR DETAILED SPECTROSCOPIC STUDIES OF THE [Fe ₄ S ₄] ⁺ AND [Fe ₄ S ₄] ³⁺ STATES

P. AURIC N. DUPRÉ J. JORDANOV	271	A CORRELATION BETWEEN THE STRUCTURAL, ELECTRONIC AND MAGNETIC PROPERTIES OF $[\text{Fe}_4\text{S}_5\text{Cp}_4]^{n+}$ ($n=0,1+,2+$) CORES, PRESENT IN A DISTORTED CUBANE-TYPE CLUSTER WITH ONE PENTA-COORDINATED IRON ATOM
NORIKAZU UEYAMA MICHIAKI FUJI ATSUSHI KAJIWARA AKIRA NAKAMURA	272	CHELATION EFFECT OF A Cys-X-Y-Cys TETRAPEPTIDE SEQUENCE FOR THE 4Fe-4S CLUSTER
UGO CORNARO FRANCO CARIATI FRANCO BONOMI	273	EVIDENCES FOR THE FORMATION OF COMPLEXES OF D,L-DIHYDROTHIOCTIC ACID (REDUCED LIPOIC ACID) WITH Ni^{II} , Co^{II} AND Fe^{III} SALTS
J. PAUL K.G. PAUL	274	A UNIFIED CONCEPT OF ELECTRONIC PERTURBATIONS OF PORPHYRINS
M. MOMENTEAU A. CROISY A. DESBOIS	276	STERIC HINDRANCE INFLUENCE OF IRON(II)-PORPHYRINS ON O_2 AND CO BINDINGS: INFRARED AND RESONANCE RAMAN STUDIES
ALAN L. BALCH GERD N. LA MAR MARK W. RENNER LECHOSLAW LATOS-GRAZYNSKI	277	REVERSIBLE OXIDATION OF IRON(II) N-METHYLPORPHYRINS. CHARACTERIZATION OF THERMALLY UNSTABLE IRON(III) N-METHYLPORPHYRINS
R. MONTIEL-MONTOYA E. BILL A.X. TRAUTWEIN H. WINKLER L. RICARD M. SCHAPPACHER R. WEISS	278	MÖSSBAUER STUDY OF OXY-MODELS FOR THE ENZYME P450. I: $[\text{Fe}(\text{O}_2)(\text{SC}_6\text{HF}_4)\text{TP}_{\text{P1V}}\text{P}][\text{NaCl}18\text{C}6]$; II: $[\text{Fe}(\text{O}_2)(\text{SC}_6\text{HF}_4)\text{TP}_{\text{P1V}}\text{P}][\text{Kc}222]$; AND III: $[\text{Fe}(\text{O}_2)(\text{SC}_6\text{HF}_4)\text{TP}_{\text{P1V}}\text{P}][\text{Nac}222]$
E. BILL A.X. TRAUTWEIN K. FISCHER K.H. PAULI N. BLAES U. GONSER R. PRESTON F. SEEL R. STAAB	280	LOW TEMPERATURE MOLECULAR DYNAMICS OF $[\text{HFe}(\text{CO})_4]^-$: A POSSIBLE MODEL FOR THE DYNAMIC BEHAVIOR OF O_2 IN IRON-PORPHYRINS
H. WINKLER E. BILL A.X. TRAUTWEIN L. ALDRIDGE H. TOFTLUND	282	SPIN-CROSSOVER DYNAMICS IN MODEL-COMPOUNDS FOR HEME PROTEINS
WILLIAM H. ARMSTRONG STEPHEN J. LIPPARD	284	NEW CHEMISTRY OF BINUCLEAR IRON COMPLEXES — MODELS FOR HEMERYTHRIN AND RELATED PROTEINS
LUIGI CASELLA MICHELE GULLOTTI ALESSANDRO PINTAR	285	MODELS FOR IRON-TYROSINATE COORDINATION IN PROTEINS. SPECTRAL AND STEREOCHEMICAL STUDIES OF IRON(III) COMPLEXES OF N-SALICYLIDENE-L-AMINO ACIDS
N. NI CHOILEAIN J.D. GLENNON	287	ANALYTICAL TECHNIQUES IN THE STUDY OF Ni AND Fe MODEL COMPLEXES OF BIOLOGICAL SIGNIFICANCE
JAYANTI CHANDRASEKARAN SABYASACHI SARKAR	288	SYNTHETIC APPROACH TO THE MONONUCLEAR ACTIVE SITES OF MOLYBDOENZYMES
J. LORÖSCH U. QUOTSCHALLA W. HAASE	289	MODELLING THE HEMOCYANIN ACTIVE SITE: A CONTRIBUTION TO MAGNETO-STRUCTURAL CORRELATIONS
JAN BECHER HANS TOFTLUND	290	BIOMIMETIC SYSTEMS FOR THE "VISIBLE" COPPER-SITE Cu_A IN CYTOCHROME c OXIDASE
J. VAN RIJN W.L. DRIESSEN J. REEDIJK	291	COPPER CHELATES OF A DINUCLEATING BENZIMIDAZOLE-CONTAINING LIGAND AS MODELS FOR TYPE III COPPER PROTEINS
NEIL A. BAILEY DAVID E. FENTON COLIN H. MCLEAN	292	IMIDAZOLE-CONTAINING SCHIFF BASE LIGANDS AS VERSATILE MODELS FOR COPPER PROTEIN ENVIRONMENTS
THOMAS N. SORRELL A. S. BOROVIK DEBORA J. ELLIS CHIEN-CHANG SHEN	293	MODELS FOR COPPER PROTEINS
STEPHEN A. KOCH RONALD FIKAR DOUGLAS CORWIN MICHELLE MILLAR	294	COBALT THIOLATE COMPLEXES: MODELS FOR THE ACTIVE SITES OF METAL-CYSTEINE PROTEINS

5. Complexes of Biochemical Interest

MARKUS BAUMGARTNER NORBERT CATHOMAS GEOFFREY B. JAMESON ERICH DUBLER	295	METAL COMPLEXES OF SULFUR-CONTAINING LIGANDS OF BIOLOGICAL INTEREST: S-METHYL-L-CYSTEINE, α -LIPIC ACID AND GLUTATHIONE
HELMUT SIGEL ROGER TRIBOLET	296	INTRAMOLECULAR HYDROPHOBIC AND STACKING INTERACTIONS IN BINARY AND TERNARY AMINO ACID COMPLEXES
J.P. LAUSSAC A. ROBERT R. HARAN B. SARKAR	298	MODELS FOR METAL-PROTEIN INTERACTION: COPPER(II) COMPLEXES WITH A CYCLIC PEPTIDE HAVING SIDE-CHAIN IMIDAZOLYL AND CARBOXYL GROUPS
L. ANTOLINI L. MENABUE G.C. PELLACANI M. SALADINI L.P. BATTAGLIA A. BONAMARTINI CORRADI	298	THE ROLE OF THE TOSYL GROUP ON THE COORDINATION ABILITY OF <i>N</i> -PROTECTED AMINOACIDS. SOLID STATE BEHAVIOR OF <i>N</i> -TOSYLVALINATE COPPER(II) COMPLEXES
GRAZYNA FORMICKA-KOZŁOWSKA LESLIE D. PETTIT	300	THE CUPRIC INTERACTION WITH OPIOID PEPTIDES
LUIGI CASELLA LUIGI RIGONI	301	MONONUCLEAR AND BINUCLEAR COPPER(I) AND COPPER(II) COMPLEXES DERIVED FROM L-HISTIDINE AND L-N ⁷ -METHYLHISTIDINE
B. DECOCK-LE-REVEREND L. ANDRIANARIJAONA C. LOUCHEUX L.D. PETTIT I. STEEL H. KOZŁOWSKI	302	CO-ORDINATION ABILITY OF AN <i>N</i> -TERMINAL TETRAPEPTIDE FRAGMENT OF FIBRINOPEPTIDE A
G. ARENA G. IMPELLIZZERI R.M. IZATT J.D. LAMB E. RIZZARELLI	303	THERMODYNAMIC AND SPECTROSCOPIC STUDY OF METAL COMPLEX FORMATION WITH CYCLOPEPTIDES: Cu(II)- AND Zn(II)-CYCLO-L-HISTIDYL-L-HISTIDYL
ERICH DUBLER ZLATAN KOPAJTIĆ GEOFFREY B. JAMESON	304	STRUCTURAL INVESTIGATIONS OF MAGNESIUM- AND COPPER(II)-HYDROGENURATES
ANA MARIA V.S.V. CAVALEIRO VICTOR M.S. GIL JULIO D. PEDROSA DE JESUS ROBERT D. GILLARD PETER A. WILLIAMS	305	MOLYBDENUM(VI) COMPLEXES OF (R)-CYSTEINE IN AQUEOUS SOLUTION
M. CASTILLO J.J. CRIADO B. MACÍAS M.V. VAQUERO	307	NEW NICKEL(II) COMPLEXES WITH DITHIOCARBAMATE-DERIVATIVES OF α -AMINOACIDS
A.G. SYKES R. LARSEN J.R. FISCHER E.H. ABBOTT	308	PREFERENTIAL CATALYSIS OF MODEL REACTIONS IN THE COBALT(III) COMPLEX OF THE VITAMIN B-6 SCHIFF BASE OF GLYCINE
L. ALAGNA T. PROSPERI A.A.G. TOMLINSON R. RIZZO	310	EXAFS STUDIES OF GEL AND SOLID FORMS OF Ca ²⁺ - α -D-POLYGALACTURONATE
ISABELLA L. KARLE	311	MODES OF COMPLEXATION OF CYCLIC PEPTIDES WITH LIGHT METAL IONS
PETER M. MAY KEVIN MURRAY DANIEL PEAPER	312	THE EFFECT OF SODIUM ION INTERFERENCE ON BIOINORGANIC FORMATION CONSTANTS DETERMINED BY GLASS ELECTRODE POTENTIOMETRY
ADRIANO BENEDETTI CARLO PRETI LORENZO TASSI GIUSEPPE TOSI	313	SYNTHESIS AND CHARACTERIZATION OF <i>d</i> -BLOCK COMPLEXES WITH BROMAZEPAM AS LIGAND
MARIANO CASU ADOLFO LAI GIUSEPPE SABA	314	DYNAMICAL PROPERTIES OF ATP/CdCl ₂ AND ATP(Cd(ClO ₄) ₂) COMPLEXES: A COMBINED ¹³ C AND ¹¹³ Cd RELAXATION STUDY
B. PISPISA A. PALLESCI G. PARADOSSI	316	CHIRAL DISCRIMINATION IN ELECTRON TRANSFER REACTIONS BETWEEN ASYMMETRIC SPECIES

L.L. FISH A.L. CRUMBLISS	318	AN INVESTIGATION OF THE KINETICS AND MECHANISM OF IRON(III) RELEASE FROM <i>N,N'</i> -DI(2-HYDROXYBENZYL)ETHYLENEDIAMINE- <i>N,N'</i> -DIACETIC ACID AS A MODEL FOR IRON EXCHANGE FROM TRANSFERRIN
ARMANDO J.L. POMBEIRO M. AMÉLIA N.D.A. LEMOS	319	NET ELECTRON ACCEPTOR/DONOR CHARACTER OF ISOCYANIDES AND DINITROGEN AT THE IRON(II) CENTRE $[\text{FeH}(\text{Ph}_2\text{PCH}_2\text{CH}_2\text{PPh}_2)_2]^+$: AN ELECTROCHEMICAL STUDY
ARMANDO J.L. POMBEIRO M. FERNANDA N.N. CARVALHO	321	ELECTRON-RICH RHENIUM AND MOLYBDENUM METAL CENTRES AS POTENTIAL INORGANIC MODELS IN THE BIO-REDUCTION OF ISOCYANIDES?
PATRICK A. TAYLOR ARTHUR E. MARTELL	323	A PROTON-NMR STUDY OF THE KINETICS OF FORMATION OF THE GENERAL INTERMEDIATE IN VITAMIN B-6-CATALYZED TRANSAMINATION
ARUP K. BASAK ARTHUR E. MARTELL	324	REACTIONS OF DIOXYGEN COMPLEXES. AUTOXIDATION OF 2-AMINOMETHYLPYRIDINE THROUGH COBALT DIOXYGEN COMPLEX FORMATION
W.L. KWIK K.P. ANG	324	COORDINATION ABILITIES OF SUBSTITUTED PHENOLATES — A SPECTROPHOTOMETRIC AND CONDUCTOMETRIC STUDY
E. CASASSAS M. FILELLA A. IZQUIERDO	326	COMPLEX FORMATION IN THE SYSTEM Ni(II) — α -MERCAPTOPHENYLACETIC ACID
H. ELIAS M. DREHER M. SCHUMANN CHR. HASSERODT-TALIAFERRO K.J. WANNOWIUS	328	KINETICS OF LIGAND SUBSTITUTION IN CHELATE COMPLEXES OF DIVALENT TRANSITION METALS OF BIOLOGICAL IMPORTANCE
M. BELICCHI FERRARI G. GASPARRI FAVA C. PELIZZI P. TARASCONI G. TOSI	328	COORDINATING PROPERTIES OF PYRIDOXAL THIOSEMICARBAZONE IN METAL COMPLEXES
A. MARZOTTO D.A. CLEMENTE	330	NMR AND SPECTROSCOPIC STUDIES ON THE PYRIDOXAL/GLYCINE /DIOXOURANIUM(VI) SYSTEM
ISABELLE SASAKI ALAIN GAUDEMER	332	SYNTHESIS OF COBALT(II) COMPLEXES WITH NON-SYMMETRIC SCHIFF BASES
SHALOM SAREL SHELLY AVRAMOVICI-GRISARU	332	COORDINATION CHEMISTRY OF IRON BIS-PYRIDOXAL ISONICOTINOYL HYDRAZONE: STEREOCHEMICAL AND ELECTROCHEMICAL CONSIDERATIONS
FRANCO BONOMI SILVIA PAGANI PAOLO CERLETTI	333	MOBILIZATION OF FERRITIN-BOUND IRON BY REDUCED D,L-LIPOATE AND REDUCED D,L-LIPOAMIDE
UGO CORNARO FRANCO CARIATI FRANCO BONOMI	335	ELECTROCHEMICAL PROPERTIES OF $[\text{Fe}_4\text{S}_4(\text{SC}_6\text{H}_5)_4]^{2-}$, ANALOGUE OF THE ACTIVE SITE OF IRON-SULFUR PROTEINS, IN AQUEOUS MICELLAR SOLUTIONS
PETER W. LINDER ALEXANDER VOYE	337	COMPLEXATION OF COPPER(II) IONS BY CAFFEIC ACID
J. RUIZ-SANCHEZ E. COLACIO-RODRIGUEZ J.M. SALAS-PEREGRIN M.A. ROMERO-MOLINA	338	INTERACTION OF 6-AMINO-1,3-DIMETHYL-5-PHENYLZOURACIL WITH Co(II), Ni(II), Cu(II) AND Ag(I) IONS
Y. OZAKI K. IRIYAMA T. KITAGAWA H. OGOSHI T. OCHIAI	340	COMPARATIVE STUDY OF METALLOCHLORINS AND METALLOPORPHYRINS BY RESONANCE RAMAN SPECTROSCOPY
M.A. CINELLU M.L. GANADU G. MINGHETTI F. CARIATI F. DEMARTIN M. MANASSERO	341	PALLADIUM(II) DERIVATIVES OF SOME 1,4-BENZODIAZEPIN-2-ONES
L. STRINNA ERRE G. MICERA P. PIU F. CARIATI	343	COPPER(II) COMPLEXES OF SOME INDOLIC ACIDS

MARIA E. CURRY DEREK J. HODGSON DRAKE S. EGGLESTON	344	CALCIUM BINDING TO METHYLMALONATE ION
M. MADALENA CALDEIRA NUNO OLIVEIRA VICTOR M.S. GIL CARLOS F.G. GERALDES	344	MULTINUCLEAR NMR STUDIES OF VANADIUM(V) COMPLEXES WITH LACTIC AND MALIC ACIDS
G. MICERA S. DEIANA A. DESSI P. DECOCK B. DUBOIS H. KOZŁOWSKI	345	SPECTROSCOPIC AND POTENTIOMETRIC STUDIES OF COPPER(II) COMPLEXES OF D-GLUCOSAMINE
M.B. YIM M.W. MAKINEN	346	ENDOR STUDY OF SMALL MOLECULE AND ENZYME COMPLEXES OF Gd^{3+} IN FROZEN SOLUTION
C.F.G.C. GERALDES M.C. ALPOIM M.P.M. MARQUES A.D. SHERRY M. SINGH	346	A NMR STUDY OF $Ln(NOTA)$ CHELATES AS AXIALLY SYMMETRIC AQUEOUS SHIFT REAGENTS
C.F.G.C. GERALDES A.D. SHERRY R.D. BROWN, III S.H. KOENIG	348	NMRD INVESTIGATION OF Mn^{2+} AND Gd^{3+} NOTA COMPLEXES, AND A COMPARISON WITH THE ANALOGOUS EDTA COMPLEXES
KELLEY WOODRING RICHARD W. TAYLOR	350	SUBSTITUENT EFFECTS ON THE DISSOCIATION KINETICS OF HEAVY METAL ION CRYPTATES
ANDREA MALDOTTI CARLO BARTOCCI ALBERTINO FERRI VITTORIO CARASSITI	352	PHOTOCHEMISTRY OF IRON(III) PROTOPORPHYRIN IX IN OXYGENATED ALKALINE AQUEOUS ETHANOL. EVIDENCE FOR SUPEROXIDE RADICAL FORMATION AND ITS INVOLVEMENT IN THE PORPHYRIN DEGRADATION
JOHN H. DAWSON ELISABETH T. KINTNER MAUREEN K. GENO	354	BINUCLEAR RUTHENIUM ALKYL DIOXIME COMPLEXES: MODELS FOR ELECTRON TRANSFER THROUGH SATURATED BARRIERS
DONALD W. JACOBSEN RALPH GREEN	355	SYNTHESIS OF METHYLCOBALAMIN FROM THE GLUTATHIONE-COBALAMIN COMPLEX
KENNETH L. BROWN JANETTE M. HAKIMI DONALD W. JACOBSEN	357	^{31}P -NMR STUDIES OF COBALAMINS
G. DUBOWCHIK D. HEILER A.D. HAMILTON	358	SYNTHETIC PORPHYRINS CONTAINING ADJACENT, REDOX-ACTIVE SPECIES; MODELS OF BIOLOGICAL ELECTRON TRANSFER SITES
B. SZPOGANICZ J.R. MOTEKAITIS A.E. MARTELL	360	METAL ION — AND VITAMIN B_6 — CATALYZED TRANSAMINATION AND DEPHOSPHONYLATION OF 2-AMINO-3-PHOSPHONOPROPIONIC ACID
V. MORENO E. MOLINS A. LABARTA A. CAUBET J. TEJADA	361	SYNTHESIS, MÖSSBAUER AND MAGNETIC CHARACTERIZATION OF SOME IRON(III)- -NUCLEIC ACID COMPONENTS (NUCLEOTIDE, NUCLEOSIDE AND BASE)
C. ROSSI N. MARCHETTINI E. PERICCIOLI A. PRUGNOLA E. TIEZZI N. NICCOLAI	362	MAGNESIUM(II)-INDUCED EFFECTS ON THE STABILITY OF THE ADENOSIDE-THYMIDINE COMPLEX IN SOLUTION
CARLOS F.G.C. GERALDES M. MARGARIDA C.A. CASTRO	364	A MULTINUCLEAR MAGNETIC RESONANCE STUDY OF THE INTERACTION OF MONONUCLEOTIDES WITH OXOCATIONS OF $Mo(VI)$, $W(VI)$ AND $V(V)$ IN AQUEOUS SOLUTION
P. PUIG A. TERRON J.J. FIOL V. MORENO	365	METAL COMPLEXES OF 3d IONS WITH 5'-AMP, 3'-AMP AND 2'-AMP: SYNTHESIS, CHARACTERIZATION AND STUDY OF RABBIT MUSCLE GLYCOGEN PHOSPHORYLASE β ACTIVATION
JANE E. FREW PETER JONES GEORGE SCHOLDS	367	REACTION OF RADIOLYTICALLY FORMED HYDROPEROXIDES ON DNA AND PRECURSOR COMPOUNDS WITH REDOX-ACTIVE METAL IONS AND COMPLEXES
N. KATSAROS A. GRIGORATOS	367	TRANSITION METAL COMPLEXES WITH 8-AZAADENINE AND 8-AZAGUANINE

JOLANTA SWIATEK KAZIMIERZ GASIOROWSKI HENRYK KOZŁOWSKI	368	POLAROGRAPHIC AND SPECTROSCOPIC STUDY ON Pb^{+2} ION INTERACTION WITH DNA
THOMAS D. TULLIUS BETH A. DOMBROSKI	369	USING A TRANSITION METAL COMPLEX TO MAKE AN IMAGE OF THE HELICAL TWIST OF DNA
ROGER TRIBOLET HELMUT SIGEL	371	SOLVENT-INFLUENCE ON THE INTRAMOLECULAR EQUILIBRIA OCCURRING IN COMPLEXES OF ADENOSINE 5'-TRIPHOSPHATE
W. KLEIBÖHMER B. WENCLAWIAK B. KREBS	373	REACTION OF $[cis-Pt(NH_3)_2Cl_2]$ WITH RIBOSE DINUCLEOSIDE MONOPHOSPHATES. HPLC INVESTIGATION ON THE TIME DEPENDENT FORMATION OF THE REACTION PRODUCTS
D. PRASEUTH M.H. LANSARD M. PERRÉE-FAUVET A. GAUDEMER I. SISSOÉFF E. GUILLÉ	374	INTERACTIONS OF WATER-SOLUBLE PORPHYRINS AND METALLOPORPHYRINS WITH NUCLEIC ACIDS AND DERIVATIVES — THE INFLUENCE OF THE METAL
ROBERT F. PASTERNAK ESTHER J. GIBBS	375	INTERACTIONS OF WATER SOLUBLE PORPHYRINS WITH Z-POLY(dG-dC)
BRUCE E. BOWLER STEPHEN J. LIPPARD	376	EFFECTS OF LINKED AND EXTERNAL INTERCALATORS ON THE BINDING OF PLATINUM ANTITUMOR DRUGS TO DNA
J.L. VAN DER VEER G.J. LIGHTVOET A.R. PETERS J. REEDIJK	377	BINDING OF <i>cis</i> PLATINUM COMPOUNDS TO NUCLEOBASES, NUCLEOTIDES AND OLIGONUCLEOTIDES
JIRÍ KOZELKA GREGORY A. PETSKO STEPHEN J. LIPPARD GARY J. QUIGLEY	378	MOLECULAR MECHANICS CALCULATIONS ON <i>cis</i> -DIAMMINEDICHLOROPLATINUM(II) ADDUCTS OF TWO d(GpG)-CONTAINING OLIGONUCLEOTIDE DUPLEXES
JACQUELINE K. BARTON AVIS DANISHEFSKY ELIAS LOLIS	379	CHIRAL DISCRIMINATION IN THE COVALENT BINDING OF BIS(PHENANTHROLINE)RUTHENIUM(II) COMPLEXES TO DNA
MICHAEL J. CLARKE BRUCE JANSEN KENNETH A. MARX RAY KRUGER	380	BIOCHEMICAL EFFECTS OF BINDING $[(H_2O)(NH_3)_5Ru^{II}]^{2+}$ AND $[(NH_3)_5Ru^{III}]$ TO DNA
HELMUT SIGEL ROGER TRIBOLET	381	SYNERGISM IN THE METAL ION PROMOTED HYDROLYSIS OF ADENOSINE 5'-TRIPHOSPHATE
6. Bioinorganic Therapy		
RUTH MARGALIT HARRY B. GRAY MICHAEL CLARKE S.C. SRIVASTAVA	382	BIOLOGICAL TISSUE DISTRIBUTION OF $Ru(NH_3)_5$ -BLEOMYCIN
M.G. BASALLOTE E.J.G. CONEJERO R. VILAPLANA F. GONZÁLEZ-VÍLCHEZ	382	PLATINUM COMPLEXES OF EDDA AND ITS ETHYL ESTER: SYNTHESIS AND ANTITUMOR PROPERTIES
J.P. ALBERTINI A. GARNIER-SUILLEROT	384	INTERACTION OF BLEOMYCIN WITH Pd(II) COMPLEXES ($[PdCl_4]^{2-}$, $[cis-Pd(NH_3)_2Cl_2]$, $[Pd(en)Cl_2]$) AND WITH $[cis-Pt(NH_3)_2Cl_2]$. ANTITUMOR ACTIVITY OF THE BLM- $[cis-Pt(NH_3)_2Cl_2]$ SYSTEM
OLE JØNS ERIK SYLVEST JOHANSEN	385	ALUMINIUM COMPLEXES WITH PICOLINIC ACID
I. CONSTANTINIDIS J.D. SATTERLEE	386	UROHEMIN INTERACTION WITH THE ANTIMALARIAL DRUGS CHLOROQUINE AND QUININE
G. ARAVAMUDAN P.N. VENKATASUBRAMANIAN	388	SELENIUM-MERCURY INTERACTIONS IN PRESENCE OF SULFHYDRYL COMPOUNDS: POSSIBLE MODEL SYSTEM FOR SELENIUM DETOXIFICATION OF MERCURY
M.L. FIALLO A. GARNIER-SUILLEROT	389	METAL ANTHRACYCLINE COMPLEXES AS NON CARDIOTOXIC ALTERNATIVES TO ANTHRACYCLINE ANTICANCER AGENTS. PHYSICO-CHEMICAL CHARACTERISTIC AND ANTITUMOR ACTIVITY OF Pd(II)-ANTHRACYCLINE COMPLEXES
C.G. PIERPONT N.S. ROWAN	390	COPPER(II) BINDING BY MITOXANTRONE

M.L. VITOLO J. WEBB G.T. HEFTER B.W. CLARE P. WILAIRAT C. SANGMA	392	PYRIDOXAL ISONICOTINOYL HYDRAZONE: A PROMISING AGENT FOR CHELATION THERAPY OF IRON OVERLOAD
J. WEBB E. DELHAIZE J.F. LONERAGAN	392	ASCORBATE OXIDASE, DIAMINE OXIDASE AND THEIR USE IN DIAGNOSIS OF COPPER DEFICIENCY IN PLANTS
ARGYRIOS VARSAMIDIS GUY BERTHON	393	MALATE AS A POTENTIAL AGENT TO PROMOTE HISTAMINE CATABOLISM
MICHEL BRION LUC LAMBS GUY BERTHON	394	DO TETRACYCLINES HAVE ANY INFLUENCE ON ZINC AND COPPER BIOAVAILABILITIES AT BLOOD THERAPEUTIC LEVELS?
A.R. KARIM I.P.L. COLEMAN N.J. BIRCH	396	LITHIUM TRANSPORT AND FACTORS AFFECTING THE MOVEMENT OF LITHIUM IN ISOLATED JEJUNAL MUCOSA OF GUINEA PIG
SUSAN J. BERNERS PRICE PETER J. SADLER REIKO KURODA MICHAEL J. DIMARTINO BLAINE M. SUTTON DAVID T. HILL	397	PREPARATION, CHARACTERIZATION AND ANTI-INFLAMMATORY ACTIVITY OF IMIDO GOLD(I) TRIETHYLPHOSPHINE COMPLEXES
L. TRINCIA G. FARAGLIA M. NICOLINI L. SINDELLARI A. FURLANI V. SCARCIA	399	PLATINUM(II) AND PALLADIUM(II) HALIDE COMPLEXES WITH DITHIOCARBAMIC DERIVATIVES AND THEIR CYTOSTATIC ACTIVITY
E.L. ANDRONIKASHVILI	400	THE ONCOGENE OF MURINE SARCOMA VIRUS V-Ki-ras MAY ARISE AS A RESULT OF CHEMICAL ACTION ON THE PROTOONCOGENE c-ras
YOSHIKAZU MATSUSHIMA YOSHIHARU KARUBE	401	TUMOR LOCALIZING METAL COMPLEXES
M.M. NANDI A.K. MISHRA MISS RUMA RAY	402	SYNTHETIC, STRUCTURAL AND ANTIBACTERIAL SCREENING STUDIES OF Co(II), Ni(II) AND Cu(II) COMPLEXES WITH BENZIMIDAZOLE DERIVATIVES
G.M. FERGUSON H.I. GEORGESCU C.H. EVANS	403	EFFECTS OF COBALT IONS ON THE SYNOVIAL PRODUCTION OF NEUTRAL PROTEINASES AND PROSTAGLANDIN E ₂
S.H. LAURIE D.E. PRATT	404	THE STRUCTURE AND REACTIVITY OF Ni(II)-ALBUMIN PROTEIN COMPLEX
ALBERT D. KOWALAK KAREN LEBOULLUEC	405	THE STABILITY CONSTANTS FOR IRON(II)ASPIRINATE(ACETYSALICYLATE)
MARK M. JONES SHIRLEY G. JONES WILLIAM M. MITCHELL	407	STRUCTURE-ACTIVITY RELATIONSHIPS IN THERAPEUTIC CHELATING AGENTS
SONIA APELGOT ALAIN JOSEPH JACQUES COPPEY ALAIN GAUDEMER ISABELLE SASAKI DANIÈLE PRASEUTH ETIENNE GUILLE JANINE GRISVARD IGOR SISSOËFF	408	LETHAL EFFECT OF EITHER ⁶⁴ CuCl ₂ OR ⁶⁴ Cu-TMPyP INCORPORATED IN HUMAN MALIGNANT CELLS
7. Chemical Elements in Living Organisms		
BARRY G. MORRELL NICHOLAS W. LEPP DAVID A. PHIPPS CARL A. HAMPSON	409	REDUCTION OF VANADIUM BY HIGHER PLANT ROOTS
PAUL G. LOGAN NICHOLAS W. LEPP DAVID A. PHIPPS	411	THALLIUM UPTAKE BY PLANT ROOTS: COMPETITIVE EFFECTS OF POTASSIUM IONS
S.H. LAURIE N.P. TANCOCK S.P. MCGRATH J.R. SANDERS	413	THE INFLUENCE OF COMPLEXATION ON MICRONUTRIENT UPTAKE BY PLANTS: A COMBINATION OF COMPUTER SIMULATION AND PLANT GROWTH EXPERIMENTS

ANA L. DA NOBRE ANTONIA D. DAS NEVES CARMEN A. DE G. TORRES MARIA DAS G.S. DE SOUZA CRISTINA M. BARRA ADILSON J. CURTIUS	414	VARIATION OF METAL CONCENTRATIONS IN DIFFERENT PARTS OF SUGARCANE
D.J. MCWEENY H.M. CREWS J.A. BURRELL R.C. MASSEY	416	TRACE ELEMENTS IN FOOD: EFFECTS OF DIGESTIVE ENZYMES ON SOLUBILITY
P. HOFFMANN K.H. LIESER	416	ANALYTICAL DETERMINATION OF METALS IN BIOLOGICAL AND ENVIRONMENTAL SAMPLES
G. BEMSKI JUDITH FELCMAN J.J.R. FRAÚSTO DA SILVA I. MOURA J.J.G. MOURA M. CÂNDIDA VAZ L.F. VILAS-BOAS	418	AMAVADINE, AN OXOVANADIUM(IV) COMPLEX OF N-HYDROXY-IMINO- α - α' -DIPROPIONIC ACID
SIMON R. HURFORD GILLIAN L. SMITH DAVID R. WILLIAMS DIANE CUMMINS PAUL I. RILEY	423	METAL IONS AND THEIR INTERACTIONS WITH BIOLOGICAL FLUIDS: SPECIATION OF TRACE METALS IN SALIVA
TANG CHIA-CHUN RUI HAI-FUN	424	STUDIES ON THE BIOCHEMICAL ACTIVITY OF SELENOCARRAGEENAN
K. WANG S.J. XU J.P. HU J. JI	425	THE FORMATION AND DISSOLUTION OF CALCIUM BILIRUBINATE. A CHEMICAL MODEL SYSTEM SIMULATING THE FORMATION AND DISSOLUTION OF CALCIUM-CONTAINING PIGMENT GALLSTONES
K. WANG R.C. LI B.W. CHEN Y.H. WU X.Y. WANG	426	INTERACTION OF CADMIUM AND BOVINE SERUM ALBUMIN AND THE MOBILIZATION OF CADMIUM FROM BOVINE SERUM ALBUMIN WITH CHELATING AGENTS

PLENARY LECTURES



PL1 — MO

I. BERTINI

Department of Chemistry
University of Florence
ItalyRELAXATION PHENOMENA IN NMR
OF PARAMAGNETIC SPECIES

The coupling between unpaired electrons and resonating nuclei affects the NMR parameters. The nature of the isotropic shifts is well understood in principle and applications in biochemistry are numerous and well documented [1,2]. We will here discuss the factors affecting nuclear relaxation from the point of view of: 1) determining the electronic relaxation times; 2) understanding which metal ions provide reasonably sharp NMR lines; 3) how to affect the electronic relaxation times; 4) providing a method for assigning the various resonances; 5) understanding which magnetic field is more suitable for a given system. This background is essential for *any* NMR experiment. The investigation of solvent ^1H T_1 as a function of magnetic field (nuclear magnetic relaxation dispersion, NMRD) in presence of paramagnetic metal ions in a large magnetic field range may provide the electronic relaxation time of the metal ion together with structural and dynamic information. Of course such information can be obtained *only* if the correct equations are used to describe the nucleus-unpaired electron(s) coupling. We have definitely shown which parameters of the spin hamiltonian cannot be neglected in the treatment of each particular case [3].

Nuclear T_1 measurements, even at a single frequency, provide a helpful tool to proceed with the assignment of the resonance lines and give a

rough idea of the correlation time for the nucleus-unpaired electron(s) coupling. Such informations are contained also in the linewidth (T_2) which, however, is affected by many other contributions. One contribution to the linewidth is due to the rotation of the time-averaged magnetic moment of a single molecule (Curie relaxation). Such value increases with the square of the applied magnetic field and affects the nuclear relaxation inversely to the sixth power of the nucleus-electron distance. NMR experiments at different (large) magnetic fields provide an independent tool for signal assignment [4].

Magnetic coupling between paramagnetic metal ions in the same molecule dramatically affects the electronic relaxation times specially of the slower relaxing metal ion. This route may allow to investigate, *via* NMR, systems which otherwise would provide signals far beyond detection. For example, in copper-zinc superoxide dismutase the isotropically shifted signals are too broad to be detected. Insertion of cobalt(II) in the place of zinc provides an excellent system to be investigated through ^1H NMR spectroscopy [5].

REFERENCES

- [1] I. BERTINI, C. LUCHINAT, «NMR of paramagnetic molecules in biological systems», Benjamin/Cummings, 1985, in press.
- [2] A.V. XAVIER, in I. BERTINI, R.S. DRAGO, C. LUCHINAT (eds.), «The Coordination Chemistry of Metalloenzymes», D. Reidel, Dordrecht, Holland, 1983.
- [3] I. BERTINI, C. LUCHINAT, M. MANCINI, G. SPINA in D. GATTESCHI, O. KAHN, R.D. WILLETT (eds.), «Magneto-Structural Correlations in Exchange Coupled Systems», D. Reidel, Dordrecht, Holland, 1985, in press;
I. BERTINI, C. LUCHINAT, M. MANCINI, G. SPINA, *J. Magn. Reson.*, **59**, 213 (1984);
I. BERTINI, F. BRIGANTI, C. LUCHINAT, M. MANCINI, G. SPINA, *J. Magn. Reson.*, in press.
- [4] G.N. LA MAR, J.T. JACKSON, R.G. BARTSCH, *J. Am. Chem. Soc.*, **103**, 4405 (1981);
L. LEE, B.D. SYKES, *Adv. Inorg. Biochem.*, **2**, 183 (1980).
- [5] I. BERTINI, G. LANINI, C. LUCHINAT, L. MESSORI, R. MONNANNI, A. SCOZZAFAVA, submitted for publication.



PL2 — MO

STURE FORSÉN

Physical Chemistry 2, Chemical Centre
 POB 124, Lund University
 S-221 00 Lund
 Sweden

THE DOMAIN STRUCTURE OF CALMODULIN: SOME RECENT BIOPHYSICAL STUDIES

1 — INTRODUCTION

Calmodulin (CaM) is an important Ca^{2+} dependent regulatory protein ($M_r = 16,700$) that is present in seemingly all eucaryotic cells [1]. The primary sequence of CaM from a number of sources has been determined and these studies show: (i) that the amino acid sequence of CaM is highly conserved throughout evolution; (ii) the presence of four homologous regions predicted to have the secondary structure «helix-loop-helix» with the loop constituting a potential Ca^{2+} binding site of the «EF-hand» type (fig. 1)

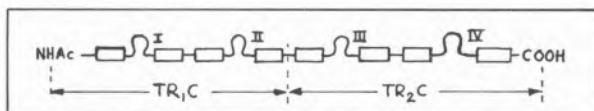


Fig. 1

Schematic structure and tryptic cleave sites of CaM

At the time of writing the X-ray structure of CaM is not yet known although considerable progress has been reported. The molecular properties of CaM have over the last few years or so been subject to study by biochemical and biophysical — primarily spectroscopic — techniques. A recent line of research that has proved to be particularly fruitful is the study of different proteolytic fragments of CaM. One of the most striking results of these studies has been that many of the physical properties of CaM can be closely represented by a superposition of the properties of the two tryptic fragments, TR_1C and TR_2C — essentially com-

prising the N-terminal and C-terminal half of the native molecule (cf. fig. 1) [2-6]. In this lecture we will discuss some recent biophysical studies of CaM and its tryptic fragment — studies that illustrate to what extent CaM indeed can be considered as consisting of two largely independent domains. We will also address the question of cooperative binding of Ca^{2+} .

2 — NMR STUDIES

NMR studies of CaM and its proteolytic fragments illustrate well the versatility of the NMR method and the complementary information that can be obtained through studies of different magnetic nuclei. ^1H NMR can be used to detect conformation changes in the protein induced by metal ion binding. ^{43}Ca NMR has provided data on the kinetics of ion binding — data that has only recently been supplemented by stopped-flow measurements. ^{113}Cd NMR is uniquely suited to determine metal ion populations at individual ion binding sites and has given convincing evidence for cooperative ion binding in CaM and TR_2C . In addition ^{113}Cd NMR is useful for monitoring conformation changes in the protein as a result of drug binding *etc.*

^1H NMR

In ^1H spectra of CaM two distinct phases are observed as Ca^{2+} is successively added to the Ca^{2+} free protein. The first two Ca^{2+} ions to bind cause conformation changes that are in slow exchange ($k_{\text{exch}} < 10 \text{ s}^{-1}$). The spectrum during this phase is a superposition of two spectra with varying relative intensities — one increasing as the other decreases [4-10]. The obvious interpretation is that only CaM and $(\text{Ca})_2\text{CaM}$ coexist to a measurable degree. A completely analogous behaviour is shown by the fragment TR_2C indicating that here only TR_2C and $(\text{Ca})_2\text{TR}_2\text{C}$ coexist in solution. By contrast ^1H spectral changes of CaM upon addition of the third or fourth Ca^{2+} or of TR_1C upon addition of two Ca^{2+} are continuous indicating conformation changes in fast exchange ($k_{\text{exch}} > 500 \text{ s}^{-1}$). Thus ^1H NMR indicates (i) the strong (slowly dissociating) Ca^{2+} sites are III and IV; (ii) Ca^{2+} binding to sites III and IV is positively cooperative in both CaM and TR_2C .

¹¹³Cd NMR

¹H NMR spectra of CaM, TR₁C and TR₂C are almost identical whether Ca²⁺ or Cd²⁺ is added thus justifying the use of Cd²⁺ as a probe for Ca²⁺. When ¹¹³Cd²⁺ is added to either CaM or TR₂C two well resolved NMR signals at about -100 ppm are observed [3,4,9]. These signals increase in intensity in parallel up to a Cd/CaM (or TR₂C) ratio of 2:1. This behaviour is observed both at low ionic strength (I ≈ 0.030) and at high ionic strength (0.15 KCl). We consider this very convincing evidence for cooperative metal ion binding to the pair of sites III and IV. The chemical shifts of the two ¹¹³Cd signals are virtually the same in CaM and TR₂C providing evidence for the structural autonomy of the C-terminal half of CaM [3].

⁴³Ca NMR

From the temperature dependence of the ⁴³Ca NMR signals in the presence of either CaM or TR₁C values of *k*_{off} for the two weakly bonded Ca²⁺ ions have in both cases been determined to ≈ 10³ s⁻¹ at 25°C [3,11].

3 — STOPPED-FLOW KINETIC STUDIES

Through the use of the newly developed fluorescent Ca²⁺ chelator «Quin 2» [12] it has recently been possible to determine directly the rates of dissociation of Ca²⁺ from CaM, TR₁C and TR₂C [13,14]. Two exponential rate processes can clearly be resolved. For CaM at 19°C and low ionic strength (20 mM pipes) the fast rate was *k*_{off}^f ≈ 550 s⁻¹ and the slow rate *k*_{off}^s ≈ 5 s⁻¹. The amplitude factors obtained convincingly show that both processes correspond to the release of two Ca²⁺ ions. Since the off rates differ by two orders of magnitude it is reasonable to attribute the two processes to dissociation of Ca²⁺ from the two strong (III and IV) and two weak binding (I and II) sites respectively. The picture does not qualitatively change in the presence of 100 mM KCl. Studies of the fragments TR₁C and TR₂C revealed several interesting facts. Under similar experimental conditions the rates of Ca²⁺ dissociation from TR₁C (*k*_{off}^{TR₁C} ≈ 400 s⁻¹) and TR₂C (*k*_{off}^{TR₂C} ≈ 10 s⁻¹) are nearly equal to those for the fast and slow processes in CaM!

4 — THERMOCHEMICAL STUDIES

A comparative study of the enthalpy change associated with the binding of Ca²⁺ to CaM, TR₁C and TR₂C has recently been made by SELLERS *et al.* [15,16]. The enthalpy change is negative at ambient temperatures in line with results for homologous Ca²⁺ binding proteins. Δ*H*^{CaM} and Δ*H*^{TR₂C} are closely linear with the Ca²⁺/CaM ratio in the range 0 to 2 — a behaviour compatible with cooperative Ca²⁺ binding. At 25°C the total enthalpy change for the binding of 4 Ca²⁺ to CaM is Δ*H*^{CaM} = -33 kJ/mol. At the same temperature the enthalpy changes accompanying the binding of 2 Ca²⁺ to tryptic fragments are: Δ*H*^{TR₁C} ≈ -16 kJ/mol and Δ*H*^{TR₂C} ≈ -14.5 kJ/mol. The sum Δ*H*^{TR₁C} + Δ*H*^{TR₂C} ≈ -30.5 kJ/mol, is strikingly close to Δ*H*^{CaM}. The entropy change associated with Ca²⁺ binding to CaM, TR₁C and TR₂C is positive in all cases.

5 — CONCLUSION

The data briefly outlined above convincingly show that the binding of Ca²⁺ ions to sites III and IV is a cooperative process in both CaM and TR₂C — of sites I and II we still know too little to say. Within a small margin CaM may in many respects be considered to be constructed from two domains comprising the N-terminal and C-terminal half of the molecule. This should however not lead one to think that the sum of the two halves equals the whole under all circumstances. In particular the interplay between CaM and other molecules, drugs and/or target proteins, will be dependent on the presence of the unbroken protein allowing for joint interaction of different regions as clearly demonstrated by the inability of fragments to activate target proteins [17].

ACKNOWLEDGEMENTS

This article summarizes the work of a large number of colleagues and coworkers at or outside Lund University, their names are found in the list of references below.

REFERENCES

- [1] C.E. KLEE, T.C. VANAMAN, *Adv. Prot. Chem.*, **35**, 213 (1982).
- [2] W. DRABIKOWSKI, H. BRZESKA, S.Y. VENYAMINOV, *J. Biol. Chem.*, **257**, 11584 (1982).

- [3] S. FORSÉN, A. ANDERSSON, T. DRAKENBERG, O. TELEMAN, E. THULIN, H.J. VOGEL, in B. DE BERNARD *et al.* (eds.), «Calcium Binding Proteins», Elsevier, Amsterdam, 1983, pp. 121-131.
- [4] E. THULIN, A. ANDERSSON, T. DRAKENBERG, S. FORSÉN, H.J. VOGEL, *Biochemistry*, **23**, 1862 (1984).
- [5] A. AULABAUGH, W.P. NIEMEZURA, W.A. GIBBONS, *Biochem. Biophys. Res. Commun.*, **118**, 225 (1984).
- [6] D.C. DALGARNO, R.E. KLEVIT, B.A. LEVINE, R.J.P. WILLIAMS, Z. DOBROWOLSKI, W. DRABIKOWSKI, *Eur. J. Biochem.*, **138**, 281 (1984).
- [7] K.B. SEAMON, *Biochemistry*, **19**, 207 (1980).
- [8] M. IKURA, T. HIRAOKI, K. HIKICHI, O. MINOWA, H. YAMAGUCHI, M. YAZAWA, K. YAGI, *Biochemistry*, **23**, 3124 (1984).
- [9] A. ANDERSSON, S. FORSÉN, E. THULIN, H.J. VOGEL, *Biochemistry*, **22**, 2309 (1983).
- [10] R.E. KLEVIT, B.A. LEVINE, R.J.P. WILLIAMS, *FEBS Lett.*, **123**, 25 (1981).
- [11] A. ANDERSSON, T. DRAKENBERG, E. THULIN, S. FORSÉN, manuscript in preparation.
- [12] R.Y. TSIEU, *Biochemistry*, **19**, 2396 (1980).
- [13] P. BAYLEY, P. AHLSTRÖM, S.R. MARTIN, S. FORSÉN, *Biochem. Biophys. Res. Commun.*, **118**, 225 (1984).
- [14] A. ANDERSSON, S.R. MARTIN, P. BAYLEY, S. FORSÉN, submitted (1984).
- [15] J. LAYNEZ, P. SELLERS, E. THULIN, Int. Symp. Thermodyn. Proteins & Biol. Membr., Granada, Spain, May 23-27 (1983).
- [16] P. SELLERS, J. LAYNEZ, E. THULIN, S. FORSÉN, manuscript in preparation.
- [17] D.L. NEWTON, M.D. OLDEWURTEL, M.H. KRINKS, J. SHILOACH, C.B. KLEE, *J. Biol. Chem.*, **259**, 4419 (1984).



PL3 — TU

JEAN-MARIE LEHN

Institut Le Bel
 Université Louis Pasteur
 Strasbourg
 and
 Collège de France
 Paris
 France

DESIGN OF CORECEPTOR MOLECULES FOR POLYNUCLEAR AND PHOTOACTIVE METAL ION COMPLEXES

Coreceptor molecules containing several metal binding subunits arranged in a macropolycyclic framework may form various types of polynuclear complexes in which the distance and arrangement of the cations, held inside the molecular cavity, may be controlled via ligand design. They allow to study cation-cation interactions (magnetic coupling, electron transfer, modified redox properties) as well as the inclusion of bridging substrates to yield cascade complexes, of potential interest for bioinorganic modelling and multicenter-multielectron catalysis.

Depending on the nature and number of binding subunits and of connecting bridges used as building blocks, a variety of macropolycyclic structures may be envisaged. Ligands containing two units of chelating, tripodal or macrocyclic type, bind two metal ions to form dinuclear cryptates of various types.

Receptors combining several subunits have the potential ability of assembling metal ions and bridging species within their molecular cavity to form cluster cryptates.

Metalloreceptors incorporating selective binding subunits for the simultaneous complexation of both metal ions and organic species form mixed-substrate supramolecular species, as shown for instance by a structure containing metalloporphyrin centers and a bound diammonium ion.

The introduction of *photoactive groups* (such as porphyrin or 2,2'-bipyridine) leads to complexes which may act as photosensitizers and units for charge separation centers in the design of systems for artificial photosynthesis.



PL4 — TU

ECKARD MÜNCK
 Gray Freshwater Biological Institute
 University of Minnesota
 P.O. Box 100, Navarre, Minnesota 55392
 U.S.A.

STRUCTURE AND MAGNETISM OF IRON-SULFUR CLUSTERS IN PROTEINS

Recent research has shown that iron-sulfur proteins provide us with an ever expanding variety of cluster structures. Although studies of the *T. thermophilus* Rieske protein [1] have yielded interesting new information (ligands other than cysteine coordinate to [2Fe-2S] clusters) the major new developments involve proteins containing 3Fe and 4Fe clusters.

Although 3Fe clusters were discovered only a few years ago, present evidence suggests that such clusters occur with different Fe/S stoichiometries and different structures. The only available X-ray crystal structure is that of ferredoxin I from *A. vinelandii*; the data reveal a [3Fe-3S] cluster which is a nearly planar ring, with Fe-Fe distances of 4.1 Å. On the other hand, EXAFS and Resonance Raman studies, as well as analyses of Fe/S stoichiometries, show that the 3Fe clusters of most proteins have the classic cubane-type structure with one Fe atom missing, and are probably of the [3Fe-4S] type [2]. Recent studies of the enzyme aconitase have demonstrated that the [3Fe-4S] cluster (electronic spin $S=1/2$) of inactive aconitase can be converted into a [3Fe-4S] clus-

ter ($S=5/2$) with a linear arrangement of iron atoms [3].

Spin-coupling models have been published for both the $S=1/2$ [4] and $S=5/2$ [3] states of oxidized 3Fe clusters. MCD studies have shown that one-electron reduced $S=1/2$ 3Fe clusters have cluster spin $S=2$, and Mössbauer studies have revealed that the cluster contains one ferric site and two irons at the 2.5⁺ oxidation level. Mössbauer studies of *D. gigas* ferredoxin II show that the pair of $Fe^{2.5+}$ is ferromagnetically coupled and that the pair, in turn, is antiferromagnetically coupled to the ferric ion [5].

In the presence of Fe^{2+} the [3Fe-4S] clusters of a variety of proteins can be converted, with good reversibility, into [4Fe-4S] clusters. The conversion has been used to label subsites of the [4Fe-4S] cluster selectively with ⁵⁷Fe and thus probe more deeply into the electronic structure of [4Fe-4S] clusters with Mössbauer spectroscopy. This labeling has been very useful for the study of the [4Fe-4S] cluster of aconitase. Studies of this enzyme in the presence of substrates and inhibitors have shown that these compounds bind to the «labile» iron of the [4Fe-4S] cluster, resulting in an expansion of the iron environment to 5- or 6-coordinate, with the development of a trapped Fe^{2+} valence [6].

Recent studies have shown that the [4Fe-4S]¹⁺ core can be stabilized in various spin states. The «normal» ground state has $S=1/2$ and yields the classical $g=1.94$ signal. Recently an $S=7/2$ state has been implicated for the Se-reconstituted [4Fe-4Se] clusters of the *C. pasteurianum* ferredoxin [7]. The Fe-protein of nitrogenase has puzzled researchers for over a decade. We have just obtained evidence from EPR, susceptibility and Mössbauer studies [8] that this protein contains a mixture of [4Fe-4S] clusters, one form with $S=1/2$ and the other with $S=3/2$. If the P-clusters of nitrogenase turn out indeed to be cubane [4Fe-4S] clusters, then the cluster can also be stabilized with an $S=5/2$ ground state.

In the enzyme sulfite reductase a [4Fe-4S] cluster is coupled via some unknown ligand to the iron atom of a siroheme, an Fe-isobacteriochlorin. This system has been studied in 14 complexation and oxidation states and the exchange coupling between the cluster and heme iron has been eva-

luated for some states [9]. It has been found that this coupling can be ferromagnetic or antiferromagnetic [9].

It is well established now that one iron atom can be abstracted from many [4Fe-4S] clusters to yield [3Fe-4S] clusters. Recently it has been suggested for *A. vinelandii* ferredoxin I [10] that a sulfur can be removed to yield a structure with a [4Fe-3S] core. A similar situation may occur in *C. pasteurianum* hydrogenase [11].

REFERENCES

- [1] J.A. FEE, K.L. FINDLING, T. YOSHIDA, R. HILLE, G.E. TARR, D.O. HEARSHEN, W.R. DUNHAM, E.P. DAY, T.A. KENT, E. MÜNCK, *J. Biol. Chem.*, **259**, 124-133 (1984).
- [2] H. BEINERT, A.J. THOMSON, *Arch. Biochem. Biophys.*, **222**, 333-361 (1983).
- [3] M.C. KENNEDY, T.A. KENT, M. EMPTAGE, H. MERKLE, H. BEINERT, E. MÜNCK, *J. Biol. Chem.*, **259**, 14463-14471 (1984).
- [4] T.A. KENT, B.H. HUYNH, E. MÜNCK, *Proc. Natl. Acad. Sci. U.S.A.*, **77**, 6574-6576 (1980).
- [5] B.H. HUYNH, J.J.G. MOURA, I. MOURA, T.A. KENT, J. LEGALL, A.V. XAVIER, E. MÜNCK, *J. Biol. Chem.*, **255**, 3242-3244 (1980).
- [6] M.H. EMPTAGE, T.A. KENT, M.C. KENNEDY, H. BEINERT, E. MÜNCK, *Proc. Natl. Acad. Sci. U.S.A.*, **80**, 4674-4678 (1983).
- [7] J.-M. MOULIS, P. AURIC, J. GAILLAND, J. MEYER, *J. Biol. Chem.*, **259**, 11396-11402 (1984).
- [8] P. LINDAHL, E.P. DAY, T.A. KENT, W.H. ORME-JOHNSON, E. MÜNCK, submitted for publication.
- [9] JODIE A. CHRISTNER, E. MÜNCK, THOMAS A. KENT, PETER A. JANICK, JOHN C. SALERNO, LEWIS M. SIEGEL, *J. Am. Chem. Soc.*, **106**, 6786-6794 (1984).
- [10] T.V. MORGAN, P.J. STEPHENS, F. DEVLIN, C.D. STOUT, K.A. MELIS, B.K. BURGESS, *Proc. Natl. Acad. Sci. U.S.A.*, **81**, 1931-1935 (1984).
- [11] E. WANG, M.Y. BENECKY, B.H. HUYNH, J.F. CLINE, M.W.W. ADAMS, L.E. MORTENSON, B.M. HOFFMAN, E. MÜNCK, *J. Biol. Chem.*, **259**, 14328-14331 (1984).



PL5 — WE

BERT L. VALLEE

Center for Biochemical and Biophysical Sciences and Medicine
Harvard Medical School
250 Longwood Avenue, Boston, MA 02115
U.S.A.

CONCURRENT CRYOKINETIC AND CRYOSPECTROSCOPIC CHARACTERIZATION OF INTERMEDIATES IN METTALLOENZYME ACTION

The detection and definition of intermediates in reaction pathways, a problem central to the delineation of structure-function relationships in enzymology, have resisted solution by and large. We have developed an approach capable of wide application to such studies through a combination of cryokinetics with cryospectroscopy. Such cryospectrokinetic studies provide concurrent structural, kinetic, and chemical data on short-lived intermediates in the course of the interactions of enzymes with their substrates and inhibitors. Sub-zero temperatures extend the lifetimes of these intermediates and, combined with rapid-mixing and rapid-scanning instrumentation, allow simultaneous measurement of both their physical-chemical and kinetic characteristics.

Carboxypeptidase A has served as our model system. The studies have been performed with a low-temperature stopped-flow instrument which also serves as a cryospectrometer [1]. The intermediates have been monitored directly through fluorescence generated by radiationless energy transfer (RET) between enzyme tryptophans and the dansyl group of enzyme-bound, rapidly hydrolyzed peptide and ester substrates which provide the basis for measurement of the rates of formation and breakdown of intermediates. *N*-Dansylated oligopeptides and their ester analogues exhibit Michaelis-Menten kinetics over the temperature range -20 to $+20^{\circ}\text{C}$ with k_{cat}/K_m values of $(0.3-3) \times 10^7 \text{M}^{-1} \text{s}^{-1}$ at $+20^{\circ}\text{C}$, pH 7.5. The cryo-

solvent, aqueous 4.5 M NaCl, alters neither the kinetic nor spectral properties of zinc or cobalt carboxypeptidases.

Sub-zero radiationless energy transfer kinetic studies of the zinc and cobalt enzymes disclose two intermediates in the hydrolysis of both peptides and esters and furnish all the rate and equilibrium constants for the reaction scheme $E+S \rightleftharpoons ES_1 \rightleftharpoons ES_2 \rightleftharpoons E+P$. The chemical and kinetic data show that neither of these is an acyl-enzyme intermediate. The cryokinetic data demonstrate for the first time the existence of two intermediates during the hydrolysis of both peptides and esters [2]. At -20°C , the formation, interconversion and breakdown of these intermediates results in three distinct fluorescence steps during substrate hydrolysis: (1) a rapid increase in signal intensity reflects the formation of the Michaelis complex, ES_1 , in <15 ms; (2) a slower exponential increase in signal intensity signifies formation of a second hitherto unknown intermediate, ES_2 ; (3) a slow decrease in signal intensity reflects separation of the dansyl product from the enzyme.

The reversible interconversion of ES_1 and ES_2 shows that the C-terminal product is not liberated prior to the rate-limiting step and, hence, deacylation cannot be rate limiting. The electronic and paramagnetic spectral properties of a chromophoric enzymatically functional cobalt carboxypeptidase A have served to identify transient intermediates in its catalysis of very rapidly hydrolyzed dansyl oligopeptides and their ester analogues [3].

They also reveal the corresponding structures of the resultant active site cobalt coordination complexes at subzero temperatures. The visible absorption spectra of these intermediates are recorded with the same rapid-scanning, low-temperature, stopped-flow spectrometer that served to establish the kinetics of previously unknown intermediate, ES_2 ; at -20°C it forms in less than 500 ms and then is converted to products over a much longer period of time.

Both the absorption and EPR spectra of the peptide and ester intermediates, ES_2 , differ significantly from one another and from those of the cobalt enzyme itself, its complexes with affinity labels, substrate analogue inhibitors, or products.

The two types of substrates generate both new and different absorption bands and maxima of the visible spectrum. The corresponding EPR spectra differ most strikingly in the resolved hyperfine splitting of their g_1 resonances but also in their three apparent g values. The absorption, electron paramagnetic resonance, and magnetic circular dichroic spectra of the intermediates identify catalysis-related, dynamic alterations in the active site metal coordination sphere clearly distinct from those observed under static conditions. The systematic changes in the cobalt spectra of carboxypeptidase when forming the peptide and ester intermediates correlate with the formation of the ES_2 complex and thus render these data the first experimental test of the entatic-state hypothesis. Both absorption and EPR spectra of the ES_2 reaction intermediates consistently demonstrate (i) the formation of transient metal complexes, (ii) differences between the effects induced by peptides and esters, and (iii) strong similarities between those induced by all peptides on the one hand and all esters on the other. The marked alterations of the cobalt spectra likely reflect the coordination of a substrate carboxyl and/or carbonyl group to the metal at a critical step in the course of catalysis [4].

In rapid quench studies at sub-zero temperatures there is a burst in product formation for ester but not for peptide hydrolysis. This indicates that the scissile bond of esters breaks prior to the rate determining step, but that of peptides does not.

These studies further predict that the peptide intermediate can be stabilized by approaching the equilibrium from the reverse direction of the reaction, *i.e.* $E+P_1+P_2 \rightleftharpoons ES_2 \rightleftharpoons ES_1 \rightleftharpoons E+S$. Cryospectroscopy in combination with HPLC analysis of the concentration of P_1 , P_2 and S confirm that an ES_2 peptide intermediate forms in this manner.

The cryospectrokinetic approach developed here in the mechanistic study of this metalloenzyme is applicable to the examination of transients of biochemical reactions in general. It will allow molecular characterization of previously elusive intermediates and greatly magnify the range of mechanistic questions that can be answered.

REFERENCES

- [1] D.S. AULD, *Methods Enzymol.*, **61**, 318 (1979).
 [2] A. GALDES, D.S. AULD, B.L. VALLEE, *Biochemistry*, **22**, 1888-1893 (1983).
 [3] K.F. GEOGHEGAN, A. GALDES, R.A. MARTINELLI, B. HOLMQUIST, D.S. AULD, B.L. VALLEE, *Biochemistry*, **22**, 2255-2262 (1983).
 [4] D.S. AULD, A. GALDES, K.F. GEOGHEGAN, B. HOLMQUIST, R.A. MARTINELLI, B.L. VALLEE, *Proc. Natl. Acad. Sci. USA*, **81**, 5041-5045 (1984).



PL6 — TH

HARRY B. GRAY
 Arthur Amos Noyes Laboratory
 California Institute of Technology
 Pasadena, California, 91125
 U.S.A.

ELECTRON TRANSFER AT FIXED DISTANCES IN METALLOPROTEINS

Work in our laboratory has shown that pentaammineruthenium(III) (a_5Ru^{3+}) can be attached to histidine 33 in horse heart cytochrome *c*, histidine 83 in *Pseudomonas aeruginosa* azurin, and histidines 12, 48, 81, and 116 in sperm whale myoglobin (Mb). Intramolecular electron transfer from Ru^{2+} to Fe^{3+} (or Cu^{2+}) in these derivatives has been studied over a range of temperatures by flash photolysis methods. In the experiment, the surface $a_5Ru(His)^{3+}$ group is reduced by electronically excited $Ru(bpy)_3^{2+}$ ($bpy = 2,2'$ -bipyridine), and in the presence of sacrificial donors (to reduce $Ru(bpy)_3^{3+}$) this event is followed by intramolecular $a_5Ru(His)^{2+} \rightarrow Fe^{3+}$ (or Cu^{2+}) electron transfer. The rate of $a_5Ru(His-33)^{2+} \rightarrow Fe^{3+}$ electron transfer in $a_5Ru(His-33)$ cytochrome *c* is between 20 and $40 s^{-1}$ over the temperature range 0 - $80^\circ C$ (above $80^\circ C$, the protein structure changes substantially, and intramolecular electron transfer is not observed). The rate of $a_5Ru(His-83)^{2+} \rightarrow Cu^{2+}$ electron transfer in $a_5Ru(His-83)$ azurin also

is temperature-independent ($2 s^{-1}$ between -10 and $55^\circ C$). Analysis of the results for $a_5Ru(His-33)$ cytochrome *c* and $a_5Ru(His-83)$ azurin suggests that the reorganizational enthalpies of the protein electron transfer sites are less than $7 kcal mol^{-1}$, which accords with the view that solvation effects are minimal in these protein interiors. Unlike the results obtained for cytochrome *c* and azurin, the intramolecular electron transfer rate in $a_5Ru(His-48)Mb$ (the closest His-48 to heme distance is 13.3 Å) is strongly dependent on temperature (k increases from $0.05 s^{-1}$ at $20^\circ C$ to $0.5 s^{-1}$ at $50^\circ C$), thereby indicating that the reorganizational enthalpy of the high-spin heme is greater than $10 kcal mol^{-1}$. It is likely that a substantial fraction of this activation is attributable to partial dissociation of the axial water ligand in the high-spin ferriheme. The rates of intramolecular $Ru^{2+} \rightarrow Fe^{3+}$ electron transfer in the other three a_5RuMb derivatives fall well below $0.01 s^{-1}$ at $25^\circ C$ (the closest His-heme distances in these derivatives are all greater than 19 Å).

The heme in each of the four a_5RuMb derivatives can be replaced with other metalloporphyrins. Preliminary results on $a_5Ru(His-48)Mb$ ($Ru^{3+}MIX$) and $a_5Ru(His-12)Mb(Ru^{3+}MIX)$ show that electron transfer from $a_5Ru(His-48)^{2+}$ to the low-spin Ru^{3+} -porphyrin is two orders of magnitude faster than the corresponding transfer to the high-spin ferriheme. The rate of electron transfer from $a_5Ru(His-12)^{2+}$ to the low-spin Ru^{3+} -porphyrin is only a factor of 50 less than that from $a_5Ru(His-48)^{2+}$, which is somewhat surprising in view of the large difference in the distance from the two donors to the Ru^{3+} -porphyrin (22 Å from His-12; 13.3 Å from His-48). Examination of the electron transfer properties of the $a_5RuMb(Ru^{3+})$ derivatives is now being extended to include experiments on $a_5Ru(His-116)Mb(Ru^{3+})$ and $a_5Ru(His-81)Mb(Ru^{3+})$.



PL7 — TH

H. ALLEN O. HILL
Inorganic Chemistry Laboratory
South Parks Road, Oxford OX1 3QR
U.K.

THE ELECTROCHEMISTRY OF REDOX PROTEINS

Over the past few years, it has been possible to devise electrodes at which the electron transfer reactions of representatives of the major classes of redox proteins proceed rapidly and reversibly. The guiding hypothesis is that the surface provided by the electrode should resemble that offered to the given redox protein by others with which it interacts *in vivo*. Thus in both instances, we are concerned with the nature of interfaces. Most current models of protein-protein complexes emphasize the electrostatic nature of the binding and pay particular attention to short-range interactions. Some proteins require no extensive electrode modification *e.g.*, *Pseudomonas aeruginosa* azurin or some cytochromes c_3 . However most require the modification of the electrode surface, or at least the electrode-solution interface, before rapid heterogeneous electron transfer rates are observed. We have been concerned principally with three types of electrode: metal (especially) gold surfaces upon which are adsorbed bi- or poly-functional molecules; oxidized pyrolytic graphite surfaces with, or without, poly-valent cations; conducting metal oxide surfaces, especially RuO_2 .

The most intensive investigations have been carried out on horse heart cytochrome *c*. This highly basic protein appears to have the following requirements: a negatively-charged surface, or at least one in which any adsorbate molecules have the negative end of the dipole disposed towards the solution; a hydrophilic surface; a surface upon which adsorption of the protein is reversible; the absence of competing poly-valent cations. These conditions are met by gold upon which is adsor-

bed molecules of the type, $X\sim Y$ where X is a group which adsorbs on to the gold and Y is a negatively-charged group (or exposes the negative end of a dipole). 4,4'-Bipyridyl is the archetype of this class of adsorbate but there are now twenty or so compounds that act, when adsorbed on gold, as effective *promoters* of the electrochemistry of horse heart cytochrome *c*. Pyrolytic graphite, when carefully oxidized, also functions well as does the metallic oxide, ruthenium dioxide.

Acidic proteins require a different surface. There are a few compounds which, when adsorbed on gold, present a positive surface to the solution. The most straightforward method of promoting the electrochemistry of proteins such as plastocyanin is to have present in solution polyvalent cations such as magnesium(II) or hexamminochromium(III). Two effects appearing to be operating: a general effect on the electrode-solution interface and a specific effect which involves binding of the cation to the protein surface. Evidence for the latter comes from NMR spectroscopy. Recently compounds have been discovered that, when adsorbed on gold, allow the electrochemistry of *either* acidic *or* basic proteins to proceed.

Having gained rapid electrode reactions of redox proteins, what use can be made of them? Examples will be given of coupling of these reactions to enzyme-catalysed reactions and their use in synthesis and sensors.



PL8 — FR

PHILIP AISEN

Departments of Physiology and Biophysics and Medicine
 Albert Einstein College of Medicine
 Bronx, New York 10461
 U.S.A.

THE BINUCLEAR IRON CENTER OF UTEROFERRIN

Uteroferrin is a single-chain glycoprotein of MW close to 35,000 found in the uterine secretions of pregnant or hormone-treated, pseudopregnant pigs and other mammals with similar placental structures. The protein bears two exchangeable iron atoms per molecule, and has been postulated to function in trans-placental iron transport. Originally thought to be a member of the transferrin class of proteins, and named accordingly, uteroferrin is now known to belong to the class of iron-tyrosinate proteins with acid phosphatase activity [1]. Whether the enzymatic properties of the protein, or its reversible iron-binding activity, are actually involved in its physiological function is not yet clear.

Perhaps the most striking feature of uteroferrin is its capacity to assume either of two interconvertible forms: purple, or oxidized, and pink, or reduced. The purple form is enzymatically inert and EPR silent, while the pink form exhibits both acid phosphatase activity and a novel $g' = 1.74$ EPR signal. The structural basis of the purple-to-pink transformation is the focus of this report.

Optical Properties

When treated with mild oxidants such as ferricyanide uteroferrin is driven to its purple form having an absorption maximum at 575 nm. The pink form, correspondingly obtained with mild reductants such as mercaptoethanol, has its absorption maximum near 510 nm, with an integrated intensity in the visible region very close to that of its purple partner. Assignment of these absorp-

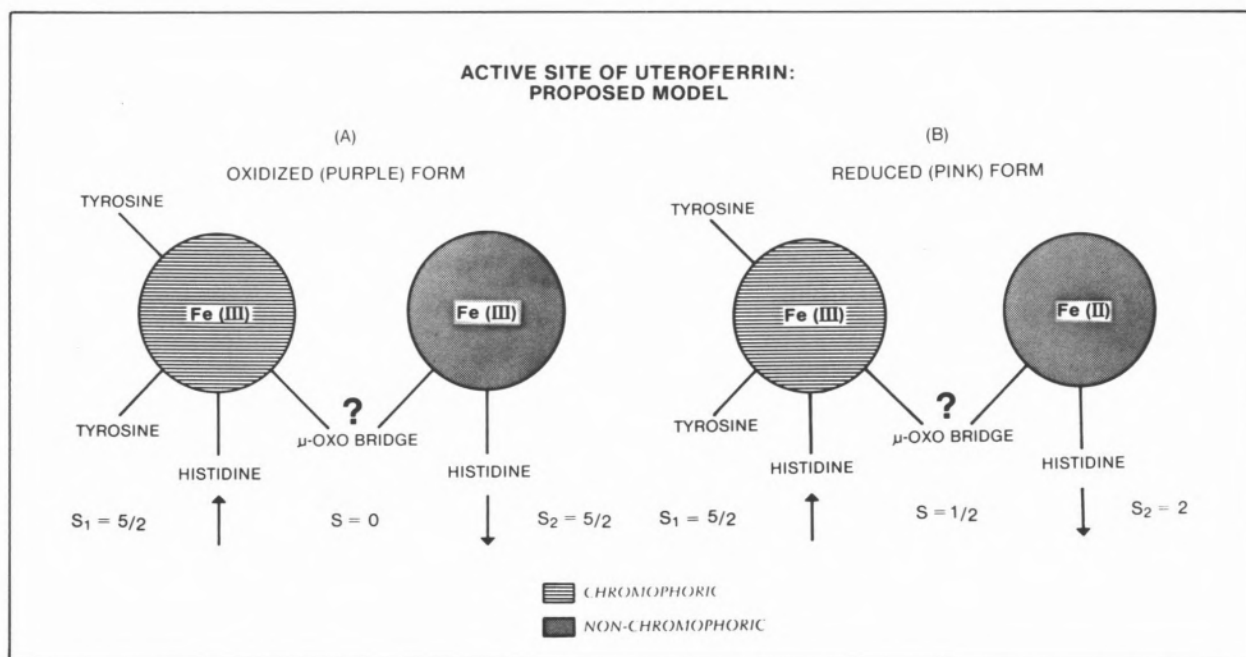
tion peaks to phenolate-to-metal charge transfer transitions is substantiated by resonance Raman spectroscopy showing characteristic tyrosyl vibrational modes [2] similar to those observed with the transferrins and intradiol dioxygenases [3]. Little change in secondary structure of uteroferrin as it undergoes conversion between pink and purple forms can be discerned from circular dichroism spectra [4].

Magnetic Studies

Like the acid phosphatase from bovine spleen, an enzyme with which it has much in common, uteroferrin in its purple form is very nearly diamagnetic and EPR silent. In its pink state, however, uteroferrin exhibits a striking EPR signal of rhombic symmetry with principal g -values 1.93, 1.74 and 1.59. The signal is observable only at temperatures below about 35 K, broadening beyond detectability above this limit. Spectroscopic and magnetic susceptibility measurements as a function of temperature suggest that the signal arises from a center with $S = 1/2$. That this center is actually a binuclear iron cluster has been elegantly demonstrated by Mössbauer spectroscopy of ^{57}Fe -enriched protein, showing all the iron to be ferric in purple, oxidized uteroferrin, but to exist as both Fe(II) and Fe(III) in the pink, reduced form [5]. An antiferromagnetically spin-coupled model, with an exchange energy near 14 cm^{-1} in the pink protein but considerably higher in the purple, appears to account for most of the magnetic properties of uteroferrin.

Further insight into the structure of the binuclear iron center has been gleaned from ^1H NMR studies. By comparison with synthetic Fe complexes, isotropically shifted resonances could be assigned to protons of tyrosine and histidine coordinated to the binuclear iron center [6]. A possible structure of the center in its pink and purple states is suggested below.

The spin-coupled iron pair of uteroferrin is sensitive to a variety of perturbants. Orthophosphate, even in the absence of detectable oxygen, forces the pink protein to its purple, oxidized, EPR-silent form. Molybdate, in contrast, quantitatively converts pink uteroferrin's initially rhombic EPR signal into an axial signal which then



remains invariant to subsequent addition of phosphate. Remarkably, however, the protein remains pink, demonstrating a dissociation between color and oxidation state. Guanidine causes a sizeable red shift in the pink protein's visible absorption maximum, thus demonstrating dissociation of color and oxidation state in a complementary way. Whether these effects reflect coordination of the perturbants to the active site of uteroferrin remains to be determined.

REFERENCES

- [1] B.C. ANTANAITIS, P. AISEN, *Adv. Inorg. Biochem.*, **5**, 111 (1982).
- [2] B.C. ANTANAITIS, T. STREKAS, P. AISEN, *J. Biol. Chem.*, **257**, 3766 (1982).
- [3] L. QUE JR., *Coord. Chem. Rev.*, **50**, 73 (1982).
- [4] B.C. ANTANAITIS, P. AISEN, H.R. LILIENTHAL, *J. Biol. Chem.*, **258**, 3166 (1983).
- [5] P.G. DEBRUNNER, M.P. HENDRICH, J. DEJERSEY, D.T. KEOUGH, J.T. SAGE, B. ZERNER, *Biochim. Biophys. Acta*, **745**, 103 (1983).
- [6] R.B. LAUFFER, B.C. ANTANAITIS, P. AISEN, L. QUE JR., *J. Biol. Chem.*, **258**, 4212 (1983).



PL9 — FR

DAVID DOLPHIN

Department of Chemistry
The University of British Columbia
Vancouver, B.C., V6T 1Y6
Canada

METALLOPORPHYRINS IN BIOCHEMISTRY

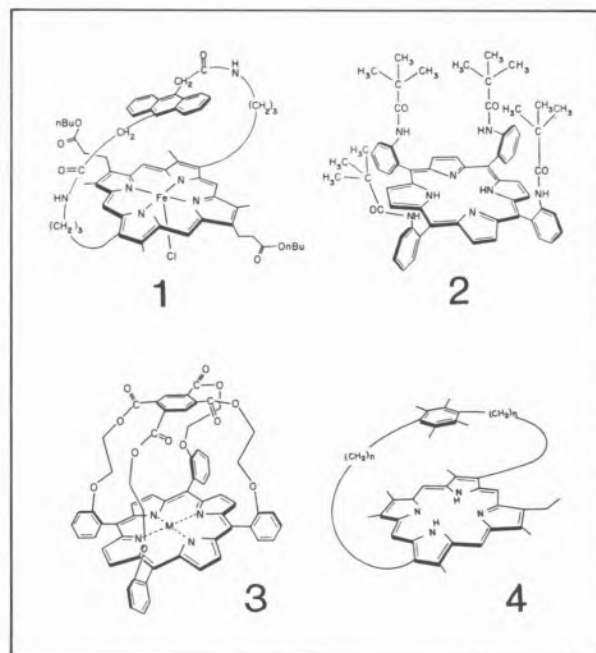
The reversible binding and storage of dioxygen is carried out by the heme proteins hemoglobin and myoglobin [1]. The activation of bound dioxygen is achieved by the cytochromes P-450 [2] and the cytochrome oxidases [3]. The former function by reducing the bound dioxygen to "peroxide", which then generates water and an active oxidizing species capable of alkane hydroxylation and alkene epoxidation, while the latter add a further two electrons and make two molecules of water

from the dioxygen. On the other hand, the catalases and peroxidases use exogenous peroxide to achieve active oxidizing species, which in the case of catalase oxidize a second equivalent of hydrogen peroxide, while the peroxidases oxidize, by one-electron processes, phenols and aromatic amines [4]. In addition, a closely related family of peroxidases, namely chloro- and myelo-peroxidase, function in a similar fashion but oxidize chloride to hypochlorite [4].

Studies on simple metalloporphyrins, devoid of the protecting protein, have expanded considerably our knowledge of the natural function of these hemoproteins. Thus, it is known for both dioxygen and carbon monoxide binding that distal side steric effects are almost entirely reflected in the control of association rate constants in both model systems and in the proteins. The dissociation rate constants, however, remain fairly constant over a wide range for heme proteins and hindered model systems. The changes in dissociation rates for dioxygen and carbon monoxide that are observed can be correlated to the size, shape and polarity of the environment around the coordinated gas molecule and a variety of model iron porphyrins such as the cylophanes (**1**) of TRAYLOR [5], the picket-pocket complexes (**2**) of COLLMAN [6], the capped (**3**) systems of BASOLO and BALDWIN [7] and the hydrophobic durene systems (**4**) of DOLPHIN [8] are but a few of the many synthetic models that have thrown light on the natural systems.

Studies on the redox chemistry of a wide variety of metalloporphyrins have shown that the porphyrin macrocycle can be readily oxidized [9] and this has led to the observation, in both green plant and bacterial photosynthesis, that the porphyrin π -cation radicals play important roles [10]. This is also true in the catalases and peroxidases, where the enzymatically important high oxidation states are shown to be oxo-iron(IV)-porphyrin cation radicals [11].

More recently, model studies with iron [12], chromium [13], manganese [14] and ruthenium porphyrins [15] have shown that the same oxo-like species are involved in the systems mimicking cytochrome P-450, suggesting that these enzymes, like the catalases and peroxidases, function via an oxo-iron(IV)-porphyrin π -cation radical. Indeed,



studies with cytochrome oxidase [16] suggest that those proteins like the catalases, peroxidases and cytochromes P-450 all function via a homolytic cleavage of the O-O bond of coordinated "peroxide" to generate a high oxidation state intermediate, which then performs its natural function under the direction and control of the protein. This "common intermediate" requires that these different proteins should, on occasion, perform the same chemistry. Such is the case, and thus catalase can mimic P-450 by causing the *N*-demethylation of methylamine [17], while P-450 can act as an oxidase and bring about the four-electron reduction of dioxygen to water [18].

REFERENCES

- [1] CHIEN HO (ed.), «Hemoglobin and Oxygen Binding», Elsevier Biomedical, New York, 1982.
- [2] B. WALKER GRIFFIN, J.A. PETERSON, R.W. ESTABROOK, in D. DOLPHIN (ed.), «The Porphyrins», vol. VII, Academic Press, New York, 1979, pp. 333-375.
- [3] CHIEN HO (ed.), «Electron Transport and Oxygen Utilization», Elsevier Biomedical, New York, 1982.
- [4] W.D. HEWSON, L.P. HAGER, in D. DOLPHIN (ed.), «The Porphyrins», vol. VII, Academic Press, New York, 1979, pp. 295-332.
- [5] T.G. TRAYLOR, D. CAMPBELL, S. TSUCHIYA, *J. Am. Chem. Soc.*, **101**, 4748-4749 (1979).
- [6] J.P. COLLMAN, J.I. BRAUMAN, B.L. IVERSON, J.L. SELLER, R.M. MORRIS, Q.H. GIBSON, *J. Am. Chem. Soc.*, **105**, 3052-3064 (1983).

- [7] J. ALMOG, J.E. BALDWIN, M.J. CROSSLEY, J.F. DE BERNARDIS, R.L. DYER, J.R. HUFF, M.K. PETERS, *Tetrahedron*, **37**, 3589-3601 (1981).
- [8] T.P. WIJESSEKERA, J.B. PAINE III, D. DOLPHIN, F.W.B. EINSTEIN, T. JONES, *J. Am. Chem. Soc.*, **105**, 6747-6749 (1983).
- [9] R.H. FELTON, in D. DOLPHIN (ed.), «The Porphyrins», vol. V, Academic Press, New York, 1978, pp. 53-125.
- [10] J. FAJER, I. FUJITA, M.S. DAVIS, A. FORMAN, L.K. HANSON, K.M. SMITH, *Adv. in Chem. Series*, **201**, (1982).
- [11] D. DOLPHIN, R.H. FELTON, *Acc. Chem. Res.*, **7**, 26-32 (1974).
- [12] J.T. GROVES, T.E. NEMO, R.S. MEYERS, *J. Am. Chem. Soc.*, **101**, 1032-1033 (1979).
- [13] J.T. GROVES, W.J. KRUPER, *J. Am. Chem. Soc.*, **101**, 7613-7615 (1979).
- [14] C.L. HILL, B.C. SCHARDT, *J. Am. Chem. Soc.*, **102**, 6374-6375 (1980).
- [15] D. DOLPHIN, B.R. JAMES, T. LEUNG, *Inorg. Chim. Acta*, **79**, 25-27 (1983).
- [16] D.F. BLAIR, C.T. MARTIN, J. GELLES, H. WANG, G.W. BRADVIG, T.H. STEVENS, S.I. CHAN, *Chem. Scr.*, **21**, 43-53 (1983).
- [17] F.F. KADLUBAR, K.C. MORTON, D.M. ZIEGLER, *Biochem. Biophys. Res. Commun.*, **54**, 1255 (1974).
- [18] L.D. GORSKY, D.R. KOOP, M.J. COON, *J. Biol. Chem.*, **259**, 6812-6817 (1984).

SESSION LECTURES



SL1 — MO

JAMES A. IBERS

Department of Chemistry
Northwestern University
Evanston, IL 60201
U.S.A.

CARBON MONOXIDE AND DIOXYGEN BINDING BY IRON(II) PORPHYRINS

A substantial body of detailed kinetic and thermodynamic data now exists on model systems for the vertebrate hemoproteins. Structural data for these model systems are much more limited. An understanding of the trends in ligand binding, especially of CO and O₂, in these models is of considerable importance in the qualitative assessment of structure-function relationships in the hemoproteins. In addition, interpretation of results from the model systems poses an interesting problem in inorganic chemistry.

Table I presents succinct results on O₂ and CO binding in selected hemoglobins as well as representative model systems. The data for the model systems have been selected for their comparability in terms of solvent and temperature.

Table I

Values of $P_{1/2}$ (in Torr) for CO and O₂ Binding to Selected Hemoglobin and Iron(II) Porphyrinato Imidazole Systems

Compound	$P_{1/2}^{O_2}$	$P_{1/2}^{CO}$	$P_{1/2}^{O_2}/P_{1/2}^{CO}$	Ref.
Hb <i>Ascaris</i>	1.4 10 ⁻³	1 10 ⁻¹	≈ 0.04	[1]
legHb	4.7 10 ⁻²	7.4 10 ⁻⁴	64	[2]
Hb ^A R	0.15-1.5	1.4 10 ⁻³	200-250	[3]
Hb ^A T	9-160	1-2.8 10 ⁻¹	32-1600	[3]
Fe(Chel-MesoP)				
(flat-open)	5.6	2.5 10 ⁻⁴	2.2 10 ⁴	[4]
Fe(TpivPP)				
(1,2-Me ₂ Im) (picket)	38	8.9 10 ⁻³	4.3 10 ³	[3,5]
Fe(PocPiv)				
(1-MeIm) (picket)	0.36	1.5 10 ⁻³	2.7 10 ²	[6]
Fe(6,6-cyclophane)				
(1,5-Cy ₂ Im) (strap)	1.4	9.1 10 ⁻⁴	1.5 10 ³	[3]
Fe(C ₂ Cap)				
(1,2-Me ₂ Im) (cap)	4.0 10 ³	2.0 10 ⁻¹	2.0 10 ⁴	[7,8]

Some interpretations of these various binding data will be offered. In these interpretations we make certain assumptions about the comparability of tetraphenylporphyrins and protoporphyrins, about tail-under porphyrins and picket-fence porphyrins, and about bases such as 1,5-disubstituted imidazoles compared with 1-methylimidazole. Factors that affect ligand binding to be discussed include (i) distal and proximal effects (Fig. 1), (ii) molecular reorganization, (iii) solvation energy effects, and (iv) intrinsic affinities. Where possible these

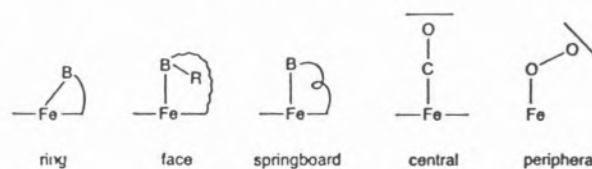


Fig. 1

Schematic Representation of Proximal and Distal Effects

various effects are related to known structural features that may be inferred from the limited structural data on these modified porphyrin systems.

ACKNOWLEDGMENT

This research was supported by the U.S. National Institutes of Health (Grant No. HL 13157).

REFERENCES

- [1] T. OKAZAKI, J.B. WITTENBERG, *Biochim. Biophys. Acta*, **111**, 503 (1965).
- [2] T. IMAMURA, A. RIGGS, Q.H. GIBSON, *J. Biol. Chem.*, **247**, 521 (1972).
- [3] J.P. COLLMAN, J.I. BRAUMAN, K.M. DOXSEE, *Proc. Natl. Acad. Sci. USA*, **76**, 6035 (1979).
- [4] T.G. TRAYLOR, M.J. MITCHELL, S. TSUCHIYA, D.H. CAMPBELL, D.V. STYNES, N. KOGA, *J. Am. Chem. Soc.*, **103**, 5234 (1981).
- [5] J.P. COLLMAN, J.I. BRAUMAN, K.M. DOXSEE, T.R. HALBERT, K.S. SUSLICK, *Proc. Natl. Acad. Sci. USA*, **75**, 564 (1978).
- [6] J.P. COLLMAN, J.I. BRAUMAN, T.J. COLLINS, B. IVERSON, J.L. SESSLER, *J. Am. Chem. Soc.*, **103**, 2450 (1981).
- [7] J.E. LINARD, P.E. ELLIS JR., J.R. BUDGE, R.D. JONES, F. BASOLO, *J. Am. Chem. Soc.*, **102**, 1896 (1980).
- [8] T. HASHIMOTO, R.L. DYER, M.J. CROSSLEY, J.E. BALDWIN, F. BASOLO, *J. Am. Chem. Soc.*, **104**, 2101 (1982).



SL2 — MO

W.E. BLUMBERG
AT&T Bell Laboratories
Murray Hill, New Jersey 07974
U.S.A.

METAL EPR TRUTH DIAGRAM REVISITED 15 YEARS LATER

In 1969 JACK PEISACH and I presented some diagrams which summarized the results of Electron Paramagnetic Resonance experiments on low spin ferric heme compounds. These diagrams presented the EPR parameters in the form of «structural parameters», but these referred to the spin Hamiltonian rather than the molecular structure in the vicinity of the iron atom. Extensive measurements on compounds of hemoglobin were presented on one diagram, and the question was asked «Do all low spin ferric heme compounds have structures analogous to those of hemoglobin?» Diagrams for other heme proteins and model compounds provided «yes» and «no» answers to the questions of structural similarity. Thus these diagrams were quickly nicknamed «Truth Diagrams». Summaries of EPR structural data have later been cast in similar formats using the same philosophy for results of experiments on other types of biological metal binding sites. Notable among these are the Cu(II) EPR experiments on copper proteins and model compounds and the EPR of paramagnetic states of the two-iron ferredoxins. As work has continued on EPR studies of paramagnetic metal sites and their model compounds, both in our own laboratories and in the laboratories of others, over the intervening 15 years numerous additions have been made to these diagrams. How have they held up after this time interval? Have they been useful in assigning molecular structure? Have they had predictive value in suggesting other types of experiments relating to molecular structure? Many published experiments can be called upon to provide answers to these questions.

The talk will give examples of these and will present extensions of this analytic technique introduced by other groups in attempts to remove ambiguities in the Truth Diagrams.



SL3 — MO

F. ANN WALKER
V.L. BALKE
J.T. WEST
Department of Chemistry
San Francisco State University
San Francisco, CA 94132
U.S.A.

THE EFFECT OF HYDROGEN-BONDING OF AMIDES ON THE STABILITY OF AXIAL LIGAND COMPLEXES OF METALLOPORPHYRINS

Several lines of evidence have recently suggested that amide groups impart unique chemical and physical properties to certain metalloporphyrin complexes: We have shown [1] that the contact shifts of the pyrrole protons of low-spin Fe(III)TPP complexes having an amide group appended to the *ortho*, *meta*, or *para* position are «anomalous» in comparison to other mono-substituted TPP complexes of LS Fe(III), and that the Fe(III)/Fe(II) redox potentials of the same complexes are also «anomalous» [2]. However, the EPR spectra of the same complexes are not distinguishably different from other LS Fe(III) complexes [3]. LEXA and coworkers have shown [4] that amide-linked «basket handle» TPP complexes of Cu, Zn, and Mg undergo simultaneous 2-electron oxidation to the porphyrin dication, while TPP complexes of these metals having substituents other than amides undergo stepwise oxidation. MOMENTEAU and LAVALETTE [5] have shown that the kinetics of dioxygen binding to several «hanging base-basket handle» TPPFe(II) derivatives

are unique when the linking group for the «basket handle» is an amide. They suggest that the difference is due to H-bonding between the amide N-H and bound O₂, which slows down the rate of dissociation of O₂. MISPELTER and coworkers [6] have presented NMR evidence for this stabilization.

Four lines of investigation in our laboratory have recently confirmed the strong tendency of amide substituents to engage in H-bond donation, not only to dioxygen in M(II)-O₂ complexes, but also to anions in M(III)L₂⁺Cl⁻ complexes of amide-substituted TPPs. The results obtained point to the latter interaction as the explanation of the «anomalous» contact shifts [1] and redox potentials [2] reported earlier. The four lines of evidence are as follows:

(1) The two-step equilibrium constants, β_2 , for addition of N-methylimidazole to (*o*-, *m*-, and *p*-NHCOCH₃)₁TPPFeCl are «anomalously» large compared to those of other TPPFeCl derivatives [7]. The pattern of enhancement in β_2 (*m* > *p* > *o*) is consistent with the steric requirements involved in H-bond stabilization of the displaced chloride, as are results from H-bond competition studies and alkyl substitution of the amide.

(2) The ligand exchange rates of N-methylimidazole from TPPFe(NMeIm)₂⁺Cl⁻ derivatives, measured by NMR techniques, are greatly enhanced for one ligand. The second ligand's exchange rate is affected less by the presence of the amide, yet in an order consistent with the acidity of the H-bonding group involved (*o*-NHCOR > *o*-OH > *o*-COOH). We thus speculate that H-bonding to displaced Cl⁻ decreases the rate of exchange of the ligand on the same side of the plane as the amide or other substituent.

(3) The binding constant of O₂ to (*o*-NHCOCH₃)₁TPPCoL is five times as large as that to (*m*- or *p*-NHCOCH₃)₁TPPCoL or (*p*-Cl)₄TPPCoL at -56°C in toluene solution (L = 3-picoline). This suggests thermodynamic H-bond stabilization of the Co-O₂ complex. Interestingly, the binding constant of O₂ to the corresponding «Picket fence» derivative (*o*-NHCOC(CH₃)₃)₁TPPCoL is twice as large as those to the TPPCoL complexes incapable of engaging in H-bond donation. This suggests that approximately a factor of 8 stabilization in the

dioxygen complex of the «Picket fence» porphyrin [8] may be attributable to H-bond interactions between the amides and bound O₂. This suggests that the importance of the «flat» vs. «protected» argument of COLLMAN *et al.* [8,9], with respect to the role of porphyrin plane solvation in determining O₂ complex stability is of less importance than assumed by these workers.

(4) The temperature dependence of the EPR spectrum of the dioxygen adduct of (*o*-NHCOCH₃)₁TPPCo(NMeIm) in toluene solution is totally different from that of the corresponding *para*-amide complex, indicating clearly that dioxygen is prevented from rotating freely around the Co-O bond axis in the former, but not the latter case. The nature of the averaging processes which produce the deceptively simple, apparently (though not truly) isotropic eight-line EPR spectra of Co-O₂ complexes over the temperature range -90° to *ca.* 0°C, which have been reported by numerous scientists over the past fifteen years, will be discussed.

REFERENCES

- [1] F.A. WALKER, V.L. BALKE, G.A. McDERMOTT, *J. Am. Chem. Soc.*, **104**, 1569-1574 (1982).
- [2] F.A. WALKER, J.A. BARRY, V.L. BALKE, G.A. McDERMOTT, M.Z. WU, P.F. LINDE, *Adv. Chem. Ser.*, **201**, 377-416 (1982).
- [3] F.A. WALKER, D. REIS, V.L. BALKE, *J. Am. Chem. Soc.*, **106**, 6888-6898 (1984).
- [4] D. LEXA, P. MAILLARD, M. MOMENTEAU, J.-M. SAVEANT, *J. Am. Chem. Soc.*, **106**, 6321-6323 (1984).
- [5] M. MOMENTEAU, D. LAVALETTE, *J. Chem. Soc., Chem. Commun.*, 341-343 (1982).
- [6] J. MISPELTER, M. MOMENTEAU, D. LAVALETTE, J.-M. LHOSTE, *J. Am. Chem. Soc.*, **105**, 5165-5166 (1983).
- [7] V.L. BALKE, F.A. WALKER, J.T. WEST, *J. Am. Chem. Soc.*, in press.
- [8] J.P. COLLMAN, T.R. HALBERT, K.S. SUSLICK, «O₂ Binding to Heme Proteins and Their Synthetic Analogs», in T.G. SPIRO (ed.) «Metal Ion Activation of Dioxygen», John Wiley & Sons, N.Y., 1980, pp. 1-71, and references therein.
- [9] J.P. COLLMAN, J.I. BRAUMAN, B.L. IVERSON, J.L. SESSLER, R.M. MORRIS, Q.H. GIBSON, *J. Am. Chem. Soc.*, **105**, 3052-3064 (1983).



SL4 — MO

G.R. MOORE

The Inorganic Chemistry Laboratory
South Parks Road
Oxford OX1 3QR
U.K.

THE INFLUENCE OF ELECTROSTATIC INTERACTIONS BETWEEN BURIED GROUPS ON THE STRUCTURE AND PROPERTIES OF GLOBULAR PROTEINS

Electrostatic interactions are generally recognised to be a central feature of the structure and function of many proteins even though they are poorly understood. One class of such interactions, those involving charges buried within a protein, are of especial importance to many metalloproteins, par-

ticularly redox proteins. This is because most redox centres are buried within the protein and carry a charge in at least one of its biochemically important oxidation states. The presence of the buried charges may have important consequences for the structure and properties of the protein and this will be demonstrated by reference to the monohaem Class I cytochromes *c*.

The most commonly studied Class I cytochrome *c* mitochondrial cytochrome *c* but there are many bacterial analogs. These are characterised by a common protein fold that results in the burial of most of the haem and its axial ligands. Not only is the iron buried, but at least one of the haem propionates is as well. In some of these cytochromes, the buried propionate is ionised. Experimental observation demonstrate the importance of these buried charges in

- 1) controlling the level of the redox potential;
- 2) coupling the change in oxidation state to the protein conformational state;
- 3) modulating the protein stability.

The general significance of these observations will be considered with reference to other kinds of redox proteins.



SL5 — MO

HITOSHI OHTAKI

Department of Electronic Chemistry
 Tokyo Institute of Technology at Nagatsuta
 4259, Nagatsuta-cho, Midori-ku, Yokohama 227
 Japan

STRUCTURES OF GLYCINATO COMPLEXES OF BIOCHEMICALLY IMPORTANT DIVALENT TRANSITION-METAL IONS IN SOLUTION

Structures of mono-, bis- and tris(glycinato) complexes of biologically important divalent transition-metal ions such as nickel(II) [1,2], copper(II) [3], and zinc(II) [2,4] ions were determined by the X-ray diffraction [1,3,4] and EXAFS [2] methods *in solution* at 25°C. The structural data of these complexes are summarized in Table I. The structure of the bis(glycinato)cop-

per(II) complex was not determinable even by the EXAFS method because of its low solubility in water.

All the complexes investigated were octahedral. The length of an $M^{2+}-OH_2$ bond increased with the introduction of glycinato ions in the coordination sphere of the M^{2+} ion, as we have seen in the case of ethylenediamine complexes of the metal ions [5-8]. Thus, water molecules coordinated to a metal ion became more labile and easier replaceable with an entering ligand at the formation of a higher complex than a lower one.

In the mono(glycinato)copper(II) complex [3], the axial $Cu-OH_2(ax)$ distance was longer than the equatorial $Cu-OH_2(eq)$, $Cu-O(eq)$ and $Cu-N(eq)$ distances (O and N denote carboxylic oxygen and amino nitrogen atoms, respectively, within a chelated glycinato ion). Therefore, the mono-complex had a distorted octahedral structure. On the other hand, the tris-complex, $Cu(gly)_3$, was regular octahedral.

All the zinc(II) complexes with glycinato ions were regular octahedral and the Zn-O and Zn-N distances were practically invariable with varying numbers of glycinato ions in the coordination sphere. On the contrary, the nickel(II) glycinato comple-

Table I

$M-OH_2$, $M-O$ and $M-N$ bond lengths (Å) in the $M(gly)_m(H_2O)_n^{(2-m)+}$ complexes in aqueous solution at 25°C

Complex	Ni ²⁺	Cu ²⁺	Zn ²⁺
$M(H_2O)_6^{2+}$	M-O : 2.04	$\begin{cases} M-O_{eq} : 1.94 \\ M-O_{ax} : 2.43 \end{cases}$	M-O : 2.08
$M(gly)(H_2O)_n^+$	$\begin{cases} n = 4 \\ M-OH_2 : 2.08 \\ M-O : 2.09 \\ M-N : 2.09 \end{cases}$	$\begin{cases} n = 4 \\ M-OH_{2,eq} : 1.98 \\ M-OH_{2,ax} : 2.27 \\ M-O : 1.99 \\ M-N : 1.99 \end{cases}$	$\begin{cases} n = 4 \\ M-OH_2 : 2.12 \\ M-O : 2.12 \\ M-N : 2.12 \end{cases}$
$M(gly)_2(H_2O)_n$	$\begin{cases} \text{Crystal} \\ n = 2 \\ M-OH_2 : 2.10 \\ M-O : 2.06 \\ M-N : 2.08 \end{cases}$	—	$\begin{cases} \text{EXAFS} \\ n = 2 \\ M-OH_2 \\ M-O : 2.07^{a)} \\ M-N \end{cases}$
$M(gly)_3^-$	$\begin{cases} M-O : 2.03 \\ M-N : 2.14 \end{cases}$	$\begin{cases} \text{EXAFS} \\ M-O : 2.01 \\ M-N : 2.10 \end{cases}$	$\begin{cases} \text{EXAFS} \\ M-O : 2.12, 2.13 \\ M-N : 2.12, 2.13 \end{cases}$

a) not separable into each distance.

xes, except for the mono-complex which was regular octahedral, had shorter Ni-O bonds than Ni-N bonds, and the differences between the Ni-O and Ni-N distances were more enhanced in the tris-complex than in the bis-complex.

Stepwise formation constants of the glycinato complexes decreased with the number of glycinato ions within the complexes. However, the stepwise formation reactions were more exothermic at a higher complex than a lower one in the case of nickel(II) and zinc(II) ions, except for the formation of $Zn(gly)_3$. A more negative value in ΔH° at a higher complex is explained in terms of weakened M-OH₂ bonds in the complex, the water molecules being more easily replaced by an entering glycinato ion. A large rate constant of formation of a higher complex may also be due to water molecules which become more labile in the complex by the elongation of the M-OH₂ bond.

The structures of the complexes thus determined were compared with those of metal complexes with other amino acids and biologically interesting ligands and with structures of carboxypeptidase, carbonic anhydrase and thermolysin in the crystalline state.

REFERENCES

- [1] K. OZUTSUMI, H. OHTAKI, *Bull. Chem. Soc. Jpn.*, **56**, 3635 (1983).
- [2] K. OZUTSUMI, T. YAMAGUCHI, H. OHTAKI, «Abstracts of the 3rd International EXAFS Conference», Stanford, U.S.A., July 15-20, 1984.
- [3] K. OZUTSUMI, H. OHTAKI, *Bull. Chem. Soc. Jpn.*, **57**, 2605 (1984).
- [4] K. OZUTSUMI, H. OHTAKI, to be published.
- [5] T. FUJITA, T. YAMAGUCHI, H. OHTAKI, *Bull. Chem. Soc. Jpn.*, **52**, 3539 (1979).
- [6] T. FUJITA, H. OHTAKI, *Bull. Chem. Soc. Jpn.*, **53**, 930 (1980).
- [7] T. FUJITA, H. OHTAKI, *Bull. Chem. Soc. Jpn.*, **55**, 455 (1982).
- [8] T. FUJITA, H. OHTAKI, *Bull. Chem. Soc. Jpn.*, **56**, 3276 (1983).



SL6 — MO

H. KOZŁOWSKI
G. FORMICKA-KOZŁOWSKA

Institute of Chemistry
University of Wrocław
Joliot-Curie 14, 50-383 Wrocław
Poland

L.D. PETTIT

I. STEEL
School of Chemistry
University of Leeds
LS2 9JT Leeds
England

CAN COPPER(II) IONS ACTIVATE BIOLOGICALLY SMALL PEPTIDE MOLECULES?

Many small peptide molecules show very high biological activity, particularly in the central nervous system where many are active as neurotransmitters or as opioids. Very frequently these peptides contain proline or tyrosine residues.

Copper is a biologically essential element which is distributed unevenly throughout the body, with relatively high concentrations being found in the brain. In some cases traces of copper have been shown to increase the activity of biologically active small molecules (e.g. aspirin and cimetidine [1,2]).

The biologically active form of oligopeptides is usually of an organized structure containing e.g. one or more beta-turns. The proline residue encourages the formation of such beta-turns [3] and is unique among biological peptide residues in that it contains a secondary nitrogen atom which, when part of a peptide chain, is not bonded to an ionizable proton and hence cannot coordinate to copper(II). It therefore acts as a «break-point» to metal coordination since it allows the two ends of the chain to coordinate independently. Since a proline residue also encourages a beta-turn, the effect is to bring the two chains close together where they can be bridged by a copper ion [4-6]. Hence the copper can be regarded as locking the

peptide into the biologically active conformation, so promoting its biological activity [7].

The specificity of a proline residue as a «break-point» is also seen in its influence on the binding capability of other amino acid residues present in the peptide sequence, such as tyrosine [8] and lysine [9] residues. The involvement of ionized tyrosine phenolate oxygen in metal ion binding may be an important factor in peptides which display opioid activity such as casomorphin [10].

Copper(II) ions can also affect adversely the biological activity of peptides by binding (and so blocking) their active residues or can promote the activity by «bridging» the peptide to its receptors. This latter situation is most likely in the case of metal-TRF system [11,12].

REFERENCES

- [1] J.R.J. SORENSON, L.W. OBERLEY, V. KISHORE, S.W.C. LEUTHAUSER, T.D. OBERLEY, A. PEZESHK, *Inorg. Chim. Acta*, **79**, 45 (1983).
- [2] F.T. GREENAWAY, L.M. BROWN, J.C. DABROWIAK, M.R. THOMPSON, V.M. DAY, *J. Am. Chem. Soc.*, **102**, 7782 (1980).
- [3] R.Y. CHOU, G.D. FASMAN, *J. Mol. Biol.*, **115**, 135 (1977); M. LISOWSKI, I.Z. SIEMION, K. SOBCZYK, *Int. J. Pept. Protein Res.*, **21**, 301 (1983) and references therein.
- [4] G. FORMICKA-KOZŁOWSKA, H. KOZŁOWSKI, I.Z. SIEMION, K. SOBCZYK, E. NAWROCKA, *J. Inorg. Biochem.*, **15**, 201 (1981).
- [5] M. BATAILLE, G. FORMICKA-KOZŁOWSKA, H. KOSŁOWSKI, L.D. PETTIT, I. STEEL, *J. Chem. Soc., Chem. Commun.*, 231 (1984).
- [6] L.D. PETTIT, I. STEEL, G. FORMICKA-KOZŁOWSKA, T. TATAROWSKI, M. BATAILLE, *J. Chem. Soc., Dalton Trans.*, in press.
- [7] L.D. PETTIT, G. FORMICKA-KOZŁOWSKA, *Neuroscience Letters*, **50**, 53 (1984).
- [8] H. KOZŁOWSKI, M. BEZER, L.D. PETTIT, M. BATAILLE, B. HECQUET, *J. Inorg. Biochem.*, **18**, 231 (1983).
- [9] M. BATAILLE, L.D. PETTIT, I. STEEL, H. KOZŁOWSKI, T. TATAROWSKI, *J. Inorg. Biochem.*, in press.
- [10] G. FORMICKA-KOZŁOWSKA, L.D. PETTIT, I. STEEL, B. HARTRODT, K. NEUBERT, P. REKOWSKI, G. KUPRYSZEWSKI, *J. Inorg. Biochem.*, **22**, 155 (1984).
- [11] G. FORMICKA-KOZŁOWSKA, L.D. PETTIT, M. BEZER, *J. Inorg. Biochem.*, **18**, 335 (1983).
- [12] T. TONOUÉ, S. MINAGAWA, N. KATO, K. OHKI, *Pharmacol. Biochem. Behav.*, **10**, 201 (1979).



SL7 — MO

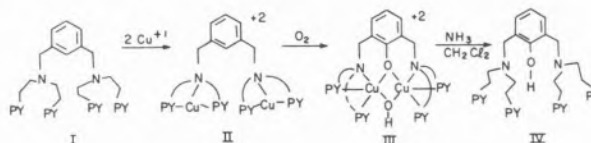
KENNETH D. KARLIN
YILMA GULTNEH
RICHARD W. CRUSE
JON C. HAYES
JON ZUBIETA

Department of Chemistry
State University of New York (SUNY) at Albany
Albany
New York, 12222
U.S.A.

DIOXYGEN BINDING AND ACTIVATION IN DINUCLEAR COPPER COMPLEX SYSTEMS

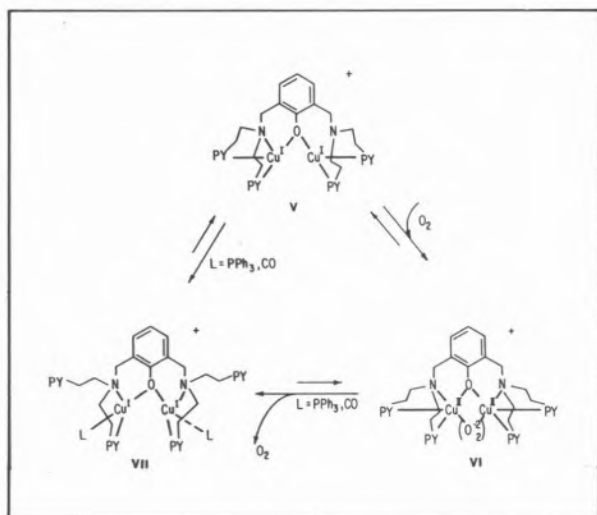
Studies of the reactivity of dioxygen with model mono- and dinuclear copper(I) centers are of interest because of their relevance to the copper proteins such as hemocyanin, a dioxygen carrier, and tyrosinase and dopamine beta-hydroxylase which are monooxygenases involved in oxygen activation [1]. Such model studies may also help in the development of synthetic reagents or catalysts for the oxidation of organic substrates. Here, we will summarize our latest findings in several systems involving Cu(I)-dioxygen interactions or reactivity. The first deals with a monooxygenase model system where the reaction of dioxygen with a dinuclear Cu(I) complex II results in the oxygenation of the ligand and concomitant formation of the phenoxo- and hydroxo- bridged dinuclear complex III. Studies using isotopically labelled dioxygen and the observed stoichiometry of reaction ($\text{Cu}:\text{O}_2 = 2:1$) demonstrate that this reaction is directly analogous to that shown by the copper mono-oxygenase enzymes [2].

Recent insights into the mechanism of this reaction will be presented. The reaction of a dinuclear



Cu(II) derivative of the ligand I with aqueous hydrogen peroxide also gives high yields of the oxygenated product III. By contrast, neither the reaction of dioxygen with a Cu(I) monomeric analog of I nor the reaction of H₂O₂ with the Cu(II) form give hydroxylated products. Together, the evidence suggests that a peroxo-bridged dinuclear Cu(II) unit is involved as an intermediate in the reaction of II \rightarrow III [3].

Thus, due to the interest in stabilizing and characterizing peroxo-Cu(II) compounds (i.e. dioxygen adducts resulting from the addition of O₂ to Cu(I)_n), we have studied the intermediate products of the reaction of dioxygen with Cu(I) complexes of dinucleating ligands such as II and IV. We have isolated and structurally characterized a Cu(I) dinuclear complex of ligand IV (V); it



contains a bridging phenoxo group and a vacant potential bridging position (Cu...Cu = 3.6 Å). Compound V reacts with O₂ resulting in the formation of a dinuclear Cu(II)-peroxo complex VI that is stable at low temperature. It is characterized by a strong charge-transfer absorption band at 505 nm. Confirmation of the complex's formulation as a peroxo species also comes from resonance Raman spectroscopy [4].

The binding of dioxygen to VI is quasi-reversible, and cycling between V and VI can be achieved and followed spectrophotometrically. Additional evidence for the reversibility of the dioxygen binding equilibrium comes from the reaction of either V or VI with CO or PPh₃. These form

adducts (VII) with VI. In addition, they can be formed by reaction with the peroxo-complex VI, resulting in the quantitative release of O₂.

REFERENCES

- [1] K.D. KARLIN, J. ZUBIETA (eds.), «Copper Coordination Chemistry: Biochemical and Inorganic Perspectives», Adenine Press, Guilderland, NY, 1983.
- [2] K.D. KARLIN, J.C. HAYES, Y. GULTNEH, R.W. CRUSE, J.W. MCKOWN, J.P. HUTCHINSON, J. ZUBIETA, *J. Am. Chem. Soc.*, **106**, 2121-2128 (1984).
- [3] N.J. BLACKBURN, K.D. KARLIN, M. CONCANNON, J.C. HAYES, Y. GULTNEH, J. ZUBIETA, *J.C.S. Chem. Commun.*, 939-940 (1984).
- [4] K.D. KARLIN, R.W. CRUSE, J.C. GULTNEH, J. ZUBIETA, *J. Am. Chem. Soc.*, **106**, 3372-3374 (1984).



SL8 — MO

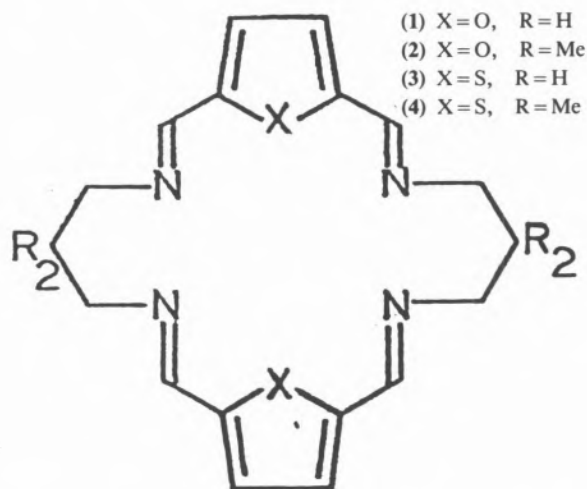
S. MARTIN NELSON

Chemistry Department
Queen's University
Belfast BT9 5AG
Northern Ireland

DI-COPPER COMPLEXES OF MACROCYCLIC LIGANDS AS MODELS FOR TYPE 3 COPPER PROTEINS

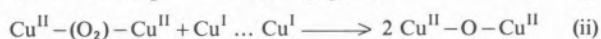
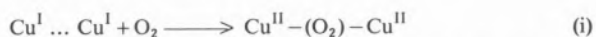
It is well established that the biological action of many metalloproteins is associated with the occurrence of the metal atoms in pairs or clusters. Prominent amongst these are the copper proteins containing di-copper (Type 3) sites such as the O₂-transport protein hemocyanin and oxygenase and oxidase proteins such as tyrosinase, dopamine β-hydroxylase, laccase, etc. [1]. Studies of synthetic di-copper complexes have contributed to our understanding of the active site chemistry of the natural systems including the nature of the interaction of O₂ and oxidisable substrates with the dimetallic site [2].

In this paper we review recent investigations of some di-copper(I) and di-copper(II) complexes of the binucleating macrocyclic ligands (1) - (4)



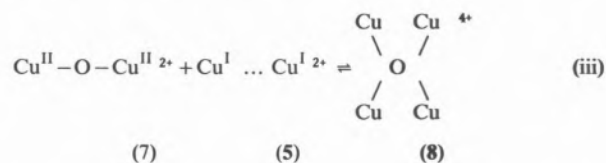
and of some related macrocyclic systems differing in ring size and in the number, nature and disposition of the potential donor atoms. X-ray structural analysis [3] has established that the Cu ... Cu separation in the complexes (1) falls in the range 2.9 - 3.4 Å. In several of the di-Cu(I) complexes the Cu(I) atoms are three-coordinate being bonded to two imino nitrogens of the macrocycle and to a monodentate ligand such as MeCN, pyridine or PPh₃. In others the metal atoms are intramolecularly linked via (one or two) small bridging ligands (SPh⁻, C≡CPh⁻, pyrazolate, pyridazine, 1,2,4-triazolate, bis(diphenylphosphino)methane) to give (usually) tetrahedral structures.

Reaction of the coordinatively unsaturated three-coordinate di-Cu(I) complexes with O₂ in *e.g.* dimethylacetamide has been monitored by gas-uptake and by accompanying changes in spectroscopic (electronic, ESR) properties. Evidence has been obtained for a two-stage reaction sequence [equations (i) and (ii)]



in which the initially formed μ -peroxo-di-Cu(II) adduct (6) undergoes a further two-electron transfer in a bimolecular reaction with a second mole-

cule of the di-Cu(I) complex (5) generating the final four-electron O₂-reduction product (7). The μ -oxo species (7) may have an aggregate (dimeric) structure. The results suggest that the reversible O₂-carrying property of hemocyanin may be due to steric prevention (by the protein superstructure) of the bimolecular reaction (ii). In this respect oxyhemocyanin may resemble oxyhemoglobin. It has also been shown that the final oxidation product (7) undergoes a reversible 1:1 association [equation (iii)] with the di-Cu(I) complex (5) to form a mixed valence species (8).



When the reaction of (5) with O₂ is carried out in the presence of an oxidisable substrate the substrate may be oxidised in preference to the irreversible oxidation of the metal ions. In several cases such as in the oxidation of catechols to quinones (*cf.* the catecholase activity of tyrosinase) the reactions are catalytic in copper complex.

REFERENCES

- [1] E.I. SOLOMON, in T.G. SPIRO (ed.) «Copper Proteins», Wiley-Interscience, New York, 1981, chap. 1.
- [2] See, for example, various chapters in K.D. KARLIN, J. ZUBIETA (eds.), «Copper Coordination Chemistry; Biochemical and Inorganic Perspectives», Adenine Press, New York, 1983.
- [3] S.M. NELSON, F. ESHO, A. LAVERY, M.G.B. DREW, *J. Am. Chem. Soc.*, **105**, 5693 (1983).



SL9 — TU

B.H. HUYNH

Physics Department
Emory University
Atlanta, Georgia
U.S.A.

L. KANG

D.V. DERVARTANIAN

H.D. PECK JR.

J. LEGALL

Biochemistry Department
University of Georgia
Athens, Georgia
U.S.A.

A COMPARISON STUDY OF SULFITE REDUCTASE FROM SULFATE-REDUCING BACTERIA: A MÖSSBAUER INVESTIGATION

INTRODUCTION

Sulfite reductase catalyzes the six-electron reduction of sulfite to sulfide. Based on physiological function, sulfite reductases may be grouped into two general categories: 1. assimilatory sulfite reductase which are involved in the synthesis of sulfur-containing cell constituents, and 2. dissimilatory sulfite reductase which participates in the respiratory pathway of sulfate reduction in sulfate-reducing bacteria. Despite the differences in their physiological functions and reaction mechanisms, both types of sulfite reductases were shown to contain siroheme and [4Fe-4S] clusters. Recent Mössbauer studies of the hemoprotein subunit of the *Escherichia coli* NADPH — sulfite reductase (SiR) disclosed that the siroheme and the [4Fe-4S] clusters are exchange-coupled [1].

RESULTS AND DISCUSSION

A dissimilatory sulfite reductase and an assimilatory-type sulfite reductase have been purified from extracts of *Desulfovibrio vulgaris*. The dissimilatory sulfite reductase is a tetramer with molecular weight of 226,000. Its optical spectrum exhibits maxima at 628, 580, 408, 390, and 279

nm [2]. The assimilatory-type sulfite reductase consists of a single polypeptide chain and has a molecular weight of 27,200. Its optical spectrum exhibits maxima at 590, 545, 400 and 280 nm. Similar to SiR, this low-molecular-weight sulfite reductase also contains siroheme and [4Fe-4S] cluster. In the oxidized form, the [4Fe-4S] cluster is in the diamagnetic +2 state. The siroheme is low-spin ferric and exhibits EPR resonances at $g=2.44$, 2.36 and 1.77. High-temperature Mössbauer measurements indicates that the ratio of siroheme to [4Fe-4S] cluster is 1:1. Low-temperature and high-field measurements unambiguously establish that the siroheme and the [4Fe-4S] cluster are exchange-coupled. The observed Mössbauer parameters ($\Delta E_Q=2.52$ mm/s, $\delta=0.25$ mm/s) and the hyperfine tensor for the siroheme resembles those found for Cytochrome P₄₅₀ [3], suggesting that the bridging ligand between the siroheme and the [4Fe-4S] cluster may be sulfur.

We have also performed Mössbauer measurements on various dissimilatory sulfite reductases (desulforubidin and desulfovibridin) isolated from different *Desulfovibrio* species. The Mössbauer spectrum of desulforubidin purified from *D. desulfuricans* (Norway) recorded at 4.2 K shows three spectral subcomponents: 1. a central doublet originating from a diamagnetic species consistent with a [4Fe-4S]²⁺ cluster, 2. a magnetic component extending from -5 mm/s to +5 mm/s attributable to the high-spin ferric siroheme, and 3. an additional magnetic component extending from -1 mm/s to +2 mm/s indicative of a [4Fe-4S] cluster that is strongly coupled to the siroheme. The absorption intensity of the siroheme-[4Fe-4S] unit is determined to be ~40% of the total absorption, indicating that desulforubidin contains one coupled siroheme-[4Fe-4S] unit per two uncoupled [4Fe-4S] clusters. These results also suggest that the coupled siroheme-[4Fe-4S] unit is a common prosthetic group for both assimilatory and dissimilatory sulfite reductases.

However, an interesting and puzzling result was observed for sulfite reductases isolated from *Thiobacillus denitrificans*, *D. desulfuricans* (27774), and *D. gigas*. All of these enzymes exhibits much less Mössbauer absorptions of siroheme than that found in desulforubidin, suggesting that these enzymes may contain sirohochlorin rather than

siroheme. Such a suggestion can also be used to explain an earlier finding that sirohydrochlorin is extracted from these enzymes while siroheme is extracted from desulforubidin and SiR under treatment of acetone/HCl. Future experiments are planned to clarify this situation.

REFERENCES

- [1] J.A. CHRISTNER, E. MÜNCK, P.A. JANICK, L.M. SIEGEL, *J. Biol. Chem.*, **258**, 11147-11156 (1983).
- [2] L.-P. LEE, J. LEGALL, H.D. PECK JR., *J. Bacteriol.*, **115**, 529-542 (1973).
- [3] M. SHARROCK, P.G. DEBRUNNER, C. SHULZ, J.D. LIPSCOMB, V. MARSHALL, I.C. GUNSALUS, *Biochim. Biophys. Acta*, **420**, 8-26 (1976).



SL10 — TU

A.X. TRAUTWEIN
Physik
Medizinische Hochschule
2400 Lübeck
W-Germany

NEW ASPECTS OF MÖSSBAUER SPECTROSCOPY

Mössbauer spectroscopy has become a well established tool in biosciences. Most of the biochemical, bioinorganic and biophysical applications deal with ^{57}Fe Mössbauer absorption experiments, to derive via isomer shifts, quadrupole splittings, and magnetic hyperfine interactions an understanding of the electronic structure and the chemical structure-function-relation of the compounds under study.

During the recent years the methodical aspects of Mössbauer spectroscopy have become wider and provide us with new applications. The purpose of the present contribution is to describe such applications.

(i) Mössbauer study of molecular dynamics:
Information about vibration, bound diffusion,

overdamped oscillation, and rotation of subgroups within a molecule (heme proteins and relevant model compounds) were derived from the T-dependence of electric field gradient tensors, line shapes and absorption areas [1-6].

(ii) Rayleigh scattering using Mössbauer radiation:

This method makes it possible to study molecular dynamics even in systems which *do not* contain any Mössbauer isotope [7].

(iii) Mössbauer studies using Synchrotron radiation:

Most recent experiments were successful in discriminating the ^{57}Fe 14.4 KeV Mössbauer resonance line ($\Gamma \sim 10^{-7}$ eV) from the "white" Synchrotron radiation beam [8]. Thus it might soon be possible to perform dynamic Mössbauer studies of chemical reactions.

(iv) Mössbauer scattering for complete three dimensional structure analysis of iron proteins:

This is a competitive tool for X-ray structure analysis. It avoids the method of multiple isomorphous replacement by applying the ^{57}Fe nucleus as heavy reference scatterer. Experiments on MbCO crystals have already been performed [9,10].

(v) Combined Mössbauer and molecular orbital investigation of oriented molecules:

The relative orientation of electric field gradient-, g-, fine structure-, and hyperfine coupling tensors with respect to the molecular frame are obtained. With this manifold of experimental and calculated results the understanding of electronic and steric structure becomes more complete. Examples with FeMoS₂-cores are presented [11-13].

REFERENCES

- [1] R.L. MÖSSBAUER, in «Proc. of the Int. Conf. on Mössbauer Spectroscopy», Alma Ata, Gordon, 1983, in press.
- [2] I. NOWIK, S.G. COHEN, E.R. BAUMINGER, S. OFER, *Phys. Rev. Lett.*, **50**, 1528 (1983).
- [3] E.W. KNAPP, S.F. FISCHER, F. PARAK, *J. Chem. Phys.*, **78**, 4701 (1983).
- [4] F. PARAK, A.X. TRAUTWEIN, in A.G. SCHNECK, C. PAUL (eds.), «Brüssels Hemoglobin Symposium», Edition de L'Université de Bruxelles, 1984, p. 299.
- [5] E. BILL, N. BLAES, K.F. FISCHER, U. GONSER, K.H. PAULY, R. PRESTON, F. SEEL, R. STAAB, A.X. TRAUTWEIN, *Z. Naturforsch.*, **39b**, 333 (1984).
- [6] R. MONTIEL-MONTOYA, E. BILL, L. RICARD, M. SCHAPACHER, A.X. TRAUTWEIN, R. WEISS, H. WINKLER, *Rev. Port. Quím.*, **27**, 278 (1985).

- [7] Y.F. KRUPSYANSKII, F. PARAK, V.I. GONDANSKIJ, R.L. MÖSSBAUER, E. GOMMAN, H. ENGELMANN, I.P. SUZDALEV, *Z. Naturforsch.*, **37c**, 57 (1982).
- [8] E. GERDAU, R. RÜFFER, H. WINKLER, W. TOLKSDORF, C.P. KLAGES, J.P. HANNON, *Phys. Rev. Lett.*, submitted for publication.
- [9] F. PARAK, R.L. MÖSSBAUER, W. HOPPE, U.F. THOMANEK, D. BADE, *J. de Physique Colloq. C6*, **37**, C6-703 (1976).
- [10] R.L. MÖSSBAUER, F. PARAK, W. HOPPE, in U. GONSER (ed.), «Topics in Current Physics», vol. 25, Springer-Verlag, Heidelberg, 1981, p. 5.
- [11] A.X. TRAUTWEIN, E. BILL, R. BLÄS, S. LAUER, H. WINKLER, A. KOSTIKAS, *J. Chem. Phys.*, in press.
- [12] H. WINKLER, E. BILL, S. LAUER, U. LAUER, A.X. TRAUTWEIN, A. KOSTIKAS, V. PAPAETHYMION, H. BÖGGE, A. MÜLLER, E. GERDAU, U. GONSER, *J. Chem. Phys.*, in press.
- [13] A.X. TRAUTWEIN, E. BILL, R. BLÄS, A. KOSTIKAS, S. LAUER, H. WINKLER, *Rev. Port. Quím.*, **27**, 186 (1985).



SL11 — TU

A. SIMOPOULOS
 A. KOSTIKAS
 V. PAPAETHYMION
 Nuclear Research Center «Demokritos»
 Aghia Paraskevi Attikis
 Greece
 D. COUCOUVANIS
 M. KANATZIDIS
 Department of Chemistry
 University of Michigan
 Michigan
 U.S.A.

ELECTRONIC AND MAGNETIC PROPERTIES OF SYNTHETIC ANALOGS FOR THE M AND P CLUSTERS OF NITROGENASE

Spectroscopic results (Mössbauer, EPR [1] and EXAFS [2]) for the Fe-Mo protein of nitrogenase have led to a structural model according to which the 30 ± 2 iron atoms of the protein are distributed into two cluster types labelled M and P respectively. The M cluster consists of two identical centers (cofactor centers) each containing six Fe

atoms and one Mo atom in a configuration which, in the native state, is EPR active with $S=3/2$. A cubane formation containing four Fe and four S atoms has been proposed for the P cluster type. Two inequivalent sites have been assigned for the Fe atoms with an occupation ratio of 3:1.

We present in this communication Mössbauer and magnetic susceptibility studies of two groups of synthetic analogs for the M and P clusters respectively.

Two binuclear (Fe-Mo) and two trinuclear (Fe-Mo-Fe and Mo-Fe-Mo) complexes with sulfur bridges between the metal centers have been studied and compared with the electronic structure and magnetic properties of the Fe-Mo cofactor of nitrogenase. The isomer shift of these complexes indicates that the MoS_4^{2-} moiety withdraws electronic charge from the Fe(II) ions resulting in their partial oxidation. This ability of the MoS_4^{2-} ligand may well represent a characteristic feature of the Fe-Mo-S aggregates of nitrogenase. Intramolecular antiferromagnetic interactions are present in the trinuclear complex $[\text{Cl}_2\text{FeS}_2\text{MoS}_2\text{FeCl}_2]^{2-}$ leading to a spin $S=0$ ground state. On the other hand, the trinuclear anion $[\text{S}_2\text{MoS}_2\text{FeS}_2\text{MoS}_2]^{3-}$, which may be described with formal valences of Fe and Mo either (I) and (V) or (III) and (IV) respectively, has a resultant spin $S=3/2$.

A number of 4Fe-4S cubane clusters with mixed terminal ligands have been investigated as possible models for the other major Fe-component of the Mo-Fe protein of nitrogenase, the «P-clusters». The latter exhibit unique spectral properties which have been attributed to significant differences in the ligation of their Fe_4S_4 cores [3]. An extensive charge delocalization prevails in the Fe_4S_4 cores of the cubanes with monodentate asymmetric ligands resulting in four essentially indistinguishable Fe sites with a formal oxidation state of +2.5. The introduction of one bidentate terminal ligand results in a differentiation of the corresponding iron site from the remaining three, leading to the 3:1 ratio similar to the P-clusters of nitrogenase. The present results indicate clearly that a differentiation of sites within the Fe_4S_4 core can be achieved with a change in their coordination number without an increase in the charge (core reduction) or charge localization within the core.

REFERENCES

- [1] B.H. HUYNH, M.T. HENZL, J.A. CHRISTNER, R. ZIMMERMAN, W.H. ORME-JOHNSON, E. MÜNCK, *Biochim. Biophys. Acta*, **623**, 124 (1980).
- [2] S.P. CRAMER, W.O. GILLUM, K.O. HODGSON, L.E. MORTENSON, E.I. STIEFEL, J.R. CHISNELL, W.J. BRILL, V.K. SHAH, *J. Am. Chem. Soc.*, **100**, 3814 (1978).
- [3] E. MÜNCK, in «Recent Chemical Applications in Mössbauer Spectroscopy», *Advances in Chemistry Series*, American Chemical Society, Washington D.C., 1981, p. 305.



SLI2 — TU

JACQUES MEYER
 JEAN-MARC MOULIS
 DRF/Biochimie (INSERM U. 191) CEN-G
 Grenoble
 France
 MARC LUTZ
 DB-Biophysique
 CEN-SACLAY
 France

RESONANCE RAMAN SPECTROSCOPY OF IRON-SULFUR PROTEINS

Resonance Raman (RR) spectroscopy allows a very selective and sensitive structural probing of chromophores in biological systems, whatever their physical state. Its application to [Fe-S] proteins has made significant progress in the last few years. Characteristic spectra are now available for [1Fe], [2Fe-2S], [3Fe-xS] and [4Fe-4S] sites in rubredoxins and ferredoxins. Thus, RR spectroscopy can be used for the unambiguous identification of [Fe-S] clusters.

Furthermore, RR spectroscopy can afford detailed structural information which is not accessible to other techniques. By measuring the frequency shifts occurring upon $^{32}\text{S} \rightarrow ^{34}\text{S}$ or $^{76}\text{Se} \rightarrow ^{82}\text{Se}$ isotopic substitutions on core chalcogenide atoms, and the depolarization ratios of the RR bands, it is in general possible to discriminate the vibrational modes of the inorganic core (Fe-S*) from those involving the cysteine ligands (Fe-Scys), and to

determine the symmetry species of the RR active modes. The symmetry point group of the [Fe-S] cluster may therefrom be inferred, *i.e.* the configuration of the active site may be determined with accuracy. Relevant investigations involving [4Fe-4X] and [2Fe-2X] (X=S,Se) proteins will be presented and discussed.

A given type of [Fe-S] cluster may assume slightly different structures depending on which polypeptide chain accommodates it. Recent studies have shown RR spectroscopy to be exceptionally efficient in detecting such differences, particularly in the cases of [2Fe-2S] and [3Fe-xS] proteins. In some instances spectral differences can be assigned to structural differences involving a given subset of Fe-S bonds of the active site.

Investigations on simple [Fe-S] proteins such as those outlined above are opening the way to similar studies of more complex proteins.



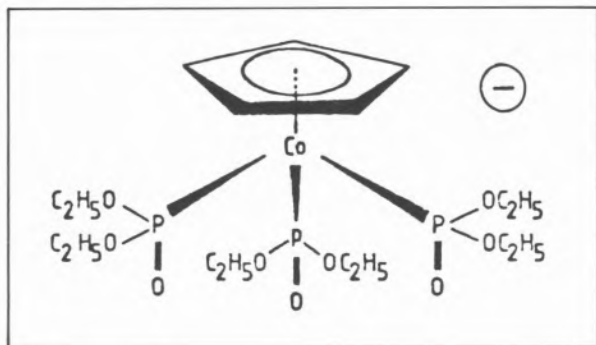
SL13 — TU

GIL NAVON
HADASSAH SHINAR
Department of Chemistry
Tel Aviv University
Ramat-Aviv 69978
Israel

WOLFGANG KLAUI
Institut für Anorganische Chemie
Technischen Hochschule Aachen
5100 Aachen
West Germany

AN ORGANOMETALLIC LITHIUM IONOPHORE

Recently there has been an intensive research for the discovery of Li^+ ionophores mainly because of the importance of Li^+ in the treatment of manic-depressive patients. It is hoped that Li^+ ionophores will assist the delivery of Li^+ ions across the blood brain barrier. Most of the Li^+ ionophores described in the literature are based on cyclic and branched polyethers. We report here that the organometallic ligand $[(\text{C}_5\text{H}_5)\text{Co}\{\text{P}(\text{O})(\text{OC}_2\text{H}_5)_2\}_3]^-$ (L^- hereafter) [1] has efficient ionophoric properties with a specificity towards Li^+ ions.



A considerable shortening of the ^{23}Na NMR longitudinal relaxation time (T_1) occurs upon binding of Na^+ to the ligand. We have used this phenomenon to measure the stability constant of the Na-L complex in aqueous solutions. The association constants of the K^+ and Li^+ complexes with L^-

were also determined by the measurement of the ^{23}Na NMR T_1 in competition experiments. Another approach was the measurement of the ^{31}P chemical shifts of L^- upon binding to the metal ions and H^+ . The results obtained by the two methods were in good agreement. The association constants in aqueous solutions follow the trend $\text{H}^+ > \text{Li}^+ > \text{Na}^+ > \text{K}^+$. The same trend was found earlier in methanol [2]. However, the association constants in methanol are greater by three orders of magnitude.

In order to follow the transport of Na^+ and Li^+ across lipid membranes we prepared large unilamellar vesicles, containing either NaCl or LiCl , suspended in a solution containing KCl and 2 mM $\text{K}_7\text{Dy}(\text{tripolyphosphate})_2$. $\text{Dy}(\text{tripolyphosphate})_2^{7-}$ is known to act as a shift reagent for $^{23}\text{Na}^+$ [3]. Thus in the presence of this reagent the $^{23}\text{Na}^+$ resonance of the extravascular solution shifts to higher field while the intravesicular $^{23}\text{Na}^+$ resonance remains unshifted. We have found this reagent to be an efficient shift reagent for $^7\text{Li}^+$ as well. In fig. 1 we present a series of spectra that were

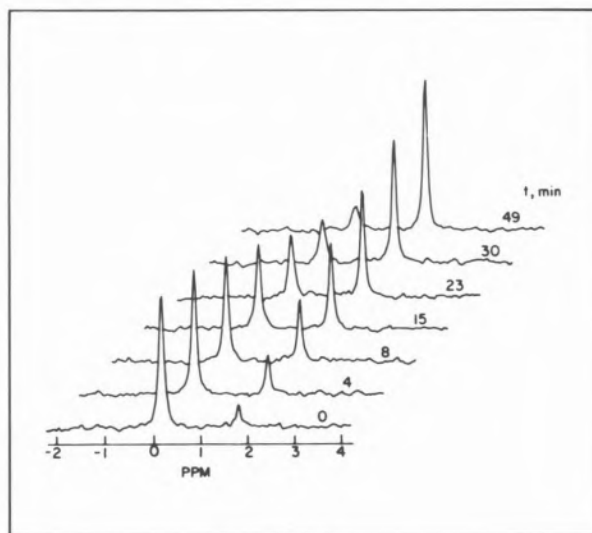


Fig. 1

taken with vesicles loaded with 150 mM LiCl and Tris-Cl-buffer pH 7.5. At time zero the carrier L^- was added to a final concentration of 200 μM . The decrease of the intravesicular $^7\text{Li}^+$ resonance and the concomitant increase of the extravascular one is clearly seen. Fig. 2 describes the time course of the transport in terms of molar concentration.

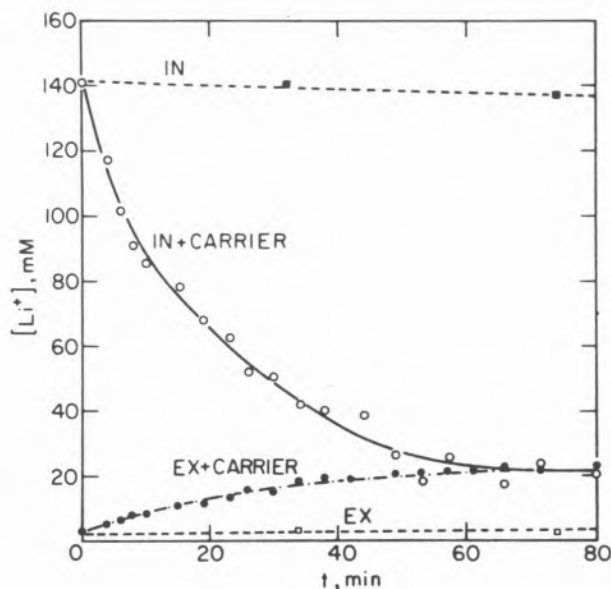


Fig. 2

The intravesicular volume in the case shown was 16%. The unfacilitated transport for the same batch of vesicles is also shown in the figure. Similar experiments with Na^+ vesicles and different concentrations of L^- gave the following values for $10^3 \times k_{\text{out}}$: 3.2, 6.2, 8.7, 13.8, 17.9, 26.7 min^{-1} for L^- concentrations of 91, 182, 300, 400, 600 and 800 μM respectively. These results clearly indicate that the transport rate constant is directly proportional to the first power of the carrier concentration giving $k/[\text{L}^-] = 33.3 \pm 3.1 \text{ S.D. } \text{M}^{-1}\text{min}^{-1}$. This leads to the conclusion that the species active in the transport is a 1:1 ligand-to-metal complex. In similar experiments with Li^+ the reduced rate constant for lithium transport was $k/[\text{L}^-] = 208 \pm 51 \text{ S.D. } \text{M}^{-1}\text{min}^{-1}$ *i.e.* larger than that of Na^+ by a factor of 6.2. This factor is much smaller than the ratio of the association constants both in methanol and water, thus indicating that the rate of the transport is kinetically limited. It is interesting to note that the rate of transport of sodium diminishes in the presence of Li^+ when both are present in the vesicles. This is a result of the competition of these two ions for complexing the carrier. Thus the selectivity may be increased in systems containing a mixture of these two ions. It is hoped that chemical modification in the structure of the present ligand may lead to the discovery of other Li^+ ionophores, which may be even more efficient and selective.

REFERENCES

- [1] W. KLAUI, *Z. Naturforsch., Teil B*, **34**, 1409 (1979).
- [2] G. ANDEREGG, W. KLAUI, *Z. Naturforsch., Teil B*, **36**, 949 (1981).
- [3] R.K. GUPTA, P. GUPTA, *J. Magn. Reson.*, **47**, 344 (1982).



SL14 — TU

K.R.K. EASWARAN
Molecular Biophysics Unit
Indian Institute of Science
Bangalore 560 012
India

IONOPHORE-METAL INTERACTIONS

Many of the biological transport processes are mediated by membrane proteins. The mechanisms underlying their transmembrane transporting properties have features of essentially two ideal transport mechanisms namely, the channel and the carrier mechanisms [1]. These mechanisms have been postulated and defined based on studies on electrical conductances of bilayer lipid membranes when ionophores are incorporated into them with special reference to cation transport. Classic examples of these ionophore molecules are valinomycin, lasalocid, nonactin and A23187 which act by a carrier mechanism [2]. Conformational studies of these carriers and their cation complexes are of primary importance for a detailed understanding of this mechanism of ion transport at the molecular level.

Valinomycin is a cyclic dodecapeptide with the sequence $\text{Cyclo(L-Val-D-HyIv-D-Val-L-Lac)}_3$. It has a remarkable selectivity for K^+ over Na^+ . This molecule exhibits solvent dependent conformations [3] with a) tight, closed structure formed by intramolecular hydrogen bonds between the ester carbonyls and the amide hydrogens in apolar solvents, b) a partially intramolecularly hydrogen bonded structure in medium polar solvents called

a propellar conformation and c) an open structure with a considerable amount of flexibility in polar solvents. Several interesting stoichiometries and conformations are known for the cation complexes of valinomycin [4]. The valinomycin-K⁺ complex has an essentially solvent independent conformation with the K⁺ ion trapped inside the bracelet structure. The stoichiometry of the complexes of valinomycin with the IA group cations (Li⁺, Na⁺, K⁺, Rb⁺ and Cs⁺) is 1:1. Whereas the K⁺, Rb⁺ and Cs⁺ complexes have bracelet structures, Li⁺ [5] and Na⁺ form an altogether different complex. This complex may be called a peripheral complex with the cation bound only to one end of the molecule. The IIA group cations Mg²⁺ [6], Ca²⁺ [7], Sr²⁺ [6] and Ba²⁺ [8-10] form more than one complexed species in solution with valinomycin. All these cations form the 1:1 peripheral complexes. In addition, 2:1 (valinomycin:cation) complexes are also formed with the cation sandwiched between two valinomycin molecules. Sr²⁺ and Ba²⁺ form, in addition to the 1:1 and 2:1 complexes, 1:2 complexes with open, labile structures. In the solid state [9,11] valinomycin forms the 1:2 complex with Ba²⁺ with an ellipsoidal structure and the bariums occupying the two focii.

Nonactin belongs to the class of macrotetrolide actins. It forms isomorphous 1:1 complexes with Na⁺, K⁺ and Ca²⁺ [12-15]. The backbone of these complexes resembles the seam of a tennis ball while positioning of the liganding oxygens is different with respect to the seam. In the K⁺ complex, K⁺ has coordination number of 8 with the cation at the center of two approximate tetrahedrons formed by carbonyls and tetrahydrofuran ring oxygens. In the Ca²⁺ complex [15,16], the four tetrahydrofuran ring oxygens are at the center while the four carbonyl oxygens tetrahedrally coordinate to the central cation.

Another very important class of ionophores is the carboxylic ionophores. The calcium ionophores, lasalocid and A23187 belong to this group. Lasalocid is a monomer in polar solvents [17] and aggregates into a dimer in apolar solvents [18]. It forms both neutral and charged complexes with 1:1 and 2:1 stoichiometries depending on the solvent, cations and the protonation state of the carboxylic group [19,20]. Lasalocid forms both 2:1 and 1:1 complexes with Li⁺ [21] and Ca²⁺ [22,23].

Other monovalent cations complex to form only the 1:1 complexes. The rare earth cations (lanthanides La³⁺ to Lu³⁺) form both 1:1 and 2:1 complexes [24]. In methanol, with lanthanide chlorides, no complexation is found whereas the nitrates form both the types of complexes. In acetonitrile, formation of the 2:1 complex is predominant. As one goes down the series from La³⁺ to Lu³⁺, the stability of the 2:1 complex increases with a corresponding decrease in the stability of the 1:1 complex in both the solvents.

The observation of 2:1 (sandwich) type conformation in many of the ionophore-cation complexes is very significant and suggests that a relay carrier mechanism might be operative in addition to carrier and channel mechanism in mediated ion transport across membranes.

REFERENCES

- [1] E. GRELL (ed.), «Membranes — A Series of Advances», vols. I-III, Marcel-Dekker, New York.
- [2] YU. A. OVCHINNIKOV, V.T. IVANOV, A.M. SHKROB, «Membrane Active Complexones», Elsevier, Amsterdam, 1974.
- [3] D.J. PATEL, A.E. TONELLI, *Biochemistry*, **12**, 486 (1973).
- [4] K.R.K. EASWARAN, in H. SIGEL, «Metal Ions in Biological Systems», vol. 19, chap. 5, Marcel Dekker, New York, 1984, in press.
- [5] M.B. SANKARAM, K.R.K. EASWARAN, *Biopolymers*, **21**, 1557 (1982).
- [6] M.B. SANKARAM, K.R.K. EASWARAN, *Int. J. Pept. Protein Res.* (1985), in press.
- [7] C.K. VISHWANATH, K.R.K. EASWARAN, *Biochemistry*, **21**, 2612 (1982).
- [8] S. DEVARAJAN, K.R.K. EASWARAN, *Biopolymers*, **20**, 891 (1981).
- [9] S. DEVARAJAN, K.R.K. EASWARAN, *Int. J. Pept. Protein Res.*, **23**, 324 (1984).
- [10] S. DEVARAJAN, K.R.K. EASWARAN, *J. Biosci.*, **6**, 1 (1984).
- [11] S. DEVARAJAN, C.M.K. NAIR, M. VIJAYAN, K.R.K. EASWARAN, *Nature*, **286**, 640 (1980).
- [12] J.H. PRESTEGARD, S.I. CHAN, *Biochemistry*, **8**, 3921 (1969).
- [13] J.H. PRESTEGARD, S.I. CHAN, *J. Am. Chem. Soc.*, **12**, 4440 (1970).
- [14] E. PRETCH, M. VASAK, M. SIMON, *Helv. Chim. Acta*, **55**, 1098 (1972).
- [15] C.K. VISHWANATH, K.R.K. EASWARAN, *Biochemistry*, **20**, 2018 (1981).
- [16] C.K. VISHWANATH, N. SHYAMALA, K.R.K. EASWARAN, M. VIJAYAN, *Acta Crystallogr.*, **C39**, 1640 (1983).
- [17] C. SHEN, D.J. PATEL, *Proc. Natl. Acad. Sci. USA*, **73**, 4277 (1976).
- [18] D.J. PATEL, C. SHEN, *Proc. Natl. Acad. Sci. USA*, **73**, 1796 (1976).

- [19] H. DEGANI, H.L. FRIEDMAN, *Biochemistry*, **13**, 5022 (1974).
 [20] S.R. ALPHA, A.H. BRADY, *J. Am. Chem. Soc.*, **95**, 7043 (1973).
 [21] B.P. SHASTRI, K.R.K. EASWARAN, *Int. J. Biol. Macromol.*, **6**, 219 (1984).
 [22] C.K. VISHWANATH, K.R.K. EASWARAN, *FEBS Lett.*, **153**, 320 (1982).
 [23] C.K. VISHWANATH, K.R.K. EASWARAN, *J. Chem. Soc., Perkin Trans. 2* (1984), in press.
 [24] B.P. SHASTRI, M.B. SANKARAM, K.R.K. EASWARAN, unpublished observations.



SL15 — TU

PETER J. SADLER

Department of Chemistry
 Birkbeck College, University of London
 Malet Street
 London WC1E 7HX
 U.K.

GOLD DRUGS

Current interest in the pharmacological use of gold compounds centres around the treatment of rheumatoid arthritis with either injectable gold(I) thiolates [1] or the orally-absorbed triethylphosphine gold(I) thiolate auranofin [2], and the possibility that gold compounds could become useful anti-cancer agents [3].

In recent studies we have made both kinetic and thermodynamic measurements of structural changes involving polymeric gold(I) thiomalate in solution [4]. We have examined its reducing activity, for example towards Fe(III) cytochrome *c*. The commercially available drug, "Myocrisin", does not appear to be a true 1:1 complex. A curious feature of Au(I) thiolate chemistry is the high stability of sulphur-bridged polymers and this may be of biological importance.

We have detected a mixed ligand complex on reaction of gold(I) thiomalate with cyanide [5]. Cyanide may even play a role in the natural meta-

bolism of gold (and some other metal ions?) and it is notable that $K[Au(CN)_2]$ exhibits significant antitumour activity [3].

The chemistry of gold compounds containing nitrogen ligands has received relatively little attention. We have prepared a new series of imido complexes of triethylphosphine gold(I) [6]. Through the use of X-ray crystallography, EXAFS and NMR spectroscopy of ^{15}N -labelled complexes they were shown to contain linear P-Au-N structures. The riboflavin complex appeared to be a rare example of an N_3 -coordinated metal flavin complex. All of the new complexes exhibited significant anti-inflammatory activity in the carrageenan-induced rat paw edema assay.

The curious ability of Et_3PAuCl and related complexes to induce spin-state transitions of a wide range of ferric haem proteins may be related to the binding of gold to active-site histidine residues [7].

Gold binding to *N* ligands is also of interest in connection with the anti-cancer activity of gold compounds. However, the chemistry of Au(III) complexes, which are isoelectronic ($5d^8$) and often isostructural (square-planar) with those of Pt(II), is much less well developed than that of Pt(II). We have gained an insight into *trans* effects and influences in triethylphosphine Au(III) imido complexes using ^{15}N -labelled imides [6].

We have used NMR methods to examine the conditions under which displacement of triethylphosphine from auranofin occurs both outside and inside cells [8].

Significant advances in our understanding of the chemistry, molecular biology and pharmacology of gold are now emerging, and it seems likely that these areas will receive increasing attention in the future.

REFERENCES

- [1] P.J. SADLER, *Struct. Bonding (Berlin)*, **29**, 171-219 (1976).
 [2] B.M. SUTTON, E. MCGUSTY, D.T. WALZ, M.J. DiMARTINO, *J. Med. Chem.*, **15**, 1095 (1972).
 [3] P.J. SADLER, M. NASR, V.L. NARAYANAN, «Platinum Coordination Complexes in Cancer Chemotherapy», Martinus Nijhoff Publishers, Boston, Massachusetts, 1984, pp. 290-304.
 [4] M.C. GROOTVELD, P.J. SADLER, *J. Inorg. Biochem.*, **19**, 51 (1983).

- [5] G. GRAHAM, J.R. BALES, M.C. GROOTVELD, P.J. SADLER, submitted for publication.
- [6] S.J. BERNERS PRICE, P.J. SADLER, R. KURODA, M.J. DiMARTINO, B.M. SUTTON, D.T. HILL, *Rev. Port. Quím.*, **27**, 397 (1985).
- [7] a) G. OTIKO, P.J. SADLER, *FEBS Lett.*, **116**, 227 (1980);
b) S.J. BERNERS PRICE, M.C. GROOTVELD, G. OTIKO, H.R. ROBBINS, P.J. SADLER, *Inorg. Chim. Acta*, **79**, 186 (1983).
- [8] M.T. RAZI, G. OTIKO, P.J. SADLER, *ACS Symposium Series*, **209**, 371 (1983).



SL16 — TU

ROBERT F. PASTERNAK

JUDITH HEMPEL

Department of Chemistry
Swarthmore College
Swarthmore, PA 19081
U.S.A.

Smith Kline & French Laboratories
Philadelphia, PA 19010
U.S.A.

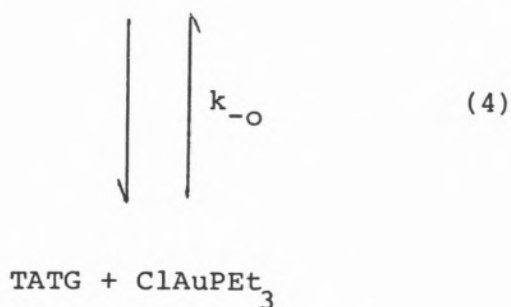
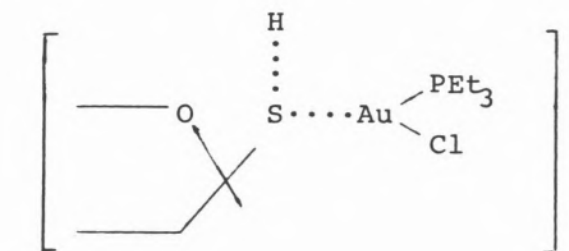
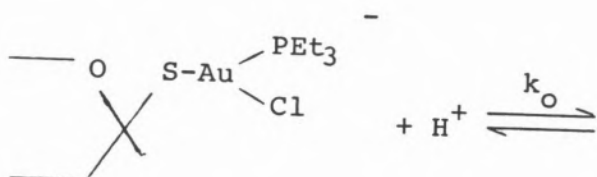
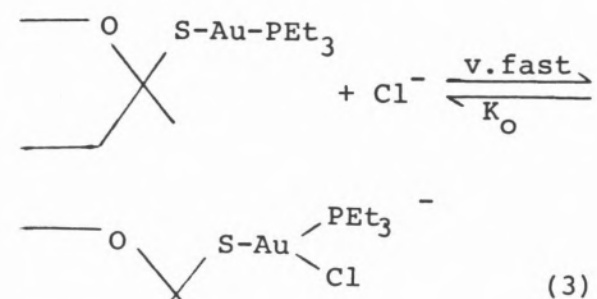
SOLUTION KINETICS OF A GOLD(I) BIOLOGICALLY ACTIVE COMPLEX

Auranofin((2,3,4,6-tetra-*O*-acetyl-1-thio- β -D-glucopyranosato-*S*)(triethylphosphine)gold(I)), an orally administered chrysotherapeutic agent, reacts with hydrochloric acid as shown below:



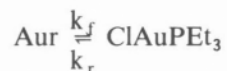
where TATG is tetraacetylthioglucose and S is a sulfonium ion with two gold centers ((2,3,4,6-tetra-*O*-acetyl-2- β -D-glucopyranosyl)bis-((triethylphosphine)aurio)sulfonium ion). The stability constants, for reactions (1) and (2) were determined at $\mu = 1.0$ M in water and methanol-water solvent systems via spectrophotometric titrations. In water at 37°C $K_1 = 4.6 \times 10^{-4}$ M⁻¹ and $K_2 = 2.0 \times 10^3$ while in a 50% by volume

methanol/water mixture, $K_1 = 7.8 \times 10^{-3}$ M⁻¹ and $K_2 = 1.3 \times 10^2$. Thus in a 50% methanol/water mixture, reaction (1) goes virtually to completion in 1.0 M Cl⁻ even for hydrogen ion concentrations as low as 0.1 M. The kinetics of this reaction as a function of [H⁺] and [Cl⁻] were studied using the stopped flow method. For the Cl⁻ dependence studies, the ionic strength was maintained at 1.0 M with NaClO₄. The pseudo-first order rate constant, k_{obs} , is linearly dependent on [H⁺] throughout the entire concentration range but the chloride profile shows saturation behavior. A mechanism consistent with our results is:



Then, $k_{\text{obs}} = \frac{k_o K_o [\text{H}^+][\text{Cl}^-]}{1 + K_o [\text{Cl}^-]}$. At 25°C $K_o = .30 \text{ M}^{-1}$
and $k_o = 1480 \text{ M}^{-1} \text{ s}^{-1}$.

Because the stability constant, K_1 , is smaller in water than in the mixed solvent system, reaction (1) does not proceed to completion in aqueous solution under the conditions of the kinetic experiments. To ensure first-order kinetic profiles, excess tetraacetylthioglucose was added to the reaction mixtures. Thus, for:



$k_{\text{obs}} = k_f + k_r$ and k_{obs} is a function of $[\text{H}^+]$, $[\text{Cl}^-]$ and $[\text{TATG}]$.

Stopped-flow experiments demonstrate that k_{obs} depends directly on each of these concentrations, *i.e.*, $k_{\text{obs}} = k_f [\text{H}^+][\text{Cl}^-] + k_r [\text{TATG}]$ so that a plot of $k_{\text{obs}}/[\text{TATG}]$ vs $[\text{H}^+][\text{Cl}^-]/[\text{TATG}]$ is linear. At 25°C, the slope of this line, $k_f = 210 \text{ M}^{-2} \text{ s}^{-1}$ and the intercept $k_r = 4.3 \times 10^5 \text{ M}^{-1} \text{ s}^{-1}$. From the activation parameters obtained in this medium, we can extrapolate these results to 37°C and obtain a kinetically derived equilibrium constant $K_1 = k_f/k_r = 4.5 \times 10^{-4} \text{ M}^{-1}$ in excellent agreement with the value obtained at this temperature via spectrophotometric titrations.



SL17 — WE

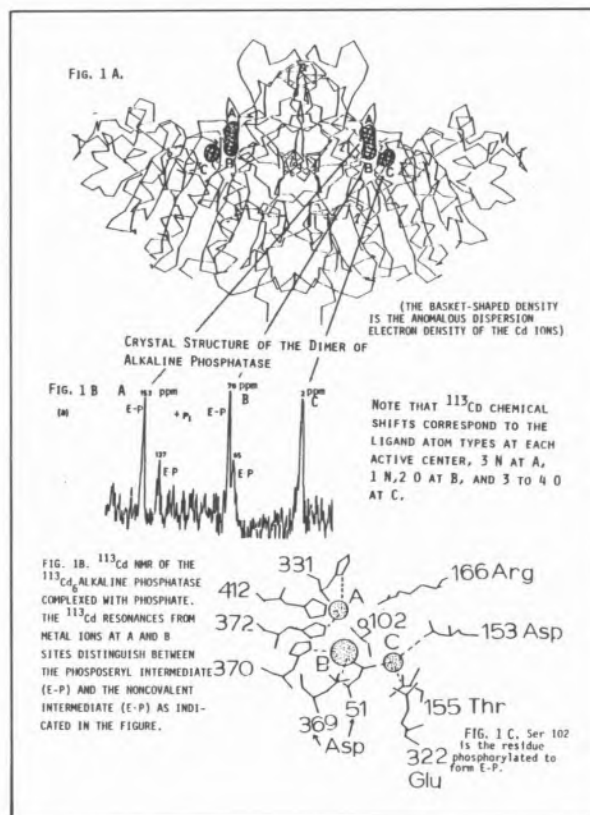
JOSEPH E. COLEMAN
PETER GETTINS
Yale University

**ALKALINE PHOSPHATASE: AN ENZYME
WITH MULTIPLE CATALYTIC METAL IONS
AT EACH ACTIVE CENTER:
 ^{31}P AND ^{113}Cd NMR IN SOLUTION
CORRELATED WITH THE CRYSTAL
STRUCTURE**

The alkaline phosphatases are Zn(II) metalloenzymes of great importance to mammalian physiology. These membrane-attached proteins participate in Ca(II) and HPO_4^{2-} uptake at the intestinal brush border, are essential for the formation of hydroxyapatite, and have less well determined functions in kidney and placenta. Although the molecular events that insert these enzymes (whose currently known function is the nonspecific hydrolysis of phosphate monoesters) into these complex processes are unknown, the periplasmic alkaline phosphatase from *E. coli* has proved to be a valid prototype for the catalytic domains of the more complex mammalian enzymes. These prototypic features include the Zn(II) ions and the formation of a phosphoserine intermediate.

The crystal structure of the dimer of alkaline phosphatase is shown in Fig. 1A and is constructed from the α -carbon backbone derived from the electron density map of the native $\text{Zn(II)}_4\text{Mg(II)}_2$ protein into which is embedded the electron density map of the 6 Cd(II) ions substituted in $\text{Cd(II)}_6\text{AP}$. The latter was determined from the anomalous dispersion of X-rays by Cd [1]. The three ^{113}Cd NMR signals, A, B and C from $^{113}\text{Cd(II)}_6\text{AP}$ in solution are shown in Fig. 1B. Each signal integrates to 2 Cd nuclei if the small upfield signals are included (see below). The assignments of A, B and C resonances to specific metal binding sites in the crystal structure is based

on ^{113}Cd chemical shift vs. ligand-type [2,4]. The detailed ligand structure taken from the electron density map is shown in Fig. 1C. The 153 ppm signal is assigned to the N,N,N site, the 70 ppm signal to the N,O,O site and the 2 ppm signal to the O,O,O site.



The reasons that a simple phosphomonoesterase requires 3 metal ions in a triad $3.9 \times 4.9 \times 7 \text{ \AA}$ at each active center have been only partially worked out. Studies with ^{31}P NMR show functions for A and B site metal ions, but a function for C remains unclear. The enzyme activity for both the Zn(II) and Cd(II) derivatives is unaffected by the absence of C site metal ion, but both A and B have profound effects on turnover rate. The chemical shift of the ^{113}Cd resonances from both A and B sites are changed by the shift from the phosphoserine intermediate (E-P) to the noncovalent phosphate intermediate (E·P). A small amount of E·P present in the $\text{Cd(II)}_6\text{AP}$ of Fig. 1B accounts for the upfield satellite signals. On the other hand, the signal from the C site which does not appear to participate directly in catalysis is not influenced by the $\text{E-P} \rightleftharpoons \text{E} \cdot \text{P}$ equilibrium.

^{31}P NMR of the Phosphoenzyme Intermediates

Typical ^{31}P NMR spectra of the phosphoenzyme intermediates formed by Zn and Cd alkaline phosphatases are shown in Fig. 2. For the Zn enzyme E-P resonates at 8.6 ppm, while $\text{E}\cdot\text{P}$ resonates at 4.2 ppm. Both resonate downfield from model compounds suggesting both intermediates to be distorted. The Cd substitution has little effect on the chemical shift of E-P ($\delta=8.4$ ppm), but a dramatic effect on the chemical shift of $\text{E}\cdot\text{P}$ ($\delta=13$ ppm) (Fig. 2). The $\text{E}\cdot\text{P}$ resonance at 13 ppm is a doublet and the phosphorous is thus coupled to one of the three Cd(II) ions at each active center. Heteronuclear decoupling at the A site ^{113}Cd resonance but not the B site resonance removes the coupling. Hence the phosphate of $\text{E}\cdot\text{P}$ is coordinated to the A site metal placing the phosphorous atom in a position to undergo nucleophilic attack by the seryl oxygen (Fig. 1C). The fact that the chemical shifts of E-P in both Zn and Cd enzymes are the same and the $\text{E}\cdot\text{P}$ ^{31}P NMR signal is not coupled, suggests that this intermediate is not coordinated to either A or B site metal ions.

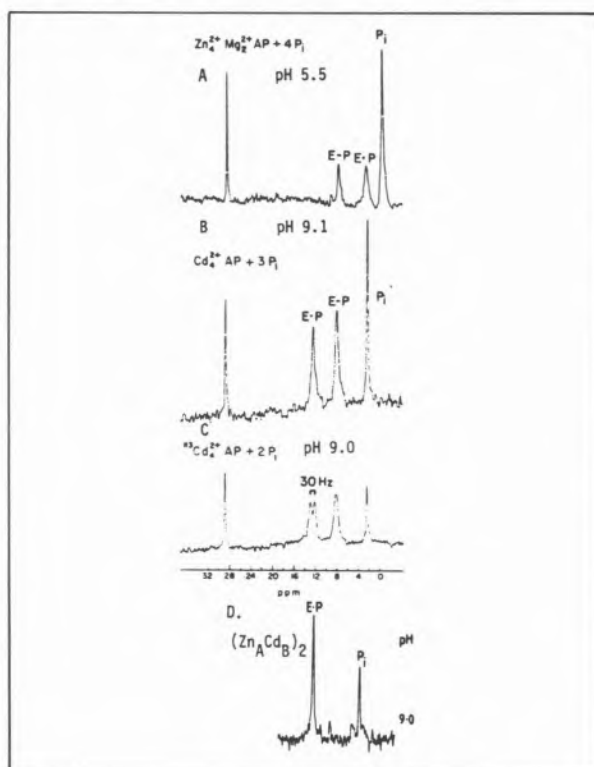


Fig. 2

^{31}P NMR of phosphoenzyme intermediates formed by Zn and Cd and hybrid alkaline phosphatases

While A site Cd(II) is coordinated to the phosphate of $\text{E}\cdot\text{P}$, it is surprising to find that the unusual downfield chemical shift of this intermediate is not due to the A site metal, but to the Cd(II) ion in B site. The ^{31}P spectrum of these intermediates in a $(\text{Zn}_A\text{Cd}_B)_2\text{AP}$ hybrid is shown in Fig. 2D. The $\text{E}\cdot\text{P}$ resonance is uncoupled, as expected since it is coordinated to Zn(II) in A site, but its chemical shift is still at 12.9 ppm reflecting a structure induced by the Cd(II) at B site. This Cd(II) has profound effects on the rate of turnover. With ^{31}P NMR it is possible to determine a detailed pH profile for the interconversion, $\text{E}\cdot\text{P} \rightleftharpoons \text{E}\cdot\text{P}$. The most striking finding is the shift in the pH where $[\text{E}\cdot\text{P}] = [\text{E}\cdot\text{P}]$ from pH 5.5 for the Zn enzyme to pH 8.5 for the Cd enzyme (nearly pH 10 if the Cd_2AP is used) [3]. We believe this dramatic shift reflects the pK_a of a solvent coordinated to A site when the phosphate has shifted to serine 102 to form $\text{E}\cdot\text{P}$. This solvent in its ionized ($\text{Zn}\text{-OH}$) form appears to be the nucleophile in the second step of the mechanism, the dephosphorylation of the phosphoserine group [3].

^{31}P transfer of magnetization and inversion transfer from P_i to the $\text{E}\cdot\text{P}$ show that dissociation of P_i from $\text{E}\cdot\text{P}$ is the slowest and rate-limiting step in the mechanism. This rate is dramatically influenced by the species of metal ion in B site and also by the binding of negatively charged anions to A site to form a five-coordinate intermediate involving both anion and phosphate coordination [3]. ^{113}Cd NMR shows that alcohols coordinate to A site metal ion, presumably as the alkoxides and compete with solvent in the second nucleophilic step producing the new ester in the transferase reaction. The comparison of multinuclear NMR in solution with the crystal structures of the same derivatives of alkaline phosphatase has allowed many conclusions about mechanism.

REFERENCES

- [1] H.W. WYCKOFF, M. HANDSCHUMACHER, H.M.K. MURTHY, J.M. SOWADSKI, *Adv. in Enzymol.*, **55**, 453-480 (1983).
- [2] J.E. COLEMAN, P. GETTINS, *Adv. in Enzymol.*, **55**, 381-452 (1983).
- [3] P. GETTINS, J.E. COLEMAN, *J. Biol. Chem.*, **259**, 4991-4997; **259**, 11036-11040 (1984).
- [4] I.M. ARMITAGE, J.E. OTVOS, in BERLINER, REUBEN (eds.), «Biological Mag. Res.», Plenum Press, 1982, p. 79-144.



SL18 — WE

SVEN LINDSKOG
 Department of Biochemistry
 University of Umeå
 S-90187 Umeå
 Sweden

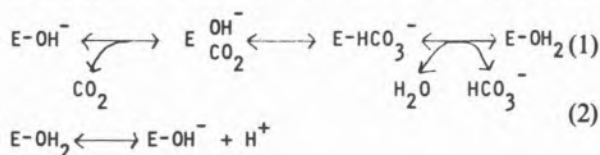
THE STRUCTURAL BASIS OF KINETIC DIFFERENCES BETWEEN CARBONIC ANHYDRASE ISOENZYMES

Mammals, birds, and reptiles have at least three genetically, immunologically, and kinetically distinct isoenzyme forms of the zinc-containing enzyme carbonic anhydrase catalyzing the reversible reaction, $\text{CO}_2 + \text{H}_2\text{O} \rightleftharpoons \text{HCO}_3^- + \text{H}^+$. Isoenzyme II (previously called C) occurs in the red blood cells and in many other tissues. It is one of the most efficient of all known enzymes with a CO_2 hydration turnover number of $1 \cdot 10^6 \text{ s}^{-1}$ at pH 9 and 25°C [1]. Isoenzyme I (or B) is found in the red blood cells of most mammals and in part of the alimentary canal. It is less efficient than isoenzyme II with a CO_2 hydration turnover number of about $2 \cdot 10^5 \text{ s}^{-1}$ at pH 9 and 25°C . Isoenzyme III occurs predominantly in red skeletal muscle. It has a low catalytic activity and CO_2 hydration turnover numbers of about $4 \cdot 10^3 \text{ s}^{-1}$ at 25°C have been estimated [2,3].

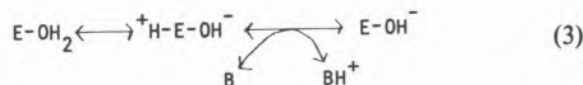
Isoenzymes I, II and III have homologous structures, and they have probably arisen by duplications of an ancestral carbonic anhydrase gene. The ligands of the zinc ion as well as several amino acid residues linked to the metal-ion center through hydrogen-bond networks are conserved in all sequenced carbonic anhydrases I, II and III [1]. Furthermore, the visible spectra of Co(II)-substituted isoenzymes I, II, and III are very similar [4]. These data indicate that the metal-ion centers have nearly identical structures in all three isoenzymes. Thus, although the metal-ion center is thought to be directly involved in the interconversion between CO_2 and HCO_3^- , the fine tuning of

the catalytic properties seems to depend on other features of the active sites. In particular, the amino acid side chains at sequence positions 64 and 200 might be important modifiers of catalytic behaviour. All sequenced type II isoenzymes have His-64 and Thr or Asn at position 200. All sequenced type I isoenzymes have histidine residues at both these positions. In fact, the presence of His-200 is the only unique feature distinguishing the active sites of isoenzymes I from those of isoenzymes II. The type III isoenzymes sequenced so far have Thr-200 and lysine or arginine at position 64 as well as additional basic residues, Arg-67 and Arg-91, in their active sites.

All known kinetic properties of the carbonic anhydrase isoenzymes fit with the idea that they have a common basic catalytic mechanism involving a $\text{CO}_2/\text{HCO}_3^-$ interconversion half reaction (eq. (1)) and a H^+ transfer half reaction (eq. (2)).



At least in isoenzymes I and II the H^+ transfer half reaction is complex presumably involving an intramolecular H^+ transfer between the metal-ion center and an amino acid side chain (His-64 in isoenzymes II and, probably, His-200 in isoenzymes I) and a subsequent H^+ transfer to buffer as indicated in eq. (3):



In the high-activity isoenzymes II $\text{CO}_2/\text{HCO}_3^-$ interconversion is very fast and at saturating substrate and buffer concentrations the intramolecular H^+ transfer step (eq. (3)) limits the rate of turnover. The most important kinetic difference between isoenzymes I and II is associated with $\text{CO}_2/\text{HCO}_3^-$ interconversion and is probably related to a stabilization of the E-HCO_3^- complex in isoenzymes I relative to isoenzymes II. This stabilization might be due to an interaction of zinc-coordinated HCO_3^- with His-200 [5]. Available kinetic data on the low-activity isoenzymes III [2,3] indicate that the maximal rate of CO_2 hydration is limited by the H^+ transfer half reaction just as in

the case of isoenzymes II. It seems that an efficient pathway for H^+ exchange between active site and reaction medium is missing. This is probably related to the absence of suitable «proton-transfer» groups in the active sites of isoenzymes III. Another important feature of isoenzymes III is that the pK_a of metal-bound H_2O appears to be well below 6 in contrast to isoenzymes I and II where the corresponding pK_a 's are near 7. This low pK_a in isoenzymes III is probably due to electrostatic interactions with the positively charged active-site residues at sequence positions 64, 67, and 91.

REFERENCES

- [1] S. LINDSKOG, in T.G. SPIRO (ed.), «Zinc Enzymes», Wiley, New York, 1983, pp. 78-121.
- [2] C. TU, G. SANYAL, G.C. WYNNS, D.N. SILVERMAN, *J. Biol. Chem.*, **258**, 8867-8871 (1983).
- [3] P. ENGBERG, E. MILLQVIST, G. POHL, S. LINDSKOG, in preparation.
- [4] P. ENGBERG, S. LINDSKOG, *FEBS Lett.*, **170**, 326-330 (1984).
- [5] I. SIMONSSON, B.-H. JONSSON, S. LINDSKOG, *Eur. J. Biochem.*, **129**, 165-169 (1982).



SL19 — WE

C. LUCHINAT
Department of Chemistry
University of Florence
Italy

A COMPARISON OF SOME pH-DEPENDENT PROPERTIES OF ZINC ENZYMES

Zinc enzymes are numerous, and more of them are being discovered. However, only relatively few are obtainable with an amount of effort and to a degree of purification to be of interest to chemists [1,2]. Zinc in zinc enzymes can be at the catalytic site, *i.e.* it can itself be involved in the catalytic

process, or can be buried into the protein and play a structural role. This kind of zinc will be no further treated here. The function of zinc at the catalytic site is essentially that of acting as a Lewis acid [3]. Despite this only role, zinc enzymes are capable of catalyzing several kinds of reactions like hydrations, redox reactions, hydrolytic processes, group transfer, polymerizations, etc.

Some zinc enzymes like carboxypeptidase A (CPA) and carbonic anhydrase (CA) are classical examples in enzymology. Besides them, liver alcohol dehydrogenase (LADH) and alkaline phosphatase (AP) will be also discussed here.

The donor atoms of catalytic zinc ions in enzymes are histidines (three in CA, two in CPA, three (?) in AP, one in LADH), carboxylate groups (one in CPA, one or two in AP), and cysteines (two in LADH). All of them contain at least one water (or hydroxide) molecule. A water molecule coordinated to the metal ion is an important acidic group, whose pK_a ranges from below 6 to well above 10-11. As inorganic chemists, we know that such pK_a will decrease with increasing the positive charge on the metal ion; the latter depends on the number and the nature of the ligands. Furthermore the pK_a depends on the solvent properties. The thermodynamic properties of «free» water in an active cavity surely play a role in determining the above pK_a , but more efforts aimed to the understanding of such role would be needed [4]. We have also related such pK_a with the presence of charged (positive or negative) groups into the cavity. The apparent anion binding affinity for the metal ion is also largely affected by the state of ionization of the coordinated water and by the presence of charged groups.

Understanding the overall acid-base behavior of the enzymes is crucial to the elucidation of the catalytic mechanism. The active species in CA, LADH, and AP are the hydroxo forms. In carbonic anhydrase the coordinated hydroxide attacks CO_2 and provides a bicarbonate adduct which essentially is released followed by a proton. In liver alcohol dehydrogenase OH^- is believed to accept a proton by the alcohol allowing an alcoholate species to bind the metal. Such intermediate eases the hydride transfer to the NAD^+ coenzyme; the release of the substrate occurs

through a five coordinate adduct with water as fifth ligand. In alkaline phosphatase it is proposed that a coordinated OH^- hydrolyzes the phosphoric ester with a serine residue, which is an earlier intermediate in the catalytic process. In carboxypeptidase, zinc binds the peptidic carbonyl oxygen, favoring the hydrolytic attack: it is not clear whether a water molecule is simultaneously bound and whether it has a role.

Spectroscopic evidences for the described properties are shown on cobalt(II) substituted derivatives.

REFERENCES

- [1] T.G. SPIRO (ed.), «Zinc Enzymes», John Wiley and Sons, New York, 1983.
- [2] H. SIGEL (ed.), «Zinc and Its Role in Biology and Nutrition», Marcel Dekker, New York, 1983.
- [3] R.J.P. WILLIAMS, *Pure Appl. Chem.*, **54**, 1889 (1982).
- [4] H. SIGEL, private communication.



SL20 — WE

MARVIN W. MAKINEN
GREGG B. WELLS
MOON B. YIM

Department of Biochemistry and Molecular Biology
The University of Chicago
Chicago, Illinois 60637
U.S.A.

MAGNETIC RESONANCE SPECTROSCOPY OF OXYGEN-17 TO PROBE THE ACTION OF METALLOENZYMES: LIVER ALCOHOL DEHYDROGENASE

The use of oxygen-17 as a spectroscopic probe of Co^{2+} -substituted metalloenzymes is discussed. Continuous wave, microwave power saturation studies of a variety of metalloprotein and small molecule complexes of paramagnetic metal ions

show that the value of the parameter $P_{1/2}$ (microwave power at which the saturation factor $(1 + \gamma^2 H_1^2 T_1 T_2)^{-1}$ equals 0.5) is sensitive to the presence of oxygen-17 enriched oxygen-donor ligands while no change is observed in the presence of oxygen-18 enriched ligands. Analysis of the results of pulse saturation and recovery experiments of high-spin metmyoglobin and methemoglobin in oxygen-17 enriched water shows that the influence of oxygen-17 results in a fast cross-relaxation event (T_{21}^*) that is comparable to the nuclear modulation effect seen in spin-echo spectroscopy. On the basis of the theory of cross-relaxation [1] and spectral diffusion [2], the saturation factor has the form $(1 + \gamma^2 H_1^2 T_2 / (1/T_1 + 1/T_{21}^*))^{-1}$. With oxygen-17 selectively incorporated into different ligands in the same metal ion complex it is seen that the change in $P_{1/2}$ is dependent upon geometrical relationships of metal-ligand bonding and the extent of metal-ligand covalency. Also, the influence of oxygen-17 is seen only in coordination complexes in which the isotopically enriched oxygen-donor ligand is in the inner coordination shell of the metal ion. Outer sphere oxygen-donor ligands do not have an influence on $P_{1/2}$. The effect has been observed thus far with high- and low-spin Fe^{3+} -heme complexes, Co^{2+} -substituted metalloenzymes and small molecule coordination complexes, as well as in polycrystalline $\text{K}(\text{Cr})\text{Al}(\text{SO}_4)_2 \cdot 12 \text{H}_2\text{O}$. These results, thus, indicate that the effect is not dependent upon the electronic ground state or the presence of a nuclear moment associated with the paramagnetic metal ion. Because the effect is observable with standard EPR spectrometers (in our laboratory an X-band Bruker ER 200D equipped with an Oxford Instruments ESR10 cryostat), the method of continuous wave, microwave power saturation can be readily applied to investigate the immediate donor-ligand atom environment of paramagnetic metal ions in metalloenzymes and proteins. Investigations of a variety of binary and ternary complexes of active-site specific Co^{2+} -substituted horse-liver alcohol dehydrogenase (COLADH) [3] have been carried out to assign the coordination number of the metal ion with use of oxygen-17 enriched ligands as spectroscopic probes. No influence of oxygen-17 enriched H_2O is observed in the CoLADH-(trifluoroethanol), CoLADH-NADH-4-(N,N-dimethylamino)-cinnamaldehyde

complex at pH 9, or in the corresponding aldehyde complex formed with the inhibitor 1,4,5,6-tetrahydro-NADH formed at neutral pH, in general agreement with expectations based on X-ray crystallographic studies. Experiments with a variety of ternary inhibitor or substrate complexes of CoLADH-NAD⁺ and CoLADH-NADH in the presence of oxygen-17 enriched water show clear evidence for metal-coordinated H₂O, indicating a penta-coordinated ligand configuration of the active site metal ion. The results confirm our earlier suggestions [4,5] that the catalytically competent environment of the active site metal ion of this enzyme in ternary enzyme-coenzyme-substrate complexes requires the participation of a metal-bound molecule. The results of these studies will be discussed in light of our previous proposal [4-6] for the mechanism of action of liver alcohol dehydrogenase.

REFERENCES

- [1] N. BLOEMBERGEN, S. SHAPIRO, P.S. PERSHAN, J.O. ARTMAN, *Phys. Rev.*, **114**, 445 (1959).
- [2] A. KIEL, *Phys. Rev.*, **125**, 1451 (1962).
- [3] W. MARET, I. ANDERSSON, H. DIETRICH, H. SCHNEIDER-BERNLÖHR, R. EINARSSON, M. ZEPPEZAUER, *Eur. J. Biochem.*, **98**, 501 (1979).
- [4] M.W. MAKINEN, M.B. YIM, *Proc. Natl. Acad. Sci. USA*, **78**, 6221 (1981).
- [5] M.W. MAKINEN, W. MARET, M.B. YIM, *Proc. Natl. Acad. Sci. USA*, **80**, 2584 (1983).
- [6] W. MARET, M.W. MAKINEN, submitted for publication.



SL21 — WE

MICHAEL ZEPPEZAUER

Fachbereich 15
Analytische und Biologische Chemie
Universität des Saarlandes
D-6600 Saarbrücken
F.R.G.

STRUCTURAL MODULATIONS OF THE CATALYTIC METAL BINDING SITE IN LIVER ALCOHOL DEHYDROGENASE DUE TO LOCAL AND GLOBAL CHANGES OF PROTEIN CONFORMATION DURING THE CATALYTIC CYCLE

The structural flexibility of the catalytic metal binding site of LADH in different phases of the catalytic cycle has been probed by spectroscopic techniques such as EPR-, Mössbauer-, NMR- and optical spectroscopy both in equilibrium and in short-lived, transitory states. As chemical probes, various metal ion species were used to replace the catalytic zinc ion in the active site, e.g. Co(II), Cu(II), Fe(II), Fe(III). The spectroscopic properties of these metal ions are changed in two ways, first by the coenzyme-induced transition of the protein structure from the open to the closed conformation, secondly by local rearrangements of the catalytic site due to charge compensations following the binding of negatively charged metal ligands, including substrate in the form of alcoxide anions. These changes have been used to analyse equilibria as well as temperature- and time-dependent transitions between the conformational and/or differently liganded states of the protein.



SL22 — WE

DAVID F. BLAIR
STEPHAN N. WITT
SUNNEY I. CHAN
Arthur Amos Noyes Laboratory
California Institute of Technology
Pasadena, California 91125
U.S.A.

THE MECHANISM OF DIOXYGEN REDUCTION BY CYTOCHROME *c* OXIDASE

The mechanism of dioxygen reduction by cytochrome *c* oxidase has been the subject of intensive investigation. Conventional spectroscopic approaches cannot be used to study the intermediates formed during the dioxygen reduction reaction under physiological conditions because the reaction is very rapid: the bimolecular rate constant for the combination of dioxygen with the enzyme is $8 \times 10^6 \text{ M}^{-1} \text{ s}^{-1}$ at room temperature and most of the intramolecular electron transfers which ensue take place within a millisecond. However, the reaction may be slowed by going to lower temperatures (160-200 K). A technique for studying the cytochrome oxidase, dioxygen reaction at low temperatures, was developed in 1975 by B. CHANCE *et al.* [1]. This method, which is called the «triple trapping» technique, involves the inhibition of the enzyme with carbon monoxide and subsequent initiation of the reaction with dioxygen by photolysis of the CO adduct at low temperature. We have examined the reaction of cytochrome *c* oxidase with dioxygen using a modification of the triple trapping technique in conjunction with EPR spectroscopy. The investigation has been extended to a broader temperature range than previous studies, and several new reaction steps have been resolved. Where possible, the temperature dependences of the rates of individual steps have been measured. Both the low potential sites (Fe_a and Cu_A) and the dioxygen reduction

site (Fe_{a_3} and Cu_B) have been monitored simultaneously, enabling clarification of the relationship between the electron transfers to the dioxygen reduction site and the events which occur there. The evidence indicates that there are two intermediates at the three-electron level of dioxygen reduction, only the first of which is EPR-detectable. The conversion between these two intermediates, which probably corresponds to the breaking of the dioxygen bond, exhibits a distribution of activation enthalpies which peaks at $18.1 \pm 1.6 \text{ kcal mol}^{-1}$. Assuming a preexponential factor of 10^{13} , the corresponding activation entropy is $21.4 \pm 8.2 \text{ cal mol}^{-1} \text{ K}^{-1}$, indicating that this process is strongly promoted by entropic factors. Experiments using enzyme reduced by only three electrons confirm the existence of two different three-electron intermediates. These experiments also indicate that the rate of electron transfer from Fe_a to the $\text{Fe}_{a_3}/\text{Cu}_B$ site depends upon the nature of the intermediate of dioxygen reduction which is present at the latter site. Finally, we have obtained evidence that one of the three-electron intermediates of dioxygen reduction, probably a ferryl ion, can react with carbon monoxide at low temperature (211K) to produce CO_2 and a partially reduced enzyme species. These results are discussed in terms of the electron transfer pathways within the enzyme and its mechanisms of dioxygen reduction and energy conservation.

REFERENCES

- [1] B. CHANCE, C. SARONIO, J.S. LEIGH, *J. Biol. Chem.*, **250**, 9226 (1975).



SL23 — WE

J.A. FEE
 T. YOSHIDA
 B. ZIMMERMAN
 D. KUILA
 W.R. RANGER
 Biophysics Research Division
 The University of Michigan
 Ann Arbor, Michigan 48109
 U.S.A.
 and Isotope and Nuclear Chemistry Division
 Los Alamos National Laboratory
 Los Alamos, New Mexico 87545
 U.S.A.

PROGRESS IN THE CHARACTERIZATION OF *THERMUS* RESPIRATORY PROTEINS

We have been purifying and characterizing respiratory proteins from the extremely thermophilic aerobe, *Thermus thermophilus*.

Cytochrome c_1aa_3

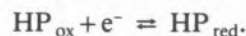
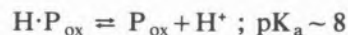
We have used the spectral properties of the tightly bound cytochrome c , as an indicator of the redox state of the components of cytochrome, aa_3 in reductive, oxidative and potentiometric titrations. During the latter, we assume all redox components are in equilibrium with the mediators: At pH 7.8 cytochrome c_1 has $E_m = 205$ mV ($n=1$), Cu_A has $E_m = 265$ mV ($n=1$), cytochrome a has $E_m = 270$ mV ($n=1$ and 60% spectral contribution at 605 nm), and cytochrome a_3/Cu_B has $E_m \sim 360$ mV ($n=2$ and 40% spectral contribution at 605 nm). Reductive and oxidative titrations are consistent with an equilibration between cytochrome c_1 , cytochrome a and Cu_A but not between cytochrome a and the cytochrome a_3/Cu_B pair. These observations are consistent with a conformational change controlling electron transfer between c_1 , a , Cu_A redox components and the a_3/Cu_B pair.

When hydrogen peroxide is added to cytochrome c_1aa_3 a difference optical spectrum (oxidized + peroxide minus oxidized) is observed with a trough at 413 nm and a peak at 433 nm ($\Delta E = 27$ mM⁻¹ cm⁻¹) and peaks at 606 nm and 580 nm. Others have observed similar changes

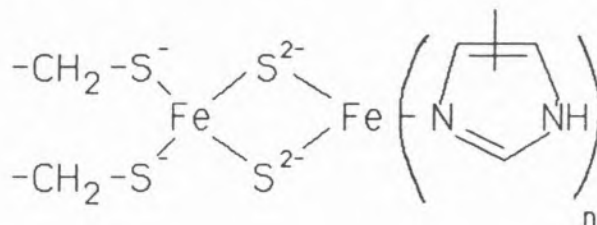
with bovine cytochrome aa_3 , suggesting that the two enzymes form similar complexes. The reaction with peroxide is slow (4.2 hr⁻¹ at 50 μ M H₂O₂), and appears to be reversed by incubation with catalase (0.35 hr⁻¹). We find no difference between the EPR spectra of oxidized and peroxy enzymes. Drs. T.A. Kent and E. Münck have recorded the Mössbauer spectrum of ⁵⁷Fe enriched peroxy complex and have found no apparent changes from the «preparation II» type spectrum. Ethyl peroxide and *t*-butyl peroxide also form complexes with cytochrome c_1aa_3 having similar spectral properties. The following dissociation constants have been measured at pH 7.8 and 25°C: = 0.5 μ M(HOOH), = 30 μ M(EtOOH), = 4 mM(*t*-BuOOH). Our results suggest that peroxides react with the cytochrome a_3 to form a complex having electronic properties very similar to those of the resting protein; an end-on complex would be consistent with our data.

Rieske Fe/S Protein

The redox potential has been measured in the pH range 6.7 to 9.2. Below pH 8, E_m is constant and equal to ~ 150 mV while above pH 8 E_m decreases ~ 60 mV/unit pH. A reversible effect of pH on the optical spectrum of oxidized protein was found and shown to be determined by an ionizing group with $pK_a \sim 8$. These observations are consistent with the following equilibria associated with the [2Fe-2S] clusters of Rieske protein:



Previous work suggested that each [2Fe-2S] cluster of Rieske protein was coordinated by only two cysteine residues. Working in collaboration with Drs. John F. Cline and Brian Hoffman it has been found that the cluster is coordinated to ¹⁴N containing ligands, and we speculate here that the structure of the Rieske cluster is



with one of the coordinating imidazole rings ionizing with $pK_a \sim 8$.

Cytochrome *o*

An additional cytochrome *c* oxidase has been purified from *Thermus* membranes. The enzyme consists of two subunits, ~ 18 and ~ 37 KD, in a 1:1 ratio and one B-type heme per molecule; no other metals are present at significant levels. The spectral properties of the enzyme are characteristic of cytochrome *o* as found previously by others. Thus, the CO compound of the reduced protein difference spectrum (CO + reduced *minus* reduced) shows a trough at 434 nm and a peak at 419 nm.

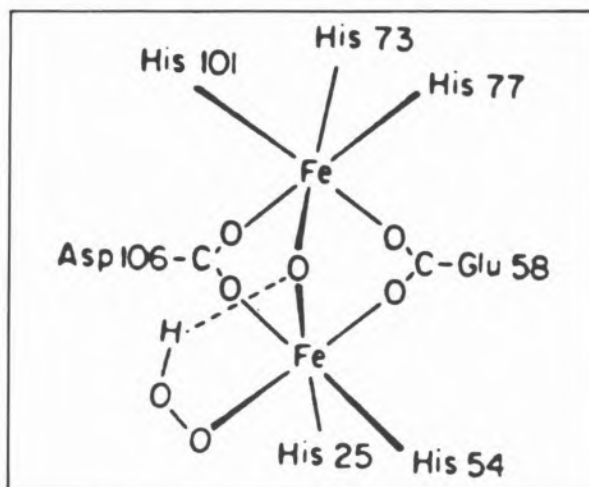


Fig. 1

Proposed structure for the binuclear iron center of oxyhemerythrin



SL24 — WE

JOANN SANDERS-LOEHR

Department of Chemical, Biological, and Environmental Sciences
Oregon Graduate Center
Beaverton, Oregon 97006
U.S.A.

OXYGEN BINDING TO THE BINUCLEAR CENTER OF HEMERYTHRIN

Hemerythrin is the non-heme iron respiratory protein of several marine invertebrates. In binding oxygen it cycles from ferrous deoxyhemerythrin to ferric oxyhemerythrin with a concomitant reduction of oxygen to peroxide [1]. In the 2.0 Å resolution crystal structure of the irreversibly oxidized (ferric) methemerythrin [2], the two active-site iron atoms are located in an α -helical framework and coordinated to histidyl and carboxylate residues (Fig. 1). The irons of the confacial biocuboctahedron are bridged by two protein carboxylates and an oxo group derived from solvent. The existence of a μ -oxo-bridged binuclear iron center in oxy- and methemerythrin was originally proposed on the basis of the strong antiferromagnetic cou-

pling ($-J \approx 100 \text{ cm}^{-1}$) of the iron atoms and the high intensity of the absorption bands in the electronic spectrum [1]. More recent confirmation of the presence of a bridging oxo group has come from X-ray absorption and resonance Raman spectroscopy. The best fits of the EXAFS data reveal a short Fe-O bond at 1.8 Å which is characteristic of an Fe-O-Fe moiety [3,4]. In the resonance Raman spectra a strongly enhanced peak at $\sim 500 \text{ cm}^{-1}$ is assigned to the symmetric stretch of an Fe-O-Fe group on the basis of its $\sim 15 \text{ cm}^{-1}$ shift to lower energy when the oxo bridge is isotopically substituted with ^{18}O [5,6].

The chemistry of the oxygen binding reaction has been a subject of intense interest. The bound dioxygen in oxyhemerythrin has been unambiguously identified as peroxide from the observation of the O-O stretching vibration at 844 cm^{-1} [5]. The actual location of the peroxide ion has been more difficult to determine due to the tendency of oxyhemerythrin crystals to auto-oxidize. In the crystal structure of azidomethemerythrin, the exogenous azide ligand is clearly bound end-on to the His-25-ligated iron atom [2]. A comparison of the EXAFS behavior of oxyhemerythrin and azidomethemerythrin shows that the two forms contain the same number and types of iron ligands, leading to the prediction that peroxide is bound in the same manner as azide [3]. Crystallographic studies on oxyhemerythrin (partial O_2 occupancy) confirm this interpretation [7]. Difference electron density maps of oxyhemerythrin

minus methemerythrin at 2.2 Å resolution (Fig. 2b) reveal positive electron density attributable to peroxide in a region similar to the positive electron density of azide in the azidomethemerythrin minus methemerythrin maps (Fig. 2a). The region of negative electron density in both of the difference maps represents the position of the lower iron atom in methemerythrin (which lacks an exo-

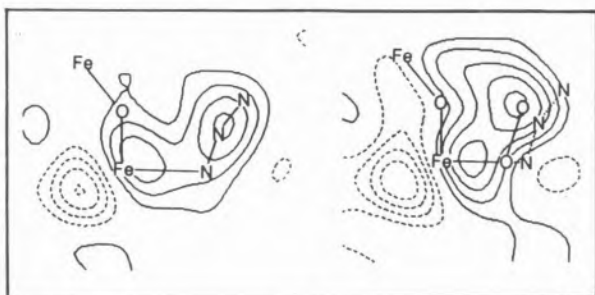


Fig. 2

Difference electron density maps in the $O(\mu\text{-oxo})\text{-Fe-N}(\text{azide})$ plane at 2.2 Å resolution [7]. Positive density (—), negative density (-----). Left: azidomethemerythrin minus methemerythrin. Atom positions from the 2.0 Å resolution refinement of azidomethemerythrin projected onto the $O\text{-Fe-N}$ plane. Right: oxyhemerythrin minus methemerythrin. Atom positions for peroxide estimated from present map.

ogenous ligand). The binding of either peroxide or azide causes a movement of this iron atom in the direction of the ligand. The most notable difference between the peroxide and azide maps is that the peroxide electron density is shifted somewhat towards the Fe-Fe axis relative to azide.

Since the peroxide appears to be coordinated in an end-on fashion in oxyhemerythrin, it is likely to be protonated. Support for this proposition comes from the deuterium isotope dependence of the peroxide stretching vibrations [6]. The O-O stretch of oxyhemerythrin at 844 shifts to 848 cm^{-1} in D_2O , while the Fe-O stretch shifts from 503 to 500 cm^{-1} in D_2O . The corresponding N-N and Fe-N vibrations of azidomethemerythrin are totally unaffected by D_2O . Thus, the deuterium isotope effects seem to be related to peroxide binding rather than to changes in protein structure. Furthermore, the 4 cm^{-1} increase in $\nu(\text{O-O})$ is unexpected for an increase in mass and is most likely due to electronic or structural changes accompanying deuteration. A model which accounts for the unusual isotope dependence as well as the unusually low frequency of the Fe-O-Fe vibration (486 cm^{-1} in oxyhemerythrin

versus $\sim 515 \text{ cm}^{-1}$ in the methemerythrin) and the location of the peroxide electron density relative to that of azide is one in which the hydroperoxide ligand is hydrogen-bonded to the $\mu\text{-oxo}$ bridge (Fig. 1). Another example of anomalous deuterium isotope behavior occurs in hydroxomethemerythrin. In this case, the shift in $\nu(\text{Fe-O-Fe})$ from 492 in H_2O to 517 cm^{-1} in D_2O may also be due to a hydrogen bond between the bound hydroxide and the $\mu\text{-oxo}$ bridge.

REFERENCES

- [1] J. SANDERS-LOEHR, T.M. LOEHR, *Adv. Inorg. Biochem.*, **1**, 235 (1979).
- [2] R.E. STENKAMP, L.C. SIEKER, L.H. JENSEN, *J. Am. Chem. Soc.*, **106**, 618 (1984).
- [3] W.T. ELAM, E.A. STERN, J.D. MCCALLUM, J. SANDERS-LOEHR, *J. Am. Chem. Soc.*, **104**, 6369 (1982).
- [4] W.A. HENDRICKSON, M.S. CO, J.L. SMITH, K.O. HODGSON, G.L. KLIPPENSTEIN, *Proc. Natl. Acad. Sci. USA*, **79**, 6255 (1982).
- [5] D.M. KURTZ, D.F. SHRIVER, I.M. KLOTZ, *Coord. Chem. Rev.*, **24**, 145 (1977).
- [6] A.K. SHIEMKE, T.M. LOEHR, J. SANDERS-LOEHR, *J. Am. Chem. Soc.*, **106**, 4951 (1984).
- [7] R.E. STENKAMP, L.C. SIEKER, L.H. JENSEN, J. MCCALLUM, J. SANDERS-LOEHR, *Proc. Natl. Acad. Sci. USA*, **82**, 713 (1985).



SL25 — WE

W.G.J. HOL

A. VOLBEDA

Laboratory of Chemical Physics
University of Groningen
Nijenborgh 16 9747 AG Groningen
The Netherlands

THE STRUCTURE OF THE COPPER-CONTAINING OXYGEN-TRANSPORTING HEMOCYANINS FROM ARTHROPODS

Hemocyanins are the large, non-heme, copper-containing oxygen-transport molecules occurring in the hemolymph of a large number of invertebrate species. The class of molluscan hemocyanins

consists of cylindrical molecules with subunits of molecular weight ~ 400.000 yielding total molecular weights of up to 10 million. Arthropodan hemocyanins, on the other hand, consist of hexamers, and usually multi-hexamers with subunits of molecular weight ~ 75.000 with total molecular weights between 0.5 and 4 million (For Reviews see refs. [1,2,3]).

The first X-ray structure of a hemocyanin molecule has been determined in our laboratory. It is the hemocyanin of the spiny lobster, *Panulirus interruptus*, an arthropod. It is a single-hexamer hemocyanin and therefore one of the smallest hemocyanins known, but the structure to be solved was still a particle with a molecular weight of about ~ 450.000 . Concurrently with the X-ray investigation, the amino acid sequence determination of this hemocyanin was carried out by the group of BEINTEMA at the University of Groningen. About 90% of the sequence has been determined presently.

The structure of *Panulirus interruptus* was elucidated at 3.2 Å resolution using crystals grown at pH 4.5 at low salt concentrations [4]. The entire hexamer was contained in the asymmetric unit. Therefore the initial isomorphous replacement phases, which yielded a rather poor electron density map, could be improved enormously by molecular averaging and phase extension techniques. The ultimate 3.2 Å map gave a clear picture of the course of the polypeptide chain, the position of the two copper ions in each subunit, the three disulfide bridges and the single carbohydrate moiety [5].

Panulirus interruptus hemocyanin can be considered as a trimer of dimers, rather than as a dimer of trimers, because the dimer contacts are more extensive, and evolutionarily better conserved than the contacts between trimers [6]. The point group symmetry of the hexamer is 32 [4].

The individual subunits of this arthropodan hemocyanin consist of three distinct domains (Fig. 1). The first domain comprises ~ 180 residues and is virtually all-helical. The single carbohydrate moiety is covalently attached to residue Asn-169 which is part of a β -strand. The second domain, consisting of ~ 220 residues, is also mainly helical but contains two 2-stranded anti-parallel β -sheets. In the centre of this domain

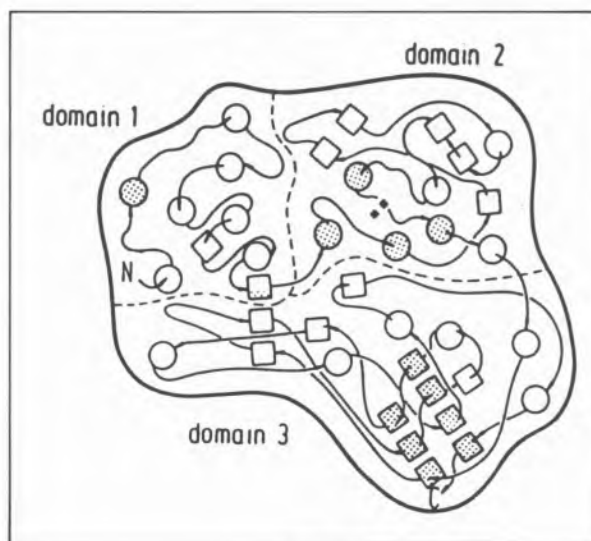


Fig. 1

Schematic drawing of the course of the polypeptide chain in a single subunit of *Panulirus hemocyanin*. Circles represent helices, squares β -strands. The small black squares are the copper positions. The three domains are separated by dashed lines. The dotted helix in domain 1 is absent in cheliceratan hemocyanins. The dotted helices in domain 2 provide the six copper ligands. The dotted β -strands in domain 3 correspond closely in structure with β -barrels of immunoglobulins and Cu,Zn superoxide dismutase

the binuclear copper site is located. Each copper is liganded by three histidine residues, two of which are provided by residues one turn apart in the same α -helix (Fig. 2). The distance between the copper positions is 3.8 ± 0.4 Å. The electron density map provides no evidence for a bridging protein ligand, but at the current resolution the possibility of a small exogenous ligand cannot be excluded.

The third domain contains ~ 260 residues and consists of a central anti-parallel β -barrel surrounded by a number of long loops containing helices and anti-parallel $\beta\beta$ -units (Fig. 1). An unexpected discovery was the identical topology of this β -barrel with those found in the immunoglobulins and in Cu,Zn superoxide dismutase [5].

In a recent study, the available amino acid sequence information from seven different species has been compared with each other and with the three-dimensional structure of *Panulirus hemocyanin* [6]. It appears that the *Panulirus hemocyanin* architecture is common to all arthropodan hemocyanins, but one helix in the first domain is absent in one class of arthropods. It also appears that

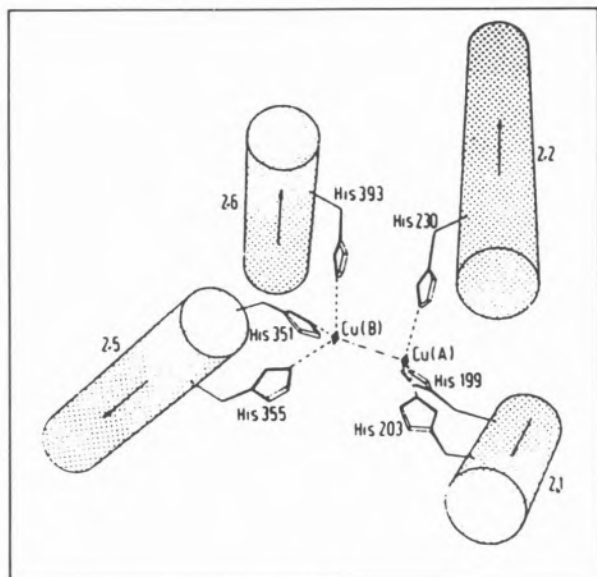


Fig. 2

Schematic representation of the binuclear copper site in arthropodan hemocyanins. The first (2.1), second (2.2), fifth (2.5) and sixth (2.6) helices of the second domain provide the six histidine ligands

the second domain is most conserved during evolution. Further, it seems that no conserved tyrosine occurs in the second domain which could serve as a bridging ligand in either the oxygenated or deoxygenated form of the molecule as is proposed by several investigators.

REFERENCES

- [1] K.F. VAN HOLDE, K.I. MILLER, *Rev. Biophys.*, **15**, 1 (1982).
- [2] H.D. ELLERTON *et al.*, *Progr. Biophys. Molec. Biol.*, **41**, 143 (1983).
- [3] E.F.J. VAN BRUGGEN *et al.*, in M. HARRIS (eds.), «Electron Microscopy of Proteins», vol. 1, Academic Press, New York, 1981, pp. 1-38.
- [4] E.J.M. VAN SCHAICK, W.G. SCHUTTER, W.P. GAYKEMA, A.M.H. SCHEPMAN, W.G.J. HOL, *J. Mol. Biol.*, **158**, 457 (1982).
- [5] W.P.J. GAYKEMA, W.G.J. HOL, J.M. VEREIJKEN, N.M. SOETER, H.J. BAK, J.J. BEINTEMA, *Nature*, **309**, 23 (1984).
- [6] B. LINZEN *et al.*, submitted for publication.



SL26 — WE

A.J. THOMSON
C.P. BARRETT
J. PETERSON
C. GREENWOOD

Schools of Chemical and Biological Sciences
University of East Anglia
Norwich NR4 7TJ
U.K.

OPTICAL DETECTION OF PARAMAGNETIC RESONANCE BY MAGNETIC CIRCULAR DICHROISM. APPLICATIONS TO METALLOPROTEINS

The intensity of the magnetic circular dichroism (MCD) spectrum of a paramagnetic molecule is inversely proportional to the spin temperature, T_s , at liquid helium temperature. Irradiation of the sample with a microwave field of constant frequency will, if resonance occurs, raise the spin temperature. This is detected by a change in the intensity of the MCD signal. Thus it is possible to measure paramagnetic resonance by optical detection (PROD) using MCD spectroscopy. This is a form of optical double magnetic resonance (ODMR) which appears not to have been carried out on proteins before. We have constructed a microwave cavity with optical access to enable the MCD spectrum of a frozen, aqueous metalloprotein solution to be measured in a microwave field in the Q-band (35 GHz) frequency range. The PROD spectra of some simple copper(II) complexes are discussed. Results have also been obtained for the copper(II) ion in the blue protein azurin as well as for Cu_2^* in mammalian cytochrome *c* oxidase. A comparison between these two centres will be made. The PROD spectrum enables the relative orientations of the ground state *g*-tensor and the optical transition-moment tensors to be determined. In this way useful information about the angular distribution of ligands about a central metal ion in an isotropic solution of a metalloprotein appears to be available. This may provide a complementary technique to that of EXAFS which, by contrast, provides no angular information.



SL27 — TH

I. PECHT
O. FARVER
A. LICHT

Department of Chemical Immunology
Rehovot 76100
Israel

ELECTRON TRANSFER PATHWAYS IN BLUE COPPER PROTEINS

Electron transfer reactions play a central role in biological energy conversion processes. The mechanisms employed by the different protein elements of these systems are now being examined at the resolution of amino acid residues involved in the reactions. Thus, specific loci on the protein's surface involved in electron-transfer and the media separating them from the metal ion active centers are investigated [1,2]. An affinity labeling procedure for such loci has been developed, taking advantage of the chemical properties of the Cr(II)/(III) couple: While Cr(II) ions are exceptionally strong reductants and exchange their ligands very fast, the Cr(III) ion exchanges its ligands rather slowly [3]. Thus, Cr(II) can coordinate to one or more amino acid residues of the protein while transferring to its active center an electron. Upon oxidation to Cr(III), it maintains the same liganding residue(s) in its coordination sphere. Hence identification of the attachment site of the Cr(III) may provide information about the electron transfer locus. The Cr(III) binding sites are determined primarily by proteolytic cleavage of the different labeled proteins [4-7]. In some cases spectroscopic methods have been useful in corroborating these assignments [8].

Several copper proteins have been examined by the above approach. These include: The blue copper containing electron carrier proteins — azurins from several bacteria (*Ps. aeruginosa* [4] and *Alc. Faecalis*). Plastocyanin (French bean) the electron mediator of the photosynthetic apparatus

[5]. Stellacyanin [6] and the oxidase laccase isolated from the Japanese lacquer tree (*Rhus vernici-fera*). Our prime interest focused on the spatial relation between the copper site and the locus of Cr(III) labeling and predominantly on the role of the labelled regions in the functions of the examined proteins.

In *Ps. azurin*, Cr(III) labeling of the neighborhood of His-35 imidazole has been found [4]. This amino acid residue has been implicated earlier in the electron-transfer function of the protein. Even anionic inorganic redox partners seem to react at this region [8]. In stellacyanin, the site of the single Cr(III) bound to the protein is currently being identified.

The cuprous ions in the Cr(III) labeled plastocyanin, azurin and stellacyanin can be fully reoxidized by inorganic or enzymatic agents without any loss of the bound chromium. The single and the same Cr(III) ion originally coordinated to azurin and stellacyanin remains bound through several Cr(II) reduction and reoxidation cycles. In contrast, one can label plastocyanin (French bean) with several Cr(III) ions by repeated redox cycles. As illustrated in the table up to 6.0 Cr(III) ions can be bound to one plastocyanin molecule in seven reduction steps. Reoxidation has been attained in these cycles with Co(III) dipicolinate and analysis of the protein's copper content established the stoichiometry.

Cr(II) Labeling Upon Multiple Reduction-Oxidation Titrations of Pc

TITR.	I	II	III	IV	V	VI	VII
Cr/Pc	0.89	1.7	2.5	3.5	4.4	5.2	6.0

The numbers represent moles of Cr(II) bound to plastocyanin after each cycle (Roman numbers).

The labeled proteins now carry the Cr(III) modification on their surface. To examine the physiological significance of the labeled sites, the reactivities of native and singly Cr(III) labeled forms of azurin and plastocyanin were compared. It became apparent that the Cr(III) label attenuated the reactivity of both azurin and plastocyanin [9,10] with only one of their respective two partners. This led to the conclusions that on both proteins:

a) There are probably two distinct and physiologically operative electron transfer sites. b) One of these sites is centered around the respective Cr(III) labeled region. c) By elimination, the second is at the exposed, homologous imidazole of His-87 or 117 in Pc and Az, respectively.

REFERENCES

- [1] O. FARVER, I. PECHT, in R. LONTIE (ed.), «Copper Proteins and Copper Enzymes», CRC Press, vol. 1, 1983, pp. 187-214.
- [2] R.A. MARCUS, N. SUTIN, *Biochim. Biophys. Acta* (1985), in press.
- [3] H. TAUBE, *Science*, **226**, 1028-1036 (1984).
- [4] O. FARVER, I. PECHT, *Isr. J. Chem.*, **21**, 13-17 (1981).
- [5] O. FARVER, I. PECHT, *Proc. Natl. Acad. Sci. USA*, **78**, 4190-4193 (1981).
- [6] G. MORPURGO, I. PECHT, *Biochem. Biophys. Res. Commun.*, **104**, 1592-1596 (1982).
- [7] G.Q. JONES, M.T. WILSON, *J. Inorg. Biochem.*, **21**, 159-168 (1983).
- [8] V.C. CHO, D.F. BLAIR, U. BANERJEE, J.J. HOPFIELD, H.B. GRAY, I. PECHT, S.I. CHAN, *Biochemistry*, **23**, 1858-1901.
- [9] O. FARVER, Y. SHAHAK, I. PECHT, *Biochemistry*, **21**, 1885-1890 (1982).
- [10] O. FARVER, Y. BLATT, I. PECHT, *Biochemistry*, **21**, 3556-3561 (1982).



SL28 — TH

K. LERCH

Biochemisches Institut der Universität Zürich
Winterthurerstrasse 190, CH-8057 Zürich
Switzerland

THE BINUCLEAR COPPER CENTER AND THE REACTION MECHANISM OF TYROSINASE

Tyrosinase is a copper-containing monooxygenase catalyzing the formation of dark colored melanin pigments [1]. Various forms of the enzyme can be obtained (met-, halfmet-, oxy- and desoxytyrosinase), depending on the oxidation state of the

active site copper. Met- and oxytyrosinase contain two tetragonal Cu(II) ions antiferromagnetically coupled through an endogenous bridge with the exogenous oxygen molecule in oxytyrosinase bound as peroxide. In halfmettyrosinase the two coppers are present in a mixed-valence state [2]. The chemical and spectroscopic properties of the different forms are surprisingly similar to those reported for the oxygen-binding hemocyanins [3]. However, differences between the tyrosinase and hemocyanin active sites are apparent from peroxide displacement and binding studies of tyrosinase substrate analogues [4]. Binding of L-mimosine and various derivatives of benzoic acid to halfmettyrosinase results in very unusual Cu(II) spectral features. They relate to a significant distortion of the Cu(II) site as shown by the rhombic splittings and perpendicular hyperfine structure of the EPR spectra [5]. In addition, these competitive inhibitors are found to bind to the enzyme with an equilibrium constant higher by one order of magnitude relative to aqueous Cu(II) [6]. It is suggested that the protein environment of the binuclear copper complex contributes significantly to the stabilization of substrate analogues binding to the active site. This stabilization and the concomitant change from a tetragonal toward a trigonal bipyramidal geometry of the Cu(II) site seem to greatly assist the catalytic hydroxylation reaction of tyrosinase. It is proposed that the binding of a monophenol substrate to oxytyrosinase leads to a distortion of the Cu(II) complex, thus labilizing the peroxide. This then leaves a reactive, polarized peroxide which in turn can hydroxylate the monophenol most likely via an electrophilic attack on the aromatic ring.

REFERENCES

- [1] K. LERCH, in H. SIGEL (ed.), «Metal Ions in Biological Systems», vol. 13, Marcel Dekker, New York, 1981, pp. 143-186.
- [2] K. LERCH, *Mol. Cell Biochem.*, **52**, 125-138 (1983).
- [3] E.I. SOLOMON, in T.G. SPIRO (ed.), «Copper Proteins», Wiley and Sons, Inc., New York, 1981, pp. 41-108.
- [4] R.S. HIMMELWRIGHT, N.C. EICKMAN, C.D. LUBIEN, K. LERCH, E.I. SOLOMON, *J. Am. Chem. Soc.*, **102**, 7339-7344 (1980).
- [5] M.E. WINKLER, K. LERCH, E.I. SOLOMON, *J. Am. Chem. Soc.*, **103**, 7001-7003 (1981).
- [6] D.E. WILCOX, A.G. PORRAS, Y.T. HWANG, K. LERCH, M.E. WINKLER, E.I. SOLOMON, submitted for publication.



SL29 — TH

PETER M.H. KRONECK
WOLFGANG JAKOB
Universität Konstanz
Fakultät für Biologie
D-7750 Konstanz
F.R.G.

ASCORBATE OXIDASE: FURTHER INVESTIGATIONS OF ITS STRUCTURE AND CATALYTIC PROPERTIES

Ascorbate Oxidase (L-ascorbate:O₂ oxidoreductase, AO, E.C. 1.10.3.3) is a multicopper enzyme widely distributed in plants. For a review of the literature prior to 1982 see ref. [1]. This article describes some recent developments in the number of Cu/M_r, the selective depletion of the type-2 Cu (t2d-AO), the preparation of the apoprotein and its reconstitution to the holoenzyme. In addition redox reactions of AO and t2d-AO with L-ascorbate, thiomolybdate(VI) and dioxygen are reported as studied by stopped flow spectrophotometry and rapid freeze EPR spectroscopy. Finally, a model is presented describing the active site of the multicopper oxidase. On the basis of this model some mechanistic aspects of the reaction of reduced AO with molecular oxygen are discussed.

Cu content, stoichiometry of the Cu types, and stability towards H⁺, OH⁻

The number of Cu atoms/M_r and stoichiometry of the three Cu types strongly depend on several environmental factors maintained during the process of purification, such as pH, ionic strength, buffer, metal ions and chelating agents in the medium. Below pH 5.5, upon dialysis against acetate buffer, the absorbance at 610 nm slightly decreases, whereas an increase in the region 300-400 nm is observed. At pH 4.0, the blue color of AO has completely disappeared accompanied by a slow precipitation of the protein. These results are confirmed by EPR which clearly show that the type-1 signals have been replaced by signals characteristic

of non-prosthetic Cu. The acid induced denaturation of AO is irreversible below pH 4.5, dialysis against buffer, pH 7.0, does not restore the original spectral properties. Above pH 8.0, the optical density at 610 nm also diminishes, but no concomitant turbidity due to protein denaturation is observed. At pH > 10.5 the typical blue color of AO has faded completely, again an increase at 330 nm (type-3 region) can be detected. The reaction at alkaline pH is biphasic with t_{1/2} 5 and 45 min. at pH 11.5, 25°C. Despite the drastic changes in the optical spectrum of AO the Cu remains bound to the protein as shown by EPR and AAS. Up to pH 10.5, this process is fully reversible, dialysis against buffer, pH 7.0, restores both the spectral properties of AO and its activity towards L-ascorbate/dioxygen. According to CLARK *et al.* [2] AO dissociates into two subunits (65,000 M_r) at pH > 10.0. Our studies on the reversibility of the OH⁻ induced processes seem to indicate that one (or several) ligand(s) of the type-1 Cu are replaced by OH⁻ producing a type-2 ligand field. Alternatively, prosthetic groups close to the Cu sites might be deprotonated, i.e. -NHCO-, -NH₃⁺ or imidazole, inducing changes of the protein conformation and the Cu coordination spheres.

Dialysis of AO against phosphate buffer, pH 7.0, containing less than 10⁻⁹ M Cu (determined by AAS), leaves the optical density at 610 nm unchanged but decreases the intensity of the 330 nm chromophore (A₃₃₀/A₆₁₀ 0.56 vs. 0.75 [1]). After addition of extraneous Cu to the dialysis medium (0.31 mM CuSO₄ corresponding to 20 Cu/AO) this effect is reversed.

t2d-AO, apo-AO and reconstitution.

Depending on pH, time of dialysis and the presence of metal chelating agents (EDTA, DMG) the type-2 Cu can be removed giving the so-called t2d-AO. Starting with 7.8 ± 0.3 Cu/M_r in native AO a t2d-AO is obtained with 6.5 ± 0.2 Cu, and a specific activity of 13%. The EPR spectrum of t2d-AO documents the loss of the type-2 Cu, the optical purity index A₃₃₀/A₆₁₀ decreases to 0.36 (vs. 0.75 in AO). The intensity of the fluorescence emission at 335 nm increases by 55 ± 5% compared to native AO.

Dialysis against CN⁻, at basic pH, in the absence of O₂, causes the complete loss of AO (0.8 ± 0.3

Cu). The apoprotein is reconstituted using $\text{Cu}(\text{CH}_3\text{CN})_4\text{ClO}_4/1.0 \text{ M CH}_3\text{CN}$ at neutral pH. The activity of the reconstituted AO peaks at approx. 60% (vs. native AO). The reconstitution seems to proceed via an «all or nothing process», i.e. no intermediate forms of AO could be isolated carrying only the type-3, type-2 or type-1 Cu.

Redox reactions of AO and t2d-AO.

Both AO and t2d-AO are reduced by L-ascorbate in the absence of O_2 . From potentiometric titrations $E'_{0,610} = 327 \pm 3 \text{ mV}$, 10°C , vs. 344 mV , 25°C (vs. SHE [1]). Determination of $E'_{0,330}$ reveals a difference of $30 \pm 10 \text{ mV}$ for $E'_{0,330} - E'_{0,610}$ at 10°C whereas at 25°C the difference is almost zero. K_2MoS_4 reduces both AO and t2d-AO. Interestingly, with $1\text{MoS}_4^-/\text{AO}$, no change in absorbance at 610 nm is observed. On the other hand, EPR clearly shows that at this point 90% of the type-2 Cu must be reduced. Upon further addition of MoS_4^- , the type-3 Cu is reduced prior to the type-1 centers. For t2d-AO the reducing equivalents are immediately transferred to the type-1 Cu. Taking into account the results of several kinetic studies (stopped flow and rapid freeze EPR) of the half reactions $\text{AO}_{\text{red}}(\text{t2d-AO}_{\text{red}}) + \text{O}_2$ and $\text{AO}_{\text{ox}}(\text{t2d-AO}_{\text{ox}}) + \text{L-ascorbate}$ a model is developed describing some structural and mechanistic aspects of AO. The picture of the active site is based on the experimental result that removal of the type-2 Cu drastically alters the reactivity of AO_{red} towards O_2 . In a first step two molecules O_2 bind at the type-3 Cu sites. Splitting of the O-O bond is triggered by electron transfer from type-1 Cu to the oxygen complex. Parallel to the release of one H_2O the second oxygen atom remains bound ($\text{O}\cdot^-$) close to the type-2 Cu. The second H_2O is formed after transfer of a second electron (from type-1 Cu) to the oxygen anion mentioned above.

REFERENCES

- [1] P.M.H. KRONECK, F.A. ARMSTRONG, H. MERKLE, A. MARCHESINI, in P.A. SEIB, B.M. TOLBERT (eds.), «Ascorbic Acid: Chemistry, Metabolism and Uses», *Adv. Chem. Ser.*, **200**, 223 (1982).
- [2] E.E. CLARK, W.N. POILLON, C.R. DAWSON, *Biochim. Biophys. Acta*, **118**, 72 (1966).



SL30 — TH

B. MONDOVI

Institute of Applied Biochemistry
University of Rome
00185 Rome
Italy

A. FINAZZI AGRÒ

G. ROTILIO
Institute of Biological Chemistry
University of Rome
00185 Rome
Italy

S. SABATINI

C.N.R. Center of Molecular Biology
00185 Rome
Italy

REDOX TITRATIONS AND REVERSIBLE REMOVAL OF COPPER FROM BOVINE PLASMA AMINE OXIDASE

INTRODUCTION

Copper-dependent amine oxidases are enzymes that contain two copper atoms per functional unit to approximately 180,000 dalton.

In spite of long and intensive study, the mechanism of action of these enzymes is still obscure. In particular the role of copper, which is essential for the enzymatic activity, has not yet been established. In fact it neither binds the substrate [1] nor undergoes valence change upon anaerobic addition of substrate [1,2]. Its redox behaviour has not been systematically studied, leaving open the question concerning its role in the electron transfer between the substrate and oxygen.

In view of the controversial picture arising from the existing knowledge of Cu-amine oxidases, a more rigorous approach to these aspects was undertaken and a new method for reversible preparation of protein was worked out as previous reports [3,4] on the matter lack proper ESR controls.

RESULTS

Redox reactions of the copper

In buffered solutions at pH 7.2, NADH slowly reduced the enzyme copper anaerobically, but only in the presence of phenazine methosulfate as mediator. Neither ferrocyanide nor ascorbate was able to reduce the copper, even in high excess and in the presence of suitable mediators such as methylene blue and toluidine blue. Reacting the enzyme with phenylhydrazine or substrate — both of which change the ESR line shape (see below) without affecting the signal intensity — had no influence on the apparent redox behaviour of the enzyme.

Under anaerobic conditions dithionite reduced the enzyme-copper with half-time in the range of several minutes. The visible absorption of the enzyme was bleached as well. Reoxidation, as monitored by reappearance of both ESR and optical spectra, was practically immediate.

Preparation and reconstitution of the copper-free-enzyme

The copper-free enzyme was prepared according to the following procedure: i) reduction by excess dithionite in air; ii) addition of 3mM KCN for 1-3 mM copper-enzyme; iii) overnight dialysis against 50 mM KCN in 0.1 M phosphate buffer pH 7.2; iv) exhaustive dialysis against 0.1 M phosphate buffer. Reconstitution was obtained by adding 1 mM CuCl₂. The mixture was left standing for 12 h and then dialyzed against 0.1 M phosphate buffer containing 2 mM EDTA. The reconstituted enzyme was dialyzed against the same buffer containing 0.1 M NaClO₄ and finally against buffer alone. This procedure always left 10-15% residual copper in the apoenzyme. The visible and ESR spectra and the enzyme activity (Table I) were almost fully recovered in the reconstituted protein.

DISCUSSION

The copper of beef plasma amine oxidase is likely to have a rather low redox potential as compared, for instance, to that of other non-blue copper-containing oxidases or related enzymes, such as superoxide dismutase [5] and dopamine- β -hydroxylase [6]. The enzyme reduced by nearly stoichiometric dithionite is promptly reoxidized by

Table I

Properties of copper-free and reconstituted bovine plasma amine oxidase. The data are the average of three preparations

	% Copper content	% Specific activity (per copper)
Native enzyme	100	100
Dithionite-cyanide- -treated enzyme	6	0
Reconstituted enzyme	63	80

oxygen. This result, though not apparently related to the role of copper in the enzymic catalysis, where its reduction by substrate is not established [7], supports a possible function of the metal in the catalytic oxygen activation by this enzyme. In fact, fast reoxidation by oxygen is not observed in reduced superoxide dismutase nor in reduced azurin and plastocyanin, which are functionally reoxidized by other molecules.

The reduced amine oxidase lost a great part of its copper if dialyzed against CN⁻ at neutral pH, while the oxidized enzyme was practically unaffected by much higher CN⁻ concentrations. This procedure allowed a study of the spectral properties of the apo- and reconstituted protein in a greater detail. It is proposed that this preparation gives a «reduced» form of the apoenzyme, possibly at the level of the second, organic cofactor.

ACKNOWLEDGEMENTS

This work has been in part supported by the Italian C.N.R. Special Project on the «Chimica Fine», Contract N. 83.00310.95 and in part by «Ministero della Pubblica Istruzione». The authors wish to thank Mr. A. Ballini for skilful technical assistance.

REFERENCES

- [1] B. MONDOVI, G. ROTILIO, M.T. COSTA, A. FINAZZI-AGRO, E. CHIANCONE, R.E. HANSEN, H. BEINERT, *J. Biol. Chem.*, **242**, 1160-1167 (1967).
- [2] R. BARKER, N. BODEN, G. NAYLEY, S.C. CHARLTON, R. HENSON, M.C. HOLMES, I.D. KELLY, P.F. KNOWLES, *Biochem. J.*, **177**, 289-302 (1979).
- [3] H. YAMADA, K.T. YASUNOBU, *J. Biol. Chem.*, **237**, 3077-3080 (1962).
- [4] J.M. HILL, P.J.G. MANN, *Biochem. J.*, **91**, 171-182 (1964).
- [5] G. ROTILIO, L. MORPURGO, L. CALABRESE, B. MONDOVI, *Biochim. Biophys. Acta*, **302**, 229-235 (1973).
- [6] T. SKOTLAND, T. LIONES, *Inorg. Persp. Biol. Med.*, **2**, 151-180 (1979).
- [7] K.T. YASUNOBU, H. ISHIZAKI, N. MINAMIURA, *Mol. Cell. Biochem.*, **13**, 3-29 (1976).



SL31 — TH

JAMES F. RIORDAN

Department of Biological Chemistry
Harvard Medical School
Boston, MA 02115
U.S.A.

ELECTRONIC ABSORPTION SPECTROSCOPY OF COBALT ANGIOTENSIN CONVERTING ENZYME

Angiotensin converting enzyme (ACE) is a metalloenzyme containing one g-atom of zinc per mole. It catalyzes the cleavage of dipeptides from the carboxyl terminus of oligopeptide substrates. An assumed role for zinc in the catalytic process has been based on analogy with other zinc peptidases, especially carboxypeptidase and thermolysin. However, the binding of zinc to ACE ($K_d = 1 \times 10^{-5}$ M at pH 7.5) is as much as 1000 times weaker than for other zinc metalloenzymes. Detailed analysis of the kinetics of metal binding to ACE indicates that the formation rate constant, $5.9 \times 10^5 \text{ M}^{-1} \text{ sec}^{-1}$, is not substantially different from that for carboxypeptidase A but that the dissociation rate is much greater ($t_{1/2} = 92.4 \text{ sec}$ vs. 28.3 min for carboxypeptidase). Differences between the stability constants of thermolysin, carboxypeptidase A and ACE suggest that metal binding in ACE may involve less than two nitrogen donor atoms.

The nature of the active site zinc atom is of particular interest in light of recent developments in hypertension chemotherapy. Since physiologically ACE is responsible for generating the potent vasoconstrictor angiotensin II, inhibitors of ACE should, and indeed do, lower blood pressure. The most effective inhibitors, such as Captopril and Enalaprilat, are designed to interact with the metal atom and it has been proposed that direct metal ligation accounts for their pronounced potency.

In order to examine the metal binding site

of ACE we have replaced the zinc atom by cobalt(II). Cobalt ACE has between 55 and 120% of the activity of the native zinc enzyme depending upon the particular peptide or ester substrate employed. The visible absorption spectrum of the cobalt protein exhibits a single maximum at 525 nm of low absorptivity ($\epsilon = 100 \text{ M}^{-1} \text{ cm}^{-1}$) suggestive of a distorted coordination geometry. Such weak absorptivity necessitated the use of relatively high concentrations (about 0.1 mM) of enzyme for spectral studies. In order to obtain the milligram quantities of enzyme for this purpose, a new high capacity affinity chromatographic procedure was developed based on the specific ligand *N*-carboxyalkyl phenylalanyl glycine immobilized on Sepharose via a 28A spacer.

The spectra of cobalt-ACE complexes with Captopril, Enalaprilat and other inhibitors display more clearly defined absorption maxima at higher wavelengths (525-637 nm) and of higher absorptivities (130 to $560 \text{ M}^{-1} \text{ cm}^{-1}$) than that of the cobalt enzyme alone. These large spectral responses indicate that binding of inhibitor induces significant changes in the cobalt coordination sphere. In particular, the coordination geometry appears to be tetrahedral-like and more regular. The presence of an $S \rightarrow \text{Co(II)}$ charge transfer band in the near UV spectrum of the cobalt ACE-Captopril complex indicates direct ligation of the thiol group of the inhibitor to the active site cobalt atom. These studies support the similarities between ACE, carboxypeptidase and thermolysin.



SL32 — TH

KATSUMI NIKI
 MITSUMASA FURUKAWA
 YOSHIAKI KAWASAKI
 Department of Electrochemistry
 Yokohama National University
 Tokiwadai, Hodogaya-ku, Yokohama 240
 Japan

CHARLOTTE HINNEN
 Laboratoire d'Electrochimie Interfaciale du C.N.R.S.
 1, Place Aristide-Briand, 92190 Meudon-Bellevue
 France

ELECTROCHEMICAL AND SPECTROELECTROCHEMICAL BEHAVIOR OF C-TYPE CYTOCHROMES AT ELECTRODE INTERFACE IN THE PRESENCE OF ELECTRON PROMOTERS

Cytochrome c_3 exhibits reversible voltammetric responses at mercury and also at solid electrodes. On the other hand, cytochrome c has been reported to exhibit an irreversible electrode reaction on certain electrodes. However, it exhibits a quasi-reversible voltammetric response on either electrodes with special characteristics or on gold electrode in the presence of an electron promoter.

In the present work, we have investigated the adsorption behavior of c -type cytochromes onto silver and gold electrodes in the absence and in the presence of electron promoters, such as 4,4'-bipyridyl (bipy), using voltammetric and surface enhanced Raman scattering (SERS) techniques.

Both cyt. c and c_3 are very strongly adsorbed from aqueous solutions onto Ag and Au surfaces. The electrode reactions of adsorbed cyt. c_3 on Ag and Au are reversible with a formal potential of -0.49 V (vs. Ag/AgCl satd. KCl) in 0.03 M phosphate buffer at pH 7.0 and 25°C . This formal potential agrees quite well with that of the bulk species. On the other hand, the electrode reaction of the adsorbed cyt. c is irreversible with a reductive peak potential by cyclic voltammetry (CV) of -0.38 V and an oxidative peak potential on the

reverse scan of -0.25 V on a gold electrode. That is, the formal potential of adsorbed cyt. c is 30 mV more negative than that of the bulk species. The redox peaks of the adsorbed cyt. c on Ag electrode are hardly observable but SERS confirms that the redox reaction takes place at -0.3 V. SERS also revealed that the redox reaction of adsorbed cyt. c_3 takes place at -0.4 V, which very likely corresponds to the most positive site of cyt. c_3 .

Adsorbed bipy on both Ag and Au surfaces can be gradually replaced by cytochromes when these electrodes are immersed in cytochrome solutions. An equilibrium exists between solution and surface adsorbed cytochromes and bipy. SERS and ac impedance experiments revealed that the Ag is covered mainly by bipy when this electrode is immersed in a mixture of cyt. c_3 ($60 \mu\text{M}$) and bipy (0.5 mM).

Bis(4-pyridyl) disulfide (PySSPy) from the solution replaces cyt. c that is adsorbed on Ag, but cyt. c does not replace the adsorbed PySSPy. Cyt. c exhibits a quasi-reversible voltammetric response on such a PySSPy covered Ag electrode. In the solution containing both cyt. c_3 ($60 \mu\text{M}$) and bipy (5 mM), the redox peaks of cyt. c_3 are not observed on Ag. However, the redox peaks of cyt. c_3 and cyt. c are observed on Au electrode under certain conditions in the solutions containing both cytochromes and bipy.



SL33 — TH

BORIS P. ATANASOV

Biophys. Chem. Proteins Laboratory
Institute of Organic Chemistry & Centre of Phytochemistry
Bulgarian Academy of Sciences
1113-Sofia
Bulgaria

ON THE MECHANISM OF ELECTRON TRANSFER BETWEEN MYOGLOBIN AND CYTOCHROME *c*

The influence of the binding site specificity, the intermolecular orientation, and the three-dimensional electrostatic field structure (3DEFS) in the formation of the "active complex" for electron transfer from ferro myoglobin to ferri cytochrome *c* was studied. Using selective chemical modifications and molecular labels the "active area" on the protein surfaces was determined. The energy of the 3DEFS reorganization in the electron relocation was evaluated by the ratio of the kinetic constants for the redox reactions and triplet quenching of partly Zn-substituted hemeproteins, as well as calculated and visualized by differential three-dimensional electrostatic field maps. The main experimental and theoretical results in this field obtained in the last 12 years in our laboratory will be presented and discussed.



SL34 — FR

JACK PEISACH

Albert Einstein College of Medicine
Bronx, NY 10461
U.S.A.

ELECTRON SPIN ECHO SPECTROSCOPY AND THE STUDY OF METALLOPROTEINS

The pulsed EPR technique based on the generation of electron spin echoes has become a valuable research tool in biophysical and biochemical studies [1-7]. The echo experiments have been of several different types but the most fruitful has involved measurement of the electron spin echo decay envelope. This envelope is modulated by nuclear precession frequencies characteristic of the nuclei coupled to the electron spin. The Fourier transform of spin echo decay envelopes yields a frequency spectrum containing the same information to that obtained from an ENDOR experiment.

A purpose for performing this type of experiment on biological materials is to identify a ligand atom bound to a paramagnetic metal ion in a protein. Many ligands contain a ^{14}N nucleus which can be detected by the appearance of characteristic modulation patterns in the echo envelope. Furthermore the identification of the ^{14}N containing ligand can be made using the ^{14}N quadrupolar frequencies, which are known for many nitrogenous ligands. A measurement of the echo envelope spectrum can thus, in favorable cases, lead at once to the identification of a metal-ion ligand. Similar experiments can be performed whenever it is possible to modify a ligand by ^2H -, ^{13}C - or ^{15}N -substitution. Other experiments can be performed to examine the interaction of metal centers with ^{31}P nuclei in phosphate derivatives. Structural information is obtained both from the appearance in the echo envelope of the appropriate nuclear modulating frequencies and from the depth of the nuclear modulation pattern. In the

case of weakly coupled nuclei, such as ^2H either belonging to a ligand or to a molecule in close proximity to a metal center, the depth of the modulation pattern is proportional to n/r^6 , where r is the metal to deuterium distance and n is the number of equivalent nuclei.

Another kind of experiment is possible when the presence of an exchangeable proton near a paramagnetic center, such as in a water molecule, is suspected. Exchange with D_2O will result in the appearance of a deep, low frequency modulation pattern at the ^2H nuclear precession frequency (1.96 MHz at 3000 gauss). The deuterium signal is entirely distinct from the ^1H modulation pattern (12.8 MHz at 3000 gauss) and it can be distinguished from ^{14}N modulation patterns by repeating the experiment at two well-separated magnetic field settings. An experimental approach involving deuterium substitution and demonstration of contact interaction addresses the positive identification of H_2O as a metal ligand, such as in metmyoglobin. The experiment is immediately suggested by the X-ray crystallographic indication of oxygen near to a metal center when the ligand cannot be named with certainty as water.

REFERENCES

- [1] J. PEISACH, W.B. MIMS, J.L. DAVIS, *J. Biol. Chem.*, **254**, 12379-12389 (1979).
- [2] W.B. MIMS, J. PEISACH, in L.J. BERLINER, J. REUBEN (eds.), «Biological Magnetic Resonance», vol. 3, Plenum Press, NY, pp. 213-263 (1981).
- [3] R.M. BURGER, A.D. ADLER, S.B. HORWITZ, W.B. MIMS, J. PEISACH, *Biochemistry*, **20**, 1701-1704 (1981).
- [4] L. AVIGLIANO, J.L. DAVIS, M.T. GRAZIANI, A. MARCHE-SINI, W.B. MIMS, B. MONDOVI, J. PEISACH, *FEBS Letters*, **156**, 80-84 (1981).
- [5] J.L. ZWEIER, J. PEISACH, W.B. MIMS, *J. Biol. Chem.*, **257**, 10314-10316 (1982).
- [6] T. SHIMIZU, W.B. MIMS, J.L. DAVIS, J. PEISACH, *Biochim. Biophys. Acta*, **757**, 29-39 (1983).
- [7] J. PEISACH, W.B. MIMS, J.L. DAVIS, *J. Biol. Chem.*, **259**, 2704-2706 (1984).



SL35 — FR

BRIAN M. HOFFMAN

Department of Chemistry
Northwestern University
Evanston, Illinois 60201
U.S.A.

ENDOR OF IRON SULFUR CENTERS

EPR studies of metalloenzymes often are restricted because hyperfine interactions from constituent or substrate nuclei are unobservable. Electron-nuclear double resonance (ENDOR) is a high-resolution extension of EPR that can often resolve these interactions, thus removing the limitation. In ENDOR, nuclear resonance transitions are observed through their influence on the strength of the EPR signal and, unlike ordinary NMR, they can be comparably observable for all magnetic nuclei. Thus, the technique offers some unique capabilities for the characterization of an enzyme catalytic center.

Inspired by the logo of ICBC2, we will discuss the applications of ENDOR to iron-sulfur centers. Systems to be discussed include the MoFe protein of nitrogenase, aconitase, and hydrogenases, and their interaction with substrates and/or inhibitors.



SL36 — FR

L.C. SIEKER

R.E. STENKAMP

L.H. JENSEN

Department of Biochemistry
University of Washington
Seattle, Washington
U.S.A.

J. LEGALL

Department of Biochemistry
University of Georgia
Athens, Georgia, 30602
U.S.A.
Groupe Commun d'Enzymologie
DB/SRA B.P. n 1, 13115 St. Paul, les-Durance
France

STRUCTURE OF A SMALL RUBREDOXIN: TENTATIVE ASSIGNMENT OF AMINO ACID SEQUENCE AND THREE DIMENSIONAL STRUCTURE OF THE RUBREDOXIN FROM *DESULFOVIBRIO DESULFURICANS* (STRAIN 27774)

The structure of rubredoxin from the sulfate and nitrate reducing strain of *Desulfovibrio desulfuricans* (strain 27774) is being studied by X-ray diffraction methods to determine its three-dimensional structure. The amino acid composition indicates a significantly shortened polypeptide chain and the first occurrence of histidine in a rubredoxin from an anaerobic organism [1]*. Fig. 1 shows the amino acid sequences of five different rubredoxins** from three different types of bacteria. The preliminary sequence of RBDD is placed in alignment at the bottom for comparison. There

* The amino acid composition listed in that report should have 5 Glu residues added to it.

** The rubredoxins from the different organisms are denoted RBCP from *Clostridium pasteurianum*, RBDV from *Desulfovibrio vulgaris*, RBDG from *Desulfovibrio gigas*, RBPE from *Peptostreptococcus elsdenii*, RBPA from *Peptococcus aerogenes* (formerly called *Micrococcus aerogenes*) and RBDD from *Desulfovibrio desulfuricans* (strain 27774).

		5		10		15
RBCP	MET-Lys-Lys-Tyr-Thr-CYS-Thr-Val-CYS-GLY-TYR-Ile-TYR-ASP-PRO-					
RBDV		Val			Glu	
RBDG	Asp Ile	Val			Glu	
RBPE	Asp	Glu	Ser Ile			Glu
RBPA	Gln	Phe Glu	Leu			
RBDD	Ala	Asp	Ser		Glu	Asp
		20		25		30
RBCP	Glu-ASP-Gly-ASP-Pro-ASP-ASP-Gly-Val-Asn-Pro-GLY-Thr-ASP-PHE-					
RBDV	Ala Glu	Thr Asn	Lys			Ser
RBDG	Lys	Ser	Ile-Lys			Ser
RBPE	Glu	---	Gly Asn	Ala Ala		Lys
RBPA	Leu Val Gly	---	Thr Pro Asp	Gln Asp	---	Ala
RBDD	Ala Glu(gly)	---	---	(gly) Lys(gly gly)	Ser	Ser
		35		40		45
RBCP	Lys-ASP-Ile-Pro-ASP-ASP-TRP-Val-CYS-PRO-Leu-CYS-GLY-Val-Gly-					
RBDV	Asp	Leu Ala		Val	Ala Pro	
RBDG	Glu	Leu	Ala	Val	Ala Ser	
RBPE	Ala	Leu Ala		Thr	Ala Asp	
RBPA	Glu	Val Ser Glu Asn			Ala	
RBDD	Gly	Leu	(trp)	Val	Asp(ala)	
		50		55		
RBCP	LYS-ASP-Glu-PHE-Glu-Glu-Val-Glu-Glu					
RBDV	Ser	Ala Ala	---	---		
RBDG		Ala	Lys Gln	---		
RBPE		Ala	Val Lys Met Asp	---		
RBPA		Glu Asp	Val Tyr	Asp		
RBDD		Ser	---	---		

The complete amino acid sequence is shown for the rubredoxin from *Clostridium pasteurianum*. The amino acids for the other rubredoxins are placed in the appropriate column where they are different. Deletions are shown as dashes in the column. The residues denoted by parentheses for RBDD are very tentative and should not be accepted as established fact.

Fig. 1

is considerable homology among the five sequences but distinct differences are obvious. A comparison of the three-dimensional structures of the upper three proteins (manuscript in preparation) shows virtually identical chain folding with the strictly conserved aromatic groups being in very similar orientations. It seems reasonable to expect a similar folding of the chain for the smaller RBDD, keeping in mind that some form of truncation of the chain will be present.

Crystals of this rubredoxin belong to the triclinic system with one molecule in the unit cell. The cell parameters are: $a = 24.922(4)$ Å, $b = 17.786(3)$ Å, $c = 19.715(3)$ Å, $\alpha = 101.02(1)^\circ$, $\beta = 83.37(1)^\circ$ and $\gamma = 104.52(1)^\circ$. Reflection data, including Friedel reflections, were measured to 1.5 Å for a total of 11,600 measurements. Computational details will be presented elsewhere in a more complete description of this work.

A Patterson synthesis calculated with the Bijvoet differences showed a single peak with hints of four closely associated peaks. Using the atom coordinates of the Fe-4S cluster, the atoms of the polypeptide backbone and of many of the strictly homologous residues of RBDV [2], a rotation function against the 26.0 to 5.0 Å data set of the

triclinic cell produced a rotation which appeared correct [3]. This partial structure was corrected for interfering side chains in the triclinic cell by deleting the offending atoms. Many of the amino acid residues were defined as alanine for the initial model.

After several cycles of restrained least squares refinement [4] and adding or deleting atoms, a 2.1 Å Fourier map was calculated by adding in higher order reflections. This map was inspected for features consistent with the known three-dimensional folding and homology of the Rbs and the amino acid composition for RBDD, taking into consideration the juxtaposition of neighboring residues from adjoining molecules in the packing arrangement within the crystal. The e.d. map clearly shows an overlap problem of the chain from residue 20 to 23 with residue 5 of an adjoining molecule. Closer inspection of this region indicates that it is possible to fit the density best by bridging this loop between residue 19 and 24 with a glycine residue, shortening the loop by three residues. This Gly20 not only fits the density but also fulfills the general rule of a Gly being located at a beta bend where chains reverse direction [5]. This arrangement in the model also retains the normal chain path for the *N*-terminus at residue 5. Another region in the e.d. map shows that the density for the chain terminates after Phe49. In fact, there is very little room for another *C*-terminal residue due to molecular packing restrictions.

An interesting aspect to shortening the «back» 17 to 28 loop by three residues in RBDD is exposure of the hydrophobic interior where the aromatic portion of Trp37 is protected in the three structures known by structure analysis. This region in RBDD contains density which is thin and diffuse and is difficult to fit tryptophan. As the structure is improved this region should become more defined. It is possible that a histidine occupies this space rather than a tryptophan. This would allow for a hydrogen bond of the carboxyl group of Asp19 to the ring N of histidine as is seen between Asp19 and N37H2 of Trp37 in RBCP [6]. Fig. 2a shows the alpha carbon chain of RBDD which can be compared to the alpha carbon chain of RBDV in 2b.

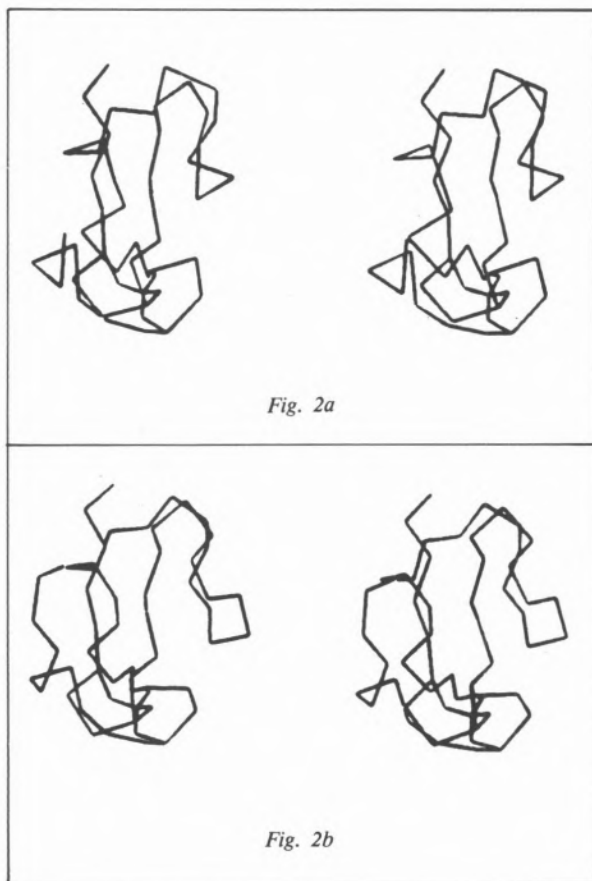


Fig. 2a

Fig. 2b

REFERENCES

- [1] L.C. SIEKER, L.H. JENSEN, B.C. PRICKRIL, J. LEGALL, *J. Mol. Biol.*, **171**, 101-103 (1983).
- [2] E.T. ADMAN, L.C. SIEKER, L.H. JENSEN, J. LEGALL, *J. Mol. Biol.*, **112**, 113-120 (1977).
- [3] R.A. CROWTHER, «The Molecular Replacement Method», in M.G. ROSSMANN (ed.), «International Science Review Series», vol. 13, Gordon & Breach, New York, 1972, pp. 173-183.
- [4] W.A. HENDRICKSON, J.H. KONNERT, in R. SRINIVASAN (ed.), «Biomolecular Structure, Function, Conformation and Evolution», vol. 1, Pergamon Press, Oxford, 1980, pp. 43-57.
- [5] J.S. RICHARDSON, *Adv. Protein Chem.*, **34**, 167-339 (1981).
- [6] K.D. WATENPAUGH, L.C. SIEKER, L.H. JENSEN, *J. Mol. Biol.*, **131**, 509-522 (1979).



SL37 — FR

P.J. STEPHENS

T.V. MORGAN

F. DEVLIN

Department of Chemistry
University of Southern California
Los Angeles, CA 90089-0482
U.S.A.

C.D. STOUT

Department of Crystallography
University of Pittsburgh
Pittsburgh, PA 15260
U.S.A.

B.K. BURGESS

Department of Molecular Biology and Biochemistry
University of California at Irvine
Irvine, CA 92717
U.S.A.

NOVEL REDOX CHEMISTRY OF *AZOTOBACTER VINELANDII* FERREDOXIN I

It was shown by X-ray crystallography [1,2] and Mössbauer spectroscopy [3] that aerobically purified *Azotobacter vinelandii* ferredoxin I contains a $[3\text{Fe-3S}]^{3+}$ cluster and a $[4\text{Fe-4S}]^{2+}$ cluster. Dithionite was reported to reduce the $[3\text{Fe-3S}]^{3+}$ cluster, but not the $[4\text{Fe-4S}]^{2+}$ cluster [3]. $\text{Fe}(\text{CN})_6^{3-}$ was believed to oxidise the $[4\text{Fe-4S}]$ cluster to the oxidised HIPIP, $[4\text{Fe-4S}]^{3+}$ state [4].

Our studies of the oxidative and reductive chemistry of ferredoxin I have both revised and extended earlier work. We have shown that:

- 1) aerobically isolated ferredoxin I, $(7\text{Fe})\text{FdI}_{\text{ox}}$, is anaerobically reconstituted from its apoprotein as $(8\text{Fe})\text{FdI}_{\text{ox}}$, a $\{2[4\text{Fe-4S}]^{1+/2+}\}$ protein of the bacterial ferredoxin type [5].
- 2) $(8\text{Fe})\text{FdI}$ is rapidly destroyed by O_2 , $(7\text{Fe})\text{FdI}_{\text{ox}}$ being produced in $\sim 10\%$ yield [5].
- 3) $\text{Fe}(\text{CN})_6^{3-}$ oxidation of $(7\text{Fe})\text{FdI}_{\text{ox}}$ is not a reversible, $[4\text{Fe-4S}]^{3+}$ -producing reaction. Instead, progressive destructive oxidation occurs leading eventually to apoprotein [6-8].
- 4) *en route* to apoprotein, $\text{Fe}(\text{CN})_6^{3-}$ oxidation creates two intermediate species, $(7\text{Fe})\text{FdI}'_{\text{ox}}$ and $(3\text{Fe})\text{FdI}_{\text{ox}}$.



SL38 — FR

BHARAT B. KAUL
CAROL J. HINSHAW
JACK T. SPENCE

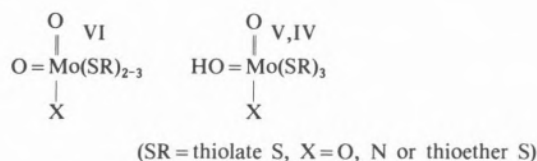
Department of Chemistry and Biochemistry
Utah State University
Logan, Utah 84322
U.S.A.

JOHN H. ENEMARK
SHANNATH L. MERBS

Department of Chemistry
University of Arizona
Tucson, Arizona 85721
U.S.A.

MODELS FOR THE MOLYBDENUM CENTERS OF THE MOLYBDENUM HYDROXYLASES

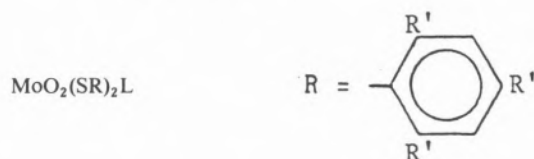
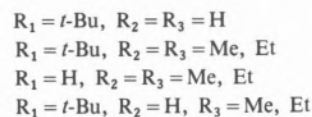
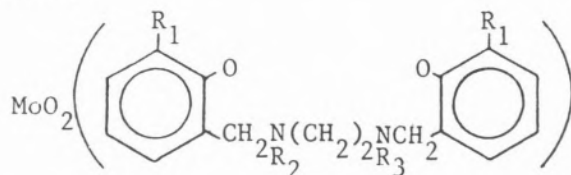
Recent EXAFS and EPR results indicate the Mo centers of sulfite oxidase and assimilatory nitrate reductase in their oxidized (Mo(VI)) and reduced (Mo(V), Mo(IV)) states have ligand sets as follows [1]:



Most Mo(VI)O₂L_n complexes (L = ligand(s) with O, N or S coordinating groups) give oxo-Mo(V) dimers upon one-electron reduction:

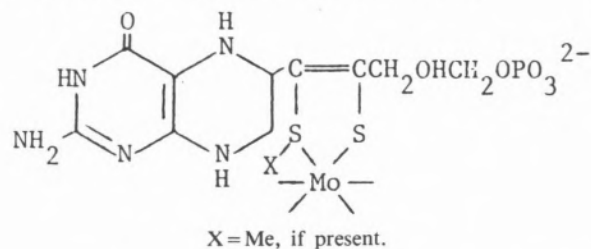


A number of MoO₂L_n complexes having sterically bulky ligands which prevent such dimer formation upon reduction have been synthesized in this laboratory:

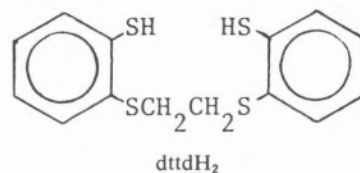


One-electron electrochemical reduction of these complexes gives Mo(V) monomeric products with structures dependent on the presence and the number of protons on the amino groups of the ligands. In some cases, the oxo-Mo(V) complexes and the oxo-Mo(IV) complexes have also been synthesized. Structures, electrochemical properties and EPR spectra of the complexes have been obtained. Their relevance as models for the enzyme Mo centers will be discussed.

Recent work has identified a novel reduced pterin with a sulfur side chain, obtained from the Mo-cofactor of the Mo hydroxylases, for which a Mo-binding site has been proposed [2]:



As possible models for Mo coordination of this kind, MoO₂(dttdd), MoOCl(dttdd) and MoO(PPh₂Et)(dttdd) have been synthesized (dttddH₂ = 2,3,8,9-dibenzo-1,4,7,10-tetrathiadecane).



MoO₂(dtttd) has been determined by X-ray crystallography to have substantially distorted octahedral geometry, with the thioether groups approximately *trans* to the oxo groups. MoO₂(dtttd) is reduced electrochemically to MoO(dtttd) without dimer formation. MoOCl(dtttd) and MoO(dtttd) form a reversible couple, but neither can be oxidized electrochemically to MoO₂(dtttd). While the oxo-Mo(V) dimer, Mo₂O₃(dtttd)₂, is thermodynamically stable, it is not formed in the coulometric reduction of MoO₂(dtttd) because the comproportionation reaction is very slow:

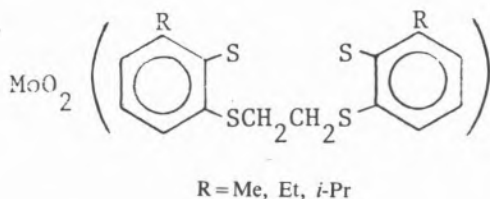


As a result, MoO₂(dtttd) reacts with PPh₂Et to give OPPh₂Et and the Mo(IV) complex without dimer formation, while MoO(dtttd) reacts with Me₂SO to give MoO₂(dtttd) and Me₂S:



MoO₂(dtttd) thus catalyzes the reduction of Me₂SO to Me₂S, mimicking the Mo enzyme, biotin sulfoxide reductase.

The electrochemical properties and EPR spectra of the complexes have been determined, and the properties of similar complexes having bulky groups on the ligand will be reported:



The plausibility of an unsaturated thiolate-thioether ligand as a model for the Mo binding site in the Mo-pterin ligand will be discussed.

REFERENCES

- [1] S.A. CRAMER, L.S. SOLOMONSON, M.W.H. ADAMS, L.E. MORTENSON, *J. Am. Chem. Soc.*, **106**, 1467 (1984).
- [2] J.L. JOHNSON, K.V. RAJAGOPALAN, *Proc. Natl. Acad. Sci. USA*, **79**, 6856 (1982).



SL39 — FR

LUIGI G. MARZILLI

Chemistry Department
Emory University
Atlanta, GA 30322
U.S.A.

NEVENKA BRESCIANI-PAHOR

LUCIO RANDACCIO
ENNIO ZANGRANDO

Istituto di Chimica
University of Trieste
Trieste
Italy

JENNY P. GLUSKER

Institute for Cancer Research
Philadelphia, PA 19111
U.S.A.

STRUCTURAL AND ¹H AND ³¹P NMR SPECTROSCOPIC STUDIES OF B₁₂ COMPOUNDS: A NEW CRYSTALLINE FORM OF VITAMIN B₁₂

Coenzyme B₁₂ (5'-deoxyadenosylcobalamin) can be considered to be an «organic radical carrier» much as the heme group in hemoglobin is a dioxygen carrier [1]. In both types of protein systems, the conformation of the protein influences the ability of the metal center to bind the carried species (radical or dioxygen) [2-4]; therefore, the relationship between the structure at the metal center and its carrying function is both intriguing and important. FINKE [5] has pointed out the need for a greater understanding of the structural factors that influence Co-C homolysis. Until recently, X-ray structural information was available for only one organometallic B₁₂ compound, namely coenzyme B₁₂ itself [6]. This structure established that the 5'-deoxyadenosyl group was attached to the cobalt *via* the 5'-carbon atom. This was the first demonstration of the existence of a naturally occurring alkyl organometallic compound.

Methyl B₁₂ (methylcobalamin) is a biologically active coenzyme and is essential for human metabolism [3]. At the First International Bio-Inorganic meeting, we presented the first report of the

structure of this other coenzyme [7] and a complete report is in press [8]. We had selected this molecule for structural and spectroscopic investigation not only because of its natural occurrence as a cofactor for a methyltransferase enzyme, but also because it serves as a spectroscopic and structural prototype for comparative studies of alkyl cobalamins. Investigations of model B₁₂ compounds, such as the cobaloximes, [LCo(DH)₂X] (DH = monoanion of dimethylglyoxime; L = neutral, two electron donor; X = mononegative electron donor), have revealed a wealth of information concerning the relationship of structure to reactivity or spectroscopic patterns [9]. Similar comparative spectroscopic and structural information on the biologically more relevant cobalamins could help elucidate conformational changes that influence the radical-carrying ability of coenzyme B₁₂ when incorporated into B₁₂ holoenzymes. Recently, we obtained a new crystalline form of vitamin B₁₂ (cyanocobalamin) which is intermediate between the «wet» and «dry» forms of the vitamin. The quality of the data suggests that more accurate values of structural parameters are likely to emerge than from previous studies of the known forms.

Current concepts in B₁₂ biochemistry will be evaluated based on our recently performed structural and ¹H and ³¹P NMR spectroscopic studies on cobalamins as well as published and ongoing studies of model organocobalt compounds.

REFERENCES

- [1] J. HALPERN, *Pure Appl. Chem.*, **55**, 1059 (1983).
- [2] P.J. TOSCANO, L.G. MARZILLI, *Prog. Inorg. Chem.*, **31**, 105 (1984).
- [3] D. DOLPHIN (ed.), «B₁₂», 2 vols., Wiley-Interscience, New York, 1982.
- [4] J.P. GLUSKER, in D. DOLPHIN (ed.), «B₁₂», vol 1, Wiley-Interscience, New York, 1982, p. 23.
- [5] R.G. FINKE, D.A. SCHIRALDI, B.J. MAYER, *Coord. Chem. Rev.*, **54**, 1 (1984).
- [6] P.G. LENHERT, D.C. HODGKIN, *Nature*, **192**, 937 (1962).
- [7] L.G. MARZILLI, P.J. TOSCANO, M.F. SUMMERS, L. RANDACCIO, N. BRESCIANI-PAHOR, J.P. GLUSKER, M. ROSSI, *Inorg. Chim. Acta, Bioinorganic Sec.*, **79**, 29 (1983).
- [8] M. ROSSI, J.P. GLUSKER, L. RANDACCIO, M.F. SUMMERS, P.J. TOSCANO, L.G. MARZILLI, *J. Am. Chem. Soc.*, (1985), in press.
- [9] N. BRESCIANI-PAHOR, M. FORCOLIN, L.G. MARZILLI, L. RANDACCIO, M.F. SUMMERS, P.J. TOSCANO, *Coord. Chem. Rev.*, in press.



SEYMOUR H. KOENIG
 RODNEY D. BROWN, III
 The IBM Thomas J. Watson Research Center
 P.O. Box 218, Yorktown Heights, NY 10598
 U.S.A.

LOKESH BHATTACHARYYA
 C. FRED BREWER

Departments of Molecular Pharmacology, and Microbiology and Immunology
 Albert Einstein College of Medicine
 Bronx, NY 10461
 U.S.A.

COMPARATIVE PROTON AND DEUTERON NMRD STUDIES OF Ca²⁺ - Mn²⁺ - CONCAVALIN A, PEA, AND LENTIL LECTINS: EVIDENCE FOR A COMMON SITE OF EXCHANGING WATER MOLECULES

We have measured the magnetic field dependence (dispersion) of the nuclear magnetic relaxation rates (NMRD profiles) of solvent protons and deuterons in solutions of Ca²⁺-Mn²⁺-Concanavalin A (CMPL), Ca²⁺-Mn²⁺-lentil lectin (CMLcH), and Ca²⁺-Mn²⁺-pea lectins (CMPSA), over the temperature range -8 to 35°C. From a comparison of proton and deuteron results, we find that CMPL has two types of solvent binding sites that differ both in their exchange times and distance from the Mn²⁺ ions. The «slow» site is an inner sphere site of the Mn²⁺ with $\tau_M \sim 10^{-5}$ s assuming a single water; the «fast» site has $\tau_M \sim 5 \times 10^{-9}$ s, and $r \sim 5$ Å. This conclusion is corroborated by measurements of the temperature dependence of the proton NMRD profiles of CMPL, which show that the profiles are composite, containing two contributions with opposite dependences on temperature (fig. 1). The rapidly exchanging waters dominate the paramagnetic NMRD profile of CMPL at -8°C, while the slowly exchanging waters dominate the profile at 35°C. Similar proton and deuteron measurements of CMLcH and CMPSA show that these two metallolectins, which are structurally related to CMPL, possess a com-

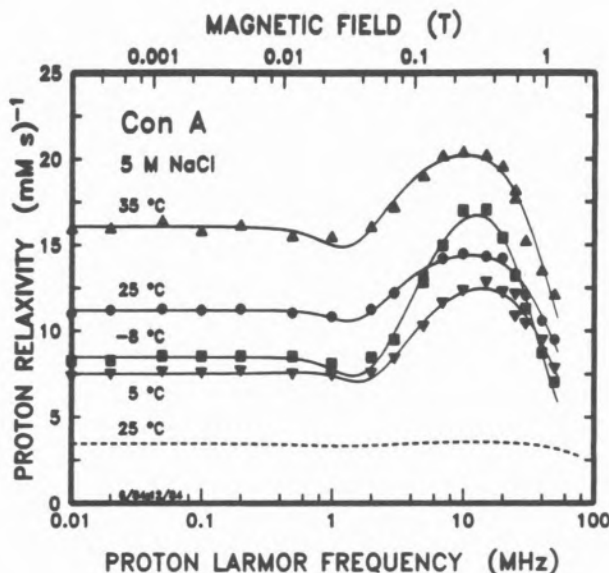


Fig. 1

The paramagnetic contributions to the proton $1/T_1$ NMRD profiles of Ca^{2+} - Mn^{2+} -Con A at four temperatures. The protein concentration was 0.56 mM, and the bound Mn^{2+} and Ca^{2+} concentrations were each 0.48 mM. 5 M NaCl was used to prevent freezing at -8°C . The solid lines through the data points are meant to serve as visual guides. The data are clearly composite, with contributions from two classes of sites with opposite dependences on temperature. The dashed line is the expected contribution of the slowly exchanging class of water molecules to the 25°C data, computed for protons from the measured deuterium CMPL profile

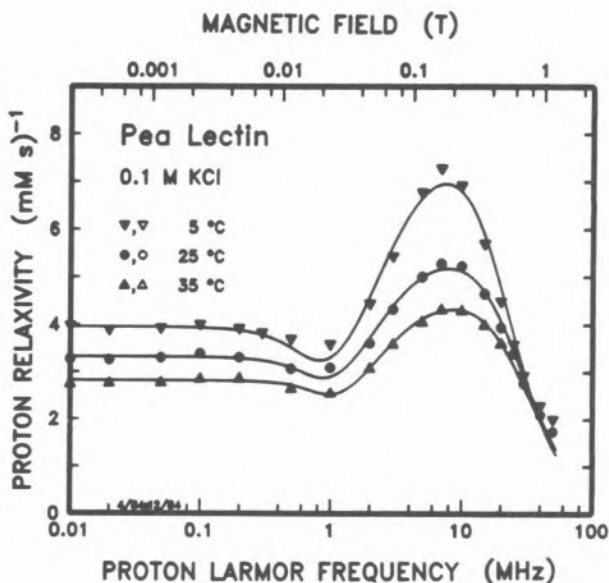


Fig. 2

The paramagnetic contributions to the proton $1/T_1$ NMRD profiles of Ca^{2+} - Mn^{2+} -pea lectin (CMPSA) at three temperatures. The solid lines through the data points are meant to serve as visual guides

mon solvent exchange site, one that corresponds to the site of rapid exchange of CMPL. These conclusions were corroborated by measurements of the temperature dependence of the proton NMRD profiles of CMLcH and CMPSA (cf. fig. 2), which are essentially identical and which exhibit the temperature dependence of the fast exchange contribution found for CMPL. We assign the site of rapid solvent exchange, common to all three lectins, to the inner coordination sphere of the Ca^{2+} ions, with the water protons $\sim 5 \text{ \AA}$ from the Mn^{2+} ion, and the additional site in CMPL to the inner sphere of the Mn^{2+} ions.



SL40 — FR

ANDREA SCOZZAFAVA
Department of Chemistry
University of Florence
Italy

THERMODYNAMIC AND STRUCTURAL PROPERTIES OF THE METAL BINDING SITES OF THE TRANSFERRINS

No X-ray structure of transferrins is up to now available at a resolution which allows a precise determination of the nature and the steric properties of the ligands present into the metal binding sites of these proteins. For this reason we have undertaken a systematic study of several metal derivatives of transferrins in presence of the natural synergistic anion carbonate or of the oxalate anion, through different spectroscopic techniques like ^1H , ^{13}C , ^{205}Tl NMR, CD and UV, VIS spectroscopies. The main results of these investigations are here briefly summarized.

Well resolved ^1H NMR spectra of the cobalt(II)-carbonate-conalbumin adduct have been obtained which allowed the identification of two histidines and two tyrosines among the protein ligands [1].

In this system the two sites appear indistinguishable both with respect to the NMR and CD spectroscopies. When the carbonate is replaced by the oxalate however, the two sites display CD spectra very different between them [2]. One site in the oxalate derivative shows dramatic spectroscopic changes upon dissociation of a protein group with $pK_a=9.5$. Also the CD and NMR spectra of the carbonate derivative show a very similar pH dependence [2].

The ^{205}Tl NMR spectra of the dithallium-carbonate-transferrin derivative shows two well resolved thallium resonances separated by 20 ppm [3]. This separation is very small on the ^{205}Tl NMR scale, therefore it can be inferred that the chromophores in the two sites are very similar to a high degree of approximation.

The role of the synergistic anion has been monitored through the study of the dialuminium-oxalate-conalbumin derivative [4]. ^{13}C NMR spectra of ^{13}C enriched oxalate show that the two oxalate ions in the two sites are almost equivalent whereas the two carboxylate residues of each oxalate group are noticeably different between them. This has been interpreted as an evidence that in each binding site the oxalate binds with only one carboxylate group to the metal, whereas the se-

cond one is interacting with some residue of the protein wall. These residues could, in our opinion, be different between the two sites and they could be responsible for the very small spectroscopic differences which are generally observed between the two sites, and for the different affinities of the two sites for the metal ions. Studies are in progress in order to ascertain whether the observed acidic equilibrium with pK_a of 9.5, which deeply affects the structural properties of one site in the cobalt(II) oxalate derivative, can be indicative of the dissociation of the group at which the synergistic anion is supposed to interact [5,6].

REFERENCES

- [1] I. BERTINI, C. LUCHINAT, L. MESSORI, A. SCOZZAFAVA, *Eur. J. Biochem.*, **141**, 375 (1984).
- [2] I. BERTINI, C. LUCHINAT, L. MESSORI, R. MONNANNI, A. SCOZZAFAVA, *Rev. Port. Quím.*, **27**, ... (1985).
- [3] I. BERTINI, C. LUCHINAT, L. MESSORI, *J. Am. Chem. Soc.*, **105**, 1347 (1983).
- [4] I. BERTINI, E. BORGHI, C. LUCHINAT, A. SCOZZAFAVA, *J. Mol. Struct.*, **113**, 191 (1984).
- [5] D.C. HARRIS, G.A. GRAY, P. AISEN, *J. Biol. Chem.*, **249**, 5261 (1974).
- [6] J.C. ZWEIER, J.B. WOOTEN, J.S. COHEN, *Biochemistry*, **20**, 3505 (1981).

MINISYMPOSIA

1. Ni-Biochemistry

Convener: J.J.G. Moura
(Lisboa)



MS1.1 — MO

J.J.G. MOURA

M. TEIXEIRA

I. MOURA

A.V. XAVIER

Centro de Química Estrutural
U.N.L., Complexo I, I.S.T.
Av. Rovisco Pais, 1000 Lisboa
Portugal

J. LE GALL

Department of Biochemistry
University of Georgia
Athens, Georgia 30602
U.S.A.

DESULFOVIBRIO GIGAS HYDROGENASE; CATALYTIC CYCLE AND ACTIVATION PROCESS

Desulfovibrio gigas [NiFe] hydrogenase (E.C. 1.12.2.1) has a molecular weight of 89 kD (two subunits of 63 kD and 26 kD) and contains 1 gatm of nickel, 11 gatm of iron and 11-12 gatm of sulfide [1].

1 — NATIVE STATE

IRON-SULFUR-CENTERS

Mössbauer and EPR spectroscopic studies established that in the purified enzyme the iron-sulfur clusters are arranged in a $[\text{Fe}_3\text{S}_x]_{\text{ox}}$ cluster (EPR active) and two $[\text{Fe}_4\text{S}_4]^{2+}$ clusters (EPR silent) [2]. The $[\text{Fe}_3\text{S}_x]_{\text{ox}}$ cluster is the origin of an almost isotropic EPR signal centered around $g=2.02$, observable below 30 K. The Mössbauer parameters of the $[\text{Fe}_4\text{S}_4]$ clusters (quadrupole splitting of

1.16 mm/s and isomeric shift of 0.46 mm/s, at 4.2 K) are typical of 4Fe centers in the +2 oxidation level [2].

NICKEL CENTER

In the native preparations, a rhombic EPR signal with g -values at 2.31, 2.23 and 2.02 (*Ni-signal A*) is observed up to 120 K (Fig. 1). This rhombic signal, assigned to nickel(III), accounts for

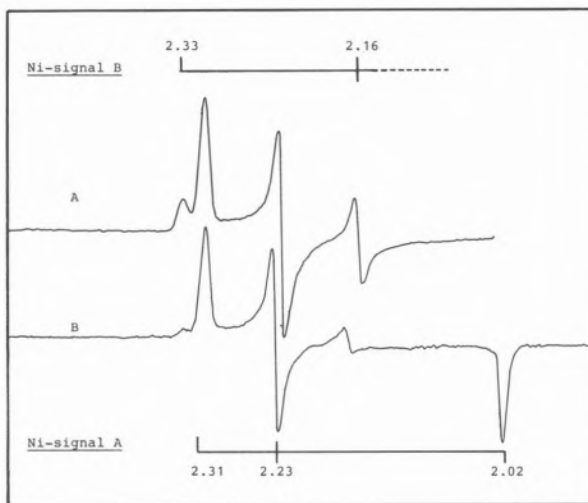


Fig. 1

EPR spectra of *D. gigas* [NiFe] hydrogenase, recorded in a Bruker ER-200 EPR spectrometer, equipped with an Oxford Instruments continuous flow cryostat.

A) and B) — Two different preparations of the enzyme. Temperature 100 K, modulation amplitude 1 mT, microwave power 2 mW, frequency 9.34 GHz

50-100% of the chemically detectable nickel depending on preparation. This assignment was confirmed by the observation of hyperfine coupling in ^{61}Ni -isotopic replaced hydrogenase [3]. A minor species can also be detected at g -values 2.33, 2.16 and ~ 2.0 (*Ni-Signal B*, Fig. 1). The relative intensities of *Ni-Signals A* and *B* varies with preparation and can be altered by anaerobic redox cycling of the enzyme. This indicates that there exists different Ni(III) environments in the oxidized enzyme.

2 — INTERMEDIATE OXIDATION STATES

The first event occurring during the anaerobic reduction of *D. gigas* with hydrogen is the disappearance of *Ni-Signals A* and *B* and the isotropic $g=2.02$ signal due to the $[\text{Fe}_3\text{S}_4]$ clusters [4]. An EPR silent state is then attained. Further reduction of the enzyme under H_2 atmosphere is accompanied by the development of a new rhombic EPR signal with g -values at 2.19, 2.16 and 2.02 (*Ni-Signal C*, Fig. 2-A). This signal was also attributed to a nickel species by the ^{61}Ni isotopic substitution [3].

During the course of the reduction experiment *Ni-Signal C* attains a maximum intensity (40-60% of the chemically detectable nickel). Longer incu-

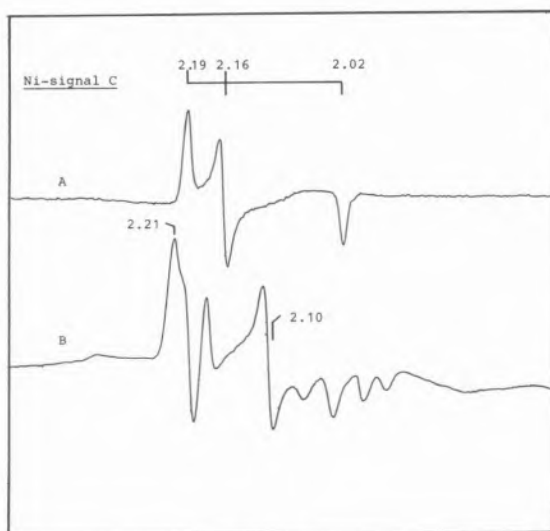


Fig. 2

EPR spectra of intermediate redox states of *D. gigas* [NiFe] hydrogenase, in the presence of hydrogen. Experimental conditions as in Fig. 1.

- A) Temperature 77 K, microwave power 2 mW.
 B) Same as A, at 4.2 K, microwave power 2 mW

bation time under H_2 yields an EPR silent state, when measured at 77 K. At low temperature (below 15 K) EPR signals typical of $[\text{Fe}_4\text{S}_4]^{1+}$ clusters are observed [5].

At redox states of the enzyme such that *Ni-Signal C* develops, low temperature studies reveal the presence of another EPR active species: below 10 K, the shape of the EPR spectra changes drastically and a new set of signals at $g=2.21$, 2.10 and broad components at higher field is clearly discernible at 4 K (Fig. 2-B). This set of g -values exhi-

bits different power dependence from that of *Ni-Signal C* (readily saturated with low microwave power, typical of a slow relaxation species). The origin of the "2.21" signals is under discussion. Since these signals are only observable at low temperature with high microwave power levels (fast relaxing species), they may originate from an iron-sulfur center. Since the g -values appear to be too high, another explanation is that they originate from the Ni-center weakly interacting with another paramagnetic center in the vicinity (e.g. iron-sulfur center).

3 — MID-POINT REDOX POTENTIALS

Redox transitions were observed at -70 mV (measured by the disappearance of the 2.02 signal) and -220 mV (measured by the disappearance of the *Ni-Signal A* (Fig. 3 - insert A)). Only the second redox transition is pH dependent, with a slope of ~ -60 mV per pH unit [6]. *Ni-Signal C* develops at a mid-point redox potential below -300 mV, reaches a maximum around -350 mV and disappears below -400 mV (Fig. 3).

LISSOLO *et al.* [7] determined the activity of the enzyme as a function of the redox potential. Their study indicates that the hydrogenase activation is a one-electron process with a mid-point redox potential around -340 mV (Fig. 3 - insert B). This value correlates with the appearance of *Ni-Signal C*, suggesting that this signal may represent an activated state of the enzyme.

4 — ACTIVATION PROCESS AND CATALYTIC CYCLE

The definition of the role of the nickel during the redox cycle of [NiFe] hydrogenases requires the assignment of the oxidation states involved, the characterization of the ligation mode of the nickel center, as well as the elucidation of possible interactions between the redox centers.

The simplest interpretation of our redox data involves a redox scheme that requires the transition from Ni(III) to Ni(0). However, nickel chemistry shows that the very high and very low oxidation states are not stable chemical species; very negative and very positive redox potentials are associated with the transitions $\text{Ni(I)} \rightleftharpoons \text{Ni(0)}$ and $\text{Ni(III)} \rightleftharpoons \text{Ni(II)}$, respectively. Also, the Ni(III)/Ni(II)

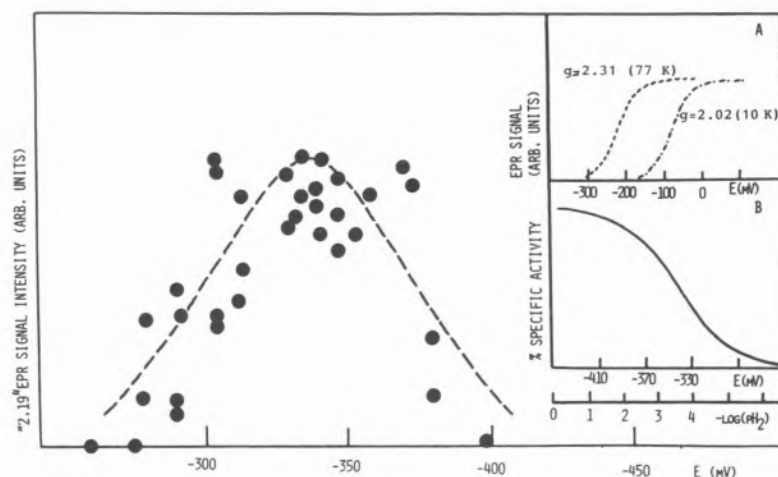


Fig. 3

EPR signal intensity (arbitrary units) of the Ni-signal C in function of the redox potential. EPR signals were measured at 77 K. No attempt was made to fit the experimental points to a Nernst equation.

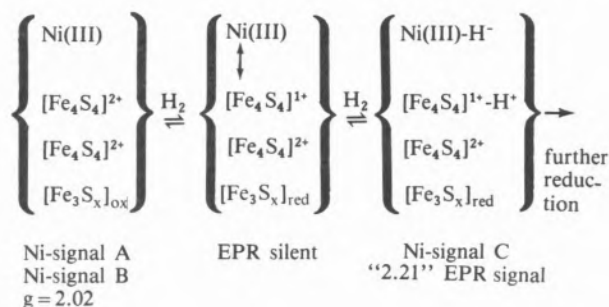
Insert A — Redox titration followed at $g=2.02$ (10 K) and $g=2.31$ (77 K), data from reference [2].

Insert B — Activation profile of *D. gigas* [NiFe] hydrogenase at different partial pressures of hydrogen, data from reference [7]

chemistry offers a wide range of versatile properties namely: facile rearrangement of ligands, spin and conformational equilibria as well as alteration of the type and number of ligand in the nickel coordination sphere. The redox potential of the Ni(III)/Ni(II) couple can be brought, in principle, to physiological levels by preferential stabilization of the Ni(III) state. Thus, the utilization of fewer redox states seems more realistic in terms of the nickel chemistry.

Another important point to consider in the reactional mechanism of hydrogenase is that the so-called "oxygen stable" [NiFe] hydrogenases (e.g. *D. gigas* hydrogenase) are not fully active in the "as isolated" state. Studies of the hydrogenase activity [7] indicate that the enzyme must go through a lag phase as well as an activation one, in order to be fully active. This complex phenomenon seems to involve the removal of oxygen (lag phase) followed by a reduction step (activation phase).

Taking into consideration the hydrogenase activity studies, the plausibility of the Ni(III) \rightleftharpoons Ni(II) redox cycling scheme, and the sequence of events observed by EPR spectroscopy upon exposure to H_2 atmosphere, a model is proposed for the mechanism of the [NiFe] hydrogenases in the context of both the catalytic and the activation processes:



The "as isolated" state is fully characterized. EPR and Mössbauer studies in the enzyme "as isolated" [2] indicate that there is no magnetic interaction between these four redox centers.

The active state of the enzyme is EPR silent. During this activation process, both the isotropic $g=2.02$ and the nickel signal disappear. The loss of the $g=2.02$ signal is attributed to the reduction of the $[\text{Fe}_3\text{S}_x]$ cluster, $E_o = -70$ mV (EPR silent $[\text{Fe}_3\text{S}_x]_{\text{red}}$).

In order to retain the Ni(III)/Ni(II) redox scheme, the disappearance of Ni Signal A and/or Ni Signal B requires a more complicated mechanism. We propose that one of the $[\text{Fe}_4\text{S}_4]$ clusters is reduced into a $[\text{Fe}_4\text{S}_4]^{1+}$ state ($S=1/2$) and the reduced cluster is spin coupled with the Ni(III) center resulting in an EPR silent state. This proposal implies that the previously determined redox potential, -220 mV, for the disappearance of Ni-Signal A [2] is actually the mid-point redox potential for

one of the $[\text{Fe}_4\text{S}_4]$ clusters. Such a mechanism is supported by the optical studies which indicate that the activation process involves the reduction of iron-sulfur clusters. Preliminary Mössbauer data (our unpublished results in collaboration with B.H. Huynh) also show that approximately one $[\text{Fe}_4\text{S}_4]$ cluster is reduced in the EPR silent state and it is possible to recognize the normal "signature" of the reduced 3Fe cluster.

The events which follow the EPR silent state are the appearance of both the *Ni-Signal C* and the "g=2.21" signal. In accordance with the heterolytic mechanism of hydrogen activation, we propose that in the presence of the natural substrate a hydride intermediate state is obtained. The nickel center is assigned as the hydride binding site and the $[\text{Fe}_4\text{S}_4]^{1+}$ cluster is the proton binding site. The spin coupling between the Ni(III) and the $[\text{Fe}_4\text{S}_4]^{1+}$ cluster is broken in this hydride intermediate, originating *Ni-Signal C*. Thus, this signal is assumed to represent the hydride-bound Ni(III) center and the g=2.21 is attributed to the proton-bound $[\text{Fe}_4\text{S}_4]^{1+}$ cluster. Alternatively, the g=2.19 EPR signal could be due to a transient Ni(III) state in a different coordination, resulting from the breaking of the coupling and the g=2.21 signal could be due to the interacting Ni(III) and $[\text{Fe}_4\text{S}_4]^{1+}$ centers bound to hydride and proton, respectively. By further incubation with H_2 the *Ni-Signal C* disappears, suggesting reduction to Ni(II) with the concomitant development of reduced $[\text{Fe}_4\text{S}_4]$ center signals.

ACKNOWLEDGEMENTS

We thank Drs. T. Lissolo, B.H. Huynh, H.D. Peck Jr., and D.V. DerVartanian for very interesting discussions. This research was supported by grants from Instituto Nacional de Investigação Científica, Junta Nacional de Investigação Científica e Tecnológica, AID Grant 936-5542-G-SS-4003-00 and NATO Grant 0341/83.

REFERENCES

- [1] J. LeGall, P.O. Ljungdahl, I. Moura, H.D. Peck Jr., A.V. Xavier, J.J.G. Moura, M. Teixeira, B.H. Huynh, D.V. DerVartanian, *Biochem. Biophys. Res. Commun.*, **106**, 610-616 (1982).
- [2] M. Teixeira, I. Moura, A.V. Xavier, D.V. DerVartanian, J. LeGall, H.D. Peck Jr., B.H. Huynh, J.J.G. Moura, *Eur. J. Biochem.*, **130**, 481-484 (1983).
- [3] J.J.G. Moura, I. Moura, B.H. Huynh, H.J. Krüger, M. Teixeira, R.C. DuVarney, D.V. DerVartanian, A.V. Xavier, H.D. Peck Jr., J. LeGall, *Biochem. Biophys. Res. Commun.*, **408**, 1388-1393 (1982).

- [4] J.J.G. Moura, M. Teixeira, I. Moura, A.V. Xavier, J. LeGall, *J. Mol. Cat.*, **23**, 303-314 (1984).
- [5] M. Teixeira, I. Moura, A.V. Xavier, B.H. Huynh, D.V. DerVartanian, H.D. Peck Jr., J. LeGall, J.J.G. Moura, *J. Biol. Chem.* (1985) in press.
- [6] R. Cammack, D. Patil, R. Aguirre, E.C. Hatchikian, *FEBS Lett.*, **142**, 289-292 (1982).
- [7] T. Lissolo, S. Pulvin, D. Thomas, *J. Biol. Chem.*, **259**, 11725-11729 (1984).



MSI.2 — MO

S.P.J. ALBRACHT
J.W. VAN DER ZWAAN
R.D. FONTIJN
E.C. SLATER
Laboratory of Biochemistry
University of Amsterdam
P.O. Box 20151, 1000 HD Amsterdam
The Netherlands

HYDROGENASE FROM *CHROMATIUM VINOSUM*: THE REDOX STATES OF NICKEL AND THE IRON-SULPHUR CLUSTER DURING CATALYSIS

The presence of nickel in a purified hydrogenase was first reported in 1981 by Graf and Thauer [1] for the enzyme from *Methanobacterium thermoautotrophicum*. EPR spectroscopy [2] showed that virtually all nickel was present as low-spin Ni(III) which could be reduced with H_2 . No signals due to Fe-S clusters were observed. Hydrogenase from *Chromatium vinosum*, also a nickel-enzyme, clearly displays two signals in the g=2 region which could be ascribed to Fe-S clusters [3]. An analysis of the 4 different EPR signals that can be detected in the enzyme as isolated led to the following hypothesis [3-5]. The preparation contains intact and defect enzyme molecules. Defect molecules, which are unreactive in the standard activity assays with viologens, contain one Ni(III) ion and one $[\text{3Fe-xS}]^{\text{ox}}$ cluster. Two forms of Ni(III), Ni-a and Ni-b, can be detected. Their ratio varies from preparation to preparation. In-

tact molecules, fully reactive in the activity assay, contain one Ni(III) ion and one $[4\text{Fe-4S}]^{3+}$ cluster. As with the defect enzyme molecules, the same two forms of nickel, in the same ratio, are present. Only one form of the $[4\text{Fe-4S}]^{3+}$ cluster is observed. The two $S=1/2$ systems of Ni(III) and $[4\text{Fe-4S}]^{3+}$ in intact molecules are spin-coupled, giving rise to complicated, frequency-dependent EPR spectra of both paramagnets. As a result of the coupling, the spin relaxation of Ni(III) increases dramatically, causing its signal to broaden above 20 K. The strength of the coupling (approximately 0.01 cm^{-1}) indicates a mutual distance of at most 1.2 nm. We have now succeeded in transforming defect enzyme molecules into intact ones and vice versa. We failed to demonstrate a dependence of added Fe or S ions during the reconstitution of defect molecules, although a conversion of a 3Fe to a 4Fe cluster is strongly suggested by changes in the EPR spectra. We have also been able to convert Ni-b to Ni-a.

The oxidised form of intact enzyme as isolated does not readily react with H_2 . Immediate activation takes place upon reduction with reduced viologens. Studies on the enzyme at oxidation-reduction potentials down to -480 mV revealed that nickel can exist in three, possibly 4, different redox states: the 3^+ , 2^+ , 1^+ and possibly the zero-valent state. The 1^+ state is unstable: oxidation to Ni(II) occurs in the absence of H_2 . If H_2 is present, reduction to another EPR silent state, possibly Ni(0), takes place. The low-valency states are re-oxidised to Ni(II) in a few milliseconds by benzyl viologen. Oxygen induces a re-oxidation to Ni(III) within 100 ms. Hydrogen, possibly as a hydride ion, is present in the direct coordination sphere of Ni(I). The EPR spectra indicate that H_2 can reduce the Fe-S cluster to the $[4\text{Fe-4S}]^+$ state.

REFERENCES

- [1] E.-G. GRAF, R.K. THAUER, *FEBS Lett.*, **136**, 165-169 (1981).
- [2] S.P.J. ALBRACHT, E.-G. GRAF, R.K. THAUER, *FEBS Lett.*, **140**, 311-313 (1982).
- [3] S.P.J. ALBRACHT, K.J. ALBRECHT-ELLMER, D.J.M. SCHMEDDING, E.C. SLATER, *Biochim. Biophys. Acta*, **681**, 330-334 (1982).
- [4] S.P.J. ALBRACHT, M.L. KALKMAN, E.C. SLATER, *Biochim. Biophys. Acta*, **724**, 309-316 (1983).
- [5] S.P.J. ALBRACHT, J.W. VAN DER ZWAAN, R.D. FONTIJN, *Biochim. Biophys. Acta*, **766**, 245-258 (1984).



MS1.3 — MO

ROBERT A. SCOTT

School of Chemical Sciences
University of Illinois
Urbana, IL 61801
U.S.A.

MELVIN CZECHOWSKI

DANIEL V. DERVARTANIAN

JEAN LEGALL

HARRY D. PECK JR.

Department of Biochemistry
University of Georgia
Athens, GA 30602
U.S.A.

ISABEL MOURA

Centro de Química Estrutural
Universidades de Lisboa
I.S.T., 1000 Lisbon
Portugal

NICKEL X-RAY ABSORPTION SPECTROSCOPY OF *DESULFOVIBRIO GIGAS* HYDROGENASE

INTRODUCTION

Several recent studies have begun to elucidate the coordination environment of the nickel active site in various hydrogenases. Ni extended X-ray absorption fine structure (EXAFS) results on the oxidized form of the *Desulfovibrio gigas* (*Dg*) hydrogenase [1] and the F_{420} -reducing hydrogenase of *Methanobacterium thermoautotrophicum* (*Mt*) [2] suggest that both of these Ni(III) sites are ligated to the protein through mainly sulfur-containing residues. H_2 reduction of the *Dg* hydrogenase caused a shift of the Ni K edge position to lower energy, indicating redox cycling of the Ni (probably Ni(III) \leftrightarrow Ni(II)) [1]. Electron spin echo envelope modulation (ESEEM) measurements on the two different *Mt* hydrogenases provided evidence for a "distant" (not directly ligated) nitrogen atom in the F_{420} -reducing enzyme but not in the methylviologen (MV)-reducing enzyme [3]. These hydrogenases also contain Fe-S clusters, with one 3Fe and two $[4\text{Fe-4S}]$ clusters having

been identified in the *Desulfovibrio desulfuricans* enzyme [4]. The presence of 3Fe clusters is of considerable interest due to the possibility that magnetic coupling between Ni(III) and a paramagnetic 3Fe cluster may give rise to the "g=11.35" electron paramagnetic resonance (EPR) signal in the partially reduced *Dg* hydrogenase [5].

As part of our continuing effort to structurally characterize the Ni site of *Dg* hydrogenase at various levels of oxidation, we report here higher quality Ni EXAFS data of the oxidized (as isolated) protein showing the presence of heterogeneity of Ni-ligand distances.

EXPERIMENTAL

All XAS data were collected at Stanford Synchrotron Radiation Laboratory (SSRL) on beam line VII-3 under dedicated operation at 3.0 GeV (*ca.* 60 mA) using Si[220] monochromator crystals. Enzyme data were collected at *ca.* 4 K as fluorescence excitation spectra using an array of NaI (Tl) scintillation detectors similar to the one previously described [6]. The Ni EXAFS data for oxidized *Dg* hydrogenase consist of an average of 13 30-minute scans on a sample containing *ca.* 4 mM Ni.

[Ni(en)₃]Cl₂·2H₂O (en = ethylenediamine) and [Ni(mnt)₂](Bu₄N) (mnt = maleonitriledithiolate) were examined as models for Ni-N (or -O) and Ni-S interactions, respectively. Ni EXAFS data on these models were collected at room temperature by transmission techniques at SSRL on beam line VII-3 under parasitic conditions at 1.88 GeV (*ca.* 15 mA) using Si[220] monochromator crystals. The empirical amplitude and phase representing Ni-N and Ni-S scattering were extracted from the EXAFS of these models by complex Fourier backtransformation [7], using the known distances and coordination numbers (Ni-N: R=2.124 Å [8], N=6; Ni-S: R=2.146 Å [9], N=4). Debye-Waller factors for the hydrogenase fits are then quoted as $\Delta\sigma^2$ values, relative to these models.

RESULTS AND DISCUSSION

Fig. 1a shows the Fourier transform (FT) of the Ni EXAFS data of oxidized (as isolated) *Dg* hydrogenase. The prominent feature in the FT is the first-shell peak at $R' \approx 1.6$ Å. This FT peak

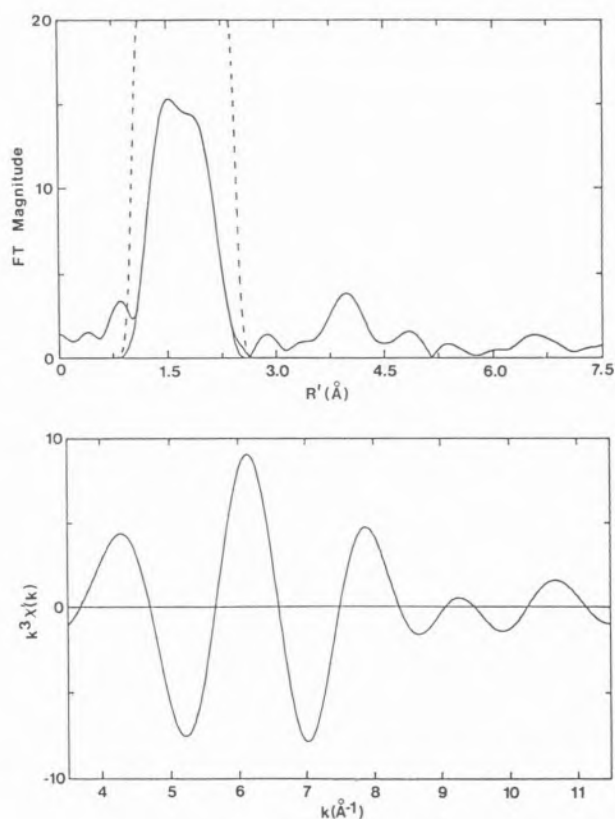


Fig. 1

Ni EXAFS of oxidized (as isolated) *Desulfovibrio gigas* hydrogenase collected at 4 K.

a) Fourier transform ($k=3.5-11.5$ Å⁻¹, k^3 weighting) of Ni EXAFS.

b) Filtered EXAFS generated by using the filter window represented by the dashed lines in a) and Fourier backtransformation

was also observed in our previous data [1] but the higher quality and extended FT range of the data in Fig. 1 reveal that this peak is actually split, indicating the existence of at least two shells of atoms in the first coordination sphere. This splitting is too small for the peaks to be individually extracted (by Fourier filtering) so that their assignment must be done by simulation (curve-fitting) which is discussed below. Fourier filtering these first-shell peaks yields the filtered EXAFS data shown in Fig. 1b. The beat pattern (node at $k \approx 9$ Å⁻¹) is another reflection of the split first-shell FT peak.

No attempt was made to analyze the FT peak at $R' \approx 4.0$ Å (Fig. 1a). This peak may or may not represent a scatterer, which would lie *ca.* 4.3-4.5 Å from the Ni atom. One would not typically ex-

pect to observe a scatterer at such a long distance unless the Debye-Waller factor is very small, which is possible in this case since these data were collected at 4 K.

Table I summarizes the results of a number of (curve-fitting) simulations to the Fourier-filtered data (Fig. 1b). These simulations were generated assuming either 6- or 4-coordination of the Ni atom with various combinations of (N,O) or S ligand atoms. (Coordination numbers were fixed as integers while the distance and $\Delta\sigma^2$ were optimized). The tabulated *f* values can be used to gauge the relative quality of the simulations, the lower *f* representing the better fit. By this criterion the only reasonable combinations of ligand atoms were two shells of S atoms (S,S' fits) or one shell of S and one shell of (N,O) atoms (S, (N,O) fits). (The single-shell S fits 1,8 (Table I) give much worse *f* values by a factor of 2-3.) Also, judging by *f* values, the 4-coordinate simulations are significantly worse than the 6-coordinate. This leaves fits 2-7 (Table I) as the most reasonable structural models of the Ni first coordination sphere. (The

distributions of ligand atoms in Table I were the ones yielding the lowest *f* values for 6-coordinate (S,S') and (S, (N,O)) fits.) The *f* values for these simulations do not allow a choice to be made among these possibilities, but examination of some of the optimized values of the parameters does.

In the (S, (N,O)) fits, the optimized Ni-(N,O) distance is in a typical range for Ni(III) [10,11], but the σ^2 values are significantly below that of the Ni(II) model, [Ni(en)₃]Cl₂·2H₂O. M-N bonds are typically very rigid showing little temperature dependence between 4 K and *ca.* 200 K (cf., Cu(II)-N interactions in cytochrome *c* oxidase [12]). Thus, unless the Ni-N interaction of Ni(en)₃²⁺ is unusually "soft", one would expect the Ni-(N,O) $\Delta\sigma^2$ values to be nearer to zero. Also, M-S σ^2 values are expected to be much more temperature dependent [12] and given a reasonable M-S vibrational frequency of *ca.* 325 cm⁻¹ [13] one can estimate a Ni-S $\Delta\sigma^2$ of -0.006 Å². The Ni-S $\Delta\sigma^2$ values of fits 5-7 (Table I) are significantly higher than this estimate which would have to be ratio-

Table I
Curve-fitting Results for the Filtered Ni EXAFS of Oxidized Dg Hydrogenase

Fit	Ni-S			Ni-S'			Ni-(N,O)			<i>f</i> ^{c)}
	R ^{a)} (Å)	N	$\Delta\sigma^2$ ^{b)} (Å ²)	R (Å)	N	$\Delta\sigma^2$ (Å ²)	R (Å)	N	$\Delta\sigma^2$ (Å ²)	
<i>Six-coordinate:</i>										
1	2.20	(6) ^{d)}	+0.0082							1.47
2	2.23	(5)	+0.0012	2.06	(1)	-0.0067				0.64
3	2.26	(4)	-0.0015	2.09	(2)	-0.0043				0.66
4	2.28	(3)	-0.0035	2.12	(3)	-0.0024				0.69
5	2.22	(4)	+0.0028				1.92	(2)	-0.0087	0.54
6	2.23	(3)	+0.0005				1.93	(3)	-0.0071	0.60
7	2.24	(2)	-0.0023				1.94	(4)	-0.0061	0.75
<i>Four-coordinate:</i>										
8	2.20	(4)	+0.0051							1.85
9	2.24	(3)	-0.0038	2.08	(1)	-0.0087				0.97
10	2.28	(2)	-0.0069	2.12	(2)	-0.0059				0.98
11	2.31	(1)	-0.0095	2.15	(3)	-0.0025				1.01
12	2.21	(3)	+0.0016				1.92	(1)	-0.0100	1.21
13	2.23	(2)	-0.0026				1.94	(2)	-0.0100	1.01
14	2.24	(1)	-0.0073				1.95	(3)	-0.0090	1.29

a) R = distance; N = coordination number.

b) $\Delta\sigma^2$ is the mean square deviation in R relative to the model compounds.

c) $f = \left[\sum_{i=1}^N [k^3 (\chi_{\text{obs}}^{(i)} - \chi_{\text{calc}}^{(i)})]^2 / (N-1) \right]^{1/2}$

d) Values in parentheses were not optimized.

nalized as a large static disorder ($\Delta R \approx 0.16 \text{ \AA}$ [13]) in the Ni-S shell. Such a static disorder is explicitly considered in the (S,S') fits 2-4 (Table I), where two shells of S atoms allow a reasonable fit of the data ($f \approx 0.7$) with reasonable distances (2.3 and 2.1 \AA) and reasonable Debye-Waller factors (for fits 3 and 4). The $\Delta\sigma^2$ values (e.g., for fit 4) are still higher than the previous estimate, but such quantitative comparisons will have to await an actual temperature-dependent EXAFS study of several Ni-S and Ni-N model compounds.

SUMMARY

The most likely composition for the first coordination sphere of the Ni(III) site in oxidized *Desulfovibrio gigas* hydrogenase is $\text{NiS}_m\text{S}'_n$, where $(m+n)=6$, $m=3$ or 4, $n=3$ or 2, $R(\text{Ni-S}) \approx 2.27 \text{ \AA}$, $R(\text{Ni-S}') \approx 2.10 \text{ \AA}$. It is possible that N- or O-containing ligands are also coordinated (with $R[\text{Ni-(N,O)}] \approx 1.93 \text{ \AA}$) but the quality of the current data does not allow valid conclusions from such three-shell fits.

REFERENCES

- [1] R.A. SCOTT, S.A. WALLIN, M. CZECHOWSKI, D.V. DERVARTANIAN, J. LEGALL, H.D. PECK JR., I. MOURA, *J. Am. Chem. Soc.*, **106**, 6864-6865 (1984).
- [2] P.A. LINDAHL, N. KOJIMA, R.P. HAUSINGER, J.A. FOX, B.K. TEO, C.T. WALSH, W.H. ORME-JOHNSON, *J. Am. Chem. Soc.*, **106**, 3062-3064 (1984).
- [3] S.L. TAN, J.A. FOX, N. KOJIMA, C.T. WALSH, W.H. ORME-JOHNSON, *J. Am. Chem. Soc.*, **106**, 3064-3066 (1984).
- [4] H.-J. KRÜGER, B.H. HUYNH, P.O. LJUNGDAHL, A.V. XAVIER, D.V. DERVARTANIAN, I. MOURA, H.D. PECK JR., M. TEIXEIRA, J.J.G. MOURA, J. LEGALL, *J. Biol. Chem.*, **257**, 14620-14623 (1982).
- [5] J. LEGALL, P.O. LJUNGDAHL, I. MOURA, H.D. PECK JR., A.V. XAVIER, J.J.G. MOURA, M. TEIXEIRA, B.H. HUYNH, D.V. DERVARTANIAN, *Biochem. Biophys. Res. Commun.*, **106**, 610-616 (1982).
- [6] S.P. CRAMER, R.A. SCOTT, *Rev. Sci. Instrum.*, **52**, 395-399 (1981).
- [7] R.A. SCOTT, *Meth. Enzymol.*, submitted for publication.
- [8] The structure of the chloride salt was assumed to be the same as that for the sulfate salt:
MAZHAR-UL-HAQUE, C.N. CAUGHLAN, K. EMERSON, *Inorg. Chem.*, **9**, 2421-2424 (1970).
- [9] R. EISENBERG, in S.J. LIPPARD (ed.), «Progress in Inorganic Chemistry», vol. 12, Wiley, New York, 1970, pp. 295-369.
- [10] M.J. VAN DER MERWE, J.C.A. BOEYENS, R.D. HANCOCK, *Inorg. Chem.*, **22**, 3489-3490 (1983).
- [11] K. NAG, A. CHAKRAVORTY, *Coord. Chem. Rev.*, **33**, 87-147 (1980).
- [12] R.A. SCOTT, J.R. SCHWARTZ, S.P. CRAMER, in «Inorganic and Biochemical Perspectives of Copper Coordination Chemistry», Proc. 2nd SUNY Albany Conf., Adenine, New York, 1985, in press.
- [13] B.-K. TEO, R.G. SHULMAN, G.S. BROWN, A.E. MEIXNER, *J. Am. Chem. Soc.*, **101**, 5624-5631 (1979).



MS1.4 — MO

DANIEL V. DERVARTANIAN
HANS J. KRUGER*
H.D. PECK, JR.
J. LEGALL

Department of Biochemistry
University of Georgia
Athens, Georgia 30602
U.S.A.

THE REACTIVITY OF THE NICKEL-CONTAINING HYDROGENASE FROM *DESULFOVIBRIO GIGAS* WITH OXYGEN, DEUTERIUM AND CARBON MONOXIDE

The periplasmic hydrogenase from *D. gigas* has been purified to homogeneity [1] and shown to contain 11-12 iron-sulfide atoms per 89 kDa [1,2]. In the native, isolated state, a rhombic EPR signal with g-values at 2.31, 2.20 and 2.00 is found which has been unequivocally identified as a Ni(III) species by the observation of hyperfine coupling in ^{61}Ni -substituted hydrogenase [3]. In the presence of hydrogen the initial Ni(III) species disappears and is replaced by a new EPR signal with g-values at 2.19, 2.16 and 2.00 assigned to a proposed Ni(III)-hydride intermediate [1,2]. In

* Present Address: Department of Chemistry, Harvard University, Cambridge, Massachusetts.

order to obtain additional information on the nature of the nickel EPR signals in the isolated and hydrogen-reduced states, hydrogenase has been reacted with oxygen, deuterium and carbon monoxide in order to probe these nickel EPR signals and ascertain their function in the catalysis of hydrogenase.

Reaction with Oxygen

The new EPR signal seen on binding of hydrogen with hydrogenase suggested that the gaseous ligand, O_2 , might also bind with hydrogenase and affect the nickel component. When O_2 (100%) was allowed to react with isolated hydrogenase for 3 hours, no immediate and significant changes were observed either on the initial Ni(III) EPR signal or that of the isotropic $g=2.02$ EPR signal (assigned by Mössbauer spectroscopy to a $3Fe-xS$ cluster, refs. 1,2). However, when the effect of increasing microwave power on the Ni(III) and $g=2.02$ EPR signals was studied, it was found that the power saturation curve (Fig. 1) for the Ni(III) signal of hydrogenase in the presence of O_2 was significantly greater than in the absence of O_2 . No such effect in the power saturation curve for the $g=2.02$ EPR signal was observed, suggesting that O_2 was sensed by the Ni(III) component but not by the $3Fe-xS$ cluster. Since O_2 is a paramagnetic species, the possible binding of O_2 to the nickel component could result in an additional spin-relaxation mechanism. A similar set of power saturation curves in the absence and presence of O_2 has been observed for the nickel-iron-sulfur containing hydrogenase from *Desulfovibrio desulfuricans* which also contains 1 nickel and 11-12 iron-sulfur atoms per 78 kDa [4].

Reaction with Deuterium

In order to ascertain whether the nickel species observed on binding of hydrogen to hydrogenase could represent a Ni(III)-hydride intermediate, studies were performed in which deuterium replaced hydrogen. A control experiment showed that extensive dialysis of hydrogenase against D_2O caused no change whatsoever to the initial Ni(III) EPR signal with g-values at 2.31, 2.20 and 2.00. Hydrogenase which had been dialyzed against

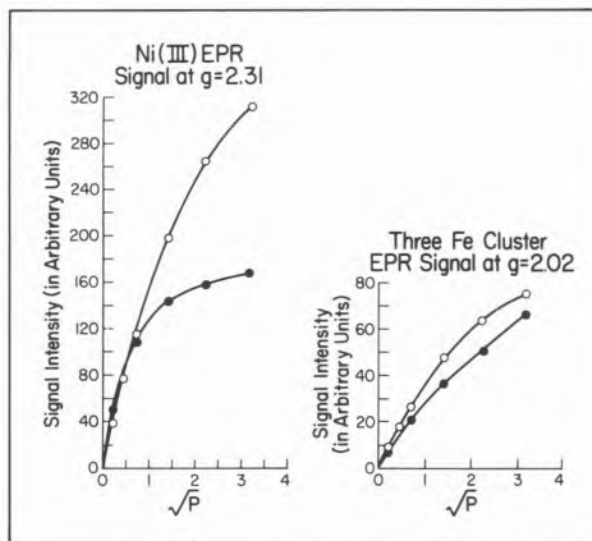


Fig. 1

Effect of microwave power on the signal intensity of the $g=2.31$ and $g=2.02$ EPR signals of *D. gigas* hydrogenase. Enzyme purified according to ref. [1] ($100 \mu M$ in protein and $150 mM$ in potassium phosphate buffer, pH 7.6) was either exposed to pure nitrogen for 3 h (●) or to pure oxygen (○) for 3 h. EPR spectroscopy was performed with a Varian E-109 spectrometer equipped with an Air-Products APD-E automatic temperature controller and interfaced with a Hewlett-Packard HP-85 microcomputer. EPR conditions: temperature, 12K; microwave frequency, 9.157 GHz; modulation amplitude, 10 gauss; time constant, 0.1 sec; scanning rate, 250 gauss per min

D_2O was then reduced for 3 hours with D_2 and compared with respect to its EPR spectra to hydrogenase dialyzed against H_2O and reduced with H_2 for 3 hours. Fig. 2A) versus 2B) shows a small narrowing in the D_2 -reduced hydrogenase relative to H_2 -reduced enzyme. The narrowing corresponds to 2 gauss in the $g=2.19$ region and 3 gauss in the $g=2.00$ region. Although the differences are quite small, the experiments have been repeated on three separate occasions, and it is now probable that the narrowing found in the D_2 -reduced hydrogenase is significant. Although other explanations for this narrowing are possible (water or hydroxide binding to the nickel component), another possible explanation is that hydrogen is bound to the Ni(III) species with g-values at 2.19, 2.16 and 2.00. This latter explanation is also consistent with the well-known heterolytic activation for hydrogenase first reported by KRASNA and RITTENBERG [5] and the dependence of this effect on D_2 .

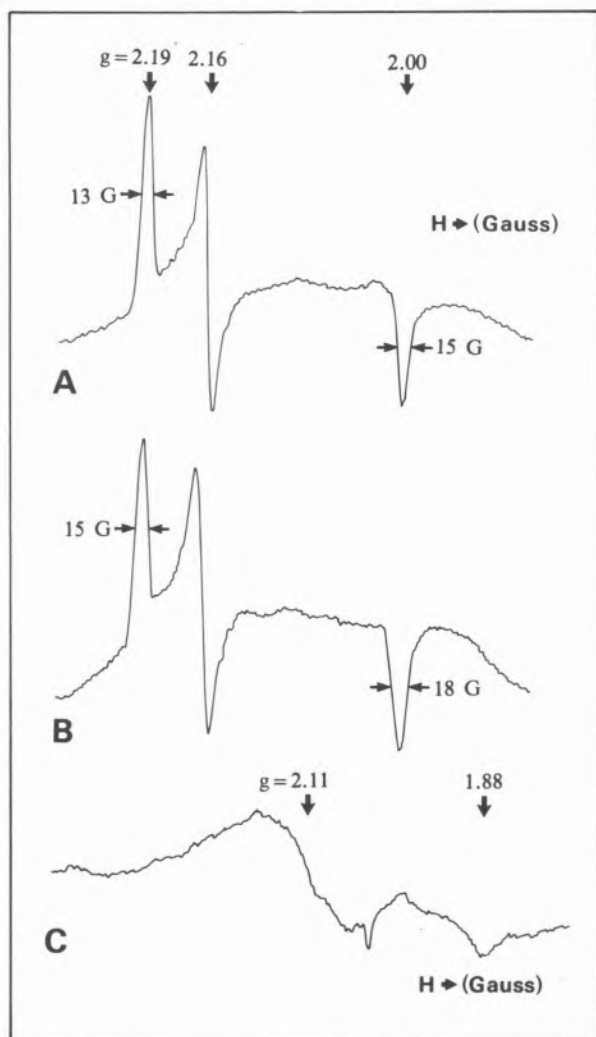


Fig. 2

- A) *D. gigas* hydrogenase (protein concentration as in fig. 1) dialyzed against D_2O , and reduced with D_2 for 3 hours
- B) As A) but dialyzed against H_2O and reduced with H_2 for 3 hours. EPR conditions for A) and B) as in fig. 1 except that temperature was 61K; microwave power, 10 mW; modulation amplitude, 5 gauss; scanning rate, 125 gauss per min and microwave frequency, 9.161 GHz
- C) *D. gigas* hydrogenase (protein concentration as in fig. 1) reduced with H_2 for 3 hours, and then reacted with CO for 10 minutes. EPR conditions as in fig. 1 except that microwave power was 10 mW

Reaction with Carbon Monoxide

Carbon monoxide has been found to be an effective competitive inhibitor for the *D. gigas* hydrogenase ($K_i=0.35 \mu M$, Lissolo and LeGall, unpublished results). A possible site of inhibition for CO might involve the nickel component of the hydrogenase. To test this possibility, CO was

reacted with both the oxidized (native) hydrogenase and the H_2 -reduced enzyme. No effect of CO was noted on the EPR signals of isolated enzyme, that is, no changes were noted in the EPR signals of the initial Ni(III) species or the isotropic $g=2.02$ species. However, when CO was added to the H_2 -reduced enzyme, there was a loss of the $g=2.19, 2.16, 2.00$ EPR signal and a new somewhat broad signal appeared with a major g -value of 2.11 (Fig. 2C). This signal could be detected as high as 90K and therefore appears to be a complex of CO with the nickel component. The effect of CO on the EPR spectrum of hydrogenase is reversible as vacuum evacuation of the CO-treated hydrogenase restores the initial EPR spectrum. When treated with H_2 , the EPR signals of the proposed Ni(III)-hydride species reappear with the same intensity as with non-CO treated hydrogenase. These observations demonstrate that the binding of CO with hydrogenase is a completely reversible process and are consistent with the kinetic finding that CO is a competitive inhibitor. They are also consistent with a role for nickel in the activation of hydrogen.

The EPR spectral changes observed when hydrogenase is reacted with O_2 , D_2 or CO implicate nickel as a possible functional binding site for these reactants as well as its substrate, H_2 . These studies are being continued with various nuclear isotopes of the reactants in order to establish in an unequivocal manner the nature of the interactions with nickel. The function of nickel in hydrogenase appears to be two-fold: i. involvement in catalytic activity as indicated by our studies with D_2 and CO, and ii. reversible inactivation of the hydrogenase as suggested by the results obtained with O_2 .

ACKNOWLEDGEMENTS

This work was supported by a grant from the National Science Foundation (PCM-8111325) to J.L., D.V.D. and H.D.P.

REFERENCES

- [1] J. LeGALL, P.O. LJUNGDAHL, I. MOURA, H.D. PECK JR., A.V. XAVIER, J.J.G. MOURA, M. TEIXEIRA, B.H. HUYNH, D.V. DERVARTANIAN, *Biochem. Biophys. Res. Commun.*, **106**, 610 (1982).

- [2] M. TEIXEIRA, I. MOURA, A.V. XAVIER, D.V. DERVARTANIAN, J. LEGALL, H.D. PECK JR., B.H. HUYNH, J.J.G. MOURA, *Eur. J. Biochem.*, **130**, 481 (1983).
- [3] J.J.G. MOURA, I. MOURA, B.H. HUYNH, H.J. KRUGER, M. TEIXEIRA, R.C. DUVARNEY, D.V. DERVARTANIAN, A.V. XAVIER, H.D. PECK JR., J. LEGALL, *Biochem. Biophys. Res. Commun.*, **108**, 1388 (1982).
- [4] H.J. KRUGER, B.H. HUYNH, P.O. LJUNGAHL, A.V. XAVIER, D.V. DERVARTANIAN, I. MOURA, H.D. PECK JR., M. TEIXEIRA, J.J.G. MOURA, J. LEGALL, *J. Biol. Chem.*, **257**, 14620 (1982).
- [5] A.I. KRASNA, D. RITTENBERG, *J. Am. Chem. Soc.*, **76**, 3015 (1951).



MS1.5 — MO

J.R. LANCASTER, JR.
K. GILLIES
K.R. ROGERS
Department of Chemistry and Biochemistry
Utah State University
Logan, Utah 84322
U.S.A.

BIOENERGETIC ROLE OF NICKEL-CONTAINING PROTEINS IN METHANOGENS

In 1978, PETER MITCHELL received the Nobel Prize in Chemistry for the postulate that free energy released from favorable electron transfer is conserved in the form of a transmembrane ion gradient, which is subsequently utilized to drive ATP synthesis for cellular energy needs [1]. This is broadly accepted as a valid general description of all systems described to date involving coupling to electron transfer.

The methanogenic bacteria are the sole biological source of methane, and most species are capable of energy conservation by coupling to the eight-electron reduction of CO₂ by H₂. In 1980, we reported the presence in the particulate fraction of *M. bryantii* of several EPR-detectable centers, including the first observation of Ni(III) in a biological system [2]. These findings were interpreted

as evidence for the existence of a membrane-bound electron transfer complex involved in energetic coupling of methanogenesis to proton translocation. The subsequent demonstration by other laboratories of the presence of similar centers in purified soluble hydrogenases from several methanogens [3-5] and our repeated failure to demonstrate energy-coupled ion gradient formation in subcellular extracts has prompted us to re-examine our earlier conclusions. We report here data which does not support the presence of a tightly membrane-bound electron transfer complex in at least one methanogen species. This raises the possibility that ATP synthesis coupled to electron transfer occurs by a direct mechanism, not involving the obligatory intermediacy of a transmembrane ion gradient.

We have verified our previous results, that ultracentrifugation of cell free extracts results in the sedimentation of several EPR-identifiable components (including substantial amounts of the Ni(III) center) and in addition virtually all of the factor F420-reducing hydrogenase, ATPase, and methane-forming activities (see below). Addition of either molecular H₂ or reduced factor F420 results in reduction of all EPR centers, indicating that all such centers are involved in electron transfer between these two species (data not shown).

Since most methanogens derive useful energy from methane production by hydrogen reduction of CO₂, it might be expected that components essential for this reaction would be present in all such organisms. Table I shows a summary of a species survey of EPR-detectable components in the particulate fraction of various methanogens cultured on several growth substrates.

Table I
Species survey of EPR-visible particulate centers in methanogens

Methanogen	g = 2.02		g = 1.94	
	(ox)	Ni(III)	Radical	(red)
<i>M. bryantii</i>	+	+	+	+
<i>M. thermoauto.</i>	+	+	+	+
<i>M. barkeri</i> (acetate)	+	+	+	+
<i>M. barkeri</i> (H ₂ -CO ₂)	+	+	—	+
<i>M. ruminantium</i>	+	—	+	—
<i>M. hugateii</i>	+	—	+	—
<i>M. voltae</i> (H ₂ -CO ₂)	+	—	—	—
<i>M. voltae</i> (formate)	+	—	—	—

The only component universally present is a $g=2.02$ oxidized species, with temperature and power saturation characteristics of an oxidized Fe³ or Fe⁴ iron-sulfur center, quite possibly due to nonphysiological oxidation by oxygen exposure. Three of the six methanogen species exhibit an oxidized Ni(III) center, along with a « $g=1.94$ »-type reduced iron-sulfur species. It should be pointed out that in most such systems the majority of nickel is EPR silent, so that lack of such an EPR signal does not necessarily indicate absence of the center. We conclude from these results that the particulate fraction of several methanogens contains EPR-identifiable electron transfer components and also that many of these components are present under differing growth conditions (cf. acetate-grown *M. barkeri* and H₂-CO₂-grown *M. bryantii*).

Electron microscopic and other studies show the presence in this particulate fraction from *M. thermoautotrophicum* of enclosed membranous structures. However, complete resolution of hydrogenase activity from the membrane (as judged by labeling with C¹⁴ mevalonic acid [6]) can be achieved by gel exclusion chromatography, showing that this electron transfer reaction is not tightly membrane-bound (data not shown). This does not, however, rule out the possibility that some portion of the complete electron transfer chain from H₂ and CO₂ to CH₄ is responsible for ion translocation and therefore membrane-bound. In order to investigate this, we examined the subcellular localization of methanogenesis from H₂ and CO₂ (fig. 1). Fig. 1A shows that all such electron transfer activity is quantitatively recovered in the crude particulate fraction, *i.e.*, the preparation described above containing the EPR-observable components. Fig. 1B shows that further centrifugation of this resuspended pellet (under conditions where approx. 80% of the membranes are sedimented) results in no loss of methanogenic activity. In addition, none of the EPR-identifiable components are sedimented (not shown). The recent elimination of internal membrane structures as responsible for methanogenesis [7] argues against the possibility that this small relative fraction of the membrane is selectively associated with electron transfer.

We conclude from these studies that while metha-

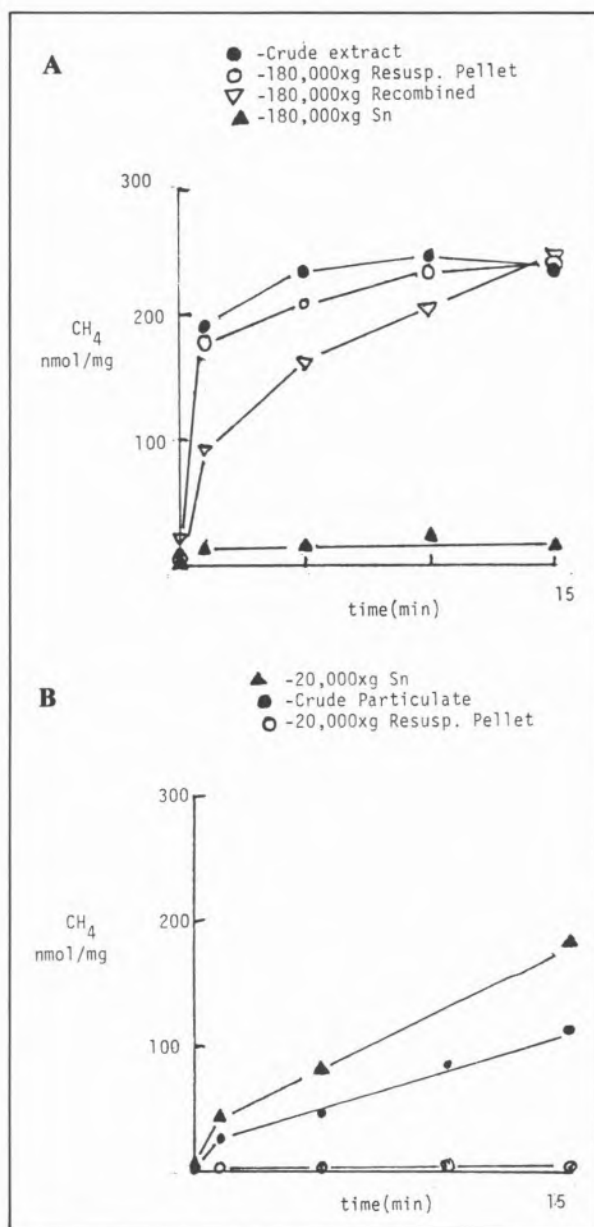


Fig. 1

Subcellular location of methanogenic activity. A) Crude particulate (180,000 xg 2 1/2 hr.). B) separation of membranes by centrifugation of resuspended pellet from A) at 20,000 xg for 1 hr. Methanogenesis measured under an atmosphere of H₂:CO₂ (80%:20%) at 60°C in 0.2M Na PIPES buffer (pH 6.9 at 25°C in air), 2 mM ATP, 2 mM MgCl₂, 2 mM methyl coenzyme M in a total volume of 0.5 mL. Protein concentration ranged from 10 to 28 mg/mL.

nogenic electron transfer can be sedimented by a relatively high-speed ultracentrifugation, there is no evidence that the membrane fraction contains a tightly-bound segment of the chain. These

results apparently explain the conflicting reports of the subcellular location of methanogenic activity [8,9].

ACKNOWLEDGEMENTS

We would like to thank W.B. WHITMAN and R.S. WOLFE for providing us with samples of the various methanogens mentioned in Table I.

This research was supported by a research grant from the Division of Biological Energy Research, U.S. Department of Energy, an American Heart Association Established Investigatorship Award, and the Department of Chemistry and Biochemistry, U.S.U.

REFERENCES

- [1] P. MITCHELL, *Biol. Rev.*, **41**, 445 (1966).
- [2] J.R. LANCASTER, *FEBS Lett.*, **115**, 285 (1980).
- [3] S.P.J. ALBRACHT, E.-G. GRAF, R.K. THAUER, *FEBS Lett.*, **140**, 311 (1982).
- [4] N. KOJIMA, J.A. FOX, R.P. HAUSINGER, L. DANIELS, W.H. ORME-JOHNSON, C. WALSH, *Proc. Natl. Acad. Sci. U.S.A.*, **80**, 378 (1983).
- [5] G. FAUQUE, M. TEIXEIRA, I. MOURA, P.A. LESPINAT, A.V. XAVIER, D.V. DER VARTANIAN, H.D. PECK JR., J. LE GALL, J.G. MOURA, *Eur. J. Bioch.*, **142**, 21 (1984).
- [6] G.D. SPROTT, K.M. SHAW, K.F. JARRELL, *J. Biol. Chem.*, **258**, 4026 (1983).
- [7] G.D. SPROTT, L.C. SOWDEN, J.R. COLVIN, K.F. JARRELL, *Can. J. Microbiol.*, **30**, 594 (1984).
- [8] R.P. GUNSALUS, R.S. WOLFE, *J. Bact.*, **135**, 851 (1978).
- [9] F.D. SAUER, S. MAHADEVAN, J.D. ERFLE, *Biochem. J.*, **221**, 61 (1984).

2. Mo-Biochemistry

Convener: R.N.F. Thorneley
(Brighton)



MS2.1 — TU

R.C. BRAY
G.N. GEORGE
School of Chemistry and Molecular Sciences
University of Sussex
Brighton, BN1 9QJ
U.K.

THE NATURE OF THE *VERY RAPID* INTERMEDIATE IN XANTHINE OXIDASE TURNOVER

Xanthine oxidase and xanthine dehydrogenase give rise during turnover to a transient molybdenum(V) EPR signal given the name *very rapid* [1]. The signal is seen with a variety of substrates. Evidence that it corresponds to a kinetically competent intermediate will be summarized. Studies of hyperfine coupling involving substitutions with deuterium, carbon-13, oxygen-17 and sulphur-33 have provided information both about the structure of the intermediate and about the origins and exchangeability of ligands of the metal in the intermediate. These and other data have permitted a likely mechanism for xanthine oxidase turnover to be proposed [2-4]. Additional experiments required to confirm the mechanism or to distinguish alternatives will be discussed. These include experiments in progress with molybdenum-95, molybdenum-97, mass spectrometry with oxygen-18 and rapid freezing EXAFS being carried out with Dr. S. Cramer, and ENDOR.

ACKNOWLEDGEMENTS

EPR facilities were provided by the M.R.C. and the work was supported by the S.E.R.C.

REFERENCES

- [1] R.C. BRAY, *Adv. Enzymol. Relat. Areas Mol. Biol.*, **51**, 107-165 (1980).
- [2] S. GUTTERIDGE, R.C. BRAY, *Biochem. J.*, **189**, 615-623 (1980).
- [3] R.C. BRAY, in R.C. BRAY, P.C. ENGEL, S.G. MAYHEW (eds.), «Flavins and Flavoproteins», de Gruyter, Berlin, 1985, pp. 707-722.
- [4] R.C. BRAY, G.N. GEORGE, *Biochem. Soc. Trans.* (1985), in press.



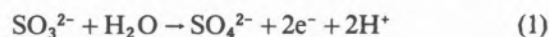
MS2.2 — TU

JOHN H. ENEMARK
W.E. CLELAND JR.
Department of Chemistry
University of Arizona
Tucson, Arizona 85721
U.S.A.

DAVID COLLISON
FRANK E. MABBS
Chemistry Department
University of Manchester
Manchester M13 9PL
England

APPROACHES TO THE MOLYBDENUM CENTERS OF «OXO-TYPE» ENZYMES

Molybdenum is an essential trace element which is found in enzymes such as xanthine oxidase, sulfite oxidase, and nitrate reductase. The chemical reactions catalyzed by these enzymes all involve a change in the number of oxygen atoms in the substrate as illustrated in (1), the oxidation of sulfite to sulfate. There is strong evidence that these

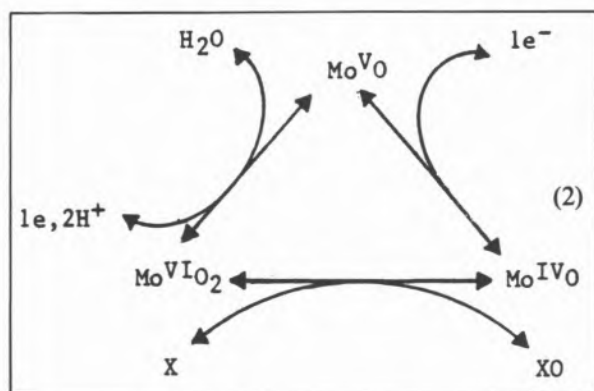


enzymes possess a common molybdenum cofactor [1]. EXAFS studies support a monomeric molybdenum center with at least one terminal oxo group and at least two -SR ligands bound to the molybdenum atom [2].

An overall chemical reaction cycle for the oxo-molybdenum centers of such enzymes involving Mo(IV), Mo(V) and Mo(VI) is shown in (2). Berg and Holm [3] have developed an elegant chemical model for the oxo-transfer reaction between

Mo(IV) and Mo(VI) shown at the bottom of (2). Our interest has been in synthetic analogs for the EPR active Mo(V) species shown at the top of (2). These Mo(V) states can be detected by rapid freeze EPR experiments and can be stabilized by certain inhibitors [4].

The isolation and characterization of Mo(V) complexes which may be synthetic analogs of the Mo(V) states in enzymes are difficult because of the propensity of oxo Mo(V) complexes to dime-



rize in the presence of trace amounts of water to give diamagnetic products. Our approach to this problem has been to create a steric pocket for the molybdenum atom in order to inhibit such dimerization reactions.

A simple pocket shaped ligand is hydrotris(3,5-dimethylpyrazolyl)borate. Complexes of this ligand were extensively studied by TROFIMENKO [5], who was the first to isolate the oxo Mo(V) complex, LMoOCl₂ [6]. We have developed a better synthetic route to LMoOCl₂ and to other related monomeric oxo Mo(V) complexes, including several complexes which contain at least two thiolate ligands coordinated to the molybdenum atom.

All of these monomeric Mo(V) complexes are stable in the presence of water, and all undergo reversible one electron reductions to stable Mo(IV) complexes. The reduction potentials for the complexes span a range of about 1.2 volts and encompass the Mo(V)/Mo(IV) reduction potentials of xanthine oxidase, xanthine dehydrogenase and sulfite oxidase. This extensive series of stable Mo(V) complexes opens the way to study the kinetics of electron transfer reactions of the biologically important Mo(V)/Mo(IV) couple.

The EPR spectra of the LMoOXY complexes are markedly dependent upon the nature of the X and Y ligands coordinated to the molybdenum atom and show large hyperfine splittings due to ⁹⁵Mo. The LMoOX₂ complexes possess C_s symmetry with the oxo group, the molybdenum atom and one of the nitrogen atoms of the pyrazolylborate ligand lying in the mirror plane. Thus, the unique direction in these complexes is the vector normal to the mirror plane, (*i.e.*, normal to the MoO bond) not a vector parallel to the MoO bond as occurs in tetragonal oxo Mo(V) complexes. The EPR spectra of several complexes have been simulated, but a detailed understanding of the actual directions of the components of the g and A tensors in relation to the molecular coordinate system will require a complete single crystal EPR experiment.

The stable monomeric oxomolybdenum(V) complexes synthesized in this study provide good starting points for structural and spectroscopic models for the inhibited states of the «oxo-type» molybdenum enzymes.

ACKNOWLEDGEMENTS

We acknowledge support by the National Institutes of Environmental Health Sciences and the North Atlantic Treaty Organization.

REFERENCES

- [1] J.L. JOHNSON, in M. COUGHLAN (ed.), «Molybdenum and Molybdenum Containing Enzymes», Pergamon Press, New York, 1980, p. 347.
- [2] S.P. CRAMER, R. WAHL, K.V. RAJAGOPALAN, *J. Am. Chem. Soc.*, **103**, 7721 (1981);
J. BORDAS, R.C. BRAY, C.D. GARNER, S. GUTTERIDGE, S.S. HASNAIN, *Biochem. J.*, **199**, 499 (1980).
- [3] J.M. BERG, R.H. HOLM, *J. Am. Chem. Soc.*, **106**, 3035 (1984).
- [4] R.C. BRAY, *Adv. Enzymol. Relat. Areas Mol. Biol.*, **51**, 107 (1980).
- [5] S. TROFIMENKO, *Chem. Rev.*, **72**, 497 (1972).
- [6] S. TROFIMENKO, *Inorg. Chem.*, **10**, 504 (1971).



MS2.3 — TU

C. DAVID GARNER
JOHN R. NICHOLSON
STUART K. HAGYARD
JOHN CHARNOCK

The Chemistry Department
Manchester University
Manchester M13 9PL
England

COLIN F. MILLS
The Rowett Research Institute
Bucksburn, Aberdeen AB2 9SB
Scotland

COPPER-MOLYBDENUM SULPHUR CLUSTERS AND RELEVANCE TO MOLYBDENUM-INDUCED COPPER-DEFICIENCY IN RUMINANTS

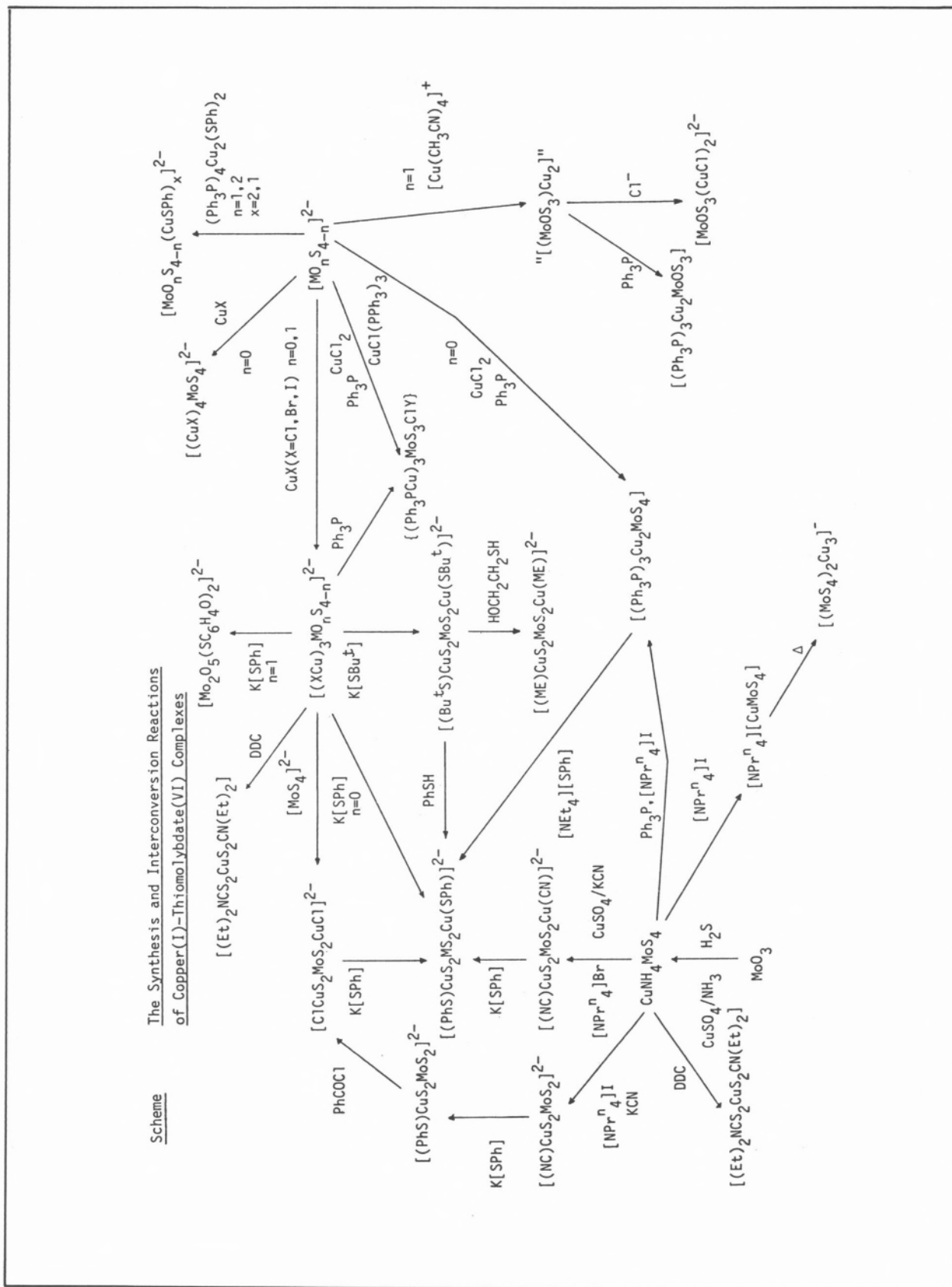
Although the tetrathiomallate(VI) ions $[MS_4]^{2-}$ ($M=Mo$ or W) were first isolated in the 1880's, their interesting ability to coordinate metal ions was not recognised until almost a hundred years later, for example when MÜLLER *et al.* prepared $[Ni(WS_4)_2]^{2-}$ [1]. The ions are extremely versatile ligands and have been shown to function as bidentate chelates to a wide variety of metal ions [2].

The first indication of the biological antagonism between Cu and molybdenum arose from the work of FERGUSON *et al.* [3] who found that the disease could be prevented or cured by feeding the animals with copper sulphate. The antagonistic effects of Mo on Cu metabolism in ruminants are synergised by a variety of dietary sources of sulphur both inorganic and organic [4], which can be metabolized *via* sulphide (*e.g.* $[SO_4]^{2-}$ or S-amino acids). The mechanisms of these interactions are not understood and the quantitative effects of dietary Mo and S sources upon absorption or retention by ruminants are poorly defined. However, the species specificity of the action of Mo as an antagonist of Cu absorption is related to the fact that, in contrast to ruminants, little opportunity exists in the digestive tract of non-ruminants for the generation of sulphide. Mo, given

as $[MoO_4]^{2-}$, is remarkably well-tolerated by non-ruminants [5]. In contrast, when $[MoS_4]^{2-}$ is given orally to rats, the effect on Cu metabolism closely reflect those found in ruminants, after ingestion of molybdenum, *i.e.* Cu absorption is inhibited and systemic inhibitory effects on Cu metabolism become evident [6]. Furthermore, $[MoO_2S_2]^{2-}$ and $[MoOS_3]^{2-}$ are capable of modifying the tissue distribution of absorbed Cu in rats. The presence of $[MoS_4]^{2-}$ has been demonstrated for *in vitro* incubations of rumen contents or microorganisms with added $[MoO_4]^{2-}$ and $[SO_4]^{2-}$ [7]. However, the formation of $[MoO_{4-n}S_n]^{2-}$ ($0 < n < 4$) *in vivo* in the rumen may be favoured over $[MoS_4]^{2-}$ by the rapid turnover rate of sulphide within this organ and the pH value of 6.5. Therefore, we have investigated the chemical interactions between Cu and $[MoO_{4-n}S_n]^{2-}$ ($n=2, 3$, or 4) ions to establish the nature of the species which are formed and their characteristic spectroscopic properties. A summary of these reactions is presented in the Scheme. The structures of key compounds have been determined by X-ray crystallography and a variety of spectroscopic studies have been accomplished. ^{95}Mo NMR, resonance Raman and EXAFS data each serve to characterise the nature of particular Cu-Mo-S aggregates and, therefore, may be useful as probes of the species formed *in vivo*.

REFERENCES

- [1] A. MÜLLER, E. DIEMANN, *J. Chem. Soc., Chem. Commun.*, 65 (1971).
- [2] A. MÜLLER, E. DIEMANN, R. JOSTES, H. BÖGGE, *Angew. Chem. Int. Ed. Engl.*, **20**, 934 (1981), and references therein.
- [3] W.S. FERGUSON, A.L. LEWIS, S.J. WATSON, *J. Agric. Sci.*, **33**, 44 (1943).
- [4] N.F. SUTTLE, in W.G. HOEKSTRA, J.W. SUTTLE, H.E. GANTHER, W. MERTZ (eds.), «Trace Element Metabolism in Animals», University Park Press, Baltimore, Maryland, p. 612.
- [5] C.F. MILLS, in «Biological Roles of Copper», Ciba Foundation 79. Published November 1980 by Excerpta Medica, pp. 49-69.
- [6] I. BREMNER, C.F. MILLS, *Phil. Trans. R. Soc. Lond.*, **B294**, 75 (1981), and references cited therein.
- [7] T.T. EL-GALLAD, C.F. MILLS, I. BREMNER, R. SUMMERS, *J. Inorg. Biochem.*, **18**, 323 (1983).





MS2.4 — TU

EDWARD I. STIEFEL

Corporate Research Science Laboratories
 Exxon Research and Engineering Company
 Clinton Township, Route 22 East Annandale, NJ 08801
 U.S.A.

MOLYBDENUM-SULFUR STRUCTURAL, REDOX AND REACTION CHEMISTRY

In all well characterized Mo enzymes molybdenum is found associated with sulfur ligands. The sulfur can be inorganic (probably S^{2-} , but possibly S_2^{2-}) or organic (thiolate or thioether ligands). Results from the literature on enzyme and model systems will be juxtaposed to identify some of the structural and mechanistic possibilities in xanthine oxidase, sulfite oxidase and nitrogenase.

Redox reactions are an important part of the reactivity of Mo-S systems. Both the Mo and the S components of the complexes are potentially redox active. In oxo molybdenum complexes this reactivity manifests itself in the reduction of Mo(VI) to Mo(V) or Mo(IV) by thiol — disulfide interchange reactions. A potential intermediate complex containing a partially oxidized dithiolate (a partial disulfide) and a partially reduced mononuclear Mo(VI) center has also been identified [1]. In di- and trinuclear Mo clusters reactions of coordinated S_2^{2-} can occur without changing the metal oxidation state and/or without significantly altering the complex geometry.

The ability of both Mo and S to change oxidation states is sometimes manifested in internal redox processes that can be induced by external redox agents. Induced internal redox behavior can lead to seemingly paradoxical reactions such as the reduction of the metal center in a complex by addition of an oxidant. For example, hexavalent $Mo^{VI}S_4^{2-}$ reacts with the oxidant R-S-S-R to yield the dinuclear pentavalent $Mo^V_2S_4(S_2)_2^{2-}$ ion [2]. MoS_4^{2-} reacts with $R_2NC(S)S-S(S)CNR_2$ (thiuramdisulfide) to give $Mo^VS_2(S_2CNR_2)_3$ an EPR active

mononuclear Mo(V) complex. The implications of internal electron transfer in Mo-S chemistry and the possible ramifications for Mo enzymes will be discussed.

The trinuclear complex $Mo_3S_4(SCH_2CH_2S)_3^{2-}$ prepared by ligand redox from $Mo_3S(S_2)_6^{2-}$ has an M_3S_4 core which is a fragment of a thiocubane structure [3]. This M_3S_4 stoichiometric unit has been identified in Fe-S proteins and vibrational spectroscopic properties of the Fe proteins compared to those of the Mo complex [3] suggest a structure for the biocluster.

Finally, Mo-S complexes display unconventional reactivity toward H_2 [4] and substituted acetylenes [4,5]. For example, substituted acetylenes have been found to insert into Mo-S₂ linkages to produce complexes with Mo-C and S-C bonds [5]. The relative reactivity of molybdenum, sulfur and multicenter sites will be considered with regard to the mode in which Mo enzymes interact with their substrates.

REFERENCES

- [1] J.M. BERG, D.J. SPIRA, K.O. HODGSON, A.E. BRUCE, K.F. MILLER, J.L. CORBIN, E.I. STIEFEL, *Inorg. Chem.*, **23**, 3412 (1984).
- [2] W.-H. PAN, M.A. HARMER, T.R. HALBERT, E.I. STIEFEL, *J. Am. Chem. Soc.*, **106**, 459 (1984).
- [3] T.R. HALBERT, K. MCGAULEY, W.-H. PAN, R.S. CZERNUSCEWICZ, E.I. STIEFEL, *J. Am. Chem. Soc.*, **106**, 1849 (1984).
- [4] M. MCKENNA, L.L. WRIGHT, L. TANNER, R.C. HALTIWANGER, M.R. DUBOIS, *J. Am. Chem. Soc.*, **105**, 5329 (1983) and references therein.
- [5] T.R. HALBERT, W.-H. PAN, E.I. STIEFEL, *J. Am. Chem. Soc.*, **105**, 5476 (1983).



MS2.5 — TU

BARBARA K. BURGESS
 JUDITH F. RUBINSON
 JAMES L. CORBIN
 MICHAEL J. DILWORTH

Department of Molecular Biology and Biochemistry
 University of California
 Irvine CA 92717
 U.S.A.

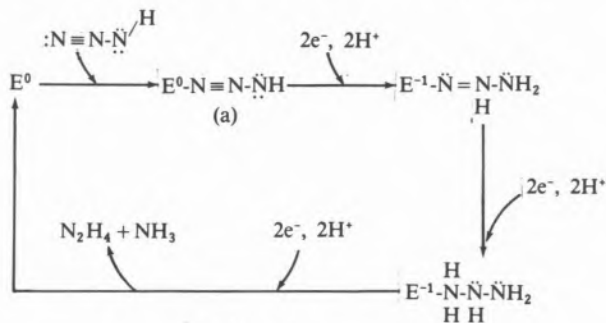
AZIDE REDUCTION BY *AZOTOBACTER VINELANDII* NITROGENASE

Nitrogenase (N_2 ase) is composed of two separately purified proteins, the molybdenum-iron (MoFe) protein and the iron (Fe) protein. Nitrogen fixation requires both proteins, a reductant, protons and MgATP. The Fe protein is generally accepted as a specific one-electron donor for the MoFe protein, which is believed to contain the site of substrate binding and reduction. N_2 ase also catalyzes the reduction of protons and a number of non-physiological substrates including azide.

The two-electron reduction of azide to $N_2 + NH_3$ by N_2 ase was first demonstrated by SCHÖLLHORN and BURRIS in 1967 [1]. In 1981 DILWORTH and THORNELEY [2] additionally demonstrated a six-electron reduction of azide to $N_2H_4 + NH_3$ and showed that a large relative excess of NH_3 was formed. The molar ratio of the products was $\sim 1 N_2H_4 : 2 N_2 : 5-6 NH_3$. We have examined the reduction of azide by the purified component proteins of *Azotobacter vinelandii* (*Av*) N_2 ase [3].

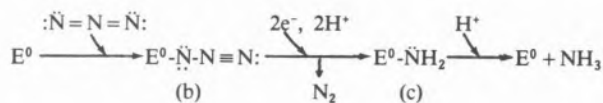
We have shown that one of the two species present in azide solutions, HN_3 , is a potent substrate ($K_m = 12 \mu M$) which is reduced by six electrons to $N_2H_4 + NH_3$. Like the six-electron reduction of N_2 , HN_3 reduction does not yield any less highly reduced products which implies the presence of tightly bound intermediates. Scheme 1 shown here is a possible mechanism for HN_3 reduction. The

substrate $:N \equiv N - \ddot{N}H$ (unlike N_3^- , see below) is expected to bind to a metal atom in the enzyme to give species (a) which has the N_2 triple bond closest to the metal atom. Scheme 1 involves three sequential, two-electron, two-proton reductions of that triple bond and is similar to mechanisms we have proposed previously for the six-electron reduction of N_2 [4], HCN [5], and CH_3NC [6].



Scheme 1

Our data demonstrate that the other species present in solution, N_3^- , is the substrate for the two electron reduction of azide to give $N_2 + NH_3$. Unlike HN_3 , the substrate N_3^- ($:\ddot{N} = N = \ddot{N}:$) is symmetrical and is expected to be polarized on binding to a metal site in the enzyme to yield species (b) (Scheme 2), where the N_2 triple bond is now remote from the metal. Species (b) could be readily reduced by two electrons and two protons to yield N_2 and a bound amido species (c), which would rapidly be protonated to yield NH_3 . N_3^- is the only known anionic N_2 ase substrate and its reduction is the only example of a N_2 ase reaction requiring inequivalent numbers of protons and electrons.



Scheme 2

Our data strongly support the suggestion [7] that some of the N_2 formed (Scheme 2) is further reduced by six-electrons to give two NH_3 (excess NH_3). The evidence includes the observations that: (i) both N_2 and excess NH_3 formation depend on $[N_3^-]$ and not on $[HN_3]$; (ii) the excess NH_3 reaction is strongly inhibited by HN_3 which, in turn, is competitively inhibited by N_2 ; (iii) inhibition of the excess NH_3 reaction by HN_3 , CO

(and possibly N_2 and C_2H_2) causes a corresponding increase in the observed N_2 and most importantly, (iv) like N_2 reduction, but unlike any other N_2 ase substrate reduction, the formation of excess NH_3 is inhibited by D_2 , which gives a corresponding increase in observed N_2 . Our data also show that the N_2 formed from N_3^- reduction, which appears to be further reduced to two NH_3 , is not in equilibrium with N_2 in the gas phase. Thus, the N_2 must be formed close enough to the N_2 -reduction site to be rapidly trapped at that site.

REFERENCES

- [1] R. SCHÖLLHORN, R.H. BURRIS, *Proc. Natl. Acad. Sci. USA*, **57**, 1317-1323 (1967).
- [2] M.J. DILWORTH, R.N.F. THORNELEY, *Biochem. J.*, **193**, 971-983 (1981).
- [3] J.F. RUBINSON, B.K. BURGESS, J.L. CORBIN, M.J. DILWORTH, *Biochemistry*, (1984), in press.
- [4] B.K. BURGESS, S. WHERLAND, E.I. STIEFEL, W.E. NEWTON, *Biochemistry*, **20**, 5140-5146 (1981).
- [5] J.-G. LI, B.K. BURGESS, J.L. CORBIN, *Biochemistry*, **21**, 4393-4402 (1982).
- [6] J.F. RUBINSON, J.L. CORBIN, B.K. BURGESS, *Biochemistry*, **22**, 6260-6268 (1983).
- [7] R.W.F. HARDY, E. KNIGHT JR., *Biochim. Biophys. Acta*, **139**, 69-90 (1967).

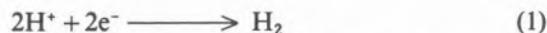


MS2.6 — TU

R.N.F. THORNELEY
D.J. LOWE
A.F.R.C. Unit of Nitrogen Fixation
University of Sussex
Brighton BN1 9RQ
U.K.

HYDROGEN AND NITROGEN INTERACTIONS AT THE ACTIVE SITE OF NITROGENASE

In the absence of N_2 , nitrogenase catalyses the reduction of protons to H_2 (eqn. 1).

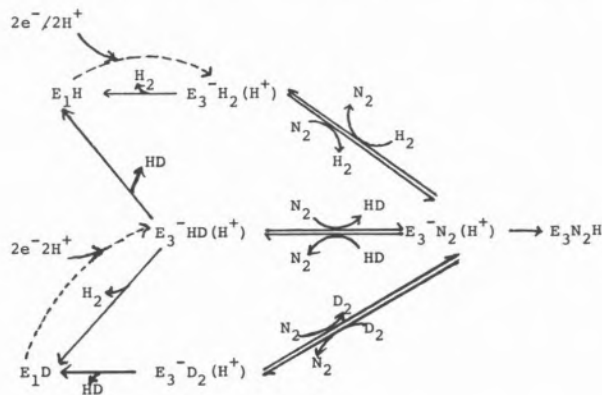


In the presence of N_2 , H_2 evolution is partially suppressed such that the limiting stoichiometry given by eqn. 2 is observed.



Nitrogenase also catalyses the formation of HD from D_2 in the presence of N_2 [1]; whether this reaction also occurs in the absence of N_2 is disputed [2]. However, Av nitrogenase does not cause significant incorporation of 3H into the aqueous phase when H_2 (50%) labelled with 3H , is used in the presence of 40% N_2 and 10% Ar [1]. Av nitrogenase functioning in the presence of N_2 and HD does not produce detectable amounts of D_2 . BURGESS [3] could not reconcile this result with N_2 binding to a site involving a metal trihydride as originally proposed by CHATT [4]. Although we consider that CHATT's view that N_2 binds H_2 displacement still provides the most likely explanation of the stoichiometry given by eqn. 2.

We have developed a comprehensive model for the mechanism of nitrogenase action [5-9]. A part of this model is shown in scheme 1 involving a metal (Mo?) dihydride species ($E_3^-H_2$) and an additional proton (H^+) bound to an adjacent group in the protein. This proton can react with the dihydride to yield H_2 but not directly with the metal centre to yield a trihydride. N_2 can displace H_2 and then D_2 can displace N_2 faster than D_2 displaces H_2 from the metal site. The relative rate of



Scheme 1

Proposed mechanism of N_2 binding and HD formation at the E_3 reduction level of *KpI*. This predicts that no D_2 is formed under HD/ N_2 , as described above, and that no T^+ enters the aqueous phase under T_2/N_2

this latter reaction will determine the extent of N_2 independent HD formation.

The total H_2 detected in a rapid quench experiment (curve a, Fig. 1) can be considered, according to scheme 2, to comprise two components (curves b and c, Fig. 1). Curve b simulates

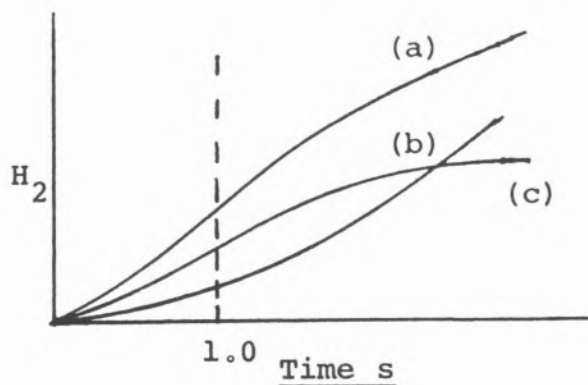
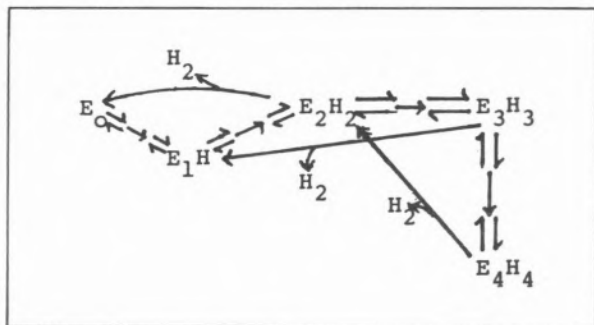


Fig. 1

Computer simulation of H_2 evolution

- a) Total H_2 on quenching; b) H_2 evolved at pH 7.4;
c) ΣH_2 from E_2 , E_3 and E_4 on quenching

the time course for H_2 evolution at pH 7.4. Curve c is the H_2 evolved after the reaction of the postulated hydridic-intermediates E_2 , E_3 and E_4 (scheme 2) with protons on quenching. If DCl/D₂O or



Scheme 2

The part of the LOWE-THORNELEY [6] scheme for nitrogenase that is concerned with H_2 evolution where $E_3H_2(H^+)$ in Scheme 1 is written as E_3H_3

NaOD/D₂O is used to quench functioning enzyme, a proportion of the products should be HD and/or D₂ providing there is rapid exchange of protons and solvent at the active site with the bulk solution.

Before quenching, only H_2 can be evolved. At time 1 s, the simulations of Fig. 1 predict that 33% H_2 would have been evolved before quenching, 33% would arise from E_2H_2 and 33% from $E_3H_3 + E_4H_4$ on quenching.

When Kp1 (110 μM), Kp2 (620 μM), with ATP (10 mM), MgCl₂ (10 mM), Na₂S₂O₄ (10 mM), Hepes (25 mM) at pH 7.4 23° was quenched after 1 s reaction under Ar or Ar + CO with DCl (1N) or NaOD (1N) to give a quenched solution containing 43% D₂O, 319 ± 20 nmol H_2 as produced. The computer prediction was 315 nmol H_2 (ΣH_2 with 1 equivalent H_2 from E_2 and E_3 , 2 equivalents H_2 from E_4H_4). No HD or D₂ was found (detection limit < 5%). We conclude that the exchange of protons and/or H₂O with the bulk H₂O at the H_2 evolution site is slow.

REFERENCES

- [1] B.K. BURGESS, S. WHERLAND, E.I. STIEFEL, W.E. NEWTON, *Biochemistry*, **20**, 5140-5146 (1981).
- [2] J.H. GUTH, R.H. BURRIS, *Biochemistry*, **22**, 5111-5122 (1983).
- [3] B.K. BURGESS, in C. VEEGER, W.E. NEWTON, (eds.) «Advances in Nitrogen Fixation Research», Nijhoff-Junk, The Hague, pp. 103-114 (1984).
- [4] J.C. CHATT, *Annu. Proc. Phytochem. Soc. Eur.*, **18**, 1-18 (1980).
- [5] R.N.F. THORNELEY, D.J. LOWE, *Biochem. J.*, **215**, 393-403 (1983).
- [6] D.J. LOWE, R.N.F. THORNELEY, *Biochem. J.*, **224**, 877-886 (1984).
- [7] R.N.F. THORNELEY, D.J. LOWE, *Biochem. J.*, **224**, 887-894 (1984).
- [8] D.J. LOWE, R.N.F. THORNELEY, *Biochem. J.*, **224**, 895-901 (1984).
- [9] R.N.F. THORNELEY, D.J. LOWE, *Biochem. J.*, **224**, 903-909 (1984).

3. Nucleic Acid Metal Ion Interactions

Convener: H. Sigel
(Basel)



MS3.1 — TU

R. BRUCE MARTIN
Chemistry Department
University of Virginia
Charlottesville, Virginia 22901
U.S.A.

METAL ION BINDING TO NUCLEOSIDES AND NUCLEOTIDES

In neutral solutions alkali and alkaline earth metal ions bind significantly to the phosphate group of nucleotides but only weakly to nucleosides. For transition metal ions the nucleotide nitrogen base and phosphate sites offer potentially competitive binding loci. Some transition metal ions such as Pd(II) and Pt(II) coordinate predominantly at nucleic base nitrogens of nucleotides while first transition row metal ions interact more strongly but not exclusively at the phosphate group. Because the phosphate group is no longer basic, it is a much weaker binding site in RNA and DNA polymers than in nucleotides [1].

In pyrimidine nucleosides metal ion binding occurs at N3. In purine nucleosides there is a dichotomy for metal ion binding between N1 and N7 that is pH dependent. For slowly exchanging diamagnetic metal ions such as Pd(II) and Pt(II), intensities of peaks in proton NMR spectra permit determination of relative mole fractions of all complexes present [2].

For rapidly exchanging metal ions of the first transition row, NMR methods are unsuitable for resolving the N1 versus N7 dichotomy. In addition, many of these metal ions are paramagnetic, and selective relaxation techniques hold pitfalls for binding site determinations in fused aromatic

rings. The N1 versus N7 dichotomy has been resolved for first transition row metal ions by recourse to linear stability constant logarithm versus pK_a plots for a variety of related ligands.

Stability constant logarithms for Ni^{2+} , Cu^{2+} , and Zn^{2+} binding at pyridine or purine N1 type nitrogens and imidazole or purine N7 type nitrogens display a linear relationship with pK_a for each metal ion and nitrogen type. The slopes of all lines vary only from 0.3 to 0.5. For all three aqueous metal ions and (dien)Pd²⁺, at the same pK_a , the stability constant for N7 binding is 0.8 to 1.2 log units stronger than for N1 binding. For neutral adenosine the N1 site is intrinsically 320 times more basic than the N7 site. However, for the above three aqueous metal ions the ratio of N1 to N7 bound adenosine complexes is projected to be 3, 2.5, and 1, respectively. Thus solutions of neutral adenosine and these aqueous metal ions contain comparable amounts of N1 metalated and N7 metalated complexes. The logarithm of intrinsic [N1]/[N7] binding ratios are listed in the Table. N7 coordination in purine bases predominates at low pH and gives way to favored N1 coordination for (dien)Pd²⁺, Cu^{2+} , and Zn^{2+} between pH 1.5 to 2.7 for adenosine, pH 6.1 to 6.7 for inosine, and pH 6.9 to 7.5 for guanosine [3,4].

Table
Intrinsic log ([N1]/[N7]) binding ratios

	Adenosine	Guanosine	Inosine
H ⁺	2.5	5.1	5.6
CH ₃ Hg ⁺	-0.1	2.7	3.3
(dien)Pd ²⁺	0.6		1.5
Ni ²⁺	0.5	0.8	1.0
Cu ²⁺	0.4	1.4	1.6
Zn ²⁺	0.0	1.0	1.2

REFERENCES

- [1] R.B. MARTIN in H. SIGEL (ed.), «Metal Ions in Biological Systems», vol. 8, M. Dekker, New York, 1979, p. 57.
- [2] K.H. SCHELLER, V. SCHELLER-KRATTINGER, R.B. MARTIN, *J. Am. Chem. Soc.*, **103**, 6833 (1981).
- [3] S.-H. KIM, R.B. MARTIN, *Inorg. Chim. Acta*, **91**, 19 (1984).
- [4] R.B. MARTIN, *Acc. Chem. Res.*, **18**, 32 (1985).



MS3.2 — TU

JEAN-CLAUDE CHOTTARD

Laboratoire de Chimie et Biochimie Pharmacologiques et Toxicologiques

UA 400

Université René Descartes

45, rue des Saints-Pères, 75270 Paris Cedex 06

France

PLATINUM OLIGONUCLEOTIDE MODELS OF PLATINUM-DNA INTERACTIONS

DNA is a primary target of the aquated forms of the antitumor drug *cis*-[PtCl₂(NH₃)₂] [1,2]. *In vitro* studies with various DNAs have shown that intrastrand crosslinking of two bases by the *cis*-Pt(NH₃)₂²⁺ moiety is the main type of reaction. The identified adducts from enzymatic digests correspond to platinum chelation by the two guanines and by the adenine and guanine of the following sequences: d(GpG) (more than 50% of the lesions) [3,4], d(ApG) [4], d(ApXpG) [4] and d(GpXpG) [4] (with X = A, C or T).

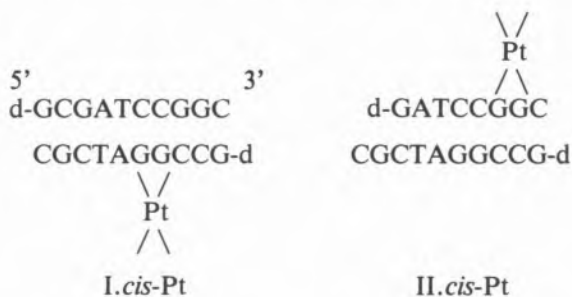
With model studies we address the following questions: i) Is platinum chelation by two adjacent bases sequence dependent? ii) To what extent does platinum chelation by two adjacent bases lead to a distortion of the DNA duplex?

i) We have compared XpG and GpX sequences. The XpG type has been studied with the CpG, d(pCpG) and ApG dinucleotides. In each case the guanine-N7 is platinated first. ApG gives only AN7-GN7 *anti,anti* platinum chelate, similar to the well known GpG adduct. CpG and d(pCpG) also give only one CN3-GN7 adduct with *Ganti*, that is a mixture of two interconverting *Csyn* and *Canti* conformers resulting of a partial rotation of the cytosine about the glycosidic and N3-Pt bonds [5].

The GpX type of sequence has been studied with the GpC, d(GpC), d(pGpC) and GpA dinucleotides. In each case the guanine-N7 is platinated first and the chelation leads to a complex mixture of adducts involving *syn* and *anti* isomers of the two bases. The GC dinucleotides give two couples

of GN7-CN3 chelates in different proportions: *Ganti*, *Csyn* and *anti*; *Gsyn*, *Csyn* and *anti* [6]. Each couple again results of a rotation of the cytosine, that could be demonstrated in the *Gsyn* case. GpA not only gives three GN7-AN7 chelates (*Ganti*, *Asyn* and *anti*; *Gsyn*, *Asyn*) but also one GN7-AN1 chelate presenting a partial rotation of the adenine about the glycosidic and N1-Pt bonds. These data together with the results of kinetic experiments show that despite the large conformational freedom of dinucleotides, *Ganti* N7-platinated XpG sequences are more prone to chelation by the adjacent X base than are the GN7-platinated GpX sequences. Examination of dinucleotide and double stranded DNA CPK models suggests that such a difference could be mainly due to the larger distance between the X binding site and the GN7-bound platinum within stacked conformations of GpX compared to XpG sequences. This could explain the identification of a d(ApG) but not a d(GpA) adduct in the platinated DNA digests [4].

ii) We have tested the possibility of duplex formation between short oligonucleotides with one of the strands bearing a d(GpG).*cis*-Pt chelate, either close to the middle or to one end of the sequence.



A stoichiometric mixture of the purified and characterized GG-platinated oligonucleotide with the complementary strand actually leads to the duplex structures I.*cis*-Pt and II.*cis*-Pt. This is shown by their UV and CD sigmoidal melting profiles and by their CD spectra of the B-DNA type. The presence of the platinum chelate lowers the T_m of the duplex structure from 58 to 49°C for I.*cis*-Pt and 55 to 28°C for II.*cis*-Pt [7]. ¹H NMR analysis of the exchangeable G-N1H and T-N3H protons in water shows the presence of the corresponding 10 and 8 hydrogen bonds respectively in I.*cis*-Pt and II.*cis*-Pt, indicating that base pairing is still pre-

sent for the platinated guanines and their adjacent bases. It also shows that for II.cis-Pt the imino protons of the three GC pairs of the platinated end are exchanged at 15°C indicating the occurrence of fraying at this end of the duplex. These results show that d(GpG) platinum chelation does not disrupt the DNA duplex structure and leads to a distortion quite similar to that of a kink [8] as can be seen with CPK models.

ACKNOWLEDGEMENTS

These results are due to the work of drs. J.-P. Girault and B. van Hemelryck, and to a tight cooperation with drs. J.-Y. Lallemand and E. Guittet (400 MHz NMR studies), G. Chottard (CD studies), J. Igolen and T. Huynh-Dinh (oligonucleotide synthesis). Support of this work by a grant from the «Association pour le Développement de la Recherche sur le Cancer» is gratefully acknowledged.

REFERENCES

- [1] J.J. ROBERTS, M.F. PERA JR., in S.J. LIPPARD (ed.), *ACS Symp. Series*, **209**, 1983, pp. 3-25.
- [2] J.-P. MACQUET, J.-L. BUTOUR, N.P. JOHNSON, H. RAZAKA, B. SALLES, C. VIEUSSENS, M. WRIGHT in M.P. HACKER, E.B. DOUPLE, I.H. KRAKOFF (eds.), «Platinum Coordination Complexes in Cancer Chemotherapy», Martinus Nijhoff Publishing, 1984, pp. 27-38.
- [3] A.-M.J. FICHTINGER-SCHEPMAN, P.H.M. LOHMAN, J. REEDIJK, *Nucl. Acid Res.*, **10**, 5345-56 (1982).
- [4] A. EASTMAN, *Biochemistry*, **22**, 3927-33 (1983).
- [5] J.-P. GIRAULT, G. CHOTTARD, J.-Y. LALLEMAND, F. HUGUENIN, J.-C. CHOTTARD, *J. Am. Chem. Soc.*, **106**, 7227-32 (1985).
- [6] J.-C. CHOTTARD, J.-P. GIRAULT, E.R. GUITTET, J.-Y. LALLEMAND, G. CHOTTARD in S.J. LIPPARD (ed.), *ACS Symp. Series*, **209**, 1983, pp. 125-145.
- [7] B. VAN HEMELRYCK, E.R. GUITTET, G. CHOTTARD, J.-P. GIRAULT, T. HUYNH-DINH, J.-Y. LALLEMAND, J. IGOLEN, J.-C. CHOTTARD, *J. Am. Chem. Soc.*, **106**, 3037-3039 (1984).
- [8] H.M. SOBELL, C.C. TSAI, S.C. JAIN, S.G. GILBERT, *J. Mol. Biol.*, **114**, 333-365 (1977).



MS3.3 — TU

JAN REEDIJK

Department of Chemistry
Gorlaeus Laboratories
State University Leiden
P.O. Box 9502, 2300 RA Leiden
The Netherlands

REACTIONS OF PLATINUM COMPOUNDS WITH NUCLEIC ACIDS AND OLIGONUCLEOTIDES

The use of *cis*-PtCl₂(NH₃)₂ and derivatives as anti-tumor drugs and the generally accepted view that binding of these drugs to DNA plays a key rôle in the cell-killing process continue to stimulate research in the area of nucleic acid-metal interactions.

Our current research program is focussed on the reaction of *cis*-PtCl₂(NH₃)₂ (abbreviated cisPt) and related compounds with DNA (from several sources; both *in vivo* and *in vitro*) and with oligonucleotides (up to 18 base pairs in well-defined sequences).

The reaction products are — after working up and purification — studied by enzymatic digestion (using exonucleases and endonucleases), HPLC in combination with AAS, NMR spectroscopy (high frequencies; proton decoupling and NOE techniques; pH dependent) and CD spectroscopy.

This paper will review our recent results in this area, not only including recent reviews [1,2] and papers [3-6], but also material not yet published. Our results obtained up to now can be summarized as follows:

1. The primary mode of attack of cisPt with DNA, G-containing oligonucleotides and in competition of nucleotides is always the N7 atom of guanine. This result has been obtained by a variety of groups.
2. The second mode of interaction (cisPt has two reactive coordination sites) with oligonucleotides of varying base sequences and with

- DNA appears to be (in decreasing order):
- A next neighbour N7 atom of a guanine (resulting in a cisPt(GG) chelate);
 - A 5' neighbour N7 atom of an adenine (resulting in a cisPt(AG) chelate);
 - Another N7 atom of a nearby guanine (resulting in either intrastrand, or inter-strand chelates cisPt(GNG) or cross-links cisPt(G)₂);
 - A cross-link with functional groups of a protein, forming a cisPt(G)(Protein) complex.
- The distortion of the double helix in case of chelation to two adjacent guanines in the same strand, *i.e.* in case of formation of cisPt(GG), is relatively small, as deduced from the fact that the Watson-Crick base pairs remain intact at ambient temperatures (seen from low field imino proton NMR spectra).
 - The kind of distortion in a double stranded helix for a decanucleotide with a GG-unit in the central part can best be described as a kink in the linear helix with an angle of about 40-70 degrees.
 - The distortion in double-stranded DNA after binding of cisPt (to a GG-unit) appears to be similar as deduced from ³¹P NMR measurements on double-stranded oligonucleotides and on DNA.
 - The distortion of the double helix in case of chelation by the unit GTG (binding through guanines) is different from a GG-chelate and apparently much more severe.

ACKNOWLEDGEMENTS

The sponsorship of our research from the Netherlands Foundation for Chemical Research (SON) and for Cancer Research (KWF) is gratefully acknowledged. Johnson & Matthey is thanked for generous loans of Platinum.

The colleagues and co-workers mentioned as co-authors in the references are kindly thanked for their valuable contributions.

REFERENCES

- A.T.M. MARCELIS, J. REEDIJK, *Recl. Trav. Chim. Pays-Bas*, **102**, 121 (1983).
- J. REEDIJK, J.H.J. DEN HARTOG, A.M.J. FICHTINGER-SCHPEMAN, A.T.M. MARCELIS, in M.P. HACKER *et al.* (eds.), «Platinum Coordination complexes in Chemotherapy», Nijhoff, Boston, 1984, p. 39.

- J.H.J. DEN HARTOG, C. ALTONA, J.H. VAN BOOM, J. REEDIJK, *FEBS Letters*, **176**, 393 (1984).
- J.H.J. DEN HARTOG, C. ALTONA, J.H. VAN BOOM, G.A. VAN DER MAREL, C.A.G. HAASNOOT, J. REEDIJK, *J. Am. Chem. Soc.*, **106**, 1528 (1984).
- J.H.J. DEN HARTOG, C. ALTONA, J.H. VAN BOOM, H. VAN DEN ELST, J. REEDIJK, *Inorg. Chem.*, submitted for publication.
- A.M.J. FICHTINGER-SCHPEMAN, J.L. VAN DER VEER, P.H.M. LOHMAN, J.H.J. DEN HARTOG, J. REEDIJK, *Biochemistry*, in press.



MS3.4 — TU

STEPHEN J. LIPPARD
Department of Chemistry
Massachusetts Institute of Technology
Cambridge, Massachusetts 02139
U.S.A.

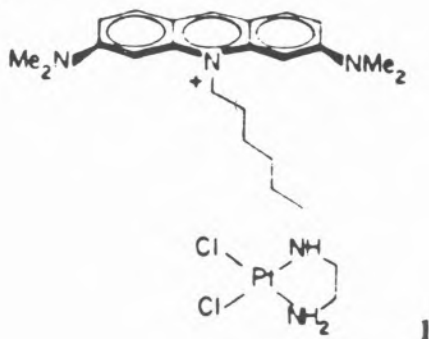
THE BINDING OF PLATINUM COMPLEXES TO DNA

The *cis* stereochemistry of the anticancer drug *cis*-diamminedichloroplatinum(II), *cis*-DDP, is essential for its biological activity [1]. The *trans* isomer is cytotoxic but has no antitumor effect. Numerous studies in our laboratory [2] and elsewhere [3] have demonstrated that the major adduct of *cis*-DDP with DNA, formed preferentially at low drug-to-nucleotide (D/N) ratios, is an intrastrand crosslink between adjacent guanosine residues. In this complex, the stereochemistry of which has been systematically probed by molecular mechanics calculations presented elsewhere at this conference [4], the [*cis*-Pt(NH₃)₂]²⁺ moiety makes two bonds to the N7 atoms of the guanine bases which coordinate in a head-to-head arrangement. The inactive *trans*-DDP complex cannot, for stereochemical reasons, form this adduct. What then are the preferred binding sites, if any, of *trans*-DDP on DNA and how might knowledge of these adducts sharpen our understanding of the

molecular mechanism of action of platinum anti-cancer drugs?

To address these questions we have used the large (Klenow) fragment of DNA polymerase I to map the binding of *trans*-DDP to M13mp8 viral DNA. Through this replication mapping approach [5] we confirmed that $(dG)_n$, $n \geq 2$, sequences are the major *cis*-DDP binding sites on DNA whereas considerably lower binding specificity is observed with the *trans* isomer. The *trans*-DDP molecules show a preference for $d(GNG)$ sequences, where N is any intervening nucleotide. Such an adduct has previously been proposed to be important for *cis*-DDP on the basis of forward mutagenesis experiments using the lac I system [6]. It is therefore curious that the replication mapping results reveal *trans*-DDP to form $d(GNG)$ adducts more readily than *cis*-DDP at comparably low D/N ratios. The stereochemistry of the binding of *trans*-DDP to short synthetic oligonucleotides has been further examined by NMR studies of chromatographically purified adducts, as will be described.

Previously we showed that the regioselectivity of the binding of *cis*-DDP to DNA depends critically upon the nucleotides flanking the $d(GpG)$ target site [7]. The binding sites can be switched and modulated by the presence of an external intercalating reagent, such as ethidium, during platination. This interesting stereochemical modulation of the sequence-dependent local structure of DNA has now been further elucidated through studies of the binding of newly synthesized platinum reagents, such as **1** below, in which the intercalator is chemically linked to *cis*-[Pt(en)Cl₂], en = ethylenediamine, by a polymethylene chain [8]. New DNA binding results with this and related «tethered» platinum complexes will be discussed.



REFERENCES

- [1] B. ROSENBERG, *Cancer Chemother. Rep.*, **59**, 589 (1975).
- [2] J.P. CARADONNA, S.J. LIPPARD, in M.P. HACKER, E.B. DOUPLE, I.H. KRAKOFF (eds.), «Platinum Complexes in Cancer Chemotherapy», Martinus Nijhoff, Boston (1984), p. 14 and refs. cited therein.
- [3] a) P.J. STONE, A.D. KELMAN, F.M. SINEX, M.M. BHARGAVA, H.O. HALVORSON, *J. Mol. Biol.*, **104**, 793 (1976);
b) J. REEDIJK, J.H.J. DEN HARTOG, A.M.J. FICHTINGER-SCHEPMAN, A.T.M. MARCELLIS, in M.P. HACKER, E.B. DOUPLE, I.H. KRAKOFF (eds.), «Platinum Complexes in Cancer Chemotherapy», Martinus Nijhoff, Boston (1984), p. 38.
- [4] J. KOZELKA, G.A. PETSKO, S.J. LIPPARD, G.J. QUIGLEY, *Rev. Port. Quím.*, **27**, ... (1985).
- [5] A. PINTO, S.J. LIPPARD, *Proc. Natl. Acad. Sci. USA*, in press.
- [6] J. BROUWER, P. VAN DE PUTTE, A.M.J. FICHTINGER-SCHEPMAN, J. REEDIJK, *Proc. Natl. Acad. Sci. USA*, **78**, 7010 (1981).
- [7] T.D. TULLIUS, S.J. LIPPARD, *Proc. Natl. Acad. Sci. USA*, **79**, 3489 (1982).
- [8] B.E. BOWLER, L.S. HOLLIS, S.J. LIPPARD, *J. Am. Chem. Soc.*, **106**, 6102 (1984).



MS3.5 — TU

G.L. EICHHORN
P. CLARK
Y.A. SHIN
J.J. BUTZOW
J.M. RIFKIND
R.P. PILLAI
P.P. CHUKNYISKI
D. WAYSBORT

Laboratory of Cellular & Molecular Biology, Gerontology Research Center
National Institute on Aging, National Institutes of Health
DHHS, Baltimore, MD 21224
U.S.A.

THE INFLUENCE OF METAL ION-NUCLEIC ACID INTERACTIONS ON GENETIC INFORMATION TRANSFER (G.I.T.)

One of the major concerns of our laboratory for many years has been the interaction of metal ions with nucleic acids, and the impact of these and

other metal interactions on genetic information transfer (GIT). All of the steps of this GIT require metal ions, and there is evidence that the metals may be involved in genetic regulation. Nevertheless, under certain conditions, these same metals are capable of introducing error into GIT. It is therefore of great importance to understand how metals can produce both the beneficial and the deleterious effects.

REACTIONS OF METALS WITH NUCLEIC ACIDS

Since the nucleic acids are the molecules primarily responsible for GIT, an understanding of the reactions of metals with nucleic acids can be of significance in understanding the effects of metals on GIT. We have found that metal ions can, in fact, have profound effects on nucleic acids, such as the degradation of RNA, the mispairing of bases, changes in macromolecular conformation; all of these have implications for GIT [1].

Different Metals.

Not all metals, however, produce all of these effects, and probably no two metals produce them at the same rate and to the same extent. The recognition of this fact leads to the realization that different metals can influence the nucleic acids very differently. And, of course, they do. Some metals stabilize double helices and other ordered structures, while other metals destabilize them. Some metal-nucleic acid complexes are in fast exchange with their products of dissociation, while others require much time for formation as well as dissociation. There are, of course, similarities among these complexes — *e.g.*, N-7 of purines is an important binding site for many metals (though not all). Yet the differences are very important.

Comparisons with Pt-DNA Reaction

The differences must be remembered in relating some of the above reactions to the chemistry of platinum-DNA complexes. These complexes have aroused great interest, as this symposium amply demonstrates, and justifiably so, because of the antitumor activity of «cisplatin». As a result, a great deal is now known about the Pt-DNA inter-

action, and it is sometimes assumed that this knowledge can be readily extrapolated to other metal-nucleic acid complexes.

RNA SYNTHESIS

GIT includes the synthesis of DNA, RNA and protein. We have focused on RNA synthesis with the *E. coli* RNA polymerase enzyme. This enzyme contains an intrinsic metal, zinc, at the initiation site, and a required activating metal — *e.g.*, magnesium — at the elongation site. At both sites a nucleoside triphosphate substrate is bound to the metal. The selection of substrate at both sites is guided by a DNA template, one of whose strands is copied through recognition of its bases by complementary substrates.

Structure at the Active Site

The distances from intrinsic metal to substrate at the initiation site and from activating metal to substrate at the elongation site have been previously determined by CHATTERJI and WU [2], and by BEAN, KOREN and MILDVAN [3], respectively. We have found that the template does not affect the structure at the elongation site, and CHATTERJI, WU, and WU [4] have shown that the template does affect the structure at the initiation site. These studies and our present ESR studies on the relationship between the metals on the two sites makes it possible to propose a map of the active site of the enzyme.

RNA Synthesis and Template Conformation

The conformational changes induced by metal binding to DNA affect RNA synthesis by RNA polymerase. We have followed the conformational change from B to Z DNA under a variety of conditions, and have found that changes in the rate of RNA synthesis precisely correlate with the conformational transition in every instance [5].

RNA Synthesis with Different Metals

A number of metal ions can satisfy the requirement for an activator at the elongation site [6]. Both *cis* and *trans*-[Pt(NH₃)₂Cl₂] inhibit RNA synthesis (*cis* much more than *trans*), and we have shown that the inhibition is due to reaction with

the DNA template [7]. The activating metals differ from each other in their ability to cause the enzyme to differentiate between correct and incorrect substrates.

INORGANIC STRUCTURE PROBES

We have shown some time ago that the ability of the enzyme to differentiate between the ribonucleoside and deoxynucleoside structures can be mimicked by the copper acetate dimer. The two oxygen ligands of a bridging acetate are displaced by two hydroxyl groups of the ribose on the ribonucleoside; the reaction cannot occur with a deoxynucleoside with only one hydroxyl. This reagent is therefore a ribonucleoside structure probe. We do not propose this reaction as a serious model for RNA polymerase in that we do not believe that the selection mechanism in the enzyme works in the same manner. Recent attempts to use a rhodium dimer in this way proved unsuccessful, but the rhodium dimer was able to differentiate between adenine and the other nucleotide bases by the formation of a π -bonded complex with the adenine.

REFERENCES

- [1] G.L. EICHORN, *Adv. Inorg. Biochem.*, **3**, 1 (1981).
- [2] D. CHATTERJI, F.Y.-H. WU, *Biochemistry*, **21**, 4657 (1982).
- [3] B.L. BEAN, R. KOREN, A.S. MILDVAN, *Biochemistry*, **16**, 3322 (1977).
- [4] D. CHATTERJI, K. WU, F.Y.-H. WU, *J. Biol. Chem.*, **259**, 284 (1984).
- [5] J.J. BUTZOW, Y.A. SHIN, G.L. EICHORN, *Biochemistry*, **23**, 4837 (1984).
- [6] V.W. ARMSTRONG, D. YEE, I. ECKSTEIN, *Biochemistry*, **18**, 4120 (1979).
- [7] R.C. SRIVASTAVA, J. FROELICH, G.L. EICHORN, *Biochimie*, **60**, 879 (1978).
- [8] N.A. BERGER, G.L. EICHORN, *Nature (New Biology)*, **239**, 237 (1972).



MS3.6 — TU

E.L. ANDRONIKASHVILI
M. KHARATISHVILI
Institute of Physics
Academy of Sciences of the Georgian S.S.R.
Tbilisi
U.S.S.R.

N. ESIPOVA
Institute of Molecular Biology
Academy of Sciences of the U.S.S.R.
Moscow
U.S.S.R.

INFLUENCE OF METAL IONS ON THE COOPERATIVITY OF DNA-PROTEIN INTERACTIONS

Complexes of numerous bivalent ions with DNA have been thoroughly studied. However, the role of metals in certain complex systems cannot be explained solely on the basis of experimental data obtained on binary DNA-Me²⁺ systems.

One should expect that gradual complication of the system under investigation may give an answer to the following question: at what level of the biological object organization the action of ions becomes sufficient for the biological effect?

In the present paper, the influence of Zn²⁺ ions on the DNA ability to enter into higher levels of structural organization is investigated by analysis of the circular dichroism (CD) spectra of DNA and its complexes with the antibiotic distamycine analogue distamycine-2 (Dm-2).

The distamycines possess high specificity with respect to A-T sequences of DNA and, owing to the presence of -CONH-groups, are widely used as a protein model in the investigations of nuclein-protein interactions. On distamycine binding with DNA, cooperative effects are observed pointing to the changes in DNA conformation making possible the further formation of the structures with higher organization level.

The results obtained in the present paper show that the joint action of Zn²⁺ ions and Dm-2 on DNA is not a mere sum of their separate actions.

This fact proves that Dm-2 alters the phase state of DNA, whereas Zn^{2+} ions cause a new «phase» transition in the latter. Here the observed changes in CD spectra may result from the DNA electronic state change occurring without any essential rearrangements in the secondary structure.

DNA undergoes a similar transition in polyethylene glycol solutions, as well, and it is known from the literature that sharp changes in CD spec-

tra are not accompanied by changes in the curves of X-ray diffuse scattering, which signifies the invariability of the DNA secondary structure.

The analysis of the observed phenomena allows us to come to the conclusion that the DNA complex with Dm-2 in the investigated conditions determines the formation of a specific phase in the system, and its state may be finely adjusted afterwards by adding Zn^{2+} .

4. *Uptake, Essentiality and Toxicity of the Chemical Elements*

Convener: J.J.R. Fraústo da Silva
(Lisboa)



MS4.1 — TH

J.J.R. FRAÚSTO DA SILVA

Centro de Química Estrutural
Instituto Superior Técnico
Lisbon
Portugal

AN INTRODUCTION TO THE MINISYMPOSIUM

This Minisymposium is concerned with the essentiality and toxicity of the chemical elements involving basic questions of the uptake, transport, metabolism and function of a group of metals and non-metals which include some of the least understood trace nutrients: vanadium, nickel, silicon, and selenium. Chromium was also in the original plan but the invited speaker was unable to be present.

Dr. Farago gives a general introduction to the Minisymposium discussing the uptake, essentiality and toxicity of metal ions towards higher plants and refers particularly to the case of metal-tolerant plants and to the internal mechanisms developed to ensure tolerance which have been the object of her work for some years. Some interesting cases of chemical speciation on the uptake are also considered.

Prof. Saltman describes what may be a fundamental mechanism for the mobilization and utilization of iron by biological systems: the direct reduction under aerobic conditions of low molecular weight Fe(III) complexes by hemoglobin and perhaps other heme proteins to form Fe(II) which can be incorporated into tetrapyrroles, iron-sulfur proteins and ferritin. The importance of ATP as a novel potential iron biological chelator is also

considered, extending the role of this bioenergetic intermediate.

Prof. Chasteen discusses, among other aspects, the oxidation state of vanadium in blood (which may have some connexions with the work of Prof. Saltman). He shows that vanadate is rapidly and quantitatively reduced *in vitro* to oxovanadium(IV) by fresh human serum and suggests that the metal is complexed and transported in this state by the iron transport protein transferrin and possibly also by albumin. Hence, the claim often made of a +5 extracellular oxidation state is not confirmed experimentally, although uptake appears to be preferred from the vanadate form.

It is perhaps worth to recall, for information, that this situation has a parallel in the two other cases in which vanadium has been shown to play an important biological role: that of the *Ascidacea* Tunicates and that of the *Amanita* mushrooms. In the case of the Tunicates, such as *Ascidia nigra* or *Phallusia mammilata*, vanadium seems to be taken up through the phosphate transport system and accumulated in the vanadocytes after reduction to VO^{2+} and then to V^{3+} , apparently as a aqua-complex. In the mushrooms, among which *Amanita muscaria* is outstanding, vanadium is again likely to be extracted from the soils as vanadate, but is present in the toadstool as a VO^{2+} complex of *N*-hydroxyiminodipropionate (amavadin). Our own work [1] has thrown some light on the reasons for the selection of this unusual ligand: possibly the more favourable competition of this low basicity polyamino carboxylate with the hydroxide ion to allow the formation of a 1:2 (ML_2) VO^{2+} complex at the pH of the mushroom. This complex may be a catalytic center of fast turnover, but its function is unknown.

Chromium is not discussed in this Minisymposium but a few comments will probably be in order. Indeed, recent research work has questioned well accepted hypothesis regarding the biological role of this metal. Chromium has been considered, for a number of years, to be a component of the "glucose tolerance factor" (GTF) and much work was devoted to the synthesis of models of GTF and to the assay of various chromium compounds and complexes as substitutes for GTF. However, it has shown that the active fractions of GTF extracted from brewers' yeast did *not* contain

chromium [2] and that the function of this substance could be reproduced by certain organic compounds containing amine groups at adequate distances and locations [3]. The possibility that chromium(III) acts only as a structural element promoting the formation of octahedral complexes with ligands which expose amino groups in *trans*-position to the outside of the coordination sphere is worth exploring. Of course, these results need to be confirmed and reconciled with the findings concerning the biological effects of chromium, particularly with the symptoms observed with animals submitted to Cr-deficient diets.

As for nickel, one of the most relevant findings in the last few years was the detection by EPR of a Ni(III) state in CO-dehydrogenase and in several bacterial hydrogenases [4], which raises some fundamental questions besides that of the actual function of this element. In urease (and also in the so called factor F-430 found in methanogenic bacteria) nickel is present in the Ni(II) state and it is considered to play a "normal" role of acid-base catalyst, although zinc is the almost universally preferred choice. The higher affinity for amines and the preference for octahedral arrangements may be determinant for the choice of nickel for the active site of urease, but the mechanisms suggested for its action do not make use of these more advantageous properties [5] and the reason why nickel was preferred to zinc remains unanswered. The detection of a Ni(III) state in bacterial hydrogenase is even more puzzling, particularly since Ni(III)/Ni(II) transitions appear to occur at very low negative redox potential (~ -0.5 V). This is hardly compatible with the extremely strong stabilisation of the Ni(III) state necessary to achieve a drop of over 4 V relative to the Ni(III)/Ni(II) couple in aqueous solution for which we have recently recalculated $E^\circ \sim 3.7$ V [6]. Further investigation of the problem is clearly necessary.

But it is again the Ni(III)/Ni(II) redox couple that is now considered to play a role in nickel carcinogenesis, following the demonstration that for peptides and human serum albumin it can participate in active oxygen biochemistry and toxicity at physiological conditions. This demonstration is part of an overview of physico-chemical, metabolic and molecular aspects of nickel carcinogenesis that Prof. Evert Nieboer presents in this Minisym-

posium, in which he provides experimental evidence supporting the hypothesis that bioavailability and compartmentalisation of Ni^{2+} are determinants of the deleterious effect of this element.

Two non-metal elements are also discussed at this Minisymposium: silicon and selenium, each of them with a well-defined and accepted general function.

Prof. Carlisle describes her extensive work on the role of silicon in the rate of bone formation and its importance in connective tissues, not limited to the structural role admitted in the past but also related to a defined function in the metabolism of glucosaminoglycans linked with the formation of cartilage and connective tissue.

It is perhaps interesting to mention here that many so called spring silicated waters in Portugal (waters in which the contents of silicate is of the order of the total amount of cations) are considered (by popular tradition or clinical observation) to have beneficial properties for the skin and to assist wound healing...

Still according to Prof. Carlisle, the fact that silicon reaches high levels in the mitochondria of osteogenic cells is also considered as an indication that this non-metal participates in the biochemistry of the sub-cellular enzyme containing structure of the cell. Again, these findings must be interpreted in the light of the thermodynamic predestination of a Si(IV) state for this element, which suggests that the metabolic role of silicon would be similar to that of phosphate, albeit more limited, even if some microorganisms, such as *Proteus mirabilis*, are able to synthesise compounds with Si-N and even Si-C bonds...

The last non-metal considered is selenium, which Dr. Shamberger has discussed extensively in a recent book [7]. With a well documented function as a biological specific anti-oxidant, associated to vitamin E, it is part of the defense system which protects unsaturated membrane phospholipids from the adverse effects of oxygen and its reduction products, particularly the $\cdot OH$ radical. Selenium has been more the concern of nutritionists than of bioinorganic chemists. The interesting aspects of its selection for biological functions is usually justified with the statement that it can catalyze 2-electron transfer reactions at a potential close to 0 V, contrary to what happens

with the transition metals (molybdenum excepted, but at lower negative potentials) [8]. Nevertheless, its current forms of occurrence (selenomethionine, Se-methylseleno-methionine, selenocysteine, selenocystine, *etc.*) point to mechanisms different from those involving two-electron cycling between *e.g.* selenate and selenite, unlikely to be naturally free in biological systems. This is undoubtedly an aspect which needs clarification and the contribution of Dr. Shamberger in the field of selenium biochemistry is timely and relevant.

These rather sketchy remarks should be regarded as no more than an introduction of the speakers and an attempt to provide a framework to the contents of this necessarily limited minisymposium, focussing, but not exclusively, on some less common biological elements. It is hoped that it will prove to be as interesting and stimulating for the participants not so much concerned with the aspects of essentiality and toxicity as it will certainly be for the researchers in this area of bioinorganic chemistry.

REFERENCES

- [1] J. FELCMAN, J.J.R. FRAÚSTO DA SILVA, M. CÂNDIDA T.A. VAZ, *Inorg. Chim. Acta*, **93**, 101 (1984).
- [2] S.J. HAYLOCK, P.D. BUCKLEY, L.F. BLACKWELL, *J. Inorg. Biochem.*, **19**, 105 (1983).
- [3] J.A. COOPER, L.F. BLACKWELL, P.D. BUCKLEY, *Inorg. Chim. Acta*, **92**, 23 (1984).
- [4] G. FAUKE, M. TEIXEIRA, I. MOURA, P. LESPINAT, A.V. XAVIER, D. DER VARTANIAN, H. PECK JR., J. LE GALL, J.J.G. MOURA, *Eur. J. Biochem.*, **142**, 21 (1984).
- [5] N.E. DIXON, P.W. RIDDLES, C. GAZZOLA, R.L. BLAKELEY, B. ZERNER, *Can. J. Biochem.*, **58**, 1335 (1980).
- [6] R. DELGADO, J.J.R. FRAÚSTO DA SILVA, «Some aspects of Ni(III) biochemistry», Lisbon, 1984.
- [7] R. SHAMBERGER, «Biochemistry of Selenium», Plenum Press, New York, 1983.
- [8] R.J.P. WILLIAMS, J.J.R. FRAÚSTO DA SILVA, «High-redox potential chemicals in biological systems», in R.J.P. WILLIAMS, J.J.R. FRAÚSTO DA SILVA (eds.), «New Trends in Bio-inorganic Chemistry», Academic Press, London, 1978.



MS4.2 — TH

M.E. FARAGO
Chemistry Department
Royal Holloway and Bedford Colleges
Egham Hill
Surrey TW20 OEX
U.K.

METAL IONS AND PLANTS

Metals are particularly important to healthy plant life; for example copper and zinc have been long known as essential for healthy growth. Excesses or deficiencies of metals have effects on growth and morphology which are well documented [1-3] and have particular relevance to agriculture.

The root is the plant organ by which most salts are taken up by the plant. However, BOWLING [4] has suggested that there are four links in the uptake chain: movement of ions or complexes in the soil to the roots; uptake into the root; transport across the root; and movement to the shoot.

In recent years there has been interest in the effects on plants of high concentrations of certain metals, brought about by natural mineralisation [5] or by metal pollution [6]. Some plants can grow on soils with metal concentrations that are normally toxic, and have been used as indicators of particular environmental conditions. The mechanisms of such plants tolerance to high metal concentrations has been the subject of much work and speculation [7-12]. Mechanisms are divided into external and internal types, the former covering the few situations in which the metal is unavailable to the root. Suggested internal mechanisms are numerous, but can be grouped loosely under four headings [11,12]:

1. Metal is available to plant root, but is not taken up
e.g. excretion of a complexing agent rendering metal unavailable;
2. Metal is taken up but rendered harmless to metabolism within the plant
e.g. deposition in cell wall or vacuole;

3. Metal is taken up but excreted
e.g. by guttation, leaching or leaf fall;
4. Metal is taken up but metabolism altered to accommodate increased concentration
e.g. increase in specific enzymes.

It has been realised recently that the chemical species of the element under consideration cannot be ignored when biological uptake is being considered. For example our work has shown that for the water hyacinth, *Eichhornia crassipes*, Pt(II) compounds are more toxic than those of Pt(IV), and that *cis* [Pt(NH₃)₂Cl₂] is taken up to a greater extent than the *trans* isomer [13]. LEPP *et al.* [14,15] have shown, in excised barley roots, that the uptake of the vanadyl cation is generally greater than the vanadate anion, and that the uptake of Tl(I) is by an active process, while that of Tl(III) is passive. The paper will present a general introduction concerned with the uptake, essentiality and toxicity of metal ions with reference to higher plants. Some of our work on Ni-, Zn-, and Cu-tolerant plants will be described, and the effects of chemical speciation on the uptake will be discussed.

REFERENCES

- [1] E.J. HEWITT, T.A. SMITH, «Plant Mineral Nutrition», English Universities Press, London (1975).
- [2] E. EPSTEIN, «Mineral Nutrition in Plants», Wiley, London (1972).
- [3] V. SAUCHELLI, «Trace Elements in Agriculture», van Nostrand, New York (1969).
- [4] D.J.F. BOWLING, «Uptake of Ions by Plant Roots», Chapman and Hall, London (1976).
- [5] R.R. BROOKS, «Geobotany and Biogeochemistry in Mineral Exploration», Harper and Row, New York (1972).
- [6] N.W. LEPP (ed.), «Effects of Heavy Metal Pollution in Plants», Applied Science, London (1981).
- [7] J. ANTONOVICS, A.D. BRADSHAW, R.G. TURNER, *Adv. Ecol. Res.*, **7**, 1 (1971).
- [8] S.J. WAINWRIGHT, H.W. WOOLHOUSE, in M.J. CHADWICK, G.T. GOODMAN (eds.), «The Ecology of Resource Degradation and Renewal», *15th Symp. Brit. Ecol. Soc.*, Blackwell, Oxford, 231 (1975).
- [9] C.D. FOY, R.L. CHANEY, M.C. WHITE, *Ann. Rev. Plant Physiol.*, **29**, 511 (1978).
- [10] H.W. WOOLHOUSE, *Chem. Brit.*, **16**, 72 (1980).
- [11] M.E. FARAGO, *Coord. Chem. Revs.*, **36**, 155 (1981).
- [12] M.E. FARAGO, *Chemtech*, **11**, 684 (1981).
- [13] M.E. FARAGO, P.J. PARSONS, *Inorg. Chim. Acta*, **79(B7)**, 233 (1983).
- [14] N.W. LEPP, B.G. MORRELL, D.A. PHIPPS, *Inorg. Chim. Acta*, **79(B7)**, 228 (1983).
- [15] N.W. LEPP, P.G. LONGAN, D.A. PHIPPS, *Inorg. Chim. Acta*, **79(B7)**, 229 (1983).



MS4.3 — TH

LOIS A. EGUCHI
PAUL SALTMAN
Department of Biology
University of California
San Diego, La Jolla, CA 92093
U.S.A.

THE AEROBIC REDUCTION OF Fe(III) COMPLEXES BY HEMOGLOBIN AND MYOGLOBIN

INTRODUCTION

The essentiality of iron in biological systems is manifest in oxygen transport, redox reactions, metalloenzymes, and the maintenance of macromolecular structure. Organisms have evolved many strategies to cope with the unique problems of the solution chemistry of this element [1-3]. Much has been learned regarding the participation of low molecular weight chelating agents and iron-specific proteins of storage and transport for maintaining the solubility, permeability and transportability of iron. Little is known regarding the mechanisms whereby Fe(III), the most stable state of iron under aerobic conditions, can be reduced to Fe(II) for incorporation into tetrapyrroles, iron-sulfur proteins, or ferritin [4,5].

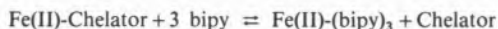
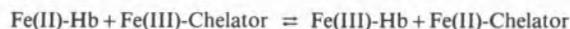
Two conditions for the facile reduction of iron *in vitro* have received much attention: 1) powerful inorganic reducing agents in the presence of O₂ (*i.e.*, dithionite) and 2) relatively high concentration of FAD.H₂ or FMN.H₂ under anaerobiosis. Neither of these conditions seems to reflect a meaningful physiological environment.

The initial observations of EGYED *et al.* [6] that hemoglobin (Hb) mediates the aerobic mobilization of iron from transferrin to 2,2'-bipyridine (bipy) suggested that Hb might serve as a biological reductant. These observations were extended to erythrocytes and reticulocytes [7], where direct participation of Hb in the reduction and mobilization of iron could be inhibited with NO₂⁻. Red

cells in an oxygenated environment were found to generate and mobilize Fe(II) in significant concentrations. Our *in vitro* experiments explore a plausible mechanism for such reduction.

DISCUSSION

Our experiments demonstrate that both Hb and Mb can reduce Fe(III) complexes and, in turn, become oxidized to their met-species. This reduction occurs at appreciable rates in the presence of O₂, although the rate is enhanced in the absence of O₂. These results suggest deoxyHb is the preferred reductant and that O₂⁻ is not involved. The lack of inhibition by SOD further supports this view. The following reaction scheme is consistent with our experiments:



Consideration of the structure of these two heme proteins [8] makes it unlikely that the Fe(III)-chelator complex can enter the heme pocket to effect a direct interaction and transfer of an electron. We speculate that electrons are passed via the peptide backbone to the surface of the protein where reduction takes place. This would be analogous to the mechanism proposed by GRAY *et al.* [14] for a redox-active derivative of Mb consisting of a Ru(III)-complex bound to a specific histidine residue (His-113) on the protein surface. The appreciable differences in reduction as a function of the presenting complex could be a function of site specific interaction(s) in the second reaction of the proposed mechanism. The rates of ligand exchange as well as the presence of polynuclear iron-oxyhydroxide complexes also influence rates of reduction.

We can only speculate about the involvement of these two O₂-binding proteins in the cellular reduction and accumulation of iron. The experiments with both erythrocytes and reticulocytes [7] demonstrate the direct participation of Hb in iron mobilization. Pretreatment of erythrocytes aerobically with 16 mM NaNO₂ does not affect Fe(II) uptake but effectively inhibits iron release from the cell to the environment. This inhibition is due

to the oxidation of Hb and can be reversed with dithionite.

The possibility that other heme proteins, including those normally involved in electron transport pathways and other redox reactions, can also contribute electrons to Fe(III) complexes is under investigation. It is no longer necessary to invoke subcellular environments of low pO₂ or high concentrations of FAD.H₂ to reduce iron. Enzymatic mechanisms for the recycling of Hb and Mb have been identified [10]. We suggest a novel role for the O₂-transport proteins as powerful reducing agents, as well as an important new chelation function for ATP, heretofore considered primarily as a bioenergetic intermediate.

ACKNOWLEDGEMENTS

This work was supported by Research Grant AM-12386 from the United States Public Health Service and L.A.E. received a predoctoral award from the United States Public Health Service, 5T32 AMO7233.

We appreciate the wisdom and counsel of Drs. Jack Hege-
nauer, Linda Strause, Vijay Sharma, and Harry Gray.

REFERENCES

- [1] T. SPIRO, P. SALTMAN, in A. JACOBS, M. WORWOOD (eds.), «Iron in Biochemistry and Medicine», Academic Press, London and New York, 1974, pp. 1-28.
- [2] A. JACOBS, in R. PORTER, D.W. FITZSIMONS (eds.), «Iron Metabolism», Ciba Foundation Symp., Elsevier, Amsterdam, 1977, pp. 91-106.
- [3] P. AISEN, in R. PORTER, D.W. FITZSIMONS (eds.), «Iron Metabolism», Ciba Foundation Symp., Elsevier, Amsterdam, 1977, pp. 1-17.
- [4] P. AISEN, I. LISTKOWSKY, *Ann. Rev. Biochem.*, **49**, 357-393 (1980).
- [5] R.R. CRICHTON, *Trends Biochem. Sci.*, **9**, 283-286 (1984).
- [6] A. EGYED, A. MAY, A. JACOBS, *Biochim. Biophys. Acta*, **629**, 391-398 (1980).
- [7] A. EGYED, P. SALTMAN, *Biol. Trace Element Res.*, (1984), in press.
- [8] R.E. DICKERSON, I. GEIS, «Hemoglobin: Structure, Function, Evolution, and Pathology», Benjamin/Cummings Pub. Co., Menlo Park, 1983, pp. 20-60.
- [9] R. MARGALIT, I. RECHT, H.B. GRAY, *J. Am. Chem. Soc.*, **105**, 301-302 (1983).
- [10] H. LEHMANN, R.S. HUNTSMAN, R. CASEY, H. LANG, P.A. LARKIN, in W.J. WILLIAMS *et al.* (eds.), «Hematology», 2nd edn., McGraw Hill, New York, 1972, pp. 524-530.



MS4.4 — TH

EDITH M. CARLISLE

School of Public Health
University of California
Los Angeles, CA 90024
U.S.A.

SILICON ESSENTIALITY AND FUNCTION

The occurrence of silicon in living systems, its physiological and biochemical roles, and its toxicology have attracted increasing research interest over the last 10 years (see [1]) because it is only within the last decade that silicon has been recognized as participating in the normal metabolism of higher animals and as an essential trace element. Silicon has been shown to be required in bone, cartilage and connective tissue formation as well as participating in several other important metabolic processes.

A series of experiments has contributed to establishing silicon's essentiality. The first of these were *in vitro* studies [2] which showed that silicon is localized in active growth areas in young bone, suggesting a physiological role for silicon in bone calcification processes. These were followed by *in vivo* studies showing that silicon affects the rate of bone mineralization. Of critical importance, it was subsequently demonstrated that silicon deficiency is incompatible with normal growth and skeletal development in the chick and rat [3,4] and that these abnormalities could be corrected by a silicon supplement. Recent studies [5] have demonstrated silicon essentiality under entirely new conditions and provide strong confirmatory evidence of silicon's essentiality for bone formation.

Later work demonstrates silicon's importance in connective tissue. Although a structural role has been proposed for silicon in connective tissue, more recent studies indicate that silicon plays an important metabolic role. The importance of silicon in bone formation is also emphasized in recent studies where skull and long bone abnor-

malities have been produced in silicon-deficient chicks under conditions promoting optimal growth using a semi-synthetic diet containing a natural protein in place of the crystalline amino acid based diet used in the earlier studies. The skull abnormalities were associated with a striking difference in the pattern of the bone matrix and a significant decrease in bone collagen content. The findings demonstrate that silicon has a significant effect on the bone matrix which in further studies has been shown to be independent of vitamin D. An *in vivo* requirement for silicon has also been established in articular cartilage and connective tissue formation. Skeletal and other abnormalities involving glycosaminoglycans in formation of cartilage matrix and connective tissue were found to be associated with silicon deficiency. These observations provided the first indication that silicon is involved with glycosaminoglycans in articular cartilage and connective tissue formation. Additional support for a role of silicon in glycosaminoglycan metabolism is the further finding that silicon is associated with animal glycosaminoglycans and their protein complexes.

The *in vivo* findings above have been corroborated in nutritional bone and cartilage studies, where the essentiality of silicon for growth in bone, and more recently, in cartilage, has been demonstrated, and where furthermore, a requirement for silicon in collagen and glycosaminoglycan formation has been established. An effect of silicon on formation of extracellular matrix components by connective tissue cells has also been demonstrated. Moreover, additional support for silicon's proposed metabolic role in connective tissue at the cellular level is provided by the earlier finding that silicon is one of the major ions of osteogenic cells, and furthermore, that silicon reaches high levels in mitochondria of these cells, indicating that silicon participates in the biochemistry of the subcellular, enzyme-containing structure of the cell.

REFERENCES

- [1] G. BENDZ, I. LINDQUIST (ed.), «Biochemistry of Silicon and Related Problems», Plenum Press, New York, 1978.
- [2] E.M. CARLISLE, *Science*, **167**, 179-280 (1970).
- [3] E.M. CARLISLE, *Science*, **178**, 119-621 (1972).
- [4] K. SCHWARZ, D.B. MILNE, *Nature*, **239**, 333-334 (1972).
- [5] E.M. CARLISLE, *Nutr. Rev.*, **40**, 193-198 (1982).



MS4.5 — TH

N.D. CHASTEEN

E.M. LORD

C.E. HOLLOWAY

Department of Chemistry
University of New Hampshire
Durham, N.H. 03824
U.S.A.

H.J. THOMPSON

Department of Animal and Nutritional Sciences
University of New Hampshire
Durham, N.H. 03824
U.S.A.

CHARACTERIZATION OF THE BIOCOMPLEXES OF VANADIUM METABOLISM IN THE RAT

Interest in the biochemistry and physiology of vanadium has grown enormously in recent years [1]. This interest stems in part from observations that vanadium is a potent inhibitor of a variety of key enzyme systems, most notably the ATPases. In a recent study, we obtained preliminary evidence that dietary vanadyl(IV) sulfate is a preventative agent against the induction by 1-methyl-1-nitrosourea of mammary gland carcinogenesis in the rat [2]. We have undertaken an investigation of the metabolism of vanadium with the long range goal of identifying the origin of the cancer preventative effect.

Sprague Dawley rats were maintained on a casein based diet, AIN-76, containing 25 ppm vanadium either as VOSO_4 or NH_4VO_3 . To identify the prevalent oxidation state of vanadium in the gastrointestinal tract EPR measurements were made on the stomach, duodenum (plus lumen) and the feces of animals. EPR spectroscopy, which is specific for the +4 oxidation state, indicated the presence of VO^{2+} , in all samples. It was further observed that the AIN-76 diet in a slurry at pH 1.5, which is the approximate pH of the stomach, quantitatively reduced vanadate(V) to VO^{2+} . These observations suggest that vanadium as VO^{2+} is the principal form in the gastrointestinal tract regardless of the oxidation state of the salt used in the

diet, although further measurements with animals are needed to confirm this observation.

To gain information about the relative rates of vanadium uptake in the +4 and +5 oxidation states, gastric intubation experiments were carried out. Solutions of 25 ppm vanadium as either VOSO_4 or NH_4VO_3 in 5% glucose solution were administered to animals which had been previously fasted for 16 hr. Uptake in the blood stream was followed using ^{48}V radioisotope with samples taken at 1/2 hr intervals for a period of two hours. Blood levels reached 50 ppb for the NH_4VO_3 treated animals and was still increasing at 2 hr. In contrast, a concentration of only 10 ppb was observed for the VOSO_4 treated animals with no further increase after 1/2 hr. These preliminary results point toward a selective mechanism of vanadium absorption which is dependent on the oxidation state of the metal, a phenomenon well known for iron.

Approximately 95% of the V was found associated with the plasma component of the blood, a result consistent with the findings of others. When the plasma was subjected to ultrafiltration on an Amicon PM10 membrane (exclusion limit $\sim 10,000$), 96.6% of the vanadium was retained, indicating that little vanadium was present as low molecular weight complexes. Polyacrylamide gel electrophoresis and size exclusion chromatography of the plasma from either V(IV) or V(V) treated animals showed association of the element with the serum transferrin component (MW $\sim 80,000$). However, recovery from the columns was only 40% indicating that weakly complexed vanadium, perhaps involving other serum proteins such as albumin (see below), was lost in the chromatography step. This vanadium eluted from the column only after extensive washing.

EPR measurements were made in an attempt to identify the oxidation state of vanadium in blood. No vanadium(IV) signals were observed, possibly owing to the low concentration of the metal or to the presence of only vanadium(V). Evidence for the oxidation state in serum was therefore obtained indirectly. When vanadate(V) was added to fresh human serum *in vitro*, rapid and quantitative reduction to VO^{2+} occurred. EPR measurements showed the characteristic signals of the well known VO^{2+} complexes with albumin and trans-

ferrin. Thus, these data suggest that the prevalent form of vanadium in serum is the VO^{2+} ion and that the metal is complexed to the iron transport protein transferrin and possibly also to albumin. It is often stated that extracellular vanadium exists in the +5 oxidation state, however, to our knowledge the redox chemistry of vanadium in serum has never been examined.

The kinetics of vanadium(IV) oxidation in the VO^{2+} -transferrin complex by molecular oxygen ($P_{\text{O}_2}=0.2$ atm, 37°C , pH 7.45) was studied by EPR and found to have a half-life of approximately 15 min. The half-life was doubled when the oxidation reaction was carried out in fresh serum, presumably due to the presence of reducing agent(s) (see above). The reaction was also significantly retarded in the presence of excess apotransferrin suggesting that vanadium first dissociates from the protein prior to oxidation. UV-difference spectroscopy and NMR showed that vanadium(V), once generated from vanadium(IV), likewise bound to the specific sites of transferrin, possibly as the *cis*- VO_2^+ cation.

Several tissues were examined by EPR. Liver, spleen, kidney, and lung exhibited prominent EPR signals due to VO^{2+} complexed with ferritin, the iron storage protein. These organs are known to accumulate vanadium and are also rich in iron. Transferrin may mediate the uptake of vanadium by these organs and by neoplastic tissues as well. Cancer cells have a high iron requirement and many transferrin receptors on their cell surfaces. Vanadium delivery to cells by transferrin could be the first step in the mechanism of antineoplastic activity of this element.

ACKNOWLEDGEMENTS

This research was supported by Grants GM 20194 and CA 38265 from the National Institutes of Health.

REFERENCES

- [1] N.D. CHASTEEN, «The biochemistry of vanadium», *Struct. Bonding (Berlin)*, **53**, 107-137 (1983).
- [2] H.J. THOMPSON, N.D. CHASTEEN, L.D. MEEKER, «Dietary vanadyl(IV) sulfate inhibits chemically-induced mammary carcinogenesis», *Carcinogenesis*, **5**, 849-851 (1984).



MS4.6 — TH

EVERT NIEBOER

Department of Biochemistry and Occupational Health Program
McMaster University
1200 Main Street West, Hamilton, Ontario, L8N 3Z5
Canada

PHYSICOCHEMICAL, METABOLIC AND MOLECULAR ASPECTS OF NICKEL CARCINOGENESIS

Recent work in our laboratory is consistent with the hypothesis that bioavailability and compartmentalization are determinants in nickel carcinogenesis. It is visualized that in target organs (namely lung and nasal mucosa), extracellular and intracellular pools of particulate nickel compounds provide a continuous intracellular flux of Ni^{2+} . Intracellular compartmentalization of Ni^{2+} is, however, balanced by extracellular transport and excretion. In the somatic mutation model of cancer, Ni^{2+} is believed to be the ultimate carcinogen. Our experimental evidence in support of these views is reviewed.

In vitro studies with nickel oxides and sulphides have shown that surface passivity of particulates (*i.e.*, smooth exterior, crystallinity, low surface charge, low surface activity such as in protein adsorption and cell lysis, and moderate solubility in biological fluids) appears to be predisposing to carcinogenicity.

Experiments with a number of human and animal cell types have demonstrated that the uptake of Ni^{2+} may be described by an "equilibrium model". Under steady state conditions, the Ni^{2+} ion distributes passively between the intracellular and extracellular ligand pools. The removal of Ni^{2+} from pre-loaded cells can be readily achieved by ligands such as EDTA, D-penicillamine, L-histidine and human serum albumin (even at physiological concentrations in the latter two cases). Evidence will also be presented that Ni^{2+} is rapidly excreted by the kidney.

Metal ions are known to stabilize left-handed Z-DNA. It has been postulated that a number of carcinogens may alter the equilibrium between right-handed B-DNA and Z-DNA *in vivo*, and that such alterations may have mutagenic consequences [1]. We have shown that the B → Z transition for poly(dG-dC).poly(dG-dC) is correlated with the ability of metal ions to complex DNA. For class B metal ions (nitrogen/sulphur seeking [2]), the metal/DNA molar ratio for mid-phase (half) conversion was small (e.g., 0.3 for Ag⁺) compared to class A ions (oxygen seeking; e.g., 450 for Ce³⁺). The following correlation was obtained: $y = -0.994 \log x + 3.54$ (correlation coefficient = 0.92, n = 20); with $y = X_{m,r}^2$, a covalent index; x = metal ion/DNA molar ratio, and n , the number of metal ions tested. It is concluded that since B → Z conversion of DNA is an intrinsic property of most metal ions, unusual intranuclear compartmentalization of Ni²⁺ must prevail if this phenomenon is relevant to nickel carcinogenesis. Finally, it has been demonstrated for peptides and human serum albumin that the Ni(III)/Ni(II) redox couple can participate in active oxygen biochemistry and toxicity at physiological conditions. Tumour promoters may contribute to cancer development by generating active oxygen compounds that damage DNA [3].

ACKNOWLEDGEMENTS

The overview presented represents both ongoing research and that completed recently by my students and staff: biological reactivity of "insoluble" nickel compounds (R.I. Maxwell and A.A. Jusys); Ni²⁺ uptake by cells (A.R. Stafford and C.R. Menon); renal excretion of nickel in man (W.E. Sanford); B → Z conversion of DNA (F.E. Rossetto); and Ni(III)/Ni(II) redox couple characterization (P.I. Stetsko).

REFERENCES

- [1] A. RICH, A. NORDHEIM, A.H.-J. WANG, *Ann. Rev. Biochem.*, **53**, 791 (1984).
- [2] E. NIEBOER, D.H.S. RICHARDSON, *Environ. Pollut., Ser. B*, **1**, 3 (1980).
- [3] J.L. MARX, *Science*, **219**, 158 (1983).



MS4.7 — TH

R.J. SHAMBERGER

The Cleveland Clinic Foundation
Cleveland, Ohio 44106
U.S.A.

SELENIUM BIOCHEMISTRY

Early interest in selenium has been primarily related to its toxicity, but was first recognized to be important in normal metabolism by SCHWARZ and FOLTZ [1] who found it prevented necrotic degeneration in the liver of vitamin E-deficient rats. This initial finding was quickly confirmed by work that showed the prevention by about 0.1 ppm of dietary selenium of a vitamin E deficiency disease of the chick, exudative diathesis. The recognition of selenium as a nutritionally important factor came with additional reports that selenium could prevent certain vitamin E deficiency diseases in animals. Other clinical disorders associated with selenium-vitamin E deficiency in domestic animals have been observed. These diseases include skeletal myopathy in cattle, chickens, horses, sheep, swine and turkeys; cardiac myopathy in cattle, swine (mulberry heart disease), and turkeys; hepatosis dietetica in swine; encephalomalacia and pancreatic necrosis in young chickens; decreased egg production and hatchability in adult chickens; gizzard and intestinal myopathy in turkeys; placental retention in cattle; unthriftiness in cattle and sheep; and infertility in ewes (embryonic death) and periodontal disease in sheep.

Because of the ability of selenium to prevent certain vitamin E deficiency diseases and because vitamin E was thought to function as a biologically specific antioxidant in the prevention of *in vivo* lipid peroxidation, hypotheses for the mode of action of selenium in animals suggested that it may also function as an antioxidant. These hypotheses were confirmed when ROTRUCK *et al.* [2] found that selenium is an important cofactor of glutathione peroxidase (EC 1.11.1.9) an enzyme

which metabolizes hydroperoxides. Glutathione peroxidase has been purified from several tissues of a number of species, and its molecular weight was estimated to be between 76,000 to 97,000. Glutathione peroxidase purified from ovine erythrocytes contains four gram-atoms of selenium per mole and does not contain heme or flavin moieties. Selenium-dependent glutathione peroxidase together with catalase, superoxide dismutase, and presumably vitamin E serve as part of an intracellular multicomponent antioxidant defense system which protects unsaturated membrane phospholipids and/or important proteins from the adverse effects of reactive oxygen and free radical initiators of the oxygen. During the reduction of molecular oxygen to water, highly reactive intermediates of oxygen reduction such as peroxides and superoxides are formed. H_2O_2 is produced by a variety of enzymes, not only within the peroxisomes where they are broken down by catalase, but also in the microsomal, mitochondrial and soluble fractions of the cell. In rat liver, up to 5% of oxygen is consumed for the production of hydrogen peroxide. Much of the hydrogen peroxide results from the dismutation of superoxide anions which means that H_2O and O_2^- may be present simultaneously in biological material. This condition favors the formation of $\cdot OH$ and singlet oxygen which may attack a variety of organic compounds. Two other selenoproteins have also been reported in animals. Selenoproteins are also important in bacterial metabolism.

Selenium occurs naturally in foods and feedstuffs in the organic molecules which are mainly selenomethionine, Se-methylselenomethionine, selenocys-

tine, and selenocysteine. The amounts of selenium in feed and food plants vary according to the concentration and bioavailability of soil selenium. While many of the regions of the world contain adequate selenium to meet the nutritional needs of animals and people, many regions of the world are deficient in selenium. Substantial differences in selenium intake exist between people in different parts of the world. Less than 60 micrograms/person/day may be consumed in New Zealand, Finland and parts of China. The severe deficiencies observed in Northeastern China seem to be responsible for an endemic cardiomyopathy (Keshan Disease) observed in children. This disease affects as many as 11% of the population in the target age groups, and the case-fatality rate is near 80%. Even though other factors may also be involved, prophylaxis with orally administered sodium selenite almost completely eliminated Keshan disease. Similar cardiomyopathies also occur in total parenteral nutrition patients who have a very low selenium intake. Epidemiological evidence also links a low selenium intake to various types of human cancer, and a large number of experiments show that selenium, at greater than nutritional levels, can inhibit carcinogenesis in several experimental animal models.

REFERENCES

- [1] K. SCHWARZ, C.M. FOLTZ, *J. Am. Chem. Soc.*, **79**, 3292 (1957).
- [2] J.J. ROTRUCK, A.L. POPE, H.E. GANTHER, A.B. SWANSON, D.G. HAFEMAN, W.G. HOEKSTRA, *Science*, **179**, 588 (1973).

5. Models of Iron Binding Sites in Biology

Convener: J.T. Groves
(Ann Arbor)



MSS.1 — TH

JOHN T. GROVES
THOMAS J. McMURRY
Department of Chemistry
The University of Michigan
Ann Arbor, Michigan 48109
U.S.A.

SYNTHETIC ANALOGS OF OXIDIZED HEME PROTEINS. PREPARATION AND CHARACTERIZATION OF IRON(IV) PORPHYRINS

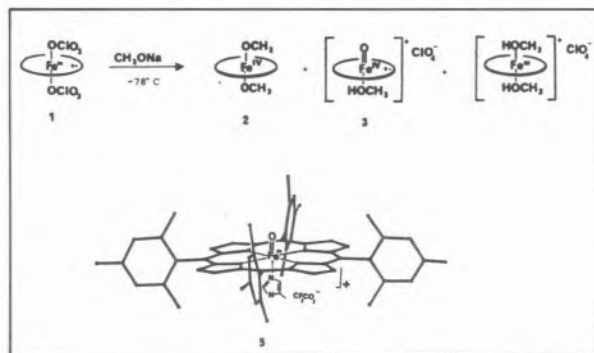
Oxidized forms of the heme-iron center have been shown to be isolable states for the peroxidases [1]. Similar intermediates have been proposed for the catalytic cycle of cytochrome P-450 [2]. It is now recognized that the one-electron oxidation of simple iron porphyrins leads to oxidation of the porphyrin ligand to give Fe(III) porphyrin radical species. The addition of methoxide ligands to the sterically hindered tetramesitylporphyrin (TMP) derivative, Fe(III)(TMP·)(ClO₄)₂ (**1**) has very recently been shown [3] to afford a dimethoxyiron(IV) complex, Fe(IV)(TMP)(OCH₃)₂ (**2**). Only two other families of monomeric iron(IV) porphyrin complexes are known; an oxoiron(IV) species Fe(IV)(O)(TPP) [4] and an oxoiron(IV) porphyrin radical complex Fe(IV)(O)(TMP·)(X) (**3**) [5]. We describe here the preparation of several derivatives of **3** in which the axial ligand X is varied and the *disproportionation* of **1** and **2** to generate **3**.

As we have previously described [6], the oxidation of Fe(TMP)(Cl) in methylene chloride-methanol with *m*-chloroperoxybenzoic acid (MCPBA) at -78°C afforded the oxoiron(IV) porphyrin radi-

cal complex **3**. The identity of the sixth ligand in this complex can now be identified as the solvent methanol on the basis of the following observations. When the reaction was carried out in toluene-methanol at -90°C with Fe(TMP)(Cl), Fe(TMP)(benzoate) or Fe(TMP)(OCH₃), three different complexes with ¹H-NMR spectra similar to **3** were initially formed (pyrrole H, δ -9.01, -15.6 and -16.2 in toluene-d₈ at -78°C, respectively). Upon standing at -67°C, all three solutions changed with time to show the NMR spectrum of **3** (pyrrole H, δ -22.8 in toluene). The most reasonable interpretation of these results is that the initially formed oxoiron(IV) complex underwent ligand solvolysis.

Attempts to coordinate imidazole derivatives to **3** by ligand metathesis led only to reduction of the complex. The dimethoxyiron(IV) complex **2** reacted with one equivalent of 4-methylimidazolium trifluoroacetate to produce an unsymmetrically ligated, low spin iron(III) porphyrin radical complex [Fe(III)(TMP·)(OCH₃)(4-MeIm)]⁺ (**4**) (pyrrole H, δ -30.5 at -77°C). The oxidation of **4** with iodosylbenzene produced the oxoiron(IV) porphyrin radical complex Fe(IV)(O)(TMP·)(4-MeIm) (**5**) (pyrrole H, δ -13.7 at -78°C). The addition of norbornene to a mixture of **4** and **5** caused the reduction of **5** in 10 minutes at -49°C but had no effect on **4**. Norbornene oxide was detected in 67% yield based on **5**.

While the addition of two equivalents of methoxide to solutions of **1** produced **2** [6], the addition of only *one* equivalent of methoxide produced a 30% yield of the oxoiron(IV) porphyrin radical complex **3**. Since there were no other oxidizing agents in this solution except the starting iron(III) porphyrin radical, the presence of **3** can only indicate that an initially formed iron(IV) complex



underwent further oxidation to **3** under these conditions. The only reasonable source of the oxo oxygen in this system is trace amounts of water in the medium. Thus, oxoiron(IV) porphyrin radical complexes can be formed by disproportionation without the need of peroxidic oxidants.

ACKNOWLEDGEMENTS

Financial support by the National Institutes of Health is gratefully acknowledged.

REFERENCES

- [1] W.D. HEWSON, L.P. HAGER, in D. DOLPHIN (ed.), «The Porphyrins», vol. VII, part B, Academic Press, New York, 1979, pp. 295-332.
- [2] R.E. WHITE, M.J. COON, *Ann. Rev. Biochem.*, **49**, 315-356 (1980).
- [3] J.T. GROVES, R. QUINN, T.J. McMURRY, G. LANG, B. BOSO, *J. Chem. Soc., Chem. Commun.*, 1455-1456 (1984).
- [4] D.H. CHIN, A.L. BALCH, G.N. LAMAR, *J. Am. Chem. Soc.*, **102**, 1446-1448 (1980); *ibid.*, **102**, 4344-4350 (1980).
- [5] J.T. GROVES, R.C. HAUSHALTER, M. NAKAMURA, T. NEMO, B.J. EVANS, *J. Am. Chem. Soc.*, **103**, 2884-2886 (1981).



MS5.2 — TH

JOHN R. LINDSAY SMITH
DAVID N. MORTIMER
Department of Chemistry
University of York
York YO1 5DD
England

TETRA(4-N-METHYLPYRIDYL)PORPHYRINATOIRON(III) PENTACATION, A POLAR CATALYST FOR MODEL SYSTEMS FOR CYTOCHROME P450 MONO-OXYGENASES

A common feature of the iodosylarene based model systems for the cytochrome P450 mono-oxygenases is that they use a metalloporphyrin

catalyst dissolved in a low polarity solvent [1]. However, the poor solubility of the iodosylarene in these solvents results in an inhomogeneous reaction mixture [2]. We report here how, by using tetra(4-N-methylpyridyl)porphyrinatoiron(III) pentacation ($\text{Fe}^{\text{III}}\text{TMPyP}$) as the catalyst, the oxidations can be carried out in protic and dipolar aprotic solvents and that in methanol the reactions are homogeneous.

The epoxidation of alkenes by $\text{Fe}^{\text{III}}\text{TMPyP}/\text{PhIO}$ in methanol shows very similar stereoelectronic requirements to the corresponding reaction of tetraphenylporphyrinatoiron(III)chloride/ PhIO ($\text{Fe}^{\text{III}}\text{TPPCl}/\text{PhIO}$) in dichloromethane (Table I) and both systems give stereospecifically the *syn*-addition product. In the hydroxylation of cyclohexane and [$^2\text{H}_{12}$]cyclohexane the two model systems show large primary kinetic isotope effects ($k_{\text{H}}/k_{\text{D}} \geq 7.0$) [3].

Table I

The reactivities of aliphatic alkenes, relative to cyclohexene, towards epoxidation with iodosylbenzene catalysed by $\text{Fe}^{\text{III}}\text{TMPyP}$ in methanol and by $\text{Fe}^{\text{III}}\text{TPPCl}$ in dichloromethane^{a)}

Substrate	Epoxide Yield (%) ^{b)}	Reactivity relative to cyclohexene	
		$\text{Fe}^{\text{III}}\text{TMPyP}^{\text{c)}$	$\text{Fe}^{\text{III}}\text{TPPCl}^{\text{c)}$
2,3-Dimethylbut-2-ene	95	8	10
1-Methylcyclohexene	55	4	4
<i>cis</i> -4-Methylpent-2-ene	55	2.2	1.5
Cyclohexene	30	1.0	1.0
<i>trans</i> -4-Methylpent-2-ene	20	0.2	0.1

a) Data obtained from competition experiments with molar ratio of each substrate to oxidant and to catalyst, 200:10:1, respectively.

b) Typical yields, based on PhIO , from reaction in MeOH.

c) Relative reactivities were unchanged when reactions were carried out under nitrogen.

The similarity in the behaviour of the two iron-porphyrin catalysts is also apparent from kinetic isotope effect measurements in oxidative *O*- and *N*-dealkylations. The data in Table II show that each model system demethylates anisole *via* a rate determining methoxy C-H cleavage [4] whilst with

tertiary amines there is a rate determining electron-transfer (small k_H/k_D) followed by a product

Table II
Kinetic isotope effects in oxidations with iodosylbenzene catalysed by $Fe^{III}TMPyP$ and by $Fe^{III}TPPCL$

Oxidising System	Kinetic isotope effects (k_H/k_D)		
	PhOCH ₃ ^{b)} PhOCD ₃	PhCH ₂ NMe ₂ PhCD ₂ NMe ₂	PhCH ₂ NCD ₂ Ph ^{a)} Me
	intermolecular		intramolecular
$Fe^{III}TPPCL$ / PhIO/PhH	$9 \pm 3^c)$	$1.3 \pm 0.1^a)$	3.0 ± 0.2
$Fe^{III}TMPyP$ / PhIO/CH ₃ CN	5.5 ± 1	$1.3 \pm 0.1^d)$	$6.0 \pm 1.0^e)$

a) Measured by g.c.-m.s.

b) Calculated from relative yields of phenol and 2-methoxyphenol [4].

c) Solvent CH₂Cl₂ [4].

d) Each substrate was oxidised in competition with 4-chloro-*N,N*-dimethylbenzylamine.

e) Solvent water.

determining proton transfer (medium to large k_H/k_D) [5]. Hammett ρ values (-0.41 ± 0.02 and -0.73 ± 0.08 for the $Fe^{III}TPPCL$ - and $Fe^{III}TMPyP$ -catalysed systems respectively) from the competitive oxidations of 3- and 4-substituted *N,N*-dimethylbenzylamines corroborate the electron-transfer oxidation of tertiary amines.

We conclude that the use of the catalyst $Fe^{III}TMPyP$ extends the range of solvents that can be used for the metalloporphyrin-catalysed model systems. The studies also reveal the negligible effect of the solvent polarity and the charge on the porphyrin ligand on the course and mechanism of these oxidations.

We are currently looking at the kinetics of these oxidations using $Fe^{III}TMPyP/PhIO$ in methanol.

REFERENCES

- [1] a) J.T. GROVES, T.E. NEMO, R.S. MYERS, *J. Am. Chem. Soc.*, **101**, 1032 (1979);
b) J.T. GROVES, W.J. KRUPER, *J. Am. Chem. Soc.*, **101**, 7613 (1979);
c) D. MANSUY, J.-F. BARTOLI, M. MOMENTEAU, *Tetrahedron Lett.*, **23**, 2731 (1982);
d) J.R. LINDSAY SMITH, P.R. SLEATH, *J. Chem. Soc., Perkin Trans. 2*, 1009 (1982);
e) J.A. SMEGAL, C.L. HILL, *J. Am. Chem. Soc.*, **105**, 3515 (1983);

- f) J.T. GROVES, R.S. MYERS, *J. Am. Chem. Soc.*, **105**, 579 (1983);
g) P.S. TRAYLOR, D. DOLPHIN, T.G. TRAYLOR, *J. Chem. Soc., Chem. Commun.*, 279 (1984).
[2] B.C. SCHARDT, C.L. HILL, *Inorg. Chem.*, **22**, 1563 (1983).
[3] a) J.T. GROVES, T.E. NEMO, *J. Am. Chem. Soc.*, **105**, 6243 (1983);
b) J.R. LINDSAY SMITH, M.W. NEE, J.B. NOAR, T.C. BRUCE, *J. Chem. Soc., Perkin Trans. 2*, 255 (1984).
[4] J.R. LINDSAY SMITH, P.R. SLEATH, *J. Chem. Soc., Perkin Trans. 2*, 621 (1983).
[5] J.R. LINDSAY SMITH, D.N. MORTIMER, *J. Chem. Soc., Chem. Commun.*, 64 (1985).



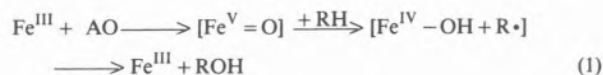
MS5.3 — TH

D. MANSUY

Laboratoire de Chimie et Biochimie Pharmacologiques et Toxicologiques
UA 400
Université Paris V
45 rue des Saints-Pères, 75270 Paris 06
France

HEME MODEL STUDIES ON OLEFIN OXIDATION BY CYTOCHROME P-450

Cytochrome P-450-dependent monooxygenases catalyze the monooxygenation of a wide range of organic compounds, including alkanes, alkenes and aromatic compounds, by O₂ in the presence of NADPH as well as by several single oxygen atom donors like PhIO, NaIO₄, alkylhydroperoxides and peracids. Model systems using simple iron-porphyrins as catalysts and PhIO [1] or alkylhydroperoxides [2] have been reported to perform epoxidation of alkenes. The mechanism generally admitted for these cytochrome P-450-dependent or model reactions is that of eq. (1):

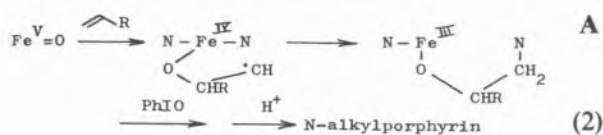


This paper describes our recent results on:
(a) the use of such model systems to interpret at

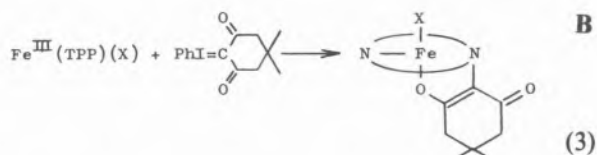
the molecular level and in detail the mechanisms of the different reactions involved in the oxidation of alkenes by cytochrome P-450.

(b) the preparation of iron-porphyrin catalysts bearing optically active amino-acids in close proximity to the iron, which are, like cytochrome P-450, able to catalyze the asymmetric epoxidation of olefins.

Monosubstituted olefins are oxidized by cytochrome P-450 leading to allylic alcohols, epoxides and aldehydes. The oxidation of non-hindered monosubstituted olefins gives *in vivo* the same products but also a slow degradation of the cytochrome P-450 heme leading to the accumulation of N-alkylated protoporphyrin IX into the liver [3]. Oxidation of the same olefins by PhIO in the presence of iron-porphyrins led us to strikingly similar results with the formation of identical oxidation products derived from the olefin [4]. Moreover, with non-hindered monosubstituted olefins, a slow degradation of the catalyst was observed, a new inactive iron complex appearing in the reaction medium. Demetalation of this complex by acidic treatment led to green pigments which were identified as N-alkylporphyrins in the case of 1-butene, 1-pentene, 4-methyl-pent-1-ene and 1-hexene. The structure of the N-alkylporphyrin derived from 1-butene was determined. The results are in agreement with the involvement of metalocycle **A** in the olefin oxidation (eq. (2)).



The instability of complexes **A** precluded so far their complete characterization. However, we could prepare the first iron-porphyrin complexes exhibiting this metalocyclic structure, upon reaction of iron-porphyrins with an iodonium ylid which is the carbon equivalent of PhIO (eq. (3)) [5].

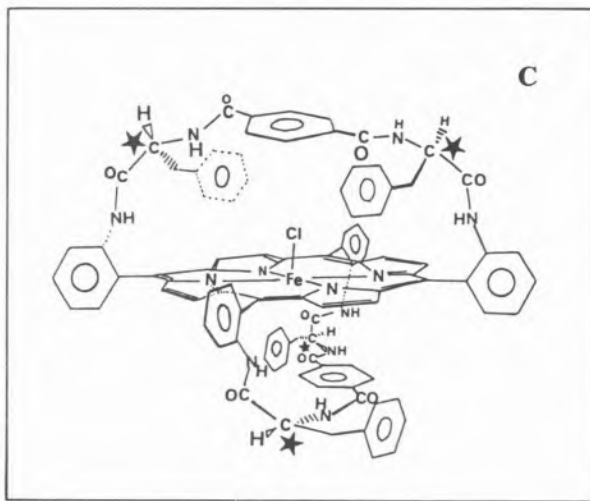


Complex **B** was isolated and completely characterized. Its visible spectrum is similar to that of complex **A** observed during oxidation of 1-alkenes.

All these data (i) clearly show that such five-membered metalocycles derived from iron-porphyrins do exist and are formed upon model- or cytochrome P-450-dependent oxidation of 1-alkenes, (ii) suggest, with other literature results, that another kind of metalocycles, four membered $\overline{\text{Fe-O-C-C}}$ metalocycles, could be involved as intermediates in these olefin oxidation and, above all, (iii) demonstrate that the different reactions observed upon cytochrome P-450-dependent oxidation of alkenes are well mimicked by iron-porphyrin model systems.

However, iron-porphyrins as simple as Fe(TPP)(Cl) are naturally unable to perform, unlike cytochrome P-450, any specific binding of alkenes and any asymmetric epoxidation of alkenes. We have prepared «picket» and «basket-handle» iron-porphyrins bearing optically active phenylalanine residues on both sides of the porphyrin plane. These optically active complexes were found able to catalyze the epoxidation of *p*-chlorostyrene with enantiomeric excess ranging from 20 to 60%. The optically active «basket-handle» iron-porphyrin (complex **C**) which exhibits the most rigid chiral environment of the iron gave the best enantiomeric excess.

These first data suggest that studies on such chiral complexes should lead to the design of efficient catalysts for chiral oxidations and to the unders-



tanding of the role of amino-acids on substrate recognition and binding in hemoprotein-catalyzed oxidations.

REFERENCES

- [1] J.T. GROVES, T.E. NEMO, *J. Am. Chem. Soc.*, **105**, 5786 (1983).
- [2] D. MANSUY, P. BATTIONI, J.P. RENAUD, *J. Chem. Soc., Chem. Commun.*, 1255 (1984).
- [3] P.R. ORTIZ DE MONTELLANO, M.A. CORREIA, *Ann. Rev. Pharmacol. Toxicol.*, **23**, 481 (1983).
- [4] D. MANSUY, J. LECLAIRE, M. FONTECAVE, M. MOMENTEAU, *Biochem. Biophys. Res. Commun.*, **119**, 319 (1984).
- [5] For preliminary results on that point, see: D. MANSUY, J.P. BATTIONI, I. AKHREM, D. DUPRÉ, J. FISCHER, R. WEISS, I. MORGENSTERN-BADARAU, *J. Am. Chem. Soc.*, **106**, 6112 (1984).



MS5.4 — TH

CHRISTOPHER A. REED
GERALD E. WUENSCHELL
PETER D. W. BOYD
JOHN R. TATE
SUSAN RASMUSSEN
Department of Chemistry
University of Southern California
Los Angeles, California 90089-1062
U.S.A.

DERIVATIZED PORPHYRINS AS MODELS FOR H-BONDED OXYHEMOGLOBIN AND CYTOCHROME OXIDASE

Hydrogen bonding by a distal protein residue was postulated as long ago as 1964 as a factor in the stabilization of coordinated dioxygen in oxyhemoglobin [1]. More recently, protein crystallography has put such H-bonding by distal histidine on a firmer basis [2,3]. NMR studies on strapped porphyrin model complexes show that the N-H bond of a secondary amide can interact with coor-

dinated oxygen and contribute about an order of magnitude to the affinity constant [4,5].

The ligand in Fig. 1 has been synthesized in order to model the effect of distal histidine. The indole picket is one of a number of rigidly appended bases which position an H-bonding moiety in the vicinity of the coordinated dioxygen in a $\text{Fe}(\text{O}_2)(\text{Porphyrin})\text{L}$ complex. Progress towards the structural characterization of such a complex and the effect of the H-bonding moiety on its O_2 affinity will be reported.

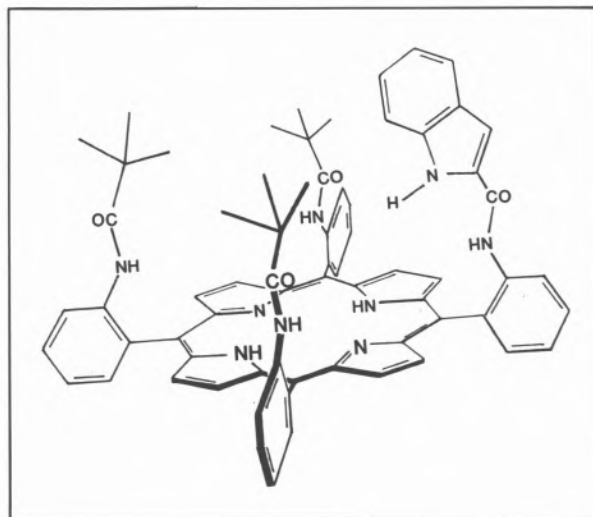


Fig. 1

Cytochrome oxidase is known to have an active site where an iron porphyrin is in close proximity to a copper center. The porphyrin illustrated in Fig. 2 has been synthesized for a model complex

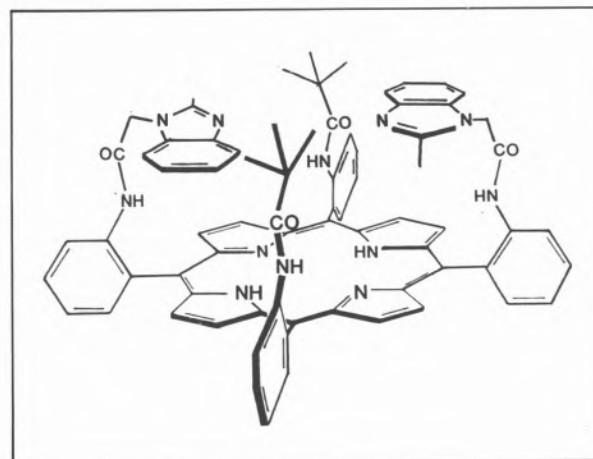


Fig. 2

approach and progress towards the definitive structural characterization of iron and copper derivatives will be presented.

REFERENCES

- [1] L. PAULING, *Nature (London)*, **203**, 182-183 (1964).
- [2] S.W.V. PHILLIPS, *J. Mol. Biol.*, **142**, 531-554(1980).
- [3] B. SHAANAN, *J. Mol. Biol.*, **171**, 31-59 (1983).
- [4] J. MISPELTER, M. MOMENTEAU, D. LAVALETTE, J.-M. LHOSTE, *J. Am. Chem. Soc.*, **105**, 5165-5166 (1983).
- [5] M. MOMENTEAU, D. LAVALETTE, *J. Chem. Soc., Chem. Commun.*, 341-343 (1982).



MS5.5 — TH

T.G. TRAYLOR
 JAMES MARSTERS
 LARRIE DEARDURFF
 Department of Chemistry
 University of California
 San Diego, La Jolla, California 92093
 U.S.A.

GEMINATE RECOMBINATION IN THE PHOTOLYTIC DISSOCIATION OF NO AND CO FROM HEMES AND HEME PROTEINS

Recently the study of recombination of NO, O₂, and CO to heme proteins by fast kinetic methods has revealed processes occurring at 10 to 10⁻¹ sec⁻¹ which are independent of ligand concentration and show spectroscopic characteristics of ligand rebinding from a geminate pair. The fact that geminate recombination of CO occurs with rate constants as low as 10⁶-10⁷ sec⁻¹, unprecedented in low viscosity solvents, suggest some special function of the protein which prevents diffusion out of the protein «geminate cage».

We have therefore searched for geminate recombination to model compounds in solvents of various viscosities. No geminate recombination of CO to

chelated protoheme was observed even in mineral oil at 0° where the viscosity exceeds one poise. This suggests that protein pockets present the equivalent of a very high viscosity. To further probe this effect, photolyses of the faster reacting NO ligand were studied using the heme/1-methylimidazole system of KASSNER and HOFFMAN.

Measurement of quantum yield of NO photolysis from protoheme compared to CO photolysis (previously shown to have a quantum yield of 1.0) revealed a quantum yield of 0.08 in water/1-methylimidazole (30%) and 0.007 in glycerol/1-methylimidazole (30%) at 20°C. Similarly, the quantum yield of mesoheme dimethyl ester was 0.19 in toluene/1-methylimidazole (20%) and 0.06 in mineral oil/1-octadecylimidazole (0.3 M) containing 10% chloroform. Thus viscosity has the expected effect of decreasing the quantum yield (see figs. 1A and B).

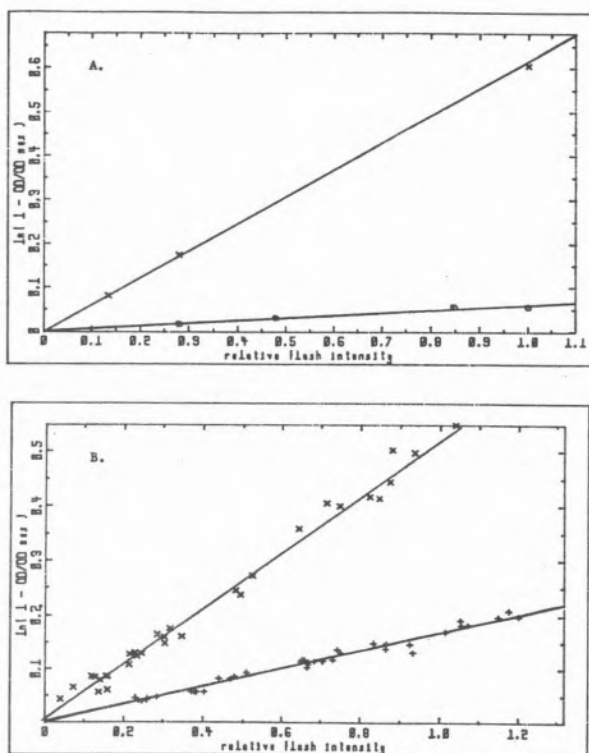


Fig. 1

Plot of the effect of solvent viscosity on NO photorelease quantum yield.

A) FePP(IX)(1-MeIm); (x) H₂O/30% 1-MeIm, (o) glycerol/30% 1-MeIm.

B) Mesoheme dimethyl ester; (x) toluene/20% 1-MeIm, (+) 0.3 M octadecyl imidazole in mineral oil/10% CHCl₃

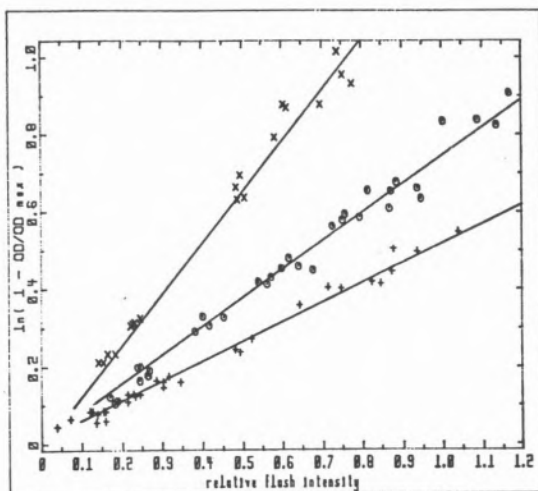


Fig. 2

Plot of the NO photorelease quantum yield for cyclophane hemes and mesoheme dimethyl ester in toluene/20% 1-MeIm; (x) pyridine-5,5-cyclophane heme, (o) adamantane-6,6-cyclophane heme, (+) mesoheme dimethyl ester

In order to probe the influence of distal side steric effects on geminate recombination, cyclophane hemes having varying size pockets were subjected to the studies described above. The results clearly show that distal side steric effects increase quantum yields (see fig. 2). Thus the lowered quantum yields in heme proteins cannot be explained with distal side steric effects. These results will be discussed in terms of effects of structure and viscosity on both diffusion and recombination rates.



MS5.6 — TH

M. SCHAPPACHER

R. WEISS

Laboratoire de Cristalchimie et Chimie Structurale (ERA 08)

Institut Le Bel

Université Louis Pasteur

4, rue B. Pascal - 67070 Strasbourg Cedex

France

R. MONTIEL-MONTOYA

A. TRAUTWEIN

Physik, Medizinische Hochschule

24, Lübeck 1

B.R.D.

A. TABARD

Laboratoire de Synthèse et d'Electrosynthèse organométalliques (LA 33)

Faculté des Sciences Gabriel

21100 Dijon Cedex

France

FORMATION OF IRON(IV) OXO DERIVATIVES VIA REDUCTION OF FERROUS PORPHYRIN DIOXYGEN ADDUCTS AND REACTION WITH CARBON DIOXIDE

The catalytic cycle of cytochrome P450 involves the binding of molecular oxygen to the ferrous heme protein and the conversion of this ferrous-dioxygen adduct to a high-valent iron-oxo derivative with two oxidation equivalents above iron(III). While synthetic metalloporphyrin-dioxygen complexes have been obtained which model the spectroscopic properties of the oxy-states of cytochrome P450 and cobalt substituted cytochrome P450_{CAM}, the conversion of ferrous dioxygen complexes into reactive iron-oxo species has so far not been achieved. In order to obtain high-valent-iron-oxo derivatives, we have studied the reduction of dioxygen adducts of iron(II) porphyrins with complex hydrides or strongly reducing thiolates and reaction with carbon dioxide, acyl chlorides and other electrophiles.

Fe(O)(THF)Po (Po = TP_{piv}P, TPP, TMP and OEP) react at -40°C in THF with sodium bis 2-methoxy-ethoxy-aluminium hydride (red-al) or Na⁺c 222 | *t*-butyl S⁻ to yield the peroxo-iron(III) porphyrin complexes [Fe^{III}(O)₂Po]⁻.

The structure of complexes of this type has been studied by EXAFS using perturbed difference Fourier analysis. The results of these studies confirm the dihapto-triangular geometry of the FeO_2 moiety with an Fe-O bond distance of 1.81 ± 0.03 Å. These peroxo-iron (III) porphyrin derivatives react at -70°C with carbon dioxide and acyl chlorides to form a novel red species which has Mössbauer properties which are similar to known iron (IV) species. The Mössbauer spectrum of the species obtained by reduction of $[\text{Fe}(\text{O}_2)(\text{THF})\text{TP}_{\text{piv}}\text{P}]$ and reaction with carbon dioxide shows the following parameters:

	δ (rel. α Fe at RT) (mms^{-1})	ΔE_Q (mms^{-1})	Γ (mms^{-1})
4.2 K	0.120	2.200	0.414
100 K	0.088	2.087	0.378
	$\pm 0.007 \text{ mms}^{-1}$		

Magnetic spectra ($H^{\text{ext}}// = 6.7$ T parallel to the γ beam) recorded at 4.2, 30 and 100 K confirm the presence of low-spin iron(IV) in this compound. The 400 MHz, ^1H NMR of the tetramesitylporphyrin analog in deuterated THF at -50°C presents as in other iron(IV) species a resonance at a very high-field ($\delta = -36,4$ ppm) and other resonances at the expected diamagnetic positions (7.33 s (*meta*-H), 2.97 s (*o*-methyl), 2.81 s (*p*-methyl)). Addition at -70°C of 1MeIm to the species obtained in THF with $\text{TP}_{\text{piv}}\text{P}$ yields another red species having a visible spectrum very similar to that known for $(\text{Fe}(=\text{O})\text{1MeIm TPP})$ ($\lambda_{\text{max}} = 426, 560, \text{ and } 590$ nm). The Mössbauer spectrum ($H^{\text{ext}} = 0$) recorded at 4.2 and 100 K presents the following parameters:

	δ (rel. α Fe at RT) (mms^{-1})	ΔE (mms^{-1})	Γ (mms^{-1})
4.2 K	0.109	1.372	0.315
100 K	0.074	1.370	0.320
	$\pm 0.007 \text{ mms}^{-1}$		

These parameters are practically identical with those for *met*-Mb- H_2O_2 and for japanese-radish peroxidase and very similar to those known for $\text{Fe}(=\text{O})\text{1MeIm TPP}$.

These results indicate that the peroxo-iron(III)-porphyrinates which form by reduction of the dioxygen adducts react with carbon dioxide to form iron(III) peroxymonocarbonate intermediates and that the O-O bond present in these intermediates is only homolytically cleaved to form low-spin iron(IV)-oxo-porphyrin derivatives.



MS5.7 — FR

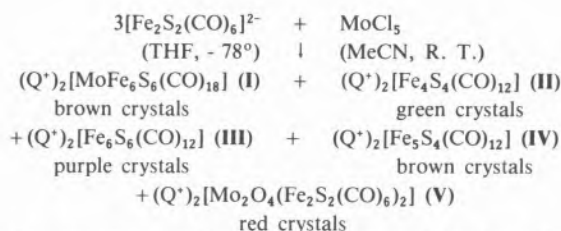
B.A. AVERILL
K.S. BOSE
P.E. LAMBERTY
J.E. KOVACS
G.L. LILLEY
X. WU
N.C. JAIN
M.E. ROGERS
E. SINN
Department of Chemistry
University of Virginia
Charlottesville, Virginia 22901
U.S.A.

SYNTHETIC APPROACHES TO THE METAL CENTERS OF NITROGENASE

The MoFe protein of nitrogenase contains two novel metal-sulfur clusters: the FeMo-cofactor and the P clusters [1]. The former is a novel Mo-Fe-S cluster of as yet unknown structure, with approximate stoichiometry $\text{MoFe}_6\text{S}_{10}$ and an $S=3/2$ ground state. The latter are apparently atypical 4Fe-4S centers in which three of the iron atoms exhibit unusual Mössbauer parameters, presumably due to the presence of non-cysteinyll or additional ligands to those iron atoms. We present results of our studies aimed at developing synthetic analogs of these clusters.

Two basic types of synthetic Mo-Fe-S cluster [2,3] containing the MoFe_3S_4 «cubane» and the «linear» MoS_2Fe [3,4] units, have been prepared as potential models for the FeMo-cofactor of nitrogenase; the synthetic route in all cases involves reaction of $[\text{MoS}_4]^{2-}$ with an iron complex. We have developed a new synthetic route in which the sulfide originates with the iron reagent, and which produces clusters containing the novel MoS_2Fe_2 structural unit in addition to a variety of novel Fe-S clusters.

Reaction of the $[\text{Fe}_2\text{S}_2(\text{CO})_6]^{2-}$ ion [5] with MoCl_5 gives at least five new clusters, as shown in the scheme below:



The structure and some properties of **II** have been reported [6], while the structure of **III** has been solved and that of **IV** is in progress. In addition, independent syntheses of all five compounds have been developed. Complex **I** has not yet yielded crystals suitable for detailed X-ray diffraction studies. Reaction of $\text{Fe}_2\text{S}_2(\text{CO})_6$ with $t\text{-BuS}^-$ produces the $[\text{Fe}_2\text{S}_2(\text{S}-t\text{-Bu})(\text{CO})_6]^-$ ion (**VI**), whose structure shows it to be the mixed organic disulfide analog of **II**. Reaction of $[\text{Fe}_2\text{S}_2(\text{CO})_6]^{2-}$ with MoOCl_3 gives the novel hexanuclear $[\text{MoOFe}_5\text{S}_6(\text{CO})_{12}]^{2-}$ ion (**VII**), the structure of which has been solved. Cluster **VII** contains the expected $\text{MoS}_2\text{Fe}_2(\text{CO})_6$ unit plus a 3Fe cluster attached to Mo via sulfide bridges. The synthesis, structures, properties, and reactivity of these novel clusters will be described.

Our approach to the synthesis of models for the P clusters of nitrogenase has centered on the preparation of large, rigid tridentate ligands capable of coordinating to three iron atoms of a 4Fe-4S cluster and stabilizing the mixed-ligand clusters in solution. Our specific goal is a trisubstituted triptycene that is capable of facile modification to permit exploration of the hypotheses presented regarding possible ligands to the P clusters. Results obtained to date via this approach will be presented.

ACKNOWLEDGEMENTS

This research was supported by the Competitive Research Grants Office of the U.S. Department of Agriculture (82-CRCR-1-1123). B.A. Averill is an Alfred P. Sloan Foundation Fellow, 1981-1985.

REFERENCES

- [1] M.J. NELSON, P.A. LINDAHL, W.H. ORME-JOHNSON, *Adv. Inorg. Biochem.*, **4**, 1(1983).
- [2] R.H. HOLM, *Chem. Soc. Rev.*, **10**, 455 (1981).
- [3] B.A. AVERILL, *Struct. Bonding (Berlin)*, **53**, 59 (1983).
- [4] D. COUCOUVANIS, *Acc. Chem. Res.*, **14**, 201 (1981).
- [5] D. SEYFERTH, R.S. HENDERSON, L.-C. SUNG, *Organometallics*, **1**, 125 (1982).
- [6] K.S. BOSE, E. SINN, B.A. AVERILL, *Organometallics*, **3**, 1126 (1984).



MS5.8 — FR

D. COUCOUVANIS
M. KANATZIDIS
A. SALIFOGLU
W.R. DUNHAM
W.R. HAGEN
Department of Chemistry
University of Michigan
Ann Arbor, Michigan 48109
U.S.A.

THE REACTIONS, STRUCTURAL CHARACTERIZATION AND ELECTRONIC PROPERTIES OF THE NEW METASTABLE $[\text{Fe}_6\text{S}_6\text{L}_6]^{3-}$ AND $[\text{Fe}_6\text{S}_6\text{L}_6]^{2-}$ COMPLEXES

The synthesis of the $[\text{Fe}_4\text{S}_4(\text{SR})_4]^{2-}$ and $[\text{Fe}_2\text{S}_2(\text{SR})_4]^{2-}$ synthetic analog clusters is accomplished readily by spontaneous self assembly from mixtures of appropriate reactants. This type of synthetic procedure is based on the premise that «... clusters derived from substitutionally labile iron (II, III) reactants, form as a consequence of being the thermodynamically most stable soluble reaction products» [1]. The «spontaneous self assembly» procedure is inappropriate for the synthesis of molecular analogues for certain «non-conventional» protein Fe/S sites that may owe their stability to the protein environment. Such metastable sites in the absence of protein constraints and given the appropriate activation energies are likely to transform to the thermodynamically stable «conventional» clusters. The synthesis of a new class of *metastable* Fe/S clusters was accomplished recently in our laboratory. The metastable $[\text{Fe}_6\text{S}_6\text{X}_6]^{3-}$ clusters ($\text{X} = \text{Cl}^-, \text{Br}^-, \text{I}^-, \text{RO}^-$) have been isolated [2,3] in crystalline form and the structures of the $[\text{Fe}_6\text{S}_6\text{Cl}_6]^{3-}$ [2] and $[\text{Fe}_6\text{S}_6(p\text{-CH}_3\text{-Ph-O})_6]^{3-}$ [3] anions have been determined by X-ray crystallography. The prismatic $[\text{Fe}_6\text{S}_6]^{3+}$ core (fig. 1) is a common feature in these clusters which possess both the conventional

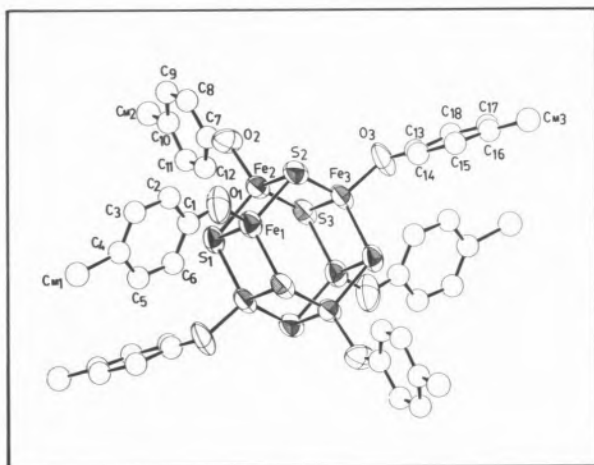


Fig. 1

The structure of the $[\text{Fe}_6\text{S}_6(\text{p-CH}_3\text{-Ph-O})_6]^{3-}$ cluster (Ref. [3])

Fe_2S_2 structural fragments ($\text{Fe-Fe} \sim 2.75 \text{ \AA}$; $\text{Fe-S-Fe} \sim 75^\circ$) and the unusual Fe_3S_3 «puckered» ring units ($\text{Fe-Fe} \sim 3.8 \text{ \AA}$; $\text{Fe-S-Fe} \sim 113^\circ$). The only other example of a Fe_3S_3 unit with similar structural parameters is available in the structure of the 3Fe site in Fd I from *A. vinelandii* [4].

The metastable nature of the $[\text{Fe}_6\text{S}_6\text{L}_6]^{3-}$ anions ($\text{L} = \text{Cl}^-, \text{Br}^-, \text{I}^-, \text{RS}^-$) is apparent in the facile, quantitative transformation (fig. 2) to $[\text{Fe}_4\text{S}_4\text{X}_4]^{2-}$ according to the reaction $2[\text{Fe}_6\text{S}_6\text{X}_6]^{3-} \rightarrow 3[\text{Fe}_4\text{S}_4\text{X}_4]^{2-}$. The $[\text{Fe}_6\text{S}_6\text{L}_6]^{3-}$

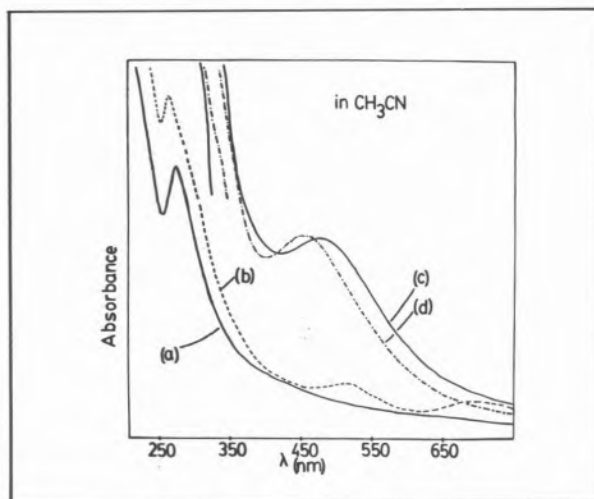


Fig. 2

Cluster transformations in CH_3CN solution. (a) $[\text{Fe}_6\text{S}_6\text{Cl}_6]^{3-}$; (b) $[\text{Fe}_4\text{S}_4\text{Cl}_4]^{2-}$, obtained by heating solution (a) to 60°C for 5 min.; (c) $[\text{Fe}_6\text{S}_6(\text{SPh})_6]^{3-}$, obtained immediately following the addition of six equivalents of PhS^- to solution (a) at ambient temperature; (d) $[\text{Fe}_4\text{S}_4(\text{SPh})_4]^{2-}$ obtained from solution (c), after standing for 10 min. at ambient temperature

clusters are paramagnetic and their EPR spectra are consistent with $S = 1/2$ ground states and g_x , g_y and g_z values within, 2.038-2.039, 1.713-1.794 and 1.209-1.287 respectively.

The $[\text{Fe}_6\text{S}_6\text{X}_6]^{3-}$ anions undergo reversible electrochemical oxidation to the $[\text{Fe}_6\text{S}_6\text{X}_6]^{2-}$ dianions. These oxidations which occur at low positive potentials can be affected chemically by a mild oxidizing agent such as the $[(\text{C}_5\text{H}_5)_2\text{Fe}]^+$ ion. Oxidation of $[\text{Fe}_6\text{S}_6\text{Cl}_6]^{3-}$ solutions with one equivalent of $[(\text{C}_5\text{H}_5)_2\text{Fe}][\text{PF}_6]$ in CH_3CN results in the formation of the $[\text{Fe}_6\text{S}_6\text{Cl}_6]^{2-}$ diamagnetic cluster [5]. The structure of the $[\text{Fe}_6\text{S}_6\text{Cl}_6]^{2-}$ anion has been determined and contains the $[\text{Fe}_6\text{S}_6]^{4+}$ core. A comparison of the structural parameters in the $[\text{Fe}_6\text{S}_6\text{Cl}_6]^{2-}$ and $[\text{Fe}_6\text{S}_6\text{Cl}_6]^{3-}$ anions (Table I) shows shorter Fe-S bonds in the former and suggests that the highest occupied M.O. in $[\text{Fe}_6\text{S}_6\text{Cl}_6]^{3-}$ is antibonding in nature.

Table I

Interatomic Distances^{a)} (A) and Angles ($^\circ$) in the $(\text{Fe}_6\text{S}_6\text{Cl}_6)^{2-}$, A and $(\text{Fe}_6\text{S}_6\text{Cl}_6)^{3-}$, B Anions

Distances	A ^{b)}	B ^{c)}
Fe-Fe ^{d)}	3.791(6,5)	3.790(3,7)
Fe-Fe ^{e)}	2.757(6,5)	2.765(3,3)
Fe-S ^{d)}	2.268(6,8)	2.284(3,3)
Fe-S ^{e)}	2.254(12,8)	2.272(6,2)
Fe-Cl	2.189(6,8)	2.224(3,2)
S-S ^{d)}	3.743(6,8)	3.801(3,8)
S-S ^{e)}	3.585(6,8)	3.618(3,5)
Angles		
S-Fe-S ^{d)}	112.0(6,9)	113.7(3,3)
S-Fe-S ^{e)}	104.8(12,5)	105.2(6,2)
Fe-S-Fe ^{d)}	114.5(6,6)	113.2(3,3)
Fe-S-Fe ^{e)}	75.1(12,4)	74.8(6,2)
Fe-Fe-Fe ^{d)}	60.0(6,4)	60.0(3,2)
Fe-Fe-Fe ^{e)}	86.9(6,5)	86.5(3,3)

a) See fig. 1 for the labeling scheme. The mean values of chemically equivalent bonds are given. In parenthesis the first entry represents the number of independent distances or angles averaged out, the second entry represents the larger of the standard deviations for an individual value estimated from the inverse matrix or of the standard deviation:

$$\sigma = [\sum_{i=1}^N (x_i - \bar{x})^2 / N(N-1)]^{1/2}$$

b) From Ref. [5].

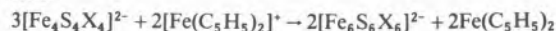
c) From Ref. [2].

d) Distances or angles within the Fe_3S_3 structural units.

e) Distances or angles within the Fe_2S_2 rhombic units.

In search of a general procedure for the synthesis of the $[\text{Fe}_6\text{S}_6\text{X}_6]^{2-}$ dianions from readily available

reagents the oxidation of the $[\text{Fe}_4\text{S}_4\text{X}_4]^{2-}$ clusters was attempted in CH_2Cl_2 according to the reaction



The reaction proceeds cleanly at ambient temperature and for $\text{X} = \text{Cl}^-$, Br^- the oxidative transformation of the $[\text{Fe}_4\text{S}_4\text{X}_4]^{2-}$ clusters to the $[\text{Fe}_6\text{S}_6\text{X}_6]^{2-}$ «prismanes» is quantitative [5].

The oxidative transformation of $[\text{Fe}_4\text{S}_4\text{Cl}_4]^{2-}$ to $[\text{Fe}_6\text{S}_6\text{Cl}_6]^{2-}$ should be contrasted with the oxidative transformation of the Fe_4S_4 centers to Fe_3S_4 centers in certain ferredoxins [6]. The apparent structural difference in the oxidation products in the two systems may reflect the ability of the protein matrix to «capture» unstable intermediates and prevent subsequent rearrangements or higher order coupling reactions.

The facile reversible reduction of $[\text{Fe}_6\text{S}_6\text{Cl}_6]^{2-}$ at low potential ($E_{1/2} = 0.32$ V, in CH_2Cl_2 vs SCE) reveals a new Fe/S redox couple and introduces the Fe_6S_6 core as a viable candidate for future consideration in the biochemistry of «unconventional» and perhaps hitherto unknown Fe/S proteins. The metastable nature of the $[\text{Fe}_6\text{S}_6]^{3+}$ and $[\text{Fe}_6\text{S}_6]^{4+}$ cores clearly indicates that core extrusion reactions are not likely to reveal the presence of such species in proteins. The facile transformation of $[\text{Fe}_6\text{S}_6]^{4+}$ to the $[\text{Fe}_4\text{S}_4]^{2+}$ and $[\text{Fe}_2\text{S}_2]^{2+}$ more stable cores [5] may indeed lead to erroneous conclusions for core extrusion experiments which involve non-heme iron proteins that may contain $[\text{Fe}_6\text{S}_6]^{3+,4+}$ centers.

ACKNOWLEDGEMENTS

This research was supported generously by a grant from the National Institutes of Health (GM-26671).

REFERENCES

- [1] R.H. HOLM, *Chem. Soc. Rev.*, **10**, 455 (1981).
- [2] a) M.G. KANATZIDIS, W.R. HAGEN, W.R. DUNHAM, R.K. LESTER, D. COUCOUVANIS, *J. Am. Chem. Soc.*, **107**, 953 (1985).
b) M.G. KANATZIDIS, W.R. DUNHAM, W.R. HAGEN, D. COUCOUVANIS, *J. Chem. Soc., Chem. Commun.*, 356-358 (1984).
- [3] D. COUCOUVANIS, M.G. KANATZIDIS, A. SALIFOGLU, submitted for publication.
- [4] D. GHOSH, S. O'DONNELL, W. FUREY JR., A.H. ROBBINS, D.C. STOUT, *J. Mol. Biol.*, **158**, 73-109 (1982).
- [5] D. COUCOUVANIS, M.G. KANATZIDIS, W.R. DUNHAM, W.R. HAGEN, *J. Am. Chem. Soc.*, **106**, 7998 (1984).
- [6] H. BEINERT, A.J. THOMSON, *Arch. Biochem. Biophys.*, **222**, 333-361 (1983), and references therein.



MS5.9 — FR

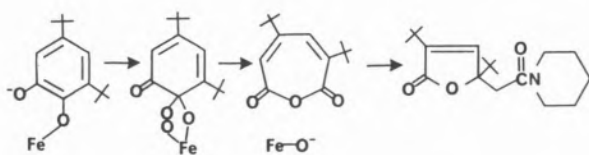
LAWRENCE QUE JR.

Department of Chemistry
University of Minnesota
Minneapolis, MN 55455
U.S.A.

IRON(III)-CATALYZED OXYGENATION OF CATECHOLS

Mechanistic studies on the intradiol cleaving catechol dioxygenases suggest that the iron center in these enzymes remains in its high-spin ferric oxidation state throughout its catalytic cycle [1]. This is due to the presence of tyrosinate ligands which stabilize the ferric state [2]. Such observations have led to a proposed mechanism involving substrate activation by the ferric center where catechol coordinated to the iron through only one of its oxygens reacts with dioxygen [3]. Several iron(III)-catecholate complexes have been synthesized and characterized to test this hypothesis. $\text{Fe}(\text{saloph})\text{catH}$ [4] and $\text{Fe}(\text{TPP})\text{catH}$ [5] are examples where catechol acts as a monodentate ligand and $[\text{Fe}(\text{salen})\text{cat}]^-$ [6] and $[\text{Fe}(\text{NTA})\text{DBC}]^{2-}$ [7] are examples of chelated catecholate complexes. The reactivity studies, conducted on the corresponding 3,5-di-*tert*-butylcatechol (DBCH_2) complexes, provide valuable insights. Of the four complexes, only $\text{Fe}(\text{salen})\text{DBC-H}$ and $[\text{Fe}(\text{NTA})\text{DBC}]^{2-}$ react with dioxygen. $\text{Fe}(\text{salen})\text{DBC-H}$ undergoes a one-electron oxidation to the corresponding chelated semiquinone complex [8], while $[\text{Fe}(\text{NTA})\text{DBC}]^{2-}$ gives rise to the desired oxidative cleavage product in good (80%) yield [7,9]. Chelated catecholate is not expected to react with dioxygen based on electrochemical studies; the chelation stabilizes the catecholate oxidation state to the extent that it is too weak a reducing agent for dioxygen. To rationalize the reactivity of $[\text{Fe}(\text{NTA})\text{DBC}]^{2-}$, some structural change must occur prior to reaction with dioxygen. It is proposed that the DBC ligand

becomes monodentate during the reaction, as suggested by the structure of the $[\text{Fe}(\text{NTA})\text{DBC}]^{2-}$ complex which shows an unsymmetrically chelated DBC ligand ($\text{Fe}-\text{O}(\text{DBC})$, 1.89 and 1.98 Å). The cleavage reaction is initiated by the breaking of the longer $\text{Fe}-\text{O}(\text{DBC})$ bond. The time required for the reaction (4 days) probably reflects the energy necessary to break this bond. The activated complex then reacts with O_2 to form a peroxide intermediate. It is proposed that the ferric center coordinates the peroxide and facilitates its decomposition to the desired cleavage product as illustrated below:



REFERENCES

- [1] L. QUE JR., *Adv. Inorg. Biochem.*, **5**, 167-199 (1983).
- [2] J.W. PYRZ, A.L. ROE, L.J. STERN, L. QUE JR., *J. Am. Chem. Soc.*, **107**, 614-620 (1985).
- [3] L. QUE JR., J.D. LIPSCOMB, E. MÜNCK, J.M. WOOD, *Biochim. Biophys. Acta*, **485**, 60-74 (1977).
- [4] R.H. HEISTAND II, A.L. ROE, L. QUE JR., *Inorg. Chem.*, **21**, 676-681 (1982).
- [5] M.R. ROGERS, L. QUE JR., unpublished results.
- [6] R.B. LAUFFER, R.H. HEISTAND II, L. QUE JR., *Inorg. Chem.*, **22**, 50-55 (1983).
- [7] L.S. WHITE, P.V. NILSSON, L.H. PIGNOLET, L. QUE JR., *J. Am. Chem. Soc.*, **106**, 8312-8313 (1984).
- [8] R.B. LAUFFER, R.H. HEISTAND II, L. QUE JR., *J. Am. Chem. Soc.*, **103**, 3947-3949 (1981).
- [9] M.G. WELLER, U. WESER, *J. Am. Chem. Soc.*, **104**, 3752-3754 (1982).



MS5.10 — FR

KENNETH N. RAYMOND
 DAVID J. ECKER
 LARRY D. LOOMIS
 BERTHOLD MATZANKE
 Department of Chemistry
 University of California
 Berkeley, California 94720
 U.S.A.

STRUCTURE, RECOGNITION AND TRANSPORT OF FERRIC ENTEROBACTIN IN *E. COLI*

The transport and uptake of iron by microbes, a process which is essential for their growth, is mediated by low-molecular-weight complexing agents called siderophores [1,2]. A siderophore produced by *E. coli*, enterochelin [3] (here called enterobactin [4]), is the most powerful iron complexing agent known and has been among the most thoroughly studied of the siderophores [5]. Ferric enterobactin transport in *E. coli* has been studied with respect to the specificity of the outer membrane protein receptor and the mechanism of enterobactin-mediated transport of ferric ion across the outer membrane. Transport kinetic and inhibition studies were performed with ferric enterobactin and synthetic structural analogs (Fig. 1) to map the parts of the molecule important for receptor binding. The ferric complex of the synthetic structural analog of enterobactin, 1,3,5-N,N',N''-tris(2,3-dihydroxybenzoyl)-tri-*o*-methylbenzene (MECAM) is transported with the same maximum velocity as ferric enterobactin. A double label transport assay with $^{59}\text{Fe}[\text{}^3\text{H}]\text{-MECAM}$ showed that the ligand and the metal are transported across the outer membrane when a large excess of extracellular complex was added to the cell suspension. At least 60% of internalized ^{59}Fe enterobactin exchanged with extracellular ^{55}Fe enterobactin (Fig. 2). Internalized $^{59}\text{Fe}[\text{}^3\text{H}]\text{MECAM}$ was released from the cell as

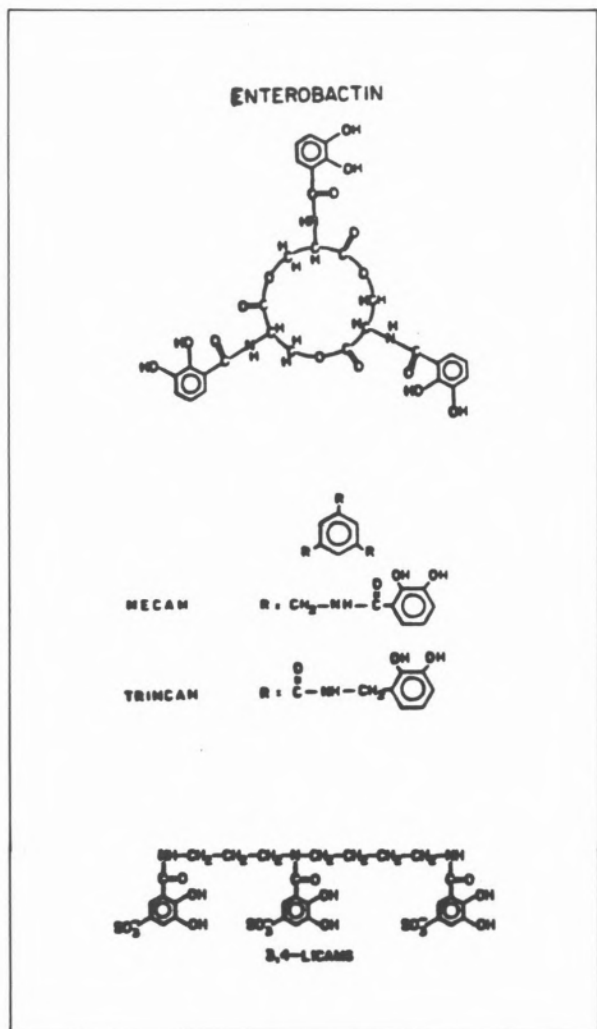


Fig. 1

The structure of enterobactin and several synthetic enterobactin analogs: MECAM[1,3,5-N,N',N''-tris(2,3-dihydroxybenzoyl)triaminomethylbenzene]; TRIMCAM[1,3,5-tris(2,3-dihydroxybenzoyl)carbamido]benzene]; and LICAMS[1,5,10-N,N',N''-tris(5-sulfo-2,3-dihydroxybenzoyl)triazadecane]

the intact complex when either unlabeled Fe MECAM or Fe enterobactin was added extracellularly. The results suggest a mechanism of active transport of unmodified coordination complex across the outer membrane with possible accumulation in the periplasm. Energy-dependent binding of ^{67}Ga enterobactin was observed, but the rate was substantially lower than the rate of ^{59}Fe enterobactin transport. The results establish important correlations between the coordination chemistry of the metal and the mechanism of receptor-mediated uptake.

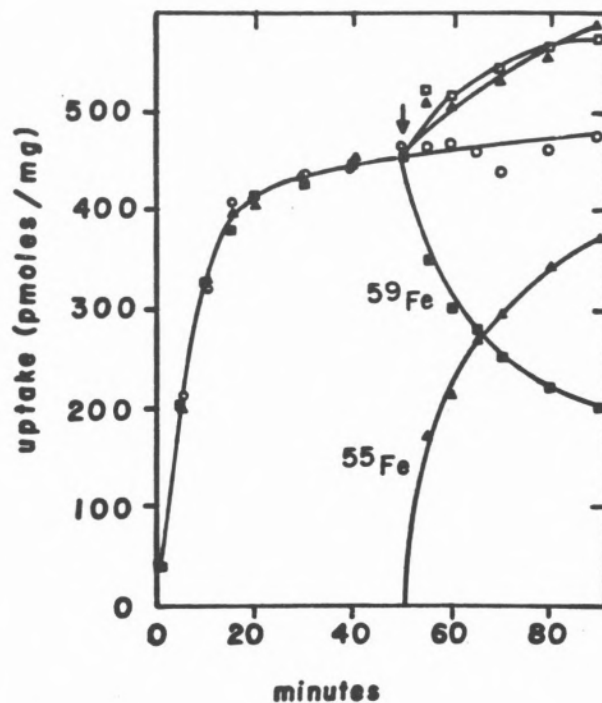


Fig. 2

Exchange of external and cellular ferric enterobactin. The cell concentration was 1.22 mg/mL and the pH was 7.4. In all experiments the initial concentration of ^{59}Fe enterobactin was $2\mu\text{M}$; \circ , ^{59}Fe enterobactin uptake with no additions; Δ , (control) ^{59}Fe enterobactin uptake with the addition (at 51 min, arrow) of the same substrate at $30\mu\text{M}$ concentrations; \blacksquare , ^{59}Fe enterobactin uptake with addition (at 51 min, arrow) of ^{55}Fe enterobactin at $30\mu\text{M}$ concentrations; \blacktriangle , ^{55}Fe enterobactin accumulation in the same experiment; \square , numerical sum of ^{55}Fe (\blacktriangle) and ^{59}Fe (\blacksquare) in the same experiment

REFERENCES

- [1] K.N. RAYMOND, G. MÜLLER, B.F. MATZANKE, *Topics in Current Chemistry*, **123**, 49-102 (1984).
- [2] J.B. NEILANDS, *Ann. Rev. Nutr.*, **1**, 27-46 (1981).
- [3] I.G. O'BRIEN, F. GIBSON, *Biochim. Biophys. Acta*, **215**, 393 (1970).
- [4] J.R. POLLACK, J.B. NEILANDS, *Biochem. Biophys. Res. Comm.*, **38**, 989 (1970).
- [5] G. MÜLLER, Y. ISOWA, K.N. RAYMOND, *J. Biol. Chem.*, (1984), submitted for publication.

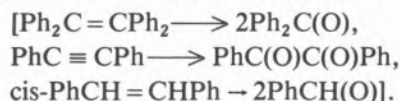


MS5.11 — FR

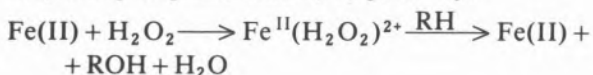
DONALD T. SAWYER
HIROSHI SUGIMOTO
Department of Chemistry
University of California
Riverside, California 92521
U.S.A.

**ACTIVATION OF HYDROPEROXIDES
BY $\text{Fe}^{\text{II}}(\text{MeCN})_4(\text{ClO}_4)_2$ AND $\text{Fe}^{\text{III}}\text{Cl}_3$
IN ACETONITRILE; MODEL SYSTEMS
FOR THE ACTIVE SITES OF PEROXIDASES,
CATALASE, AND MONOXYGENASES**

Addition of $\text{Fe}^{\text{II}}(\text{MeCN})_4(\text{ClO}_4)_2$ to solutions of hydrogen peroxide in dry acetonitrile catalyzes the rapid disproportionation of H_2O_2 via initial formation of a $\text{Fe}^{\text{II}}(\text{H}_2\text{O}_2)^{2+}$ adduct, which, in turn, oxidizes a second H_2O_2 to yield dioxygen. The intermediate of the latter step dioxygenates diphenylisobenzofuran, 9,10-diphenylanthracene, and rubrene, which are traps for singlet-state dioxygen. This intermediate also dioxygenates electron-rich unsaturated carbon-carbon bonds



In the presence of organic substrates such as 1,4-cyclohexadiene, 1,2-diphenylhydrazine, catechols, and thiols, the $\text{Fe}(\text{II})\text{-H}_2\text{O}_2/\text{MeCN}$ system yields dehydrogenated products (PhH , $\text{PhN}=\text{NPh}$, quinones, and RSSR) with conversion efficiencies that range from 100% to 17%. Although the $\text{Fe}(\text{II})$ catalyst does not promote the disproportionation of Me_3COOH or $m\text{-ClPhC}(\text{O})\text{OOH}$, these hydroperoxides are activated for the dehydrogenation of organic substrates. With substrates such as alcohols, aldehydes, methyl styrene, thioethers, sulfoxides, and phosphines, the $\text{Fe}^{\text{II}}(\text{H}_2\text{O}_2)^{2+}$ adduct promotes their monooxygenation to aldehydes, carboxylic acids, epoxide, sulfoxides, sulfones, and phosphine oxides, respectively.



The reaction efficiencies for the group of substrates with the $\text{Fe}(\text{II})$ adducts that are formed by H_2O_2 , Me_3COOH , and $m\text{-ClPhC}(\text{O})\text{OOH}$ have been evaluated. Also, the reaction rates for the substrate- $[\text{Fe}^{\text{II}}(\text{H}_2\text{O}_2)^{2+}]$ dehydrogenations and monooxygenations relative to that for Ph_2SO have been determined, as have the substituent effects for the monooxygenation of 4-X- PhCH_2OH and 4-X- $\text{PhCH}(\text{O})$. The $\text{Fe}^{\text{II}}(\text{H}_2\text{O}_2)^{2+}$ adduct is an efficient catalyst for the autooxygenation of $\text{PhCH}(\text{O})$ to $\text{PhC}(\text{O})\text{OOH}$. In all of these processes the iron(II) catalyst remains in its reduced state.

Solutions of $\text{Fe}^{\text{III}}\text{Cl}_3$ in dry acetonitrile also catalyze the rapid disproportionation of H_2O_2 to O_2 and H_2O , but the catalyst remains in the $\text{Fe}(\text{III})$ state. In the presence of triphenylphosphine, dimethyl sulfoxide, and olefins the $\text{Fe}^{\text{III}}\text{Cl}_3\text{-H}_2\text{O}_2/\text{MeCN}$ system yields monooxygenated substrates (Ph_3PO , Me_2SO_2 , and epoxides). The epoxidation of olefins is especially favored by the $\text{Fe}^{\text{III}}\text{Cl}_3\text{-H}_2\text{O}_2$ adduct.

Both of these catalyst systems [$\text{Fe}^{\text{II}}(\text{MeCN})_4(\text{ClO}_4)_2$ and $\text{Fe}^{\text{III}}\text{Cl}_3$] in dry acetonitrile activate hydroperoxides for the dehydrogenation and monooxygenation of organic substrates, and do not promote radical processes (Fenton chemistry). Their ability to facilitate these reactions via the oxene chemistry of ferryl (FeO^{2+}) and perferryl (FeCl_3O) make them useful reaction mimics for the active sites of *peroxidases*, *catalase*, and *monooxygenases*.



MS5.12 — FR

K. WIEGHARDT

K. POHL

U. BOSSEK

Lehrstuhl für Anorganische Chemie I

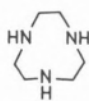
Ruhr-Universität

D-4630 Bochum

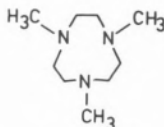
F.R.G.

SYNTHESES OF IRON MODEL COMPOUNDS WITH MACROCYCLIC N-DONOR LIGANDS

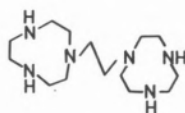
Small macrocyclic N-donor ligands have been used to assemble inorganic model compounds for the met form of vertebrate respiratory protein hemerythrin from mononuclear Fe^{III} complexes. These ligands include the following examples:



tcn



mtcn

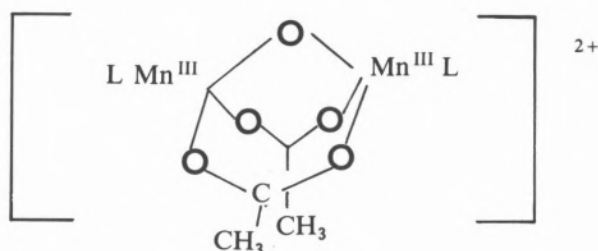


dtcn

A series of iron(III) complexes containing the (μ -oxo)bis(μ -carboxylato)diiron(III) core with the above ligands have been synthesized and characterized by X-ray crystallography. Their spectroscopic

and magnetic properties are compared with the natural proteins. The reactivity of the core has also been investigated. The reactions of the model compounds with N_3^- , NCS^- etc. afford binuclear oxo-bridged species, e.g. $[(tcn)(N_3)_2]Fe-O-Fe(N_3)_2(tc n)$, and $[(tcn)Fe(N_3)_3]$ indicating the facile degradation of the (μ -oxo)-bis(carboxylato) unit.

Analogous compounds containing Mn^{III} have also been prepared. Their structures, spectroscopic, magnetic and chemical properties will be briefly discussed.



The mixed valence Mn^{III}Mn^{IV} binuclear complexes are readily obtained by oxidation of the above complex with $AgBF_4$ in acetonitrile. These complexes may serve as models for the water-oxidation enzyme photosystem II.

Finally, an octameric cation, $[Fe_8(tc n)_6(\mu_3-O)_2(\mu_2-OH)_{12}]^{8+}$, has been prepared and characterized by X-ray crystallography. The quantitative assembly of this species in aqueous solution at ambient temperature and pH 7-8 starting from mononuclear $(tcn)FeCl_3$ may serve as a model reaction for the iron storage protein ferritin.

6. *Proteins of Iron Storage and Transport*

Convener: E.C. Theil
(Raleigh)



MS6.1 — FR

E.C. THEIL

Department of Biochemistry
Box 7622, North Carolina State University
Raleigh, NC 27695-7622
U.S.A.

FERRITIN: A GENERAL VIEW OF THE PROTEIN, IRON CORE, AND THE IRON-PROTEIN INTERFACE

The need for ferritin arose 2.5 billion years ago when oxygen generated during photosynthesis converted Fe^{2+} to insoluble Fe^{3+} . Most contemporary organisms, with representatives among plants, animals, and bacteria, use ferritin to provide a soluble, concentrated reservoir of iron. Ferritin consists of three parts: the outer protein cover, the inner iron core, and the iron-protein interface.

Apoferritin, the protein without any iron, consists of 24 subunits arranged in a hollow sphere. Conservation of protein structure is indicated by immunological crossreactivity, spanning vertebrate classes from fish to mammals, by similarity of sequence and crystals of apoferritin from different sources. The subunits are of similar or identical size, but subtle differences in primary structure of the subunits identifies apoferritin from different organisms; moreover, within an organism small differences in the primary structure of the subunits is associated with particular types of cells, particular physiological states, and with variations in the bioavailability of stored iron. The variations in the structure of the ferritin protein suggest that the information for the primary structure of the subunits is coded for, in part at least, in a

multigene family which is differentially used in each cell type. Evidence which supports such a hypothesis has recently been obtained.

Cell-specific variations in the protein are exemplified by comparing liver and red cell ferritin from bullfrog tadpoles in which the number of serine residues varies from 9/subunit to 15/subunit, respectively. Although both proteins may be phosphorylated in the assembled state, more of the serine residues in the red cell protein are accessible and some of them reside in unique regions, as judged by autoradiograms of tryptic peptides of the proteins phosphorylated using ^{32}P [1]. Iron stored in red cell ferritin appears to be more available than that in liver or macrophage cells.

Physiological variations have been observed in spleen macrophage ferritin from normal and iron-loaded lamb, where apoferritin from the normal cells contains protein subunits that are covalently crosslinked to form intramolecular dimer pairs [2]. Similar crosslinks may be introduced into the apoferritin from iron-loaded tissue with 1,5-difluoro-2,4-dinitrobenzene. A relative decrease in the rate of iron core formation (0.52) and a relative increase in the rate of iron release (1.68) were associated with natural or synthetic crosslinks when the proteins were examined *in vitro*. The differences in the relative rates observed *in vitro* predicated a relative difference in steady state iron content of 0.31. The observed difference in the iron content of the two types of ferritin as isolated from the spleen is 0.39, which is sufficiently good agreement to indicate that the effect of the subunit crosslinks observed *in vitro* corresponds to the effect *in vivo*. Thus, physiologically significant modifications of apoferritin structure, e.g. formation or disruption of crosslinked protomers, allow adjustment of the storage properties of ferritin to the needs of the cell, i.e. when iron is in excess, the apoprotein is modified to retain more iron in the stored form.

The iron core of ferritin is a polynuclear complex of hydrous ferric oxide with small amounts of phosphate and an average formula: $[(\text{FeO}\cdot\text{OH})_8\text{FeO}\cdot\text{OPO}_3\text{H}_2]$. Variations in the core size range from 0-4500 Fe atoms, which within an individual molecule may be arrayed in single large or multiple small crystallites. The crystalline properties of the iron core depend on the presence of

the protein and are very similar to the mineral ferrihydrate. Since ferrihydrate has no phosphate, phosphate appears to reside in disordered regions of the core. The actual arrangement in the core is unknown, but accessibility to chelators suggests that it is distributed throughout the core. The presence of phosphate during reconstitution of the core diminishes both the polydispersity and the size of the magnetic domain. Polynuclear iron complexes of Fe(III) and ATP also have phosphate throughout the cluster, judged by EXAFS analysis, and thus serve as models for the ferritin core [3].

An interface between iron and apoferritin has been observed by electron microscopy. Binding of metals such as V, Cr, Zn, and Tb has been detected by proton release, X-ray diffraction, X-ray absorption, and EPR and visible [4] spectroscopy. Recently a complex of Fe(III) and apoferritin, with an iron environment distinct from that in the core, has been observed by EXAFS analysis [5]. Properties of the complex suggest an environment with carboxylate ligands provided by apoferritin. Ability to trap iron in an environment distinct from the polynuclear iron core allows examination of the role of apoferritin in initiation of formation of the iron core and of the effect of variations in apoferritin structure.

ACKNOWLEDGEMENT

The work of the author reported here was supported in part by the N.C. Agricultural Research Service and National Institutes of Health Grant AM20251.

REFERENCES

- Much of the information reported is reviewed by E.C. THEIL in E.C. THEIL, G.L. EICHORN, L.G. MARZILLI (eds.), «Advances in Inorganic Biochemistry», vol. 5, Elsevier, New York, 1983, pp. 1-38. Only more recent publications are cited below.
- [1] K. IHARA, K. MAEGUCHI, C.T. YOUNG, E.C. THEIL, *J. Biol. Chem.*, **259**, 278-283 (1984).
 - [2] J.R. MERTZ, E.C. THEIL, *J. Biol. Chem.*, **258**, 11719-11726 (1983).
 - [3] E.C. THEIL, D.E. SAYERS, A.N. MANSOUR, F.J. RENNICK, C. THOMPSON, «Proceedings of the 3rd International EXAFS Conference», July 16-20, 1984, Stanford University, Springer-Verlag, New York (in press).
 - [4] A. TREFFRY, P.M. HARRISON, *J. Inorg. Biochem.*, **21**, 9-20 (1984).
 - [5] D.E. SAYERS, E.C. THEIL, F.J. RENNICK, *J. Biol. Chem.*, **258**, 14076-14079 (1983).



MS6.2 — FR

R.R. CRICHTON

Unité de Biochimie
Université Catholique de Louvain
Place L. Pasteur, 1, B-1348 Louvain-la-Neuve
Belgium

PRIMARY STRUCTURE STUDIES ON APOFERRITINS: IRON UPTAKE AND RELEASE

The ferritins are a group of non-haem iron binding proteins which are widely distributed in living organisms (from man to bacteria). Their role is to conserve iron in a soluble, non-toxic and bio-available form within cells (in animals ferritin is also present in variable amounts in serum). The apoferritin molecule is composed of 24 subunits, of MW around 20,000 for the best characterized mammalian proteins, forming a compact, roughly spherical protein shell of external diameter 12 nm which encloses a cavity (diameter 7-8 nm) within which iron is deposited essentially as polymeric ferric oxyhydroxide.

The amino acid sequence of apoferritins from horse spleen, human spleen and liver have been determined by classical protein sequencing techniques while those of rat liver apoferritin and of a human liver apoferritin (of the heavy or H type) have been determined by cDNA techniques. The latter appears to resemble closely the sequence of H type apoferritin found in HeLa cells (unpublished studies from the author's laboratory). The sequences of four of these apoferritins are compared in fig. 1. We can immediately remark that whereas the three L type sequences are closely similar, the human H type sequence is considerably different from the L sequences. A detailed analysis of amino acid substitutions reveals that with the exception of an 8 residue insertion in the region between the D and E helices in rat liver apoferritin and of a His for a Leu at position 169 in the E helix of the human H sequence, the residues

which line the 3-fold and 4-fold axes, through which iron may penetrate to the interior of the molecule, are conserved, as are the putative iron oxidation sites on the internal face of the B-helix.

```

0           10           20           30
A)SSQIRQNYSTEVFAAVNRLVNLVLRASYTY
B)xxxxxxxxxxDxxxxxxxxYxxxxxxxxYxxxxx
C)TxxxxxxxxxxExxxxxxxxRxxxxHxRxxxxx
D)xxxVxxxxHQxSxxxIxRQIxExxxxxVx

           40           50           60
A)LSLGFYFDRDDVALEGVCHFFRELAEEKRE
B)xxxxxxxxSxxxxxxxxSxxxxxxxxxxxxxx
C)xxxxxFxxxxxxxxxxGxxxxxxxxxxxxxx
D)xxMSYYxDxxxxxxxxKNFAKYxLHQSHxExx

           70           80           90
A)GAERLLKMQRGRALFQDLQKPSQDEWG
B)xyxxxxxxxxxxxxxxxxxxxxxxxxIKxxAxxxx
C)xAxxxxLxxExxxxxxxxxVQxxSQxxxx
D)HxxKxMxxxxxxxxxIFLxxIKxxDCxDxE

           100          110          120
A)TTLDAMKAAIVLEKSLNQALLDLHALGSAQ
B)KxPxxxxxxxxMxxxxKxxxxxxxxxxxxxxxxR
C)xxLExxxxxLxxxxNxxxxxxxxxxxxxxxxQ
D)SGxNxxExxHxxxxVxxSxxExxKxATDK

           130          140          150
A)ADPHLCDFLESHFLDEEVKLIKMGDHLTN
B)TxxxxxxxxTxxxxxxxxxxxxxxxxxxxxxx
C)AxxxxxxxxSxxxxKxxxxxxxxNxxxxx
D)NxxxxxxxxIxTxTxNEQxxAxELxDxVxx

           160          170          180
A)IQRLVGSQAGLGEYLFERLTLKHD
B)LHKxGxPExxxxxxxxxxxxxxxxxxxxx
C)xRRWQxxxSxxxxxxxxxxxxxxxxxx
D)xxKMGAxESGxAxxxxDKHxWETVIMKAKP
RANFP

```

Fig. 1

Comparison of Amino Acid Sequences of Apoferritins
 A) Horse spleen, B) Human spleen, C) Rat liver, D) Human H chain. Sequences which are identical with that in the line immediately above are marked x. The human H chain sequence extends 11 residues further than the other sequences, while the rat liver apoferritin has an 8 residue insertion at position 158 (marked as †)

The mechanisms involved in iron deposition and mobilisation are assumed to involve oxidation of Fe^{2+} and reduction of hydrolysed (and non-ionic) ferric iron respectively. Our current understanding of these processes will be discussed in the light of comparative sequence studies and the role of ferritins in intracellular iron metabolism will be analysed.



MS6.3 — FR

P.M. HARRISON
 G.C. FORD
 D.W. RICE
 J.M.A. SMITH
 A. TREFFRY
 J.L. WHITE
 Department of Biochemistry
 The University of Sheffield
 Sheffield S10 2TN
 U.K.

THE THREE-DIMENSIONAL STRUCTURE OF APOFERRITIN: A FRAMEWORK CONTROLLING FERRITIN'S IRON STORAGE AND RELEASE

Ferritin is a giant clathrate compound comprising a protein cage encompassing an «iron-core» of the mineral ferrihydrite complexed with phosphate [1]. The space for this mineral is a sphere of *ca.* 80 Å diameter allowing the storage of up to about 4500 Fe^{3+} atoms. The cage, apoferritin, is a nearly spherical protein shell of thickness about 25 Å. This shell is composed of 24 polypeptide chains arranged in 432 symmetry [1] (Fig. 1). Each chain is folded into a roughly cylindrical subunit (*ca.* 25 × 55 Å), and antiparallel pairs of these subunits form the 12 faces of a rhombic dodecahedron. The apoferritin subunit is a bundle of 4 long antiparallel helices, A,B,C and D, with a shorter helix, E, lying at about 60° to this bundle. There is also a long strand running the length of the bundle which forms a short stretch of antiparallel β-sheet with a 2-fold related subunit. Subunits are arranged such that one end lies beside a molecular 3-fold axis and the other points towards a 4-fold axis. Around the latter axes four nearly parallel E helices from four subunits are in close contact and form another, shorter bundle, with a small hydrophobic central channel (diameter *ca.* 3-4 Å, length *ca.* 15 Å) which passes through the protein shell. In the L-chains the amino acids lining these channels, twelve leucines from four subunits are con-

presented as a framework for the discussion of mechanisms of iron incorporation into ferritin and mobilization of iron from its iron-core.

ACKNOWLEDGEMENTS

We thank the Medical Research Council, the Science and Engineering Research Council and the Wellcome Trust for financial support. G.C.F. is a Wellcome Trust Senior Lecturer.

REFERENCES

- [1] G.C. FORD, P.M. HARRISON, D.W. RICE, J.M.A. SMITH, A. TREFFRY, J.L. WHITE, J. YARIV, *Phil Trans. Roy. Soc.*, **B304**, 551-565 (1984).
- [2] G.C. FORD, E. GODBEHERE, T.H. LILLEY, D.W. RICE, A. TREFFRY, J.L. WHITE, P.M. HARRISON, *Abs. Wa. 34-4*, XIIIth International Conference on Co-ordination Chemistry, Boulder, Colorado, U.S.A. (1984).



MS6.4 — FR

N. DENNIS CHASTEEN
CARL P. THOMPSON
DONNA M. MARTIN
Department of Chemistry
University of New Hampshire
Durham, N.H. 03824
U.S.A.

THE EFFECT OF HISTIDINE MODIFICATION ON THE IRON BINDING CENTERS OF HUMAN SERUM TRANSFERRIN

The transferrins are a class of iron-binding proteins which include serum transferrin, ovotransferrin from egg white, and lactoferrin found in milk and other fluids. These proteins have molecular weights near 80,000 and reversibly bind two Fe^{3+} ions in separate but structurally similar domains. String models, based on the amino acid sequences of the various transferrins as well as on results

from chemical modification studies and spectroscopic data, have been proposed for the iron binding regions of these proteins [1-3]. Likely candidates for the protein ligands in the *N*-terminal domain of human serum transferrin include His-119, His-249, Tyr-185, and Tyr-188. Examination of the portion of the sequence where these groups are clustered reveals several other amino acid residues which may also participate in the uptake and release of iron by the protein. These residues have cationic side chains and include several lysines, arginines and one or two histidines. The present investigation was undertaken to study the effect of histidine modification on the kinetics of iron removal from diferric transferrin by chelating agents.

The modification reaction with ethoxyformic anhydride (EFA) was initially studied. The reaction followed biphasic kinetics consisting of a fast reacting pool of 10 histidines and a slowly reacting pool of 5 histidines.

The iron removal reaction was studied at pH 6.9 in 0.1 M HEPES, 0.02 M NaHCO_3 using pyrophosphate (3 mM) as a mediating chelator and desferrioximine B (0.9 mM) as a terminal iron acceptor while monitoring the absorbance decrease at 295 nm. Semilogarithmic plots of the absorbance data showed that the reaction was biphasic, the fast and slow rates corresponding to loss of iron from the *N*-terminal and *C*-terminal binding sites respectively. This assignment was established by conducting urea-PAGE on samples of the reaction mixture at various times. The rate of iron removal from the *C*-terminal monoferric protein was also measured and found to closely correspond to the slower rate of the diferric protein. The two macroscopic pseudo first-order rate constants were obtained by curve fitting the absorbance data to the sum of two exponentials. Under the conditions of the experiment, iron was removed from the *N*-terminal site at a rate approximately three times faster than from the *C*-terminal site. The four microscopic rate constants were obtained from nonlinear least-squares curve fitting of the time dependence of the concentrations of the four transferrin species, *i.e.* $[\text{Tf}]$, $[\text{Fe}_N\text{Tf}]$, $[\text{TfFe}_C]$, and $[\text{FeTfFe}]$, to the general equations for sequential iron removal from the diferric protein by two parallel pathways. The microscopic constants were

in accord with the macroscopic constants from the spectrophotometric data.

The effect of histidine modification on the macroscopic rate constants was investigated. As diferric transferrin was progressively ethoxyformylated, both rate constants decreased in proportion to the number of fast reacting histidines modified. The data for both sites plotted in the form of a Tsou Chen-Lu graph gave straight lines for $i=1$. These results suggest that a single histidine, presumably one in each iron binding domain, is involved in the release of iron from the protein.

It is well known that the rate of iron removal from transferrin is greatly accelerated below pH 7, following first-order kinetics in $[H^+]$. The effect of histidine modification on iron release was therefore investigated as a function of pH. Modification imparted increased kinetic stability to the protein in the pH range 5 to 7 with the effect greatest at pH 5. The kinetics at pH 5 were studied using citrate, pyrophosphate, orthophosphate, ATP GTP, and DPG as mediating chelators. In every case protein modification significantly slowed the rate by factors ranging from 2 to 10. Evidently the reduction in pK_a of histidine upon ethoxyformylation imparts kinetic stability to the protein in acid, perhaps by eliminating the formation of a protonated imidazole group near the iron. Such a group may be the site of binding of chelates and other anions to the protein.

The structural features of transferrin which play a role in the mechanism of iron release are largely unknown. Until now, amino acids which are not ligands have received little attention. The chemical modification studies presented here implicate the involvement of a key histidine, presumably not bound to the metal, in this process. We speculate that His-207 in the *N*-terminal domain of serum transferrin, which has counterpart residues in the *C*-domain and in both domains of ovotransferrin, is responsible for the effects reported here. Lactoferrin has unusual stability in acid and lacks histidine in this location in the *N*-domain [1-3]. The corresponding portion of the *C*-domain has not been sequenced.

ACKNOWLEDGEMENTS

This research was supported by Grant GM 20194 from the National Institutes of Health.

REFERENCES

- [1] J. MAZURIER, M.-H. METZ-BOUTIGUE, J. JOLLÈS, G. SPIK, J. MONTREUIL, P. JOLLÈS, *Experientia*, **39**, 135-141 (1983).
- [2] N.D. CHASTEEN, in E.C. THEIL, G.L. EICHHORN, L.G. MARZILLI (eds.), «Iron Binding Proteins without Cofactors or Sulfur Clusters», *Adv. Inorg. Biochem.*, vol. 5, Elsevier, N.Y., 1983, pp. 202-235.
- [3] N.D. CHASTEEN, *Trends Biochem. Sci.*, **8**, 272-275 (1983).



MS6.5 — FR

PHILIP AISEN

Departments of Physiology and Biophysics, and Medicine
Albert Einstein College of Medicine
Bronx, New York 10461
U.S.A.

TRANSFERRIN AND IRON TRANSPORT

The critical role of transferrin in the regulation of iron metabolism has long been appreciated, but the molecular mechanisms underlying the protein's activities are still largely obscure. Transferrin functions as an iron donor to cells requiring this essential metal for the biosynthesis of hemoglobin and other vital iron proteins, and as an iron acceptor from cells where the metal is absorbed, released from stores, or recovered from the hemoglobin of senescent red blood cells. Thus, both limbs of the metabolic iron cycle — plasma-to-cell and cell-to-plasma — hinge upon transferrin. Without functional transferrin, neither the maintenance of zero iron balance, nor the delivery of iron to cells, is successfully regulated by the organism.

Many of the processes underlying the interaction of transferrin with iron-requiring cells have been clarified in recent years [1,2]. Iron transfer from protein to cell is receptor-mediated, entails internalization of the receptor-transferrin complex to an acidic, pre-lysosomal compartment where the

iron-protein bond is disrupted and iron becomes available to the cell, and culminates with release from the cell of iron-depleted but otherwise intact transferrin. Relatively little is known, however, of the processes entailed by the return to transferrin of iron recovered from the hemoglobin of catabolized red blood cells. To approach these mechanisms, we have used an *in vitro* model in which immunosensitized red cells are phagocytosed by rat macrophages. In this model, more than half of the iron initially in hemoglobin can be processed for release to the medium, making it suitable for the study of iron delivery from cell to protein. When apotransferrin is present in the culture medium, from 40-70% of the iron released by macrophages is rapidly bound to the protein, with most of the remainder in a ferritin-like form. Macrophages induced by inflammation, or stimulated by preincubation with methemalbumin, release much less iron than non-stimulated macrophages, in accord with the clinical observation of hypoferrinemia in inflammatory states. Iron excreted by macrophages exhibits no distinct preference for either site of transferrin, so that our experiments offer no explanation for the observed differences in site occupancies of transferrin in the circulation [3,4]. The absence of transferrin in the culture medium depresses iron release only slightly, with much of the excreted iron then in a form that readily binds to apotransferrin *in vitro*. Treatment of macrophages with pronase, which largely abolishes their ability to bind apotransferrin [5], depresses iron release no more than 10-15%. It appears, therefore, that binding of apotransferrin to macrophages may not be essential for iron excretion by the cells [6]. The chemistry underlying sequestration of released iron by transferrin remains an enigma.

REFERENCES

- [1] P.A. SELIGMAN, *Prog. Hemat.*, **13**, 131-147 (1983).
- [2] A. DAUTRY-VARSAT, A. CIECHANOVER, H.F. LODISH, *Proc. Natl. Acad. Sci. USA*, **80**, 2258 (1982).
- [3] A. LEIBMAN, P. AISEN, *Blood*, **53**, 1058 (1979).
- [4] J. WILLIAMS, K. MORETON, *J. Biochem.*, **185**, 483 (1980).
- [5] T. NISHISATO, P. AISEN, *Blood*, **52**, 631 (1982).
- [6] K. SAITO, T. NISHISATO, J.A. GRASSO, P. AISEN, (1984), submitted for publication.



MS6.6 — FR

J. WEBB

K.S. KIM

V. TALBOT

School of Mathematical and Physical Sciences
Murdoch University
Perth WA 6150
Australia

D. J. MACEY

School of Environmental and Life Sciences
Murdoch University
Perth WA 6150
Australia

S. MANN

J.V. BANNISTER

R.J.P. WILLIAMS

Inorganic Chemistry Laboratory
University of Oxford
Oxford
England

T.G. ST. PIERRE

D.P.E. DICKSON

Department of Physics
University of Liverpool
Liverpool
England

R. FRANKEL

Francis Bitter National Magnet Laboratory
Massachusetts Institute of Technology
Cambridge, Massachusetts
U.S.A.

COMPARATIVE CHEMICAL AND BIOLOGICAL STUDIES OF INVERTEBRATE FERRITINS

Ferritin has been isolated from the hemolymph of several molluscan species and characterised with respect to its protein composition, the nature of the iron cores present and to its biological function(s). In the case of the chiton *Clavari zona hirtosca*, ferritin is the major iron binding protein present in the hemolymph as determined by the chromatographic fractionation of hemolymph both according to its iron content and according to the distribution of presented Fe-59. The hemolymph concentration of ferritin is remarkably high, ca. 400 $\mu\text{mol/mL}$, a level that can be associated with its role of delivering Fe to the mineralising front of those tissues where magnetite,

Fe_3O_4 is extensively deposited. Ferritin from *C. hirtosa* has a MW of 550,000, subunit MWs of 28000 and 25000, pI values of 4.2 - 4.5 and is immunologically distinct from horse spleen ferritin. The iron core contains on average 2000 Fe atoms. Very high resolution electron microscopy has been used to determine the particle size distribution of the core and the extent of the crystallinity present within the core structure. Temperature dependent Mössbauer spectra indicate that the cores exhibit superparamagnetic behaviour with a blocking tem-

perature between 20 and 40 K. Comparable behaviour has also been observed in the case of the mollusc *Patella vulgata*, whose hemolymph ferritin has a core of limited crystallinity that has a blocking temperature of about 20 K. In the case of the tropical rock oyster *Saccostrea cucullata*, ferritin has been identified as the major iron binding protein present in the body mass. Moreover, in oysters containing elevated tissue levels of Zn, ferritin, as isolated, accounts for significant amounts of protein-bound zinc.

7. Kinetics in Bioinorganic Chemistry

Convener: H.B. Dunford
(Edmonton).



MS7.1 — FR

H. BRIAN DUNFORD
ANNE-MARIE LAMBEIR

Department of Chemistry
University of Alberta
Edmonton
Canada

CORNELIA BOHNE
WILHELM BAADER

Department of Biochemistry
University of São Paulo
São Paulo
Brazil

STEADY STATE AND BURST KINETIC STUDIES ON PEROXIDASES

Despite the tremendous advances in mechanistic studies brought about by transient-state and relaxation kinetics, many problems remain more amenable to treatment by steady state and burst techniques. Two examples follow:

1 — THE CHLORINATION OF MONOCHLORODIMEDONE

The overall reaction is

$$\text{Cl}^- + \text{HCID} + \text{H}_2\text{O}_2 + \text{H}^+ \xrightarrow{\text{CIP}} \text{Cl}_2\text{D} + 2\text{H}_2\text{O}$$
 where HCID represents monochlorodimedone with its replaceable H atom, Cl₂D dichlorodimedone and CIP chloroperoxidase from *Caldariomyces fumago*. Thus the reaction involves three substrates, Cl⁻, HCID and H₂O₂. One of the substrates, Cl⁻, also inhibits the enzyme. A question of some importance is the mechanism of chlorination. An earlier conclusion, based largely on specificity studies, indicated that enzyme-activated hypochlorous acid is the active chlorinating reagent [1]. However recent work on chloroperoxidase supports a free-radical mechanism [2] and a study on

myeloperoxidase led to the conclusion that free hypochlorous acid is the active reagent [3]. Our steady-state kinetic results, which will be presented, provide clear evidence that under the conditions of our experiments chloroperoxidase-activated hypochlorous acid is the active reagent [4].

2 — CHEMILUMINESCENCE FROM ISOBUTYRALDEHYDE

When isobutyraldehyde is added to horseradish peroxidase an apparently spontaneous reaction occurs in which triplet acetone and formic acid are formed, with resultant emission of light from the electronically excited acetone. Experimental results were obtained by use of an oxygen-monitoring electrode and a photon counter. The light emission proceeds through a burst phase into a steady state phase.

From a variety of conditions it was possible to demonstrate that the reaction is initiated by the autoxidation of isobutyraldehyde to a peracid which forms compound I of peroxidase. Subsequent steps proceed through a normal peroxidatic cycle, not a chain reaction. An almost-complete mechanism will be presented for this reaction [5,6] which provides both a model and a probe for light emitting reactions in biology [7].

REFERENCES

- [1] R.D. LIDDY, J.A. THOMAS, L.W. KAISER, L.P. HAGER, *J. Biol. Chem.*, **257**, 5030-5037 (1982).
- [2] B.W. GRIFFEN, P.L. ASHLEY, *Arch. Biochem. Biophys.*, **233**, 188-196 (1984).
- [3] P.C. ANDREWS, N.I. KRINSKY, *J. Biol. Chem.*, **257**, 13240-13245 (1982).
- [4] A.-M. LAMBEIR, H.B. DUNFORD, *J. Biol. Chem.*, **258**, 13558-13563 (1983).
- [5] H.B. DUNFORD, W.J. BAADER, C. BOHNE, G. CILENTO, *Biochem. Biophys. Res. Commun.*, **122**, 28-32 (1984).
- [6] W.J. BAADER, C. BOHNE, G. CILENTO, H.B. DUNFORD, submitted for publication.
- [7] G. CILENTO, *Pure Appl. Chem.*, in press.



MS7.2 — FR

M. BRUNORI
A. COLOSIMO
C. SILVESTRINI
M.G. TORDI

Institute of Chemistry and CNR Centre for Molecular Biology
Faculty of Medicine
University of Rome La Sapienza
and
Department of Expt. Medicine and Biochemical Sciences
University of Rome Tor Vergata
Rome
Italy

KINETIC STUDIES OF THE REACTION OF PSEUDOMONAS CYTOCHROME OXIDASE (*c-d₁*)

Pseudomonas A., grown under suitable conditions, synthesizes a soluble enzyme containing heme *c* and heme *d₁*, which is referred to as Ps nitrate-reductase or oxidase since it is employing as a terminal electron acceptor both nitrate and dioxygen. The functional properties of this enzyme have been investigated by equilibrium and kinetic methods, involving largely absorption spectroscopy. The transient and steady state kinetics with both macromolecular substrates, *i.e.* azurin and cytochrome *c₅₅₁*, have been extensively investigated; the bimolecular steps involved in electron transfer with these two metalloproteins, as well as the internal electron transfer (*c* ⇌ *d₁*), have been carefully characterized. Likewise, the reaction of the reduced enzyme with dioxygen has been investigated, and a mechanism has been proposed, keeping in mind the formation of water as the final product of oxygen reduction.

The results are presented and discussed with special reference to the dimeric structure of the enzyme, also in view of recently acquired data on the kinetic properties of a monomeric state of the macromolecule obtained by chemical modification.



MS7.3 — FR

J.D. SINCLAIR-DAY
A.G. SYKES

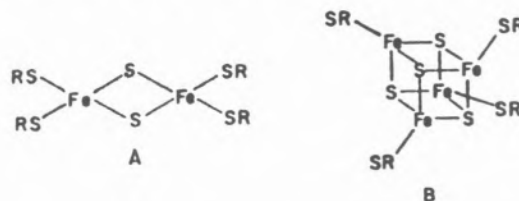
Department of Inorganic Chemistry
The University
Newcastle upon Tyne, NE1 7RU
England

BINDING SITES FOR INORGANIC REDOX PARTNERS ON [2Fe-2S] AND 2[4Fe-4S] FERREDOXINS

Reactions of [2Fe-2S] parsley ferredoxin (M.Wt. 10,500), and bacterial 2[4Fe-4S] ferredoxin from *Clostridium pasteurianum* (M.Wt. 6,000) with inorganic redox partners will be considered. The [2Fe-2S] ferredoxins have a single peptide chain of 98 amino-acid residues and an active site bound by four cysteine side chains (RS) as in (A). They are one-electron redox active ($E^{\circ} = -0.42$ V), [1],



A crystal structure of the [2Fe-2S] protein from *Spirulina platensis* has been reported. Studies on the 2[4Fe-4S] ferredoxin from *Peptococcus aerogenes* have confirmed a structure in which a single peptide chain of 55 amino-acids binds two 4Fe-4S clusters as in (B), with the centres 12 Å apart.



Each cluster is one-electron redox active ($E^{\circ} = -0.40$ V), (2),



Rate constants were determined by stopped-flow spectrophotometry with the inorganic reactant in large (> 10-fold) excess of the protein ($\sim 10^{-5}$ M). All studies reported were at 25°C with ionic

strength $I=0.10$ M (NaCl). The buffer was Tris/HCl in the range $\text{pH}=7.0-9.0$.

Reductants with Parsley [2Fe-2S]. The Cr(II) complex of the 1,4,8,12-tetraazacyclopentadecane saturated macrocycle ligand, here designated as $[\text{Cr}(\text{15aneN}_4)(\text{H}_2\text{O})_2]^{2+}$ ($E^\circ = -0.58$ V), has labile axial ligands. Following reduction of the 2- state protein product analyses have demonstrated that Cr(III) remains attached, and therefore that the reaction falls within the definition of inner-sphere electron transfer. The reaction site is not blocked by redox inactive $[\text{Cr}(\text{en})_3]^{3+}$, and is therefore different to that used by the positively charged oxidants. The rate constant at $\text{pH } 8.0$ ($1.03 \times 10^3 \text{ M}^{-1} \text{ s}^{-1}$) increases by 30% on decreasing the pH to 7. The reductants $[\text{Co}(\text{sep})]^{2+}$ and $[\text{Co}(\text{9aneN}_3)_2]^{2+}$ give (outer-sphere) rate constants of $2.8 \times 10^2 \text{ M}^{-1} \text{ s}^{-1}$ (conventional spectrophotometry) and $1.06 \times 10^3 \text{ M}^{-1} \text{ s}^{-1}$ respectively. Experiments to determine the effect of pH and with $[\text{Cr}(\text{en})_3]^{3+}$ are in progress.

Oxidants with Parsley [2Fe-2S]. Experimental first-order rate constants (k_{obs}) gave linear dependences on oxidant concentrations with negative and zero charged oxidants, enabling k ($\text{M}^{-1} \text{ s}^{-1}$) to be determined. With 2+ through 5+ charged oxidants a non-linear dependence on oxidant consistent with the reaction sequence (3) - (4) is obtained.



Table I

Oxidant	K (M^{-1})	k_{et} (s^{-1})	k ($\text{M}^{-1} \text{ s}^{-1}$)
$[(\text{NH}_3)_5\text{CoNH}_2\text{Co}(\text{NH}_3)_5]^{5+}$	26,400 ^{a)}	214 ^{a)}	$5.6 \times 10^{6b)}$
$[\text{Pt}(\text{NH}_3)_6]^{4+}$	21,000	3.29	$6.9 \times 10^{4b)}$
$[\text{Co}(\text{NH}_3)_6]^{3+}$	998	19.2	$1.9 \times 10^{4b)}$
$[\text{Co}(\text{NH}_3)_5\text{Cl}]^{2+}$	(194)	(2300)	$4.1 \times 10^{5b)}$
$[\text{Co}(\text{NH}_3)_5\text{C}_2\text{O}_4]^{2+}$			5.7×10^3
$[\text{Co}(\text{acac})_3]$			4.3×10^3
$[\text{Co}(\text{edta})]^-$			7.2×10^3
$[\text{Co}(\text{C}_2\text{O}_4)_3]^{3-}$			3.9×10^3

^{a)} Extrapolated from data 0-7°C

^{b)} $k = Kk_{\text{et}}$

No dependence on pH was observed over the range $\text{pH } 7.0-9.0$. Positively charged redox

inactive complexes associate with the protein, $[\text{Cr}(\text{NH}_3)_6]^{3+}$ ($K = 464 \text{ M}^{-1}$), and $[\text{Cr}(\text{en})_3]^{3+}$ ($K = 590 \text{ M}^{-1}$), and block reaction with the positively charged oxidants. They only partially block reaction with neutral complexes, and accelerate the reaction with $[\text{Co}(\text{edta})]^-$. The variation of K values with charge is consistent with a binding site of charge 3- on the protein.

Reactions of Other [2Fe-2S] Proteins. Similar data has been obtained for [2Fe-2S] ferredoxins from parsley, spinach, and the blue-green algae *Spirulina platensis* with $[\text{Co}(\text{NH}_3)_6]^{3+}$ as oxidant, Table II.

Table II

Source of [2Fe-2S]	K (M^{-1})	k_{et} (s^{-1})
Parsley	998	19.2
Spinach	993	15.9
<i>Spirulina platensis</i>	2070	4.9

Since there is a 35% variation in residues between parsley and *Spirulina platensis*, conservation of binding site or sites seems likely.

Location of Binding Sites. Conserved 3- negative patches at 67-69 and 94-96 are close to the active site. From NMR line broadening studies using *Anabaena variabilis* [2Fe-2S] MARKLEY *et al.* have designated negatively charged residues 22-24 and nearby 63 as a possible binding site. Spinach [2Fe-2S] is now known to consist of a mixture of ferredoxin I and II components which are difficult to separate. They have 25 residues different. If this observation applies to other [2Fe-2S] proteins then all data reported will be for I and II components. We have not observed any instances of biphasic kinetics, and if mixtures are present the dominance of conserved binding sites between I and II components is implied.

Similar studies with 2[4Fe-4S] have been carried out.



MS7.4 — FR

Z. BRADIĆ
 K. TSUKAHARA
 P.C. WILKINS
 R.G. WILKINS
 Department of Chemistry
 New Mexico State University
 Las Cruces, NM 88001
 U.S.A.

REDUCTION BY RADICALS OF METMYOGLOBIN, METHEMERYTHRIN AND DERIVATIVES

Myoglobin and hemerythrin are oxygen-binding proteins. Myoglobin is a heme-iron protein which undergoes a one-electron transfer process between the met (Fe(III)) and deoxy (Fe(II)) forms. Hemerythrin contains a well characterized binuclear iron site which can exist in the met (Fe(III)Fe(III)), semi-met (Fe(III)Fe(II)) and deoxy (Fe(II)Fe(II)) forms. The two proteins show interesting similarities, as well as contrasts in their redox chemistry. We have previously examined the reduction by dithionite of metmyoglobin, methemerythrin and anionic adducts [1,2]. In general, the effective reducing agent is the SO_2^- radical which is present in small concentrations in solutions of dithionite. We have now extended these studies by using as a reducing agent the diquat radical ($\text{DQ}^{\cdot+}$) produced by one-electron reduction of DQ^{2+} (1,1'-ethylene-2,2'-bipyridylum ion).

Metmyoglobin and derivatives. The reduction by $\text{DQ}^{\cdot+}$ is compared with that by SO_2^- [1,2] in Table I. Some of the features shown by SO_2^- and already discussed [1,2] are shared with the organic radical. The rate constant/pH profiles for Mb^+ with SO_2^- and $\text{DQ}^{\cdot+}$ are similar, and the basic form (Mb^+OH^-) is at least 10^2 less reactive than the acid form, Mb^+OH_2 . Although all three myoglobin adducts can be *directly* reduced by $\text{DQ}^{\cdot+}$, that of the imidazole is by far the most reactive. Only Mb^+imid is directly reduced by SO_2^- [1].

This may suggest a difference in mechanism for reduction by the two radicals. It is believed that SO_2^- attacks the imidazole ligand and transfers its

Table I
 Second-order rate constants ($\text{M}^{-1}\text{s}^{-1}$) for reduction by $\text{DQ}^{\cdot+}$
 and SO_2^- of metmyoglobin (Mb^+) derivatives at 25°C and
 $I = 0.5 \text{ M}$

Protein	$k(\text{DQ}^{\cdot+})$	$k(\text{SO}_2^-)$
Mb^+OH_2	1.3×10^7	4.5×10^6
Mb^+OH^-	$\leq 10^5$	$\leq 10^4$
Mb^+imid	3.4×10^7	8.8×10^7
Mb^+N_3^-	6.1×10^3	$< 10^3$
Mb^+F^-	1.1×10^3	$< 2 \times 10^2$
HRP^+	1.5×10^5	5.0×10^5

electron through the π -system to the metal ion [1]. The much bulkier viologen radical by contrast may react at some point on the periphery of the protein and then this is followed by electron transfer to the metal ion.

Methemerythrin and derivatives. Most of the early work on reduction of methemerythrin (Hr^+) by dithionite was carried out at pH 8.2 [3]. The reaction is quite complex and this is now understood to reside in (a) the base form of Hr^+ being reduced only slowly by $\text{S}_2\text{O}_4^{2-}$ and (b) the conversion of base to acid form of Hr^+ (pH=7.8) also being slow, $k \sim 10^{-3}\text{s}^{-1}$. Reduction of Hr^+ at pH=6.0 is cleaner, the acid form of Hr^+ being easily reduced by SO_2^- ($k = 1.5 \times 10^5 \text{M}^{-1}\text{s}^{-1}$) to the Fe(III)Fe(II) form [3]. Further reduction of Fe(III)Fe(II) at all pH's is slow, independent of $[\text{S}_2\text{O}_4^{2-}]$ concentration, $k \sim 10^{-3}\text{s}^{-1}$, and may also be associated with a conformational change in the protein. Reduction of anionic adducts of Hr^+ by dithionite occurs only *via* the dissociated fragment [4]. No direct reduction occurs. Even at pH=8.5, reduction of Hr^+SCN^- produces a form of Hr^+ (the acid form?) which is easily reduced. The role of the semi-met form in these reductions and in the autoxidation of oxyhemerythrin is currently being explored.

The reduction of Hr^+ by $\text{DQ}^{\cdot+}$ and other viologen radicals is also being examined. The rate constant for the one-electron reduction by 4,4'-diMeDQ $^{\cdot+}$

is $5.4 \times 10^6 \text{ M}^{-1}\text{s}^{-1}$ at 25° and pH 6. Further reduction is slower ($k = 9.1 \times 10^4 \text{ M}^{-1}\text{s}^{-1}$) but appears to be direct, unlike the behavior with SO_2^- ion.

REFERENCES

- [1] E. OLIVAS, D.J.A. DE WAAL, R.G. WILKINS, *J. Biol. Chem.*, **252**, 4038 (1977); D.R. EATON, R.G. WILKINS, *J. Biol. Chem.*, **253**, 908 (1978).
- [2] R.J. BALAHURA, R.G. WILKINS, *Biochim. Biophys. Acta*, **724**, 465 (1983).
- [3] P.C. HARRINGTON, D.J.A. DE WAAL, R.G. WILKINS, *Arch. Biochem. Biophys.*, **191**, 444 (1978).
- [4] E. OLIVAS, D.J.A. DE WAAL, R.G. WILKINS, *J. Inorg. Biochem.*, **11**, 205 (1979).



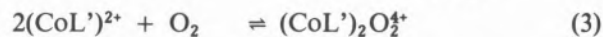
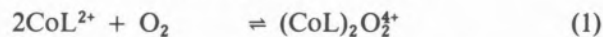
MS7.5 — FR

ARTHUR E. MARTELL
CARL J. RALEIGH
Department of Chemistry
Texas A&M University
College Station, Texas 77843
U.S.A.

KINETICS AND REACTION PATHWAYS FOR THE AUTOXIDATION OF COBALT POLYAMINE COMPLEXES

The two types of autoxidation reactions of binuclear cobalt dioxygen complexes that have been identified involve oxidative dehydrogenation of the ligand with regeneration of a cobalt(II) complex, and conversion to an inert cobalt(III) complex of the unchanged ligand with release of hydrogen peroxide. Examples of ligands which form dioxygen complexes exhibiting these two types of characteristic reactions are the pentadentate polyamines, tetraethylenepentamine (TETREN, **1**), 1,9-bis(2-pyridyl)-2,5,8-triazanonane (PYDIEN, **2**), and 2,6-bis(2-(3,6-diazahexyl)pyridine (EPYDEN, **3**). The stabilities and properties of the cobalt dioxygen complexes of ligands **1**, **2**, and **3** have been described [1-4].

It has been found that the cobalt(II) complex of PYDIEN forms a peroxo-bridged binuclear dioxygen adduct which undergoes facile autoxidation through successive oxygenation and dehydrogenation (anaerobic) steps, as follows:

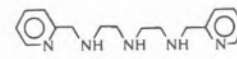


The kinetics of reaction (2) have been studied in detail, and have been found to follow the rate law:

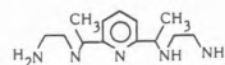
$$-d[\text{O}_2 \text{ complex}]/dt = k_1 [\text{O}_2 \text{ complex}] + k_2 [\text{O}_2 \text{ complex}] [\text{OH}^-] \quad (7)$$



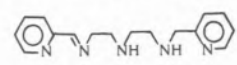
TETREN 1



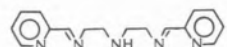
PYDIEN 2



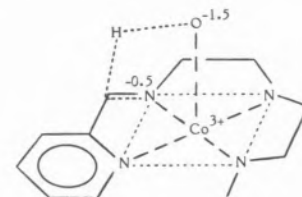
EPYDEN 3



Monoimine, 4, L'



Diimine, 5, L''



Transition state, 6

Decomposition of the cobalt(II) complexes formed in reactions (2) and (4) with strong acid results in the formation of pyridine-2-carboxaldehyde, which was identified quantitatively as the 2,4-dinitrophenylhydrazone. The reaction mechanism suggested for the autoxidation steps (2) and (4) involve the formation of a deprotonated coordinated amino nitrogen in a pre-equilibrium step, followed by electron and hydrogen atom shifts through a transition state **6** in which the following transformations occur in a concerted fashion: O-O fission, shift of α -proton to oxygen, and electron transfer through the metal ion from the α -carbon to the oxygen.

The final autoxidation step (6) is entirely different in nature, and involves the conversion of the metal ion to an inert Co(III) complex, with dissociation of hydrogen peroxide. This reaction is also base-catalyzed, with a pre-equilibrium ligand deprotonation step. The rate law is similar in form to (7), but involves an entirely different mechanism with respect to the fate of dioxygen.

The autoxidation reactions of the cobalt dioxygen complexes formed from TETREN and EPYDEN are assigned a similar rate law (7) and reaction mechanism, involving the displacement of the peroxy ligand after deprotonation of a coordinated amino nitrogen in a pre-equilibrium step. The lack of dehydrogenation in the autoxidation of the cobalt dioxygen complex formed from EPYDEN has been found to be due to the fact that the ligand has a folded conformation in the dioxygen complex that does not allow generation of an imine double bond conjugated with the pyridine ring

[5]. This interpretation is supported by crystal structure determinations [6,7]. The lack of dehydrogenation in the autoxidation of the cobalt dioxygen complex containing TETREN is considered due to the lack of an aromatic ring to stabilize the imine by conjugation.

REFERENCES

- [1] W.R. HARRIS, I. MURASE, J.H. TIMMONS, A.E. MARTELL, *Inorg. Chem.*, **17**, 889 (1978).
- [2] W.R. HARRIS, J.H. TIMMONS, A.E. MARTELL, *J. Coord. Chem.*, **8**, 251 (1979).
- [3] A.E. MARTELL, *Acc. Chem. Res.*, **15**, 155 (1982).
- [4] E.C. NIEDERHOFFER, J.H. TIMMONS, A.E. MARTELL, *Chem. Rev.*, **84**, 137 (1984).
- [5] C.J. RALEIGH, A.E. MARTELL, *J. Chem. Soc., Chem. Commun.*, 335 (1984).
- [6] J.H. TIMMONS, R.H. NISWANDER, A. CLEARFIELD, A.E. MARTELL, *Inorg. Chem.*, **18**, 2977 (1979).
- [7] C.J. RALEIGH, A.E. MARTELL, *J. Coord. Chem.*, in press.

ROUND TABLES

1. *Metals in Medicine*

Convener: K.H. Falchuck
(Boston)



RT1.1 — MO

KENNETH H. FALCHUK

Center for Biochemical and Biophysical Science and Medicine
Harvard Medical School
and

Department of Medicine
Brigham and Women's Hospital
Boston, Massachusetts 02115
U.S.A.

CLINICAL DISORDERS OF ZINC METABOLISM AND THEIR TREATMENT

The importance of metals to biochemistry, biology, pathology, and clinical and veterinary medicine is now generally recognized. In intact cells, under normal conditions, these elements participate in enzymatic catalysis, oxidation reduction reactions, nerve conduction, muscle contraction, cytokinesis, karyokinesis, transport across membranes, intracellular organelle stabilization, among other biochemical and biological processes. However, under pathological conditions, they induce diseases in humans, animals and plants. The signs and symptoms of the diseases each metal produces vary; they are dependent on the tissues of organs affected and whether the mechanisms underlying the resultant disorders are the consequences of a deficiency, imbalance or excess.

The pathophysiology of the various diseases associated with disorders of zinc metabolism has been studied and serves to illustrate these comments concerning metals, in general.

In a 70 kg human, there are 2 to 3 g of zinc. Over 99% of this zinc is found within cells and appears

to be inaccessible to the organism for use in the synthesis of new zinc dependent enzymes, proteins, *etc.* Less than 1% of the total is found in serum at concentrations between 90-120 μg per ml. Approximately 30% of the serum zinc is associated with α_2 macroglobulin and the remainder with one or more proteins of molecular weight $> 100,000$ dalton. The identity of this latter specific zinc binding protein(s) is unknown, though many believe it is albumin. The zinc associated with α_2 macroglobulin is relatively stable under normal and diseased states. The zinc content of the other fraction is "labile". It is determined normally by a physiological balance between) the availability of this metal from dietary sources, b) its absorption into the blood through the small intestine, particularly the jejunum and ileum, c) the effect of hormones, d) the amounts taken up by newly formed or growing cells, and e) its losses through *e.g.* the urinary system. The zinc in this fraction represents the sole pool of this element accessible to cells and, hence, provides the zinc required for all the new metabolic/biological needs of the organism.

Reductions in this "labile" zinc fraction lead to zinc deficiency within days. The classical signs and symptoms of zinc deficiency in both animals and man derive from abnormalities in organs with a high cellular turnover; for example, skin (parakeratosis, acrodermatitis), intestine (loss of mucosal cell lining, fibrosis), gonads (hypogonadism and aspermia) or in organs which are undergoing rapid growth (dwarfism). In addition, in the developing fetus these are extensive malformations (over 90%) of all organs.

In humans, diseases due to zinc deficiency can be a) hereditary in nature (acrodermatitis enteropathica), b) acquired by individuals whose daily requirements are normal: due to failure to ingest at least 15 mg zinc/day, concurrent ingestion of fibers, clay, chelators, or other compounds which bind to and prevent zinc absorption, during malabsorption states associated with diseases of the small intestine, following surgical removal of the small intestine, following administration of hyperalimentation fluids with no added zinc, *etc.* or c)

acquired by individuals with increased need for zinc: such as in pregnancy, during the acute phase of many common illness or in a number of illnesses including cirrhosis, trauma, burns, *etc.* In the latter, excessive amounts of the metal are lost in the urine. Independent of the origin of the illness, all are successfully treated by appropriate zinc replacement.

Disorders secondary to imbalances in the amount of metal present in the diet or through metal-metal interactions in the blood have been described. Prominent in this category are those reported for interactions between zinc and either calcium, copper or cadmium.

Effects of increased zinc in organs are limited since conditions leading to excessive absorption of zinc are not known. Oral ingestion of large doses of zinc has led to gastric irritation and ulceration. Furthermore, inhalation of the metal into the lungs causes "zinc fume fever" a condition characterized by pulmonary inflammation and fibrosis.

The metabolic bases for the clinical disorders induced by zinc deficiency still need to be defined. It has not been possible to account for them on the basis of alterations of the functions of zinc in any one, or combinations, of its known metalloenzymes. Recent studies with experimental, model systems, however, suggest a role for zinc in the regulation of the structure, composition and function of the genome which differs from that of its function in enzymatic catalysis. The identification of this role for zinc suggests that effects on genome function induced by its deficiency might provide the molecular mechanism to account for the above clinical manifestations.



RT1.2 — MO

WARREN E.C. WACKER
HENRY K. OLIVER
University Health Services
Harvard University
Cambridge, MA 02138
U.S.A.

MAGNESIUM DEFICIENCY STATES

Since magnesium is the second most abundant intracellular cation and is required in many biochemical reactions, one would expect deficiencies in this element to occur in man.

Magnesium was first found to be required for normal growth of mice in 1926. In 1932 magnesium deficiency was induced in young rats and appeared clinically as neuromuscular hyper-irritability, described as tetany, which culminated in seizures and death after three to four weeks of the deficient diet. In the same year, naturally occurring clinical magnesium deficiency was observed in lactating cows and sheep and was given the name grass tetany or grass staggers. This form of magnesium deficiency continues to be a serious problem in the field of animal husbandry. While there were early anecdotal reports of magnesium deficiency in humans as early as 1934, it was not until the 1950's that clinical magnesium deficiency, accompanied by a decrease in the serum magnesium concentration and manifested by a variety of neuromuscular abnormalities, was definitely established by a number of investigators including Flink and his co-workers and Vallee and his co-workers.

The clinical manifestations vary, and the severity does not correlate with the concentration of magnesium in serum. The disorder may be characterized by tetany, athetotic movements, nystagmus, convulsions, agitation, tremors, hallucinations, neuromuscular weakness, dysphagia, cardiac arrhythmias or with any combination of these signs and symptoms. While clinical deficiency can occur in the presence of a normal serum magne-

sium concentration, a decrease in serum magnesium concentration is usually present.

It is extremely difficult to produce experimental magnesium deficiency in adult humans. Only by reducing the oral intake virtually to zero, has it been possible to induce symptomatic experimental magnesium deficiency in humans. Thus, clinical magnesium deficiency in man is a «conditioned deficiency». The conditioning factors consist of either decreased absorption or increased excretion of magnesium usually in the presence of an inadequate dietary intake. It occurs as a complication of many diseases and as the result of drug therapy, which either decreases absorption or increases renal excretion.

Specific congenital absorption and excretion defects leading to symptomatic magnesium deficiency have been identified in humans.

Despite the availability of adequate means for the measurement of magnesium in serum and other body fluids for over 20 years, magnesium deficiency in man, even when it is symptomatic, frequently goes undetected. This is particularly so in patients with cardiovascular disease, who are receiving large doses of potent diuretics. In such patients magnesium deficiency causes hyper-irritability of the heart and enhanced toxicity of the digitalis glycosides which may lead to severe ventricular tachyarrhythmias and death.



RT.1.3 — MO

KARL H. BEYER JR.*
The Milton S. Hershey Medical Center
Hershey, Pennsylvania 17033
U.S.A.

FROM THEORY TO THERAPY: HOW TO MAKE A NEW DRUG OUT OF A NEW IDEA

I remember iron, quinine and strychnine tablets as a sort of Spring tonic, along with sassafras tea, at our house when I was a child. Calomel («mild

mercurous chloride»), the old pharmacy texts called it) was prescribed, but I don't know why except that the tablets or powders were said to be laxative at doses of 1/2 to 3 grains. Today, these things are abhorred by physician and regulatory agency alike.

Times have changed and so has the discovery and development of new drugs. Today, we conceive the way to new therapy as Designed Discovery; the fitting of chemical structure to the clinical correlates of disease that we express one way or another in our laboratory methodology. Luck and serendipity still find expression where there is keen perception and unusual discernment. These less precise ways are not adequate, of themselves, to justify complex research programs and structures that require the investment of many careers and hundreds of millions of dollars.

Whether it be inorganic, organometallic, or organic compound, simple or complex, of least or great size, bringing a biologically active agent from theory to therapy becomes increasingly complex as our ability to conceive and ask relevant questions regarding utility and safety increases.

Biological activity of an agent can be delineated, simply, as 1) its primary attribute, that for which it is to be used — as for blood pressure lowering, or antidepressant or antiulcer activity; 2) its secondary attributes, the pharmacological effects that have to be contended with — for example, bronchoconstriction in an antihypertensive agent, dryness of the mouth in an antihistaminic drug for the relief of some allergies; 3) The third attribute has to do with safety.

Just as the first two attributes have to do with a) what's good about it? and

b) «yes, but»,

the third attribute relates to what is bad about the exciting new agent.

To the regulatory agency a new use for an otherwise old agent makes it new from the standpoint of its overall assessment. This would be the case for the assessment of an element, such as helium or lithium, potassium, calcium, or barium, which may be made available in some state of purity as such or as an inorganic or organic salt.

You may be interested in developing an immunoassay for your favorite copper-containing enzy-

* Visiting Professor of Pharmacology

me. It may work, but if the assay picks up both relevant and irrelevant isozymes it maybe worse than useless. It may be misleading.

Organisms have made use of organic compounds having elemental reactive sites since their inception. We have used more simple organometallic compounds in medicine almost as long as chemists have synthesized them. Such complexes of mercury, antimony, and gold have stood us in good stead for many decades for the treatment of syphilis, as diuretics for the relief of edema, the treatment of schistosomiasis and the management of arthritis.

You may know that safety of such compounds is almost as important as efficacy, but you probably have no idea how to go about bringing an interesting agent from theory to therapy. The purpose of this lecture is to explain how you might go about making a new drug out of an interesting agent today; the excitement, the pitfalls, the time, the cost and «what's it to you».



RT1.4 — MO

N.J. BIRCH
Biomedical Research Laboratory
School of Applied Sciences
The Polytechnic, Wolverhampton
WV1 1LY
England

LITHIUM IN MEDICINE

Lithium has been used in medicine since the middle of the nineteenth century. However, it has been used extensively only in psychiatry and only since 1949 when CADE [1] first discovered the "anti manic" action. Latterly this was exploited by SCHOU [2,3] who recognised the significant prophylactic, or preventative, action against recurrent mood swings in periodic affective disorders, the manic depressive psychoses. Currently some 25,000 patients in the United Kingdom (1 in 2000 of the population) receive lithium therapy.

The biochemical basis of the action of lithium, and indeed the aetiology of the disease itself, has been extensively studied but so far a solution eludes us [4]. A number of side effects of lithium has been frequently described and these, themselves, have become the bases for a number of medical uses of lithium. In particular its use in granulocytopenia, a deficiency of specific white blood cells, granulocytes, has been documented in a major review volume by ROSSOF & ROBINSON [5] Lithium has also been used in attempts to elucidate mechanisms and provide a diagnostic test in essential hypertension where it may interact with sodium transport mechanisms [6].

In psychiatric practice lithium is always given orally, a dose of up to 1 g lithium carbonate per day being usual and with the objective of maintaining the blood plasma concentration of lithium in the range 0.6-1.2 mmol/l. Excessive plasma lithium is an indication of impending toxicity which may result from overdosage (accidental or with suicidal intent) reduced fluid or salt intake, excessive sweating or dietary restriction. Toxicity is best treated by haemodialysis which must be maintained until the body burden of lithium is significantly reduced. Practical aspects of therapy have been comprehensively discussed by JOHNSON [7].

In an attempt to prevent the wide daily excursions in plasma lithium shown following the administration of conventional lithium carbonate preparations on a normal regime, slow release formulations have been used in which the lithium carbonate is either embedded in a waxy or cellulose matrix or very highly compressed. The efficacy of these has been questioned and we have carried out a series of studies to identify the mode of transfer of lithium across the gastrointestinal tract [8,9].

Recent fears that lithium might cause permanent renal damage in long-term therapy have now been largely discounted though there still remains some doubt of the safety of combinations of lithium with other major psychotropic drugs over a prolonged period. Combination of lithium therapy with other long-term psychotropic therapy therefore is best avoided.

It has been suggested that lithium may act by interference with magnesium dependant processes due to the chemical similarity between the two ele-

ments resulting from the diagonal relationship in the periodic table [10]. Kinetic studies of magnesium dependant enzymes and investigation by NMR of interactions of lithium and magnesium with nucleotides [11], have shown only weak effects of lithium on magnesium regulated processes and the working hypothesis must therefore be reconsidered.

Lithium carbonate is a useful and inexpensive drug which has an important role to play in current therapeutics. Its mode of action is not well defined and much scope therefore remains for further study in this area of Inorganic Pharmacology.

REFERENCES

- [1] J.F.J. CADE, *Med. J. Australia*, **36**, 349-352 (1949).
- [2] M. SCHOU, *Brit. J. Psychiatry*, **109**, 803-809 (1963).
- [3] M. SCHOU, «Lithium treatment of Manic-Depressive Illness: A Practical Guide», 2nd edn., Karger, Basel, 1983.
- [4] N.J. BIRCH, in H. SIGEL (ed.), «Metal Ions in Biological Systems», vol. 14, Marcel Dekker, New York, 1982, pp. 257-313.
- [5] A.H. ROSSOF, W.A. ROBINSON, «Lithium effects on granulopoiesis and immune function», Plenum, New York, 1980, p. 475.
- [6] M. CANESSA *et al.*, *Clin. & Exp. Hypertension*, **3**, 783-795 (1981).
- [7] F.N. JOHNSON, «Handbook of Lithium Therapy», M.T.P. Press, Lancaster, 1980.
- [8] A.R. KARIM *et al.*, *Gastroenterol. Clin. et Biol.*, **8**, 867-868 (1984).
- [9] N.J. BIRCH, I.P.L. COLEMAN, A.R. KARIM, *Brit. J. Pharmacol.* (1985) in press.
- [10] N.J. BIRCH, *Brit. J. Pharmacol.*, **47**, 586-594 (1973).
- [11] J.W. AKITT, N.J. BIRCH, manuscript in preparation.



RT1.5 — MO

I.R. JUDSON

A.H. CALVERT

Department of Biochemical Pharmacology
Institute of Cancer Research
The Royal Cancer Hospital
Clifton Avenue, Belmont, Sutton, Surrey SM 25 PX
U.K.

CLINICAL APPLICATIONS OF PLATINUM METAL COMPLEXES

In the late 1960's ROSENBERG noted that the growth of bacteria exposed to an electric field became filamentous, suggesting the presence of an antiproliferative agent in the culture medium. This observation led to the identification of *cis*-dichloro-diammine platinum II (cisplatin) as a possible anticancer agent [1]. Subsequent clinical studies performed initially in the USA and England, but later throughout the world have established cisplatin as one of the most important new anticancer drugs to enter clinical practice in the last ten years [2]. Its use in combination in the treatment of testicular tumours has transformed the prognosis. Even for patients with disseminated disease cure rates in the region of 90% are now achieved in most major centres [3]. Cisplatin is also the prime agent in ovarian cancer [4] and is active in a variety of other tumours.

Cisplatin is capable of forming adducts to nucleophilic sites on biological molecules, the chlorine atoms acting as leaving groups. In common with a number of other anticancer drugs, cisplatin will cross-link DNA via the guanine residues. The property of cisplatin which endows it with its special activity is not known. However, cisplatin is capable of forming intrastrand cross-links [5] and it is tempting to speculate that these differentiate its activity from that of other drugs. The analogue transplatin possesses most of the biological properties and toxicities of cisplatin but is both devoid of antitumour effect and incapable of forming intrastrand cross-links.

Although cisplatin has been one of the most active anticancer drugs to be introduced recently, it is also one of the most toxic. Cisplatin causes severe emesis and is toxic to the kidneys and the peripheral nervous system. It can also cause deafness, anaemia and convulsions, the latter mediated by hypomagnesaemia. The acute renal failure which occurred in the early trials of cisplatin may be averted by forced hydration and diureses, although a progressive decline in renal function still occurs and limits both the maximal single dose and the total dose which may be given. OZOLS *et al.* [6] have shown that hyperhydration and the administration of hypertonic saline will allow higher doses of cisplatin to be given without a marked decline in renal function, possibly due to a common ion effect in the renal tubule stabilising the leaving groups of cisplatin. However, the incidence of the other complications, particularly deafness and peripheral neuropathy, was markedly increased.

Another approach has been to search for analogues. In a collaborative programme with the Johnson Matthey Company we have evaluated about 300 analogues of cisplatin as potential alternatives to the parent drug. Of these, eight were selected which showed antitumour activity similar to that of cisplatin in experimental systems. An intensive toxicity study of these eight led to the selection of 2 analogues without nephrotoxicity. These were *cis*-diammine-1,1-cyclobutane dicarboxylate platinum II (JM8, CBDCA, Carboplatin) and *cis*-dichloro-*trans*-dihydroxy-diisopropylamine platinum IV (CHIP, JM9, Iproplatin) [7]. Carboplatin has been extensively evaluated in the Royal Marsden Hospital and latterly in other centres [8]. It has activity similar to that of cisplatin in carcinoma of the ovary, but is devoid of renal toxicity and ototoxicity [9]. It also causes significantly less emesis. Carboplatin is also highly active in small cell lung cancer [10] and has shown encouraging activity in a number of other tumours. The dose-limiting toxicity of carboplatin is to the bone-marrow. Iproplatin is at an earlier stage, but has been evaluated in Rosewell Park (USA) and Manchester (England). It also possesses reduced non-haematological toxicity compared to cisplatin and has shown encouraging signs of antitumour activity. It is interesting that there is

some clinical evidence that Carboplatin and Iproplatin may be active in patients whose tumours are resistant to cisplatin [11]. These observations suggest that the pursuit of cisplatin analogues may lead to the discovery of drugs with an enhanced or different spectrum of antitumour activity in addition to having a more acceptable toxicity profile.

REFERENCES

- [1] B. ROSENBERG, «Platinum Complexes for the Treatment of Cancer», *Interdisciplin. Sci. Rev.*, **3**, 134-147 (1978).
- [2] A.W. PRESTAYKO, S.T. CROOKE, S.K. CARTER (eds.), «Cisplatin: Current Status and New Developments», Academic Press, New York, 1980.
- [3] E.S. NEWLANDS, R.H. BEGENT, G.J. RUSTIN *et al.*, *Lancet*, **1** (8331), 948-951.
- [4] E. WILTSHAW, B. CARR, *Recent Results Cancer Res.*, **48**, 178-182 (1974).
- [5] J.P. CARDONNA, S.J. LIPPARD, in M.P. HACKER, E. DOUPLE, I.H. KRAKOFF (eds.), «Platinum Coordination Complexes in Cancer Chemotherapy», Martinus Nijhoff, Boston, 1984.
- [6] R.E. OZOLS, B.J. CORDEN, J. COLLINS, R.C. YOUNG, in M.P. HACKER, E. DOUPLE, I.H. KRAKOFF (eds.), «Platinum Coordination Complexes in Cancer Chemotherapy», Martinus Nijhoff, Boston, 1984.
- [7] K.R. HARRAP *et al.*, in A.W. PRESTAYKO, S.T. CROOKE, S.K. CARTER (eds.), «Cisplatin: Current Status and New Developments», Academic Press, New York, 1980.
- [8] A.H. CALVERT, S.J. HARLAND, D.R. NEWELL *et al.*, *Cancer Chemother. and Pharmacol.*, **9**, 140-147 (1982).
- [9] E. WILTSHAW, B.D. EVANS, A.C. JONES, J.W. BAKER, A.H. CALVERT, *Lancet*, **1**, 587 (1983).
- [10] I.E. SMITH, S.J. HARLAND, B.A. ROBINSON *et al.*, *Cancer Treat. Rep.*, (1985) in press.
- [11] B.D. EVANS, K.S. RAJU, A.H. CALVERT *et al.*, *Cancer Treat. Rep.*, **67**, 997-1000.

2. Environmental Bioinorganic Chemistry

Convener: J.M. Wood
(Minneapolis-St. Paul)



RT2.1 — MO

J.M. WOOD
Gray Freshwater Biological Institute
University of Minnesota
Navarre, MN 55392
U.S.A.

ENVIRONMENTAL ASPECTS OF NICKEL TRANSPORT AND NICKEL TOXICITY IN SELECTED ALGAL SPECIES

More than ten years ago it was shown that nickel can function as an essential element by Zerner's group in Queensland, Australia. In a series of seven papers in *Biochemistry*, a detailed study of the structure, kinetics and mechanism of Jack Bean urease was reported by this group who showed that nickel is present at the active site of this enzyme. Since that time nickel has been found to play a very important role in the metabolism of carbon-1 (C_1) compounds in the anaerobic bacteria. Nickel containing coenzymes function in the active sites of the enzymes which fix molecular hydrogen (*i.e.* the hydrogenases), in the terminal enzyme for methane biosynthesis (*i.e.* a nickel-containing B_{12} -analog or nitrin macrocycle), and in the hydration of carbon monoxide by those organisms which utilize CO as sole carbon and energy source.

In sediments nickel forms stable and insoluble complexes with sulfide ions and with thiolates to give nickel sulfides and stable oxidation complexes with organic compounds which contain thiol-groups. However, at the sediment/water interface, nickel forms weaker coordination complexes with oxygen donors such as carboxylate, hydroxyl, and other oxy-ligands (*e.g.* humic acids, fulvic acids, clays, metal oxides, *etc.*). Slightly stronger complexes are formed with oxygen

donors at the cell surfaces of bacteria and algae which have many anionic functional groups from both proteins and polysaccharides (*e.g.* polygalacturonic acids at the surface of green algae). These complexes, to the weaker oxygen donors, are unstable enough for nickel to be exchanged with the fast exchange ions Ca^{2+} and Mg^{2+} releasing Ni^{2+} into the water. Thus, Ni^{2+} has an intermediate exchange rate with Ca^{2+} and Mg^{2+} , and so Ni^{2+} cannot be removed entirely from industrial wastewater by traditional treatment methods.

Since algae are known to bioaccumulate nickel directly from the aqueous environment, we conducted a basic study to determine some of the parameters necessary for nickel removal by, and nickel resistance in, these photosynthetic organisms. I shall present here a summary of the results of this study by selecting two axenic cultures of cyanobacteria, (*Synechococcus* ATCC 17146 and *Oscillatoria* UTEX 1270) compared with two strains of green algae (*Scenedesmus* ATCC 11460 and *Chlamydomonas* UTEX 89). Nickel tolerance was found to vary widely among these four species, with the two species of green algae (*Eukaryotes*) being much more resistant to nickel poisoning than the two species of cyanobacteria (*Prokaryotes*). Using $^{63}Ni^{2+}$, and a microplate technique, we examined nickel transport through cell membranes, nickel complexation at the cell surface, as well as inside cells, and nickel efflux from cells in these four algal species. Also we examined a variety of environmental factors which regulate nickel bioaccumulation and toxicity. *Chlamydomonas* tolerates up to 10 ppm of Ni^{2+} without any effect on its growth rate. In fact this organism will even grow slowly in the presence of up to 150 ppm Ni^{2+} . *Scenedesmus* tolerates up to 5 ppm, but *Oscillatoria* only tolerates 1 ppm and *Synechococcus* is very sensitive accepting only 0.02 ppm. With the exception of *Chlamydomonas*, these algae all accumulate Ni^{2+} optimally at pH 8.0. *Chlamydomonas* does not accumulate Ni^{2+} in the pH range 7.0 to 9.0. A detailed study of Ni^{2+} bioaccumulation in *Scenedesmus* indicated that Ni^{2+} uptake is not affected by either competing cations or competing anions, however, the rate of Ni^{2+} uptake was affected by the age of the culture and by light *versus* dark conditions. Ni^{2+} was found to be primarily complexed at the cell surfa-

ces which accommodated a 3×10^3 fold increase in concentration over the external environment. Nickel transport in *Chlamydomonas* was found to be dependent on the concentration of Mg^{2+} in the culture medium. Competition experiments between Mg^{2+} and Ni^{2+} showed that Mg^{2+} prevents Ni^{2+} toxicity. Similar competition between Ca^{2+} and Ni^{2+} could not be shown, indicating that Ni^{2+} is probably transported in *Chlamydomonas* by way of the ATP-dependent Mg^{2+} channel. In the absence of Mg^{2+} , at equivalent concentration to Ni^{2+} , growth inhibition then occurs for a period of time until cells develop an efflux mechanism which pumps out the intracellular nickel. Similar efflux mechanisms have been discovered in *Prokaryotes* for the specific removal of Cd^{2+} (*Staphylococcus aureus*) and for the removal of arsenicals and antimonials (*Escherichia coli*). *Synechococcus* was found to be the most sensitive organism to Ni^{2+} in this series of experiments. Therefore, attempts were made to select for more tolerant mutants. This was accomplished by selecting surviving colonies from solid culture media containing 10^{-5} M nickel sulfate. After approximately two weeks colonies appeared which resisted nickel poisoning by the selection of two different mechanisms. One class of mutants was found to synthesize large quantities of an intracellular polymer which complexed Ni^{2+} approximately 300 fold over the internal cytoplasm concentration. The second class of mutants did not accumulate nickel as is the case with the parent culture *Synechococcus* ATCC 17146. This ability to resist both nickel complexation at the cell surface, and nickel uptake, was brought about by the synthesis and excretion of a low molecular weight polar ligand which complexes nickel outside the cell and prevents its uptake. Although we have not yet determined the structure of this ligand, we have isolated its $^{63}Ni^{2+}$ -complex and found that it has a molecular weight of less than 1000. Fast atom bombardment mass spectroscopy failed to fragment this complex due to its extreme hydrophobicity. When this ligand is added back to cultures of the parent strain of *Synechococcus*, nickel toxicity is prevented.

The experiments described above show that several direct mechanisms are available to the algae for both the bioaccumulation of and resistance to nickel.



RT2.2 — MO

KURT J. IRGOLIC

Department of Chemistry
Texas A&M University
College Station, Texas 77843
U.S.A.

ARSENIC IN THE ENVIRONMENT

Arsenic is an ubiquitous element notorious as a poison and at the same time essential for life. During the past decade the transformation of arsenic compounds in the environment that take part in the cycling of arsenic were investigated. Most of the arsenic is present in the environment in inorganic form as arsenides, arsenite, and arsenate. Organic arsenic compounds are dispersed into the environment by man and are synthesized by organisms from inorganic precursors through largely unknown pathways.

Biological methylation of inorganic arsenic compounds is ubiquitous in nature. The mechanism of this reaction and the required methyl donors are not yet known with certainty. Algae, shrimp, lobsters, crabs, and other marine organisms accumulate arsenic in form of organic compounds more complex than simple methylarsenic derivatives. Arsenobetaine, $(CH_3)_3 As^+ - CH_2 - COO^-$, was identified in several marine organisms. Dimethyl(ribose)arsine oxide was found in kelp. Growth experiments with algae indicated that algae are capable of synthesizing arsenolecithins, in which nitrogen is replaced by arsenic. Arsenocholine — the expected hydrolysis product of arsenic-containing lipids — has not yet been identified in organisms. Experiments to synthesize arsenocholine, arsenobetaine, arsenocholine phosphate, arsenic-containing lipids, and arsenoriboses have been rather successful. Within a year synthetic samples of all these compounds should be available in quantities sufficient to evaluate the toxicity of these arsenic compounds and to develop chromatographic techniques for their detection in extracts. A thorough understanding of the role of arsenic

and its compounds can be achieved only, when the identities and concentrations of arsenic compounds in the environment are known, when their transformations have been studied, and when their interactions with biologically important molecules and structures have been elucidated. For this purpose, liquid chromatographic techniques were developed for the separation of arsenic compounds that use graphite furnace atomic absorption spectrometers and inductively coupled plasma emission spectrometers as element-specific detectors. Progress in the environmental bioinorganic chemistry of arsenic will only be achieved when many more investigators replace total arsenic determinations by determinations of arsenic compounds.



RT2.3 — MO

MICHAEL R. HOFFMANN

W.M. Keck Laboratories
Engineering & Applied Science
California Institute of Technology
Pasadena, California 91125
U.S.A.

KINETICS AND MECHANISM OF PHOTO-ASSISTED REACTIONS ON IRON OXIDE SURFACES

The kinetics and mechanisms of the photo-induced reductive dissolution of hematite ($\alpha\text{-Fe}_2\text{O}_3$) by S(IV) oxyanions and S(IV) autoxidation in aqueous suspensions of hematite have been investigated. Experimental quantum yields for $\text{Fe(II)}_{\text{aq}}$ production are reported for anoxic hematite suspensions containing S(IV). Quantum yield studies together with spectroscopic information indicate that $\equiv\text{Fe(III)-S(IV)}$ surface complexes undergo a photo-induced ligand to metal charge transfer reaction resulting in the reductive dissolution of hematite and production of $\text{Fe(II)}_{\text{aq}}$.

An experimental rate expression for the photo-induced reductive dissolution of hematite has been formulated as:

$$\frac{d[\text{Fe(II)}]_{\text{aq}}}{dt} = \phi_{\text{Fe(II)}} I_0 (A/V)$$

Direct excitation of charge transfer bands in $\equiv\text{Fe(III)-S(IV)}$ surface complexes provide the simplest explanation which is consistent with experimental observations, although excitation of the low energy $\text{O}^{2-} \rightarrow \text{Fe}^{3+}$ charge transfer band in the bulk solid cannot be totally excluded.

The autoxidation of S(IV) in oxalic hematite suspensions exhibits autocatalytic behavior. This behavior is interpreted in terms of three general processes: i) production of $\text{Fe(II)}_{\text{aq}}$ from photo-induced ligand to metal charge transfer reactions of $\equiv\text{Fe(III)-S(IV)}$ surface complexes, ii) oxidation of $\text{Fe(II)}_{\text{aq}}$ to $\text{Fe(III)}_{\text{aq}}$ and, iii) the $\text{Fe(III)}_{\text{aq}}$ catalyzed autoxidation of S(IV). A numerical model, based on these processes, is developed to predict the disappearance of S(IV) in oxygenated hematite suspensions under illumination.

Irradiation of a wide variety of semi-conductor solids with visible and near UV light results in the acceleration of rates of surface redox reactions. Similar processes may possibly play important roles in the atmospheric transformation of SO_2 , aldehydes, ketones, and aldehyde addition products. Whereas, in natural waters photo-induced reduction of iron (hydrated) oxides will increase the dissolved concentrations of $\text{Fe(II)}_{\text{aq}}$ and $\text{Fe(III)}_{\text{aq}}$ above the levels that would be predicted to exist in oxygenated waters at equilibrium with the atmosphere. The net effect of surface photo-redox reactions may be to increase the rate of iron cycling in surface and atmospheric waters and to increase the concentrations of iron species which may be preferred for biological uptake. Furthermore, reactions which are catalyzed by $\text{Fe(III)}_{\text{aq}}$, such as S(IV) autoxidation, may proceed at much higher rates than those predicted by models which constrain $\text{Fe(III)}_{\text{aq}}$ to be in equilibrium with an iron (hydrated) oxide phase. In addition, photo-induced reductions of Mn(III,IV) and Fe(III) (hydrated) oxides by naturally occurring organics are likely to play important roles in the geochemical cycling of these elements.

The overall reaction rate for a given surface photo-chemical reaction of interest in natural waters

will depend on: i) the relative abundance of the solid in natural waters, ii) the wavelength dependent quantum yield of surface complexes and/or of the solid for the given chemical reaction, and iii) the wavelength dependent light intensity in the water of interest.

The band model has proven to be a useful model for understanding the electronic properties of some solids. In order to assess the potential of a wide variety of naturally occurring solids for participating in surface photochemical reactions, an examination of the band gap energies of some well characterized solids may be useful, provided one realizes that the band theory may not be the most appropriate model for the electronic properties of all solids. Within the framework of band theory, for a solid to participate in surface photochemical reactions of interest in natural waters, its band gap energy must be constrained to values less than 4.20 eV, which corresponds to light of wavelength 295 nm. The minimum energy required to activate the solid may be altered by surface coordination, stoichiometric deficiencies, impurities, and crystal defects, all of which may introduce energy levels within the band gap.



RT2.4 — MO

FRANÇOIS M.M. MOREL

Ralph M. Parsons Laboratory
Department of Civil Engineering
Massachusetts Institute of Technology
Cambridge, Massachusetts 02139
U.S.A.

IRON UPTAKE AND PHYTOPLANKTON GROWTH

The kinetics of iron uptake have been studied in cultures of the coastal diatom *Thalassiosira weissflogii*, both in chelated (buffered) and unchelated media. The availability of the iron is governed by

the effective free ferric ion concentration near the cell surface as controlled by coordination and redox reactions, and by transport processes. In media containing high concentrations of chelating agents, uptake rates in the dark are simply proportional to the equilibrium free ferric ion concentration in the bulk solution. Many Fe(III) chelates are photoreactive, so that in the light, a rapid reduction of the chelated Fe(III) to Fe(II) and reoxidation of Fe(II) by oxygen can take place, leading to an increase in the effective free ferric ion activity and in uptake rate. In the absence of chelating agents, iron transport can become limited by the dissolution rate of iron oxide or by the diffusion rate near the cell surface depending on concentrations and mixing conditions. The kinetics of uptake are also directly affected by other trace metals (e.g. Cd) which compete with iron for cellular transport sites.

Under all conditions, a sizeable fraction of the cellular iron (20-80%) is bound to the surface of the cells, and can be readily removed by acidification, reduction or chelation. Under steady conditions, that iron is not measurably transported into the cell and thus the surface bound iron does not then serve as an iron storage mechanism. However, upon decreases in pH, a fraction of the surface bound iron is released, a large portion of which is transported into the cell. There is thus a two step mechanism providing for surface accumulation of iron at high pH (e.g. during the day when the algae photosynthesize and deplete the CO₂ locally) and subsequent uptake at low pH (e.g. during the night when the algae respire and increase the local CO₂ concentration).

The maximum iron uptake rate is dependent on the previous iron nutrition of the algae. Under iron limitation, one can observe increases in maximum (short term) uptake rates, decreases in cellular iron, and/or decreases in growth rates depending on the free ferric ion concentration. The general relationship among these physiological parameters has been elucidated quantitatively. At a "median" free ferric ion concentration (ca. a 10⁻²⁰ M) both the short term uptake rate and the cellular iron concentration are near their maximum values and result in maximum growth rate. At higher free ferric ion concentrations, the maxi-

imum short term uptake rate is decreased in such a way that the actual steady iron uptake rate, the iron cellular quota and the growth rate all remain constant (and maximum). At lower free ferric ion concentration, the cellular quota decreases in such a way as to maintain maximum growth rate. When the cellular iron quota reaches some minimum value, the growth rate itself decreases proportionally to the free ferric iron concentration. The mathematical model corresponding to these interactive processes appears generally applicable to all limiting phytoplankton nutrients. The model can be further applied to formulate the uptake and growth kinetic effects of toxicants and to predict the stable ambient nutrient and toxicant concentrations in systems under geobiological control.



RT2.5 — MO

J.E. CROSS
D. READ
G.L. SMITH
D.R. WILLIAMS
Department of Applied Chemistry
UWIST PO Box 13
Cardiff CF1 3XF
U.K.

PLUTONIUM SPECIATION FROM DISPOSAL VAULT INTO MAN

Plutonium is one of the most important components of radioactive waste arising from the nuclear power programme. It is the major transuranic by-product of the nuclear fuel cycle and, although a considerable proportion of the radioelement is removed during reprocessing, nuclear wastes may contain significant quantities of this element. The chemistry of plutonium — its long half-life (2.41×10^4 years for Pu-239 and 6.55×10^3 years for Pu-240), its high specific activity of α -emission and its chemical toxicity — make this element of paramount importance in radiological assessments. Hence, the predicted

chemical behaviour of plutonium in any proposed radioactive waste disposal site must be carefully considered.

The disposal of any radioactive material involves the encapsulation of the waste within a suitable matrix and its subsequent placement in either a natural or engineered repository, known as the vault. It is intended that this barrier will contain the waste until such a time that it no longer poses an environmental threat [1]. However, the situation in which the vault fails, and the radioactive material enters the surrounding geosphere and is ultimately incorporated into biosphere food chains, must be considered when assessing the safety of a proposed site.

In order to evaluate the behaviour of plutonium along the pathway from the vault through the geosphere to the biosphere, a knowledge of its physical and chemical forms at each stage is required. Computer simulation modelling may be used to predict such information concerning the speciation of plutonium. Chemical speciation models use thermodynamic formation constant data for all possible complexes which may be present and compute the equilibrium species distribution in a given scenario, enabling the most important plutonium species to be identified. To model a particular system, it must be fully characterised in terms of component concentrations, Eh and pH, together with the physical properties of the disposal environment pertaining to ion exchange and sorption phenomena.

Cement is being considered as a matrix for waste containment for low and intermediate level waste disposal facilities [2]. Hence, as a first approximation, the flooded vault may be considered as a cement solution. Calculation of the speciation of plutonium in this media has shown that the behaviour of this radioelement in the vault is dominated by the high pH encountered therein. Subsequent release of this solution into the geosphere is accompanied by a decrease in pH to the near neutral conditions typically encountered in groundwaters. In this situation, competitive complexing by inorganic ligands, such as carbonate and fluoride, and by organic material, becomes important.

The bioavailability of a metal is dependent on its chemical speciation. Thus, the extent to which plutonium is taken up by man will be determined

by its chemical form in the biosphere. Plutonium can become concentrated in food chains, particularly in the presence of chelating agents, such as citrate and DTPA, and may be subsequently ingested by man. In addition, another important assimilation route is the inhalation of plutonium particulates. Again, the chemical form of the plutonium entering the lungs will determine its rate of removal [3]. Insoluble compounds, *e.g.* oxides and fluorides, may take years, whilst soluble compounds and labile complexes, *e.g.* nitrates and citrates, may take only a few weeks. The distribution of plutonium *in vivo* mimicks that of iron, being primarily complexed to ferritin, hemosiderin, transferrin and citrate [4]. A variety of chelating agents have been developed for plutonium decontamination therapy [5]. However, such drugs are generally only effective if given immediately after intoxication since plutonium is rapidly incorporated into tissues and bones where it is inaccessible to the treatment.

In conclusion, a knowledge of the chemical speciation of plutonium along the disposal pathway from vault to man is essential for a full understanding of its behaviour. Such information allows accurate predictions of the consequences of radioactive waste disposal over the long timescale involved.

REFERENCES

- [1] «Consultation Document on Disposal Facilities on Land for Low and Intermediate Level Radioactive Wastes. Draft Principles for the Protection of the Human Environment», Department of the Environment, London, October 1983.
- [2] R.H. FLOWERS, «The Packaging of Intermediate and Low Level Radioactive Wastes», Proceedings of Conference, Radioactive Waste Management, BNES, London, 1984.
- [3] Task Group on Lung Dynamics, *Health Physics*, **12**, 173 (1966).
- [4] G. BOOCOCK, C.J. DANPURE, D.S. POPPLEWELL, D.M. TAYLOR, *Radiat. Res.*, **42**, 381 (1970).
- [5] V. VOLF, «Treatment of Incorporated Transuranium Elements», Technical Reports Series No. 184, IAEA, Vienna, 1978.

3. *Biological Mineralization*

Convener: R.J.P. Williams
(Oxford)



RT3.1 — TU

R.J.P. WILLIAMS
Inorganic Chemistry Laboratory
University of Oxford
South Parks Road, Oxford OX1 3QR
U. K.

BIO-MINERALS

In the last ten years a few of us have been developing a new branch of bio-inorganic chemistry, that of the solid state. Bio-minerals are not a small class but include Ca, Fe, Si, P, Mn, Sr, Ba, Al, S, F, Zn, Cu compounds some of which are amorphous. The minerals are used as structural units (bone and shell), as protective devices (glass needles), and as sensors of fields (gravitational and magnetic). The minerals are usually formed together with an organic matrix to make a composite material of highly desirable physical properties. In my opening introduction and in the discussion I hope that the way in which biological systems control allotropy, crystal morphology and crystal packing will become clear. Material science has a great deal to learn from these bio-minerals since evolution has imposed upon them a perfection of the relation between composition, structure and function. This was necessary for example in the two-way competition between grasses and species which eat grass.

A point of equal interest is the recent development of methods for the analysis of the microcrystalline or amorphous materials. The electron microscope used in various modes is the main tool for seeing the objects and also for diffraction and lattice imaging. Elemental analysis has to be carried out on extremely small volumes and here the electron microscope can be used

together with proton induced X-ray emission (PIXE). For amorphous materials solid state NMR and EXAFS have obvious advantages. We shall illustrate many of the methods.

A reference for those who know little about the subject is the book [1] "Mineral Phases in Biology".

REFERENCES

- [1] D.C. PHILLIPS, R.J.P. WILLIAMS (eds.), «Mineral Phases in Biology», Royal Society (London) 1984 (also published in *Phil. Trans. R. Soc. London, Ser. B*, **304**, 411-510 (1984).



RT3.2 — TU

J. WEBB
School of Mathematical and Physical Sciences
Murdoch University
Perth WA 6150
Australia
T.G. ST.PIERRE
D.P.E. DICKSON
Department of Physics
University of Liverpool
Liverpool
England
S. MANN
C.C. PERRY
R.J.P. WILLIAMS
Inorganic Chemistry Laboratory
University of Oxford
Oxford
England
G. GRIME
F. WATT
Department of Nuclear Physics
University of Oxford
Oxford
England

MÖSSBAUER AND PIXE STUDIES OF IRON BIOMINERALS

Biomineralisation of iron is now known to be a widespread phenomenon, having been reported in all five living Kingdoms, ranging from Animalia to Monera. The spatial organisation of these bio-

minerals and their biosynthesis are of particular interest since they represent in many cases composite bioinorganic materials of exquisite morphology and design.

The mature teeth along the radula or tongue of the limpet *Patella vulgata* contain hard mineralised phases of iron and silicon oxides within an organic matrix. Mineralisation of the radula teeth is a continuing process and thus the radula exhibits a spatial and temporal sequence of element deposition. The distribution of chemical elements in these teeth has been determined using proton induced X-ray emission (Pixe). The focussed proton beam of energy 4 MeV and intensity 100 pA/ μm^2 was operated in the scanning mode with a spatial resolution of *ca.* 2 μm . The early unmineralised teeth show little evidence of organized distribution of elements in the already fully formed organic structure. Progressive mineralisation however leads to distinct localisation of many elements including Fe, Si, Ca, P and Cu. The

data can be represented as high-resolution colour-coded elemental maps that provide unique insights into the compositional development of these biomineralised structures.

As an approach complementary to the Pixe studies, Fe-57 Mössbauer spectroscopy has been used to determine the chemical form, stoichiometry and crystallinity of iron present in the teeth. The spectrum of mature teeth at 1.3 K is composed of 2 magnetically split sextets. The intensity of the minor sextet decreases as the temperature is raised and a doublet appears in the centre of the spectrum. These and related data indicate that the biomineralised iron occurs as massive crystals of goethite (α -FeOOH) and as small superparamagnetic particles that appear to be poorly ordered. Comparable spectral analyses of the early maturing teeth and of morphologically distinct teeth fragments confirm that well-formed crystals of α -FeOOH constitute a significant amount of the iron species present.

4. *Electron Transfer Processes* Convener: B.G. Malmström (Göteborg)



RT4.1 — TH

C.M. GROENEVELD
 G.W. CANTERS

Department of Chemistry, Gorlaeus Laboratories
 State University Leiden, P.O. Box 9502, 2300 RA Leiden
 The Netherlands

THE pH DEPENDENCE OF THE ELECTRON SELF EXCHANGE RATE OF AZURIN FROM *PSEUDOMONAS AERUGINOSA* AS STUDIED BY NMR

Several research groups have found that the time course of the reduction of oxidised cytochrome c_{551} by reduced azurin (Az) from *Ps. aeruginosa* shows a fast and a slow phase [1,2]. The occurrence of two phases has been interpreted as being due to the presence of a redox active and a redox inactive form of the Az, which interconvert on a time scale of 10-100 msec. Later it was concluded from kinetic experiments that the interconversion is related to a proton association/dissociation equilibrium with pK around 7 [3]. Subsequently the interconversion was linked to the titration behaviour of a particular histidine (His-35). In a series of NMR experiments it has been shown that His-35 participates in an acid/base equilibrium with the same pK and the same kinetics as the interconversion of the «active» and «inactive» forms [4,5]. Protonation/deprotonation of His-35, moreover, appeared to be connected with a conformational change of the protein which quite clearly affected a number of the Cu ligands [6,7]. Recently GORIN *et al.* [8] have argued on the basis of T-jump experiments that the low and high pH forms of reduced as well as oxidised azurin may exhibit different redox activities towards cytochrome

c_{551} , but that the biphasic nature of the reaction kinetics does not necessarily imply that one form of the Az is two or more orders of magnitude more reactive than the other forms, as assumed previously [3].

As suggested by SILVESTRINI *et al.* [3], a particularly telling experiment would be the determination of the pH dependence of the electron self exchange rate of azurin.

In principle this rate can be obtained from the NMR spectrum of slightly oxidised solutions of Az. As long as the so-called «strong pulse» or «slow exchange» conditions obtain, the exchange rate can be extracted from the broadening of a few selected peaks in the NMR spectrum. It has been demonstrated that the ligand peaks are well suited to this purpose [9]. Thus the electron self exchange rate of azurin has been measured under a variety of conditions. The results will be reported on the poster. The main conclusion, surprisingly, is that at room temperature the self exchange rate does not depend strongly on pH or buffer. There is a clear effect on both the entropy and enthalpy of activation, but the effect is of an isokinetic nature, with an isokinetic temperature of about 300 K and an isokinetic exchange rate of about $9 \times 10^5 \text{ M}^{-1} \text{ s}^{-1}$. The implications for the redox characteristics of azurin will be indicated on the poster.

REFERENCES

- [1] M.T. WILSON, C. GREENWOOD, M. BRUNORI, E. ANTONINI, *Biochem. J.*, **145**, 449 (1975).
- [2] P. ROSEN, I. PECHT, *Biochemistry*, **15**, 775 (1976).
- [3] M.C. SILVESTRINI, M. BRUNORI, M.T. WILSON, V.M. DARLEY-USMAR, *J. Inorg. Biochem.*, **14**, 327 (1981).
- [4] K. UGURBIL, R. BERSOHN, *Biochemistry*, **16**, 3016 (1977).
- [5] H.A.O. HILL, B.E. SMITH, *J. Inorg. Biochem.*, **11**, 79 (1979).
- [6] E.T. ADMAN, G.W. CANTERS, H.A.O. HILL, N.A. KITCHEN, *FEBS Lett.*, **143**, 287 (1982);
 E.T. ADMAN, G.W. CANTERS, H.A.O. HILL, N.A. KITCHEN, *Inorg. Chim. Acta*, **79**, 252 (1983).
- [7] G.W. CANTERS, H.A.O. HILL, N.A. KITCHEN, E.T. ADMAN, *Eur. J. Biochem.*, **138**, 141 (1984).
- [8] A.F. GORIN, R. BERSOHN, P.E. COLE, *Biochemistry*, **22**, 2032 (1983).
- [9] G.W. CANTERS, H.A.O. HILL, N.A. KITCHEN, E.T. ADMAN, *J. Magn. Reson.*, **57**, 1 (1984).



RT4.2 — TH

B. REINHAMMAR

Department of Biochemistry & Biophysics
Chalmers University of Technology
S-412 96 Göteborg
Sweden

ELECTRON TRANSFER AND PROTONATION STEPS IN THE REDUCTION OF DIOXYGEN TO WATER BY LACCASE

There are only two classes of oxidases which can catalyze the complete reduction of molecular oxygen to two water molecules. These enzymes are the blue copper-containing oxidases and cytochrome oxidase. They are shown to share many properties which are of importance in their ability to reduce dioxygen without the release of any intermediate. For example, their minimal functional units contain four transition metal ions which all take part in the catalytic electron transfer between one-electron donating reductants and dioxygen. Earlier studies have elucidated some of the steps in the electron flow mediated by the proteins [1,2]. However, in order to understand the mechanism of dioxygen reduction it is also necessary to know how protons are involved in these reactions. Such studies are difficult to perform and have therefore not been done for any of these proteins.

Recent studies in this laboratory have shown that it is possible to observe two discrete proton consumption steps during reoxidation of tree laccase with dioxygen [3].

This has led to a better understanding of how molecular oxygen is reduced and the nature of the oxygen intermediate.

It was earlier reported that when reduced laccase is reoxidized with dioxygen two reaction steps can be observed [4]. In the first, rapid step, type 1 Cu(I) is reoxidized at the same time as an oxygen radical is formed. This radical intermediate decays

in a much slower reaction which involves the reoxidation of type 2 Cu(I). The type 3 copper pair, as a rule, acts as a two-electron, acceptor-donor and no EPR signals are therefore observed from this site during the reoxidation of the enzyme. It is therefore not fully established whether the pair is reoxidized or not in the rapid reaction. If it is not reoxidized, the oxygen radical would be a superoxide ion which is probably bound to the copper pair. If the pair is also reoxidized, the intermediate could be an O^- radical, as suggested earlier [4]. It could also be a type 3 (Cu_2-O_2) complex with 0-2 H^+ on the dioxygen if the O-O bond has not been broken.

The results from the proton consumption studies have allowed a distinction between these possible intermediate species. Two protons are used up in the rapid reaction with dioxygen. The oxygen intermediate can therefore not be O_2^- , O_3^- or HO_2^- . A H_2O_2 radical is also less likely since it would not appear to be as stable as the oxygen intermediate has been found to be [5]. It is therefore suggested that the intermediate is an O^- radical. The following reaction sequence appears to be supported by the data: Dioxygen first binds to the reduced type 3 copper pair and then receives two electrons to form a peroxide complex with the reoxidized metal pair. An electron from type 1 Cu(I) is then rapidly transferred to this peroxide complex. This electron presumably first reduces one of the type 3 Cu(II) ions before the charge is further transferred to dioxygen. The increased charge on dioxygen will then result in the cleavage of the O-O bond and one water molecule and an O^- radical are formed. The radical would be bound to the copper pair until it is slowly reduced by electron transfer from type 2 Cu(I) as two more protons are consumed and fully reoxidized laccase is formed. This mechanism of dioxygen reduction is also occurring during turnover with the exception of the last step. The fourth electron is there delivered by the re-reduced type 1 copper.

ACKNOWLEDGEMENTS

This work has been supported by grants from the Swedish Natural Science Research Council.

ACKNOWLEDGEMENTS

JHD is the recipient of a Camille and Henry Dreyfus Teacher/Scholar Award, an Alfred P. Sloan Foundation Research Fellowship and a National Institutes of Health Research Career Development Award.

REFERENCES

- [1] Over the last two decades, publications from the laboratories of Chance, DeVault, Hopfield, Jortner, Mauzerall, Sutin, Hush, Marcus, and Miller have extensively discussed the biological and theoretical aspect of this subject. See, for example: (a) B. CHANCE, D. DEVAULT, H. FRAUENFELDER, R.A. MARCUS, J.R. SCHREIFFER, N. SUTIN (eds.), «Tunneling in Biological Systems», Academic Press, New York, 1979; (b) «Electron and Proton Transfer», *Faraday Discuss. Chem. Soc.*, **74**, (1982).
- [2] M.J.K. GENO, J.H. DAWSON, *Inorg. Chem.*, **23**, 1182 (1984).
- [3] M.J.K. GENO, J.H. DAWSON, submitted for publication.
- [4] Elegant experiments by Isied, Gray, and coworkers have measured rates of intramolecular electron transfer with known driving forces in «semisynthetic» metalloproteins, see for example: K.M. YOCOM, J.B. SHELTON, J.R. SHELTON, W.A. SCHROEDER, G. WOROSILA, S.S. ISIED, E. BORDIGNON, H.B. GRAY, *Proc. Natl. Acad. Sci., U.S.A.*, **79**, 7052 (1982).
- [5] B. ANDERES, D.K. LAVALLEE, *Inorg. Chem.*, **22**, 2665 (1983).
- [6] S.S. ISIED, A. VASSILIAN, *J. Am. Chem. Soc.*, **106**, 1732 (1984).



RT4.4 — TH

R. WEVER

A.C.F. GORREN

Laboratory of Biochemistry
University of Amsterdam
P.O. Box 70151, 1000 HD Amsterdam
The Netherlands

R. BOELEN

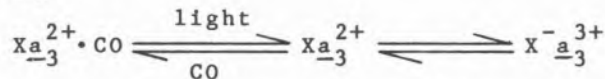
Laboratory of Physical Chemistry
University of Groningen
The Netherlands

ELECTRON TRANSFER REACTIONS
IN CYTOCHROME C OXIDASE

Cytochrome *c* oxidase (ferrocytochrome *c*: oxygen oxydoreductase) catalyses the electron transfer from cytochrome *c* to oxygen. In the mitochondrion the enzyme during its oxidation-reduction process pumps protons [1] across the mitochon-

drial membrane. The proton gradient generated is used by the ATP-ase to produce ATP. Cytochrome *c* oxidase contains four redox centres which are all involved in the enzyme mechanism: two haem *a* groups associated with cytochrome *a* and cytochrome *a*₃, respectively, and two copper ions. The haem iron in cytochrome *a* and one of the copper ions (Cu_A) are involved in the uptake of electrons from cytochrome *c* and the electron transfer to the dioxygen-binding site. The haem iron of cytochrome *a*₃ and the other copper ion (Cu_B) are able to bind dioxygen and to reduce it to water. X-ray edge absorption spectra of oxidized cytochrome *c* oxidase have demonstrated [2] that the distance between these two metal ions is 3.75 Å. This value is in agreement with the distance of 4.5 Å which was obtained [3] from simulations of the triplet EPR spectra of the cytochrome *c* oxidase species formed in the presence of azide and NO. The binuclear copper-iron site is able to bind two ligands simultaneously as was concluded from photodissociation experiments on the various NO complexes of cytochrome *c* oxidase [4]. These observations lead to further support for the notion that during turnover of cytochrome *c* oxidase both metal ions are involved in binding and reduction of dioxygen and/or intermediates.

Relatively little is still known about the pathways during turnover via which electrons are transferred from cytochrome *a* to the cytochrome *a*₃ - Cu_B pair. It has been shown [5] that in the mixed-valence CO complex upon dissociation or binding of the CO molecule the various redox centres in the enzyme change their redox state according to:



where X is cytochrome *a* or Cu_A. These electron redistributions are explained by the changes in the apparent midpoint potential of cytochrome *a*₃ when CO binds to or photodissociates from the reduced cytochrome *a*₃ [6]. These light-induced electron transfer reactions can be studied optically by a steady-state illumination technique or by laser photolysis. Data will be presented that show that in the partially reduced enzyme a pathway is present between Cu_A and the cytochrome *a*₃ - Cu_B pair, via which electrons are transferred rapidly ($k = 7 \cdot 10^3 \text{ s}^{-1}$).

There is evidence that during turnover dioxygen is reduced to peroxy intermediates [7] via a 2-electron transfer process. How these intermediates are subsequently reduced to water is not clear. We have therefore studied the reaction of mixed-valence carboxy-cytochrome *c* oxidase, which contains 2 electrons, with hydrogen peroxide. This reaction can be studied by photolysis of the CO compound after mixing with H₂O₂ under anaerobic conditions. The results show that H₂O₂ reacts rapidly ($k=2.5 \cdot 10^4 \text{ M}^{-1} \cdot \text{s}^{-1}$) with the partially reduced enzyme to form the fully oxidized enzyme. On the time scale of our experiments no other intermediates were observed. This demonstrates that under suitable conditions partially reduced cytochrome *c* oxidase can use hydrogen peroxide as a 2-electron acceptor instead of the 4-electron accepting dioxygen molecule. These results are in line of those of ORII [8], who showed that cytochrome *c* oxidase may act as a cytochrome *c* peroxidase.

REFERENCES

- [1] M.K.F. WICKSTRÖM, *Nature*, **266**, 271-273 (1979).
- [2] L. POWERS, B. CHANCE, Y. CHING, P. ANGIOLILLO, *Biophys. J.*, **34**, 465-498 (1981).
- [3] R. BOELEN, H. RADEMAKER, R. WEVER, B.F. VAN GELDER, *Biochim. Biophys. Acta*, **756**, 196-209 (1984).
- [4] R. BOELEN, R. WEVER, B.F. VAN GELDER, H. RADEMAKER, *Biochim. Biophys. Acta*, **724**, 176-183 (1983).
- [5] R. BOELEN, R. WEVER, *FEBS Lett.*, **116**, 223-226 (1980).
- [6] R. BOELEN, R. WEVER, *Biochim. Biophys. Acta*, **547**, 296-310 (1979).
- [7] B. CHANCE, C. SARONIO, J.S. LEIGH JR., *J. Biol. Chem.*, **250**, 9226-9237 (1975).
- [8] Y. ORII, *J. Biol. Chem.*, **257**, 9246-9248 (1982).



RT4.5 — TH

A.V. XAVIER
H. SANTOS
J.J.G. MOURA
I. MOURA

Centro de Química Estrutural
U.N.L., Complexo I, I.S.T.
1000 Lisboa
Portugal

J. LEGALL
Department of Biochemistry
University of Georgia
Athens, GA 30602
U.S.A.

MECHANISM AND REGULATION FOR A COUPLED TWO-ELECTRON TRANSFER IN A TETRAHAEM CYTOCHROME

The need for a two-electron transfer process is a recurrent and elusive problem in biochemistry [1]. Analysis of the relative microscopic midpoint redox potentials for the four haems of *Desulfovibrio gigas* cytochrome *c*₃ [2] provides evidences that this molecule has the potential properties to optimize this function.

The oxidation of cytochrome *c*₃ can be considered to involve five steps which are obtained by successive loss of one electron [2]: Step 0 (all haems reduced) through Step IV (all haems oxidized). A full description of the redox equilibria involves 16 oxidation states and 32 microscopic midpoint redox potentials e_i^{jkl} (the presence of the upperscripts *j*, *k*, *l*, indicates those haems which are oxidized). The relative values, $\Delta e_{ij} = e_i - e_j$, as well as the haem-haem interacting potentials $I_{ij} = e_i - e_j^i = e_j - e_j^i$, were obtained for *D. gigas* cytochrome *c*₃ by a thorough NMR study (see Table 3 of reference [2]). The microscopic redox potentials are such that for a dynamic equilibrium (e.g., in an electron transfer chain) a situation optimized for a two-electron transfer can be generated. In order to explain the mechanism by which this phenomenon is achieved, let us follow

the successive alterations of the microscopic midpoint redox potentials of each haem throughout the oxidation at pH=7.2, starting with the fully reduced protein ($\Delta e_{12} = -35$ mV, $\Delta e_{13} = -36$ mV, and $\Delta e_{14} = -61$ mV). Oxidation of the haem with lowest midpoint redox potentials (haem 1, e_1) modifies the microscopic midpoint redox potentials of the other haems (e_i^1 , $i=2, 3$ or 4). It is important to notice that although I_{12} is positive (+19 mV), I_{13} is negative (-29 mV), altering the values of e_2 and e_3 in such way that $e_2^1 < e_2$, $e_3^1 > e_3$ and $e_3^1 \gg e_2^1$. Haem 2 is now easier to oxidize and haem 3 becomes more difficult to oxidize. Subsequent oxidation of haem 2 has a similar but even more drastic effect on haem 3 ($I_{23} = +42$ mV) and haem 4 ($I_{24} = -24$ mV). I_{23} is so large and positive that e_3^{12} becomes equal to e_3^1 , within experimental error. Thus, oxidation of haem 2 impels the concomitant oxidation of haem 3. Haem 4 is now more difficult to oxidize ($I_{34} = -18$ mV). Using the values given in the table cited above [2] it is easily seen that a similar situation is also observed both for the reduction at pH=7.2 as well as for the oxidation/reduction at pH=9.6 of *D. gigas* cytochrome c_3 .

The above analysis depicts a situation of strong cooperativity (coupling) between the redox centers, of *Desulfovibrio gigas* cytochrome c_3 , where oxidation (reduction) of haem 1 (haem 4) triggers a process by which two electrons are selected to be released (captured) in an essentially simultaneous way.

It is worth stressing that by purely electrostatic considerations, the values of the interacting poten-

tials, I_{ij} , should be always negative and could never be of use for a similar mechanism. Redox-linked conformational modifications must be involved. These conformational changes result in the presence of regulatory redox centers as well as redox centers actually implicated in the electron transfer chain.

This regulatory role may be quite general. In particular, the present knowledge on *D. gigas* hydrogenase [3] for which cytochrome c_3 is a coupling protein, suggests the use of redox centers with a similar role.

Furthermore, the postulation of these centers makes it possible to reconcile the need for fast electron transfer with that of avoiding "short-circuits" [4]. The ready state for the redox centers involved in the electron transfer chain, e.g., an entatic state [5], can only be generated after a signal has been emitted by the dispatcher redox center.

ACKNOWLEDGEMENTS

This work is supported by INIC, JNICT and USAID.

REFERENCES

- [1] R.J.P. WILLIAMS, *Biochim. Biophys. Acta*, **505**, 1-44 (1978).
- [2] H. SANTOS, J.J.G. MOURA, I. MOURA, J. LEGALL, A.V. XAVIER, *Eur. J. Biochem.*, **141**, 283-296 (1984).
- [3] M. TEIXEIRA, I. MOURA, A.V. XAVIER, B.H. HUYNH, D.V. DERVARTANIAN, H.D. PECK JR., J. LEGALL, J.J.G. MOURA, *J. Biol. Chem.* (1985) in press.
- [4] J. KRAUT, *Biochem. Soc. Trans.*, **9**, 197-202 (1981).
- [5] B.L. VALLEE, R.J.P. WILLIAMS, *Proc. Natl. Acad. Sci. USA*, **59**, 498-505 (1968).

POSTER SESSIONS

1. Metalloproteins



PS1.1 — MO

DEAN E. WILCOX
 ARTURO G. PORRAS
 MARK D. ALLENDORF
 LUNG-SHAN KAU
 DARLENE J. SPIRA
 EDWARD I. SOLOMON

Department of Chemistry
 Stanford University
 Stanford, California 94305
 U.S.A.

STRUCTURE/FUNCTION CORRELATIONS OF THE COUPLED BINUCLEAR COPPER ACTIVE SITE

Chemical and spectroscopic studies of the coupled binuclear copper active site [1] in hemocyanin and tyrosinase have led to a spectroscopically effective model of this metalloprotein site (Fig. 1A). Two tetragonal cupric ions at ~ 3.6 Å separation with imidazole protein ligands have an endogenous bridge (RO^-) which provides a pathway for strong superexchange coupling between the equatorial $d_{x^2-y^2}$ valence orbitals, leading to the EPR-nondetectability of the coppers. Exogenous ligands (*i.e.* O_2^{-2} in the oxygenated form) bind at the site and bridge the coppers and axial exchangeable coordination positions allow for associative ligand substitution. Our recent studies of metalloproteins containing this coupled binuclear copper site have focused on correlations between the geometric and electronic structure of the binuclear copper unit and the chemical activity of these sites.

The coupled binuclear copper site in tyrosinase catalyzes the ortho-hydroxylation of monophenols to *o*-diphenols and their subsequent oxidation to *o*-quinones. Carboxylic acids are competitive inhi-

bitors of these tyrosinase reactions and, in collaboration with Konrad Lerch of Universität Zürich, we have studied [2] the mechanistic and spectroscopic perturbations of carboxylate binding to the tyrosinase active site. Carboxylate inhibitors are found to divide into two types. A group of relatively poor inhibitors (acetate, phenyl acetate, etc.) have binding affinity for the copper site not different from that for aqueous Cu(II); when ligated to the half met $[\text{Cu(II)Cu(I)}]$ tyrosinase derivative, they produce normal tetragonal Cu(II) EPR and ligand field spectral features indicative of equatorial coordination. In contrast, a group of good competitive inhibitors (benzoate, *p*-toluate, etc.), which are substrate analogues in the sense that the coordinating carboxylate is conjugated to an aromatic ring forming a planar structure, binds to the site with a much higher affinity. Ligation of these carboxylates to half met tyrosinase produces unusual EPR and ligand field spectral features which reflect d_{z^2} mixing into the groundstate and indicate a distorted trigonal bipyramidal copper geometry. A ligand field analysis of the C_s distortion coordinate for associative ligand substitution reactions of tetragonal complexes indicates that these carboxylate substrate analogues are binding midway along this coordinate and the protein pocket is implicated in providing the higher affinity and trigonal bipyramidal geometry. Stabilization of substrate in this manner is suggested to lower the barrier for formation of the ternary ($[\text{Cu(II)}]_2$, O_2^{-2} , substrate) complex and provide a favorable geometric and electronic structure for facile ortho-hydroxylation of phenol in the tyrosinase coupled binuclear copper site (Fig. 1B).

Laccase is a multicopper oxidase containing one coupled binuclear copper unit (type 3), one normal copper (type 2) and one Blue copper (type 1). Recent chemical and spectroscopic studies [3] of the native and the type-2-depleted form have indicated that, in contrast to hemocyanin and tyrosinase, exogenous ligands do not bridge the coupled binuclear copper ions. Azide binding to laccase has now been studied [4] in considerable detail using variable temperature absorption, MCD and

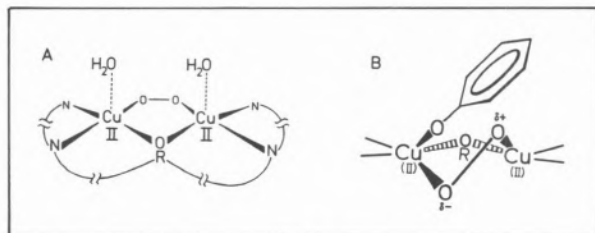


Fig. 1

A(left): Spectroscopically effective model of the coupled binuclear copper active site; B(right): Proposed geometric and electronic structure of the ternary intermediate in ortho-hydroxylation of phenol by the tyrosinase coupled binuclear copper site

EPR to probe the geometric and electronic features of ligand binding by this multicopper enzyme. Specifically, the combination of low temperature MCD and absorption spectroscopies has allowed us to differentiate the charge transfer (CT) features (temperature dependent MCD) associated with N_3^- binding to the paramagnetic type 2 Cu(II) from those (temperature independent MCD) associated with N_3^- binding to the antiferromagnetically coupled, and therefore diamagnetic, binuclear type 3 copper unit. Further, in a limited fraction of type 3 sites, N_3^- and H^+ competitively displace and protonate the endogenous bridge, eliminating the superexchange pathway, resulting in a pair of paramagnetic, dipolar-coupled Cu(II) centers whose associated N_3^- -to-Cu(II) CT transitions are observed in the low temperature MCD spectrum. A correlation of these spectroscopic studies strongly suggests that low affinity N_3^- bridges between the paramagnetic type 2 and the diamagnetic type 3 binuclear coppers in fully oxidized laccase. High affinity N_3^- is indicated to bind to the paramagnetic type 2 Cu(II) in a limited fraction of the native protein where the type 3 coppers are reduced. Finally, this study has led to a proposed model (Fig. 2) for exogenous ligand binding to a trinuclear copper laccase active site, involving both the type 2 and type 3 coppers, which may enable the irreversible reduction of dioxygen to water by this multicopper oxidase.

REFERENCES

- [1] EDWARD I. SOLOMON, in T.G. SPIRO (ed.), «Copper Proteins», Wiley, New York, 1981, Chapter 2.
- [2] D.E. WILCOX, A.G. PORRAS, Y.T. HWANG, K. LERCH, M.E. WINKLER, E.I. SOLOMON, *J. Am. Chem. Soc.*, in press.

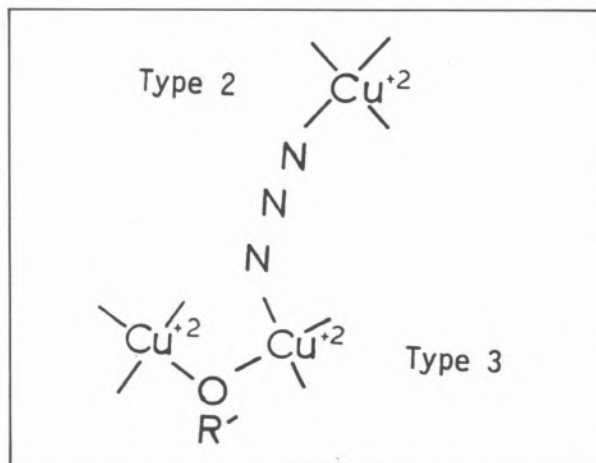


Fig. 2

Proposed trinuclear copper active site model for N_3^- binding by native laccase

- [3] a) D.J. SPIRA, M.E. WINKLER, E.I. SOLOMON, *Biochem. Biophys. Res. Commun.*, **107**, 721-726 (1982);
b) D.J. SPIRA, E.I. SOLOMON, *Biochem. Biophys. Res. Commun.*, **112**, 729-736 (1983).
- [4] M.D. ALLENDORF, D.J. SPIRA, E.I. SOLOMON, *Proc. Natl. Acad. Sci. USA*, in press.



PS1.2 — TU

JUDITH M. NOCEK
DONALD M. KURTZ JR.

Department of Chemistry
Iowa State University
Ames, Iowa 50011
U.S.A.

J. TIMOTHY SAGE
PETER DEBRUNNER

Department of Physics
University of Illinois
Urbana, Illinois 61801
U.S.A.

**A NITRIC OXIDE ADDUCT
OF THE BINUCLEAR IRON CENTER
IN DEOXYHEMERYTHRIN
FROM *PHASCOLOPSIS GOULDII*.
ANALOGUE OF A PUTATIVE
INTERMEDIATE IN THE OXYGENATION
REACTION**

The preparation and characterization of a nitric oxide adduct of the binuclear iron site in the non-heme oxygen-carrying protein, hemerythrin (Hr) [1] are reported. Addition of gaseous NO to an anaerobic solution of deoxyHr results in a nitric oxide adduct. The optical spectrum of this adduct is different from that of any other adduct of Hr in [Fe(II),Fe(II)] (deoxy), [Fe(III),Fe(III)] (oxy or met) or [Fe(II), Fe(III)] (semi-met) oxidation levels (Fig. 1). Samples of deoxyHr frozen within

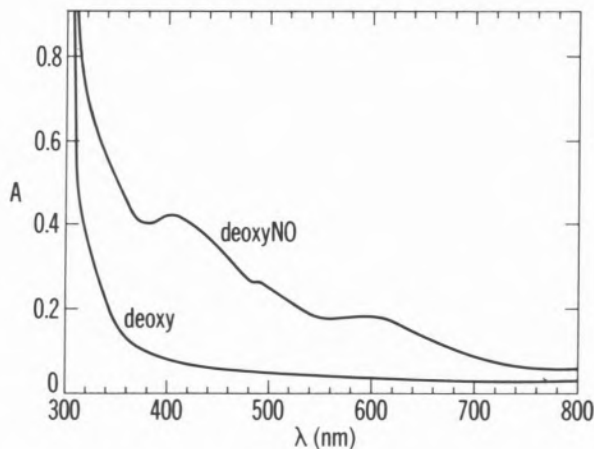


Fig. 1

a few minutes after addition of gaseous NO yield an axial EPR spectrum with $g_{\parallel} = 2.76$, $g_{\perp} = 1.84$ (Fig. 2). Double integration of the spectrum yields 0.9 spins/2 Fe. Addition of excess N_3^- or CNO^- but not several other anions results in immediate

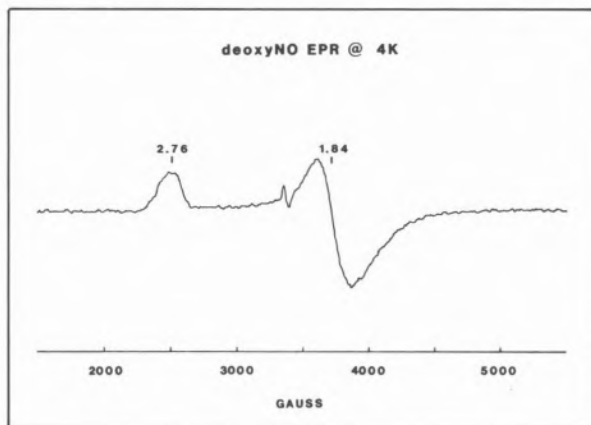
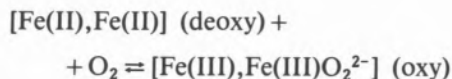


Fig. 2

bleaching of the optical spectrum and disappearance of the EPR spectrum. The anion specificity is similar to that observed for bleaching of the oxyHr color and demonstrates the reversibility of the NO reaction. The ^{57}Fe Mössbauer spectrum of the NO adduct consists of two quadrupole doublets at 100 K but shows magnetic hyperfine splitting of both doublets at 4.2 K. The parameters of one of the doublets are characteristic of high spin Fe(II). The parameters of the remaining doublet are close to those of a non-heme ferrous nitrosyl complex having $S = 3/2$. The g values of the EPR spectrum can be fit by assuming antiferromagnetic coupling of the high spin Fe(II) ($S = 2$) with the $\{\text{FeNO}\}^7$ ($S = 3/2$) leading to a ground state, $S' = 1/2$. X-ray crystallography suggests that O_2 has direct access to only one of the iron atoms in Hr and binds with a bent Fe-O-O geometry [2]. These data suggest a $[\text{Fe(II),Fe(III)NO}^-]$ formulation for the NO adduct of deoxyHr. This formalism is analogous to that of a presumed $[\text{Fe(II),Fe(III)O}_2^-]$ intermediate in the oxygenation reaction:



Our results suggest either that the iron atoms in deoxyHr are antiferromagnetically coupled or

become coupled after addition of NO or O₂ to the exposed iron, but prior to formal oxidation of the second iron.

REFERENCES

- [1] I.M. KLOTZ, D.M. KURTZ JR., *Acc. Chem. Res.*, **17**, 16-22 (1984).
 [2] R.E. STENKAMP, L.C. SIEKER, L.H. JENSEN, *J. Am. Chem. Soc.*, **106**, 618-622 (1984).



PS1.3 — TH

C.L. COYLE
 W.G. ZUMFT
 Lehrstuhl für Mikrobiologie der Universität
 D-7500 Karlsruhe 1
 F.R.G.
 W. JAKOB
 P.M.H. KRONECK
 Fachbereich Biologie der Universität
 D-7750 Konstanz
 F.R.G.

CHARACTERIZATION OF A NOVEL COPPER ENZYME: BACTERIAL NITROUS OXIDE REDUCTASE

The respiratory capability of bacteria is highly diverse considering the terminal oxidants being used other than dioxygen. About 25 genera of taxonomically different groups of bacteria respire nitrate to N₂, NO or N₂O. Three or four terminal oxido-reductases accomplish this respiratory redox process. When dinitrogen is the final product of nitrate respiration, it is formed from N₂O, involving catalysis by a novel Cu protein. The enzyme from denitrifying *Pseudomonas perfectomarina* (ATCC 14405) has been isolated and purified to homogeneity [1]. Nitrous oxide reductase contains about eight copper atoms per molecular weight 120 000. The protein is a dimer of two presumably identical subunits. Several spectroscopically

distinct forms of the enzyme have been identified. A "pink" form of the enzyme is obtained when the purification is done aerobically. The specific activity of this species is 15-35 nkat per mg protein as measured by the nitrous oxide-dependent oxidation of photochemically reduced benzyl viologen. The spectrum of the pink form has absorption maxima at 480, 530, 620 and 780 nm (Fig. 1a).

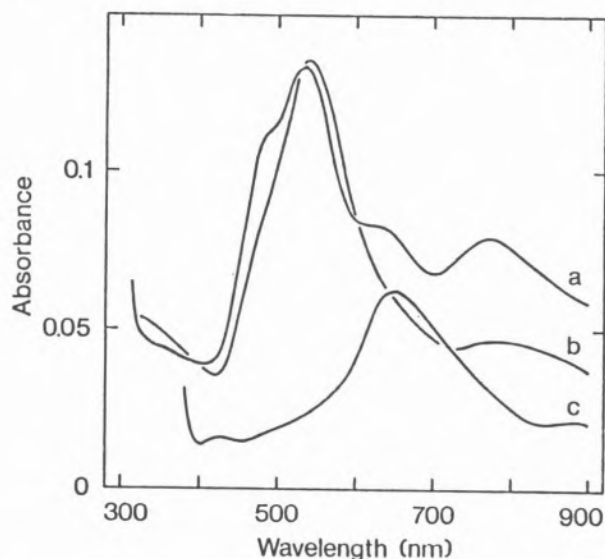


Fig. 1

Electronic spectra of (a) pink form of enzyme as isolated; (b) purple form as isolated; (c) dithionite-reduced form

Cells that were broken anaerobically and fractionated excluding oxygen from all chromatographic steps, yielded a "purple" form of the copper protein whose catalytic activity was consistently three to fivefold higher than that of the pink form. The spectrum of the purple form is shown in Fig. 1b. This form, as isolated, had absorption maxima at 540 and 780 nm. Maxima at 480 and 620 nm observed in the pink form were found only as slight shoulders.

EPR spectra of the pink and purple forms of the enzyme were similar, with the purple form providing better resolution. A representative spectrum of the oxidized purple protein is shown in Fig. 2a. The data suggest the presence of an unusual type 1 Cu. The type 1 Cu is unusual in the sense that although there is a relatively narrow hyperfine splitting ($A_{\parallel} = 35.33$ Gauss; $g_{\parallel} = 2.215$, $g_{\perp} = 2.033$) it does not appear to be associated

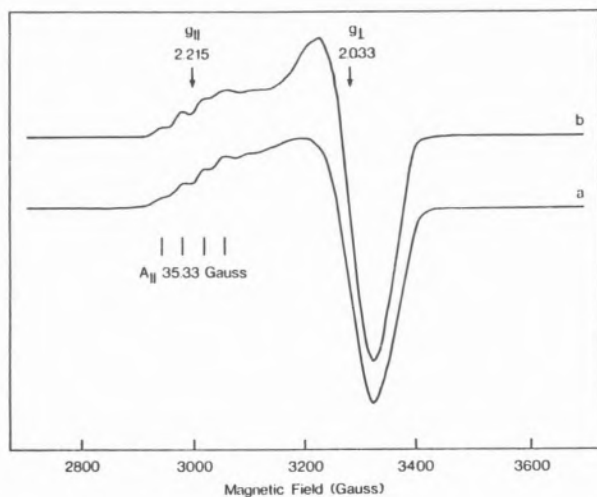


Fig. 2

EPR spectra of (a) purple form of enzyme as isolated in 50 mM phosphate, pH 7.1; (b) pink form after 28 hrs dialysis against 10 mM EDTA, Tris buffer, pH 7.5 (EDTA was removed by further dialysis)

with the absorption band at 620 nm. The 620 nm absorption is ruled out as the LMCT band from $S \rightarrow Cu$ because it is not bleached upon the addition of reducing agents.

Little change was observed in the absorption spectrum or copper content of the pink enzyme form that had been extensively dialyzed against EDTA. The EPR spectrum of this material, which is enzymatically inactive, is shown in Fig. 2b. Dialysis of the protein against KCN removed 80-90% of the copper and inactivated the enzyme. The addition of $Cu(en)_2SO_4$ to the cyanide-treated enzyme resulted in the partial regeneration of the electronic spectrum of the pink form. The regenerated form of the enzyme, however, remained enzymatically inactive.

A "blue" form of the enzyme was obtained by reduction of the purple or pink form by dithionite or ascorbate. The spectrum of the reduced form had a single absorption maximum at 640 nm and is shown in Fig. 1c. The pink form as isolated accepted eight electrons in an anaerobic titration with dithionite. Similar results were obtained when the absorbance decreases at 530 nm, 470 nm and 780 nm were monitored. Upon reduction with dithionite, the type 1 Cu EPR signal disappeared. A rather broad signal with no hyperfine structure ($g_{av} \approx 2.068$) remained even in the presence of excess reductant.

Attempts to remove part of the copper from the purple form of the enzyme by procedures which deplete type 2 Cu [2,3], produced a reduced species that showed no loss in copper content. The reoxidation of this species yielded the pink form of the enzyme.

The pink and purple forms of the enzyme can be activated by base. The activity increased about ten-fold from pH 6 to 10, to give a maximal specific activity around 330 nkat per mg protein. Enzyme inhibitors were cyanide, azide, EDTA, acetylene and fluoride. In addition to measuring activity by the nitrous oxide dependent oxidation of benzyl viologen, a direct measurement of nitrous oxide reduction and dinitrogen evolution was done by gas chromatography. Under these conditions the enzyme became inactivated or inhibited after a few turnovers. Further characterization of the copper chromophore should provide a better understanding of the structure and reactivity of copper sites in enzymes.

REFERENCES

- [1] W.G. ZUMFT, T. MATSUBARA, *FEBS Lett.*, **148**, 107-112 (1982).
- [2] M.T. GRAZIANI, L. MORPURGO, G. ROTILIO, B. MONDOVI, *FEBS Lett.*, **70**, 87-90 (1976).
- [3] L. MORPURGO, M.T. GRAZIANI, A. DESIDERI, G. ROTILIO, *Biochem. J.*, **187**, 361-366 (1980).



PS1.4 — MO

DUARTE MOTA DE FREITAS

Department of Chemistry
Loyola University of Chicago
6525 North Sheridan Road, Chicago
Illinois 60626
U.S.A.

JOAN SELVERSTONE VALENTINE

Department of Chemistry and Biochemistry and Molecular Biology Institute
University of California at Los Angeles
405 Hilgard Avenue, Los Angeles
California 90024
U.S.A.

**ANION BINDING SITES OF REDUCED
BOVINE COPPER-ZINC
SUPEROXIDE DISMUTASE:
A CI-35 AND HIGH-RESOLUTION
H-1 NMR STUDY**

Bovine erythrocyte Cu, Zn superoxide dismutase (Cu, Zn-SOD) in its oxidized form has been shown by X-ray crystallography [1] to be a dimer of two equivalent subunits, with one copper(II) and one zinc(II) ion per subunit. This protein is an extremely efficient catalyst of superoxide dismutation ($2\text{O}_2^- + 2\text{H}^+ \rightarrow \text{O}_2 + \text{H}_2\text{O}_2$) and it has been proposed that this activity is its primary physiological function *in vivo* [2]. Although the site of reactivity for superoxide and several anions with oxidized Cu, Zn-SOD has been established as being the copper(II) ion, the anion binding sites of reduced protein are still a matter of controversy [3]. This is an important question since the substrate, O_2^- , is also an anion and is known to react with the enzyme in both oxidized and reduced forms [2].

FEE and WARD [4] observed that the nuclear magnetic relaxivities of solutions of Cl^- was larger in the presence of reduced Cu, Zn-SOD than in the presence of apoprotein and that addition of CN^- lowered the relaxivity of reduced protein to that of the apoprotein. The binding of halides to reduced yeast Cu, Zn-SOD was also studied by high-field H-1 NMR [5]. Five resonances were assigned to C-2 protons of histidyl imidazoles at the

active site of the reduced protein and three of these were observed to shift upon addition of halide ions. Although both of these observations are in agreement with coordination of halide ions to the copper(I) ion in reduced Cu, Zn-SOD [4,5], they are also consistent with binding of halide ions to a protein side chain close to the metal binding region.

We reanalyzed these data in light of the present understanding of electrostatic interactions in the reaction mechanism of bovine Cu, Zn-SOD. It has been shown from the SOD activity and anion affinity of proteins chemically modified at Arg-141 with phenylglyoxal [6,7] or at Lys-120 and Lys-134 with succinic anhydride, acetic anhydride or cyanate [8-11] that these residues are important anion binding sites in the oxidized protein [12].

We observed that reduced arginine-modified and reduced lysine-modified SOD (2.1×10^{-4} M) caused less broadening of the Cl^- resonance than did reduced native protein when measured under the same conditions. We also found that the C-2 proton resonances of histidyl imidazoles of reduced native SOD and reduced lysine-modified SOD were shifted upon addition of Cl^- whereas this anion had no effect in the H-1 NMR spectrum of reduced arginine-modified SOD (even at Cl^- concentrations as high as 1M). We therefore conclude that the major anion binding sites in reduced bovine Cu, Zn-SOD are Arg-141, Lys-120, and Lys-134 and not the copper(I) ion. Implications of these findings for the mechanism of superoxide dismutation of this protein will also be discussed.

REFERENCES

- [1] J.A. TAINER, E.D. GETZOFF, K.M. BEEM, J.S. RICHARDSON, D.C. RICHARDSON, *J. Mol. Biol.*, **160**, 181 (1982).
- [2] I. FRIDOVICH, *Annu. Rev. Biochem.*, **44**, 147 (1975).
- [3] J.S. VALENTINE, M.W. PANTOLIANO, in T.G. SPIRO (ed.), «Copper Proteins», Ed. Wiley, New York, 1981, pp. 291-358.
- [4] J.A. FEE, R.L. WARD, *Biochem. Biophys. Res. Commun.*, **71**, 427 (1976).
- [5] A.E.G. CASS, H.A.O. HILL, V. HASEMANN, J.T. JOHANSEN, *Carlsberg Res. Commun.*, **43**, 439 (1978).
- [6] D.P. MALINOWSKI, I. FRIDOVICH, *Biochem.*, **18**, 5909 (1979).
- [7] O. BERMINGHAM-McDONOGH, D. MOTA DE FREITAS, A. KUMAMOTO, J.E. SAUNDERS, D.M. BLECH, C.L. BORDERS JR., J.S. VALENTINE, *Biochem. Biophys. Res. Commun.*, **108**, 1376 (1982).

- [8] F. MARMOCCHI, I. MAVELLI, A. RIGO, R. STEVANATO, F. BOSSA, G. ROTILIO, *Biochem.*, **21**, 2853 (1982).
 [9] D. COCCO, I. MAVELLI, L. ROSSI, G. ROTILIO, *Biochem. Biophys. Res. Commun.*, **111**, 860 (1983).
 [10] A. CUDD, I. FRIDOVICH, *J. Biol. Chem.*, **257**, 11443 (1982).
 [11] D. COCCO, L. ROSSI, D. BARRA, F. BOSSA, G. ROTILIO, *FEBS Lett.*, **150**, 303 (1982).
 [12] D. MOTA DE FREITAS, J.S. VALENTINE, *Biochem.*, **23**, 2079 (1984).



PS1.5 — TU

K. CICHUTEK
 H. WITZEL

Institute of Biochemistry
 University of Münster
 Domagkstr. 85, D-4400 Münster
 F.R.G.

F. PARAK

Institute of Physical Chemistry
 University of Münster
 Schlossplatz 7 D-4400 Münster
 F.R.G.

IRON A AND IRON B IN PURPLE BOVINE SPLEEN ACID PHOSPHATASE

The two-iron-centre of purple bovine spleen phosphatase, in the reduced form hydrolyzing activated phosphoesters, has been studied by Mössbauer-spectroscopy. In presence of dithionite iron A is released with a first order rate constant $k_A = 0.110 \text{ s}^{-1}$, iron B with $k_B = 0.005 \text{ s}^{-1}$, measured by complex formation with 1,10-phenanthroline. Interruption of the release at different times and addition of $^{57}\text{Fe(III)}$ to the protein allows to reconstitute an enzyme species with predominantly ($^{57}\text{Fe-Fe}$)-centre and a species with ($^{57}\text{Fe-}^{57}\text{Fe}$)-centre. The actual ^{57}Fe -enrichment, which can be calculated from the absorption areas for iron A and B, is in agreement with the theoretical enrichment, calculated by the rate constants of Fe-removal.

The oxidized, inactive form of the enzyme contains two high spin Fe(III) with $\Delta E_Q = 0.95 \text{ mm/s}$ and $\delta S = 0.50 \text{ mm/s}$ for iron A and $\Delta E_Q = 1.45 \text{ mm/s}$ and $\delta S = 0.60 \text{ mm/s}$ for iron B (relative to $\alpha\text{-Fe}$ at 298 K).

Reductive activation by one-electron transfer changes iron A, characterized now by $\Delta E_Q = 2.65 \text{ mm/s}$ and $\delta S = 1.20 \text{ mm/s}$, which is typical for high spin Fe(II). Iron B remains high spin Fe(III) with $\Delta E_Q = 1.25 \text{ mm/s}$ and $\delta S = 0.65 \text{ mm/s}$.

After reduction the visible absorption maximum of the tyrosinate-Fe(III)-charge transfer band shifts from 550 nm (purple) to 505 nm (pink), connected with a resonance Raman shift of the C-O-stretching mode from 1288 cm^{-1} to 1296 cm^{-1} . Therefore tyrosine must be coordinated to iron B.

The results are discussed in regard to the results of DEBRUNNER *et al.* obtained on uteroferrin.



PS1.6 — TH

M. SAHLIN
 A. EHRENBORG
 A. GRÄSLUND

Department of Biophysics
 University of Stockholm
 Arrhenius Laboratory
 S-106 91 Stockholm
 Sweden

B.-M. SJÖBERG

Department of Molecular Biology
 The Swedish University of Agricultural Sciences
 Biomedical Center
 Box 590, S-751 24 Uppsala
 Sweden

PARAMAGNETIC ^1H NMR SPECTRA OF RIBONUCLEOTIDE REDUCTASE FROM *ESCHERICHIA COLI*

Ribonucleotide reductase from *E. coli* consists of two non-identical subunits, proteins B1 and B2. Protein B2 contains a dimeric iron center with two antiferromagnetically coupled ferric ions, and

a tyrosyl free radical, essential for the enzymatic activity [1]. Protein B2 can be prepared in its native state, or in a state with an intact iron center but without radical (non-radical state), or as an apoprotein with neither iron nor radical.

The 400 MHz ^1H NMR spectra of protein B2 (approximately 1 mM in 50 mM phosphate buffer, pH 7.5, 10°C) show paramagnetically shifted resonances in the native and non-radical states (not present in the apoprotein spectrum). In D_2O solvent a peak (half-width ~ 4 ppm) appears around 19 ppm which is due to non-exchangeable proton(s). In H_2O solvent an additional peak (half-width ~ 8 ppm) is seen around 24 ppm, due to exchangeable proton(s). A super-WEFT pulse sequence was used to suppress the water signals [2]. Hemerythrin, a respiratory protein of lower invertebrates, with a known 3-dimensional structure, contains an iron center with many spectroscopic properties in common with that of protein B2 [3]. The paramagnetically shifted resonances of protein B2 appear in the same region as those of hemerythrin from *Phascolopsis gouldii*. In hemerythrin, the exchangeable proton signals were assigned to imidazole groups on the histidine liganded to the iron ions [4]. There may be a similar origin for the exchangeable proton signal(s) of protein B2. Histidine ligands to the iron center of protein B2 have also been implicated through observation of 4 histidines, which are invariant residues in the amino acid sequences of subunits equivalent to protein B2 in ribonucleotide reductases from widely different species [5].

REFERENCES

- [1] A. GRÄSLUND, M. SAHLIN, B.-M. SJÖBERG, «Free radical metabolites of toxic chemicals and related ESR investigations», in «Environmental Health Perspectives», to be published in 1985.
- [2] T. INUBISHI, E.D. BECKER, *J. Magn. Reson.*, **51**, 128-133 (1983).
- [3] R.G. WILKINS, P.C. HARRINGTON, in E.C. THEIL, G.L. EICHHORN, L.G. MARZILLI (eds.), «Advances in Inorganic Biochemistry», vol. 5, Elsevier, New York, 1983, pp 51-85.
- [4] M.J. MARONEY, R.B. LAUFFER, L. QUE JR., *J. Am. Chem. Soc.*, **106**, 6445-6446 (1984).
- [5] B.-M. SJÖBERG, H. EKLUND, J.A. FUCHS, J. CARLSSON, N.M. STANDART, J.V. RUDERMAN, S.J. BRAY, T. HUNT, *FEBS Lett.*, (1985), submitted for publication.



PS1.7 — MO

MICHAEL J. MARONEY
A. LAWRENCE ROE
LAWRENCE QUE JR.
Department of Chemistry
University of Minnesota
Minneapolis, MN 55455
U.S.A.

JUDITH C. NOCEK
GUDRUN S. LUKAT
DONALD M. KURTZ JR.
Department of Chemistry
Iowa State University
Ames, IA 50011
U.S.A.

NMR AND EXAFS STUDIES OF HEMERYTHRIN COMPLEXES

The binuclear iron site of hemerythrin can be prepared in three oxidation states — Fe(III)-Fe(III), Fe(III)-Fe(II), and Fe(II)-Fe(II) [1]. The first of these is associated with the met and oxy forms of the protein; the second with the semimet forms; and the third with the deoxy form. All these forms exhibit isotropically shifted NMR resonances which can be assigned to the N-H protons of coordinated histidines [2]. Such protons are normally observed near 100 and 65 ppm downfield for imidazoles coordinated to high-spin ferric and ferrous centers, respectively [3]. In the met, metazido, metsulfido, and oxy forms, these protons are observed near 20 ppm downfield; the significant decrease in the isotropic shift results from the strong antiferromagnetic coupling between the ferric centers ($J \sim -100 \text{ cm}^{-1}$) [4]. The similarity of the shifts observed for methemerythrin and methemerythrin sulfide indicates that the presence of the sulfide does not significantly change the extent of coupling between the two ferric centers. EXAFS studies on the metsulfido complex reveal the replacement of the oxo bridge with a sulfido bridge, in agreement with resonance Raman arguments [5]. The iron atoms are found to be both coordinated to the sulfur with an Fe-S bond distance of 2.22(3) Å. The Fe-Fe distance is estimated to be 3.4 Å, giving rise to an Fe-S-Fe angle

of approximately 100°. These structural changes are expected for the substitution of the oxo bridge with sulfide.

NMR studies on the semimet and deoxy forms reveal the N-H signals to be further downfield, indicating that the extent of antiferromagnetic coupling between the iron atoms is significantly decreased. For the semimet azido complex, the N-H resonances are found at 73 and 54 ppm downfield with relative intensities of 2:3; these have been assigned to the histidine N-H protons coordinated to the ferric and ferrous sites, respectively. Thus the azide is coordinated to the ferric site, in agreement with resonance Raman data showing the persistence of the azide-to-Fe(III) charge transfer transition in this complex [6]. The temperature dependence of these shifts is best fitted with a J value of -10 cm^{-1} .

The NMR spectrum of the semimet sulfido complex is somewhat more complex. Five N-H resonances are observed in the region of 23-54 ppm downfield with relative intensities of 3:2:2:2:1. The temperature dependences of these peaks show both Curie and anti-Curie behavior, similar to that observed for the $\beta\text{-CH}_2$ resonances of the cysteines in reduced Fe_2S_2 -ferredoxins [7]. The data may be interpreted in terms of both possible mixed-valent complexes with the unpaired electron localized on one of the iron atoms, *i.e.* electron transfer is slow on the NMR time scale.

Deoxyhemerythrin exhibits N-H resonances at 44, 46, and 62 ppm downfield. These signals are perturbed upon addition of azide with new resonances observed at 47, 66, and 77 ppm downfield. These spectral comparisons show that azide can coordinate to the iron sites in deoxyhemerythrin.

REFERENCES

- [1] R.G. WILKINS, P.C. HARRINGTON, *Adv. Inorg. Biochem.*, **5**, 51-85 (1983).
- [2] M.J. MARONEY, R.B. LAUFFER, L. QUE JR., D.M. KURTZ JR., *J. Am. Chem. Soc.*, **106**, 6445-6446 (1984).
- [3] R.B. LAUFFER, B.C. ANTANAITIS, P. AISEN, L. QUE JR., *J. Biol. Chem.*, **258**, 14212-14218 (1983).
- [4] J.W. DAWSON, H.B. GRAY, H.E. HOENING, G.R. ROSSMAN, J.M. SCHREDDER, R.H. WANG, *Biochemistry*, **11**, 461-465 (1972).
- [5] G.S. LUKAT, D.M. KURTZ JR., A.K. SHIEMKE, T.M. LOEHR, J. SANDERS-LOEHR, *Biochemistry*, (1984), in press.
- [6] M.J. IRWIN, L.J. DUFF, D.F. SHRIVER, I.M. KLOTZ, *Arch. Biochem. Biophys.*, **224**, 473-478 (1983).
- [7] I. BERTINI, G. LANINI, C. LUCHINAT, *Inorg. Chem.*, **23**, 2729-2730 (1984).



PS1.8 — TU

ANDREW K. SHIEMKE
JOANN SANDERS-LOEHR
THOMAS M. LOEHR

Department of Chemical, Biological, and Environmental Sciences
Oregon Graduate Center
19600 N.W. Walker Road, Beaverton, Oregon 97006
U.S.A.

RESONANCE RAMAN STUDY OF THE HYDROXIDE ADDUCT OF HEMERYTHRIN

Hemerythrin is the non-heme iron-containing respiratory protein of several marine invertebrates. When O_2 binds to the binuclear active site, the two iron atoms are oxidized to the ferric state and dioxygen is reduced to peroxide [1]. Methemerythrin, the unligated form of the protein in which both irons are oxidized to the Fe(III) state, no longer binds O_2 , but readily binds small anions such as N_3^- , SCN^- , OCN^- , and CN^- . At high pH, it binds hydroxide to form hydroxomethemerythrin. X-ray crystallographic studies show that the binuclear iron site of met- and oxyhemerythrin contains a μ -oxo bridge [2]. This Fe-O-Fe moiety gives rise to intense near-UV charge transfer transitions [3]. Excitation within these charge transfer bands gives strong, selective enhancement of a Raman peak near 500 cm^{-1} which has been assigned as the symmetric Fe-O-Fe vibration, $\nu_s(\text{Fe-O-Fe})$ [4,5]. Whereas most methemerythrin have only a single Raman peak in the $\nu_s(\text{Fe-O-Fe})$ region, hydroxomethemerythrin has a strong peak at 492 cm^{-1} , and a smaller peak at 565 cm^{-1} (Fig. 1a). Substitution of ^{18}O into the oxo bridge position causes the 492 cm^{-1} peak to shift to 478 cm^{-1} (Fig. 1c), prompting assignment of this peak as $\nu_s(\text{Fe-O-Fe})$. Preparation of hydroxomethemerythrin in H_2^{18}O , under conditions where the bridge does not exchange, results in a shift of the 565 cm^{-1} feature to 538 cm^{-1} (Fig. 1b). This shift agrees with the calculated value (540 cm^{-1}) for the replacement of ^{16}O by ^{18}O in the iron-oxygen

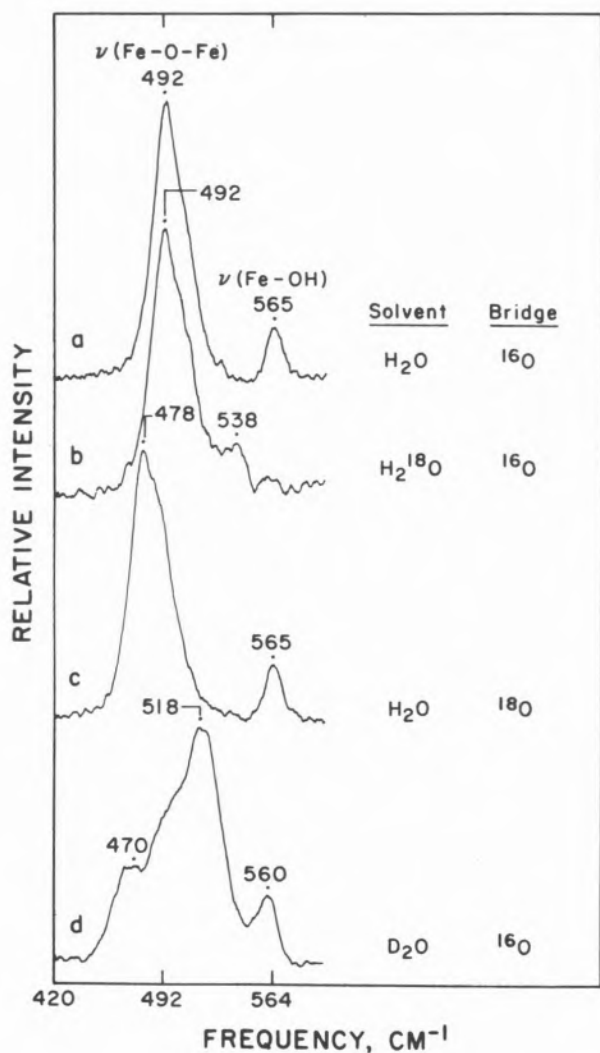


Fig. 1

stretch of a bound hydroxide, and we now assign it as such.

In contrast to the straightforward results from the oxygen isotope experiments, preparation of hydroxomethemerythrin in D₂O causes several anomalous shifts in the resonance Raman spectrum (Fig. 1d) [6]. The major peak at 492 cm⁻¹ in H₂O ($\nu_s(\text{Fe-O-Fe})$) shifts to 517 cm⁻¹ in D₂O. This shift cannot be due to deuterium-induced conformation changes of the protein since analogous peaks of deuterium-substituted met-, azidomet-, and perchloromethemerythrin do not shift. In addition, the iron-oxygen stretch of the bound hydroxide at 565 cm⁻¹ shifts only 5 cm⁻¹ in D₂O, which is less than half the shift expected for the substitution of OH⁻ by OD⁻ (calc. shift to 553 cm⁻¹). This indica-

tes that the hydroxide ligand is involved in the anomalous D₂O effect on $\nu_s(\text{Fe-O-Fe})$.

Although the spectral shifts of hydroxomethemerythrin in D₂O are unusual, similar results have been obtained for oxyhemerythrin [5]. Both hydroxomet- and oxyhemerythrin show anomalous deuterium isotope effects on ligand as well as Fe-O-Fe vibrations. In addition, these forms of the protein have $\nu_s(\text{Fe-O-Fe})$ frequencies (492 and 486 cm⁻¹ for hydroxomet- and oxyhemerythrin, respectively) which are considerably lower than those of the other ferric hemerythrin (507-516 cm⁻¹) [4,5]. We have proposed that these effects in oxyhemerythrin are the result of a hydrogen bond between the proton of the hydroperoxide ligand and the oxygen of the oxo-bridge. Because hydroxide is the only other methemerythrin ligand that is capable of forming a hydrogen bond analogous to that proposed for oxyhemerythrin, it is not unreasonable to propose a similar model for hydroxomethemerythrin. In this case, we suggest that the proton of the bound hydroxide is hydrogen bonded to the oxo-bridge. Though this appears to be a strained structure, the strain may be responsible for the large deuterium effect on $\nu_s(\text{Fe-O-Fe})$. We are currently studying model compounds which contain elements of this proposed hydroxomethemerythrin structure.

REFERENCES

- [1] J. SANDERS-LOEHR, T.M. LOEHR, *Adv. Inorg. Biochem.*, **1**, 235 (1979).
- [2] a) R.E. STENKAMP, L.C. SIEKER, L.H. JENSEN, *J. Am. Chem. Soc.*, **106**, 618 (1984);
b) R.E. STENKAMP, L.C. SIEKER, L.H. JENSEN, J.D. MCCALLUM, J. SANDERS-LOEHR, *Proc. Natl. Acad. Sci. USA*, **82**, 713 (1985).
- [3] K. GARBETT, D.W. DARNALL, I.M. KLOTZ, R.J.P. WILLIAMS, *Arch. Biochem. Biophys.*, **135**, 419 (1969).
- [4] S.M. FREIER, L.L. DUFF, D.F. SHRIVER, I.M. KLOTZ, *Arch. Biochem. Biophys.*, **205**, 449 (1980).
- [5] A.K. SHIEMKE, T.M. LOEHR, J. SANDERS-LOEHR, *J. Am. Chem. Soc.*, **106**, 4951 (1984).
- [6] J.D. MCCALLUM, A.K. SHIEMKE, J. SANDERS-LOEHR, *Biochemistry*, **23**, 2819 (1984).



PSI.9 — TH

J.M.A. SMITH
G.C. FORD
J.L. WHITE
P.M. HARRISON
Department of Biochemistry
The University
Sheffield S10 2TN
U.K.

PRELIMINARY STRUCTURAL STUDIES ON BACTERIOFERRITIN

Bacterioferritin is a novel multimeric cytochrome which appears to function both as an electron transport protein and as a means of storing iron. A cytochrome, named b_1 , was isolated from *Escherichia coli* by DEEB and HAGER [1] who suggested it was a key component of membrane electron transport systems in this organism. A similar cytochrome (named cytochrome $b_{557.5}$), but which also contained non-haem iron was purified from *Azotobacter vinelandii* by BULEN and co-workers [2] and subsequently characterised more fully by STIEFEL and WATT [3]. These authors showed that the protein resembled mammalian ferritin in several respects and identified it as a bacterioferritin. A protein from *E. coli* could be similarly described [4], since it contained an «iron-core» surrounded by a shell of protein, although its diameter, measured from electron micrographs, was somewhat smaller than that of ferritin and the magnetic properties of its inorganic complex differed from those of ferritin's iron-core.

We report here preliminary X-ray crystallographic data for three crystalline forms of bacterioferritin isolated from *E. coli* grown anaerobically on nitrate. These crystals are monoclinic, tetragonal and cubic in form. The monoclinic crystals grown from aqueous solutions containing $MnCl_2$ have cell dimensions $a = 122.2 \text{ \AA}$, $b = 209.6 \text{ \AA}$, $c = 118.6 \text{ \AA}$, $\beta = 118.3^\circ$ and space group $P2_1$. Tetragonal crystals grown from 2 M $(NH_4)_2SO_4$ solution, also containing $MnCl_2$, have

$a = b = 210.6 \text{ \AA}$, $C = 145.0 \text{ \AA}$ and space group $P4_22_12$ but show marked pseudo-cubic symmetry. Soaking the tetragonal crystals in tetrakisacetoxymercurimethane solution causes conversion to a cubic form with $a = 146.9 \text{ \AA}$, space group $I432$. We interpret these data in terms of a unit cell containing two molecules each having 24 protein subunits arranged in 432 molecular point symmetry to give a packing diameter of 127 \AA . This now clearly shows that bacterioferritin does indeed closely resemble horse spleen ferritin which has a similar diameter and the same number of subunits and symmetry, although it contains no haem. Crystals of all three forms of *E. coli* bacterioferritin diffract to high resolution (at least 1.6 \AA) and are all suitable for three dimensional structure determination. This is now being undertaken.

Structural relationships between the three crystalline forms of *E. coli* bacterioferritin, between the *E. coli* and *A. vinelandii* proteins and between ferritin and bacterioferritin will be outlined and the functions of these exciting proteins discussed.

ACKNOWLEDGEMENTS

We thank the Science and Engineering Research Council, The Medical Research Council and the Wellcome Trust for support. G.C.F. is a Wellcome Trust Senior Lecturer.

REFERENCES

- [1] S.S. DEEB, L.P. HAGER, *J. Biol. Chem.*, **239**, 1024-1031 (1964).
- [2] W.A. BULEN, J.R. LECOMTE, S. LOUGH, *Biochem. Biophys. Res. Commun.*, **54**, 1274-1281 (1973).
- [3] E.I. STIEFEL, G.D. WATT, *Nature*, **279**, 81-83 (1979).
- [4] J. YARIV, A.J. KALB, R. SPERLING, E.R. BAUMINGER, S.G. COHEN, S. OFER, *Biochem. J.*, **197**, 171-175 (1981).



PS1.10 — MO

MORTEN J. BJERRUM
ERIK LARSEN
Chemistry Department
The Royal Veterinary and Agricultural University
Copenhagen
Denmark

MANGANESE CONTAINING SUPEROXIDE DISMUTASE. STRUCTURAL AND SPECTROSCOPIC INVESTIGATIONS

The known primary structures of three manganese containing superoxide dismutases (Mn-SOD's) from *S. cerevisiae*, *B. stearothermophilus* and *E. coli* have been analyzed by the methods of CHOU and FASMAN [1], GARNIER *et al.* [2] and of LIM [3,4] in order to predict the secondary structures of the three enzymes. The three theoretical models show satisfactory agreement and predict that the enzymes have a mixed α -helix, β -sheet structure and that they have homologous structures. The former conclusion is also reached from an analysis of the CD of Mn-SOD from *S-cerevisiae*. The 180-240 nm CD spectra of this enzyme are compared with the spectra of Mn-SOD from *E. coli* [5] to demonstrate the homologous structures.

The absorption and CD spectra of Mn-SOD are analyzed and discussed in connection with data for model compounds.

REFERENCES

- [1] P.Y. CHOU, G.D. FASMAN, *Adv. Enzymol.*, **47**, 45 (1978).
- [2] J. GARNIER, D.J. OSGUTHORPE, B. ROBSON, *J. Mol. Biol.*, **120**, 97 (1978).
- [3] V.J. LIM, *J. Mol. Biol.*, **88**, 857 (1974).
- [4] V.J. LIM, *J. Mol. Biol.*, **88**, 873 (1974).
- [5] B.B. KEELE, C. GIOVAGNOLI, G. ROTILIO, *Physiol. Chem. Phys.*, **7**, 1 (1975).



PS1.11 — TU

ROBERT W. HENKENS
KATHLEEN H. GROOVER
RITA A. SHEFFEY
Chemistry Department
Duke University
Durham, North Carolina 27706
U.S.A.
TAFFY J. WILLIAMS
Naval Medical Research Institute
Bethesda, Maryland 20814
U.S.A.

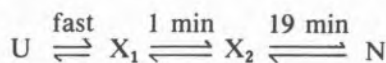
ACTIVE SITE FORMATION IN THE LAST STAGES OF FOLDING OF CARBONIC ANHYDRASE

Carbonic anhydrase (EC 4.2.1.1) is a zinc metalloenzyme catalyzing the reaction: $\text{CO}_2 + \text{H}_2\text{O} \rightleftharpoons \text{HCO}_3^- + \text{H}^+$. The enzyme consists of a single polypeptide chain with no disulfide links that is folded into a globular structure containing a distinct active site crevice. The zinc ion is coordinated at the bottom of the crevice to three histidine residues from adjacent strands of a large β -sheet that passes through the core of the structure. Carbonic anhydrase is denatured by guanidinium chloride, forming a random coil at high concentrations of the denaturant. Below 1 M guanidinium chloride the enzyme is able to refold from the random coil to reform the native structure. The protein (mol. wt. 30,000) is about twice as large as most proteins for which there is information on the folding pathway. A unique advantage of carbonic anhydrase for investigation of the principles that govern protein folding, over the usual small proteins that have been investigated (*e.g.* RNase, lysozyme, cytochrome *c*), is that the high degree of folding cooperativity that makes direct observation of kinetic intermediates exceptionally difficult is not present in this protein. Intermediates in the folding are known [1-6].

Our objective in this project is to determine changes in structure and bonding that occur in the active site in the last stages of the folding process.

For this purpose, we have modified the carbonic anhydrase by substitution of cobalt(II) for zinc(II). The Co(II) enzyme, unlike all other metal-substituted derivatives, has catalytic properties closely similar to the native zinc enzyme. We have studied the folding of the Co(II) enzyme and have made some comparisons between the folding kinetics of the Co(II) and Zn(II) enzymes. Measurements have been made on both the type I and type II carbonic anhydrases.

Using ^{13}C NMR spectroscopy, we have investigated 1) catalysis of the exchange reaction $\text{CO}_2 + \text{H}_2\text{O} \rightleftharpoons \text{HCO}_3^- + \text{H}^+$ and 2) the binding of HCO_3^- in the active site of the Co(II) modified enzyme during the folding process. Using UV and visible spectroscopy, we have also studied 3) the changes in coordination geometry of the metal during folding, 4) the transfer of aromatic side chains from contact with the solvent to form the globular structure and 5) the time course for the recovery of esterase catalytic activity. Overall, the data indicate that the folding of Co(II) carbonic anhydrase proceeds via a stepwise acquisition of folded structure through at least two well populated intermediate states: X_1 and X_2 .



The results provide clear evidence that the active site is completed during the last and slowest phase of the protein folding process, and rule out any possibility that the slow phase arises from slow *cis-trans* isomerizations of proline peptide bonds in the fully unfolded state U as has been suggested for other proteins. This paper concentrates on the structural changes occurring in the active site during the $X_2 \rightarrow \text{N}$ reaction.

The distinctive visible absorption bands produced by the Co(II) in cobalt carbonic anhydrase provide a sensitive intrinsic probe of the geometry of the metal site during folding. Previous folding experiments demonstrate the utility of this probe [7,8]. The native state of the enzyme has a distorted tetrahedral metal coordination geometry, reflected in an unusual visible absorption spectrum (cf. top curve in Fig. 1). The spectral changes observed during the $X_2 \rightarrow \text{N}$ reaction are illustrated in fig. 1. Judged by the spectral changes, the distorted tetrahedral coordination geometry is for-

med in the last stage of folding. Prior to the last stage, the protein exhibits low absorbance a characteristic of octahedral coordination. At any wavelength, the kinetics fits a single exponential curve with a corresponding half-life of 19 min.

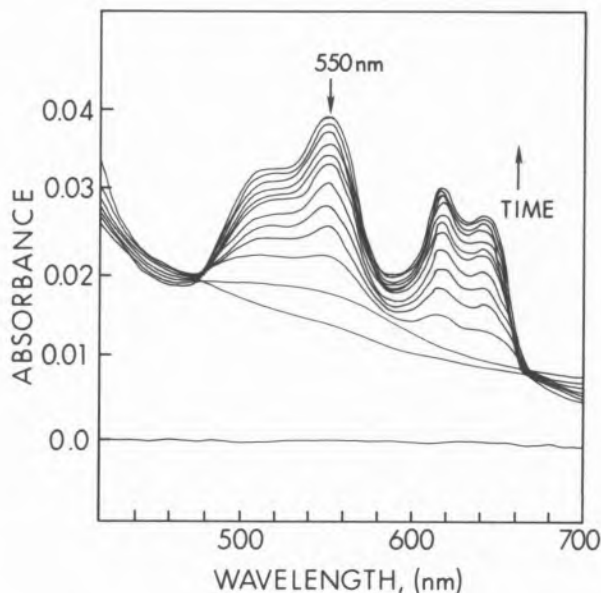


Fig. 1

Changes in the visible absorption spectrum during the folding of cobalt(II) carbonic anhydrase II. The first curve is for the enzyme denatured in 4.9 M guanidinium chloride. The other curves are measured 7 min. apart during the folding process. Measurements made in 10 cm cell containing the sample at pH 7.5, room temperature

By measuring the NMR linewidth for both CO_2 and HCO_3^- at two field strengths, we have determined both the paramagnetic effects that reflect substrate binding and the exchange effects due to catalysis at chemical equilibrium. The following results were obtained for the refolded type I enzyme at 14°C and pH 6.3: 1) HCO_3^- is bound to the catalytically competent enzyme with the carbon 3.2 Å from the cobalt, 2) the catalyzed exchange rate is $1.0 \times 10^4 \text{ s}^{-1}$. From this and previous NMR data [9,10], we conclude that carbonic anhydrase functions as an efficient catalyst of the $\text{CO}_2 + \text{H}_2\text{O} \rightleftharpoons \text{HCO}_3^- + \text{H}^+$ reaction through an inner sphere mechanism that involves direct coordination of the HCO_3^- to the metal ion in the active site. The NMR results obtained during folding (fig. 2) indicate that this catalytic ability is formed

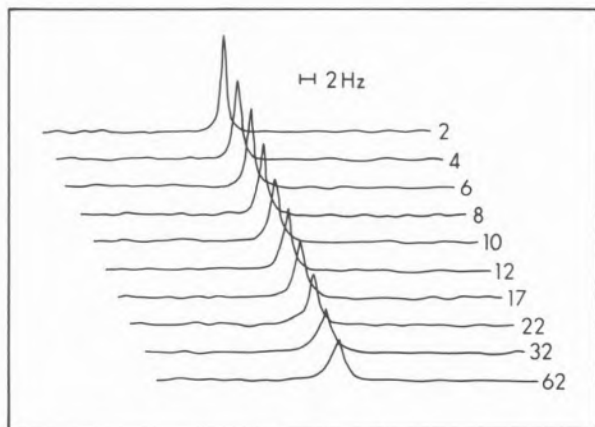


Fig. 2

Changes in the linewidth of the $H^{13}CO_3$ resonance during the folding of zinc carbonic anhydrase II. The linewidth is used to measure the recovery during refolding of catalytic activity for the $^{13}CO_2 + H_2O \rightleftharpoons H^{13}CO_3^- + H^+$ exchange reaction. Measurements made at pH 6.8, 24°C. The numbers at the side of each curve indicate the time of refolding in min.

in the $X_2 \rightarrow N$ reaction coincidentally with the formation of the distorted metal geometry in the last stage of the folding process.

ACKNOWLEDGEMENTS

This research was supported by National Institute of General Medical Sciences Grant 1 R01 GM 31510-01A1, the Naval Medical Research and Development Command, Research Work Unit MF 585271 C.0001, the Office of Naval Research Contract N00014-84-C-0183 and the North Carolina Biotechnology Center. This is paper No. 4 from the North Carolina Biomolecular Engineering and Materials Applications Center.

REFERENCES

- [1] A. YAZGAN, R.W. HENKENS, *Biochemistry*, **11**, 1314-1318 (1972).
- [2] B.P.N. KO, A. YAZGAN, P.L. YEAGLE, S.C. LOTTICH, R.W. HENKENS, *Biochemistry*, **16**, 1720-1725 (1977).
- [3] U. CARLSSON, R. AASA, L.E. HENDERSON, B.-H. JONSSON, S. LINDSBERG, *Eur. J. Biochem.*, **52**, 25-36 (1978).
- [4] P.J. STEIN, R.W. HENKENS, *J. Biol. Chem.*, **253**, 8016-8018 (1978).
- [5] L.F. MCCOY, E.S. ROWE, K.P. WONG, *Biochemistry*, **19**, 4738-4743 (1980).
- [6] R.W. HENKENS, B.B. KITCHELL, S.C. LOTTICH, P.J. STEIN, T.J. WILLIAMS, *Biochemistry*, **21**, 5918-5923 (1982).
- [7] N. BERGENHEM, U. CARLSSON, G. LIND, I.-M. ASTRAND, *Acta. Chem. Scand., Ser. B*, **37**, 244-246 (1983).
- [8] N. BERGENHEM, U. CARLSSON, *Ann. N.Y. Acad. Sci.*, **429**, 137-139 (1984).
- [9] T.J. WILLIAMS, R.W. HENKENS, *Biochemistry*, in press.
- [10] R.W. HENKENS, S.P. MERRILL, T.J. WILLIAMS, *Ann. N.Y. Acad. Sci.*, **429**, 143-145 (1984).



PS1.12 — MO

L. BANCİ
I. BERTINI
F. BRIGANTI
C. LUCHINAT
Department of Chemistry
University of Florence
Italy

WATER PROTON RELAXATION PROPERTIES OF MANGANESE(II) PROTEINS: A NEW THEORETICAL FRAMEWORK

Water proton relaxation data as a function of magnetic field (NMRD) performed on manganese(II) containing proteins have since now escaped rationalization on the ground of existing theories [1]. Interesting attempts have been made to circumvent inadequacies of the theory [2] by the combined use of high field 1H and 2H relaxation data, but the presence of strong contributions from second sphere and outer sphere water to the overall relaxation of solvent nuclei complicates the analysis of the data.

A theoretical treatment has been recently developed in our laboratory [3-5] to take into account in a general way all the meaningful perturbations of the electron spin levels in the spin-hamiltonian formalism and to evaluate their effects on the longitudinal relaxation of nearby nuclei brought about by dipolar coupling with the unpaired electrons.

We have separately evaluated here the effects on water proton relaxation of a possible small zero-field splitting of the manganese(II) $S = 5/2$ manifold, and of hyperfine coupling (assumed isotropic) of the unpaired electrons with the $I = 5/2$ ^{55}Mn nucleus. Both are theoretically found to decrease the low field (0.01-0.1 MHz) relaxation rates, and to leave the high field relaxation rates unaltered. According to this finding, fitting of the available data to the standard theory has

lead to an underestimate of the zero-field electronic relaxation time τ_0 and hence to an overestimate of the hydration number of the protein-bound manganese(II) ion. As previously noted from more qualitative considerations, however, inclusion of zero field splitting alone still leads to a fitting of the data with an unreasonably large hydration number [1].

If the effect of the hyperfine coupling is taken into account a sensible improvement of the overall picture is obtained. The performed calculations and the best fit parameters obtained for various manganese(II) proteins will be discussed in detail, together with some considerations on the combined effects of both zero-field splitting and hyperfine coupling being operative in the same system. It will be shown that in any case the treatment gives a satisfactory description of the overall NMRD profiles.

REFERENCES

- [1] S.H. KOENIG, R.D. BROWN, in I. BERTINI, R.S. DRAGO (eds.), «ESR and NMR of Paramagnetic Species in Biological and Related Systems», D. Reidel, Dordrecht, Holland, 1980, chapter 4.
- [2] T. KUSHNIR, G. NAVON, *J. Magn. Reson.*, **56**, 373 (1984).
- [3] I. BERTINI, C. LUCHINAT, M. MANCINI, G. SPINA, in D. GATTESCHI, O. KAHN, R.D. WILLETT (eds.), «Magneto-Structural Correlations in Exchange Coupled System», D. Reidel, Dordrecht, in press.
- [4] I. BERTINI, C. LUCHINAT, M. MANCINI, G. SPINA, *J. Magn. Reson.*, **59**, 213 (1984).
- [5] I. BERTINI, F. BRIGANTI, C. LUCHINAT, M. MANCINI, G. SPINA, *J. Magn. Reson.*, in press.



PS1.13 — MO

C. FRED BREWER

LOKESH BHATTACHARYYA

Departments of Molecular Pharmacology, and Microbiology and Immunology
Albert Einstein College of Medicine
Bronx, NY 10461
U.S.A.

RODNEY D. BROWN, III

SEYMOUR H. KOENIG

IBM Thomas J. Watson Research Center
Yorktown Heights, NY 10598
U.S.A.

EXTENDED SITE BINDING INTERACTIONS BETWEEN CONCAVALIN A AND GLYCOPEPTIDES AND OLIGOSACCHARIDES

We have previously provided evidence that simple mono- and oligosaccharides bind to Concanavalin A (Con A) via single glycoside interactions, *i.e.*, to a one residue size binding site. More recently, we have shown that a high mannose type glycopeptide interacts with the protein differently than simple mono- and oligosaccharides. We have extended these studies, using solvent nuclear magnetic resonance dispersion measurements, by investigating the effects of binding several high-mannose type glycopeptides isolated from ovalbumin on the conformation of Con A, as well as several synthetic oligosaccharides which resemble portions of the carbohydrate moieties of high mannose and complex type glycopeptides. We show that a trimannosyl moiety, which is a structural feature of both high mannose and complex type glycopeptides, is the predominant recognition site of binding to Con A in these glycopeptides.



PSI.14 — TU

JONAS ÅNGSTRÖM

Department of Biochemistry and Biophysics
Chalmers Institute of Technology and University of Göteborg
S-412 96 Göteborg
Sweden

JACQUES BAUDIER

Laboratoire de Biophysique, ERA C.R.N.S. 551
Université Louis Pasteur
U.E.R. de Sciences Pharmaceutiques
B.P. No 10, 67048 Strasbourg-Cedex
France

EFFECTS OF Ca^{2+} AND Zn^{2+} ON THE ^1H NMR PROPERTIES OF BOVINE S100b

The S100b protein belongs to the Ca^{2+} binding protein family which includes proteins such as calmodulin, troponin-C and the intestinal calcium binding protein (ICaBP). The latter protein is closely related to the β subunit of S100b ($\beta\beta$) in that it, too, possesses a modified EF hand structure in addition to a regular EF hand. Recent studies show that S100b not only binds four Ca^{2+} ions strongly but also four Zn^{2+} ions with very high affinity and that Zn^{2+} increases the protein affinity for Ca^{2+} . Likely candidates for Zn^{2+} binding are the five His residues found per S100b monomer in contrast to other calcium binding proteins containing one His at the most.

In the aromatic region of the NMR spectrum of S100b only five His C-2 resonances are found (Fig. 1). From this follows that the two subunits have identical environments. The pH dependence of the C-2 resonances reveals a wide spread in pKa values: three of these residues are markedly basic (8.0, 8.6 and 9.1) and must therefore have an acidic environment; one His shows a normal pKa (<6.5) whereas the last His is acidic (<6.0). These values are approximate since complete titration curves are not obtained. The pKa values of all five His appear to be lowered by approximately 0.5 pH units in the presence of 60 mM NaCl. Monovalent cations are known to antagonize Ca^{2+}

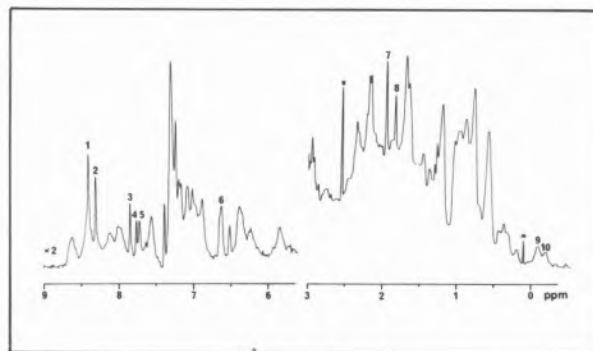


Fig. 1

^1H NMR convolution difference spectrum at 270 MHz of 0.25 mM S100b in 10 mM Tris- ^2HCl , 72 mM NaCl, pH* 7.6. The following resonances have been labeled in the spectrum: His C-2 resonances (1-5); the 3,5-ring proton doublet of the single Tyr residue (6); the Met methyl resonances (7,8) and two ring current shifted methyl resonances (9,10). The two resonances marked with an asterisk do not belong to the protein

binding to S100b, and since Ca^{2+} binding is pH dependent, the effect of NaCl on the protein may thus be rationalized as an indirect effect on a pH dependent conformational equilibrium involving different Ca^{2+} affinities for the protein.

A pH dependent conformation change is also manifested in the chemical shifts of several Phe resonances having secondary shift contributions and ring current shifted methyl resonances upfield of 0 ppm, mostly all of which shift toward their primary positions as the pH is lowered. Full titration curves are not obtained but the pKa for this process must be below 7. The effect of NaCl on these resonances is similar to that observed for the His resonances.

Calcium drastically alters the appearance of the aromatic region of the NMR spectrum at pH 8.25. Several Phe resonances with secondary shifts disappear under the main envelope of Phe resonances. The largest effect is seen for the first two Ca^{2+} ions, which appear to bind slowly on the NMR time scale, whereas the next two equivalents only have minor effects at this pH. Addition of 120 mM NaCl to the Ca^{2+} saturated protein indicates that it is the Ca^{2+} in the high affinity Ca^{2+} sites that is mostly antagonized by this salt.

Zinc also affects the NMR spectrum of S100b profoundly. The first two equivalents of Zn^{2+} bind to S100b in the slow exchange limit causing three His C-2 resonances to disappear and several Phe resonances to shift to new positions still retaining

some of the secondary shift contributions. It is noteworthy that the 3,5-ring proton resonance of the single Tyr residue also is perturbed, in contrast to Ca^{2+} binding. In the aliphatic region the methyl resonances upfield of 0 ppm disappear with a concomitant appearance of two new resonances between 0-0.5 ppm. Also notable is that the three resonances stemming from the Met residues in α -helices III and IV are significantly perturbed in this case.

The next two equivalents of Zn^{2+} cause all Phe resonances with secondary shifts to disappear under the main Phe envelope. The remaining two His C-2 resonances also disappear. The former observation agrees well with UV difference spectroscopy showing that the Phe residues are exposed to the solvent. Corresponding changes in the aliphatic region show that the Met residues now have approximately identical environments. Also Zn^{2+} ions three and four bind to S100b with slow exchange on the NMR time scale. Addition of four equivalents of Ca^{2+} to the Zn^{2+} saturated protein results in the appearance of at least three His C-2 and C-4 resonances at new positions, indicating that the protein structure now is more well defined or that motional averaging is more effective. From these data, Co^{2+} binding studies (this ion competes with Zn^{2+} for binding sites three and four as found by flow dialysis) and the assumption that the folding of the peptide backbone essentially follows that of the structurally related ICaBP, it is possible to assign the His residues involved in Zn^{2+} binding. A schematic structural model for the effects of pH, salt and Zn^{2+} binding on the Ca^{2+} binding of S100b has been formulated.

ACKNOWLEDGEMENTS

This work was supported by grants from the Swedish Natural Science Research Council and a short term EMBO fellowship (J.B.).



PS1.15 — TH

OU YAOHUA
ZHANG YUN
WEI YUEWANG
ZHOU XIN

Department of Biological Sciences and Biotechnology
Tsinghua University
Beijing
P.R.C.

FT-IR STUDIES OF THE ACTIVE SITES IN AMINOACYLASE

Aminoacylase is a Zn enzyme consisting of two subunits and containing one Zn(II) ion in each subunit which is necessary for the activity. Research has been done on the chemical modifications of some amino acid residues in aminoacylase. But there has been no direct information about the structure and function of the active sites concerning Zn. IR spectroscopy is a powerful tool for studying molecular structures. But the applications of IR spectroscopy to biological molecules have long been limited because of difficulties like spectral interpretation, interference of water, and low concentration. And there has been no report on the study of active sites in metallo-enzymes by use of IR spectroscopy.

In this paper, an attempt is made to study the IR absorptions of aminoacylases in aqueous solution, and to acquire information about Zn(II) and its coordination surrounding on the active sites of aminoacylase. As far as we know, this is the first attempt of its kind. Our results indicate that direct information of Zn can be clearly demonstrated in the IR spectra, and this method could be used for advanced studying about the structure and function of aminoacylase or other metallo-enzymes.

MATERIALS AND METHODS

The aminoacylase, isolated from porcine kidney, and purified by chromatography on Sephadex G-150 and DEAE cellulose, was homogeneous as

judged by gel electrophoresis. Its specific activity, measured at 37°C, pH=7.0, with *N*-acetylalanine as substrate, was about 80 U/mg protein. The Zn free apoaminoacylase was obtained by chelating Zn out with *O*-phenanthroline [1]. The Co substituted aminoacylase, and Co substituted aminoacylase in 0.1 M phosphate buffer containing 1 mM Co(II) was obtained by adding Co(II) to metal free apoaminoacylase [1].

The solution samples of aminoacylases were run in liquid film with polyvinyl plates as windows. Their far IR absorptions were measured with a Nicolet 170 XS Fourier Transform Infrared Spectrophotometer, in the frequency range of 530 cm⁻¹ to 100 cm⁻¹. The spectrum of water was obtained in the same way.

The far IR absorption spectra of aminoacylase, metal-free aminoacylase, and Co substituted aminoacylase in aqueous solution were obtained by digitally subtracting the absorbance contribution of water from the solution spectra of the samples, and that of the Co substituted aminoacylase existing in the environment with free Co(II) ions was obtained similarly.

RESULTS AND DISCUSSION

As shown in Fig. 1, the absorbance spectra of water and of aminoacylases aqueous solutions are almost indistinguishable from each other. The reason is that the absorption of water is so strong that it masks the absorptions of enzymes. But the

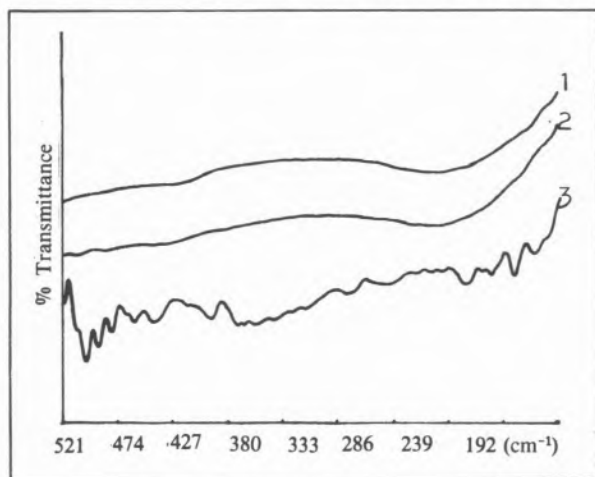


Fig. 1

The far IR spectra of redistilled water¹, aqueous solution of aminoacylase (8 mg/ml)², and the subtracted spectrum of aminoacylase in aqueous solution (10 mg/ml)³

absorptions of the enzymes can be clearly demonstrated in the difference spectra (Fig. 1 and Fig. 2). Because it is impossible to find independent peaks of the samples and of the solvent, we chose the subtracting factors according to the criterion that the difference absorptions are near zero at the wavenumbers where the solutions have their minimum absorptions. The absorbance spectrum of water is relatively flat at the far IR range, so the error of this method could be permissible for qualitative considerations.

Absorptions of proteins in far IR range have seldom been studied and are said to be caused by vibrations of the backbone. Up to now, there has been only one report on using far IR spectroscopy in the study of enzymes. In the case of metallo-enzymes, the metal ions are much heavier than ordinary atoms in proteins. So the vibrational absorptions concerning metal ions should appear in the far IR range if they could be strong enough. Our experiments show that (see Fig. 2) a peak between 510 cm⁻¹ and 500 cm⁻¹ appears only when

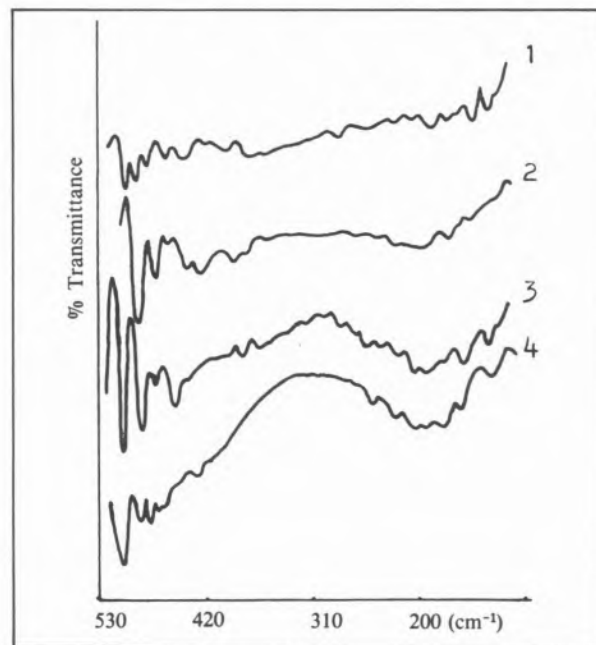


Fig. 2

The subtracted far IR spectra of Zn-aminoacylase¹, metal-free apoaminoacylase², Co-substituted aminoacylase³, and Co-substituted aminoacylase existing in the environment with free Co(II)⁴

the metal ion exists, whether it is Zn(II) or Co(II). And this peak of Co substituted aminoacylase is shifted to higher wavenumbers (about 2 cm⁻¹)

comparing with that of the Zn aminoacylase. For these reasons, we tentatively assign the peak to the vibrational absorptions of the metal ions and the coordinated atoms in the active sites of aminoacylase. One prerequisite for this assignment is that the conformation of the aminoacylase remains the same when Zn is removed or when Co is put in. And an experimental evidence which supports this hypothesis is that the fluorescence emission spectra of aminoacylase with metal ions are fundamentally the same as that of the apoaminoacylase, while it has been known that aminoacylase has twelve tryptophan residues, and one of them is necessary for the activity.

The specific activity of the Co-substituted aminoacylase is higher in the presence of free Co(II) ions than in their absence. For Zn aminoacylase, the existence of some free Co(II) ions can also increase its specific activity [1]. These facts indicate that there are some metal ions, other than those firmly situated in the active sites, which can activate aminoacylases somehow. It can be found from Fig. 2 that the Co-substituted aminoacylase has very similar absorbance spectra under the two different conditions mentioned above. The positions of the peak which is believed to reflect the vibration between metal ions and the coordinated atoms are the same in the two cases. This indicates that free Co(II) ions do not influence the environment of the Co(II) ions in the active sites very much. More experiments will be needed to explain how free Co(II) ions influence the activity of aminoacylase.

REFERENCE

- [1] OU YAOHUA, ZHANG YUN, WEI YUEWANG, ZHOU XIN, «Co-substituted Aminoacylase», Collection of Papers, The First National Conference of Bio-inorganic Chemistry, Nov., 1984.



PS1.16 — MO

R. WEVER
H. PLAT
E. DE BOER
Laboratory of Biochemistry
University of Amsterdam
P.O. Box 20151, 1000 HD Amsterdam
The Netherlands

BROMOPEROXIDASES FROM SEAWEED: A NOVEL CLASS OF ENZYMES CONTAINING VANADIUM?

Marine organisms, and in particular algae, accumulate a wide variety of halogenated compounds which show antimicrobial activity and which may have a function in systems involved in chemical defence [1,2]. In the biosynthesis of the brominated compounds bromoperoxidases participate. Bromoperoxidases from red [3] or green algae [4] have been studied in some detail, but little is known about the enzyme found in brown algae [5,6]. In this contribution data are presented on the properties of bromoperoxidase from the brown algae *Ascophyllum nodosum* which was recently purified by us [7].

It is known [8] that bromoperoxidases from marine origin show a pH optimum in the bromination reaction and this was also observed in the bromoperoxidase from *Ascophyllum nodosum*. The enzyme shows distinct pH optima, the position of which was determined by the concentration of H_2O_2 and Br^- .

At low pH values, the enzyme is inhibited by an excess of Br^- . However, high concentrations of H_2O_2 (1-5 mM) do not inhibit the enzyme. The complex steady-state kinetics correspond to a ping-pong mechanism in which H_2O_2 first has to oxidise the enzyme before Br^- or H^+ are bound. When Br^- or H^+ are bound to the enzyme before H_2O_2 has reacted, these substrates act as inhibitors.

Surprisingly, although the brominating activity (90 μ moles monochlorodimedone brominated per min

per mg of protein) is comparable to that of other haloperoxidases that contain haem, the bromoperoxidase even at high protein concentration (10 mg/ml) does not exhibit a Soret peak typical of a haemoprotein. Recently, it was reported [6] that the bromoperoxidase activity, after inactivation of the enzyme at low pH, could be restored at high pH by addition of vanadium. This observation [6], which we could confirm, prompted us to determine the vanadium content of our preparation. Indeed, analysis demonstrated that a considerable amount of vanadium was present in our purified bromoperoxidase preparation. The amount of vanadium per mg of protein was high enough to be studied by EPR at low temperature.

In the oxidised state, the enzyme as isolated does not show signals that can be attributed to vanadium. Also, addition of Br⁻ or H₂O₂ was without effect. However, upon reduction with dithionite, an EPR spectrum was observed which showed the typical hyperfine splitting of vanadium (I=7/2). EPR experiments are in progress to determine whether the valence of this metal ion changes during catalysis. If this should be the case, a novel class of enzymes that contain vanadium as a prosthetic group has been discovered.

ACKNOWLEDGEMENTS

We gratefully acknowledge the support by DSM B.V., Geleen, and the grant support from the Foundation for Technical Sciences (S.T.W.) under the auspices of the Netherlands Foundation for Chemical Research (S.O.N.).

REFERENCES

- [1] J.F. SIUDA, J.F. DE BERNARDIS, *Lloydia*, **36**, 107-143 (1973).
- [2] W. FENICAL, *J. Phycol.*, **11**, 245-259 (1975).
- [3] R.F. THEILER, J.S. SIUDA, L.P. HAGER in P.N. KAUL, C.J. SINDERMANN (eds.), «Drugs and Food from the Sea, Myth or Reality», The University of Oklahoma, Norman, Oklahoma, 1978, pp. 153-169.
- [4] J.A. MANTHEY, L.P. HAGER, *J. Biol. Chem.*, **256**, 11232-11238 (1981).
- [5] S. RÖNNERSTRAND, *Kungl. Fysiograf. Sällskapets I Lund Förhandl.*, **16**, 117-130 (1946).
- [6] H. VILTER, *Phytochemistry*, **23**, 1387-1390 (1984).
- [7] R. WEVER, H. PLAT, E. DE BOER, *Biochim. Biophys. Acta* (1985), submitted for publication.
- [8] W.D. HEWSON, L.P. HAGER, *J. Phycol.*, **16**, 340-345 (1980).



PS1.17 — TU

VINCENT L. PECORARO
GERBEN ZYLSTRA
RONALD H. OLSEN

Department of Chemistry
University of Michigan
and
Department of Microbiology and Immunology
University of Michigan Medical School
Ann Arbor, MI 48109
U.S.A.

ISOLATION OF THE DNA SEQUENCE CODING FOR *PSEUDOMONAS AERUGINOSA* AZURIN

The mechanism of electron transfer by metalloenzymes has been the basis of extensive research. One of the unanswered questions in the field is the importance of relative metal ion and protein orientations to the electron transfer rate. Important data have been accumulated for protein-protein interactions [1,2] and for protein-small molecule electron transfer reactions [3-5] with the "blue" copper proteins. Azurin, a "blue" copper protein isolated from *P. aeruginosa*, is an ideal donor/acceptor protein to study because: a) the protein sequence is known [6]; b) the X-ray structure is reported [7]; and c) electron transfer rates between azurin and other proteins and small molecules are tabulated [1-5].

Our entry into this field hopes to exploit the new biotechnology known as site specific mutagenesis. The single "blue" copper atom in azurin is coordinated in a distorted tetrahedral geometry by nitrogen atoms from His-46 and His-117 and sulfur atoms of Cys-112 and Met-121 [7]. We propose to develop a retroazurin in which residues 112 and 121 are changed to Met and Cys, respectively. This alteration of the protein sequence will result in a change in the long axis (Cu-Met) in the distorted tetrahedral environment of the copper. Besides generating a unique modification of the

original site in the protein which is accessible to physical studies, the effect of the metal ion orientation on the electron transfer process can be addressed.

The first step in developing a new protein is to isolate and sequence the native DNA for the azurin gene. This report describes our progress in this endeavor.

We have used a DNA synthesizer to construct an oligonucleotide which is complementary to the mRNA encoding for amino acids 11-17 of azurin. The probe (shown below) is 20 nucleotide bases long and 32 fold redundant.

CTP-GTA-TAC-GTQ-AAP-TTP-TG
(where P=A or G and Q=C or T)

Purification of the probe was accomplished with a 0.1 M triethylammonium acetate pH 7.1/acetonitrile gradient which varied linearly from 15 to 40% acetonitrile over a 20 minute period. The probe eluted from the C-18 reverse phase column after 13 minutes (Fig. 1). The probe was then labelled with ^{32}P using T4 polynucleotide kinase and ATP [$\gamma\text{-}^{32}\text{P}$]. This radioactive probe is being used in southern

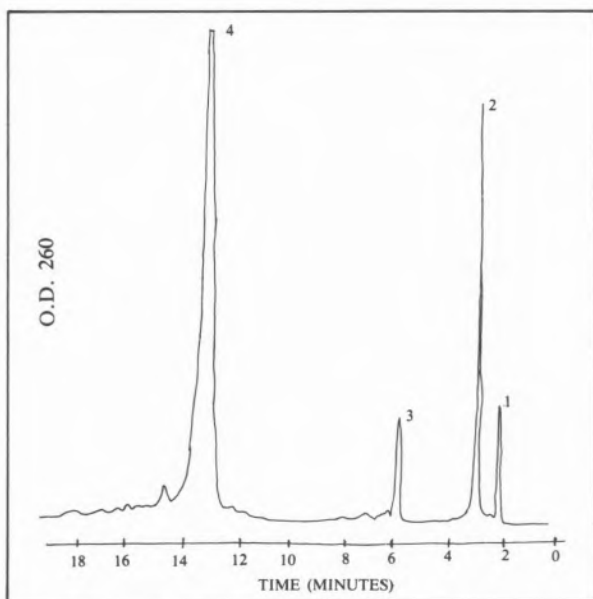


Fig. 1

HPLC elution profile of oligonucleotide probe used in southern blotting experiments. The probe elutes after 13 minutes. Peak 1, solvent front; Peak 2, failure sequences (i.e., probes of improper length); Peak 3, benzamide; Peak 4, desired oligonucleotide probe

blotting experiments against gene banks of the *P. aeruginosa* chromosome [8] to determine which group of clones contain the azurin gene. In addition, colony blotting experiments will allow isolation of the cloned gene. With these data in hand, we will isolate and sequence the DNA coding for the azurin gene. Our progress in the isolation of the proper clone, the determination of the DNA sequence of the azurin gene and determination of the sequence homology between the native DNA sequence and that predicted from the amino acid sequence will be reported.

REFERENCES

- [1] S. WHERLAND, I. PECHT, *Biochemistry*, **17**, 2585 (1978).
- [2] M.A. AUGUSTIN, S.K. CHAPMAN, D.M. DAVIES, A.D. WATSON, A.G. SYKES, *J. Inorg. Biochem.*, **20**, 281 (1984).
- [3] R.A. HOLWERDA, S. WHERLAND, H.B. GRAY, *Annu. Rev. Biophys. Bioeng.*, **5**, 363 (1976).
- [4] J.V. MCARDLE, C.L. COYLE, H.B. GRAY, G.S. YONEDA, R.A. HOLWERDA, *J. Am. Chem. Soc.*, **99**, 2483 (1977).
- [5] D. CUMMINS, H.B. GRAY, *J. Am. Chem. Soc.*, **99**, 5158 (1977).
- [6] M.D. DAYHOFF (ed.), «Atlas of Protein Sequence and Structure», vol. 5, suppl. 2, National Biomedical Research Foundation, 1978.
- [7] E.T. ADMAN, L.H. JENSEN, *Isr. J. Chem.*, **21**, 8 (1981).
- [8] R.H. OLSEN, G. DEBUSSCHER, W.R. MCCOMBIE, *J. Bacteriol.*, **150**, 60 (1982).



PS1.18 — TH

SERGIO PAULO SEVERO DE SOUZA DINIZ *
Department of Pharmacy and Biochemistry
Maringá State University
CP 331 — 87.100 Maringá — Paraná
Brazil

THE EFFECT OF MOLYBDENUM ON NITROGEN FIXING ORGANISMS

Biological nitrogen fixation is carried out by prokaryotic organisms and blue-green algae, mediated by the enzyme nitrogenase. Molybdenum is a

constituent of the MoFe protein of the nitrogenase complex. The absence of Mo has been shown to prevent the synthesis of nitrogenase, but it is not clear how Mo regulates or how MoO_4^{2-} accumulation is regulated.

Nitrogenases from different bacteria have very similar properties. The enzyme consists of the two oxygen-labile proteins — component I (which has two copies each of two different subunits and contains iron and molybdenum atoms) and component II (which has two copies of a single subunit and contains the site of substrate binding and substrate reduction). The active site of nitrogenase resides in an iron-molybdenum cofactor (FeMo-co) that is a part of component I. The role of component II is to reduce component I.

MoFe proteins are complex metalloproteins with MW around 220,000, containing two molybdenum atoms with about 30 iron atoms and a slightly smaller number of acid-labile sulphur atoms per molecule. Mössbauer studies have resulted in identification of three types of metal centre named "P" clusters (16 Fe), the FeMo centres (12-16 Fe) and "S" atoms (2 Fe).

Mo-uptake is energy-dependent and is repressed by NH_4^+ (2 mM) and high concentrations of MoO_4^{2-} (1 mM) in *Clostridium pasteurianum*. In *Azotobacter vinelandii*, Mo-uptake was not inhibited in the presence of NH_4^+ , although the rate of uptake of MoO_4^{2-} was slower. During derepression of *Klebsiella pneumoniae* both uptake and nitrogenase activity were maximal at 1 μM MoO_4^{2-} and uptake was inhibited by NH_4^+ . *Azospirillum brasilense* showed the maximal nitrogenase activity *in vivo* at a MoO_4^{2-} concentration of 2 μM . *C. pasteurianum* and *A. vinelandii* have Mo-storage proteins which bind MoO_4^{2-} transported into the cell, but *K. pneumoniae* does not. The steps in the transformation of MoO_4^{2-} to the Mo-S environment of FeMo-co may be expected to be very similar in all nitrogen fixing organisms.

ACKNOWLEDGEMENTS

These studies were supported by the Maringá State University, Paraná, Brazil, and by the Ministry of Education of Japan (Monbusho).

* Present address: Department of Agricultural Chemistry, Faculty of Agriculture; Tohoku University — Sendai 980, Japan.



PS1.19 — TH

RICHARD C. REEM
JAMES W. WHITTAKER
EDWARD I. SOLOMON
Department of Chemistry
Stanford University
Stanford, California 94305
U.S.A.

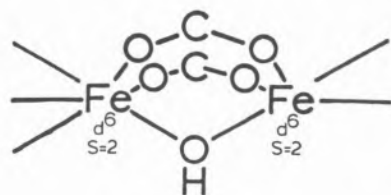
SPECTROSCOPIC STUDIES OF NONHEME IRON ACTIVE SITES

Nonheme iron active sites are involved in the interactions with O_2 in oxygen transport (hemerythrin, Hr), superoxide dismutation (iron superoxide dismutase, FeSD) and lipid peroxidation (soybean lipoxygenase, SBL). We have used a combination of variable temperature absorbance, CD, MCD, and EPR spectroscopies to obtain information on active site electronic structure relating to biological function of these iron sites in both ferric and ferrous oxidation states.

The structure of the binuclear iron active site in $\text{Met} < \text{Fe(III)Fe(III)} > \text{Hr}$ is known to high resolution from X-ray crystallographic studies, which show two irons bridged by an oxo anion as well as aspartate and glutamate carboxylates. One iron is hexacoordinate, bound by three histidyl residues in addition to the bridging ligands; the other iron is pentacoordinate in the Met protein (three bridging ligands plus two histidyl residues) and binds exogenous ligands such as N_3^- , or O_2^{2-} in the oxygenated protein. The results of variable temperature absorbance and CD spectroscopy allow us to distinguish for the first time electronic transitions associated with each iron in the active site and to observe the changes which occur at each iron with temperature and exogenous ligand binding. This, coupled with polarized single crystal absorbance data leads to detailed insight into the electronic structure of the site and perturbation by binding of peroxide.

In contrast to the well defined geometric structure of the Met Hr iron site which has emerged, the

deoxy Hr active site is known at a lower resolution. In addition, previous spectroscopic studies have been impaired by the absence of absorbance features clearly associated with the iron in the accessible spectral range. The application of variable temperature CD and MCD have allowed us to detect the Fe(II) ligand field transitions of deoxy Hr near 1000 nm and use them as probes of the iron site in this oxidation state. The MCD spectrum of deoxy Hr is shown in Fig. 1A. At 5 K, the zero field CD spectrum is coincident with the 5 T MCD spectrum. As the temperature is raised, while keeping the field constant, an MCD signal is observed, reaching a maximum intensity near 65 K and declining at higher temperatures. Assuming a largest reasonable value for the zero field splitting to be $D=12\text{ cm}^{-1}$ this MCD data requires an antiferromagnetic exchange interaction $-J>13\pm 5\text{ cm}^{-1}$ within the binuclear center. Model studies have shown that the carboxylate bridges cannot account for an exchange of this magnitude. A hydroxo or oxo bridge would provide the required coupling, and, although the possibility of a protein conformational change which introduces a new bridging ligand cannot be ruled out, a hydroxo bridge is most likely present in deoxy hemerythrin. This data, combined with CD data which indicates the presence of one 5- and one 6-coordinate iron, allows us to present the following model for the deoxy Hr active site:



CD studies of the Fe(II) ligand field bands in deoxy Hr show that N_3^- and OCN^- bind at the pentacoordinate iron in deoxy Hr, each with a single binding constant of about 70 M^{-1} . F^- also binds with $K_B \sim 7\text{ M}^{-1}$, but no other anions have been found to bind with $K_B > 0.5\text{ M}^{-1}$. Binding of anions generates large changes in the CD and MCD spectra of deoxy Hr, as illustrated in Fig. 1. The MCD spectrum of deoxy N_3^- Hr (Fig. 1B) indicates a groundstate paramagnetism which saturates at low temperature with $g > 8$. We also observe an unusual Fe(II) EPR signal (Fig. 1C)

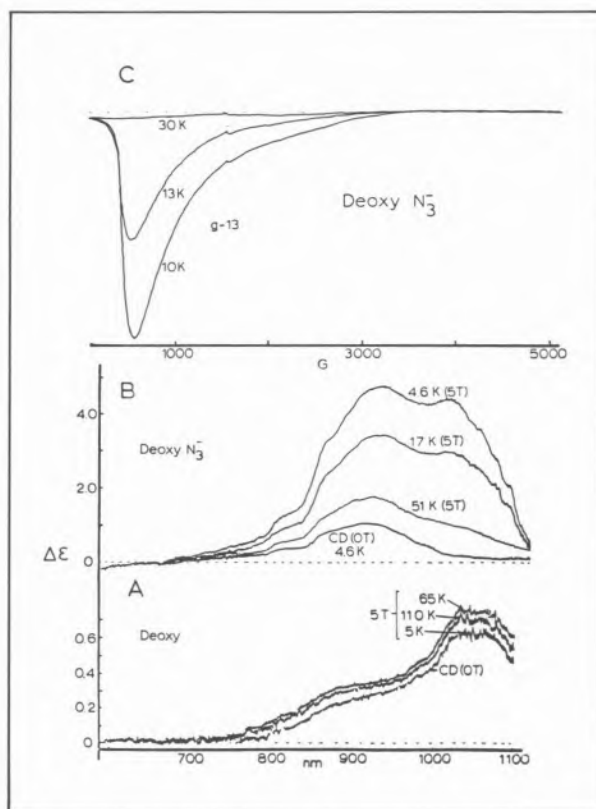


Fig. 1
EPR and MCD Spectra of Deoxy and Deoxy- N_3^- Hemerythrin

with $g_{\text{eff}} \sim 13$. The observation of paramagnetism indicates that the groundstate magnetic properties of the binuclear ferrous site are no longer dominated by antiferromagnetic coupling. The most probable explanation of this effect is the breaking of, or perturbation of the hydroxo bridge. This could result in labilization of the oxo bridge which would be consistent with the observed rapid exchange of the bridge oxygen with solvent water in the presence of N_3^- or OCN^- . Similar studies on the ligand field spectra of the ferrous mononuclear iron active sites in FeSD and SBL are providing information on the environment and accessibility of the iron in this oxidation state. Transitions observed near 1000 nm in CD and MCD spectra reflect the coordination environment of the iron centers and have been used to probe ligand binding to the ferrous sites. In addition, we have used low temperature MCD spectroscopy to probe the mononuclear iron sites in the ferric enzymes and their interactions with exogenous ligands.



PSI.20 — MO

B. BARATA

I. MOURA

A.V. XAVIER

J.J.G. MOURA

Centro de Química Estrutural
FCL, UNL, Complexo I, IST
Av. Rovisco Pais, 1000 Lisboa
Portugal

J. LIANG

B.H. HUYNH

Department of Physics
Emory University
Atlanta, Georgia 30322
U.S.A.

J. LEGALL

Department of Biochemistry
University of Georgia
Athens, Georgia 30602
U.S.A.

EPR AND MÖSSBAUER STUDIES ON *DESULFOVIBRIO GIGAS* Mo(Fe-S) PROTEIN

The Mo(Fe-S) protein from *Desulfovibrio gigas*, a sulfate reducing organism, was shown to contain one Mo and approx. 12 Fe per molecule and a molecular weight of 120 KDa. No evidence was found for the presence of subunits. Its physiological role has not yet been determined. Optical, EPR and CD data strongly suggest the presence of [2Fe-2S] clusters. At ~70 K the EPR spectrum of the dithionite reduced sample exhibits a Mo signal centered around $g=1.97$ and signals at $g=2.02$, 1.94 and 1.93, corresponding to one type of [2Fe-2S] centers, named (Fe-S I). At lower temperature ($T < 40$ K) an additional signal appears at $g=2.06$ and 1.90, indicating the presence of a second [2Fe-2S] center (Fe-S II). Redox titration studies revealed yet another Fe-S center with type I EPR signal. The two type I centers are termed (Fe-S I A) and (Fe-S I B).

When observed at temperatures lower than 40 K, the type I Fe-S EPR features at $g=2.02$ split into two peaks separated by approx. 15 G. Such splitting can be explained either by coupling of the pa-

ramagnetic site to a nearby $I=1/2$ nucleus, such as a proton, or a slight difference in the resonances of Fe-S I A and I B centers. The EPR signals of the Fe-S centers and molybdenum of the reduced protein are compared in H_2O and D_2O .

Recently, the protein was purified from ^{57}Fe grown cells. The quality of the Mössbauer data obtained in the native and partially reduced Mo(Fe-S) protein enabled us to pursue the characterization of the [Fe-S] centers in correlation with the previously reported EPR data.

In the native state, the Mössbauer parameters of the only quadrupole doublet observed at 4.2 K with an external field of 500 G applied parallel to the gamma beam ($\Delta E_Q = (0.63 \pm 0.02)$ mm/s, and $\delta = (0.27 \pm 0.02)$ mm/s), are typical of high-spin ferric ions with tetrahedral sulfur coordination.

Partially reduced states of the protein show two types of doublets, at 150 K. The central quadrupole doublet is similar to that of the oxidized Mo(Fe-S) protein. The outer doublet represents the ferrous site in the reduced [2Fe-2S] clusters. The shape of the ferrous doublet indicates that it consists of at least two unresolved doublets. This observation is consistent with the EPR finding that the Mo(Fe-S) protein contains more than one type of [2Fe-2S] cluster. The Mössbauer parameters for the two ferrous sites are $\Delta E_Q = (3.27 \pm 0.02)$ mm/s, $\delta = (0.57 \pm 0.02)$ mm/s and $\Delta E_Q = (2.79 \pm 0.02)$ mm/s, $\delta = (0.59 \pm 0.02)$ mm/s.

Low temperature studies are being carried out in order to compare the above data with [2Fe-2S] clusters of reduced ferredoxin from spinach and Rieske centers.

ACKNOWLEDGEMENTS

This work was supported by INIC, JNICT and NATO.

REFERENCES

- J.J.G. MOURA, A.V. XAVIER, R. CAMMACK, D.O. HALL, M. BRUSCHI, J. LEGALL, *Biochem. J.*, **173**, 419-425 (1978).



PS1.21 — TU

A.R. LINO

A.V. XAVIER

I. MOURA

Centro de Química Estrutural

and

UNL, Complexo I,

IST, Av. Rovisco Pais, 1000 Lisboa

Portugal

J. LEGALL

L.G. LJUNGDAHL

Department of Biochemistry

University of Georgia

Athens, Georgia 30602

U.S.A.

COBALT CONTAINING B₁₂ COFACTORS FROM METHANOGENIC BACTERIA — SPECTROSCOPIC CHARACTERIZATION

Methanogens are primitive organisms that use the reduction of CO₂ by H₂ to methane as a terminal metabolic electron transfer reaction [1]. They belong to a bacterial group designated as "archaeobacteria", which are distantly related in the evolutionary scale to eucaryotes and to the strict anaerobic bacteria such as clostridia and sulfate reducing bacteria.

Several electron carriers and factors, unique to methanogens, have been isolated from these bacteria (including F₄₂₀, coenzyme M, factors F₄₃₀ and F₃₄₂).

Recently, a B₁₂ containing protein was isolated from *Methanosarcina barkeri* (DSM 800) [2]. This protein contains bound aquocobalamine and when the cofactor is reduced and methylated with ¹⁴C-methyl iodide, the resultant ¹⁴C-methyl B₁₂ protein is extremely active in the biosynthesis of ¹⁴C-labeled methane [2].

Two B₁₂ proteins have now been isolated from *M. barkeri* (DSM 800 and 804). The visible spectra of native B₁₂ proteins from both strains are very similar and characteristic of bound aquocobalamine (Fig. 1). The enzyme cofactor can be

reduced with mercaptoethanol or borohydride and methylated by methyl iodide, producing the methyl B₁₂ form of the protein (Fig. 1). The methylated form of the enzyme can be converted by photolysis to a stable low-spin Co^{II} complex.

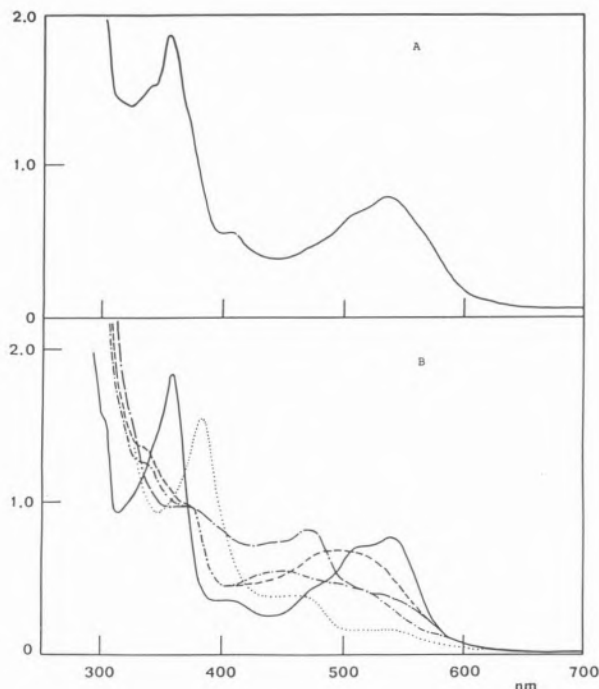
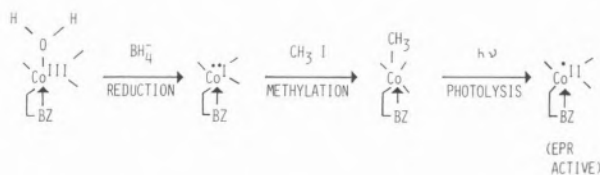


Fig. 1

(A) Absorption spectra of B₁₂ containing protein from *M. barkeri* (DSM 804) in the native form. (B) Absorption spectra of B₁₂ containing protein from *M. barkeri* (DSM 800) in the native form (—), reduced with BH₄⁻ after 2 hours of reduction (·····), methylated with CH₃I (----) and after photolysis under reducing conditions (-·-·-)



Amino-acid composition, cobalt and molecular weight of both proteins is shown in Table I. The proteins show similar amino-acid composition and the same Co content per monomer, in spite of their different oligomerization forms.

The corrinoids were extracted and purified from cell extracts and also from the purified proteins in their cyano form according to BERNHAUER *et al.* [3]. Different corrinoids are present in the cell ex-

Table I
Amino Acid Composition of *M. barkeri* (DSM 800 and 804)
 B_{12} Protein

Amino-acids	B_{12} protein from <i>M. barkeri</i> (DSM 800)		B_{12} Protein from <i>M. barkeri</i> (DSM 804)	
	from analysis	nearest integer	from analysis	nearest integer
Lysine	12.8	13	12.2	12
Hystidine	3.9	3	3.8	4
Arginine	4.2	4	4.6	5
Tryptophan	n.d.	n.d.	n.d.	n.d.
Aspartic Acid	17.2	17	18.4	18
Threonine	8.0	9	9.5	10
Serine	6.5	7	7.4	8
Glutamic Acid	20.9	21	18.7	19
Proline	7.1	7	7.1	7
Glycine	1.5	15	15.0	15
Alanine	18.3	18	15.3	15
Cysteine (Half)	n.d.	n.d.	3.2	4
Valine	11.9	12	12.5	13
Methionine	6.0	7	5.4	6
Isoleucine	10.0	10	9.9	10
Leucine	13.0	13	12.5	13
Tyrosine	4.4	5	4.5	5
Phenylalanine	5.6	6	4.5	5
Total Residues		168		169
Cobalt		1		1
Mol. Weight (subunit)		72 000 (18 100)		50 000 (17 800)
		α_4		α_3

tract. The major one ($\sim 90\%$ of total) was completely purified and analysed. The visible spectra of dicyano and monocyano complexes of this corrinoid are shown in Fig. 2. The nuclear magnetic resonance spectra of this corrinoid as well as that of the corrinoid from the holoenzyme, are shown in Fig. 3. The NMR spectra of the corrinoids present six resonances in the aromatic region. Two of these resonances come from a *meso* (C-H) and a ribose (C₁-H) proton. The other four are assigned to base protons showing that the 5,6-dimethylbenzimidazole is replaced by 5-hydroxybenzimidazole. No resonance is observed in the region between 2 and 4 ppm, which could account for a methoxy group, showing that in *M. barkeri* factor III (and not factor III_m) is the corrinoid present in larger quantities. The corrinoid extracted from the purified B_{12} containing protein

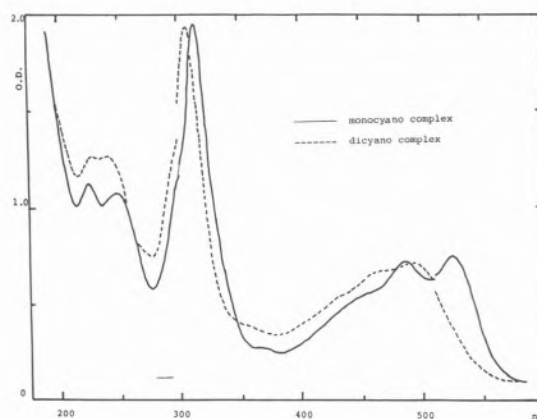


Fig. 2
Absorption spectra of 5-hydroxybenzimidazolcobalamine extracted from cells of *M. barkeri* (DSM 800) in the monocyano and dicyano complex forms

is spectroscopically identical to that isolated from the cells. The NMR spectra shown in Fig. 3 closely resembles the one published for factor III by HENSENS *et al.* [4].

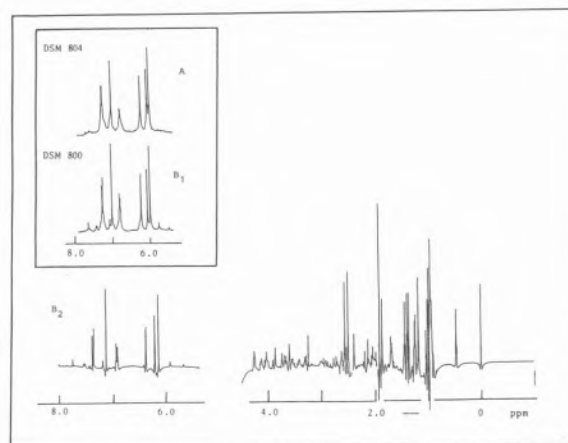


Fig. 3
300 MHz ^1H NMR spectra of factor III (5-hydroxybenzimidazolcobalamine) from *M. barkeri*. (A) Corrinoid extracted from the purified B_{12} protein from *M. barkeri* (DSM 804); (B1) Corrinoid extracted from the purified B_{12} protein from *M. barkeri* (DSM 800); (B2) Corrinoid extracted from cells of *M. barkeri* (DSM 800)

When the methyl B_{12} protein (from both strains) or the methyl extracted corrinoids are photolysed under reducing conditions, an EPR spectra at 77 K depicts typical signals of a stable Co^{II} complex (Fig. 4). Triplets are observed from the N-hyperfine interaction of the coordinated benzimidazole base showing that the nucleotide base is coordina-

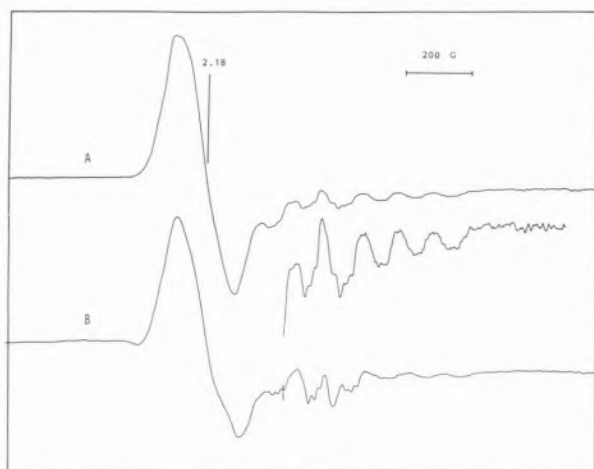


Fig. 4

(A) EPR spectra of B_{12} containing protein from *M. barkeri* (DSM 800); (B) EPR spectra of the extracted corrinoid from cells of *M. barkeri* (DSM 800).

Both methyl B_{12} protein and methyl extracted corrinoids were photolyzed under reducing conditions.

EPR Conditions: Microwave frequency 9.28 GHz; Temperature 77 K; Microwave power 20 mW; Field modulation 2 mT; Gain 8×10^4

ted to the cobalt both in its bound form to the protein and in the free form.

M. barkeri is until now the only methanogen where the presence of a B_{12} protein was reported [2,5]. In these bacteria it was shown that factor III is the most abundant corrinoid in the cells and that it is also the corrinoid associated with the B_{12} protein.

Although the physiological role of these proteins is not yet clearly established, they seem to be involved in the biosynthesis of CH_3S-CoM or CH_4 from CH_3OH [2].

ACKNOWLEDGEMENTS

Work supported by INIC, JNICT, U.S.A.I.D. and Quatrum.

REFERENCES

- [1] J.G. ZEIKUS, *Bact. Rev.*, **41**, 515-541 (1977).
- [2] J.M. WOOD, I. MOURA, J.J.G. MOURA, H. SANTOS, A.V. XAVIER, J. LEGALL, M. SCANDELLARI, *Science*, **216**, 303-305 (1982).
- [3] K. BERNHAUER, G. WILHARM, *Arch. Biochem. Biophys.*, **83**, 248 (1959).
- [4] O.D. HENSENS, H.A.O. HILL, C.E. MCCLELLAND, R.J.P. WILLIAMS, in D. DOLPHINS (ed.), « B_{12} », vol. 1, Wiley, New York, 1092, pp. 463-500.
- [5] P. VAN DER MEIJDEN, H.J. HEYTHUYSEN, A. POWELS, F.P. HOWEN, C. VAN DER DRIFT, G.D. VOGLY, *Arch. Microbiol.*, **134**, 238-242 (1983).



PS1.22 — TH

TINY VAN HOUWELINGEN

G.W. CANTERS

J.A. DUINE

J. FRANK, JZN.

G. STOBBELAAR

Department of Chemistry

Gorlaeus Laboratories

State University Leiden

P.O. Box 9502, 2300 RA Leiden

The Netherlands

and

Biochemical Laboratory

Technical University Delft

Julianalaan 67-67a, 2628 BC, Delft

The Netherlands

A BLUE COPPER PROTEIN FROM *THIOBACILLUS VERSUTUS*

The multifarious coordinating capabilities of copper are reflected by the variety of metalloproteins in which Cu occupies the catalytically active site. The usual classification of copper proteins distinguishes between three or four types [1].

As more and more copper proteins are discovered and characterised, it is becoming clear that within each class diversity reigns. For instance, for the type I blue copper proteins, the most extensively studied class up till now, it has been found that redox potentials may vary from 180 to 760 mV, molecular weights from 10 to 20 kD and pI points from 4 to 11. Most intriguing is the coordination of the Cu. It has been demonstrated by crystallographic techniques in a number of cases that the metal is surrounded in a distorted tetrahedral fashion by an N_2SS^* coordination [2-4]. The nitrogens are provided by two histidines and the sulfurs derive from a methionine and a cysteine. However, stellacyanin lacks methionine and Russian researchers have reported a blue copper protein which does not seem to contain cysteine [5,6]. It is not understood how the details of the Cu coordination relate to the spectroscopic properties and the redox potential of the protein and further structural studies and a search for new type I copper proteins are needed.

Here the isolation of a blue copper protein from *Thiobacillus versutus* (previously called *Thiobacillus sp.* strain A2, see [7]) grown on methylamine is reported. This protein is part of a redox chain that consists of probably 4 proteins and that takes care of the conversion of methylamine into the aldehyde. The primary enzyme is a methylamine dehydrogenase (MADH) of which the prosthetic group is a pyrrolo-quinoline quinone (PQQ) [8]. The next two links in the chain are the blue copper protein mentioned above and a cytochrome, followed probably by a final oxidase. Isolation and purification of the blue copper protein will be described on the poster. A detailed characterization is nearly completed (ESR, NMR, optical spectra, redox potential, pI, molecular weight, etc.) and the results will be reported as well. The data obtained so far ($E_0 = 256$ mV, maximum of the visible absorption band at 596 nm, type I ESR spectrum, MW = 12,000 - 13,000) justify the conclusion that the protein is an amicyanin type blue copper protein [9].

REFERENCES

- [1] E.T. ADMAN, in PAULINE HARRISON (ed.), «Topics in Molecular and Structural Biology», MacMillan.
- [2] P.M. COLMAN, H.C. FREEMAN, J.M. GUSS, M. MURATA, V.A. NORRIS, J.A.M. RAMSHAW, M.P. VENKATAPPA, *Nature*, **272**, 319 (1978).
- [3] E.T. ADMAN, R.E. STENKAMP, L.C. SIEKER, L.H. JENSEN, *J. Mol. Biol.*, **123**, 35 (1978).
- [4] G.E. NORRIS, B.F. ANDERSON, E.N. BAKER, *J. Mol. Biol.*, **165**, 501 (1983).
- [5] C. BERGMAN, E.K. GANVIK, P.O. NYMAN, L. STRID, *Biochem. Biophys. Res. Commun.*, **77**, 1052 (1977).
- [6] V.T. AIKAZYAN, R.M. NALBANDYAN, *Biochim. Biophys. Acta*, **677**, 421 (1981).
- [7] A.P. HARRISON JR., *Intern. J. System. Bacteriol.*, **33**, 211 (1983).
- [8] J.A. DUINE, J. FRANK JZN., *Trends Biochem. Sci.*, **6**, 278 (1981).
- [9] J. TOBARI, Y. HARADA, *Biochem. Biophys. Res. Commun.*, **101**, 502 (1981).



PS1.23 — TH

M.C. FEITERS
Chemistry Department
University of Manchester
U.K.
and
Daresbury Laboratory
Warrington
U.K.

C.M. GROENEVELD
G.W. CANTERS
Department of Chemistry
University of Leiden
The Netherlands
S.S. HASNAIN
Daresbury Laboratory
Warrington
U.K.

EXAFS STUDIES ON OXIDIZED AND REDUCED AZURIN AT HIGH AND LOW pH

X-ray fluorescence spectra [1] at the Cu K-edge were taken of the blue copper protein, azurin, from *Pseudomonas aeruginosa*, in reduced and oxidized state, and at high and low pH, to assess the effect of these conditions on the coordination sphere of the copper.

There is no change in either edge position or XANES (X-ray absorption near edge structure) when the pH is changed. However, there are changes in the XANES upon oxidation or reduction at both high and low pH. The edge position of the oxidized protein is at higher energy than that of the reduced protein. This is in agreement with what is expected because of the valence change of the copper.

The EXAFS (extended X-ray absorption fine structure) of oxidized protein is strongly reminiscent of that of lyophilized azurin [2]. There is almost no change when the pH is altered; the major shells can be fitted with the same set of parameters, involving 2 N atoms and 1 S atom, from His-46, His-117 and Cys-112, respectively, except for a small correction in E_0 .

There are pronounced changes upon reduction:

one of the imidazole nitrogens disappears while at the same time a second S atom, presumably from Met-121, shows up. There is a small pH effect on the position of the latter atom (of the order of 0.1 Å).

These results are compared with recent results from other spectroscopic investigations [3-5].

REFERENCES

- [1] S.S. HASNAIN, P.D. QUINN, G.P. DIAKUN, E.M. WARDELL, C.D. GARNER, *J. Phys. E.*, **17**, 40-43 (1984).
- [2] T.D. TULLIUS, P. FRANK, K.O. HODGSON, *Proc. Natl. Acad. Sci. U.S.A.*, **75**, 4069-4073 (1978).
- [3] E.T. ADMAN, G.W. CANTERS, H.A.O. HILL, N.A. KITCHEN, *FEBS Lett.*, **143**, 287-292 (1982).
- [4] G.W. CANTERS, H.A.O. HILL, N.A. KITCHEN, E.T. ADMAN, *J. Magn. Reson.*, **57**, 1-23 (1984).
- [5] G.W. CANTERS, H.A.O. HILL, N.A. KITCHEN, E.T. ADMAN, *Eur. J. Biochem.*, **138**, 141-152 (1984).



PS1.24 — MO

K.K. RAO
D.O. HALL
Department of Plant Sciences
King's College
London
U.K.
P. CUENDET
M. GRÄTZEL
Institute de Chimie Physique
EPFL, CH-1015, Lausanne
Switzerland

WATER PHOTOLYSIS USING SEMICONDUCTOR-BOUND HYDROGENASES

Aqueous suspensions of TiO_2 powders in the presence of a bacterial hydrogenase and an electron donor evolved hydrogen on irradiation with a sunlight simulator lamp, both in the presence and in the absence of added electron mediators. Hydrogenases from *Clostridium pasteurianum* and *Desulfovibrio desulfuricans*, strains Norway 4 and 9974 were used in these studies with EDTA or methyl alcohol as electron source. Electron relays tested were ferredoxin, cytochrome c_3 , methyl viologen and rhodium trisbipyridyl.

The rates and duration of photoproduction of hydrogen were dependent on the nature of the hydrogenase, nature of electron donor and the pH of the reaction medium. Hydrogen evolution at very high rates, lasting up to 24 h, was observed from a mixture of hydrogenase, TiO_2 -bound $\text{Rh}(\text{bipy})_3$ and methyl alcohol in carbonate buffer at pH 9; with *C. pasteurianum* hydrogenase initial rate of H_2 evolution per g TiO_2 was 1066 μmoles per hour and 15730 μmoles of H_2 were produced in 24 h.

Photohydrogen production from TiO_2 -hydrogenase mixtures was also observed in the absence of any added electron relays, the rates of hydrogen production being higher at pH 9 than at pH 7

and also better with methyl alcohol as electron donor compared to EDTA.

Data on relative rates of H_2 evolution from various combinations of hydrogenases and relays will be presented.



PS1.25 — TU

VÍCTOR M. FERNÁNDEZ
Instituto de Catálisis
Serrano 119, Madrid
Spain
CLAUDE HATCHIKIAN
Laboratoire de Chimie Bacterienne-CNRS
132-77 Marseille
France
DAULAT PATIL
RICHARD CAMMACK
King's College
68 Half Moon Lane
London SE24 9JF
U.K.

EPR SPECTRA OF THE NICKEL CENTRE AND IRON-SULPHUR CLUSTERS DURING ACTIVATION AND DEACTIVATION OF *DESULFOVIBRIO GIGAS* HYDROGENASE

Hydrogenases of certain *Desulfovibrio* species contain nickel, and display relatively low activity when first isolated. They can be activated up to ten-fold by prolonged treatment with hydrogen or with dithionite [1,2]. Some degree of activation can also be achieved by milder reductants like dithiothreitol plus a mediator dye such as indigotrisulphonate.

On treatment of *Desulfovibrio gigas* hydrogenase with strong reducing agents, the EPR signals of oxidized three-iron cluster and Ni(III) [3] immediately disappeared [4,5]. We have observed a new broad EPR signal, at temperatures below 15 K

(Fig. 2, left), which we interpret as due to interacting [4Fe-4S] clusters.

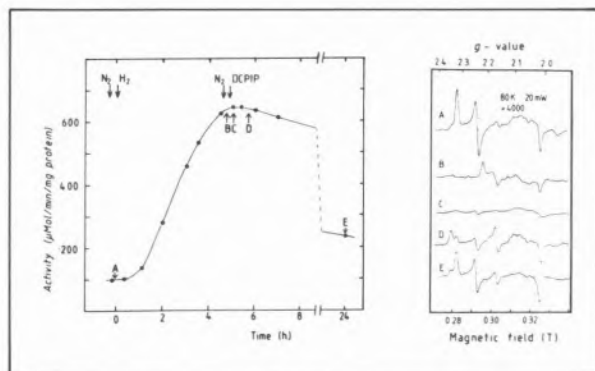


Fig. 1

Left: Changes in activity of *D. gigas* hydrogenase during incubation under hydrogen, at pH 8.5, then reoxidation with DCPIP. Activity was measured by hydrogen-dependent methyl viologen reduction.

Right: EPR spectra of samples removed from the incubation, recorded at 80 K

Longer incubation at low redox potentials produced a considerable increase of the activity (Fig. 1, left), and in parallel the development of another Ni signal (Fig. 1, B, right) as previously described by MOURA *et al.* [6]. We postulate that this signal represents the oxidation level Ni(I). This Ni(I) signal differed from the other nickel signals in that it showed extremely rapid electron-spin relaxation and became split at low temperatures (Fig. 2, right). The splitting was only observed under con-

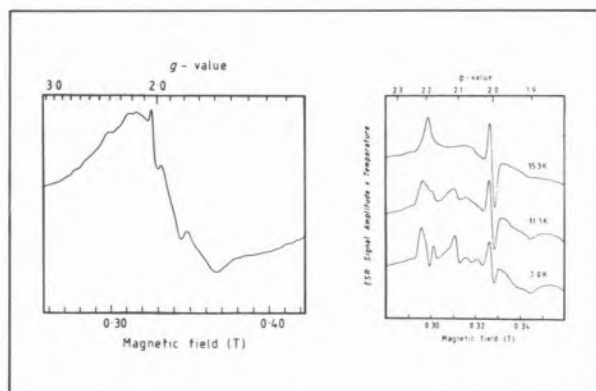


Fig. 2

Left: EPR spectrum of the broad signal of *D. gigas* hydrogenase after reduction with hydrogen for 5 minutes, recorded at 7 K.

Right: Spectra of the nickel signal produced after reduction with hydrogen for 4 hours, recorded at the temperatures indicated. At 80 K the spectrum was as Fig. 1, right

ditions where the broad signal was detected, and we interpret it as due to spin-spin interaction between Ni(I) and the reduced [4Fe-4S] clusters. The Ni(I) signal disappeared on prolonged reduction at very low redox potentials. One possible explanation for this effect is the production of a nickel hydride, Ni(II).H⁻ which would be undetectable by EPR. This species could well participate in the catalytic cycle of the enzyme. A third type of nickel EPR spectrum was obtained by oxidizing the activated *D. gigas* hydrogenase anaerobically with dichlorophenol-indophenol (DCPIP) (Fig. 1, D). The enzyme in this state, although inactive towards hydrogen, could be fully reactivated within seconds by reducing agents (with the reappearance of the Ni(I) signal). In some conditions this oxidized state was stable under air at room temperature for months. Therefore it seems that there are at least three oxidation states of the nickel in the active form, and two in the inactive form:

Enzyme before activation:

Ni(III) $g = 2.32, 2.23, 2.01$

Ni(II) No EPR signal

Activated enzyme:

Ni(III) $g = 2.34, 2.16, 2.01$

Ni(II) No EPR signal

Ni(I) $g = 2.19, 2.15, 2.01$

The results are consistent with a function for nickel in hydrogen activation in *D. gigas* hydrogenase. The interaction between Ni(I) and [4Fe-4S]⁺ could provide a way for internal electron transfer from hydrogen to the natural electron acceptor, cytochrome c₃ [7].

ACKNOWLEDGEMENTS

This work was supported by grants from the S.E.R.C. and Nuffield Foundation. V.M.F. and R.C. are the recipients of a British-Spanish Joint Action Fellowship.

REFERENCES

- [1] V.M. FERNÁNDEZ, R. AGUIRRE, E.C. HATCHIKIAN, *Biochim. Biophys. Acta*, **790**, 1-7 (1984).
- [2] T. LISSOLO, S. PULVIN, D. THOMAS, *J. Biol. Chem.*, **259**, 11725-11729 (1984).
- [3] J.J.G. MOURA, M. TEIXEIRA, I. MOURA, A. XAVIER, J. LEGALL, *J. Mol. Catal.*, **23**, 303-314 (1984).
- [4] R. CAMMACK, D. PATIL, R. AGUIRRE, E.C. HATCHIKIAN, *FEBS Lett.*, **142**, 289-292 (1982).

- [5] M. TEIXEIRA, I. MOURA, A.V. XAVIER, D.V. DERVARTANIAN, J. LEGALL, H.D. PECK JR., B.H. HUYNH, J.J.G. MOURA, *Eur. J. Biochem.*, **130**, 481-484 (1983).
- [6] J.J.G. MOURA, I. MOURA, B.H. HUYNH, H.J. KRÜGER, M. TEIXEIRA, R.C. DU VARNEY, D.V. DERVARTANIAN, A.V. XAVIER, H.D. PECK JR., J. LEGALL, *Biochem. Biophys. Res. Commun.*, **408**, 1338-1393 (1982).
- [7] J.M. ODOM, H.D. PECK JR., *Annu. Rev. Microbiol.*, **38**, 551-592 (1984).



PS1.26 — TH

MICHAEL K. JOHNSON
ISABEL C. ZAMBRANO
Department of Chemistry
Louisiana State University
Baton Rouge, LA 70803
U.S.A.

MELVIN H. CZECHOWSKI
HARRY D. PECK JR.
DANIEL V. DERVARTANIAN
JEAN LEGALL
Department of Biochemistry
University of Georgia
Athens, GA 30602
U.S.A.

LOW TEMPERATURE MAGNETIC CIRCULAR DICHROISM SPECTROSCOPY AS A PROBE FOR THE OPTICAL TRANSITIONS OF PARAMAGNETIC NICKEL IN HYDROGENASE

The electronic transitions localized on nickel in hydrogenase should provide a sensitive monitor of metal coordination number, geometry and ligand-type. However, they are obscured in the UV-visible spectra of hydrogenases by intense S-Fe charge transfer transitions originating from Fe-S clusters. Here we demonstrate that low temperature MCD spectroscopy is uniquely capable of identifying and monitoring the optical transitions arising from paramagnetic Ni in hydrogenase.

A partially purified sample of hydrogenase from *Methanobacterium thermoautotrophicum* Δ H strain has been investigated by room temperature UV-visible absorption, and low temperature

MCD and EPR spectroscopy. In agreement with previous studies [1], the as isolated hydrogenase exhibits a rhombic EPR signal ($g=2.300, 2.230,$ and 2.014) which is attributed to Ni(III). Quantitation at 70 K versus a CuEDTA standard affords a spin concentration of $120 \pm 10 \mu\text{M}$ for the Ni(III) signal in the sample used for MCD studies. No EPR signals attributable to oxidized, paramagnetic Fe-S clusters were observed over the temperature range 8-150 K.

Fig. 1 shows the room temperature UV-visible absorption and low temperature MCD spectra of *Methanobacterium thermoautotrophicum* hydrogenase in the range 300-800 nm. The broad, featureless absorption spectrum with a shoulder at approximately 400 nm is typical of that exhibited by Fe-S proteins. The MCD shows temperature dependent transitions in the regions 530-670 nm and 300-460 nm which must originate from a paramagnetic chromophore. MCD magnetization plots at 650, 600 and 363 nm (not shown) are all

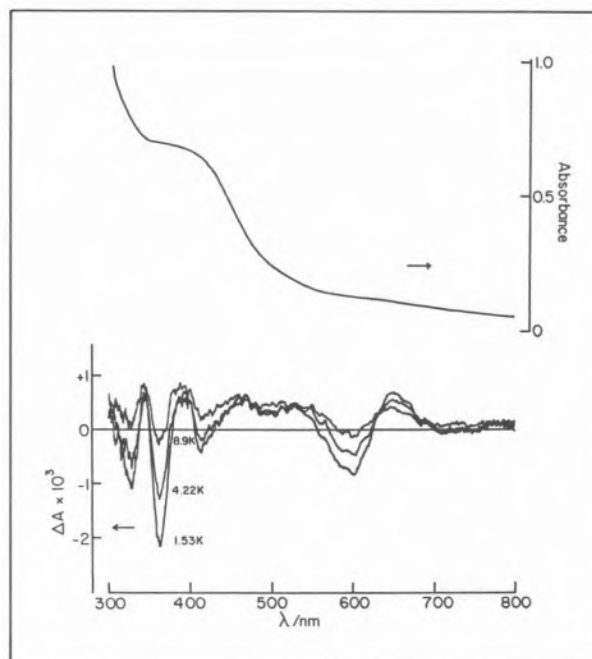


Fig. 1

Room temperature absorption and low temperature MCD spectra of *Methanobacterium thermoautotrophicum* hydrogenase as isolated. Upper panel: room temperature absorption, 1 mm pathlength. Lower panel: MCD spectra at 1.53, 4.22 and 8.9 K, magnetic field = 4.5 Tesla, pathlength = 1.67 mm. Ni(III) concentration = $120 \pm 10 \mu\text{M}$ (from EPR spin quantitation). Sample in 0.15 M Tris/HCl pH 7.5 buffer with 50% v/v ethylene glycol

consistent with the electronic transitions arising from an EPR-active $S=1/2$ ground state with g-values around 2 and are fitted well by theoretical magnetization curves based on the EPR-determined g-values for the Ni(III) center. Thus both the unique form of the MCD spectrum (compared to that of any Fe-S cluster thusfar investigated) and the magnetization properties identify the temperature dependent MCD transitions as originating from the Ni(III) center in hydrogenase. Recent studies in this laboratory indicate that an analogous Ni(III) MCD spectrum is observed in as isolated *Desulfovibrio gigas* hydrogenase albeit superimposed on the MCD signal from a paramagnetic, oxidized [3Fe-xS] center.

In light of the recent EXAFS results for Ni in hydrogenase [2,3], both S-Ni charge transfer and Ni d-d transitions would be expected in the UV-visible spectral region. Studies of appropriate model complexes are required for detailed assignment of the MCD transitions. Once this is accomplished low temperature MCD spectroscopy will become an invaluable technique for identifying changes in Ni coordination and redox state during catalytic turnover.

REFERENCES

- [1] J.J.G. MOURA, M. TEIXEIRA, I. MOURA, A.V. XAVIER, J. LEGALL, *J. Mol. Cat.*, **23**, 304-314 (1984).
- [2] P.A. LINDAHL, N. KOJIMA, R.P. HAUSINGER, J.A. FOX, B.K. TEO, C.T. WALSH, W.H. ORME-JOHNSON, *J. Am. Chem. Soc.*, **106**, 3062-3064 (1984).
- [3] R.A. SCOTT, S.A. WALLIN, M.H. CZECHOWSKI, D.V. DERVARTANIAN, J. LEGALL, H.D. PECK JR., I. MOURA, *J. Am. Chem. Soc.*, **106**, 6864-6865 (1984).



PS1.27 — TH

MICHAEL K. JOHNSON
JOYCE E. MORNINGSTAR
DEBORAH E. BENNETT

Department of Chemistry
Louisiana State University
Baton Rouge, LA 70803
U.S.A.

BRIAN A.C. ACKRELL
EDNA B. KEARNEY

Molecular Biology Division
Veterans Administration Medical Center
San Francisco, CA 94121

and
Department of Biochemistry and Biophysics
University of California
San Francisco, CA 94143
U.S.A.

SPECTROSCOPIC EVIDENCE FOR [2Fe-2S], [3Fe-xS], AND [4Fe-4S] CLUSTERS IN RECONSTITUTIVELY ACTIVE MAMMALIAN SUCCINATE DEHYDROGENASE

Succinate dehydrogenase (SDH) has been investigated by low temperature MCD and EPR as well as room temperature CD and UV-visible absorption spectroscopy. Both reconstitutively active (prepared as in ref. [1]) and reconstitutively inactive (prepared as in ref. [2] but in the absence of succinate) samples have been studied. The low temperature MCD measurements, including magnetization data at discrete wavelengths, provide the first definitive assessment of the nature of all the Fe-S clusters in this complex multicomponent enzyme. Reconstitutively active SDH is found to contain three Fe-S clusters: S1, S2, and S3. In agreement with previous studies, MCD and CD spectroscopy confirm S1 to be a [2Fe-2S]^{2+,1+} center that is reduced in the presence of succinate. The EPR and MCD characteristics of the reduced center are most similar to those of hydroxylase-type [2Fe-2S] centers.

Center S2 is identified by MCD as a [4Fe-4S]^{2+,1+} cluster which has a lower redox potential than S1

and is reducible with dithionite. This result is contrary to previous studies which have been interpreted in terms of center S2 being either a low potential [2Fe-2S] cluster [3] or non-existent [4]. EPR power saturation studies confirm that centers S1 and S2 are magnetically interacting in the dithionite-reduced enzyme. However, center S2 is not EPR silent but can be detected as weak shoulders to high and low field of the reduced S1 EPR spectrum at temperatures below 20 K in dithionite-reduced Complex II, as well as reconstitutively active and inactive SDH. This new signal is most clearly observed in dithionite-reduced Complex II and difference spectra under conditions where S1 is power saturated show the principal g-values to be 2.06, 1.95, and 1.85. These g-values are characteristic of [4Fe-4S]¹⁺ centers in bacterial ferredoxins.

S1 and S2 are present in both reconstitutively active and inactive SDH. The third cluster, S3, is only present in significant amounts in reconstitutively active enzyme. In both succinate and dithionite-reduced reconstitutively-active SDH both the form of the MCD spectrum and the magnetization data identify this cluster as a paramagnetic, EPR-silent reduced [3Fe-xS] center. This result confirms the recent linear electric field effect EPR measurements on the isotropic g=2.01 signal observed in oxidized Complex II [5], which indicated that this signal originates from an oxidized [3Fe-xS] center rather than a tetranuclear high potential Fe-S cluster, [4Fe-4S]³⁺. Moreover the MCD data suggest that center S3 is a necessary requirement for reconstitutive activity and indicate that bulk conversion of this center to a [4Fe-4S] cluster does not occur on addition of substrate.

Although the results do not completely rule out the possibility of partial [3Fe-xS] to [4Fe-4S] conversion on addition of substrate, it seems likely that the [3Fe-xS] center in SDH is able to sustain Q-reductase activity.

These results resolve many of the long standing controversies concerning the Fe-S cluster content of SDH and for the first time enable rationalization of all the published spectroscopic data in addition to the analytical and core extrusion studies [6].

REFERENCES

- [1] B.A.C. ACKRELL, E.B. KEARNEY, C.J. COLES, *J. Biol. Chem.*, **252**, 6963-6965 (1977).
- [2] K.A. DAVIS, Y. HATEFI, *Biochemistry*, **10**, 2509-2516 (1971).
- [3] T. OHNISHI, J.C. SALERNO, in T.G. SPIRO (ed.), «Iron-Sulfur Proteins», John Wiley and Sons, New York, 1982, pp. 285-327.
- [4] S.P.J. ALBRACHT, *Biochim. Biophys. Acta*, **612**, 11-28 (1980).
- [5] B.A.C. ACKRELL, E.B. KEARNEY, W.B. MIMS, J. PEISACH, H. BEINERT, *J. Biol. Chem.*, **259**, 4015-4018 (1984).
- [6] C.J. COLES, R.H. HOLM, D.M. KURTZ, W.H. ORME-JOHNSON, J. RAWLINGS, T.P. SINGER, G.B. WONG, *Proc. Natl. Acad. Sci. U.S.A.*, **76**, 3805-3808 (1979).



PS1.28 — TU

K. NAGAYAMA

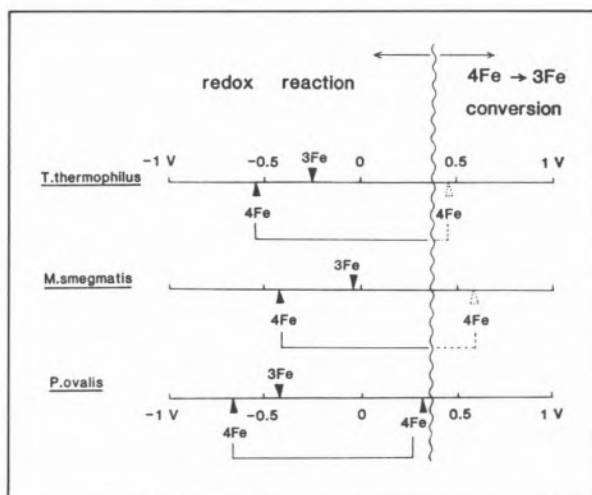
Biometrology Lab, JEOL Ltd.
Nakagami, Akishima, Tokyo 196
Japan

REDOX STATE STUDIES OF TWO IRON-SULFUR CENTERS IN 7Fe FERREDOXINS BY PROTON MAGNETIC RESONANCE

- 1) Two types of iron-sulfur clusters, [3Fe-XS] and [4Fe-4S], were identified by ¹H-NMR in the intact ferredoxins (Fd) extracted from *Thermus thermophilus*, *Mycobacterium smegmatis* and *Pseudomonas ovalis*. The [4Fe-4S] clusters always showed the redox couples which had potentials lower than that of the [3Fe-XS] clusters.
- 2) The oxidizability of a redox couple, [4Fe-4S], in a 7Fe ferredoxin extracted from *P. ovalis* was monitored by ¹H-NMR. The iron-sulfur cluster in the ferredoxin was not only reducible, but also oxidizable in its native form. This result provided the first verification of Carter's 3 redox theory for a redox center in ferredoxin, 4Fe, in the native form of the protein.

3) The redox couples in 7Fe ferredoxins treated with ferricyanide were monitored by $^1\text{H-NMR}$. An excess amount of ferricyanide was found to effect conversion of one of the two redox centers, the 4Fe core, to a 3Fe core in the ferredoxins extracted from *T. thermophilus*, *M. smegmatis* and *P. ovalis*. On long term incubation in air, the converted 3Fe core showed even further change in NMR spectra.

4) With above three results the complicated change observed during the reduction-reoxidation process in NMR spectra of *Thermus thermophilus* Fd was interpreted in the term of the redox reaction and 3Fe-4Fe interconversion.



Figure

Redox potentials of 3Fe and 4Fe redox centers and potential range of 4Fe to 3Fe interconversion

REFERENCES

- [1] K. NAGAYAMA, D. OHMORI, T. IMAI, T. OSHIMA, *FEBS Lett.*, **158**, 208-212 (1983).
- [2] K. NAGAYAMA, D. OHMORI, *FEBS Lett.*, **173**, 15-18 (1984).
- [3] K. NAGAYAMA, T. IMAI, D. OHMORI, T. OSHIMA, *FEBS Lett.*, **169**, 79-84 (1984).



PS1.29 — TH

E. BILL

A.X. TRAUTWEIN

H. WINKLER

Physik

Medizinische Hochschule

2400 Lübeck 1

W. Germany

F.-H. BERNHARDT

Physiologische Chemie

Rheinisch-Westfälische Technische Hochschule

5100 Aachen

W. Germany

NITROSYL-BINDING TO THE MONONUCLEAR NON-HEME IRON OF PUTIDAMONOXYIN: A MODEL FOR THE CORRESPONDING PEROXO COMPLEX

Putidamonooxin (PMO), the terminal oxygenase of a 4-methoxybenzoate monooxygenase enzyme system (EC 1.14.99.15), consists of three identical subunits, the active centers of which contain one [2Fe-2S] cluster and one mononuclear non-heme (cofactor) iron [1-6]. The activation of molecular oxygen by the reduced PMO is achieved by binding O_2 to the cofactor iron, and by successive transfer of two electrons to the O_2 -molecule, one from the reduced [2Fe-2S] cluster and one from the reduced non-heme iron, respectively. Because of the relatively fast kinetics of this process (≤ 10 ms) we were so far not able to follow the stepwise transfer of these electrons or to detect the "mononuclear non-heme iron peroxo complex" $[\text{FeO}_2]^+$ via ESR or Mössbauer spectroscopy. The corresponding nitrosyl-complex, however, is more stable and therefore accessible for ESR and Mössbauer measurements.

We have recorded Mössbauer spectra of the nitrosyl complex (using different substrates) in the temperature range 1.5 K to 200 K with varying applied magnetic fields H^{ext} . One of our results is that we did not observe any substrate dependence. Additionally, we find from the spin-Hamiltonian

analysis of our experimental spectra that the nitrosyl complex is characterized by a $S=3/2$ spin state. The actual spin-Hamiltonian parameters are almost the same as those reported for EDTA·Fe(II)·NO [7].

There are two alternative electronic configurations d^5 and d^7 , which would provide a $S=3/2$ spin state; they are represented by a variety of compounds which exhibit isomer shifts (relative to α -Fe at room temperature) in the range of about 0.2 mms^{-1} - 0.6 mms^{-1} for d^5 and 1.7 mms^{-1} - 2.00 mms^{-1} for d^7 [8]. Since our measured 4.2 K value is 0.68 mms^{-1} we conclude that the situation in the ternary "enzyme·substrate·NO" complex is most likely reflected by the ferric $S=3/2$ spin state for the mononuclear non-heme iron. This conclusion is in agreement with titration-results: titration of the NO complex with ferricyanide under anaerobic conditions does not change the typical ESR spectrum of this complex, indicating that the cofactor iron cannot be further oxidized and therefore is in the ferric state [9].

In summary we conclude that our data obtained from the ternary "enzyme·substrate·NO" complex indicate that the cofactor iron (i) is in the ferric intermediate spin state ($S=3/2$) and (ii) is penta-coordinated, which means that upon NO binding to the reduced cofactor iron at least one ligand has to be released, because in the binary "enzyme·substrate" complex (reduced and oxidized) the cofactor iron has a coordination number also higher than four [4,10]. Comparing our data with literature values suggests that the cofactor iron in the binary as well as in the ternary NO complex is not directly bound to a sulfur atom, though biochemical arguments seem to indicate the opposite. The detailed results of this Mössbauer investigation together with an ESR study of the cofactor iron of PMO will be published elsewhere [9,10].

ACKNOWLEDGEMENTS

This work was supported by Deutsche Forschungsgemeinschaft.

REFERENCES

- [1] F.-H. BERNHARDT, E. HEYMANN, P.S. TRAYLOR, *Eur. J. Biochem.*, **92**, 209 (1978).

- [2] W. ADRIAN, F.-H. BERNHARDT, E. BILL, K. GERSONDE, E. HEYMANN, A.X. TRAUTWEIN, H. TWILFER, *Hoppe-Seyler's Z. Physiol. Chem.*, **361**, 211 (1980).
 [3] F.-H. BERNHARDT, H.M. MEISCH, *Biochem. Biophys. Res. Commun.*, **93**, 1247 (1980).
 [4] E. BILL, F.-H. BERNHARDT, A.X. TRAUTWEIN, *Eur. J. Biochem.*, **121**, 39 (1981).
 [5] F.-H. BERNHARDT, H. KUTHAN, *Eur. J. Biochem.*, **120**, 547 (1981).
 [6] H. TWILFER, F.-H. BERNHARDT, K. GERSONDE, *Eur. J. Biochem.*, **119**, 595 (1981).
 [7] D.M. ARCIERO, J.D. LIPSCOMB, B.H. HUYNH, T.A. KENT, E. MÜNCK, *J. Biol. Chem.*, **258**, 14981 (1983).
 [8] N.N. GREENWOOD, T.C. GIBB, «Mössbauer Spectroscopy», Chapman and Hall, London, 1971.
 [9] H. TWILFER, F.-H. BERNHARDT, K. GERSONDE, *Eur. J. Biochem.*, **147**, 171 (1985).
 [10] E. BILL, F.-H. BERNHARDT, A.X. TRAUTWEIN, H. WINKLER, *Eur. J. Biochem.*, **147**, 177 (1985).



PS1.30 — TH

A.X. TRAUTWEIN

E. BILL

R. BLÄS

S. LAUER

H. WINKLER

Physik

Medizinische Hochschule

2400 Lübeck 1

W. Germany

A. KOSTIKAS

Nuclear Research Center «Demokritos»

Aghia Paraskevi

Greece

EXPERIMENTAL AND THEORETICAL ELECTRONIC STRUCTURE STUDIES OF IRON SULFUR AND IRON MOLYBDENUM SULFUR COMPOUNDS VIA MÖSSBAUER SPECTROSCOPY AND MOLECULAR ORBITAL THEORY

The electronic structures of mononuclear Fe-S complexes with a Fe^{11}S_4 core and of binuclear Fe-Mo-S complexes containing the $\text{Fe}_2\text{S}_2\text{Mo}$ core have been derived from a semiempirical molecular

orbital method (Iterative Extended Hückel Theory), followed by a spin-orbit coupling calculation on the five highest occupied iron-like molecular orbitals. Fine structure and hyperfine structure tensors and parameters (g , D , E , A , and electric field gradient) have been calculated and compared with data from spin-Hamiltonian analysis of Mössbauer measurements.

For the mononuclear complex anions $[\text{Fe}(\text{SPh})_4]^{2-}$ and $[\text{Fe}(\text{dts})_2]^{2-}$ it was found from our molecular orbital (MO) calculations that the main component of the electric field gradient (efg) tensor, V_{22} , is negative, D positive, and that the magnetic anisotropy places the preferred direction of the hyperfine magnetic field perpendicular to the V_{22} direction, in agreement with spin-Hamiltonian results. The similarity of parameters of $[\text{Fe}(\text{SPh})_4]^{2-}$ and reduced rubredoxin (Rd_{red}) confirms the suggestion that this anion has a ground electronic state practically identical to Rd_{red} . The complex anion $[\text{Fe}(\text{dts})_2]^{2-}$ shows smaller anisotropy, and due to the fact that the orbital groundstate is energetically not well separated from higher states in this case a strong temperature dependence of the quadrupole splitting is observed (Fig. 1).

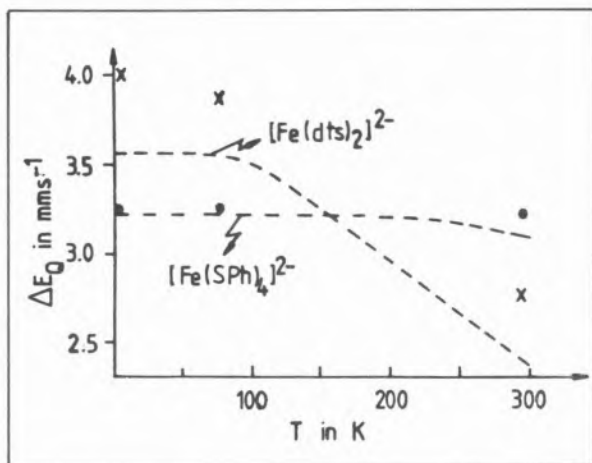


Fig. 1

ΔE_Q^{exp} of $[\text{Fe}(\text{SPh})_4]^{2-}$ (•) and $[\text{Fe}(\text{dts})_2]^{2-}$ (×). The dashed curves correspond to MO spin-orbit coupling calculations

For the binuclear complex anions $[(\text{SPh})_2\text{FeS}_2\text{MoS}_2]^{2-}$, $[\text{S}_5\text{FeS}_2\text{MoS}_2]^{2-}$ and $[\text{Cl}_2\text{FeS}_2\text{MoS}_2]^{2-}$ it was found from our MO calculations and the spin-Hamiltonian analysis that D is negative and V_{22} is positive. A specific feature of our MO results derived for these binuclear

Fe-Mo-S complexes is that V_{22} is directed perpendicular to the Fe-Mo line, and the preferred direction of the magnetic hyperfine field is close to the V_{22} axis. The correlation of calculated values of electron densities at the iron nuclei, $\rho(\text{O})$, and isomer shifts δ for mononuclear and binuclear compounds confirms the role of MoS_4^{2-} as a charge withdrawing ligand (Fig. 2).

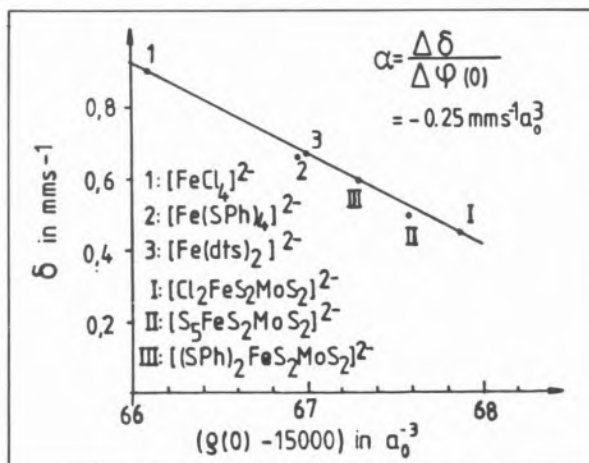


Fig. 2

Correlation between δ^{exp} (at 4.2 K, rel. to $\alpha\text{-Fe}$ at 300 K) and ρ^{calc} (°) for iron-sulfur compounds and for $[\text{FeCl}_4]^{2-}$

In order to probe our MO results derived for the binuclear Fe-Mo-S complexes, *i.e.* V_{22} being directed perpendicular to the Fe-Mo-line, we have investigated a single crystal of $[(\text{C}_6\text{H}_5)_4\text{P}][(\text{C}_6\text{H}_5\text{CH}_2)-(\text{CH}_3)_3\text{N}][\text{Cl}_2\text{FeS}_2\text{MoS}_2]$ by Mössbauer spectroscopy with various orientations of the crystal with respect to the γ -beam. From this investigation we derive that V_{22} is positive and oriented indeed perpendicular to the Fe-Mo direction. This result was confirmed by additional single crystal measurements applying an external magnetic field, and by magnetically perturbed spectra of polycrystalline samples. A full presentation of our theoretical and experimental results will be given elsewhere [1,2].

ACKNOWLEDGEMENTS

This work was supported by Stiftung Volkswagenwerk.

REFERENCES

- [1] A.X. TRAUTWEIN, E. BILL, R. BLÁS, S. LAUER, H. WINKLER, A. KOSTIKAS, *J. Chem. Phys.*, in press.
- [2] H. WINKLER, E. BILL, S. LAUER, U. LAUER, A.X. TRAUTWEIN, A. KOSTIKAS, V. PAPAETHYMIU, H. BÖGGE, A. MÜLLER, E. GERDAU, U. GONSER, *J. Chem. Phys.*, in press.



PS1.31 — TU

JACQUES GAILLARD
 PIERRETTE AURIC
 DRF-G-Service de Physique
 Centre d'Études Nucléaires de Grenoble
 85X - 38041 Grenoble Cedex
 France

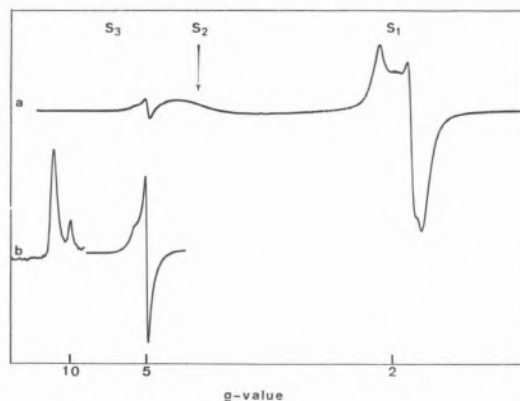
JEAN-MARC MOULIS
 JACQUES MEYER
 DRF-G-Laboratoire de Biochimie
 Centre d'Études Nucléaires de Grenoble
 85X - 38041 Grenoble Cedex
 France

EVIDENCE FOR HIGH MULTIPLICITY SPIN STATES IN THE 2 [4Fe-4Se]⁺ FERREDOXIN FROM CLOSTRIDIUM PASTEURIANUM

The electronic and magnetic properties of the reduced 2[4Fe-4Se]⁺ Se-substituted ferredoxin (Fd) from *Clostridium pasteurianum* have been investigated by EPR and Mössbauer spectroscopy. The occurrence of three spin states, $S_1 = 1/2$, $S_2 = 3/2$, $S_3 = 7/2$, has been inferred from the experimental data (figure).

The signal corresponding to S_1 ($g_{1,2,3} = 2.103, 1.940, 1.888$) is reminiscent of the EPR signal of reduced native Fd and accounts for 0.7 to 0.8 spin/molecule.

A broad signal ($g_{1,2,3} \cong 4.5, 3.5, 2$) is assigned to the ground doublet of $S_2 = 3/2$ and has an intensity, at 6 K, which is nearly equal to that of S_1 . The $S_3 = 7/2$ state gives rise to an isotropic signal at $g = 5.17$ and two weak peaks at $g = 10.11$ and $g = 12.76$. These signals are originating from excited levels, the ground doublet of which is EPR silent. This ground doublet is observable in Mössbauer spectra as a magnetic component accounting for 20% of the total iron, and involving two antiferromagnetically coupled subsites in approximately a 3:1 ratio which display fully developed paramagnetic hyperfine interactions at 4.2 K. The corresponding iron sites experience hyperfine



Figure

EPR spectra of reduced Se-substituted Cp Fd: a) 6 K; b) 15 K (low field part of a). EPR conditions: microwave power: a) 50 μ W, b) 2 mW; modulation amplitude 0.8 mT; field modulation: 100 kHz; frequency: 9.25 GHz. In b), the amplifier gain was increased by a factor 100 for recording the two low field peaks

fields of about -26 T and 20 T. The crystal field parameters of S_3 have been calculated: $\lambda = E/D = 0.12$ and $D/k = -3 \text{ K} \pm 1$.

EPR signals corresponding to the S_2 and S_3 states have also been observed in spectra of reduced Se-substituted ferredoxins from *C. acidurici* and *C. thermosaccharolyticum* but not in the spectrum of reduced Se-substituted *B. stearothermophilus* Fd, which displays only the signal of the S_1 state. The latter Fd is larger (81 amino-acids) than clostridial ferredoxins (55 amino-acids) and accommodates only one [4Fe-4X] (X=S, Se) cluster. Thus the $S = 3/2$ and $S = 7/2$ spin states arise from specific interactions between the clostridial type ferredoxins and their [4Fe-4Se]⁺ active sites.

REFERENCE

J.M. MOULIS, P. AURIC, J. GAILLARD, J. MEYER, *J. Biol. Chem.*, **259**, 11396 (1984).



PS1.32 — MO

J. LAMPREIA

I. MOURA

A. XAVIER

J.J.G. MOURA

Centro de Química Estrutural

Complexo I, UNL

Av. Rovisco Pais, 1000 Lisboa

Portugal

H.D. PECK JR.

J. LeGALL

Department of Biochemistry

University of Georgia

Athens, GA 30602

U. S. A.

EPR STUDIES ON ADENYLYL SULFATE (APS) REDUCTASE — A FLAVIN, IRON-SULFUR CONTAINING PROTEIN

Sulfate reducing bacteria (SRB) utilize sulfate as terminal electron acceptor (anaerobic "respiration") with concomitant accumulation of sulfite. This metabolic process, known as dissimilatory sulfate reduction is carried out by a complex enzymatic system as indicated schematically in Fig. 1 [1]. Adenylyl sulfate (APS) reductase is a key enzyme in the overall process, carrying out the reduction of APS the activated form of sulfate, to sulfite with the release of AMP [2].

ORGANISMS

APS reductases were purified to homogeneity from the following sulfate reducing bacteria: *Desulfovibrio gigas* (NCIB 9332), *D. desulfuricans* (ATCC 27774), *D. desulfuricans* (strain Berre eau), *D. baculatus* (strain 9974) and *D. vulgaris* (strain Hildenborough).

ACTIVE SITE COMPOSITION

The enzyme (molecular mass 440 KD, dimer) contains 12-16 gatom of iron (arranged in [Fe-S] clusters) and 1 FAD per monomeric unit. The chemical analysis (as well as the spectroscopic data, see

SULFATE REDUCTION DISSIMILATORY PROCESS

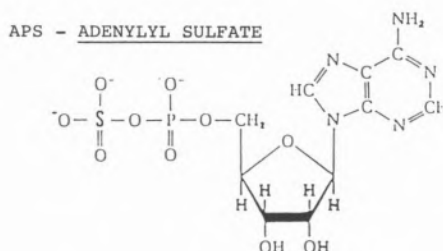
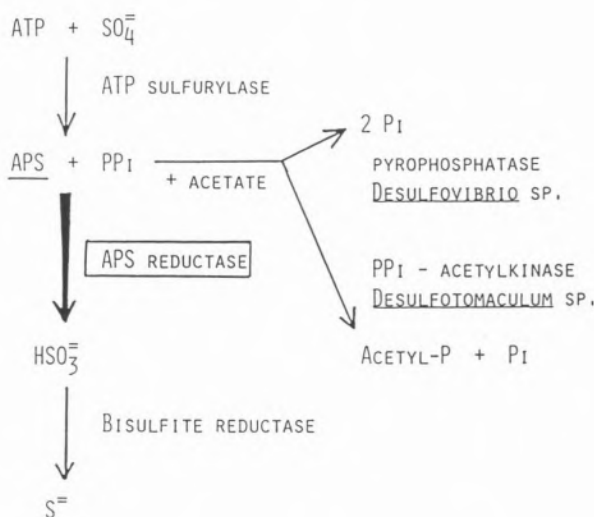


Fig. 1

Schematic representation of dissimilatory sulfate reduction pathway. Relevant enzymes

below) are quite similar, despite the microbial origin of the enzyme.

EPR SPECTROSCOPIC DATA — CHARACTERIZATION OF THE IRON-SULFUR CLUSTERS

Low temperature EPR studies were undertaken in order to characterize the redox centers present. In the native state all the samples examined so far show an almost isotropic EPR signal, centered around $g=2.02$, only detectable below 25 K — Center I (Fig. 2-A). This signal shows measurable line broadening when the enzyme is isolated from ⁵⁷Fe grown cells (the experiments were conducted with ⁵⁷Fe *D. gigas* enzyme). The signal is compatible with the presence of a paramagnetic iron-sulfur cluster (see also below). The integration of this EPR signal varies slightly from preparation to preparation of the enzyme and also with its bacterial origin, but accounts always to less than one

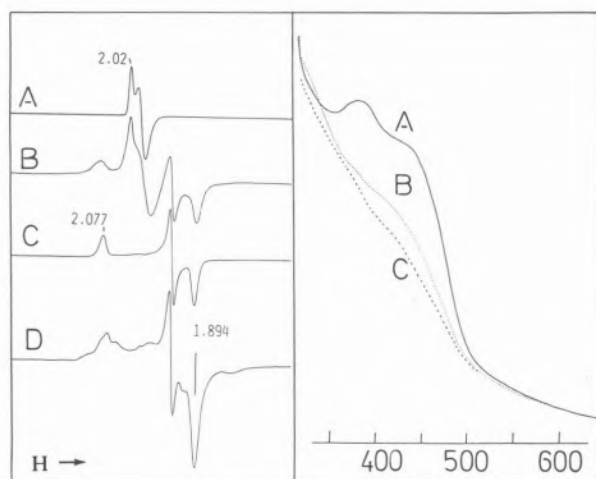


Fig. 2

Left part — EPR spectra of APS reductase from *D. desulfuricans* (strain 9974).

A — Native form; B — SO_3^{2-} + AMP; C — Dithionite reduced (20 sec.); D — Dithionite reduced (30 min.)

Spectrum B is represented with twice the gain of spectra A and C. Spectrum D is represented with 1.25 of the gain of spectra A and C. Temperature 8 K; modulation amplitude 1 mT; power 2 mW.

Right part — Visible spectra of APS reductase from *D. desulfuricans* (strain 9974).

A — Native protein; B — Enzyme reacted with SO_3^{2-} ; C — Enzyme reacted with SO_3^{2-} + AMP

spin per monomeric unit (0.1-0.25 spin). The catalytic events occurring in the presence of natural interacting substrates (sulfite and AMP) as well as chemical reductants (ascorbate, dithionite and H_2 reduced methylviologen) can be followed by EPR in conjunction with visible spectroscopy. Different redox states of the enzyme can be attained using different reduction times.

Center II, EPR g -values 2.077, 1.935 and 1.894, integrates to approx. 0.7-0.9 spins per monomeric unit and is only observable below 25 K. These EPR features are trapped after a short dithionite reduction time (Fig. 2-C) or in the presence of H_2 reduced methylviologen. Sulfite plus AMP only reduce partially Center II and affect drastically the isotropic EPR signal (Fig. 2-B). Sulfite bleaches the flavin chromophore contribution (Fig. 3-A/B) but do not affect appreciably iron-sulfur centers. A complex EPR spectrum develops after a long reduction time, which accounts for at least three iron-sulfur clusters (Fig. 2-D). Center I and II seem to be catalytically involved with the substrate ($\text{AMP} + \text{SO}_3^{2-}$) as seen by EPR and visible

spectroscopies. EPR redox titrations, in the presence of dye mediators, indicate that Center II has a relatively high midpoint redox potential (~ -50 mV). Preliminary Mössbauer spectroscopic studies on *D. gigas* ^{57}Fe APS reductase (in collaboration with B.H. Huynh, Emory University, Atlanta USA) indicate that the spectrum of the native enzyme is essentially dominated by diamagnetic quadrupole doublets typical of $[\text{Fe}_4\text{S}_4]$ clusters in the +2 oxidation state. The paramagnetic species detected by EPR ($g=2.02$) may be in the limiting range for Mössbauer detection, due to its spin concentration. The presence of an extra metal center has been ruled out by a careful screening of the metal content of the enzyme. Further studies are in progress in order to fully characterize the APS reductase iron-sulfur centers.

ACKNOWLEDGEMENTS

Work supported by INIC, JNICT and USAID.

REFERENCES

- [1] H.D. PECK JR., J. LEGALL, *Philos. Trans. R. Soc. London, Ser. B*, **298**, 443-466 (1982).
- [2] R.N. BRAMLETT, H.D. PECK JR., *J. Biol. Chem.*, **250**, 2979-2986 (1975).



PS1.33 — TH

PAUL A. LINDAHL
WILLIAM H. ORME-JOHNSON
Chemistry Department
Massachusetts Institute of Technology
Cambridge, Massachusetts 02139
U.S.A.

THOMAS A. KENT
EDMUND P. DAY
ECKARD MÜNCK
Gray Freshwater Biological Institute
University of Minnesota
Navarre, Minnesota 55392
U.S.A.

A [4Fe-4S] CLUSTER WITH SPIN $S = 3/2$: STUDIES OF THE NITROGENASE Fe-PROTEIN FROM *A. VINELANDII* IN THE PRESENCE OF 0.4 M UREA

The Fe protein of nitrogenase contains a [4Fe-4S] cluster which exhibits an EPR signal with g -values at 1.88, 1.94 and 2.05 in the reduced state. Several groups (see ref. [1]) have quantitated this "g = 1.94" signal and have consistently obtained a spin concentration of approximately 0.3 spins/4Fe, substantially less than the 1 spin/4Fe expected. ZUMFT *et al.* [2] noted that the $g = 1.94$ signal declines sharply when the sample contains 0.5 M urea. We noticed that their spectra exhibit feeble resonances between $g = 6$ and $g = 4$, the intensity of which seemed to be inversely related to that of the $g = 1.94$ feature. HAAKER *et al.* [3] reported that the addition of ethylene glycol to the *A. vinelandii* Fe-protein (denoted Av2) increases the $g = 1.94$ signal intensity. Using EPR, Mössbauer spectroscopy and magnetic susceptibility, we have investigated the solvent dependence of the electronic states of Av2. The details of these studies are reported elsewhere [4]. Here we focus on Mössbauer and EPR studies of reduced Av2 in 0.4 M urea (Av2/urea) and give evidence for the presence of a [4Fe-4S]¹⁺ cluster with a novel $S = 3/2$ ground state.

RESULTS

Sample preparations and experimental methods are described elsewhere [4]. Fig. 1 shows EPR spectra of dithionite-reduced Av2 in Tris HCl buffer (A) or 0.4 M urea (B). Both spectra display a $g = 1.94$ signal. This signal for the Tris HCl sample (Av2/Tris HCl) accounts for 0.35 spins/4Fe

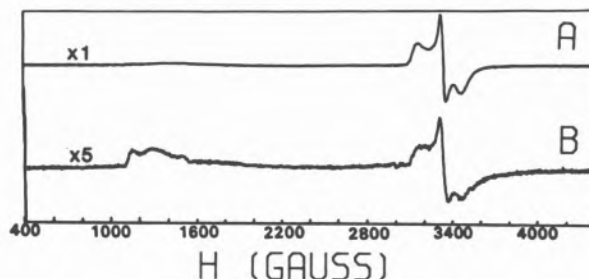


Fig. 1

X-band EPR spectra of reduced Av2/Tris HCl (Fig. 1A) and reduced Av2/urea. The spectra were recorded at 9 K; microwave power, 0.2 mW

and that of the urea sample for 0.1 spins/4Fe. Fig. 2 shows an expanded scan of the $g = 5$ region. Both samples exhibit resonances in that region but those of the urea sample are more intense and sharper. For Av2/urea the intensity at $g = 5.8$ increases relative to that at $g = 5.1$ as the temperature is lowered from 20 K to 5 K. This suggests that these two resonances arise from different doublets within an $S \geq 3/2$ multiplet, with the

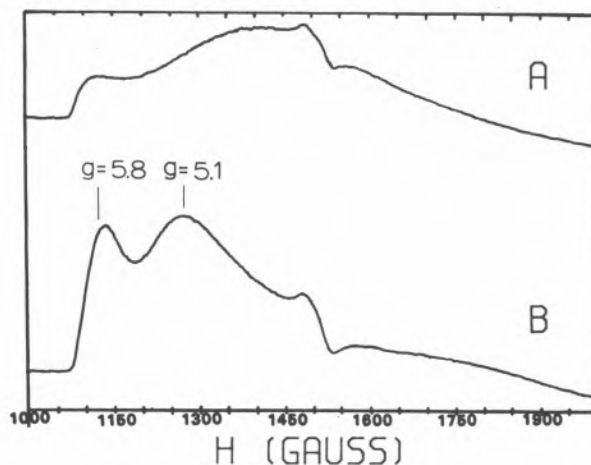


Fig. 2

Low-field features of EPR spectra of reduced Av2/Tris HCl (A) and reduced Av2/urea (B). Spectra recorded at 9 K; microwave power, 5 mW

$g=5.8$ doublet being lower in energy. We describe the multiplet with the spin Hamiltonian

$$H = D[S_z^2 - S(S+1)/3] + \frac{E}{D}(S_x^2 - S_y^2) + 2\beta\vec{H}\cdot\vec{S} \quad (1)$$

For $S=3/2$, $D = -2 \text{ cm}^{-1}$, $E/D=0.22$ and $\beta H \ll |D|$, EPR resonances would occur at $g=1.4, 1.1, 5.7$ for the ground doublet and at $g=2.6, 5.1, 1.7$ for the excited state [5]. (This is the only obvious choice for S which explains the data.) According to a method developed by AASA and VANNGARD [6], the intrinsic intensity of the absorption type peak at $g=5.8$ is 20 times less than that at $g=2.05$. Hence, the roughly equal areas of the resonances at $g=5.8$ and $g=2.05$ in Fig. 1B indicate that the concentration of the $S=3/2$ center is large compared with that of the $g=1.94$ species.

The Mössbauer spectra of Fig. 3 show that the majority of the iron in Av2/urea belongs to an unusual [4Fe-4S] cluster. They also provide strong evidence that this cluster is the EPR-active $S=3/2$ center. Fig. 3A shows spectra of Av2 in 50% ethylene glycol (Av2/ethylene glycol). These spectra are typical of those observed for all previously studied [4Fe-4S] $^{1+}$ clusters which have $S=1/2$, and which yield the $g=1.94$ signal. Such spectra can be fitted by assuming two pairs of iron sites; one pair with negative internal fields, H_{int} , and one with positive internal fields. A positive H_{int} signifies that the magnetic splittings of the Mössbauer spectrum increase as the applied field H is increased. The outermost lines in Fig. 3A do move outward with increasing H .

Fig. 3B shows a 6.0 T spectrum of Av2/urea. The spectrum of Fig. 3A, scaled to 15% of the total absorption, is plotted over the data. There is no evidence for adventitiously bound Fe^{2+} or Fe^{3+} which would be expected if any cluster conversions or decompositions with iron release had occurred upon addition of urea. Approximately 80% of the iron belongs to the rather featureless paramagnetic component between -1 mm/s and $+2 \text{ mm/s}$.

Fig. 3C shows 0.06 T and 6.0 T difference spectra of Av2/urea sample obtained by subtracting from the raw data 15% of the corresponding spectra of Av2/ethylene glycol (and 5% of oxidized Av2). The striking feature of Fig. 3C is that no spectral

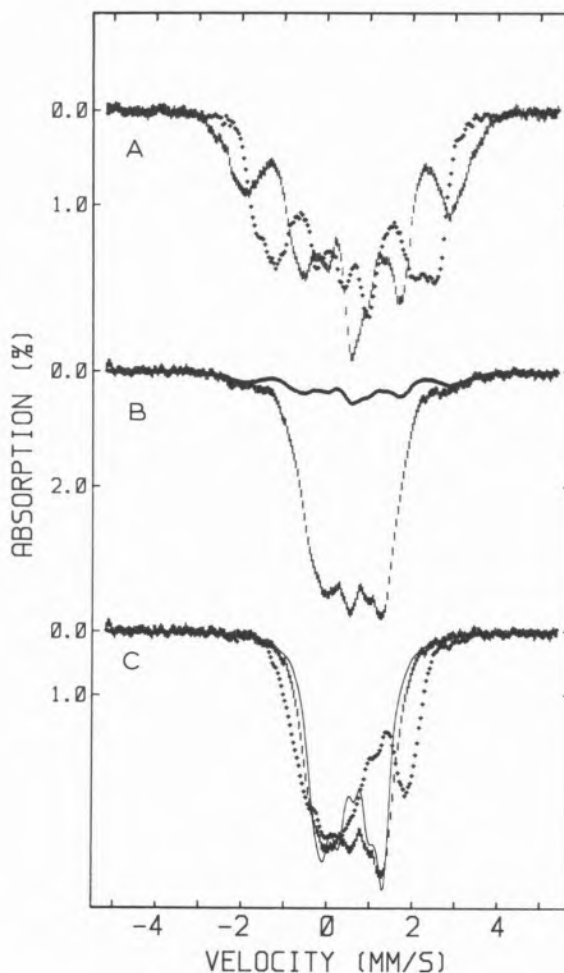


Fig. 3

4.2 K Mössbauer spectra of reduced Av2 in 50% ethylene glycol (A) and 0.4 M urea (B). The spectra in (A) were recorded in applied field of 0.06 T (full circles) and 6.0 T (hash marks). The spectrum in (B) was recorded in a 6.0 T field (hash marks). Indicated is also a 15% contribution of a species as observed in (A). In (C) the 6.0 T spectrum (hash marks) of (B) is compared with data recorded in a 0.06 T field (full circles). The solid line in (B) is a theoretical spectrum based on Eq. (1) with $S=3/2$, $D = -2 \text{ cm}^{-1}$, $E/D=0.22$, $H=6.0 \text{ T}$, assuming two sites with magnetic hyperfine coupling constants $A_1 = -4 \text{ MHz}$ and $A_2 = -8 \text{ MHz}$. Further details and computer analyses of all spectra displayed here are given in [4]

component of the 6.0 T data has a splitting larger than that of the 0.06 T data. That is, all the irons have negative (or unusually small) internal fields. Clearly, this cluster has an electronic structure very distinct from those of the clusters with the familiar $S=1/2$ ground state. However, the Av2/urea spectra clearly exhibit magnetic hyperfine structure in zero applied field and, therefore,

must belong to a Kramers system. The only EPR-active Kramers system in this sample, other than the $g=1.94$ species, is the $S=3/2$ system with $g=5.1$ and $g=5.8$.

DISCUSSION

Our data establish a $S=3/2$ ground state for the [4Fe-4S] cluster of Av2/urea. The EPR resonances at $g=5.8$ and 5.1 and the unique Mössbauer spectra (with all components having negative internal fields) characterize this unusual state. The observed quadrupole splittings and isomer shifts (spectra not shown here) are similar to those of the more familiar $S=1/2$ clusters, suggesting that the new state primarily arises from changes in the exchange interactions among the irons and not from a significant rearrangement of charge.

As indicated by the EPR data of Figs. 1 and 2, Av2/Tris HCl contains a mixture of $S=1/2$ and $S=3/2$ clusters. Saturation magnetization data (not shown) are dominated by the spin $S=3/2$ cluster and rule out significant concentrations of any higher spin. Combined saturation magnetization, Mössbauer and EPR data show that the mixture of $S=1/2$ and $S=3/2$ clusters is roughly half and half. This observation explains the low concentration of the $g=1.94$ EPR center ($S=1/2$) that had perplexed many investigators, including us, for a long time.

The observation of negative internal fields of all Mössbauer spectral components of Av2/urea places a severe restriction on any theoretical model of the Av2/urea electronic structure. For all iron sulfur clusters studied thus far the iron sites are intrinsically high-spin. H_{int} of an isolated high-spin iron is dominated by the negative contribution of the Fermi contact term. In an exchange-coupled Fe-S cluster, the sign of H_{int} at a particular iron nucleus is opposite to the sign of the projection of the local spin of that iron onto the system spin (see for instance, ref. [7]). In Av2/urea all local spins must have positive projections onto the $S=3/2$ system spin. Therefore, a successful theoretical model must yield local spin expectation values that are parallel, not antiparallel, to the system spin.

ACKNOWLEDGEMENTS

This work was supported by grants from NSF # PCM 8204764 (W.H. Orme-Johnson) NSF # PCM 8442497 (E. Münck) and USDA # 83-CRCR1-1284 (E.P. Day).

REFERENCES

- [1] B.K. BURGESS, in C. VEEGER, W.E. NEWTON (eds.), «Advances in Nitrogen Fixation Research», Nijhoff/Junk, The Hague, 1984.
- [2] W.G. ZUMFT, G. PALMER, L.E. MORTENSON, *Biochim. Biophys. Acta*, **292**, 413-421 (1973).
- [3] H. HAAKER, A. BRAAKSMA, J. CORDEWENER, J. KLUGKIST, H. WASSINI, H. GREUDE, R.R. EADY, C. VEEGER, in C. VEEGER, W.E. NEWTON (eds.), «Advances in Nitrogen Fixation Research», Nijhoff/Junk Publishers, The Hague, 1984.
- [4] P.A. LINDAHL, E.P. DAY, T.A. KENT, W.H. ORME-JOHNSON, E. MÜNCK, *J. Biol. Chem.*, submitted for publication.
- [5] B.H. HUYNH, T.A. KENT, in B.V. THOSAR, P.K. IYENGAR (eds.), «Advances in Mössbauer Spectroscopy», Elsevier, 1983, p. 500.
- [6] R. AASA, T. VANNGARD, *J. Magn. Reson.*, **19**, 308-315 (1975).
- [7] M.C. KENNEDY, T.A. KENT, M. EMPTAGE, H. MERKLE, H. BEINERT, E. MÜNCK, *J. Biol. Chem.*, **259**, 14463-14471 (1984).



PS1.34 — TU

M. TEIXEIRA
 I. MOURA
 A.V. XAVIER
 J.J.G. MOURA
 Centro de Química Estrutural
 Complexo I, U.N.L.
 Av. Rovisco Pais, 1000 Lisboa
 Portugal
 G. FAUQUE
 B. PICKRIL
 J. LEGALL
 A.R.B.S., E.C.E.
 CEN Cadarache
 13115 Saint Paul lez Durance
 France

NICKEL-IRON-SULFUR-SELENIUM CONTAINING HYDROGENASES ISOLATED FROM *DESULFOVIBRIO BACULATUS* STRAIN 9974

Hydrogenases from the periplasmic, cytoplasmic and membrane fractions of *Desulfovibrio baculatus* strain 9974 (DSM 1743) have been purified to apparent electrophoretic homogeneity.

PHYSICO-CHEMICAL DATA

Table I indicates the results of metal analysis as well as other physico-chemical data, namely the specific activity of the enzyme in respect to hydrogen evolution ($\mu\text{moles H}_2/\text{min.mg.}$). Plasma emission metal analysis detects the presence of iron, and of nickel and selenium in equimolecular amounts. The U.V. and visible spectra show broad bands around 277 and 390-400 nm, typical of iron-sulfur containing proteins.

EPR DATA

The EPR spectra of the native ("as isolated") enzymes are shown in Fig. 1 A-C. All the enzymes show a weak isotropic EPR signal centered around $g=2.02$ observable at low temperatures (below 20 K) that accounts for about 0.002 to 0.03 spins per molecule. The periplasmic and membrane bound enzymes also show additional

Table I
 Physico-chemical data on *D. baculatus* (9974) hydrogenases

	Cytoplasmic	Periplasmic	Membrane bound
Specific Activity ($\mu\text{moles H}_2$ evolved/min.mg.)	466	527	120
Molecular weight (kDa)	100 ^{a)} 81(54, 27) ^{b)c)}	110 ^{a)} 75(49, 26) ^{b)c)}	100 ^{a)} 89(62, 27) ^{b)c)}
Metal content			
Fe	7.7 (14.1) ^{d)}	9.25(13.5)	10.3(11.4)
Ni	0.54(1.0)	0.69(1.0)	0.90(1.0)
Se	0.56(1.03)	0.66(0.96)	0.86(0.95)
Ratio $A_{390/280}$	0.28	0.25	0.10

- a) Molecular mass determined by high pressure liquid chromatography.
 b) Molecular mass determined in the presence of SDS.
 c) Molecular mass of subunits are indicated between brackets.
 d) Values in () were converted per 1 nickel per minimal molecular weight.

EPR signals with g -values greater than 2.0 assigned to nickel(III), which are detectable up to 77 K. The periplasmic hydrogenase shows EPR features at 2.20, 2.06 and ~ 2.00 (Fig. 1-B); the signals of the membrane bound enzyme can be

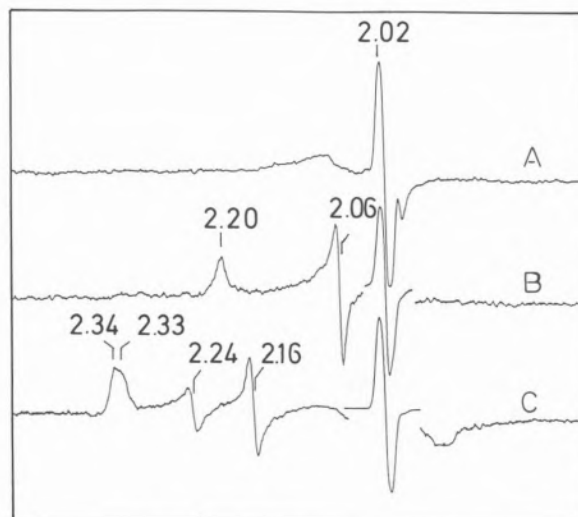


Fig. 1

EPR spectra of *D. baculatus* (strain 9974) native hydrogenase:
 A — Cytoplasmic fraction; B — Periplasmic fraction;
 C — Membrane bound fraction.

Experimental conditions: temperature 8 K; microwave power 2 mW; modulation amplitude 1 mT; microwave frequency 9.41 GHz

decomposed into two sets of EPR signals with g-values at 2.34, 2.16 and ~ 2.00 (component I) and at 2.33, 2.24 and ~ 2.00 (component II) (Fig. 1-C).

In the hydrogen reduced state all the hydrogenase fractions show identical EPR spectra: signals typical of reduced iron-sulfur centers with $g_{\text{med}} \sim 1.94$, and additional EPR features with g-values greater than 2.0 that were assigned to nickel. The conjunction of EPR studies performed at different temperatures and microwave powers, as well as the observation of EPR signals in reduced samples (reduced either with H₂ gas or sodium dithionite, during different times), enables the identification of two sets of iron-sulfur centers: *center I* (2.03, 1.89 and 1.86) detected below 10 K and *center II* (2.06, 1.95 and 1.88) easily saturated at low temperature.

DISCUSSION

The hydrogenase fractions isolated from *D. baculatus* (strain 9974) show unusual spectroscopic properties which should be relevant for the understanding of the role of EPR detectable nickel in hydrogenases. The samples show a very weak EPR signal due to iron-sulfur centers in the oxidized state. Iron-sulfur EPR signals have been observed in the native state of other hydrogenases. *D. gigas* hydrogenase has an almost isotropic EPR signal centered around $g = 2.02$ assigned to a [Fe₃S₄] center on the basis of complementary EPR and Mössbauer spectroscopic studies [1]. This signal integrates from 0.7 up to 1.0 spin/molecule depending on the preparation. However, the *D. vulgaris* (Hildenborough) enzyme also shows a very weak signal in the native state which only accounts for up to 0.05 spin/molecule [2] and the soluble *D. desulfuricans* (Norway strain) hydrogenase is EPR silent as isolated [3]. The cytoplasmic fraction of *D. baculatus* (strain 9974) hydrogenase is practically EPR silent (the isotropic signal accounts for 0.002 spin/molecule). Additionally, EPR signals assigned to Ni(III) are observed in the periplasmic and the membrane bound form. The nickel EPR g-values observed in the membrane fraction are typical of Ni(III) as observed for other nickel containing hydrogenases as isolated. However the rhombic EPR signal observed for the periplasmic fraction as isolated is

quite unusual. Similar g-values (2.20, 2.06 and 2.0) were also observed in the *D. desulfuricans* (Norway strain) enzyme isolated from the soluble fraction [3]. Other complex nickel EPR signals have been reported [4] and assigned as being the result of the interaction between the nickel and an iron-sulfur center.

Upon reduction under hydrogen atmosphere (or by addition of dithionite) the three hydrogenases gave the same type of EPR spectra despite its native state. These observations indicate that native hydrogenases isolated from different bacterial sources or from different fractions (soluble or membrane bound) yield different Ni(III) EPR signals [5]. They may contain the redox centers in different oxidation states depending on the enzyme conditions. In order to express full activity, certain enzymes (e.g. *D. gigas* yielding a 2.31, 2.23 and 2.0 native EPR nickel(III) signal) require an activation/reductive step. Others, as in the case of *D. baculatus* (strain 9974) do not show a lag time dependent activation step. The state of the nickel in the native preparation may be determinant for the behaviour of the enzyme towards the full expression of activity.

Remarkable is also the presence of selenium in equimolecular amounts to nickel. Selenium is also found in *Methanococcus vannielii* [6] and *D. desulfuricans* (Norway strain) hydrogenases [3].

ACKNOWLEDGEMENTS

This work was supported by INIC, JNICT, NATO and USAID.

REFERENCES

- [1] M. TEIXEIRA, I. MOURA, A.V. XAVIER, D.V. DERVARTANIAN, J. LEGALL, H.D. PECK JR., B.H. HUYNH, J.J.G. MOURA, *Eur. J. Biochem.*, **130**, 481-484 (1983).
- [2] B.H. HUYNH, M.H. CZECHOWSKI, H.J. KRÜGER, D.V. DERVARTANIAN, H.D. PECK JR., J. LEGALL, *Proc. Natl. Acad. Sci. USA*, **81**, 3728-3732 (1984).
- [3] S.H. BELL, D.P.E. DICKSON, R. RIEDER, R. CAMMACK, D.S. PATIL, D.O. HALL, K.K. RAO, *Eur. J. Biochem.*, **145**, 645-651 (1984).
- [4] S.D.J. ALBRACHT, J.W. VAN DER ZWAAN, R.D. FONTIJN, *Biochim. Biophys. Acta*, **766**, 245-258 (1984).
- [5] M. TEIXEIRA, I. MOURA, A.V. XAVIER, B.H. HUYNH, D.V. DERVARTANIAN, H.D. PECK JR., J. LEGALL, J.J.G. MOURA, 1985, submitted for publication.
- [6] S. YAMAZAKI, *J. Biol. Chem.*, **257**, 7926-7929 (1982).



PS1.35 — TU

M. CZECHOWSKI
G. FAUQUE
Y. BERLIER
P.A. LESPINAT
J. LeGALL

Centre d'Etudes Nucléaires de Cadarache
A.R.B.S.-E.C.E., B.P. 1
13115 Saint Paul lez Durance
France

**PURIFICATION OF AN HYDROGENASE
FROM AN HALOPHILIC SULFATE
REDUCING BACTERIUM:
DESULFOVIBRIO SALEXIGENS
STRAIN BRITISH GUIANA**

Hydrogenases have been purified to apparent homogeneity from many bacterial species [1]. They are involved in either hydrogen consumption which is used to supply reductant for CO₂ fixation or energy generation via electron transport, or for hydrogen production which enables the bacteria to dispose of excess electrons [1,2].

Desulfovibrio (D.) salexigens strain British Guiana (NCIB 8403) is the only well known halophilic strain in the genus *Desulfovibrio*. A few electron transfer proteins have been isolated and characterized from *D. salexigens*: a cytochrome *c*₃ (Mr 13 000) [3], a flavodoxin and a rubredoxin [4] and a blue protein containing molybdenum and iron-sulfur centers [5]. We report on the purification

of an hydrogenase from *D. salexigens* strain British Guiana.

D. salexigens was grown at 37°C on a standard lactate-sulfate medium [6] supplemented with 3% sodium chloride. The cells were then lysed and frozen until used. They were slowly defrosted and centrifuged at 20 000 rpm for 1.5 hr. The supernatant from 250 g of cells (wet weight) was then centrifuged twice at 40 000 rpm for 2 hr.

All purification procedures were carried out in air at 4°C and the pH of the buffers (Tris-HCl and phosphate: KPB) was 7.6 (measured at 5°C). A summary of the steps of the purification is presented in Table 1.

The centrifuged extract was loaded onto a hydroxylapatite (Biorad) column (5×29 cm) and the column washed with 500 ml of 0.2 M Tris-HCl. A reverse gradient of 500 ml of 0.2 M Tris-HCl to 500 ml of 0.01 M Tris-HCl was set up. The column was then washed with 300 ml 0.01 M KPB and a phosphate linear gradient of 1 000 ml 0.01 M KPB to 1 000 ml 0.4 M KPB was set up. No hydrogenase was found in the eluent. The column was further washed with 500 ml 0.4 M KPB and the hydrogenase finally eluted from the column. About 80% of the hydrogenase activity (in the H₂ evolution) was recovered. The hydrogenase enzyme was then concentrated to 8 ml in a diaflow apparatus using a YM 30 membrane. It was then dialyzed against 4 500 ml 0.01 M Tris-HCl. The dialysis resulted in the formation of a precipitate which redissolved in 1 M Tris-HCl. The hydrogenase activity was then redetermined in the supernatant and found to have decreased by 50%. The resuspended pellet was checked for activity and very little was found. A spectrum of the resuspended pellet showed only cytochromes.

Table 1
Purification of hydrogenase from *D. salexigens*

Fraction	Protein (mg)	Total Activity (μmoles H ₂ /min)	Specific Activity (μmoles H ₂ /min/mg)	Exchange Activity (μmoles HD+H ₂ /min/mg)
Crude extract	12 690	54 000	4.3	2
Hydroxylapatite column	N.d.	42 492	N.d.	N.d.
Dialysis and Centrifugation	210	19 522	93	28
DEAE-Bio-Gel	27	16 245	602	175

Hydrogenase activity measured by the hydrogenase evolution assay [9] or the D₂-H⁺ exchange reaction [7].

Protein determined by a modified Lowry procedure [10].

N.d.: Not determined.

The dialyzed protein was diluted 1:4 with 0.01 M Tris-HCl and then applied to a DEAE-Biogel A column (5×33.5 cm). The column was washed with 200 ml of 0.01 M Tris-HCl and then a linear gradient was constructed (1 000 ml of 0.01 M Tris-HCl to 1 000 ml of 0.3 M Tris-HCl).

The hydrogenase was collected at a concentration of about 0.25 M Tris-HCl. About 85% of the hydrogenase was recovered in the last step of purification. The 400 nm/280 nm ratio was 0.275 and the specific activity was 602 μ moles H₂ produced/min/mg protein.

In the D₂–H⁺ exchange reaction, in contrast to the hydrogenases from *D. gigas* [7], *D. vulgaris* Hildenborough and *Methanosarcina barkeri* [8] where the initial HD evolution is initially higher than the H₂ production, the H₂/HD ratio found with *D. salexigens* hydrogenase was higher than 1, as it has also been observed with the periplasmic and cytoplasmic hydrogenases from *D. baculatus* strain 9974 (our unpublished results).

ACKNOWLEDGEMENTS

We are indebted to Dr. M. Scandellari and R. Bourrelli for growing the bacteria and we thank N. Galliano for careful technical assistances.

REFERENCES

- [1] M.W.W. ADAMS, L.E. MORTENSON, J.S. CHEN, *Biochim. Biophys. Acta*, **594**, 105-176 (1981).
- [2] H.G. SCHLEGEL, K. SCHNEIDER, in H.G. SCHEGEL, K. SCHNEIDER (eds.), «Hydrogenases: Their catalytic activity, structure and function», E. Goltze KG, Gottingen, 1978, pp. 15-44.
- [3] H. DRUCKER, E.B. TROUSIL, L.L. CAMPBELL, *Biochemistry*, **9**, 3395-3400 (1970).
- [4] I. MOURA, J.J.G. MOURA, M. BRUSCHI, J. LEGALL, *Biochim. Biophys. Acta*, **591**, 1-8 (1980).
- [5] G. FAUQUE, M. CZECHOWSKI, N. GALLIANO, J. LEGALL, unpublished results.
- [6] R.L. STARKEY, *Arch. Microbiol.*, **9**, 268-304 (1938).
- [7] Y. BERLIER, G. FAUQUE, P.A. LESPINAT, J. LEGALL, *FEBS Lett.*, **140**, 185-188 (1982).
- [8] G. FAUQUE, «Relations structure — fonction de différentes protéines d'oxydo-réduction isolées de bactéries sulfato-réductrices et méthanigènes», Thèse d'Etat, U.T. Compiègne, France, 1985, p. 222.
- [9] H.D. PECK JR., J. GEST, *J. Bacteriol.*, **71**, 70-80 (1956).
- [10] M.A. MARKWELL, S.M. HAAS, L.L. BIEBER, N.E. TOLBERT, *Anal. Biochem.*, **87**, 206-210 (1978).



PS1.36 — TH

G. CHOTTARD

Département de Recherches Physiques
 Université Pierre et Marie Curie
 Tour 22, 4 place Jussieu, 75230 Paris Cedex 05
 France

J.P. MAHY

P. BATTIONI

D. MANSUY

Laboratoire de Chimie
 École Normale Supérieure
 72231 Paris Cedex 05
 France

A RESONANCE RAMAN STUDY OF THE MYOGLOBIN COMPLEXES FORMED BY REACTION WITH MONOSUBSTITUTED HYDRAZINES

Hydrazines are effective inducers of hemoglobin precipitation in the form of Heinz bodies. It has been shown that monosubstituted hydrazines, typically $C_6H_5NHNH_2$ and CH_3NHNH_2 react with myoglobin (Mb) and hemoglobin (Hb) to yield Fe^{III} σ bonded phenyl and methyl derivatives respectively [1,2]. In the case of the reaction of methylhydrazine an intermediate Mb (Hb) methyl-diazene complex can be isolated [2].

We report here the results of a Resonance Raman (RR) study of these complexes using Soret excitation, which point to the very different behavior of the phenyl and methyl Mb derivatives.

σ bonded phenyl derivative Mb Fe^{III} C_6H_5

In the 1300-1650 cm^{-1} the main porphyrin vibrations are observed: the intense oxidation state marker band is located at 1372 cm^{-1} and two weaker bands are observed at 1586 and 1640 cm^{-1} . These frequencies are indicative of a Fe^{III} low spin derivative [3]. In the low frequency region a fairly strong band occurs at 640 cm^{-1} , which does not correspond to a previously reported porphyrin vibration. By comparison with spectra of substituted phenyl derivatives, we assign this band (together with the 1049 and 1075 cm^{-1} bands) to a

vibration of the axial phenyl ligand. The origin of the observed enhancement of the axial ligand internal vibrations is studied.

σ bonded methyl derivative Mb Fe^{III} - CH_3

Under Soret excitation (430-455 nm), the complex Mb Fe^{III} - CH_3 undergoes photoreduction leading to deoxy Mb. Under the same excitation but in the presence of excess CH_3NHNH_2 , the observed Raman spectrum is that of the Mb Fe^{II} ($NH=NCH_3$) complex, which has been previously described as an intermediate in the formation of Mb Fe^{III} - CH_3 from Mb Fe^{III} and NH_2NHCH_3 [2]. These photoreduction reactions can be followed by visible and Raman spectroscopy; they preclude the observation of the RR spectrum of Mb Fe^{III} - CH_3 .

Methyldiazene derivative Mb Fe^{II} - $NH=NCH_3$

The RR spectrum of the methyldiazene complex shows an oxidation state marker band at 1370 cm^{-1} and low spin marker bands at 1584 and 1639 cm^{-1} . The low frequency bands are under investigation. These RR data will be compared to those obtained for the isoelectronic complexes MbO₂ and MbCH₃NO.

REFERENCES

- [1] a) K.L. KUNZE, P.R. ORTIZ DE MONTELLANO, *J. Am. Chem. Soc.*, **105**, 1380 (1983).
 b) D. RINGE, G.A. PETSKO, D.E. KERR, P.R. ORTIZ DE MONTELLANO, *Biochemistry*, **23**, 2 (1984).
- [2] D. MANSUY, P. BATTIONI, J.P. MAHY, G. GILLET, *Biochem. Biophys. Res. Commun.*, **106**, 30 (1982).
- [3] M.C. CALLAHAN, G.T. BABCOCK, *Biochemistry*, **20**, 952 (1981).



PSI.37 — MO

JAN MINTOROVITCH
 JAMES D. SATTERLEE
 Department of Chemistry
 University of New Mexico
 Albuquerque, New Mexico 87131
 U.S.A.

**THE INFLUENCE OF DISTAL AMINO ACIDS
 UPON LIGAND BINDING AS DETERMINED
 FROM CYANIDE ION BINDING
 TO SPERM WHALE MET-MYOGLOBIN
 AND THE MONOMER FRACTION
 GLYCERA DIBRANCHIATA
 MET-HEMOGLOBINS**

INTRODUCTION

The monomer hemoglobin fraction from the marine annelid *Glycera dibranchiata* has been shown to possess a three-dimensional structure similar to vertebrate hemoglobins with the exception that the distal histidine (primary sequence position E-7) is replaced by leucine [1,2]. Several authors have discussed the influence that such a substitution may have on ligand binding [3,4].

In our studies of the effects and importance of the E-7 (His → Leu) replacement in the *Glycera dibranchiata* monomer hemoglobin, we want, ultimately, to investigate the thermodynamics and kinetics of ligand binding for each separated component of the monomer fraction [5,6]. As a starting point cyanide ion binding to the met form of the unseparated monomer fraction is being studied. Thermodynamics of the binding of this same ligand to sperm whale myoglobin has been carried out as a reference.

EXPERIMENTAL

The *Glycera dibranchiata* hemoglobin monomer was prepared and separated as described before [5,6]. Sperm whale myoglobin was purchased from Sigma and used without further purification. All chemicals used were reagent grade quality. All

solutions were prepared in 0.3 M potassium phosphate buffer, pH 6.8. The spectrometer used for the ligand-binding titration was a Perkin-Elmer UV-Vis 559A with a temperature controlled cell compartment. Binding studies of cyanide ion with the monomer fraction hemoglobin were carried out in the difference mode as shown for the *Glycera dibranchiata* monomer fraction in Fig. 1.

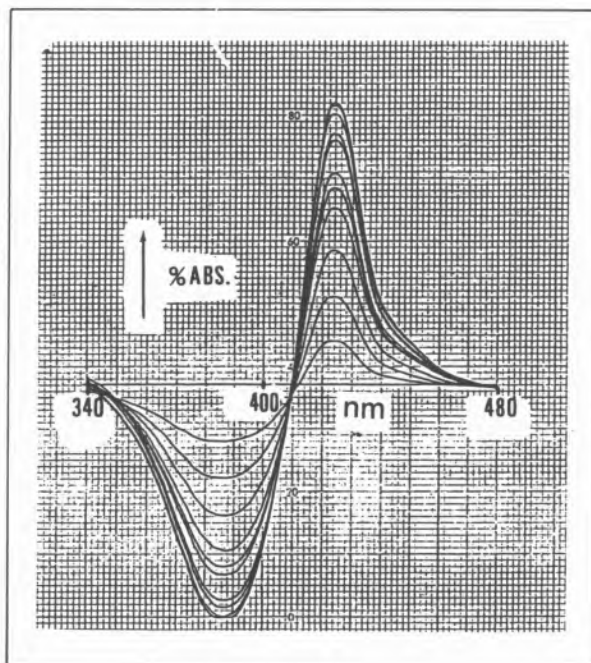


Fig. 1
 Visible difference spectra for CN^- binding to glycera monomer HB

RESULTS AND DISCUSSION

The results presented here are for our initial studies of cyanide ion (as KCN) binding to the oxidized (met) forms of the proteins. For myoglobin the values for K_{Diss} and Hill coefficient were in accordance with the current literature [7] (Fig. 2). For the glycera hemoglobin, however, the results were not comparable to the literature values [4] (Fig. 2). For both proteins we found that the rate at which cyanide ion is bound is not instantaneous. With our conditions (pH 6.8, 0.3 M phosphate buffer) the reaction proceeds to equilibrium within 30 minutes for the sperm whale myoglobin, but takes over ten hours for the *Glycera dibranchiata* monomer fraction. When both reactions are analyzed, using the Hill parameter formalism [8], both yield $n=1.0 \pm 0.1$ as shown in Fig. 2.

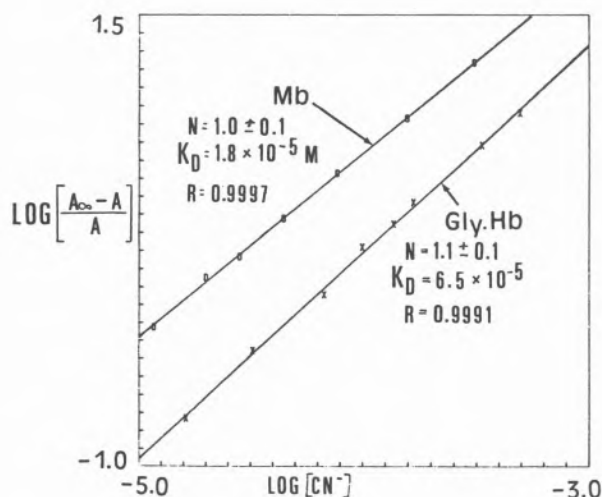


Fig. 2

Hill plots for CN^- binding to glycera monomer HB and myoglobin

This is what is to be expected for a noncooperative protein that binds a ligand such as cyanide ion according to an equilibrium such as: $\text{P} + \text{CN}^- \rightleftharpoons \text{P-CN}$.

ACKNOWLEDGEMENTS

This research is supported by a grant from the National Institutes of Health (AM 30912) and the Alfred P. Sloan Foundation. J.D.S. is a Fellow of the Alfred P. Sloan Foundation 1983-1985.

REFERENCES

- [1] E. PADLAN, W. LOVE, *J. Biol. Chem.*, **249**, 4067-4078 (1974).
- [2] T. IMAMURA, T. O. BALDWIN, A. RIGGS, *J. Biol. Chem.*, **247**, 2785-2797 (1972).
- [3] B. SEAMONDS in B. CHANCE, T. YANETANI, A. MILDVAN (eds.), «Probes of Structure and Function of Macromolecules and Membranes», vol. II, Academic Press, N.Y., 1971, pp. 317-320.
- [4] B. SEAMONDS, R.E. FORSTER, P. GEORGE, *J. Biol. Chem.*, **246**, 5391-5397 (1971).
- [5] R. L. KANDLER, J. D. SATTERLEE, *Comp. Biochem. Physiol. B*, **75**, 499-503 (1983).
- [6] R. L. KANDLER, I. CONSTANTINIDIS, J.D. SATTERLEE, *Biochem. J.*, **225**, (1984), in press.
- [7] E. ANTONINI, M. BRUNORI, «Hemoglobin and Myoglobin in Their Reaction with Ligands», Elsevier Press, Amsterdam, 1971, p. 230.



PSI.38 — TU

J.T.J. LECOMTE
S.D. EMERSON
G.N. LA MAR
Department of Chemistry
University of California
Davis, CA 95616
U.S.A.

ASSIGNMENT OF PROTEIN RESONANCES IN THE PROTON NMR SPECTRUM OF METCYANOMYOGLOBIN

To take full advantage of the potentials of high resolution proton NMR in solution, signals must be assigned unequivocally to specific protons in the molecule. Sperm whale myoglobin in its metcyano form (MbCN) is a low-spin ferric complex which shows the resonances from the immediate surroundings of the active site well resolved from the diamagnetic envelope. In particular, many relatively sharp peaks appear below 10 ppm. The large spread of the chemical shifts illustrated in Fig. 1,A is due to the low in-plane symmetry of the heme environment. So far, most of the assignments were reached by comparing the spectrum of native MbCN to the spectra of holoMbCNs reconstituted from apoMb and selectively deuterated hemins. Consequently, they bear only on the prosthetic group since such a method does not provide a direct handle on the protein resonances. A few of the latter have been identified through the variation of the chemical shift with pH, however, this applies to titratable groups. The value of the non-selective spin-lattice relaxation time has also proved useful as this parameter depends on the distance to the paramagnetic center. Using X-ray coordinates and T_1 data, the distal His (E7) ring NH as well as the proximal His (F8) ring NH and peptide NH have been located in the spectrum. They are labeled **A**, **B**, and **D** respectively in Fig. 1,A. Another promising approach consists in the observation and analysis of homonuclear Overhauser effects

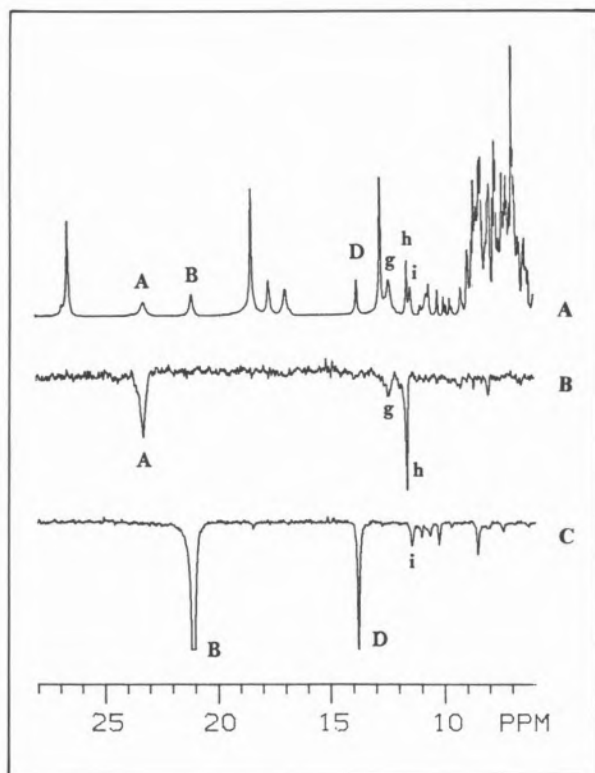


Fig. 1

Downfield region of the 500 MHz proton spectrum of sperm whale MbCN in 90% H₂O/10% ²H₂O, 0.2 M NaCl, at 30°C, pH 9.2.

A) Reference spectrum recorded with H₂O presaturation.
B) Steady-state NOE difference spectrum resulting from the saturation of the distal His (E7) ring NH (labeled A); h is assigned to the corresponding C₄H.

C) Steady-state NOE difference spectrum resulting from saturation of the proximal His (F8) ring NH (labeled B); the origin of D is confirmed as the F8 peptide NH, this NOE and others suggest that i is one of the F8 β-H₂.

The NOE experiments were performed using a Redfield train as observe pulse

(NOE). In combination with T₁ data the NOE has been utilized successfully to identify the spin system of Ile FG5, a residue belonging to the heme cavity [1].

Here we report on further NOE studies. By performing the experiments in H₂O, the known histidine NH resonances can be taken as spatial references and the signals experiencing an NOE are classified as arising from distal- or proximal-side residues (Fig. 1, B and C). H₂O and/or ²H₂O NOE data collected on MbCN containing modified hemes and various metcyanomyoglobins presenting amino acid replacements inside the heme

cavity (*i.e.* horse Mb and elephant Mb) are examined to verify the consistency of the assignments. The time dependence of the effect is studied in order to evaluate possible structural fluctuations. Furthermore, the pseudo-contact contribution to the chemical shift of an assigned resonance ($\Delta H/H_{p.c.}$) can be estimated. With several $\Delta H/H_{p.c.}$ values, it is possible to determine the principal components of the magnetic susceptibility tensor χ and the orientation of the magnetic axes via the formula for non-axial anisotropy

$$\Delta H/H_{p.c.} = c r^{-3} \{ [\chi_{zz} - \frac{1}{2}(\chi_{xx} - \chi_{yy})] (1 - 3\cos^2\Omega) + \frac{3}{2}(\chi_{xx} - \chi_{yy}) \sin^2\Theta \cos\Omega \}$$

where Ω is the polar angle between the iron-proton vector and the z-direction and Θ is the angle between its projection in the xy plane and the x axis. In turn, those parameters allow to predict the chemical shift of yet unassigned protein protons under the influence of the paramagnetic center.

REFERENCE

- [1] S. RAMAPRASAD, R.D. JOHNSON, G.N. LA MAR, *J. Am. Chem. Soc.*, **106**, 5330-5335 (1984).



PSI.39 — TH'

A.W. ADDISON
J.J. STAPHANOS (STEPHANOS)
Chemistry Department
Drexel University
Philadelphia, PA 19104
U.S.A.

NITROSYLIRON(III) HEMOGLOBIN: AUTOREDUCTION AND SPECTROSCOPY

INTRODUCTION

The reactions of heme proteins with nitric oxide continue to be extensively investigated. We report here the results of our studies on the reactions of NO with myoglobin (Mb), *Glycera dibranchiata* hemoglobins (mHb, hHb), and human hemoglobin (A₁Hb) and its subunits. With the noteworthy heme pocket alterations in comparison with other

Hb and Mb [His(E7)→Leu, Gly(E6)→Asp], monomeric mHb offers itself as an interesting model Hb for probing the chemical influences of the distal histidine.

MATERIALS AND METHODS

Polymeric and monomeric Hb's were separated by chromatography on Sephadex G-75. Mb was Sigma type-III equine, AHb was Sigma type-IV. Hb-subunits were prepared according to BUCCI and FRONTICELLI [1], and WAKS [2]. The nitrosyl complexes were obtained by direct reaction of NO with the iron(III) proteins. After autoreduction, samples of reduced AHb(II)NO were recycled (oxidised) with an excess of potassium hexacyanoferrate(III) to produce Hb(III)NO-H₂O. The hexacyanoferrates were removed on a Sephadex G-75 column.

RESULTS

The ESR spectrum of mHb(II)NO (Fig. 1) shows that it is low-spin and paramagnetic and has an ESR spectrum similar to that of other Hb,

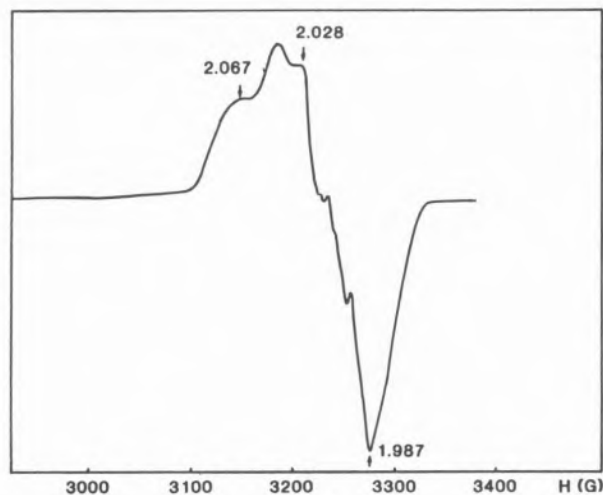


Fig. 1
Low temperature first derivative ESR spectrum of mHb(II)NO at pH 7

Mb(II)NO systems and the hexacoordinate iron(II) model complex, Fe(OEP)NO(BzIM), ($g = 1.97, 2.03$ and 2.06). The pronounced hyperfine splitting in Fe(OEP)NO indicates the pentacoordinate structure. The ferric heme is ESR silent, while a hexacoordinate structure in solution is indicated for Fe(OEP)NO(ClO₄). On addition of DPG, IHP,

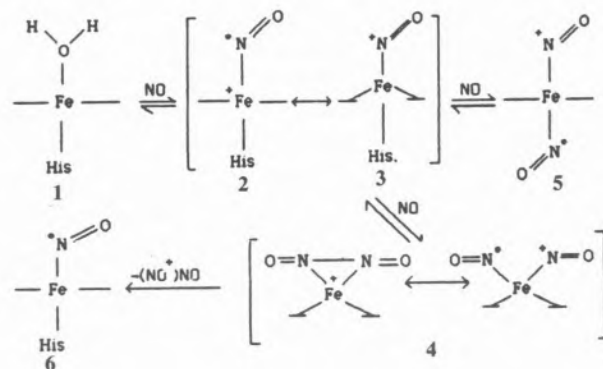
SDS, or hexacyanoferrate, or lowering of the pH to 5.5, the spectrum of mHb(II)NO does not change, thus the possibility [3] of induced change of the coordination state under such conditions is excluded.

The splitting of the α - and β -bands in the optical spectrum of Mb(III)NO contrasts markedly with the sharp, single bands observed in mHb(III)NO. We attribute the nondegeneracy of the d_{xy} and d_{yz} orbitals in Mb(III)NO to the influence of the distal His.

CD spectra were obtained for mHb(II)NO, mHb(III)NO, hHb(II)NO, hHb(III)NO, Mb(II)NO, Mb(III)NO. The vicinal chiral center contribution which governs the heme protein CD leads to low Kuhn anisotropies ($g = 0.001$ for magnetic dipole allowed), which we have used to assign certain electronic transitions.

The Hb(III)NO spectrum is not stable but transforms into that of Hb(II)NO. This autoredox process follows kinetics which are first order in Fe(III)NO. The rates of autoreduction (25°C, 1 atm NO) are: Mb(III)NO < mHb(III)NO < α Hb(III)NO < AHb(III)NO. At high NO concentration or after "recycling" of AHb, the rate of reduction becomes very slow.

The first step in the reaction of NO with the ferric heme 1 is the reversible formation of heme(III)NO 2. The optical and ESR spectra suggest that a one-electron transfer between NO and metal ion results in the formation of a spin-paired nitrosonium-heme 3, which reacts with another molecule of NO in the rate-determining step to produce the *cis*- and *trans*-nitrosonium nitrosyl hemes 4, 5. The fact that DPG accelerates the rate of reduction in the case of AHb suggests that His(F8) vacates the axial position in the rate-determining step. The removal of (NO⁺)NO from the *cis*-form



4 followed by the attack of another NO gives the final heme(II)NO 6.

By following the rate of reduction at different temperatures the activation parameters E_a , ΔG^\ddagger , ΔH^\ddagger and ΔS^\ddagger have been obtained.

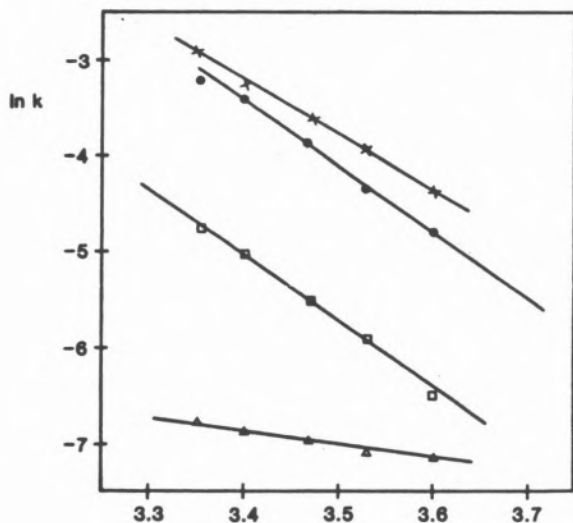


Fig. 2

Arrhenius plots for • mHb, □ Mb, × Hb, △ AHb

REFERENCES

- [1] E. BUCCI, C. FRONTICELLI, *J. Biol. Chem.*, **240**, 551 (1965).
- [2] M. WAKS, Y.K. YIP, S. BEYCHOCK, *J. Biol. Chem.*, **248**, 646 (1975).
- [3] H.C. MEKIN, B. BENKO, N.T. YU, K. GERSONDE, *FEBS Lett.*, **158**, 199 (1983).



PS1.40 — MO

LAURA A. ANDERSSON
V. RENGANATHAN
ANDREW A. CHIU
THOMAS M. LOEHR
MICHAEL H. GOLD

Department of Chemical, Biological, and Environmental Sciences
Oregon Graduate Center
1960 N.W. Walker Road, Beaverton, Oregon, 97006
U.S.A.

SPECTRAL CHARACTERIZATION OF DIARYLPROPANE OXYGENASE, A NOVEL PEROXIDE-DEPENDENT, LIGNIN-DEGRADING HEME ENZYME

Diarylpropane oxygenase (DAPOX), an H_2O_2 -dependent lignin-degrading enzyme from the basidiomycete fungus *Phanerochaete chrysosporium*, catalyzes the oxygenation of a variety of lignin model compounds with incorporation of a single atom of dioxygen (O_2) into the products [1]. DAPOX is also capable of oxidizing some alcohols to aldehydes and/or ketones [2]. This enzyme has an M_r of 41,000 and a single iron protoporphyrin IX prosthetic group [2]. The Soret maximum of its ferrous-CO complex is at ~ 420 nm, as seen for ferrous-CO myoglobin (Mb), hemoglobin (Hb) and horseradish peroxidase (HRP), and unlike the typical ~ 450 nm Soret maximum of the ubiquitous heme mono-oxygenase, cytochrome P-450. The electronic absorption spectra of native (ferric), cyano, and ferrous DAPOX most closely resemble those of the analogous myoglobin complexes. Thus, from absorption spectroscopy it appears likely that native DAPOX contains a high-spin, hexacoordinate ferric iron, while that of ferrous DAPOX is high-spin, pentacoordinate. The EPR g -values of native DAPOX, 5.83 and 1.99, are also in good agreement with those of «axial» aquometMb, supporting the high-spin, hexacoordinate assignment; they correlate less well with those of «rhombohedral» HRP, catalase, cyto-

chrome *c* peroxidase (CCP), and P-450. Comparative EPR spectroscopy of HRP, catalase, CCP, Mb and Hb revealed that the heme environments differed between the two functionally-distinct types of heme proteins [3]. According to its EPR spectral properties, DAPOX would fit into the oxygen-binding category.

Resonance Raman spectra of ferric DAPOX, obtained with 406.7 and 488.0 nm excitation lines, have their spin- and oxidation-state marker bands at 1612, 1558, 1479, and 1372 cm^{-1} , frequencies analogous to those of high-spin, hexacoordinate aquometMb. The RR spectra of ferrous DAPOX have key bands at 1603, 1554, 1470, and 1357 cm^{-1} , frequencies highly similar to those of deoxyMb, and hence also indicative of a high-spin, pentacoordinate ferrous iron for the reduced form of the enzyme. The RR spectra of both ferric and ferrous DAPOX are less similar to those of HRP, catalase, or CCP, and are clearly distinct from those of cytochrome P-450 (see Table I).

Thus, our spectral analysis strongly supports a neutral histidine, as found in myoglobin, as the fifth ligand to the heme iron in native DAPOX. This work also implies that the heme ligand is most likely not the tyrosinate of catalase, or the histidinate (or strongly hydrogen-bonded histidine) of horseradish peroxidase. Furthermore, the data clearly indicate that the fifth ligand of DAPOX is *not* the cysteinate found in cytochrome P-450. Our work also suggests that the heme

environment of DAPOX must be similar to that of the oxygen-binding myoglobin, rather than that of the peroxidases, catalase, or cytochrome P-450. Given the functional similarity between DAPOX and P-450, this work implies that the mechanism of oxygen insertion for the two systems is different.

REFERENCES

- [1] M. KUWAHARA, J.K. GLENN, M.A. MORGAN, M.H. GOLD, *FEBS Lett.*, **169**, 247 (1984).
- [2] M.H. GOLD, M. KUWAHARA, A.A. CHIU, J.K. GLENN, *Arch. Biochem. Biophys.*, **234**, 353 (1984).
- [3] J. PEISACH, W.E. BLUMBERG, in B. CHANCE (ed.), «Probes of Structure and Function of Macromolecules and Membranes», vol. 2, 1971, p. 231.

Table I
Comparison of Key Resonance Raman Bands for Diarylpropane Oxygenase and Other Heme Systems

System	Soret Excitation			Visible Excitation		Ligands	
	$\nu(\text{C}=\text{C})(\text{p})$	$\nu_3(\text{p})$	$\nu_4(\text{p})$	$\nu_{10}(\text{dp})$	$\nu_{19}(\text{ap})$	5th	6th
<i>High-spin Fe(III)</i>							
DAPOX ^{a)}	1627	1479	1372	1612	1558	His ^{b)}	H ₂ O ^{b)}
AquometMb ^{a)}	1620	1483	1369	1614	1562	His	H ₂ O
HRP	1632	1500	1376	1608	1576	His ⁻	—
P-450-cam	1626	1488	1368	1623	1567	Cys ⁻	—
<i>High-spin Fe(II)</i>							
DAPOX ^{a)}	1626	1470	1357	1603	1554	His ^{b)}	—
DeoxyMb	1618	1473	1357	1607	1552	His	—
HRP	1627	1472	1358	1605	1553	His ⁻	—
P-450-cam	1620	1467	1346	1604		Cys ⁻	—

a) This work. b) Tentative identification.



PSI.41 — TU

JOHN H. DAWSON
MASANORI SONO
KIM SMITH EBLE
Department of Chemistry
University of South Carolina
Columbia, South Carolina 29208
U.S.A.

LOWELL P. HAGER
Department of Biochemistry
University of Illinois at Urbana-Champaign
Urbana, Illinois 61801
U.S.A.

SPECTROSCOPIC PROPERTIES OF CHLOROPEROXIDASE COMPOUNDS II AND III — POSSIBLE STRUCTURAL MODELS FOR ANALOGOUS CYTOCHROME P-450 DERIVATIVES

Previous spectroscopic studies of analogous derivatives of chloroperoxidase (CPO) and cytochrome P-450 (P-450) have demonstrated that close similarities exist in their UV-visible absorption [1], magnetic circular dichroism (MCD) [2], EPR [3], Mössbauer [4], and extended X-ray absorption fine structure [5] properties. In particular, both enzymes exhibit unique hyperporphyrin («split Soret») spectra in their ferrous-CO [1] and ferric-thiolate [6] adducts, strongly suggesting the coordination of an endogenous thiolate ligand in CPO, as has well been established for P-450 [7]. These extensive parallels between the coordination properties of CPO and P-450 have motivated us to generate other CPO derivatives as potential analogs for catalytic intermediates of P-450, especially its oxygen complexes.

We report herein the generation of a unique, stable CPO-dioxygen adduct (CPO•O₂, CPO Compound III) and of CPO Compound II (CPO-II), and their characterization with UV-visible absorption and MCD spectroscopy. The CPO dioxygen adduct is formed by bubbling O₂ into a dithionite-reduced enzyme solution at -30°C in cryogenic mixed solvents. CPO-II is generated at

ambient temperature (~4°C) by adding peroxides and ascorbic acid to ferric CPO (1-2 μM) in a molar ratio of 100:2000:1. The UV-visible absorption and MCD spectra of CPO•O₂ and CPO-II are displayed in figs. 1 and 2, respectively.

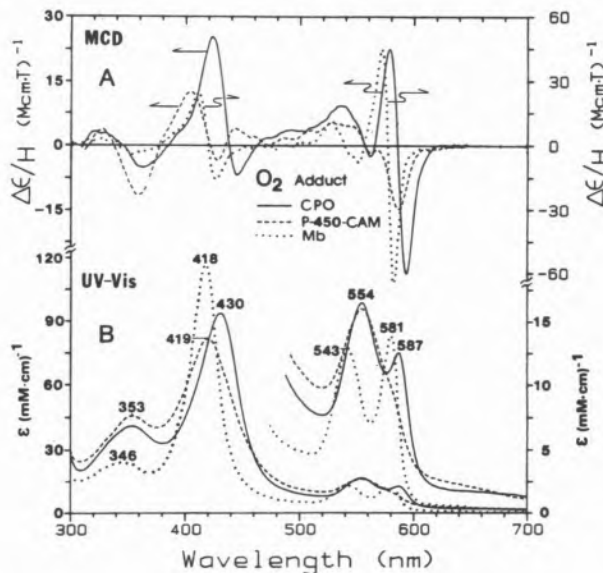


Fig. 1

UV-visible absorption (bottom) and MCD (top) spectra of oxygenated CPO (—), P-450-CAM (---) and Mb (·····). The spectra were obtained in 65% (v/v) ethylene glycol/0.035 M potassium phosphate buffer (pH 6.0, 7.4 and 7.0 before mixing, respectively) at -30°C with 30-40 μM protein concentrations. The P-450-CAM sample contained 100 mM KCl and 4 mM d-camphor

The absorption spectrum of CPO•O₂ at -30°C (Fig. 1B) [$\lambda_{nm}(\epsilon_{mM})$:354(41), 430(94), 554(16.5), 587(12.5)] has two noticeable distinctions from that of P-450•O₂: (a) the Soret peak of CPO•O₂ is red-shifted about 10 nm from that of P-450•O₂, and (b) a distinct α -peak is seen at 587 nm in the CPO case that is not observed for P-450•O₂. However, the overall spectral features of CPO•O₂ are more similar to those of P-450•O₂ [$\lambda_{nm}(\epsilon_{mM})$:353(46), 419(82), 554(16)] than of oxygenated myoglobin. Oxygenated CPO is EPR silent at 77 K. The bound O₂ in oxygenated CPO can be replaced by CO; upon bubbling CO into the CPO•O₂ solution at -30°C, the diagnostic hyperporphyrin spectrum of ferrous-CO CPO ($\lambda_{max,nm}$:362, 445, 549) is generated. CPO•O₂ undergoes autoxidation to form native ferric CPO without any detectable intermediates with a half life comparable to that of P-450•O₂. In fig. 2,

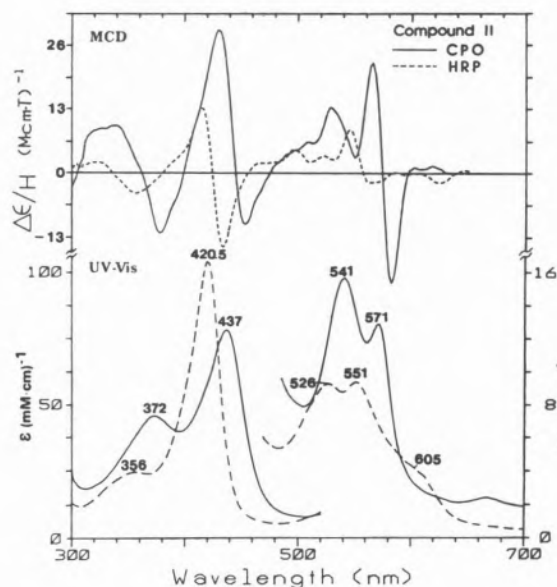


Fig. 2

UV-visible absorption (bottom) and MCD (top) spectra of Compound II derivatives of CPO (—) and HRP (----). The measurements for CPO (1.5–2 μ M) were made in 0.1 M potassium phosphate buffer, pH 6.0, with peroxides (~0.15 mM) and ascorbic acid (~3 mM) and those for HRP (10–15 μ M) in 0.005 M sodium carbonate buffer, pH 10.5, with equivalent amounts of EtOOH and ascorbic acid, at ~4°C. The MCD spectrum of CPO Compound II is the average of 3 measurements

UV-visible absorption (bottom) and MCD (top) spectra of horseradish peroxidase Compound II (HRP-II) are overplotted with those of CPO-II. Considerable differences are seen between the spectra of HRP-II and CPO-II, presumably because the endogenous axial ligands are not the same: histidine imidazole for HRP and thiolate, most likely, for CPO.

In conclusion, the dioxygen adducts of CPO and P-450 are clearly distinguishable from that of Mb, a histidine-ligated heme protein, in their UV-visible absorption and MCD spectral properties [8]. Considerable spectral differences are also seen between the Compound II states of CPO and HRP. The small, but nonetheless significant, spectroscopic dissimilarities between the dioxygen adducts of CPO and P-450 (Fig. 1A, B) are somewhat surprising, since the analogous ferric and ferrous ligand adducts of CPO and P-450 show great similarities [1,6,9]. The reason for these differences are not clear at the present.

ACKNOWLEDGEMENTS

This work was supported by NIH Grants GM26730 (JHD) and GM07768 (LPH). JHD is the recipient of a Camille and Henry Dreyfus Teacher/Scholar Award, an Alfred P. Sloan Foundation Research Fellowship and a National Institutes of Health Research Career Development Award.

REFERENCES

- [1] P.F. HOLLENBERG, L.P. HAGER, *J. Biol. Chem.*, **248**, 2630 (1973).
- [2] J.H. DAWSON, J.R. TRUDELL, G. BARTH, R.E. LINDER, E. BUNNENBERG, C. DJERASSI, R. CHIANG, L.P. HAGER, *J. Am. Chem. Soc.*, **98**, 3709 (1976).
- [3] P.F. HOLLENBERG, L.P. HAGER, W.E. BLUMBERG, J. PEISACH, *J. Biol. Chem.*, **255**, 4801 (1980).
- [4] P.M. CHAMPION, E. MÜNCK, P.G. DEBRUNNER, P.E. HOLLENBERG, L.P. HAGER, *Biochemistry*, **12**, 426 (1973).
- [5] S.P. CRAMER, J.H. DAWSON, K.O. HODGSON, L.P. HAGER, *J. Am. Chem. Soc.*, **100**, 7287 (1978).
- [6] M. SONO, J.H. DAWSON, L.P. HAGER, *J. Biol. Chem.*, **259**, 13209 (1984).
- [7] M. SONO, L.A. ANDERSSON, J.H. DAWSON, *J. Biol. Chem.*, **257**, 8308 (1982).
- [8] J.H. DAWSON, S.P. CRAMER, *FEBS Lett.*, **88**, 127 (1978).
- [9] J.H. DAWSON, M. SONO, L.P. HAGER, *Inorg. Chim. Acta*, **79**, 184 (1983).



PSI.42 — TH

RICHARD J. KASSNER
MICHAEL G. KYKTA
Department of Chemistry
University of Illinois at Chicago
Chicago, Illinois 60680
U.S.A.

ANION BINDING TO A CYTOCHROME *c'*

The cytochromes *c'* are mono- and diheme proteins reported to comprise the largest and most widespread class of bacterial cytochromes known [1]. These proteins are similar to the low-spin

cytochromes *c* in their heme binding sequence pattern, but exhibit optical spectra resembling those of high-spin metmyoglobin and methemoglobin. The ferric cytochromes *c'* are characterized by paramagnetic susceptibilities intermediate between those of high-spin and low-spin hemoproteins, while the ferrous cytochromes *c'* have paramagnetic susceptibilities which are very similar to those of high-spin hemoglobins and myoglobins [2]. X-ray crystallographic studies have established earlier suggestions that the heme iron in ferric cytochromes *c'* is pentacoordinate with a histidyl imidazole group providing the single axial ligand to the heme iron [3]. The ferrous cytochromes *c'* are also thought to be pentacoordinate based on a comparison of their properties to deoxymyoglobins: Although earlier studies [4] indicated that only CO and NO bind to the ferrous cytochromes *c'* and that no anionic ligands bind to the oxidized state, in direct contrast to the ligand binding properties of hemoglobins and myoglobins, recent studies from our laboratory demonstrated the binding of ethylisocyanide to the reduced cytochromes *c'* [5,6]. We now wish to report the binding of an anionic ligand to the ferric cytochrome *c'* from *Chromatium vinosum*. In the presence of 50 mM potassium cyanide the cytochrome *c'* exhibits a single visible absorption band and a red shifted Soret band similar to the low-spin complex observed for cyanide binding to ferric myoglobin in contrast to the high-spin type spectrum characteristic of each of these proteins in the absence of cyanide as indicated in Table I. These results indicate that addition of cyanide to the cytochrome *c'* results in the conversion of the pentacoordinate heme to a low-spin hexacoordinate complex. This finding suggests that the heme binding site in this

cytochrome *c'* is significantly more accessible to ligands than previously indicated and that CN⁻ may provide an important new probe for structural studies of the heme environment and properties of this protein.

ACKNOWLEDGEMENTS

This work was supported by grants AM28188 and HL26216 from the National Institutes of Health.

REFERENCES

- [1] T.E. MEYER, M.D. KAMEN, *Adv. Protein Chem.*, **35**, 105-212 (1982).
- [2] M.H. EMPTAGE, A.V. XAVIER, J.M. WOOD, B.M. AL-SAAD, G.R. MOORE, R.C. PITT, R.J.P. WILLIAMS, R.P. AMBLER, R.G. BARTSCH, *Biochemistry*, **20**, 58-64 (1981).
- [3] P.C. WEBER, A. HOWARD, N.H. XUONG, F.R. SALEMME, *J. Mol. Biol.*, **153**, 399-424 (1981).
- [4] S. TANIGUCHI, M.D. KAMEN, *Biochim. Biophys. Acta*, **74**, 438-455 (1963).
- [5] R.J. KASSNER, S.C. RUBINOW, M.A. CUSANOVICH, *Biochim. Biophys. Acta*, **743**, 195-199 (1983).
- [6] S.C. RUBINOW, R.J. KASSNER, *Biochemistry*, **23**, 2590-2595 (1984).
- [7] R.G. BARTSCH in H. GEST, A. SAN PIETRO, L.P. VERNON (eds.), «Bacterial Photosynthesis», Antioch Press, Yellow Springs, Ohio, 1963.
- [8] E. ANTONINI, M. BRUNORI, «Hemoglobin and Myoglobin in Their Reactions with Ligands», North Holland, Amsterdam, 1971.

Table I

Absorption Maxima of Ferric Cytochrome *c'* Metmyoglobin and Their Cyanide Derivatives

Protein	Absorption Maxima (nm)			Ref.
<i>Chromatium</i> cytochrome <i>c'</i> ^{a)}	635	445	400	[7]
<i>Chromatium</i> cytochrome <i>c'</i> -CN	538	417		
Horse Mb ^{b)}	630	502	408	[8]
Horse Mb-CN	540	422		[8]

a) pH=7.0. b) pH=6.4.



PS1.43 — MO

CARLOS O. AREAN*
 GEOFFREY R. MOORE
 GLYN WILLIAMS
 ROBERT J.P. WILLIAMS
 The Inorganic Chemistry Laboratory
 University of Oxford
 South Parks Road, Oxford OX1 3QR
 U.K.

**SELECTIVITY OF THE INTERACTION
 BETWEEN CYTOCHROME *c*
 AND TRANSITION METAL ION
 COMPLEXES OF EDTA
 AND RELATED LIGANDS**

INTRODUCTION

The monohaem electron-transfer protein, mitochondrial cytochrome *c*, has a highly positively charged surface that binds anionic inorganic redox reagents at a variety of sites. Some of these sites are kinetically important for the accompanying electron-exchange reactions and they may be identified by the use of NMR spectroscopy [1-3] in combination with the X-ray crystal structures [4]. The experimental procedure is straightforward. First, the perturbations introduced into the NMR spectra of cytochrome *c* by the paramagnetic reagents are measured. Second, assigned NMR resonances are grouped into those unaffected by the added reagent and those perturbed by it with the second group being rated according to the extent of the perturbation. Third, the pattern of resonance perturbation is compared with the X-ray structure and the probable binding sites located. Using this procedure we have identified three anion binding sites on cytochrome *c* close to its exposed haem edge [1-3]. These sites bind the reagents $[\text{Fe}(\text{CN})_6]^{3-}$ and $[\text{Fe}(\text{edta})(\text{H}_2\text{O})]^-$ but they do so with differing relative affinities that are not determined solely by the overall charge of the reagent but by its chemical composition and structure. We have investigated these factors by varying

the nature of metal-polyaminocarboxylate (pac) complexes and in the present communication we report that subtle differences between the pac complexes significantly affect their binding preferences on cytochrome *c*.

RESULTS AND DISCUSSION

In Fig. 1 the paramagnetic difference NMR spectra (PDS) for binding of $[\text{Fe}(\text{edta})(\text{H}_2\text{O})]^-$ and $[\text{Fe}(\text{dtpa})]^{2-}$ to ferricytochrome *c* are shown. The $[\text{Fe}(\text{dtpa})]^{2-}$ PDS is similar to the previously reported $[\text{Cr}(\text{CN})_6]^{3-}$ PDS [1] and significantly different from the $[\text{Fe}(\text{edta})(\text{H}_2\text{O})]^-$ PDS (Fig. 1). The PDS for the edta and dcta complexes of Mn(III) are similar to that for $[\text{Fe}(\text{edta})(\text{H}_2\text{O})]^-$ but the PDS for the heedta complex of Fe(III) is similar to the $[\text{Fe}(\text{dtpa})]^{2-}$ PDS (not shown).

Most of the spectral perturbations revealed by the PDS are caused by binding of the paramagnetic reagent to three sites on the surface of cytochrome *c*. These sites are illustrated in Fig. 2. The different resonance patterns of the PDS result from a change in the relative affinities of the three sites for the different reagents. $[\text{Fe}(\text{dtpa})]^{2-}$ binds at sites 2 and 3 with about the same affinity but $[\text{Fe}(\text{edta})(\text{H}_2\text{O})]^-$ has a greater affinity for site 2 than for site 3. This selectivity is not caused simply by the change in net charge of the reagent. From the range of compounds studied the following points emerge:

- 1) Trinegative, spherically symmetric complexes, such as $[\text{Cr}(\text{CN})_6]^{3-}$, have a marked preference for site 3.
- 2) Reduction in the net negative charge of spherically symmetric complexes reduces the selectivity of the sites.
- 3) Some asymmetric complexes have a preference for site 2.

The reasons why some asymmetric complexes prefer site 2 to site 3 are not entirely clear. In solution, $[\text{Fe}(\text{edta})(\text{H}_2\text{O})]^-$ may have an unligated carboxylate group whereas the dtpa and heedta complexes do not. Perhaps by interacting directly with a lysine residue of the protein, a free carboxylate assists binding at site 2. Also, site 2, unlike site 3,

* Present address: Departamento de Química Inorgánica, Facultad de Química, Oviedo, Spain

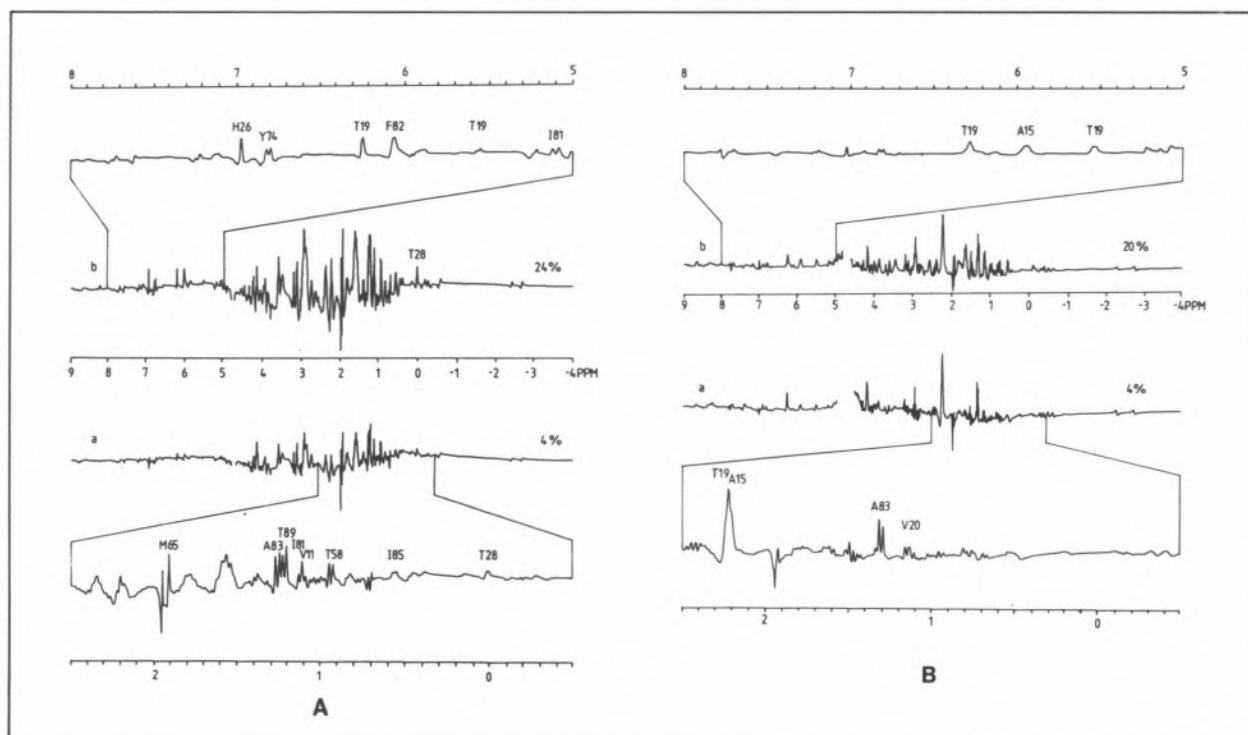


Fig. 1

300 MHz NMR paramagnetic difference spectra (PDS) for the binding of $[Fe(dtpa)]^{2-}$ to 4 mM horse ferricytochrome c at pH* 5.3 and 27°C (A) and $[Fe(edta)(H_2O)]^-$ to 4 mM tuna ferricytochrome c at pH* 5.5 and 27°C (B).

Experimental details for obtaining such spectra have been reported elsewhere [1-3]. The percentage figures are mol %. Horse and tuna cytochromes c show the same binding preferences at their main binding surfaces.

Resonance labels are: V11, Val-11; A15, Ala-15; T19, Thr-19; V20, Val-20; H26, His-26; T28, Thr-28; Y58, Thr-58; M65, Met-65; Y74, Tyr-74; I81, Ile-81; F82, Phe-82; A83, Ala-83; I85, Ile-85; T89, Thr-89.

Complexes studied in the present work are the 1:1 Fe(III) and Mn(III) complexes of: dtpa, diethylenetriamine-*N,N,N',N',N''*-pentaacetic acid; edta, ethylene-*N,N,N',N'*-tetraacetic acid; dcta, *trans*-1,2-diaminocyclohexane-*N,N,N',N'*-tetraacetic acid; heedta, *N*-(2-hydroxyethyl)ethylenediamine-*N,N',N'*-triacetic acid

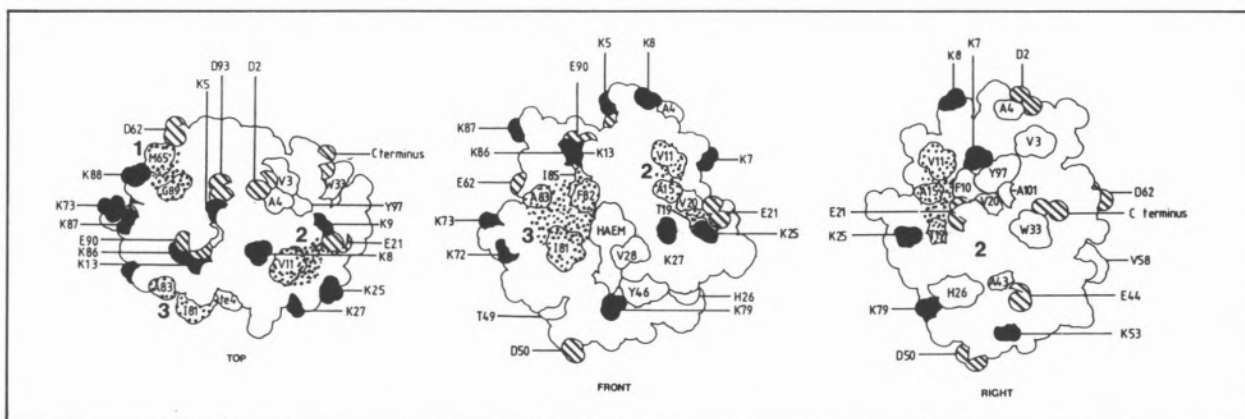


Fig. 2

Representation of the three major anion binding sites on cytochrome c.

The space-filling diagrams for tuna cytochrome c illustrate the positions of negatively charged groups (striped) and positively charged groups (solid). Important residues with assigned NMR resonances are shown in outline. Top, front and right refer to the conventional orientation of cytochrome c [4]. The stippled residues are those affected by low concentrations of the paramagnetic reagents and 1-3 refer to the binding sites

includes a protein carboxylate (Fig. 2), Glu-21, and it is possible that this plays an important role either by binding to the central metal ion of the reagent or by hydrogen bonding to its ligated H_2O . Whatever the exact cause of the selectivity these studies demonstrate that proteins do have the capacity for selecting between similar complexes. They also emphasize the need for care in interpreting reactivity parameters for redox reactions between proteins and small molecules especially in cases where there appears to be more than one possible reaction pathway, as with cytochrome *c*. Using chemically modified lysine derivatives of cytochrome *c* we hope to unravel the observed binding selectivities.

ACKNOWLEDGEMENTS

This work was supported by the Science and Engineering Research Council (SERC) and the Medical Research Council (MRC). GW thanks the MRC for a Training Fellowship and GRM thanks the SERC for an Advanced Fellowship.

REFERENCES

- [1] C.G.S. ELEY, G.R. MOORE, G. WILLIAMS, R.J.P. WILLIAMS, *Eur. J. Biochem.*, **124**, 295-303 (1982).
- [2] G. WILLIAMS, C.G.S. ELEY, G.R. MOORE, M.N. ROBINSON, R.J.P. WILLIAMS, *FEBS Lett.*, **150**, 293-299 (1982).
- [3] G.R. MOORE, C.G.S. ELEY, G. WILLIAMS, *Adv. Inorg. Bioinorg. Mech.*, **3**, 1-96 (1984).
- [4] T. TAKANO, R.E. DICKERSON, *J. Mol. Biol.*, **153**, 79-115 (1981).



PS1.44 — TH

I. MOURA

A.V. XAVIER

J.J.G. MOURA

Centro de Química Estrutural, UNL
Complexo IIST, Av. Rovisco Pais, 1000 Lisboa
Portugal

M.Y. LIU

G. PAI

H.D. PECK JR.

J. LE GALL

Department of Biochemistry
University of Georgia

Athens, Georgia 30602

U.S.A.

W.J. PAYNE

Department of Microbiology
University of Georgia

Athens, Georgia 30602

U.S.A.

NMR STUDIES OF A MONOHEME CYTOCHROME FROM *WOLINELLA SUCCINOGENES*, A NITRATE RESPIRING ORGANISM

An ascorbate reducible monoheme *c*-type cytochrome (8.2 KDa, $E'_0 \sim +100$ mV) was purified from the nitrate "respiring" organism *Wolinella succinogenes* (VPI 10659). The optical spectrum in the ferro and ferric forms are typical of a *c*-type heme coordination. The oxidized state shows the 695 nm band taken as indicative of methionyl axial coordination, but additional optical bands are also observed at 619 nm and 498 nm (shoulder) reminiscent of the absorption bands of cytochrome *c'* [1]. These peculiarities of the optical spectrum prompted us to study this situation of spin-equilibrium by nuclear magnetic resonance (NMR) spectroscopy.

The NMR spectrum of the reduced state is shown in Fig. 1. The heme mesoproton resonances (9.88, 9.59, 9.30 and 9.25 ppm) and the resonances originated from the bound axial methionine (S-CH₃ at -3.72 ppm and methylene protons at -3.85, -1.66 and -0.70 ppm) are readily discernible.

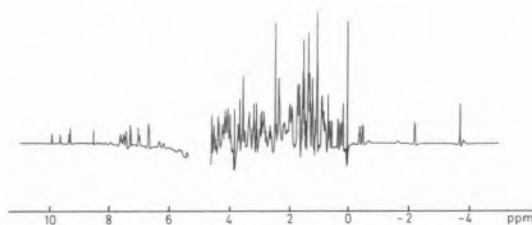


Fig. 1

Deconvoluted ^1H NMR spectrum of *W. succinogenes* ferricytochrome at 303 K, pH 7.2

The pH dependence of the NMR spectrum of ferricytochrome is shown in Fig. 2. As expected for a paramagnetic protein, several hyperfine shifted resonances are observable downfield of 10 ppm. The 3-proton intensity resonances designated M_i ($i=1,4$) are assigned to heme methyl groups. The-

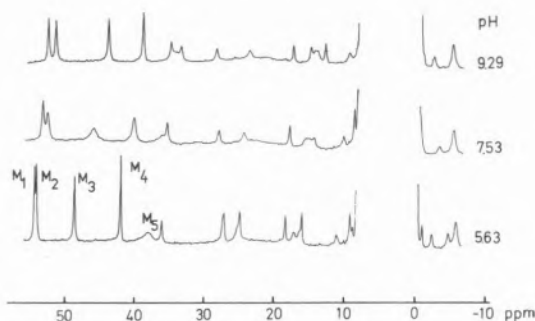


Fig. 2

^1H NMR spectra of *W. succinogenes* ferricytochrome at 303 K for three different pH values

se resonances have downfield shifts greater than 38 ppm which is unusual for a low-spin c -type situation. The temperature dependence of the ferricytochrome resonances shows that M_2 and M_4 are almost temperature invariant, M_1 shows a temperature dependence according to Curie's law and M_3 is anti-Curie dependent. Resonance 5 is extremely temperature dependent ($\delta_{50^\circ\text{C}} - \delta_{0^\circ\text{C}} = 7.15$ ppm at pH = 7.5) and also anti-Curie dependent.

The pH profile gives a pK_a value at ~ 7.3 and the linewidth variation is compatible with an intermediate rate for the exchange process between two forms.

Magnetic susceptibility measurements by a NMR method [2] were performed as a function of the pH. The results are indicated in Table I.

Table I

Magnetic susceptibility data for ferricytochrome at 308 K

pH	$\chi_M^P (\times 10^3)$	μ_{eff}
4.90	7.59	4.31
7.50	4.64	3.38
9.98	2.52	2.48

The visible spectra, NMR and magnetic susceptibility measurements are indicative of a spin equilibrium which shifts towards the high-spin form when the pH is lowered. This is compatible with the increase in chemical shifts of the heme methyl resonances at low pH.

The assembly of these preliminary studies, indicates that there is a spin equilibrium in the ferric form. The high-spin/low-spin transition is relatively fast in the nuclear magnetic resonance time scale, since only four heme methyl resonances are observed in the lowfield region of the spectrum. The methyl resonance from the bound methionine axial ligand is not observed in the upfield spectral region. Thus, the high spin state could be produced by loss of the sixth axial ligand (methionine sulfur) to the ferric ion.

The chemical exchange between the situation of bound and unbound axial ligand could induce a large chemical shift to the methionine methyl resonance [3]. Resonance M_5 is a plausible candidate for this S-CH_3 methionine, due to its chemical shift and strong temperature dependence.

ACKNOWLEDGEMENTS

This work was supported by grants from the Instituto Nacional de Investigação Científica, Junta Nacional de Investigação Científica e Tecnológica, Portugal and AID grant n. 936-5542-G-SS-4003-00.

REFERENCES

- [1] R.G. BARTSCH, M.D. KAMEN, *J. Biol. Chem.*, **230**, 41-63 (1958).
- [2] W.D. PHILIPS, M. POE, *Methods in Enzymol.*, **24**, 304-317 (1972).
- [3] R. TIMKOVICH, M.S. CORK, *Biochemistry*, **23**, 851-860 (1984).



PS1.45 — TH

I. MOURA

A.V. XAVIER

J.J.G. MOURA

Centro de Química Estrutural

Complexo I, U.N.L.

Av. Rovisco Pais, 1000 Lisboa

Portugal

G. FAUQUE

J. LEGALL

A.R.B.S., E.C.E., CEN Cadarache

13115 Saint Paul lez Durance

France

G.R. MOORE

Inorganic Chemistry Laboratory

University of Oxford

South Parks Road, Oxford OX1 3QR

U.K.

B.H. HUYNH

Department of Physics

Emory University

Atlanta, Georgia

U.S.A.

STRUCTURAL HOMOLOGY OF TETRAHEME CYTOCHROME c_3

Low potential tetraheme cytochromes c_3 (molecular mass 13 KDa) are found in sulfate reducing bacteria belonging to the genus *Desulfovibrio*. They seem to play an important role in electron transfer processes, but at the present moment their physiological role is still controversial. Cytochrome c_3 can act as an electron carrier for hydrogenase (although recently direct electron transfer was shown to occur between some of the electron carrier proteins, e.g., *D. gigas* FdII and flavodoxin, and hydrogenase) and in some species involved in the reduction of elemental sulfur. Each heme, in this class of cytochromes, is bound to the protein by two thioether linkages involving cysteine residues, and the fifth and sixth ligands of each heme iron are histidinyll residues. Table I indicates all the tetraheme cytochromes c_3 that have been isolated until now as well as some of their physicochemical properties. The amino acid compositions are quite different from cytochrome to cytochrome originating very different isoelectric

Table I *

Desulfovibrio species	State of physico-chemical characterization	Isoelectric point	Number of residues	Molecular mass
<i>D. gigas</i>	P,A,S,NMR, EPR,MB	5.2	111	14400
<i>D. vulgaris</i> (Hildenborough)	P,A,S,NMR, EPR,MB	10.2	107	14100
<i>D. vulgaris</i> (Miyazaki)	P,A,S,X-ray, NMR,MB	10.6	107	14000
<i>D. desulfuricans</i> (Norway 4)	P,A,S,X-ray, NMR,EPR	7	118	15100
<i>D. baculatus</i> (strain 9974)	P,A,NMR, EPR	7	(118)	15100
<i>D. desulfuricans</i> (strain 27774)	P,A,NMR,EPR	n.d.	(103)	13500
<i>D. desulfuricans</i> (Berre eau)	P,NMR,EPR	8.6	n.d.	14000
<i>D. desulfuricans</i> (El Alghela Z)	P,A,S,NMR,EPR	10.0	102	13400
<i>D. salexigens</i> (British Guiana)	P,A,S,NMR	10.8	106	14000
<i>D. desulfuricans</i> (Cholinicus)	P,A	8.0	(108)	14300
<i>D. africanus</i> (Benghazi)	P,A	8.5	(109)	14900

P — Purified

A — Amino acid analysis

S — Sequence

NMR — Nuclear Magnetic Resonance

EPR — Electron Paramagnetic Resonance

MB — Mössbauer Spectroscopy

* Table composed from references [1-5] and references therein.

points. Tetraheme cytochromes are conserved in all the *Desulfovibrio* species analysed so far. It is interesting to note that even when the terminal acceptor is modified (i.e. nitrate by sulfate in *D. desulfuricans* (strain 27774) this multiheme cytochrome is still conserved. Cytochrome $c_{551.5}$ (c_7), a three heme containing cytochrome isolated from the sulfur reducing bacterium *Desulfuromonas acetoxidans*, is a close relative to cytochrome c_3 . The four hemes in cytochrome c_3 , are localized in nonequivalent protein environments (see below the comparison of the NMR and EPR spectral data) and each heme exhibits different redox midpoint potentials. The midpoint redox potentials of all the hemes are negative but the span in redox potential between the lowest and the highest one varies in this class of homologous proteins. As an example, in *D. vulgaris* cytochrome c_3 this difference is 80 mV, in *D. gigas* cytochrome c_3 100

mV, and in *D. desulfuricans* (Norway strain) cytochrome c_3 this value is 200 mV (using the microscopic redox potentials determined by EPR) [6-8].

A comparison of the NMR and EPR characteristics of this class of homologous proteins is presented in order to better understand the structure — function relationships.

Fig. 1 shows the low field region of the NMR spectra of several cytochromes c_3 isolated from different *Desulfovibrionas*. An obvious common feature is the low downfield chemical shifts expe-

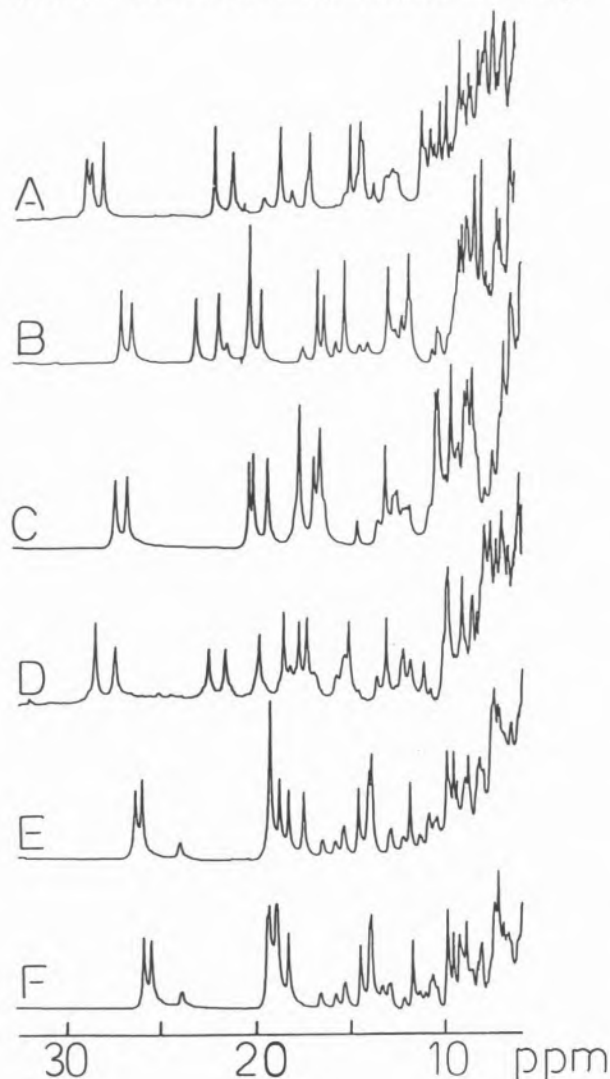


Fig. 1

Low-field NMR spectra of several ferricytochromes c_3 at 313 K. A — *D. gigas*; B — *D. salexigens*; C — *D. vulgaris* (strain Hildenborough); D — *D. desulfuricans* (El Algeila Z); E — *D. desulfuricans* (Norway 4); F — *D. baculatus* (strain 9974)

rienced by the heme methyl groups in this low spin paramagnetic state of the protein. The differences observed in the distribution of resonances are also striking. There is a wide variation in the distribution of heme methyl resonances between the different cytochromes c_3 . These differences fall largely into three regions: the region downfield of 25 ppm, the region between 15 ppm and 25 ppm and the region upfield of 15 ppm. The presence of resonances downfield of 25 ppm is common to all cytochromes c_3 . The fact that there are not many resonances in any of the spectra of Fig. 1 downfield of 25 ppm suggests that these proteins have similar structures. However, there is a striking difference: *D. gigas* cytochrome c_3 has three resonances in this region while the remaining five proteins have only two resonances. Similar differences can be seen in the regions between 15 ppm and 25 ppm. The heme methyl resonances in these regions of the spectra of some of the proteins, such as that from *D. desulfuricans* (Norway strain) are bunched together and cover a small range of chemical shift values whilst for other proteins, such as that from *D. salexigens*, they are better resolved and cover a wider range of chemical shift values. All of these differences may result from two causes: differences in the relative spatial orientations of the four heme groups, and differences in the electronic properties of the four heme groups.

Despite of the emphasis upon the differences between the spectra of cytochromes c_3 it is relevant to notice that there is a high degree of similarity between them. For instance, in all cases there are 10 to 12 heme methyl resonances with chemical shift values >12 ppm.

Fig. 2 compares the EPR spectra of several cytochromes c_3 from different *Desulfovibrio* species. The cytochromes c_3 exhibit quite different EPR characteristics. Cytochrome c_3 from *D. desulfuricans* (Norway strain), *D. baculatus* (strain 9974) and *D. desulfuricans* (strain Berre eau) show quite similar characteristics. They all have broad features at $g \approx 3.3$, a resonance around $g = 3.0$ and a shoulder on this peak to lower g -values. For other cytochromes, like *D. gigas* and *D. desulfuricans* (El Algeila Z) cytochromes c_3 , the broad peak around $g \approx 3.30$ is missing and only one prominent EPR signal is observed with a g_{\max} around

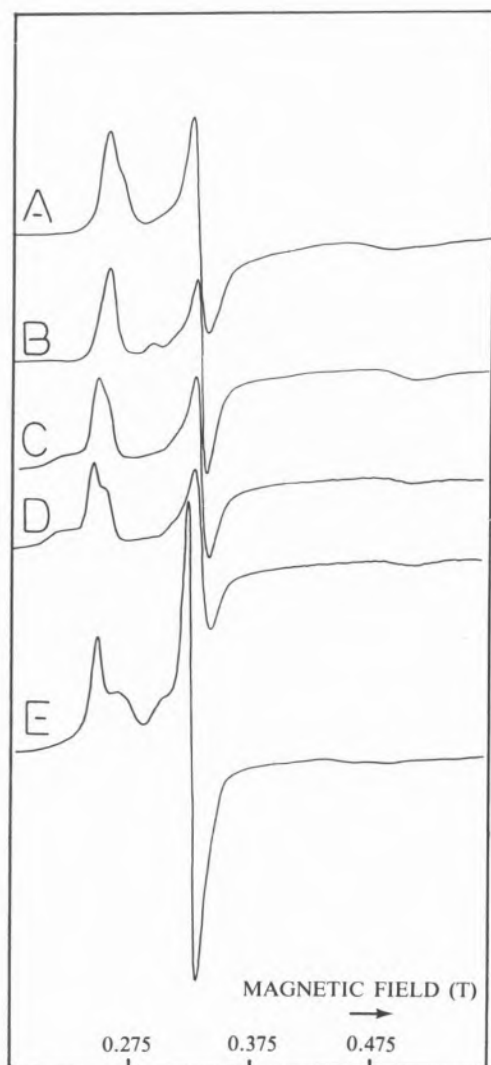


Fig. 2

EPR spectra of several cytochromes c_3 at 10 K, microwave power 0.63 mW and modulation amplitude 0.5 mT.

A — *D. gigas*; B — *D. desulfuricans* (El Algeila); C — *D. desulfuricans* (Norway 4); D — *D. baculatus* (strain 9974); E — *D. vulgaris* (strain Hildenborough)

$g \approx 3.0$ -2.9, showing in some cases a shoulder. *D. vulgaris* cytochrome c_3 is still different since three g_{\max} values are quite discernible at g -values 3.12, 2.97 and 2.87. The g_{med} is sharper when compared to the g_{med} signals from other cytochromes c_3 . It was recently shown that in heme model compounds where the two imidazoles are perpendicular to each other, the EPR signals are extremely anisotropic with g_{\max} values of the order of 3.4 [9,10]. The X-ray structure of cytochromes c_3 from *D. vulgaris* (strain Miyazaki) and *D. desulfuricans* (strain Norway) show that three of the heme groups have the two axial histidines in the

same plane. Only one heme in both these cytochromes has the two axial histidines perpendicular to each other. This heme is also the one most exposed to the solvent [10].

In this context, re-examination of the EPR data indicates that the heme originating g -features above 3.0 in *D. vulgaris* (Hildenborough) and *D. desulfuricans* (Norway strain) should be assigned to the heme having two axial histidyl residues perpendicular to each other. Also this heme has the lowest redox potential (-325 mV) in *D. desulfuricans* (strain Norway 4). However, in *D. gigas* and *D. desulfuricans* (El Algeila Z), the EPR characteristics are different and the signal with high g_{\max} is not present. It is possible that in these proteins all the histidines are coplanar. The X-ray structures have not yet been determined.

Preliminary Mössbauer studies indicate that in the native state there is a weak magnetic interaction between the different hemes at 4.2 K in the absence of an external magnetic field. Also, measurable spectral differences that correlate with the EPR data are observed within this group of multiheme proteins. Comparison of Mössbauer spectra of *D. gigas* cytochrome c_3 (without high g_{\max} features) and *D. vulgaris* (Hildenborough) cytochrome c_3 (having a g_{\max} feature greater than 3.0) show that the magnetic component with the largest magnetic hyperfine constant is present in *D. vulgaris* cytochrome c_3 and absent in the *D. gigas* protein.

The screening of the EPR and NMR characteristics of this class of cytochromes would probably permit a division of this type of proteins into sub-groups with more similar properties, using structural criteria.

ACKNOWLEDGEMENTS

This work was supported by INIC, JNICT, NATO and USAID.

REFERENCES

- [1] H. SANTOS, J.J.G. MOURA, I. MOURA, J. LEGALL, A.V. XAVIER, *Eur. J. Biochem.*, **141**, 283-296 (1984).
- [2] J.J.G. MOURA, H. SANTOS, I. MOURA, J. LEGALL, G.R. MOORE, R.J.P. WILLIAMS, A.V. XAVIER, *Eur. J. Biochem.*, **127**, 151-155 (1982).
- [3] W. SHINKAI, T. HASE, T. YAGI, H. MATSUBARA, *J. Biochem. (Tokyo)*, **87**, 1747-1756 (1980).
- [4] Y. HIGUCHI, M. KUSUNOKI, Y. MATSUURA, N. YASUOKA, M. KAKUDO, *J. Mol. Biol.*, **172**, 109-139 (1984).

- [5] M. PIERROT, R. HASER, M. FREY, F. PAYAN, J.P. ASTIER, *J. Biol. Chem.*, **257**, 14341-14348 (1982).
- [6] A.V. XAVIER, J.J.G. MOURA, J. LEGALL, D.V. DERVARTANIAN, *Biochimie*, **61**, 689-695 (1979).
- [7] D.V. DERVARTANIAN, A.V. XAVIER, J. LEGALL, *Biochimie*, **60**, 321-326 (1978).
- [8] R. CAMMACK, G. FAUQUE, J.J.G. MOURA, J. LEGALL, *Biochim. Biophys. Acta*, **784**, 68-74 (1984).
- [9] G. PALMER, «Annual Summer Meeting of the Biochemical Society on Electron Spin/Paramagnetic Resonance in Biochemistry», Leeds, July 1984.
- [10] A. WALKER, unpublished results cited in ref. [9].
- [11] K. NIKI, personal communication.



PS1.46 — TH

A.R. LINO
J.J.G. MOURA
A.V. XAVIER
I. MOURA

Centro de Química Estrutural, UNL
Complexo I, IST
Av. Rovisco Pais, 1000 Lisboa
Portugal

G. FAUQUE
J. LEGALL

Centre d'Etudes Nucleaires de Cadarache
Departement of Biologie, SRA, Bl. no. 1,
13115 Saint-Paul-lez-Durance
France

CHARACTERIZATION OF TWO LOW-SPIN BACTERIAL SIROHEME PROTEINS

Sulfite reductase catalyses the rather unusual six-electron reduction of SO_3^- to S^- .

Two low molecular weight proteins with sulfite reductase activity have been isolated from *M. barkeri* (DSM 800) [1,2], 23 KD and *Drm. acetoxidans* (strain 5071) [2], 23.5 KD. The enzymes contain one siroheme (iron-tetrahydroporphyrin prosthetic group) and one $[\text{Fe}_4\text{S}_4]$ cluster per minimal molecular weight.

The visible spectrum characteristics of both enzymes are very similar to those of siroheme containing enzymes; however, no band at 715 nm, characteristic of high-spin Fe^{3+} complexes of isobacteriochlorins is observed [3]. Low temperature

EPR studies show that as isolated the proteins siroheme is in a low-spin ferric state ($S=1/2$) with g-values at 2.40, 2.30 and 1.88 for the *M. barkeri* enzyme and g-values at 2.44, 2.33 and 1.81 for the *Drm. acetoxidans* enzyme.

EPR studies on model complexes have shown that ferric isobacteriochlorins with a single axial ligand are always high-spin while ferric isobacteriochlorins with two axial ligands are low-spin. The fact that in these sulfite reductases the siroheme is low-spin ferric suggests that it is six-coordinated. The siroheme of all the other sulfite reductases characterized so far has been shown to be in a high-spin ferric state with EPR features at 6.63, 5.24 and 1.98 [4].

The sulfite reductase from *M. barkeri* and *Drm. acetoxidans* together with the assimilatory sulfite reductase from *D. vulgaris* (strain Hildenborough) [5] which also shows a siroheme in the low-spin state belong to a new class of sulfite reductases. They are small molecular weight proteins with one siroheme and a $[\text{Fe}_4\text{S}_4]$ center per polypeptide chain. In the native state their siroheme is low-spin ferric. The physiological significance of this observation is not known and deserves further investigation.

ACKNOWLEDGEMENTS

This work was supported by Junta Nacional de Investigação Científica e Tecnológica, Instituto Nacional de Investigação Científica (Portugal) and U.S.A.I.D. Grant No. 936-5542-G-SS-4003-00.

REFERENCES

- [1] J.J.G. MOURA, I. MOURA, H. SANTOS, A.V. XAVIER, M. SCANDOLLARI, J. LEGALL, *Biochem. Biophys. Res. Commun.*, **108**, 1002-1009 (1982).
- [2] I. MOURA, A.R. LINO, J.J.G. MOURA, G. FAUQUE, A.V. XAVIER, J. LEGALL, *J. Biol. Chem.* (1985), in press.
- [3] A.M. STOLZENBACH, S.H. STRAUSS, R.H. HOLM, *J. Am. Chem. Soc.*, **103**, 4763-4778 (1981).
- [4] L.M. SIEGEL, D.C. RUEGER, M.J. BARBER, R.J. KRUEGER, N.R. ORME-JOHNSON, W.H. ORME-JOHNSON, *J. Biol. Chem.*, **257**, 6343-6350 (1982).
- [5] B.H. HUYNH, L. KANG, D.V. DERVARTANIAN, H.D. PECK JR., J. LEGALL, *J. Biol. Chem.*, **259**, 15373-15376 (1984).

2. Mechanisms of Metalloprotein Action



PS2.1 — MO

A. FERRI

Istituto di Chimica Biologica
Università
Ferrara
Italy

C. BARTOCCI

A. MALDOTTI

V. CARASSITI

Istituto Chimico
Centro di Studio Sulla Fotochimica e Reattività
degli Stati Eccitati dei Composti di Coordinazione
Università
Ferrara
Italy

MET-80 INVOLVEMENT IN PHOTOREDOX PROCESSES OF CYTOCHROME *c*

The irradiation with light from 280 to 360 nm of deaerated neutral solutions of Fe(III)-Cyt *c* (horse heart) induces the reduction of Fe(III)- to Fe(II)-Cyt *c*. The primary photochemical event is an electron transfer from the sulfur atom of Met-80 (the 6th axial ligand) to iron.

We are currently investigating the possible relation existing between this event and the role of Cyt *c* in biological electron transport systems.

When the photochemically obtained Fe(II)-Cyt *c* was reoxidized by chemical agents, the resulting protein showed a typical low spin absorption spectrum lacking in the 695 nm band. This indicates that a strong-field ligand replaces Met-80 in the sixth coordination position of the central iron [1]. This explanation agrees well with previous observations on more simple systems such as Fe(III)-porphyrin complexes where under irradiation there is an intramolecular electron transfer process between axial ligands and iron [2].

The addition of large excess of azide to a Fe(III)-Cyt *c* solution gave a stable species in which the

added N_3^- replaced the Met-80 sulfur as the iron axial ligand. This clearly indicates that both in the case of Met-80 and N_3^- as the sixth ligand, irradiation gives rise to a ligand to metal electron transfer process.

We have also investigated the behaviour of deaerated solutions of Fe(III)-Cyt *c* in the presence of NADH.

Either in the presence of N_3^- or NADH, the reduction of Fe(III)- to Fe(II)-Cyt *c* was observed, and the Fe(III)-Cyt *c* obtained by reoxidation of the photoproduct had spectroscopic and chromatographic characteristics identical with those of the native one.

The three different systems examined have some important peculiarities:

1) Irradiation of Fe(III)-Cyt *c* in the presence of an external ligand, as N_3^- , capable of replacing Met-80 in the sixth coordination position of Fe(III), leads to the direct oxidation of the ligand and Cyt *c* behaves as a reversible electron acceptor.

2) In the absence of exogenous axial ligands, irradiation induces the reduction of iron, leading at the same time to an irreversible modification of the protein moiety. In fact, after reoxidation, this modified species shows i) a diminished affinity for weak cation exchange resin (CM-Cellulose), ii) a different dependence on pH of high-low spin equilibrium, iii) a more negative E_0 , and iv) a characteristic ESR spectrum. Preliminary data of the aminoacid analysis show that Met-80 results unmodified; this suggests that its sulfur is able to recapture an electron, perhaps from a neighbouring aminoacid residue, finally originating a structurally and functionally modified cytochrome.

3) When NADH is added to Cyt *c* solutions, despite the fact that spectroscopic data indicate that NADH does not replace Met-80 in the sixth axial position (probably because of steric hinderance), the Fe(III) photoreduction quantum yield ($\phi = 4 \times 10^{-3}$) is tenfold that obtained in the absence of NADH.

Since in the conditions used Cyt *c* absorbs more than 90% of the incident light, the above results suggest that, although the primary photochemical act is the electron transfer from Met-80 to Fe(III),

either in the presence or in the absence of NADH, the way by which the oxidized methionine takes back the electron is different in the two cases.

REFERENCES

- [1] C. BARTOCCI, A. MALDOTTI, V. CARASSITI, O. TRAVERSO, A. FERRI, *Inorg. Chim. Acta*, in press.
 [2] See for example:
 C. BARTOCCI, F. SCANDOLA, A. FERRI, V. CARASSITI, *J. Am. Chem. Soc.*, **102**, 7067 (1980).



PS2.2 — TU

HAROLD M. GOFF
 D.V. BEHERE
 ENRIQUE GONZALEZ-VERGARA
 Department of Chemistry
 University of Iowa
 Iowa City, IA 52242
 U.S.A.

THE HEME ENVIRONMENT OF PEROXIDASES: ^{15}N NMR OF BOUND C^{15}N^-

Cyanide ion potentially can provide a useful NMR spectroscopic probe of the heme environment in ferric hemoproteins. Both carbon-13 and nitrogen-15 cyanide signals have been detected for model cyanoiron(III) porphyrin complexes [1-3]. Nitrogen-15 signals suffer less paramagnetic broadening, and accordingly the resonances have also been observed in a far downfield region in hemoglobin, myoglobin, and cytochrome *c* [3]. Coordinated cyanide ^{15}N chemical shifts for peroxidases are reported here for the first time. Chemical shift values are highly distinctive for these enzymes as compared with those for other hemoproteins. Table I presents a summary of ^{15}N chemical shift data for ferric hemoproteins. The striking upfield shift for peroxidase cyanide signals appears to be directed by both strong distal

Table I
 Nitrogen-15 Chemical Shift Values

Compound	CN^- Chemical Shift (ppm) ^{a)}
Myoglobin(CN)	948 ^{b)}
Hemoglobin(CN)	975, 1047 ^{b)}
Cytochrome <i>c</i> (CN)	847 ^{b)}
Horseradish Peroxidase(CN)	578
Lactoperoxidase(CN)	423
Chloroperoxidase(CN)	412
Cytochrome <i>c</i> Hemopeptide-11(CN)	749
ProtDMEFe(CN)(Imidazole)	1015 ^{c)}
ProtDMEFe(CN)(Imidazolate)	738 ^{c)}

a) Rel. to NO_3^- , 25°C, pH 7 to 8. b) Ref. [3]. c) DMSO solvent.

hydrogen bonding effects and by presence of a polar amino acid ligand *trans* to the cyanide residue.

A *trans* ligand influence is seen for the model cyano-imidazole iron(III) protoporphyrin dimethyl ester complex upon deprotonation of the imidazole ligand. An upfield ^{15}N shift of 277 ppm follows generation of the imidazolate species. Putative ligation of a deprotonated cysteinyl sulfur residue in chloroperoxidase can thus be invoked to explain in part the relatively far upfield ^{15}N cyanide resonance in this enzyme. Partial imidazolate character (through proximal imidazole hydrogen bonding) in horseradish peroxidase likewise may influence the upfield character of the coordinated cyanide ion in this enzyme. The relatively high-field ^{15}N signal for lactoperoxidase could be taken to imply presence of a charged *trans* amino acid residue. Although histidyl imidazolate coordination cannot be dismissed for the iron(III) state, separate ^{13}C NMR experiments using CO as a probe are consistent with *trans* imidazole coordination in the carbonmonoxy state.

On the basis of model studies, distal hydrogen bonding of the bound cyanide ion in peroxidases can also be invoked as contributing to the upfield bias for ^{15}N NMR signals in these enzymes. The role of protic solvents in directing an upfield bias for cyanide signals of model compounds has been noted previously [3]. We have also demonstrated that addition of a non-coordinating imidazole to a benzene solution of dicyanoiron(III) protoporphyrin dimethyl ester effects an upfield shift of 82 ppm presumably through Im-H---N-C-Fe hydro-

gen bonding. An upfield shift of 98 ppm for the cytochrome *c* hemopeptide resonance as compared with that of cytochrome *c* may reflect the influence of exposure of the distal site of the model compound to aqueous (hydrogen-bonding) solvent. The striking upfield bias of cyanide resonances for peroxidases as compared with other hemoproteins must parallel the reactivity and heme pocket differences among the biomolecules. Neither hydrogen bonding nor *trans* ligand effects alone provide for exact model compound simulation of the ^{15}N resonance values in peroxidases. Hence both contributions must dictate the level of unpaired spin delocalization at the cyano nitrogen atom. Likewise, these effects may be responsible for the very efficient heterolytic cleavage of peroxides by peroxidase enzymes. The unique ^{15}N chemical shifts for peroxidases are supportive of the concept that a distal hydrogen bonding network [4] and perhaps a polar, basic *trans* ligand are essential for O-O bond activation by peroxidases and by cytochrome P-450.

REFERENCES

- [1] H. GOFF, *J. Am. Chem. Soc.*, **99**, 7723 (1977).
- [2] I. MORISHIMA, T. INUBUSHI, *J. Chem. Soc., Chem. Commun.*, 616 (1977).
- [3] I. MORISHIMA, T. INUBUSHI, *J. Am. Chem. Soc.*, **100**, 3568 (1978).
- [4] H.B. DUNFORD, *Adv. Inorg. Biochem.*, **4**, 41 (1982).



PS2.3 — TH

JAMES D. SATTERLEE

Department of Chemistry
University of New Mexico
Albuquerque, New Mexico 87131
U.S.A.

JAMES E. ERMAN

Department of Chemistry
Northern Illinois University
DeKalb, Illinois 60115
U.S.A.

ELEMENTS OF THE PROPOSED PEROXIDASE MECHANISM ELUCIDATED FROM NMR AND IR STUDIES OF CYTOCHROME *c* PEROXIDASE FORMS

INTRODUCTION

Cytochrome *c* peroxidase (EC 1.11.1.5, ferricytochrome *c*: oxidoreductase; CcP) is a ferriheme enzyme typical of the class of peroxidases. Isolated from baker's yeast, CcP's physiological role is thought to be catalysis of the hydrogen peroxide oxidation of ferrocyclochrome *c* [1,2]. The catalytic cycle of CcP involves heme iron in the +4 oxidation state (oxidized intermediates I,II), and recently the precise steps in the CcP catalytic mechanism have come under intense study [3-6]. The result has been the proposal of a specific mechanism for CcP [6]. In this work we present the results of our recent NMR and infrared spectroscopy studies of ferric and ferrous CcP forms that elucidate specific parts of the Poulos-Kraut mechanism [6].

EXPERIMENTAL

Cytochrome *c* peroxidase was isolated and purified as previously described [7]. Proton Nuclear Magnetic Resonance and infrared spectroscopies were performed as previously described [8,9].

RESULTS AND DISCUSSION

The proposed catalytic mechanism of cytochrome *c* peroxidase (Poulos-Kraut mechanism) involves a

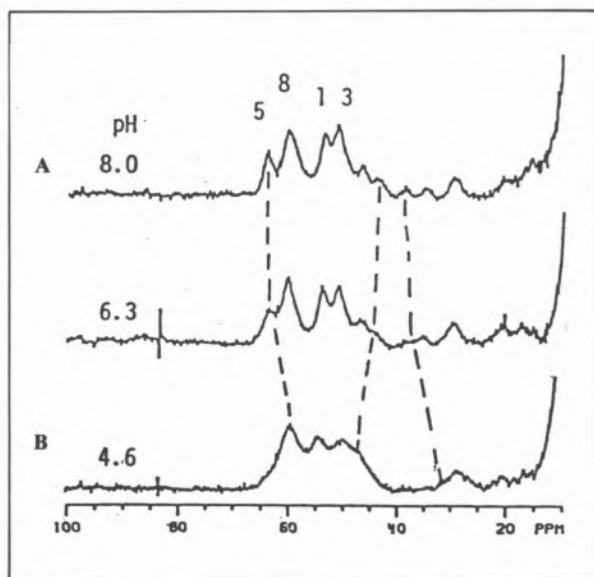


Fig. 1

pH Dependence of CcP-F Hyperfine Proton Resonances

«catalytic triad» of distal amino acid residues that participate in the decomposition of heme coordinated hydrogen peroxide [5,6]. These amino acids, Arg-48, Trp-51, His-52, may function as hydrogen bond donors in fulfilling their function. Elsewhere, we have detected the presence of hydrogen bonding to a heme bound ligand [8], indicating the validity of such a role for the distal amino acids. We show here the effect of pH upon the visible and infrared spectra of CcP-CO and determine the pK of the hydrogen bonded proton as ~ 8.4 . Another aspect of CcP function is the pK at 5.5 that regulates the native enzyme's reactivity and ligand-binding properties. Recently it has been shown that the X-ray difference maps of CcP vs. CcP-F indicate a specific movement of Arg-48 to a position that enables it to hydrogen bond to heme coordinated fluoride ion [10,11]. When we compare these results to our recent NMR data on CcP-F we find that three proton hyperfine resonances (a methyl group and two single protons, Fig. 1A-B) exhibit specific titrations with pK values ~ 5.5 . One of these resonances is an assigned heme methyl group at position 5 of the heme ring [12]. The specificity of this effect indicates that we are probably observing a pH-dependent movement of Arg-48 within the heme pocket. We would like to draw attention to the similarity of the CcP-F pH dependence with that

reported for the native enzyme [9]. It may well be that both pH dependences relate to positioning the Arg-48 so that it may participate in the hydrogen peroxide decomposition [5].

ACKNOWLEDGEMENT

This work has been supported by the National Institutes of Health grant AM30912 and by the Alfred P. Sloan Foundation. J.D.S. is a Fellow of the Alfred P. Sloan Foundation.

REFERENCES

- [1] J. BEETLESTONE, *Arch. Biochem. Biophys.*, **89**, 35 (1960).
- [2] P. NICHOLLS, *Arch. Biochem. Biophys.*, **106**, 25 (1964).
- [3] P.S. HO, B. M. HOFFMAN, C.H. KANG, E. MARGOLIASH, *J. Biol. Chem.*, **258**, 4356-4363 (1983).
- [4] J.E. ERMAN, D.S. KANG, *Fed. Proc.*, **41**, 1207 (1982).
- [5] J. KRAUT, *Biochem. Soc. Trans.*, **9**, 197 (1981).
- [6] T.L. POULOS, J. KRAUT, *J. Biol. Chem.*, **255**, 8199 (1980).
- [7] J.D. SATTERLEE, J.E. ERMAN, *J. Biol. Chem.*, **256**, 1091-1093 (1981).
- [8] J.D. SATTERLEE, J.E. ERMAN, *J. Am. Chem. Soc.*, **106**, 1139-1140 (1984).
- [9] J.D. SATTERLEE, J.E. ERMAN, *Arch. Biochem. Biophys.*, **202**, 608 (1980).
- [10] S. EDWARDS, Ph.D. Dissertation, University of California, San Diego, 1983.
- [11] S. EDWARDS, J. KRAUT, (1984), privileged communication.
- [12] J.D. SATTERLEE, J.E. ERMAN, G.N. LAMAR, K.S. SMITH, K.C. LANGRY, *Biochim. Biophys. Acta*, **743**, 246-255 (1983).



PS2.4 — MO

DAVID MYERS
GRAHAM PALMER
Department of Biochemistry
Rice University
P.O. Box 1892, Houston, TX 77251
U.S.A.

MCD STUDIES ON THE HEME AND TRYPTOPHAN COMPONENTS OF CYTOCHROME *c* PEROXIDASE

We have measured the magnetic circular dichroism of cytochrome *c* peroxidase (CCP) and some of its derivatives from 250-350 nm. Comparison of the changes observed on conversion to the catalytic intermediate (CCP-I) with spectra obtained from horseradish peroxidase and its derivatives and model compounds of protoheme leads us to the conclusion that the observed changes in the MCD spectra reflect conversion of the heme to the ferryl state. No evidence was found for modification of tryptophan in CCP-I.



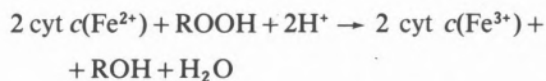
PS2.5 — TU

ELKA V. ELENKOVA
MASANORI SONO
JOHN H. DAWSON
Department of Chemistry
University of South Carolina
Columbia, SC 29208
U.S.A.
ANN M. ENGLISH
Department of Chemistry
Concordia University
Montreal H3G 1M8
Canada

MAGNETIC CIRCULAR DICHROISM STUDIES OF CYTOCHROME *c* PEROXIDASE AND ITS LIGAND COMPLEXES

INTRODUCTION

Yeast cytochrome *c* peroxidase (CCP) is a soluble heme protein, located in the mitochondrial intermembrane space, that catalyzes the two-electron reduction of hydroperoxides by ferrocycytochrome *c* in the following reaction:



CCP contains a noncovalently bound protoheme IX prosthetic group and has a known amino acid sequence. The crystal structure of CCP has recently been published [1]. Despite the above information, questions still remain about the relationship between the physical structure of CCP and its catalytic properties. We have used magnetic circular dichroism (MCD) spectroscopy to probe the electronic, and therefore indirectly the physical, structure of native ferric and ferrous CCP and its complexes with CN^- , N_3^- , F^- , CO , NO and of CCP-Compound I. In order to provide a basis for comparison, the MCD data on CCP, reported here for the first time, have been compared to analogous data from other imidazole-ligated heme proteins such as myoglobin (Mb) and horseradish peroxidase (HRP).

EXPERIMENTAL PROCEDURES

CCP was purified from baker's yeast [2] to $A_{408}/A_{280} = 1.28$. The enzyme concentration was determined from $E_{408}^{mM} = 93$ [3]. Absorption and MCD spectra were obtained as previously described [4]. Samples were examined in 0.1 M potassium phosphate buffer, pH 7.0, at 4°C except where noted.

RESULTS

The MCD spectra of native ferric and alkaline ferric CCP differ from those of the analogous forms of Mb and HRP (data not shown, [5]), presumably as a result of different ligands at the sixth coordination site. Therefore, we have looked at complexes of native ferric CCP, HRP and Mb with known sixth ligands such as F^- , CN^- , N_3^- . The MCD spectrum of the ferric CCP cyanide complex is very similar to the spectra of analogous Mb and HRP ligand adducts [5]. As shown in Fig. 1, the MCD spectra of the azide complexes of CCP, HRP and Mb are very similar in the

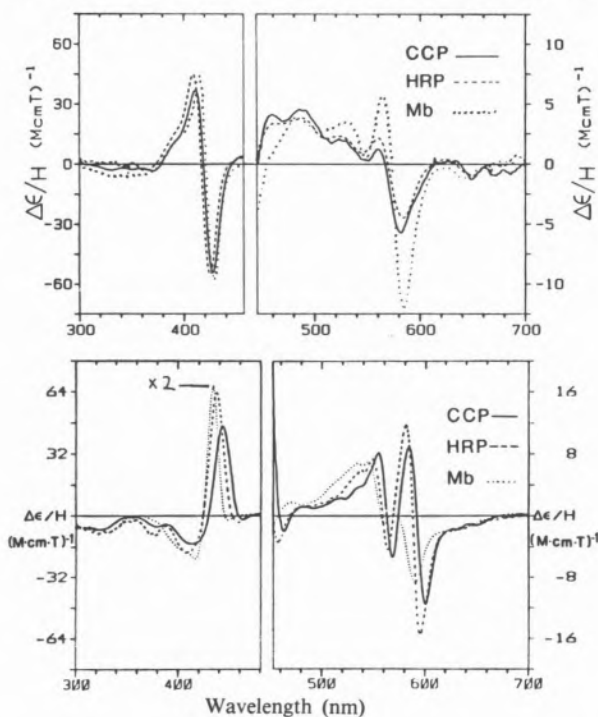


Fig. 1

Top: MCD spectra of the azide complexes of ferric CCP (—), HRP (---) at pH 4.0 and Mb (.....). Enzyme concentrations were 20-35 μM . Bottom: MCD spectra of high spin ferrous CCP (—), HRP (---) and Mb (.....). Enzyme concentrations were 50-65 μM

Soret region, but differ in the visible region, where the spectrum of Mb- N_3 is somewhat different. Ferric CCP-F also has an MCD spectrum that is much more similar to HRP-F than to Mb-F. The native ferrous forms of all three heme proteins are high spin with imidazole at the fifth coordination site. Once again, the MCD spectra of all three proteins are quite similar in the Soret region but, in the visible region, the spectrum of Mb differs noticeably from those of CCP and HRP (Fig. 1). On the other hand, the low-spin ferrous complexes of all three heme proteins with CO and NO display very similar MCD spectra [5]. Lastly CCP-Compound I exhibits a MCD spectrum that is reasonably similar to HRP-Compound II and differs significantly from that of HRP-Compound I (Fig. 2).

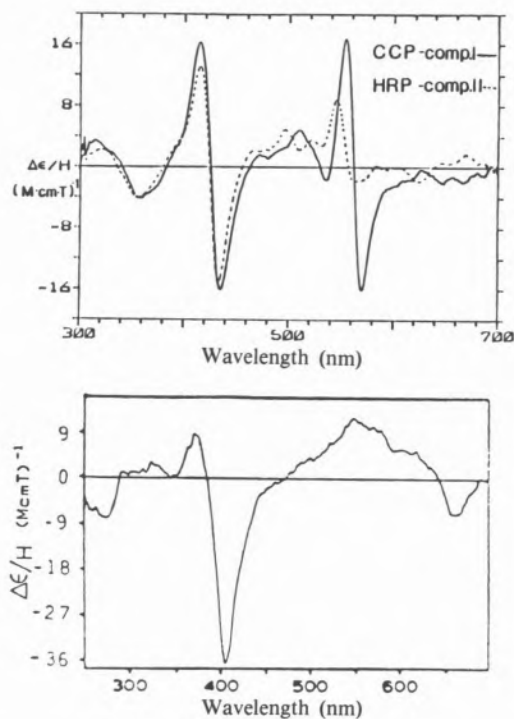


Fig. 2

Top: MCD spectra of 10.3 μM CCP-Compound I (—) and of 13.6 μM HRP-Compound II (---) in 5 mM potassium carbonate, pH 10.5, with equivalent amounts of EtOOH and ascorbate. Bottom: MCD spectrum of HRP-Compound I at 0°C (taken from [7])

CONCLUSIONS

a) Despite similar ligand environments, some differences do exist among the electronic structures of the three imidazole coordinated heme proteins.

When differences exist, CCP and HRP are similar and Mb is different.

b) CCP-Compound I has a similar electronic structure to HRP-Compound II, an Fe(IV) heme iron complex, and differs substantially from HRP-Compound I, which is thought to have an Fe(IV) iron coupled to a porphyrin π cation radical [6]. This result is consistent with the assignment of CCP-Compound I as a Fe(IV) heme iron with an adjacent oxidized amino-acid side chain radical [6].

ACKNOWLEDGEMENTS

This research was supported by NIH Grant GM 26730.

REFERENCES

- [1] B.C. FINZEL, T.L. POULOS, J. KRAUT, *J. Biol. Chem.*, **259**, 13027 (1984).
- [2] C.E. NELSON, E. VL. SITZMAN, C.H. KNAG, E. MARGOLIASH, *Anal. Biochem.*, **83**, 622 (1977).
- [3] T. YONETANI, *J. Biol. Chem.*, **240**, 4509 (1965).
- [4] M. SONO, L.A. ANDERSSON, J.H. DAWSON, *J. Biol. Chem.*, **257**, 8308 (1982).
- [5] E.V. ELENKOVA, M. SONO, J.H. DAWSON, A.M. ENGLISH, in preparation.
- [6] B.M. HOFFMAN, in H.B. DUNFORD, D. DOLPHIN, K.N. RAYMOND, L. SIEKER (eds.), «The Biological Chemistry of Iron», Reidel Publishing Co., Dordrecht, Holland, 1982, p. 391.
- [7] W.R. BROWETT, M.J. STILLMAN, *Biochim. Biophys. Acta*, **660**, 1 (1981).



PS2.6 — TH

JAMES TERNER
 CATHERINE M. RECZEK
 ANDREW J. SITTER
 Department of Chemistry
 Virginia Commonwealth University
 Richmond, VA 23284
 U.S.A.

OBSERVATION OF THE Fe^{IV}=O STRUCTURES OF HORSE RADISH PEROXIDASE COMPOUND II AND FERRYL MYOGLOBIN BY RESONANCE RAMAN SPECTROSCOPY

The formation of intermediate enzymatic states upon reaction of peroxides with heme proteins such as peroxidases and catalases are well known [1]. These intermediate states are commonly known as compounds I and II, which are respectively two and one oxidation equivalents above the resting state of the enzyme (an Fe^{III} heme). Our recent resonance Raman spectroscopy investigations have been aimed towards an understanding of the heme structure of horseradish peroxidase compound II, as well as the similar compound, which is formed upon reaction of hydrogen peroxide with metmyoglobin, known as "ferryl myoglobin" [2].

We have observed the Fe^{IV}=O stretching vibrations on the heme groups of both horseradish peroxidase compound II [3] and ferryl myoglobin [4], giving direct evidence for an Fe^{IV}=O (oxy-ferryl) heme structure. In horseradish peroxidase compound II we have identified the Fe^{IV}=O stretch at 779 cm⁻¹. Upon ¹⁸O substitution the band is observed to shift to 743 cm⁻¹. Additionally we have observed the Fe^{IV}=O stretching vibration at 797 cm⁻¹ in ferryl myoglobin. This is confirmed by a shift to 771 cm⁻¹ upon reaction of samples with ¹⁸O-labelled H₂O₂ [5]. No change in the Fe^{IV}=O frequencies were observed when horseradish peroxidase compound II or ferryl myoglobin were prepared with ²H₂O₂. The frequency

region from 700 to 1000 cm^{-1} is known to contain double bonded metal-oxide stretching frequencies [6]. The 779 cm^{-1} band assigned as the $\text{Fe}^{\text{IV}}=\text{O}$ stretch is considerably higher than the iron-oxygen stretch of ferrimyoglobin hydroxide at 490 cm^{-1} [7] or oxyhemoglobin at 567 cm^{-1} [8]. The $\text{Fe}^{\text{IV}}=\text{O}$ resonance Raman stretching frequency has been previously reported by BAJDOR and NAKAMOTO [9] who observed the $\text{Fe}^{\text{IV}}=\text{O}$ frequency at 852 cm^{-1} for the heme model compound ferryl-tetraphenylporphyrin at 15 K in an O_2 matrix.

The oxyferryl structure for peroxidase compound II was one of several proposed by GEORGE [10]. Until a number of years ago it had been assumed that only ferrous and ferric forms existed in aqueous solution and that the ferryl ion was unstable in the presence of water or proteins. It had been argued that oxidation states of above iron(III) could be described in terms of ferrous or ferric electronic configurations exclusively. In the last decade it was nevertheless shown that stable $\text{Fe}(\text{IV})$ porphyrins could be prepared. There have been a number of proposals regarding the coordination of the oxygen to the iron in $\text{Fe}(\text{IV})$ hemes, such as $\text{Fe}^{\text{IV}}\text{-OH}$, $\text{Fe}^{\text{IV}}\text{-OOH}$, or simply Fe^{IV} . The prevalent configuration, though, has been the $\text{Fe}^{\text{IV}}=\text{O}$ formulation since the double bonded oxygen is known to stabilize transition metals in high oxidation states. We have not been able to observe sensitivity to deuterium substitution, when the ferryl form is prepared by reaction with $^2\text{H}_2\text{O}_2$, for any of the resonance Raman bands of ferryl myoglobin or horseradish peroxidase compound II. LA MAR *et al.* [11] have given NMR evidence for an $\text{Fe}^{\text{IV}}=\text{O}$ group in ferryl myoglobin and horseradish peroxidase compound II based on comparison with low spin $\text{Fe}^{\text{IV}}=\text{O}$ heme model complexes. PENNER-HAHN *et al.* [12] have presented X-ray absorption evidence for an $\text{Fe}^{\text{IV}}=\text{O}$ group in terms of a short iron-oxygen distance.

The resonance Raman data on compound II of horseradish peroxidase [3,13] and ferryl myoglobin [4] show a number of significant differences. The 797 cm^{-1} $\text{Fe}^{\text{IV}}=\text{O}$ frequency of ferryl myoglobin is higher than the observed 779 cm^{-1} $\text{Fe}^{\text{IV}}=\text{O}$ frequency of horseradish peroxidase compound II. The ferryl myoglobin $\text{Fe}^{\text{IV}}=\text{O}$ frequency appears to have a greater amount of cou-

pling with other out-of-plane motions as suggested by a smaller ^{18}O -induced frequency shift. The ferryl myoglobin porphyrin center-to-nitrogen distance, calculated from the resonance Raman band frequencies, is found to be 0.198 nm, which is less than the corresponding figure of 0.199 nm for compound II of horseradish peroxidase. Since the protoporphyrin IX hemes are identical for both ferryl myoglobin and horseradish peroxidase compound II, these differences in structure, as well as the functional differences are likely induced by the differing protein influences in the two species. The smaller porphyrin center-to-nitrogen distance of ferryl myoglobin suggests that the iron atom might be slightly displaced out of the porphyrin plane relative to the iron atom of horseradish peroxidase compound II.

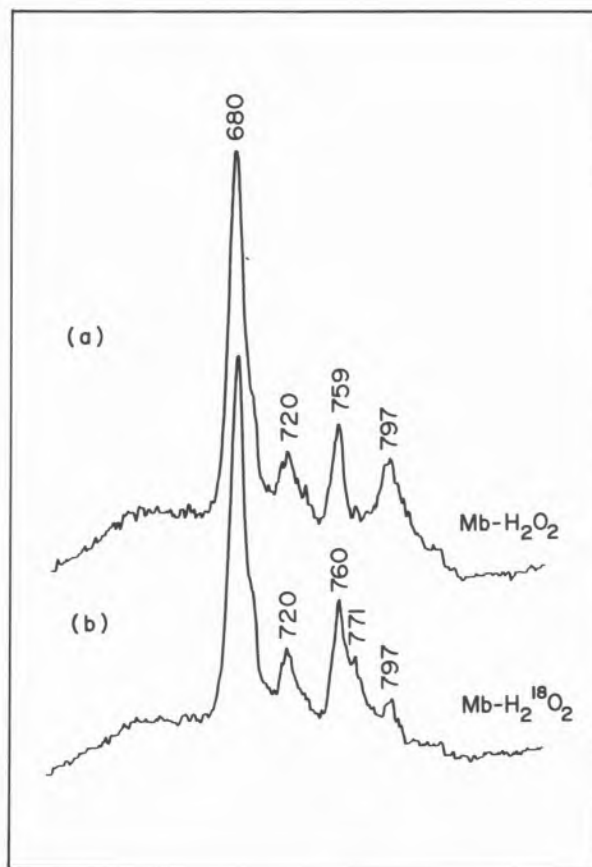


Fig. 1

Resonance Raman spectra in the frequency region from 600 to 1000 cm^{-1} using 406.7 nm excitation, of a) ferryl myoglobin 0.1 M, pH 8.6, 0.05 M tris-acetate; and b) ^{18}O -labelled ferryl myoglobin, showing the shift of the $\text{Fe}^{\text{IV}}=\text{O}$ stretch at 797 cm^{-1} (a) to 771 cm^{-1} (b) upon ^{18}O substitution

ACKNOWLEDGEMENTS

Financial support is acknowledged from the Research Corporation, the donors of the Petroleum Research Fund as administered by the American Chemical Society, and the Jeffress Memorial Trust.

REFERENCES

- [1] W.D. HEWSON, L.P. HAGER, in D. DOLPHIN (ed.), «The Porphyrins», vol. VII, Academic Press, N.Y., 1979, pp. 295-332.
- [2] H. THEORELL, A. EHRENBERG, *Arch. Biochem. Biophys.*, **41**, 442-461 (1952).
- [3] J. TERNER, A.J. SITTER, C.M. RECZEK, *Biochim. Biophys. Acta*, **828**, 73-80 (1985).
- [4] A.J. SITTER, C.M. RECZEK, J. TERNER, *Biochim. Biophys. Acta* (1985), in press.
- [5] A.J. SITTER, J. TERNER, *J. Labelled Compd. Radiopharm.*, (1984), in press.
- [6] D.M. ADAMS, «Metal-Ligand and Related Vibrations», St. Martin's Press, New York, 1968, pp. 235-267.
- [7] S.A. ASHER, T.M. SCHUSTER, *Biochemistry*, **18**, 5377-5387 (1979).
- [8] H. BRUNNER, *Naturwissenschaften*, **61**, 129-131 (1974).
- [9] K. BAJDOR, K. NAKAMOTO, *J. Am. Chem. Soc.*, **106**, 3045-3046 (1984).
- [10] P. GEORGE, *Biochem. J.*, **54**, 267-276 (1953).
- [11] G.N. LA MAR, J.S. DE ROPP, L. LATOS-GRAZYNSKI, A.L. BALCH, R.B. JOHNSON, K.M. SMITH, D.W. PARISH, R. CHENG, *J. Am. Chem. Soc.*, **105**, 782-787 (1983).
- [12] J.E. PENNER-HAHN, T.J. MCMURRY, M. RENNER, L. LATOS-GRAZYNSKY, K.S. EBLE, I.M. DAVIS, A.L. BALCH, J.T. GROVES, J.H. DAWSON, K.O. HODGSON, *J. Biol. Chem.*, **258**, 12761-12764 (1983).
- [13] J. TERNER, D.E. REED, *Biochim. Biophys. Acta*, **789**, 80-86 (1984).



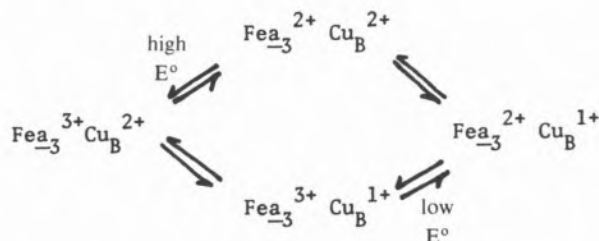
PS2.7 — MO

WALTHER R. ELLIS
 DAVID F. BLAIR
 HSIN WANG
 HARRY B. GRAY
 SUNNEY I. CHAN
 Arthur Amos Noyes Laboratory
 California Institute of Technology
 Pasadena, California 91125
 U.S.A.

**THIN-LAYER
 SPECTROELECTROCHEMISTRY
 OF THE CYT a AND CYT a_3
 SITES IN BEEF HEART
 CYTOCHROME c OXIDASE**

The nature of the intermediates generated in the reduction of fully oxidized cytochrome c oxidase is the subject of intense research in many laboratories. Any mechanistic model for the redox reactions of the four metal sites in this enzyme must be consistent with the information derived from a careful analysis of reduction potential measurements. With this in mind, we report the results of anaerobic spectroelectrochemical [1,2] experiments using optically transparent thin-layer electrode (OTTLE) cells. Attention is focused on the cyt a and cyt a_3 sites in the native enzyme, for which reduction potentials and their dependences on pH, ionic strength, and temperature are presented. The pH-dependence studies (6.8-8.4 range, 10°C, $\mu=0.1$ M) are especially illuminating and may be summarized as follows: 1) the E° value of cyt a exhibits a comparatively weak pH dependence which indicates coupling to a group with $pK_{a,red}$ close to 7.0; 2) cyt a_3 exhibits two distinct E° values — the higher of these is markedly pH-dependent over the entire range examined while the lower is pH-dependent only above pH 7.5. (The details of the spectral deconvolutions will be given in the full paper). Previous interpretations of the redox behavior of these sites have focused on a putative heme-heme interaction (for reviews, see

[3] and [4]). Our measurements of E° for cyt *a* (+350 mV) indicate interactions with Cu_A and Cu_B (this work and our results previously reported for the CO derivative [5]). The problem of two distinct E° values (+240 mV, and +170 mV at pH 8.0) for the cyt a_3 site cannot be explained by interaction with cyt *a*. Instead, we suggest that the metal centers (Cu_B -cyt a_3) at the O_2 -binding site participate in an anticooperative interaction which causes the cyt a_3 center to titrate at two potentials:



An earlier paper [6] noted that the redox state of Cu_B strongly influences the optical properties of one or both of the cytochromes.

Studies of the cytochrome reduction potentials as a function of ionic strength are consistent with a buried cyt *a* site and more solvent-exposed cyt a_3 site.

The temperature dependences of the cyt *a* and cyt a_3 reduction potentials yield ΔS° and ΔH° values, which are compared with results [7] for a variety of high- and low-spin hemoproteins.

Finally, we comment on a recent report [8] that «pulsed» cytochrome *c* oxidase is a peroxide derivative of the fully oxidized enzyme. Anaerobic experiments in oxidative and reductive directions yield slightly different Nernst plots at applied potentials greater than *ca.* +340 mV vs. NHE. Difference spectra clearly show that this behavior is due to the «pulsed» vs. «resting» phenomenon. From these experiments we conclude that «pulsed» cytochrome *c* oxidase can be produced in the absence of O_2 , as previously suggested [9].

REFERENCES

- [1] V.T. TANIGUCHI, W.R. ELLIS, V. CAMMARATA, J. WEBB, F.C. ANSON, H.B. GRAY in K. KADISH (ed.), «Spectrochemical and Electrochemical Studies of Biological Redox Components», Washington, D.C., American Chemical Society, 1972, pp. 51-68.

- [2] W.R. ELLIS, T.V. MORGAN, V.T. TANIGUCHI, P.J. STEPHENS, H.B. GRAY, submitted for publication.
 [3] B.G. MALMSTRÖM, *Quart. Revs. Biophys.*, **6**, 389 (1974).
 [4] M. WIKSTRÖM, K. KRAB, M. SARASTE, «Cytochrome Oxidase», Academic Press, London, 1981.
 [5] a) W.R. ELLIS, D.F. BLAIR, H. WANG, H.B. GRAY, S.I. CHAN, «Abstracts 23rd Int. Conf. Coord. Chem.», 1984, p. 518;
 b) W.R. ELLIS, D.F. BLAIR, H. WANG, H.B. GRAY, S.I. CHAN, submitted for publication.
 [6] D.F. BLAIR, D.F. BOCIAN, G.T. BABCOCK, S.I. CHAN, *Biochemistry*, **21**, 6928 (1982).
 [7] W.R. ELLIS, V.T. TANIGUCHI, unpublished results.
 [8] C. KUMAR, A. NAQUI, B. CHANCE, *J. Biol. Chem.*, **259**, 2073 (1984).
 [9] M. BRUNORI, A. COLOSIMO, P. SARTI, E. ANTONINI, M.T. WILSON, *FEBS Lett.*, **126**, 195 (1981).



PS2.8 — TU

DAVID BICKAR
 A.L. LEHNINGER
 Johns Hopkins Univ. Sch. Med.
 Baltimore MD 21205
 U.S.A.

DIFFERENTIATION OF THE ALLOSTERIC AND REDOX PROPERTIES OF CYTOCHROME *c*

A general procedure has been developed to prepare derivatives of cytochrome *c* in which the iron atom has been replaced with another metal. These derivatives were used to distinguish the allosteric effects of cytochrome *c* binding to cytochrome *c* oxidase from those due to electron transfer. The internal electron transfer from cytochrome *a* to cytochrome a_3 of cytochrome *c* oxidase, a reaction which would seem to be cytochrome *c* independent but which is nonetheless accelerated by cytochrome *c*, was chosen as a test case. Only those cytochrome *c* derivatives which were capable of a reversible one-electron redox reaction facilitated the electron transfer from cytochrome *a* to cytochrome a_3 . This suggests that the effect of cyto-

chrome *c* on the electron transfer from cytochrome *a* to cytochrome a_3 is not due to an allosteric effect but instead involves the electron carrying capacity of cytochrome *c*.

METHODS

Porphyrin cytochrome *c* (p-cytc) was prepared according to the method of DICKINSON and CHIEN [1], except the protein was initially dissolved in 50 mM Hepes, pH 8.0, and later equilibrated with 10 mM Hepes, pH 7.4 by passing down a Sephadex G-25 column.

The metal to be incorporated was prepared by dissolving 100 mM of the divalent metal salt in 250 mM imidazole, and the pH adjusted to 7.0. Dimethylformamide was added to a final concentration of 10% v/v. An equal volume of p-cytc was added, and the solution warmed to 60°C in a foilcovered test tube. Metal incorporation was monitored spectrally, and was usually complete within an hour. After the reaction was complete the reaction mixture was passed down a Sephadex PD-10 column equilibrated with 10 mM Hepes, 1 mM EDTA, pH 7.0. The cytochrome *c* was collected and passed down a Bio-Rad P-10 column, 1.5 × 18 cm, equilibrated with 10 mM Hepes, pH 7.0, with a flow rate of 12 ml/hr. Most samples passed as a single, tight band, although occasionally a band of p-cytc preceded the metal-containing cytochrome *c*.

Internal electron transfer from cytochrome *a* to cytochrome a_3 of cytochrome *c* oxidase was monitored at 431 nm by following the rate of cytochrome a_3 reduction after the addition of 20 mM $\text{Na}_2\text{S}_2\text{O}_4$ to a deoxygenated solution of 2.3 μM cytochrome *c* oxidase in 100 mM Hepes, pH 7.4 [2]. The cytochrome *c* derivative, if present, was added before the dithionite. At 431 nm, the rapid reduction of cytochrome *a* and the slower reduction of cytochrome a_3 cause absorbance changes which are approximately equal in magnitude and opposite in sign.

RESULTS AND DISCUSSION

In Fig. 1 a comparison of the spectral change upon reduction of cytochrome *c* oxidase by dithionite with and without cytochrome *c* is shown. The very rapid initial absorbance decrease is due

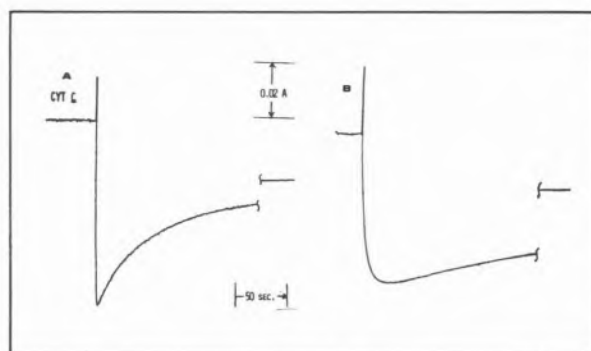


Fig. 1

Acceleration of electron transfer from cytochrome *a* to cytochrome a_3 by cytochrome *c*

to the reduction of cytochrome *a*, while the slower absorbance increase is due to the reduction of cytochrome a_3 . Clearly, in the presence of cytochrome *c* (Fig. 1A), the reduction of cytochrome a_3 is significantly faster than in the absence of cytochrome *c* (Fig. 1B).

Table I shows the effects of different derivatives of cytochrome *c* on the rate of electron transfer to cytochrome a_3 . Only those derivatives capable of a reversible one-electron redox reaction were able to facilitate the electron transfer from cytochrome *a* to cytochrome a_3 . None of the derivatives which were not able to accept and give an electron (p-cytc, Cu-cytc, Zn-cytc, Sn-cytc) showed any significant enhancement of the rate of internal electron transfer, even when present in large excess.

Table I
Catalysis of cytochrome a_3 reduction by cytochrome *c*

Cytochrome <i>c</i>	Rate of Cytochrome a_3 Reduction (% of rate with Fe-cyt <i>c</i>)
Fe-cyt <i>c</i>	100
None	12
Porphyrin cyt <i>c</i>	12
Cu-cyt <i>c</i> (20-fold excess)	14
Zn-cyt <i>c</i>	12
Sn-cyt <i>c</i>	12
Co-cyt <i>c</i>	106
Mn-cyt <i>c</i>	105
Fe-cyt <i>c</i> (reconstit.)	102

Cytochrome *c* oxidase concentration (a_3) = 2.3 μM .
Sodium Dithionite = 20 mM. Cyt *c* was equimolar to oxidase unless noted.

It appears then that the acceleration of electron transfer from cytochrome *a* to cytochrome *a*₃ by cytochrome *c* is not due to an allosteric interaction. Alternative possibilities include a direct involvement of the redox site of cytochrome *c* in the internal transfer of cytochrome *c* oxidase [3,4], or an as yet undefined electron transfer step between cytochrome *a* and cytochrome *a*₃ which is thermodynamically unfavorable. We are currently exploring these possibilities.

REFERENCES

- [1] L.C. DICKINSON, J.C. CHIEN, *Biochemistry*, **14**, 3526-3533 (1975).
- [2] G.D. JONES, M.G. JONES, M.T. WILSON, M. BRUNORI, P. SARTI, A. COLOSIMO, *Biochem. J.*, **209**, 175-182 (1983).
- [3] S.D. FULLER, V.M. DARLEY-USMAR, R. CAPALDI, *Biochemistry*, **20**, 7046-7055 (1981).
- [4] B.C. HILL, C. GREENWOOD, *FEBS Lett.*, **166**, 362-366 (1984).



PS2.9 — TH

STEPHEN L. MAYO
 JUDITH L. CAMPBELL
 JOHN H. RICHARDS
 HARRY B. GRAY
 Department of Chemistry
 California Institute of Technology
 Pasadena, California 91125
 U.S.A.

THE USE OF «NON-PERTURBATIVE» SITE-DIRECTED MUTAGENESIS FOR THE STUDY OF ELECTRON TRANSFER MECHANISMS IN METALLOPROTEINS

Recent advances in genetic engineering methodology have led to the design of proteins that provide new routes to the study of electron transfer mechanisms. Using site-directed mutagenesis [1-3], we have optimized yeast iso-1 cytochrome *c* [4,5] for studying intramolecular electron transfer me-

chanisms via the ruthenium modification method [6-9]. Each mutation was designed [10] to maintain the structural and functional integrity of the protein while providing for the efficient study of the effect of donor/acceptor distance, intervening medium, and donor/acceptor orientation on intramolecular electron transfer rates [11]. Currently, we have completed the generation, isolation, and characterization of three isostructural/isofunctional mutants of yeast iso-1 cytochrome *c*. The first two mutations, Cys-102/Ser and Ser-102/Thr, were designed to circumvent complications in the physical characterizations caused by the cysteine sulfhydryl [12,13]. And the third mutation, His-39/Lys (performed on the Thr-102 mutant), was designed to provide convenient access to the other naturally occurring surface histidine (His-33). This poster is concerned with the design rationale and experimental manifestation of the above mutations and the biological and physical characterization of these systems. It also addresses future directions in this work as well as the potential of using protein engineering and computer graphics methodologies for the design of novel, metalloprotein based, redox catalysts (for example, see [14]).

REFERENCES

- [1] M.J. ZOLLER, M. SMITH, *Methods in Enzymology*, **100**, 468 (1983).
- [2] G. MCFARLAND-DALBADIE, J.H. RICHARDS, *Annual Reports in Medicinal Chemistry*, **18**, 237 (1983).
- [3] J. MESSING, *Methods in Enzymology*, **101**, 20 (1983).
- [4] D.L. MONTGOMERY, B.D. HALL, S. GILLIAM, M. SMITH, *Cell*, **14**, 673 (1978).
- [5] M. SMITH, D.W. LEUNG, S. GILLIAM, C.R. ASTELL, D.L. MONTGOMERY, B.D. HALL, *Cell*, **16**, 753 (1979).
- [6] K.M. YOCOM, J.B. SHELTON, J.R. SHELTON, W.E. SCHROEDER, G. WOROSILA, S.S. ISIED, E. BORDIGNON, H.B. GRAY, *Proc. Natl. Acad. Sci. USA*, **79**, 7052 (1982).
- [7] D.G. NOCERA, J.R. WINKLER, K.M. YOCOM, E. BORDIGNON, H.B. GRAY, *J. Am. Chem. Soc.*, **106**, 5145 (1984).
- [8] R. MARGALIT, N.M. KOSTIĆ, C.-M. CHE, D.F. BLAIR, H.-J. CHIANG, I. PECHT, J.B. SHELTON, J.R. SHELTON, W.A. SCHROEDER, H.B. GRAY, *Proc. Natl. Acad. Sci. USA*, in press.
- [9] N.M. KOSTIĆ, R. MARGALIT, C.-M. CHE, H.B. GRAY, *J. Am. Chem. Soc.*, **105**, 7765 (1983).
- [10] Mutants were designed on an Evans and Sutherland PS300 (an interactive computer graphics system) using the protein engineering simulation capabilities of program BIOGRAF/I (written by S.L. MAYO, B.D. OLAFSON, and W.A. GODDARD III).

- [11] *Prog. Inorg. Chem.*, **30** (1983).
 [12] M. AYROVAINEN, W.R. ELLIS, H.B. GRAY, unpublished results.
 [13] G. PIELAK, A.G. MAUK, M. SMITH, personal communication.
 [14] R. MARGALIT, I. PECHT, H.B. GRAY, *J. Am. Chem. Soc.*, **105**, 301 (1983).



PS2.10 — MO

ALISON BUTLER
 MICHAEL ALBIN
 HARRY B. GRAY
 Arthur Amos Noyes Laboratory
 California Institute of Technology
 Pasadena, California 91125
 U.S.A.

Cu(II)-LADH: A MULTI-SITE REDOX SYSTEM

In pursuit of our goal to understand the factors that govern the redox chemistry of multi-site metalloenzymes, we are investigating various metallo-substituted derivatives of liver alcohol dehydrogenase (LADH). LADH is a dimeric protein (MW ~ 80,000) comprised of identical subunits, each of which contains two Zn²⁺ ions — one at a catalytic site (c) and the other at a structural site (n) [1]. The catalytic Zn²⁺ is coordinated to 2 cysteines, 1 histidine and a water molecule and the other is bound to 4 cysteine residues.

The Cu(II)-substituted derivative, Cu₂(c)Zn₂(n)LADH, has been shown to be a spectroscopic analog of type 1, blue copper sites in proteins [2,3]. We have undertaken the electrochemical and spectroscopic characterization of this and other metal-substituted derivatives, including ones in which a coenzyme such as NAD⁺ has replaced the coordinated water molecule at the active site. These data will be compared with results obtained for other blue copper proteins [4]. In the course of our investigations we have found it necessary

to develop a new purification scheme for the commercially available native protein involving preparative scale isoelectric focusing. The characterization of the separated species (>6) will be presented. Moreover, a modification of a recent preparation [5] allows us to prepare electrophoretically pure derivatives of the type M₂(c)Zn₂(n)LADH. Our approach to understanding long range electron transfer has been through the use of covalent modification (using [Ru(NH₃)₅(H₂O)]^{2+/3+}) of surface histidines of structurally well-characterized proteins to provide specific redox pathways. The structure of LADH [6], examined using computer graphics, reveals five such groups that are available for modification. The distance between these residues and the catalytic site (containing Cu^{II} — fig. 1), including a description of the interposing medium, is given in Table I. We have been able to modify the histidines, enabling the electron transfer energetics between Ru^{II} and Cu^{II} to be evaluated.

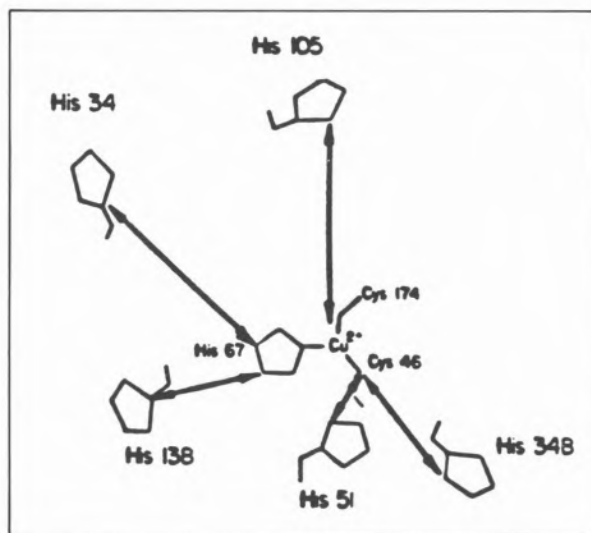


Fig. 1
 Active Site of Cu^{II} substituted LADH illustrating nearest surface histidine residues

Table I
 Structural Data for Cu₂(c)Zn₂LADH

Histidine Residue	Cu-histidine (Å)	«medium»
51	7.4	nothing
348	14.9	Thr-370, Arg-369
138	15.1	Phe-140
105	21.7	Ash-109, Phe-319
34	22.3	Ser-156, Thr-142

REFERENCES

- [1] H. EKLUND, C.-I. BRÄNDÉN in T.G. SPIRO (ed.), «Zinc Enzymes», Wiley-Interscience, 1983.
- [2] W. MARET, H. DIETRICH, H.-H. RUF, M. ZEPPEZAUER, *J. Inorg. Biochem.*, **12**, 241 (1980).
- [3] W. MARET, M. ZEPPEZAUER, J. SANDERS-LOEHR, T.M. LOEHR, *Biochemistry*, **22**, 3202 (1983).
- [4] E.I. SOLOMON, J.W. HARE, D.M. DOOLEY, J.H. DAWSON, P.J. STEPHENS, H.B. GRAY, *J. Am. Chem. Soc.*, **102**, 168 (1980).
- [5] W. MARET, I. ANDERSSON, H. DIETRICH, H. SCHNEIDER-BERNLÖHR, R. EINARSSON, M. ZEPPEZAUER, *Eur. J. Biochem.*, **98**, 501 (1979).
- [6] H. EKLUND, B. NORDSTRÖM, E. ZEPPEZAUER, G. SÖDERLUND, I. OHLSSON, T. BOVIE, B.O. SÖDERBERG, O. TAPIA, C.I. BRÄNDÉN, *J. Mol. Biol.*, **102**, 27 (1976).



PS2.11 — TU

MICHAEL P. DOYLE
SURENDRA N. MAHAPATRO
Department of Chemistry
Trinity University
San Antonio, Texas 78284
U.S.A.

ELECTRON TRANSFER BETWEEN HEMOGLOBIN AND ARENEDIAZONIUM SALTS

Hemoglobin is oxidized to methemoglobin by *p*-nitrobenzenediazonium tetrafluoroborate with first order rate dependence on both the hemoglobin and diazonium salt concentrations [1]. Detailed product analyses have suggested that electron transfer occurs peripheral to the hemo-protein. We now present evidence from substituent dependence in reductive electron transfer to arenediazonium salts for a unique mechanistic duality in reactions with hemoglobin.

Potassium ferrocyanide was employed for comparative evaluation of outer-sphere electron transfer to diazonium salts. Oxidations were performed

under anaerobic conditions in aqueous phosphate-buffered solutions at pH 7.0 and 25.0°C. First order kinetic dependences on both ferrocyanide and diazonium salt were established, and rate constants were obtained from a minimum of four determinations for reactions with each of a representative series of monosubstituted arenediazonium tetrafluoroborates. Excellent correlation was obtained with Hammett σ -constants ($\rho = +4.7$, corr. coef. 0.99) for these second-order rate constants spread from the *p*-methoxy- to the *p*-nitrobenzenediazonium salts over a range of 10^5 .

Second order rate constants were obtained for oxidations of deoxyhemoglobin with the same series of diazonium salts under the same reaction conditions. The plot of these rate constants against those obtained from reactions with ferrocyanide exhibits a break in this expected correlation for *p*-methyl and *p*-methoxy substituents that points to a distinct change in mechanism from that with ferrocyanide. Consistent with this interpretation, reactions of deoxyhemoglobin with *p*-nitro- and *p*-cyanobenzenediazonium tetrafluoroborates, based on the stoichiometry of eq. (1),



resulted in the production of only the corresponding arenes, whereas those with *p*-chloro- through *p*-methoxybenzenediazonium tetrafluoroborates formed only the σ -arylhiron(III) complexes of hemoglobin. The red σ -aryl-heme complexes were separated from globin by previously reported extraction procedures [2] and identified from their characteristic electronic spectra [2,3]. Exposure of these oxygen-sensitive compounds to air resulted in the formation of their corresponding *N*-arylhemin derivatives whose well-defined green zinc(II) complexes were further confirmed by chromatographic and spectroscopic characterization [4,5]. An attractive explanation for the divergent influence of arenediazonium ion substituents on the rates for oxidation of hemoglobin is that hemoglobin provides a channel to iron(II) for those diazonium salts that would undergo electron transfer slowly, if at all, outside of the heme cavity. Once inside the hydrophobic channel, electron transfer produces a neutral arylidazo radical that is more likely to expel dinitrogen and combine with iron(III) than to reenter the hydrophilic

region outside of the heme cavity where hydrogen abstraction is the product-forming process.

The rate for electron transfer is dependent on the distance between the reaction centers [6]. In the case of diazonium salts, "tunneling" to the iron(II) center reduces the distance for approach of the diazonium salt so that the rate for oxidation becomes a function of the kinetic barrier for entrance to the heme cavity. If this kinetic barrier reflects the hydrophilic to hydrophobic crossover, correlation with hydrophobic parameters should be evident. Accordingly, the semilog plot of second order rate constants for those diazonium salts that produced σ -arylrion(III) complexes against π gave a reasonable correlation (slope = 0.67, corr. coef. 0.90), whereas no correlation exists with σ_p or other electronic parameters. In addition, reaction of $^-OOCCH_2C_6H_4N_2^+-p$ with hemoglobin results in a rate for electron transfer that is three times slower than that for the p -toluyldiazonium ion whereas their rates for reduction by ferrocyanide are nearly identical, and the product of electron transfer from hemoglobin to $^-OOCCH_2C_6H_4N_2^+-p$ is phenylacetic acid rather than the σ -arylrion(III) complex.

ACKNOWLEDGEMENTS

We are grateful to the National Institute of Environmental Health Sciences for their support of this research (ES01673 and ES03609).

REFERENCES

- [1] M.P. DOYLE, S.N. MAHAPATRO, S.V. TRAN, *Inorg. Chim. Acta*, **92**, 123 (1984).
- [2] K.L. KUNZE, P.R. ORTIZ DE MONTELLANO, *J. Am. Chem. Soc.*, **105**, 1380 (1983).
- [3] D. LANCON, P. COCOLIOS, R. GUILARD, K.M. KADISH, *J. Am. Chem. Soc.*, **106**, 4472 (1984).
- [4] O. AUGUSTO, K.L. KUNZE, P.R. ORTIZ DE MONTELLANO, *J. Biol. Chem.*, **257**, 6231 (1982).
- [5] S. SAITO, H.A. ITANO, *Proc. Natl. Acad. Sci. USA*, **78**, 5508 (1981).
- [6] a) R. MARGALIT, I. PECHT, H.B. GRAY, *J. Am. Chem. Soc.*, **105**, 301 (1983);
b) H. COHEN, S. EFRIMA, D. MEYERSTEIN, M. NUTKOVICH, K. WEIGHARDT, *Inorg. Chem.*, **22**, 688 (1983).



PS2.12 — TH

MARY AYROVAINEN

HARRY B. GRAY

Arthur Amos Noyes Laboratory
California Institute of Technology
Pasadena, California 91125
U.S.A.

INTRAMOLECULAR ELECTRON TRANSFER IN Ru(NH₃)₅-MODIFIED CYTOCHROMES *c*

In an effort to elucidate the factors governing the rates of electron transfer in biological systems, specifically the roles of distance, relative redox-center orientation and thermodynamic driving force, we have extended our series of semi-synthetic metalloproteins [1] to include derivatives of the cytochromes *c* of tuna and the yeasts *Saccharomyces cerevisiae* and *Candida krusei*.

Well characterized, single site metalloproteins that have been modified at histidine residues by (NH₃)₅Ru³⁺ can be made to undergo intramolecular electron transfer in a flash photolysis experiment utilizing Ru(bpy)₃²⁺* as an external reductant [2]. The yeast cytochromes differ from previously studied systems in that they each contain several potential sites for inorganic modification. Thus, electron transfer in modified derivatives of a single protein, driven by the same free energy change, can be compared, and the problems associated with comparing rates for dissimilar proteins avoided.

Peptide mapping experiments have shown that the iso-1 cytochrome *c* of the yeast *S. cerevisiae* is labeled by the (NH₃)₅Ru³⁺ moiety at His-26, His-33, and His-39. The intramolecular electron transfer rates for the 1:1 Ru:Fe His-33 and His-39 derivatives may yield information regarding the importance of the orientation of redox centers, as the «through-space» pathway from His-33 is perpendicular to the plane of the heme, the native prosthetic group, while His-39 lies in the heme plane at a distance of ~ 13 Å from the heme edge.

The His-33 residue is slightly closer to the Fe³⁺ center, being 11.8 Å from the «pyrrole» nitrogen of the His-18 residue, a ligand to the iron.

Differences between the electron transfer rates of the His-33 derivative of the yeast cytochrome and that of the horse heart cytochrome analog should reflect any medium effects, as only 50% of the amino acid residues in the sequences of these homologous proteins are identical.

The cytochrome of *Candida krusei*, which contains the same accessible residues, His-33 and His-39, has also been modified. It lacks the Cys-102 of the iso-1 cytochrome, which allows for protein dimerization and is a binding site for pentaammine ruthenium.

Tuna cytochrome *c* offers the possibility of studying an intramolecular electron transfer at a higher driving force ($\Delta E^\circ \approx 0.24$ V vs. 0.17 V for the Ru-His derivatives), since it can be modified at the methionine residue 65 and lacks accessible surface histidine residues.

Methods for the synthesis and characterization of the above-mentioned derivatives will be reported.

REFERENCES

- [1] a) K.M. YOCOM, J.B. SHELTON, J.R. SHELTON, W.A. SCHROEDER, G. WOROSILA, S.S. ISIED, E. BORDIGNON, H.B. GRAY, *Proc. Natl. Acad. Sci. USA*, **79**, 7052 (1982);
 b) R. MARGALIT, N.M. KOSTIC, C.-M. CHE, D.F. BLAIR, H.-J. CHIANG, I. PECHT, J.B. SHELTON, J.R. SHELTON, N.A. SCHROEDER, H.B. GRAY, *Proc. Natl. Acad. Sci. USA*, **81**, 6554 (1984).
 c) K. YOCOM, Ph. D. Thesis, California Institute of Technology, 1982.
- [2] a) N.M. KOSTIC, R. MARGALIT, C.-M. CHE, H.B. GRAY, *J. Am. Chem. Soc.*, **105**, 7765 (1983);
 b) K.M. YOCOM, J.R. WINKLER, D.G. NOCERA, E. BORDIGNON, H.B. GRAY, *Chem. Scr.*, **21**, 29 (1983);
 c) D.G. NOCERA, J.R. WINKLER, K.M. YOCOM, E. BORDIGNON, H.B. GRAY, *J. Am. Chem. Soc.*, **106**, 5145 (1984).

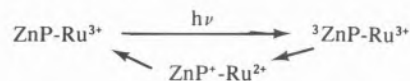


PS2.13 — MO

ANDREW W. AXUP
 ROBERT J. CRUTCHLEY
 HARRY B. GRAY
 Arthur Amos Noyes Laboratory
 California Institute of Technology
 Pasadena, California 91125
 U.S.A.

INTRAMOLECULAR ELECTRON TRANSFER BETWEEN METAL REDOX SITES IN RUTHENIUM-MODIFIED MYOGLOBINS

To understand the parameters affecting intramolecular electron transfer, we have expanded our studies that utilize ruthenium-modified myoglobins. Substitution of zinc-mesoporphyrin IX into modified myoglobin allows the long-lived zinc triplet excited state to act as an electron donor. The protein-bound pentaammineruthenium(III) is then reduced, and the resulting porphyrin cation radical oxidizes the ruthenium(II), returning the system to its initial state.



Triplet decay rates for the zinc-meso substituted native- and pentaammineruthenium(III)(histidine-81)-myoglobins are both 100 s⁻¹. This result indicates that any electron transfer across a distance of 20 Å proceeds at a rate less than 10 s⁻¹. Triplet lifetime quenching is observed in the pentaammineruthenium(III)(histidine-48)-myoglobin(Zn), suggesting rapid electron transfer across a distance of 13 Å. The difference spectrum of the zinc triplet and ground state reveals four isobestics at which direct evidence of the porphyrin cation radicals may be observed. By monitoring the disappearance of the cation radical, the electron transfer rate for the back reaction may be evaluated. A distinguishing feature of these semi-synthetic metalloproteins is the unimolecular nature of the system, enabling the temperature dependence of the electron transfer process to be investigated over a very wide range.



PS2.14 — TU

FRASER A. ARMSTRONG
 H. ALLEN O. HILL
 B. NIGEL OLIVER
 Inorganic Chemistry Laboratory
 Oxford University
 South Parks Road, Oxford OX1 3QR
 England

TOWARDS THE DESIGN OF ELECTROCHEMICAL INTERFACES WHICH PERMIT RAPID AND SPECIFIC HETEROGENEOUS ELECTRON TRANSFER TO REDOX ENZYMES

As a consequence of low electron-transfer probabilities across long distances, rates of redox processes involving biological molecules and membranes may depend upon the promotion of relatively long-lived intermolecular interactions. Selective lowering of activation requirements, through non-covalent stabilisation of molecular orientations which effectively minimise donor-acceptor separation, can provide the basis for recognition and regulation in electron transfer. We are currently approaching the study of these processes through the design of «model» electrochemical interfaces which permit the observation of direct (unmediated) protein electrochemistry. Pyrolytic graphite (PG) has proved to be an intriguing electrode material at which a wide range of redox proteins exhibit well-behaved quasi-reversible electrochemistry upon appropriate «tuning» of solution conditions. The various surfaces of this anisotropic material exhibit widely differing properties.

In a recent communication [1] we drew attention to the contrasting electrochemical reactivity of mitochondrial cytochrome *c* at polished «edge» and freshly cleaved «basal plane» surfaces of PG. Electrochemistry of cytochrome *c* at the hydrophilic «edge» is well-behaved, whereas at the hydrophobic «basal plane», a largely irreversible response is obtained. In subsequent surface analysis

with ESCA we have been able to establish that a high (ca. 50%) surface coverage of various oxygen functionalities (probably including phenols and carboxyls) is readily generated at the «edge» upon polishing in air. By contrast the oxygen coverage at a freshly cleaved «basal» surface is very low. We have now investigated the electrochemical effects of «edge» surface protonation equilibria through titrations of the faradaic current observed at constant overpotential using the rotating disc electrode technique. We have examined the responses of cytochrome *c* (overall positive charge) and spinach plastocyanin (overall negative charge) over the pH range 4-8 (addition of acid or base components to acetate-MES-Tris buffer with 1 mM NaCl background) and compared these with the response of a «marker» probe $\text{Fe}(\text{CN})_6^{3-/4-}$. Results are shown in Fig. 1.

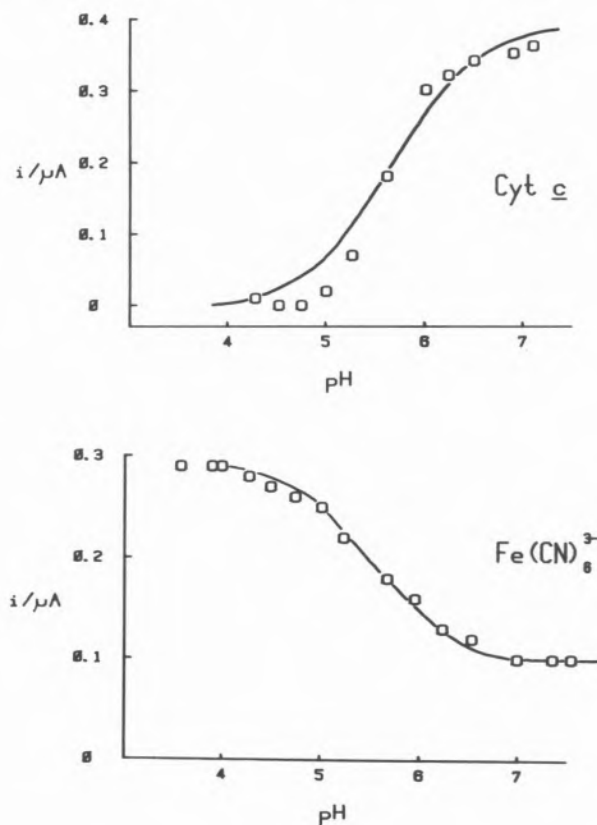


Fig. 1

Current, which registers fast heterogeneous electron transfer to cytochrome *c*, is clearly «switched off» as the pH drops below 6. By contrast, electron-transfer to plastocyanin or $\text{Fe}(\text{CN})_6^{3-/4-}$ (which itself exhibits no intrinsic protonation

equilibria within the range pH 4-8) is «switched on». From these observations we conclude that productive interactions between protein and the hydrophilic «edge» surface may be regulated simply and effectively by electrode surface protonation.

We have previously shown [2] that direct electrochemistry of several negatively charged proteins could be promoted at polished PG by the addition of multivalent cations such as Mg^{2+} or $Cr(NH_3)_6^{3+}$. In order to define the relationship between protein, cation and surface more closely, we have examined the behaviour of «edge» graphite surfaces that have been covalently modified with a variety of Cr(III) complexes. As an illustration of this, voltammetric cycling through potential domains < -800 mV vs. SCE, which induces reduction of $Cr(NH_3)_6^{3+}$ in concentrated aqueous NH_3 , results in the rapid formation of stable Cr(III)-surface complexes. The Cr(III) coverage with reference to carbon, as analysed by ESCA, is 5-10%. The resulting electrode surface is now *inactive* towards cytochrome *c* at pH 8. However, this electrode (but not one with which Cr(III) precycling has not been taken below -800 mV to activate Cr(II-III) «lock-on») shows *well-behaved* electrochemistry with plastocyanin. The roles of surface hydrophobicity and charge in the promotion of fast heterogeneous electron-transfer reactions of proteins are thus clearly evident. Our views on charge may be summarised in Fig. 2, in which a «charge-modified edge» surface (H^+ or discrete Cr(III) sites) is compared with the «native edge», with regard to the responses displayed by cytochrome *c* (positive charge around heme edge) and plastocyanin (negative charge conservatively localised at side of molecule).

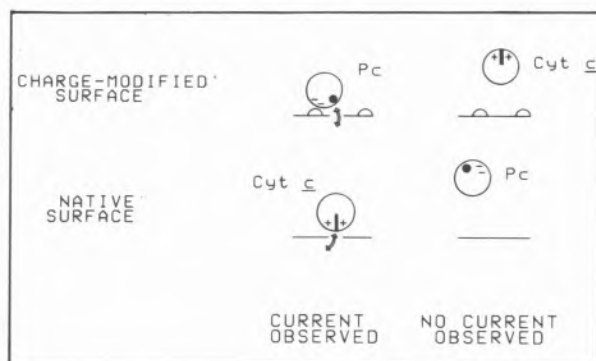


Fig. 2

Experiments currently in progress are directed towards a closer definition of these interactions and, in particular, a detailed understanding of specific charge and steric requirements for efficient and selective electron transfer.

REFERENCES

- [1] F.A. ARMSTRONG, H.A.O. HILL, B.N. OLIVER, *J. Chem. Soc., Chem. Commun.*, 976, (1984).
- [2] F.A. ARMSTRONG, H.A.O. HILL, B.N. OLIVER, N.J. WALTON, *J. Am. Chem. Soc.*, **106**, 921 (1984).



PS2.15 — TH

LARS-GUNNAR FRANZÉN

ÖRJAN HANSSON

LARS-ERIK ANDRÉASSON

Department of Biochemistry and Biophysics

Chalmers Institute of Technology and University of Göteborg

S-412 96 Göteborg

Sweden

EPR STUDIES ON THE FUNCTION OF THE 16, 24 AND 33 kDa SUBUNITS ON THE PHOTOSYSTEM II DONOR SIDE

The three extrinsic subunits (16, 24 and 33 kDa) of Photosystem II (PS II) do not contain any prosthetic groups, but are nevertheless necessary for the function of the oxygen-evolving complex (OEC). The effect of their selective removal from oxygen-evolving PS II particles was examined by monitoring the multiline manganese EPR signal and the decay time of the oxidized secondary donor, Z^+ (EPR Signal II). After washing with 1 M NaCl, which removes the two lighter proteins, only a small Signal II_f is observed. This indicates that rapid electron transfer from the OEC to Z still occurs, *i.e.* that some S state transitions are still functional, despite the loss of oxygen evolution. However, the multiline signal of state S₂ of

the OEC can not be detected in NaCl-washed PS II particles. In contrast, PS II particles inhibited by chloride depletion do show a large multiline signal.

Washing with 1 M $MgCl_2$, which solubilizes all three proteins, leads to the formation of a large Signal II_f after a light flash. After readdition of purified 33 kDa protein, Signal II_f decreases to the control level. Also, the addition of Ca^{2+} results in an acceleration of the reduction of Z^+ . Thus, the 33 kDa subunit seems to be essential for the rapid electron transfer from the OEC to Z. The 16 and 24 kDa subunits are necessary for the higher S state transitions and complete turnover of the OEC.



PS2.16 — MO

PIERRE SÉTIF
H. BOTTIN
T. VÄNNGÅRD
P. MATHIS

Service de Biophysique
Département de Biologie
Centre d'Etudes Nucléaires de Saclay
91191 Gif sur Yvette Cedex
France

ABSORPTION AND EPR STUDIES OF PHOTOSYSTEM I PHOTOCHEMISTRY

The electron transfer chain of the photosystem I reaction center is composed of several membranous components. The primary donor is a specialized chlorophyll molecule called P700, whereas five different electron acceptors have been identified so far: the primary acceptor A_0 , which is presumably a chlorophyll molecule, an acceptor named A_1 , of unknown chemical nature, and F_X , F_B and F_A , all of which are probably iron-sulfur centers. Upon photoexcitation, P700 ejects an electron towards the primary acceptor A_0 . This primary photoact is then followed by electron trans-

fer to a secondary acceptor and so on, thus stabilizing the separation of charges. *In vivo*, the reducing power generated on PS I acceptor(s) is used to reduce $NADP^+$ through soluble ferredoxin while P700⁺ is reduced by plastocyanin, the source of electrons being photosystem II and ultimately water. A cyclic electron transfer around PS I is also probably functioning.

Low temperature study of electron transfer to secondary acceptors [1]

This study was made at 10-30 K on PS I particles which contain only the membranous electron carriers, in order to elucidate the dynamics of electron transfer in PS I, which are poorly understood up to now. By parallel EPR and absorption experiments conducted under different redox conditions, it was possible to put forward an heterogeneity in the pathways for electron transfer and to evaluate the proportions of reaction centers undergoing the different reactions.

Under moderate redox conditions (P700 initially reduced, acceptors initially oxidized in the dark), it was shown by parallel EPR and absorption studies that illumination induces a progressive and irreversible accumulation of the state (P700⁺ ... F_A^-) up to a maximum which represents about two thirds of the reaction centers. In these centers, the irreversible reduction of F_A competes with a recombination reaction ($t_{1/2} = 120 \mu s$) which takes place probably between P700⁺ and the acceptor A_1^- . Heterogeneity for the rate of center F_A reduction was also shown. In the other third of reaction centers, only the recombination reaction of $t_{1/2} = 120 \mu s$ takes place.

Under highly reducing conditions (F_B and F_A initially reduced), the charge separation becomes completely reversible: after a saturating laser flash excitation, 70-80% of the reaction centers undergo a fast recombination with $t_{1/2} = 120 \mu s$ while 10-15% of the centers relax more slowly by recombination between P700⁺ and F_X^- ($t_{1/2} = 50-400 ms$). A quantitative analysis of our data, together with results published in [2,3] show that the electron transfer occurs probably in parallel from A_1 to F_X , F_B and F_A at low temperature.

Yield of P700 triplet state formation [4]

In PS I reaction centers prepared with SDS (CP 1 particles), in which the secondary acceptors are lacking, the primary charge separation giving the biradical ($P700^+ \dots A_0^-$) is followed at any temperature by a recombination process producing some P700 triplet state by the so-called radical pair mechanism. The quantum yield of P700 triplet state formation under low-intensity laser flash excitation has been measured to be 0.45 and 0.35 respectively at 294 K and 6-20 K. From these quantum yield measurements, the yield of P700 triplet state formation from the primary biradical ($P700^+ \dots A_0^-$) was estimated to be about 0.6 at both temperatures whereas superior limits were derived for this yield from double laser flash experiments (0.84 at 294 K and 0.79 at 20 K).

REFERENCES

- [1] P. SÉTIF, T. VÄNNGÅRD, P. MATHIS, *Biochim. Biophys. Acta*, in press.
- [2] M.S. CROWDER, A. BEARDEN, *Biochim. Biophys. Acta*, **722**, 23-35 (1983).
- [3] S.K. CHAMOROVSKY, R. CAMMACK, *Biochim. Biophys. Acta*, **679**, 146-155 (1982).
- [4] P. SÉTIF, H. BOTTIN, P. MATHIS, 1984, submitted for publication.



PS2.17 — TU

DAVID F. BLAIR
JEFF GELLES
SUNNEY I. CHAN

Arthur Amos Noyes Laboratory
California Institute of Technology
Pasadena, California 91125
U.S.A.

**PROTON PUMPING BY CYTOCHROME *c* OXIDASE:
THE IMPORTANCE AND MECHANISMS
OF ELECTRON GATING**

In one important component of the mitochondrial respiratory chain, cytochrome *c* oxidase, exothermic electron transfer reactions are used to drive vectorial proton transport against an electrochemical hydrogen ion gradient across the mitochondrial inner membrane. Previous examinations of the possible mechanisms of this coupled transport phenomenon have focused on the role of redox-linked pKa changes and proton "gates" (mechanisms for controlling the flow of protons). We have explored the question of how electron transfer may be coupled to proton pumping, with particular emphasis upon the role of *electron gating*. The approach involves the solution of the steady state rate equations pertinent to proton pump models which include, to various degrees, the uncoupled (*i.e.*, not linked to proton pumping) electron transfer processes which will necessarily occur in any real electron transfer-driven proton pump. This analysis furnishes a quantitative framework for examining the effects of variations in pKas and reduction potentials, the relationship between efficiency and turnover rate, and the level of electron gating efficiency which is required. Some novel conclusions emerge from the analysis, including: 1) an efficient electron transfer-driven proton pump need not exhibit a pH-dependent reduction potential, for a variety of reasons; 2) very efficient electron gating is a requisite of efficient

electron transfer-driven proton pumping, especially when a reasonable correlation of electron transfer rate and exothermicity is assumed; and 3) a consideration of the importance and possible mechanisms of electron gating suggests that copper sites in proteins are more attractive than heme sites as candidates for a proton pumping function. The ideas derived from the kinetic analysis of a proton pumping cycle have been used to construct a model for proton pumping by cytochrome *c* oxidase which emphasizes the role and possible mechanisms of electron gating. In this model, Cu_A is the site of proton pumping, and electron gating is effected by protonation-linked changes in the coordination environment of this copper ion. A consideration of the nature of the dioxygen reduction reaction demonstrates that *uncoupling* electron transfer from proton pumping may be desirable at particular steps in this reaction; a mechanism for this uncoupling which involves branched electron transfer pathways is suggested.



PS2.18 — TH

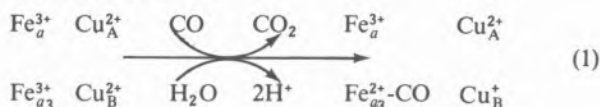
STEPHAN N. WITT
 DAVID F. BLAIR
 JOEL E. MORGAN
 SUNNEY I. CHAN

Arthur Amos Noyes Laboratory
 California Institute of Technology
 Pasadena, California 91125
 U.S.A.

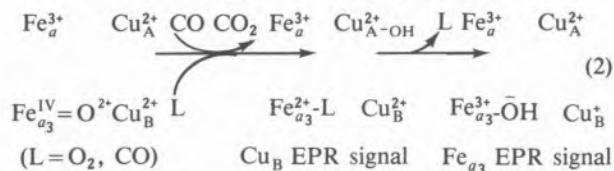
REACTIONS OF CYTOCHROME *c* OXIDASE WITH CARBON MONOXIDE

Cytochrome *c* oxidase oxidizes carbon monoxide to carbon dioxide via three distinct reactions. The «resting» oxidized form of cytochrome *c* oxidase is known to oxidize carbon monoxide very slowly to produce the mixed-valence CO compound ($t_{1/2} = 400$ min. at 277 K) [1,2]. We have observed that the «pulsed» form of cytochrome oxidase also oxidizes carbon monoxide to yield the mixed-valence CO compound. The latter reaction occurs

much faster than with the resting enzyme ($t_{1/2} = 4$ min. at 277 K) [2]. Both reactions may be represented as follows:



In low temperature kinetic experiments using electron paramagnetic resonance (EPR) to follow the reduction of dioxygen by fully reduced cytochrome oxidase, we have recently trapped a highly reactive intermediate at the dioxygen reduction site in which dioxygen is reduced by three electrons. Upon incubation of samples containing this intermediate at 211 K and higher, we observed the formation, within 20 minutes, of two new EPR signals. One EPR signal is due to Cu_B and has been observed previously [3] under different conditions of sample preparation. The other EPR signal is attributable to low spin ferric cytochrome *a*₃. Both of the EPR signals are diagnostic of a partially reduced Fe_{a₃}/Cu_B site. The EPR evidence thus indicates that the three electron-reduced dioxygen intermediate is being reduced by an electron donor other than the metal centers of the protein. Significantly, carbon monoxide is the only available reductant in the low temperature kinetic experiments [4]. Because CO provides two reducing equivalents, and since the Fe_{a₃}/Cu_B site becomes only half reduced, the intermediate that oxidizes CO is by implication a ferryl cytochrome *a*₃/cupric Cu_B couple which is one oxidizing equivalent above the oxidized enzyme (equation (2)). The ferryl cytochrome *a*₃ intermediate is apparently highly reactive, exhibiting significant carbon monoxide oxygenase activity even at 211 K.



REFERENCES

- [1] D. BICKAR, C. BONAVENTURA, J. BONAVENTURA, *J. Biol. Chem.*, **259**, 10777 (1984).
- [2] J.E. MORGAN, D.F. BLAIR, S.I. CHAN, *Bioinorg. J.*, in press.
- [3] B. REINHAMMAR, R. MALKIN, P. JENSEN, B. KARLSSON, L. ANDRÉASSON, R. AASA, T. VÄNNGÅRD, B. MALMSTRÖM, *J. Biol. Chem.*, **255**, 5000 (1980).
- [4] B. CHANCE, C. SARONIO, J.S. LEIGH, *J. Biol. Chem.*, **250**, 9226 (1975).



PS2.19 — MO

ANN M. ENGLISH
TUN-CHEONG CHEUNG
JACK A. KORNBLATT

Enzymology Research Group
Chemistry and Biology Departments
Concordia University
1455 de Maisonneuve Blvd., West, Montreal H3G 1M8, Quebec
Canada

ELECTRON TRANSFER BETWEEN FERROCYTOCHROME *c* PEROXIDASE (CCP^{II}) AND FERRICYTOCHROME *c* (C^{III}): IONIC STRENGTH EFFECTS

CCP (EC 1.11.1.5) catalyzes the peroxidation of C^{II} [1]. The proteins form a tight complex [1,2], and electron transfer within the complex is believed to be rapid because of the large turnover number of CCP [1]. A recent study [3] also reported fast electron transfer ($k = 1.7 \times 10^4 \text{ s}^{-1}$) in the C^{III}:CCP^{II} complex ($\Delta E^\circ = 0.46 \text{ V}$) [4] following photoinduced electron transfer from C^{II} to CCP^{III}. However, when we attempted to corroborate this rate by a more direct measurement, we obtained a value of 0.2 s^{-1} [5], which is surprisingly slow. Since the crystal structures of both proteins and a computer model of the complex have been published [6,7], this is an ideal model to examine the structural factors important in controlling protein-protein electron transfer; thus, we decided to further probe the redox reactivity of the complex.

The stability of the C:CCP complex is reported to decrease significantly at high ionic strength [2]. Therefore, we expected a changeover from unimolecular to bimolecular electron transfer on increasing the salt concentration. We report here our findings on the ionic strength dependence of electron transfer from CCP^{II} to C^{III}.

EXPERIMENTAL

CCP was isolated by the method of NELSON *et al.* [8] and C was obtained from Sigma (type VI).

The reactions were carried out at room temperature as follows: CCP ($3.3 \mu\text{M}$) in 5-200 mM phosphate, pH 7.0, containing 0.008% acetophenone and 2% isopropyl alcohol, was sealed in a 1-cm cuvette and degassed. CCP^{II} was formed in situ by UV-irradiation [9] and 50-200 μl of C^{III} were added. Absorbance changes at 440 and 421 nm were followed using a rapid response spectrophotometer (HP Model 8451A; response time 0.1 s). The former wavelength monitors the decrease in CCP^{II} and the latter, an isosbestic point in the CCP spectrum, monitors the reduction of C^{III}.

RESULTS AND DISCUSSION

In 10 mM phosphate the decay at 440 nm and the growth at 421 nm are both exponential, and give rise to identical rate constants as we reported previously [5]. Initial C/CCP ratios of 0.5:1, 1:1, 2:1, and 3:1 were used and the observed rate constants fall within $0.22 \pm 0.02 \text{ s}^{-1}$. Essentially identical results were obtained at 5 mM phosphate. However, when the phosphate concentration was increased to 15 mM, the observed trace of absorbance vs. time indicated that a second, slower process was occurring. At 25 mM phosphate, the fraction of electron transfer occurring via the slow phase had increased at the expense of the fast phase, and at 50 mM phosphate only the slow phase was apparent. Increasing the phosphate concentration up to 200 mM phosphate caused no further changes in the observed kinetics. The absorbance changes occurring on the slow time scale were also found to be strictly first order and the measured rate constants are again independent of the C/CCP concentration within ratios of 0.5:1-3:1. These results are consistent with the scheme:



where k_t is 0.22 and 0.02 s^{-1} at low and high salt, respectively.

For the reaction to be unimolecular, complex formation between the reactants must be extensive. Since K_D for C^{III}:CCP^{III} is micromolar at low ionic strength [1,2], it is reasonable to suppose that K_D for the reactants is equally small. However, at high ionic strength, extrapolated values of K_D (obtained from absorbance changes on complexa-

tion [2]) are greater than millimolar which should give rise to bimolecular kinetics. This raises the possibility of a second C binding site on CCP which is further removed from the peroxidase heme and therefore does not give rise to spectral perturbations. Alternatively, the slow process could be a rate-limiting conformation change of the peroxidase followed by bimolecular electron transfer.

ACKNOWLEDGEMENTS

This work was supported by grants from FCAC (Quebec) and NSERC (Canada).

REFERENCES

- [1] T. YONETANI, *The Enzymes*, **8**, 345 (1976), and references therein.
- [2] a) J.E. ERMAN, L.B. VITELLO, *J. Biol. Chem.*, **255**, 6224 (1980).
b) C.H. KANG, S. FERGUSON-MILLER, E. MARGOLIASH, *J. Biol. Chem.*, **252**, 919 (1977).
- [3] M.J. POTASEK, *Science*, **201**, 151 (1978).
- [4] $E^\circ (C^{III}/I) = 0.26$ V from G.R. MOORE, D.E. HARRIS, F.A. LEITCH, G.W. PETTIGREW, *Biochim. Biophys. Acta*, **764**, 331 (1984);
 $E^\circ (CCP^{III}/I) = -0.20$ V from C.W. CONROY, P. TYMA, P.H. DAUM, J.E. ERMAN, *Biochim. Biophys. Acta*, **537**, 62 (1978).
- [5] T.C. CHEUNG, Y. HO, A.M. ENGLISH, J.A. KORNBLATT, G. MCLENDON, K. TAYLOR, J.R. MILLER, in preparation.
- [6] a) T.L. POULOS, S.J. FREER, R.A. ALDEN, S.L. EDWARDS, U. SKOGLAND, K. TAKIO, B. ERICKSSON, N. XUONG, T. YONETANI, J. KRAUT, *J. Biol. Chem.*, **255**, 575 (1980);
b) R. SWANSON, B.L. TRUS, N. MANDEL, G. MANDEL, O.B. KALLAI, R.E. DICKERSON, *J. Biol. Chem.*, **252**, 759 (1977).
- [7] T.L. POULOS, J. KRAUT, *J. Biol. Chem.*, **255**, 10322 (1980).
- [8] C.E. NELSON, E.V. SITZMAN, C.H. KANG, E. MARGOLIASH, *Anal. Biochem.*, **83**, 622 (1977).
- [9] B. WARD, C.K. CHANG, *Photochem. Photobiol.*, **35**, 757 (1982).



PS2.20 — TU

PETER JENSEN
MICHAEL T. WILSON*
ROLAND AASA
BO G. MALMSTRÖM

Department of Biochemistry and Biophysics
Chalmers University of Technology and University of Göteborg
S-412 96 Gothenburg
Sweden

CYANIDE-INHIBITION STUDIES ON CYTOCHROME *c* OXIDASE USING RAPID-FREEZE/EPR

It has been known for a long time that cyanide inhibition of partially reduced cytochrome *c* oxidase occurs with a higher rate than with the oxidized or reduced enzyme. This partial reduction has been suggested to cause a conformational change, leading to a transition to a more active enzyme form and thus rendering its cytochrome a_3 site more available to cyanide binding. An enzyme model with only 2 conformational states, *resting* and the more active *pulsed* form, was found to be inadequate and the model had to be extended to include an *open* and a *closed* conformational state of both the pulsed and the resting form. A partial reduction of the 4 redox centers in the oxidase (cytochrome *a* and a_3 , Cu_A and Cu_B) was proposed to be the trigger mechanism for the transition from closed to open conformation, enabling fast cyanide binding.

To investigate the number of electrons necessary to trigger this conformational change, a rapid freeze/EPR investigation was performed. The data shows that the majority of the enzyme molecules in both resting and pulsed state are rapidly inhibited by cyanide when cytochrome *a* and Cu_A have been reduced and this prevents entry of more

* Visiting scientist of the Nobel Institute for Chemistry, 1983.
Permanent address: Department of Chemistry, University of Essex, Wivenhoe Park, Colchester, Essex CO4 3SQ, U.K.

than 2 electrons to the redox sites in the enzyme. In a small fraction (approx. 20%) of the oxidase molecules, however, 3 electron equivalents can enter the enzyme. This is evidenced by the appearance of the low-spin Fe^{3+} HCN-cytochrome a_3 signal at $g=3.55$, indicating that Cu_B must be reduced. Thus, only the fraction of the molecules that has accepted 3 electron equivalents shows a cyanide EPR signal whereas in the remaining 80% of the molecules no cyanide signals could be found. Such heterogeneities due to mixtures of different enzyme forms have been widely reported. The absence of cyanide signals can be explained if cyanide binds as a bridging ligand between the antiferromagnetically coupled cytochrome a_3 and Cu_B sites.

A mechanism with open and closed enzyme forms could have a functional significance in facilitating 2-electron reduction of O_2 , bound at the a_3 - Cu_B site, as a way of avoiding the formation of toxic superoxide ions. Alternatively, such conformational changes could be part of the energy transduction system, e.g. the mechanical part of a proton pump.

Note: A full description of the experiments can be found in *Biochem. J.* (1984), in press.



PS2.21 — TU

LOUISE KARLE HANSON
Department of Applied Science
Brookhaven National Laboratory
Upton, New York 11973
U.S.A.

REDOX PATHWAYS IN *c*-TYPE CYTOCHROMES. POSSIBLE ROLE OF THE BRIDGING SULFUR

Rates of reduction of various classes of heme proteins by small organic reductants have been correlated with the degree of exposure of the heme to solvent [1]. For the *c*-type cytochromes (cyt), the heme edge about ring II is exposed in a cleft. That this exposed heme edge may be important

for electron transfer to and from the heme iron has been considered by many researchers whose suggestions have generally focussed on the peripheral aromatic carbons of the porphyrin. Examination of the van der Waals surfaces of the *c*-type cytochromes of known crystal structure reveals [2] that the sulfur of the thioether bridge that covalently links ring II to the protein (the sulfur of Cys-17 of cyt *c*) protrudes from the heme edge and the protein surface. If delocalization of ring π and iron d orbitals occurs onto this sulfur, then it effectively extends electron density from the aromatic edge of the heme by ~ 2.4 Å. For self-exchange reactions this would decrease the distance over which the electron has to tunnel. For reactions with small molecule reductants and oxidants, the sulfur could provide an accessible site on the protein surface.

The possibility that such delocalization may occur was examined theoretically with charge-iterative extended Hückel calculations. Low-spin Fe(III) and Fe(II) porphins, substituted at the 2- and 4-positions with $\text{C}(\text{CH}_3)\text{HSCH}_3$ groups, and ligated to imidazole and dimethylsulfide were calculated. In the Fe(III) calculations, the acceptor t_{2g} orbital of the iron (either d_{xz} or d_{yz}) was found to be delocalized ~ 25 -30% onto the porphyrin macrocycle, including the bridging sulfurs. The amount of unpaired spin density calculated for a sulfur, 1-4%, is comparable to values obtained for individual aromatic ring carbons. In the Fe(II) case, the t_{2g} orbitals are much less delocalized. However, the porphyrin $a_{1u}(\pi)$ orbital contains a large contribution from the bridging sulfur. Thus, since both porphyrin π and Fe(III) t_{2g} orbitals are predicted to delocalize out to the bridging cysteinyl sulfurs, the calculations suggest that the exposed sulfur off ring II may indeed facilitate electron transfer.

ACKNOWLEDGEMENTS

This work was supported by the Division of Chemical Sciences, U.S. Department of Energy, Washington, D.C., under Contract No. DE-AC02-76CH00016.

REFERENCES

- [1] T.E. MEYER, C.T. PRZYSIECKI, J.A. WATKING, A. BHATTACHARYYA, R.P. SIMONSEN, M.A. CUSANOVICH, G. TOLLIN, *Proc. Natl. Acad. Sci. U.S.A.*, **80**, 6740 (1983).
- [2] G. TOLLIN, M.A. CUSANOVICH, private communication.



PS2.22 — MO

GERALD T. BABCOCK

Department of Chemistry
Michigan State University
East Lansing, Michigan 48824
U.S.A.

GRAHAM PALMER

Department of Biochemistry
Rice University
P.O.B. 1892, Houston, Texas 77251
U.S.A.

JOHN M. JEAN**LEAH N. JOHNSTON****WILLIAM H. WOODRUFF**

Structure and Dynamics Group
Isotope and Nuclear Chemistry Division
Los Alamos National Laboratory
Los Alamos, New Mexico 87545
U.S.A.

TIME-RESOLVED RESONANCE RAMAN STUDY OF THE OXIDATION OF CYTOCHROME OXIDASE BY DIOXYGEN

Cytochrome oxidase catalyzes the rapid and efficient reduction of dioxygen to water. The sequence of events which occurs in this mechanistically complex reaction has been difficult to elucidate owing to the rapid rates of O_2 binding ($\sim 10^8 M^{-1} s^{-1}$) and electron transfer ($\sim 10^5$ - $10^3 s^{-1}$) [1]. To overcome this kinetic obstacle, flash photolysis of the carbon monoxide complex of the reduced protein has been used to initiate the oxygen reduction reaction. This «flow-flash» approach was pioneered by GIBSON and GREENWOOD for room temperature spectrophotometry [2], and adapted by CHANCE and coworkers to low temperature optical, EPR and EXAFS spectroscopies [3]. Although these approaches have clarified the kinetics of the reaction [4], basic structural questions concerning the reaction sequence remain unresolved. Owing to this situation and to uncertainties in extrapolating the low temperature results to room temperature [5], we have combined flow-flash and time-resolved resonance Raman techni-

ques to study the cytochrome oxidase/oxygen reaction at room temperature.

Cytochrome oxidase was prepared from beef heart [6a] and, following anaerobic reduction, combined with carbon monoxide. The solution was loaded into one syringe and oxygenated buffer into a second syringe. These were mounted on a syringe pump and connected to a Gibson-type, four-jet tangential mixer [7]. The mixed solution flowed into the Raman cuvette upon which the Q-switched pulses (10 ns duration) of two Quanta Ray Nd:YAG lasers were focussed. The pulse from the first laser was the 532 nm Nd:YAG second harmonic. Its energy was sufficient to photolyze the CO cytochrome oxidase complex and initiate the O_2 reduction reaction. Raman scattered light from the second, time delayed pulse at 416 nm was dispersed and detected by an EG&G/PARC 1420 diode array detector [8]. The delay times between the green photodissociation and violet probe pulses were variable from 10 ns to approximately 1 ms.

Fig. 1 shows Raman spectra of cytochrome oxidase at various times after initiation of the reoxi-

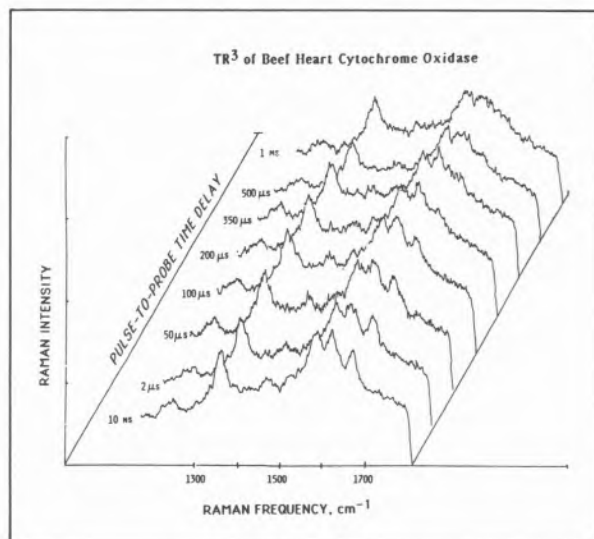


Fig. 1

Raman spectra of cytochrome oxidase at the indicated times following initiation of the oxygen reduction reaction at room temperature

dation reaction. The 10 ns spectrum is that of the photodissociation product of the reduced carbon monoxy enzyme. The oxidation state marker ($\bar{\nu}_4$, $1355 cm^{-1}$) and the a_3^{2+} formyl stretching frequency ($\bar{\nu}_{C=O}$, $1666 cm^{-1}$) [6] are well-resolved

and agree with those recently obtained in an anaerobic study of this species [9]. As the reaction proceeds, the 1355 cm^{-1} mode shifts to higher frequency [10] and the 1666 cm^{-1} mode decreases in intensity, indicating that oxidation of the protein is occurring.

The data in Fig. 1 and the difference spectrum in Fig. 2a indicate that little change in the observed vibrational frequencies occurs during the first $50\text{ }\mu\text{s}$. This observation is surprising in view of time-resolved optical data [2,4] which have clearly established that oxygen addition and, possibly, partial oxidation of the metal centers should have occurred in this time range. The initial oxygen adduct, however, has been suggested to be an oxygenated heme *a* species similar in electronic properties to oxyhemoglobin and oxymyoglobin [3,4,11], which may photodissociate as do the oxygenated O_2 transport proteins [12]. Accordingly, the high light intensity used to record the spectra in Fig. 1 may have photodissociated the oxygen adduct. Evidence that this, in fact, occurs is supplied by the $40\text{ }\mu\text{s}$ difference spectrum (Fig. 2b) obtained by using a low intensity, defocused probe pulse [13]. Under these conditions, the intermediate(s) at $40\text{ }\mu\text{s}$ are shown to have an oxidation state marker ($\bar{\nu}_4$) at 1378 cm^{-1} and spin state marker ($\bar{\nu}_2$) [6] at 1588 cm^{-1} . These frequencies are similar to those reported for oxymyoglobin and oxyhemoglobin. This observation, together with the photolability of the $40\text{ }\mu\text{s}$ transient, provides the best evidence to date that the reoxidation of cytochrome oxidase involves an oxycytochrome *a*₃ species at early times in the reaction.

The difference spectrum in Fig. 2c ($100\text{ }\mu\text{s}$ spectrum minus 10 ns spectrum) was obtained under high light intensity conditions. As opposed to the $40\text{ }\mu\text{s}$ spectrum obtained under these conditions, frequencies characteristic of oxidized, low- or intermediate-spin heme *a* species ($\bar{\nu}_4$, 1374 cm^{-1} ; $\bar{\nu}_2$, 1587 cm^{-1}) are apparent demonstrating that non-photolabile intermediates are formed at $100\text{ }\mu\text{s}$.

The results establish a number of points [14] regarding the reoxidation of cytochrome oxidase by O_2 . First, time-resolved resonance Raman, which is more general and offers greater structural insight than other spectroscopic probes, can be profitably applied to the study of the reaction. Second, the initial intermediates in the reaction

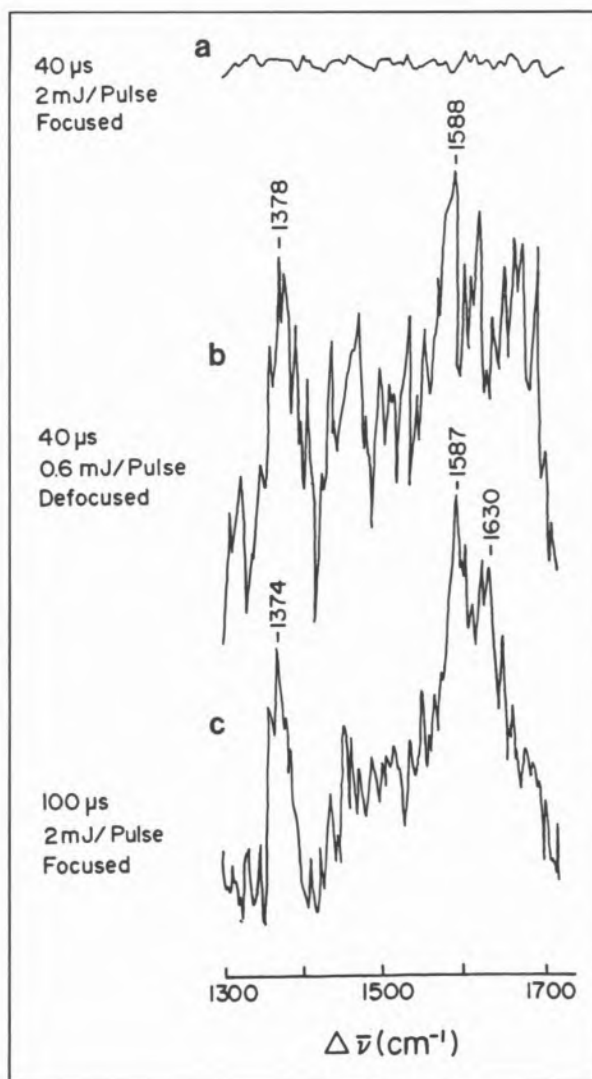


Fig. 2

Estimates of the Raman properties of intermediate species formed during the reoxidation of cytochrome oxidase by O_2 at $40\text{ }\mu\text{s}$ (a,b) and $100\text{ }\mu\text{s}$ (c) after initiation. For spectra (a) and (c) data taken under the high power density conditions of Fig. 1 were used. The scaled spectrum of the reduced photodissociated enzyme (the 10 ns spectrum in Fig. 1) was subtracted from the experimental spectra so that cancellation of the reduced oxidation state marker (1355 cm^{-1}) occurred. In the $40\text{ }\mu\text{s}$ spectrum of (b), the energy of the photolysis pulse was 2.5 mJ , but the probe energy was decreased to 0.6 mJ . A loose line focus at the sample plus a beam mask were used to decrease probe power density further. We estimate that the probe power density used to record spectrum (b) was 30-fold less than in (a), or 1-2 photons per molecule of enzyme in the illuminated volume

mechanism are photolabile. This conclusion may seem to be at odds with low temperature work reported by CHANCE *et al.* [3] who described their compound A as «non-photolabile», but their ob-

servation most likely results from the fact that oxyheme species have much lower photolysis quantum yields than carbon monoxy heme species. Third, at reasonably early times in the reaction ($\sim 100 \mu\text{s}$) the system evolves to a state in which is photostable. Fourth, we note the apparent disappearance at later times ($> 200 \mu\text{s}$) of the $1666/1676 \text{ cm}^{-1}$ cytochrome a_3 formyl C=O stretch. This mode is always observed in stable forms of the enzyme [6] and its absence may suggest unusual reactivity of the formyl group in the turnover dynamics of the enzyme.

ACKNOWLEDGEMENTS

The authors are most grateful to EG&G/Princeton Applied Research Corporation for the loan of the diode array detector OMA system and to Mr. R.T. Ingle for his efforts in supplying the oxidase. Research support from NIH (GM25480 to GTB, GM21337 to GP and AM33679) and the University of Texas Research Institute for partial sabbatical support (GTB) is acknowledged.

REFERENCES AND NOTES

- [1] a) B.G. MALMSTRÖM, *Biochim. Biophys. Acta*, **549**, 281 (1979);
b) M. WIKSTROM, K. KRAB, M. SARASTE, «Cytochrome Oxidase: A Synthesis», Academic Press, London, 1981.
- [2] a) Q. GIBSON, C. GREENWOOD, *Biochem. J.*, **86**, 541 (1963);
b) C. GREENWOOD, Q. GIBSON, *J. Biol. Chem.*, **242**, 1782 (1967).
- [3] a) B. CHANCE, C. SARONIO, J.S. LEIGH JR., *J. Biol. Chem.*, **250**, 9226 (1975);
b) B. CHANCE, C. KUMAR, L. POWERS, Y.C. CHING, *Biophys. J.*, **44**, 358 (1983).
- [4] a) B.C. HILL, C. GREENWOOD, *Biochem. J.*, **218**, 913 (1984);
b) Y. ORII, *J. Biol. Chem.*, **259**, 7187 (1984);
c) G.M. CLORE, L.-E. ANDREASSON, B. KARLSSON, R. AASA, B.G. MALMSTRÖM, *Biochem. J.*, **185**, 139 (1980);
d) J.K.V. REICHARDT, Q.H. GIBSON, *J. Biol. Chem.*, **257**, 9268 (1982).
- [5] F.G. FIAMINGO, R.A. ALTSCHULD, P.P. MOH, J.O. ALBEN, *J. Biol. Chem.*, **257**, 1639 (1982).
- [6] For frequency assignments in the Raman spectrum of cytochrome oxidase see
a) G.T. BABCOCK, P.M. CALLAHAN, J.J. McMAHON, M.R. ONDRIAS, I. SALMEEN, *Biochemistry*, **20**, 959 (1981);
b) W.H. WOODRUFF, R.J. KESSLER, N.S. FERRIS, R.F. DALLINGER, K.R. CARTER, T.M. ANTALIS, G. PALMER, *Adv. Chem. Ser.*, **201**, 625 (1982);
c) S. CHOI, J.J. LEE, Y.H. WEI, T.G. SPIRO, *J. Am. Chem. Soc.*, **105**, 3692 (1983).
- [7] Q.H. GIBSON, L. MILNES, *Biochem. J.*, **91**, 161 (1964).
- [8] W.H. WOODRUFF, S. FARQUHARSON, *ACS Symp. Ser.*, **85**, 215 (1978).
- [9] E.W. FINDSEN, M.R. ONDRIAS, *J. Am. Chem. Soc.*, **106** (1984), in press.
- [10] The apparent oxidation state marker (ν_4) frequencies (cm^{-1}) for the spectra in Fig. 1, in order of increasing probe delay, are as follows: 1355, 1355, 1357, 1364, 1365, 1368, 1369, 1369.
- [11] G.T. BABCOCK, C.K. CHANG, *FEBS Lett.*, **97**, 358 (1979).
- [12] See, for example,
a) T. YAMAMOTO, G. PALMER, D. GILL, I.T. SALMEEN, L. RIMAL, *J. Biol. Chem.*, **248**, 5211 (1973);
b) T.G. SPIRO, T.C. STREKAS, *J. Am. Chem. Soc.*, **96**, 338 (1974);
c) W.H. WOODRUFF, S. FARQUHARSON, *Science*, **201**, 831 (1978);
d) M. NAGUMO, M. NICOL, M.A. EL-SAYED, *J. Phys. Chem.*, **85**, 2435 (1981);
e) J.M. FRIEDMAN, D.L. ROUSSEAU, M.R. ONDRIAS, R.A. STEPENOSKI, *Ann. Rev. Phys. Chem.*, **33**, 471 (1982).
- [13] Control experiments in which the same illumination geometry as that used for Fig. 2b was used to study oxymyoglobin showed that the oxy species, rather than the photodissociation product, predominated in the spectrum. The poor signal-to-noise ratio in Fig. 2b results from the suboptimal illumination conditions necessary to record the spectrum.
- [14] G.T. BABCOCK, J.M. JEAN, L.N. JOHNSTON, G. PALMER, W.H. WOODRUFF, *J. Am. Chem. Soc.*, **106**, 8305 (1984).



PS2.23 — TU

PER-ERIC THÖRNSTRÖM

BASSAM SOUSSI

LARS ARVIDSSON

BO G. MALMSTRÖM

Department of Biochemistry & Biophysics

Chalmers University of Technology

S-412 96 Göteborg

Sweden

**STEADY-STATE KINETICS
OF CYTOCHROME *c* OXIDASE
IN PHOSPHOLIPID VESICLES:
THE EFFECTS OF pH,
IONIC STRENGTH AND D₂O**

The steady-state kinetics of cytochrome *c* oxidase (E.C. 1.9.3.1) reconstituted into phospholipid vesicles has been investigated with a spectrophotometric method, using the high activity region of the reaction between reduced cytochrome *c* and the enzyme. k_{cat} and k_{cat}/K_m were evaluated at high ionic strength ($I=0.5$) in the pH range 5.2-8.6, and the effects of varied ionic strength and D₂O were studied in a more limited pH range. Throughout the investigation, the zwitterionic buffers Hepes [4-(2-hydroxyethyl)-1-piperazine-ethane sulfonic acid] and Mes [2-(*N*-morpholino) ethane sulfonic acid] were used at a concentration of 0.05 M. The ionic strength was changed by inclusion of various amounts of K₂SO₄. The orientation was found to be 65% cytochrome *a* on the outside of the vesicle. Consequently, 65% of the total concentration was used when the kinetic parameters were calculated.

Principal results and conclusions are as follows: At high ionic strength ($I=0.5$) k_{cat} increases with decreasing pH from 35 s⁻¹ at pH 8.6 to 1000 s⁻¹ at pH 5.2. This result is qualitatively in accordance with one earlier study, with the enzyme in detergent solution, whereas most other investigators have reported a pH maximum for k_{cat} . The pH dependence of k_{cat} cannot be simulated with less

than three pK_a values, which suggests at least three sites, each increasing the activity on protonation. Our estimated pK_a values (7.8, 6.8 and 4.5) are within experimental uncertainty the same as those found in detergent solution.

Variation of the ionic strength from $I=0.05$ to $I=0.5$ has little effect on k_{cat} but k_{cat}/K_m , and thus K_m , is a function of ionic strength. The velocity at a given cytochrome *c* concentration generally decreases with increasing ionic strength. At low pH (6.2) the effect seems to be more complicated as our results show a maximum of k_{cat}/K_m around $I=0.25$. k_{cat}/K_m was essentially constant at high ionic strength ($I=0.5$) in the pH range 5.2-8.6, *i.e.* K_m also increases with decreasing pH. This suggests that the pH effect is mainly on the rates of catalytic steps, rather than on the combination between enzyme and substrate. It is not obvious which particular steps are affected.

The effects of D₂O were studied in the pD range 5.8-7.2. Taking into account both the difference between pH and pD and the D₂O-induced shift in pK_a ($pK_a^D = pK_a^H + 0.54$) we found that D₂O decreases k_{cat} by a factor of about 2. k_{cat}/K_m is, on the other hand, approximately the same in H₂O and D₂O. From the D₂O-data we conclude that an intramolecular proton transfer step is at least partially rate limiting. This contradicts the common assumption that the product dissociation step of the reaction is rate limiting.

Based on our results and a minimal mechanism involving 13 consecutive steps in the catalytic cycle of cytochrome oxidase, we argue that an intramolecular step which involves both electron and proton transfer is rate limiting. The step is suggested to be important in the function of cytochrome oxidase as a proton pump.



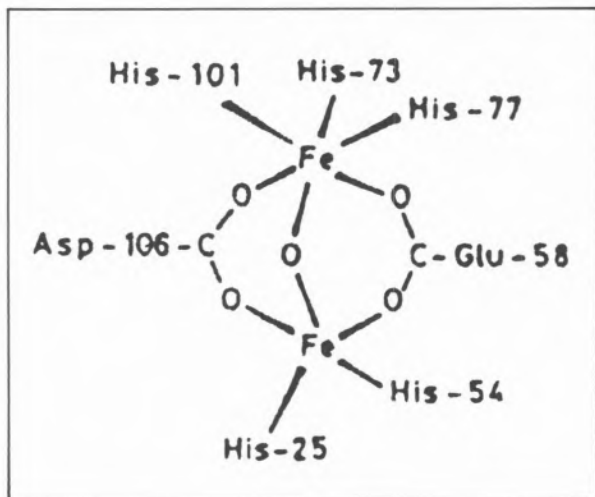
PS2.24 — TH

G.D. ARMSTRONG
T. RAMASAMI
A.G. SYKES
Department of Inorganic Chemistry
The University
Newcastle upon Tyne NE1 7RU
England

ACTIVE SITE CHEMISTRY OF OCTAMERIC AND MONOMERIC HEMERYTHRIN FROM *THEMISTE ZOSTERICOLA*

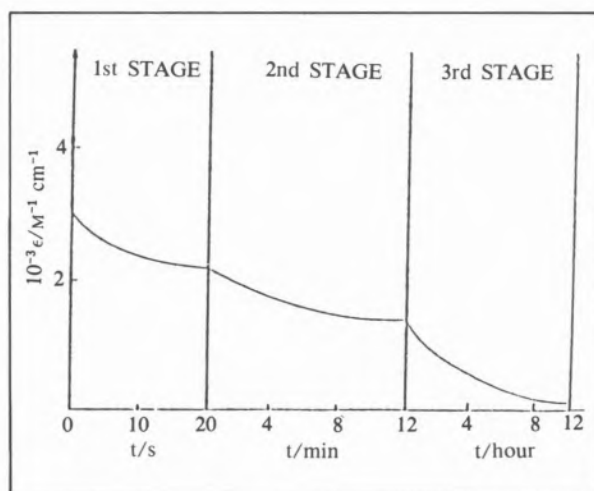
Hemerythrin [1,2] was obtained from the coelomic fluid of *Themiste Zostericola* as the octamer (M.Wt. 108,000), which has eight identical subunits, and from the retractor muscle as the monomer, metmyohemerythrin (M.Wt. 13,900). Each subunit is known to contain a binuclear Fe active site capable of binding O₂.

The structure of the active site of the met, Fe(III,III), form is as shown [3]. Coordination of hydroxide (corresponding to an acid dissociation of pK_a ca. 8.0) is known to occur at the five-coordination iron. Using EXAFS [4] it has been demonstrated that the deoxy, Fe(II,II), form has no μ -oxo bridge and there is an increase in the Fe-Fe distance.



Reduction of octameric methemerythrin has been studied by WILKINS *et al.* using dithionite and a semi-met, Fe(II,III)₈, intermediate has been successfully characterised. It has also been proposed that further reduction proceeds by long-distance intramolecular electron-transfer (ca. 30 Å yielding Fe(II,II) and Fe(III,III) subunits [5], the latter being rapidly re-reduced to Fe(II,III).

To further augment this study, and monitor precisely the latter stages of reduction, detailed investigations of the reduction of methemerythrin and metmyohemerythrin using as one-electron reductants the Sargeson cage complexes [Co(sep)]²⁺ (E° -0.30 V) and [Co(sarCl₂)]²⁺ (E° -0.13 V), the triazacyclononane complex [Co(9-aneN₃)]²⁺ (E° -0.40 V) and [Cr(bipy)₃]²⁺ (E° -0.26 V) have been carried out. Three stages are clearly seen in the reduction of methemerythrin (pH 6.3 - 9.0). The figure shown is for a reaction monitored at 400 nm with MetHr = 1.0 × 10⁻⁴ M (expressed as monomer), [Co(sep)]²⁺ = 1.4 × 10⁻³ M, pH 6.3, I = 0.15 M (Na₂SO₄). The rate of the first stage shows a first-order dependence on reductant. Rate constants for stages 2 and 3 (3.7 × 10⁻³ and 1.2 × 10⁻⁴ s⁻¹ respectively, pH 8.2) show no dependence on the concentration or nature of the reductant consistent with an intramolecular process. Hydrogen-ion dependencies are observed for the first and second stages. Rate constants for stage 3 are however independent of [H⁺].



Consumption of reductant in the different stages was determined using [Cr(phen)₃]²⁺ which has an intense absorbance at 850 nm ($\epsilon = 6500 \text{ M}^{-1} \text{ cm}^{-1}$).

It was found that eight equivalents (per octamer) of reductant are consumed in the first stage followed by four equivalents in each of stages 2 and 3. These results were confirmed using the strong reductant $[\text{Cr}(\text{edta})]^{2-}$ ($E^\circ - 1.0 \text{ V}$) which enabled spectra to be recorded more precisely at the end of each stage.

Reduction of metmyohemerythrin also occurs in three stages at pH 8.2. The first stage gives a first-order dependence on reductant. The rate constants for stages 2 and 3 (4.0×10^{-3} and $9.0 \times 10^{-4} \text{ s}^{-1}$ respectively) show no dependence on the nature or concentration of the reductant. Further detail of these different stages will be presented.

The existence of a quarter-met intermediate in the reduction of methemerythrin (product of the second stage) indicates that the Fe(II,III) units generated at the end of the first and second stages are not identical. Furthermore, comparison of the rate constants for the second stage of the reduction of methemerythrin and metmyohemerythrin suggests a common rate-controlling conformational change in both cases.

REFERENCES

- [1] I.M. KLOTZ, D.M. KURTZ, *Acc. Chem. Res.*, **17**, 16 (1984).
- [2] R.G. WILKINS, P.C. HARRINGTON, *Adv. Inorg. Biochem.*, **5**, 52 (1983).
- [3] R.E. STENKAMP, L.C. SIEKER, L.H. JENSEN, *J. Amer. Chem. Soc.*, **106**, 618 (1984).
- [4] W.T. ELAM, E.A. STERN, J.D. MCCALLUM, J.S. LOEHR, *J. Amer. Chem. Soc.*, **105**, 1919 (1983).
- [5] R.G. WILKINS, P.C. HARRINGTON, *J. Amer. Chem. Soc.*, **103**, 1550 (1981).



PS2.25 — MO

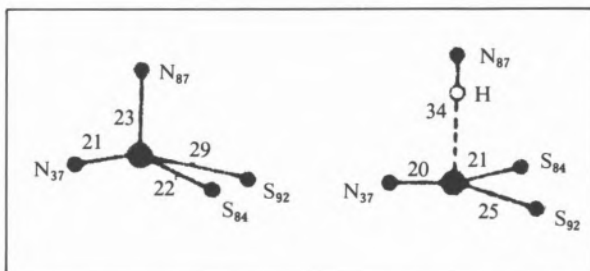
J.D. SINCLAIR-DAY

A.G. SYKES

Department of Inorganic Chemistry
The University
Newcastle upon Tyne
England

ACID DISSOCIATION CONSTANTS FOR THREE PLASTOCYANINS

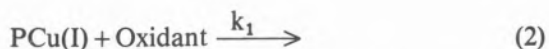
The metalloprotein plastocyanin (M.Wt. 10,500) consists of 99 amino acids and a single (Type I) Cu active site [1]. It is involved in electron transport ($E^\circ \sim 360\text{mV}$) in the chloroplast where it functions as an oxidant for cytochrome f and a reductant for P700. The Cu atom is coordinated by His37, Cys84, His87 and Met92 (NSNS donor atom set) in a distorted tetrahedral arrangement for both Cu oxidation states. Proton induced deactivation of the active site [2] has been shown to correspond to dissociation of His87 yielding a redox-inactive three-coordinate structure [3].



The acid dissociation constant, K_a , can be determined using NMR



spectroscopy [4] which allows direct observation of the relevant protonation. The kinetic method employs oxidants such as $[\text{Fe}(\text{CN})_6]^{3-}$ and $[\text{Co}(\text{phen})_3]^{3+}$ to probe the reactivity of the protein in the pH range of interest, where PCu(I) but not HPCu(I) is redox active (2).



The dependence (3) enables K_a to be determined.

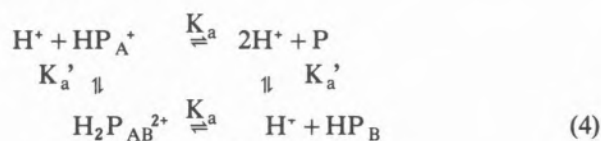
$$k(\text{M}^{-1}\text{s}^{-1}) = \frac{k_1 K_a}{[\text{H}^+] + K_a} \quad (3)$$

Kinetic determination of pK_a 's using $[\text{Fe}(\text{CN})_6]^{3-}$ as an oxidant are in satisfactory agreement with those by NMR. However, the use of $[\text{Co}(\text{phen})_3]^{3+}$ yields pK_a 's which are consistently higher, see Table.

Table
Experimentally determined pK_a 's for different plastocyanins

Source	NMR	$[\text{Fe}(\text{CN})_6]^{3-}$	$[\text{Co}(\text{phen})_3]^{3+}$
Parsley	5.7	5.5	6.1
Spinach	4.9	4.9	5.7
<i>A. variabilis</i>	5.1	4.8	5.5

The results may be explained by introducing a second protonation effective in the oxidation by $[\text{Co}(\text{phen})_3]^{3+}$ as in (4)-(6). Sites for the two independent protonations are designated A and B where A refers to the active site protonation at His87.

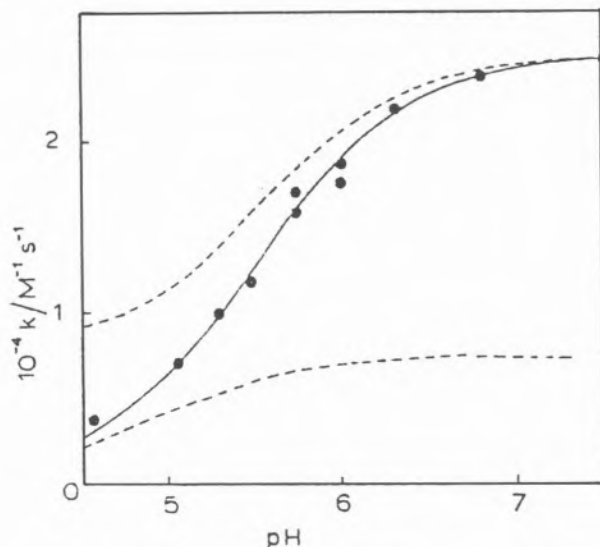


This scheme gives (7)

$$k(\text{M}^{-1}\text{s}^{-1}) = \frac{k_1 K_a K_a' + k_2 K_a [\text{H}^+]}{K_a K_a' + K_a' [\text{H}^+] + K_a [\text{H}^+] + [\text{H}^+]^2} \quad (7)$$

The figure shows the best fit for spinach PCu(I) using K_a as determined by NMR, and indicates the component profiles arising from each protonation. This procedure gives pK_a ' values for parsley (5.8), spinach (5.7) and *A. variabilis* (5.7).

The effect of K_a' is consistent in simple electrostatic terms with a proton associating at, or near, the site of electron transfer for a positively charged oxidant. The involvement of K_a' in the oxidation by $[\text{Fe}(\text{CN})_6]^{3-}$ is small or negligible indicating



that oppositely charged complexes use different binding locations on plastocyanin. These conclusions are consistent with earlier NMR studies [5,6] which define binding sites close to His87 and Tyr83 for $[\text{Fe}(\text{CN})_6]^{3-}$ and $[\text{Co}(\text{phen})_3]^{3+}$ respectively. We therefore propose the protonation corresponding to K_a' is at the binding site near to Tyr83.

The pK_a' value of ~ 5.7 is higher than expected for a single carboxylate residue but may be explained in terms of two carboxylates sharing one proton. There are a number of carboxylate residues close to Tyr83, notably the highly conserved 42-45 residues in plant plastocyanins, also Asp42 and Glu85 in *A. variabilis* plastocyanin. These could provide an adequate site for protonation and association of $[\text{Co}(\text{phen})_3]^{3+}$. The amino-acid sequence for parsley plastocyanin indicates deletions at 58 and 59 which could explain the higher pK_a value.

REFERENCES

- [1] A.G. LAPPIN, in H. SIGEL (ed.), «Metal Ions in Biological Systems», vol. 13, pp. 15-71.
- [2] M.G. SEGAL, A.G. SYKES, *J. Am. Chem. Soc.*, **100**, 4585 (1978).
- [3] H.C. FREEMAN, in J.P. LAURENT (ed.), «Coordination Chemistry», vol. 21, Pergamon, Oxford, 1981, p. 29.
- [4] J.L. MARKLEY, C.L. KOJIRO, *FEBS Lett.*, **162**, 54 (1983).
- [5] P.M. HANDFORD, H.A.O. HILL, R.W.-K. LEE, R.A. HENDERSON, A.G. SYKES, *J. Inorg. Biochem.*, **13**, 83 (1980).
- [6] D.J. COOKSON, M.T. HAYES, P.E. WRIGHT, *Biochim. Biophys. Acta*, **591**, 162-176 (1980).



PS2.26 — TH

M.E. SANDER
H. WITZEL
Institute of Biochemistry
University of Münster
F.R.G.

CARBOXYPEPTIDASE A, EVIDENCE FOR AN ANHYDRIDE INTERMEDIATE

In the reaction of carboxypeptidase A, a Zn^{2+} containing exopeptidase, it is still in discussion, whether Glu-270 forms a covalent anhydride intermediate with the acyl group of the substrate or is involved in a general base catalysis mechanism. Evidence for an acyl enzyme has been obtained at $-60^{\circ}C$ only spectroscopically with one ester substrate, the *O*-(*trans*-*p*-chlorocinnamoyl)-L-phenyllactate (Makinen).

Since it should be possible to trap such an anhydride intermediate with nucleophiles under conditions where accumulation can be expected, we incubated the enzyme at $-75^{\circ}C$ with several hippuric esters or -peptides in the presence of hydroxylamine and *O*-methylhydroxylamine. Thus the enzyme could be inactivated, while it was still active in the blank probe with the same concentration of hydroxylamine. Inactivation was most efficient with hippuryl glycolic acid, a relatively slow substrate for the carboxypeptidase A. A hydroxamate group within the protein could be identified by the visible spectrum of its Fe^{3+} -complex, which was characteristic for that of a glutamic acid. Such a hydroxamate group, responsible for the inactivity of the enzyme and produced only in the presence of a substrate, can be expected, if this glutamic acid forms an anhydride intermediate.

Furthermore we could stabilize the acyl enzyme by adding denaturing agents at $-60^{\circ}C$ during the reaction with hippuryl-L-phenylalanin or *O*-(*trans*-*p*-chlorocinnamoyl)-L-phenyllactate. This loaded enzyme was reduced with $[^3H]NaCNBH_3$. After complete hydrolysis of the protein the $[^3H]$ α -ami-

no- δ -hydroxyvaleric acid, which is formed as the reduction product of an acylated glutamic acid, could be identified by high voltage paper electrophoresis and paper chromatography. These results can also be interpreted only on the basis of an anhydride intermediate.

A tryptic digest of the reduced protein gives evidence that the glutamic acid in question is Glu-270.



PS2.27 — TH

JUNZO HIROSE
MASAHIDE NOJI
YOSHINORI KIDANI
Faculty of Pharmaceutical Sciences
Nagoya City University
Tanabe-dori 3-1, Mizuho-ku, Nagoya 467
Japan
RALPH G. WILKINS
Department of Chemistry
New Mexico State University
Las Cruces, N.M. 88003
U.S.A.

THE INTERACTION OF ZINC IONS WITH ARSANILAZOTYROSINE-248-CARBOXYPEPTIDASE A

Arsanilazotyrosine-248-carboxypeptidase A([(Azo-CPD)Zn]) [1] is a derivative modified with chromophoric arsanilazotyrosine-248 residue. [(Azo-CPD)Zn] has almost the same activity as native carboxypeptidase A. It has proven particularly useful for studying the conformation of the enzyme [2] and metal binding to the apo-enzyme [3]. At pH 7.5-8.8, the arsanilazotyrosine-248 residue forms an intramolecular complex with the zinc ion at the active site and gives a characteristic optical absorption at 510 nm.

When excess zinc ions were added to [(Azo-CPD)Zn], the characteristic red color, which arose from the intramolecular complex of the arsanilazotyrosine-248 residue with the active

site zinc of the enzyme, changed to yellow (Fig. 1) Excess zinc ions also inhibited the peptidase activity of [(Azo-CPD)Zn]. The interaction between

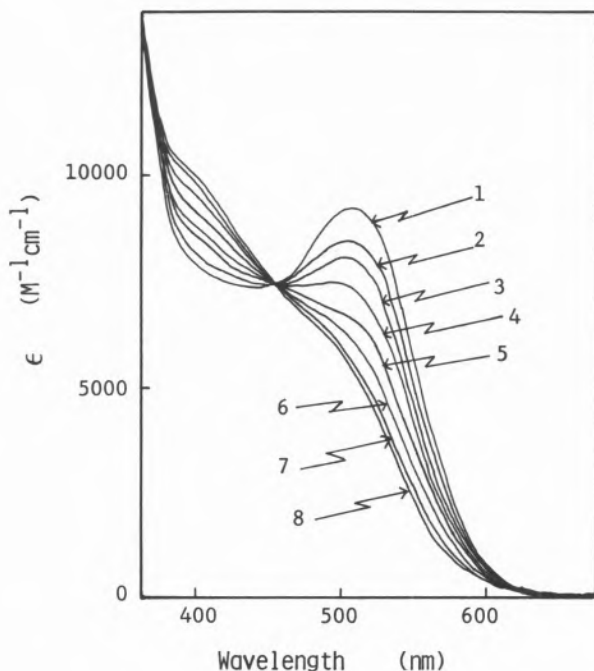
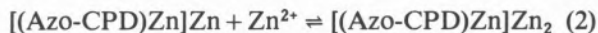
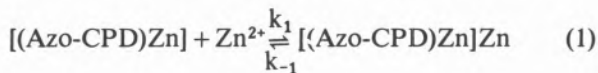


Fig. 1

Effect of excess zinc ions on the absorption spectrum of arsanilazotyrosine-248-carboxypeptidase A. [(Azo-CPD)Zn] = 3.4×10^{-5} M, Temp 25°C. pH 8.2, 0.05 M Tris-HCl buffer (0.5 M NaCl).

1, without zinc ions; 2, $Zn^{2+} = 10^{-5}$ M; 3, $Zn^{2+} = 2.0 \times 10^{-5}$ M; 4, $Zn^{2+} = 3.0 \times 10^{-5}$ M; 5, $Zn^{2+} = 5.0 \times 10^{-5}$ M; 6, $Zn^{2+} = 7.0 \times 10^{-5}$ M; 7, $Zn^{2+} = 1.5 \times 10^{-4}$ M; 8, $Zn^{2+} = 3.5 \times 10^{-4}$ M

excess zinc ions and [(Azo-CPD)Zn] has been studied by the stopped flow and spectrophotometric methods at pH 8.2, 7.7, I=0.5M (NaCl) and 25°C. [(Azo-CPD)Zn] has two binding sites for excess zinc ions and the binding constant of the first site ($3.9 \times 10^5 M^{-1}$ at pH 8.2, $7.1 \times 10^4 M^{-1}$ at pH 7.7) is much larger than that of the second site ($1.8 \times 10^3 M^{-1}$ at pH 8.2, $7 \times 10^2 M^{-1}$ at pH 7.7), as shown in the following equations.



The binding of excess zinc ions to the first site was completely correlated with both the inhibition of the peptidase activity and the color change of

the enzyme. The results can be explained in terms of the zinc ion reaction with only one of three conformational states of [(Azo-CPD)Zn] [2]. The second order rate constants (k_1) for binding of excess zinc ions to [(Azo-CPD)Zn] were 4.3×10^6 and $8.4 \times 10^5 M^{-1} \text{sec}^{-1}$, at pH 8.2 and 7.7, respectively, and the first order rate constants (k_{-1}) for the dissociation of zinc ions from [(Azo-CPD)Zn]Zn are 11 and 12 sec^{-1} , respectively. It has been proven that excess zinc ions promote the inhibition of the peptidase activity and the color change from red to yellow through specific binding of zinc ions to one conformational state of [(Azo-CPD)Zn].

REFERENCES

- [1] J.T. JOHANSEN, B.L. VALLEE, *Biochemistry*, **14**, 649 (1975).
- [2] L.W. HARRISON, D.S. AULD, B.L. VALLEE, *Proc. Natl. Acad. Sci. USA*, **72**, 4356 (1975).
- [3] J. HIROSE, R.G. WILKINS, *Biochemistry*, **23**, 3149 (1984).



PS2.28 — TH

P. GRUNWALD

Institut für Physikalische Chemie der Universität
 Laufgraben 24, 2000 Hamburg 13
 F.R.G.

KINETIC SALT EFFECT OF ALKALINE EARTH CHLORIDES ON THE UREASE CATALYZED UREA HYDROLYSIS

The kinetics of the Ni-containing [1] enzyme urease have turned out to be very complex. In order to get some informations about the reaction mechanism of the urease catalyzed urea hydrolysis we investigated the reaction in presence of the alkaline earth chlorides MgCl_2 , CaCl_2 , SrCl_2 , and BaCl_2 in a concentration range of 10^{-6}

$M < c_{Me^{2+}} < 10^{-4}$ M where the Debye-Hückel Limiting Law is valid and where the alkaline earth carbonates do not precipitate. The activities were determined by conductivity measurements [2] in buffer free solutions [3].

The result of all measurements is that the activities A as a function of ionic concentration c fit the equation

$$\ln A = \ln A_0 - B \sqrt{c} \quad (1)$$

The sign of the slope being negative expresses that the urea hydrolysis is inhibited by the added salts. The value for B changes only slightly if $BaCl_2$ ($B = -38.05 \pm 1.73$) instead of $MgCl_2$ ($B = -37.01 \pm 1.33$) is present, although the radii of the metal ions differ from each other by about 0.7 Å and the degree of hydration is 13.9 (Mg^{2+}) and 8.4 (Ba^{2+}). Further the B -value is only insignificantly affected by the course of the reaction: $B = -38.17 \pm 1.76$ (Mg^{2+}) and -40.92 ± 1.73 (Ba^{2+}) for a conversion of 1.3×10^{-3} mole urea. This points out that the reaction is mainly influenced by the concentration of the added ions. Therefore, an interpretation of the results on the basis of the Debye-Hückel Limiting Law and the activated complex theory seemed to be meaningful. Applying the theory of transition state to reactions in solution, the equation for the rate constant k is

$$k = \frac{k_B \cdot T}{h} \cdot K^\ddagger \cdot \frac{f_A \cdot f_B}{f_{AB^\ddagger}} \quad (2)$$

At infinite dilution the activity coefficients f for the reactants, A, B and for the activated complex AB^\ddagger are unity and $k = k_0$. Inserting the Debye-Hückel Limiting Law for ionic activity coefficients into the logarithmic form of equation (2) gives

$$\lg(k/k_0) = 1.02 z_A z_B \sqrt{I} \quad (T = 298 \text{ K}) \quad (3)$$

This expression, that has been derived by Brønsted and Bjerrum, shows that if the charges z of the reactants are both positive or both negative $\lg(k/k_0)$ will increase with increasing ionic strength I , whereas the plot of the $\lg(k/k_0)$ versus $I^{1/2}$ has a negative slope if ions of opposite charge are reacting.

An evaluation of the data by use of equation (3) again leads to linear relationships. In all cases the

extrapolation of $\lg(k/k_0)$ to zero ionic strength yields values close to zero and the gradient $1.02 \cdot z_A \cdot z_B$ of every line is about -10 .

From that, it follows that one of the reactants must have a negative charge. No conclusion can be drawn from the experiments concerning the size of z_A or z_B , but we assume that this kind of kinetic salt effect results from the reaction of urease with positively charged metal-urea complexes and that the active site of the enzyme carries a negative charge. This is contrary to the reaction model that has been published by ZERNER [4].

REFERENCES

- [1] N.E. DIXON, C. GAZZOLA, J.J. WATERS, R.L. BLAKELEY, B. ZERNER, *J. Am. Chem. Soc.*, **97**, 4130 (1975).
- [2] A.J. LAWRENCE, G.R. MOORES, *Eur. J. Biochem.*, **24**, 538 (1972).
- [3] P. GRUNWALD, *Biochem. Educ.*, **12**, 170 (1984).
- [4] N.E. DIXON, P.W. RIDDLES, C. GAZZOLA, R.L. BLAKELEY, B. ZERNER, *Can. J. Biochem.*, **58**, 1335 (1980).



PS2.29 — TH

P. GRUNWALD

Institut für Physikalische Chemie der Universität
Laufgraben 24, 2000 Hamburg 13
F.R.G.

DEPENDENCE OF THE UREASE CATALYZED UREA HYDROLYSIS ON SUBSTRATE CONCENTRATION AND TEMPERATURE IN THE PRESENCE OF ALKALINE EARTH HALIDES

The alkaline earth halides $MgCl_2$, $CaCl_2$, $SrCl_2$, and $BaCl_2$ inhibit the urease catalyzed urea hydrolysis. The interpretation of the inhibition by a model, that has first been developed by Brønsted and Bjerrum on the basis of the Debye-

-Hückel Limiting Law and the transition state theory, leads to the assumption that the active site of urease carries a negative charge.

In order to confirm the hypothesis set up, Michaelis constants have been determined for three different metal concentrations (3×10^{-6} , 1.5×10^{-5} , and 9×10^{-5} M) in a urea concentration range from 0.1 M to 1.6×10^{-3} M. The data are compiled in Table 1 and have to be compared

-values are reduced up to 50% and more compared with those measured below 30°C. These results also indicate that the added alkaline earth halides directly influence the reaction between urea and the active site of the enzyme urease.

REFERENCES

- [1] G. TALSKEY, *Angew. Chem.*, **83**, 553 (1971).

Table 1

c_{MeCl_2} (mole/l)	Michaelis constant $K_{M(\text{app})} \cdot 10^3$ (mole/l)			
	MgCl ₂	CaCl ₂	SrCl ₂	BaCl ₂
$3 \cdot 10^{-6}$	3.22 ± 0.20	3.18 ± 0.16	2.90 ± 0.30	2.89 ± 0.09
$1.5 \cdot 10^{-5}$	3.13 ± 0.15	2.77 ± 0.07	2.70 ± 0.11	2.58 ± 0.07
$9 \cdot 10^{-5}$	2.85 ± 0.13	2.60 ± 0.10	2.52 ± 0.07	2.07 ± 0.09

with K_M for pure urease preparations 0.00328 ± 0.00011 M. The data show, that K_M decreases with increasing concentration as well as with increasing ionic radius of the inhibiting metal ion. The inhibitory effect caused by a 3×10^{-6} M BaCl₂ solution is of the same magnitude as that of a MgCl₂ solution with a 30 fold metal ion concentration. The corresponding Lineweaver Burk plots show that the kind of inhibition changes from a predominantly noncompetitive inhibition for low MgCl₂ concentrations to completely uncompetitive inhibition in the presence of BaCl₂. From this it can be deduced that the active site of urease reacts with metal ion — urea complexes.

The temperature dependence of the urea hydrolysis catalyzed by urease is quite complex. If the reaction rate is determined in small temperature intervals, the measuring points no longer fall close to a straight $\ln v/T^{-1}$ — Arrhenius plot, but fit a wave like curve due to subsequent conformational changes with increasing temperature [1]. This anomalous temperature behaviour of urease is distinctly intensified in the presence of alkaline earth chlorides. Measurements, that have been performed in ΔT intervals of 1 K between 3°C and 80°C, further show that the temperature optimum of urease is raised from 60°C up to 73°C if the reaction solution contains 5×10^{-4} M SrCl₂. The mean activation energies decrease with increasing temperature, especially above 30°C where the E_A -



PS2.30 — TH

M. STEPHENSON

Unilever Research
Port Sunlight Laboratory
Quarry Road East
Bebington, Wirral L63 3JW
England

PROTEIN INTERACTION WITH THE COPPER(II)/ASCORBIC ACID/OXYGEN SYSTEM: EVIDENCE FOR A NON-SITE SPECIFIC REACTION

The ability of ascorbic acid, in the presence of low levels of copper(II), to deactivate enzymes such as catalase [1], alkaline phosphatase [2], Na,KATPase [3] and acetylcholinesterase [4] has been well documented. Recent investigations [4] have used the catalytic effect of copper(II) on enzyme deactivation as evidence for the "site specific" mechanism of biomolecule deactivation. In

this mechanism a metal-ion bound to the biomolecule acts as a centre for the production of hydroxyl radicals (via a modified Haber-Weiss cycle) which react rapidly with the surrounding biomolecule producing "site specific" deactivation [5].

In this presentation we aim to show that this type of experiment does not allow one to state with certainty that the "site specific" mechanism is operating. We show that a heterogeneous copper(II) catalyst (which does not form biomolecule/metal-ion complexes) is as effective as a homogeneous catalyst at deactivating the enzyme acetylcholinesterase in sharp contrast to the predictions of the "site specific" mechanism.

REFERENCES

- [1] C.W.M. ORR, *Biochem.*, **6**, 2995 (1967).
- [2] C.A.D. MIGGIANO, A. MORDENTE, G.E. MARTORANA, E. MEUCCI, A. CASTELLI, *Biochim. Biophys. Acta*, **789**, 343 (1984).
- [3] K. GOTO, R. TANAKA, *Brain Res.*, **201**, 239 (1981).
- [4] E. SHINAR, T. NAVOK, M. CHEVION, *J. Biol. Chem.*, **258**, 14778 (1983).
- [5] B. HALLIWELL, J.M.C. GUTTERIDGE, *Biochem. J.*, **219**, 1 (1984).



PS2.31 — MO

DAVID K. LAVALLEE
DEBASISH KUILA
Chemistry Department
Hunter College of the City University of New York
695 Park Avenue, New York 10021
U.S.A.

REACTIVITY PATTERNS IN THE NUCLEOPHILIC DEALKYLATION OF *N*-SUBSTITUTED METALLOPORPHYRINS

The reactions of *N*-substituted porphyrins are of interest in two quite different respects: for explanations of the variable efficiency in the formation

of *N*-alkylporphyrins by drugs that interact with cytochrome P-450 and for applications to synthesis of radiolabelled porphyrins for diagnostic imaging or therapy.

There are two types of mechanism for dealkylation of *N*-substituted metalloporphyrin that have precedence in the literature. One possible process involves reduction of a Co(II) or Fe(II) *N*-substituted metalloporphyrin to form a σ -alkyl Co(III) or Fe(III) complex [1-3]. The complexes could then lose the σ -alkyl group by several different types of reaction mechanisms, *i.e.*, through carbocationic, carboanionic or radical intermediates as have been documented for the Co(III) σ -alkyl corins [4]. A second type of reaction involves nucleophilic removal of the *N*-substituent through a carbocationic intermediate. This type of reaction has been a focus of our work [5-9]. In this article, we will present an overview of our previous results and present some new findings which are relevant.

Features of the nucleophilic dealkylation reaction which could affect the overall rate include the nature of the *N*-substituent, the nucleophile, the solvent, the porphyrin and the metal ion. We have found that the *N*-substituent has a profound effect on the dealkylation rate. The types of substituent which we have investigated are acyl (ethylacetato), alkyl (benzyl, methyl, and ethyl) and aryl (phenyl). For the sake of comparison, we used the same solvent (CH₃CN), metal ion (copper (II)) and nucleophile (di-*n*-butylamine). At 25°C, the relative rates for dealkylation of the *N*-substituted tetraphenylporphyrinocopper(II) complex to form CuTPP are 100 (benzyl) [8]: 1 (methyl) [8]: 0.1 (ethyl) [8]: 0.15 (ethylacetato, $k_{\text{obsd}} = 1.1 \times 10^{-4} \text{ s}^{-1}$): $< 10^{-4}$ (phenyl) [8]. The activation parameters for this series are too few to be definitive but the trends they suggest are reasonable: the activation enthalpy is least for the *N*-benzyl complex and the activation entropy of the *N*-methyl complex is the least unfavorable. The first of the two features and the extremely slow loss of the *N*-phenyl group are consistent with S_N1 character. For this type of mechanism, the ability of the benzyl group to delocalize positive charge would stabilize a carbocationic activated complex relative to the other *N*-substituents and the phenyl group would be disfavored. The more unfavorable

entropy for groups bulkier than the methyl group is consistent with S_N2 character since nucleophilic attack is an important feature of the mechanism. One substituent about which we report herein for the first time is the ethylacetato group. The *N*-ethylacetatotetraphenylporphine ligand has been reported previously [10] and the Cu(II) complex (formed *in situ* from $\text{Cu}(\text{CF}_3\text{SO}_3)_2$ and *N*- $\text{CH}_2\text{CO}_2\text{C}_2\text{H}_5$ HTPP in CH_3CN) shows a visible spectrum typical of a Cu(II) *N*-substituted porphyrin complex [8]. Although we expected that the carbonyl functionality might inhibit carbocation formation and thereby increase the activation enthalpy, the reactivity of this complex is very similar to the corresponding *N*-ethyl TPP complex. The acetato group is a versatile functionality and we might expect to be able to synthesize a variety of *N*-substituted porphyrins that could have similar dealkylation reactivity.

The contributions of factors other than the *N*-substituent are consistent with S_N1 characteristics in some cases and with S_N2 reactions in other cases. The dependence of the rate of dealkylation on the metal ion is characteristic of S_N1 reactions. The rate is highly dependent on the metal ion. Under comparable conditions, the rate order is [5-9] $\text{Pd(II)} > \text{Cu(II)} > \text{Ni(II)} > \text{Co(II)} \gg \text{Zn(II)} > \text{Mn(II)}$ which parallels the stability order of the product (non-*N*-substituted) metalloporphyrin. This result and the dependence on carbocationic stabilization noted above infer that the activated complex resembles the product and that bond-breaking is important in determining the rate. The dependence of the rate on the nucleophile and the solvent are characteristic of an S_N2 mechanism. Although these factors have not been studied in detail, it is quite clear that the dealkylation rates are highly dependent on solvent [7]. Highly polar solvents appear to stabilize the nucleophile and retard reaction, as expected. It must be noted here that we are discussing the dependence of the dealkylation step itself. The solvent can also have a profound effect by changing the rate determining step of the mechanism, as illustrated by the reactions of $\text{Pd}(\text{N-CH}_3\text{TPP})^+$ in CH_3CN (in which complexation is fast and dealkylation slow) and in DMF (in which complexation is slow relative to dealkylation) [9]. In reactions of $\text{Cu}(\text{N-CH}_3\text{TPP})^+$, ion-pairing of the complex with a nucleophilic anion

may be the origin of the observed first order rather than second order rate law [7,11]. The nucleophilicity of amines is much greater than pyridine which is, in turn, much more nucleophilic than water or alcohols [4], but this aspect has not been studied extensively.

The rate of dealkylation is not affected greatly by the nature of the porphyrin ring [7], so results deduced from synthetic porphyrins can be transferred to naturally-derived porphyrins (*e.g.* under comparable conditions, the rate constants for dealkylation of $\text{Cu}(\text{N-CH}_3\text{TPP})^+$, $\text{Cu}(\text{N-CH}_3\text{TPPS}_4)^{3-}$ and $\text{Cu}(\text{N-CH}_3$ deuteroporphyrin IX dimethylester) are 2.9×10^{-3} , 3.7×10^{-3} , $1.4 \times 10^{-3} \text{ M}^{-1} \text{ sec}^{-1}$ (25°C , CH_3CN as solvent, di-*n*-butylamine as nucleophile) [7]. The results of kinetic studies of dealkylation of *N*-substituted metalloporphyrins to date suggest that the rate can vary over wide limits which are controllable in synthetic schemes by choice of *N*-substituent, metal ion, solvent and/or nucleophile. In biological reactions of *N*-substituted hemes or hemins it might be expected that dealkylation by nucleophilic attack would be different except in cases of very favorable carbocationic stabilization. In the presence of strong reductants *in vivo*, migration to form σ -iron(III) species could result in removal of the *N*-substituent. It is not surprising that *N*-aryl and *N*-alkyl porphyrins are not dealkylated after their formation from myoglobin or hemoglobin [12,13] in light of the relative stability of such complexes against dealkylation and the relative ease of hydrolysis of iron complexes of these *N*-substituted species [14].

REFERENCES

- [1] P.R. ORTIZ DE MONTELLANO, K.L. KUNZE, H. S. BEILAN, C. WHEELER, *J. Am. Chem. Soc.*, **104**, 3545 (1982).
- [2] P. BATTIONI, J.P. MAHY, G. GILLET, D. MANSUY, *J. Am. Chem. Soc.*, **105**, 1399 (1983).
- [3] D. DOLPHIN, D.J. HALKO, E. JOHNSON, *Inorg. Chem.*, **20**, 4348 (1981).
- [4] J.M. PRATT, «Inorganic Chemistry of Vitamin B₁₂», Acad. Press, N. Y., 1972.
- [5] D.K. LAVALLEE, *Inorg. Chem.*, **15**, 691 (1976).
- [6] D.K. LAVALLEE, *Inorg. Chem.*, **16**, 955 (1977).
- [7] D. KUILA, D.K. LAVALLEE, *Inorg. Chem.*, **22**, 1095 (1983).
- [8] D.K. LAVALLEE, D. KUILA, *Inorg. Chem.*, in press.

- [9] J.D. DOI, C. COMPITO-MAGLIOZZO, D.K. LAVALLEE, *Inorg. Chem.*, **23**, 448 (1984).
 [10] H.J. CALLOT, T. TSCHAMBER, *Bull. Soc. Chim. Fr.*, **11**, 3192 (1973).
 [11] C. STINSON, P. HAMBRIGHT, *Inorg. Chem.*, **15**, 3181 (1976).
 [12] K.L. KUNZE, P.R. ORTIZ DE MONTELLANO, *J. Am. Chem. Soc.*, **105**, 1380 (1983).
 [13] D. MANSUY, P. BATTIONI, J.P. MAHY, G. GILLET, *Biochem. Biophys. Res. Commun.*, **106**, 30 (1982).
 [14] D.K. LAVALLEE, J. CARRERO, work in progress.



PS2.32 — TU

CECILIA FORSMAN
 LENA TIBELL
 INGVAR SIMONSSON
 SVEN LINDSKOG
 Department of Biochemistry
 University of Umeå
 S-901 87 Umeå
 Sweden

INHIBITION OF HUMAN CARBONIC ANHYDRASE II BY SOME ORGANIC COMPOUNDS

In addition to monovalent inorganic anions a variety of organic compounds inhibit carbonic anhydrase-catalyzed reactions by binding at or near the zinc ion in the active center. The best known of these are certain aromatic and heterocyclic sulfonamides [1].

We have studied the inhibition of human carbonic anhydrase II by four organic compounds, tetrazole, 1,2,4-triazole, 2-nitrophenol and trichloroacetaldehyde hydrate (chloral hydrate). These inhibitors can be classified in two categories depending on their effects on CO₂ hydration at pH near 9. The first category is represented by tetrazole and 2-nitrophenol giving rise to predominantly uncompetitive inhibition patterns. At this pH these compounds are anions and their behaviour is comple-

tely analogous to the behaviour of simple inorganic anions [2,3]. We also show that tetrazole is a competitive inhibitor of HCO₃⁻ dehydration in analogy with the behaviour of anions [9]. The second category is represented by 1,2,4-triazole and chloral hydrate yielding noncompetitive inhibition patterns at high pH. 1,2,4-triazole was also studied at pH 7.2 and found to be a noncompetitive inhibitor of both CO₂ hydration and HCO₃⁻ dehydration. However, at chemical equilibrium 1,2,4-triazole and CO₂/HCO₃⁻ bind to the enzyme in a mutually competitive fashion.

A third category of organic inhibitors is represented by phenol which has been shown to be a competitive inhibitor of CO₂ hydration and a non-competitive inhibitor of HCO₃⁻ dehydration by SIMONSSON *et al.* [4]. The diverse kinetic patterns of these organic inhibitors can be explained by the mechanism model of Fig. 1, an extended version

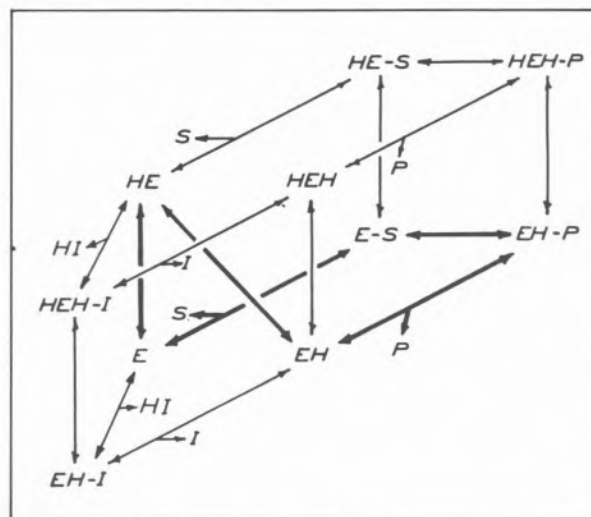


Fig. 1

Kinetic mechanism scheme for carbonic anhydrase. **H** to the right of **E** represents a protonated catalytic group and **H** to the left of **E** represents a protonated proton-transfer group. **S** represents CO₂, **P** represents HCO₃⁻, **I** represents the anionic form of the inhibitor, and **HI** represents a neutral inhibitor. Reaction steps indicated by thick lines represent the catalytic pathway that is thought to dominate at high pH. The diagonal line corresponds to the intramolecular H⁺ transfer step. Vertical lines correspond to buffer-facilitated H⁺ transfer steps

of the scheme originally proposed by STEINER *et al.* [5]. In this scheme **H** to the right of **E** represents a protonated catalytic group believed to be a zinc-bound H₂O molecule ionizing to OH⁻. **H** to the left of **E** represents a protonated proton trans-

fer group, thought to be His-64. At high substrate and buffer concentrations the intramolecular proton transfer ($\text{EH} \rightleftharpoons \text{HE}$) is probably rate limiting. pK_i/pH profiles for tetrazole, 1,2,4-triazole and chloral hydrate suggest that enzyme-inhibitor complexes with the stoichiometric composition $(\text{H})\text{EHI}$ are formed. (H) denotes that binding occurs regardless of the ionization state of the proton transfer group. The complex between enzyme and tetrazole or 2-nitrophenol is formed mainly by a combination of $(\text{H})\text{EH}$ and the anionic form of the inhibitor, I . The competitive inhibition of CO_2 hydration by phenol suggested that $(\text{H})\text{EHI}$ is formed mainly in a reaction between $(\text{H})\text{E}$ and neutral inhibitor HI . The noncompetitive patterns obtained for 1,2,4-triazole and chloral hydrate could then be explained by assuming that both of these pathways for the formation of $(\text{H})\text{EHI}$ are kinetically significant.

REFERENCES

- [1] S. LINDSKOG, *Adv. Inorg. Biochem.*, **4**, 115-170 (1982).
- [2] Y. POCKER, T.L. DEITS, *J. Am. Chem. Soc.*, **104**, 2424-2434 (1982).
- [3] L. TIBELL, C. FORSMAN, I. SIMONSSON, S. LINDSKOG, *Biochim. Biophys. Acta*, **789**, 302-310 (1984).
- [4] I. SIMONSSON, B.-H. JONSSON, S. LINDSKOG, *Biochem. Biophys. Res. Commun.*, **108**, 1406-1412 (1982).
- [5] H. STEINER, B.-H. JONSSON, S. LINDSKOG, *Eur. J. Biochem.*, **59**, 253-259 (1975).



PS2.33 — TH

GEROLAMO DEVOTO

Cattedra di Chimica
Facoltà di Medicina e Chirurgia
Università di Cagliari
Italy

ENRICO SANJUST

GIOVANNI FLORIS
Istituto di Chimica Biologica
Università di Cagliari
Italy

INHIBITORY ACTIVITY OF Cu(II) , Co(II) AND Ni(II) COMPLEXES WITH 1,4-BIS(3-AMINOPROPYL)PIPERAZINE AND 3,3'-DIAMINO-N-METHYLDIPROPYLAMINE TOWARD LENTIL SEEDLINGS DIAMINEOXIDASE

Diamine oxidases (amine: oxygen oxidoreductase, deaminating E.C. 1.4.3.6) are enzymes evenly distributed among living organisms. They catalyse the oxidation of one primary amino group of the substrate according to the following reaction $\text{R-CH}_2\text{-NH}_2 + \text{O}_2 + \text{H}_2\text{O} \rightarrow \text{R-CHO} + \text{NH}_3 + \text{H}_2\text{O}_2$. An important tool in studying the function of an enzyme is to find out specific inhibitors and to follow their effects.

Recently a DAO from Lentil seedlings (LSAO) has been purified to homogeneity [1]. This enzyme is similar to other plant amine oxidases.

LSAO is inhibited *in vitro* by various complexes of type $\text{M(L)}_2\text{X}_2$ where $\text{M} = \text{Cu(II)}$, Co(II) and Ni(II) ; $\text{L} = 1,4\text{-Bis(3-Aminopropyl)piperazine (APP)}$, $3,3'\text{-Diamino-N-methyldipropylamine (AMPA)}$; $\text{X} = \text{Cl}^-$, Br^- , SO_4^{2-} .

The inhibition constants were determined by Dixon's and Lineweaver Burk plots.

All inhibitors tested are non competitive and their inhibition constant change with the nature of the metal and anion of the complex. No inhibition is revealed with the Co(II) complexes. $\text{Cu(AMPA)}_2\text{Br}_2$ in aqueous solution ($3.7 \times 10^{-5} \text{ M}$) gives the most high inhibitor value [2].

REFERENCES

- [1] G. FLORIS, G. GIARTOSIO, A. RINALDI, *Phytochemistry*, **22**, 187 (1983).
- [2] G. DEVOTO, M. MASSACESI, G. PONTICELLI, R. MEDDA, G. FLORIS, *Experientia*, in press.



PS2.34 — TU

R.C. BRAY

G.N. GEORGE

School of Chemistry and Molecular Sciences
University of Sussex
Brighton, BN1 9QJ
U.K.

F.F. MORPETH

National College of Food Technology
University of Reading
Whiteknights Park, Reading
U.K.

D.H. BOXER

Department of Biochemistry
Medical Sciences Institute
The University
Dundee, DD1 4HN
U.K.

THE NATURE OF THE HIGH-pH/LOW-pH TRANSITION IN SULPHITE OXIDASE AND IN NITRATE REDUCTASE

It has been known [1] for some years that the molybdenum centres of liver sulphite oxidase and of *E. coli* nitrate reductase, when in the Mo(V) oxidation state, exist in high-pH and low-pH forms, distinguished by different EPR spectra. The low-pH EPR signals show well resolved hyperfine coupling from a single proton (A_{av} about 1 mT) exchangeable with the solvent, whereas the high-pH spectra show no such coupling and have slightly different g -values with lower values of g_{av} . pK values for interconversion between the species were given [2,3] as 8.2 and 8.3 respectively for sulphite oxidase and nitrate reductase. The precise nature of this transition, in structural terms, and its significance in relation to the catalytic reactions of the enzymes has remained uncertain. We now summarise recent studies [4-6] which provide new information.

Data on the two enzymes will be considered together. The low-pH form has been shown [4,5] to bear an anion ligand which can be varied, with, particularly for nitrate reductase, different ligands giving slightly different g -values. With fluoride, hyperfine coupling to ^{19}F can be seen. The proton is believed to be in the form of an -OH ligand of

molybdenum. Coupling of the proton is comparable to that in such a ligand [7] in irradiated molybdate, and furthermore coupling to ^{17}O has been observed (*cf.* [8]) in sulphite oxidase (but not yet in nitrate reductase).

Interconversion between the species depends [4,5] on the anion concentration as well as on the pH, concentration effects being less readily interpretable for nitrate reductase than for sulphite oxidase. Recently it has become apparent that the high-pH forms of the enzymes, like the low-pH forms, bear a coupled proton, though its presence is much less obvious in their EPR spectra. In nitrate reductase the proton (A_{av} 0.34 mT) causes broadening only [5] of the high-pH spectrum, with no resolved hyperfine splitting. For sulphite oxidase, only spin-flip transitions related to the proton hyperfine coupling show up [6], in the form of shoulders on the high-pH EPR spectrum.

Assuming the proton «seen» in the high-pH and low-pH forms to be identical and in an -OH ligand in both, the question then arises as to where in the low-pH form the proton controlling the pK -value is located. This proton clearly shows no resolved hyperfine coupling. Structures of the signal-giving species will be discussed in relation to relevant work on model compounds. The question of whether a proton plays a part in the catalytic reaction will also be discussed.

ACKNOWLEDGEMENTS

EPR facilities were provided by the MRC and the work was supported by the SERC; FFM thanks the University of Reading Research Board for travel funds and DHB was a Nuffield Foundation Science Research Fellow.

REFERENCES

- [1] R.C. BRAY, *Adv. Enzymol. Relat. Areas Mol. Biol.*, **51**, 107-165 (1980).
- [2] H.J. COHEN, I. FRIDOVICH, K.V. RAJAGOPALAN, *J. Biol. Chem.*, **246**, 374-382 (1971).
- [3] S.P. VINCENT, R.C. BRAY, *Biochem. J.*, **171**, 639-647 (1978).
- [4] R.C. BRAY, S. GUTTERIDGE, M.T. LAMY, T. WILKINSON, *Biochem. J.*, **221**, 277-236 (1983).
- [5] G.N. GEORGE, R.C. BRAY, F.F. MORPETH, D.H. BOXER, *J. Biochem.*, **227**(3) (1985), in press.
- [6] G.N. GEORGE, *J. Magn. Reson.* (1985), submitted for publication.
- [7] T. YAMASE, R. SASAKI, T. IKAWA, *J. Chem. Soc., Dalton Trans.*, 628-634 (1981).
- [8] R.C. BRAY, S. GUTTERIDGE, *Biochemistry*, **21**, 5992-5999 (1982).

3. Metal Substituted Metalloproteins



PS3.1 — MO

CHRISTIAN SARTORIUS
MICHAEL ZEPPEZAUER

Fachbereich 15, Analytische und Biologische Chemie
Universität des Saarlandes
6600 Saarbrücken
F.R.G.

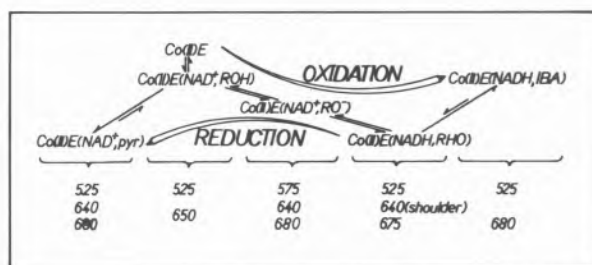
MICHAEL F. DUNN

Department of Biochemistry
University of California
Riverside, California 92521
U.S.A.

DETECTION AND CHARACTERIZATION OF INTERMEDIATES IN THE REACTION CATALYZED BY Co(II)-SUBSTITUTED HORSE LIVER ALCOHOL DEHYDROGENASE

Substitution of the active site zinc ion of horse liver alcohol dehydrogenase by certain divalent transition metal ions such as Co(II), Ni(II), Cu(II), and Fe(II) yields enzyme derivatives which are of special interest due to their spectroscopic properties [1]. Since the binding of substrates during catalysis occurs via inner-sphere coordination to the catalytic metal ion [1-3], changes in the ligand-to-metal charge-transfer (LMCT) and the d-d electronic transitions can be used as indicators for intermediates occurring during the catalytic cycle [1,4,5]. The Co(II)-substituted horse liver alcohol dehydrogenase (Co(II)-E) has so far proven the best model for native alcohol dehydrogenase because its structure as well as its catalytic behavior is highly similar to the native enzyme. We have attempted to resolve the redox step, *i.e.* the interconversion of the ternary complexes (Co(II)-E, NAD', alcohol) and (Co(II)-E, NADH, aldehyde) into fast intermediary steps by means of rapid-scanning stopped-flow (RSSF) UV-spectroscopy [6]. Under conditions of single turnover [7] the reduction of aldehydes was shown to occur in

two kinetically detectable relaxations at pH 7. The fast relaxation shows spectral changes which correspond to the oxidation of bound NADH and to the appearance of a new d-d-transition at 575 nm. This process is accompanied by perturbations of the LMCT bands around 350 nm. The slow relaxation is characterized by apparent isoabsorptive points at 300 nm and 375 nm and consists of the conversion of the species formed in the fast phase to the ternary complex (Co(II)-E, NAD', alcoxide) with the alcoxide inner-sphere coordinated to the catalytic metal ion. These findings are essentially, the same for all investigated aromatic aldehydes. The assumption of metal-bound alcoxide is supported by the fact that the intermediate does no longer appear if the pH is lowered below the pK_a of the presumed enzyme-bound alcohol. The oxidation of alcohols in single turnover at pH 8 is characterized by essentially the same spectral changes for aromatic alcohols as well as for ethanol and methanol. A fast relaxation which leads to the same intermediate as the fast phase of the aldehyde reduction is followed by a slow relaxation which consists of the appearance of NADH and a conversion of the ternary complex (Co(II)-E, NAD', alcoxide) to the ternary complex (Co(II)-E, NADH, IBA). In the presence of the



Scheme 1

Transient-spectroscopy of single-turnover runs Co(II)-substituted horse liver alcohol dehydrogenase. Discernible species of the alcohol oxidation are Co(II)-E or (Co(II)-E, NAD', ROH), (Co(II)-E, NAD', RO⁻) and (Co(II)-E, NADH, IBA). The following species can be separated in the reduction of aldehydes: (Co(II)-E, NADH, ROH), (Co(II)-E, NAD', RO⁻) and (Co(II)-E, NAD', pyr). Numbers below the species indicate the wavelenghts (in nm) of characteristic absorption maxima of the complexes

inhibitor 2,2,2-trifluoroethanol, the reaction with Co(II)-E and NAD' progresses in a single phase leading to a product whose spectrum corresponds to the spectrum of the assumed ternary complex

(Co(II)-E,NAD', alcoxide). Decreasing the pH below the pK_a of the presumed enzyme-bound alcohol again prevents the formation of this ternary complex.

We have tentatively assigned the absorption bands centered at 650 nm and 680 nm to the active site Co(II)-ion in the open and closed conformation, respectively, of the protein. Irrespective of the conformation state, binding of an anionic ligand to the Co(II)-ion creates the transition at 575 nm. Scheme I summarizes the transients observed hitherto and their spectral characteristics.

REFERENCES

- [1] M. ZEPPEZAUER, I. ANDERSSON, H. DIETRICH, M. GERBER, W. MARET, G. SCHNEIDER, H. SCHNEIDER-BERNLÖHR, *J. Mol. Cat.*, **23**, 377 (1984).
- [2] M.F. DUNN, J.S. HUTCHISON, *Biochemistry*, **12**, 4882 (1973).
- [3] E. CEDERGREN-ZEPPEZAUER, J.-P. SAMANA, H. EKLUND, *Biochemistry*, **21**, 4895 (1982).
- [4] S.C. KOERBER, A.K.H. MAC GIBBON, H. DIETRICH, M. ZEPPEZAUER, M.F. DUNN, *Biochemistry*, **22**, 3424 (1983).
- [5] S.C. KOERBER, M.F. DUNN, *Biochimie*, **63**, 97 (1981).
- [6] M.F. DUNN, S.A. BERNHARD, D. ANDERSON, A. COPELAND, R.G. MORRIS, J.P. ROQUE, *Biochemistry*, **18**, 2346 (1979).
- [7] J.T. MCFARLAND, S.A. BERNHARD, *Biochemistry*, **11**, 1486 (1972).



PS3.2 — TH

I. BERTINI
 G. LANINI
 C. LUCHINAT
 Department of Chemistry
 University of Florence
 Italy
 C. HAAS
 W. MARET
 M. ZEPPEZAUER
 Department of Biochemistry
 University of Saarland
 Saarbrücken
 F.R.G.

¹H NMR INVESTIGATION OF INHIBITOR BINDING TO COBALT(II) SUBSTITUTED LIVER ALCOHOL DEHYDROGENASE (LADH)

It is known from X-ray studies that imidazole and pyrazole bind at the catalytic zinc ion in LADH [1]. They substitute the coordinated water molecule whereas the remaining residues are essentially in unchanged positions. We have substituted cobalt(II) for zinc(II) at the catalytic site and allowed the two ligands to interact with the new derivative [2]. The electronic spectra in the 12,000-25,000 cm^{-1} region show some changes indicating that binding occurs at the metal ion. The ¹H NMR spectra in H₂O [3] show as sharp signals in the downfield region up to 50 ppm from water the NH signal of the coordinated histidine, the NH of imidazole and the corresponding *meta*-like proton, or the *meta*-like protons of pyrazole. The signals of the cysteine β -CH₂'s and of the *ortho*-like protons of the two ligands are quite broad and often shifted very far downfield. Such spectra provide definitive evidence that the metal-coordinated residues system does not change upon water substitution by either ligand. Furthermore, the ligand exchange is slow on the NMR time scale. The very same considerations apply to the ternary systems with imidazole and NADH on one side and pyrazole and NAD⁺ on the other.

^{13}C NMR studies have been performed on $\text{CH}_3\text{-}^{13}\text{CO}_2^-$ in presence of cobalt(II) substituted LADH. Evidence is provided that acetate binds at the metal ion, presumably substituting the water molecule, with an affinity constant that has been estimated to be $5 \pm 1 \text{ M}^{-1}$ through electronic spectroscopy.

REFERENCES

- [1] H. EKLUND, J.P. SAMAMA, L. WALLÉN, *Biochemistry*, **21**, 4888 (1982).
- [2] W. MARET, I. ANDERSSON, H. DIETRICH, H. SCHNEIDER-BERNLÖHR, R. EINARSSON, M. ZEPPEAUER, *Eur. J. Biochem.*, **98**, 501 (1979).
- [3] I. BERTINI, G. LANINI, C. LUCHINAT, W. MARET, S. RAWER, M. ZEPPEAUER, *J. Am. Chem. Soc.*, **196**, 1826 (1984).



PS3.3 — TH

I. BERTINI
G. LANINI
C. LUCHINAT
M.S. VIEZZOLI
Department of Chemistry
University of Florence
Italy
M. POLSINELLI
E. GALLORI
Institute of Genetics
University of Florence
Italy
F. PAOLETTI
Institute of General Pathology
University of Florence
Italy

^1H NMR SPECTRA OF ACTIVE SITE RESIDUES IN COBALT(II) ALKALINE PHOSPHATASE

Dimeric alkaline phosphatase (AP) contains a total of three pairs of metal binding sites [1], which are occupied by four zinc(II) and two magnesium(II) ions in the native enzyme. Extensive

work mostly based on metal substitution has shown a very complicated pattern of metal binding to such sites both from the thermodynamic and kinetic points of view [2].

On the ground of the experience gained by some of us in the use of cobalt(II) as an NMR shift probe for zinc metalloenzymes we have reacted cobalt(II) with apo AP obtained from the *E. coli* enzyme. Extensive checks were performed through electronic spectroscopy on the binding sequence of cobalt(II) ions as a function of pH. It was established that in the pH region 5-7 the first two cobalt(II) ions selectively bind to one set of sites which, by means of comparison with mixed copper-cobalt derivatives and by obvious extension of literature data [3,4] have been assigned as A sites. Titration of cobalt(II) into AP solutions at pH 5-6.5 results in the development of ^1H NMR signals sizeably isotropically shifted outside the region of the bulk protein signals and relatively well resolved. The titration was first limited to one cobalt(II) ion per protein, *i.e.* half occupancy of A sites, to minimize possible anticooperative effects between A sites. From these initial sets of data, which include measurement of longitudinal relaxation times of the isotropic shifted signals, it can be already established that the number and shape of signals in the downfield region of the spectrum confirms the presence of three histidines in the coordination sphere of cobalt(II) in the A site. The ^1H NMR spectra in D_2O solution indeed show the disappearance of three signals from the exchangeable NH protons of the coordinated histidines. Such spectra also indicate that at least one, and possibly two, of the three histidines are coordinated through N1.

Work is in progress to investigate the effect of higher cobalt(II)-protein ratios on the NMR spectra and the pH dependence of the latter.

REFERENCES

- [1] H.W. WYCKOFF, M. HANDSCHUMAKER, H.M. KRISHNA MURTHY, J.M. SOWADSKI, in A. MEISTER (ed.), «Advances in Enzymology and Related Areas of Molecular Biology», John Wiley & Sons, New York, 1983, p. 453.
- [2] J.E. COLEMAN, P. GETTINS, in T.G. SPIRO (ed.), «Metal Ions in Biology», vol. 5, John Wiley & Sons, New York, 1983, p. 153.
- [3] R.A. ANDERSON, F. SCOTT KENNEDY, B.L. VALLEE, *Biochemistry*, **15**, 3710 (1976).
- [4] M.L. APPLEBURY, J.E. COLEMAN, *J. Biol. Chem.*, **244**, 709 (1969).



PS3.4 — TH

I. BERTINI
 C. LUCHINAT
 L. MESSORI
 R. MONNANNI
 A. SCOZZAFAVA
 Department of Chemistry
 University of Florence
 Italy

CD AND ^1H NMR STUDIES ON COBALT(II) SUBSTITUTED OVOTRANSFERRIN-OXALATE COMPLEXES

Although the X-ray structure of the transferrins is not as yet available, other spectroscopic techniques allowed to identify the nature of the metal ligands that probably are two tyrosines, two histidines, the synergistic anion and a water or hydroxo moiety [1].

The ^1H NMR spectra of mono and dicobalt ovotransferrin at pH 8.3 in presence of bicarbonate as synergistic anion show rather well resolved signals. The pattern of the signals is in good agreement with the above proposed chromophore; no difference between the sites is observed [2].

By substituting oxalate for bicarbonate as synergistic anion the two sites become spectroscopically non equivalent. The CD spectra relative to each site are deeply different as shown in Fig. 1.

^1H NMR spectra of ovotransferrin oxalate derivatives are able to differentiate between the two sites; the existence of different conformational states of the chromophore in equilibrium among them can also be assessed.

The pH dependent properties of the chromophore were also studied. In the low pH region the C-terminal site appears to be more stable than the N-terminal one. In the high pH region there is evidence for a pH dependent equilibrium with a pK_a value of about 9.5. Deprotonation of a third tyrosine group in the proximity of the chromophore is suggested to be responsible for such equilibrium.

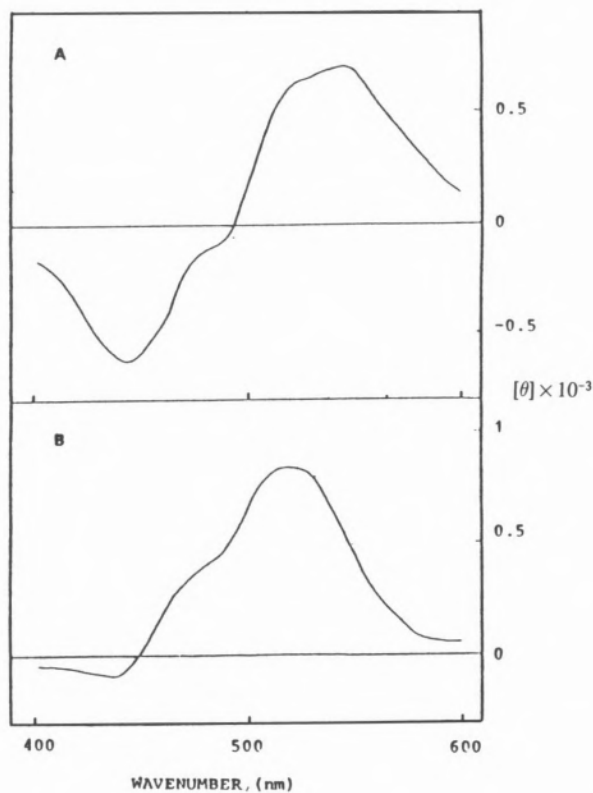


Fig. 1
 Visible CD spectra of the C-terminal (A) and N-terminal site (B) of cobalt(II)₂-ovotransferrin-oxalate

REFERENCES

- [1] N.D. CHASTEEN, in E.C. THEIL, G.L. EICHHORN, L.G. MARZILLI (eds.), «Advances in Inorganic Biochemistry», vol. 5, Elsevier, New York, 1983, pp. 201-233.
- [2] I. BERTINI, C. LUCHINAT, L. MESSORI, A. SCOZZAFAVA, *Eur. J. Biochem.*, **141**, 373-378 (1984).



PS3.5 — TU

J. LORÖSCH
U. QUOTSCHALLA
W. HAASE

Institut für Physikalische Chemie
Technische Hochschule Darmstadt
Petersenstr. 20, 6100 Darmstadt
F.R.G.

MAGNETIC AND EPR INVESTIGATIONS ON Co(II)-HEMOCYANIN: A MODEL FOR DEOXY-HEMOCYANIN

Magnetic exchange interaction of the binuclear copper active sites found in hemocyanin, tyrosinase and in some multi-copper oxidases is still an unresolved problem. Strong antiferromagnetic coupling between the two Cu(II)-ions of the oxy-form is concluded from the diamagnetic behaviour in magnetic and EPR investigations [1]. From series of dimeric model complexes it has been shown that a greater spin of the metal centers results in a decrease of the antiferromagnetic coupling [2]. This leads to a strong increase of the magnetic effect, which is an important advantage for the magnetic investigations in proteins because of the small concentration of metallic centers. Owing to this, metal substitution at the active site in these enzymes seems to be a useful tool to investigate their magnetic behaviour.

In this study we report on the magnetic and EPR properties of the Co(II)-derivative of *Limulus polyphemus* hemocyanin, where both Cu-ions of the active site were replaced by Co(II). Co(II)-hemocyanin was prepared by a modification of the method developed by S. SUZUKI and co-workers [3].

Because of the small concentration of magnetic centers we have developed two methods for sample preparation which will be presented. Using sedimentation and lyophilisation techniques we have obtained enzyme concentrations up to 35% by weight.

Initial information about the Co(II)-coordination arises from absorption and near-infrared spectra

suggesting tetrahedral coordination in Co(II)-hemocyanin which would be comparable to tetrahedral low molecular weight complexes. From the $\nu_3(^4A_2 - ^4T_1(P))$ and $\nu_2(^4A_2 - ^4T_1(F))$ transitions we have determined a strong tetrahedral ligand field comparable to Co(II)-tyrosinase [4]. The splitting of the ν_3 transition into four components reflects distortions from tetrahedral symmetry. Since Cu(I)-complexes often show tetrahedral coordination [5], the Co(II)-derivative of *Limulus polyphemus* hemocyanin may reflect the coordination geometry of the deoxy-form.

Magnetic measurements have been carried out between 4.2 and 315 K with a Faraday-system described previously [6]. The magnetic behaviour of oxyhemocyanin and its Co(II)-derivative will be presented.

The exchange coupling is discussed in relation to the limits of the used instrumental equipment. The general application of temperature dependent measurements of the magnetic susceptibility to proteins containing active sites with exchange coupled metal centers will be pointed out.

Temperature dependent X-band EPR spectra have been recorded between 4.2 and 80 K. At 4.2 K a broad signal has been observed which can be estimated on the basis of axial symmetry of the EPR spectra [7]. The signal typical for high-spin Co(II) complexes [8] is broadened significantly with increasing temperature and disappears at 76 K in the most concentrated sample measured. This is caused by the rapid spin-lattice relaxation typical for Co(II). The EPR spectra will be discussed in relation to the exchange coupling and to structural features of the Co(II)-derivative of hemocyanin.

From the results of the Co(II)-hemocyanin it can be concluded that Co(II) replaces Cu(I) in the active site in a distorted tetrahedral environment. Therefore this derivative can be used as a model for the deoxy-form which can be studied by common techniques in contrast to a Cu(I)-site.

REFERENCES

- [1] D.M. DOOLEY, R.A. SCOTT, J. ELLINGHAUS, E.I. SOLOMON, H.B. GRAY, *Proc. Natl. Acad. Sci. USA*, **75**, 3019 (1978).
- [2] S.L. LAMBERT, D.N. HENDRICKSON, *Inorg. Chem.*, **18**, 2683 (1979).
- [3] S. SUZUKI, J. KINŌ, A. NAKAHARA, *Bull. Chem. Soc. Jpn.*, **55**, 212 (1982).

- [4] C. RÜEGG, K. LERCH, *Biochemistry*, **20**, 1256 (1981).
 [5] F.A. COTTON, G. WILKINSON, «Advanced Inorganic Chemistry», 3rd ed., Interscience Publishers, N.Y., 1972, pp. 875, 904.
 [6] L. MERZ, Dissertation, Darmstadt, 1980.
 [7] L. BANCI, A. BENCINI, C. BENELLI, D. GATTESCHI, C. ZANCHINI, *Struct. Bonding (Berlin)*, **52** (1982).
 [8] R.L. CARLIN, «Transition Metal Chemistry», vol. 1, Marcel Dekker, N.Y., 1965, p. 1.



PS3.6 — TH

W. MARET

C. HAAS

M. ZEPPEZAUER

Fachbereich 15.2, Analytische und Biologische Chemie

Universität des Saarlandes

6600 Saarbrücken

F.R.G.

H. DIETRICH

Institut für Getränketechnologie

Forschungsanstalt Geisenheim

6222 Geisenheim

F.R.G.

R. MONTIEL-MONTOYA

E. BILL

A.X. TRAUTWEIN

Institut für Physik

Medizinische Hochschule Lübeck

2400 Lübeck

F.R.G.

Fe(II)- AND Fe(III)-SUBSTITUTED HORSE LIVER ALCOHOL DEHYDROGENASE

The catalytic metal binding site in $H_4Zn(n)_2$ -HLADH (HLADH = horse liver alcohol dehydrogenase, EC 1.1.1.1), a derivative lacking the catalytic zinc ions, provides a pseudotetrahedral geometry for various metal ions [1]. Recently, Fe(II) ions have been inserted into this site. In the absence of added oxidizing or reducing agents, Fe(II) is quickly oxidized to a violet Fe(III)-enzyme; in a subsequent slow reaction the Fe(III)-enzyme is bleached ($t_{1/2} \sim 15$ min). In the presence of oxidizing or reducing agents

Fe-HLADHs can be prepared, in which iron is exclusively in the di- or trivalent state. The electronic structure of the iron ion is influenced by ligand binding and binding of coenzyme to the enzyme. In this communication we characterize Fe-HLADH by EPR-, Mössbauer-, UV/Vis-, CD- and resonance Raman [2] spectroscopy.

Fe(II)-HLADH

The reduced Fe-HLADH does not absorb in the visible region and is EPR-silent at low temperatures. Mössbauer spectra reveal two Fe(II) species in the high spin state ($S = 2$). The Mössbauer parameters ($\delta(1) = 0.86$; $\delta(2) = 1.31$; $\Delta E_Q(1) = 3.80$; $\Delta E_Q(2) = 3.35$, $\{mm \cdot s^{-1}\}$) indicate a coordination number of five for both species.

Fe(III)-HLADH

The oxidized Fe-HLADH shows a broad electronic absorption band with a maximum at 560 nm ($\epsilon = 1500 M^{-1} cm^{-1}$), consistent with a $S \rightarrow Fe(III)$ ligand-to-metal charge transfer. A shoulder is detected at 336 nm ($\epsilon = 4000 M^{-1} cm^{-1}$). In the CD-spectrum the visible absorption band is resolved into at least three transitions. Resonance Raman spectra are produced by excitation at 514 nm ($\nu_1 = 309$ (w), $\nu_2 = 357$ (s), $\nu_3 = 387$ (w) and $\nu_4 = 428$ (s) cm^{-1}). They are very similar to those of Ni- and Cu-HLADH [3]. The EPR spectrum of Fe(III)-HLADH at 10 K is characterized by absorptions at $g = 9.5$ and $g = 4.25$ and is typical for a rhombic symmetry of Fe(III) in the high spin state ($S = 5/2$). At least two species with slightly different parameters are responsible for these signals. This heterogeneity is revealed by Mössbauer spectroscopy only in the paramagnetic hyperfine structure ($\Delta E_M(1) = 390$ kG; $\Delta E_M(2) = 470$ kG). The Mössbauer parameters are in the range expected for tetra- and pentacoordinate iron.

CONCLUSIONS

Fe(II)- and Fe(III)-HLADH do not show appreciable enzymatic activity in ethanol oxidation. Iron binds in the active site of HLADH to two sulfur atoms of cysteines, one histidine and one water molecule. The identity of the fifth ligand in the pentacoordinate structure is under scrutiny. Thus, Fe-HLADH illustrates a certain coordinati-

ve flexibility of the metal binding site in this enzyme. In view of the peculiar structure and chemistry of the catalytic metal binding site in HLADH, we can explore Fe-HLADH as a model system for native Fe/S proteins.

ACKNOWLEDGEMENTS

Financial support was given by Deutsche Forschungsgemeinschaft, Bundesministerium für Forschung und Technologie, Wissenschaftliche Gesellschaft des Saarlandes, Vereinigung der Freunde der Universität, Universität des Saarlandes, Fonds der Chemischen Industrie, EMBO, FEBS and NATO.

REFERENCES

[1] M. ZEPPEAUER, I. ANDERSSON, H. DIETRICH, M. GERBER, W. MARET, G. SCHNEIDER, H. SCHNEIDER-BERNLÖHR, *J. Mol. Catal.*, **23**, 377-387 (1984).
 [2] W. MARET, M. ZEPPEAUER, A.K. SHIEMKE, T.M. LOEHR, J. SANDERS-LOEHR, in preparation.
 [3] W. MARET, M. ZEPPEAUER, J. SANDERS-LOEHR, T.M. LOEHR, *Biochemistry*, **22**, 3202-3206 (1983).



PS3.7 — MO

C. SYVERTSEN
 R. GAUSTAD
 T. LJONES
 Department of Chemistry
 University of Trondheim
 7055 Dragvoll
 Norway

Cu²⁺ BINDING TO DOPAMINE β-MONOOXYGENASE

Dopamine β-monooxygenase contains four subunits and binds copper ions, which are necessary for catalytic activity. The questions of the stoichiometry of binding of copper ions to the enzyme, and of the number of copper ions necessary for catalytic activity have not been completely resolved [1,2]. We have now determined the stoichiometry of high affinity sites for copper in do-

pamine β-monooxygenase and the formation constants for binding to these and other sites by using a Cu²⁺ specific electrode. The electrode has been used to measure the concentration of free unbound copper during a titration of the enzyme with Cu²⁺. The Cu²⁺ electrode shows a linear response according to the Nernst equation from 1.0 to 1 × 10⁻¹⁹ M of free Cu²⁺ [3]. Both native and apo(metal free) dopamine β-monooxygenase have been titrated, and the stoichiometry of high affinity binding sites for Cu²⁺ are seen in Fig. 1 to be four per enzyme tetramer. We calculated the stoichiometric formation constants using a computer program which fits the titration data by least squares regression analysis. The values are shown in Table I.

To verify the results obtained with dopamine β-monooxygenase three other metal-binding proteins have been titrated. Bovine serum albumin, apo-carbonic anhydrase and ovotransferrin bind copper with high affinity, and the binding parameters are shown in Fig. 1 and Table I. The first formation constants of the Cu²⁺-bovine serum albumin and Cu²⁺-(apo)carbonic anhydrase complexes agree well with published values obtained with equilibrium dialysis methods. Also, the stoichiometry of two copper sites with approximately similar affinity per ovotransferrin is in agreement with the metal binding properties of that protein.

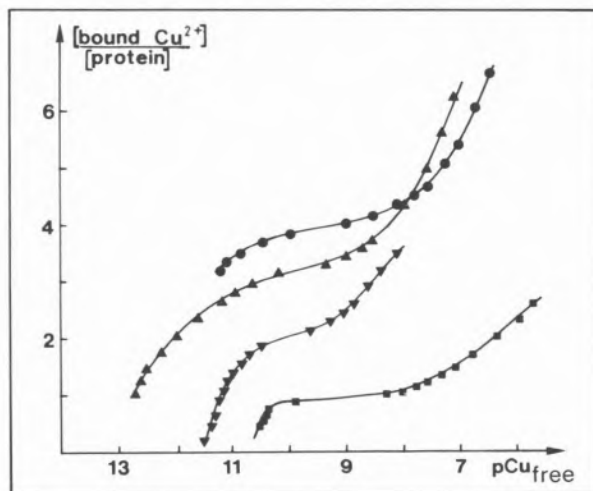


Fig. 1
 Semilogarithmic plot for binding of Cu²⁺ to: (●) native dopamine β-monooxygenase, (▲) apo dopamine β-monooxygenase, (▼) ovotransferrin, (■) apo carbonic anhydrase. For dopamine β-monooxygenase the curves refer to binding to enzyme tetramer

Table I

Successive formation constants of Cu^{2+} -protein complexes. 0.1 M KNO_3 or KCl , pH 5.8-6.0 in Mes or acetate buffer. For dopamine β -monoxygenase the constants refer to binding to enzyme subunits

		CuP logK ₁	Cu ₂ P logK ₂	Cu ₃ P logK ₃	Cu ₄ P logK ₄
Dopamine β -mono- oxygenase	apo	11.2	7.1	6.4	
	native		6.4	5.5	
Bovine serum albumin		11.2	8.7	7.0	6.0
Apo carbonic anhydrase		10.4	7.1	5.8	
Ovotransferrin*		11.2	11.4	9.1	7.8

* pH 7.9, 15 mM NaHCO_3 .

Regarding dopamine β -monoxygenase, the results establish the stoichiometry of four high affinity binding sites for Cu^{2+} ($\log K_f \sim 11$) per enzyme tetramer, and more binding sites of lower affinity ($\log K_f \sim 5-7$). While the first four Cu^{2+} represent binding to a separate class of binding sites, the next four Cu^{2+} and so forth have the same affinity as for binding of excess copper to the other three proteins analysed. Additional copper ions in excess of four per enzyme tetramer may still be necessary for maximal activity under the conditions of catalysis (presence of substrates and a reducing agent), but they should then be regarded as activating copper ions rather than being an integral part of the enzyme.

REFERENCES

- [1] T. SKOTLAND, T. LJONES, *Eur. J. Biochem.*, **94**, 145-151 (1979).
- [2] J.P. KLINMAN, M. KRUEGER, M. BRENNER, D.E. EDMONDSON, *J. Biol. Chem.*, **259**, 3399-3402 (1984).
- [3] A. AVDEEF, J. ZABRONSKY, H.H. STUTING, *Anal. Chem.*, **55**, 304-307 (1983).



PS3.8 — TU

STEFAN DAHLIN
BENGT REINHAMMAR
JONAS ÅNGSTRÖM

Department of Biochemistry and Biophysics
University of Göteborg and Chalmers Institute of Technology
S-412 96 Göteborg
Sweden

NMR STUDIES OF Ni(II)- AND Co(II)-SUBSTITUTED STELLACYANIN

Stellacyanin is a small metalloprotein which, as it occurs in nature, contains a single copper(II) ion. The metal has a distorted tetrahedral coordination that gives the protein its intense blue colour. This so-called «type 1 copper» is also found in various other small proteins and in the more complex copper oxidases; laccase, ceruloplasmin and ascorbate oxidase. It is now widely accepted that the structure of the type 1 site in all proteins is essentially the same and that the copper is coordinated to two histidine imidazole nitrogens, a cysteinyl sulfur and, at least in two small proteins, to a methionine sulfur. Stellacyanin, however, contains no methionine and the nature of the fourth ligand is still enigmatic. Since stellacyanin is known to deviate considerably in many spectroscopic and chemical properties compared to the other blue copper-containing proteins, it has attracted much interest and a great number of spectroscopic methods have been used in attempts to identify the fourth ligand and to explore the complicated structure of this copper site.

To derive more information from spectroscopic measurements, it is useful to study metal substituted proteins in which the native copper is replaced by a suitable metal ion [1]. Popular candidates for this replacement are cobalt(II) and nickel(II) and optical absorption studies of stellacyanin derivatives of these metals have been reported earlier [2]. In this work, NMR studies of Co(II)- and Ni(II)-substituted stellacyanin have been performed.

The majority of resonances are found between about 10 and -10 ppm but, as can be seen in Fig. 1, several resonances exhibit large hyperfine shifts. Such large shifts indicate that both Co(II) and Ni(II) are in their high-spin state. As expected, the shifts are temperature dependent and Curie-plots for both derivatives show that several of the resonances in Fig. 1 deviate from linearity, indicating some conformational changes at about 30°C that occur in, or near, the metal site. In order to understand this temperature dependent transition, further NMR experiments are needed and the results of such experiments together with the results of magnetic susceptibility measurements will be presented on the poster.

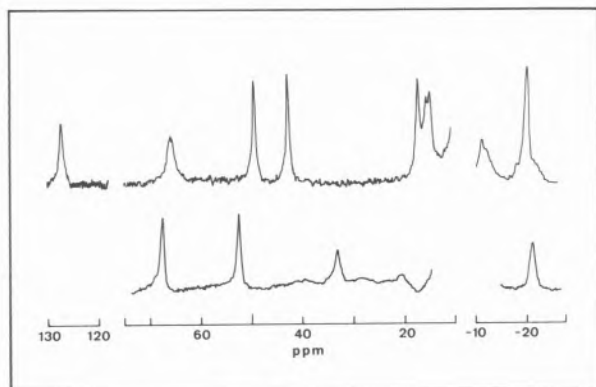


Fig. 1

Hyperfine resonances in the NMR spectra of Co(II)-stellacyanin (upper spectrum) and Ni(II)-stellacyanin (lower spectrum). The part appearing at negative ppm in the upper spectrum has been attenuated twice. Interjacent parts are omitted for clarity. For both derivatives, the concentration was 2 mM in D₂O, pH 7.4. Spectra were recorded using a Bruker WH 270 MHz spectrometer. A «water elimination Fourier transform» (WEFT) pulse sequence was employed

Varying the pH between about 4 and 9 indicated that none of the resonances in Fig. 1 are pH dependent.

It is useful to compare these spectra with the NMR spectra of Ni(II)- and Co(II)-substituted azurin obtained earlier [3]. The differences spotted in the out-shifted regions, in spectra of the two proteins reconstituted with the same metal, might give some clues to the structure of the site in stellacyanin since the fourth ligand in azurin is believed to be a methionine. The NMR spectrum of the Ni(II) derivative does not reveal any hyperfine shifted methyl resonances, thus confirming the absence of methionine in the coordination

sphere of the metal in stellacyanin. However, no clear candidates for the fourth ligand are obvious from the spectra.

REFERENCES

- [1] B.L. HAUENSTEIN JR., D.R. McMILLIN in H. SIGEL (ed.), «Metal Ions in Biological Systems», Marcel Dekker Inc., New York, 1981, chapter 10.
- [2] D.R. McMILLIN, R.A. HOLWERDA, H.B. GRAY, *Proc. Natl. Acad. Sci. USA*, **71**, 1339 (1974); D.R. McMILLIN, R.C. ROSENBERG, H.B. GRAY, *Proc. Natl. Acad. Sci. USA*, **71**, 4760 (1974); V. LUM, H.B. GRAY, *Isr. J. Chem.*, **21**, 23 (1981).
- [3] H.A.O. HILL, B.E. SMITH, C.B. STORM, R.P. AMBLER, *Biochem. Biophys. Res. Commun.*, **70**, 783 (1976); J.A. BLASZAK, E.L. ULRICH, J.L. MARKLEY, D.R. McMILLIN, *Biochemistry*, **21**, 6253 (1982).



PS3.9 — TH

PETER P. CHUKNYISKI

JOSEPH M. RIFKIND

Laboratory of Cellular and Molecular Biology

Gerontology Research Center

National Institute on Aging

National Institutes of Health

DHHS, Baltimore, Maryland 21224

U.S.A.

KENNETH ALSTON

Department of Natural Sciences

Benedict College

Columbia, South Carolina 29204

U.S.A.

CONFORMATION AND TEMPERATURE DEPENDENT SPECTRAL CHANGES IN NICKEL HEMOGLOBIN

INTRODUCTION

It has been shown [1] that normal human adult hemoglobin (HbA) reconstituted with Ni(II) protoporphyrin IX does not bind oxygen and is in a T-like conformation. It was recognized that the value of studies on this stable non-reactive T-like hemoglobin would be greatly enhanced by the pre-

paration of an R-like hemoglobin with the same Ni(II) metal center.

In this paper we demonstrate the formation of such an R-like structure by utilizing the reaction of carboxypeptidase A (CPA). The visible spectra as well as the temperature dependent spectral changes of both of these Ni(II) hemoglobins are compared.

MATERIALS AND METHODS

CPA reacted NiHbA was prepared by the initial treatment of Fe(II)HbA according to the procedure of ANTONINI *et al.* [2] and the subsequent replacement of Fe-porphyrin by Ni-porphyrin [1]. Absolute and difference spectra were recorded on a Cary 14 spectrophotometer. The sample and reference cell holders were thermostated independently using Lauda R-4/RD circulating baths (Brinkman Instruments) and the temperature was measured with a thermister (Yellow Springs Instrument Co., Model 425c).

RESULTS AND DISCUSSION

The T-like NiHbA has two maxima in the Soret region at 398 nm and 420 nm (Fig. 1A). Reaction of CPA with Fe(II)HbA produces only very small perturbations in the visible spectrum in both liganded and unliganded states [3]. However, the CPA treatment produces a major alteration of the Soret band of NiHbA with the peak at 399 nm almost completely eliminated and only one major peak at 420 nm (Fig. 1B). CPA treatment also changes the other visible bands with the 557 nm band replaced by major peaks at 542 nm and 576 nm. The changes in the visible spectrum associated with this reaction suggest an alteration in the metal coordination [4] which does not take place for the Fe(II) hemoglobins undergoing an analogous change in protein conformation [3].

It has previously been shown [5,6] that temperature dependent spectral changes in hemoproteins depend on the internal molecular dynamics and anharmonicity of the heme group and its surrounding atoms.

For Fe(II) hemoglobins this temperature depen-

dence was shown to be 17% smaller in R state hemoglobins than T-state hemoglobins. A comparison of this temperature dependence for R-like and T-like Ni(II) hemoglobins is shown in Fig. 1. Analogous to the results found for Fe(II) hemoglobins the temperature dependence for CPA treated NiHbA is 86% relative to that of the untreated HbA.

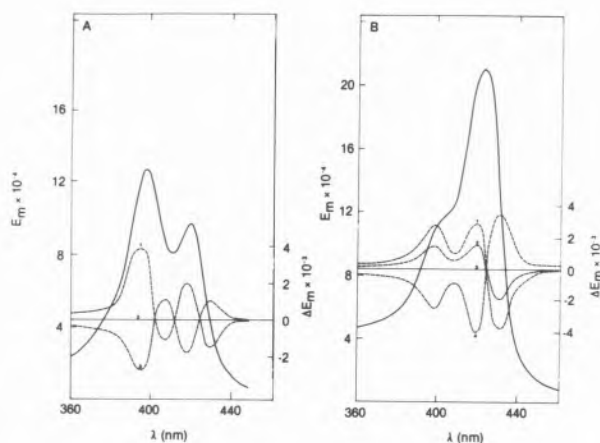


Fig. 1

A) Absorption spectrum (Soret Band) of NiHbA at 21°C-solid line. Temperature induced difference spectra 1,2,3 at 0,21,40°C, respectively.

B) Absorption spectrum (Soret band) of CPA treated NiHbA at 21°C-solid line. Temperature induced difference spectra 1,2,3,4 at 0,10,21,40°C, respectively.

For both A) and B) experimental conditions were concentration per heme 5.8 μM , reference sample at 21°C, 0.1 M phosphate and pH=7.00

This finding is a further [4] confirmation that the CPA treated hemoglobin is in an R-like state. Furthermore, the similarity of the magnitude of the temperature dependence for Fe(II) and Ni(II) hemoglobins [6] as well as the similar increase in the temperature dependence associated with the R→T transition suggests that this phenomenon is determined by the conformation of the globin in the region of the heme, and not the metal ion coordination which is seen to be different in Ni and Fe hemoglobins.

The studies on stable Ni-hemoglobins which do not bind oxygen in both the R and T conformation are found to be valuable in understanding the relationship between protein conformation and heme environment.

REFERENCES

- [1] K. ALSTON, H. SCHECHTER, J. ARCOLEO, J. GREER, G. PARR, F. FRIEDMAN, *Hemoglobin*, **8**, 41 (1984).
- [2] E. ANTONINI, J. WYMAN, R. ZITO, A. ROSSI FANNELLI, A. CAPUTO, *J. Biol. Chem.*, **236**, PC 60 (1961).
- [3] M. BRUNORI, E. ANTONINI, J. WYMAN, S. ANDERSON, *J. Mol. Biol.*, **34**, 357 (1968).
- [4] P.T. MANOHARAN, K. ALSTON, J.M. RIFKIND, in K. KARLIN, J. ZUBIETA (eds.), «Copper Coordination Chemistry», Adenine Press, in press.
- [5] P.L. SAN BIAGIO, E. VITRANO, A. CUPANE, F. MADONIA, M.U. PALMA, *Biochem. Biophys. Res. Commun.*, **77**, 1158 (1977).
- [6] P. CHUKNYISKI, P. MANOHARAN, J. RIFKIND, *Biophys. J.*, **45**, 29a (1984).



PS3.10 — MO

NICOLAY GENOV
MARIA SHOPOVA
RAINA BOTEVA

Institute of Organic Chemistry with a Centre of Phytochemistry
Bulgarian Academy of Sciences
Sofia 1040
Bulgaria

STUDIES ON THE LANTHANIDE COMPLEXES OF SUBTILISINS

A large number of proteins contain strongly bound calcium ions, Ca(II), which are essential for their conformational stability and biological function. The electronic transitions of Ca(II) can not be studied by conventional spectroscopic techniques and this makes it difficult to study the respective binding sites. The trivalent lanthanide ions, Ln(III), possess physico-chemical and spectroscopic properties which make them suitable replacement probes for Ca(II) in calcium-binding proteins.

Subtilisins are a group of extracellular alkaline proteases of bacterial origin. They are stabilized by calcium against autolysis and thermal denaturation. In the present paper circular dichroism (CD) and proteolytic activity determinations were used for studying changes in the conformational and thermal stabilities of four subtilisins; mesentericopeptidase and subtilisins Novo, Carlsberg and DY.

EXPERIMENTAL

Mesentericopeptidase and subtilisin DY were isolated in homogeneous state as described in [1] and [2], respectively. Subtilisins Novo and Carlsberg were received as a gift from Professor IB SVENDSEN (Carlsberg Laboratory, Denmark). The proteolytic activity was determined with casein as substrate. Circular dichroism was measured with a Rousel Jonan Dichrographe III instrument. The thermostability of the enzymes was measured in the sense of heat inactivation at 50°C. The solutions were incubated at 50°C for 24 h in the presence of 10⁻² M CaCl₂ or TbCl₃ or NdCl₃.

RESULTS AND DISCUSSION

The replacement of Ca(II) by Tb(III) or Nd(III) did not affect the dichroic properties and catalytic activity of subtilisins at neutral pH and room temperature, as judged from the CD spectra and proteolytic activity determinations. The retention of the biological activity can serve as an additional evidence that the native conformation has not been appreciably altered due to the substitutions. Fig. 1 shows that the Tb(III) or Nd(III) substitutions have no significant effect on the conformational stability of mesentericopeptidase at acidic pH. The behaviour of the other three subtilisins, after the respective replacements, was similar. The heat inactivation kinetics at 50°C showed that the substitution of the two lanthanides for Ca(II) lowers significantly the stability of all four subtilisins. This is illustrated in the case of mesentericopeptidase in Fig. 2. For example, after 5 h of incubation in the presence of Ca(II) at neutral pH, this enzyme preserves 78% of its caseinolytic activity, but it retains only 15-18% of the initial acti-

vity for the same period after the substitution. Probably, Ca(II) ions are better accommodated at the respective binding site than the lanthanides.

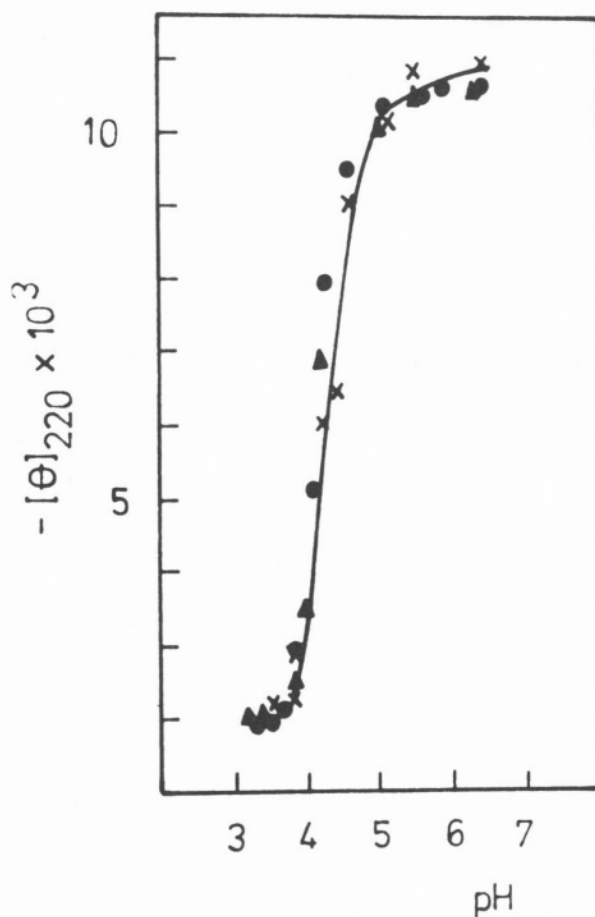


Fig. 1

Effect of replacement of Tb(III) (×—×) or Nd(III) (▲—▲) for Ca(II) (●—●) on the ellipticity at 220 nm of mesentericopeptidase at room temperature

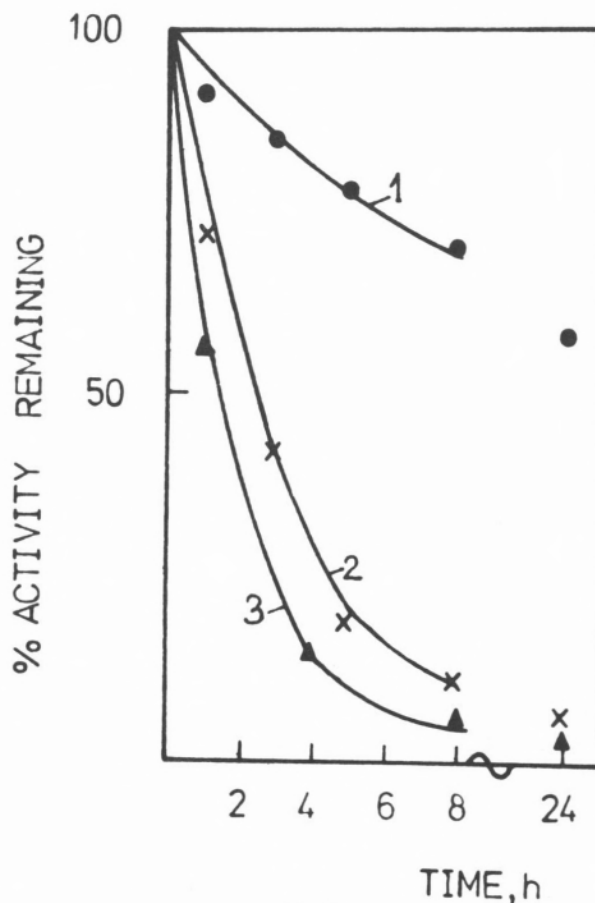


Fig. 2

Effects of 10^{-2} M CaCl_2 (●—●), TbCl_3 (×—×) and NdCl_3 (▲—▲) on the heat inactivation at 50°C of mesentericopeptidase. Casein was used as a substrate

REFERENCES

- [1] M. KARADJOVA, A. BAKURDJIEVA, P. VELCHEVA, *Compt. Rend. Acad. Bulg. Sci.*, **23**, 431-434 (1970).
- [2] N. GENOV, M. SHOPOVA, R. BOTEVA, G. JORI, F. RICCHELLI, *Biochem. J.*, **207**, 193-200 (1982).

4. Models for Metalloproteins



PS4.1 — MO

H. TSAI

W.V. SWEENEY

Department of Chemistry

Hunter College

695 Park Avenue, N.Y. 10021

U.S.A.

C.L. COYLE

Exxon Research and Engineering

Clinton Township, Route 22 East, Annandale, N.J. 08801

U.S.A.

TRANSPORT OF HYDROGEN IONS BY A 4Fe-4S MODEL COMPOUND IN A DIRECTIONAL ELECTRON TRANSPORT SYSTEM.

The ability of $[\text{Fe}_4\text{S}_4(\text{SC}_6\text{H}_5)_4]^{2-/-3-}$ to cotransport electrons and hydrogen ions in a directional electron transport system has been examined. A sequential electron transport system was used, where aqueous Cr(II)edta was the electron donor, and $(\text{CH}_3\text{N}((\text{CH}_2)_7\text{CH}_3)_3)_2[\text{Fe}_4\text{S}_4(\text{SC}_6\text{H}_5)_4]$ in toluene solution mediated the terminal reduction of methyl viologen in aqueous solution. The iron-sulfur complex, $(\text{CH}_3\text{N}((\text{CH}_2)_7\text{CH}_3)_3)_2[\text{Fe}_4\text{S}_4(\text{SC}_6\text{H}_5)_4]$ was prepared by the addition of $(\text{CH}_3\text{N}((\text{CH}_2)_7\text{CH}_3)_3)\text{Cl}$ (Aldrich), to the sodium salt of the cluster in methanol. The complex was isolated after storage at -40°C and recrystallized from warm $\text{CH}_3\text{CN}/\text{MeOH}$. The complex is freely soluble in toluene, and as such is the first reported $[\text{Fe}_4\text{S}_4(\text{SR})_4]^{n-}$ complex soluble in a water immiscible solvent.

Reduction of the Fe-S complex was accomplished by vigorously agitating a mixture of aqueous Cr(II)edta with a toluene solution of the model for several minutes. In a typical experiment, 4.05 ml of 37 mM Cr(II)edta (pH 7.5) and 0.3 ml of 3 mM Fe-S complex were used, although the exact concentrations and volumes used varied between experiments. After waiting 10-20 minutes to allow

the immiscible aqueous and toluene phases to separate, a portion of the toluene phase was carefully transferred to a tube containing 3.00 ml of 10 mM methyl viologen in 0.5 mM tris/100 mM KCl buffer (pH 8). This mixture was agitated for approximately three minutes, and the immiscible phases were allowed to separate. The toluene phase was then removed from the top of the methyl viologen solution. Reduction was evidenced by the appearance of a deep blue color in the methyl viologen phase. The number of moles of reduced methyl viologen generated was measured optically. In all cases a drop in the pH was observed to be coincident with the reduction of methyl viologen. The average molar ratio of reduced methyl viologen to transported hydrogen ions (MV/H^+) for these eleven experiments was 1.18 ± 0.24 . The reduction potential of methyl viologen is pH independent, so it is assumed that methyl viologen does not bind hydrogen ions on reduction.

Evidence suggesting that electron transport between Cr(II)edta and methyl viologen was actually mediated by the Fe-S complex was obtained in several ways. After exposure of the Fe-S model to the aqueous Cr(II)edta phase, an EPR spectrum characteristic of reduced 4Fe-4S complex was obtained. While the g-values for this approximately axial spectrum ($g = 2.02$, $g = 1.90$) are not identical with reported values obtained in other solvents, some variation between solvents has been previously noted [1]. This observation of reduced Fe-S complex is consistent with optical experiments which show the characteristic bleaching expected for reduction of $[\text{Fe}_4\text{S}_4(\text{SR})_4]^{2-}$ complexes [2]. After reoxidation by exposure to methyl viologen, the original optical spectrum was regained, with recoveries of the original absorbance typically between 85 and 100%.

Electron transfer experiments were performed in the absence of the Fe-S complex, and these yielded no reduction of methyl viologen. If $(\text{CH}_3\text{N}((\text{CH}_2)_7\text{CH}_3)_3)\text{Cl}$ is included in the toluene phase (as a test of possible solubilization of the negatively charged Cr(II)edta complex), there still is no reduction of methyl viologen observed.

Optical studies were performed to quantitate the number of moles of reduced model compound after exposure to Cr(II)edta, and the number of moles of reduced methyl viologen ultimately pro-

duced. The experimentally obtained ratios of 0.88 and 1.01 agree quite well with the expected value of 1.0. This indicates that the only major species mediating electron transport between Cr(II)edta and methyl viologen was the Fe-S complex.

The observed change in pH suggests that the Fe-S complex is cotransporting electrons and hydrogen ions by a mechanism of reduction-linked proton binding. Another possible origin for the observed pH changes that should be considered is proton transport by the Fe-S complex driven by separation of charge between toluene and aqueous phases. This can be tested using valinomycin, a ring carrier ionophore which can permit K^+ ion to pass into the hydrophobic toluene phase. If under normal experimental conditions a potential was developed, addition of valinomycin should collapse the potential. Thus the rates of electron transport and the ratio of electron/proton transported would be greatly increased on addition of valinomycin. Because no significant increases were observed, it is concluded that proton transport driven by the separation of charge is not the dominant mechanism.

These results indicate that the Fe-S complex does cotransport protons and electrons. Further, the transport of the proton is not a process driven solely by the separation of charge between the aqueous and toluene phases. The actual site of binding of the hydrogen ion to the reduced Fe-S complex is not yet established. Studies are currently in progress to determine the site or sites of association.

ACKNOWLEDGEMENTS

We wish to thank M.A. Greaney, P. Mandel, and E.I. Stiefel for technical assistance and helpful discussions.

REFERENCES

- [1] E.J. LASKOWSKI, R.B. FRANKEL, W.O. GILLUM, G.C. PAPAETHYMIU, J. RENAUD, J.A. IBERS, R.H. HOLM, *J. Am. Chem. Soc.*, **100**, 5322 (1978).
- [2] a) R.B. FRANKEL, T. HERSKOVITZ, B.A. AVERILL, R.H. HOLM, P.J. KRUSIC, W.D. PHILLIPS, *Biochem. Biophys. Res. Commun.*, **58**, 974 (1974);
b) J. CAMBRAY, R.W. LANE, A.G. WEDD, R.W. JOHNSON, R.H. HOLM, *Inorg. Chem.*, **16**, 2565 (1977).



PS4.2 — TU

MICHELLE MILLAR
TIMOTHY O'SULLIVAN
Department of Chemistry
New York University
New York, NY 10003
U.S.A.

SYNTHESIS AND STUDY OF AN ANALOG FOR THE $[Fe_4S_4]^{3+}$ CENTER OF OXIDIZED HIGH POTENTIAL IRON-SULFUR PROTEINS

Although many examples of synthetic analogs for the $[Fe_4S_4]^{n+}$ ($n=1,2$) oxidation levels of iron-sulfur proteins have been prepared and characterized, no previous attempt to synthesize a compound with the $n=3$ oxidation level has been successful. Electrochemical studies have shown that $[Fe_4S_4(S-2,4,6-(i-Pr)_3C_6H_2)_4] [(n-Bu)_4N]_2$, (**1**) and $[Fe_4S_4(S-2,3,5,6-Me_4C_6H_4)_4] [(n-Bu)_4N]_2$, (**2**), can be reversibly oxidized in CH_3CN and CH_2Cl_2 by one electron to the corresponding $[Fe_4S_4(SR)_4]^{1-}$ compounds, **3** and **4**. The $-1/-2$ and $-2/-3$ redox couple potentials measured by normal and reverse pulse voltammetry in CH_2Cl_2 versus SCE are respectively: -0.12 V and -1.20 V for **1** and -0.05 V and -1.10 V for **2**. The oxidation of **1** with $[(C_5H_5)_2Fe]BF_4$ produces $[Fe_4S_4(S-2,4,6-(i-Pr)_3C_6H_2)_4] [(n-Bu)_4N]$, (**3**), in 35% yield. Formulation of **3** as the first example of a synthetic compound containing the $[Fe_4S_4]^{3+}$ core, was confirmed by an X-ray crystal structure. The $[Fe_4S_4-(S-\alpha-C)_4]$ unit of **3** (Fig. 1) has crystallographic C_2 symmetry and approximate D_{2d} symmetry. The average Fe-S (2.26 Å) and Fe-SR (2.21 Å) bond distances are similar to the distances reported for the X-ray structure of the $[Fe_4S_4]^{3+}$ center of the oxidized high potential iron-sulfur protein from *Chromatium vinosum*. Also, the $[Fe_4S_4]$ core of **3** is tetragonally compressed with four short Fe-S bonds and eight long Fe-S bonds. The observed shift to longer wave-

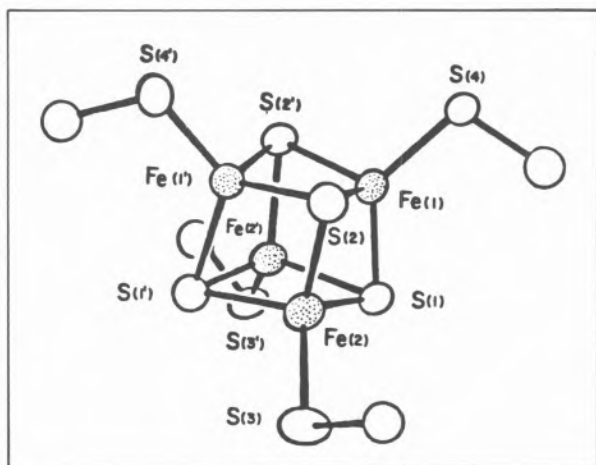


Fig. 1
The $[\text{Fe}_4\text{S}_4(\text{S}-\alpha\text{-C})_4]$ unit of 3

length of the lowest energy band in the electronic spectrum of 1 and 2 upon oxidation to 3 and 4 parallels the behavior of the high potential protein. Further spectroscopic and synthetic studies of $[\text{Fe}_4\text{S}_4]^{3+}$ centers will also be presented.



PS4.3 — TH

J. GLOUX*
P. GLOUX**
B. LAMOTTE
G. RIUS

Centre d'Etudes Nucleaires de Grenoble
Département de Recherche Fondamentale
Service de Physique
85 X - 38041 Grenoble, Cedex
France

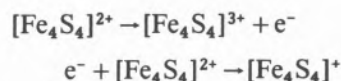
**ESR IN SINGLE CRYSTALS
OF 4 IRON 4 SULFUR SYNTHETIC
CUBANES: A NEW WAY FOR DETAILED
SPECTROSCOPIC STUDIES
OF THE $[\text{Fe}_4\text{S}_4]^+$ AND $[\text{Fe}_4\text{S}_4]^{3+}$ STATES**

Electron Spin Resonance (ESR) represents certainly one of the best methods in order to identify and study the redox states of iron-sulfur cores in

proteins as well as in synthetic models. For the 4 Iron 4 Sulfur cubanes, the two paramagnetic states are the $[\text{Fe}_4\text{S}_4]^+$ state which corresponds to the reduced ferredoxins and the $[\text{Fe}_4\text{S}_4]^{3+}$ state which corresponds to the oxidized high potential iron-sulfur proteins.

These ESR studies have always been made in non-oriented systems, *i.e.* frozen solutions or polycrystalline powders. Thus, it is the comparison between only the principal values of the \tilde{g} -tensors of the proteins and of their synthetic models which is used to check the similarity between the active sites of these proteins and their synthetic analogs. But from such an approach it is not possible to deduce precise data concerning the electronic and magnetic cubane structures which are only poorly understood till now. A better knowledge would require first the acquisition of more spectroscopic informations, *i.e.* the complete \tilde{g} -tensors, by ESR studies in single crystals.

We want to report here that we have succeeded to create in single crystals of the compound $[\text{Fe}_4\text{S}_4(\text{SC}_6\text{H}_5)_4](\text{NBu}_4)_2$, first synthesized by HOLM *et al.* [1], the two paramagnetic states $[\text{Fe}_4\text{S}_4]^+$ and $[\text{Fe}_4\text{S}_4]^{3+}$. This has been made by inducing by irradiation with gamma rays the following *in situ* reactions in the single crystals:



Moreover, these paramagnetic species are then created in the best conditions permitting detailed ESR studies since they are diluted at low concentration in the crystal built on $[\text{Fe}_4\text{S}_4]^{2+}$ cores which are diamagnetic at low temperature.

The ESR spectra show anisotropic lines spreading over about 500 Gauss and centered around $g=2$. We have been able to obtain the complete angular variations of the two main sets of lines in the three perpendicular planes ab , bc^* and c^*a defined with respect to the monoclinic unit cell and

* USM-G
** CNRS

thus to deduce the \tilde{g} -tensors. Their principal values are the following:

$$\begin{aligned} \text{A center: } g_1 &= 2.089 & g_2 &= 1.969 \\ & g_3 & &= 1.877 \\ \text{B center: } g_1 &= 2.108 & g_2 &= 2.006 \\ & g_3 & &= 1.987 \end{aligned}$$

Comparing with known experimental data in proteins, we can assign respectively the A center to the $[\text{Fe}_4\text{S}_4]^+$ of reduced ferredoxins [2] and the B center to the $[\text{Fe}_4\text{S}_4]^{3+}$ of oxidized high potential proteins [3].

REFERENCES

- [1] B.A. AVERILL, T. HERSKOWITZ, R.H. HOLM, J.A. IBERS, *J. Am. Chem. Soc.*, **95**, 3523 (1973).
- [2] N.A. STOMBAUGH, R.H. BURRIS, W.H. ORME-JOHNSON, *J. Biol. Chem.*, **248**, 7951 (1973).
- [3] B.C. ANTANAITIS, T.H. MOSS, *Biochim. Biophys. Acta*, **405**, 262 (1975).



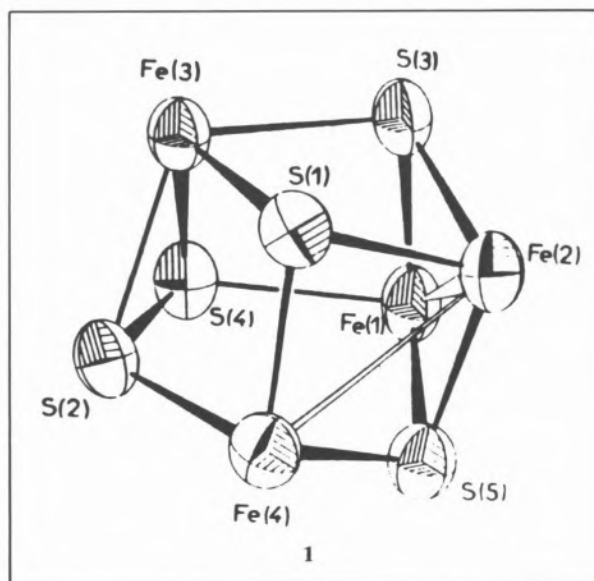
PS4.4 — MO

P. AURIC
N. DUPRÉ
J. JORDANOV

Laboratoire de Chimie et Physicochimie Moléculaire
Laboratoires de Chimie
Département de Recherche Fondamentale
Centre d'Etudes Nucléaires
85X, 38041 Grenoble
France

A CORRELATION BETWEEN THE STRUCTURAL, ELECTRONIC AND MAGNETIC PROPERTIES OF $[\text{Fe}_4\text{S}_5\text{Cp}_4]^n$ ($n=0,1+,2+$) CORES, PRESENT IN A DISTORTED CUBANE-TYPE CLUSTER WITH ONE PENTA-COORDINATED IRON ATOM

The Fe-S cluster **1** contains an electron-rich disulfide ligand which has the ability to form donor-acceptor complexes, either by S coordination or by S-S reductive cleavage.



Moreover, the X-ray analysis of $\text{Fe}_4\text{S}_5\text{Cp}_4^+$ revealed a new structural Fe-S cluster type, where one Fe atom is five-coordinate, and accounts thus for the distortion from a «conventional» Fe_4S_4 core. It was of interest to assess the spin-density delocalisation and the nature of the interaction between the ligands and the metal sites, and thus to achieve a better knowledge of the chemical reactivity of this entity and its oxidised homologues. Therefore, a detailed structural and bonding comparison of this series has been made, using both X-ray and EXAFS data. This analysis has then been correlated to the Mössbauer, EPR and magnetic susceptibility measurements.

Also, a more detailed Mössbauer study enabled us to predict the iron sites from which the electrons are probably abstracted upon the successive oxidations, and to visualise a spin-state change, at the five-coordinate Fe site, between $\text{Fe}_4\text{S}_5\text{Cp}_4^+$ and $\text{Fe}_4\text{S}_5\text{Cp}_4^{2+}$.

REFERENCES

- [1] G.J. KUBAS, P.J. VERGAMINI, *Inorg. Chem.*, **20**, 2667 (1981).
- [2] N. DUPRÉ, H.M.J. HENDRIKS, J. JORDANOV, *J. Chem. Soc., Dalton Trans.*, 1463 (1984).
- [3] N. DUPRÉ, H.M.J. HENDRIKS, J. JORDANOV, J. GAILLARD, P. AURIC, *Organometallics*, **3**, 800 (1984).



PS4.5 — TU

NORIKAZU UHEYAMA

MICHIAKI FUJI

ATSUSHI KAJIWARA

AKIRA NAKAMURA

Department of Macromolecular Science

Faculty of Science

Osaka University

Osaka 560

Japan

CHELATION EFFECT OF A Cys-X-Y-Cys TETRAPEPTIDE SEQUENCE FOR THE 4Fe-4S CLUSTER

Physical and chemical properties of the 4Fe-4S cluster in simple alkane- or arylthiolato model complexes have been established by HOLM's group [1,2]. The differences between native ferredoxin and the model complexes have been discussed in terms of redox potential, electron transfer rate, and redox stability. These differences are caused by a peptide chain of native ferredoxin. For example, invariant amino acid residues in the protein sequence of *P. aerogenes* ferredoxin play a crucial role in the construction of an unusual 4Fe-4S core environment. Previously we reported the importance of a Cys-Gly-Ala fragment of $[\text{Fe}_4\text{S}_4(\text{Z-cys-Gly-Ala-OMe})_4]^{2-}$ (Z = benzyloxy-carbonyl) with NH---S hydrogen bonding which is supported in a nonpolar solvent [3]. This paper presents a study on the chelation effect of an invariant Cys-X-Y-Cys sequence to a 4Fe-4S cluster and the effect of two amino acid residues placed between two Cys residues. A simple 4Fe-4S model complex with Cys-Gly-Gly-Cys ligands has already been synthesized by QUE *et al.* [4].

$[\text{Fe}_4\text{S}_4(\text{Z-cys-Gly-Ala-cys-OMe})_2]^{2-}$, **1**, and $[\text{Fe}_4\text{S}_4(\text{Z-cys-Ile-Ala-cys-OMe})_2]^{2-}$, **2**, having a conservative sequence of *P. aerogenes* ferredoxin were synthesized from the ligand exchange reaction of $[\text{Fe}_4\text{S}_4(\text{S-}t\text{-Bu})_4]^{2-}$ and the corresponding tetrapeptides. The $^1\text{H-NMR}$ spectrum of **1** in $\text{Me}_2\text{SO-d}_6$ exhibits two $\beta\text{-CH}$ signals of Cys resi-

dues at 11.0 and 12.3 ppm which are observed separately, with different contact shifts from the 4Fe-4S core to the $\beta\text{-CH}$ groups of two Cys thiolato ligands. The redox potential of **1** was -0.95 V (SCE) with a positive shift (0.04 V) from that (-1.00 V, SCE) of $[\text{Fe}_4\text{S}_4(\text{Z-cys-Gly-Ala-OMe})_4]^{2-}$ in *N,N*-dimethylformamide (DMF) and -0.91 V (SCE) in dichloromethane. These values may be compared with that (-0.98 V, SCE) of $[\text{Fe}_4\text{S}_4(\text{Z-cys-Gly-Ala-OMe})_4]^{2-}$ at room temperature. This positive shift in DMF is ascribed to a chelation effect by Cys-X-Y-Cys to the 4Fe-4S cluster. A decrease in the temperature for **1** in dichloromethane results in a positive shift of the redox potential; it attains -0.85 V (SCE) at 243 K, which is similar to the redox potential of $[\text{Fe}_4\text{S}_4(\text{Z-cys-Gly-Ala-OMe})_4]^{2-}$ at 233 K, indicating a preferable conformation for the NH---S hydrogen bonding, frozen at low temperature (233 K). In the case of **2**, the Cys-Ile-Ala-Cys sequence was found to chelate to the 4Fe-4S core in spite of the disadvantageous hairpin turn structure of the Cys-Ile-Ala sequence [5].

Redox behaviors of **1** and **2** in aqueous micellar solutions will be discussed as a model for a metalloprotein which acts as an electron transfer mediator.

REFERENCES

- [1] R.H. HOLM, *Acc. Chem. Res.*, **10**, 427 (1977).
- [2] J.M. BERG, R.H. HOLM, in T.G. SPIRO (ed.), «Iron-Sulfur Proteins», Wiley, New York, 1982, p. 1.
- [3] N. UHEYAMA, T. TERAKAWA, M. NAKATA, A. NAKAMURA, *J. Am. Chem. Soc.*, **105**, 7098 (1983).
- [4] L. QUE JR., J.R. ANGLIN, M.A. BOBRIK, A. DAVISON, R.H. HOLM, *J. Am. Chem. Soc.*, **96**, 6042 (1974).
- [5] N. UHEYAMA, T. TERAKAWA, T. SUGAWARA, M. FUJI, A. NAKAMURA, *Chem. Lett.*, 1287 (1984).



PS4.6 — TH

UGO CORNARO

FRANCO CARIATI

Department of Inorganic and Metallo-organic Chemistry

University of Milan

Italy

FRANCO BONOMI

Department of General Biochemistry

University of Milan

Italy

EVIDENCES FOR THE FORMATION OF COMPLEXES OF D,L-DIHYDROTHIOCTIC ACID (REDUCED LIPOIC ACID) WITH Ni^{II}, Co^{II} AND Fe^{III} SALTS

We wish to report here very preliminar evidences about the complexing ability of D,L-dihydrothioctic acid (D,L-dihydrolipoate, DHL) towards some metallic ions. The occurrence of the Fe^{III}-DHL complex was first noticed in studies dealing with the enzymatic synthesis of iron-sulfur structures [1,3], and DHL was found able to remove ferritin-bound iron to an extent which compares more than favourably with the figures obtained by using other iron-chelators [4]. The possibility of using complexes of DHL with Ni^{II} and Co^{II} in the enzymic biosynthesis of hetero-metallic, sulfur-coordinated clusters, such as those known to occur in some bacterial hydrogenases [5] and nitrogenases [6], suggested the present preliminary investigation.

All experimental operations were performed anaerobically. DHL was prepared by NaBH₄ reduction of an aqueous solution of D,L-thioctic acid brought to pH 9.0 with NaOH. After acidification to destroy the excess reductant, DHL was extracted with chloroform, dried with sodium sulphate, and its concentration determined by sulfhydryl titration [7]. The same procedure was used for the synthesis of D,L-dihydrothioctamide, starting with an ethanolic solution of D,L-thioctamide.

Fig. 1 shows the electronic spectra of mixtures of DHL and of halides of the investigated metals.

All the spectra show two major charge-transfer absorption bands, and the Fe^{III}-DHL complex gave, on a metal-content basis, the most intense absorption. The iron complex can be reduced with dithionite to give an almost colorless solution. Careful air-oxidation of this dithionite-reduced

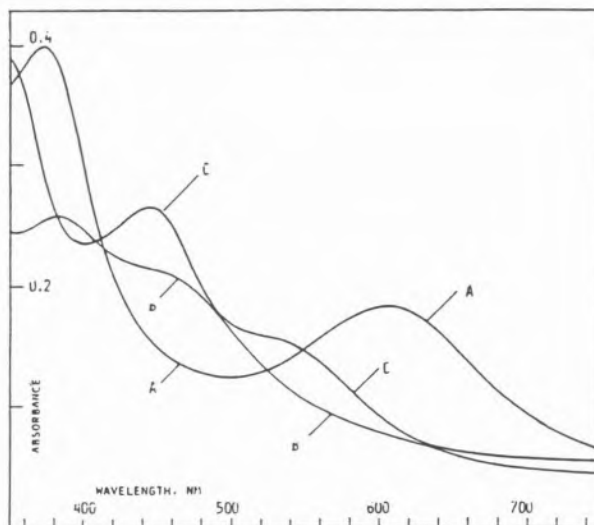


Fig. 1

Electronic spectra of buffered solutions of DHL in the presence of different metal ions. Spectra were recorded in 0.05 cm cuvettes and in 0.2 M Tris/sulfate pH 9.00. A — 20 mM DHL and 1 mM FeCl₃; B — 1 mM DHL and 2.2 mM CoCl₂; C — 1 mM DHL and 1.8 mM NiCl₂

sample allows recovery of the spectral features of the starting mixture (not shown). This and other evidences (3) suggest that iron is bound to DHL in the ferric form. When aqueous-detergent micellar solutions of D,L-dihydrothioctamide replaced DHL in the reaction with Fe^{III}, the same results were obtained, whereas D,L-thioctic acid and its amide did not display any chelating ability. These observations rule out the possible involvement of the carboxylate moiety of DHL as a ligand. Fig. 2 shows that, whatever the ion used, complexes are formed at an approximate 1/1 molar ratio between DHL and the metal. On the basis of the diamagnetic behaviour of the Fe^(II,III)-DHL complexes, and of the strong resemblance of the electronic spectra of Fe^{III}-DHL to those of Fe₂(ethanedithiolate)₄²⁻, we are inclined to assign to the Fe-DHL complex the structure Fe₂(DHL)₄⁶⁻. The apparent 1/1 stoichiometry observed in the titration experiments could be explained by the reduction of some of the iron with concomitant oxidation of the thiol groups of DHL.

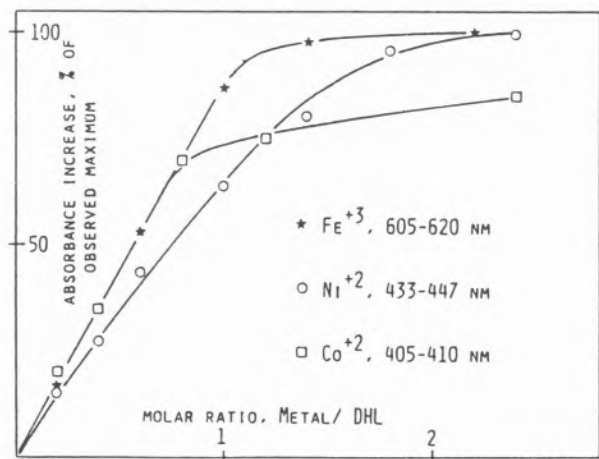


Fig. 2

Spectrophotometric titrations of DHL with increasing concentrations of different metal ions. To 50-100 ml of an anaerobic solution of DHL in 0.2 M Tris/sulfate pH 9.00, small volumes of concentrated aqueous solutions of the metal chlorides were added in the given molar ratios. Samples were anaerobically withdrawn for measuring the absorbance spectra 5 minutes after each addition

Work is in progress in order to crystallize and isolate all these compounds, to determine their structure and their electrochemical properties and to test their ability as substrates in the biosynthesis of naturally-occurring structures.

REFERENCES

- [1] S. PAGANI, F. BONOMI, P. CERLETTI, *Eur. J. Biochem.*, **142**, 361-366 (1984).
- [2] F. BONOMI, S. PAGANI, D.M. KURTZ JR., *Eur. J. Biochem.*, in press.
- [3] F. BONOMI, M.K. WERTH, D.M. KURTZ JR., submitted for publication to *Inorg. Chem.*
- [4] F. BONOMI, S. PAGANI, P. CERLETTI, *Rev. Port. Quím.*, **27**, 333 (1985).
- [5] A.V. XAVIER, M. TEIXEIRA, J.J.G. MOURA, I. MOURA, J. LE GALL, *Inorg. Chim. Acta*, **79**, 13-14 (1983).
- [6] R. EADY, B.E. SMITH, K.A. COOK, J.R. POSTGATE, *Biochem. J.*, **72**, 655-675 (1972).
- [7] G.L. ELLMAN, *Arch. Biochem. Biophys.*, **82**, 70-77 (1959).



PS4.7 — MO

J. PAUL

Exxon Research and Engineering Company
Clinton Township, Annendale, NJ 08801
U.S.A.

K.G. PAUL

Department of Physiological Chemistry
University of Umeå
S-901 87 Umeå
Sweden

A UNIFIED CONCEPT OF ELECTRONIC PERTURBATIONS OF PORPHYRINS

This communication addresses the problem whether different observables on porphyrins, or hemes, are understandable within a unified model or whether each experimental technique expresses itself in its own language. Does a pattern exist such that an observed quantity of one parameter immediately predicts a quantity of another?

The effects of 2,4-substitutions on a number of observables are collected in Table 1. For most of them a working model based upon delocalized electron density suffices to give a unified view. Removing electron density from the annular structure weakens the N-H bond, increases its H-donor capacity (E_H), and lowers its pK_3 . It also diminishes its Soret band energy (increases λ_{Soret}) and reduces the electron availability at the iron atom. The latter effect, which is observed as a more positive FeIII/II reduction potential (ΔE_m), will also increase ν_{CO} and decrease ν_{FeC} of liganded CO. The trend of these observables persists in the succession R=CHO, COCH₃, CHCH₂, H, and C₂H₅ but for a 0,5 nm shift of the Soret band upon H for C₂H₅ substitution. The trend holds also for another two observables, the melting point T_m of the esters and the 1-CH₃ proton chemical shift δ_1 . In these cases, however, the mechanism is less obvious.

On the assumption that T_m reflects the strength of intermolecular attraction certain classes of tunable forces are plausible [1]. The basicity of the pyrrolic nitrogen atoms could modulate the strength of

an intermolecular hydrogen bond. Alternatively, the altered electron density could affect van der Waal's forces. In a first approximation this should correlate the dominant oscillator frequency, i.e. the Soret band energy, to T_m . Such a correlation does exist but opposite to that required to explain the T_m data. Dipole type interactions between the static charge displacements of the substituted porphyrins provide a third possible intermolecular force. Quantum chemical calculations on carbonyl hemes indicate a considerable change of the dipole moment from CH_2CH_3 to CHO even in the plane of the porphyrin.

The 1- CH_3 proton resonance obeys a contact shift as a result of spin density, ρ^{spin} , in the aromatic ring [2]. These shifts correspond to a net spin of 5×10^{-3} electrons at the nearest carbon atom whereas the total shift of electron density, ρ^{electron} , is in the order of some tenths of an electron. Hence it is crucial to reveal whether ρ^{spin} parallels ρ^{electron} or only reflects irregular ripples of ρ^{electron} . Unlike 2,4-substituents protein moieties induce C_2 symmetry changes such that 5- CH_3 resonances parallel 1- CH_3 resonances [3]. Also the protein-induced shifts follow a trend which relates larger chemical shifts to lower reduction potentials. This correlation becomes understandable if one postulates that an enhanced rhombic distortion gives a lower reduction potential. The enhanced x-y asymmetry will then also induce a larger pseudo-contact shift of the proton resonances.

The elucidation of correlations such as those in Table 1 requires a physical description of their

origin. Much information can, however, also be revealed by a statistical evaluation. A route to pattern recognition is offered by the SIMCA programmes [4].

REFERENCES

- [1] J. PAUL, K.G. PAUL, C. HOLMBERG, *Chem. Scr.*, (1984), submitted for publication.
- [2] G.N. LAMAR, D.B. VISCIO, K.M. SMITH, W.S. CAUGHEY, M.L. SMITH, *J. Am. Chem. Soc.*, **100**, 8085 (1978).
- [3] M.L. SMITH, J. PAUL, B. NORDÉN, K.G. PAUL, *Biochim. Biophys. Acta*, (1985), submitted for publication.
- [4] S. WOLD, M. SJÖSTRÖM, *ACS Symposium Series*, **52**, 245 (1977).
- [5] J.E. FALK, «Porphyrins and Metalloporphyrins», Elsevier, Amsterdam, 1964.
- [6] M. SONO, T. ASAKURA, *Biochemistry*, **13**, 4386 (1974).
- [7] M.L. SMITH, J. PAUL, P.I. OHLSSON, K.G. PAUL, *Biochemistry*, (1984), in press.
- [8] J. PAUL, M.L. SMITH, K.G. PAUL, to be submitted for publication.

Table 1
Observables of 2,4-di(R)deuteroporphyrins

R	$T_m^a)$ (°C)	$E_H^b)$ (kJ/mol)	$pK_3^c)$ —	$\lambda_{\text{Soret}}^d)$ (nm)	$\Delta E_m^e)$ (mV)	$\Delta\nu_{\text{CO}}^f)$ (cm^{-1})	$\Delta\nu_{\text{FeC}}^g)$ (cm^{-1})	$\delta_1^h)$ (ppm)
C_2H_5	215	9.65	5.85	400	0	0	0	-12.63
H	219	9.69	5.50	399.5	+0.5	+3	—	-9.99
C_2H_3	228	10.28	4.80	407	+18	+3.5	-3	-9.31
COCH_3	235	10.36	3.35	421	+148	+10.5	-18	-0.72
CHO	289	10.69	-3.0	437	—	+20	—	(+0.10)

a) Melting points of porphyrin dimethyl esters, [1] plus refs. therein.

b) H-bond strengths of substituted pyrroles, $\text{RH}_3\text{C}_4\text{N}\cdots\text{H-F}$ [1].

c) Porphyrin dimethyl esters in detergents [5].

d) Porphyrin dimethyl esters in CHCl_3 [5,6].

e) Reconstituted Mb and HRPC_2 , relative C_2H_5 [7].

f) Reconstituted MbCO and HRPC_2CO and free carbonyl-hemes [7,8].

h) $S=1/2$ Fe(III) biscyano complexes of 2,4-substituted hemes (except for CHO), 1- CH_3 [2].



PS4.8 — TU

M. MOMENTEAU

A. CROISY

Institut Curie, Section de Biologie, Laboratoire 112

Centre Universitaire, 91405

Orsay

France

A. DESBOIS

Institut de Biologie Physico-chimique

Laboratoire de Biophysique

13 rue Pierre et Marie Curie, 75005 Paris

France

STERIC HINDRANCE INFLUENCE OF IRON(II)-PORPHYRINS ON O₂ AND CO BINDINGS: INFRARED AND RESONANCE RAMAN STUDIES

In designing model compounds for the active site of oxygen carrier hemoproteins, it is important to know the influence of steric hindrance on the O₂ and CO bindings. Indeed if in natural compounds the CO moiety adopt an end-on bent or tilted geometry from the perpendicular to the porphyrin plane [1], in various model complexes CO has been found to adopt a linear geometry [2]. This difference is attributed to distal group steric effect in the formers. On the contrary in both systems the Fe-O-O is bent [3-4].

As part of our studies of stereochemical influence on the formation and reactivity of carbonylated and oxygenated model compounds, we have prepared a new series of porphyrin derivatives specifically designed to investigate such a distal steric effect. The first observations of their infrared (IR) and resonance Raman (RR) spectroscopic studies are reported here.

All the single-face hindered porphyrins are derived from 5,10,15,20 tetraphenylporphyrin. The efficient protection of CO and O₂ coordination site is provided by a polymethylene chain anchored through amide linkage in *ortho* position of two *meso* phenyl groups in a cross configuration. The two other *meso* phenyl groups are substituted in

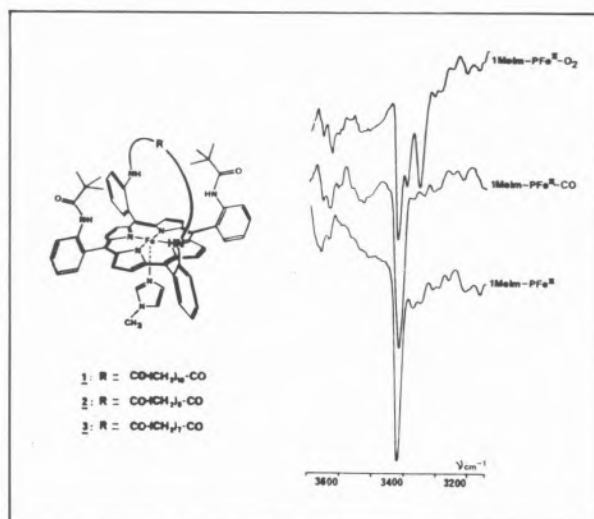


Fig. 1

IR NH stretching of compound 3

ortho position by a pivalamido residue. The presence of these "pickets" inhibits the sideways displacement of the anchoring "handle" in comparison with symmetrical "basket handle" porphyrins previously developed in our laboratory [5], as shown by the strong up-field shifts of methylene protons in ¹H NMR spectra of four-coordinated iron(II) derivatives which are affected by pseudo-contact interaction [6].

IR spectra of iron(II) CO and O₂ complexes were recorded on a Nicolet 5MX FT/IR spectrometer at 4 cm⁻¹ resolution. All RR spectra were obtained with excitation at 441,6 nm using a He/Cd laser (Liconix, model 4050). Samples were prepared by bubbling (1 atm) ¹²CO, ¹³CO (CEA, France, 99 atome %), ¹⁶O₂ and ¹⁸O₂ (CEA, France, 98 atome %) in a toluene or benzene solution of iron(II) derivatives (10⁻⁴ M) and *N*-methylimidazole (10⁻² M). IR spectra of carbonylated derivatives reveal a gradual shift of ¹²C-O stretching vibrations from 1960 cm⁻¹ (1) to 1948 cm⁻¹ (3) which are very different from the observed frequency at 1970 cm⁻¹ of unhindered ferrous-porphyrins CO [7]. It should be noted that compound 3 exhibits ν_{CO} not significantly different from those observed for carboxyhemoglobin and carboxymyoglobin [8]. RR spectra of ¹²CO-1 and ¹²CO-3 show a specific band at 488 cm⁻¹ and 506 cm⁻¹ respectively corresponding to the Fe-¹²CO stretching mode. These bands are sensitive to ¹³CO isotopic substitution and are shifted to 484 and 501 cm⁻¹. The decrease in the C=O stretching frequencies as well as the

increase in the Fe-CO stretching frequencies may be caused by a tilted or bent configuration of the carbonyl compounds due to increasing steric hindrance. This is in agreement with previous results obtained by YU *et al.* [9].

RR and IR spectra of oxy derivatives have also been recorded. RR bands at 562 and 559 cm^{-1} in the spectra of $^{16}\text{O}_2$ -1 and $^{16}\text{O}_2$ -3 are shifted by 23 cm^{-1} to the low frequency region upon substitution by $^{18}\text{O}_2$ and clearly arise from the Fe-O₂ stretching modes. The Fe-O₂ frequency was observed at 568 cm^{-1} for $^{16}\text{O}_2$ -iron(II) "picket fence" porphyrin [10]. The significant difference of 6 cm^{-1} between our less hindered compound 1 and Collman's model can be attributed both to the steric effect and the hydrogen bond between the oxygen atom not liganded to the iron and the NH group of one of the "handle" amides in 1 [11].

The comparison of IR spectra of 1, 2 and 3 and their O₂ and CO adducts gives further evidence for the latter interaction. All show the presence of one intense band at 3422-3425 cm^{-1} due to amide NH-stretching vibration (Fig. 1). An additional weaker band is observed only with oxygenated complexes in the 3372-3355 cm^{-1} range. The intrinsic shift induced by the presence of the oxygen molecule for the NH stretch is thus larger than 50 cm^{-1} and is consistent with an intramolecular hydrogen bond formation. However, the balance between these frequencies may depend upon a change in O₂ configuration due to steric hindrance within the coordination cavity.

Studies with the aim of correlating spectral properties of these compounds with their O₂ and CO affinities are now in progress in this laboratory.

REFERENCES

- [1] J.M. BALDWIN, *J. Mol. Biol.*, **136**, 103 (1980).
- [2] S.M. PENG, J.A. IBERS, *J. Am. Chem. Soc.*, **98**, 8032 (1976).
- [3] S.E.V. PHILLIPS, *J. Mol. Biol.*, **142**, 531 (1980); B. SHAANAN, *Nature (Lond.)*, **296**, 683 (1982).
- [4] J.P. COLLMAN, R.R. GAGNE, C.A. REED, W.T. ROBINSON, G.A. RODLEY, *Proc. Natl. Acad. Sci. USA*, **71**, 1326 (1974).
- [5] D. LAVALETTE, C. TÊTREAU, J. MISPELTER, M. MOMENTEAU, J.M. LHOSTE, *Eur. J. Biochem.*, **145**, 555 (1984); M. MOMENTEAU, J. MISPELTER, B. LOOCK, J.M. LHOSTE, *J. Chem. Soc., Perkin Trans. I*, 221 (1985).
- [6] J. MISPELTER, M. MOMENTEAU, J.M. LHOSTE, *J. Chem. Phys.*, **72**, 1003 (1980).

- [7] J.H. WANG, A. NAKAHARA, E.E. FLEISHER, *J. Am. Chem. Soc.*, **80**, 1109 (1958); J.P. COLLMAN, J.I. BRAUMAN, T.R. HALBERT, K.S. SUSLICK, *Proc. Natl. Acad. Sci. USA*, **73**, 3333 (1976).
- [8] M. TSUBAKI, R.B. SRIVASTAVA, N.T. YU, *Biochemistry*, **21**, 5236 (1982).
- [9] N.T. YU, E.A. KERR, B. WARD, C.K. CHANG, *Biochemistry*, **22**, 4534 (1983).
- [10] H. HORI, T. KITAGAWA, *J. Am. Chem. Soc.*, **102**, 3608 (1980).
- [11] J. MISPELTER, M. MOMENTEAU, D. LAVALETTE, J.M. LHOSTE, *J. Am. Chem. Soc.*, **105**, 5165 (1983).



PS4.9 — TH

ALAN L. BALCH
GERD N. LA MAR
MARK W. RENNER

Department of Chemistry
University of California
Davis, CA 95616
U.S.A.

LECHOSŁAW LATOS-GRAZYNSKI

Institute of Chemistry
University of Wrocław
Wrocław
Poland

REVERSIBLE OXIDATION OF IRON(II) N-METHYLPORPHYRINS. CHARACTERIZATION OF THERMALLY UNSTABLE IRON(III) N-METHYLPORPHYRINS

Oxidation of $\text{NCH}_3\text{TPPFeX}$ and $\text{NCH}_3\text{OEPFeX}$ ($\text{X} = \text{Cl}^-$, Br^- , I^- ; NCH_3TPP is anion of *N*-methyltetraphenylporphyrin, NCH_3OEP is anion of *N*-methyloctaethylporphyrin) yields the Fe(III) complexes of the respective *N*-methylporphyrin (*i.e.* $[\text{NCH}_3\text{TPPFeX}]\text{X}'$ 1 and $[\text{NCH}_3\text{OEPFeX}]\text{X}'$ 2). The following oxidizing agents have been used: Cl_2 , Br_2 , I_2 . The oxidation is reversible. The oxidation product is thermally unstable and decomposes to several compounds depending on the X ligand. TPPFeX , CH_3X , NCH_3TPPH , Fe(III) and a μ -oxo dimer have been identified.

Complexes **1** and **2** have been characterized on the basis of ^1H NMR, ^2H NMR, ESR spectroscopies and electronic spectra.

The proton NMR resonances of **1** and **2** have been assigned by means of specific deuteration, intensity and linewidth analysis.

The *N*-methyl resonance appears at 285 ppm (-60°C , CDCl_3) and could be observed only by ^2H NMR on deuterium labeled samples.

Four pyrrole resonances of **1** and eight methylene resonances of **2** confirm a C_5 symmetry imposed by *N*-methylation. The characteristic downfield resonance positions of pyrroles (133.2, 95.8, 79.5 ppm; -60°C) and ESR parameters ($g_{\perp}^{\text{eff}} = 5.9$, $g_{\parallel}^{\text{eff}} = 2.1$) prove that the oxidation has taken place on the iron. The ^6A ground state has been proposed.

The electron exchange between Fe(II) and Fe(III) complexes has not been observed.

The results of the paper should be relevant to the explanation of the green pigment formation in the course of cytochrome P-450 inactivation.



PS4.10 — MO

R. MONTIEL-MONTOYA

E. BILL

A.X. TRAUTWEIN

H. WINKLER

Physik

Medizinische Hochschule

2400 Lübeck 1

W. Germany

L. RICARD

M. SCHAPPACHER

R. WEISS

Cristallochimie

Université Louis Pasteur

67070 Strasbourg

France

MÖSSBAUER STUDY OF OXY-MODELS FOR THE ENZYME P450.

I: $[\text{Fe}(\text{O}_2)(\text{SC}_6\text{HF}_4)\text{TP}_{\text{PIV}}\text{P}][\text{Nac18C6}]$;

II: $[\text{Fe}(\text{O}_2)(\text{SC}_6\text{HF}_4)\text{TP}_{\text{PIV}}\text{P}][\text{Kc222}]$;

AND III: $[\text{Fe}(\text{O}_2)(\text{SC}_6\text{HF}_4)\text{TP}_{\text{PIV}}\text{P}][\text{Nac222}]$

Mössbauer data have been recorded in the temperature range between 4.2 K and 295 K, with and without externally applied magnetic field. Quadrupole splittings ΔE_Q have been plotted *versus* temperature in Fig. 1 to visualize the different tempe-

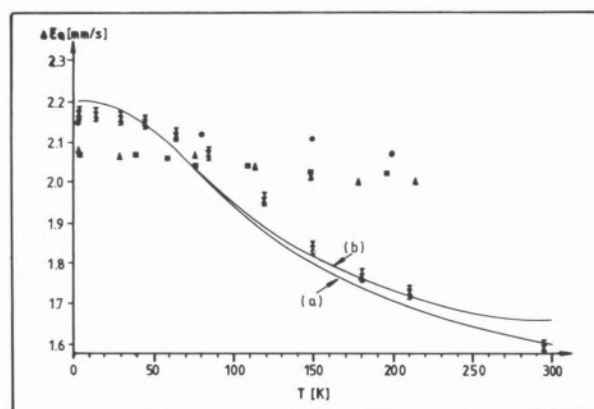


Fig. 1

Temperature dependent experimental quadrupole splittings for compounds I (X), II (■), III (▲), and P450 O_2 (●). The values for P450- O_2 are taken from M. SHARROCK et al. [4]. The solid lines correspond to (a) $V_{xx}^* = -0.95$, $V_{zz} = 1$, and (b) $V_{xx}^* = -0.95$, $V_{zz} = 1.5$ in eq. (1)

temperature dependences. From a computer simulation of magnetic spectra the sign of the main component of the electric field gradient tensor (efg) V_{zz} turns out to be negative for **I** and **II**, and the asymmetry parameter η takes the values $\eta \sim 0$ at 4.2 K and $\eta \sim 0.5$ at 173 K for **I**, and $\eta \sim 0.3$ at 4.2 K for **II**.

Our interpretation of the pronounced temperature dependence in ΔE_Q of **I** is based on the three-di-

$$V_{pq} = \left[\begin{pmatrix} -2.2 & 0 & 0 \\ & 1.1 & 0 \\ & & 1.1 \end{pmatrix} + 2 \begin{pmatrix} V_{xx}^* & 0 & 0 \\ & -V_{xx}^* & V_{zz} \\ & & V_{zz} \end{pmatrix} \exp(-190/kT) \right] / [1 + 2\exp(-190/kT)]. \quad (1)$$

mensional structure of this material, as derived from X-ray studies (Fig. 2). The occupation of sites 02A, 02B, and 02C at -100°C turned out to be approximately 0.5, 0.25, and 0.25, respectively.

From these numbers we estimate the energy barrier Δ which separates 02A from 02B and 02C: $\Delta \sim 190$ K. We now employ the assumption that sites 02B and 02C are equivalent, *i.e.* their efg tensors differ only by interchanging signs within elements V_{xz} and V_{yz} . Adding the two tensors thus

yields $2 \begin{pmatrix} V_{xx} & V_{xy} & 0 \\ & V_{yy} & 0 \\ & & V_{zz} \end{pmatrix}$. Appropriate rotation

about the z-axis (which we choose parallel to the heme-normal) finally yields $\begin{pmatrix} V_{xx}^* & 0 & 0 \\ & V_{yy}^* & 0 \\ & & V_{zz} \end{pmatrix}$.

The efg tensor of 02A is the only contribution to ΔE_Q at 4.2 K. In agreement with the findings of SPARTALIAN *et al.* [1] from their study of a similar model compound, with the findings from our single crystal study of MbO_2 [2], and with the results obtained from molecular orbital calculations [3], we choose V_{zz} such that it lies in the heme plane (x-y-plane). After testing several orientations for V_{zz} within this plane, we find the best possible fit of our experimental data for a mini-

imum amount of free parameters when we choose V_{zz} parallel to V_{xx}^* . Thus the efg tensor of 02A

$$\text{becomes} \quad \begin{pmatrix} -2.2 & 0 & 0 \\ & 1.1 & 0 \\ & & 1.1 \end{pmatrix}$$

The overall efg tensor for the situation that 02B and 02C become Boltzmann-populated with temperature (and assuming fast relaxation among the three sites) is then given by:

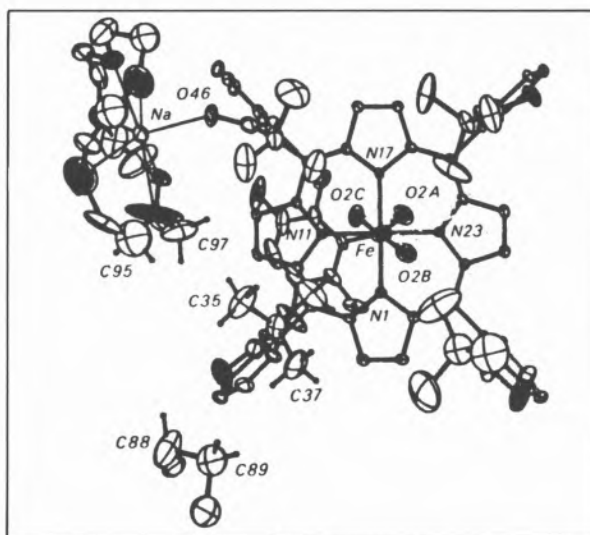


Fig. 2

ORTEP-plots for **I** obtained from X-ray studies at -100°C

All V_{pq} -values in eq. (1) are given in mms^{-1} .

Eq. (1) with the remaining parameters V_{xx}^* and V_{zz} explains the decrease of ΔE_Q and the increase of η with increasing temperature, and additionally the negative sign of V_{zz} at 4.2 K as well as at 173 K (curves a and b in Fig. 1).

Compound **II** shows only negligible temperature dependence in ΔE_Q . This is directly obvious from comparing the efg tensors of 02A and 02B of compound **II** (Fig. 3), which, under approximately C_2 -operation, result from each other. The overall efg tensor would then be:

$$V_{pq} = \left[\begin{pmatrix} V_{xx} & V_{xy} & V_{xz} \\ & V_{yy} & V_{yz} \\ & & V_{zz} \end{pmatrix} + \begin{pmatrix} V_{xx} & V_{xy} & -V_{xz} \\ & V_{yy} & -V_{yz} \\ & & V_{zz} \end{pmatrix} \exp(-\Delta/kT) \right] / [1 + \exp(-\Delta/kT)]. \quad (2)$$

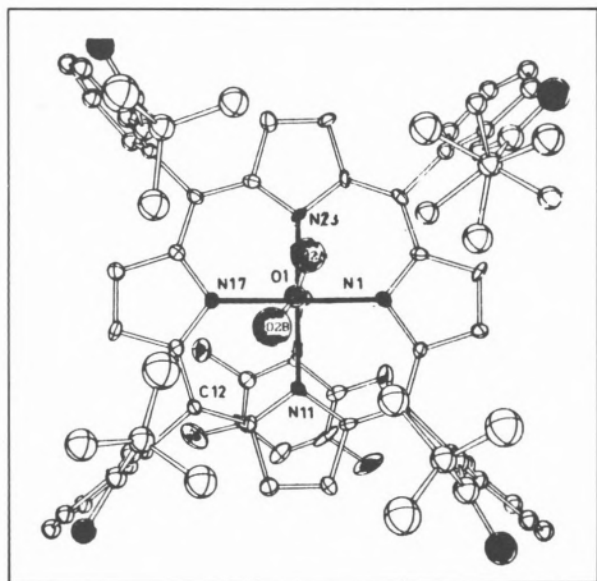


Fig. 3

ORTEP-plot for II obtained from X-ray studies at room temperature

From eq. (2) it is clear that in this case the temperature has only a minor influence in V_{pq} and hence in ΔE_Q .

REFERENCES

- [1] K. SPARTALIAN, G. LANG, J.P. COLLMAN, R.R. GAGNE, CH.A. REED, *J. Am. Chem. Soc.*, **63**, 5375 (1975).
- [2] Y. MAEDA, T. HARAMI, Y. MORITA, A.X. TRAUTWEIN, U. GONSER, *J. Chem. Phys.*, **75**, 36 (1981).
- [3] A.X. TRAUTWEIN, unpublished results.
- [4] M. SHARROCK, P.G. DEBRUNNER, C. SCHULZ, J.D. LIPSCOMB, V. MARSHALL, I.C. GUNSALES, *Biochim. Biophys. Acta*, **420**, 8 (1976).



PS4.11 — MO

E. BILL
 A.X. TRAUTWEIN
 Physik
 Medizinische Hochschule
 2400 Lübeck 1
 W. Germany
 K. FISCHER
 K.H. PAULI
 Kristallographie
 Universität des Saarlandes
 6600 Saarbrücken 11
 W. Germany
 N. BLAES
 U. GONSER
 R. PRESTON
 Angewandte Physik
 Universität des Saarlandes
 6600 Saarbrücken 11
 W. Germany
 F. SEEL
 R. STAAB
 Anorganische Chemie
 Universität des Saarlandes
 6600 Saarbrücken 11
 W. Germany

LOW TEMPERATURE MOLECULAR DYNAMICS OF $[\text{HFe}(\text{CO})_4]^-$: A POSSIBLE MODEL FOR THE DYNAMIC BEHAVIOR OF O_2 IN IRON-PORPHYRINS

Recently we have described the structure of compounds which have been synthesized from pentacarbonyl iron and *N*-substituted imidazole groups [1]. One of these compounds contains as cation hexa (1-ethylimidazole) iron(II) and as anion hydrido tetracarbonylferrate (-I), for which we use the shorthand notations $[\text{FeIm}_6]^{2+}$ and $[\text{HFe}(\text{CO})_4]^-$. In Fig. 1 we show the experimental Mössbauer spectra obtained at 288.7 K and 4.2 K. From the computer fits of these spectra using Lorentzian lines we derived isomer shifts and quadrupole splittings which are typical for high-spin ($S=2$) iron (curve 1) corresponding to $[\text{FeIm}_6]^{2+}$, and low-spin iron (curve 2) corresponding to $[\text{HFe}(\text{CO})_4]^-$. The zero quadrupole splitting at

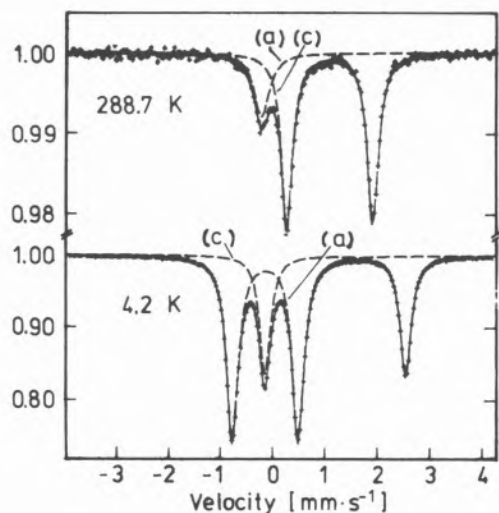


Fig. 1

Mössbauer spectra of the cation iron (curve 1) and anion iron (curve 2)

288.7 K may be due either to exact static tetrahedral (T) point-symmetry for the iron site in the anion, or due to dynamic effects. Decreasing the sample temperature from 288.7 K to 4.2 K has dramatic influence on the point-symmetry within the anion. At about 210 K the compound undergoes a reversible transition which increases the quadrupole splitting of the anion iron from zero to about 1.35 mms⁻¹ within a temperature range of 30 K (Fig. 2), while the cation iron shows a temperature dependence of ΔE_Q without abrupt changes, but characteristic for hexacoordinated high-spin ($S=2$) iron [2].

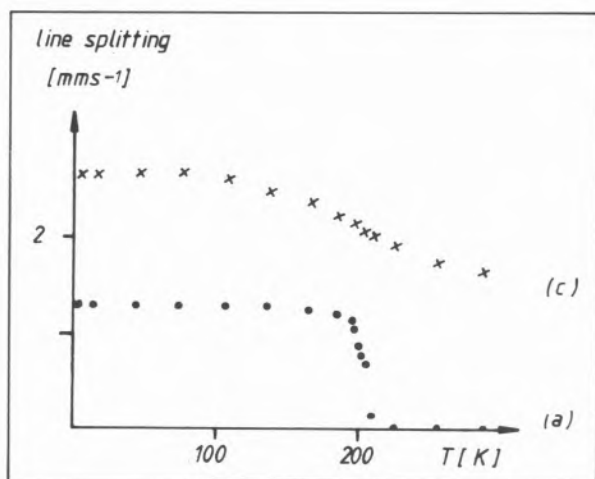


Fig. 2

Temperature dependence of experimental quadrupole splittings of the cation iron (x) and the anion iron (•), respectively

The peculiar temperature behavior of ΔE_Q^{anio} indicates that we are concerned with dynamic effects rather than static tetrahedral point-symmetry of the iron site in the anion above 200 K.

Comparing the resonance absorption of cation iron (area A_1 under curve 1 of Fig. 1) and anion iron (area A_2 under curve 2 of Fig. 1) indicates that $A_1:A_2$ is 4.35:1 at 288.7 K, in strong contradiction to the crystallographic result that the ratio Fe(cation):Fe(anion) is 1:2. The reason for this drastic discrepancy lies in the considerable difference of the temperature behavior of the two Debye-Waller factors, $f(\text{cation})$ and $f(\text{anion})$. At 4.2 K the crystallographic result for the ratio Fe(cation):Fe(anion) is much better reflected by the corresponding Mössbauer absorption areas A_1 and A_2 (Fig. 1). Thus we conclude that the ratio of different iron sites within a compound is not reflected in a Mössbauer measurement at one single temperature only.

X-ray studies which were obtained at room temperature and at 225 K indicate peculiar structural properties of the anion (Fig. 3). Three of the four CO-groups exhibit mean-square displacements

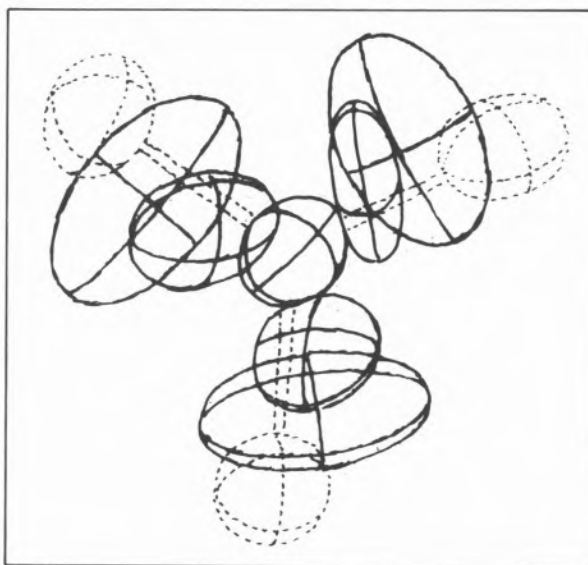


Fig. 3

ORTEP-plot of the anion projected onto the plane of the three static CO-groups. The picture indicates that the fourth CO-group is distributed equally between three equivalent positions

which may be considered as normal. The fourth CO-group, however, turns out to occupy — with equal probability — three equivalent positions,

each of them being characterized by large mean-square displacement. Similar to this the central iron undergoes relatively large displacements. The symmetry of the three equal CO-positions is such that the weighted average of the three corresponding electric field gradient tensors yields zero-quadrupole splitting. (This conclusion is also in agreement with results which we have derived from corresponding semiempirical molecular orbital calculations). From this consideration and from the temperature-dependence of our Mössbauer parameters, we conclude that the structure of the anion is, with respect to the nuclear lifetime of ^{57m}Fe , static with low point-symmetry below 180 K. Above 210 K one of the four CO-groups undergoes fast enough transitions between the three equivalent positions. We have analyzed this specific dynamic behavior in full detail by inspecting the temperature dependence of the Mössbauer lineshape of $[\text{HFe}(\text{CO})_4]^-$ under relaxation conditions [3,4]. We have found that the relaxation of one of the four CO-groups among its three equivalent sites is associated with a corresponding jump behavior of Fe; however, the triangular displacement body of Fe with jump distance of about 0.30 Å is considerably smaller than that of the CO group.

ACKNOWLEDGEMENTS

This work was supported by Deutsche Forschungsgemeinschaft.

REFERENCES

- [1] F. SEEL, R. LEHNERT, E. BILL, A.X. TRAUTWEIN, *Z. Naturforsch., Teil B*, **35**, 631 (1980).
- [2] H.E. MARCOLIN, A.X. TRAUTWEIN, Y. MAEDA, F. SEEL, P. WENDE, *Theor. Chim. Acta*, **41**, 223 (1976).
- [3] M. BLUME, *Phys. Rev.*, **174**, 351 (1968).
- [4] E. BILL, N. BLAES, K.F. FISCHER, U. GONSER, K.H. PAULY, R. PRESTON, F. SEEL, R. STAAB, A.X. TRAUTWEIN, *Z. Naturforsch., Teil B*, **39**, 333 (1984).



PS4.12 — MO

H. WINKLER
E. BILL
A.X. TRAUTWEIN
L. ALDRIDGE
Physik
Medizinische Hochschule
2400 Lübeck 1
W. Germany
H. TOFTLUND
Chemistry
Odense University
4230 Odense M
Denmark

SPIN-CROSSOVER DYNAMICS IN MODEL-COMPOUNDS FOR HEME PROTEINS

Besides oxygenation and carboxylation of myoglobin and hemoglobin also electron transfer reactions of heme proteins are often associated with a change of the spin state of iron from high-spin to low-spin and vice versa. Investigating this transition may yield information about how the spin-crossover mechanism determines the reaction rate. Fe(II) complexes with hexadentate ligands of the type given in Fig. 1 may serve as appropriate models, because they exhibit spin-crossover beha-

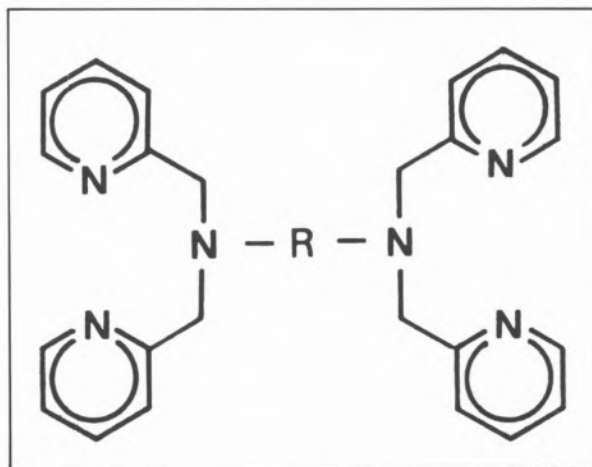


Fig. 1

The tetrakis(2-pyridyl-methyl)-R ligand type

viator in the temperature range $100 \text{ K} \leq T \leq 400 \text{ K}$ as identified by magnetic susceptibility measurements [1]. We have performed experimental Mössbauer studies on $\text{Fe}_{0.1}\text{Zn}_{0.9}(\text{tpchxn})(\text{ClO}_4)_2 \cdot n\text{H}_2\text{O}$ (tpchxn = tetrakis(2-pyridyl-methyl)-trans-1,2-cyclohexadiamine), where the transition rates are expected to fall into the time window of ^{57}Fe Mössbauer spectroscopy because according to GÜTLICH [2] dilution of ferrous spin-crossover systems with Zn causes in general an enhancement.

In Fig. 2 some representative Mössbauer spectra are displayed. At 100 K clearly two doublets can be distinguished: 1) with $\Delta E_Q = 0.48 \text{ mms}^{-1}$ and $\delta^* = 0.42 \text{ mms}^{-1}$ from low-spin Fe(II); 2) with $\Delta E_Q = 3.63 \text{ mms}^{-1}$ and $\delta^* = 0.96 \text{ mms}^{-1}$ from high-spin Fe(II). At 250 K an additional line is discernible which may be attributed to a third doublet 3) with $\Delta E_Q = 1.40 \text{ mms}^{-1}$ and $\delta^* = 0.03 \text{ mms}^{-1}$. (* = rel. to $\alpha\text{-Fe}$).

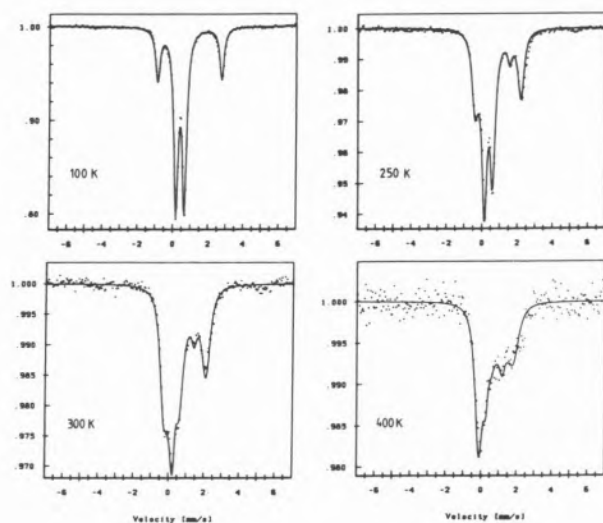


Fig. 2

Mössbauer spectra of $\text{Fe}_{0.1}\text{Zn}_{0.9}(\text{tpchxn})(\text{ClO}_4)_2$ at four different temperatures. The solid lines are simulations with the relaxation model described in the text

The appearance of such an «intermediate site» has recently been reported by EDWARDS *et al.* [3] also for $\text{Fe}(\text{phen})_2(\text{NCBH}_3)_2$. The Mössbauer resonances exhibit indeed line broadenings and shifts which are characteristic for relaxation processes. Therefore the attempt has been made to simulate the spectra with the random-frequency-modulation model of WICKMAN [4] which has been applied successfully by DZIOBKOWSKY *et al.* [5], *e.g.*, also to describe effects of electron hopping in the mixed-valence complex $[\text{Fe}(\text{II})\text{Fe}(\text{III})_2\text{O}(\text{CH}_3\text{COO})_6(\text{H}_2\text{O})_3]$. Common to the present case is the gradual averaging of different quadrupole splittings when the temperature is raised. For the sake of simplicity the two relaxation processes $\text{LS} \rightleftharpoons \text{HS}$ and $\text{LS} \rightleftharpoons \langle i \rangle$ were taken as completely separated from one another as sketched in Fig. 3. The results for the four spectra displayed in Fig. 2 are given in Table I, where A_I

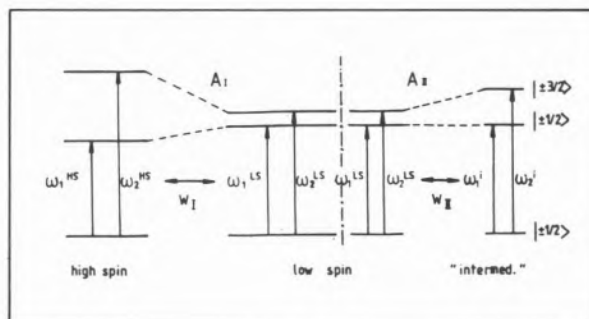


Fig. 3

Scheme of the assumed relaxation model

and A_{II} denote the relative portions of the two processes (Fig. 3), whereas w_I and w_{II} are the corresponding relaxation rates defined as sum of the forward and backward transition probabilities. The symbols p_{HS} and p_i represent the occupation probabilities of the HS- and $\langle i \rangle$ -state. The temperature dependence of ΔE_Q is shown in Fig. 4. The isomer shift of the LS-doublet is nearly constant

Table I
Relaxation parameters used for the simulations in Fig. 2 (uncertainty of about 1 in the last given digit)

T[K]	A_I	p_{HS}	w_I [MHz]	A_{II}	p_i	w_{II} [MHz]
100	1.00	0.23	0.01	0.00	—	—
250	0.86	0.41	1.1	0.14	0.41	0.06
300	0.83	0.53	3.5	0.17	0.53	0.7
400	0.75	0.58	8	0.25	0.58	0.9

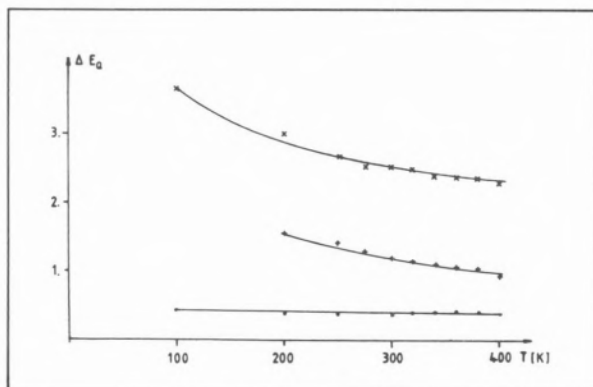


Fig. 4

Quadrupole splittings for high-spin (x) low-spin (•) and «intermediate» (+) doublet as a function of temperature

with increasing temperature while the other two doublets show a continuous decrease explainable by second order Doppler shift.

ACKNOWLEDGEMENTS

This work was supported by Deutsche Forschungsgemeinschaft.

REFERENCES

- [1] H. TOFTLUND, S. YDE-ANDERSEN, *Acta Chem. Scand., Ser. A*, **35**, 575 (1981).
- [2] P. GÜTLICH, in J.G. STEVENS, G.K. SHENOY (eds.), «Mössbauer Spectroscopy and Its Chemical Applications», American Chemical Society, Washington, 1981.
- [3] M.P. EDWARDS, C.D. HOFF, B. CURNUTTE, J.S. ECK, K.F. PURCELL, *Inorg. Chem.*, **23**, 2613 (1984).
- [4] H.H. WICKMAN, in I.J. GRUVERMAN (ed.), «Mössbauer Effect Method», vol. 2, Plenum Press, New York, 1966.
- [5] C.T. DZIOBKOWSKI, J.T. WROBLESKI, D.B. BROWN, *Inorg. Chem.*, **20**, 679 (1981).



PS4.13 — MO

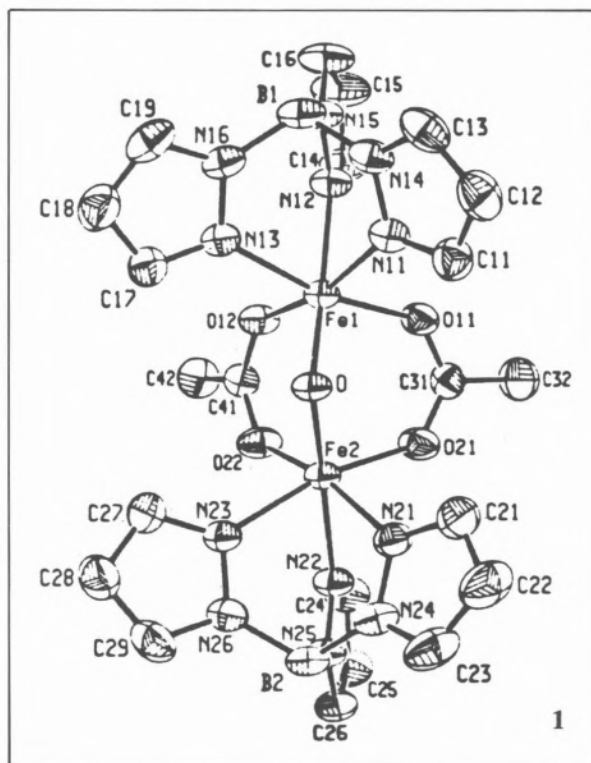
WILLIAM H. ARMSTRONG

STEPHEN J. LIPPARD

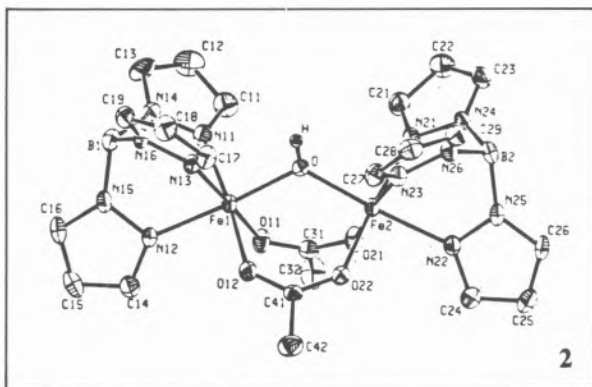
Department of Chemistry
Massachusetts Institute of Technology
Cambridge, Massachusetts 02139
U.S.A.

NEW CHEMISTRY OF BINUCLEAR IRON COMPLEXES — MODELS FOR HEMERYTHRIN AND RELATED PROTEINS

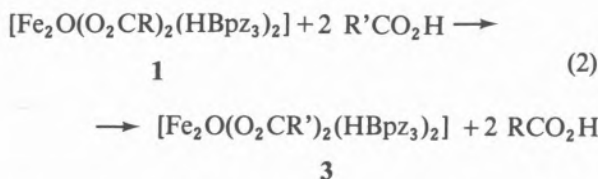
Previously we described the synthesis of $[\text{Fe}_2\text{O}(\text{O}_2\text{CR})_2(\text{HBpz}_3)_2]_2$ complexes [R = Me, Et, Ph; HBpz₃ = hydrotris(1-pyrazolyl)borate], **1**, and showed that their magnetic and spectroscopic properties closely resemble those of the met forms of hemerythrin as well as ribonucleotide reductase [1]. The analogs where HBpz₃ is replaced



by TACN (1,4,7-triazacyclononane) exhibit similar behavior [2]. The discovery [3] that **1** can be reversibly protonated to form $[\text{Fe}_2(\text{OH})(\text{O}_2\text{CR})_2(\text{HBpz}_3)_2]_2^+$, **2**, eq. (1), suggested that it might be possible to exchange the brid-



ging carboxylate groups in **1** with other carboxylic acids, eq. (2). This exchange reaction has now been demonstrated by NMR and optical spectroscopic studies. The mechanism presumably involves



protonation of the oxo bridge to form **2**, a reaction that lengthens the Fe-O bridge bond by 0.18 Å [3], followed by hydroxide bridge cleavage upon attack by the $\text{R}'\text{CO}_2^-$ anion on one of the iron centers. Closure of the $\text{R}'\text{CO}_2^-$ bridge displaces one oxygen of an originally bridging RCO_2^- ligand, and loss of RCO_2H together with closure of the Fe-O-Fe bridge completes the first substitution reaction. This process is then repeated to form the product **3**. Using related chemistry we have prepared and structurally characterized by X-ray crystallography the phosphate bridged analog of **1**, $[\text{Fe}_2\text{O}\{\text{O}_2\text{P}(\text{OPh})_2\}_2(\text{HBpz}_3)_2]$, **4**. These results demonstrate that carboxylate groups and phosphate esters can be readily exchanged into the bridging positions of the μ -oxodiiron(III) center, presumably by means of μ -hydroxodiiron(III) intermediates. This new chemistry raises interesting

possibilities for the catalytic mechanisms of ribonucleotide reductase, uteroferrin, and the purple acid phosphatases.

REFERENCES

- [1] a) W.H. ARMSTRONG, S.J. LIPPARD, *J. Am. Chem. Soc.*, **105**, 4837 (1983);
b) W.H. ARMSTRONG, A. SPOOL, G.C. PAPAETHYMIU, R.B. FRANKEL, S.J. LIPPARD, *J. Am. Chem. Soc.*, **106**, 3653 (1984).
- [2] a) K. WIEGHARDT, K. POHL, W. GEBERT, *Angew. Chem., Int. Ed. Engl.*, **22**, 727 (1983);
b) A. SPOOL, I.D. WILLIAMS, S.J. LIPPARD, submitted for publication.
- [3] W.H. ARMSTRONG, S.J. LIPPARD, *J. Am. Chem. Soc.*, **106**, 4632 (1984).
- [4] W.H. ARMSTRONG, S.J. LIPPARD, submitted for publication.



PS4.14 — TU

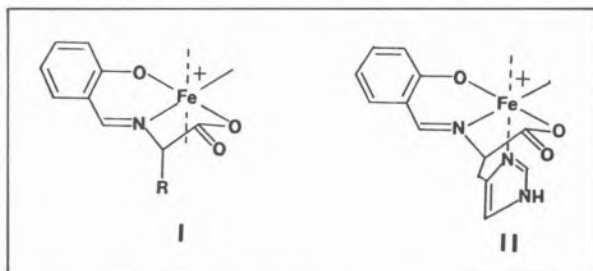
LUIGI CASELLA
MICHELE GULLOTTI
ALESSANDRO PINTAR
Dipartimento di Chimica Inorganica e Metallorganica
Centro CNR
Via Venezian 21, 20133 Milano
Italy

MODELS FOR IRON-TYROSINATE COORDINATION IN PROTEINS. SPECTRAL AND STEREOCHEMICAL STUDIES OF IRON(III) COMPLEXES OF *N*-SALICYLIDENE-L-AMINO ACIDS

The iron-tyrosinate proteins are a heterogeneous group of non-heme iron proteins that includes the transferrins, the catechol dioxygenases and the purple acid phosphatases [1]. These proteins display, as a common spectral feature, a moderately intense absorption band that dominates the visible spectrum and is attributed to a charge transfer transition from the tyrosinate residue to iron(III).

The position and intensity of this band depend on many factors, such as the metal geometry and the number of phenolate groups bound to iron(III), but it is also sensitive to the nature of the other ligands in the iron environment. Only limited information is available on the nature and number of these additional ligands in the various proteins; hence the importance of model studies [2-5] that serve to provide the necessary data for a correct interpretation of the spectral features of the metal sites in the proteins.

We have synthesized and characterized a series of high spin iron(III) complexes of the *N*-salicylidene derivatives of L-amino acids, Fe(sal-L-aa)Cl, having the structure **I** when the amino acid is non



polar or **II** in the case of histidine. The stereochemical properties of these complexes have been deduced on the basis of detailed studies performed on the corresponding zinc(II), copper(II) and cobalt(II) systems [6-8]. Systems of this type seem particularly convenient for the investigation of adduct formation with additional ligand molecules, since both equatorial and axial coordination positions are in principle available to the added ligands. The electronic spectra in methanol of the complexes of type **I** (aa = ala, val, phe) display the phenolate-to-iron charge transfer band in the narrow range 530-540 nm ($\epsilon \sim 1200 \text{ M}^{-1} \text{ cm}^{-1}$), while additional absorptions occur at ~ 430 ($\epsilon \sim 1000$), 318 (~ 5000), 295 (~ 5000), 262 (~ 13000) and 235 nm (~ 17000). Coordination of a pseudoaxial imidazole group, as in **II**, produces an ipsochromic shift of the visible bands, particularly that near 500 nm, but has almost negligible effects on the other electronic transitions. Shifts to higher energy of the phenolate-to-iron charge transfer bands can be observed in the spectra of either **I** or **II** upon addition of various bases, the extent of the shift being dependent on the nature of the added base. Comparable changes occur in the CD

spectra of the systems. Of particular interest are the adducts between **I** or **II** and the catecholate monoanion (catH) that may be compared with other models proposed [3] for substrate binding to the catechol dioxygenase enzymes [1]. The adducts [Fe(sal-L-ala)(catH)] and [Fe(sal-L-his)(catH)] exhibit phenolate-to-iron charge transfer bands at 480 and 470 nm, respectively, with a broad shoulder between 650 and 700 nm, that is attributed to a catecholate-to-iron charge transfer band [9]. Although the match may be accidental, the similarity between these spectra and those of the corresponding dioxygenase-substrate complexes (465 and ~ 680 nm for catechol dioxygenase, 475 and ~ 690 nm for protocatechuate 3,4-dioxygenase) [1] is surprisingly good (for [Fe(salen)(catH)] the corresponding bands occur at 418 and ~ 590 nm) [1] and bear on the relevance of the Fe(sal-L-aa)X complexes in model studies of iron-tyrosinate proteins.

REFERENCES

- [1] L. QUE JR., *Coord. Chem. Rev.*, **50**, 73 (1983).
- [2] E.W. AINSCOUGH, A.M. BRODIE, J.E. PLOWMAN, K.L. BROWN, A.W. ADDISON, A.R. GAINSFORD, *Inorg. Chem.*, **19**, 3655 (1980).
- [3] R.H. HEISTAND II, R.B. LAUFFER, E. FIKRIG, L. QUE JR., *J. Am. Chem. Soc.*, **104**, 2789 (1982).
- [4] S.A. KOCH, M. MILLAR, *J. Am. Chem. Soc.*, **104**, 5255 (1984).
- [5] A.L. ROE, D.J. SCHNEIDER, R.J. MAYER, J.W. PYRZ, J. WIDOM, L. QUE JR., *J. Am. Chem. Soc.*, **106**, 1676 (1984).
- [6] L. CASELLA, M. GULLOTTI, *J. Am. Chem. Soc.*, **103**, 6338 (1981).
- [7] L. CASELLA, M. GULLOTTI, G. PACCHIONI, *J. Am. Chem. Soc.*, **104**, 2386 (1982).
- [8] L. CASELLA, M. GULLOTTI, submitted for publication.
- [9] R.B. LAUFFER, R.H. HEISTAND II, L. QUE JR., *J. Am. Chem. Soc.*, **103**, 3947 (1981).



PS4.15 — TH

N. NI CHOILEAIN
J.D. GLENNON
Chemistry Department
University College Cork
Cork
Ireland

ANALYTICAL TECHNIQUES IN THE STUDY OF Ni AND Fe MODEL COMPLEXES OF BIOLOGICAL SIGNIFICANCE

There is increasing awareness of the need for analytical probes that can determine the complex species of a metal without disturbance of the matrix. The task is made somewhat easier by using model compounds, designed to mimic the properties of the complex of interest. The elucidation of the Ni(II)-binding site of human serum albumin involved the use of computer-assisted potentiometric analysis of the interaction of the *N*-terminal native-sequence tripeptide, L-aspartyl-L-alanyl-L-histidine *N*-methylamide with Ni(II). The low-molecular-weight Ni(II) binding constituent in human serum, L-histidine, forms only two major complex species in the pH range 4-9, Ni(Hist) and Ni-(Hist)₂ [1]. The species distribution is verified by examining the system by differential pulse polarography at the same metal:ligand ratio. Fig. 1 shows in a single scan the two kinetically inert complex species, at pH 6.2, and serves as a useful comparison of the information that can be obtained by the application of current-measuring and potentiometric methods of analysis.

As an extension of our previous studies on Fe(III)-monohydroxamate complexes, investigations into the synthesis and analysis of simple model compounds of the naturally occurring rhodoturulic acid were undertaken [2,3]. A strong indication of similar Fe(III)-binding comes from an examination of the visible absorption spectra of the Fe(III) complexes of the synthesised dihydroxamic

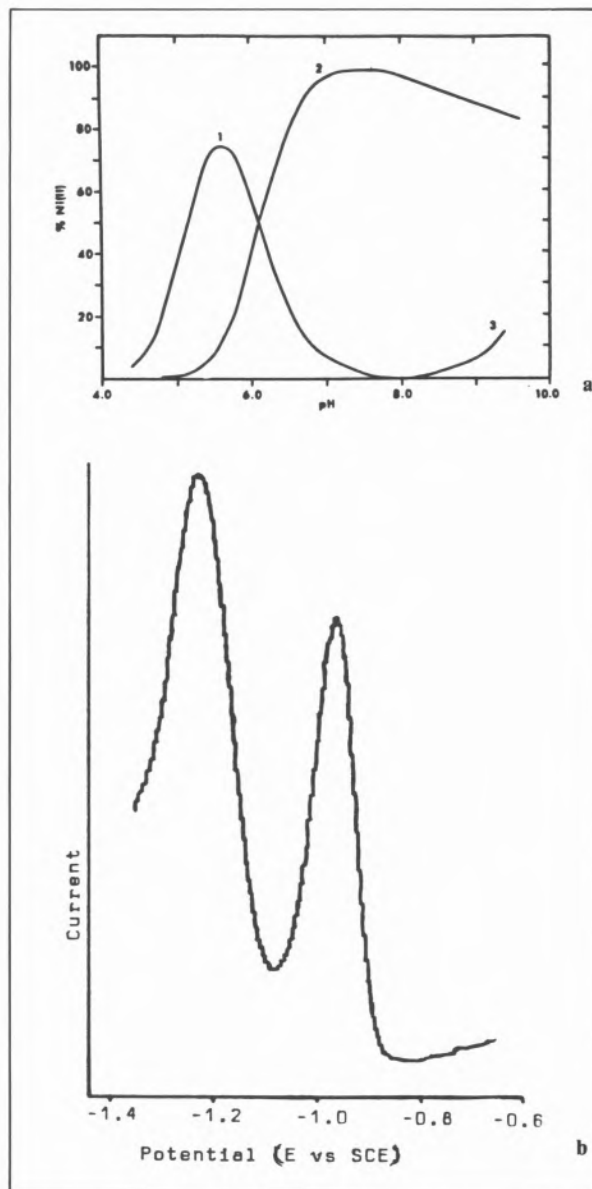


Fig. 1

- a) Species distribution diagram for the Ni(II)-L-His system, $C_M = 1.09 \times 10^{-4} M$, $C_L = 4.81 \times 10^{-4} M$, curve 1, ML ; curve 2, ML_2 ; curve 3, $MH_{-1}L_2$
b) Differential pulse polarogram of Ni(II)-L-His system in $0.6 M NaNO_3$ at pH 6.2

acids, HOHN-CO-(CH₂)_n-CONHOH [4]. A clear isobestic point at 480 nm is evident suggesting that two complex species exist in the pH range 3.6 to 9.0. Results from the potentiometric analysis for $n=3$ indicates a levelling of \bar{n} at a value of 1.5 supporting a formulation of Fe_2L_3 (Fig. 2). The insolubility of the orange complex at higher concentrations is also atypical of simple hydro-

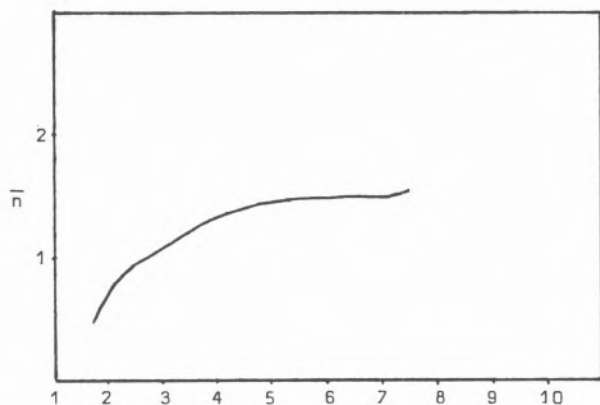


Fig. 2

Plot of \bar{n} versus pH for the Fe(III)-glutaryl dihydroxamic acid system ($n=3$)

xamate complexation of Fe(III). Further investigations are being carried out.

REFERENCES

- [1] J.D. GLENNON, B. SARKAR, *Biochem. J.*, **203**, 12-23 (1982).
- [2] D.A. BROWN, M.V. CHIDAMBARAM, J.D. GLENNON, *Inorg. Chem.*, **19**, 3260-3264 (1980).
- [3] S.J. BARCLAY, B.H. HUYNH, K.N. RAYMOND, *Inorg. Chem.*, **23**, 2011-2018 (1984).
- [4] D.A. BROWN, R. GERATY, N. NI CHOILEAIN, J.D. GLENNON, unpublished observations.

of central molybdenum oxidation states from VI to IV (*via* V) indicate the minimal coordination spheres $\text{Mo}^{\text{VI}}\text{O}_2(\text{SR})_{2,3}$ and $\text{Mo}^{\text{IV}}\text{O}(\text{SR})_{3,4}$ for the oxidised and fully reduced forms, respectively. Numerous molybdenum-containing model complexes have been prepared to mimic the structural as well as the functional properties of the molybdoenzymes [1]. To date none of these model complexes appears to have all these properties very similar to the molybdoenzymes. We have synthesized some monomeric complexes of the general formula: $[\text{MoS}(\text{S}_2)(\text{DTC})]$, $[\text{MoO}(\text{DTC})(\text{cat})]$ and $[\text{MoO}_2(\text{DTC})(\text{cat})]^-$ (DTC = dialkyldithiocarbamate, cat = catecholatedianion). These complexes catalyze the oxidation of xanthine and sulfite and can reduce molecular oxygen to superoxide. Typical EPR parameters for the complex $[\text{MoOEt}_2(\text{DTC})(\text{cat})]$ (g_{xx} , 1.951; g_{yy} , 1.979; g_{zz} , 1.995; $\langle g \rangle = 1.975$; $\langle A \rangle$, 31.0) suggest the structural closeness of this model compound to xanthine oxidase [2]. EPR and other spectral data along with C.V. results are presented and their relevance to enzymatic processes is discussed.

REFERENCES

- [1] W.E. NEWTON, S. OTSUKA (eds.), «Molybdenum Chemistry of Biological Significance», Plenum Press, N.Y., 1980.
- [2] R.C. BRAY, «Molybdenum Iron-Sulfur Flavin Hydroxylases and Related Enzymes», in P.D. BOYER (ed.), «The Enzymes», 3rd edn., vol. XII, Academic Press, N.Y., 1975, p. 299.



PS4.16 — MO

JAYANTI CHANDRASEKARAN
SABYASACHI SARKAR

Department of Chemistry
Indian Institute of Technology
Kanpur 208 016
India

SYNTHETIC APPROACH TO THE MONONUCLEAR ACTIVE SITES OF MOLYBDOENZYMES

EXAFS results for several molybdoenzymes responsible for oxidation of substrates X/XO by oxygen atom transfer with concomitant changes



PS4.17 — TH

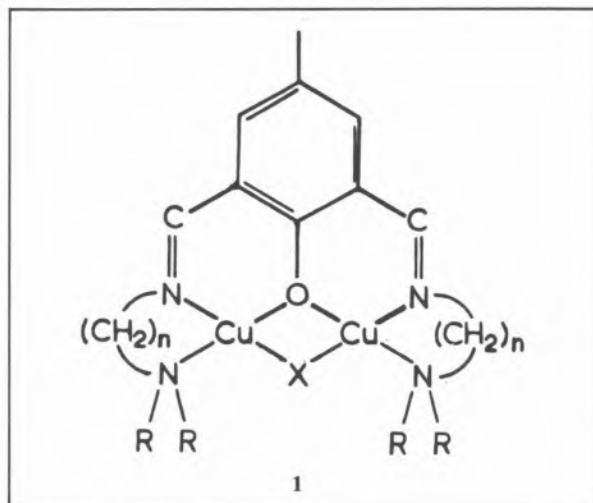
J. LORÖSCH
 U. QUOTSCHALLA
 W. HAASE
 Institut für Physikalische Chemie
 Technische Hochschule Darmstadt
 Petersenstr. 20, 6100 Darmstadt
 F.R.G.

MODELLING THE HEMOCYANIN ACTIVE SITE: A CONTRIBUTION TO MAGNETO-STRUCTURAL CORRELATIONS

The dioxygen carrying protein hemocyanin is the best investigated enzyme containing a binuclear Cu(II)-active site. In the oxidized form the Cu(II)-ions are tetragonally coordinated and bridged by an endogenous protein group for which authors [1] favour a phenolate group from tyrosine. For the oxy-form dioxygen is known to form an exogenous bridge, whereas azide, chloride, etc. are found in the artificial met-forms.

Magnetic investigations of these protein forms referred to strong antiferromagnetic coupling between the two Cu(II)-ions resulting in diamagnetism [2]. To understand this magnetic behaviour magneto-structural correlations for two particular features of the hemocyanin active site are needed. Model complexes containing (i) asymmetric bridged Cu(II)-ions and (ii) a large Cu-O-Cu bridging angle at the endogenous ligand have to be investigated. Because it is quite impossible to vary continuously the bridging angle in a single asymmetric bridged model system the problem has to be resolved separately and then correlated.

As a part of our investigations in the magnetic behaviour of the hemocyanin active site we present in this study different asymmetric bridged Cu(II)-dimers. For modelling the asymmetric bridging character of the active site we have synthesized a five-dentate macrocyclic ligand forming binuclear Cu(II)-complexes (1).



The structures of three complexes with an exogenous OH-bridge ($n=2$, $R=Et$ and $n=3$, $R=Me$) [3,4] and an exogenous N_3 -bridge ($n=3$, $R=Me$) [5], respectively, will be presented.

The copper coordination polyhedra in all complexes are similar. The 4+1 coordination can be described as a square planar basis plane with an additional ligand perpendicular to this plane and more elongated. In the azido-bridged dimer the azido-group is bound end-on. In this compound the bridging angles Cu-O-Cu and Cu-N-Cu are similar (103°) whereas in the OH-bridged complexes a significant difference of several degrees between the two Cu-O-Cu bridging angles has been observed.

A first attempt to obtain magneto-structural correlations for asymmetric bridged dimers will be discussed. We propose a model to relate the strong antiferromagnetic coupling found in all three asymmetric bridged complexes ($-500 \text{ cm}^{-1} > 2J > -900 \text{ cm}^{-1}$) to magneto-structural data from symmetric dimers. Exchange coupling has been found to depend mainly on the properties of that bridge (electronegativity, bridging angle) which would give the stronger antiferromagnetic coupling in symmetric dimers. The energy gap between the levels $S=0$ and $S=1$ can be described as having approximately the same magnitude as has been found for the corresponding symmetric complexes.

The magnetic behaviour of the discussed asymmetric bridged dimers leads to the following conclusions about exchange coupling in hemocyanin:

- exchange coupling of the hemocyanin active site depends mainly on the bridging tyrosine oxygen;
- asymmetric model complexes with increased bridging angle up to 140° are needed to obtain more information about the exchange coupling of the hemocyanin active site.

REFERENCES

- [1] E.I. SOLOMON in T.G. SPIRO (ed.), «Metal Ions in Biology», vol. 3, Wiley-Interscience, New York, 1981, pp. 41-108.
- [2] D.M. DOOLEY, R.A. SCOTT, J. ELLINGHAUS, E.I. SOLOMON, H.B. GRAY, *Proc. Natl. Acad. Sci. USA*, **75**, 3019 (1978).
- [3] J. LORÖSCH, U. QUOTSCHALLA, W. HAASE, to be published.
- [4] J. LORÖSCH, H. PAULUS, W. HAASE, submitted for publication.
- [5] J. LORÖSCH, H. PAULUS, W. HAASE, *Inorg. Chim. Acta*, in press.



PS4.18 — MO

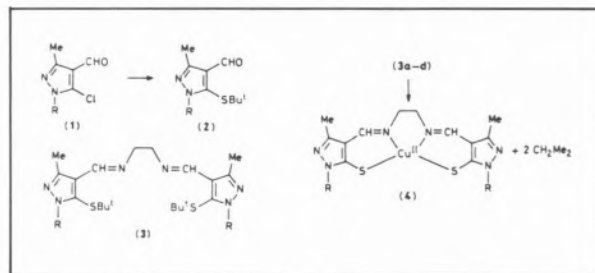
JAN BECHER
HANS TOFTLUND
Department of Chemistry
University of Odense
DK-5230 Odense M
Denmark

BIOMIMETIC SYSTEMS FOR THE "VISIBLE" COPPER-SITE Cu_A IN CYTOCHROME *c* OXIDASE

Recent work on the structure of the Cu_A site of cytochrome *c* oxidase suggests that two cysteines and two histidines are ligated to the central copper ion. We have demonstrated that *t*-butyl sulfides are convenient sources of copper(II) thiolato complexes as Cu^{2+} is a sufficiently strong Lewis acid to cleave the sulfur *t*-butyl-bond. This method has been used to pre-

pare a series of S_2N_2 copper(II) complexes of Schiff-base ligands derived from 2-mercaptoaldehydes and diamines. From the spectral properties of these systems we have suggested that a red shift of the LMCT bands, as well as a decrease in A_{\parallel} , for the thiolato copper(II) complexes may be caused by two independent factors: either through an increase in the electron density at sulfur or through an increase in the tetrahedral distortion of the Cu(II) chromophore.

By variation in the molecules, we have prepared a number of ligands based on different heterocycles for the study of Cu(II) protein models. An example with pyrazole is shown in the scheme:



The β -chloroaldehydes as well as the protected β -mercaptoaldehydes are also useful as starting materials for the preparation of annelated heterocycles.

REFERENCE

- J. BECHER, H. TOFTLUND, P.H. OLESEN, *J. Chem. Soc., Chem. Commun.*, 740 (1983).



PS4.19 — TU

J. VAN RIJN

W.L. DRIESSEN

J. REEDIJK

Department of Chemistry

State University Leiden

P.O. Box 9502, 2300 RA Leiden

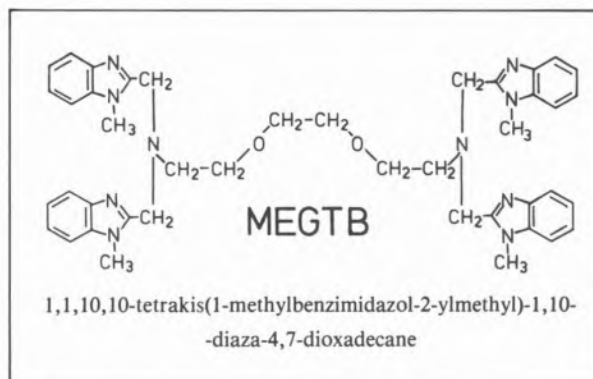
The Netherlands

COPPER CHELATES OF A DINUCLEATING BENZIMIDAZOLE-CONTAINING LIGAND AS MODELS FOR TYPE III COPPER PROTEINS

The active site in Type III copper proteins is generally believed to contain two copper ions close together and each coordinated by at least two imidazole groups of histidine residues [1]. The coordination geometry, imposed by the structure of the protein, is known to influence the specific properties, like O_2 transport or oxidative catalysis. To help elucidating the structures and understanding the reactivities of these proteins, low molecular weight compounds are studied as models. The steric constraints in polydentate ligands, *e.g.* the size of the bite and the presence of bulky substituents, are used as tools in tuning the model system. The incorporation of benzimidazole groups has the advantages of a biomimetic group being easily synthesized and having a bulky substituent.

The ligand megtb (see figure) has the potential to bind two metal ions with several possibilities for the metal-metal distances, both with and without exogenous bridging ligands. The ligand has been prepared in two steps, *i.e.* a ring closure reaction by condensation of *o*-diaminobenzene with the polyaminocarboxylic acid EGTA (ethylene glycol bis-(β -aminoethyl ether) *N,N,N',N'*-tetraacetic acid), followed by *N*-methylation [2].

The coordination compounds with copper(II) appear to have two general formulae: a) $Cu_2LX_4 \cdot nH_2O$ with different kind of anions and



$Cu_2LX_2Y_2 \cdot nH_2O$ for X=halide and Y=a non-coordinating anion; b) $Cu_2LXY_3 \cdot nH_2O$ for X=1,3-azolate and Y=a non-coordinating anion. The crystal structures of $Cu_2(megtb)F_2(BF_4)_2 \cdot 3H_2O$ and $Cu_2(megtb)Cl_4 \cdot 6H_2O$ show a coordination geometry close to a square pyramid with 3 N atoms and the halide anion in the equatorial plane and an O ether atom on the apical position. The halide anion is also a sixth donor atom for a neighbouring Cu(II) ion at a larger, non-bonding distance. The resulting intermolecular Cu-Cu distance is slightly shorter than the intramolecular one. The magnetic exchange is weak in these compounds.

When bridging ligands are used in a sub-stoichiometric ratio, together with non-coordinating anions, intramolecular dicopper species can be obtained. They have a typical spin-triplet EPR spectrum both in the solid state and in solution, and J-values characteristic for copper dimers with bridging 1,3-azolates.

With Cu(I) both stable mononuclear compounds with non-coordinating anions, as well as dinuclear compounds with coordinating (pseudo)halides, are formed. Reaction with carbon monoxide results in a stable 1:1 (Cu:CO) product. The compounds react stepwise with dioxygen and are active in the oxidative coupling of 2,6-dialkylphenols. This reaction is used as a test reaction to investigate the catalytic properties of these and related systems.

REFERENCES

- [1] W.P.J. GAYKEMA, W.G.J. HOL, J.M. VEREIJKEN, N.M. SOETER, H.J. BAK, J.J. BEINTEMA, *Nature*, **309**, 23 (1984).
- [2] J. VAN RIJN, J. REEDIJK, *Recl. Trav. Chim. Pays-Bas*, **103**, 78 (1984).



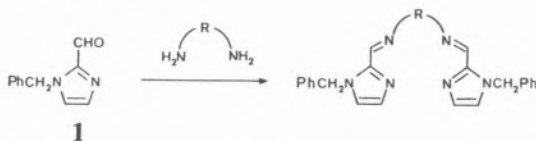
PS4.20 — TH

NEIL A. BAILEY
 DAVID E. FENTON
 COLIN H. McLEAN
 Department of Chemistry
 The University of Sheffield
 Sheffield S3 7HF
 U.K.

**IMIDAZOLE-CONTAINING SCHIFF BASE
 LIGANDS AS VERSATILE MODELS
 FOR COPPER PROTEIN ENVIRONMENTS**

The active sites of cuproproteins, for which crystal structures are available, contain copper(II) ion bound by one or more histidine imidazole groups [1]. Consequently it is of interest to prepare complexes of ligands containing imidazole groups as small molecule models for these copper(II) sites.

The condensation of 1-benzylimidazole-2-carboxaldehyde, **1**, with primary diamines leads to ligands able to complex a central metal ion in an N₄ donor set:



Visible spectroscopy of the copper(II) complexes of these ligands has been used to examine the effect of the length and nature of the ligand backbone (R) on the geometry of the central metal ion. The crystal structure of the copper(II) complex where R = (CH₂)₄, Cu(Bzic₂tmd)(ClO₄)₂, has been solved, (Figure).

4-Methyl-5-[(2-aminoethyl)thiomethyl]imidazole, **2**, (an intermediate in the production of the antiulcer drug cimetidine [2]), and related aminothioetherimidazoles, have been employed in the design and synthesis of Schiff Base chelates capable of providing N₃S, N₂S₂, or N₂SO donor sets around a central metal ion.

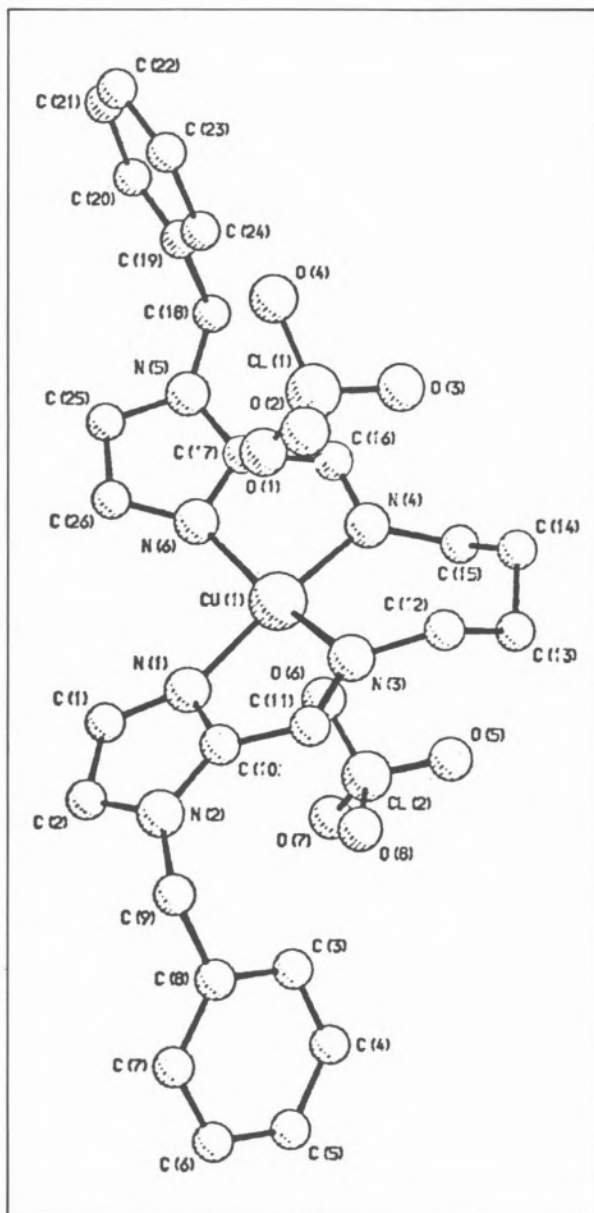
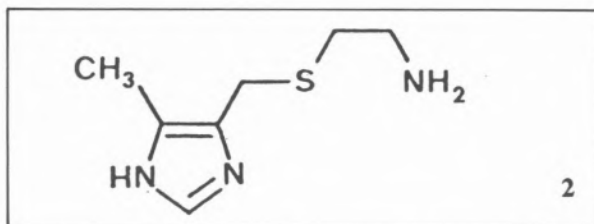


Figure
 The crystal structure of Cu(Bzic₂tmd)(ClO₄)₂



Mononuclear copper(II) complexes of these ligands can be related to Type I copper protein environments, while homo- and hetero-binuclear

imidazolate-bridged complexes can be prepared as models for the bimetallic active sites of metallo-proteins such as superoxide dismutase.

REFERENCES

- [1] E.I. SOLOMON, K.W. PENFIELD, D.E. WILCOX, *Struct. Bonding (Berlin)*, **53**, 1 (1983).
- [2] G.J. DURANT, J.C. EMMETT, C.R. GANELLIN, *British Patent*, 1 338 169 (1973).



PS4.21 — MO

THOMAS N. SORRELL
A.S. BOROVIK
DEBORA J. ELLIS
CHIEN-CHANG SHEN
Department of Chemistry
University of North Carolina
Chapel Hill, NC 27514
U.S.A.

MODELS FOR COPPER PROTEINS

Copper proteins are widespread in biology, performing many functions related to oxygen metabolism; and binding and activation of dioxygen by hemocyanin and tyrosinase have attracted much recent attention [1]. In many respects, this focussed interest has largely ignored the rich inorganic chemistry of the binuclear active-site in hemocyanin which encompasses reactions of the reduced form of the protein with carbon monoxide, nitric oxide, and other small ligands; generation of mixed-valence derivatives; and reactions of the oxidized form of the protein with small anionic ligands.

We have pursued studies in several directions with the aim of exploring the chemistry, spectroscopy, and physical properties of mono- and binuclear copper complexes. Much of this work involves the synthesis of multidentate ligands that are able to chelate the copper ion in an environment that mi-

mics the structural features of the hemocyanin active site.

We prepared the binucleating ligand bpeac (2,6-bis{bis[2-(1-pyrazolyl)ethyl]amino}-*p*-cresol) and both its copper(II) [2] and copper(I) [3] derivatives. The copper(II) complex thus formed contains two Cu(II) ions bridged by a phenolate group and bound by three nitrogen donors each. In addition, another anionic ligand (acetate or azide) bridges the two copper ions, completing the coordination sphere. The azide derivative is especially interesting since the two copper(II) ions are antiferromagnetically coupled, and the singlet-triplet splitting, $2J$, is equal to -1800 cm^{-1} , rendering the complex diamagnetic at room temperature. Other spectroscopic properties of this azido-bridged dimer are similar to those for the azido derivative of hemocyanin, strengthening the proposals for the structure of its active site. The copper(I) derivative of bpeac represents one of only two phenolato-bridged copper(I) dimers having no other bridging group. However, the reaction of this compound with O_2 , even at low temperature, results in irreversible oxidation of the copper(I) ions and illustrates the possible importance for isolation of the active site by the protein in hemocyanin in order to eliminate intermolecular interactions. Studies of the copper(I) derivatives of more hindered analogs of bpeac will be reported.

The unusual luminescence of the carbonyl derivative of hemocyanin has provided us with another interesting lead to follow to understand the structure of the hemocyanin active site [4]. We have prepared a number of mononuclear copper(I) complexes and examined their absorption spectra and luminescence properties both in the absence and presence of carbon monoxide. The results of these investigations will be reported, and their implications discussed.

REFERENCES

- [1] E.I. SOLOMON, in T.G. SPIRO (ed.), «Copper Proteins», John Wiley & Sons, Inc., New York, 1981, chapter 2.
- [2] T.N. SORRELL, C.J. O'CONNOR, O.P. ANDERSON, J.H. RIEBENSPIES, *J. Am. Chem. Soc.*, in press.
- [3] T.N. SORRELL, A.S. BOROVIK, *J. Chem. Soc., Chem. Commun.*, 1489-1490 (1984).
- [4] A. FINAZZI-AGRO, L. ZOLLA, L. FLAMIGNI, H.A. KUIPER, M. BRUNORI, *Biochemistry*, **21**, 415-418 (1982).



PS4.22 — TH

STEPHEN A. KOCH

RONALD FIKAR

DOUGLAS CORWIN

Department of Chemistry

State University of New York at Stony Brook

Stony Brook, New York

U.S.A.

MICHELLE MILLAR

Department of Chemistry

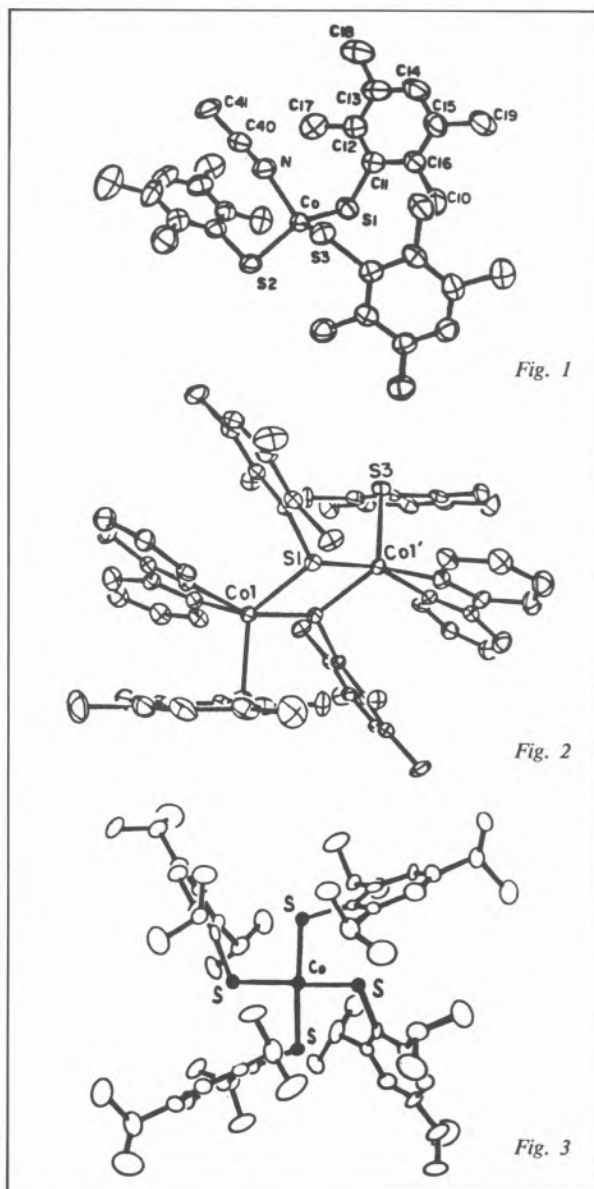
New York University

New York, NY 10003

U.S.A.

COBALT THIOLATE COMPLEXES: MODELS FOR THE ACTIVE SITES OF METAL-CYSTEINE PROTEINS

Cobalt has been extensively substituted for native metals in metalloproteins to serve as a spectral probe. A series of cobalt thiolate complexes have been prepared to serve as models for the cobalt-cysteine coordination found in cobalt-substituted proteins, including alcohol dehydrogenase, blue copper proteins, and metallothionein. We have used the steric capacity of the thiolate ligands to control the coordination number and the molecularity of the cobalt thiolate complexes. The reaction of three equivalent of 2,3,5,6-tetramethylbenzenethiolate with CoCl_2 gives a monomeric, four-coordinate complex $[\text{Co}(\text{S-2,3,5,6-Me}_4\text{C}_6\text{H})_3(\text{CH}_3\text{CN})]^-$ (Fig. 1); with less sterically encumbered thiolate ligands, the $[\text{Co}_4(\text{SR})_{10}]^{2-}$ adamantane cluster is obtained. We have found that $\text{Co}(\text{SR})_2\text{L}_2$ complexes have a strong tendency to become five-coordinate by adding another ligand. For the case of $[\text{Co}(\text{S-2,3,5,6-Me}_4\text{C}_6\text{H})_2(\text{bipy})]$, this is achieved by dimerization to give a structure with an unsymmetric μ -di-thiolate bridge (Fig. 2). In the case where the thiolate is 2,4,6-triisopropylbenzenethiolate, the coordination shell is expanded by the addition of an CH_3CN to give the five coordinate monomeric complex $[\text{Co}(\text{SR})_2(\text{L}_2)(\text{CH}_3\text{CN})]$ ($\text{L}_2 = \text{bipy, phen}$). The analogous zinc compound, $[\text{Zn}(\text{S-2,4,6-}i\text{-Pr}_3\text{C}_6\text{H}_2)_2(\text{bipy})]$, does not add an



CH_3CN ligand and remains four coordinate. The possible relevance of these findings to the question of the occurrence of five coordinate intermediates in alcohol dehydrogenase will be presented. EXAFS and ESR studies of the newly discovered nickel center in certain hydrogenase enzymes suggest that this center contains Ni(III) in a tetragonal ligand environment with four sulfur ligands. We have been studying nickel and related cobalt thiolate complexes to serve as models for this novel biological active site. With these objectives in mind, we have synthesized a quite interesting Co(III) tetrathiolate anion (Fig. 3) which is a rare example of a square planar Co(III) complex.

5. Complexes of Biochemical Interest



PSS.1 — MO

MARKUS BAUMGARTNER
 NORBERT CATHOMAS
 GEOFFREY B. JAMESON
 ERICH DUBLER
 Institute of Inorganic Chemistry
 University of Zürich
 8057 Zürich
 Switzerland

METAL COMPLEXES OF SULFUR-CONTAINING LIGANDS OF BIOLOGICAL INTEREST: S-METHYL-L-CYSTEINE, α -LIPOIC ACID AND GLUTATHIONE

S-methyl-L-cysteine (SMC) offers three possible binding sites for metal atoms: The carboxylate group, the amino nitrogen atom and the thioether linkage. Since sulfur atoms are soft bases, they are expected to interact most favorably with soft acids as Hg(II), Pt(II), Ag(I) or Cu(I), but to a less extent with borderline acids as *e.g.* Cu(II).

We have grown single crystals of a copper(II) complex $Cu(SMC)_2$ from solution on the surface of solid copper(II) hydroxy salts. The crystal structure determination ($R=0.045$, $R_w=0.052$) confirms spectroscopic evidence that the thioether sulfur is not coordinated to copper(II), even though there is a potentially favorable five-membered chelate ring with sulfur and nitrogen as coordinating atoms. Bridging of the copper centers by carboxylate groups leads to a two-dimensional polymeric structure approximately isostructural with its cadmium analogue [1]. The copper(II) atom exhibits a (4+2) tetragonally elongated CuN_2O_4 coordination octahedron.

α -Lipoic acid (LIP, DL-6,8-thiooctic acid) is a biomolecule widely distributed in animals and plants. Obviously there are two binding sites for metal

atoms: The carboxylate group and the disulfide moiety.

Single crystals of a zinc complex, $Zn(LIP)_2 \cdot 2H_2O$, were grown on the surface of solid zinc hydroxy salts. The crystal structure determination ($R=0.068$, $R_w=0.084$) proves the occurrence of isolated molecules $[Zn(LIP)_2(H_2O)_2]$ with the carboxylate groups acting as bidentate ligands. As suggested [2] there is no interaction of the disulfide moiety of α -lipoic acid with the metal atom. The coordination geometry of the zinc(II) atom is a ZnO_6 octahedron with pronounced distortion. This is the first crystal structure reported of a metal complex of lipoic acid.

Glutathione (GSH): A copper(II) complex with the formula $Cu(II)_2GSSG \cdot 6H_2O$ could be isolated. From the interpretation of UV- and EPR-spectra it seems plausible that this complex exhibits a dimeric structure with the disulfide moiety linking two copper(II) atoms as it is found in $Cu(II)_2GSSGNa_4 \cdot 6H_2O$ [3].

REFERENCES

- [1] P. DE MEESTER, D.J. HODGSON, *J. Am. Chem. Soc.*, **99**, 6884 (1977).
- [2] H. SIGEL, *Angew. Chem., Int. Ed. Engl.*, **21**, 389 (1982).
- [3] K. MIYOSHI, Y. SUGIURA, K. ISHIZU, Y. IITAKA, H. NAKAMURA, *J. Am. Chem. Soc.*, **102**, 6130 (1980).



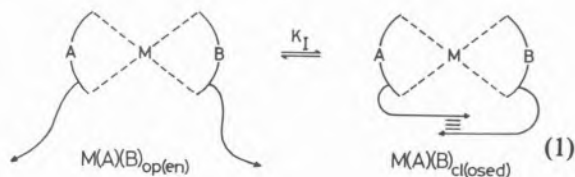
PS5.2 — TH

HELMUT SIGEL
 ROGER TRIBOLET
 Institute of Inorganic Chemistry
 University of Basel
 Spitalstrasse 51, CH-4056 Basel
 Switzerland

INTRAMOLECULAR HYDROPHOBIC AND STACKING INTERACTIONS IN BINARY AND TERNARY AMINO ACID COMPLEXES

Selectivity is one of the outstanding features of biological systems; it is often caused by non-covalent interactions, like aromatic-ring stacking or hydrophobic interactions [1]. After our recent observations [2-4] that both these types of intramolecular ligand-ligand interactions in mixed ligand complexes may be promoted by the addition of ethanol or dioxane to an aqueous solution of these complexes, we screened the stability data available in the literature for evidence of such intramolecular interactions in binary and ternary amino acid complexes.

The considered intramolecular equilibrium is schematically represented in (1).



The position of this equilibrium is independent of the concentration; it is quantified by the dimensionless equilibrium constant K_1 (eq. (2)),

$$K_1 = \frac{[M(A)(B)_{cl}]}{[M(A)(B)_{op}]} \quad (2)$$

and this constant may be calculated from the stability data obtained from potentiometric pH titrations; the percentage of the «closed» isomer follows from K_1 [1,5,6].

There are two careful studies available, which deal with the effect of dioxane on the stability of amino acid complexes: in one [7] the Cu^{2+} /alaninate (Ala^-) system is described and in the other [8] the Cu^{2+} /leucinate (Leu^-) system. For both systems complex stability increases with increasing amounts of dioxane, but the $\text{Cu}(\text{Leu})_2$ complex is in the dioxane-water mixtures by 0.2 to 0.7 log units more stable than expected [3]. This additional stability increase may be attributed to intramolecular hydrophobic interactions between the isopropyl residues in $\text{Cu}(\text{Leu})_2$; the extent of this interaction (eq. (1): $A=B=\text{Leu}$) changes in dependence on the amount of dioxane added to water: $\text{Cu}(\text{Leu})_{2/cl}$ reaches 21% in water, 81% in 50% (v/v) dioxane-water, and 64% in 70% (v/v) dioxane-water ($I=0.1$; 25°C) [3]. This shows that addition of some dioxane favors the intramolecular hydrophobic interaction in $\text{Cu}(\text{Leu})_2$, while high concentrations of the organic solvent (>60%) destabilize it. This observation of an initial promotion of the interaction contrasts with the common experience made at simple unbridged adducts: they are always destabilized by the addition of dioxane or other organic solvents [4,9]. In several mixed ligand complexes [3,4], however, intramolecular stacking is also promoted by the addition of ethanol or dioxane.

The stability data of other binary and ternary metal ion/amino acid systems are summarized in the Table; they provide further evidence that hydrophobic and aromatic-ring stacking interactions in complexes of amino acids with suitable side chains are quite common.

It must be mentioned in this connection that the increased stability in aqueous solution of the Cu^{2+} bis-complexes of phenylalanine, tyrosine and similar amino acids has been repeatedly attributed to Cu^{2+} /aromatic-ring interactions [10,11]. However, the often used argument based on the solid-state structures is not conclusive, because even in the solid state the interaction is weak, if it exists at all; this follows from two different crystal structure analyses of the bis(L-phenylalaninato) copper(II) complex: in one case [12] the phenyl ring is located below Cu^{2+} , while in the other it is not [13]. In addition, in a recent study [14] of Pd^{2+} complexes it is shown that the decreasing interaction energies in the complexes follow the order phenyl-aromatic > phenyl-propyl (or

Table

Evidence from Stability Data for Intramolecular Hydrophobic and Aromatic-ring Stacking Interactions in Some Binary ($A = B$) and Ternary Amino Acid Complexes in Aqueous Solution (25°C; $I = 0.05-0.1$)^{a)}

Complex	% M(A)(B) _{cl} for			
	Co ²⁺	Ni ²⁺	Cu ²⁺	Zn ²⁺
<i>binary:</i>				
M(Nva) ₂	13	~2	17	
M(Phe) ₂	46	38	61	53
M(Tyr) ₂	66	38	67	67
M(Trp) ₂			87	
<i>ternary:</i>				
M(Phe)(Nva)	21	~5	11	
M(Tyr)(Nva)	22	9	24	
M(Phe)(Tyr)	50	25	36	

a) These results are abstracted from the data given in Tables VI and VII of references [3] and [5], respectively; where available, the average of several calculations is listed. Abbreviations: Nva, norvalinate; Phe, phenylalaninate; Trp, tryptophanate; Tyr, tyrosinate.

larger alkyl residue) > ... > Pd²⁺-aromatic ≫ Pd²⁺-aliphatic ~ 0. This means, the Pd²⁺-aromatic interactions are already weaker than intramolecular hydrophobic or stacking interactions, and a Cu²⁺-aromatic interaction is expected to be even weaker than the Pd²⁺-aromatic one. Indeed, in our studies [2-4] of phenylalkanecarboxylate-Cu²⁺ complexes we could not discover any hint for such an interaction in solution.

The following points which are partly based on the data of the Table argue also *against* a significant Cu²⁺-aromatic interaction in solution but *for* intramolecular ligand-ligand interactions in many amino acid complexes: (i) Always the stability constant for the bis-complex is larger than expected, which is convincingly explained by an intramolecular stack formation. (ii) The increased stability can *not* result from an influence of the second ligand on Cu²⁺, making it more suitable for a Cu²⁺-aromatic interaction (as suggested [10,11]), because, *e.g.*, M(Phe)(Gly) or M(Phe)(Ala) show no increased stability, while M(Phe)(Nva) or M(Phe)(Tyr) do so (Table). (iii) Thermodynamic results also support the postulation of intramolecular ligand-ligand interactions: ΔH_1 for the reaction between Cu²⁺ and Trp⁻ or Ala⁻ are very similar, while ΔH_2 for the addi-

tion of the second Trp⁻ to Cu(Trp)⁺ is about 5 kJ/mol more exothermic than for the reaction Cu(Ala)⁺ + Ala⁻ → Cu(Ala)₂ [15]; this agrees with other studies showing that formation of stacking adducts is not solely entropy driven [16]. (iv) The mentioned Cu²⁺/leucinate results could not be explained without a ligand-ligand interaction. (v) The increased binding tendency of the second ligand is a general feature and occurs with many other metal ions aside from Cu²⁺: for the complexes with Co²⁺, Ni²⁺ and Zn²⁺ the increased stability can hardly be attributed to metal ion-aromatic or metal ion-hydrophobic interactions. Indeed, the data of the Table reveal that the situation is governed by the ligands and *not* by the metal ions. In conclusion: most of the indicated results, if considered for themselves, would not provide very convincing arguments. It is the wealth of data pointing into the same direction which, if combined, provide strong evidence that hydrophobic and aromatic-ring stacking interactions indeed occur in binary and ternary complexes of amino acids with suitable side chains.

ACKNOWLEDGEMENTS

The support of this work by the Swiss National Science Foundation is gratefully acknowledged.

REFERENCES

- [1] H. SIGEL, B.E. FISCHER, E. FARKAS, *Inorg. Chem.*, **22**, 925-934 (1983).
- [2] R. MALINI-BALAKRISHNAN, K.H. SCHELLER, U.K. HÄRING, R. TRIBOLET, H. SIGEL, *Inorg. Chem.*, **24**, (1985), in press.
- [3] H. SIGEL, R. TRIBOLET, K.H. SCHELLER, *Inorg. Chim. Acta*, **100**, 151-164 (1985).
- [4] H. SIGEL, R. MALINI-BALAKRISHNAN, U.K. HÄRING, submitted for publication.
- [5] B.E. FISCHER, H. SIGEL, *J. Am. Chem. Soc.*, **102**, 2998-3008 (1980).
- [6] H. SIGEL, *Angew. Chem., Int. Ed. Engl.*, **21**, 389-400 (1982).
- [7] A. GERGELY, T. KISS, *J. Inorg. Nucl. Chem.*, **39**, 109-114 (1977).
- [8] V. ZELANO, E. ROLETTO, A. VANNI, *Ann. Chim. (Rome)*, **73**, 113-121 (1983).
- [9] a) K.A. CONNORS, S.-R. SUN, *J. Am. Chem. Soc.*, **93**, 7239-7244 (1971);
b) B. FARZAMI, Y.H. MARIAM, F. JORDAN, *Biochemistry*, **16**, 1105-1110 (1977);
c) P.R. MITCHELL, *J. Chem. Soc., Dalton Trans.*, 1079-1086 (1980).

- [10] L.D. PETTIT, *Pure Appl. Chem.*, **56**, 247-292 (1984).
 [11] A. ODANI, O. YAMAUCHI, *Inorg. Chim. Acta*, **93**, 13-18 (1984).
 [12] H. MUHONEN, R. HÄMÄLÄINEN, *Finn. Chem. Lett.*, 120-124 (1983).
 [13] D. VAN DER HELM, M.B. LAWSON, E.L. ENWALL, *Acta Crystallogr.*, **B27**, 2411-2418 (1971).
 [14] S.-H. KIM, R.B. MARTIN, *J. Am. Chem. Soc.*, **106**, 1707-1712 (1984).
 [15] J.L. MEYER, J.E. BAUMAN JR., *J. Chem. Eng. Data*, **15**, 404-407 (1970).
 [16] a) I. SÓVÁGÓ, R.B. MARTIN, *FEBS Lett.*, **106**, 132-134 (1979);
 b) G. ARENA, R. CALI, V. CUCINOTTA, S. MUSUMECI, E. RIZZARELLI, S. SAMMARTANO, *Thermochim. Acta*, **74**, 77-86 (1984).



PS5.3 — TH

J.P. LAUSSAC
 A. ROBERT
 R. HARAN

Laboratoire de Chimie de Coordination du CNRS
 Unité n.° 8241 liée par convention à l'Université Paul Sabatier
 205, route de Narbonne, 31 400 Toulouse
 France

B. SARKAR

The Research Institute of the Hospital for Sick Children
 Toronto
 Canada
 and
 Department of Biochemistry
 University of Toronto
 Canada

**MODELS FOR METAL-PROTEIN INTERACTION:
 COPPER(II) COMPLEXES WITH A CYCLIC PEPTIDE HAVING SIDE-CHAIN IMIDAZOLYL AND CARBOXYL GROUPS**

Considerable effort has been devoted to the study of macrocyclic ligands and their metal complexes. Thus, introduction of a metal ion into functionalized cyclic peptides may be an appropriate model for the studies of binding by metalloenzymes. Such cyclic peptides can be designed to incorporate amino acid side chains that are important for the function of various enzymes. For example, the imidazolyl and the carboxyl groups of histidine

and glutamic acid seem to play an important role in the coordination of proteins or naturally occurring peptides to metal ions. The investigation of simple cyclic peptides having side-chain imidazolyl and carboxyl groups as model might be of significant value in elucidating the details of enzyme mechanisms, particularly in aqueous solution.

We chose to synthesize cyclo-(Gly-L-Glu-Gly-L-His-Gly-Gly-L-His-Gly) (hereinafter denoted G5H2Gu). Complexation of G5H2Gu with the transition metal ion Cu(II) in aqueous solution over a wide pH range and with different peptide/metal ratios, has been studied by using carbon-13 and proton NMR, ESR and Visible Spectroscopy.

The results obtained are discussed in terms of different complexes depending on the pH and are compared with a cyclic peptide having different side-chains and a different cavity size.



PS5.4 — MO

L. ANTOLINI
 L. MENABUE
 G.C. PELLACANI
 M. SALADINI

Istituto di Chimica Generale e Inorganica
 University of Modena
 Italy

L.P. BATTAGLIA

A. BONAMARTINI CORRADI

Istituto di Chimica Generale e Inorganica
 Centro di Studio per la Strutturistica Diffraattometrica del C.N.R.
 University of Parma
 Italy

THE ROLE OF THE TOSYL GROUP ON THE COORDINATION ABILITY OF N-PROTECTED AMINOACIDS. SOLID STATE BEHAVIOR OF N-TOSYLVALINATE COPPER(II) COMPLEXES

Among *N*-protected aminoacids, as *N*-acetyl-, *N*-benzoyl-, *N*-benzyloxycarbonyl and *N*-toluenesulfonyl-aminoacids, only the latter class of deri-

vatives has been proved to coordinate in aqueous and alcoholic solution to the copper(II) ion, acting as carboxylate ligand, or, undergoing amide nitrogen deprotonation at $\text{pH} > 5$, as naturally occurring L- α -aminoacids.

In this communication we report the results of an investigation concerning the interactions between N-tosylvaline and copper(II) ion. At pH lower than 5 two solid simple complexes, one green and one blue, having formula $\text{CuL}_2 \cdot 3\text{H}_2\text{O}$ and $\text{CuL}_2 \cdot 2\text{H}_2\text{O} \cdot 2\text{MeOH}$, respectively, have been separated. For the blue complex the crystal structure was determined. It consists (Fig. 1) of monomeric units in which the copper atom, lying on the symmetry centre, is surrounded by two carboxylic oxygens ($\text{Cu-O1} = 1.954(4) \text{ \AA}$) and two water molecules ($\text{Cu-O2} = 1.989(3) \text{ \AA}$) in a square planar arrangement. Two long contacts with two methanol molecules ($\text{Cu-O3} = 2.492(4) \text{ \AA}$) complete the coordination to elongated tetragonal bipyramid. The second carboxylic oxygen is not involved in the coordination ($\text{Cu} \cdots \text{O4} = 3.137(4) \text{ \AA}$). These data reinforce the assignment of this type of geometry, based on spectroscopic results, for the $\text{Cu}(\text{tsgly})_2 \cdot 4\text{H}_2\text{O}$ ($\text{tsgly} = N$ -toluensulfonyl-glycine monoanion) [1].

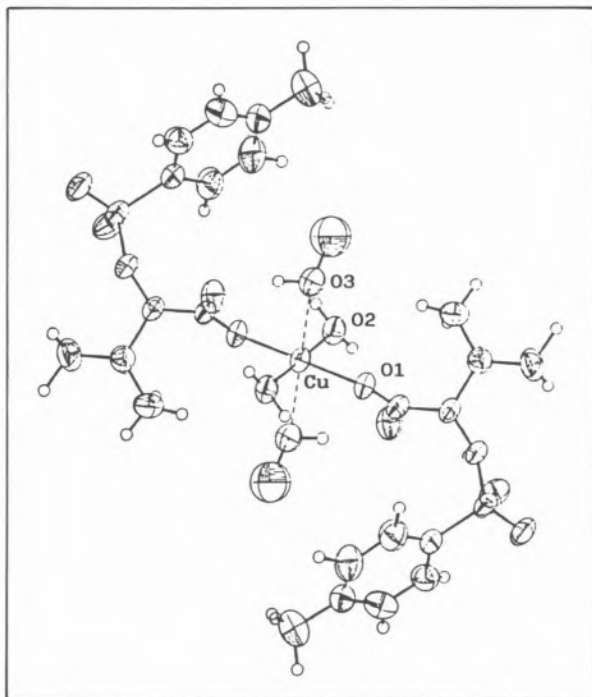


Fig. 1

ORTEP view of the $[\text{Cu}(\text{tsval})_2 \cdot 2\text{H}_2\text{O} \cdot 2\text{MeOH}]$

The green compound shows physical properties indicating a dimeric structure with strong antiferromagnetic interactions between the copper(II) within the pairs.

By treating these two complexes in aqueous or alcoholic solution with an equimolar amount of 2,2'-bipyridine, a deep blue compound of formula $\text{Cu}(\text{tsval})_2 \text{bipy}$ ($\text{tsval} = N$ -toluensulfonylvalinate monoanion; $\text{bipy} = 2,2'$ -bipyridine) was separated. Since it presents unusual spectroscopic properties, the crystal structure was determined. In the unit cell, two crystallographically independent and chemically inequivalent copper(II) ions are present. Each copper atom is surrounded by two carboxylic oxygen atoms, belonging to two different aminoacids, and two bipyridine nitrogen atoms, $[(\text{Cu-O})_{\text{mean}} = 1.938(4) \text{ \AA}$, $(\text{Cu-N})_{\text{mean}} = 2.001(4) \text{ \AA}]$. The five coordination positions are occupied for one copper atom by a carboxylic oxygen of an adjacent aminoacid ($\text{Cu-O} = 2.457(3) \text{ \AA}$) giving rise to a dimeric unit with a monoatomic bridge, and for the other copper atom by a sulphonic oxygen ($\text{Cu-O} = 2.407(3) \text{ \AA}$) of one of the two aminoacids coordinated through one carboxylic oxygen to the same copper atom giving rise to a discrete molecule.

REFERENCES

- [1] L. ANTOLINI, L.P. BATTAGLIA, G. BATTISTUZZI GAVIOLI, A. BONAMARTINI CORRADI, G. GRANDI, G. MARCOTRI-GIANO, L. MENABUE, G.C. PELLACANI, *J. Am. Chem. Soc.*, **105**, 4327-33 (1983).



PS5.5 — TU

GRAZYNA FORMICKA-KOZŁOWSKA

Institute of Chemistry
University of Wrocław
Joliot-Curie 14, 50-383 Wrocław
Poland

LESLIE D. PETTIT

School of Chemistry
The University of Leeds
Leeds LS2 9JT
U.K.

THE CUPRIC INTERACTION WITH OPIOID PEPTIDES

The role of peptides as classical hormones has long been known. More recently it has been appreciated a different role of some peptides acting in the central nervous system (*e.g.* thyroliberin, somatostatin, opiate related peptides, etc.). It is thought that they act as local tissue regulators and in some instances also as neurotransmitters [1]. Control of sleep, memory, perception are possible functions for these peptides.

All these peptides may serve as special chelate agents for trace elements, widely distributed in the body, especially for copper present in brain. It has been proved that some of the neuropeptides retain their biological activity in the form complexed by transition metal ions [2].

Since a few years we have been interested in metal (especially Cu(II)) interaction with some neuropeptides [3,4] and their chemical analogs [5]. All these peptides proved to be very specific ligands for metal ions.

Recently we have been studying the cupric complexation by some opiate related peptides *i.e.* β -casomorphin-5 and its di-, tri- and tetra-peptide fragments and enkephalin analogs.

β -casomorphin-5 is the opioid isolated from β -casein with the following sequence: Tyr-Pro-Phe-Pro-Gly. For our studies besides the β -casomorphin-5 itself, we have used a series of peptides: Tyr-Pro-Phe-Pro, Tyr-Pro-Phe, Tyr-Pro, Pro-Phe-Pro-Gly, Pro-Phe-Pro. Spectroscopic

(CD, EPR) and potentiometric studies have shown that the Cu(II) interaction with the β -casomorphin fragments depends strongly on the *N*-terminal amino acid. With Pro in this position typical peptide complexes containing the Cu-N⁽⁻⁾ bond are formed. With Tyr in this position a dimeric species, Cu₂L₂, becomes a major complex at physiological pH values, with the copper(II) bound to the -NH₂, CO groups of one ligand and to the phenolic oxygen of a second ligand.

The proline residue in the second and fourth positions in β -casomorphin-5 acts as a «break-point» to Cu(II) coordination and destroys completely the coordination ability of amino acid residues after the first Pro. In other systems with a proline residue inside the peptide chain the *N* and *C* terminals either interact separately [6] or form a macro-chelate with the peptide bent in a β -conformation [7].

Similar to the β -casomorphin, the enkephalin peptides with opiate activity contain the L-tyrosine residue on the *N*-terminus. This position of Tyr residue is a common feature to most endorphins and it is an important factor for their biological activity. Only the 2nd and 5th positions of enkephalin analogs can be safely manipulated to give a peptide with potent activity. Enkephalins and their structural analogs are of great interest to physicians and pharmacologists, because their properties might give the information on the mechanism of the development of drug addiction. Besides the pharmacologists are looking for enkephalin analogs which elicit analgesia but are less addicting with the hope to find the addiction-free pain relievers.

The following peptides have been studied: Tyr-Gly-Gly-Phe-Met (Met-enkephalin), Tyr-D-Ala-Gly-Phe-Met-NH-CH₂-CH₂-NH₂, Tyr-D-Ala-Gly-Phe-Met-N-(CH₃)₂, Tyr-D-Ala-Gly-Phe-Leu-ol. Spectroscopic and potentiometric data have indicated that all peptides mentioned above form similar four nitrogen complexes with cupric ions. Only in some cases a weak interaction of the phenolic oxygen with Cu(II) has been observed.

It is interesting to compare the role of a Tyr residue placed in a different position of a peptide chain. In β -casomorphin-5 the Tyr residue plays an important role in the formation of a major dimeric complex, while in enkephalin analogs the

N-terminal tyrosine interacts with cupric ion only through the amino and carbonyl groups. In earlier studies a Tyr residue plays a critical role in the formation of a dimeric cupric complex of Gly-Pro-Tyr-Gly [6], while a similar dimeric complex is only a minor species in the Tyr-Pro-Gly-Gly system and it is undetectable in the Gly-Pro-Gly-Tyr case [6].

REFERENCES

- [1] H.D. NIALL, in M. GOODMAN, J. MEIENHOFER (eds.), «Peptides: Proc. of the 5th Am. Peptide Symposium», Halsted Press, N.Y., 1977, p. 96.
- [2] T. TONOUE, S. MINAGAWA, N. KATO, K. OHKI, *Pharmacol. Biochem. Behav.*, **10**, 201 (1979).
- [3] G. FORMICKA-KOZŁOWSKA, H. KOZŁOWSKI, G. KUPRYSZEWSKI, *Inorg. Chim. Acta*, **46**, 29 (1980).
- [4] G. FORMICKA-KOZŁOWSKA, H. KOZŁOWSKI, M. BEZER, L.D. PETTIT, G. KUPRYSZEWSKI, J. PRZYBYLSKI, *Inorg. Chim. Acta*, **56**, 79 (1981).
- [5] G. FORMICKA-KOZŁOWSKA, M. BEZER, L.D. PETTIT, *J. Inorg. Biochem.*, **18**, 335 (1983).
- [6] H. KOZŁOWSKI, M. BEZER, L.D. PETTIT, M. BATAILLE, B. HECQUET, *J. Inorg. Biochem.*, **18**, 231 (1983).
- [7] M. BATAILLE, G. FORMICKA-KOZŁOWSKA, H. KOZŁOWSKI, L.D. PETTIT, I. STEEL, *J. Chem. Soc., Chem. Commun.*, **231** (1984).



PS5.6 — TH

LUIGI CASELLA
LUIGI RIGONI

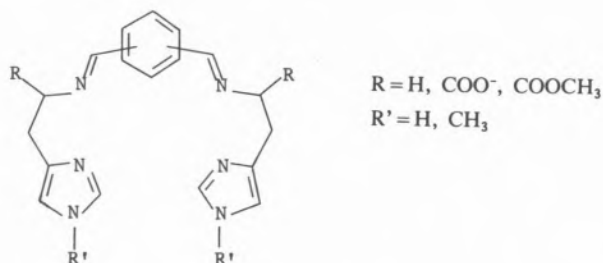
Dipartimento di Chimica Inorganica e Metallorganica
Università di Milano
Via Venezian 21, 20133 Milano
Italy

MONONUCLEAR AND BINUCLEAR COPPER(I) AND COPPER(II) COMPLEXES DERIVED FROM L-HISTIDINE AND L-N⁷-METHYLHISTIDINE

The imidazole groups of histidine residues appear systematically involved in metal binding at the active site of copper proteins and enzymes, parti-

cularly those that function as oxygen carriers or promote some kind of oxygen activation [1]. Recently some copper(I) complexes containing the imidazole groups of histamine or histidine residues have been reported, also by us, to exhibit an apparent partially reversible oxygenation behavior in solution [2,3]. Though, in general, the oxygenated species in these or other systems [4] do not mimic the spectral features of the corresponding protein derivatives.

We have synthesized a series of mononuclear and binuclear copper(I) and copper(II) complexes of the ligands derived from the condensation of phthalic dicarboxaldehydes and two molecules of histamine, L-histidine, or their *N*⁷-methylated derivatives:



The binuclear copper(I) complexes are formally two-coordinate, while additional ligand molecules are required to obtain the corresponding copper(II) complexes. By changing the type of substitution of the xylyl residues and the nature of the additional ligands we expect to vary the distance between the metal ions in the binuclear complexes, while the substituents R and R' affect the donor properties and charge of the ligands. The characterization of the complexes and the reactivity to dioxygen and other molecules of the copper(I) systems will be discussed.

REFERENCES

- [1] T.G. SPIRO (ed.), «Copper Proteins», Wiley, New York, 1981.
- [2] M.G. SIMMONS, C.L. MERRILL, L.J. WILSON, L.A. BOTTOMLEY, K.M. KADISH, *J. Chem. Soc., Dalton Trans.*, 1827 (1980).
- [3] L. CASELLA, M.E. SILVER, J.A. IBERS, *Inorg. Chem.*, **23**, 1409 (1984).
- [4] K.D. KARLIN, R.W. CRUSE, Y. GULTNEH, J.C. HAYES, J. ZUBIETA, *J. Am. Chem. Soc.*, **106**, 3372 (1984).



PS5.7 — MO

B. DECOCK-LE-REVEREND

L. ANDRIANARIJAONA

C. LOUCHEUX

Laboratoire de Chimie Macromoléculaire

Laboratoire associé au C.N.R.S. No. 351

Université des Sciences et Techniques de Lille

F-59655 Villeneuve d'Ascq

France

L.D. PETTIT

I. STEEL

School of Chemistry

The University

Leeds LS2 9JT

England

H. KOZŁOWSKI

Institute of Chemistry

University of Wrocław

Joliot-Curie 14, PL-50-383 Wrocław

Poland

CO-ORDINATION ABILITY OF AN *N*-TERMINAL TETRAPEPTIDE FRAGMENT OF FIBRINOPEPTIDE A

Spectroscopic and potentiometric studies of the interaction of Cu(II) with an *N*-terminal fragment of fibrinopeptide A have shown considerable specificity of an aspartic acid residue (Asp-2) in

metal ion binding. In the system Cu(II) — Ala-Asp-Ser(Bzl)-Gly four distinct species are formed involving all together the NH₂ group (Ala) and three amide nitrogens (see Fig. 1). Correlation of the spectroscopic and potentiometric data (Table I) allows assignment of the species CuL to co-ordination between Cu and NH₂(Ala) and the neighbouring peptide oxygen, CuH₁L to NN co-ordination (NH₂, N⁻), CuH₂L to NNN co-ordi-

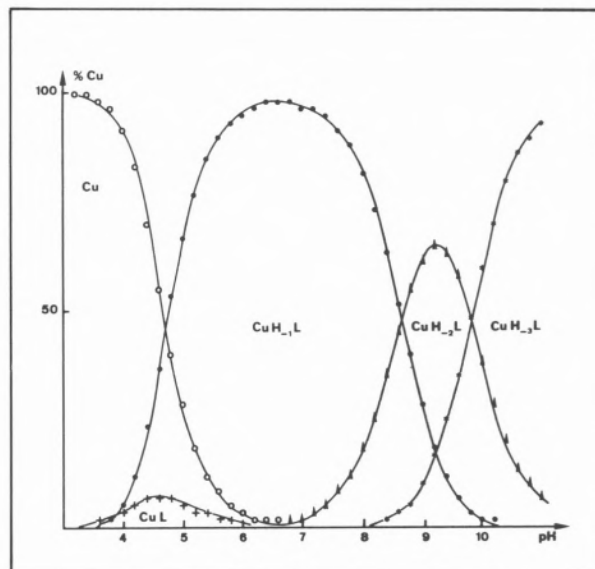


Fig. 1

The distribution of species as a function of pH for solutions containing Copper(II) and Ala-Asp-Ser(Bzl)-Gly with 1:1 metal to peptide molar ratio.

Table I
Formation constants and spectroscopic data of proton and Cu(II) complexes with Ala-Asp-Ser(Bzl)-Gly

Species	log β (or K)	Absorption spectra d-d $\lambda_{[nm]}$ ($\epsilon 1. M^{-1} cm^{-1}$)	CD spectra $\lambda_{[nm]}$ ($\Delta\epsilon$)	EPR spectra g \parallel A \perp (G)
LH	8.332(NH ₃ ⁺)			
LH ₂	3.700(β COOH)			
LH ₃	2.510(α COOH)			
CuL	6.18			
CuH ₁ L	2.28	635(84)	618(+0.09)B + E ^{a)} 298(-0.78)N ⁻ → Cu(II) ^{b)} 264(+0.58)NH ₂ → Cu(II) ^{b)}	2.245 192
CuH ₂ L	- 6.39	625(130)	590(-0.26)B + E 298(-0.48)N ⁻ → Cu(II) 259(+1.9)NH ₂ → Cu(II)	
CuH ₃ L	-16.2	510(180)	520(-1.8)B + E 300(+0.84)N ⁻ → Cu(II) 272(-0.4)NH ₂ → Cu(II)	2.179 210

a) d-d transitions. b) charge transfer transitions.

nation (NH_2 , N^- , N^-) and CuH_3L to NNNN co-ordination (NH_2 , N^- , N^- , N^-).

Comparison of the formation constants of CuH_1L and CuH_2L complexes (Table I) with those of the comparable species in the Cu(II) — tetraglycine system shows the influence of Asp-2 in the system studied. For example the CuH_1L complex ($\log \beta = 2.28$) is significantly more stable than with tetraglycine ($\log \beta = -0.4$, ref. [1]). This comparison indicates clearly the involvement of COO^- of the Asp-2 residue in metal ion binding. The formation of the additional chelate ring when COO^- is bound to the Cu(II) ion in this NN species leads to the creation of a very stable complex with a maximum concentration reaching 100% around pH 7 (see Fig. 1).

REFERENCES

- [1] H. SIGEL, R.B. MARTIN, *Chem. Rev.*, **82**, 385 (1982).



PS5.8 — TU

G. ARENA
G. IMPELLIZZERI
Chemistry Department
University of Catania
Italy

R.M. IZATT
J.D. LAMB

E. RIZZARELLI
Chemistry Department and Thermochemical Institute
Brigham Young University
Provo, Utah
U.S.A.

THERMODYNAMIC AND SPECTROSCOPIC STUDY OF METAL COMPLEX FORMATION WITH CYCLOPEPTIDES: Cu(II)- AND Zn(II)-CYCLO-L-HISTIDYL-L-HISTIDYL

Cyclic peptides can be very useful models for the study of protein-metal ion interactions. Cyclic peptides have the advantage over linear peptides

that no free terminal amino and carboxylate groups are present to bind to the cation. Thus, cyclopeptide complexes of metal ions represent simple model compounds for the study of metal ion interaction with amido groups and side chains in proteins and polypeptides.

We have investigated copper(II) and zinc(II) complexation with cyclo-L-histidyl-L-histidyl (cyhis). Our interest in this type of ligand is well justified in light of work reported previously in the literature. LANGEBECK *et al.* [1] found that cyhis catalyzes the oxidation of DOPA and that the addition of Cu(II) to the reaction system accelerates the oxidation. HORI *et al.* [2] have obtained the crystal structure of $\text{Cu}(\text{cyhis})_2(\text{ClO}_4)_2 \cdot 4\text{H}_2\text{O}$ by X-ray crystallography. On this basis it was proposed that cyhis may be a good model for elucidating interactions between metal ions and the imidazole group of the histidine residue of some enzymes.

In light of the problems associated with extrapolating solid state properties to solution species, we began an investigation of the coordination chemistry of the title ligand in aqueous solution. Specifically, we determined by potentiometric titration the stability constants of the species formed between the ligand and either copper(II) or zinc(II). The species $\text{M}(\text{cyhis})_2^{2+}$ was present in the pH range 4.0 to 5.5 and was the principal complex species observed.

The ligand protonation constants determined potentiometrically were 6.53 and 5.49, for $\log K_1$ and $\log K_2$ respectively, at 25°C and $I = 0.1 \text{ mol dm}^{-3}$ (KNO_3).

Calorimetric measurements were also carried out to determine ΔH and ΔS values for the formation of the metal complexes. These data helped in ascertaining whether or not the imidazole nitrogen is involved in the complexation process.

REFERENCES

- [1] G. LOSSE, A. BARTH, W. LANGEBECK, *Chem. Ber.*, **94**, 2271 (1961).
[2] F. HORI, Y. KOJIMA, K. MATSUMOTO, S. OOI, H. KUROYA, *Bull. Chem. Soc. Jpn.*, **25**, 1080 (1973).



PS5.9 — TH

ERICH DUBLER
 ZLATAN KOPAJTIC
 GEOFFREY B. JAMESON
 Institute of Inorganic Chemistry
 University of Zürich
 8057 Zürich
 Switzerland

STRUCTURAL INVESTIGATIONS OF MAGNESIUM- AND COPPER(II)- -HYDROGENURATES

Uric acid, uric acid dihydrate, sodium hydrogenurate monohydrate and ammonium hydrogenurate occur as crystalline solids in human urinary calculi. Sodium hydrogenurate monohydrate microcrystals in addition are the cause (or a consequence?) of gouty arthritis. Beside these well known facts some chemical but no structural information is available about the interaction of uric acid with bio-metals, e.g. Ca, Mg, Fe, Co, Cu or Zn.

We have grown single crystals of two different phases of $Mg(\text{hydrogenurate})_2 \cdot 8H_2O$ and of $Cu(\text{hydrogenurate})_2 \cdot 6H_2O$, determined their crystal structures and investigated the thermal decomposition of the compounds with different methods of thermal analysis. Relevant crystal data are: $Mg(C_5H_3N_4O_3)_2 \cdot 8H_2O$ phase I, $a = 9.573(2)$, $b = 14.627(3)$, $c = 7.170(1)$ Å, $\beta = 101.91(1)^\circ$, space group $P 2_1/c$; $Mg(C_5H_3N_4O_3)_2 \cdot 8H_2O$ phase II, $a = 10.397(2)$, $b = 14.306(3)$, $c = 6.732(1)$ Å, $\beta = 104.64(2)^\circ$, space group $P 2_1/c$; $Cu(C_5H_3N_4O_3)_2 \cdot 6H_2O$, $a = 6.929(4)$, $b = 18.229(4)$, $c = 14.559(5)$ Å, $\beta = 102.70(3)^\circ$, space group $P 2_1/n$.

The structures of both phases of $Mg(C_5H_3N_4O_3)_2 \cdot 8H_2O$ contain isolated, slightly distorted octahedral $[Mg(H_2O)_6]^{2+}$ cations, hydrogenurate anions and two molecules of water of crystallization per formula unit. A structural formula representing these facts is

$[Mg(H_2O)_6](\text{hydrogenurate})_2 \cdot 2H_2O$. No bonding interaction between magnesium and hydrogenurate is observed. According to literature data the first deprotonation site of uric acid in solution should be N(9). The hydrogenurate phases described here however are deprotonated at N(3) (the positions of the hydrogen atoms could be located in difference fourier maps). Differences in details of the geometry between the hydrogenurate anion and uric acid may be described in terms of three additional resonance structures distributing the formal negative charge at N(3) within the pyrimidine (but not the imidazole) ring of uric acid. In both phases pairs of hydrogen-bonding of the type N(1)-H(1)...O(8) and O(6)...H(9)-N(9) result in infinite chains of hydrogenurate molecules along the b-axis of the cell.

$Cu(\text{hydrogenurate})_2 \cdot 6H_2O$ represents the first example of a hydrogenurate d-metal complex as evidenced by its crystal structure analysis. Deprotonation of uric acid has occurred at N(9), and copper exhibits a distorted square-pyramidal coordination by two N(9) atoms of hydrogenurate and three water molecules. There are three additional molecules of water of crystallization per formula unit. The hydrogen-bonding scheme is different from that of the magnesium salts and is dominated by pairs of the type N(1)-H(1)...O(8) and O(2)...H(7)-N(7).



PS5.10 — MO

ANA MARIA V.S.V. CAVALEIRO
VICTOR M.S. GIL
JULIO D. PEDROSA DE JESUS

Department of Chemistry
University of Aveiro
Portugal

ROBERT D. GILLARD
PETER A. WILLIAMS

Department of Chemistry
University College
P.O. Box 78, Cardiff CF1XL
Wales U.K.

MOLYBDENUM(VI) COMPLEXES OF (R)-CYSTEINE IN AQUEOUS SOLUTION

Complex formation between molybdate ions and (R)-cysteine has been studied, in aqueous solution, over a range of concentrations and pH, at 298K and $I=1 \text{ mol dm}^{-3}$ (NaCl), using UV, CD and NMR techniques. One main species is evident for $\text{pH} > 6.5$, in which cysteine is bonded as a tridentate ligand to Mo(VI), forming a 1:1 complex. This compound has a formation constant $\log K_f = 18.23 \pm 0.12$, determined by CD measurements. In solutions with pH values between 4.5 and 6.5, apart from this complex, there is evidence for at least three other species.

INTRODUCTION

Complexes of molybdenum(VI) with (R)-cysteine have been studied by a number of authors [1-5], as possible models for molybdenum-containing enzymes.

An early report [1], based on spectrophotometric studies, claimed the formation of complexes where ligand:Mo(VI) ratio varies from 3:1 to 1:1, in aqueous solutions, at pH values between 4.6 and 6.5. Conflicting results about the nature of the species formed and the pH region adequate for their study, have been subsequently reported [4,5]. Circular dichroism proved to be a very informative technique and was used over a wide pH range (4.5-9.5), with varying metal and ligand concentrations. A number of UV and NMR experiments linked our work with previous studies. We found

that redox chemistry, although being important in all conditions in which this and previous work have been carried out, has not been properly considered in previous studies.

At pH values higher than 6.5, a single complex, with Mo(VI):cysteine ratio equal to 1:1, has been identified and its formation constant determined. This species, and at least a second complex of Mo(VI), is present at lower pH values. However, in more acidic solutions (pH between 4.5 and 6.5) reduction of Mo(VI) is much faster, resulting in the formation of the known compound $[\text{Mo}_2\text{V}_4\text{O}_4(\text{cys})_2]^{2-}$.

RESULTS AND DISCUSSION

SPENCE and CHANG [1] have studied the complexes formed over a pH range from 4 to 6. Using Job's method of continuous variation they have suggested the formation of species where ligand:metal ratio varies from 3:1 to 1:1 and have estimated the formation constant for the first complex. We have used the same method for studying the species present in solutions with pH varying from 6.4 to 8.5 and concentrations of Mo(VI) and cysteine similar to those used by Spence and Chang. Some of the results are shown in Fig. 1. The molar ratios corresponding to the maxima of the curves vary with pH, total concentration and wavelength chosen. These results could be inter-

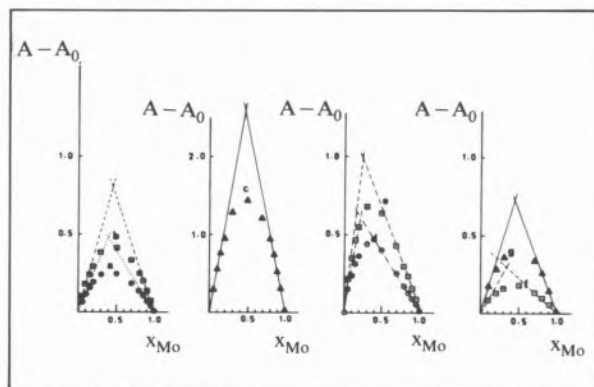


Fig. 1

Job's plots of absorbances for solutions of sodium molybdate and (R)-cysteine where

- $C_{\text{Mo}} + C_{\text{cys}} = 0.04 \text{ mol dm}^{-3}$, $\text{pH} = 8.5$, $l = 10 \text{ mm}$, and
(a) $\lambda = 370 \text{ nm}$, (b) $\lambda = 360 \text{ nm}$, (c) $\lambda = 340 \text{ nm}$;
- $C_{\text{Mo}} + C_{\text{cys}} = 0.04 \text{ mol dm}^{-3}$, $\text{pH} = 6.4$, $l = 5 \text{ mm}$, and
(d) $\lambda = 380 \text{ nm}$, (e) $\lambda = 360 \text{ nm}$;
- $C_{\text{Mo}} + C_{\text{cys}} = 0.016 \text{ mol dm}^{-3}$, $\text{pH} = 6.4$, $l = 5 \text{ mm}$,
(f) $\lambda = 360 \text{ nm}$, (g) $\lambda = 340 \text{ nm}$

preted as meaning that complexes with ligand:metal ratios varying from 1:1 to 3.5:1 have been formed. However we have other evidence for the occurrence of fast redox processes in these solutions, with formation of Mo(V) complexes of cysteine, namely the well known $[\text{Mo}_2\text{O}_4(\text{cys})_2]^{2-}$ compound. This complex absorbs strongly in the region of our measurements, and at higher wavelengths than the Mo(VI) species. It has also been found that the reduction is faster for higher total concentrations, higher ligand:metal ratios and lower pH values. All these results explain the deviation of the Job's plot maximum from a molar ratio close to 1:1, when we increase total concentration and/or decrease pH. This means that these results should not be used by themselves to support the presence of species with Cys:Mo(VI) ratio higher than 1:1.

CALLIS and WENTWORTH [5] studied this system using ^1H NMR and found that reduction of Mo(VI) occurred for $\text{pH} < 8.5$. Using solutions with $\text{pH} = 9.40$, they have claimed evidence for the formation of a 1:1 and a 3:1 complex. Having studied the first species in detail, they have found that the ligand should be tridentate and calculated a formation constant, $\log K_f = 19.88 \pm 0.06$, for the complex $[\text{MoO}_3(\text{cys})]^{2-}$. Using analogous conditions, we have obtained NMR spectra similar to those described by Callis *et al.* However, other signals were always present which could be assigned for cysteine and $[\text{Mo}_2\text{O}_4(\text{cys})_2]^{2-}$.

Solutions of (R)-cysteine and Mo(VI), with pH values between 6.5 and 9.2 give CD spectra which can be assigned to a single species. The spectra recorded for solutions where $C_M = 10^{-2} \text{ mol dm}^{-3}$, $C_L:M_{\text{Mo}}$ varied from 0.4 to 6 and $I = 1 \text{ mol dm}^{-3}$ (NaCl) were used to calculate a formation constant value, $\log K_f = 18.23 \pm 0.12$, for a complex 1:1. This compound had the stoichiometry confirmed by applying ASMUS's method [6] in the treatment of these results, and we believe that it is the species $[\text{MoO}_3(\text{cys})]^{2-}$ described by other authors [1,5].

In solutions where pH varies from 4.5 to 6.5, quite distinct CD spectra ($\lambda > 250 \text{ nm}$) are observed. These spectra were resolved into four components: One, made of one negative ($\lambda_{\text{max}} = 277 \text{ nm}$) and one positive ($\lambda_{\text{max}} = 325 \text{ nm}$) band, is the spectrum of the species 1:1 observed at $\text{pH} > 6.5$.

A second component is a new positive band ($\lambda_{\text{max}} = 412 \text{ nm}$) and is tentatively assigned to a dimeric complex of Mo(VI), $[\text{Mo}_2\text{O}_5(\text{cys})_2]^{2-}$. Two negative bands, centred at 357 and 385 nm, respectively, are associated with Mo(V) complexes of (R)-cysteine. This last assignment is further supported by the developments in the spectrum with time, which eventually turn it into that of $[\text{Mo}_2^{\text{V}}\text{O}_4(\text{cys})_2]^{2-}$.

ACKNOWLEDGEMENTS

We wish to thank NATO for a travel grant (n.º 1752) and INIC (Centro de Química do Meio Aquático da Universidade de Aveiro) for financial support.

REFERENCES

- [1] J.T. SPENCE, H.Y. CHANG, *Inorg. Chem.*, **2**, 1963 (1963).
- [2] A. KAY, P.C.H. MITCHELL, *Nature*, **219**, 267 (1968).
- [3] A. KAY, P.C.H. MITCHELL, *J. Chem. Soc. (A)*, 2421 (1970).
- [4] J.F. MARTIN, J.T. SPENCE, *J. Phys. Chem.*, **74**, 2863 (1970).
- [5] G.E. CALLIS, R.A.D. WENTWORTH, *Bioinorg. Chem.*, **7**, 57 (1977).
- [6] E. ASMUS, U. HINZ, K. OHLS, W. RICHLI, *Z. Anal. Chem.*, **178**, 104 (1960).



PS5.11 — TU

M. CASTILLO

Departamento de Química Inorgánica
Facultad de Química
Universidad de Sevilla
Spain

J.J. CRIADO

B. MACÍAS

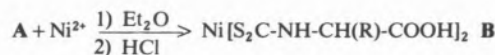
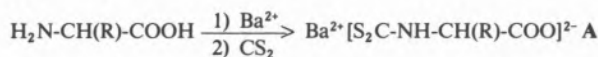
M.V. VAQUERO

Departamento de Química Inorgánica
Facultad de Farmacia
Universidad de Salamanca
Spain

NEW NICKEL(II) COMPLEXES WITH DITHIOCARBAMATE-DERIVATIVES OF α -AMINOACIDS

Although little is known about the role of nickel *in vivo*, it has been recognized that it is essential in the growth of experimentation animals [1] and its deficiency impairs iron absorption, reducing the haemoglobin level; on the other hand, its ability in changing its coordination geometry (D_{4h} , T_d , O_h) may make it important in a fine control over metabolic activity, and is also useful as a substituent for Mg^{2+} because of their close radii [2,3].

In an attempt to fathom its biochemistry, complexes formed by Ni(II) and dithiocarbamate derivatives of α -aminoacids have been synthesized according to:



All reagents were from Fluka (*p.a.*) and were used without any further purification.

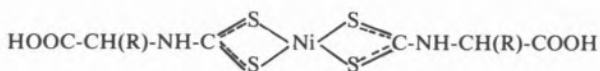
Synthesis of compounds **A** has been described elsewhere [4,5]. To obtain compounds **B**, an aqueous solution of $NiCl_2 \cdot 6H_2O$ is dropwise added on **A** dissolved in H_2O ($Ni:Ba = 1:2$ molar ratio). Addition of Et_2O and then HCl 0.1 M

(stoichiometrically to yield $BaCl_2$ formation) leads to extraction of compounds **B** in the organic phase. A fine olive-green powder is obtained after room temperature evaporation of Et_2O . The product is purified by recrystallization in Et_2O and acetone (final yield 70%). However, when glycine is used, if addition of HCl and Et_2O is not carried out, evaporation of water yields $Ba[Ni(S_2C-NH-CH_2-COO)_2]$, while decomposition products are obtained with alanine and 2-aminobutyric acid ($R = Me, Et$).

Chemical analysis (C,H,N,S,Ni) data agree with the expected formula. Characterization of the complexes has been carried out by IR spectroscopy (KBr pellets, Beckman Acculab-10), UV-Vis spectroscopy (in H_2O or Et_2O , Shidmazu UV-240), 1H NMR (Hitachi Perkin-Elmer R-24B) and magnetic measurements (at room temperature, Stanton MC-5 Gouy-type balance).

Nickel(II) (d^8) complexes may exhibit three different geometries: square planar (D_{4h}), octahedral (O_h) and tetrahedral (T_d), the former being diamagnetic.

Compounds **B** are diamagnetic, and our IR results (see below) indicate the presence of free $-COOH$ groups. With these results, the structure below can be suggested.



The main features of the *IR spectra* have been collected in the Table.

Table

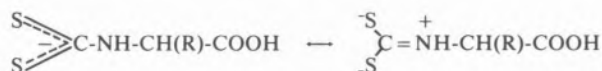
Compound	ν_{COOH}	ν_{COO^-}		ν_{CS}	ν_{NiS}
		ν_a	ν_s		
Ba(gly dtc)	—	1620(s)	1410(s)	620(m)	—
Ni(gly dtc) ₂	1700(s)	—	—	615(m)	380(w)
Ba[Ni(gly dtc) ₂]	—	1580(s)	1410(s)	645(m)	380(w)
Ba(DL-ala dtc)	—	1615(s)	1405(s)	620(m)	—
Ni(DL-ala dtc) ₂	1700(s)	—	—	625(m)	370(w)
Ba(DL-2-am.but dtc)	—	1625(s)	1400(s)	635(m)	—
Ni(DL-2-am.but dtc) ₂	1695(s)	—	—	655(m)	370(w)

s = strong; m = medium; w = weak.

The ν_a and ν_s bands of the COO^- groups in the ligands (compounds **A**) have been recorded at 1625-

-1615 cm^{-1} and 1410-1400 cm^{-1} , respectively, while for compounds **B** only one band at 1700-1695 cm^{-1} , due to ν_{CO} in COOH groups, is recorded. ν_{NH} and ν_{CN} bands are recorded in both series of compounds **A** and **B** at the expected positions 3330-3270 and 1545-1500 cm^{-1} and do not change significantly between each pair of compounds **A** and **B**, while the ν_{NIS} band is recorded at 380-370 cm^{-1} .

The position of the band corresponding to the ν_{CS} vibration in dithiocarbamates has been a matter of controversy, and largely depends on the bond order in such a moiety. Taking into account the feasibility of a resonance of the type



(i.e., lowering the C-S bond order), BECK *et al.* [4] have ascribed to this vibration a band at ca. 630 cm^{-1} in compounds similar to those studied here, although other authors argue that it is recorded around 1000 cm^{-1} [6].

Electronic spectra of compounds **A** show three very intense bands at 205, 250 and 275 nm. For compounds **B**, bands are recorded at $\nu_1 = 230$ nm (broad, sometimes splitted) and $\nu_2 = 320$ nm ($\epsilon = 8000 \text{ dm}^3 \text{ mol}^{-1} \text{ cm}^{-1}$ in both cases), with lower intensity bands at $\nu_3 = 390$ nm ($\epsilon = 1800$), $\nu_4 = 480$ -475 nm ($\epsilon = 20$) and $\nu_5 = 640$ -630 nm ($\epsilon = 30$).

Bands ν_1 and ν_2 should be originated by intra-ligand transitions, and the shift observed if compared with those of the free ligands may be originated by electronic effects. Bands ν_4 and ν_5 are due to d-d transitions (Laporte-forbidden), while band ν_3 is M-L charge transfer in origin [7].

For d^8 systems in D_{4h} geometry three spin allowed, Laporte forbidden bands are expected, corresponding to transitions $E_g(xz, yz) \rightarrow B_{1g}(x^2 - y^2)$, $A_{1g}(z^2) \rightarrow B_{1g}(x^2 - y^2)$ and $B_{2g}(xy) \rightarrow B_{1g}(x^2 - y^2)$. Taking into account that the ligands are bidentate, the symmetry would be D_{2h} and band splitting is expected, although usually a mere broadening of the band is observed.

The lowest energy d-d transition is usually recorded above 1000 nm, and so, bands ν_4 and ν_5 at 480-475 and 640-630 nm may be ascribed to transitions $A_{1g} \rightarrow B_{1g}$ and $E_g \rightarrow B_{1g}$, respectively.

Finally, $^1\text{H NMR spectra}$ coincide with those expected for the formula above depicted.

A structural (X-ray diffraction) determination of glycine-compounds **A** and **B** is under progress.

REFERENCES

- [1] A. SCHNEGG, M. KIRCHGESSNER, *Ubers. Tierernaher.*, **7**, 179 (1979).
- [2] D.A. PHIPPS, «Metals and Metabolism», Clarendon Press, Oxford, 1978, p. 120.
- [3] P.M. HARRISON, R.J. HOARE, «Metals in Biochemistry», Chapman and Hall, London, 1980, p. 17.
- [4] W. BECK, M. GIRNTH, M. CASTILLO, H. ZIPPEL, *Chem. Ber.*, **111**, 1246 (1978).
- [5] M. CASTILLO, J.J. CRIADO, B. MACÍAS, *Inorg. Biochem. Discuss. Group, Chem. Soc.*, London, Dec. 1984.
- [6] E.C. ALYEA, G. FERGUSON, A. SOMOGYVARI, *Inorg. Chem.*, **21**, 1372 (1982).
- [7] A.B.P. LEVER, «Inorganic Electronic Spectroscopy», 2nd ed., Elsevier, Amsterdam, 1984, p. 536.



PS5.12 — TH

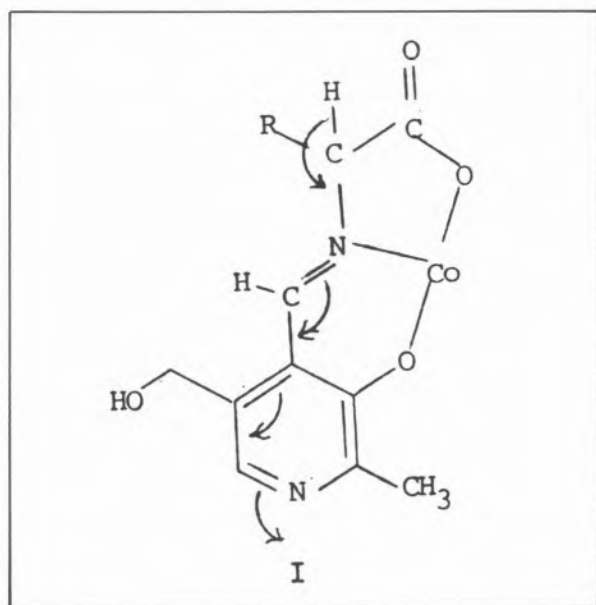
A.G. SYKES
R. LARSEN
J.R. FISCHER
E.H. ABBOTT
Department of Chemistry
Montana State University
Bozeman, Montana 59717-0001
U.S.A.

PREFERENTIAL CATALYSIS OF MODEL REACTIONS IN THE COBALT(III) COMPLEX OF THE VITAMIN B-6 SCHIFF BASE OF GLYCINE

Vitamin B-6 is an essential cofactor to a large number of enzymes which catalyze many diverse reactions of amino acids. The heterocyclic aldehyde, pyridoxal is one of the forms of the cofactor. It has been recognized for many years that pyri-

doxal can catalyze non-enzymic reactions of amino acids and that these reactions are often subject to strong additional catalysis by metal ions [1]. Such model reactions have provided a wealth of mechanistic information which has been of great assistance in determining the mechanism of the enzymic reactions.

The vitamin B-6 catalyzed reactions are based on transformations of a schiff base formed from the amino acid and pyridoxal. They occur through electron shifts cleaving a substituent to the amino acid α -carbon atom as illustrated in I.



Dunathan has suggested that selective catalysis of bond breaking at the amino acid will occur when the bond to be broken is oriented so that it best overlaps with the π orbital terminating at the azomethine nitrogen [2].

Using amino acid glycine, it is possible to synthesize cobalt(III) complexes of vitamin B-6 schiff bases which can be used to test Dunathan's hypothesis and determine the magnitude of catalysis resulting from the proper orientation of the bond to be broken [3]. The complex tetramethylammonium bis(pyridoxylidene-glycinato)cobaltate(III) has been synthesized and its structure determined by X-ray crystallographic methods. The complex crystallizes in a triclinic unit cell and belongs to the space group $P\bar{1}$. 3,007 reflections were collected. The position of the cobalt ion was revealed by a Patterson synthesis and the positions of all

non-hydrogen atoms were determined by least squares refinement. With anisotropic thermal parameters for all non-hydrogen atoms, the structure refined to an R value of 0.117. The magnitude of the R values is a consequence of disorder associated with the tetramethylammonium cation and from hydrogen bonding involving the waters of crystallization. The standard deviations of the bond lengths and angles are quite satisfactory and agree closely for the two independent but identical ligands. Formula I illustrates the coordination of the cobalt ion by one of two ligands. Complete crystallographic data are available upon request from the author.

The structure reveals a distortion of the chelate rings which renders the glycine protons strongly non-equivalent and places them at different dihedral angles with respect to the azomethine π system. The distortion is illustrated in fig. 1.

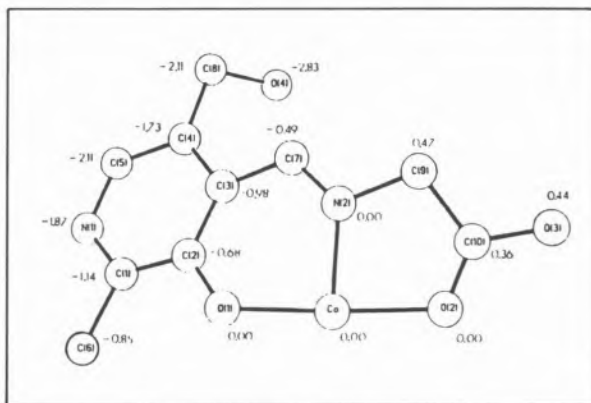


Fig. 1

Location of ligand atoms with respect to the plane determined by the cobalt ion and the atoms coordinated to it. Distances are in angstroms. C-9 is the α -carbon atom of the amino acid. This is a partial structure

Different dihedral angles for the two methylene protons is supported by their different four-bond, pseudoallylic NMR coupling to the proton on the azomethine carbon atom. Values of 1.95 Hz and 1.17 Hz are observed.

Chemically, there is an important consequence of the non-equivalence of the methylene protons on the amino acid α -carbon atom. The rates of deuteration were measured for these two protons as a mean for evaluating the kinetic differences in breaking each bond. The carbon-hydrogen bond which best overlaps the π orbital of the azomethi-

ne nitrogen is the one most easily broken. For the fast proton $\Delta H^\ddagger = 9.9$ Kcal/M and $\Delta S^\ddagger = -28$ eu. For the slower reacting proton $\Delta H^\ddagger = 14.5$ Kcal/M and $\Delta S^\ddagger = -17$ eu. This shows that the stereochemistry of the schiff base plays an important role in the reactivity of the amino acid substituents and that proper orientation of the bond to be broken results in a lower barrier for the reaction and shows how the enzyme might bring about its rapid rates of reaction.

REFERENCES

- [1] D.E. METZLER, M. IKAWA, E.E. SNELL, *J. Am. Chem. Soc.*, **76**, 648 (1954).
- [2] H.C. DUNATHAN, *Proc. Natl. Acad. Sci. USA*, **55**, 712 (1966).
- [3] J.R. FISCHER, E.H. ABBOTT, *J. Am. Chem. Soc.*, **101**, 2781 (1979).



PS5.13 — MO

L. ALAGNA
T. PROSPERI
A.A.G. TOMLINSON
I.T.S.E.

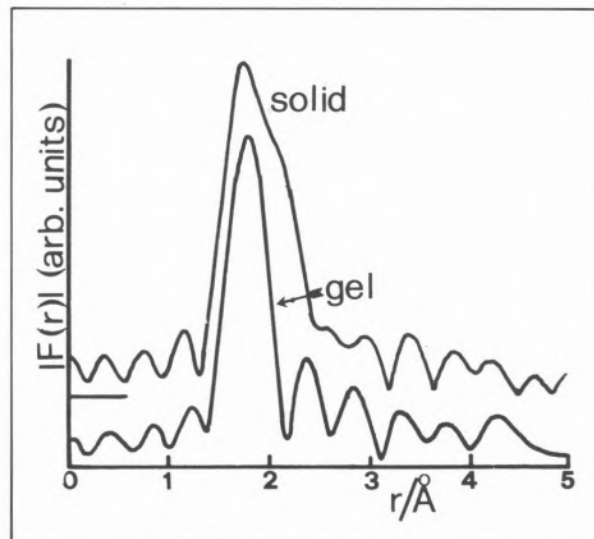
Area della Ricerca di Roma, C.N.R.
C.P. 10 Monterotondo Staz., 00016 Rome
Italy

R. RIZZO
Dipartimento di Chimica
Università di Roma "La Sapienza"
00185, Rome
Italy

EXAFS STUDIES OF GEL AND SOLID FORMS OF Ca^{2+} - α -D-POLY GALACTURONATE

Knowledge of the structural assemblies involved in the biologically important Ca^{2+} polysaccharides is still fragmentary. We have measured the EXAFS spectra of the gel and solid forms of Ca^{2+} - α -D-polygalacturonate, the major intercellular component of deacetylated pectin [1]. Calcium ascorbate

dihydrate and the 2-keto-D-gluconate were used as model compounds [2]. Filtered Fourier transforms of the extracted EXAFS (widest common k range possible; k^3 -weighted; not phase-shift corrected) are shown in the figure.



The first shell peak is clearly different in the two materials, *i.e.* the Ca-O bond distance distributions differ. The gel gives a well-defined peak, whereas the solid has a shoulder at higher Ca-O distance. (EXAFS of the models confirm that an asymmetry can be identified when the spread of Ca-O bond distances is at least 0.2 Å, as in the 2-keto-D-gluconate).

Further structure is visible out to 3.5 Å, and is again different in the two forms. Full parameter fits are in course and should provide information on the possible 2_1 and 3_1 configurations put forward in the literature [3].

REFERENCES

- [1] E.R. MORRIS, D.A. POWELL, M.J. GRINDLEY, D.A. REES, *J. Mol. Biol.*, **155**, 507 (1982).
- [2] M.L. DHEU-ANDRIES, L.S. PEREZ, *Carbohydr. Res.*, **124**, 324 (1983).
- [3] M.D. WALKINSHAW, S. ARNOTT, *J. Mol. Biol.*, **153**, 1075 (1981).



PS5.14 — TU

ISABELLA L. KARLE
 Laboratory for the Structure of Matter
 Naval Research Laboratory
 Washington, D.C. 20375-5000
 U.S.A.

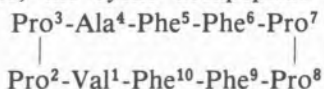
MODES OF COMPLEXATION OF CYCLIC PEPTIDES WITH LIGHT METAL IONS

The structures and conformations of a number of free cyclic peptides and the same peptides complexed with Li^+ , Na^+ , K^+ or Mg^{2+} ions have been established by X-ray diffraction analyses of single crystals. The different modes of complexation that have been found are: 1) an infinite sandwich in which the metal ion and the cyclic peptide alternate [1]; 2) a discrete sandwich in which the metal ion is between two cyclic peptide molecules [2-4]; 3) incomplete encapsulation of the metal ion by one peptide molecule [5,6]; 4) complete encapsulation by one peptide molecule [7,8]; and 5) the metal ion partially *exo* to the polar cavity formed by the peptide [9]. Modes 1)-4) appear to be a function of the size of the cyclic peptide, beginning with a pentapeptide for 1) and progressing to a dodecapeptide for 4). Mode 5) can occur when the size of the metal ion is mismatched with the size of the cyclic peptide.

The complexation of cyclic oligopeptides with metal ions requires the formation of ligands between the metal ion and carbonyl oxygens. If the peptide is too small, even acting in pairs, then the incomplete coordination sphere about the metal ion is completed by ligands to the oxygens of water molecules [1] or to O or N atoms of solvent molecules [5,6] such as CH_3CN , $\text{C}_2\text{H}_5\text{OH}$, $(\text{CH}_3)_2\text{CO}$ or to counterions [1] such as SCN^- . The Mg^{2+} ion has shown an almost exclusive preference for octahedral coordination [1,2], with all O- Mg^{2+} -X angles (X=O or N) very near to 90° . The Li^+ and Na^+ ions adjust their coordination to the local geometry, as for example, in the complexes with antamanide and antamanide analogs, the Li^+ and

Na^+ ions have pentacoordination with ligands to four carbonyl O atoms in a square array and the fifth ligand to a polar atom of a solvent molecule at the apex of the coordination pyramid [5,6]. In every case, the ligands to O or N atoms radiate from the metal ion in all directions and a polar envelope about the metal ion is provided that separates it from the lipophilic regions of the peptide.

The free cyclic peptide is not in a conformation ready to accept and encapsulate a metal ion. Severe conformational changes occur upon complexation. To demonstrate that complexation is responsible for the conformational changes rather than other changes in the crystal environment such as packing, intermolecular interactions, and/or solvent inclusion, a number of crystal structure analyses were performed on the uncomplexed peptides, or closely related analogs of the peptide. To illustrate, the cyclic decapeptide antamanide



and the biologically active analog [$\text{Phe}^4, \text{Val}^6$] antamanide were crystallized from solutions containing water and common organic solvents such as $\text{C}_2\text{H}_5\text{OH}$, CH_3CN , acetone, DMFA, *etc.*, and from completely nonpolar solvents such as *n*-hexane. The resulting crystals had different packing arrangements of the peptides, different solvent inclusions (both polar and nonpolar) and several different side chains on the peptides. Nevertheless, the folding of the backbone and the twisting of the side chains are almost identical in all the crystals [10-12]. Similarly, the conformations of the cyclic pentapeptides (Gly-Pro-Gly-D-Ala-Pro) and (D-Phe-Pro-Gly-D-Ala-Pro) are superimposable despite a different side chain and different packing in the respective crystals [13,14]. Similarly, uncomplexed valinomycin crystallized from different solvents and occurring in different crystalline packing arrangements has a unique elongated conformation [15-17].

The process of forming complexes with Li^+ , Na^+ and Mg^{2+} with each of the cyclic peptides involves major changes such as the rotation of one or more peptide units by as much as 180° . On complexation in antamanide, not only does the flattened elongated cyclic backbone become folded, but sequences 4,5,6 and 9,10,1 turn inside out so that

the *exo* carbonyl groups turn into the cavity to form ligands with the metal ion [5,6,10-12]. In addition, *cis/trans* isomerism of amide bonds may occur [2,18], intramolecular hydrogen bonds are broken [1,2,18], and elongated peptide ring backbones become folded. Examples will be presented.

REFERENCES

- [1] I.L. KARLE, *Int. J. Pept. Protein Res.*, **23**, 32-38 (1984).
- [2] I.L. KARLE, J. KARLE, *Proc. Natl. Acad. Sci. USA*, **78**, 681-685 (1981).
- [3] G. KARTHA, K.I. VARUGHESE, S. AIMOTO, *Proc. Natl. Acad. Sci. USA*, **79**, 4519-4523 (1982).
- [4] Y.H. CHIU, L.D. BROWN, W.N. LIPSCOMB, *J. Am. Chem. Soc.*, **99**, 4799-4802 (1977).
- [5] I.L. KARLE, *J. Am. Chem. Soc.*, **96**, 4000-4006 (1974).
- [6] I.L. KARLE, *Biochemistry*, **13**, 2155-2162 (1974).
- [7] M. PINKERTON, L.K. STEINRAUF, P. DAWKINS, *Biochem. Biophys. Res. Commun.*, **35**, 512-518 (1969).
- [8] K. NEUPERT-LAVES, M. DOBLER, *Helv. Chim. Acta*, **58**, 432-442 (1975).
- [9] L.K. STEINRAUF, J.A. HAMILTON, M.N. SABESAN, *J. Am. Chem. Soc.*, **104**, 4085-4091 (1982).
- [10] I.L. KARLE, E.N. DUESLER, *Proc. Natl. Acad. Sci. USA*, **74**, 2602-2606 (1977).
- [11] I.L. KARLE, *J. Am. Chem. Soc.*, **91**, 5152-5157 (1977).
- [12] I.L. KARLE, TH. WIELAND, H. FAULSTICH, H.C.J. OTTENHEYM, *Proc. Natl. Acad. Sci. USA*, **76**, 1532-1536 (1979).
- [13] I.L. KARLE, *J. Am. Chem. Soc.*, **100**, 1286-1289 (1978).
- [14] I.L. KARLE, in A. EBERLE, R. GEIGER, TH. WIELAND (eds.), «Perspectives in Peptide Chemistry», S. Karger, Basel, 1981, pp. 261-271.
- [15] W.L. DUAX, H. HAUPTMAN, C.M. WEEKS, D.A. NORTON, *Science*, **176**, 911 (1972).
- [16] I.L. KARLE, *J. Am. Chem. Soc.*, **97**, 4379-4386 (1975).
- [17] G.D. SMITH, W.L. DUAX, D.A. LANGS, G.T. DE TITTA, J.W. EDMONDS, D.C. ROHRER, C.M. WEEKS, *J. Am. Chem. Soc.*, **97**, 7242-7247 (1975).
- [18] M. CZUGLER, K. SASVÁRI, M. HOLLÓSI, *J. Am. Chem. Soc.*, **104**, 4465-4469 (1982).



PSS.15 — TH

PETER M. MAY
KEVIN MURRAY
DANIEL PEAPER

Department of Applied Chemistry
UWIST
Cardiff
U.K.

THE EFFECT OF SODIUM ION INTERFERENCE ON BIOINORGANIC FORMATION CONSTANTS DETERMINED BY GLASS ELECTRODE POTENTIOMETRY

Recently, a library of computer programs for the determination of metal-ligand formation constants, called ESTA (Equilibrium Simulation for Titration Analysis), has been developed [1]. These programs permit various corrections which are important in the measurement of thermodynamic parameters required by those modelling metal-ion interactions in biological fluids (*e.g.* blood plasma, intestinal juice and saliva [2]). Changes in ionic activities, liquid junction potentials and ion-selectivity of the electrodes used for potentiometric titrations can be calculated [3].

Such corrections become necessary when the background ionic strength of a titration is not high enough to remain reasonably constant. This is often the case in work of biological relevance, where ionic strengths less than 200 mmol dm⁻³ are commonplace. Moreover, the formation constants of many bioinorganic systems are such that pH measurements need to be made in relatively alkaline solutions where sodium ion interference with the glass electrode response is most pronounced. The object of the present work was to quantify the effect of this interference and to assess the seriousness of neglecting it in a typical study of a metal-ligand interaction with bioinorganic interest.

In the first stage, potential differences arising from the presence of sodium ions in the titration

solutions were characterised in terms of two parameters, K and α . K is the selectivity coefficient in the NICOLSKI equation [4] when $\alpha = 1$. Data were collected experimentally and from the literature [5].

In the second stage, experimental titration data for the binding between zinc(II) and the amino acid, cysteine [6,7] were analysed using the ESTA program. Sodium ion interference was found to introduce a systematic error, rising to several millivolts towards the end of each titration. As a result, the first protonation constant of cysteine ($\log \beta_{101} = 10.01$) was lowered by 0.03 log units by omitting from the numerical analysis the effects of sodium ion in the background electrolyte. Larger differences were found for the metal-ligand formation constants (e.g. $\Delta \log \beta_{210} = 0.06$; $\Delta \log \beta_{330} = 0.1$). Generally, the errors were about ten times larger than the calculated standard deviations for the corresponding formation constants.

It may be concluded that significant systematic errors have affected many bioinorganic formation constants determined in sodium ion background electrolyte solutions. However, with modern glass electrodes, the magnitude of these errors is probably about the same as other systematic effects (such as those arising from errors in the analytical concentrations of the solutions being titrated). Nevertheless, they are sufficiently serious to warrant attention in any precise determination of formation constants for bioinorganic purposes.

REFERENCES

- [1] K. MURRAY, P.M. MAY, «ESTA User's Manual», Department of Applied Chemistry, UWIST, Cardiff, 1984.
- [2] P.M. MAY, R.A. BULMAN, *Prog. Med. Chem.*, **20**, 225 (1983).
- [3] P.M. MAY, K. MURRAY, D.R. WILLIAMS, *Talanta*, **32**(6) (1985), in press.
- [4] B.P. NICOLSKY, *Acta Physiochim. USSR*, **7**, 597 (1937).
- [5] N. LINNET, «pH Measurements in Theory and Practice», Radiometer, Copenhagen, 1970.
- [6] C. FURNIVAL, P.M. MAY, D.R. WILLIAMS, unpublished data.
- [7] G. BERTHON, P.M. MAY, D.R. WILLIAMS, *J. Chem. Soc., Dalton Trans.*, 1433 (1978).

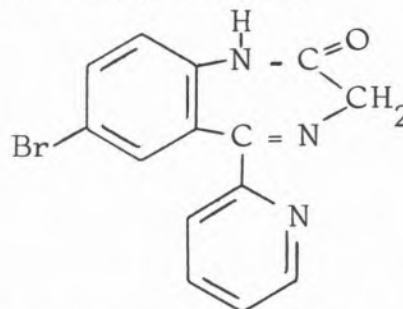


PS5.16 — MO

ADRIANO BENEDETTI
CARLO PRETI
LORENZO TASSI
GIUSEPPE TOSI
Instruments Centre
Department of Chemistry
University of Modena
Via G. Campi, 183, 41100 Modena
Italy

SYNTHESIS AND CHARACTERIZATION OF d-BLOCK COMPLEXES WITH BROMAZEPAM AS LIGAND

Working in the field of 1,4-benzodiazepines of biological and pharmacological interest as ligands, we report the complexes of ruthenium(III), osmium(III), rhodium(III), iridium(III), palladium(II) and platinum(II) halides with 7-bromo-1,3-dihydro-5-(2-pyridil)-2H-1,4-benzodiazepin-2-one (bromazepam).



These new derivatives, of the ML_3X_3 and MLX_2 type, have been characterized on the basis of elemental analyses, IR and electronic spectra, multinuclear NMR studies, conductivity measurements, magnetic susceptibility data and thermal analyses. These studies suggest a pseudo-octahedral structure for rhodium and iridium derivatives and a square planar geometry for the palladium and platinum ones. The ligand behaves always as bidentate through the nitrogen in 4-position of the diazepine ring and the nitrogen of the pyridine ring.

Assignments for the metal-ligand and metal-halide bands have been made.

The results will be compared with those obtained with other 1,4-benzodiazepines.

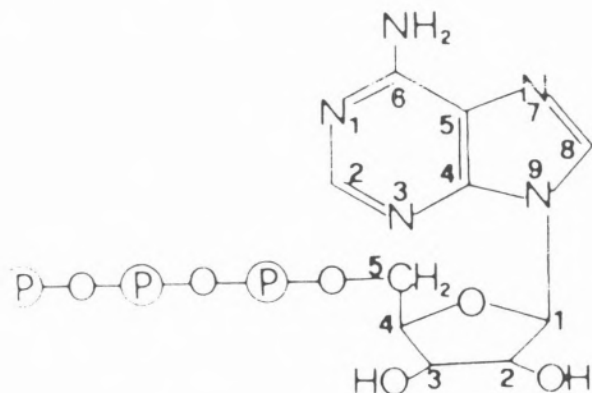


PS5.17 — TU

MARIANO CASU
ADOLFO LAI
GIUSEPPE SABA
Dipartimento di Scienze Chimiche
Via Ospedale 72, 09100 — Cagliari
Italy

**DYNAMICAL PROPERTIES OF ATP/CdCl₂
AND ATP/Cd(ClO₄)₂ COMPLEXES:
A COMBINED ¹³C AND ¹¹³Cd
RELAXATION STUDY**

In the past and recent years a great deal of investigations were undertaken on the binding mode between ATP and divalent metal ions, especially because of the intrinsic relevant biological importance.



Nuclear Magnetic Resonance has been thoroughly applied in most of these works; however, despite the overall NMR parameters employed, a number of questions on the binding sites on the nucleotide and on the metal ion coordination sphere has still to be answered [1]. Here we present the results of ¹³C and ¹¹³Cd spin-lattice relaxation and ¹³C-¹H and ¹¹³Cd-¹H nuclear overhauser studies of ATP in presence of the diamagnetic salts CdCl₂ and Cd(ClO₄)₂ (Table 1).

The pertinent data were obtained by means of the following formulas:

$$\frac{1}{T_{1 \text{ obs}}} = \frac{1}{T_{1 \text{ DD}}} + \frac{1}{T_{1 \text{ others}}} \quad (1)$$

$$\frac{1}{T_{1 \text{ DD}}} = \frac{\eta_{\text{obs}}}{\eta_{\text{max}}} \cdot \frac{1}{T_{1 \text{ obs}}} \quad (2)$$

$$\frac{1}{T_{1 \text{ DD}}} = \frac{n_{\text{H}}}{10} \hbar^2 \gamma_{\text{X}}^2 \gamma_{\text{H}}^2 r_{\text{XH}}^6 \tau_{\text{c}} \left[\frac{1}{1 + (\omega_{\text{H}} - \omega_{\text{X}})^2 \tau_{\text{c}}^2} + \frac{3}{1 + \omega_{\text{X}}^2 \tau_{\text{c}}^2} + \frac{6}{1 + (\omega_{\text{H}} + \omega_{\text{X}})^2 \tau_{\text{c}}^2} \right] \quad (3)$$

where

n_{H} = number of relaxators (protons)

$\gamma_{\text{X}}, \omega_{\text{X}}$ = gyromagnetic ratio and angular frequency of the pertinent nucleus (¹³C, ¹¹³Cd) at 1.88 T

r_{XH} = distance of the relaxator from the pertinent nucleus;

Table 1

¹³C Spin-lattice relaxation data and viscosity (η) measurements of ATP/CdCl₂ and ATP/Cd(ClO₄)₂ systems in aqueous solution

pH	ATP		ATP/CdCl ₂		ATP/Cd(ClO ₄) ₂		
	C2	C8	C2	C8	C2	C8	
2	T_1 (sec)	0.223	0.207	0.095	0.082	0.071	0.067
	η_{obs}	2.06	1.97	1.26	1.37	1.22	1.23
	η_{max}	1.99		1.99		1.99	
	$T_{1 \text{ DD}}$ (sec)	0.223	0.207	0.150	0.121	0.120	0.108
	τ_{c} (sec) ^{a)}	1.9·10 ⁻¹⁰		3.5·10 ⁻¹⁰		4.2·10 ⁻¹⁰	
	η (cp)	1.47		1.58		1.49	
6.5	T_1 (sec)	0.203	0.171	0.070	0.058		
	η_{obs}	2.06	1.96	1.07	1.13		
	η_{max}	1.99		1.99			
	$T_{1 \text{ DD}}$ (sec)	0.203	0.171	0.130	0.103		
	τ_{c} (sec) ^{a)}	2.3·10 ⁻¹⁰		4.1·10 ⁻¹⁰			
	η (cp)	1.57		1.70			

a) Arithmetic averages over the two carbon atoms.

On these basis information was obtained on the dynamics of the complexes and on the number of water molecules coordinated to the metal ion [2,3] (Table 2).

Table 2
¹¹³Cd Spin-lattice relaxation data for ATP/CdCl₂ and
 ATP/Cd(ClO₄)₂ in aqueous solution

	pH=2 ATP/Cd(ClO ₄) ₂	pH=2 ATP/CdCl ₂	pH=6.5 ATP/CdCl ₂
T ₁ (sec)	1.26	2.37	3.20
η _{obs}	-0.45	-0.54	-0.35
η _{max}	-2.19	-2.21	-2.19
T _{1 DD} (sec)	6.13	9.68	20.03
n _H ^{a)}	10.2	7.6	3.2

a) Values calculated from eq. (3) with r_{Cd-H} = 2.98 Å

It was found that the number of coordinated water molecules strongly depends on the metal ion accompanying counterion (Cl⁻ or ClO₄⁻), while the dynamics' data are discussed in terms of increased nucleotide self-association induced by the presence of the metal ion.

REFERENCES

- [1] S. BIAGINI, R. CAMINITI, M. CASU, G. CRISPONI, A. LAI, *Chem. Phys.*, **93**, 461 (1985).
- [2] C.F. JENSEN, S. DESHMUKH, H.J. JAKOBSEN, R.R. INNERS, P. ELLIS, *J. Am. Chem. Soc.*, **103**, 3659 (1981).
- [3] T.L. JAMES, «Nuclear Magnetic Resonance in Biochemistry», Academic Press, New York, 1975, pp. 39.



PS5.18 — MO

B. PISPISA
 A. PALLESCHI
 G. PARADOSSI
 Dipartimento di Chimica
 Università di Napoli
 80134 Napoli
 and
 Dipartimento di Chimica
 Università di Roma
 00185 Roma
 Italy

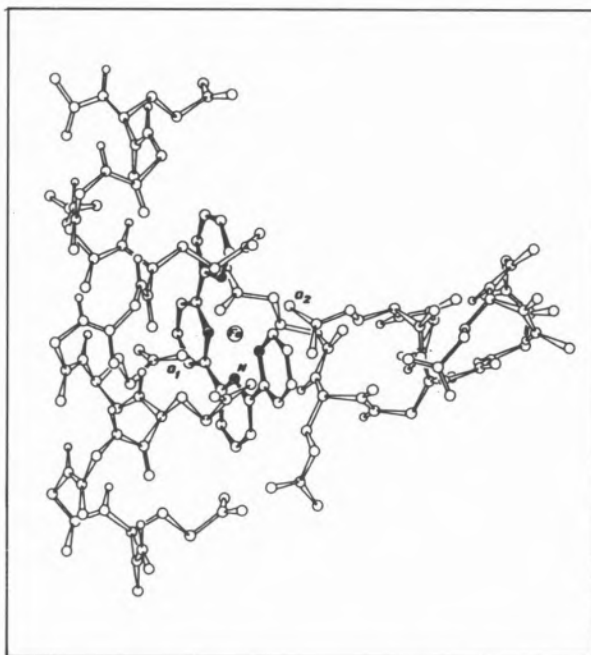
CHIRAL DISCRIMINATION IN ELECTRON TRANSFER REACTIONS BETWEEN ASYMMETRIC SPECIES

A simple, though realistic, synthetic model of enzymic material for stereoselective oxidation reactions has been prepared by us anchoring hemin-like $[\text{Fe}(\text{tetpy})(\text{OH})_2]^+$ ions to poly(L-glutamate) (FeTL) or poly(D-glutamate) (FeTD) ($\text{tetpy} = 2,2',2'',2'''$ -tetrapyrrolyl) [1,2]. The structural features of FeTL system, under conditions where it exhibits stereoselective activity, are illustrated in Figure. The molecular model was obtained by conformational energy calculations, partially based on available X-ray data, and is fully consistent with a number of experimental findings [3].

Oxidation of chiral catecholamines, such as L-dopa and L-adrenaline, by FeTL and FeTD enantiomeric systems was found to proceed stereoselectively [2], as shown in Table, where thermodynamic data for the formation of the diastereomeric precursor complexes are also reported. From the results, it appears that: i) stereoselectivity is largely controlled by kinetic effects, $\Delta(\Delta G^\ddagger)$ being definitely higher than $\Delta(\Delta G^0)$, and ii) the energetics of chiral discrimination, $\Delta(\Delta H)$, is of the order of magnitude that one would have been expected on the basis of $\Delta(\Delta G^0)$ values, on

the reasonable assumption that the entropies of association of the diastereomeric pairs are nearly identical.

We have also investigated the geometric and steric constraints which control the formation of the diastereomeric adducts by conformational energy calculations, based on nonbonding, electrostatic and hydrogen bonding energy terms [3]. The most relevant molecular parameters of the hypothetical models of the diastereomeric noncovalent electron-transfer complexes, corresponding to the deepest minimum in the total interaction energy, are reported in the same Table. Inspection of the Table indicates that: i) the redox centers in the diastereoisomers experience a different separation distance (and mutual orientation), as one would predict for kinetically-controlled stereoselectivity, ii) the difference in the total energy between LL



and DL pairs agrees surprisingly well (both in magnitude and sign) with the experimentally determined $\Delta(\Delta H)$ values, and iii) stereoselectivity calculated [3] by the molecular parameters of the models is in satisfactory agreement with that observed.

These findings, and the indirect tests carried out in searching vainly an agreement between calculated and experimental stereoselectivity using molecular parameters corresponding to other relative

Table
Kinetic, Calorimetric and Molecular Parameters of the Diastereomeric Electron-Transfer Complexes

Reductant	Diaster.	$G_{LL}^\ddagger - G_{DL}^\ddagger$ a,b)	$G_{LL}^o - G_{DL}^o$ c,b)	$\Delta H_{LL} - \Delta H_{DL}$ d)	$\bar{R}^{e,f)}$	$R'^{g,f)}$	$U_{LL} - U_{DL}$ h,f)	Stereoselectivity		
								cld ^{i,l)}	cld ^{i,m)}	exp ⁿ⁾
L-dopa	DL	568 ± 110	253 ± 120	130 ± 50	7.0 ± 0.1	7.1 ± 0.1	60 ± 90	4.2 ± 0.8	2.6 ± 0.5	3.9 ± 0.8
	LL				5.8 ± 0.1	7.5 ± 0.1				
L-adrenaline	DL	711 ± 100	161 ± 110	250 ± 100	7.0 ± 0.1	7.5 ± 0.1	245 ± 185	4.3 ± 0.8	4.6 ± 0.7	4.5 ± 1.1
	LL				7.5 ± 0.1	7.8 ± 0.1				

- a) Difference (cal/mol) in the standard free energies of the diastereomeric transition states of the electron-transfer step;
 b) from kinetic data in the steady-state approximation (25.9°C);
 c) difference (cal/mol) between the standard free energies of the diastereomeric precursor complexes;
 d) difference (cal/mol) between the enthalpies of formation of the diastereomeric pairs, from differential calorimetric measurements at 25°C, under conditions where the association of substrates is virtually complete;
 e) closest catecholic-O \cdots Fe separation distance (Å);
 f) from conformational energy calculations in the deepest minimum of total interaction energy, given as a sum of all pairwise non-bonded, electrostatic and hydrogen bonding interactions (average values as obtained using two types of nonbonded potential functions and four different sets of values for the interatomic interaction parameters);
 g) closest catecholic-O \cdots Fe separation distance (Å) *via* tetrapyrrolyl ring, estimated from the molecular geometry of the models;
 h) difference (cal/mol) in the total potential energy between LL and DL diastereoisomers in the deepest minimum of total energy;
 i) overall stereoselectivity calculated by $(R_{DL}/R_{LL})^2 \exp [(U_{LL} - U_{DL})/RT](k_{etDL}/k_{etLL})$, where $R_{DL(LL)}$ refers to \bar{R} or R' and k_{et} is the specific rate for the intramolecular electron-transfer process, as obtained by kinetic data in the steady-state conditions;
 l) using \bar{R} values;
 m) using R' values;
 n) 25.9°C, pH 7, 0.05 M Tris buffer, [C]/[P]=0.20, α -helical fraction in the polypeptide matrices \approx 0.70, as determined by chiroptical measurements.

minima of the total energy as well, lead us to consider the present hypothetical models as a good representation of the actual diastereomeric electron-transfer complexes. They confirm the idea that chiral discrimination in the reactions investigated is coupled with a remote attack mechanism on the central metal ion *via* the peripheral tetrapyrrolyl ligand of the active site [2,3]. In the sense that FeTL (or FeTD) system contains both binding and catalytic sites, it may be considered as an enzymic model.

REFERENCES

- [1] M. BRANCA, M.E. MARINI, B. PISPISA, *Biopolymers*, **15**, 2219 (1976);
 M. BRANCA, B. PISPISA, *J. Chem. Soc., Faraday Trans. I*, **73**, 213 (1977).
 [2] M. BARTERI, B. PISPISA, *J. Chem. Soc., Faraday Trans. I*, **78**, 2073, 2085 (1982);
 B. PISPISA, M. BARTERI, M. FARINELLA, *Inorg. Chem.*, **22**, 3166 (1983);
 B. PISPISA, M. FARINELLA, *Biopolymers*, **23**, 1465 (1984).
 [3] B. PISPISA, A. PALLESCHI, M. BARTERI, S. NARDINI, *J. Phys. Chem.*, in press.



PS5.19 — TU

L.L. FISH
A.L. CRUMBLISS
Chemistry Department
Duke University
Durham, N.C. 27706
U.S.A.

AN INVESTIGATION OF THE KINETICS AND MECHANISM OF IRON(III) RELEASE FROM *N,N'*-DI(2-HYDROXY-BENZYL)ETHYLENEDIAMINE-*N,N'*-DIACETIC ACID AS A MODEL FOR IRON EXCHANGE FROM TRANSFERRIN

The kinetics and mechanism of the release of iron(III) from *N,N'*-di(2-hydroxybenzyl)ethylenediamine-*N,N'*-diacetic acid (HBED) [1] has been investigated. Because the donor groups of HBED (phenol, carboxylate, amine) provide a hexadentate binding site which has a high affinity for iron(III) and which has certain similarities to transferrin [2], this reaction may serve to mimic iron dissociation reactions from transferrin. Our initial study of this complex was made by investigating the following iron(III) exchange reaction,



The rate law for this exchange reaction over the pH range from 2.5 to 6.0 expressed in terms of EDTA^{4-} is as follows.

$$\text{Rate} = (k_2[\text{H}^+]^2 + k_3[\text{H}^+]^3 + k_4[\text{H}^+]^4 + k_5[\text{H}^+]^5)[\text{FeHBED}^-][\text{EDTA}^{4-}] \quad (2)$$

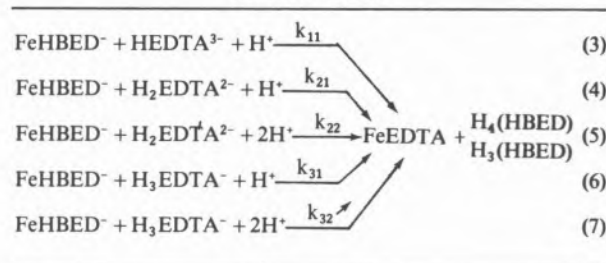
These observations are consistent with five parallel paths to products as shown in the Reaction Scheme.

The values for the microscopic rate constants and pH range where each path contributes significantly to product formation are as follows: (3) pH 6.0-4.5, $k_{11} = 1.4 \text{ M}^{-2}\text{s}^{-1}$; (4) pH 6.0-2.5, $k_{21} = 1.0 \text{ M}^{-2}\text{s}^{-1}$; (5) pH 4.5-2.5, $k_{22} \leq 7.5 \times 10^2 \text{ M}^{-3}\text{s}^{-1}$;

(6) pH 3.8-2.5, $k_{31} = 1.6 \text{ M}^{-2}\text{s}^{-1}$; (7) pH 3.8-2.5, $k_{32} \leq 2.5 \times 10^3 \text{ M}^{-3}\text{s}^{-1}$. Apparently the microscopic rate constants are not influenced by the degree of protonation of EDTA. This is consistent with a carboxylate group, unprotonated over the entire pH range, being the site of primary attack by the EDTA leading to ternary complex formation. Protonation of one or both of the phenolate groups of HBED further assists the iron exchange.

The influence of acetohydroxamic acid as a catalyst for reaction (1) was investigated. A significant rate enhancement was observed at physiological pH. Possible mechanisms for this catalytic effect will be discussed.

Reaction Scheme



In order to determine the usefulness of HBED as a kinetic model for transferrin, certain experiments previously reported for transferrin [3,4] were duplicated using FeHBED^- . Initial rate studies for iron(III) exchange between FeHBED^- and EDTA, thioglycolate, and pyrophosphate were carried out at physiological pH. These results are compared with results from the corresponding transferrin reactions in the Table. Also included in the Table are redox reactions using dithionite and thioglycolate reductants and bathophenanthroline-disulfonic acid (BPS) as a trap for the dissociated iron(II). The transferrin system reacts 10^2 to 10^5 times faster than FeHBED^- toward competing chelating agents. In the reduction reactions, however, the thioglycolate reaction proceeds at comparable rates and the dithionite reaction is 10^2 faster for FeHBED^- than transferrin. Furthermore, the FeHBED^- system exhibits a wider reactivity range than does transferrin (variation in k by 10^6 for FeHBED^- and 40 for transferrin). Apparently HBED is not a good kinetic model for transferrin, despite the binding site similarities.

Table
Comparison of ligand exchange kinetics for FeHBED and Fe-Transferrin at pH 7.4^{a)}

	X = HBED	X = Transferrin	
	$k_{\text{HBED}}, \text{s}^{-1}$	$k_{\text{Tf}}, \text{s}^{-1}$	$k_{\text{Tf}}/k_{\text{HBED}}$
FeX + L \longrightarrow FeL + X			
L = 0.05 M EDTA	2.7×10^{-9}	4.1×10^{-4} ^{b)}	1.5×10^5
L = 0.1 M Thioglycolate	3.5×10^{-6}	3.6×10^{-4} ^{c)}	1.0×10^2
L = 0.06 M Pyrophosphate	1.3×10^{-7}	1.9×10^{-3} ^{c)}	1.5×10^4
Fe ^{III} X + BPS $\xrightarrow{\text{R}}$ Fe ^{II} (BPS) ₃ + X			
R = 0.03 M Dithionite	5.7×10^{-3}	4.3×10^{-5} ^{c)}	7.5×10^{-3}
R = 0.1 M Thioglycolate	4.2×10^{-5}	3.6×10^{-4} ^{c)}	8.6

a) All data 25°C, I = 0.1 M KNO₃. b) [3]. c) [4].

The implications of this observation in terms of the role of the protein and/or HCO₃⁻/CO₃⁼ in influencing the lability of the iron in transferrin will be discussed.

REFERENCES

- [1] F. L'EPLATTENIER, I. MURASE, A.E. MARTELL, *J. Am. Chem. Soc.*, **89**, 837 (1967).
- [2] N.D. CHASTEEN, *Adv. Inorg. Biochem.*, **5**, chapter 8, (1983).
- [3] D.A. BALDWIN, D.M.R. DE DOUSE, M.A. VON WANDRUSZKA, *Biochim. Biophys. Acta*, **719**, 140 (1982).
- [4] N. KOJIMA, G. BATES, *J. Biol. Chem.*, **254**, 8847 (1979).



PS5.20 — TU

ARMANDO J.L. POMBEIRO
M. AMÉLIA N.D.A. LEMOS
Centro de Química Estrutural, Complexo I
Instituto Superior Técnico
Av. Rovisco Pais, 1096 Lisboa Codex
Portugal

NET ELECTRON ACCEPTOR/DONOR CHARACTER OF ISOCYANIDES AND DINITROGEN AT THE IRON(II) CENTRE {FeH(Ph₂PCH₂CH₂PPh₂)₂}⁺: AN ELECTROCHEMICAL STUDY

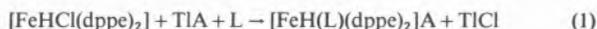
1 — INTRODUCTION AND RESULTS

Isocyanides (C≡NR) have been used as probes for the study of the electronic and chemical properties of dinitrogen activated by a transition metal centre [1].

Hence, *e.g.*, an analogy of chemical behaviour between N₂ and CNR was detected when they bind a d⁶ Mo or W phosphinic centre, both substrates being activated towards ready electrophilic attack. The net electron donor/acceptor character

of N_2 and CNR and their chemical reactivities were also compared [2,5] when they ligate $\{ReCl(dppe)_2\}$ and in the present work we extend to a group VIII centre, $\{FeH(dppe)_2\}^+$, the comparison between these two substrates.

Complexes *trans*- $[FeH(L)(dppe)_2]A$ ($L = N_2$ or CNR with $R = C_6H_4NO_2-4$, C_6H_4Me-4 , C_6H_5 , C_6H_4OMe-4 , Me, Et or Bu^1 ; $A^- = BF_4^-$ or PF_6^-), which were prepared according to reaction (1) [3],



undergo a partial reversible or an irreversible electrochemical oxidation at a Pt electrode, in thf (or NCMe)/ $[Bu_4N][BF_4]$ or in thf/ $LiClO_4$, and the values of $E_{p/2}^{ox}$ were compared with those obtained by other authors [4] for the analogous carbonyl, nitrile and thiocyanate compounds *trans*- $[FeH(L')(dppe)_2]^n$ ($n = +1$; $L' = CO$, NCMe or NCPH. $n = 0$; $L' = SCN^-$ or Cl^-). The following order of $E_{p/2}^{ox}$ is then observed: $CO > aryl \text{ isocyanides} > alkyl \text{ isocyanides} > NCPH > NCMe = N_2 > SCN^- > Cl^-$ —which corresponds to the order of decreasing net electron π acceptor – σ donor character of these ligands.

2 — DISCUSSION

2.1 — Isocyanide and dinitrogen ligand P_L parameter at the $\{FeH(dppe)_2\}^+$ centre

A linear relationship between $E_{1/2}^{ox}$ of complexes $[FeH(L')(dppe)_2]^n$ (see above) and the P_L ligand parameter for L' —defined [4] as $P_L = E_{1/2}^{ox} [Cr(CO)_5L] - E_{1/2}^{ox} [Cr(CO)_6]$ —was previously reported by other authors [4]. In the present study, this relationship is expressed for $E_{p/2}^{ox}$ by equation (2) which allows to estimate the P_L values for the isocyanide and the dinitrogen ligands

$$E_{p/2}^{ox} \approx 1 + P_L \text{ (volt)} \quad (2)$$

at the $\{FeH(dppe)_2\}^+$ centre (from the knowledge of the corresponding $E_{p/2}^{ox}$ which were obtained experimentally in this work): $P_L(CNR)$ falls in the range -0.1 to -0.2 V (depending on R) and $P_L(N_2) = -0.5$ V.

2.2 — Dependence of the net electron acceptor/donor character of isocyanides and dinitrogen on the electron-richness of the binding metal centre

The electron-richness, E_s , of a metal centre $\{M_s\}$, defined [4] as $E_s = E_{1/2}^{ox} [M_s(CO)]$ (a higher electron-richness corresponds to a lower E_s value), constitutes a relevant electrochemical parameter for the study of the electronic releasing ability of the metal centre. Isocyanide and dinitrogen ligand P_L values at the $\{FeH\}^+$ centre ($Fe = Fe(dppe)_2$) were compared with those estimated for metal centres with clearly distinct electron-rich characters, such as $\{Mo(N_2)\}$ and $\{Cr(CO)_5\}$ (Table) and a few observations may be presented:

— For both N_2 and CNR, the net electron acceptor/donor character (P_L) appears to be dependent on the electron-richness (E_s) of the metal centre: a decrease in the former may result from lowering the latter.

— A higher P_L dependence on E_s is observed for N_2 rather than for CNR: for the very high electron-rich $\{Mo(N_2)\}$ centre, N_2 is a strong net acceptor ligand (even better than isocyanide), whereas at $\{FeH\}^+$ the former presents a much lower electron acceptor character (weaker than isocyanide) and binds only weakly to the metal site;

Table

P_L ligand parameter for CNR and N_2 at metal centres with different electron-richness (E_s)

Metal centre ^{a)}	E_s/V	$P_L(CNR)/V$	$P_L(N_2)/V$
$\{Mo(N_2)\}$	-0.13^b	$-0.23(CNBu^1)^c$	-0.07^b
$\{FeH\}^+$	$+1.04^b$	<i>ca.</i> -0.1 to -0.2 (<i>e.g.</i> , -0.2 for $CNBu^1$) ^{c)}	<i>ca.</i> -0.5^c
$\{Cr(CO)_5\}$	$+1.53^b$	<i>ca.</i> -0.33 to -0.44 (<i>e.g.</i> , -0.44 for $CNBu^1$) ^{b,d)}	— ^{e)}

a) $M = M(dppe)_2$. b) Ref. [4]. c) Estimated in the present study. d) Ref. [5]. e) Does not bind N_2 .

the least electron-rich centre, $\{Cr(CO)_5\}$, is even unable to bind N_2 (the isocyanides present then a considerably lower net electron-acceptance than when ligating the other more electron-rich centres which can bind N_2).

— Isocyanides appear to present a nearly constant (at least compared to the carbonyl reference ligand) net electron acceptor character when bound

to the centres which can ligate N_2 , $\{Mo(N_2)\}$ and $\{FeH\}^+$, in spite of their so different E_s values which may perhaps be accounted for by the electronic effects of the *trans* ligand.

ACKNOWLEDGEMENTS

The support given by the Calouste Gulbenkian Foundation, INIC and JNICT is gratefully acknowledged. The authors are also indebted to Dr. C.J. PICKETT of the Unit of Nitrogen Fixation for helpful discussion.

REFERENCES

- [1] A.J.L. POMBEIRO, in J. CHATT, L.M.C. PINA, R.L. RICHARDS (eds.), «New Trends in the Chemistry of Nitrogen Fixation», Academic Press, 1980, chapter 6; A.J.L. POMBEIRO, *Rev. Port. Quím.*, **26**, 30 (1984).
- [2] A.J.L. POMBEIRO, *Rev. Port. Quím.*, **23**, 179 (1981).
- [3] M.B.M. BAPTISTA, A.J.L. POMBEIRO, «4th Annual Meeting Portug. Chem. Soc.», Lisbon, 1981, PC 133.
- [4] J. CHATT, C.T. KAN, G.J. LEIGH, C.J. PICKETT, D.R. STANLEY, *J. Chem. Soc., Dalton Trans.*, 2032 (1980).
- [5] A.J.L. POMBEIRO, C.J. PICKETT, R.L. RICHARDS, *J. Organomet. Chem.*, **224**, 285 (1982).



PS5.21 — TU

ARMANDO J.L. POMBEIRO
M. FERNANDA N.N. CARVALHO
Centro de Química Estrutural, Complexo I
Instituto Superior Técnico
Av. Rovisco Pais, 1096 Lisboa Codex
Portugal

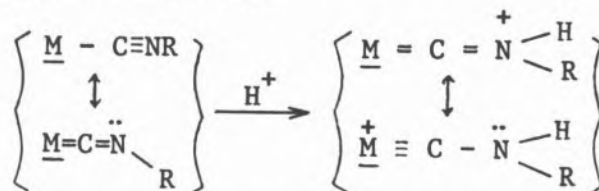
ELECTRON-RICH RHENIUM AND MOLYBDENUM METAL CENTRES AS POTENTIAL INORGANIC MODELS IN THE BIO-REDUCTION OF ISOCYANIDES?

Isocyanides ($C\equiv NR$) are organic species which are isoelectronic with dinitrogen (N_2) and can also be reduced by the enzyme nitrogenase with com-

plete cleavage of the unsaturated bond to afford amines and methane, e.g., according to reaction (1) (C_2 and C_3 hydrocarbons are also formed in lower yields).



The mechanism of the $C\equiv N$ bond cleavage is yet unknown, but the study of the activation of isocyanides by transition-metal centres in well defined coordination compounds may provide some useful information for the understanding of the process. When bound to a transition metal centre with a low π -electron releasing ability, isocyanides can undergo attack by a nucleophile at the ligating carbon; however, the isocyanide ligand can be activated towards electrophilic attack (which occurs at the N atom) by a metal centre with a high electron-richness (high π -electron donor character). The latter type of reaction occurs typically for d^6 $Mo(0)$ or $Re(I)$ centres of the types $\{Mo(dppe)_2\}$ or $\{ReCl(dppe)_2\}$ (where $dppe = Ph_2PCH_2CH_2PPh_2$), e.g., in complexes *trans*- $[Mo(CNMe)_2(dppe)_2]$ and *trans*- $[ReCl(CNMe)(dppe)_2]$, respectively, and carbyne-type ligands are formed by protonation of isocyanide ligand according to the following general VB scheme [1]:



where the weakening of the unsaturated CN bond is evident, although without occurrence of the complete rupture of this bond. However, protonation of the isocyanide may proceed until CN bond cleavage, at a related electron-rich metal centre with labile co-ligands such as monophosphines or phosphites. Hence, in complexes $[M(CNMe)_n L_{6-n}]$ ($M = Mo$ or W ; $n = 2$ or 3 ; $L = PMe_2Ph$) [2] and $[ReCl(N_2)(CNR)\{P(OMe)_3\}_3]$ ($R = Me, Et, t-Bu, C_6H_4Me-4$ or C_6H_4Cl-4) [3], the isocyanide ligand undergoes protic attack (by HA acid) to afford the corresponding primary ammonium salt. The presence of labile ligands plays a fundamental role due to their facile replacement by a stronger electron donor anion, A^- , which promotes further protonation at CNR to give complete reduction to amine.

Hydrocarbons are also detected in some of these systems, although in minor yields; hence, it is yet unknown the fate of most of the terminal CNR carbon atom, although species with carbon hydrides or $\equiv\text{CA}$ ligating the metal atom seem likely intermediates.

The protonation of the isocyanide ligand occurs with concomitant oxidation of the metal (which behaves as the reducing agent), and the systems are not catalytic (the maximum yield for the reductive cleavage of the isocyanide corresponds to the consumption of nearly all the available metal six d electrons).

Hence, *electron-richness* of the metal centre and the presence of a *labile co-ligand* appear to play a fundamental role in the activation of isocyanides towards reductive cleavage to primary amines upon protonation which occurs in a stepwise way. However, these systems fail to mimic the formation (in a considerable amount) of the other products (hydrocarbons) of the enzymatic reduction. The poisoning of the ligating carbon atom (which possibly exhibits an electrophilic character) by the anion of the acid may conceivably occur, and the use of an *auxiliary reducing agent* (or the imposition, by electrochemical techniques, of a suitable cathodic potential) would be required to reduce the oxidized central metal and, hence, activate the ligating carbon atom towards protonation and also regenerate an active electron-rich metal centre, although in a discontinuous process — Fig. 1 where L is a labile ligand (may be more than one) such as phosphine or phosphite and A^- is a stronger net electron donor species such as OR^- or an halide.

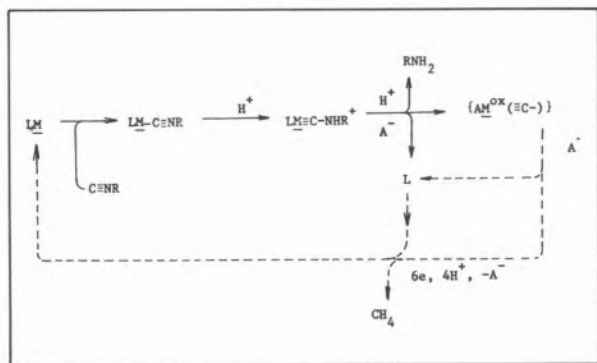


Fig. 1

Hypothetical catalytic cycle for the protic reduction of isocyanide to amine and methane at an electron-rich metal centre

The metal centre M may be a poly-hydridic moiety which would account for H_2 evolution by protic reduction. It may also bind other substrates such as dinitrogen which may be activated to reduction affording ammonia by protonation (as it is observed [4] for the Mo or W monophosphine centres). In the natural systems, water may behave as the protic source.

We are pursuing this work namely by attempting to isolate metallic intermediates, to increase the yield of hydrocarbon formation and by extending this type of study to other activating centres (*e.g.*, with a group VIII transition metal site) and to other substrates (such as nitriles).

REFERENCES

- [1] A.J.L. POMBEIRO, R.L. RICHARDS, *Transition Met. Chem.*, **5**, 55 (1980);
J. CHATT, A.J.L. POMBEIRO, R.L. RICHARDS, *J. Chem. Soc., Dalton Trans.*, 492 (1980);
A.J.L. POMBEIRO, M.F.N.N. CARVALHO, P.B. HITCHCOCK, R.L. RICHARDS, *J. Chem. Soc., Dalton Trans.*, 1629 (1981).
- [2] A.J.L. POMBEIRO, R.L. RICHARDS, *Transition Met. Chem.*, **5**, 281 (1980).
- [3] M.F.N.N. CARVALHO, A.J.L. POMBEIRO, U. SCHUBERT, O. ORAMA, C.J. PICKETT, R.L. RICHARDS, *J. Chem. Soc., Dalton Trans.*, submitted for publication.
- [4] J. CHATT, A.J. PEARMAN, R.L. RICHARDS, *J. Chem. Soc., Dalton Trans.*, 1852 (1977).



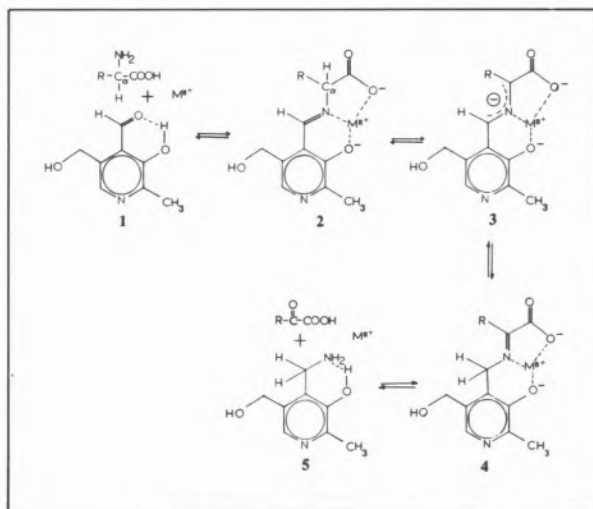
PS5.22 — TH

PATRICK A. TAYLOR
 ARTHUR E. MARTELL
 Department of Chemistry
 Texas A&M University
 College Station, Texas 77843
 U.S.A.

A PROTON-NMR STUDY OF THE KINETICS OF FORMATION OF THE GENERAL INTERMEDIATE IN VITAMIN B-6-CATALYZED TRANSAMINATION

The rates of the transamination reactions of α -amino acids and α -keto acids have been determined by measurement of the 200 MHz proton NMR spectra of the functional groups of the Al(III) complexes of the Schiff bases **2**, **4** formed with pyridoxal **1** and pyridoxamine **5** respectively. Reaction systems measured in D_2O at $10^\circ C$ consisted of 1:1:1 molar ratios of pyridoxal: α -amino acid:Al(III) or pyridoxamine: α -keto acid:Al(III). Amino and keto acids employed are alanine, α -aminoisobutyric acid, valine, phenylglycine, pyruvic acid, and α -ketobutyric acid. A negative deprotonated intermediate **3** was detected in all systems that undergo transamination (*i.e.*, except α -aminoisobutyric acid). The intermediate resembles the aldimine with NMR resonances shifted upfield in accordance with its greater negative charge. With Al(III) and pyridoxal as catalysts the equilibrium concentrations of the intermediate formed from α -amino acids are reached in the time required to reach transamination equilibrium and is maintained in solution at a fraction (± 10 -20%) of the aldimine Schiff base concentration. In the reverse reaction with Al(III) and pyridoxamine as catalysts, α -keto acids produce the intermediate initially at higher concentrations than those of the aldimine reaction product. The ratios of these species change as equilibrium is reached, to give the same fraction of Al(III)-stabi-

lized intermediate as that obtained in the forward reaction. The relative changes in concentration of the α -deprotonated carbanion **3** and reaction products (the Schiff base chelates **2** and **4**) with time clearly demonstrate it to be the common mandatory intermediate in both the forward and reverse metal ion-catalyzed transamination reactions.



For the metal-free enzyme systems it is suggested that the active intermediate is an analogous deprotonated intermediate with a proton coordinated to the azomethine nitrogen in place of the metal ion in **3**. This type of intermediate, first suggested by ABBOTT and MARTELL [1], is suggested as the transamination intermediate in place of the quinoid-type Schiff base tautomer previously suggested [2,3].

REFERENCES

- [1] E.H. ABBOTT, A.E. MARTELL, *J. Am. Chem. Soc.*, **95**, 5014 (1973).
- [2] D.E. METZLER, M. IKAWA, E.E. SNELL, *J. Am. Chem. Soc.*, **76**, 648 (1954).
- [3] A.E. MARTELL, *Adv. in Enzymol.*, **53**, 163 (1982).

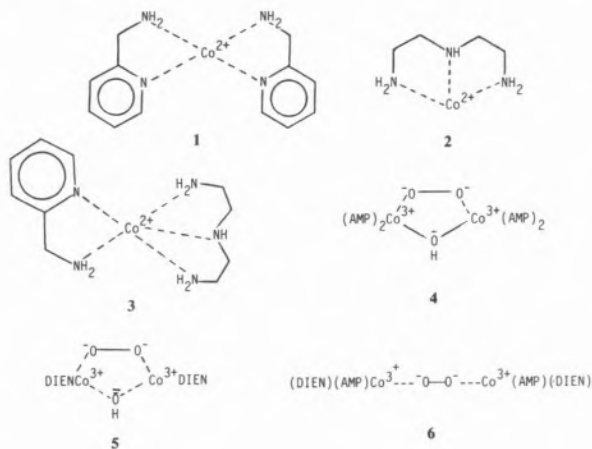


PS5.23 — TH

ARUP K. BASAK
ARTHUR E. MARTELL
Department of Chemistry
Texas A&M University
College Station, Texas 77843
U.S.A.

REACTIONS OF DIOXYGEN COMPLEXES. AUTOXIDATION OF 2-AMINOMETHYL- PYRIDINE THROUGH COBALT DIOXYGEN COMPLEX FORMATION

The metal complex formation constants and the oxygenation constants of the cobalt(II) complexes of diethylenetriamine (DIEN) and 2-aminomethylpyridine (AMP) have been determined by potentiometric measurements under N_2 and O_2 . In the mixed ligand system three cobalt complexes are formed which are capable of combining with dioxygen: the 2:1 AMP complex, **1**, the 1:1 DIEN complex, **2** and the 1:1:1 mixed ligand DIEN, AMP complex, **3**. The corresponding dioxygen complexes are indicated by formulas **4**, **5**, and **6**. The equilibrium constants for the mixed ligand system have been employed to determine the conditions under which the concentration of **3** has its maximum value, and the conditions that favor the formation of the mixed ligand dioxygen complex **6**.



The kinetics of oxidative dehydrogenation of **3** through the formation and degradation of **6** have been measured spectrophotometrically and rate constants are reported. The reaction has been found to be second order, first order in the concentration of the dioxygen complex and first order in the concentration of hydroxide ion. The reaction product in the two-electron oxidation of AMP is the corresponding imine, which under the reaction conditions employed is converted to pyridine-2-carboxaldehyde, determined quantitatively as the 2,4-dinitrophenylhydrazone. The proposed reaction mechanism involves deprotonation of the amino group, through the influence of the Co^{3+} center, as a pre-equilibrium step. This is followed by a concerted process involving homolytic fission of dioxygen, shift of an electron through the metal ion to the coordinated oxygen, and transfer of the α -proton to the oxygen atom. The two-electron oxidation of each AMP ligand is thus balanced by conversion of half of the dioxygen to water, with regeneration of cobalt(II). The proximity of the dioxygen to the α - CH_2 of the ligand is considered an important requirement for this concerted mechanism.



PS5.24 — TH

W.L. KWIK
K.P. ANG
Department of Chemistry
National University of Singapore
Singapore

COORDINATION ABILITIES OF SUBSTITUTED PHENOLATES — A SPECTROPHOTOMETRIC AND CONDUCTOMETRIC STUDY

The copper(II) — phenolate oxygen interaction in several mixed-ligand complexes of copper(II) containing a heterocyclic amine and a phenol has been studied by electronic spectral,

conductometric and EPR spectral measurements. Electronic spectral results demonstrate the dependence of such interaction on the nature of the phenolic substituents as well as the solvents. Partial dissociation of the phenolate from the complex was detected in methanol at low concentrations ($\leq 1 \times 10^{-4}$ M). In DMSO the complexes remain intact. The X-band EPR spectral data obtained at ambient temperature and at 77 K are consistent with the results from the electronic spectral and conductometric study.

INTRODUCTION

Metal-phenolate oxygen interaction has been known to exist in Fe(III), Cu(II) and several trivalent metal transferrers [1]. An investigation of model compounds of Cu(II) containing a phenolate ligand could be useful in providing an insight into the geometry of the naturally occurring metal enzymes. Several studies [2-4] have reported the binding of phenolate oxygen to Cu(II) in solution. This present study reports some characteristic features of the Cu(II) — phenolate oxygen interaction in several mixed-ligand complexes [Cu(terpy)(RArO)Cl] (terpy = 2,2',2'-terpyridine; RArO = phenolate with substituent R).

RESULTS AND DISCUSSION

The complexes of this study display in both methanol and DMSO, broad d-d absorption bands at 680-720 nm, indicative of tetragonal geometry around Cu(II). An intense band/shoulder is found in the 380-450 nm region ($\epsilon = 400-600 \text{ dm}^3 \text{ mol}^{-1} \text{ cm}^{-1}$) (Table I). This is characteristic of the Cu(II) — phenolate oxygen coordination [3,4,6]. Unlike the d-d transitions, this band is solvent dependent, shifting to lower energy in going from methanol to DMSO. Moreover among the complexes contain-

ing the *p*-methoxy-, *p*-chloro-, *p*-bromo-, *p*-fluoro-, *o*-NO₂- and *m*-NO₂-phenolate, the position of this band points to varied phenolate-Cu(II) interaction as one goes from the electron-donating to the increasingly stronger electron-withdrawing phenolic substituents. Among the complexes containing the *p*-NO₂-, 2,4-dinitro- and 2,5-dinitrophenolate, the absorption in the 380-450 nm region appears as an exceedingly strong and well-defined band ($\epsilon = 1 \times 10^3 - 1 \times 10^4 \text{ dm}^3 \text{ mol}^{-1} \text{ cm}^{-1}$) in both methanol and DMSO. Although a similar band of lower intensity is found in the corresponding phenol ($\epsilon = 1 \times 10^2 - 1 \times 10^3 \text{ dm}^3 \text{ mol}^{-1} \text{ cm}^{-1}$), the observed band in the complex is characteristic of the complex as the molar absorptivity remains, in each case, as a constant over a concentration range of $1 \times 10^{-3} - 1 \times 10^{-4}$ M. This contrasts with the decreasing values of the «apparent» ϵ evaluated for the uncoordinated phenol as concentration increases. This would be expected if the strong band in the 380-450 nm is due to the phenolate ion. Thus the strong absorption band in each of the three nitrophenolate complexes is tentatively assigned to a $\pi \rightarrow \pi^*$ transition of the coordinated phenolate which is most probably nonbridging. Values of the molar conductance of all the complexes at concentration $\geq 1 \times 10^{-4}$ M, fall in the range of 90-110 $\Omega^{-1} \text{ cm}^{-1} \text{ mol}^{-1}$ in methanol and of 20-40 $\Omega^{-1} \text{ cm}^{-1} \text{ mol}^{-1}$ in DMSO, suggesting that these complexes behave as 1:1 electrolytes in both solvents. However as the concentration is lowered further ($< 1 \times 10^{-4}$ M) the molar conductance of the complexes in methanol rises sharply to 400-450 $\Omega^{-1} \text{ cm}^{-1} \text{ mol}^{-1}$, accompanied by significant increases in intensities of the phenolate band. These changes indicate partial dissociation

Table I
EPR Parameters and Electronic Spectra (380-450 nm) for Selected Copper(II) Complexes

Complex (L = ArO)	g_{\perp}	g_{\parallel}	$A_{\parallel} \text{ cm}^{-1}$	$\nu_{\text{max}}, \text{ nm}(\epsilon)$	
				CH ₃ OH	DMSO
[Cu(terpy)(<i>o</i> -NO ₂ L)Cl]	2.09	2.22	0.0162	410(Sh)	450(500)
[Cu(terpy)(<i>m</i> -NO ₂ L)Cl]	2.11	2.23	0.0164	430(Sh)	460(200)
[Cu(terpy)(<i>p</i> -NO ₂ L)Cl]	2.12	2.22	0.0166	390(1×10^4)	434(1.5×10^4)
[Cu(terpy)(<i>p</i> -FL)Cl]	2.11	2.23	0.0163	405(Sh)	460(600)
[Cu(terpy)(<i>p</i> -CIL)Cl]	2.09	2.22	0.0165	405(Sh)	455(200)
[Cu(terpy)(<i>p</i> -BrL)Cl]	2.08	2.21	0.0165	400(Sh)	455(150)
[Cu(terpy)(<i>p</i> -OCH ₃ L)Cl]	2.08	2.23	0.0163	400(Sh)	405(200)
[Cu(terpy)(2,4-di-NO ₂ L)Cl]	2.12	2.22	0.0166	380(Sh)	432(1.2×10^4)
[Cu(terpy)(2,5-di-NO ₂ L)Cl]	2.13	2.23	0.0167	433(3×10^2)	494(3×10^3)

tion of the complexes in methanol, probably yielding Cu(terpy)^{2+} and phenolate at low concentrations. In DMSO, however, both the molar conductance and absorptivity remain nearly constant even at low concentration. For the five complexes containing *p*-methoxy, *p*-Cl, *p*-Br, *p*-F, *o*-NO₂ or *m*-NO₂-phenolate, no distinct phenolate absorption appears in the visible region, rendering it impractical to monitor the behaviour of these complexes at low concentration. However the molar conductivities display sharp increases at low concentrations ($<1 \times 10^{-4}$ M) in methanol, indicative of similar behaviour as for the nitrophenolates.

The solution and frozen-glass EPR spectra of these complexes in 5:1 methanol:water at low concentrations lend further support to the presence of non-bridging phenolate in these complexes as well as to the partial dissociation. Thus at 77 K the spectra are well-resolved, indicating that these complexes are monomeric (Table I). Furthermore the spin-Hamiltonian parameters [g_{\parallel} , g_{\perp} , A_{\parallel} (^{63/65}Cu)] are typical of tetragonal Cu(II) complexes. Substantial covalency of the Cu-N bond is evidenced by the seven well-defined N-14-superhyperfine structure on the g_{\perp} component, demonstrating the equivalence of the three pyridyl N. At ambient temperature, however the spectra are poorly resolved, displaying striking resemblance to that reported recently for $[\text{Cu(tery)}]^{2+}$ [6]. In the latter the poorly resolved spectrum has been attributed to dynamic Jahn-Teller effect.

REFERENCES

- [1] B.P. GAHER, J. MISKOWSKI, T.G. SPIRO, *J. Am. Chem. Soc.*, **96**, 6868 (1974).
- [2] J.M. PASTOR, A. GARNIER, L. TOSI, *Inorg. Chim. Acta*, **37**, L549 (1979).
- [3] H. KOZLOWSKI, M. BEZER, L.D. PETTIT, *J. Inorg. Biochem.*, **18**, 231 (1983).
- [4] R.J.W. HEFFORD, L.D. PETTIT, *J. Chem. Soc., Dalton Trans.*, 1331 (1981).
- [5] W.L. KWIK, K.P. ANG — Synthesis and Characterisation of these complexes were presented at ICCS XXIII, July 29-August 3, 1984.
- [6] A. GERGELY, T. KISS, *Inorg. Chim. Acta*, **16**, 51 (1976).
- [7] R.B. BONOMO, F. RIGGI, *Transition Met. Chem.*, **9**, 308 (1984).



PS5.25 — TU

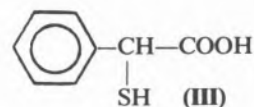
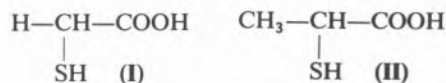
E. CASASSAS
M. FILELLA
A. IZQUIERDO
Departament de Química Analítica
Universitat de Barcelona
Spain

COMPLEX FORMATION IN THE SYSTEM Ni(II) — α -MERCAPTOPHENYLACETIC ACID

INTRODUCTION

The complex chemical significance of biologically active ligands like L-cysteine and D-penicillamine is determined by the mercaptosulphur donor atom, which is quite soft in character. The ability of these ligands to act as chelating agents of metal ions is due to the presence of other electron donor groups in their molecule. A deeper understanding of this type of chelate formation requires extension of research into studies of the effect of different substituents in the chelation properties of a ligand. The aim of the present work is to study the influence of the presence of a phenyl group in the Ni(II) complexing activity of aliphatic α -mercaptoacids.

It has been reported that α -mercaptoacetic acid (I) forms polynuclear — Ni₃L₄, Ni₄L₆ — and mononuclear — NiL₂ — complexes [1-3]. The same species excluding the Ni₄L₆ have been considered for α -mercaptoacetic acid (II) [4]. In this study formation constants for the Ni(II) complexes of α -mercaptoacetic acid (III) have been determined.



EXPERIMENTAL

The protonation constants of the ligand and the formation constants of the metal complexes have been determined at 25°C and 1 M ClO₄⁻ in 50% ethanol/water (v/v) using glass electrode potentiometry. The study has been carried out in an ethanol-water mixture because of the insolubility of the ligand in water.

The following cell, which includes a Wilhelm bridge [5], was used:

Ag,AgCl(s)	0.010 M NaCl 0.990 M NaClO ₄ (50% eth./w.)	1 M NaClO ₄ (50% eth./w.)	TS	Glass electrode
------------	---	---	----	-----------------

The electrode system was calibrated in terms of hydrogen ion concentration by performing strong acid *versus* strong base titrations [6].

In the determination of the protonation constants the hydrogen ion concentration was varied by addition of a T1 solution to a TS solution:

T1: -H₁ M H⁺; 1 M ClO₄⁻
(50% ethanol/water (v/v))

TS: A₀ M H₂L; H₀ M H⁺; 1 M ClO₄⁻
(50% ethanol/water(v/v))

In the study of the metal complexation, the total metal concentration was kept constant by adding equal volumes of T1 and T2 to a new TS solution:

T2: 2B₀ M Ni²⁺; H₂ M H⁺; 1 M ClO₄⁻
(50% ethanol/water (v/v))

TS: B₀ M Ni²⁺; A₀ M H₂L; H₀ M H⁺; 1 M ClO₄⁻
(50% ethanol/water (v/v))

Protonation curves for the ligand were obtained at a variety of different total ligand concentrations. Metal complex formation curves were obtained at different ligand:metal ratios and for diffe-

rent total ligand and metal concentrations. Experimental data was treated using the ESTA library [7] as described previously [8]. All calculations were performed on a VAX 11/780 computer (UWIST, Cardiff).

RESULTS AND DISCUSSION

Formation constants obtained in the present work are listed in Table 1. The finding of the Ni₃L₄, Ni₂L₃ and NiL₂ complexes confirms that ligands

containing a mercapto group tend to form complexes where sulphur bridges link two or more metal ions. The lack of formation of the Ni₄L₆ complex, reported for α-mercaptoacetic acid, can be caused by steric hindrance due to the presence of a phenyl group in the molecule. It also may be noted that this presence gives the complexes greater stability.

REFERENCES

- [1] D.L. LEUSSING, R.E. LARAMY, G.S. ALBERTS, *J. Am. Chem. Soc.*, **82**, 4826-4830 (1960).
- [2] D.D. PERRIN, I.G. SAYCE, *J. Chem. Soc. (A)*, 82-89 (1967).
- [3] H.F. DE BRABANDER, L.C. VAN POUCKE, Z. EECKHAUT, *Anal. Chim. Acta*, **70**, 401-410 (1974).
- [4] H.F. DE BRABANDER, A.M. GOEMINNE, L.C. VAN POUCKE, *J. Inorg. Nucl. Chem.*, **37**, 799-803 (1975).
- [5] W. FORSLING, S. HIETANEN, L.G. SILLEN, *Acta Chem. Scand.*, **6**, 901-909 (1952).
- [6] P.M. MAY, D.R. WILLIAMS, P.W. LINDER, R.G. TORRINGTON, *Talanta*, **29**, 249-256 (1984).
- [7] K. MURRAY, P.M. MAY, «ESTA. Equilibrium Simulation for Titration Analysis», UWIST, Cardiff, 1984.
- [8] M. FILELLA, D.R. WILLIAMS, *Inorg. Chim. Acta*, **106**, 49-57 (1985).

Table 1

	p	q	r	lg β _{pqr}	U	S.S.R.	Points	Titration
H ⁺	0	1	1	10.366 ± 0.001	521.5	2.180 E-06	498	9
	0	1	2	14.420 ± 0.002				
Ni ²⁺	3	4	0	40.437 ± 0.013	131.7	3.894 E-06	615	15
	2	3	0	28.819 ± 0.008				
	1	2	0	16.717 ± 0.003				

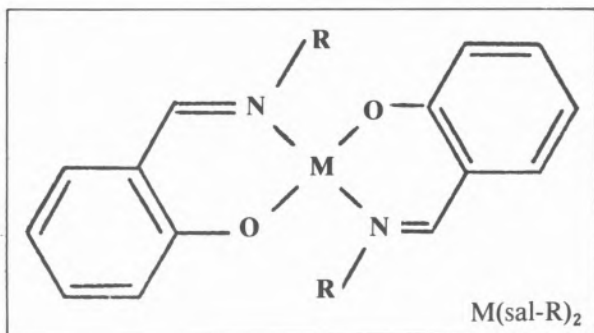


PS5.26 — TH

H. ELIAS
M. DREHER
M. SCHUMANN
CHR. HASSERODT-TALIAFERRO
K.J. WANNOWIUS
Anorganische Chemie III, Eduard-Zintl-Institut
Technische Hochschule Darmstadt, 6100 Darmstadt
Federal Republic of Germany

KINETICS OF LIGAND SUBSTITUTION IN CHELATE COMPLEXES OF DIVALENT TRANSITION METALS OF BIOLOGICAL IMPORTANCE

The bis chelate complexes $M(\text{sal-R})_2$ of divalent transition metals M^{2+} ($M = \text{Co}, \text{Ni}, \text{Cu}, \text{Zn}$) with various *N*-alkyl salicylaldimines Hsal-R ($R = \text{Et}, n\text{-Pr}, i\text{-Pr}, t\text{-Bu}, neo\text{-Pe}, \text{Ph}$) have been prepared by standard procedures and characterized.



Stopped-flow spectrophotometry has been used to study the reactivity of these complexes towards ligand substitution with acetylacetonate (Hacac) in methanol under pseudo first-order conditions ($[\text{Hacac}]_0 \gg [\text{M}(\text{sal-R})_2]_0$) according to (1):



The experimental rate law is a two-term rate law:

$$\text{rate} = (k_S + k_{\text{Hacac}}[\text{Hacac}])[\text{M}(\text{sal-R})_2] \quad (2)$$

The substitution of the first ligand in $M(\text{sal-R})_2$ is rate determining, *i.e.*, the conversion

$M(\text{sal-R})(\text{acac}) \rightarrow M(\text{acac})_2$ is a fast consecutive step.

The relative contributions of the terms k_S and $k_{\text{Hacac}}[\text{Hacac}]$ in (2) to the overall rate are mainly controlled by two factors, namely, (i) by the type of the *N*-alkyl group R for a given metal M, and, (ii) by the type of metal M for a given *N*-alkyl group R.

The data obtained for k_S and k_{Hacac} at 25°C for the 24 reactions studied are presented. The rate constants range from $k_S \approx 0$ ($M = \text{Ni}$; $R = \text{Et}, i\text{-Pr}, neo\text{-Pe}$) to $k_S = 18.5 \text{ s}^{-1}$ ($M = \text{Zn}$; $R = \text{Ph}$) and from $k_{\text{Hacac}} \approx 0$ ($M = \text{Cu}, \text{Zn}$; $R = t\text{-Bu}$) to $k_{\text{Hacac}} = 2070 \text{ M}^{-1} \text{ s}^{-1}$ ($M = \text{Ni}$; $R = \text{Et}$). The trends observed for the reactivity of the various complexes are correlated with their coordination geometry (as controlled by the *N*-alkyl group R) and with the intimate mechanism of both the solvent-induced pathway k_S and the ligand-dependent pathway $k_{\text{Hacac}}[\text{Hacac}]$.



PS5.27 — MO

M. BELICCHI FERRARI
G. GASPARRI FAVA
C. PELIZZI
P. TARASCONI
G. TOSI

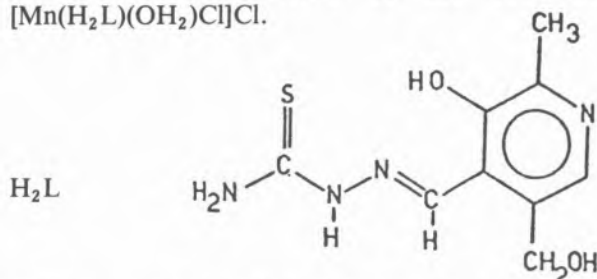
Istituto di Chimica Generale ed Inorganica
Centro di Studio per la Strutturistica Diffraattometrica del C.N.R.
Via M. D'Azeglio, 85, I-43100 Parma
Italy

COORDINATING PROPERTIES OF PYRIDOXAL THIOSEMICARBAZONE IN METAL COMPLEXES

The study of transition metal complexes of thiosemicarbazones is of great interest because of their pharmacological properties [1-3]. As part of a continuing interest in the chelating behaviour of ligands which have biological activities and the

coordinating properties of *S,N*-containing ligands [4], chemical and structural investigations of metal complexes of thiosemicarbazones are now in progress in our laboratory.

The present communication deals with the synthesis and the spectroscopic characterization of a series of Mn, Co, Ni, Cu, and Zn complexes with pyridoxal thiosemicarbazone (H_2L) and the X-ray crystal structure of the complex $[Mn(H_2L)(OH_2)Cl]Cl$.



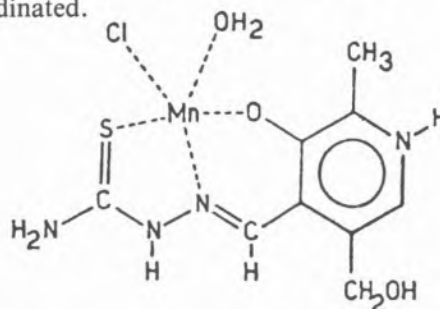
The combination of the pyridoxal moiety, which shows biological activity in several enzymatic reactions, with the thiosemicarbazone system confers to the final product interesting chelating properties.

H_2L was synthesised by the reaction of thiosemicarbazide with pyridoxal in alcoholic medium. Characterization of the ligand was made by IR and 1H NMR spectroscopies and mass spectrometry.

Metal complexes were obtained by reacting H_2L with the equimolar amount of the metal salt (nitrate, chloride or acetate) in ethanol solution. Analytical and spectroscopic data revealed different formulae in connection with the nature of the metal and the inorganic anion. In particular, three types of complexes of formula $M(H_2L)X_2$ ($M=Mn, Zn$; $X=Cl, NO_3$), $M(HL)X$ ($M=Co, Zn$; $X=CH_3COO$; $M=Ni$; $X=NO_3$), and ML ($M=Cu, Ni$) were isolated. Identification of the complexes was mainly made on the basis of the IR spectra, which show bands characteristic of $\nu(NH)$, $\nu(OH)$, $\nu(C=N)$, $\nu(C=S)$. Conspicuous changes were found in the vibrational absorptions of the ligand upon coordination effect. Although definitive assignments for $\nu(C=S)$ vibrations are difficult, the band in the region between 950 and 1050 cm^{-1} is attributable to the stretching vibration of the $C=S$ bond.

In order to gain more information about the structure and stereochemistry of such type of complexes the X-ray crystal structure of

$[Mn(H_2L)(OH_2)Cl]Cl$ was carried out. The crystals are monoclinic, space group $P2_1/n$ with unit-cell dimensions $a=13.902(4)$, $b=9.316(1)$, $c=11.982(3)$ Å, $\beta=107.61(2)^\circ$ and $Z=4$. The structure consists of $[Mn(H_2L)(OH_2)Cl]^+$ cations and Cl^- anions. The ligand behaves as terdentate and the manganese atom is uncommonly five-coordinated.



The cation has a pyramidal tetragonal geometry with a chlorine atom in apical position, the phenolic oxygen atom, a nitrogen atom, the sulphur atom of the organic ligand and the water molecule in the basal plane. This plane shows slight tetrahedral distortion, the manganese atom being 0.59 Å out of the mean basal plane towards the chlorine atom at the apex of the pyramid. The pyridoxal ring corresponds to a dipolar ion, owing to the shift of the proton from the phenolic oxygen atom to the pyridinic nitrogen atom. Bond distances and angles in thiosemicarbazide side chain agree well with those found in various aryl thiosemicarbazones which can be treated as extensively delocalized systems [5]. Packing consists of parallel layers of complex molecules linked by $NH_2...Cl$, $NH...Cl$, $O_w...Cl$, $O_w...OH$ hydrogen bonds. These layers are joined together by other hydrogen bonds of the type $N_{py}...Cl$, $OH...Cl$ to form an intricate network.

Bearing in mind that the nature terdentate of the thiosemicarbazones appears to be a potential feature for antitumor activity, studies on other similar sulphur-ligands and their metal complexes are in progress in our laboratory.

REFERENCES

- [1] M.J.M. CAMPBELL, *Coord. Chem. Rev.*, **15**, 279 (1975).
- [2] R. RESTIVO, G.J. PALENIK, *Acta Cryst.*, **B26**, 1397 (1970).
- [3] J.N. BROWN, K.C. AGRAWAL, *Acta Cryst.*, **B34**, 1002 (1978).
- [4] M. BELICCHI FERRARI, G. GASPARRI FAVA, C. PELIZZI, P. TARASCONI, *Inorg. Chim. Acta*, **97**, 99 (1985).
- [5] G.J. PALENIK, D.F. RENDLE, W.S. CARTER, *Acta Cryst.*, **B30**, 2390 (1974).



PS5.28 — TU

A. MARZOTTO
D.A. CLEMENTE

Istituto di Chimica Generale ed Inorganica dell'Università
Via Loredan 4 — 35100 Padova
Italy

NMR AND SPECTROSCOPIC STUDIES ON THE PYRIDOXAL/GLYCINE/ /DIOXOURANIUM(VI) SYSTEM

In previous communications we have reported some results on formation of dioxouranium(VI) complexes of pyridoxal and pyridoxylidene-glycine [1-5].

As it is known, pyridoxal and its derivatives are able to catalyze, in the presence of metal ions, important metabolic reactions of aminoacids through the intermediary formation of Schiff bases metal complexes [6-10].

The pyridoxal/glycine/dioxouranium(VI) system is studied both in the solid state and in solution by IR, electronic, ^1H and ^{13}C NMR spectra.

The results obtained in the solid state are in accord with the formation of a 1:1:1 ternary complex: $\text{UO}_2(\text{C}_{10}\text{H}_{11}\text{N}_2\text{O}_4)\text{XH}_2\text{O}$ (where $\text{X} = \text{CH}_3\text{COO}^-$ or NO_3^-). IR spectra exhibit changes in the regions where the azomethine $\text{C}=\text{N}$ stretching ($\nu_{\text{CN}} = 1610 \text{ cm}^{-1}$), phenolic $\text{C}=\text{O}$

($\nu_{\text{CO}} = 1510 \text{ cm}^{-1}$) and the asymmetric carboxyl stretching ($\nu_{\text{COO}^-} = 1570 \text{ cm}^{-1}$) respectively occur. The electronic spectra of an equimolar methanol solution of pyridoxal and glycine exhibit bands near 360 nm and 320 nm. Such absorptions markedly increase as a function of time when dioxouranium(VI) is added in equimolar amount and are shifted to 390 nm and 343 nm respectively. Furthermore two isosbestic points are formed at 290 nm and 275 nm. The final spectrum is very near to that of the complex prepared at the solid state. The ^1H and ^{13}C NMR spectra of the pyridoxal/glycine/dioxouranium(VI) system has been then examined in D_2O at pH 3.55 (at higher pH values precipitation occurs) in order to verify the formation of aldimine complexes induced by UO_2^{2+} .

Tables I and II show respectively proton and ^{13}C chemical shifts of pyridoxal and glycine solutions at varying molar ratios with uranyl nitrate. Large chemical shift changes are observed for C-4'-H, C-6-H and 2'- CH_3 pyridoxal protons and for $\alpha\text{-CH}_2$ glycine protons (Table I) upon complex formation and metal ion binding. In order to gain informations on the pyridoxylidene-glycine complex, ^1H chemical shifts were measured in DMSO-d_6 . In addition to the remarkable proton chemical shift variation, in particular of the aldehydic C-4'-H hydrogen ($\Delta = 1.14 \text{ ppm}$), the progressive disappearance of the $-\text{NH}_2$ resonance signal is in accord with the formation of the Schiff base and metal ion complexation. Furthermore, a new signal of intensity one appears at 9.60 ppm, characteristic of a proton bound to the pyrimidine nitrogen donor.

Table I

^1H NMR chemical shifts (δ/ppm)^{a)} of free pyridoxal hydrochloride (HPL)/glycine (Gly) system and UO_2 nitrate solutions in D_2O at pH=3.55

Compound	molar ratio	C-6-H	C-4'-H	5'- CH_2	$\alpha\text{-CH}_2$	2'- CH_3
HPL + Gly	1:1	8.08,1H	6.67,1H	5.22,2H	3.69,2H	2.60,3H
HPL + Gly + UO_2 nitrate	1:1:0.25	8.00,1H	6.62,1H	5.18,2H	3.66,2H	2.60,3H
HPL + Gly + UO_2 nitrate	1:1:0.50	7.90,1H	6.85,1H	5.20,2H	3.60,2H	2.70,3H
HPL + Gly + UO_2 nitrate	1:1:1	7.78,1H	7.30,1H	5.12,2H	3.56,2H	2.87,3H
HPL + Gly + UO_2 nitrate	1:1:2	7.77,1H	7.28,1H	5.28,2H	3.37,2H	2.86,3H
$\Delta \text{ ppm}$	=	-0.31	+0.61	+0.06	-0.32*	+0.26

a) ^1H NMR chemical shifts are measured downfield from TMS, using dioxane as an internal standard.

Table II

¹³C NMR chemical shifts (δ/ppm)^{a)} of free pyridoxal hydrochloride (HPL)/glycine (Gly) system and UO₂ nitrate solutions at pH=3.55

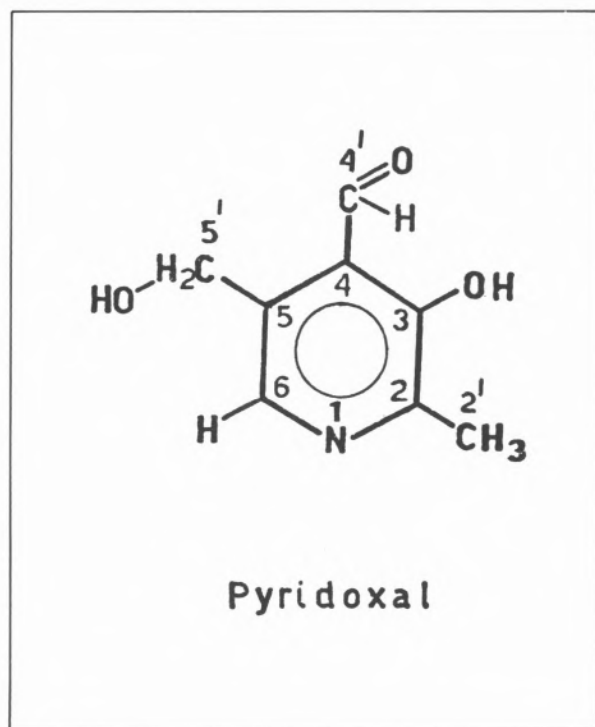
Compound	molar ratio	-COO ⁻	C-3	C-2	C-4	C-5	C-6	C-4'	C-5'	α-CH ₂	C-2'
HPL + Gly	1:1	172.70	150.75	144.85	140.45	138.70	125.40	99.35	70.60	42.06	15.00
HPL + Gly + UO ₂ nitrate	1:1:0.25	172.82	155.80	145.08	140.79	138.64	125.82	163.20	70.60	58.90	15.00
HPL + Gly + UO ₂ nitrate	1:1:0.50	173.14	163.40	146.00	141.21	138.57	126.50	163.20	70.62	58.92	15.13
HPL + Gly + UO ₂ nitrate	1:1:1	177.97	163.69	146.69	141.90	138.35	126.68	163.30	70.68	59.17	15.50
HPL + Gly + UO ₂ nitrate	1:1:2	179.73	163.81	147.48	142.47	138.34	128.21	163.40	70.70	59.91	15.87
Δ ppm	=	+ 7.03	+ 13.06	+ 2.63	+ 2.02	- 0.36	+ 2.81	+ 64.05	+ 0.10	+ 17.85	+ 0.87

a) ¹³C NMR chemical shifts are measured downfield from TMS, using dioxane as an internal standard.

Such results are supported by the ¹³C NMR data reported in Table II. The downfield shift of the C-4' pyridoxal carbon from 99.35 ppm to 163.40 ppm (that is to the resonance value exhibited by a large number of pyridoxal aldimines [11]) and of phenolic C-3 carbon (Δ=13.06 ppm) together with the significant displacement of the resonance signals of α-CH₂ (Δ=17.85 ppm) and -COO⁻ glycine carbon atoms (Δ=7.03 ppm) point out the direct involvement of the uranyl ion to promote the aldimine formation between pyridoxal and glycine and to give rise to the pyridoxylidene-glycine metal complex too.

REFERENCES

- [1] A. MARZOTTO, F. BRAGA, III Conv. Naz. Radiochim., 167 (1980).
- [2] A. MARZOTTO, *Inorg. Chim. Acta*, **40**, X72 (1980).
- [3] A. MARZOTTO, XXI Internat. Conf. Coord. Chem., 120 (1980).
- [4] A. MARZOTTO, *Inorg. Chim. Acta*, **62**, 183 (1982).
- [5] A. MARZOTTO, H. KOZLOWSKI, *Inorg. Chim. Acta*, **94**, 96 (1984).
- [6] D.E. METZLER, E.E. SNELL, *J. Am. Chem. Soc.*, **74**, 979 (1952).
- [7] D.E. METZLER, M. IKAWA, E.E. SNELL, *J. Am. Chem. Soc.*, **76**, 648 (1954).
- [8] G.L. EICHORN, J.W. DAWES, *J. Am. Chem. Soc.*, **76**, 5663 (1954).
- [9] H.N. CHRISTENSEN, *J. Am. Chem. Soc.*, **79**, 4073 (1957).
- [10] S. MATSUMOTO, Y. MATSUSHIMA, *J. Am. Chem. Soc.*, **96**, 5228 (1974).
- [11] R.C. HARRUFF, W.T. JENKINS, *Org. Magn. Resonance*, **8**, 548 (1976).





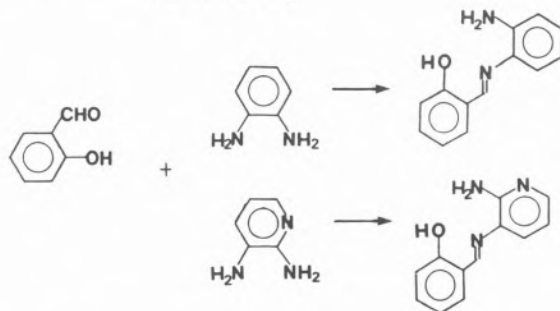
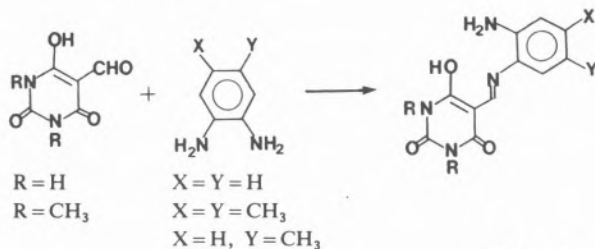
PS5.29 — TH

ISABELLE SASAKI
ALAIN GAUDEMER

Laboratoire de Chimie de Coordination Bioorganique
Université Paris-Sud
Centre d'Orsay 91405 Orsay
France

SYNTHESIS OF COBALT(II) COMPLEXES WITH NON-SYMMETRIC SCHIFF BASES

As models for oxygenases, we have undertaken the synthesis of copper and cobalt complexes with Schiff bases derived from pyrimidine bases [1-3]. In order to study the influence of the aromatic ring on the half-wave potentials and on their catalytic efficiency, we have prepared non-symmetric Schiff bases with aromatic diamines. Condensation of the carbonyl function with only one end of the diamine is obtained in the presence of a tertiary amine with 5-formyl barbituric acid, 5-formyl 1,3-dimethyl barbituric acid or with salicylaldehyde.



Further condensation of these half-units with various aromatic hydroxy aldehydes leads to non-symmetric Schiff bases.

The corresponding cobalt(II) complexes have been prepared and studied by usual spectroscopic methods. Their ability to catalyse the oxidation of phenols will be described.

REFERENCES

- [1] I. SASAKI, M.N. DUFOR, A. GAUDEMER, *Nouv. J. Chim.*, **6**, 341 (1982).
- [2] I. SASAKI, M.N. DUFOR, A. GAUDEMER, A. CHIÁROI, C. RICHE, D. PARQUER-DECROUZ, P. BOUCLY, *Nouv. J. Chim.*, **4**, 237 (1984).
- [3] I. SASAKI, A. GAUDEMER, A. CHIARONI, C. RICHE, *J. Chem. Soc., Dalton Trans.*, submitted for publication.



PS5.30 — MO

SHALOM SAREL
SHELLY AVRAMOVICI-GRISARU
Department of Pharmaceutical Chemistry
The Hebrew University of Jerusalem
P.O.B. 12065, Jerusalem
Israel

COORDINATION CHEMISTRY OF IRON BIS-PYRIDOXAL ISONICOTINOYL HYDRAZONE: STEREOCHEMICAL AND ELECTRO-CHEMICAL CONSIDERATIONS

Izoniazid can interact with the body pyridoxal to form pyridoxal isonicotinoyl hydrazone (PIH) shown to be an efficient iron chelator which can deplete the body of iron and cause an anemia («pyridoxine-responsive anemia»). It was identified recently as a promising candidate for removal of toxic accumulation of iron from the body when given orally [1]. This is an advantage over desferrioxamine (desferal) a drug in current use being administered by injection.

We report the synthesis and the X-ray crystal structure of a 2:1 PIH:Fe(III) complex which emerged from a neutral aqueous solution

(pH ~ 7.0) containing PIH and $\text{FeSO}_4 \cdot 7\text{H}_2\text{O}$. It analyzed as a $[\text{Fe}(\text{C}_{14}\text{H}_{14}\text{N}_4\text{O}_3)_2]_2\text{SO}_4$ crystalline compound of space group $\text{C}2/c$, $z=8$, $a=14.487$, $b=18.586$, $c=27.508 \text{ \AA}$, and $v=7224 \text{ \AA}^3$.

PIH is shown to function as a neutral tridentate ligand, forming a non-planar tricyclic system which comprises pyridoxal, an hexatomic and a pentatomic chelate rings with dihedral angles of 13.01° and 8.45° , respectively, between them. The coordination plane deviates from coplanarity, showing significant departure from the ideal octahedron. The hydrazidic central donor atoms are *trans* related to each other and the two phenolate and enolate oxygens mutually *cis*. The coordinated ligands retain the neutrality characteristic of its free form by a transfer of protons from the phenolic oxygens and the hydrazidic nitrogens to the pyridine nitrogens. The sulphate ion is a counterion [2]. The transition of Fe(II) to Fe(III) occurs even in presence of a strong reducing agent, suggesting that PIH lends itself to reversible two-stage redox reaction. This was fully corroborated by polarographic measurements, allowing its likening to «viologenes» of potential biological importance.

REFERENCES

- [1] C. HERSHKO, R.W. GRADY, G. LINK, S. SAREL, S. AVRAMOVICI-GRISARU in P. SALTMAN, J. HEGENAUER (eds.), «The Biochemistry and Physiology of Iron», Elsevier North Holland, 1982, pp. 627-648.
- [2] S. AVRAMOVICI-GRISARU, S. SAREL, S. COHEN, R.E. BAUMINGER, sent for publication.



PS5.31 — TU

FRANCO BONOMI
SILVIA PAGANI
PAOLO CERLETTI
Department of General Biochemistry
University of Milan
Italy

MOBILIZATION OF FERRITIN-BOUND IRON BY REDUCED D,L-LIPOATE AND REDUCED D,L-LIPOAMIDE

The mobilization of ferritin-bound iron, an issue of great physiological and clinical relevance [1], was investigated by studying several iron chelators [2], either in the absence or in the presence of iron-reducing agents [3] and of activators of the removal process [4].

In the course of other studies, we noticed the unusual ease of formation and stability of a complex between iron(III) and D,L-dihydrolipoate (DHL-COOH). This complex was characterized to some extent and the tentative formula $[\text{Fe}_2(\text{DHL-COO}^-)_4]^{-6}$ was attributed to it [5,6]. In view of the unusually high stability of this complex, of considerations about the amphiphilic nature of the ligand and about the molecular architecture of ferritin, we tested the ability of both DHL-COOH and D,L-dihydrolipoamide (DHL-NH₂) in the mobilization of ferritin-bound iron.

Fig. 1 shows the electronic spectra obtained upon incubation of horse-spleen ferritin (HSF) with DHL-NH₂, DHL-COOH and with dithiothreitol as a control dithiol. Progressive appearance of the spectral features of $[\text{Fe}_2(\text{DHL-R})_4]^{(-6,-4)}$ is evident, whatever the amidation state of the ligand. DHL-NH₂ appears to react faster than DHL-COOH. Nevertheless, after 20 hours incubation, an identical absorbance at 620 nm was attained in both reactions. By assuming $\epsilon_{620} = 4,000 \text{ (g atom iron)}^{-1}\text{cm}^{-1}$ for $[\text{Fe}_2(\text{DHL-R})_4]^{(-6,-4)}$, the amount of iron released

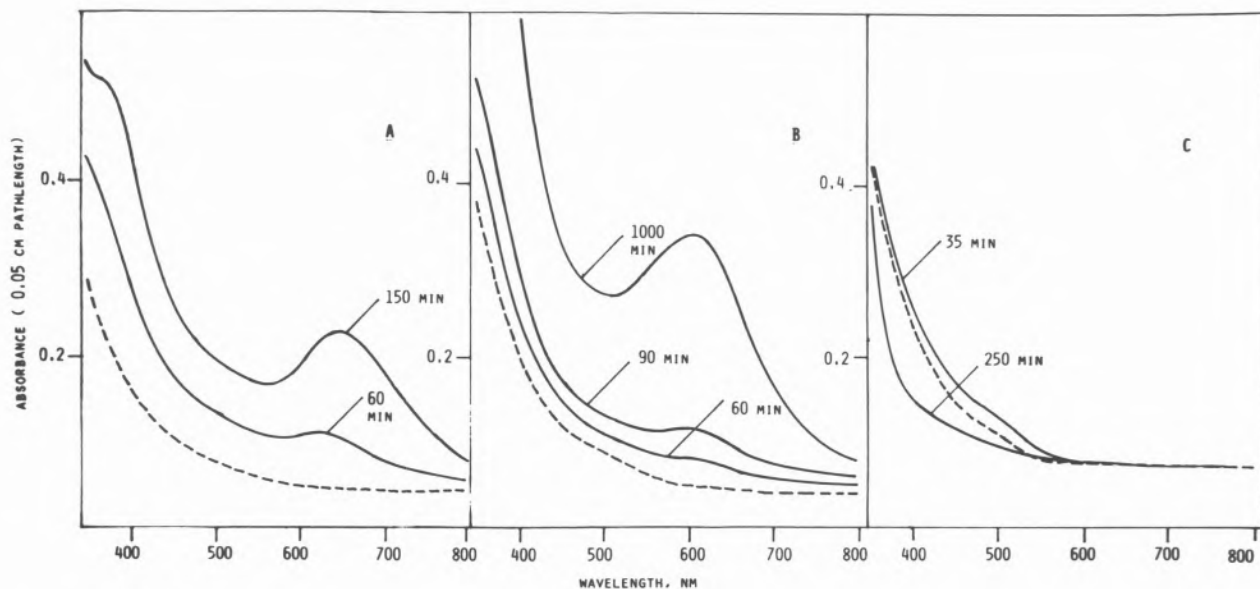


Fig. 1

Absorbance spectra of HSF incubated with different dithiols. HSF (Calbiochem, 2.2 mg/ml in 0.3 M Tris/HCl pH 9.0) was incubated at 20°C with: 4.55% (v/v) Triton X-100 and 32 mM dithiothreitol (C). Spectra were recorded before the addition of the dithiol (dashes) and at the times given

ranged between 49 and 52% of the original content of HSF (20% iron, by weight). Samples taken during the course of the incubation with DHL-COOH were chromatographed on an Ultrogel AcA54 column. This procedure separated a faintly-reddish ferritin band from the dark-green band of the iron-DHL complex, thus indicating that the complex actually leaves the ferritin molecule. Fig. 2 compares the time course of iron removal by different concentrations of either DHL-COOH or DHL-NH₂. The addition of detergent, which is mandatory in order to solubilize DHL-NH₂ at the high concentrations used in the present study, does not affect the rate of iron release. The initial lag in the time course of the reaction can be ascribed to the process of penetration of the ligand into the protein shell, whereas the biphasicity of the reaction could be explained either by the presence of different forms of ferritin-bound iron [7] or by the attainment of a dynamic equilibrium among molecules of ligand entering the protein and molecules of the complex leaving it. DHL-NH₂ appears more effective than DHL-COOH, likely because it is more hydrophobic and diffuses more easily through the channels between the subunits of HSF.

Distinctive features of the present study are: *i* — a physiological, non-toxic, inexpensive com-

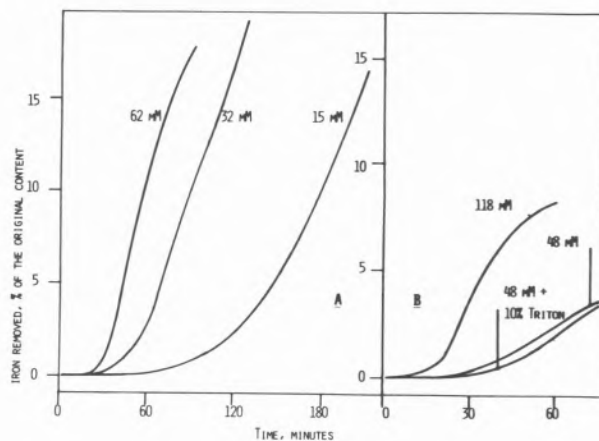


Fig. 2

Time-course of the removal of iron from HSF by DHL-NH₂ (A) or DHL-COOH (B). HSF was incubated as detailed in the legend to Fig. 1 with the given concentrations of dithiol. The absorbance increase at 620 nm was monitored continuously, and the percentage of iron-removal calculated as given in the text

pound is used as the iron-removing agent; *ii* — iron is released by either DHL-COOH or DHL-NH₂ in the ferric form; *iii* — after 5-hours incubation, the iron removal with DHL-COOH is 16.8%, thus higher than the figures at 5 hours reported for other iron-removing agents: 2.6% for

desferoxiamine B+ ascorbate, 5-7% for cathecolamides+ ascorbate and 2.7% for EDTA [2,3].

REFERENCES

- [1] R.R. CRICHTON, *Trends Biochem. Sci.*, **9**, 283-286 (1984).
- [2] L. PAPE, J.S. MULTANI, C. STITT, P. SALTMAN, *Biochemistry*, **7**, 613-616 (1968).
- [3] T.P. TUFANO, V.L. PECORARO, K.N. RAYMOND, *Biochim. Biophys. Acta*, **668**, 420-428 (1981).
- [4] E.J.F. DEMANT, *FEBS Lett.*, **176**, 97-100 (1984).
- [5] F. BONOMI, D.M. KURTZ JR., submitted for publication to *Biochemistry*.
- [6] U. CORNARO, F. CARIATI, F. BONOMI, *Rev. Port. Quím.*, **27**, 273 (1985).
- [7] S. SIRIVECH, E. FRIEDEN, S. OSAKI, *Biochem. J.*, **143**, 311-315 (1974).



PS5.32 — TU

UGO CORNARO
FRANCO CARIATI
Department of Inorganic and Metallo-organic Chemistry
University of Milan
Italy
FRANCO BONOMI
Department of General Biochemistry
University of Milan
Italy

ELECTROCHEMICAL PROPERTIES OF $[\text{Fe}_4\text{S}_4(\text{SC}_6\text{H}_5)_4]^{-2}$, ANALOGUE OF THE ACTIVE SITE OF IRON-SULFUR PROTEINS, IN AQUEOUS MICELLAR SOLUTIONS

In order to elucidate the mechanism by which the protein region of iron-sulfur proteins modulates the redox potentials of otherwise identical 4Fe-4S clusters, we investigated the properties of the title cluster (t^{-2}) in water, the physiological solvent for proteins. The title cluster is water-insoluble, but becomes soluble in the presence of detergents [1], and by using detergents differing in structure and

in charge we attempted to simulate different protein-cluster interactions.

Synthesis of $[(\text{Et})_4\text{N}]_2[\text{Fe}_4\text{S}_4(\text{SC}_6\text{H}_5)_4]$ was performed in aqueous solution as described by KURTZ *et al.* [2,3]. A stock solution of t^{-2} was anaerobically prepared in DMF, and t^{-2} concentration determined using $\epsilon_{457} = 17,700 \text{ M}^{-1} \text{ cm}^{-1}$. For electrochemical measurements the stock solution of t^{-2} in DMF was anaerobically diluted in 5% (v/v) detergent in 0.2 M Tris/sulfate buffer pH 9.00, to a final concentration of 1.34 mM t^{-2} and 5% (v/v) DMF. A three-electrodes configuration was used. All the potentials quoted here refer to saturated calomel electrode (SCE). Fig. 1 shows the cyclic voltammograms of t^{-2} dissolved in buffer/detergent mixtures of different composition and in the presence of excess thiophenol.

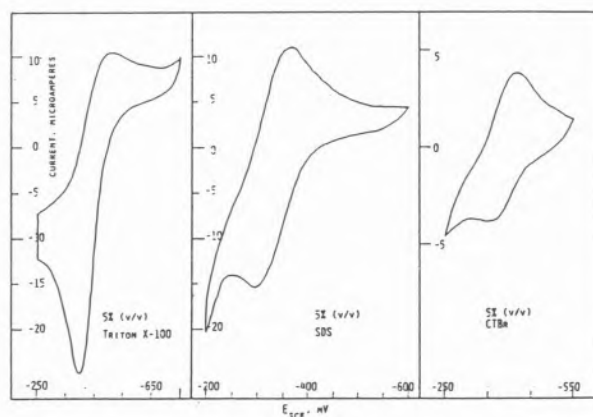


Fig. 1

Cyclic voltammograms of aqueous solutions of t^{-2} in the presence of different detergents. Cyclic voltammograms of 1.34 mM t^{-2} (in 0.2 M Tris/sulfate pH 9.0, 5% (v/v) DMF, 100 mM thiophenol containing also detergents as given in the figure) were recorded at a scan rate of 50 mV/sec

In the absence of this latter no oxidation (anodic) peak can be detected, likely because of the hydrolytic decomposition of the t^{-3} species generated in the reduction process. Excess thiophenol prevents the hydrolytic process, thus allowing the monoelectronic, quasi-reversible redox process involving the t^{-2}/t^{-3} couple to be observed. Both anodic and cathodic currents (i_a and i_c) were found to be directly proportional to the concentration of t^{-2} . In aqueous detergents, the measured values of E_0 are by far higher than those reported for the same compound dissolved in DMF

(-1.04 V vs. SCE [4]) or for water solutions of $[\text{Fe}_4\text{S}_4(\text{SCH}_2\text{CH}_2\text{OH})_4]^{2-}$ (-0.75 V vs. SCE [5,6]). Table I compares electrochemical figures

agents on E_o , and to test the reactivity of water-micellar solutions of t^{-2} towards physiological redox couples.

Table I

detergent	scan rate (ν) mV/sec	E_c mV	i_c μA	E_a mV	i_a μA	E mV	i_c/i_a	$i_c/\nu^{1/2}$
SDS	10	-364	4.3	-307	6.2	57	0.69	1.36
	20	-364	6.9	-300	9.9	64	0.70	1.54
	50	-364	11.5	-295	15.2	69	0.73	1.58
CTBr	10	-404	1.8	-336	2.7	68	0.68	0.59
	20	-413	2.9	-348	3.2	65	0.92	0.66
	50	-417	4.1	-338	4.3	79	0.97	0.59
Triton X-100	10	-510	5.4	-416	10.2	94	0.53	1.71
	20	-510	8.3	-406	17.9	104	0.46	1.86
	50	-516	10.9	-397	24.8	119	0.44	1.54
BRIJ 35	10	-497	4.3	-412	5.4	85	0.79	1.34
	20	-496	5.5	-409	8.7	87	0.63	1.23
	30	-495	7.5	-400	13.6	95	0.55	1.07

obtained with solutions of t^{-2} in the presence of different detergents, and shows that the electrochemical process is quasi-reversible and diffusion-controlled. A comparison among the values of $i_c/\nu^{1/2}$ in Table I provides also evidences about the actual inclusion of t^{-2} in the micelles. A comparison among the different micellar environments shows that the charge of the micelle plays a minor role in the modification of E_o of the enclosed t^{-2} , whereas exclusion of solvent water appears to have a major effect. With Triton X-100 and Brij 35 (having highly solvated poly-oxyethylenic hydrophilic chains) the lowest E_o values were measured.

E_o increases with CtBr (cetyltetrammonium bromide) likely as a consequence of either the positive charge carried by the micelles and/or their compactness. The influence of the micellar compactness (*i.e.* of their ability to screen the cluster from water) is further made evident when considering that the negatively-charged, highly-compact SDS (sodium dodecyl sulfate) micelles allow the highest value of E_o to be measured. Work is in progress to discriminate more properly among charge and hydrophobicity effects of the deter-

REFERENCES

- [1] D.M. KURTZ JR., *Biochem. Biophys. Res. Commun.*, **104**, 437 (1981).
- [2] D.M. KURTZ JR., W.C. STEVENS, *J. Am. Chem. Soc.*, **106**, 1523 (1984).
- [3] W.C. STEVENS, D.M. KURTZ JR., *J. Am. Chem. Soc.*, in press.
- [4] J.J. MAYERLE, S.E. DENMARK, B.V. DEPHAMPHILIS, J.A. IBERS, *J. Am. Chem. Soc.*, **97**, 1032 (1975).
- [5] J.G. REYNOLDS, R.H. HOLM, *Inorg. Chem.*, **19**, 3257 (1980).
- [6] C.L. HILL, G. RENAUD, R.H. HOLM, L.E. MORTENSON, *J. Am. Chem. Soc.*, **99**, 2549 (1977).
- [7] M. R'LAIGNI, E.C. HATCHIKIAN, D. BEULIAU, *Biochem. Biophys. Res. Commun.*, **92**, 1258 (1980).



PSS.33 — MO

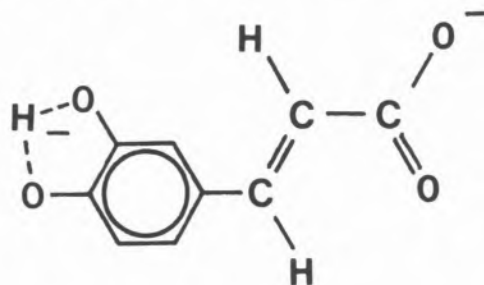
PETER W. LINDER
ALEXANDER VOYE
University of Cape Town
South Africa

COMPLEXATION OF COPPER(II) IONS BY CAFFEIC ACID

The bioavailability to plants of metal ions, either as micro-nutrients or as toxins, is strongly influenced by coordinating ligands which may be present in the soil or the artificial nutrient solution in which the plant grows [1]. In order to contribute to the understanding of the role of coordination equilibria in the transport of metal ions to plant roots, we are undertaking chemical speciation studies of soil and nutrient solutions by means of computer simulation [2,3]. Amongst the information needed for our computer models are formation constants for the manifold metal-ligand-proton complexes that can be found. Of special interest are various phenolic ligands which are known to be exuded by plant roots under certain conditions and which are believed to participate in the transport of iron from the surrounding soil or nutrient solution to the root membrane [4]. The root-exuded phenolic compound of major importance is caffeic acid. Indeed, it has been postulated that under the conditions prevailing in soils, caffeic acid tends to reduce iron (III) to iron (II), the necessary state of oxidation for iron ions to be absorbed by plant roots [4]. Since caffeic acid can potentially form complexes with all the types of metal ion which occur in soil and nutrient solutions, it is an essential component for inclusion in our speciation models. Moreover, since there is a paucity of formation constant data reported in the literature for caffeate-metal-proton complexes, we are undertaking an extensive programme of investigation into the solution equilibria of these systems. On our poster, we intend to present re-

sults obtained by glass electrode potentiometry and NMR for copper (II).

In its own right, caffeic acid is an interesting coordinating ligand purely from the inorganic chemical point of view. This arises from the two coordination sites, one at each end of the molecule. Taking the ligand species to be the dianion,



(denoted hereafter by L^{2-}) protonation constants have been determined, yielding the results in the Table. Note that whereas one of the catecholic oxygens is reasonably acidic, with a pK_a of 8.72, the second is very strongly basic (cf. catechol: $pK_{a1} = 13.0$, $pK_{a2} = 9.23$) [6]. This has been attributed to hydrogen bonding between the hydroxyl and phenoxide groups [7]. We have made no attempt to determine the first protonation constant of the trianion of caffeic acid.

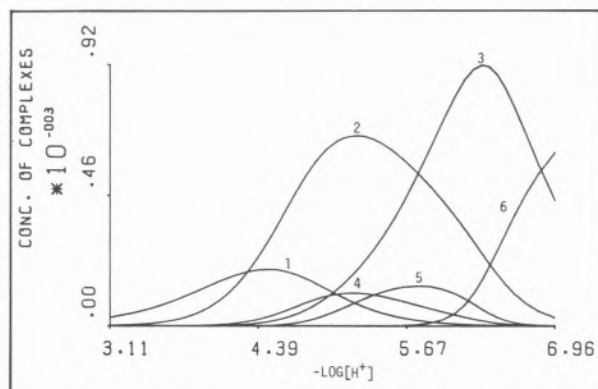
Table

Logarithms of protonation constants (β_H) determined for L^{2-} at 25°C and $I = 0.100 \text{ mol dm}^{-3}$ (Na) [Cl]. d = the standard deviation in $\log \beta_H$. n = the number of experimental observations

Reaction	$\log \beta_H$	d	n
$L^{2-} + H^+ \rightleftharpoons LH^-$	8.72	.003	389
$L^{2-} + 2H^+ \rightleftharpoons LH_2$	13.13	.004	389

Preliminary results obtained for the complexation titrations have been used to construct the diagram in the Figure. The latter shows the distribution of caffeate-copper(II)-proton complexes detected in aqueous solutions with total concentrations of the components that are typical of the titrations in this study.

Although we can be reasonably certain of the stoichiometry of the species in the figure, the structures are not known at this stage and may be merely speculated upon. Thus the following are suggested



Figure

Concentrations of complexes present as a function of pH for the caffeic acid-copper (II) system when the total concentrations in mmol dm^{-3} of L^{2-} and Cu^{2+} are 8.6 and 2.0, respectively. Temperature = 25°C and $I = 0.100 \text{ mol dm}^{-3}$ (Na) $[\text{Cl}]$. Species: (1) LCuH^+ ; (2) LCu ; (3) $(\text{LH}_{-1})\text{Cu}$; (4) $(\text{LH}_{-1})\text{Cu}_2$; (5) $(\text{LH}_{-1})_2\text{Cu}_3$; (6) $(\text{LH}_{-1})_3\text{Cu}_2$

as being plausible. (1) LCuH^+ : copper coordinated to the carboxylate; (2) LCu and (3) $(\text{LH}_{-1})\text{Cu}$: copper coordinated to the catechol moiety; (4) $(\text{LH}_{-1})\text{Cu}_2$: one copper at each end of the molecule; (5) $(\text{LH}_{-1})_2\text{Cu}_3$ and (6) $(\text{LH}_{-1})_3\text{Cu}_2$: oligonuclear species with copper acting as bridges between adjacent caffeate moieties.

REFERENCES

- [1] W.L. LINDSAY, «Chemical Equilibria in Soils», Wiley, New York, 1979.
- [2] K. MURRAY, P.W. LINDER, *J. Soil Sci.*, **34**, 511 (1983)
- [3] K. MURRAY, P.W. LINDER, *J. Soil Sci.*, **35**, 217 (1984).
- [4] R.A. OLSEN, J.C. BROWN, J.H. BENNETT, D. BLOOM, *J. Plant Nutrition*, **5**, 433 (1982).
- [5] C.F. TIMBERLAKE, *J. Chem. Soc.*, 2795 (1959).
- [6] A.E. MARTELL, R.M. SMITH, «Critical Stability Constants», vol. 3, Plenum, New York, 1977.
- [7] L. PAULING, «The Nature of the Chemical Bond», 3rd edn., Cornell University Press, New York, 1960, p. 494.



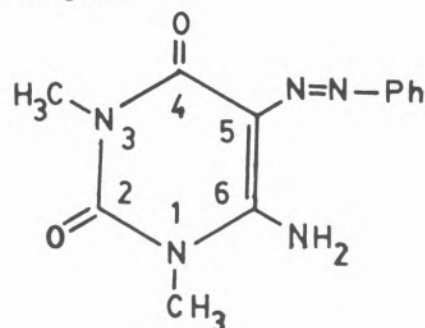
PS5.34 — TU

J. RUIZ-SANCHEZ
E. COLACIO-RODRIGUEZ
J.M. SALAS-PEREGRIN
M.A. ROMERO-MOLINA
Department of Inorganic Chemistry
Faculty of Sciences
University of Granada
18071 Granada
Spain

INTERACTION OF 6-AMINO-1,3-DIMETHYL-5-PHENYLAZOURACIL WITH Co(II), Ni(II), Cu(II) AND Ag(I) IONS

INTRODUCTION

Compounds containing pyrimidine rings are widely distributed in living cells and play a significant role in many biological systems (the ring system being an integral part of several nucleic acids, vitamins, etc.); these facts have stimulated research into the coordination modes of pyrimidines, in order to know the role of metal ions in such systems [1-4]. As an arylazo group is of interest in promoting potential antineoplastic activity [5], the pyrimidine molecules having an arylazo group are of interest. For this reason and as part of our work on the interaction of pyrimidine-derived ligands with metal ions [6-9], in the present paper, the synthesis, spectroscopic characterization and thermal behaviour of the 6-amino-1,3-dimethyl-5-phenylazouracil (DZH) and its Co(II), Ni(II), Cu(II) and Ag(I) complexes have been investigated.



DZH

EXPERIMENTAL

DZH was synthesized according to Rose [10], using 6-amino-1,3-dimethyluracil and phenylamine as starting materials.

IR and $^1\text{H-NMR}$ spectra were recorded on a Beckman 4250 spectrophotometer and a Hitachi-Perkin Elmer R-600 FT-NMR spectrometer. Thermal studies were carried out on a Mettler TG-50 thermobalance and a Mettler differential scanning calorimeter model DSC-20.

The complexes $\text{Co}(\text{DZ})_2\text{NO}_3 \cdot \text{H}_2\text{O}$; $\text{Ni}(\text{DZ})_2$; $\text{Cu}(\text{DZ})\text{NO}_3 \cdot \text{H}_2\text{O}$ and AgDZ were obtained by mixing an ethanolic solution containing 0.4 mmoles of DZH with an ethanolic solution of the respective metal nitrate (0.20 mmoles). The mixture was heated at 70-80°C with continuous stirring for about one hour. The resulting clear solution was allowed to cool slowly to room temperature. After a few days precipitates appeared. All the complexes were washed consecutively with water and ethanol and ether dried. $\text{Cu}(\text{DZ})_2\text{py}$; $\text{Cu}(\text{DZ})_2\text{DMSO}$ and $\text{Cu}(\text{DZ})_2 \cdot 2\text{H}_2\text{O}$ were obtained using the above experimental method, but pyridine, dimethylsulfoxide and 1:1 ethanol- NH_4OH mixture were used as solvents, respectively.

RESULTS AND DISCUSSION

From spectroscopic data it can be suggested that, in solid phase, DZH is in amine-ketonic form (scheme I) (bands at 3290 and 3260 cm^{-1} , corresponding to $\nu(\text{N-H})$ of the amine group and 1705 and 1610 cm^{-1} due to $\nu(\text{C}_2=\text{O})$ and $\nu(\text{C}_4=\text{O})$, respectively). However, in the isolated complexes, the anion DZ is coordinated to metal ions in imino-phenolic form, since IR spectra show only one band $\nu(\text{N-H})$, as well as a new $\nu(\text{C}=\text{N})$ band, both corresponding to the iminic group.

On the other hand, the $\nu(\text{N}=\text{N})$ band is shifted towards lower frequencies upon metal complexes formation, which suggests that a nitrogen atom of the diazo group is involved in the coordination, probably the one joined to the phenyl group, since the $\nu(\text{C-N})$ band is also shifted towards lower frequencies. Likewise, the IR spectra of the complexes show bands in the region 435-420 cm^{-1} , which are not observed in the ligand spectrum;

these bands are attributed to $\nu(\text{M-O})$ vibration (oxygen atom joined to C_4).

Elemental analysis, magnetic measurements and spectral studies [11] suggest the following molecular structures for the isolated complexes: $[\text{Co}(\text{DZ})_2(\text{H}_2\text{O})_2]\text{NO}_3$ (distorted octahedral); $\text{Ni}(\text{DZ})_2$ (tetrahedral); $\text{Cu}(\text{DZ})(\text{H}_2\text{O})\text{NO}_3$ (tetrahedral with a monodentate nitrate group); $\text{Ag}(\text{DZ})$ (linear polymeric); $\text{Cu}(\text{DZ})_2(\text{H}_2\text{O})_2$ (distorted octahedral); $\text{Cu}(\text{DZ})_2\text{py}$ and $\text{Cu}(\text{DZ})_2\text{DMSO}$ (square-pyramidal).

The thermal behaviour of these complexes has been studied by IR, TG and DSC. IR spectroscopy applied to the study of the complexes heated at 225°C allowed to clarify the decomposition steps and the nature of the intermediate products.

REFERENCES

- [1] D.J. HODGSON, *Prog. Inorg. Chem.*, **23**, 211 (1977).
- [2] L.G. MARZILLI, *Prog. Inorg. Chem.*, **23**, 255 (1977).
- [3] R.W. GELLERT, P. BAU in H. SIGEL (ed.), «Metal Ions in Biological Systems», vol. 8, M. Dekker, New York, 1979, pp. 1-56.
- [4] R.B. MARTIN, Y.H. MARIAM in H. SIGEL (ed.), «Metal Ions in Biological Systems», vol. 8, M. Dekker, New York, 1979, pp. 57-126.
- [5] S. HIBNO, *Cancer Chemother. Rep.*, **13**, 141 (1961).
- [6] J.M. SALAS, M.N. MORENO, J.D. LOPEZ, C. VALENZUELA, *J. Thermal. Anal.*, **26**, 251 (1983).
- [7] M.N. MORENO, J.M. SALAS, A. MATA, *J. Thermal. Anal.*, **29**, 553 (1984).
- [8] M.N. MORENO, J.M. SALAS, *J. Thermal. Anal.*, **29**, 1047 (1984).
- [9] J.M. SALAS, M.N. MORENO, M.A. ROMERO, E. COLACIO, *Rev. Chim. Miner.*, **29**, 233 (1984).
- [10] F.L. ROSE, *J. Chem. Soc.*, 3448 (1952).
- [11] J. RUIZ-SANCHEZ, Thesis of Licenciante, University of Granada (1984).



PSS.35 — TH

Y. OZAKI

K. IRIYAMA

Division of Biochemistry
The Jikei University School of Medicine
Nishi-Shinbashi, Minato-ku, Tokyo 105
Japan

T. KITAGAWA

Institute for Molecular Science
Myodaiji, Okazaki, Aichi 444
Japan

H. OGOSHI

T. OCHIAI

Department of Chemistry and Chemical Engineering
Technological University of Nagaoka
Nagaoka, Niigata 940-21
Japan

COMPARATIVE STUDY OF METALLOCHLORINS AND METALLOPORPHYRINS BY RESONANCE RAMAN SPECTROSCOPY

Basic studies on metallochlorins have recently become increasingly important, because it was found that not only chlorophylls but also some hemoproteins contain the metallochlorin as a prosthetic group (*e.g.* [1]). In order to elucidate the reason for the existence of chlorin prosthetic groups in some hemoproteins it is essential to investigate what features of molecular and electronic structures of metallochlorins are different from those of metalloporphyrins. Thus we have undertaken comparative study of metallochlorins and metalloporphyrins using resonance Raman (RR) spectroscopy [2] which is known to be a powerful structure probe for hemoproteins as well as their model compounds [3,4].

RESULTS AND DISCUSSION

Fig. 1 shows the 488.0 nm-excited RR spectra of Fe(OEC)Br (5-coordinate, high-spin; OEC = octaethylchlorin), Fe(OEC)(Me₂SO)₂ (6-coordinate, high-spin; Me₂SO = dimethyl sulfoxide), and Fe(OEC)(Im)₂Br (6-coordinate, low-

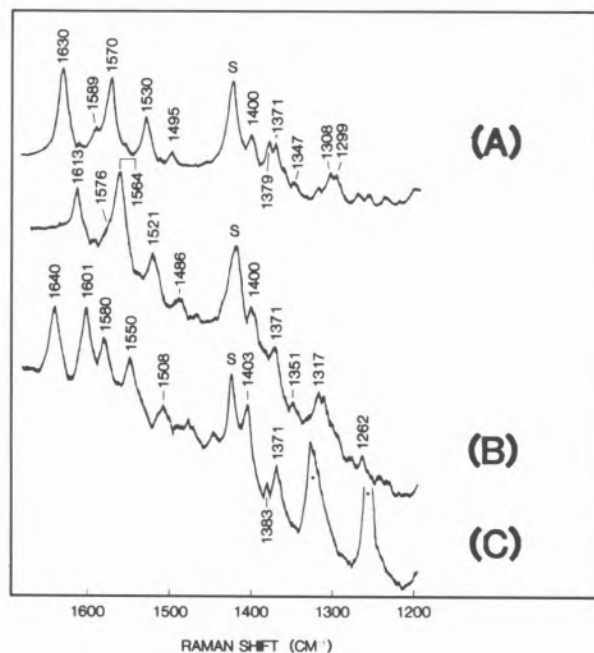


Fig. 1

Resonance Raman spectra of (A) Fe(OEC)Br, (B) Fe(OEC)(Me₂SO)₂, and (C) Fe(OEC)(Im)₂Br.

Experimental conditions: excitation wavelength, 488.0 nm; laser power, 200 mW; spectral slit width, 6 cm⁻¹. S denotes Raman lines due to solvents (CH₂Cl₂ for Fe(OEC)Br and Fe(OEC)(Im)₂Br and 1:1 mixture (V/V) of CH₂Cl₂/Me₂SO for Fe(OEC)(Me₂SO)₂). Bands marked with an asterisk are due to imidazole

-spin; Im = imidazole). RR bands at 1630, 1570, and 1494 cm⁻¹ of Fe(OEC)Br can be assigned to the modes involving mainly the methine bridge stretching vibration, that is, ν_{10} , ν_{19} , and ν_3 modes [2], respectively. These frequencies are very close to those of the corresponding modes of Fe(OEP)Br. Since the frequencies of ν_{10} , ν_{19} , and ν_3 modes are correlated with the center-to-pyrrole-N distance of the porphyrin cavity [4], the close similarities in the frequencies of these modes between Fe(OEC)Br and Fe(OEP)Br indicate the similarity in their core sizes. RR bands of Fe(OEC)Br at 1589 and 1530 cm⁻¹ may be due to the modes involving substantially the C _{β} C _{β} stretching character [2]. The corresponding modes of Fe(OEP)Br were observed at 1581 and 1558 cm⁻¹. Although it was expected that the two C _{β} C _{β} stretching modes would show large downward shifts upon saturation of one of C _{β} C _{β} bonds, the 1581 cm⁻¹ band did exhibit an upward shift by 8 cm⁻¹. Two C _{β} C _{β} stretching modes of Fe(OEP)Br with

C_{4v} symmetry belong to different symmetry species (A_1 for 1581 cm^{-1} and B_1 for 1558 cm^{-1}), but they belong to the same symmetry species (A_1) for $\text{Fe}(\text{OEC})\text{Br}$ with C_{2v} symmetry. Therefore it seems very likely that vibrational coupling of two A_1 modes causes a large splitting of the two $C_\beta C_\beta$ stretching modes for $\text{Fe}(\text{OEC})\text{Br}$. The so-called oxidation-state marker (ν_4) is seen at 1371 cm^{-1} in the RR spectrum of $\text{Fe}(\text{OEC})\text{Br}$.

The middle spectrum of Fig. 1 was obtained by dissolving $\text{Fe}(\text{OEC})\text{Br}$ in a 1:1 mixture (V/V) of $\text{CH}_2\text{Cl}_2/\text{Me}_2\text{SO}$. The RR spectrum resembles that of $\text{Fe}(\text{OEP})(\text{Me}_2\text{SO})_2$ regarding the frequencies of the methine bridge stretching modes [5], suggesting that ferric chlorin forms the hexa-coordinated high-spin complex with dimethyl sulfoxide at two axial positions as in the case of porphyrin.

Upon the high- to low-spin conversion of ferric chlorins all the RR bands above 1450 cm^{-1} showed large upward shifts. The ν_{10} , ν_{19} , and ν_3 modes of $\text{Fe}(\text{OEC})(\text{Im})_2\text{Br}$ were observed at 1640 , 1580 , and 1508 cm^{-1} , respectively. These frequencies are again close to those of the corresponding modes of $\text{Fe}(\text{OEP})(\text{Im})_2\text{Br}$.

The reduction of the iron atom resulted in numerous changes in both positions and intensities of RR bands. However, the frequency shift of the ν_4 mode was rather small (*ca.* 4 cm^{-1}) compared with porphyrins ($7\text{--}17\text{ cm}^{-1}$) [3,4]. The frequency decrease of the ν_4 mode upon the change from Fe^{3+} to Fe^{2+} has been attributed to the increased π -back donation of d_π electrons to porphyrin π^* orbital [3,4]. Therefore, the relatively small frequency shift of ν_4 mode indicates that π -back donation is less significant in ferrous chlorins than in ferrous porphyrins.

REFERENCES

- [1] S.S. SIBBETT, J.K. HURST, *Biochemistry*, **23**, 3007 (1984).
- [2] Y. OZAKI, T. KITAGAWA, H. OGOSHI, *Inorg. Chem.*, **18**, 1772 (1979).
- [3] T. KITAGAWA, Y. OZAKI, Y. KYOGOKU, *Adv. Biophys.*, **11**, 153 (1978).
- [4] T.G. SPIRO, in «Iron Porphyrins», part II, Reading, Massachusetts, 1982, pp. 89-159.
- [5] J. TERAOKA, T. KITAGAWA, *J. Phys. Chem.*, **84**, 1928 (1980).



PS5.36 — MO

M.A. CINELLU
M.L. GANADU
G. MINGHETTI

Istituti Chimici
Università di Sassari
07100 Sassari
Italy

F. CARIATI
Dipartimento di Chimica Inorganica e Metallorganica
Università di Milano
20133 Milano
Italy

F. DEMARTIN
M. MANASSERO
Laboratorio di Strutturistica
Facoltà di Scienze, Centro CNR
Università di Milano
20133 Milano
Italy

PALLADIUM(II) DERIVATIVES OF SOME 1,4-BENZODIAZEPIN-2-ONES

The reaction of PdCl_2 and $\text{Na}_2[\text{PdCl}_4]$ with two 1,4-benzodiazepin-2-ones, L, (DIAZEPAM and PRAZEPAM) has been investigated. Complexes of the types $\text{trans-(L)}_2\text{PdCl}_2$, $[(L-H)\text{PdCl}]_2$, $(L-H)(\text{Ph}_3\text{P})\text{PdCl}$ and $(L-H)\text{Pd}(\text{acac})$ have been characterized by IR and NMR spectroscopy. An X-ray structure determination of $(\text{PRAZEPAM})_2\text{PdCl}_2$ has shown that the ligand is coordinated to the metal through the 4-nitrogen atom.

RESULTS

Previously we have shown that the reaction of some 1,4-benzodiazepin-2-ones, (L) (*e.g.* DIAZEPAM, PRAZEPAM, NIMETAZEPAM, LORAZEPAM, NITRAZEPAM) with gold(III) chloride affords 1:1 adducts $(\text{L})\text{AuCl}_3$. For the complex $(\text{PRAZEPAM})\text{AuCl}_3$ the coordination mode of the ligand has been ascertained by an X-ray structure determination and found to occur through the 4-nitrogen atom [1].

We report now some preliminary results on the interaction of PdCl_2 and $\text{Na}_2[\text{PdCl}_4]$ with DIAZEPAM and PRAZEPAM (scheme I):

- 1) $\text{PdCl}_2 + n\text{L} \xrightarrow{\text{CHCl}_3} \text{trans-(L)}_2\text{PdCl}_2$
 $n = 1, 2, 3$
- 2) $\text{Na}_2[\text{PdCl}_4] + \text{L} \longrightarrow [(\text{L-H})\text{PdCl}]_2 +$
 $+ (\text{L-H})(\text{L})\text{PdCl}$
- 3) $[(\text{L-H})\text{PdCl}]_2 +$
 $2 \text{Ph}_3\text{P} \longrightarrow 2 (\text{L-H})(\text{Ph}_3\text{P})\text{PdCl}$
- 4) $[(\text{L-H})\text{PdCl}]_2 +$
 $+ 2 \text{Ti}(\text{acac}) \longrightarrow 2 (\text{L-H})\text{Pd}(\text{acac}) + 2 \text{TiCl}$

Reaction 1) was carried out in mild conditions (room temperature, CHCl_3): in any case only 1:2 adducts were obtained, even when excess ligand was employed. The *trans*-arrangement of the ligands was assigned on the basis of the IR and X-ray data. The complex $(\text{PRAZEPAM})_2\text{PdCl}_2$ exists in two crystalline modifications: one of them is pictured in Fig. 1. The ligand is bonded to the metal through the 4-nitrogen atom: the overall geometry to the organic molecule [2] does not appear to be remarkably affected by the comple-

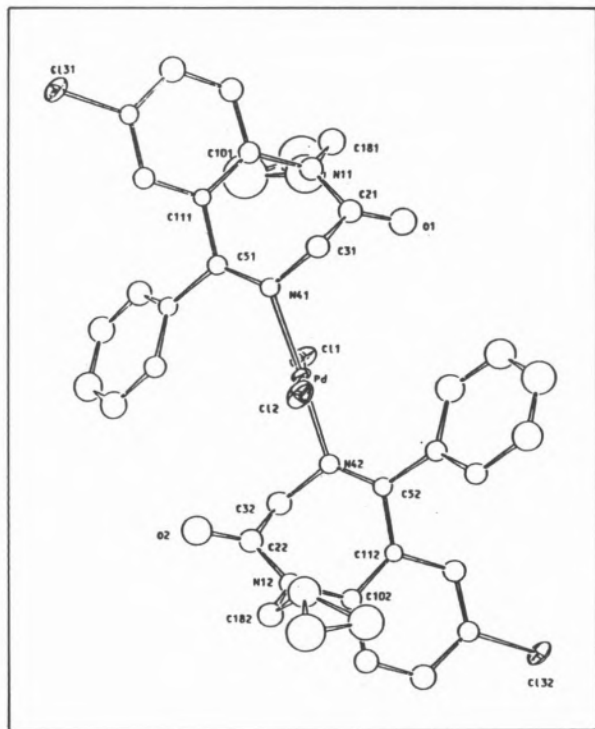


Fig. 1

ORTEP view of compound $(\text{PRAZEPAM})_2\text{PdCl}_2$. The hydrogen atoms have been omitted for clarity.

$\text{Pd-Cl}(1)$ 2.299(5), $\text{Pd-Cl}(2)$ 2.310(4), $\text{Pd-N}(41)$ 2.026(12), $\text{Pd-N}(42)$ 2.024(12), $\text{C}(51)\text{-N}(41)$ 1.293(18), $\text{C}(52)\text{-N}(42)$ 1.281(18), $\text{N}(41)\text{-C}(31)$ 1.487(19), $\text{N}(42)\text{-C}(32)$ 1.418(18) Å

xation to the metal, as observed previously in the gold(III) complex and in a copper(II) derivative, $(\text{DIAZEPAM})_2\text{CuCl}_2$ [3], the only complexes of these ligands so far investigated by X-ray analysis. Reaction 2) gave, as the main product, the species $[(\text{L-H})\text{PdCl}]_2$ plus a small amount of $(\text{L-H})(\text{L})\text{PdCl}$. The former are dinuclear complexes where the benzodiazepine ligand is likely to be coordinated through the 4-nitrogen atom and the *ortho*-carbon atom of the phenyl ring, to give a five-membered cyclometallated system. The dinuclear species are easily split by classical reactions such as 3) and 4) [4]. At the best of our knowledge these are the first complexes where a 1,4-benzodiazepin-2-one acts as an anionic chelating ligand.

Work is in progress to collect X-ray evidence of such a behaviour.

REFERENCES

- [1] a) G. MINGHETTI, C. FODDAI, F. CARIATI, M.L. GANADU, M. MANASSERO, *Inorg. Chim. Acta*, **64**, L235 (1982);
 b) G. MINGHETTI, M.L. GANADU, C. FODDAI, M.A. CINELLI, F. CARIATI, F. DEMARTIN, M. MANASSERO, *Inorg. Chim. Acta*, **86**, 93 (1984).
- [2] G. BRACHTEL, M. JANSEN, *Cryst. Struct. Commun.*, **10**, 669 (1981).
- [3] A. MOSSET, J.P. TUCHAGUES, J.J. BONNET, H. HARAN, P. SHARROCK, *Inorg. Chem.*, **19**, 290 (1980).
- [4] I. OMAE, *Chem. Rev.*, **79**, 287 (1979).



PSS.37 — TU

L. STRINNA ERRE

G. MICERA

P. PIU

Istituto di Chimica Generale ed Inorganica

Università di Sassari

Via Vienna 2, 07100 Sassari

Italy

F. CARIATI

Dipartimento di Chimica Inorganica e Metallorganica

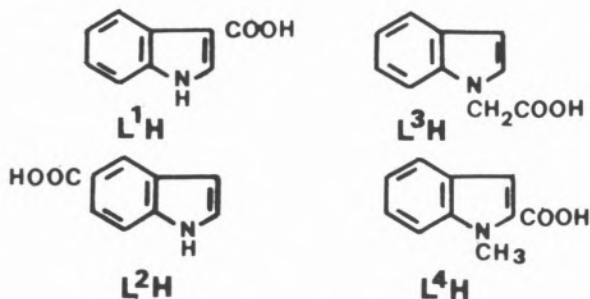
Università di Milano

Via G. Venezian 21, 20133 Milan

Italy

COPPER(II) COMPLEXES OF SOME INDOLIC ACIDS

Indolecarboxylic acids are a class of plant auxins which are responsible for metal complex formation in plant tissues [1]. As a continuation of our previous studies on the metal complexes of indolic auxins [2], we report here the synthesis and the characterization of the copper(II) complexes formed by the following ligands:



The complexes obtained, along with their solid-state magnetic properties and electronic absorption data, are listed in Table I.

Table I
Magnetic properties and electronic absorption data

Compound		λ_{\max} (nm)
Cu(L ¹) ₂ ·H ₂ O	dimer	685
Cu(L ²) ₂ ·1.5 H ₂ O	dimer	690
Cu(L ³) ₂ ·2 CH ₃ OH	dimer	700
Cu(L ³) ₂	dimer	685
Cu(L ⁴) ₂ ·1.5 H ₂ O	dimer	710
Cu(L ⁴) ₂ ·2 H ₂ O	monomer	700

Indole-3-carboxylic and indole-5-carboxylic acids yield compounds having formulae Cu(L¹)₂·H₂O and Cu(L²)₂·1.5 H₂O, respectively, which exhibit spectral properties typical of tetracarboxylate-bridged dimers of the copper(II) acetate monohydrate-type.

Also indole-*N*-acetic acid yields dimeric compounds, Cu(L³)₂·2CH₃OH and Cu(L³)₂, the latter one exhibiting an ESR powder spectrum supportive of interdimeric exchange interactions as is often the case of anhydrous copper(II) carboxylates.

On the other hand, *N*-methyl-indole-2-carboxylic acid yields, in addition to the dimeric complex Cu(L⁴)₂·1.5 H₂O, a monomeric compound, Cu(L⁴)₂·2 H₂O, whose spectral properties are consistent with a tetragonally elongated coordination involving two water molecules and two bidentate carboxylate groups behaving in a strongly asymmetrical fashion.

By taking into account also the results obtained previously for the complexes of indole-3-acetic, -3-butanolic, -3-propanoic and -2-carboxylic acids [2], it may be suggested that indolic acids behave as simple carboxylic ligands and that monomeric arrangements for the copper(II) complexes are allowed only when the carboxylic group is in *ortho* to the ring nitrogen atom.

REFERENCES

- [1] R. SAHAI, S.S.S. KUSHWAHA, A.K. CHAUDHARY, *J. Indian Chem. Soc.*, **57**, 844 (1980).
- [2] G. MICERA, L. STRINNA ERRE, A. PANZANELLI, P. PIU, F. CARIATI, *J. Coord. Chem.*, **13**, 231 (1984).



PS5.38 — TH

MARIA E. CURRY
DEREK J. HODGSON

Department of Chemistry
University of North Carolina
Chapel Hill, NC 27514
U.S.A.

DRAKE S. EGGLESTON

Smith Kline & French Laboratories
P.O. Box 7929, Philadelphia, PA 19101
U.S.A.

CALCIUM BINDING TO METHYLMALONATE ION

In an endeavor to model the binding of calcium(II) ions to γ -carboxyglutamic acid (gla) residues, we have determined the crystal and molecular structure of the calcium(II) complex of methylmalonic acid, which is an excellent structural model for the functional groups at the γ -carbon center of gla. The complex crystallizes as a hydrate of formulation $\text{Ca}_3(\text{Memal})_3 \cdot 4\text{H}_2\text{O}$, where Memal is the methylmalonato dianion, $\text{C}_4\text{H}_4\text{O}_4^{2-}$. The complex crystallizes in the monoclinic space group $C2/c$ with four formula units in a cell of dimensions $a=16.886$ (7), $b=18.959$ (10), $c=6.640$ (8) Å, $\beta=90.76$ (8)°. The structure contains two independent and distinct types of calcium atom. One calcium atom is eight-coordinate, binding to two water molecules and to six carboxylate oxygen atoms; the only chelation at this center involves oxygen atoms from a single carboxylate group. The other calcium atom is seven-coordinate, coordinating to one water molecule and six carboxylate oxygen atoms. In this case, however, one of the two chelates is formed by atoms from the two different carboxylate groups of a single methylmalonato ion; this type of chelation is not available to glutamic or aspartic acid residues, but is available to gla residues and may be significant in the binding of calcium to gla-containing proteins.



PS5.39 — MO

M. MADALENA CALDEIRA

NUNO OLIVEIRA

VICTOR M.S. GIL

CARLOS F.G. GERALDES

Department of Chemistry
University of Coimbra
Portugal

MULTINUCLEAR NMR STUDIES OF VANADIUM(V) COMPLEXES WITH LACTIC AND MALIC ACIDS

Complexation of vanadium(V) with lactic and malic acids, in aqueous solution, is being investigated using ^1H , ^{13}C and ^{51}V NMR spectroscopy [1]. Two main complexes are formed in each case, with relative concentrations depending on pH and on ionic strength. The vanadium-lactic acid complexes have 1:2 and 1:1 composition, the acid acting as a bidentate ligand in both. The two dominant vanadium-malic acid complexes have a 1:1 stoichiometry, the ligand being bidentate in one (involving the OH and the α carboxyl group) and terdentate in the other (involving also the other carboxyl group). These latter results are established on the basis of the ^{13}C shifts and the vicinal HH coupling constants observed on complexation:

	$\text{HO}_2\text{C}-\text{CH}_2-\text{CH}(\text{OH})-\text{CO}_2\text{H}$				J_{AX}	J_{BX}
	(A,B)	(X)				
a. Bidentate	0.4	0.4	6.1	5.8 ppm	4.2	9.8 Hz
b. Terdentate	4.6	2.0	10.0	6.0	1.9	4.9

An attempt is made to interpret the vanadium shifts observed on complexation.

Formation constants are being estimated and exchange and metal reduction phenomena investigated.

REFERENCE

- [1] For similar studies see M. MADALENA CALDEIRA, VICTOR M.S. GIL, *Can. J. Chem.*, **62**, 2094-2100 (1984), and references therein.



PS5.40 — TU

G. MICERA

Istituto di Chimica Generale e Inorganica
Università di Sassari
Via Vienna 2, 07100 Sassari
Italy

S. DEIANA**A. DESSI**

Istituto per l'Applicazione delle Tecniche Chimiche Avanzate ai Problemi
Agrobiologici, C.N.R.
Via Vienna 2, 07100, Sassari
Italy

P. DECOCK**B. DUBOIS**

Laboratoire de Chimie Minérale et Méthodologie Analytique
Université des Sciences et Techniques de Lille
59655 Villeneuve d'Ascq
France

H. KOZŁOWSKI

Institute of Chemistry
University of Wrocław
14 F. Joliot-Curie Street, 50383 Wrocław
Poland

SPECTROSCOPIC AND POTENTIOMETRIC STUDIES OF COPPER(II) COMPLEXES OF D-GLUCOSAMINE

Because of the involvement in many bioinorganic systems, the interaction of metal ions with simple amino sugars such as D-glucosamine has been studied [1,2], but no precise description of the complexes is really available. We have investigated the Cu(II)-D-glucosamine system in aqueous solution by using spectroscopic (ESR, absorption and CD) and potentiometric techniques.

According to the potentiometric results, five distinct complex species are formed over the pH range 5-9.5 (Table I).

The CuL_2 complex, the major species around pH 7 (~55% at pH 6.9), is easily distinguished by spectral measurements. Indeed, the *d-d* absorption maximum (660 nm, $\epsilon=44$), the ESR parameters ($g_{\parallel}=2.317$, $A_{\parallel}=175 \times 10^{-4} \text{ cm}^{-1}$) and the CD data (640 nm, $\Delta\epsilon=+0.06$) strongly support the involvement of two nitrogen atoms in metal coordination [3-4].

Above pH 7 two other complexes, namely

Table I

Logarithm of stability constants ($\log \beta_{pqr}$) of complex species $M_p H_q L_r$ ($M=\text{Cu(II)}$, $L=\text{D-glucosamine}$) in 0.15 M NaCl at 25°C

p	q	r	$\log \beta_{pqr}$
0	1	1	7.70
1	0	1	3.06
1	0	2 (CuL_2)	8.76
1	-1	2	0.83
1	-2	2 (CuH_2L_2)	-5.82
1	-3	2	-15.08

CuH_2L_2 (~10% at pH 7.4) and CuH_3L_2 (~90% at pH 8.1), are formed. The minor species, CuH_2L_2 , which is not shown by any used spectroscopic technique, results from the deprotonation of one of the hydroxyl groups of a glucosamine ligand and, thereby, involves a chelate (N,O) ring. The CuH_2L_2 species ($\lambda_{\text{max}}=620 \text{ nm}$, $g_{\parallel}=2.255$, $A_{\parallel}=196 \times 10^{-4} \text{ cm}^{-1}$) involves two chelate (N,O) rings because of the coordination of two amino groups and two deprotonated hydroxyls. The formation of CuH_2L_2 gives rise to strong negative CD effects centered around 730 nm ($\Delta\epsilon=-0.15$).

Positive Cotton effects, attributable to $\text{NH}_2 \rightarrow \text{Cu(II)}$ charge transfer transitions, are observed in the UV region (CuL_2 : 315 nm, $\Delta\epsilon=+0.6$; CuH_2L_2 at pH ~8: 300 nm, $\Delta\epsilon=+2.2$).

The formation of CuH_3L_2 , which predominates above pH 10, does not result in any distinguishable variation of absorption or ESR spectra.

REFERENCES

- [1] Z. TAMURA, M. MIYAZAKI, *Chem. Pharm. Bull.*, **13**, 345-353 (1965).
- [2] Y. INAKI, M. OTSUKU, K. TAKEMOTO, *J. Macromol. Sci., Chem.*, **A12**, 953 (1978).
- [3] G. FORMICKA-KOZŁOWSKA, H. KOZŁOWSKI, B. BJEZOWSKA-TRZEBIATOWSKA, *Inorg. Chim. Acta*, **25**, 1 (1977).
- [4] G. FORMICKA-KOZŁOWSKA, H. KOZŁOWSKI, I.Z. SIEMION, K. SOBECZYK, E. NEWROCKA, *J. Inorg. Biochem.*, **15**, 201 (1981).



PS5.41 — TH

M.B. YIM

M.W. MAKINEN

Department of Biochemistry and Molecular Biology
The University of Chicago
Chicago, Illinois 60637
U.S.A.

ENDOR STUDY OF SMALL MOLECULE AND ENZYME COMPLEXES OF Gd^{3+} IN FROZEN SOLUTION

Electron-nuclear double resonance (ENDOR) spectroscopy is applied to the investigation of the coordination structure of Gd^{3+} in small molecule and enzyme complexes in frozen solution. Proton ENDOR spectra of $GdCl_3$ in frozen methanol-water mixtures obtained with H_0 at the turning point of the EPR absorption exhibit single crystal-type line pairs. With use of selectively deuterated solvents, we have assigned the chemical origins of each pair of ENDOR lines. There are two distinguishable sets of protons due to metal-coordinated water and one set belonging to the methyl group of metal-coordinated methanol. Similarly, from the proton ENDOR spectrum of $Gd(CH_3COO)_3$ in frozen solution, we have also identified the set of lines belonging to the methyl group of metal-bound acetate. On the basis of the field dependence of the ENDOR spectra, we have determined the hyperfine coupling (hfc) components of each of the metal-bound ligands.

The hfc components of the protons of Gd^{3+} -bound acetate exhibit axial symmetry, and under the point-dipole approximation, the calculated metal-proton distance is $4.53 \pm 0.20 \text{ \AA}$. This is in reasonably good agreement with the value of 4.73 \AA deduced from crystallographic data. The hfc components of the water and methanol protons do not exhibit axial symmetry, indicating significant spin delocalization. Nonetheless, the metal-proton distances, calculated as lower limit estimates on the basis of the largest anisotropic

hfc component, are in surprisingly reasonable agreement with crystallographic data. Application of this method is made to investigate the environment of lanthanide binding sites in enzymes and proteins.



PS5.42 — MO

C.F.G.C. GERALDES

M.C. ALPOIM

M.P.M. MARQUES

Chemistry Department
University of Coimbra
3000 Coimbra
Portugal

A.D. SHERRY

M. SINGH

Chemistry Department
The University of Texas at Dallas
P.O. Box 830688, Richardson, Texas 75080
U.S.A.

A NMR STUDY OF LN(NOTA) CHELATES AS AXIALLY SYMMETRIC AQUEOUS SHIFT REAGENTS

The trivalent lanthanide ethylenediaminetetraacetate ($Ln(EDTA)$) chelates are very useful water soluble NMR shift and relaxation probes of the dynamic structure of biological molecules at $pH \sim 7$ [1], including nucleotides [2,3], carboxylates [4,5] and aminoacids [6]. The $Ln(EDTA)$ complexes suffer several disadvantages as aqueous NMR shift reagents including lack of solubility near neutral pH, exchange broadening of the resonances of some ligands to the heavier $Ln(EDTA)$ chelates [6] and structural changes along the series, which complicates the separation of pseudocontact and contact shifts [7,8].

In this work we report ^{13}C and 1H NMR studies of the 1:1 complexes of the axially symmetric macrocyclic ligand 1,4,7-triazacyclononane- N,N',N'' -triacetic acid (NOTA) with the diamagnetic and

paramagnetic lanthanides. The proton and ^{13}C spectra of the $\text{La}(\text{NOTA})$ and $\text{Lu}(\text{NOTA})$ species were studied as a function of pH and temperature. The aqueous complexes show spectra characteristic of a flexible triaza cycle, displaying fast interconversion between the two staggered δ and λ conformations of the ethylenediamine rings even at room temperature. Above pH 9.5, the hydroxo complexes are formed, and their spectra show evidence for a much more rigid triaza macrocycle. At room temperature the conformational interconversions are slow in the NMR time scale. Proton and ^{13}C NMR dynamic studies gave a value of $\Delta G^\ddagger = 63.6 \text{ KJ mol}^{-1}$ for the activation energy of this process.

LIS values have been measured for all proton and carbon resonances in nine paramagnetic $\text{Ln}(\text{NOTA})$ complexes (Fig. 1). The ethylene protons appear as a pair of resonances forming an

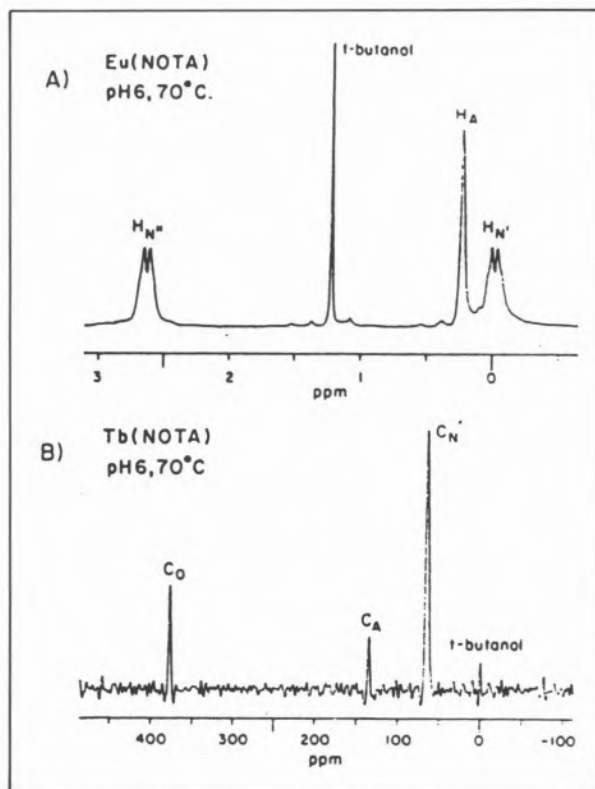


Fig. 1

Proton(A) and carbon(B) NMR spectra of $\text{Ln}(\text{NOTA})$ complexes

$\text{AA}'\text{XX}'$ splitting pattern (visible only in the $\text{Eu}(\text{NOTA})$ spectrum) while the acetate protons remain a singlet. The observed LIS's are domi-

nated by contact interactions in most of the $\text{Ln}(\text{NOTA})$ complexes.

The ^{13}C spectrum of $\text{Pr}(\text{NOTA})$, studies of the effect of added LiCl on the observed LIS's and observed breaks in plots of experimental LIS data versus theoretical pseudocontact and contact shift values, suggest that the early members of the lanthanide ion series form mixed complexes with NOTA in aqueous solution, some with NOTA bound as a hexadentate chelate and some as a pentadentate species with one unbound acetate group. The smaller trivalent lanthanide cations ($\text{Dy}-\text{Yb}$) appear to form complexes containing only hexadentate chelated NOTA .

The pseudocontact shifts for the $\text{Dy}-\text{Yb}$ complexes agree reasonably well with those calculated using the axial symmetry model and the crystal coordinates of $\text{Cr}(\text{NOTA})$ (Fig. 2). The proton and ^{13}C relaxation rates determined for three $\text{Ln}(\text{NOTA})$ complexes indicate that the smaller lanthanide cations fit into the triazamacrocyclic cavity better than do the larger ions, resulting in structurally more rigid $\text{Ln}(\text{NOTA})$ complexes.

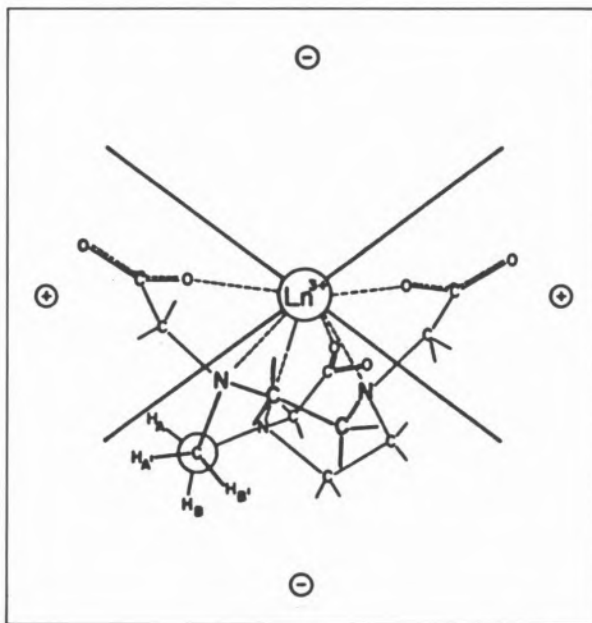


Fig. 2

The structure of $\text{Ln}(\text{NOTA})$ complexes indicating the dipolar angle and the sign of the axial dipolar geometric term

We also studied the induced LIS's of the ligand protons and ^{13}C nuclei of cyclopropane carboxylate (CPC), adenosine 5'-monophosphate (AMP) and the dicarboxylate ligand *cis*-5-norbornene-

-endo-2,3-dicarboxylic acid upon binding of the Ln(NOTA) paramagnetic complexes. Fast exchange was observed and the measured paramagnetic shifts were purified of existing contact contributions and compared with theoretical values calculated from assumed structures. The results obtained indicate that Ln(NOTA) chelates should be very useful NMR paramagnetic probes to be used in conformational analysis of small ligands or in binding to protein surfaces.

REFERENCES

- [1] R.J.P. WILLIAMS, *Struct. Bonding (Berlin)*, **50**, 79 (1982).
- [2] C.M. DOBSON, R.J.P. WILLIAMS, A.V. XAVIER, *J. Chem. Soc., Dalton Trans.*, 1762 (1974).
- [3] C.F.G.C. GERALDES, R.J.P. WILLIAMS, *Eur. J. Biochem.*, **97**, 93 (1979).
- [4] G.A. ELGAVISH, J. REUBEN, *J. Am. Chem. Soc.*, **98**, 4755 (1976).
- [5] M. SINGH, A.D. SHERRY, *J. Less Common Met.*, **94**, 351 (1983).
- [6] A.D. SHERRY, C.A. STARK, J.R. ASCENSO, C.F.G.C. GERALDES, *J. Chem. Soc., Dalton Trans.*, 2078 (1981).
- [7] C.N. REILLEY, B.W. GOOD, J.F. DESREUX, *Anal. Chem.*, **47**, 2110 (1975).
- [8] C.N. REILLEY, B.W. GOOD, R.D. ALLENDOERFER, *Anal. Chem.*, **48**, 1446 (1976).



PS5.43 — MO

C.F.G.C. GERALDES *

A.D. SHERRY

Chemistry Department
University of Texas at Dallas
P.O. Box 688, Richardson, TX 75080
U.S.A.

R.D. BROWN, III

S.H. KOENIG

IBM T.J. Watson Research Center
P.O. Box 218, Yorktown Heights, N.Y. 10598
U.S.A.

NMRD INVESTIGATION OF Mn²⁺ AND Gd³⁺ NOTA COMPLEXES, AND A COMPARISON WITH THE ANALOGOUS EDTA COMPLEXES

It is well established that the longitudinal (spin-lattice) and transverse (spin-spin) relaxation rates of solvent protons in solutions of complexes of paramagnetic ions, *e.g.*, metalloproteins or small chelates, depend on the strength of the applied static magnetic field and on the chemical environment of the ions [1,2]. The magnetic field dependence of the proton relaxation rates of water, called nuclear magnetic relaxation dispersion (NMRD) profiles, have been previously studied in detail for complexes of Gd³⁺ and Mn²⁺ with the chelates ethylenediaminetetraacetic acid (EDTA) and diethylenetriaminepentaacetic acid (DTPA) [2]. In this work, we report a study of the 1/T₁ NMRD profiles of Gd³⁺ and Mn²⁺ ions complexed with the cyclic triazamacrocyclic ligand 1,4,7-triazacyclononane-*N,N',N''*-triacetic acid (NOTA), and compare them with results for the analogous EDTA complexes. We also discuss their potential utility as paramagnetic contrast agents in NMR imaging.

Fig. 1 shows the NMRD profiles of solvent protons of Mn(EDTA) and Mn(NOTA) complexes, which are independent of pH in the range of

* Permanent Address: Chemistry Department, University of Coimbra, 3000 Coimbra, Portugal

5.8 to 10.5. Addition of excess EDTA to the Mn(NOTA) solution does not affect the rates, showing that Mn^{2+} forms at least a 50-fold stronger complex with NOTA than it does with EDTA. The Mn(NOTA) NMRD profile shows that its relaxivity is very low, probably arising only from outer sphere effects. The absence of inner sphere water molecules in Mn(NOTA) would agree quite well with X-ray crystal structures of the Cr^{3+} , Fe^{3+} , and Cu^{2+} NOTA complexes [3]. On the other hand, the results strongly suggest that Mn(EDTA) is indeed seven coordinated, with one inner sphere water molecule, as discussed previously [4-6].

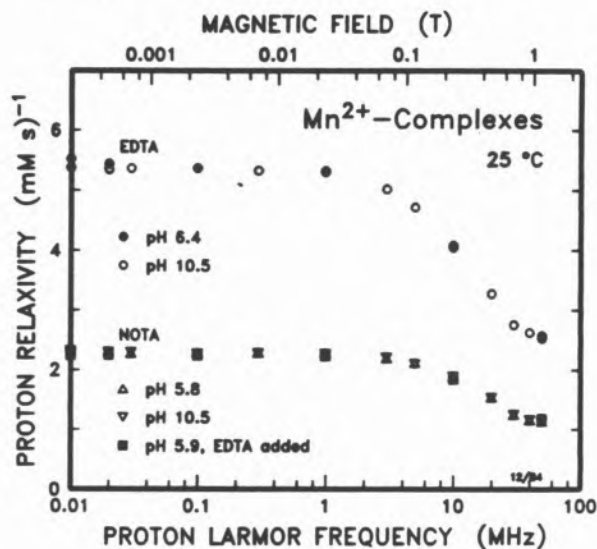


Fig. 1

$1/T_1$ NMRD profiles of solvent protons of solutions of Mn^{2+} complexes with EDTA and NOTA

Fig. 2 shows the Gd(NOTA) NMRD profiles under various conditions and compares them with the Gd(EDTA) results. At pH near neutrality, the Gd(NOTA) NMRD curve has a lower relaxivity than Gd(EDTA), particularly at low fields, due to a combination of a decreased correlation time for the dipolar interaction and a decrease of water coordination number. A water coordination number of 3.3 has been proposed for Eu(NOTA) on the basis of optical [7] and NMR results [8,9] and the present data are certainly compatible with this view. Addition of equimolar quantities of EDTA restores the NMRD profile of Gd(EDTA), indicating that EDTA competes successfully with NOTA for Gd^{3+} at neutral pH, and that the Gd(NOTA)

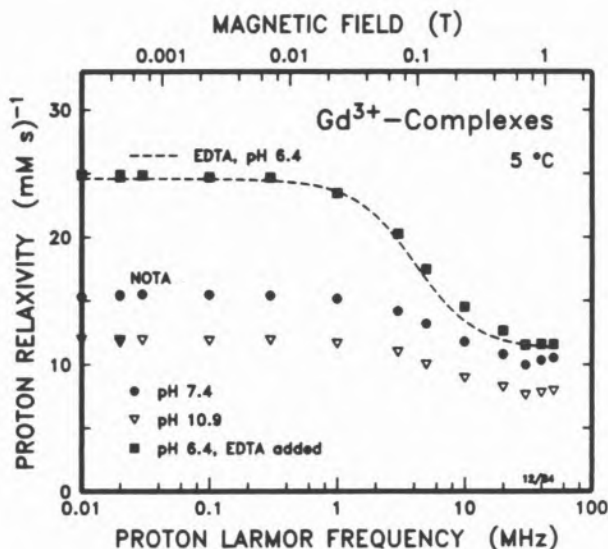


Fig. 2

$1/T_1$ NMRD profiles of solvent protons of solutions of Gd^{3+} complexes with EDTA and NOTA. The dashed line is computed from a least squares comparison of theory and experimental data [2]

complex is substantially weaker than Gd(EDTA). We also see a gradual decrease of relaxivity of Gd(NOTA) as the pH is increased from 7.4 to 10.9, equivalent to an effective decrease of approximately one proton. This is not due to $Gd(OH)_3$ precipitation, and we propose that inner sphere water molecules of Gd(NOTA) are involved at high pH, giving mixed $Gd(NOTA)(H_2O)_m(OH)_n$ species. This is in agreement with high resolution NMR observations on the La^{3+} and Lu^{3+} NOTA complexes [10].

In conclusion, the very stable Mn(NOTA) complex, although allowing an estimate of outer sphere effects for other Mn^{2+} complexes, probably would not be an efficient relaxation enhancement agent. The Gd(NOTA) complex is quite an efficient relaxation agent, particularly at high frequencies, but could be quite a toxic contrast agent in NMR imaging due to its ready release of the Gd^{3+} caused by a relatively modest stability constant.

REFERENCES

- [1] S.H. KOENIG, R.D. BROWN III, *Magn. Reson. Med.*, **1**, 478 (1984).
- [2] S.H. KOENIG, C. BAGLIN, R.D. BROWN III, C.F. BREWER, *Magn. Reson. Med.*, **1**, 496 (1984).

- [3] K. WIEGHARDT, V. BOSSEK, P. CHAUDHARI, W. HERMANN, B.C. MENKE, J. WEISS, *Inorg. Chem.*, **21**, 4308 (1982).
- [4] J. KING, N. DAVIDSON, *J. Chem. Phys.*, **29**, 787 (1958).
- [5] J. OAKES, E.G. SMITH, *J. Chem. Soc., Faraday Trans. 2*, **77**, 299 (1981).
- [6] J. OAKES, E.G. SMITH, *J. Chem. Soc., Faraday Trans. 1*, **79**, 543 (1983).
- [7] C.C. BRYDEN, C.N. REILLEY, *Anal. Chem.*, **54**, 610 (1982).
- [8] C.C. BRYDEN, C.N. REILLEY, J.F. DESREUX, *Anal. Chem.*, **53**, 1418 (1981).
- [9] A.D. SHERRY, M. SINGH, C.F.G.C. GERALDES, submitted for publication to *J. Am. Chem. Soc.*
- [10] C.F.G.C. GERALDES, M.C. ALPOIM, M.P.M. MARQUES, A.D. SHERRY, M. SINGH, submitted for publication to *Inorg. Chem.*



PS5.44 — TH

KELLEY WOODRING
RICHARD W. TAYLOR
Department of Chemistry
University of Oklahoma
Norman, OK. 73019
U.S.A.

SUBSTITUENT EFFECTS ON THE DISSOCIATION KINETICS OF HEAVY METAL ION CRYPTATES

The dissociation kinetics of the cryptates of 2.2.2, 2.2.2_D, 2_B.2_B.2 and 2_C.2_C.2 with Tl⁺ and Pb²⁺ have been studied in water and methanol-water (90:10) at 25.0°C. The dissociation reactions generally displayed parallel solvolytic (*k_s*) and acid-catalyzed (*k_H*) pathways consistent with the rate law:

$$-d[\text{MCryp}^{n+}]/dt = (k_d + k_H[\text{H}^+]) [\text{MCryp}^{n+}]$$

The introduction of a decyl side chain (2.2.2_D) produced only minor variations in the values of *k_d* and *k_H* when compared with the parent cryptand, 2.2.2. Larger effects are observed with the dibenzo-derivative (2_B.2_B.2) with Tl⁺ and for the dicyclohexano-derivative (2_C.2_C.2) with both Pb²⁺ and Tl⁺. The rate constants for the uncatalyzed and acid-catalyzed pathways in methanol-water decrease by 20- to 200-fold compared with the corresponding values obtained in water.

INTRODUCTION

The macrobicyclic polyoxa-diamines (cryptands) introduced by LEHN and co-workers form stable complexes with alkali-, alkaline-earth- and heavy metal cations [1,2]. The relative rigidity of these ligands results in peak type selectivity related to the ratio of ligand cavity to metal cation diameter. In addition to cavity size, parameters such as donor atom type and ligand backbone substituents also affect the complexation properties of the cryptands [1-3]. The introduction of hydrophobic decyl-, benzo-, and cyclohexano-moieties into the cryptand (see Fig. 1) structure increases their ability to solubilize salts in non-polar media [4] and

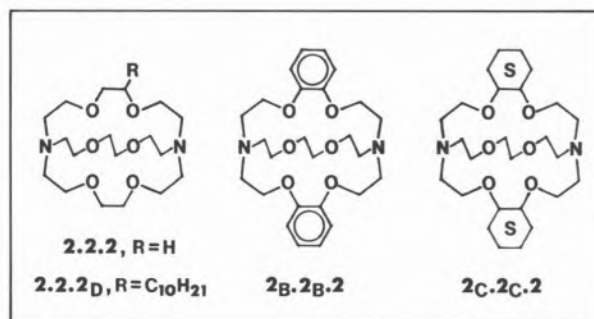


Fig. 1
Structures of 2.2.2 Cryptands

membranes [5,6]. In view of the demonstrated ability of the parent compound, cryptand 2.2.2, to enhance elimination of toxic heavy metal ions [7,8] an evaluation of substituent effects on the complexation properties with Pb²⁺ and Tl⁺ was carried out and the results are reported in this communication.

EXPERIMENTAL

Cryptands 2.2.2, 2.2.2_D, 2_B.2_B.2 and 2_C.2_C.2 were obtained from E. Merck and used without further purification. Stock cryptand solutions were analyzed spectrophotometrically [9]. Kinetic studies were carried out by mixing equal volumes of the appropriate cryptate (3.0-7.0 × 10⁻⁵ M) with a solution of known HClO₄ concentration (1.12-74.5 mM). The reactions were monitored in the wavelength region of 245-255 nm on either a Durrum stopped-flow or a Hitachi 80-100 spectrophotometer. The cell temperature was maintained at 25.0 (±0.1)°C using a thermostated water bath.

All reactions were pseudo-first-order and rate constants were obtained using standard least squares technique.

RESULTS AND DISCUSSION

In strongly acidic media the cryptate complexes dissociate via parallel uncatalyzed and proton-catalyzed pathways. The data are consistent with the rate law:

$$-d[\text{MCryp}^{n+}]/dt = (k_d + k_H[\text{H}^+])[\text{MCryp}^{n+}] \quad (1)$$

where $M^{n+} = \text{TI}^+$ or Pb^{2+} and k_d and k_H are the rate constants for the uncatalyzed and acid-catalyzed pathways, respectively. The influence of ionic strength on k_H was accounted for by the relationship:

$$k_{\text{obs}} = k_d + k_H^0[\text{H}^+]\gamma_{\text{H}}\gamma_{\text{MC}}/\gamma_{\neq} \quad (2)$$

where k_H^0 is the rate constant value at zero ionic strength and γ_{H} , γ_{MC} and γ_{\neq} are the activity coefficients of the proton, cryptate and transition-state complex, respectively. Values of γ_i were calculated using the Davies equation [10]. The values of k_d and k_H^0 obtained from plots of equation (2) are listed in Table 1.

The values of k_d in methanol-water are less than the corresponding values in water as expected [11]. In methanol-water the k_d values of the thallium cryptates increase in the sequence:

$2.2.2 < 2.2.2_{\text{D}} \ll 2_{\text{B}}.2_{\text{B}}.2 < 2_{\text{C}}.2_{\text{C}}.2 \ll 2.2 \text{ C}_8$. The introduction of the decyl-side chain has little effect on the dissociation kinetics of the TI^+ and Pb^{2+} complexes in agreement with the results reported for the analogous alkali-cation cryptates [12]. The introduction of the benzo-groups into the cryptand structure has three effects; (i) increased rigidity resulting in a smaller effective cavity, (ii) decreased donor ability of the catechol-ether oxygen atoms and (iii) increased shielding of the cation from the solvent [1]. These factors combine to weaken the cryptand with TI^+ [13] and this decrease in stability is reflected in the large increase in the value of k_d . Similar behavior has been reported for the Ba^{2+} cryptates of 2.2.2 and $2_{\text{B}}.2_{\text{B}}.2$ [14]. Saturation of the rings has little effect on the value of k_d compared to the value for $2_{\text{B}}.2_{\text{B}}.2$ with thallos ion in methanol-water. A much larger effect is noted when the k_d values for the lead ion cryptates of $2_{\text{C}}.2_{\text{C}}.2$ and 2.2.2 are compared. This may be due to the higher charge of Pb^{2+} and the increased shielding provided by cyclohexano-groups which would hinder solvation of the cryptate. The trends for the k_H^0 values of the cryptates are not as distinct as those for the k_d values. However, for both cations, the k_H^0 values for $2_{\text{C}}.2_{\text{C}}.2$ are much larger than those of the other cryptands. The values of k_H^0 are 50- to 200-fold lower in methanol-water than the corresponding values in water, with the larger difference being

Table 1
Rate Constant Values for Acid-Catalyzed Dissociation of TI^+ and Pb^{2+} Cryptates at 25°C^{a)}

Ligand	Solvent ^{b)}	TI^+		Pb^{2+}	
		k_d , sec ⁻¹	k_H^0 , M ⁻¹ sec ⁻¹	k_d , sec ⁻¹	k_H^0 , M ⁻¹ sec ⁻¹
2.2.2	H ₂ O ^{c)}	5.5 ± 0.6	1050 ± 95	1.8 × 10 ⁻⁵	0.71
	M/W	0.10 ± 0.01	26 ± 1	< 10 ⁻⁵	4.0 × 10 ⁻³
	M/W ^{d)}	0.12 ± 0.01	20 ± 1		
2.2.2 _D	H ₂ O	—	—	< 10 ⁻⁴	0.44
	M/W	0.45	37	< 10 ⁻⁵	3.0 × 10 ⁻³
2 _B .2 _B .2	H ₂ O	102	4100	< 10 ⁻⁴	0.057
	M/W	6.2	63	—	—
2 _C .2 _C .2	H ₂ O	—	—	~ 0.002	13.3
	M/W	17.7	3500	~ 3 × 10 ⁻⁵	0.056

a) k_d values at $\mu = 0.1$ (Et_4NClO_4), k_H^0 values at $\mu \rightarrow 0$.

b) M/W = methanol-water (90:10).

c) [15].

d) [16].

observed for the lead cryptates. This result is most likely a consequence of the lower dielectric constant of the methanol-water mixture compared with water.

ACKNOWLEDGEMENTS

This work was supported in part by the Petroleum Research Fund, administered by the American Chemical Society and the University of Oklahoma Research Council.

REFERENCES

- [1] J.M. LEHN, *Struct. Bonding (Berlin)*, **16**, 1 (1973).
- [2] J.M. LEHN, F. MONTAVON, *Helv. Chim. Acta*, **61**, 67 (1978).
- [3] B. DIETRICH, J.M. LEHN, J.P. SAUVAGE, *J. Chem. Soc., Chem. Commun.*, 15 (1973).
- [4] M. CINQUINI, F. MONTANARI, P. TUNDO, *Gazz. Chim. Ital.*, **107**, 11 (1977).
- [5] M. KIRCH, J.M. LEHN, *Angew. Chem., Int. Ed. Engl.*, **14**, 555 (1975).
- [6] R. GUNTHER, O. HAUSWIRTH, R. ZISKOVEN, *J. Physiol.*, **284**, 145P (1978).
- [7] W.H. MULLER, W.A. MULLER, *Naturwissenschaften*, **61**, 455 (1974).
- [8] PH. BAUDOT, M. JACQUE, M. ROBIN, *Toxicol. Appl. Pharmacol.*, **41**, 113 (1977).
- [9] J.A. DRUMHILLER, J.L. LAING, R.W. TAYLOR, *Anal. Chim. Acta*, **162**, 315-321 (1984).
- [10] C.W. DAVIES, «Ion Association», Butterworths, London, 1962, pp. 39-41.
- [11] B.G. COX, J. GARCIA-ROSAS, H. SCHNEIDER, *J. Am. Chem. Soc.*, **103**, 1054 (1981).
- [12] B.G. COX, P. FIRMAN, I. SCHNEIDER, H. SCHNEIDER, *Inorg. Chim. Acta*, **49**, 153 (1981).
- [13] M.K. CHANTOONI JR., I.M. KOLTHOFF, *Proc. Natl. Acad. Sci. USA*, **78**, 7245 (1981).
- [14] J.M. BEMTGEN, M.E. SPRINGER, V.M. LOYOLA, R.G. WILKINS, R.W. TAYLOR, *Inorg. Chem.*, **23**, 3348 (1984).
- [15] J.A. DRUMHILLER, D.L. LUTON, R.W. TAYLOR, *J. Am. Chem. Soc.*, submitted for publication.
- [16] R. GRESSER, D.W. BOYD, A.M. ALBRECHT-GARY, J.P. SCHWING, *J. Am. Chem. Soc.*, **102**, 651-653 (1980).



PS5.45 — MO

ANDREA MALDOTTI
CARLO BARTOCCI
ALBERTINO FERRI
VITTORIO CARASSITI

Istituto Chimico and Istituto di Chimica Biologica dell'Università di Ferrara
Centro di Studio sulla Fotochimica e Reattività degli Stati Eccitati
dei Composti di Coordinazione del C.N.R.
Via L. Borsari, 46 I 44100 Ferrara
Italy

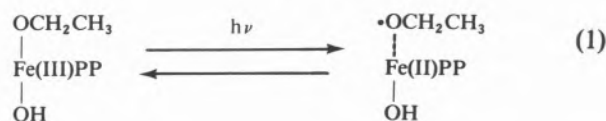
PHOTOCHEMISTRY OF IRON(III) PROTOPORPHYRIN IX IN OXYGENATED ALKALINE AQUEOUS ETHANOL. EVIDENCE FOR SUPEROXIDE RADICAL FORMATION AND ITS INVOLVEMENT IN THE PORPHYRIN DEGRADATION

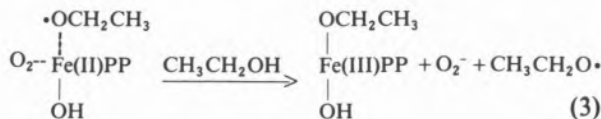
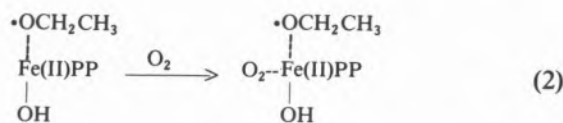
The interest for the formation of superoxide in biological aerobic processes is on steady increase in connection with the auto-oxidation of dioxygen carrier hemoproteins as well as with its toxic effect on living systems.

In recent years, a number of very interesting studies on both the mechanism of formation of superoxide and its reactivity with respect to biological substrates have been reported [1].

We have recently published an ESR-spin trapping investigation on the photochemical behaviour of Fe(III) Protoporphyrin IX chloride (Fe(III)PPCl) in oxygenated water-ethanol mixed solvents [2]. The results obtained in that study allowed us to conclude that Fe(II) porphyrin and an ethoxy radical were formed in the primary photochemical process and that the oxygen interacted somehow with Fe(II) thus hindering a rapid cage back electron transfer. The mechanism proposed is reported in Scheme 1.

Scheme 1





The most interesting aspects in the above scheme are: i) the oxygen should oxidize Fe(II) intermediate when this is still bound to some extent to the ethoxy radical; and ii) superoxide ion should be formed as a product of oxygen reduction.

In the present paper we re-investigate the photochemical behaviour of Fe(III)PPCl in aqueous ethanol for the twofold purpose of having experimental evidence of the superoxide formation and of studying the effect of O_2^- on the porphyrin complex.

Fe(III)PPCl in 40% ethanol/water solvent at pH 12 was irradiated in oxygen atmosphere in an ESR cavity with light of $\lambda > 305$ nm, at room temperature. After 10 minutes of irradiation the solution was quickly cooled to 95 K. In these conditions, an ESR spectrum ($g_{\parallel} = 2.055$, $g_{\perp} = 2.004$), typical of the superoxide radical [3] was obtained. The signal rapidly disappeared when the temperature was raised again to the initial value. These results at the same time confirm the above proposed mechanism and represent the first experimental evidence of superoxide formation upon irradiation of an iron porphyrin. The results obtained in flash-photolysis experiments are also in agreement with the above reported mechanism: in deaerated solution no appreciable photoreduction was observed in a time scale of milliseconds; in oxygenated solution, evidence of formation of Fe(II) porphyrin, which was completely re-oxidized in less than 50 μ sec, was obtained. This indicates that the re-oxidation process occurs via the reaction of oxygen with the coordinatively unsaturated Fe(II) porphyrin intermediate rather than through a bimolecular reaction between dioxygen and a Fe(II) porphyrin complex in some way stabilised prior to oxidation. Prolonged irradiations of Fe(III)PPCl in the above conditions gave rise to an absorbance decrease

in the whole UV-Vis scanned spectral range (300-800 nm). Moreover, the Soret band underwent an evident broadening. This spectral behavior can be taken as an indication of an irreversible modification of the Fe(III) porphyrin complex, consisting in a porphyrin ring opening. Photochemical experiments carried out in alkaline aqueous ethanol containing an excess of imidazole also support the degradation hypothesis: in fact, an absorption band at 670 nm, which could be ascribed to a degradation product of an imidazolate Fe(III) porphyrin complex [4], was observed to be formed under irradiation. It is likely that hydrogen peroxide, formed from the dismutation of superoxide, is responsible for the ring opening process. A similar degradation of an iron porphyrin was demonstrated previously by other authors [5].

REFERENCES

- [1] D. DOLPHIN, B.R. JAMES, H.C. WELBORN, in K.M. KADISH (ed.) «Electrochemical and Spectrochemical Studies on Biological Redox Components», ACS Advances in Chem. Ser. n.° 201, ACS, Washington D.C., 1982, p. 563 and references therein.
- [2] A. MALDOTTI, C. BARTOCCI, R. AMADELLI, V. CARASSITI, *Inorg. Chim. Acta*, **74**, 275 (1983).
- [3] G.W. EASTLAND, M.C.R. SYMONS, *J. Phys. Chem.*, **81**, 1502 (1977).
- [4] S. SANO, Y. SUGIURA, *J. Chem. Soc., Chem. Commun.*, 750 (1982).
- [5] R.F. PASTERNAK, B. HALLIWELL, *J. Am. Chem. Soc.*, **101**, 1026 (1979).



PS5.46 — TH

JOHN H. DAWSON
 ELISABETH T. KINTNER
 MAUREEN K. GENO
 Department of Chemistry
 University of South Carolina
 Columbia, South Carolina 29208
 U.S.A.

BINUCLEAR RUTHENIUM ALKYL DIOXIME COMPLEXES: MODELS FOR ELECTRON TRANSFER THROUGH SATURATED BARRIERS

A question of particular interest to the study of the mechanism of electron transfer in metalloproteins is the nature of the intervening groups and the distance separating redox-active transition metals. We are interested in the distance dependence of intramolecular electron transfer through saturated barriers. The electron density surrounding the metal centers of existing models [1] for electron transfer through saturated barriers is very different from that found in the Fe-Porphyrin or Fe-S prosthetic groups of electron transfer proteins [2]. We have used the (bpy)₂Ru(II) (bpy = 2,2'-bipyridine) moiety instead of (NH₃)₅Ru(II) [3] in order to better mimic the electron density of the protein prosthetic group. Thus we have synthesized a series of binuclear ruthenium alkyl dioxime complexes in which the bridging ligands are the monocyclic 1,4-cyclohexanedione dioxime (cyclodiox), the bicyclic 1,4- and 1,5-substituted *trans* decalindione dioximes (decadiox), and the tetracyclic 5 α -3,17-androstanedione dioxime (androdiox). This provides a series of binuclear metal complexes with the metals separated by a barrier of variable distance. The results of cyclic voltammetric studies of these complexes are shown in Table I. The potential differences for the mono- and bicyclic 1,4-bridged complexes are 471 and 325 mV, respectively with the latter being an irreversible process. The

tetracyclic and 1,5-bicyclic dimers display reversible redox behavior. In the steroid case the two waves nearly coalesce. Overall these data suggest that as the distance between the ruthenium centers increases, the difference in potential decreases.

Table I
 Cyclic voltammetry of Ru dimers

Bridge	E _{1/2} (V vs SCE)	
1,4-cyclohexanedione dioxime	.685,	.214
1,4-decalindione dioxime	.950,	.625
1,5-decalindione dioxime	.960,	.770
5 α -3,17-androstanedione dioxime	.900,	.827

Addition of one equivalent of Ce(IV) to the doubly reduced species generates a mixed-valence Ru^{II}-Ru^{III} dimer which is expected to display near-IR intervalence charge transfer (IT) bands. Results for the mono- and tetracyclic Ru dimers are shown (Table II). The extent of delocalization of the exchanging electron (α^2) can be estimated from the properties of the IT band [5] according to the equation (1) [6]

$$\alpha^2 = \frac{4.2 \times 10^{-4} \epsilon_{\max} \tilde{\nu}_{1/2}}{d^2 \tilde{\nu}_{\max}} \quad (1)$$

where *d* is the Ru-Ru internuclear separation (in Å, based on crystal structure data of the oximes), ϵ_{\max} is the molar absorptivity at the wavelength maximum and $\tilde{\nu}_{1/2}$ is the bandwidth at half-height. The values of α^2 for the mono- and tetracyclic ruthenium dimers (Table II) differ by three orders of magnitude, suggesting that the mixed-valence state is more delocalized in the monocyclic diruthenium complex than in the ruthenium steroid dimer.

Table II

Ru dimer	ΔE (Volts)	$\tilde{\nu}_{\max}$ (nm)	ϵ (M cm) ⁻¹	α^2 (Å ² M cm) ⁻¹
Ru ₂ (μ 1,4-cyclodiox)	.471	910	42	1.3 × 10 ⁻³
Ru ₂ (μ 3,17-androdiox)	.073	718	3.5	2.6 × 10 ⁻⁶

These Ru₂(bpy)₂-dioxime dimers represent a new series of ligand complexes with which to study the distance dependence of intramolecular electron transfer through saturated barriers. As the dis-

tance between the ruthenium ions increases, the difference in reduction potential of the two rutheniums decreases as does the degree of delocalization of the mixed valence state. At the same time, the energy of the IT band increases with concomitant decrease in molar absorptivity.

ACKNOWLEDGEMENTS

JHD is the recipient of a Camille and Henry Dreyfus Teacher/Scholar Award, an Alfred P. Sloan Foundation Research Fellowship and a National Institutes of Health Research Career Development Award.

REFERENCES

- [1] a) D.K. LAVALLEE, B. ANDERES, *Inorg. Chim. Acta*, **79**, 213 (1983);
b) B. ANDERES, D.K. LAVALLEE, *Inorg. Chem.*, **22**, 2665 (1983).
- [2] M. ERECINSKA, in B. CHANCE, D. DeVULT, H. FRAUENFELDER, R.A. MARCUS, J.R. SCHREIFFER, N. SUTIN (eds.), «Tunneling in Biological Systems», Academic Press, New York, 1979, p. 453, and references therein.
- [3] S.K.S. ZAWACKY, H. TAUBE, *J. Am. Chem. Soc.*, **103**, 3379 (1981).
- [4] M.K. GENO, J.H. DAWSON, *Inorg. Chem.*, **23**, 1182 (1984).
- [5] a) N.S. HUSH, *Prog. Inorg. Chem.*, **8**, 391 (1967);
b) N.S. HUSH, *Electrochem. Acta*, **13**, 1005 (1968);
c) M.B. ROBIN, P. MAY, *Adv. Inorg. Chem. Radiochem.*, **10**, 247 (1967).
- [6] a) R.W. CALLAHAN, R.F. KEENE, T.J. MEYER, D.J. SALMON, *J. Am. Chem. Soc.*, **99**, 1064 (1977).
b) R.W. CALLAHAN, T.J. MEYER, G.M. BROWN, *J. Am. Chem. Soc.*, **96**, 7829 (1974).



PS5.47 — TH

DONALD W. JACOBSEN

Department of Cardiovascular Research
The Cleveland Clinic Foundation
9500 Euclid Avenue, Cleveland, Ohio 44106
U.S.A.

RALPH GREEN

Department of Laboratory Hematology
The Cleveland Clinic Foundation
9500 Euclid Avenue, Cleveland, Ohio 44106
U.S.A.

SYNTHESIS OF METHYLCOBALAMIN FROM THE GLUTATHIONE-COBALAMIN COMPLEX

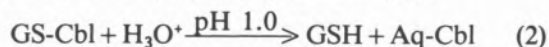
Mechanistic details on the conversion of vitamin B12 (cyanocobalamin, CN-Cbl) to its coenzyme forms adenosylcobalamin (Ado-Cbl) and methylcobalamin (Me-Cbl) by mammalian cells are largely unknown. Some information is available on Ado-Cbl formation by prokaryotes (reviewed in [1]), but the origin of Me-Cbl, the principal circulating Cbl in man, is obscure. Twenty years ago WAGNER and BERNHAUER proposed that the glutathione-cobalamin complex GS-Cbl might serve as a precursor for Cbl coenzymes based on its reactivity with alkylating agents [2]. We have recently obtained evidence that GS-Cbl is a naturally occurring intracellular Cbl in murine L1210 cells [3]. This paper concerns the reactivity of synthetic GS-Cbl in model systems for Me-Cbl formation.

GS-Cbl was prepared by reacting a 10-fold molar excess of glutathione (GSH) with hydroxocobalamin (HO-Cbl) in 0.10 M sodium acetate pH 4.5 (Reaction (1)). This complex was purified from excess



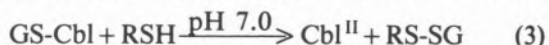
GSH by gel filtration on a 2.5 × 50 cm P2 polyacrylamide (Bio-Rad) column, or for smaller levels (<1 μmole) of GS-Cbl, on Sep-Pak C₁₈ cartridges (Waters/Millipore). The isolated complex had principal absorbance bands at 534, 428, 372,

and 289 nm (pH 7.0) and was relatively stable if stored anaerobically in the dark at pH 4.5. At lower pH (<2) the complex rapidly hydrolyzed to aquocobalamin (Aq-Cbl) (Reaction (2)).



At elevated temperature (80°C), GS-Cbl underwent thermolytic decomposition to Aq-Cbl. Since intracellular Cbls are usually extracted at elevated temperatures, this may explain why GS-Cbl has not been observed in the past.

In the presence of other thiols, GS-Cbl is very unstable and decomposes to what appears to be cob(II)alamin (Cbl^{II}) spectrophotometrically (Reaction (3)). If Reaction (3) is carried out in the



presence of methyl iodide (MeI), the final spectrum appears to be a complex mixture of products (Fig. 1). When analyzed by HPLC, the major Cbl

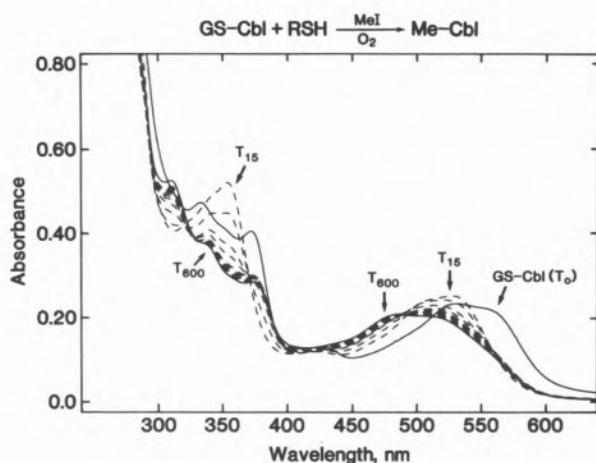


Fig. 1

Formation of Me-Cbl from GS-Cbl in the presence of MeI. The main cuvette compartment contained 2.5 ml of 25 μM GS-Cbl in 0.1 M NaHCO_3 (pH 9.0). The reaction was initiated by adding MeI and 2-mercaptoethanol to final concentrations of 25 mM and 50 mM, respectively. Spectra were recorded every 15 sec on a Hewlett-Packard 8450A diode array UV-visible spectrophotometer

product was identified as Me-Cbl (Fig. 2). Further proof of its formation was obtained by photolyzing the reaction mixture prior to HPLC. After photolysis the Me-Cbl peak disappeared and the Aq-Cbl peak increased proportionately (Fig. 2). Me-Cbl can also be formed in this model system

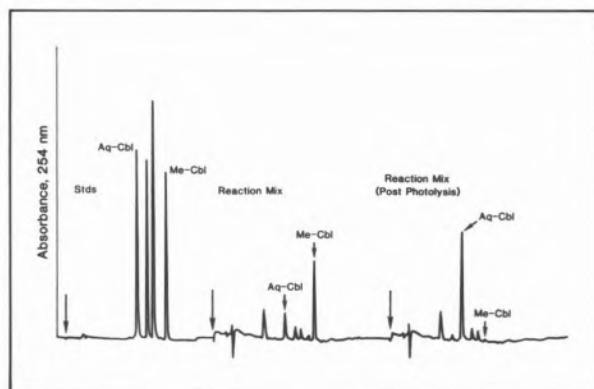
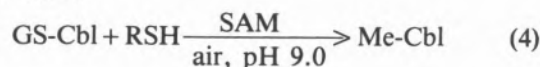


Fig. 2

Identification of Me-Cbl in Reaction Mixtures by HPLC. The reaction mixture from Fig. 1 was passed through an activated Sep-Pak C_{18} cartridge. Corrinoids were then eluted with 50% acetonitrile and concentrated to dryness. The residue was dissolved in 100 μl of water, clarified by centrifugation and analyzed (20 μl aliquots) by gradient HPLC according to JACOBSEN et al. [3]. A portion of the reaction mixture was exposed to light from a tungsten-filament bulb (300 W) for 30 min prior to HPLC

in the presence of the physiological methyl donor S-adenosylmethionine (SAM) (Reaction (4)). These studies demonstrate that intracellular GS-Cbl could serve



as a substrate for Me-Cbl biosynthesis in mammalian cells.

REFERENCES

- [1] F.M. HUENNEKENS, K.S. VITOLS, K. FUJII, D.W. JACOBSEN, in D. DOLPHIN (ed.), «B12», vol. I, Wiley, New York, 1982, pp. 145-167.
- [2] F. WAGNER, K. BERNHAUER, *Ann. N.Y. Acad. Sci.*, **112**, 580 (1964).
- [3] D.W. JACOBSEN, R. GREEN, E.V. QUADROS, Y.D. MONTEJANO, *Anal. Biochem.*, **120**, 394 (1982).



PS5.48 — MO

KENNETH L. BROWN
JANETTE M. HAKIMI

Department of Chemistry
The University of Texas at Arlington
Arlington, Texas 76019
U.S.A.

DONALD W. JACOBSEN
Division of Biochemistry
Department of Basic and Clinical Research
Scripps Clinic and Research Foundation
La Jolla, California 92037
U.S.A.

³¹P-NMR STUDIES OF COBALAMINS

³¹P-NMR observations of aquocobalamin (H₂OCbl) in H₂SO₄/H₂O mixtures show that both the base-on and base-off species may be observed and quantitated. Correlation of the base-off ³¹P-chemical shifts with a generalized acidity function [1] gives values of -1.59 and -0.09 for

the two macroscopic pK_a's for phosphodiester deprotonation, virtually identical to the values previously obtained for base-off CNCbl and CH₃Cbl (Table, [2]). Similar observations of several other base-off cobalamins (Table) show that all the base-off cobalamins have the same phosphodiester macroscopic pK_a's (-1.59 ± 0.02 and -0.04 ± 0.02) and the same chemical shifts for the phosphodiester protonated (-339.88 ± 3.80 Hz) and deprotonated (-36.70 ± 2.80) base-off species. However, the base-on species of these cobalamins have chemical shifts that vary (from -50.16 to +9.37 Hz) in a regular way with the apparent free energy of coordination of the dimethylbenzimidazole ligand (ΔG_{Co}, Table) so that Δδ_{31P} (the difference in chemical shift between the base-on and base-off species) is a linear function of -ΔG_{Co} (slope = 7.93 ± 0.40 Hz kcal⁻¹mol, intercept = -28.06 ± 1.90 Hz, correlation coefficient r² = 0.964). In addition, both the chemical shift of the base-on species and the value of Δδ_{31P} are linearly related to the axial Co-N bond length for adenosylcobalamin (AdoCbl), d_{Co-N(Bz)} = 2.24 Å [3], CH₃Cbl, 2.14 Å [4] and CNCbl, 2.06 Å [5].

These results may be interpreted in terms of the

Table
³¹P-Chemical Shifts and Phosphodiester Macroscopic pK_a's of Cobalamins^{a)}

Cobalamin	pK _{base-off} ^{b)}	ΔG _{Co} ^{c)}	Base-Off Species					Δδ _{31P} ^{e)}
			pG ₄	pG ₅	Phosphodiester Protonated δ _{31P} ^{d)}	Phosphodiester Deprotonated δ _{31P} ^{d)}	Base-on δ _{31P} ^{d)}	
CH ₃ (CH ₂) ₂ Cbl	4.10	- 1.97	-1.58	-0.05	-337.76	-38.10	-50.16	-11.98
AdoCbl	3.67	- 2.57	—	—	—	-36.70	-47.15	-10.44
NC(CH ₂) ₃ Cbl	3.50	- 2.81	-1.60	-0.02	-342.14	-36.63	-43.66	- 7.03
CH ₃ Cbl	2.89	- 3.64	-1.62	-0.02	-335.43	-38.47	-35.66	2.81
CF ₃ CH ₂ Cbl	2.60	- 4.04	-1.56	-0.02	-345.50	-33.51	-32.91	0.60
CF ₂ HCbl	2.15	- 4.66	-1.61	-0.03	-342.31	-33.47	-25.58	7.89
NCCH ₂ Cbl	1.81	- 5.19	-1.60	-0.02	-342.14	-34.33	-25.91	8.42
CF ₃ Cbl	1.44	- 5.62	—	—	—	-36.70	-11.99	24.71
CNCbl	0.10	- 7.44	-1.57	-0.04	-335.81	-37.40	- 1.72	35.68
H ₂ OCbl	-2.13	-10.48	-1.59	-0.09	-337.10	-41.64	- 0.37	51.01
Average:			-1.59 ± 0.02	-0.04 ± 0.02	-339.88 ± 3.80	-36.70 ± 2.80		

a) 25 ± 1°C.

b) Apparent pK_a of the base-on-base-off reaction.

c) Apparent free energy of coordination of the free-base benzimidazole ligand.

d) In Hz, from external 85% H₃PO₄ (negative shifts upfield from the reference) at 80.988 MHz.

e) Difference in chemical shift (in Hz) between the base-on and base-off species.

work of GORENSTEIN [6-8] who has shown that the ^{31}P -chemical shift of phosphate compounds is controlled by O-P-O bond angles. Thus, in base-on CH_3Cbl or $\text{CF}_3\text{CH}_2\text{Cbl}$ (Table) the conformation of the phosphodiester is apparently the same as that of all the base-off species and there is no difference in chemical shift between the base-on and base-off species. When coordination of the axial ligand is weaker (e.g., AdoCbl), lengthening of the axial Co-N bond causes a decrease in the RO-P-OR' bond angle and an upfield shift of the base-on ^{31}P -resonance. When the axial ligand coordination is tighter (e.g., CNCbl) the shortened axial Co-N bond causes an increase in the RO-P-OR' bond angle and a downfield shift in the base-on ^{31}P -resonance.

ACKNOWLEDGEMENTS

This research was supported by the Robert A. Welch Foundation, Houston, Texas, Grant Y-749 (K.L.B.) and the National Institutes of Health, Grant #AM25406 (D.W.J.).

REFERENCES

- [1] R.A. COX, K. YATES, *J. Am. Chem. Soc.*, **100**, 3861-3867 (1978).
- [2] K.L. BROWN, J.M. HAKIMI, *Inorg. Chem.*, **23**, 1756-1764 (1984).
- [3] P.G. LENHART, *Proc. R. Soc. London, Ser. A*, **303**, 45-84 (1968).
- [4] L.G. MARZILLI, P.J. TOSCANO, M. SUMMERS, L. RONDACCIO, N. BRESCIANI-PAHOR, J.P. GLUSKER, M. ROSSI, *Inorg. Chim. Acta*, **79**, 29 (1983), as presented at the 1st International Conference on Bioinorganic Chemistry, Florence, Italy, June 13-17, 1983.
- [5] D.C. HODGKIN, J. LINDSEY, R.A. SPARKS, K.N. TRUEBLOOD, J.G. WHITE, *Proc. R. Soc. London, Ser. A*, **266**, 494-517 (1962).
- [6] D.G. GORENSTEIN, *J. Am. Chem. Soc.*, **97**, 898-900 (1975).
- [7] D.G. GORENSTEIN, D. KAR, *Biochem. Biophys. Res. Commun.*, **65**, 1073-1080 (1975).
- [8] D.G. GORENSTEIN, *J. Am. Chem. Soc.*, **99**, 2254-2258 (1977).



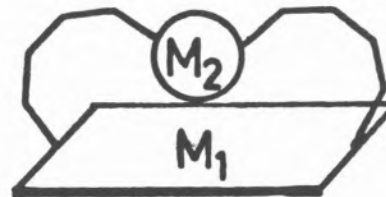
PS5.49 — TU

G. DUBOWCHIK
D. HEILER
A.D. HAMILTON
Department of Chemistry
Princeton University
Princeton, N.J. 08544
U.S.A.

SYNTHETIC PORPHYRINS CONTAINING ADJACENT, REDOX-ACTIVE SPECIES; MODELS OF BIOLOGICAL ELECTRON TRANSFER SITES

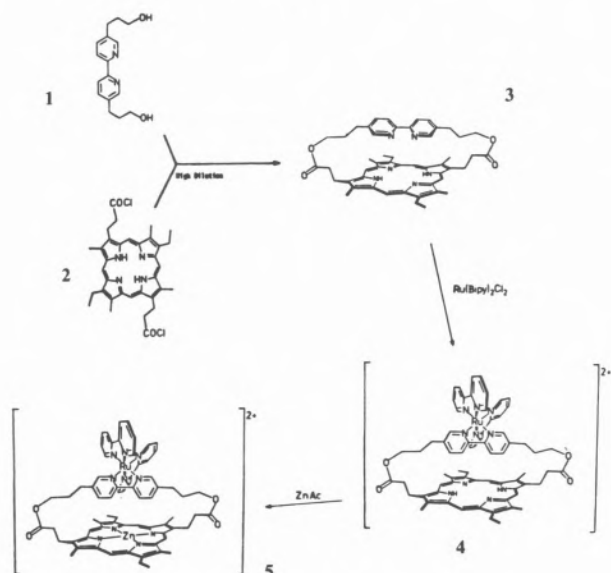
The remarkable diversity of function of hemes and chlorophylls in biochemistry is due, in large part, to changes in the surrounding protein environment. In systems which are involved in electron transport the nearby protein environment often includes other metal centers held in close proximity to the tetrapyrrole.

In an attempt to mimic some of the electron transport and photochemical charge separation properties of these centers we have prepared a series of model systems in which transition metals are covalently held a short distance from a metalloporphyrin.



The first binucleating ligand involves a 2,2'-bipyridine unit strapped across the face of a porphyrin. 5,5'-bis(3-hydroxypropyl)-2,2'-bipyridine (**1**) is prepared in six steps from β -picoline. Reaction of **1** with mesoporphyrin-II diacid chloride under high dilution conditions yields the bipyridine-bridged porphyrin **3** in good yield. Heterobinuclear complexes of **3** can be readily formed in a two step sequence. Refluxing **3** with $\text{Ru}(\text{bipy})_2\text{Cl}_2$ in

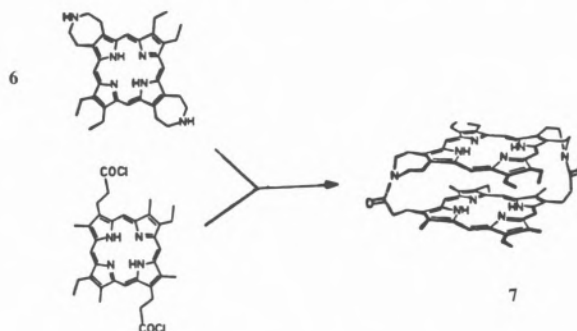
methanol gives the $\text{Ru}(\text{bipy})_3$ -porphyrin complex **4** with no insertion of ruthenium into the porphyrin. Treating **4** with zinc acetate affords heterobinuclear $\text{Ru}(\text{bipy})_3$ -zinc porphyrin (**5**).



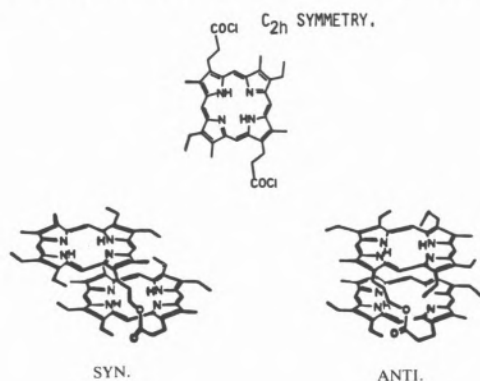
Electrochemical studies (cyclic voltammetry and differential pulse polarography) indicate that both metal centers are redox active. In addition, spectroscopic measurements indicate a strong interaction between the two chromophores. While the porphyrin luminescence is unperturbed, the emission from the lowest lying metal to ligand charge transfer band is quenched. The synthesis, physical properties and biological relevance of these novel binuclear complexes will be presented. Also the extension of this work to other transition metal complexes and to tri-, tetra- and polynuclear homologues will be discussed.

The second binucleating ligand relates to the multi-chlorophyll structures of photosynthetic reac-

tion centers and involves two or more covalently linked tetrapyrroles. In order to overcome the problems of diastereoisomerism that result when porphyrins of C_{2h} symmetry are cofacially linked (e.g. Fig. 2) we have synthesized diaminoporphyrin (**6**). This species has D_{2h} symmetry and when coupled to mesoporphyrin-II diacid chloride (**2**) provides a diastereomerically pure cofacial porphyrin dimer (**7**). The NMR spectrum of **7** shows the porphyrin NH proton signals at -8 ppm, equivalent to an inter-porphyrin distance of 4.5 \AA . The optical spectrum exhibits a blue-shif-



ted Soret peak (by 16 nm) characteristic of strong exciton coupling between the macrocycles. Various transition metal complexes of **7** have been prepared. They will be discussed in addition to the synthesis and properties of dimer **7**. The synthesis of cofacial porphyrin trimers using this strategy is under active investigation.





PS5.50 — MO

B. SZPOGANICZ

J.R. MOTEKAITIS

Departamento de Química
Universidade Federal de Santa Catarina
88000-Florianópolis-SC
Brazil

A.E. MARTELL

Department of Chemistry
Texas A & M University
College Station, Texas 77843
U.S.A.

**METAL ION — AND VITAMIN B₆ —
CATALYZED TRANSAMINATION
AND DEPHOSPHONYLATION
OF 2-AMINO-3-PHOSPHONOPROPIONIC
ACID**

Kinetic studies have been carried out for reactions of Schiff bases (SB) formed from pyridoxal 5'-phosphate (PLP) and 2-amino-3-phosphonopropionic acid (APP): 1:1:x Zn(II)-SB-PDA system where PDA is 2,6-pyridinedicarboxylic acid; 1:2 Ga(III)-SB system; and 1:2 Al(III)-SB system). Formation and disappearance of a ketimine intermediate and its complexes were followed by proton NMR and ³¹P NMR. The reaction occurs in two distinct sequential steps: transamination and dephosphonylation. The specific rate constants for individual species of the metal-free systems are: $k_{H_4SB} = 1.64 \times 10^{-4} \text{ s}^{-1}$, $k_{H_3SB} = 7.56 \times 10^{-5} \text{ s}^{-1}$, and $k_{H_2SB} = 2.34 \times 10^{-5} \text{ s}^{-1}$ for the transamination step. The values for k_{HSB} and k_{SB} are about zero. The corresponding dephosphonylation rate constants $k'_{H_4SB} = 4.27 \times 10^{-6} \text{ s}^{-1}$, $k'_{H_3SB} = 1.26 \times 10^{-6} \text{ s}^{-1}$ and $k'_{H_2SB} = 6.84 \times 10^{-7} \text{ s}^{-1}$ were determined for the dephosphonylation step. The values for k'_{HSB} and k'_{SB} are about zero. Transamination and dephosphonylation proceed more rapidly for the Ga(III) complexes than for those of Al(III) and Zn(II). The specific rate constants in the transamination step for the individual species of 1:2 Ga(III)-SB system are: $k_{Ga(H_3SB)_2} = 4.66 \times 10^{-4} \text{ s}^{-1}$, $k_{Ga(H_5SB)_2} = 3.51 \times 10^{-4}$

s^{-1} ; $k_{Ga(H_2SB)_2} = 3.13 \times 10^{-4} \text{ s}^{-1}$ and $k_{Ga(SB)_2} = 3.12 \times 10^{-5} \text{ s}^{-1}$. The specific rate constants for the dephosphonylation step are: $k'_{Ga(H_5SB)_2} = 5.2 \times 10^{-6} \text{ s}^{-1}$; $k'_{Ga(H_2SB)_2} = 5.20 \times 10^{-6} \text{ s}^{-1}$; $k'_{Ga(H_3SB)_2} = 5.17 \times 10^{-6} \text{ s}^{-1}$; $k'_{Ga(HSB)_2} = 5.09 \times 10^{-6} \text{ s}^{-1}$; $k'_{GaH(SB)_2} = 2.53 \times 10^{-6} \text{ s}^{-1}$ and $k'_{Ga(SB)_2} = 4.92 \times 10^{-7} \text{ s}^{-1}$. The results show that the most active species are those in which the carboxylate group of the amino acid moiety of the SB ligand is coordinated to the metal ion and the phosphonate is not coordinated.

ACKNOWLEDGEMENT

B.S. thanks CNPq (Brazil) for financial support.

REFERENCES

- [1] B. SZPOGANICZ, A.E. MARTELL, *J. Am. Chem. Soc.*, **106**, 5513 (1984).
- [2] B. SZPOGANICZ, A.E. MARTELL, *Inorg. Chem.*, in press.
- [3] B. SZPOGANICZ, A.E. MARTELL, *Inorg. Chem.*, submitted for publication.
- [4] B. SZPOGANICZ, A.E. MARTELL, *Inorg. Chem.*, submitted for publication.



PS5.51 — TU

V. MORENO

Departamento de Química Inorgánica
Facultad de Ciencias
Tarragona
Spain

E. MOLINS

A. LABARTA

A. CAUBET

J. TEJADA

Facultad de Física
Universidad de Barcelona
Spain

SYNTHESIS, MÖSSBAUER AND MAGNETIC CHARACTERIZATION OF SOME IRON(III)-NUCLEIC ACID COMPONENTS (NUCLEOTIDE, NUCLEOSIDE AND BASE)

New synthesis of iron(III)-nucleic acid components have been carried out. The characterization of these compounds has been done by means of Mössbauer and magnetic measurements, UV-Visible and infrared spectra.

The study of the different mechanisms of interactions between the central cation (Fe^{3+}) and the components of nucleic acids is of major interest in life science [1]. Therefore it is very important to relate the data obtained by using microscopic and macroscopic techniques in order to establish the correlation between physical properties and biological behaviour [2].

In this paper we show some results [3] of our research in the field of metal-DNA compounds interaction.

In Table I we list the compounds which have been studied.

Table I

Compound	Q.S. (mm/s)	I.S. (mm/s)
Fe-adenosine	0.59	0.28
Fe-cytosine	0.64	0.26
Fe-hipoxantine	0.65	0.29
Fe-guanine	0.61	0.28
Fe-ATP	0.59	0.29

An aqueous solution of $\text{FeCl}_2 \cdot 4\text{H}_2\text{O}$ was mixed with a nucleotide, nucleoside or base solution keeping the pH values below 6. All the complexes were precipitated by addition of EtOH, filtered and dried "in vacuo".

UV-Visible and infrared spectra were recorded for all the compounds obtained.

Mössbauer spectroscopic measurements at room temperature were registered using a conventional apparatus. The single line source used was ^{57}Co (10 mCi) in a Rh matrix.

Magnetic susceptibility measurements were made in a Faraday type balance in the temperature range 80-300 K and in fields up to 10 kG.

In Fig. 1 we show Mössbauer spectra of some of the synthesized compounds. All the spectra consist of two lines with identical intensity and width and have been interpreted in terms of the existence of a quadrupole doublet corresponding to Fe^{3+} .

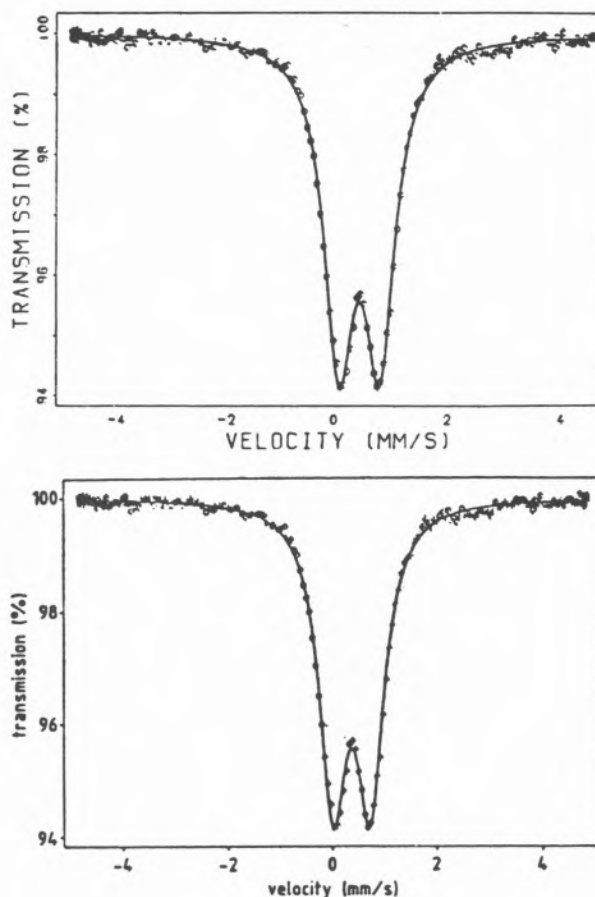


Fig. 1

Mössbauer spectra of a) Fe-Hipoxantine and b) Fe-ATP

The corrected molar susceptibilities $\chi_M^{-1}(T)$ have been fitted in the framework of the Curie-Weiss law. The values of the atomic dipolar magnetic moments (μ) and the Curie temperatures (θ) of the different compounds have been obtained from a least squares computed fit of $\chi_M^{-1}(T)$.

Both the isomer shift values (I.S.) and the dipolar magnetic moment values correspond to a high spin Fe(III)- $6S_{5/2}$ configuration. The positive values of the Curie temperatures suggest that an antiferromagnetic interaction between the Fe ions in these compounds does exist.

REFERENCES

- [1] a) D.J. HODGSON, *Prog. Inorg. Chem.*, **23**, 211-54 (1977);
 b) L.G. MARZILLI, *Prog. Inorg. Chem.*, **23**, 255-378 (1977);
 c) A. MOSSET, J.J. BONNET, J. GALY, *C.R. Acad. Sci. Paris*, **283**, 127 (1976).
- [2] G.L. EICHHORN (ed.), «Inorganic Biochemistry», Elsevier, 1973.
- [3] V. MORENO, A. TERRÓN, A. CAUBET, E. MOLINS, A. LABARTA, J. TEJADA, *Transition Met. Chem.*, in press.



PS5.52 — TH

C. ROSSI
 N. MARCHETTINI
 E. PERICCIOLI
 A. PRUGNOLA
 E. TIEZZI
 N. NICCOLAI
 Department of Chemistry
 University of Siena
 53100-Siena
 Italy

MAGNESIUM(II)-INDUCED EFFECTS ON THE STABILITY OF THE ADENOSIDE-THYMIDINE COMPLEX IN SOLUTION

Proton-carbon selective NOE measurements have been used to prove previously suggested conformations of model compounds [1] and biologi-

cal macromolecules [2,3]. The observation of through-space selective dipolar couplings between carbon and proton atoms allowed the derivation of the intermolecular distance in solution [3,4]. In this study the observed heteronuclear NOE values have been used to monitor the presence of Adenosine-Thymidine complexes. A particular attention has been devoted to value the presence of Watson-Crick-type and Hoogsteen-type base pairing. ^1H - ^{13}C heteronuclear Overhauser effects, obtained by selective perturbation of the resonance line of protons involved in hydrogen bonding, allowed the identification of intermolecular interaction patterns. These studies have been extended to monitor the effects induced on the stability of Adenosine-Thymidine complexes by the addition of magnesium ions to the solution.

Adenosine and Thymidine were obtained from Sigma Chemical Co., both nucleosides having been dissolved in 99.98% DMSO- d_6 to yield 0.5 M solutions. $\text{Mg}(\text{ClO}_4)_2$ (Merck) 0.25 M was used as the source of magnesium ions. All NMR measurements were made on a Varian XL-200 spectrometer. The temperature was held constant at 40°C. The nuclear Overhauser effect, which occurs whenever spectra are recorded under conditions of continuous broad-band proton decoupling (BB), causes intensity enhancements of carbon resonances. The observed NOEs are related to the relaxation parameters by the following equation:

$$\text{NOE}_{^{13}\text{C}}(\text{BB}) = (I_z - I_0) / I_0 = \frac{\gamma_H}{\gamma_C} \frac{\sum \sigma_i}{R_C} \quad (1)$$

where γ are the magnetogyric ratios, I_z and I_0 are peak intensities measured under continuous and gated decoupling conditions, R_C is the spin-lattice relaxation rate of the proton decoupled carbon resonance and σ_i are the cross-relaxation contributions which occur between carbon and proton nuclei.

Upon selective saturation of a proton H_a which dipolarly interacts with a ^{13}C nucleus C_b , at a distance r_{ab} , the $\text{NOE}_{^{13}\text{C}_b}(\text{H}_a)$ can be described by the equation:

$$\begin{aligned} \text{NOE}_{^{13}\text{C}_b}(\text{H}_a) &= \\ &= \frac{1}{R_{^{13}\text{C}}} \frac{\hbar^2 \gamma_H^3 \gamma_C}{10 r_{\text{C-H}_a}^6} \left[\frac{6\tau_c}{1 + (\omega_H + \omega_c)^2 \tau_c^2} - \frac{\tau_c}{1 + (\omega_H - \omega_c)^2 \tau_c^2} \right] \end{aligned} \quad (2)$$

Selective proton-carbon NOEs, shown in Fig. 1A, were obtained by selective saturation of the NH_2 proton signal of Adenosine. The ^{13}C -NMR spectrum of the Adenosine-Thymidine system when no proton signal was perturbed is shown in Fig. 1B.

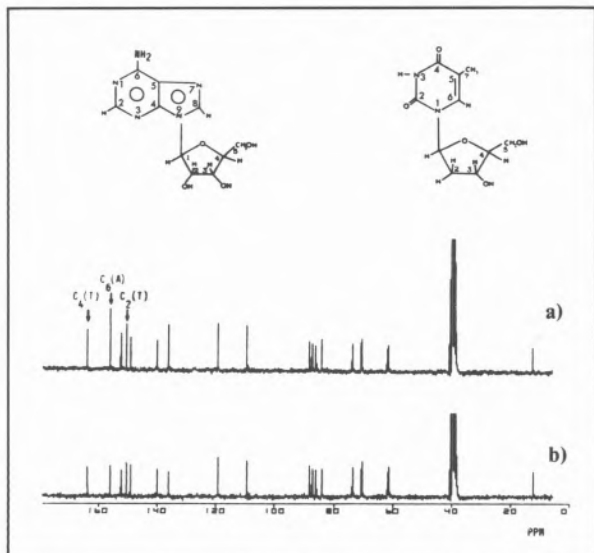


Fig. 1

^{13}C -NMR spectra of Adenosine-Thymidine in DMSO, a) obtained with the selective low power decoupler positioned at the $\text{NH}_2(\text{A})$ proton frequency and b) on a region where no proton signals were perturbed

The selective saturation of $\text{NH}_2(\text{A})$ protons generated carbon NOEs only on dipolarly coupled nuclei. These effects evidenced the presence of a magnetic interaction between $\text{NH}_2(\text{A})$ and $\text{C}_6(\text{A})$, and an intermolecular interaction between the irradiated $\text{NH}_2(\text{A})$ and the Thymidine carbonyl carbons $\text{C}_2(\text{T})$ and $\text{C}_4(\text{T})$. Such a possibility of detecting simultaneously the donor and acceptor moieties of hydrogen bonds is of primary importance for structural investigation on the Adenosine-Thymidine complex in solution.

The selective NOEs dependence on proton irradiation frequency observed for $\text{C}_4(\text{T})$ atom in the Adenosine-Thymidine and $\text{Mg}(\text{II})$ -Adenosine-Thymidine systems is shown in Fig. 2. Two maxima were observed when $\text{H}_3(\text{T})$ and $\text{NH}_2(\text{A})$ protons were irradiated. The latter effect confirmed the presence of an hydrogen bond between the $\text{C}_4(\text{T})$ carbonyl and the $\text{NH}_2(\text{A})$ aminic groups.

The addition of magnesium ions caused a strong reduction of the observed NOE on $\text{C}_4(\text{T})$ upon irradiation of $\text{NH}_2(\text{A})$. This fact suggested a com-

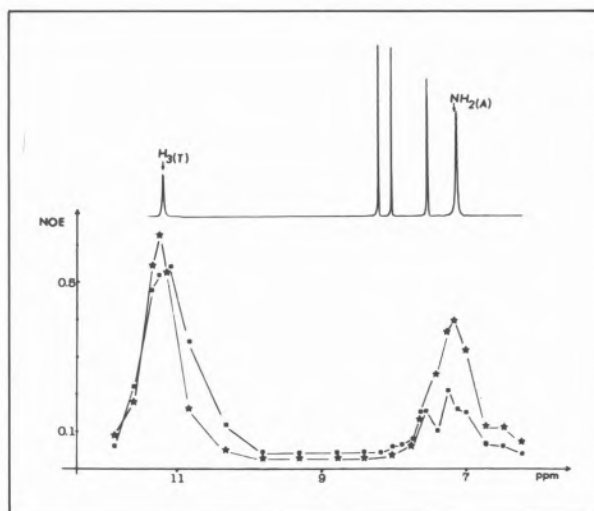


Fig. 2

Variation of the NOE effects on the $\text{C}_4(\text{T})$ carbon atom of Thymidine as a function of the proton irradiation frequency in the (★) Adenosine-Thymidine and (■) $\text{Mg}(\text{II})$ -Adenosine-Thymidine systems

petition between the $\text{NH}_2(\text{A})$ protons and the magnesium ions towards electron donor groups. As a consequence a drastic reduction of the stability of the Adenosine-Thymidine complex is observed.

It may be concluded that the carbon NOEs observed by selective irradiation of proton signals may yield powerful information on the specific interactions that take place between macromolecules in solution.

REFERENCES

- [1] N. NICCOLAI, L. POGLIANI, E. TIEZZI, C. ROSSI, *Nuovo Cimento Soc. Ital. Fis., D*, **3**, 993 (1984).
- [2] N. NICCOLAI, C. ROSSI, V. BRIZZI, W.A. GIBBONS, *J. Am. Chem. Soc.*, **106**, 5732 (1984).
- [3] N. NICCOLAI, C. ROSSI, P. MASCAGNI, P. NERI, W.A. GIBBONS, *Biochem. Biophys. Res. Commun.* (1984), in press.
- [4] P. MASCAGNI, N. NICCOLAI, C. ROSSI, W.A. GIBBONS, *J. Chem. Soc., Chem. Commun.* (1984), submitted for publication.



PSS.53 — TU

CARLOS F.G.C. GERALDES
 M. MARGARIDA C.A. CASTRO
 Chemistry Department
 University of Coimbra
 3000 Coimbra
 Portugal

A MULTINUCLEAR MAGNETIC RESONANCE STUDY OF THE INTERACTION OF MONONUCLEOTIDES WITH OXOCATIONS OF Mo(VI), W(VI) AND V(V) IN AQUEOUS SOLUTION

Metal ions play an important role in nucleic acid processes. Studies of the interaction between metal ions and nucleosides, nucleotides and related compounds [1] are therefore quite important. Nuclear Magnetic Resonance (NMR) is a powerful technique that has been extensively used in the determination of metal binding sites in these systems. The interaction of nucleosides and nucleotides with paramagnetic ions such as Mn^{2+} , Co^{2+} or Ni^{2+} has been extensively studied [1-5]. Diamagnetic systems have also been studied [1]; among these the study of the interaction of adeni- ne mononucleotides with the oxocation uranyl, UO_2^{2+} , using NMR [6] bears a special interest for the present work.

In this work we report proton, ^{13}C and ^{31}P NMR results on the interaction of purine and pyrimidine 5'-mononucleotides with oxocations of Mo(VI), W(VI) and V(V) in aqueous solution. Fig. 1 shows the 1H , ^{13}C and ^{31}P spectra of aqueous solutions containing 5'-AMP and sodium molybdate in different conditions of pH and ligand to metal ratio. These spectra show separate resonances for the

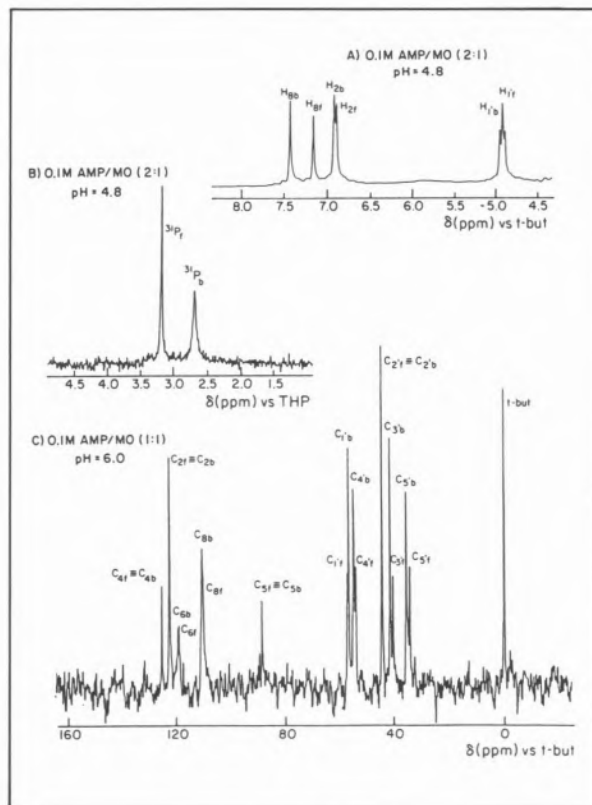


Fig. 1

Proton, carbon and phosphorus NMR spectra of 5'-AMP/Molybdate in aqueous solution as a function of pH and ligand-to-metal ratio

free and bound forms of AMP, in slow exchange. The area of the bound relative to the free signals increase when pH is dropped from 7.5 to 4.0, when the metal to ligand ratio is increased and when the total concentration of metal and ligand decreases. However a 1:1 mole solution of AMP and molybdate does not form a fully bound complex under any condition, indicating that complex formation and molybdate polymerization are competing processes [7]. The stoichiometry of the Mo(VI)-AMP complex is 1:1 as shown by the Job method using NMR signal areas.

The chemical shifts, Δ , induced by Mo(VI) binding to AMP are shown in Table 1. Most of the

Table 1
 Chemical shifts induced by Mo(VI) binding to 5'-AMP (pH=5.4)

Nucleus	H ₈	H ₂	H ₁ '	C ₈	C ₆	C ₅	C ₄	C ₂	C ₁ '	C ₂ '	C ₃ '	C ₄ '	C ₅ '	^{31}P
Δ (ppm) ^{a)}	-0.29	-0.03	-0.04	-0.37	-0.54	0	0	0	+0.58	0	-1.10	-0.81	-1.32	+0.50

a) A - sign indicates a low field shift.

shifts are to low field, and must be due to a combination of charge, magnetic anisotropy and polarization effects of the angular MoO_2^{2+} species. The relative magnitude of the shifts indicates that MoO_2^{2+} binds to an oxygen atom of the phosphate group, the oxygen atom of the ribose ring and possibly interacts with the adenine base through the N_7 and/or NH_2 group. However, molybdate does not bind to adenine in D_2O . UO_2^{2+} has been found [6] to bind to the phosphate and $-\text{OH}$ groups of 5'-AMP but not to the base. Further studies are in progress, using nucleosides, ribose, ribose-phosphates and the bases in order to define the binding sites of 5'-mononucleotides to molybdate.

We have observed similar interactions of 5'-AMP with tungstate, WO_4^{2-} , and vanadate, VO_4^- , in solution. However the percentage of metal complexes formed is always much smaller than with molybdate, possibly due to the more extensive polymerization of tungstate and vanadate in aqueous solution [7].

REFERENCES

- [1] G.L. EICHHORN, «Inorganic Biochemistry», Elsevier, N.Y., 1973.
- [2] M. COHN, T.R. HUGHES JR., *J. Biol. Chem.*, **237**, 176 (1962).
- [3] H. STERNLICH, D.E. JONES, K. KUSTIN, *J. Am. Chem. Soc.*, **90**, 7110 (1968).
- [4] G.P.P. KUNTZ, T.A. GLASSMAN, C. COOPER, T.J. SWIFT, *Biochemistry*, **11**, 538 (1972).
- [5] G. KOTOWYCZ, O. SUZUKI, *Biochemistry*, **12**, 3434 (1973).
- [6] R.P. AGARWAL, I. FELDMAN, *J. Am. Chem. Soc.*, **90**, 6635 (1968).
- [7] C.F. BAES, R.E. MESMER, «The Hydrolysis of Cations», Wiley, N.Y., 1976.



PSS.54 — TU

P. PUIG
A. TERRON
J.J. FIOL
Facultad de Ciencias
Universidad de Palma de Mallorca
Spain
V. MORENO
Facultad de Ciencias de Tarragona
Universidad de Barcelona
Tarragona
Spain

METAL COMPLEXES OF 3d IONS WITH 5'-AMP, 3'-AMP AND 2'-AMP: SYNTHESIS, CHARACTERIZATION AND STUDY OF RABBIT MUSCLE GLYCOGEN PHOSPHORYLASE b ACTIVATION

INTRODUCTION

As a follow-up to work on the synthesis and characterization of compounds of metal ions with nucleotides [1-4], complexes of Co(II), Co(III), Ni(II), Cu(II) and Zn(II) with 5'-, 3'- and 2'-AMP were prepared and were enzyme tested on rabbit muscle glycogen phosphorylase b as analogues of the allosteric activator.

RESULTS

The complexes were synthesized in a water medium and a dimethylsulfoxide medium. They were characterized by elementary C,H,N,P and metal analysis and by infrared, ultraviolet-visible and fluorescent spectroscopy.

The bonding of cations to nucleotides may be effected through the phosphate group, the ribose ring and the base. The Ns of the purine ring are right for the formation of covalent bonds with the metal ions; on the other hand, few complexes were observed between the ribose ring oxygens and a 3d cation. The nucleotide metal stability constants have a large component of electrostatic attraction

between the metal cation and the phosphate group [5]. In earlier studies [2] it was seen that the position of the phosphate group (5', 3' or 2') influenced the stability of the metal-N bond of the adenine ring.

From the study of the infrared spectra of the synthesized complexes, shiftings and changes in intensity were observed on the bands due to the purine ring, which seem to indicate metal ion-base interaction, probably through N(7), in accordance with crystallographic data [6].

On the 5'-AMP bands peculiar to the phosphate group, shiftings and splittings of the mode of stretching $\nu\text{-PO}_3^{2-}$ (deg) were observed in all the complexes except the $\text{Co}(5'\text{-AMP})\cdot 7\text{H}_2\text{O}$ and $\text{Co}(5'\text{-AMP})\text{NO}_3\cdot \text{C}_2\text{H}_6\text{SO}\cdot 5\text{H}_2\text{O}$ derivatives. This might indicate coordination to the phosphate group in the cases where splitting occurs.

For the complexes obtained with 3'-AMP it was observed that in the phosphate group vibration zone the only complex which does not present splitting of the $\nu\text{-PO}_3^{2-}$ (deg) band is the formula $\text{Co}(3'\text{-AMP})\cdot 3\text{H}_2\text{O}$ complex. This rules out direct metal-phosphate interaction in this complex and implies it in the others where splitting does occur. For the derivatives of 2'-AMP it was observed that, in the zone corresponding to the phosphate group, the only complex in which splitting of the band ascribable to the phosphate group degenerate stretching band occurs is the formula $\text{Co}(2'\text{-AMP})\cdot (\text{OH})_2\cdot 3\text{H}_2\text{O}$ complex. So this is the only one which seems to present direct metal cation-phosphate group interaction. Variations of the adenine bands were observed in all the cases. The ultraviolet-visible and fluorescent spectroscopy study is in conformity with the coupling of the metal ion to the purine ring in all cases [7].

ENZYME TEST

The test for the activity of rabbit muscle glycogen phosphorylase b in the presence of the 17 new synthesized complexes and of the $\text{Ni}(5'\text{-AMP})\cdot 6\text{H}_2\text{O}$ [6] and $\text{Cu}(5'\text{-AMP})\cdot 2\text{H}_2\text{O}$ [8] complexes already described in the literature resulted in the activation of the enzyme in the presence of the formula $\text{Co}(5'\text{-AMP})\cdot 7\text{H}_2\text{O}$, $\text{Ni}(5'\text{-AMP})\cdot 6\text{H}_2\text{O}$ and $\text{Co}(5'\text{-AMP})\text{NO}_3\cdot \text{C}_2\text{H}_6\text{SO}\cdot 5\text{H}_2\text{O}$ complexes.

The structural data in the literature [6] for the Ni(II) complex report the absence of direct Ni(II)-phosphate interaction and the infrared study leads to the same conclusion for the derivatives of cobalt which activate the enzyme. Since the structures of Cu(II) and Zn(II) complexes with nucleotides reveal the presence of direct metal cation phosphate group bonding, it may be concluded that there exists a direct correlation between the activation of the enzyme and the free phosphate group. The complexes synthesized with 3'-AMP and 2'-AMP do not activate the enzyme as it is an essential condition for the phosphate group to be coordinated in the 5'-position [9,10] as shown in earlier studies.

The conclusion of this study is that the activation of rabbit muscle glycogen phosphorylase b occurs through the 5'-AMP phosphate group in the presence of metal ions not directly coordinated to it.

REFERENCES

- [1] A. TERRON, V. MORENO, *Inorg. Chim. Acta*, **56**, L57 (1981).
- [2] A. TERRON, V. MORENO, *Inorg. Chim. Acta*, **80**, 213 (1983).
- [3] J.J. FIOL, A. TERRON, V. MORENO, *Inorg. Chim. Acta*, **83**, 69 (1984).
- [4] V. MORENO, A. TERRON, M. VICENS *et al.*, *Transition Met. Chem. (Weinheim, Ger.)*, in press.
- [5] T.M. THEOPHANIDES (ed.), «Infrared and Raman Spectroscopy of Biological Molecules», D. Reidel, Dordrecht, 1978.
- [6] A.D. COLLINS, P. DE MEESTER, D.M.L. GOODGAME, A.C. SPAPSKY, *Biochim. Biophys. Acta*, **402**, 1 (1975).
- [7] S. WATANABE, L. EVENSON, I. GULZ, *J. Biol. Chem.*, **238**, 324 (1984).
- [8] K. MASKOS, *Acta Biochim. Pol.*, **25**, 311 (1978).
- [9] GUTIÉRREZ MERINO, Tesis Doctoral, Universidad Complutense, Madrid.
- [10] T. OKAJAKY, A. NAZAKAWA, O. HAYAISHI, *J. Biol. Chem.*, **243**, 5266 (1968).



PS5.55 — TH

JANE E. FREW
 PETER JONES
 GEORGE SCHOLES
 Radiation and Biophysical Chemistry Laboratory
 The University
 Newcastle upon Tyne NE1 7RU
 U.K.

REACTION OF RADIOLYTICALLY FORMED HYDROPEROXIDES ON DNA AND PRECURSOR COMPOUNDS WITH REDOX-ACTIVE METAL IONS AND COMPLEXES

The exposure of oxygenated aqueous solutions of nucleic acids and related compounds to ionising radiation leads to the formation of peroxidic products (H_2O_2 and organic hydroperoxides). Analytical techniques [1] previously developed for determination of peroxides at concentrations of 10^{-6} – 10^{-5} mol dm^{-3} have allowed study of the post-radiolytic decay of such species in systems ranging in complexity from the pyrimidine bases to RNA and DNA.

The metal ion-catalysed decomposition of peroxides is a well documented phenomenon, and the possible involvement of contaminating metal ions in the decay processes was considered. The influence of both chelating agents and a variety of redox-active metal ions on peroxide stability has therefore been examined.

Preliminary data concerning the interaction of the glycopeptide antibiotic, bleomycin, with DNA hydroperoxide have been obtained. The results may have important implications with regard to synergism in the DNA-cleaving activities of bleomycin combined with ionising radiation.

REFERENCE

- [1] J.E. FREW, P. JONES, G. SCHOLES, *Anal. Chim. Acta*, **155**, 139 (1983).



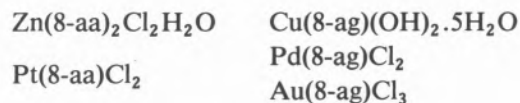
PS5.56 — MO

N. KATSAROS
 A. GRIGORATOS
 Chemistry Department
 Nuclear Research Center "Demokritos"
 Aghia Paraskevi, Athens
 Greece

TRANSITION METAL COMPLEXES WITH 8-AZAADENINE AND 8-AZAGUANINE

The biological properties of the azaderivatives of nucleic acid bases and nucleosides have been extensively studied and a number of them were found to be active chemotherapeutic agents. However very few reports have been published on complexes of metal ions with azapurines.

We have prepared and characterized a number of complexes of transition metal ions with 8-azaadenine and 8-azaguanine. These complexes were prepared by mixing equimolar aqueous solutions of the azapurines with the metal chloride or nitrate solution at an appropriate pH. On standing precipitated the complexes which were of the following composition:



These complexes were characterized by elemental analyses, conductivity and magnetic measurements, diffuse reflectance spectra and infrared spectroscopy. In the complexes prepared the 8-azapurines are acting as monodentate or bridging ligands, binding through the nitrogen of the imidazole ring.



PS5.57 — TU

JOLANTA SWIATEK
 KAZIMIERZ GASIOROWSKI
 Medical Academy of Wrocław
 Department of Basic Medical Sciences
 14 Kochanowskiego str., 51-601 Wrocław
 Poland
 HENRYK KOZŁOWSKI
 Institute of Chemistry
 University of Wrocław
 14 F. Joliot-Curie str., 50-383 Wrocław
 Poland

POLAROGRAPHIC AND SPECTROSCOPIC STUDY ON Pb^{+2} ION INTERACTION WITH DNA

The toxic effects of lead pollution seem to be already well established especially in the industrial countries [1]. The complexity of lead poisoning [2,3] was recently completed by the discovery of its carcinogenic actions in animals (for a review article, see ref. [4]). From the isotopic studies authors were not able, however, to establish whether metal ions are directly involved in DNA binding and if so which is the mode of lead binding to nucleic acid [5].

In this communication we present the polarographic and spectroscopic studies on the possible modes of interaction in the Pb^{+2} – DNA system.

RESULTS AND DISCUSSION

The lead-free DNA during a polarographic process in acetate buffer undergoes a reduction around -1.39 V. This process is usually assigned as a reduction of the adenine and cytosine residues of a double-stranded DNA molecule [6]. The relative height of a polarographic wave (h_{DNA}) is suggested to be a measure of a double-helical structure of nucleic acid [7,8].

Pb^{+2} – DNA solutions in 0.15 M acetate buffer

In the 0.15 M sodium acetate h_{DNA} reaches a value close to the maximum, which could indicate that

most of the studied DNA is in a double-helical structure. The increase of Pb^{+2} to phosphate molar ratio (P) changes distinctly the reduction potential of DNA from -1.398 V ($P=0.05$) to -1.443 V ($P=10$). The fact that the presence of Pb^{+2} ions causes a slight increase of h_{DNA} with time of solution storage and variation of the reduction potential of DNA may indicate that lead ions compete with sodium ions in the interaction with DNA and that the main interaction site is the phosphate site.

Pb^{+2} – DNA solutions in 0.05 M acetate buffer

Addition of Pb^{+2} ions to 0.05 M acetate buffer causes a distinct increase of h_{DNA} which depends on the Pb^{+2} ion concentration as well as on the time of DNA exposition on metal ions (Fig. 1). These results could clearly indicate the direct involvement of lead ions in the stabilization of a double-helical structure of DNA (increase of h_{DNA}).

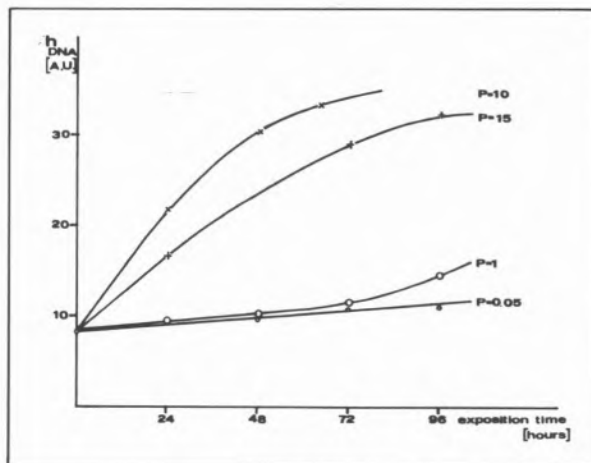


Fig. 1
 Dependence of h_{DNA} on Pb^{+2} concentration and on exposition time (solution storage) ($c_{DNA} = 25$ μ g/ml, 0.05 M acetate buffer)

The kinetics of this interaction is rather slow. The stabilizing effects of Pb^{+2} ions are supported by CD spectra. The results of CD spectra for $P > 10$ suggest the destabilizing effect of Pb^{+2} ions *i.e.* interaction with the base donors of DNA [9,10]. These results are supported also by the melting profiles for Pb^{+2} – DNA solutions (Table I). The data presented in Table I clearly show the stabilizing effects of lead ion of DNA for $P < 10$ and

for high excess of Pb^{+2} , decrease in T_m values, e.g. $69.2^\circ C$ for $P = 50$ (Table I), generally indicates the interaction of metal ion with bases of DNA, which destabilizes a double-helical structure [9]. A new phase transition appearing around $40^\circ C$ may indicate more specific interaction of Pb^{+2} ion with DNA.

Table I
 T_m values for Pb^{+2} -DNA solutions

P	T_m [$^\circ C$]
0	72.4
1	75.7
10	74.6
15	74.3
	$T_{m_1}^a = 37.0$
50	69.2
	$T_{m_1}^a = 41.0$

a) T_{m_1} temperature of the first phase transition.

CONCLUSIONS

Pb^{+2} ions interact with DNA in two different ways, i.e. via phosphate chain leading to stabilization of DNA and via base donors destabilizing a double-stranded structure. These results are supported also by the recent X-ray studies on Pb^{+2} interaction with RNA which has proved the involvement of base donors in metal ion binding [11].

REFERENCES

- [1] K.R. MAHAFFEY, *Federation Proc.*, **42**, 1730 (1983).
- [2] J.A. VALCIUKAS, R. LILIS, M. PETROCCI, *Amer. J. Industrial Med.*, **2**, 261 (1981).
- [3] J.A. VALCIUKAS, R. LILIS, *Int. Arch. Occup. Environ. Health*, **51**, 1 (1982).
- [4] M.R. MOORE, P.A. MEREDITH, *Arch. Toxicol.*, **42**, 87 (1979).
- [5] E. SABBIONI, E. MAFARANTE, *Chem.-Biol. Interactions*, **15**, 1 (1976).
- [6] V. BRABEC, *Bioelectrochem. Bioenerg.*, **8**, 437 (1981).
- [7] E. PALECEK in W.E. COHN (ed.), «Progress in Nucleic Acid Research and Molecular Biology», Academic Press, N.Y., vol. 18, 1976, p. 151.
- [8] E. PALECEK, F. JELEN, *J. Electroanal. Chem., Interfacial Electrochem.*, **116**, 317 (1980).
- [9] G.L. EICHORN, Y. AE SHIN, *J. Am. Chem. Soc.*, **90**, 7323 (1968).
- [10] Y.I. IVANOV, L.E. MINCHENKOVA, A.K. SCHYOLKINA, A.I. POLETAYEV, *Biopolymers*, **12**, 89 (1973).
- [11] R.S. BROWN, B.E. HINGERTY, J.C. DEWAN, A. KLUG, *Nature*, **303**, 543 (1983).



PS5.58 — TH

THOMAS D. TULLIUS
BETH A. DOMBROSKI
Department of Chemistry
The Johns Hopkins University
Baltimore, Maryland 21218
U.S.A.

USING A TRANSITION METAL COMPLEX TO MAKE AN IMAGE OF THE HELICAL TWIST OF DNA

We have developed a new method for determining the helical twist along a molecule of DNA of particular sequence. In this technique, a transition metal complex produces an image of the helicity of DNA, by fragmenting a DNA molecule bound to a flat inorganic surface. This method offers a rapid way of surveying the structure of any DNA molecule of moderate size, up to a few hundred base pairs in length. Such studies can be used to determine common motifs in the three-dimensional conformation of DNA that are not apparent at the level of simple base sequence. It is possible that regions of DNA important in biological regulation (promoters, for example) exist in conformations that have different helical twists from those of neighboring sequences [1], and could thus be recognized by proteins involved in regulatory processes.

RESULTS AND DISCUSSION

Our experiment is based on the determination by Rhodes and Klug of the helicity of DNA in solution, in which the enzyme deoxyribonuclease I (DNase I) was used to cut random sequence nucleosomal DNA bound to an inorganic surface (crystalline calcium phosphate, for example) [2]. The idea behind this experiment is that only certain bonds in the phosphodiester backbone are accessible to the nuclease; the backbone bonds near the inorganic surface are shielded from the enzyme, and are thus cut with much lower frequency

than the bonds exposed to the solvent. This modulation of enzyme cutting frequency results in a modulation of the band intensities in a gel electrophoretic separation of the reaction products. Such gels are capable of separating DNA molecules different in length by only one base, so all products are visualized. The periodicity of the sinusoidal modulation of cutting frequency (most easily visualized in a densitometer tracing of the autoradiograph of the electrophoresis gel) is directly related to the number of base pairs per turn of the DNA molecule. Rhodes and Klug found by their method that the helical twist of random sequence DNA is 10.6 base pairs per turn.

This method can't be used to map helicity along restriction fragments of particular sequence, though, because of the sequence specificity of DNase I. The many phosphodiester bonds of a particular DNA molecule are each cut to a different extent by DNase I, resulting in a highly non-uniform digestion pattern. We have found that the hydroxyl radical, produced by $\text{Fe}(\text{EDTA})^{2-}$ and hydrogen peroxide, is well suited as a DNA cutting reagent in such an experiment. Hydroxyl radical degrades DNA with no regard to sequence, by attacking the sugars of the DNA backbone and thereby breaking the chain [3].

In order to develop our method, we repeated the Rhodes and Klug experiment, using random sequence nucleosomal DNA bound to calcium phosphate crystals, and compared as cutting reagents DNase I and ferrous EDTA. Both reagents gave a sinusoidal modulation pattern of cutting, and both gave a helical periodicity of around 10.5 base pairs per turn. Fig. 1 shows a densitometer tracing of two of the lanes of an autoradiograph of the electrophoresis gel from this experiment, showing the comparison between the two cutting reagents. The iron reagent gives a pattern with shallower peaks and valleys than the DNase I pattern, undoubtedly due to the smaller size of hydroxyl radical. We found that it was critical to use a negatively-charged iron complex in this experiment; ferrous ion alone will fragment DNA bound to a surface, but with no modulation pattern. We think that positively-charged iron complexes can electrostatically associate with DNA, allowing hydroxyl radical production close enough to the DNA that even backbone bonds near the

surface can be cut. In contrast, the negatively-charged $\text{Fe}(\text{EDTA})^{2-}$ complex can't associate with the DNA, and the hydroxyl radical therefore can react only with the most sterically-accessible sites on the DNA molecule before the radical is quenched.

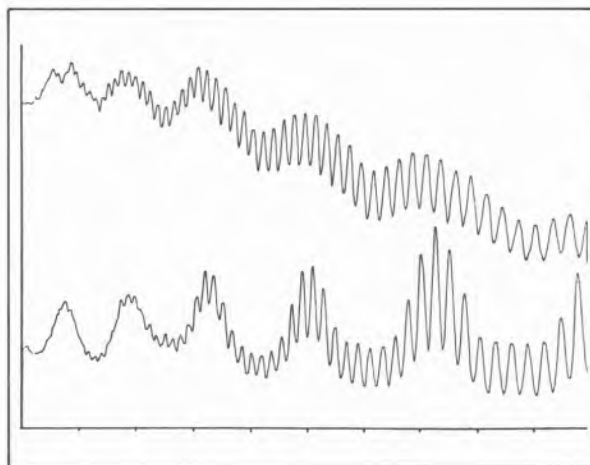


Fig. 1

Densitometer traces of two lanes of an autoradiograph of an electrophoresis gel, showing modulation patterns produced by $\text{Fe}(\text{EDTA})^{2-}$ (top) and DNase I (bottom) fragmentation of radioactively labeled nucleosomal DNA bound to a calcium phosphate precipitate

A key feature of our method is the lack of interaction of the cutting reagent with the DNA molecule. During our measurement of helical twist we wish to perturb the DNA structure as little as possible. Several other workers also have developed transition metal-based DNA cutting reagents [3-5], but their complexes each consist of a DNA intercalating group in close conjunction to a transition metal. These reagents, which depend for their utility on binding to DNA by intercalation, would not be suitable for our purpose, because the reagent itself would modify DNA structure upon binding.

Because of the uniformity of DNA backbone cutting by hydroxyl radical produced by $\text{Fe}(\text{EDTA})^{2-}$, our method can be used to determine the helical twist along DNA restriction fragments of particular sequence. Preliminary experiments have shown that we can indeed obtain smooth helical modulation patterns for such DNA molecules. These results will be reported in a subsequent publication.

EXPERIMENTAL SECTION

The reaction mixtures initially consisted of 2 μL of carrier DNA (1 μg), 3 μL of nucleosomal DNA (146 base pairs in length) labeled at the 5' ends with radioactive phosphorous, and 65 μL of a suspension of calcium phosphate precipitate. The calcium phosphate precipitate was prepared by mixing solutions of calcium chloride and potassium phosphate, in a Tris-chloride buffer of pH 8.0, to final concentrations of 26 mM phosphate and 16 mM calcium. The DNA was allowed to adsorb to the calcium phosphate precipitate for 1 hour; control experiments show that this is sufficient time for all DNA to be bound. To the mixture was then added the cutting reagent: either 0.2 units of DNase I, or 20 μL of 25 mM ferrous ammonium sulfate, 50 mM EDTA. To the iron-containing mixtures was then added 10 μL of 0.3% H_2O_2 to initiate the reaction. The reaction mixtures were incubated at 37°C for the appropriate times, quenched by addition of excess EDTA and thiourea (a hydroxyl radical scavenger), ethanol precipitated, dissolved in formamide-dye mixture, denatured, and electrophoresed.

ACKNOWLEDGEMENTS

We are grateful to the Chicago Community Trust/Searle Scholars Program, the Research Corporation, and the Biomedical Research Support Grant Program, Division of Research Resources, National Institutes of Health (Grant SO7 RR07041) for support of this work.

REFERENCES

- [1] C.R. CANTOR, A. EFSTRATIADIS, *Nucleic Acids Res.*, **12**, 8059 (1984).
- [2] D. RHODES, A. KLUG, *Nature*, **286**, 573 (1980).
- [3] R.P. HERTZBERG, P.B. DERVAN, *Biochemistry*, **23**, 3934 (1984).
- [4] J.K. BARTON, A.L. RAPHAEL, *J. Am. Chem. Soc.*, **106**, 2466 (1984).
- [5] B.E. BOWLER, L.S. HOLLIS, S.J. LIPPARD, *J. Am. Chem. Soc.*, **106**, 6102 (1984).



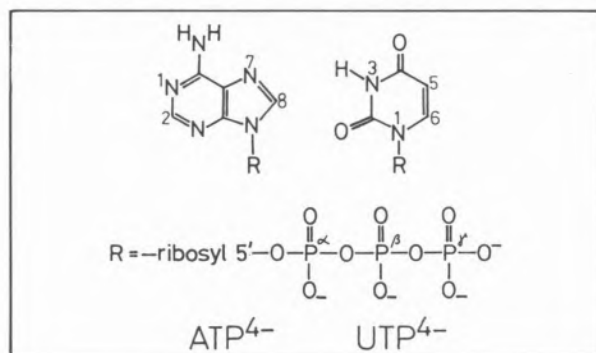
PSS.59 — MO

ROGER TRIBOLET
HELMUT SIGEL
Institute of Inorganic Chemistry
University of Basel
Spitalstrasse 51, CH-4056 Basel
Switzerland

SOLVENT-INFLUENCE ON THE INTRAMOLECULAR EQUILIBRIA OCCURRING IN COMPLEXES OF ADENOSINE 5'-TRIPHOSPHATE

Metal ion complexes of nucleotides are substrates for many enzymic reactions. In fact, nucleotides, especially adenosine 5'-triphosphate (ATP^{4-}), are quite versatile ligands [1-3]. Part of this versatility is connected with the occurrence of intramolecular equilibria in their binary and ternary complexes. To learn how the position of these equilibria is influenced by the polarity of the solvent, we have studied the effect of dioxane on the stability and structure of the complexes formed in the Cu^{2+} /1,10-phenanthroline (Phen)/ATP system. Such knowledge is important, because enzymic reactions usually take place in active-site cavities of proteins, and there is evidence [4] that the polarity in these cavities is decreased compared with the polarity of aqueous solutions.

The following results and conclusions are based on potentiometric pH titrations carried out in water and in 30% or 50% (v/v) dioxane-water mixtures ($I = 0.1$, NaClO_4 ; 25°C) [5]. For the eva-



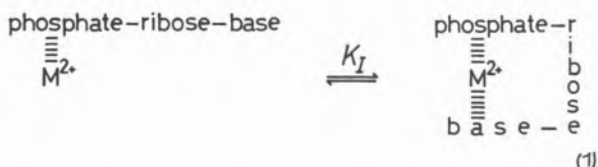
luation of many of the data it was necessary to study not only $\text{Cu}^{2+}/\text{Phen}/\text{ATP}$, but to include also the $\text{Cu}^{2+}/\text{Phen}/\text{uridine } 5'\text{-triphosphate (UTP}^{4-})$ system [5]. We are considering in the following the position of three intramolecular equilibria occurring with ATP complexes; all are affected by dioxane:

1) Location of the Proton in $\text{Cu}(\text{H}\cdot\text{ATP})^-$

The proton in $\text{Cu}(\text{H}\cdot\text{ATP})^-$ may be at N-1 of the adenine moiety or at the terminal γ -phosphate group; *i.e.* there is an equilibrium between isomeric complexes. In aqueous solution the isomer with the proton at N-1 is dominating, while in water-dioxane mixtures the complexes with the proton at the γ -phosphate are favored. This indicates, as one might expect, that with decreasing solvent polarity the formation of non-charged sites is promoted.

2) Extent of Macrochelate-Formation in $\text{Cu}(\text{ATP})^{2-}$

Equilibrium (1) involves for $\text{Cu}(\text{ATP})^{2-}$ an isomer with phosphate-coordination only, and a macrochelate, $\text{Cu}(\text{ATP})_{\text{cl}}^{2-}$, in which N-7 is also coordina-



ted to Cu^{2+} . The formation degree of this macrochelated isomer is influenced by dioxane as indicated:

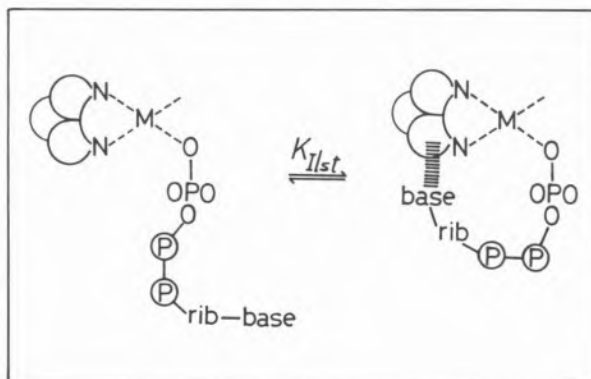
% (v/v) Dioxane:	0	30	50
% $\text{Cu}(\text{ATP})_{\text{cl}}^{2-}$:	68 ± 4	45 ± 6	24 ± 9

(the error limits correspond to an uncertainty of ± 0.05 in the log K values; see [5])

The concentration of the macrochelated isomer decreases evidently with increasing amounts of dioxane in the solvent mixture. This is probably the result of an increasing hydrophobic solvation of the adenine moiety of ATP^{4-} by the ethylene groups of dioxane, rendering the metal ion coordination to N-7 more difficult.

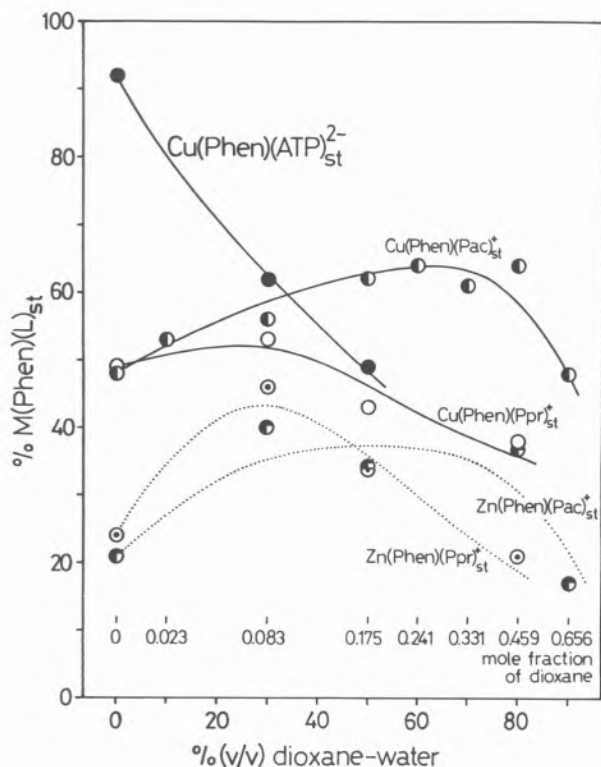
3) Intramolecular Stack-Formation in $\text{Cu}(\text{Phen})(\text{ATP})^{2-}$

The formation of an intramolecular, *i.e.* metal ion-bridged, stack between the aromatic rings of 1,10-phenanthroline and the adenine residue of ATP^{4-} is indicated in equilibrium (2):



The formation of the stacked isomer, $\text{Cu}(\text{Phen})(\text{ATP})_{\text{st}}^{2-}$, is affected by dioxane, but by far not as much as the binary adduct formed between Phen and ATP^{4-} . A change from water to 50% (v/v) dioxane-water decreases the stability of the binary $(\text{Phen})(\text{ATP})^{4-}$ adduct by a factor of $< 1/10$, while the metal ion-bridged ternary adduct is disfavored only by a factor of about $1/2$ (see figure).

The observation that dioxane influences the formation of intramolecular stacks differently than simple unbridged stacks is interesting and should be viewed in a wider frame: In the figure the formation degree of the intramolecular stack according to equilibrium (2) is plotted in dependence on the percentage of dioxane (added to an aqueous solution) for $\text{Cu}(\text{Phen})(\text{ATP})^{2-}$, as well as for $\text{M}(\text{Phen})(2\text{-phenylacetate})^+$ and $\text{M}(\text{Phen})(3\text{-phenylpropionate})^+$, where $\text{M} = \text{Cu}^{2+}$ or Zn^{2+} . It is evident that dioxane (or ethanol) [6] is even able to *promote* intramolecular stack formation in ternary Cu^{2+} or Zn^{2+} complexes; this contrasts with any experience regarding binary stacking adducts [5-7]. The reason for this observation must be connected with the presence of the metal ion; it appears that under certain structural conditions (the distance in the ligand between the coordinating atom and the stacking moiety is obviously important; see [5,6,8]) the stacked isomer is stabilized by the organic solvent molecules.



Figure

Formation degree of the intramolecular aromatic-ring stack (eq. (2)) in $\text{Cu(Phen)(ATP)}_2^{2-}$ and several other ternary complexes containing Cu^{2+} (full lines) or Zn^{2+} (dotted lines) in dependence on the percentage of dioxane added to the aqueous reagent mixture. The data are taken from refs. [5] and [6] ($I=0.1$; 25°C). Abbreviations: L, ligand; M, metal ion; Pac, 2-phenylacetate; Phen, 1,10-phenanthroline; Ppr, 3-phenylpropionate

ACKNOWLEDGEMENTS

The support of this work by the Swiss National Science Foundation is gratefully acknowledged.

REFERENCES

- [1] K.H. SCHELLER, F. HOFSTETTER, P.R. MITCHELL, B. PRIJS, H. SIGEL, *J. Am. Chem. Soc.*, **103**, 247-260 (1981).
- [2] K.H. SCHELLER, H. SIGEL, *J. Am. Chem. Soc.*, **105**, 5891-5900 (1983).
- [3] H. SIGEL, K.H. SCHELLER, R.M. MILBURN, *Inorg. Chem.*, **23**, 1933-1938 (1984).
- [4] H. SIGEL, R.B. MARTIN, R. TRIBOLET, U.K. HÄRING, R. MALINI-BALAKRISHNAN, submitted for publication.
- [5] R. TRIBOLET, R. MALINI-BALAKRISHNAN, H. SIGEL, *J. Chem. Soc., Dalton Trans.* (1985), in press.
- [6] H. SIGEL, R. MALINI-BALAKRISHNAN, U.K. HÄRING, submitted for publication.
- [7] a) K.A. CONNORS, S.-R. SUN, *J. Am. Chem. Soc.*, **93**, 7239-7244 (1971);
b) B. FARZAMI, Y.H. MARIAM, F. JORDAN, *Biochemistry*, **16**, 1105-1110 (1977).
- [8] H. SIGEL, R. TRIBOLET, K.H. SCHELLER, *Inorg. Chim. Acta*, **100**, 151-164 (1985).



PS5.60 — TU

W. KLEIBÖHMER

B. WENCLAWIAK

B. KREBS

Institute of Inorganic Chemistry

University of Münster, D-4400 Münster

F.R.G.

REACTION OF $[\text{cis-Pt}(\text{NH}_3)_2\text{Cl}_2]$ WITH RIBOSE DINUCLEOSIDE MONOPHOSPHATES. HPLC INVESTIGATION ON THE TIME DEPENDENT FORMATION OF THE REACTION PRODUCTS

The coordination of the aquated antitumor drug $[\text{cis-Pt}(\text{NH}_3)_2\text{Cl}_2]$ to the chromosomal DNA in the cell is generally accepted to be its primary way of action. Early investigations have shown that the preferred binding site is the N7 atom or occasionally the N1 atom of the purine bases and the N3 atom of the pyrimidine bases.

Even the reaction of $[\text{cis-Pt}(\text{NH}_3)_2\text{Cl}_2]$ (*cis*-DDP) with short DNA fragments like ApA, ApG, GpA and GpG results in a variety of products. The time dependent formation of these products has been investigated by reversed phase liquid chromatography. 1:1 mmolar ratios of the dinucleotides and *cis*-DDP have been reacted for several hours at 37°C in dark vials. Every hour a certain injection onto the column was chromatographed. The HPLC measurements of the reaction system ApA/*cis*-DDP show that two major products are formed during a reaction time of 48 hours. In the reaction system of GpA and *cis*-DDP we observe the formation of an intermediate with highest intensity after 13 hours. It was eluted after 30 minutes, whereas the major product peak is eluted after 16 minutes. The formation of an intermediate is also observed in the ApG/*cis*-DDP system. It has its maximum absorbance after 8 hours and is eluted after the main product peak. GpG forms

with *cis*-DDP only one product [1]. During a reaction time of 16 hours no intermediate can be observed. The major products were characterized with spectroscopic and other analytical methods.

REFERENCE

- [1] B. WENCLAWIAK, W. KLEIBÖHMER, B. KREBS, *J. Chromatogr.*, **296**, 395 (1984).



PS5.61 — TH

D. PRASEUTH
M.H. LANSARD
M. PERRÉE-FAUVET
A. GAUDEMER

Laboratoire de Chimie de Coordination Bioorganique, LA 255
Université Paris-Sud
91405 Orsay
France

I. SISSOÉFF
E. GUILLÉ

Laboratoire de Biologie Moléculaire Végétale, LA 40
Université Paris-Sud
91405 Orsay
France

INTERACTIONS OF WATER-SOLUBLE PORPHYRINS AND METALLOPORPHYRINS WITH NUCLEIC ACIDS AND DERIVATIVES — THE INFLUENCE OF THE METAL

Water-soluble cationic porphyrins and some of their metal derivatives are able to bind to DNA by intercalation and by external electrostatic association [1].

We have shown by thermal denaturation measurements and use of restriction enzymes that the intercalation is dependent on the geometry of the porphyrin: tetradentate metalloporphyrins bind more strongly than pentadentate ones, and specifically into G-C sequences. This is in agreement with the results obtained by PASTERNAK [2].

In order to define the nature and the strength of

the binding of cationic porphyrins and metalloporphyrins to DNA, the interactions of these porphyrins with DNA fragments have been investigated by an ^1H NMR method. High values are found for the association constants. It can be concluded that complexes with purine derivatives are more stable than complexes with pyrimidine ones and metalloporphyrins give more stable complexes than porphyrins free bases. Their stability is due to hydrophobic interactions in addition to electrostatic attractions. The complexes have all approximately the same geometry.

Water-soluble cationic porphyrins and metalloporphyrins have been tested in the photodegradation of the plasmid pBR 322 DNA, using visible light. Only the diamagnetic metalloporphyrins (Zn, Sn, Pd) and the porphyrins free bases are able to cleave pBR 322 DNA. This is in agreement with their $^1\text{O}_2$ quantum yield [3].

These results strongly suggest the possibility of using such porphyrins in the phototherapy of tumors.

REFERENCES

- [1] R.J. FIEL, B.R. MUNSON, *Nucleic Acids Res.*, **8**, 2835 (1980).
[2] R.F. PASTERNAK, E.J. GIBBS, J.J. VILAFRANCA, *Biochemistry*, **22**, 2406 (1983).
[3] J.B. VERLHAC, A. GAUDEMER, I. KRALJIC, *Nouv. J. Chim.*, **8**, 401 (1984).



PS5.62 — MO

ROBERT F. PASTERNAK

ESTHER J. GIBBS

Department of Chemistry

Swarthmore College

Swarthmore, PA 19081

and

Department of Chemistry

Goucher College

Towson, Maryland 21204

U.S.A.

INTERACTIONS OF WATER SOLUBLE PORPHYRINS WITH Z-POLY(dG-dC)

Two water soluble porphyrins, tetrakis(4-*N*-methylpyridyl)porphine and its copper(II) derivative (H₂TMpyP and CuTMpyP, respectively) have

been shown to interact with Z-poly(dG-dC) and to convert it back to the B-form. The fraction of Z-poly(dG-dC) remaining in a mixture depends linearly on the concentration of porphyrin per nucleotide base pair. Thus, there appears to be no "drug-drug" interaction in the conversion.

The kinetics of the conversion of Z- to B-DNA were studied via circular dichroism and ultraviolet absorption. The kinetics are biphasic and independent of porphyrin concentration until near-saturation conditions are approached. A very high order dependence on porphyrin ($n > 10$) is obtained under these conditions.

The kinetics of interaction of the porphyrins with Z-DNA were studied via stopped-flow with monitoring in the Soret region. At comparable concentrations of porphyrin and base pairs, the kinetic profile is monophasic and simple first order. As the concentration of base pairs is raised, the kinetics become second-order. These results will be interpreted in the poster.

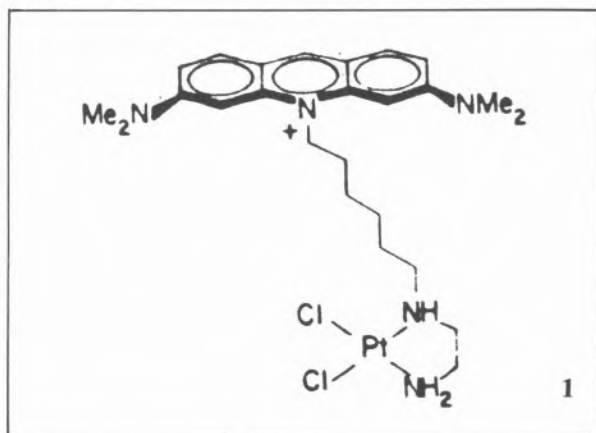


PSS.63 — TU

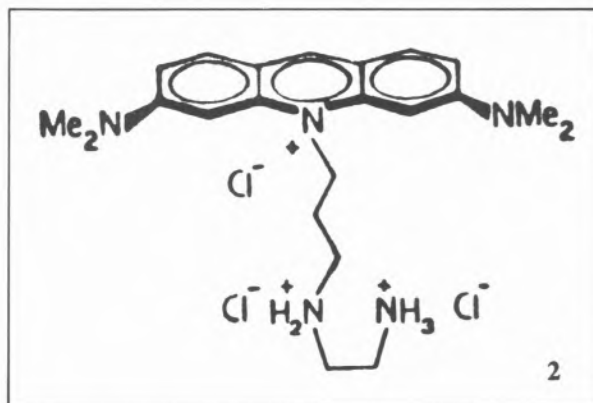
BRUCE E. BOWLER
STEPHEN J. LIPPARD
Department of Chemistry
Massachusetts Institute of Technology
Cambridge MA 02139
U.S.A.

EFFECTS OF LINKED AND EXTERNAL INTERCALATORS ON THE BINDING OF PLATINUM ANTITUMOR DRUGS TO DNA

Previously we showed that DNA intercalators, such as ethidium bromide, could alter the mode and position of binding of the platinum antitumor drug, *cis*-diamminedichloroplatinum(II) (*cis*-DDP), to the double helix [1]. These results led us to synthesize a molecule with an intercalative drug linked to a platinum complex by a hexamethylene chain [2], **1**, as a more sensitive probe of these effects. We have more recently synthe-



sized the related platinum binding ligand, **2**, in which a trimethylene chain links the acridine orange and ethylenediamine portions of the molecule [3]. When attached to platinum this new compound will allow us to probe the effects of chain length on the interaction of both ends of the molecule with DNA.



Exonuclease III mapping [4] was used to obtain information about the DNA binding sites of compound **1** on the same 165 base-pair (bp) restriction fragment from plasmid pBR322 employed in our previous *cis*-DDP/DNA mapping experiments [1a,4]. As a control we studied the binding sites of dichloroethylenediamineplatinum(II), [Pt(en)Cl₂], which is closely related to **1**, on the 165 bp fragment. We find that [Pt(en)Cl₂] binds to this restriction fragment at virtually the same oligo(dG) regions as does *cis*-DDP. Data for compound **1** also reveal binding at the same oligo(dG) sequences. Two other interesting results are observed, however. The 165 bp fragment contains a G₆CG₂ sequence near the 3'-end which is not observed as an exonuclease III stop at low levels of bound *cis*-DDP or [Pt(en)Cl₂] per nucleotide. Only when bound in the presence of the intercalator ethidium bromide are low levels of *cis*-DDP able to stop Exo III digestion at this sequence. Low levels of compound **1**, bound in the absence of ethidium bromide, definitely show stopping at this site. Thus the attached intercalator enhances platinum binding in this region in a manner similar to that by which externally added ethidium bromide enhances *cis*-DDP binding. This result probably involves relaxation of the steric requirements for platinum binding at this sequence through the conformational changes induced by intercalator binding to the DNA.

The other intriguing result is that additional stops are seen with compound **1** that correlate with (dG)₂ sequences on the unlabeled strand. For *cis*-DDP binding to the 165 bp restriction fragment, Exo III was found to map only those oligo(dG) binding sites on the labeled strand. The presence of the linked intercalator facilitates detection of

platinum bound on the unlabeled strand. This difference is ascribed to the more extensive interactions, both covalent (Pt) and intercalative (acridine), of compound 1.

In summary, exonuclease III mapping of compound 1 binding to DNA has shown that the attached intercalator alters the binding pattern of the platinum moiety in a manner analogous to that of an externally added intercalator. The presence of the attached intercalator also allows detection of binding sites on the unlabeled strand.

REFERENCES

- [1] a) T.D. TULLIUS, S.J. LIPPARD, *Proc. Natl. Acad. Sci. USA*, **79**, 3489 (1982);
b) C.M. MERKEL, S.J. LIPPARD, *Cold Spring Harbor Symp. Quant. Biol.*, **47**, 355 (1982).
- [2] B.E. BOWLER, L.S. HOLLIS, S.J. LIPPARD, *J. Am. Chem. Soc.*, **106**, 6102 (1984).
- [3] E. WHANG, B.E. BOWLER, S.J. LIPPARD, unpublished results.
- [4] T.D. TULLIUS, S.J. LIPPARD, *J. Am. Chem. Soc.*, **103**, 4620 (1981).



PS5.64 — TH

J.L. VAN DER VEER
G.J. LIGTVOET
A.R. PETERS
J. REEDIJK

Department of Chemistry
Gorlaeus Laboratories
State University Leiden
P.O. Box 9502, 2300 RA Leiden
The Netherlands

BINDING OF CIS-PLATINUM COMPOUNDS TO NUCLEOBASES, NUCLEOTIDES AND OLIGONUCLEOTIDES

For a better understanding of the specific interactions of *cis*-platinum(II) and *cis*-platinum(IV) compounds with DNA, detailed studies of the binding of such Pt compounds to nucleobases,

nucleotides and oligonucleotides are of great interest [1].

Although it is now generally accepted that binding of platinum compounds has a kinetic preference to guanine N7 sites, other bindings do also occur and may play an important rôle under certain conditions [2]. Using 9-ethylguanine as a simple analog of the GMP part in DNA, it was possible to study Pt(II) binding to guanine N1 and the — unexpected — rapid isomerisation to the N7 binding mode at acid pH values. Studying reactions of Pt(IV) compounds with 9-methylhypoxanthine and 5'-GMP, the major products appeared to be N7-coordinated Pt(II) adducts, although in a few cases spectroscopic indications for Pt(IV) adducts were found. Although it is not yet clear whether the reduction occurs before, during or after the platinum coordination to 5'-GMP, these results support the idea that *in vivo* reduction is essential for the antitumor activity of potential Pt(IV) antitumor drugs. To obtain more information about the chelation and kinetics of the so-called «GNG-*cis*Pt chelates» (platinum bound to both G's with a non-coordinating nucleobase in between), the DNA-trinucleotides pGpGpG, GpApG and GpTpG were reacted with *cis*-PtCl₂(NH₃)₂ (*cis*Pt). NMR studies indicate that the pGpGpG trimer yields only pGpGpG(N7(1),N7(3)) while GpApG gives 80% GpApG(N7(1),N7(3)) and 20% GpApG(N7(2),N7(3)). HPLC studies showed that this ratio is temperature independent. Reaction of the monofunctional platinum compound [Pt(dien)Cl]Cl with these two trimers gives 100% pGpGpG(N7(1)), while 30% GpApG(N7(1)) and 70% GpApG(N7(3)) was obtained in the second case. *cis*Pt reaction with GpTpG resulted in only one chelate: GpTpG(N7(1),N7(3)). Apparently a GG-chelate is preferred by *cis*Pt over a GNG-chelate, but if no neighbouring G is available after the first binding, kinetic preference determinates the ultimate chelate, *i.e.* binding to AG may occur.

In vitro studies concerning *cis*Pt-DNA interactions indicate that next to GG-, AG-chelation is most favoured [3]. This led to the study of the reactivity of *cis*Pt towards the decamer TpCpTpCpApGpTpCpTpC, and the stability of this decamer with its complement GpApG-

pApCpTpGpApGpA as compared to the unplatinated decamer duplex. Enzymatic degradation, atomic absorption spectroscopy together with HPLC showed that the AG-chelate is the major product.

ACKNOWLEDGEMENTS

The investigations were supported in part by the Netherlands Foundation of Chemical Research (SON) with financial aid from the Netherlands Organisation for the Advancement of Pure Research (ZWO), through grant 11-28-17.

REFERENCES

- [1] A.T.M. MARCELIS, J. REEDIJK, *Recl. Trav. Chim. Pays-Bas*, **100**, 1210 (1983).
- [2] R.B. MARTIN in S.J. LIPPARD (ed.), «Platinum, Gold and other metal chemotherapeutic agents», *ACS Symposium Series*, **209**, 231-244 (1983).
- [3] A.M.J. FICHTINGER-SCHEPMAN, J.L. VAN DER VEER, J.H.J. DEN HARTOG, P.H.M. LOHMAN, J. REEDIJK, *Biochemistry*, in press.



PS5.65 — MO

JIŘÍ KOZELKA

GREGORY A. PETSKO

STEPHEN J. LIPPARD

Department of Chemistry
Massachusetts Institute of Technology
Cambridge, Massachusetts 02139
U.S.A.

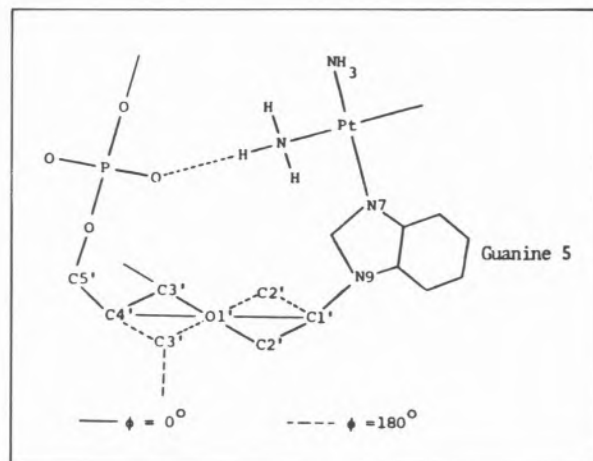
GARY J. QUIGLEY

Department of Biology
Massachusetts Institute of Technology
Cambridge, Massachusetts 02139
U.S.A.

MOLECULAR MECHANICS CALCULATIONS ON *cis*-DIAMMINEDICHLOROPLATINUM(II) ADDUCTS OF TWO d(GpG)-CONTAINING OLIGONUCLEOTIDE DUPLEXES

There is increasing evidence that the antitumor drug *cis*-diamminedichloroplatinum(II) (*cis*-DDP) [1] binds predominantly to d(GpG) units of DNA

[2,3]. Since *cis*-DDP binding to DNA destroys substrate recognition for nucleases [3] and shortens the double helix [4], severe structural changes (e.g., unwinding) of DNA have been suggested [4]. On the other hand, NMR work on platinated octa- and decanucleotides, while confirming d(GpG)-Pt binding, offered evidence for duplex structure up to 28°C [5]. We have performed molecular mechanics calculations on two oligonucleotides, [d(GGCCGGCC)]₂ and d(TCTCGGTCTC)•d(GAGACCGAGA) in both A- and B-DNA conformations, as well as on adducts in which a [Pt(NH₃)₂]²⁺ fragment is coordinated to the N7 atoms of adjacent guanosine residues. The main results of the calculations are: i) the 5'-end coordinated guanine is predicted to tilt out of the base stack, destroying at least one of the amino hydrogen bonds involved in GC base pairing and considerably weakening the imino hydrogen bond; ii) a hydrogen bond, formed between one ammine ligand of the platinum atom and the 5'-phosphate group of the d(pGpG) unit, is indicated for both A- and B-DNA. This hydrogen bond closes a ring (shown below) in which the 5'-sugar is constrained to either of two twisted conformations with phase angles [6] close to 0° or



180°, respectively; iii) in B-DNA models, the coordination of *cis*-[Pt(NH₃)₂]²⁺ on a d(GpG) unit causes the 5'-guanosine to switch the sugar pucker to C(3')-endo. This conformation is stabilized by a stronger attraction between the platinum residue and the phosphate of d(GpG); iv) in B-DNA models, formation of a non-Watson-Crick inter-strand hydrogen bond between two guanines is

indicated. Implications of these results for the interpretation of spectroscopic data on *cis*-DDP-oligonucleotide adducts are discussed.

ACKNOWLEDGEMENTS

This work has been supported by the Schweizerischer Nationalfonds zur Forderung der wissenschaftlichen Forschung and the U.S. National Cancer Institute.

REFERENCES

- [1] a) B. ROSENBERG, L. VAN CAMP, J.E. TROSKO, V.H. MANSOUR, *Nature (London)*, **222**, 385-386 (1969);
b) Review:
S.J. LIPPARD, *Science*, **218**, 1075-1082 (1982).
- [2] a) P.J. STONE, A.D. KELMAN, F.M. SINEX, *Nature (London)*, **251**, 736-737 (1974);
b) T.D. TULLIUS, S.J. LIPPARD, *J. Am. Chem. Soc.*, **103**, 4620-4622 (1981).
- [3] G.L. COHEN, J.A. LEDNER, W.R. BAUER, H.M. USHAY, C. CARAVANA, S.J. LIPPARD, *J. Am. Chem. Soc.*, **102**, 2487-2488 (1980).
- [4] G.L. COHEN, W.R. BAUER, J.K. BARTON, S.J. LIPPARD, *Science*, **203**, 1014-1016 (1979).
- [5] a) J.H.J. DEN HARTOG, C. ALTONA, J.H. VAN BOOM, G.A. VAN DER MAREL, C.A.G. HAASNOOT, J. REEDIJK, *J. Am. Chem. Soc.*, **106**, 1528-1530 (1984);
b) B. VAN HEMELRYCK, E. GUITTET, G. CHOTTARD, J.P. GIRAULT, T. HUYNH-DINH, J.Y. LALLEMAND, J. IGOLEN, J.C. CHOTTARD, *J. Am. Chem. Soc.*, **106**, 3037-3039 (1984).
- [6] D. CREMER, J.A. POPLE, *J. Am. Chem. Soc.*, **97**, 1354-1358 (1975).



PS5.66 — TU

JACQUELINE K. BARTON
AVIS DANISHEFSKY
ELIAS LOLIS
Department of Chemistry
Columbia University
New York, NY 10027
U.S.A.

CHIRAL DISCRIMINATION IN THE COVALENT BINDING OF BIS(PHENANTHROLINE)RUTHENIUM(II) COMPLEXES TO DNA

Isomers of bis(phenanthroline)dichlororuthenium(II) display striking enantioselectivity in binding covalently to right-handed B-DNA. Incubation of racemic (phen)₂RuCl₂ with calf thymus DNA yields ruthenium-bound complexes having a maximum binding ratio of 0.06 ruthenium per nucleotide. Much as for the analogous dichlorodiammineplatinum(II) complexes, binding studies with various synthetic polymers reveal a preference for guanine. Circular dichroism of the supernatants following ethanol precipitation of the ruthenium-DNA complexes show substantial optical activity and, importantly, a sequence dependence in the level of enrichment. Interestingly, in contrast to stereoselective intercalation, covalent binding of (phen)₂Ru²⁺ to simple B-DNA appears to favor the lambda isomer. Coordination of the (phen)₂Ru²⁺ moiety to the helix seems to require a structure of complementary symmetry. Curiously, incubation with poly d(GC) or Z-form polymers leads to the preferential covalent binding of the opposite (delta) ruthenium isomer. The conformation and sequence specificity of these chiral octahedral complexes suggests the possible utility of chiral bis(amine) complexes in DNA site-specific drug design.



PS5.67 — TH

MICHAEL J. CLARKE
 BRUCE JANSEN
 KENNETH A. MARX
 RAY KRUGER

Departments of Chemistry
 Boston College
 Chestnut Hill, MA 02167
 and
 Dartmouth College
 Hanover, NH, 03755
 U.S.A.

BIOCHEMICAL EFFECTS OF BINDING $[(\text{H}_2\text{O})(\text{NH}_3)_5\text{Ru}^{\text{II}}]^{2+}$ AND $[(\text{NH}_3)_5\text{Ru}^{\text{III}}]$ TO DNA

The reaction of $[(\text{H}_2\text{O})(\text{NH}_3)_5\text{Ru}^{\text{II}}]^{2+}$ with calf thymus and salmon sperm DNA has been studied over a wide range of transition metal ion concentrations in order to determine the binding sites of the metal ion to the heterocyclic bases. Kinetic studies revealed a biphasic reaction with an initial fairly rapid coordination of the metal ion being followed by slower reactions. Under these conditions a true equilibrium could not be reached; however, it was possible to study metal ion coordination under pseudo-equilibrium conditions after the initial reaction was complete and before subsequent reactions had progressed substantially. For covalently bound Ru levels up to 0.26 Ru per DNA nucleotide, ($\text{Ru}_{\text{DNA}}/\text{P}_{\text{DNA}}$), the predominant binding site on helical DNA is in the major groove at the N-7 of guanine. Spectra of $[(\text{NH}_3)_5\text{Ru}^{\text{III}}]_n$ -DNA prepared by incubation of $[(\text{H}_2\text{O})(\text{NH}_3)_5\text{Ru}^{\text{II}}]^{2+}$ with DNA (where $[\text{P}_{\text{DNA}}] = 1.5 \text{ mM}$ and reactant $[\text{Ru}^{\text{II}}]/[\text{P}_{\text{DNA}}]$ ratios are in the range 0.1 to 0.3) followed by air oxidation yielded intense charge transfer bands which could only be attributed to $[(\text{NH}_3)_5\text{Ru}^{\text{III}}]$ coordination to N-7 dG sites. HPLC of acid-hydrolyzed samples of $[(\text{NH}_3)_5\text{Ru}^{\text{III}}]_n$ -DNA, which had been prepared by this method with helical DNA, also revealed the significant presence of only $[(\text{Gua})(\text{NH}_3)_5\text{Ru}^{\text{III}}]$ for

$0.1 < [\text{Ru}^{\text{II}}]/[\text{P}_{\text{DNA}}] < 0.5$, which was verified by UV-Vis identification of the isolated chromatographic band. An earlier X-ray molecular structure determination has established the coordination site as the imidazole N-7 of dG, which is exposed in the major groove of the DNA.

At $[\text{Ru}^{\text{II}}]/[\text{P}_{\text{DNA}}] \leq 0.5$ T_m values for the DNA decreased linearly with increasing ruthenium concentration and an increase in the intensity of the 565 nm charge transfer band was noted upon melting. The UV and CD spectra of these samples indicated no extensive destacking or alteration in geometry (B family) compared to unsubstituted DNA. At $[\text{Ru}^{\text{II}}]/[\text{P}_{\text{DNA}}] > 0.5$ or when single stranded DNA was used, increased absorbance at 530 nm and 480 nm suggested additional binding to the exocyclic amine sites of adenine and cytosine residues. HPLC and individual spectrophotometric identification of the products derived from hydrolysis of these species yielded both $[(\text{Gua})(\text{NH}_3)_5\text{Ru}^{\text{III}}]$ and $[(\text{Ade})(\text{NH}_3)_5\text{Ru}^{\text{III}}]$. Earlier crystallographic, spectroscopic and electrochemical studies have established the adenosine binding site of $[(\text{NH}_3)_5\text{Ru}^{\text{III}}]$ to be the exocyclic amine (N-6). Coordination to the exocyclic amines of adenine and cytosine, is indicative of double helix disruption since these amines are involved in hydrogen bonding on the interior of B-DNA. A highly metallated ($\text{Ru}_{\text{DNA}}/\text{P}_{\text{DNA}} = 0.26$) DNA sample found to be rapidly sedimenting and unable to electrophorese into an agarose gel appeared to have undergone counterion induced collapse, which is a phenomenon that has not been previously demonstrated for DNA covalently coordinated by a transition metal ion.

Agarose gel electrophoresis of superhelical PBR322 plasmid DNA after exposure to various amine complexes of $[(\text{NH}_3)_5\text{Ru}^{\text{III}}]$ in the presence of a reductant and air generally revealed moderately efficient cleavage of the DNA, presumably due to the generation of hydroxyl radical via Fenton's chemistry. However, similar studies involving $[(\text{NH}_3)_5\text{Ru}^{\text{III}}]$ directly coordinated to the DNA showed no strand cutting. Polyacrylamide gel electrophoresis of a 381 bp, $3'$ - ^{32}P -labeled fragment of PBR322 plasmid DNA containing low levels of bound $[(\text{NH}_3)_5\text{Ru}^{\text{III}}]$ further indicated negligible DNA cutting by the coordinated metal ion.



PS5.68 — TU

HELMUT SIGEL

ROGER TRIBOLET

Institute of Inorganic Chemistry

University of Basel

Spitalstrasse 51, CH-4056 Basel

Switzerland

SYNERGISM IN THE METAL ION PROMOTED HYDROLYSIS OF ADENOSINE 5'-TRIPHOSPHATE

The enzyme-catalyzed transfers of phosphoryl or nucleotidyl groups depend on the presence of divalent metal ions, and the various stages of information transfer in genetic processes, DNA replication, RNA synthesis, and protein synthesis all require metal ions [1]. Hence, it is not surprising that the metal ion promoted dephosphorylation of nucleoside 5'-triphosphates, especially of adenosine 5'-triphosphate (ATP⁴⁻), has long been recognized [2]. The simplest of these processes is the transfer of a phosphoryl group to water, and some insight into the mechanism of this reaction with ATP has been gained [3,4].

Many enzyme-nucleotide systems involve two (or more) metal ions [1]. Therefore, we are attempting to elucidate the influence of different metal ion mixtures on the dephosphorylation rate of ATP [5]. So far, the initial rates of dephosphorylation (*i.e.*, $v_0 = d[PO_4]/dt$) of ATP (10^{-3} M) in the mixed metal ion systems Cu²⁺/ATP/Mg²⁺, Ni²⁺ or Zn²⁺ with the ratio 1:1:5 have been measured at pH 5.5 and compared with the binary ATP/M²⁺ 1:6 systems (see Table).

The remarkable result is that addition of Mg²⁺ to a Cu²⁺/ATP 1:1 system accelerates the dephosphorylation rate significantly more than the same amounts of Mg²⁺ accelerate the reaction in a Mg²⁺/ATP 1:1 system. The same synergism, based also on the Cu²⁺/ATP 1:1 system is observed with Ni²⁺, but not with Zn²⁺. We attribute this observation, based on previous results [4], to the formation of a pre-reactive complex in the Cu²⁺/ATP 1:1 system, *i.e.* of a [Cu(ATP)]₂⁺ dimer which involves purine-stacking and a Cu²⁺/N-7 interaction; the inherent reactivity in this dimer may be triggered by the addition of Mg²⁺ or Ni²⁺. Furthermore, we suggest that in the Zn²⁺/ATP 1:1 system a cor-

Table

Evidence for Synergistic Effects in the Dephosphorylation of ATP (10^{-3} M) at pH 5.5 by Mixed Metal Ion Systems ($I = 0.1$, NaClO₄; 50°C). The Effect of the Second Metal Ion on M²⁺/ATP 1:1 Systems is Expressed by Rate Enhancement Factors (= REF)^{a)}. All Initial Rates are Given as $v_0 \times 10^8$ M s⁻¹

Effect of	system		v ₀ for		REF ^{a)}
	1:1	1:1:5	1:1	1:1:5	
Mg ²⁺	Mg/ATP		0.096		
		Mg/ATP/Mg		0.13	1.4
Cu/ATP			2.5		
		Cu/ATP/Mg		9.7	4
Ni ²⁺	Ni/ATP		0.075		
		Ni/ATP/Ni		0.18	2.4
Cu/ATP			2.5		
		Cu/ATP/Ni		9.5	4
Zn ²⁺	Zn/ATP		0.15		
		Zn/ATP/Zn		0.92	6
Cu/ATP			2.5		
		Cu/ATP/Zn		14	6

a) REF = v₀ of a 1:1:5 system divided by v₀ of the corresponding 1:1 system; *e.g.*, 0.13/0.096 = 1.4 or 9.7/2.5 = 4. The rate data are summarized from several of our studies [3-7].

responding pre-reactive state is formed and that therefore no synergism with Cu²⁺ is observed.

In accord with this interpretation are the results of preliminary experiments which suggest that there is also a very pronounced synergism in Zn²⁺/ATP/Mg²⁺ systems at pH 7.5. This is interesting because, *e.g.*, DNA and RNA polymerase [1] contain tightly bound Zn²⁺ and use nucleoside 5'-triphosphates as substrates, but for activity the enzymes require in addition Mg²⁺.

ACKNOWLEDGEMENTS

The support of this work by the Swiss National Science Foundation is gratefully acknowledged.

REFERENCES

- [1] a) G.L. EICHHORN, *Met. Ions Biol. Syst.*, **10**, 1-21 (1980);
b) F.Y.-H. WU, C.-W. WU, *Met. Ions Biol. Syst.*, **15**, 157-192 (1983).
- [2] C. LIÉBECQ, M. JACQUEMOTTE-LOUIS, *Bull. Soc. Chim. Biol.*, **40**, 67-85 and 759-765 (1958).
- [3] H. SIGEL, P.E. AMSLER, *J. Am. Chem. Soc.*, **98**, 7390-7400 (1976).
- [4] H. SIGEL, F. HOFSTETTER, R.B. MARTIN, R.M. MILBURN, V. SCHELLER-KRATTIGER, K.H. SCHELLER, *J. Am. Chem. Soc.*, **106**, 7935-7946 (1984).
- [5] H. SIGEL, R. TRIBOLET, results to be published.
- [6] R.M. MILBURN, M. GAUTAM-BASAK, R. TRIBOLET, H. SIGEL, *J. Am. Chem. Soc.*, **107**, (1985), in press.
- [7] P.E. AMSLER, H. SIGEL, *Eur. J. Biochem.*, **63**, 569-581 (1976).

6. *Bioinorganic Therapy*

PS6.1 — MO

RUTH MARGALIT
HARRY B. GRAY
Arthur Amos Noyes Laboratory
California Institute of Technology
Pasadena, California 91125
U.S.A.

MICHAEL CLARKE
Department of Chemistry
Boston College
Chestnut Hill, Massachusetts
U.S.A.

S.C. SRIVASTAVA
Department of Chemistry
Brookhaven National Laboratory
Upton, New York
U.S.A.

BIOLOGICAL TISSUE DISTRIBUTION OF Ru(NH₃)₅-BLEOMYCIN

The reaction of Ru(NH₃)₅H₂O²⁺ with the chemotherapeutic agent bleomycin at pH 7.2 gives a Ru-modified derivative. The modified bleomycin has been purified and characterized (by ¹H NMR and differential pulse electrochemistry) as Ru(NH₃)₅³⁺-(pyrimidine)-BLM.

A model compound, Ru(NH₃)₅His³⁺, was found to be effective in the scission of DNA strands, *in vitro*, when combined with a reducing agent. The activity of Ru(NH₃)₅BLM in DNA strand scission will be presented and discussed. The distribution of the radioactive drug ¹⁰⁶Ru(NH₃)₅BLM in normal and tumor-bearing mice has been studied.



PS6.2 — TU

M.G. BASALLOTE
E.J.G. CONEJERO
R. VILAPLANA
F. GONZÁLEZ-VÍLCHEZ
Departamento de Química Inorgánica
Facultad de Ciencias
Apto. 40, Puerto Real, Cádiz
Spain

PLATINUM COMPLEXES OF EDDA AND ITS ETHYL ESTER: SYNTHESES AND ANTITUMOR PROPERTIES

Structure-activity relationship for antitumor properties of platinum complexes is still not clear, although *cis*-[PtA₂X₂] compounds seem to be active when A ligands are inert and X ligands can be easily replaced in biological media. The nature of A is of great importance for the antitumor activity of the complex, with little changes in its structure leading sometimes to main changes in activity. Therefore we are testing complexes of this type with new structures in order to obtain *cis*-DDP analogs with higher therapeutic indexes.

We have shown recently activity against Ehrlich ascites tumor for some platinum complexes with aminopolycarboxylic ligands [1]. However, [Pt(EDDA-H₂)Cl₂] was showed to be inactive in a previous study by SPEER *et al.* [2]. One interesting problem in structure-activity relationship is that related to the effect of the charge of the complex, active compounds being normally neutral complexes. So esterification of carboxylic groups in ligands must lead to an increase in the activity of the complexes. However, the results of previous studies with similar ligands [3,4] by other authors are contradictory and new data must be obtained for solving the problem. In this sense, we report in this paper the results of a new test of this compound and of its analog with the ethyl ester of the ligand.

SYNTHESIS AND CHARACTERIZATION

[Pt(EDDA-H₂)Cl₂] was synthesized from K₂PtCl₄ by the method of LIU [5]. The compound was obtained as yellow crystals with a yield of 55%. Elemental analysis results were: C:16.18 (16.30); H:2.71 (2.73); N:6.38 (6.33); Cl:16.79 (16.04) where theoretical values are shown in parenthesis. The infrared spectrum shows bands at 3110 cm⁻¹ (N-H), 1700 cm⁻¹ (COOH) and 330 cm⁻¹ (Pt-Cl). A band is observed in the electronic spectrum of this compound in aqueous solution (262 nm), its position being similar to the one observed for platinum complexes with EDTA [6]. The value for COOH in the ¹³C-NMR spectrum is also similar (169.64 ppm) to those of EDTA complexes [1].

EDDA-Et₂·2HCl was obtained by refluxing a solution of EDDA-H₂ in ethanol, and with HCl stream. After three hours, the solution was concentrated and precipitation of a white solid occurred. The solid was washed with water and ethanol and dried at 60°C. The yields were variable, ranging from 27 to 71%. Elemental analysis results were: C:38.85 (39.35); H:7.95 (7.96); N:8.68 (9.17); Cl:22.78 (23.23). The bands due to N-H and C=O stretching appear in the IR spectrum at 3400 cm⁻¹ and 1740 cm⁻¹. In the ¹H-NMR spectrum, the ethyl groups give signals at 1.24 ppm (CH₃) and 4.17 ppm (CH₂) (J = 7 Hz). Two significant signals in the ¹³C spectrum are those of C=O (166.12 ppm) and CH₃ (13.86 ppm).

[Pt(EDDA-Et₂)Cl₂] was obtained from K₂PtCl₄ and EDDA-Et₂ in dilute HCl solution. The solution was heated and stirred for about 2 hours. Concentrated HCl was added to cause precipitation, and then a pale yellow solid was obtained. It was washed with water and ethanol and dried at 60°C (yield = 30%). The elemental analysis results were the following: C:23.43 (24.00); H:4.10 (4.04); N:5.67 (5.02); Cl:15.22 (14.23).

In the IR spectrum, the N-H band is displaced to 3110 cm⁻¹ while the C=O band appears also at 1730 cm⁻¹. The Pt-Cl band appears in this case at 325 cm⁻¹. The electronic spectrum of this compound shows bands at 282 and 306 nm. This displacement to longer wavelengths is due to the HCl used for the dissolution of the complex and has been observed for Pt-EDTA complexes [6]. The NMR spectra also show changes with coordination.

ANTITUMOR ACTIVITY

Antitumor tests were performed against Ehrlich ascites tumor in Swiss mice and the results are shown in Table I. [Pt(EDDA-H₂)Cl₂] was dissolved in saline, and [Pt(EDDA-Et₂)Cl₂] in saline-DMSO 1:1. Control and test groups were of 10 and 8 animals respectively. The compounds were injected i.p. in day 1, and the experience was finished in day 90. T/C values have been calculated from the median survival times of the test and control groups.

Table I

Compound	Dose (mg/Kg)	T/C
[Pt(EDDA-H ₂)Cl ₂]	100	85
	50	100
	25	98
[Pt(EDDA-Et ₂)Cl ₂]	100	122
	50	91
	25	109

The values of Table I show no activity for both compounds. This result is in agreement with that of SPEER [2] for the case of the EDDA complex. Moreover, for the EDDA-Et₂ complex no significant increase in activity is observed.

REFERENCES

- [1] F. GONZÁLEZ VILCHEZ, M. GARCÍA BASALLOTE, R. VILAPLANA SERRANO, E.J. GONZÁLEZ CONEJERO, Second International Conference on the Chemistry of the Platinum Group Metals, Edinburgh (U.K.), 1984.
- [2] R.J. SPEER, H. RIDGWAY, L.M. HALL, D.P. STEWARD, K.E. HOWE, D.Z. LIEBERMAN, A.D. NEWMAN, J.M. HILL, *Cancer Chemother. Rep.*, **59**, 629 (1975).
- [3] C. YOSHIMUKI, T. FUJII, K. SAITO, M. FUJII, K. NIIMURA, European Patent. Appl. N.º 41792, 1981.
- [4] K. INAGAKI, Y. KIDANI, K. SUZUKKI, T. TASHIRO, *Chem. Pharm. Bull.*, **28**, 2286 (1980).
- [5] C.F. LIU, *Inorg. Chem.*, **3**, 680 (1964).
- [6] N.A. EZERSKAYA, J. KISELEVA, B.V. ZHADANOV, *Russ. J. Inorg. Chem.*, **15**, 533 (1970).



PS6.3 — TH

J.P. ALBERTINI

A. GARNIER-SUILLEROT

Laboratoire de Chimie bioinorganique
U.E.R. de Médecine et Biologie Humaine
Université Paris Nord
93012 Bobigny Cedex
France

**INTERACTION OF BLEOMYCIN
WITH Pd(II) COMPLEXES
($[\text{PdCl}_4]^{2-}$, $[\text{cis-Pd}(\text{NH}_3)_2\text{Cl}_2]$,
 $[\text{Pd}(\text{en})\text{Cl}_2]$) AND WITH $[\text{cis-Pt}(\text{NH}_3)_2\text{Cl}_2]$.
ANTITUMOR ACTIVITY OF THE BLM-
 $[\text{cis-Pt}(\text{NH}_3)_2\text{Cl}_2]$ SYSTEM**

Bleomycin (BLM) and *cis*-diamminodichloroplatinum(II) (*cis*-DDPt) are used in combination chemotherapy to treat malignant tumors [1-3]. The two drugs exhibit synergism. The biological target for both *cis*-DDPt and bleomycin is believed to be DNA.

In this communication we address the question of whether prior covalent binding of *cis*-DDPt to BLM might alter the interaction of these two drugs with DNA and their antitumor activity.

Because of the slowness of Pt(II) ligand exchange reactions, parallel studies were conducted on the corresponding Pd(II) complexes which react 10^5 times faster.

In this communication we report experiments showing that $[\text{PdCl}_4]^{2-}$ as well as $[\text{cis-Pd}(\text{NH}_3)_2\text{Cl}_2]$ and $[\text{Pd}(\text{en})\text{Cl}_2]$ reacts with bleomycin in a three steps process forming a 1:1 BLM.Pd(II) complex. In the same way a similar complex is obtained between BLM and $[\text{cis-Pt}(\text{NH}_3)_2\text{Cl}_2]$; its antitumor activity has been tested.

Interaction of BLM with Pd(II) complexes

The addition of $[\text{PdCl}_4]^{2-}$ to an aqueous BLM solution gives rise to the immediate formation of

a first complex (**I**). The most striking features of this formation are i) the release of two protons, ii) the quenching of the pyrimidine fluorescence, iii) the appearance of a CD band at 367 nm which can be assigned to d-d transition. As time elapses this complex evolves to a second one (complex **II**); this occurs without any modification of the pH value but with noticeable change in the CD spectrum. The half life time of complex **I** is about 7 minutes. The last step, giving rise to the ultimate complex (**III**), is slower. Here again this occurs without modification of the pH value and, at pH 3, about three days are necessary to reach its complete formation. However if the pH is raised to about 7 the transformation of complex **II** to **III** occurs at once (it should be noticed that complex **III** is obtained directly by addition of $[\text{PdCl}_4]^{2-}$ to BLM in a pH 7 Hepes buffer).

When either $[\text{cis-Pd}(\text{NH}_3)_2\text{Cl}_2]$ or $[\text{Pd}(\text{en})\text{Cl}_2]$ are substituted for $[\text{PdCl}_4]^{2-}$ one still observes a three steps process (complexes **I'**, **II'** and **III'**).

On the contrary when $[\text{PdCl}_4]^{2-}$ is added to depyruvamide bleomycin (depBLM) one still observes the release of two protons but no evolution with time: only one complex (**d**) is observed.

The striking feature is that the CD spectra of complexes **III**, **III'** and **d** are similar strongly suggesting that the same four ligands are involved in the coordination square, most probably the secondary amine nitrogen, the pyrimidine nitrogen and the two peptide nitrogens. It must be pointed out that these ligands are different from those usually found in metal bleomycin complexes (the metal being copper, iron and cobalt) [4,5].

Interaction of BLM.Pd(1:1) complex (III) with DNA

The addition of DNA to complex **III** gives rise to a quenching of the bithiazole fluorescence suggesting that it is still able to intercalate between the base pairs of DNA. Moreover an immediate modification in the 320-340 nm region (d-d transition) of the CD spectrum is observed which can be assigned to a modification of the ligand field around the Pd(II) ion. However no release of Pd(II) from the complex could be detected.

BLM.[cis-Pt(NH₃)₂Cl₂] system

The interaction of *cis*-DDPt with BLM is very slow and incomplete. After one week, at pH 7, only 30% of the 1:1 complex is obtained.

Antitumor activity of the BLM-CisDDPt complex

A mixture containing BLM and *cis*-DDPt in a 3:1 molar ratio was used. In that conditions we have estimated that all the Pt(II) ions are complexed to BLM. The mixture has been screened for anticancer activity against Lewis pulmonary carcinoma and L 1210 leukemia in a comparative study with BLM and *cis*-DDPt respectively. The percentage of inhibition by the BLM-*cis*DDPt (1:1) complex is reduced to 65% and 55% with regard to free BLM and *cis*-DDPt respectively.

REFERENCES

- [1] M.P. CORDER, G.H. CLAMON, *Cancer*, **54**, 202-206 (1984).
- [2] R. VRISENDORP, J.G. AALDERS, D.T. SLEIJFER, P.H.B. WILLEMSE, J. BOUMA, N.H. MULDER, *Cancer Treat. Rep.*, **68**, 779-781 (1984).
- [3] P.K. MASCHARAK, U. SUGIURA, J. KUWAHARA, T. SUZUKI, S.J. LIPPARD, *Proc. Natl. Acad. Sci., USA*, **80**, 6795-6798 (1983).
- [4] J.P. ALBERTINI, A. GARNIER-SUILLEROT, *Biochemistry*, **21**, 6777-6782 (1982).
- [5] J.P. ALBERTINI, A. GARNIER-SUILLEROT, *Biochemistry*, **23**, 47-53 (1984).



PS6.4 — MO

OLE JØNS

ERIK SYLVEST JOHANSEN

Royal Danish School of Pharmacy

Department of Pharmaceutical Chemistry AD

2 Universitetsparken, DK-2100 Copenhagen

Denmark

ALUMINIUM COMPLEXES
WITH PICOLINIC ACID

Aluminium has long been regarded biologically inert, but the aluminium absorption and consequent accumulation in the brain of patients with dialysis dementia is now well documented [1]. Aluminium intoxication has also been implicated in various neurological disorders such as Alzheimer dementia. Little is known about the mechanism of aluminium uptake. It is supposed that only dissolved aluminium is able to cross the mucosa barrier in the gastrointestinal tract [2]. Experiments with rats fed on diets containing suboptimal levels of zinc and elevated levels of aluminium showed increased aluminium concentrations in the rat brains. Probably aluminium in gut competes for binding sites on zinc or iron binding ligands. Investigation has showed that picolinic acid (2-pyridiniumcarboxylic acid) probably plays an important role in the absorption process of zinc [3]. The aim of the present work is to investigate the ability of aluminium to form complexes with picolinate ions.

EXPERIMENTAL

Potentiometric titrations with glass electrode were performed in 0.150 M KNO₃ at 25.0°C. Concentration of each component were of the order 10⁻³ M. The metal-to-ligand ratio varied between 1:1 and 1:4, and the mixtures were titrated in the pH range 3 to 7.

RESULTS AND DISCUSSIONS

The equilibrium analysis of the present system shows that the major aluminium-picolinate species are AlL_2^+ and $AlL_2(OH)$ with $\log(\beta_{120} \pm 3\sigma) = 8.27 \pm 0.02$ and $\log(\beta_{12-1} \pm 3\sigma) = 17.668 \pm 0.008$ respectively in mixtures with excess of picolinate (L^-).

In a 1:1 mixture the species AlL_2^+ , $\log(\beta_{110} \pm 3\sigma) = 4.497 \pm 0.007$ and $Al_2L_2(OH)_3$, $\log(\beta_{22-3} \pm 3\sigma) = 39.27 \pm 0.02$ dominated. Minor species in the system are $AlL(OH)^+$ and $AlL_2(OH)$.

The least squares computer calculations were performed with the program TITRER [4]. Distribution diagrams visualizing the relative amounts of the different species were produced using the program DISTPLOT.

The results of the present investigation show that competitive interaction between aluminium and zinc is possible.

REFERENCES

- [1] A.C. ALFREY, G.R. LE GENDRE, W.D. KAEHNY, *New Engl. Med.*, **294**, 184 (1976).
- [2] W.D. KAEHNY, W.D. HEGG, A.C. ALFREY, *ibid.*, **296**, 1389 (1977).
- [3] G.W. EVANS, *Nutr. Rev.*, **38**, 137 (1980).
- [4] E.S. JOHANSEN, O. JØNS, *Talanta*, **31**, 743 (1984).



PS6.5 — TU

I. CONSTANTINIDIS

J.D. SATTERLEE
 Department of Chemistry
 University of New Mexico
 Albuquerque, New Mexico 87131
 U.S.A.

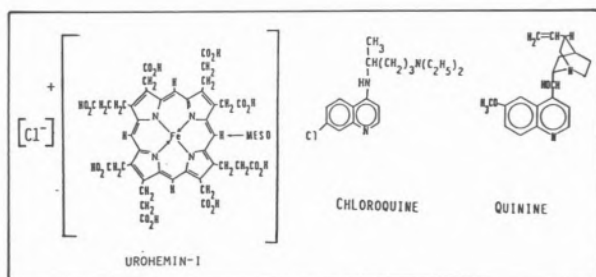
UROHEMIN INTERACTION WITH THE ANTIMALARIAL DRUGS CHLOROQUINE AND QUININE

INTRODUCTION

Despite numerous years of research the actual mode by which antimalarial drugs operate remains obscure. Recently though, it has been proposed that drugs such as chloroquine and quinine form complexes with the protoporphyrin IX of hemoglobin inside red blood cells [1]. The precise mechanism is unknown, but presumably the complexes are formed with the heme that has been released from proteolytically digested hemoglobin. It has also been suggested that protohemin IX is a specific receptor for several malaria drugs and the cause of the rapid uptake of these drugs by the erythrocyte. Due to this implied high affinity of ferric porphyrins for antimalarial drugs, we have begun binding studies in aqueous solution. In this report we present some of our initial results concerning the interaction of chloroquine and quinine with iron porphyrins in aqueous solution. Urohemine-I was chosen due to its high solubility in aqueous solutions and because recent Raman and Nuclear Magnetic Resonance (NMR) work allowed us to thoroughly characterize its solution dynamics [2,3].

EXPERIMENTAL

Urohemine was purchased from Porphyrin Products, Logan, Utah, and was further purified by column chromatography as previously described [2]. Chloroquine and quinine were purchased



from Sigma and were used without further purifications. Titrations of urohemine with the drugs were carried out at pH=6.0 (unbuffered) and at 20°C employing a Perkin Elmer 559A UV-Vis spectrophotometer with a thermostated cell compartment. pH was monitored throughout the experiment using a Beckman pH meter and a Fisher combination electrode. Ultraviolet-visible difference spectra were recorded in the Soret region of the visible spectrum. The differences here reflect the drug binding to urohemine. Data were handled using the Hill plot and Scatchard plot formalisms [4].

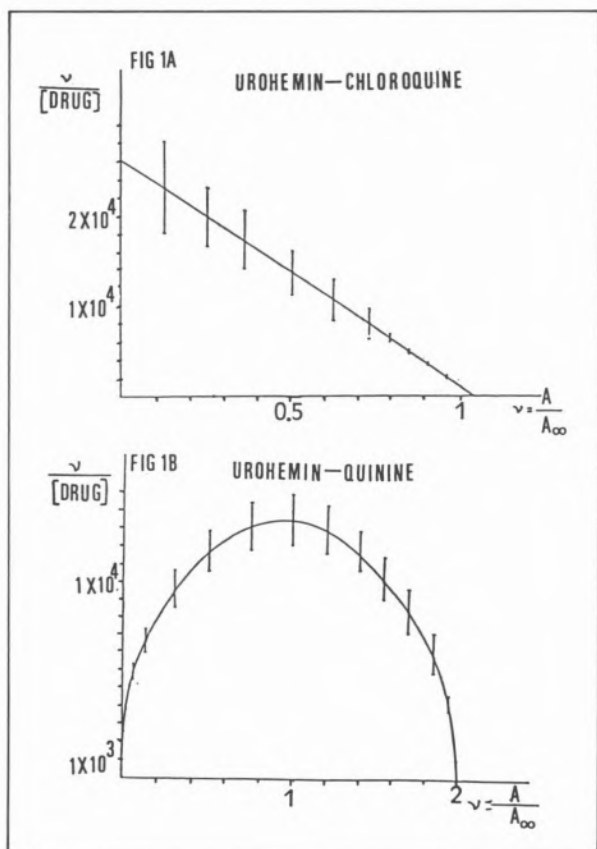


Fig. 1

Scatchard plots for drug binding to urohemine-I

RESULTS AND DISCUSSIONS

Figs. 1A and 1B show Scatchard plots for the association of urohemine to chloroquine and quinine, respectively. These results indicate that chloroquine associates in a noncooperative manner with urohemine, exhibiting a Hill coefficient of 1.0 and a $K_{\text{ass}} = (3.6 \pm 0.3) \times 10^4 \text{ M}^{-1}$ while quinine displays a cooperative association, a Hill coefficient of two, and a $K_{\text{ass}} = (1.5 \pm 0.2) \times 10^8 \text{ M}^{-2}$.

These results are interesting in view of the similar structures of the two drugs. Both possess quinoline rings with side chains at the fourth position. Since proton NMR data do not indicate axial coordination at the urohemine iron ion [4], it seemed reasonable to expect that both drugs would have similar stoichiometries. Furthermore, from our UV-Vis and proton NMR data we can conclude that urohemine forms π -complexes with both drugs [5].

Further work on malaria drug interaction with free hemins and heme proteins is in progress in our laboratory.

ACKNOWLEDGEMENTS

J.D. Satterlee is a Fellow of the Alfred P. Sloan Foundation (1983-1985) and would like to acknowledge their support of this work.

REFERENCES

- [1] A.C. CHOU, R. CHENLI, C.D. FITCH, *Biochemistry*, **19**, 1543-1549 (1980).
- [2] J.D. SATTERLEE, J.A. SHELNUTT, *J. Phys. Chem.*, **23**, 5487-5492 (1984).
- [3] J.A. SHELNUTT, M.M. DOBRY, J.D. SATTERLEE, *J. Phys. Chem.*, (1984), in press.
- [4] K.E. VAN HOLDE, «Physical Biochemistry», Prentice-Hall, Englewood Cliffs, N.J., 1971.
- [5] J.D. SATTERLEE, I. CONSTANTINIDIS, unpublished data.



PS6.6 — TH

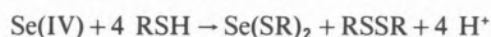
G. ARAVAMUDAN
Chemistry Department
Indian Institute of Technology
Madras 600 036
India

P.N. VENKATASUBRAMANIAN
Chemistry Department
University of Texas at Dallas
Richardson, TX 75080
U.S.A.

SELENIUM-MERCURY INTERACTIONS IN PRESENCE OF SULFHYDRYL COMPOUNDS: POSSIBLE MODEL SYSTEM FOR SELENIUM DETOXIFICATION OF MERCURY

Since PARIZEK and OSTADALOVA [1] first demonstrated that selenite markedly decreased the toxicity of mercuric chloride in rats, it has been shown that mercury too counteracted selenium toxicity [2]. However, the mechanism of their mutual detoxification has not been studied. Both mercury and selenium are closely linked to the soft sulfhydryl donor groups in amino acids in the metabolism and therefore this phenomenon might likely be associated with such compounds. We have studied the interactions of selenite, Hg(II) and the sulfhydryl compounds, cysteine and

3-mercaptopropionic acid, HS(CH₂)₂COOH (3-MPA). The results are presented in Table 1. Reactions were carried out in sulfuric acid medium to eliminate complications such as hydrolysis of mercury at higher pH in absence of chloride. A wide spectrum of products, depending upon the molar ratios of the reactants, was obtained. Similar products were formed with 3-MPA and cysteine proving the involvement of the sulfhydryl group in these interactions. The products contained selenium in several oxidation states. Formation of mixed metal complexes, featuring sulfhydryl bridging between Hg and Se in positive oxidation states, was noticeably absent. RSH reduces selenite to the unstable Se(II) and stabilises it by complexation.



Se(SR)₂ has been isolated and characterized for both 3-MPA and cysteine [3]. In most cases we studied, Se(SR)₂ is the interacting selenium species.

Hg²⁺, not coordinated to thiol, and Hg(SR)⁺ react with Se(SR)₂ by abstracting one of the Se-bound thiols. The thiol in Se(SR)⁺ now reduces it to Se²⁻. Reaction between selenide and [Hg(SR)_x]^{2-x} (x ≤ 2) leads to the formation of a complex product with the empirical formula Hg₂Se(SR)(SO₄)_{0.5}. This interaction means that the RS⁻ complexes of Hg(II) and Se(II) have comparable first formation constants. Further evidence for this is in the formation of this product when Se(IV) is added to Hg(SR)₂. Se(IV), however, has no action on Hg(II) bound to a single thiol as in Hg(SR)⁺.

There is interaction between Se(SR)₂ and even

Table 1
Results of Selenite — RSH — Hg(II) Interactions

Mole ratio of Se(IV):RSH:Hg(II)	Interacting Hg(II) species	Interacting selenium species	Product
1 4 3	aquo Hg ²⁺	Se ^{II} (SR) ₂	Hg ₂ Se(SR)(SO ₄) _{0.5}
1 4 1	aquo Hg ²⁺	Se(SR) ₂	"
1 5 1	Hg(SR) ⁺	Se(SR) ₂	"
*1 2 1	Hg(SR) ₂	Se(IV)	"
*1 1 1	Hg(SR) ⁺	Se(IV)	no reaction
1 8 1	Hg(SR) ₂	Se(SR) ₂	HgSe
1 4 1	HgCl ₂	Se(SR) ₂	Hg ₂ Se(SR)Cl
1 4 0.1	aquo Hg ²⁺	Se(SR) ₂	Se(O)

Sodium selenite and RSH were mixed in 1N H₂SO₄. Hg(II) solution was added to the Se(SR)₂ solution at room temperature.

* Sodium selenite was added to a mixture of Hg(II) and RSH.

coordination-saturated Hg(II)! Hg(SR)₂ reacts with Se(SR)₂ in presence of excess RSH, yielding HgSe. Higher mercapto complexes of Hg, higher than the bis-complex, were not observed to be formed [3]. The only plausible mechanism seems to be a direct interaction between Hg(II) and Se(II) themselves. The Hg...Se interaction causes the shift of the electronic equilibrium between S (bound to Se) and Se towards Se(II) which results in the reduction of the latter to selenide.

When HgCl₂ is the reacting species, some Hg₂Se(SR)Cl was formed. However, higher chlorocomplexation of mercury affects its reactivity with Se(SR)₂ markedly. Reactions were very slow and the yields obtained, very poor.

Addition of a very small amount of Hg(II) brings about the quantitative reduction of much larger amounts of Se(SR)₂ to elemental selenium. This destabilization is most probably caused by the formation of free Se(II) and its interaction with Se(SR)₂ in a sequence of reactions.

Our studies of Hg(II), selenite and thiol interactions provide by no means an unravelling of the exact mechanism behind the mutual antagonism between mercury and selenium in biological systems. But the broad spectrum of results obtained only suggests that the complexity of these interactions in the biological systems could be of much greater magnitude.

REFERENCES

- [1] J. PARIZEK, I. OSTADALOVA, *Experientia*, **23**, 142 (1967).
- [2] C.H. HILL, *Environ. Health Perspect. Exptl. Issue*, **4**, 104 (1973).
- [3] P.N. VENKATASUBRAMANIAN, Ph.D. Thesis, Indian Institute of Technology, Madras, India, 1977.



PS6.7 — MO

M.L. FIALLO

A. GARNIER-SUILLEROT

Laboratoire de Chimie Bioinorganique

U.E.R. de Médecine et Biologie Humaine

Université Paris Nord

93012 Bobigny

France

METAL ANTHRACYCLINE COMPLEXES AS NON CARDIOTOXIC ALTERNATIVES TO ANTHRACYCLINE ANTICANCER AGENTS. PHYSICO-CHEMICAL CHARACTERISTIC AND ANTITUMOR ACTIVITY OF Pd(II)-ANTHRACYCLINE COMPLEXES

Adriamycin (Adr) and Daunorubicin (Dr) are anthracycline antibiotics widely used in the treatment of various human cancers. However their clinical use is limited due to clinical and histopathological evidence of cardiotoxicity [1]. Recent studies have suggested that the cardiac toxicity of anthracyclines may be related to the formation of semiquinone free radical intermediates *in vivo* [2] and it has been demonstrated that a component of mitochondrial NADH dehydrogenase actively reduces Adr [3].

Thus the hope of finding a non cardiotoxic but yet active anthracycline has prompted the development of a large number of semisynthetic analogues [4].

We have recently demonstrated that Fe(III) anthracycline complexes retain antitumor activity against P 388 leukemia on one hand, and unlike the free drugs does not catalyze the flow of electrons from NADH to molecular oxygen through NADH dehydrogenase on the other [5,6]. These results suggest that iron-anthracycline complexes and more generally metal-anthracycline complexes could be non cardiotoxic alternatives to other currently available anthracycline anticancer agents.

In this context we have focused our attention on

the interaction of adriamycin and daunorubicin with Pd(II). In this communication we report the results of a detailed potentiometric and spectroscopic investigation undertaken to characterize Pd(II)-anthracycline complexes. Their stability constants have been determined as well as their interaction with DNA, their antitumor activity and their ability to catalyze the flow of electrons from NADH to molecular oxygen when they are inserted into the NADH-NADH dehydrogenase system.

Physico-chemical characterization

The addition of PdCl_4^{2-} to Adr (or Dr) at 1:1 molar ratio yields a complex with the concomitant release of two protons ($\text{pK}=2.4$). Our potentiometric and spectroscopic titrations strongly suggest that in this complex the four ligands of Pd(II) are i) one carbonyl and one phenolate oxygen forming a six membered chelate, ii) the deprotonated amine of the sugar portion, and iii), depending on pH, either a water molecule or OH^- group. The kinetics of formation of this complex is rather slow and follows a second order rate law with $k_2=3.9 \text{ s}^{-1} \text{ M}^{-2}$. The value of the constant of formation defined as $K = \frac{[\text{Pd}(\text{AdH}, \text{NH}_2)]}{[\text{Pd}][\text{AdH}, \text{NH}_2]}$ is 1.3×10^{22} . (AdH, NH_2)

stands for adriamycin with the anthraquinone moiety half deprotonated and the sugar amine deprotonated. Similar results have been obtained with daunorubicin.

Similar complexes are obtained when either $\text{Pd}(\text{NH}_3)_4^{2+}$ or $\text{cis-Pd}(\text{NH}_3)_2\text{Cl}_2$ is added to adriamycin instead of PdCl_4^{2-} ; however in that case the fourth position of the square of coordination is occupied by an amine group.

Interaction with DNA

The complex has been added to DNA at molar ratio $[\text{Nucleotide}]/[\text{Complex}] \approx 10$. A very slow evolution of the CD spectrum of the system is observed: in two weeks about 25% of the complex has disappeared suggesting that due to the high affinity of Adr and Pd^{2+} for DNA the complex partially dissociates.

Antitumor activity

The *in vitro* inhibition of P 388 leukemia cell growth by the complexes compares with that induced by the free drugs. They display antitumor activity against P 388 leukemia; no significant differences from the free drugs in terms of therapeutic efficacy were observed.

Effect of the complex on superoxide production by NADH dehydrogenase

Adr and Dr increased superoxide formation by NADH dehydrogenase in a dose-dependent fashion that appeared to follow saturation kinetics. On the contrary the Pd(II)-anthracycline complexes do not increase superoxide formation over control level.

REFERENCES

- [1] V.J. FERRANS, *Cancer Treat. Rep.*, **62**, 955-961 (1978).
- [2] S. SATO, M. IWAIZUMI, K. HANDA, Y. TAMURA, *Gann.*, **68**, 603-608 (1977).
- [3] K.J.A. DAVIES, J.M. DOROSHOW, P. HOCHSTEIN, *FEBS Lett.*, **153**, 227-230 (1983).
- [4] F. ARCAMONE, *Lloydia (Cinci)*, **40**, 45-66 (1977).
- [5] H. BERALDO, A. GARNIER-SUILLEROT, L. TOSI, F. LAVALLE, *Biochemistry*, in press.
- [6] M.L. FIALLO, A. GARNIER-SUILLEROT, submitted for publication.



PS6.8 — TU

C.G. PIERPONT
N.S. ROWAN
Department of Chemistry
University of Colorado
Boulder, CO 80309
U.S.A.

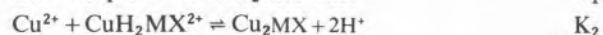
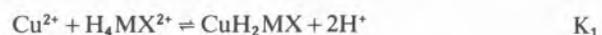
COPPER(II) BINDING BY MITOXANTRONE

The compound 1,4-dihydroxy-5,8-bis(2[(2-hydroxyethyl)amino]ethylamino)-9,10-anthracenedione dihydrochloride (Mitoxantrone (H_2MX), or No-

vantrone) has been developed as an antineoplastic agent and will soon be available commercially. The molecule is structurally similar to adriamycin and daunomycin and consequently, is thought to behave similarly. Because one of the major side effects of adriamycin is cardiotoxicity and the cardiotoxicity is thought to be associated with metal binding by the adriamycin molecule [1], we have been investigating the metal binding properties of the mitoxantrone molecule. However, there is also evidence that cardiotoxicity is not metal ion related [2]. Because of its biological abundance initial metal binding studies were made using Cu(II). For comparison, information for Cu-adriamycin and Cu-bleomycin complexes is available as is information about the distribution of copper in biological fluids [3-5]. Potentiometric titrations of the doubly charged form of mitoxantrone show that the first pK_a for the molecule is 6.8 and the second is 7.8 which agrees with earlier results [6]. There is almost no UV-vis spectrophotometric change associated with the first deprotonation, but a large change associated with the second. (Measured at 610 nm the extinction coefficient for the protonated form is 1.8×10^4 and for the deprotonated form 1.1×10^4). The differences in pK_a and the spectrophotometric results imply that the deprotonations occur at two different sites. Because of the lack of spectrophotometric change, the first probably occurs on the ethylenediamine side arm and the second with the large spectrophotometric change at a hydroxyl proton on the hydroxyanthraquinone ring.

Results of a spectrophotometric (700 to 600 nm) titration of the mitoxantrone molecule with Cu^{2+} at pH 4.8 show that little copper binds. However, if the titration is repeated at pH 7.2 then the absorbance changes show that two coppers bind per mitoxantrone molecule. Job's studies at pH 7 also show that two coppers bind per drug molecule. Because the binding was so strong in the concentration ranges used for these studies, no binding constants could be determined. Solid Cu_2MX complex was isolated using tetraphenyl borate as the counterion and analysis results confirm that two coppers bind per mitoxantrone molecule and show that the complex has a +1 charge. The complex with a +1 charge at pH 7.2 was also found from potentiometric titration curves. Com-

parison of titration curves for mitoxantrone alone and the same concentration of mitoxantrone containing two equivalents of copper showed that the copper binds strongly to the mitoxantrone even at low pH and each copper that binds releases two hydrogen ions. Using the titration data equilibrium constants were calculated according to the following equations:



The calculated values of K_1 and K_2 are 3.65×10^{-7} and 1.7×10^{-5} respectively. A fifth proton is also lost from the complex with a pK_D of 5.9 (potentiometrically) and 5.5 (spectrophotometrically). There is a large spectrophotometric change associated with this deprotonation. Copper binding constants for various antibiotics and blood serum components are given in Table 1. At pH 7 competition studies done spectrophotometrically show

Table 1

Compound	Complex	Log β	Ref.
Mitoxantrone(MX)	Cu_2MX^+	17.8 ^{a)}	this work
Adriamycin(Adria)	Cu-Adria	12.08	[3]
Bleomycin(Bleo)	Cu-Bleo	12.63	[4]
Human Serum Albumin(HSA)	Cu-HSA	16.2	[5]
Histidine(his)	$Cu(his)_2$	17.5	[5]

$$a) \text{ pH } 7.2 \quad \beta = K_1 K_2 K_D \frac{([H^+]^2 + [H^+] K_{a1} + K_{a1} K_{a2})}{[H^+]^5 K_{a1} K_{a2}}$$

that the mitoxantrone binds copper more strongly than CH_3CN , imidazole, and pyridine but less strongly than bipyridine.

Electrochemical, EPR and X-ray structure determinations will be attempted to further characterize the Cu_2MX complex.

REFERENCES

- [1] H. ELIOT, L. GIANNI, C. MEYERS, *Biochemistry*, **23**, 928 (1984).
- [2] E.O. KHARASCH, R.F. NOVAK, *Arch. Biochem. Biophys.*, **224**, 682 (1983).
- [3] H. BERALDO, A. GARNIER-SUILLEROT, L. TOSI, *Inorg. Chem.*, **22**, 4117 (1983).
- [4] H. UMEZAWA, T. TAKITA, *Struct. Bonding (Berlin)*, **40**, 73 (1980).
- [5] B. SARKAR, in H. SIEGEL (ed.), «Metal Ions in Biological Systems», vol. 12, 1981, p. 233.
- [6] J. KAPUSCINSKI, Z. DARZYNKIEWICZ, F. TRAGANOS, M.R. MELAMED, *Biochem. Pharmacol.*, **30**, 231 (1981).



PS6.9 — TH

M.L. VITOLO

J. WEBB

G.T. HEFTER

B.W. CLARE

School of Mathematical and Physical Sciences

Murdoch University

Perth WA 6150

Australia

P. WILAIRAT

C. SANGMA

Faculty of Science

Department of Chemistry

Mahidol University

Bangkok

Thailand

**PYRIDOXAL ISONICOTINOYL
HYDRAZONE:
A PROMISING AGENT FOR CHELATION
THERAPY OF IRON OVERLOAD**

The chemistry of pyridoxal isonicotinoyl hydrazone (PIH) has been investigated with emphasis on the chemical characteristics pertinent to the assessment of its value as a biological iron chelator. In acidic environments, PIH is remarkably stable, with a decomposition of $\leq 3\%$ after 72 hr at pH 2, 37°C. The acid dissociation constants of the several ionisable groups present in PIH have been determined by potentiometric titration and the formation of the iron complexes studied by potentiometry and UV-Vis spectrophotometry. The systems are quite complex due to the number of dissociable protons in both the free and coordinated ligands, the high affinity of these compounds towards iron(III) and the formation of sparingly soluble species at pH 5.

At pH 7.4, $[\text{Fe}^{3+}] = 10^{-6}$ M and a 1000-fold excess of ligand, PIH has a pM value of 27.7 which, when compared to 25.6 for transferrin, indicates that PIH is thermodynamically capable of removing iron from transferrin.

The distribution of the complex species as a function of pH shows that in each case a significant fraction is present as the electrically neutral Fe(L)(HL) at pH 7.4. A model of the coordina-

tion geometry of this species, supported by spectroscopic data, is proposed.

The affinity of PIH for iron(II) is significantly lower than for iron(III), as indicated by a formation constant of 7.0 for $[\text{Fe(II)(HL)}_2]$ compared to 12.47 for $[\text{Fe(III)(HL)}_2]$.

PIH therefore possesses many chemical features desirable in an effective iron chelating drug. Furthermore, this chelating agent has been reported to be effective in several cellular and animal bioassays and is currently a highly promising pharmacological agent for the treatment of iron overload.



_ PS6.10 — TH

J. WEBB

School of Mathematical and Physical Sciences

Murdoch University

Perth WA 6150

Australia

E. DELHAIZE

J.F. LONERAGAN

School of Environmental and Life Sciences

Murdoch University

Perth WA 6150

Australia

**ASCORBATE OXIDASE, DIAMINE OXIDASE
AND THEIR USE IN DIAGNOSIS
OF COPPER DEFICIENCY IN PLANTS**

Copper deficiency in soils and crops is a cause of concern in many agricultural industries. In general, copper deficiency leads to significant decreases in crop yield and plant fertility. However, it is often difficult to diagnose deficiency without complex laboratory procedures and at a sufficiently early stage in the plant's growth to allow remedial measures to be adopted, *e.g.* by including copper compounds in fertiliser. Analysis of the range of copper compounds present in plants,

as a function of copper supply, has revealed that several enzymes are particularly sensitive to copper deficiency and can act as an early warning signal of deficiency. These enzymes include ascorbate oxidase and diamine oxidase. Their assays have been shown to be at least as sensitive and indeed more reliable than atomic absorption analysis of copper content. In a simplified assay, ascorbate oxidase activity has been used to provide a field test that is quick, reliable and robust.



_PS6.11 — TU

ARGYRIOS VARSAMIDIS

GUY BERTHON

Centre de Technologie Biomédicale INSERM SC 13

Laboratoire de Chimie Bioinorganique

Université Paul Sabatier

38, rue des Trente-six ponts, 31400 Toulouse

France

MALATE AS A POTENTIAL AGENT TO PROMOTE HISTAMINE CATABOLISM

The most of the histamine present in the human body is stored in mast cells in tissues and in basophils in blood [1]. Its release from these sites may be triggered by immune reactions involving IgE antigens, or may directly result from non immunological stimuli such as the incorporation of so-called "histamine liberator" substances inside the membrane of the storage cells [1,2].

When localized, this release will lead to slight disorders like itching, redness and skin edema. When generalized, it may cause profound changes to the cardiovascular system and induce anaphylactic — or anaphylactoid, depending on the respective type of stimuli above — shock [1-3]. Concerning this, the demonstration of a close correlation between the plasma concentration of histamine and the seriousness of the symptoms

observed constituted an important breakthrough in the understanding of the physiological action of this mediator [4-6].

It has been known for a long time that histamine undergoes a rapid destruction in tissues [3]. It thus appears that increasing its rate of diffusion from blood into the environmental tissues may help alleviate its toxic effects. However, account being taken of the complexity of the system of labile equilibria characterizing the species potentially involved, it is impossible to discriminate the predominant forms under which histamine is present in blood plasma on an experimental basis.

A series of studies was thus devoted to the simulation of the distribution of histamine in this biofluid [7-11], which led to the following conclusions: (i) the most important fraction of histamine (about 99%) is constituted by its electrically charged mono- and di-protonated forms, and as such is not likely to passively diffuse through cell membranes, (ii) about 1% of histamine remains free, but its molecular form is highly polar [3], which also makes its passive diffusion unlikely, (iii) a small fraction whose percentage is inferior to 1% represents the binary and ternary metal complexes of histamine [11]. In the normal state, more than 70% of this fraction consists of the electrically neutral zinc-histamine-cysteinate complex, the majority of the remainder involving charged ternary copper complexes.

The hypothesis was thus put forward that zinc could indirectly favour histamine diffusion from plasma to tissues, hence its catabolism rate, whereas copper would in contrary exert an antagonistic effect [11]. This interpretation of the simulation results is in line with the roles previously attributed to zinc and copper in the evolution of the pharmacological effects of histamine in mice [12]. Subsequently, applications of the principles of the hypothesis above were developed using the aforementioned blood plasma simulation model [13,14]. Firstly, an attempt was made at increasing the concentration of the naturally occurring zinc-histamine-cysteinate complex by raising that of cysteine, but this proved unsuccessful [11]. A second study used aspartate and glutamate as successive partner ligands for zinc and histamine, but the increase of the neutral complexed fraction of histamine due to each of these two ligands was

almost totally compensated for by a correlative decrease in the concentration of the cysteinat ternary complex above [15].

Our latest investigation on the subject deals with the formation of ternary complexes of zinc and histamine with a series of dicarboxylic acids. Indeed, these substances are likely to meet the following requirements: (i) to have a low affinity for zinc on their own, (ii) to induce the formation of stable ternary complexes of this metal with histamine. In this respect, ligands with O donors are well known to form particularly stable mixed-ligand complexes of 3d metal ions with aromatic amines [16], especially those including an imidazole moiety [17].

Among oxalate (studied as a reference), fumarate, succinate and malate, only the latter can be expected to promote a significant increase of the neutral metal-complexed fraction of histamine in blood plasma.

REFERENCES

- [1] J. DRY, F. LEYNADIER, A. PRADALIER, D. HERMAN, *Sem. Hôp. Paris*, **53**(2), 77-79 (1977).
- [2] W. KAZIMIERCZAK, B. DIAMANT, *Prog. Allergy*, **24**, 295-365 (1978).
- [3] M.A. BEAVEN, «Histamine: its role in physiological and pathological processes», S. Karger, Basel, 1978.
- [4] W. LORENZ, *Agents Actions*, **5**(5), 402-416 (1975).
- [5] A. DOENICKE, W. LORENZ, *Ann. Anesth. Franç.*, **XVIII**(7/8), 691-700 (1977).
- [6] W. LORENZ, A. DOENICKE, B. SCHONING, E. NEUGEBAUER in THORNTON (ed.), «Adverse Reactions of Anaesthetic Drugs», Elsevier/North Holland Biomedical Press, 1981, pp. 169-238.
- [7] A. KAYALI, G. BERTHON, *J. Chim. Phys., Phys.-Chim. Biol.*, **77**, 333-341 (1980).
- [8] A. KAYALI, G. BERTHON, *Polyhedron*, **1**, 371-376 (1982).
- [9] A. KAYALI, G. BERTHON, *J. Chem. Soc., Dalton Trans.*, 2374-2381 (1980).
- [10] M.J. BLAIS, A. KAYALI, G. BERTHON, *Inorg. Chim. Acta*, **56**, 5-14 (1981).
- [11] G. BERTHON, A. KAYALI, *Agents Actions*, **12**(3), 398-407 (1982).
- [12] W.R. WALKER, R. REEVES, D.J. KAY, *Search*, **6**, 134-135 (1975).
- [13] P.M. MAY, P.W. LINDER, D.R. WILLIAMS, *J. Chem. Soc., Dalton Trans.*, 588-595 (1977).
- [14] G. BERTHON, P.M. MAY, D.R. WILLIAMS, *J. Chem. Soc., Dalton Trans.*, 1433-1438 (1978).
- [15] G. BERTHON, P. GERMONNEAU, *Agents Actions*, **12**(5), 619-629 (1982).
- [16] I. SOVAGO, A. GERGELY, *Inorg. Chim. Acta*, **37**, 233-236 (1979).
- [17] H. SIGEL, *Inorg. Chem.*, **19**, 1411-1413 (1980).



PS6.12 — TU

MICHEL BRION
LUC LAMBS
GUY BERTHON

Centre de Technologie Biomédicale INSERM SC 13
Laboratoire de Chimie Bioinorganique
Université Paul Sabatier
38, rue des Trente-six Ponts, 31400 Toulouse
France

DO TETRACYCLINES HAVE ANY INFLUENCE ON ZINC AND COPPER BIOAVAILABILITIES AT BLOOD THERAPEUTIC LEVELS?

Growing attention has recently been paid to the possible interference of organic pharmaceuticals with essential trace metal bioavailabilities [1-3]. Indeed, a vast majority of these substances contain donor groups likely to bind metal ions to such an extent that the normal distribution of the latter may be significantly upset. This may either lead to the expected activity of the drug or result in the occurrence of undesirable side effects [1-5]. As far as tetracyclines are concerned, their interactions with metal ions have been reported to play a critical part in important biological processes such as their deleterious impact on mineralizing tissues [6], their antibacterial activity [7] and their gastrointestinal absorption [8].

Analysing these interactions on a quantitative basis is not straightforward since, (i) account being taken of both antibiotic therapeutic doses and trace metal levels occurring *in vivo*, the concentrations of the complexes formed by tetracycline derivatives are very low, (ii) attempts at concentrating these species would upset their labile equilibria, hence their particular distribution in the biological fluid. In such cases, the only available investigation technique consists of the use of computer models which permit to simulate the distribution of all the coexisting complexes. Such models [9-11] are built up from (i) the analytically measurable overall concentrations of the reac-

tants, (ii) the parameters which relate these overall concentrations to the individual concentrations of all the species present in the medium, *i.e.* the corresponding stability constants determined beforehand under suitable experimental conditions.

This kind of technique has already been used for analysing the influence of the interactions between calcium, magnesium and various tetracyclines on the bioavailability of these antibiotics in blood plasma [12-15].

Zinc and copper are essential trace metals whose properties may be related to bacterial infection and its consequences. Zinc is the necessary cofactor of many enzymes involved in the biosynthesis of proteins and nucleic acids [16], whereas copper is known to exert antiinflammatory effects [17]. Besides, these two metals have been reported to be directly involved in tetracycline activity. The antagonistic role played by zinc ions against the gastrointestinal absorption of tetracyclines is well documented [8,18]. Moreover, both zinc and copper would mediate the binding of tetracyclines to macromolecules, especially DNA [19,20].

The coordination of zinc(II) and copper(II) with tetracycline (TC) and five of its derivatives, namely oxytetracycline (OTC), doxycycline (DOXY), minocycline (MINO), chlorotetracycline (CTC) and demethylchlorotetracycline (DMC), was investigated by potentiometry under biological conditions of temperature and ionic strength (37°C, NaCl 0.15 M). Full details on these studies will be published elsewhere [21]. It is only worth mentioning that 26 and 24 complexes were characterized for zinc and copper, respectively.

The formation constants of the above-mentioned complexes were introduced into the blood plasma databank relative to the ECCLES simulation programme [9]. Then the plasma concentration of each antibiotic considered in succession was scanned between 1×10^{-7} M and 1×10^{-3} M, whereas the relative importance of each tetracycline-containing complex in the distribution of both zinc and copper was examined. These scanning limits were chosen so as to encompass the average therapeutic concentration of antibiotic in plasma, generally close to 1×10^{-5} M [12]. The PMI parameter expressing the evolution of the low-molecular-weight fraction of metal in the presence of drug with respect to normal plasma [22] was also monitored.

For the therapeutic concentration above, the percentages of the most predominant complexes of zinc or copper involving each tetracycline derivative in turn never reached 1%; they even revealed themselves quite negligible for DOXY, MINO and DMC. Accordingly, the corresponding log PMI values relative to zinc and copper were found to be nil for all tetracyclines. Moreover, the same parameter reached only 0.10 for zinc with DOXY, 0.09 for zinc with TC and CTC, and 0.14 for copper with OTC, at a concentration of 1×10^{-3} M of antibiotic.

No significant influence of any of the present tetracycline derivatives can thus be expected on zinc and copper bioavailabilities in blood plasma. Nevertheless, further work would be required to determine the stoichiometry of the complexes predominating in the intracellular fluid and to assess their significance.

REFERENCES

- [1] D.R. WILLIAMS, *Proc. Sum. Conf. Computer Simulation, Boston*, **2**, 792-797 (1984).
- [2] H. AL-FALAH, P.M. MAY, A.M. ROE, R.A. SLATER, W.J. TROTT, D.R. WILLIAMS, *Agents Actions*, **14**(1), 113-120 (1984).
- [3] F. AKRIVOS, M.J. BLAIS, J. HOFFELT, G. BERTHON, *Agents Actions* (1984), paper 496 in press.
- [4] A. COLE, P.M. MAY, D.R. WILLIAMS, *Agents Actions*, **11**(3), 296-305 (1984).
- [5] Ref. 14 in ref. [1].
- [6] I. KAITILA, J. WARTIOVAARA, O. LAITINEN, L. SAXEN, *J. Embryol. Exp. Morphol.*, **23**, 185-211 (1970).
- [7] H. POIGER, C. SCHLATTER, *Naunyn-Schmiedeberg's Arch. Pharmacol.*, **306**, 89-92 (1979).
- [8] K.E. ANDERSON, L. BRATT, H. DENCKER, C. KAMME, E. LANNER, *Eur. J. Clin. Pharmacol.*, **10**, 59-62 (1976).
- [9] P.M. MAY, P.W. LINDER, D.R. WILLIAMS, *J. Chem. Soc., Dalton Trans.*, 588-595 (1977).
- [10] G. BERTHON, P.M. MAY, D.R. WILLIAMS, *J. Chem. Soc., Dalton Trans.*, 1433-1438 (1978).
- [11] G. BERTHON, C. MATUCHANSKY, P.M. MAY, *J. Inorg. Biochem.*, **13**, 63-73 (1980).
- [12] M. BRION, J.B. FOURTILLAN, G. BERTHON, *Inorg. Chim. Acta*, **55**, 47-56 (1981).
- [13] G. BERTHON, M. BRION, L. LAMBS, *J. Inorg. Biochem.*, **19**, 1-18 (1983).
- [14] L. LAMBS, M. BRION, G. BERTHON, *Agents Actions*, **14**(5), 743-750 (1984).
- [15] L. LAMBS, M. BRION, G. BERTHON, *Inorg. Chim. Acta*, in press.
- [16] J.F. RIORDAN, B.L. VALLEE, in A.S. PRASAD, D. OBERLEAS (eds.), «Trace Elements in Human Health and Disease», vol. 1, Academic Press, New-York, 1976, pp. 227-256.

- [17] J.R.J. SORENSON, in H. SIGEL (ed.), «Metal Ions in Biological Systems», vol. 14, Marcel Dekker Inc., New-York, 1982, pp. 77-124.
- [18] O. PENTTILÄ, H. HURME, P.J. NEUVONEN, *Eur. J. Clin. Pharmacol.*, **9**, 131-134 (1975).
- [19] P. MIKELENS, W. LEVINSON, *Bioinorg. Chem.*, **9**, 421-429 (1978).
- [20] K.W. KOHN, *Nature (London)*, **191**, 1156-1158 (1961).
- [21] M. BRION, L. LAMBS, G. BERTHON, in preparation.
- [22] P.M. MAY, D.R. WILLIAMS, *FEBS Lett.*, **78**, 134-138 (1977).



PS6.13 — TH

A.R. KARIM

I.P.L. COLEMAN

N.J. BIRCH

Biomedical Research Laboratory

School of Applied Sciences

The Polytechnic

Wulfruna St., Wolverhampton WV1 1LY

U.K.

LITHIUM TRANSPORT AND FACTORS AFFECTING THE MOVEMENT OF LITHIUM IN ISOLATED JEJUNAL MUCOSA OF GUINEA PIG

Lithium carbonate is widely used in the prophylactic treatment of manic-depressive psychoses [1] and is always administered orally. Lithium (Li^+) absorption from small intestine (Mucosal to Serosal) is passive both *in vitro* [2-4], and *in vivo* [5]. It is not affected by temperature, substrate depletion and metabolic inhibitors [6]. One criticism of these earlier studies is that a multicompartiment system with muscle and connective tissue is present and we now report studies in a three compartment system and also in isolated epithelial cells. Isolated jejunal mucosa of guinea pig was prepared and mounted to occlude a «porthole» separating two flux chambers [7]. Both sides were exposed to oxygenated Krebs-Tris buffer at 37°C.

Lithium replaced sodium, total $\text{Na}^+ + \text{Li}^+$ concentration being 106 mM.

Viability was tested by observation of active transport, potential difference, ^3H -PEG900 permeation and histological integrity. Bi-directional transfer of Li^+ across the epithelium was measured using stable isotopes ^6Li and ^7Li [8]. Lithium was determined using either an IL Video 22 or IL 357 atomic absorption spectrometer. Bi-directional fluxes of ^6Li and ^7Li showed no asymetry suggesting that there was no active component involved. Luminal and basolateral surfaces handled Li^+ isotopes similarly. Li^+ movement was independent of glucose transport and there appears to be no significant interaction between Li^+ and either Ca^{2+} or Mg^{2+} .

Acidification of the serosal side alone (pH 5.4) stimulated Li^+ absorption ($P < 0.01$) whereas mucosal acidification alone had no effect on transport. Neither treatment affected tissue uptake. Lithium, therefore, might be substituting for Na^+ in the Na^+/H^+ exchanger [9]. The pH gradient dependent increase in absorption was abolished by 1 mM Amiloride ($P < 0.0004$).

In further studies using ^3H -PEG900 as a measure of paracellular permeation, permeation of lithium correlated with that of PEG suggesting that movement of lithium in either direction occurred via the same PEG permeable, extracellular pathway. Confirmation for this route was obtained using solutions of high osmolarity, which collapsed the tight junctions [10]: lithium absorption was reduced ($P < 0.02$).

The transmucosal fluxes and tissue uptake of lithium in the absorptive (M to S) and secretory (S to M) directions were linearly related to the lithium concentration. Furthermore, the uni-directional fluxes both in the absorptive and secretory direction were similar. Total lithium transport after 45 minutes into serosal or mucosal compartments was 3-4 times greater than that found in the tissue. The plasma membrane of epithelial cells offers greater resistance to the movement of lithium than intact epithelium which suggests that the majority of ions pass via «pores» in the epithelium.

ACKNOWLEDGEMENTS

We thank «Sanity, a charity supporting biochemical research in psychiatry» for financial assistance, Instrumentation Laboratories for use of the Video 22 and Prof. F. Lauterbach for his advice.

REFERENCES

- [1] N.J. BIRCH in H. SIGEL (ed.), «Metal Ions in Biological Systems», vol. 14, M. Dekker, New York, 1982, pp. 257-313.
- [2] N.J. BIRCH, I.P.L. COLEMAN, A.R. KARIM, *Brit. J. Pharmacol.*, **80**, 443P (1983).
- [3] N.J. BIRCH, I.P.L. COLEMAN, H.E. HILBURN, A.R. KARIM, *Brit. J. Pharmacol.*, **81**, 168P (1984).
- [4] A.R. KARIM, I.P.L. COLEMAN, N.J. BIRCH, *Gastroenterol. Clin. et Biol.*, **8**(11), 867-868 (1984).
- [5] B.E. EHRLICH, J.M. DIAMOND, *Lancet*, **1**, 306 (1983).
- [6] N.J. BIRCH *et al.*, *Biochem. Soc. Trans.*, **13**, 250 (1985).
- [7] F. LAUTERBACH, *Arch. Pharmacol.*, **297**, 201-212 (1977).
- [8] N.J. BIRCH, D. ROBINSON, R.A. INIE, R.P. HULLIN, *J. Pharm. Pharmacol.*, **30**, 683-685 (1978).
- [9] D.J. BENOS, *Am. J. Physiol.*, **242**, C131-C145 (1982).
- [10] J.L. MADARA, *J. Cell Biol.*, **97**, 125-136 (1983).



PS6.14 — MO

SUSAN J. BERNERS PRICE

PETER J. SADLER

Department of Chemistry
Birkbeck College
University of London
Malet Street, London WC1E 7HX
U.K.

REIKO KURODA

Cancer Research Campaign Biomolecular Structures Research Group
Department of Biophysics
King's College
London WC2B 5RL
U.K.

MICHAEL J. DiMARTINO

BLAINE M. SUTTON

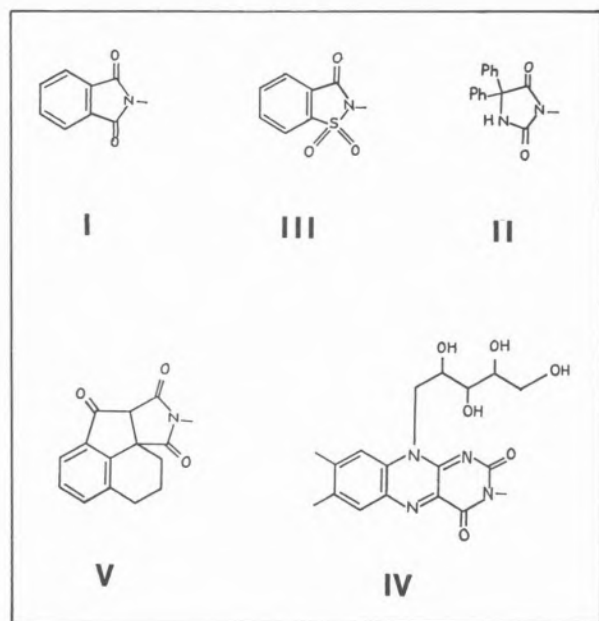
DAVID T. HILL

Smith Kline and French Laboratories
1500 Spring Garden Street, Philadelphia Pa 19101
U.S.A.

PREPARATION, CHARACTERIZATION AND ANTI-INFLAMMATORY ACTIVITY OF IMIDO GOLD(I) TRIETHYLPHOSPHINE COMPLEXES

The orally-administered gold(I) compound auranofin ("Ridaura", Smith Kline and French Laboratories) [(2,3,4,6-tetra-*O*-acetyl-1-thio- β -D-glucopyranosato-S)(triethylphosphine)gold] exhibits anti-inflammatory activity in animal models and is currently undergoing Phase IV clinical testing [1]. Structure-activity correlations with the series of complexes $R_3P-Au-SR'$ (where SR' is a sugar thiolate) have shown optimum activity when the phosphine is PEt_3 [2]. We report here the preparation, characterization and biological testing of a series of new imido complexes of triethylphosphine gold(I).

There have been very few previous reports of Au(I) complexes with nitrogen ligands. Gold(I)-N bonds are usually considered to be relatively weak. Five complexes of general formula $Et_3PAu(imide)$ containing the imido ligands shown in the Figure were prepared in good yield and gave satisfactory elemental analyses. The structure of one of them $Et_3P-Au-(phthalimide)$ was determined by X-ray crystallography and



Figure

Structure of the imido ligands in complexes of general formula $\text{Et}_3\text{PAuN}(\text{imide})$

shown to contain linear P-Au-N bonds (P-Au 2.24 Å, Au-N 2.05 Å) [3]. The X-ray absorption spectra of the Au L_{III} edges suggested that the gold coordination was similar in all of these new complexes [4]. All have a distinctive spike in the near-edge region attributable to an electronic transition involving vacant π -acceptor orbitals on the imide ligand.

The structures of these complexes in solution were investigated by the use of ^{31}P and ^{15}N NMR spectroscopy. Two-bond ^{15}N - ^{31}P spin-spin couplings were observed from solutions of $\text{Et}_3\text{P-Au-(}^{15}\text{N)}$ phthalimide confirming the existence of P-Au-N bonding in solution.

The phthalimide complex was tested first in the oxazolone-induced contact sensitivity assay in mice and was found to produce activity (66% stimulation) at a dose of 1 mg gold/kg, *i.v.*, comparable to that of Et_3PAuCl (72% stimulation). All of the complexes were tested in the carrageenan-induced rat paw edema assay [5], and the results are shown in the Table. When administered orally all complexes were effective in inhibiting the edema volume of the hind paw.

Thus it would appear that the presence of a thiolate, as in auranofin, is not essential for oral anti-inflammatory activity in animal models. How-

Table
Anti-inflammatory activity of triethylphosphine gold(I) imide complexes [3]

Imide	Dose ^{a)}	% Inhibition ^{b)c)}
I Phthalimide	15	42**
II Diphenylhydantoin	10	36*
III Saccharin	20	38**
IV Riboflavin	20	65**
V Tetrahydrosuccinimido-acenaphthenone	20	50**
Auranofin	5	17*
	10	24**
	20	56**

a) mg Au/kg.

b) % inhibition of paw volume in the rat carrageenan assay.

c) *, $P < 0.05$, **, $P < 0.01$ as significant differences from control using Student's *t* test.

ver, the *in vivo* displacement of the imido ligand by a naturally-occurring thiolate such as glutathione would be expected to be a very favourable reaction. This was confirmed by *in vitro* reactions.

The most active complex was that of riboflavin (vitamin B_2 , ligand IV). The variations in the activities observed may be partly related to the extent of oral absorption. The imides II, III, IV, and V are all biologically-active ligands in their own right as anticonvulsants (II and V), sweetener (III) and vitamin (IV). The anti-inflammatory activities of the imides alone were not determined.

This work demonstrates that stable Au(I) phosphine imide complexes can be readily prepared and exhibit anti-inflammatory activity. Further interest in the stability of P-Au-N bonds arises from the reported anticancer activity of auranofin in P388 leukaemia [6]. Using the ^{15}N - ^{31}P NMR methods described here it may be possible to map out possible Et_3PAu^+ binding sites on nucleic acid bases and DNA [7].

ACKNOWLEDGEMENTS

We thank the MRC, SERC, CRC, Smith Kline and French Laboratories and University of London Intercollegiate Research Service for support.

REFERENCES

- [1] Articles in, *J. Rheumatol.* (1982), Suppl. 8.
 [2] B.M. SUTTON, E. MCGUSTY, D.T. WALZ, M.J. DIMARTINO, *J. Med. Chem.*, **15**, 1095 (1972).
 [3] S.J. BERNERS PRICE, M.A. MAZID, P.J. SADLER, R. KURODA, M.J. DIMARTINO, D.T. HILL, *Inorg. Chem.*, submitted for publication.
 [4] S.J. BERNERS PRICE, I.M. ISMAIL, M.A. MAZID, M.T. RAZI, P.J. SADLER, G.N. GREAVES, «Proceedings of Conf. on Biological Systems: Structure and Analysis», March 1984, Daresbury, U.K., in press.
 [5] D.T. WALZ, M.J. DIMARTINO, C.L. GRIFFIN, A. MISHNER, *Arch. Int. Pharmacodyn.*, **185**, 337 (1970).
 [6] T.M. SIMON, D.H. KUNISHIMA, G.J. VIBERT, A. LORBER, *Cancer*, **44**, 1965 (1979).
 [7] C.E. BLANK, J.C. DABROWIAK, *J. Inorg. Biochem.*, **21**, 21 (1984).



PS6.15 — TU

L. TRINCIA
 G. FARAGLIA
 M. NICOLINI
 L. SINDELLARI

Istituto di Chimica Generale dell'Università
 via Loredan 4, 35100 Padova
 Italy

A. FURLANI
 V. SCARCIA

Istituto di Farmacologia e Farmacognosia dell'Università
 via Valerio 32, 34100 Trieste
 Italy

**PLATINUM(II) AND PALLADIUM(II)
 HALIDE COMPLEXES
 WITH DITHIOCARBAMIC DERIVATIVES
 AND THEIR CYTOSTATIC ACTIVITY**

The elevated toxicity is a severe dose-limiting factor in cisplatin antitumor therapy. Nephrotoxicity is one of the most important effects and it seems due to some metabolic pathways of the drug. It can be prevented by the contemporary administration of diuretics [1]. Protection by sulfur containing compounds could be an alternate mean of

preventing toxicity [2]. So far sodium diethyldithiocarbamate (DDTC) is the most promising one. Moreover DDTC exhibits a protective effect against chemical induced tumors. Its immunostimulating properties have been recently evidenced also [3]. The efficacy of cisplatin-DDTC combination is dose and time dependent in *in vivo* experiments.

Owing to the importance of DDTC metabolites and their possible interaction with cisplatin, we prepared and studied Pt(II) and Pd(II) complexes with dithiocarbamic esters. A number of them showed *in vitro* cytotoxicity (Table I), but the generally low solubility prevented to carry out a study in solution [4].

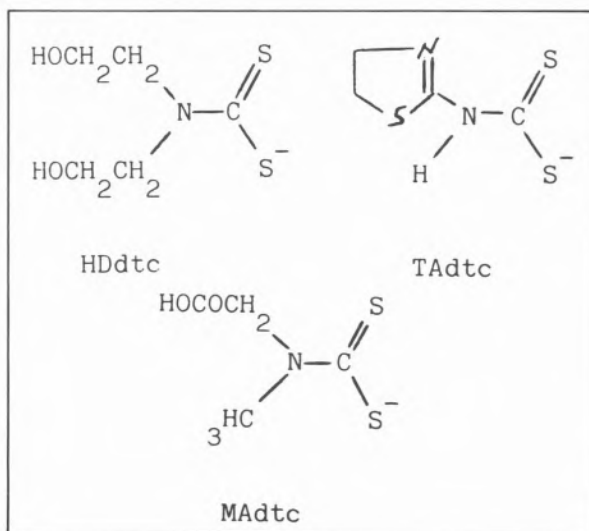
Table I
 "In vitro" Cytostatic Activity against KB cells

		Complexes	ID ₅₀ (µg/ml)*
$\begin{array}{c} \text{R} \\ \diagdown \\ \text{N}-\text{C}=\text{S} \\ \diagup \\ \text{R} \end{array}$	R = R' = Me	TMDT Pd(DMDTE)Cl ₂	**
	R = R' = Et	TEDT Pd(DMDTE)Br ₂	3.6
	R = Me, R' = Et	DMDTE Pd(TEDT)Cl ₂	0.17
	R = Et, R' = Me	DEDTM Pd(TMDT) ₂ Cl ₂	1.02
			Pd(DMDTE) ₂ Br ₂
		Pt(TEDT) ₂	3.8
		Pt(TMDT) ₂ Br ₂	2.8
		Pt(DMDTE) ₂ Br ₂	0.4

* The results of the cytostatic activity are expressed as dose at which the cells showed a 50% growth inhibition (ID₅₀). ID₅₀ value for cisplatin is 0.11 µg/ml.

** The complex is active but the value was not determined since dose-response relationship was not observed.

The following anions and some related esters have been synthesized:



Their reactions with platinum(II) and palladium(II) halides will be reported and discussed, together with the preliminary cytotoxicity data. Except for $M(\text{HDdte})_2$ and unlike the corresponding $M(\text{DEdte})_2$, where DEdte is the diethyldithiocarbamate anion, M is Pt or Pd, $M(\text{TAdtc})_2$ and $M(\text{MAdtc})_2$ are very soluble in several organic solvents, so that these compounds are promising for future biological studies.

ACKNOWLEDGEMENTS

L.T. was supported by a RECORDATI Industria Chimica e Farmaceutica S.p.A. grant.

REFERENCES

- [1] P.T. DALEY-YATES, D.C.H. MCBRIEN, *Biochem. Pharmacol.*, **33**, 3063 (1984).
- [2] R.F. BORCH, D.L. BODENNER, J.C. KATZ in M.P. HACKER, E.B. DOUPLE, I.H. KRAKOFF (eds.), «Platinum Coordination Complexes in Cancer Chemotherapy», Martinus Nijhoff Publ., Boston, 1984, p. 256.
- [3] G. RENOUX, *J. Pharmacol.*, **13**, suppl. I, 95 (1982).
- [4] G. FARAGLIA, L. SINDELLARI, L. TRINCIA, A. FURLANI, V. SCARCIA, *Inorg. Chim. Acta*, in press.



PS6.16 — TH

E.L. ANDRONIKASHVILI
Institute of Physics
Academy of Sciences of the Georgian S.S.R.
Tbilisi
U.S.S.R.

THE ONCOGENE OF MURINE SARCOMA VIRUS V-Ki-ras MAY ARISE AS A RESULT OF CHEMICAL ACTION ON THE PROTOONCOGENE c-ras

The processes of nucleotide transition and transversion leading to point mutations in DNA play a certain role in the malignant transformation. The cause of such transformations may consist either

in bivalent transition metals, e.g. $G \cdot \text{Me}^{2+} \rightarrow A$ (where G is guanine and A is Adenine) as E.L. ANDRONIKASHVILI and N.G. ESIPOVA [1] have shown, or in the methylation processes considered in detail by G. KLOPMAN and A. RAY [2] from the view-point of quantum biochemistry. Thus, for instance, at CH_3 group binding with guanine 06 the electronic structure of this nucleotide becomes similar to that of adenine, whereas thymine alkylation in 04 transforms it into cytosine-like state.

On the other hand, as a result of the investigations carried out by R. WEINBERG [3], M. BARBACID [4] and their collaborators, it has become evident that the point mutation in coding GGC triplet occupying the 12th position in the normal cellular gene c-ras (which is also called protooncogene) is characteristic of human bladder carcinoma (of chemical origin). This mutation transforms GGC triplet into GTC triplet.

However, the same 12th triplet of protooncogene undergoing GGC — AGC mutation becomes a characteristic feature of Kirsten viral murine sarcoma. The respective oncogene is called V-Ki-ras. However, in order to cause G → A transition, as it has been shown in refs. [1] and [2], the interference of a certain chemical agent is sufficient. Such an agent may be both a bivalent transition metal ion and a methyl group CH_3 .

Thus, in order to cause the formation of oncogene typical of murine sarcoma virus from a normal cellular gene of c-ras type, it is sufficient that the first guanine of the 12th GGC triplet would trap a bivalent transition metal ion or that alkylguanine would arise instead of guanine.

The oncogene of virus causing malignant diseases formed as a result of chemical action will act subsequently in accordance with viro-genetic theory. It should be emphasized that other mutations of the GGC triplet under consideration, as well as those of coding triplets of other types, being characteristic of one or another neoplasia, may have no connection with viral transformation.

Clearly, at the present stage of carcinogenesis theory development, we have no reasons to make a sharp distinction between viro-genetic and chemical theories.

REFERENCES

- [1] E.L. ANDRONIKASHVILI, N.G. ESIPOVA, *J. Mol. Catal.*, **23**, 195 (1984).
- [2] G. KLOPMAN, A. RAY, *Cancer Biochem. Biophys.*, **6**, 31-35 (1982).
- [3] C.J. TABIN, S.M. BRADLEY, C.J. BARGMAN, R.A. WEINBERG, *Nature (London)*, **300**, 143-149 (1982).
- [4] E.P. REDDY, R.K. REYNOLDS, E. SANTOS, M. BARBACID, *Nature (London)*, **300**, 149-152 (1982).



PS6.17 — MO

YOSHIKAZU MATSUSHIMA

Kyoritsu College of Pharmacy
Shibakoen, Tokyo 105
Japan

YOSHIHARU KARUBE

Faculty of Pharmaceutical Sciences
Fukuoka University
Nanakuma, Fukuoka 815
Japan

TUMOR LOCALIZING METAL COMPLEXES

We reported [1] that the radioactivity was concentrated in tumor tissues in experimental animals a few hours after the administration of the complexes of ethylenediamine-*N,N*-diacetic acid (EDDA) and related chelating agents with ^{99m}Tc . The tumor tissues were clearly visualized in scintigrams [2].

Complexes of EDDA with other radioactive metal ions and ^3H -labeled EDDA were prepared and the biodistribution of the radioactivity in mice bearing Ehrlich tumor was studied. The tumor/blood and tumor/muscle ratios of the radioactivity indicated that ^{57}Co EDDA was concentrated in the tumor tissues. The higher affinity for the tumor was noted with $\mu\text{-OXO } ^{57}\text{Co}$ EDDA, which was prepared by treatment of ^{57}Co EDDA with hydrogen peroxide. The ^{51}Cr , ^{59}Fe , ^{64}Cu and ^{67}Ga complexes of EDDA as well as ^3H -labeled EDDA were not concentrated in the tumor.

The tumor localizing EDDA complexes (^{99m}Tc EDDA and $\mu\text{-OXO } ^{57}\text{Co}$ EDDA) and related radioactive compounds, which are not tumor localizing, were injected intravenously to rats. The compounds studied were $\text{Na}^{99m}\text{TcO}_4$, $^{57}\text{CoCl}_2$, and the complexes of *N'*-acetythylenediamine-*N,N*-diacetic acid (AcEDDA) with ^{99m}Tc and ^{57}Co . Hepalinized blood was collected 1 h after the injection and was analyzed by density gradient centrifugation and dialysis.

Most of the radioactivity was present in blood plasma and cellular fractions contained less than 10% of the radioactivity. Results of dialysis of the blood against physiological saline were significantly different between the tumor localizing and not localizing complexes. Most of the radioactivity was dialyzable in the blood of rats administered with $^{99m}\text{TcO}_4^-$ and more than 80% was dialyzed in 24 h in those of the EDDA complexes. In those of the other radioactive compounds, more than 60% radioactivity was remaining undialyzed indicating that the radioactivity was firmly bound to plasma proteins.

The radioactive compounds were administered to mice bearing Ehrlich tumor. The tumor tissues were removed at selected times, homogenized, separated into nuclear, mitochondrial, microsomal, and supernatant fractions by centrifugation, and measured the radioactivity of the fractions. The results showed that the EDDA complexes were concentrated in the nuclear fraction, whereas the other compounds in the supernatant fraction. From the results above mentioned, the following conclusions may be drawn on the tumor localizing EDDA complexes. The EDDA complexes of ^{99m}Tc and ^{57}Co were not firmly bound to plasma proteins *in vivo*. Hence they were rapidly transferred into tumor tissues and rapidly cleared through kidneys from blood. Relatively high radioactivity in tumor tissues and low radioactivity in blood should give clear scintigrams of the tumor tissues.

REFERENCES

- [1] Y. MATSUSHIMA, Y. KARUBE, presented at 1st ICBC, *Inorg. Chim. Acta*, **79**, 285 (1983).
- [2] Y. KARUBE *et al.*, *Chem. Pharm. Bull.*, **29**, 2385 (1981); **30**, 2529 (1982); **31**, 3242 (1983); **32**, 4049 (1984).



PS6.18 — TU

M.M. NANDI

A.K. MISHRA*

MISS RUMA RAY

Inorganic Chemistry Laboratory

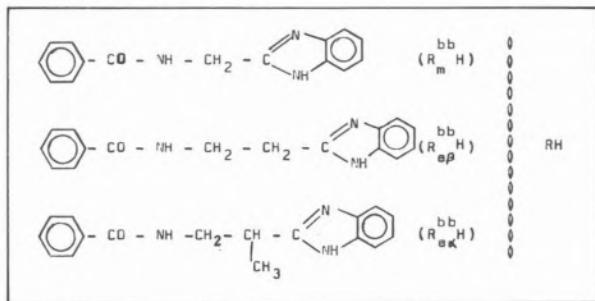
Calcutta University Post Graduate Centre

Agartala — 799004, Tripura

India

SYNTHETIC, STRUCTURAL AND ANTIBACTERIAL SCREENING STUDIES OF Co(II), Ni(II) AND Cu(II) COMPLEXES WITH BENZIMIDAZOLE DERIVATIVES

Recently several benzamido benzimidazoles have been synthesised and some of the compounds are found to be active against gram +ve microorganisms [1] whereas corresponding sulphonamido benzimidazoles which can function as chelating agents [2] are active against gram -ve microorganisms [3]. Now metal complexes of the type $M(RH)_2Cl_2$ [$M = Co(II), Ni(II)$ and $Cu(II)$] have been prepared and characterized by IR, PMR and electronic spectra, conductivity and magnetic moment data.



All the $Cu(II)$ complexes show low magnetic moment values at room temperature which suggests antiferromagnetic interaction between two $Cu(II)$ centres bridged by chloride [4,5]. The presence of

chlorine bridged structure is indicated by IR data. Magnetic moment data and electronic spectra of $Co(II)$ complexes support tetrahedral structure [6,7]. $Ni(R_m^{bb}H)_2Cl_2$ and $Ni(R_{op}^{bb}H)_2Cl_2$ are polymeric in nature and possess octahedral stereochemistry. Due to the presence of a CH_3 group in $R_{o\alpha}^{bb}H$, polymerisation is sterically hindered and $Ni(R_{o\alpha}^{bb}H)_2Cl_2$ is assumed to be in octahedral \rightleftharpoons planar equilibrium and low magnetic moment value is observed [8].

These metal complexes are active against gram +ve and gram -ve microorganisms and the activity is more than the free ligand or metal ion. $Co(II)$ complexes are found to be more active than $Ni(II)$ and $Cu(II)$ complexes.

REFERENCES

- [1] M.M. NANDI, MISS RUMA RAY, *Indian J. Chem.*, Communicated.
- [2] M.M. NANDI, Ph. D. Dissertation, University of Calcutta (1976).
- [3] M.M. NANDI, A.K. MISHRA, *Trans. Bose Res. Inst.*, **44**, 19 (1981).
- [4] E. SINN, *Coord. Chem. Rev.*, **5**, 313 (1970).
- [5] W.D. MCFADYEN, R. ROSON, H.S. CHAPP, *Inorg. Chem.*, **11**, 1777 (1972).
- [6] F.A. COTTON, G. WILKINSON, «Advanced Inorganic Chemistry», John Wiley and Sons, New York, 1980, p. 771.
- [7] R. SASIEGO, J.A. COSTAMAGNA, *J. Inorg. Nuclear Chem.*, **33**, 1528 (1971).
- [8] C.S. CHAMBERLAIN, R.S. DRAGO, *Inorg. Chim. Acta*, **32**, 75 (1979).

* Present address: Bose Institute, Microbiology Department, Calcutta-700009, India.



PS6.19 — TH

G.M. FERGUSON
H.I. GEORGESCU
C.H. EVANS

Departments of Orthopaedic Surgery and Biochemistry
University of Pittsburgh
986 Scaife Hall, Pittsburgh, Pennsylvania 15261
U.S.A.

EFFECTS OF COBALT IONS ON THE SYNOVIAL PRODUCTION OF NEUTRAL PROTEINASES AND PROSTAGLANDIN E₂

INTRODUCTION

Artificial joint replacements contain much metal. For a number of years the metal of choice has been an alloy based on cobalt, although newer prostheses are being made from titanium. The major cause of failure of these devices is aseptic loosening. Recent evidence suggests that loosening is secondary to a localized loss of bone in the area which surrounds the implant. Examination of the femoral component of failed artificial hip joints reveals the presence of a membrane growing at the surface where the surrounding bone meets the cement used to secure the prosthesis [1]. This membrane bears striking histological and cellular similarities to the synovial membrane which lines all articulating joints. Furthermore, it secretes collagenase and prostaglandin E₂ (PGE₂) in culture, thus implicating this pseudo-synovial membrane in the localized osteolysis that promotes aseptic loosening. If so, it is important to identify the local stimuli that provoke the production of collagenase and PGE₂ by cells of the synovial type. Working on the hypothesis that metal ions released by the prosthesis may be responsible, we are engaged in screening various implant metals for their ability to stimulate the production of PGE₂ and three neutral proteinases, including collagenase, by synovial cell cultures. Here we report the effects of Co²⁺.

METHODS

Synovia were obtained from human or lapine knee joints and cultured by standard methods [2]. Sterile, aqueous solutions of CoCl₂ were added to confluent cultures to give final metal ion concentrations from 0 to 10⁻³ M. After 3 days further incubation, the conditioned media were assayed for their neutral proteolytic activity, using ³H-collagen, -gelatin or -casein as substrates and aminophenylmercuric acetate (1 mM) as activator. Prostaglandin E₂ levels were measured by radioimmunoassay.

RESULTS AND DISCUSSION

The production of all three neutral proteolytic activities was stimulated by Co²⁺. For lapine cells, the maximum stimulation of 10-30 fold occurred in the presence of 10⁻⁷ M Co²⁺ (Table 1). Human cells required 10⁻⁴ to 10⁻⁵ M Co²⁺ to achieve a maximum stimulation of 10-15 fold. Production of PGE₂ by lapine cells was elevated 1.5-2 fold at concentrations of Co²⁺ that maximally provoked enzyme release, whereas all concentrations of Co²⁺ slightly depressed the synthesis of PGE₂ by human synovial cells.

Table 1

Production of neutral proteinases and PGE₂ by lapine synovial cells in response to Co²⁺

Metal Ion Added	Enzymic Activity (Units/day/10 ⁶ cells*)			
	Collagenase	Gelatinase	Caseinase	PGE ₂ (ng/culture)
None	0.40	0.27	0.050	193
Co ²⁺ (10 ⁻⁷ M)	13.23	3.96	0.613	285

* 1 Unit of neutral proteinase activity degrades 1μg of the appropriate substrate per min at 37°C.

Suitable control experiments confirmed that Co²⁺ mediated its apparent effects on the production of these neutral proteinases by stimulating the cellular synthetic machinery. Concentrations of Co²⁺ that maximally enhanced apparent enzyme production had no effect when added directly to the proteinase assays. In addition, dialysis of control conditioned media against various concentrations of Co²⁺ failed to stimulate the enzymes' activity post-synthetically. Furthermore, cells whose pro-

duction of neutral proteinases had been previously stimulated by the ionophore A23187 failed to become «hyperstimulated» in the presence of Co^{2+} (data not shown).

As the concentrations of Co^{2+} needed to produce these effects are found in patients with prosthetic joints [3,4], the cellular reactions we describe here deserve further scrutiny.

REFERENCES

- [1] S.R. GOLDRING, A.L. SCHILLER, M. ROELKE, D.A. O'NEILL, W.H. HARRIS, *J. Bone Joint Surg.*, **65A**, 575-584 (1983).
- [2] C.H. EVANS, J.D. RIDELLA, *Anal. Biochem.*, **142**, 411-420 (1984).
- [3] R.F. COLEMAN, J. HERRINGTON, J.T. SCALES, *Br. Med. J.*, **1**, 527-529 (1973).
- [4] H.S. HOBBS, M.J. MINSKI, *Biomaterials*, **1**, 193-198 (1980).



PS6.20 — MO

S.H. LAURIE
D.E. PRATT
School of Chemistry
Leicester Polytechnic
P.O. Box 143, Leicester
England

THE STRUCTURE AND REACTIVITY OF Ni(II)-ALBUMIN PROTEIN COMPLEX

There is much concern regarding the toxic effects of ingested nickel, particularly among workers in nickel refineries [1,2]. For this reason the biochemical studies undertaken by SARKAR and his co-workers [3,4] in relation to ingested Ni are of particular importance. They have shown that the main Ni(II)-binding constituents in human blood are the amino acid histidine (His) and the protein albumin. This distribution resembles that for Cu(II) except the albumin has a much stronger affinity [4] for Cu(II) than Ni(II). Nevertheless,

these studies have established that the two metal ions bind to the same site in the albumin, and this, from Cu(II) studies, is known to involve the *N*-terminal amino acid residues. The proposed near square-planar geometry formed from the amino *N*, deprotonated peptide *N* atoms, and a histidine *N* is depicted in Fig. 1.

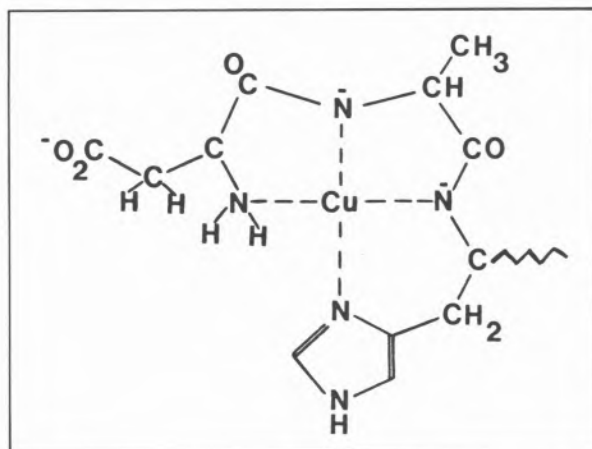


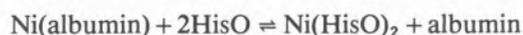
Fig. 1

The proposed Cu(II) coordination site

The ability of Ni(II) to cause peptide *N* deprotonation is known to be less than that of Cu(II), and a structure such as that in Fig. 1 would require a high pH for its formation. In keeping with this the UV/Vis absorption spectrum of 1:1 Ni(II):albumin shows an intense absorption band at 420 nm, characteristic of a square-planar environment, which reaches a maximum absorption at $\text{pH} > 9$ [4].

We have examined the bovine albumin binding of Ni(II) by means of UV/Vis absorption and CD spectroscopy. In agreement with GLENNON and SARKAR [4] the square-planar type spectra reach a maximum at $\text{pH} > 9$. The spectra, shown in Fig. 2, reveal that at the pH of blood (7.4) 70% of the Ni is bound as in Fig. 1. The remaining 30% must be octahedrally co-ordinated since, under the conditions used, this would be spectroscopically silent. The rapidity of interconversion between the two forms as the pH is altered suggests that the octahedral site must also be at the *N*-terminal end of the protein chain.

We have also found that the rate of ligand exchange for Ni(albumin), as in



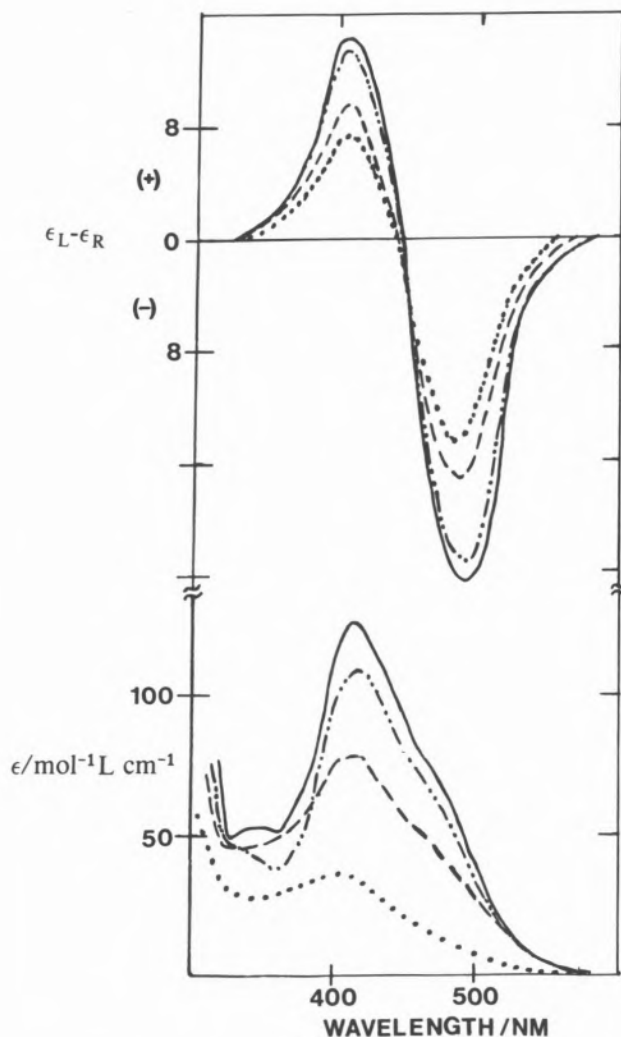


Fig. 2

The CD (upper) and UV/Vis absorption (lower) spectra of Ni(II)-albumin solutions at pH 6.9 (.....), pH 7.4 (-----), pH 8.1 (-·-·-·-), and pH 9.3 (—)

is very slow, requiring > 90 min to achieve equilibrium at 37°C and pH 7.4 (0.15 M NaCl solution), the octahedral species reacting more rapidly (via a dissociative mechanism) than the square-planar form which reacts associatively. The difference in kinetic behaviour between Ni(albumin) and Cu(albumin) could be an important factor in their different metabolic properties [4].

REFERENCES

- [1] M.D. McNEELY, M.W. NECKAY, F.W. SUNDERMAN JR., *Clin. Chem. Winston-Salem, N.C.*, **18**, 992 (1972).
- [2] F.W. SUNDERMAN JR., *Ann. Clin. Lab. Sci.*, **7**, 377 (1977).
- [3] M. LUCASSEN, B. SARKAR, *J. Toxicol. Environ. Health*, **5**, 897 (1979).
- [4] J.D. GLENNON, B. SARKAR, *Biochem. J.*, **203**, 15 (1982).



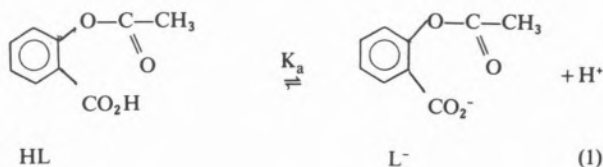
PS6.21 — TU

ALBERT D. KOWALAK
KAREN LeBOULLUEC
University of Lowell
Lowell, Massachusetts 01854
U.S.A.

THE STABILITY CONSTANTS FOR IRON(II)ASPIRINATE(ACETYLSALICYLATE)

The use of acetylsalicylic acid, aspirin, to relieve pain, reduce fever plus a wide variety of other ailments is well known. However, the theories to explain the effects of aspirin are vague. One theory postulates that the body under stress will have a two fold or greater increase of copper ions in the blood stream with a loss of essential copper from the organs. The role of the aspirin is the formation of a copper chelate which facilitates the return of copper to the deficient cells [1]. The chemistry of the coordination of aspirin with metal ions is therefore necessary to have a complete understanding of the therapeutic role of aspirin. Copper(II)aspirinate has been prepared and structural studies of the solid [2] report a polymeric material of units of $[\text{Cu}(\text{C}_9\text{H}_7\text{O}_4)_2]_2$ with the carboxylic group acting as a bridging ligand between two Cu(II) ions as well as Cu-Cu bonding. The aspirin complex in the solid state does not exhibit chelation. There are no other studies that have been reported on the interaction of aspirin with copper; in fact, very little has been reported on the interaction of aspirin with metal ions. We wish to report the results for the determination of the stability constants for the iron(II)-aspirin system.

The aspirin as ligand is monobasic:



with the possibility of the L^- forming a chelate with Fe(II);



The formation of the complex affects the ligand acid dissociation and the complexation may be followed by pH titration with base. The effect of complexation on pH is independent on whether the aspirin is bound to the iron only through the carboxylate group or if a chelate is formed.

Solutions of reagent grade iron(II) chloride or perchlorate with acetylsalicylic acid of known concentrations were prepared. The ionic strength was held constant with 0.1 M KNO_3 . The solutions were titrated with standardized NaOH under a nitrogen gas atmosphere. The $[\text{H}^+]$ was calculated from the pH with correction for the H^+ activity coefficient. The stability constants are based on concentrations.

The following equations were used for the determination of the stability constants:

$$\bar{n} = \frac{[\text{FeL}^+] + 2[\text{FeL}_2] + \dots}{[\text{Fe}^{2+}] + [\text{FeL}^+] + [\text{FeL}_2] + \dots} = \frac{n \Sigma \beta_n [\text{L}^-]^n}{\Sigma \beta_n [\text{L}^-]^n} \quad (4)$$

$$\bar{n}_{\text{exp}} = \frac{C_L - [\text{L}^-] - [\text{HL}]}{C_M} = \frac{C_L - [\text{L}^-]}{C_M} [1 + [\text{H}^+]/K_a] \quad (5)$$

$$[\text{L}^-] = \left[\frac{\text{wt. HL/mol. wt.}}{V_t} - \frac{(V N)_{\text{NaOH}}}{V_t} + \frac{K_w}{[\text{H}^+]} - [\text{H}^+] \right] \frac{K_a}{[\text{H}^+]} \quad (6)$$

The stability constants were calculated by a least squares program for equation (4) with $[\text{L}^-]$ and n_{exp} obtained by computer. K_1 and K_2 were also

determined graphically from plots of n vs pL at $n=0.5$ and 1.5 respectively. Higher order constants were not obtained as at high pH hydroxide species must be considered. In some cases Fe(OH)_2 precipitation occurs.

The pK_a of acetylsalicylic acid was determined to be 3.58. We were also concerned that hydrolysis of the ligand may have occurred. Acidification of various reaction mixtures resulted in a white solid precipitate which melted in the range $128-132^\circ\text{C}$ characteristic of the ligand. The results for the constants are shown in the Table.

The values of $\log K_1$ for the formation of $\text{Fe}(\text{C}_9\text{H}_7\text{O}_4)^+$ appear to be reasonably precise while $\log K_2$ is somewhat questionable particularly at higher ferrous ion concentrations. The deviations may be due to complications caused by hydroxide formation or the formation of dimeric complexes which need further study.

REFERENCES

- [1] J. SCHUBERT, *Sci. Amer.*, **214**, 40 (1966).
- [2] L. MANOJLOVIC-MUIR, *Chem. Commun.*, **20**, 1057 (1967).

Table

$10^3[\text{FeCl}_2]$, M	$10^3[\text{Aspirin}]$, M	$\log K_1^*$	$\log K_2^*$	$\log K_1^\#$	$\log K_2^\#$
2.60	4.51				2.60
1.00	»				2.38
2.13	»				2.79
2.76	»	2.98	2.41	3.04	2.42
3.23	»	3.05		2.98	2.87
3.94	»	2.77		2.76	
3.02	4.22	2.57		2.64	1.02
3.22	»	2.74		2.74	
2.64	»	2.74		2.77	
2.78 ($\text{Fe}(\text{ClO}_4)_2$)	»	2.74		2.77	

* graphical

computer values



PS6.22 — TH

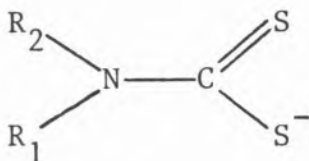
MARK M. JONES
 SHIRLEY G. JONES
 WILLIAM M. MITCHELL
 Departments of Chemistry and Pathology
 and
 Center in Molecular Toxicology
 Vanderbilt University
 Nashville, Tennessee 37235
 U.S.A.

STRUCTURE-ACTIVITY RELATIONSHIPS IN THERAPEUTIC CHELATING AGENTS

The examination of the action of a number of structurally related dithiocarbamates as antagonists for acute and chronic cadmium intoxication reveals a number of relationships involving structural parameters and various measures of antagonist efficacy. The structural features also have a pronounced effect on the histopathology of the liver and kidney in treated animals.

The report by GALE *et al.* [1] of the ability of sodium diethyldithiocarbamate to antagonize the acute toxicity of cadmium chloride led us to examine this action in some detail [2-6]. We found that while sodium diethyldithiocarbamate was, in fact, an effective antagonist, its use led to increased levels of cadmium in the brain. Subsequently, preparation and testing of a large number of structurally related dithiocarbamates led to the discovery that alterations in the brain levels of cadmium were strongly dependent on the groups attached to the dithiocarbamate moiety and that the transport of cadmium into the brain could be reduced by the use of substituents with more polar components.

All of the compounds examined had the chelating group



present, with R_1 and R_2 varied. The differences in the relative polarities of compounds in this series were estimated as roughly equivalent to the differences in the sums of the π constants for the groups R_1 and R_2 . Each compound was thus characterized by the term $(\pi_1 + \pi_2)$ where π_1 is the π constant of HANSCH and LEO [7] for R_1 and π_2 that for R_2 . It was found that compounds with strongly polar (or ionic groups) as well as those with very non-polar substituents were both less effective as antagonists than compounds whose R groups were of intermediate polarity (*i.e.* those bearing $-OH$ groups). The measures of activity used include the following: survival ratios in acute cadmium chloride intoxication and relative cadmium levels in various organs (brain, liver or kidney) as well as composite measures which had two or more of these factors given various relative weights.

The pathological changes (in animals with chronic cadmium intoxication) subsequent to the use of these chelating agents to mobilize the cadmium are also very strongly dependent upon the structure of the chelating agent utilized to effect the mobilization.

Because the organ distribution of various toxic metals is not identical, different relationships between structure and activity of chelating agents can be anticipated, and indeed are found [8,9] for other toxic metallic species.

REFERENCES

- [1] G.R. GALE, A.B. SMITH, E.M. WALKER JR., *Ann. Clin. Lab. Med.*, **11**, 476 (1981).
- [2] S.G. JONES, M.A. BASINGER, M.M. JONES, S.J. GIBBS, *Res. Commun. Chem. Pathol. Pharmacol.*, **38**, 271 (1982).
- [3] S.G. JONES, M.M. JONES, M.A. BASINGER, L.T. BURKA, L.A. SHINOBU, *Res. Commun. Chem. Pathol. Pharmacol.*, **40**, 155 (1983).
- [4] L.A. SHINOBU, S.G. JONES, M.M. JONES, *Acta Pharmacol. Toxicol.*, **54**, 189 (1984).
- [5] L.A. SHINOBU, S.G. JONES, M.M. JONES, *Arch. Toxicol.*, **54**, 235 (1983).
- [6] S.G. JONES, M.M. JONES, *Environ. Health Persp.*, **54**, 285 (1984).
- [7] C. HANSCH, A. LEO, «Substituent Constants for Correlation Analysis in Chemistry and Biology», John Wiley & Sons, New York, 1979.
- [8] G.R. GALE, L.M. ATKINS, A.B. SMITH, E.M. WALKER JR., M.M. JONES, *Res. Commun. Chem. Pathol. Pharmacol.*, **45**, 119 (1984).
- [9] G.R. GALE, L.M. ATKINS, A.B. SMITH, M.M. JONES, *Res. Commun. Chem. Pathol. Pharmacol.*, in press.



PS6.23 — MO

SONIA APELGOT
ALAIN JOSEPH
JACQUES COPPEY
Institut Curie
11, rue Pierre et Marie Curie 75231
Paris Cédex 05
France

ALAIN GAUDEMER
ISABELLE SASAKI
DANIÈLE PRASEUTH
Laboratoire de Chimie de Coordination Bioorganique
LA 255, Université Paris-Sud
91405 — Orsay
France

ETIENNE GUILLE
JANINE GRISVARD
IGOR SISOËFF
Laboratoire de Biologie Moléculaire Végétale
LA 40, Université Paris-Sud
91405 — Orsay
France

LETHAL EFFECT OF EITHER $^{64}\text{CuCl}_2$ OR $^{64}\text{Cu-TMPyP}$ INCORPORATED IN HUMAN MALIGNANT CELLS

This study was performed with A549 human malignant cells. The cells were in contact with the radioactive compound for 14, 24 or 43 hours, then washed and numerated. The incorporated radioactivity was determined as well as the Cloning

Forming Capability (C.F.C) of the cells. A clear lethal effect was observed. When the survival is expressed as a function of the radioactivity present in the growth medium ($\mu\text{Ci/ml}$) at the beginning of the contact period, exponential curves were obtained either for $^{64}\text{CuCl}_2$ or for $^{64}\text{Cu-TMPyP}$ (TMPyP = Tetra methyl pyridine porphine). The slope of the curve obtained when $^{64}\text{Cu-TMPyP}$ was used is 1.5 time greater than that with $^{64}\text{CuCl}_2$.

This study and control experiments show that:

- 1) The lethal effect observed is not a consequence of the irradiation by the particules emitted by ^{64}Cu but a consequence of the decay itself.
- 2) Each survival curve is characterized as a single exponential curve although the cells are in non-synchronized growth conditions. This result implies that the incorporation of ^{64}Cu in the compartment implicated in the lethal effect is independent of DNA synthesis.
- 3) All experiments performed to study the lethal effect of intracellular decay of radioactive isotopes have shown that an exponential survival curve is always related to decays occurring inside the DNA molecule only.
- 4) We detected ^{64}Cu bound to DNA whatever $^{64}\text{CuCl}_2$ or $^{64}\text{Cu-TMPyP}$ was used. Experiments are still in progress in order to evaluate the number of ^{64}Cu atoms bound to the DNA molecule and to evidence a relationship with the different lethal efficiency of this two compounds. A lethal effect of ^{65}Zn via decay has been also observed for A549 cells labelled with $^{65}\text{ZnCl}_2$.

7. Chemical Elements in Living Organisms



PS7.1 — MO

BARRY G. MORRELL
NICHOLAS W. LEPP

Department of Biology
Liverpool Polytechnic
Byrom Street, Liverpool L3 3AF
U.K.

DAVID A. PHIPPS
CARL A. HAMPSON
Department of Chemistry and Biochemistry
Liverpool Polytechnic
Byrom Street, Liverpool L3 3AF
U.K.

REDUCTION OF VANADIUM BY HIGHER PLANT ROOTS

INTRODUCTION

The mobilisation of metals in soils and their subsequent uptake by plants is a complex process. Within the soil there is a wide range of processes both biotic and abiotic which can alter the chemical form of the metal and hence its pattern of translocation. Precipitation and solubilisation are markedly affected by both complex formations and by redox reactions; these processes are themselves substantially affected by pH changes. Consequently, it is essential to consider such changes when attempting to examine the uptake of metals from soils by plants, since availability depends on chemical form. However, even if it is possible to establish the nature of the chemical species within the soil solution, there is no assurance that the same species will exist within the plant. Changes in both complex structure and redox state of the metal ion both occur readily and indeed, as is known for iron, the latter may play a significant part in the uptake process [1,2].

By using solution culture techniques it is possible to remove the effect of the soil components and to focus attention on the effect of plant roots on the uptake of the metal.

Vanadium is an element which exhibits a multiplicity of forms in soil systems. In parent materials, it is generally present as the reduced trivalent form, where it replaces Fe(III). Weathering of the parent material will lead to release of vanadium in the fully oxidized pentavalent form. This fully oxidized form (VO_3^-) is generally considered to be a mobile form of vanadium in soil solutions. There is, however, strong evidence of reduction, $\text{V}^{\text{V}} \rightarrow \text{V}^{\text{IV}}$, by soil organic matter [3]. This reduced vanadium is thought to exist as an anionic complex [4]; its presence in an uncomplexed form is highly unlikely since the VO^{2+} entity is only stable at pHs below 2.4 [5].

Previous studies on the uptake of vanadium utilizing excised roots and whole plants [6] have revealed a striking similarity between the uptake patterns of the two vanadium forms (V^{IV} , V^{V}). Such similarities would not be expected because of the dissimilarity of the ions. Vanadium injected into rats always adopts the V^{IV} state independent of injected form [7]. Thus it might be that vanadium in plants could always have a common form. This paper describes some initial work examining the form of vanadium in plants.

METHODS AND MATERIALS

Barley seeds (*Hordeum vulgare* L. cv. Maris Mink) were soaked for 12 hours in double distilled H_2O and then spread onto moistened tissue paper and allowed to germinate. After two days growth the seeds were transferred to beakers containing the appropriate uptake solution. The seeds were supported in glass tubes with a slight constriction at the neck. All solutions were aerated and changed every two days. Solution 1 contained 0.5 mM CaCl_2 , solution 2 0.5 mM CaCl_2 and 0.1 mM VO^{2+} , solution 3 0.5 mM CaCl_2 and 0.1 mM VO_3^- . After 9 days growth the roots were removed from the solution, blotted and freeze dried to a constant weight.

Plant material was analysed using a Bruker EPR spectrophotometer.

RESULTS

Roots which had been in CaCl_2 alone produced no spectra. Roots which had been in a solution containing VO^{2+} produced an eight peak spectra (fig. 1a) characteristic of the VO^{2+} entity. Roots which had been exposed to VO_3^- also produced a similar eight peak spectra (fig. 1b).

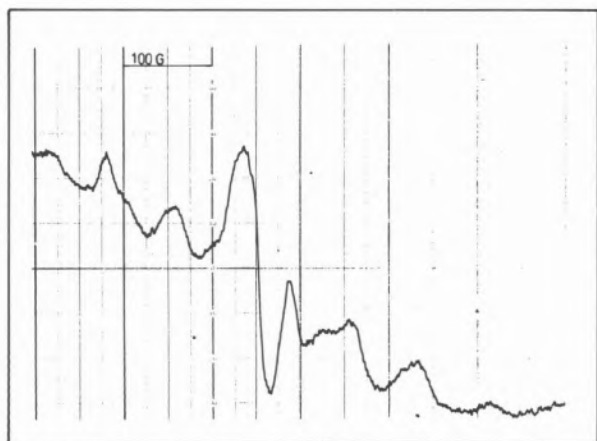


Fig. 1a

EPR spectra for roots grown in 0.1 mM $\text{VOSO}_4 + 0.5$ mM CaCl_2

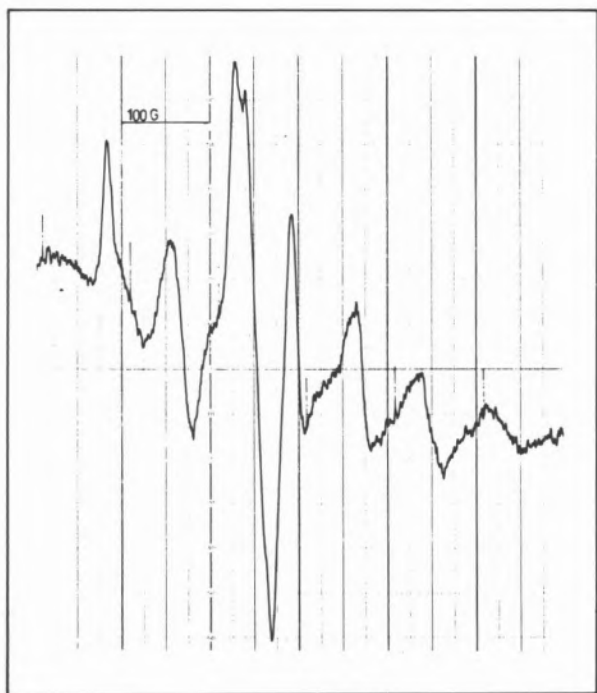


Fig. 1b

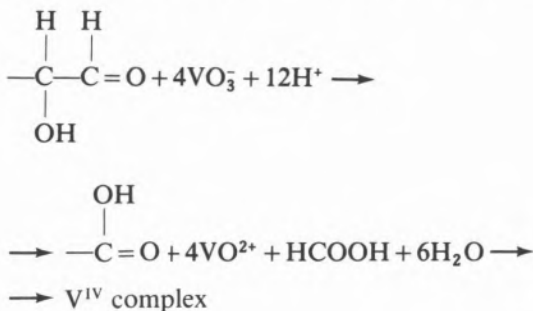
EPR spectra for roots grown in 0.1 mM $\text{NH}_4\text{VO}_3 + 0.5$ mM CaCl_2

DISCUSSION

Only substances with an unpaired electron will produce an EPR spectrum. V^{IV} with an outer electronic configuration of $4d^3 3s^1$ is thus EPR active and produces a characteristic eight peak EPR spectrum. The appearance of such a spectrum from root material exposed only to fully oxidized vanadium therefore indicates reduction has taken place. The reduction is unlikely to have occurred in the solution given its high pH and the constant aeration. The most probable explanation is that the roots have caused this reduction.

Reduction of metal ions by the roots of higher plants is a well documented phenomenon. UREN [8] has shown reduction of insoluble manganese oxides by the roots of sunflower seedlings. The reduction of Fe^{III} to Fe^{II} is also well understood [1,2]. CHANEY *et al.* [1] have proposed a mechanism of Fe reduction which involves reduction of an Fe^{III} chelate at the plasmalemma and subsequent uptake of the dissociated reduced ion. RÖHMELD and MARSCHNER [2] supported this hypothesis, as opposed to reduction in the intracellular space by secreted reductants.

The mechanism of vanadium reduction in plant roots is probably different to these, involving cell wall polyuronates as proposed by DEIANA *et al.* [9]. Polygalacturonic acid, a component of plant cell walls, will readily react with soil mineral species such as V^V because of the reducing properties of the polysaccharide end units. Reduction and subsequent complexation of the reduced species will occur, and DEIANA *et al.* [9] have proposed a mechanism for reduction of V^V to V^{IV} .



DEIANA *et al.* [9] pointed to the significance of these processes in maintaining a micro-nutrient supply for higher plant roots, especially in the case of Fe which can only be absorbed in

the reduced form. In the case of vanadium it is probably the reverse in that reduction and subsequent complexation of vanadium reduces its availability. Complexation no doubt prevents accumulation of V^V in the cell where its adverse effects on enzyme systems might cause severe cellular disruption.

REFERENCES

- [1] R.L. CHANEY, J.C. BROWN, L.O. TIFFIN, *Plant Physiol.*, **50**, 208-213 (1972).
- [2] V. RÖHMELD, H. MARSCHNER, *Plant Physiol.*, **71**, 949-959 (1983).
- [3] A. SZALAY, M. SZILAGYI, *Geochim. Cosmochim. Acta*, **31**, 1-6 (1967).
- [4] C. BLOOMFIELD, W.F. KELSO, *J. Soil Sci.*, **24**, 368-379 (1973).
- [5] G.A. DEAN, J.F. HERRINGSHAW, *Talanta*, **10**, 793-799 (1963).
- [6] B.G. MORRELL, N.W. LEPP, D.A. PHIPPS, *Minerals and Environ.*, **5**, 79-81 (1983).
- [7] E. SABBIONI, E. MARANANTE, L. AMATINI, L. UBERTALLI, C. BIRATTORI, *Bioinorganic Chemistry*, **8**, 503-515 (1978).
- [8] N.C. UREN, *J. Plant. Nutr.*, **4**, 65-71 (1981).
- [9] S. DEIANA, A. DESSI, G. MICERA, C. GESSA, M.L. DE CHERCHI, *Inorg. Chim. Acta*, **79**, 231-232 (1983).



PS7.2 — MO

PAUL G. LOGAN
NICHOLAS W. LEPP
Department of Biology
DAVID A. PHIPPS
Department of Chemistry and Biochemistry

Liverpool Polytechnic
Byrom Street, Liverpool L3 3AF
U.K.

THALLIUM UPTAKE BY PLANT ROOTS: COMPETITIVE EFFECTS OF POTASSIUM IONS

INTRODUCTION

Thallium is a rare but toxic element, with a mean crystal abundance of approximately 1 ppm. Biologically, thallium is of interest due to its mimicry of K^+ in many biological systems [1]. Thallium shows many physico-chemico similarities to potas-

sium, with the ionic radius of Tl^+ being very similar to the alkali metal cations Rb^+ and K^+ ($K^+ = 133$ pm, $Tl^+ = 144$ pm, $Rb^+ = 148$ pm). Tl^+ has been shown to be more effective than K^+ , Rb^+ or Cs^+ at activating certain (Na^+/K^+) ATPases [2,3], whilst MULLINS and MOORE [4] have shown that both the kinetics of exchange and the electrochemical influences of Tl^+ and K^+ are virtually identical in the cells of the frog sartorius.

Levels reported in soils vary in the literature, between 0.05 and $0.5 \mu\text{g.g}^{-1}$ dry weight, although recent studies by German workers report levels exceeding this value [5].

Thallium levels in plants have been reported as between 0.01 and 3800 ppm ash weight, with 0.5 ppm being typical for most species [1]. Plants with elevated thallium levels have been found in areas of natural thallium mineralization, and have been reported as toxic to grazing sheep and cattle [6].

The aim of this study is to examine the kinetics of uptake of thallium by excised barley roots, and to compare it with findings for K^+ by other workers.

MATERIALS AND METHODS

Low salt barley roots were grown hydroponically as described by EPSTEIN [7]. Barley seeds (*Hordeum vulgare* c.v. Maris Mink) were soaked in aerated distilled water for 4 hours, germinated and grown in the dark at 25°C for 7 days. Roots were excised, rinsed in distilled water, thoroughly mixed, and placed in aerated 0.5 mM CaCl_2 solution, prior to experimental use.

Uptake experiments were carried out as described by HARRISON *et al.* [8]. Roots were placed in aerated thallos acetate solutions at various concentrations, spiked with the isotope ^{204}Tl . After 15 minutes roots were removed, rinsed in chilled distilled water, and placed in chilled (2°C) unspiked thallos acetate solution for 30 minutes, after which they were removed, blotted to remove excess moisture, and weighed into digestion flasks. Samples were digested in 5 ml of a sulphuric acid/hydrogen peroxide mixture as described by ALLEN [9]. Samples were poured into scintillation vials, the flasks rinsed with 5 ml distilled H_2O , and the washings added to the samples. Activity was measured directly by measuring Cerenkov ra-

diation in a Packard Tricarb liquid scintillation counter.

In competition studies K^+ was added as KCl, and the above procedure followed.

RESULTS

The initial uptake velocity of Tl^+ by excised roots showed a hyperbolic profile with respect to the concentration of the ion in the bathing solution (Fig. 1). The maximum velocity was calculated (from the curve) at 27.5 mol/gram fresh wt./hour, and from this the K_m of 80 μM was obtained.

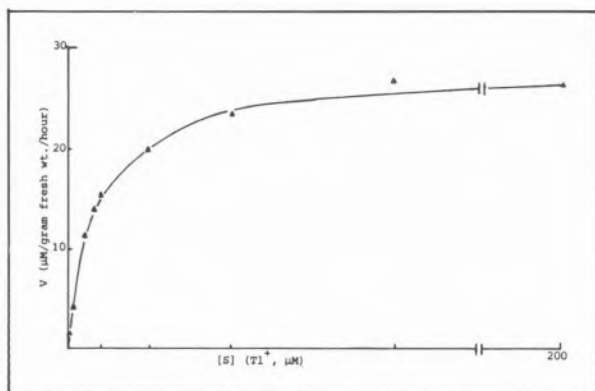


Fig. 1

Initial rate of uptake (V) against concentration of thallium $[S]$.
Uptake for 15 minutes. Desorption 30 minutes.
 $V_{max} = 27.5$; $K_m = 80 \mu M$

Competition studies with potassium showed a strongly competitive effect of the cation on thallium absorption (Fig. 2). The results are presented

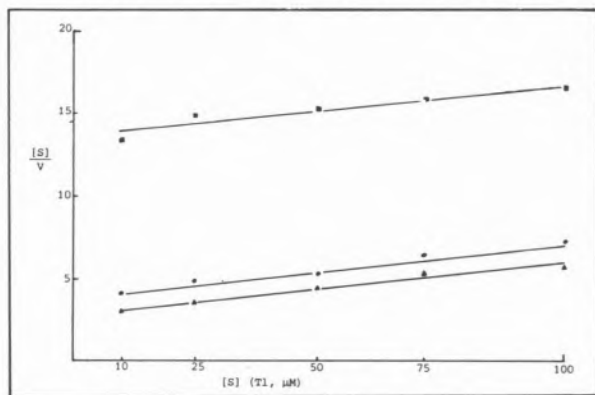


Fig. 2

Hanes plot of uptake of thallium at various concentrations in the presence and absence of inhibitors.
▲ = control; $K_m = 87$; ● = 100 $\mu M K^+$; $K_m = 106$; ■ = 500 $\mu M K^+$; $K_m = 414$

in Hanes plot showing S/V against S . The competitive nature of the inhibition is marked by an increase in the apparent K_m value in the presence of the inhibitor, with no overall change in the maximum velocity (K_m control = 87.17; K_m (100 $\mu M K^+$) = 106.21; K_m (500 $\mu M K^+$) = 414.72 μm . $V_{max} = 30.12 \pm 1.95 \mu M Tl/gram$ fresh weight/hour. The inhibition constant, K_i , was calculated from the graph as 122 μM .

DISCUSSION

The results obtained show a contrasting picture. The competition studies carried out suggest that K^+ is a competitive inhibitor of Tl^+ uptake, possibly indicating that they are both taken up by the same carrier system. The results from thallium uptake studies show that for increasing thallium concentrations a single hyperbola is obtained in accordance with Michaelis-Menten kinetics. Potassium has been shown to deviate from simple Michaelis-Menten kinetics, with a dual pattern of uptake. This involves two mechanisms [10]; mechanism I a high affinity carrier; and mechanism II, a low affinity carrier. The K_m value for K^+ uptake is given as approximately 20 μM [11] which is considerably less than that obtained for Tl uptake (80 μM). This suggests that K^+ has a greater affinity for the carrier than Tl^+ , and would therefore explain why, over the concentration range studied, a single hyperbola describes Tl^+ uptake. It could be concluded that the lower affinity of Tl^+ for the carrier means that saturation kinetics for type I sites are not reached until much higher Tl^+ concentrations, i.e. beyond the range studied here, and that thallium uptake over the range studied* is almost exclusively by mechanism I of the potassium carrier system.

REFERENCES

[1] I.C. SMITH, B.L. CARSON, «Trace metals in the environment, vol. I. Thallium», Ann Arbor Press, 1977.
[2] J.S. BRITTEN, M. BLANK, *Biochem. Biophys. Acta*, **159**, 160 (1968).
[3] CH. E. INTURUSSI, *Biochem. Biophys. Acta*, **173**, 567 (1969).
[4] L.J. MULLINS, R.D. MOORE, *J. Gen. Physiol.*, **43**, 759-773 (1960).
[5] R. SEEGER, M. GROSS, *Z. Lebensm. Unters. Forsch.*, **173**, 9-15 (1981).

- [6] V. ZYKA, *Sb. Geol. Technol. Geochem.*, **12**, 157-160 (1974).
 [7] E. EPSTEIN, *Plant Physiol.*, **36**, 437-444 (1961).
 [8] S.J. HARRISON, N.W. LEPP, D.A. PHIPPS, *Z. Pflanzenphysiol.*, **90**, 443-450 (1978).
 [9] S.E. ALLEN (ed.), «Chemical analysis of ecological material», Blackwell Scientific Publishers, London, 1977.
 [10] E. EPSTEIN, *Int. Rev. Cytol.*, **34**, 123-168 (1973).
 [11] E. EPSTEIN, «Mineral Nutrition of Plants. Principles and Perspectives», John Wiley and Sons, New York, 1972.



PS7.3 — TH

S.H. LAURIE
 N.P. TANCOCK
 School of Chemistry
 Leicester Polytechnic
 P.O. Box 143, Leicester, LE1 9BH
 England
 S.P. McGRATH
 J.R. SANDERS
 Rothamsted Experimental Station
 Harpenden, Herts
 England

THE INFLUENCE OF COMPLEXATION ON MICRONUTRIENT UPTAKE BY PLANTS: A COMBINATION OF COMPUTER SIMULATION AND PLANT GROWTH EXPERIMENTS

Chelation of the micronutrient metal ions (Cu, Fe, Mn and Zn) is known to be an important factor in the efficacy of their uptake by plants [1,2]. Chelation may occur by plant exudates [3], in substances released from decaying organic matter [4], and in bacterial excretions [5]. It is reasonable to postulate that chelation is essential (i) for the solubilization of the metal ions, particularly under alkaline conditions; (ii) for metal transportation; and (iii) for selectivity between the metal ions.

Over the past 30 years there has been a large number of studies on the application of synthetic

chelating agents to overcome plant nutritional problems, most noticeably the use of EDTA and related chelating agents to overcome plant iron deficiencies [6]. In other cases, e.g. with Cu, chelation with EDTA reportedly decreases plant uptakes [7]. In fact, there is little agreement on the influence and mechanism of chelation of the micronutrient metal ions in relation to the subsequent plant growth and health. Many of these conflicts can be attributed to a lack of knowledge or consideration of the metal speciation and to ignoring the mutual influence of one metal upon another.

Fortunately, plants may be grown from aqueous solutions which contain known levels of metal salts and chelating agents. The speciation in such solutions can now readily be calculated via computer simulation, provided the relevant thermodynamic data are available. A number of computer programs are available for assessing metal speciation in multi-metal multi-ligand systems (e.g. ECCLES, GEOCHEM, PSEUDOPLOT), such programs lead to the same results in general [8]. We have begun a series of studies on the influence of complexation upon metal ion uptakes from nutrient solutions and the effects upon plant growth and health. The emphasis is on a multi-metal study. Thus, barley seeds are allowed to germinate under carefully controlled conditions and then grown in nutrient solutions containing EDTA. A «continuous replenishment» method is being used to avoid changes in solution concentrations and pH. The solutions used differ in EDTA level and/or pH. The plants are harvested at set times, washed, weighed, and then the roots and tops separately analysed for all elements with an ICP instrument. The complexation of each metal ion in each of the solutions is determined by computer simulation. By small changes in EDTA and/or pH quite wide variations in the degrees of chelation can be obtained for one or more of the metal ions. In our initial studies solutions of the same nutrient composition (Long Ashton nutrient solutions) and pH but with varying EDTA concentrations were used. The barley plants were grown in these solutions at 20°C under regulated lighting conditions and humidity. The computed speciation of the metal ions is shown in the Table. The data in column 1 show that the assumption that

Table
Computed Percentages of Metal Ions Complexed by EDTA.
Temp. 20°C, pH 5.2, EDTA the only variable

EDTA/Fe Ratio:	1.0	1.05	1.10	1.15	1.20
Ca	0	0	0	0.1	0.2
Cu	53.8	100	100	100	100
Fe	99.5	100	100	100	100
Mg	0	0	0	0	0
Mn	0	21.6	53.4	73.2	83.1
Zn	0.8	99.3	99.8	100	100

EDTA only binds Fe, when FeNaEDTA salt is used, is invalid. Statistical analyses show that increasing EDTA results in decreased Fe and P uptakes but enhanced Cu and Mn uptakes. Al, Ca, Mg, Na, K, Mo and Zn levels were not affected neither were the plant growths. Both complexation and mutual metal ion interactions are seen to influence the metal uptakes. Further work is proceeding.

ACKNOWLEDGEMENTS

This work is supported by the Agricultural Research Council, U.K.

REFERENCES

- [1] W.L. LINDSAY, in E.W. CARSON (ed.), «The Plant Root and its Environment», University Press of Virginia, Charlottesville, 1974, p. 507.
- [2] D.A. ROBB, W.S. PIERPOINT (eds.), «Metals and Micro-nutrients», Academic Press, 1983.
- [3] F.J. STEVENSON, M.S. ARDAKANI, in J.J. MORTVEDT, P.M. GIORDANO, W.L. LINDSAY (eds.), «Micronutrients in Agriculture», Soil Science Society of America, Wisconsin, 1972, p. 79.
- [4] S.M. ELGAWHARY, W.L. LINDSAY, W.D. KEMPER, *Soil Science Society of Am. Proc.*, **34**, 211 (1970).
- [5] T. EMERY, in J.B. NEILANDS (ed.), «Microbial Iron Metabolism: A Comprehensive Treatise», Academic Press, London, 1974, p. 107.
- [6] A. WALLACE, G.A. WALLACE, *Proc. 9th Int. Plant Nutr. Colloq.*, **2**, 696 (1982).
- [7] B.A. GOODMAN, D.J. LINEHAM, in J.L. HARLEY, R. SCOTT RUSSELL (eds.), «The Soil-Root Interface», Academic Press, London, 1979, p. 67.
- [8] D.J. LEGGETT, *Talanta*, **24**, 535 (1977).



PS7.4 — MO

ANA L. DA NOBRE
ANTONIA D. DAS NEVES
CARMEN A. DE G. TORRES
MARIA DAS G.S. DE SOUZA
CRISTINA M. BARRA

Departamento de Química
UFRRJ

Rio de Janeiro
Brasil

ADILSON J. CURTIUS

Departamento de Química

PUC-RJ
Rio de Janeiro
Brasil

VARIATION OF METAL CONCENTRATIONS IN DIFFERENT PARTS OF SUGARCANE

The average concentrations and the relative standard deviations for K, Ca, Mg, Mn, Cu, Fe and Zn in different parts of 10 samples of sugarcane were obtained. The relative standard deviations ranged from 12 to 87%.

The low productivity of sugarcane crops in the Northeast of Brazil is attributed to deficiency of nutrients, including some metals, in the soil. Knowledge about the absorption of nutrients by a plant would be useful for an efficient soil correction. It is also important to verify the antagonistic effects of these elements, since the excess of one can imply in the deficiency of the other. Some metals also play an important role in the fermentation of molasses in the production of ethanol.

Several authors have studied metals in sugarcane: ORLANDO *et al.* [1,2] studied the influence of age and soil and HUMBERT [3] the effect of variety. A review on the subject was done by MALAVOLTA *et al.* [4]. CAMPOS and CURTIUS [5] studied the distribution of metals in different internodes of three varieties of sugarcane. They found that generally, the upper internodes are enriched in metals, and that different samples of a same variety, showed, for the same internode and metal, very different

concentrations. In the present work a more complete study of this variation was done.

Ten sugarcane plants of the variety CB 45-3 grown in the same soil and with the same age, 15 months, were collected. Individual parts were prepared and analysed. After cleaning, the plants were cut with a plastic knife, dried, and ashed at 500-550°C. The ashes were dissolved in an acid solution. After filtering, the K was determined by flame photometry, and the other metals by atomic absorption spectrophotometry. Experimental details are given elsewhere [5].

In this work, leaf 1 is the farthest from the root, that, at the basis makes an angle different from zero with the stem. Internode 1 is just below leaf 1. The number of internodes increases from the top of the plant to the root.

The results are shown in Table 1.

were found for K which also is the major element among those studied.

When studying plants, it is necessary to be aware that such strong individuality is common. Therefore, it is difficult to interpret the variations of metal concentrations in terms of the effects of climate, soil, variety, *etc.* The possibility of using an element as an internal standard should be considered.

The authors have also applied these findings to the study of metal distribution in sugarcane of different ages grown in soils enriched in Zn or in K.

ACKNOWLEDGEMENTS

The authors are thankful to FINEP and CNPq for financing this project.

Table 1
Average concentration (in ppm, dry material) standard deviation and relative standard deviation (in %) for sugarcane parts (10 plants)

		K	Ca	Mg	Mn	Cu	Fe	Zn
Leaf 1	\bar{x}	9200	5190	2230	220	3,7	73	75
	s	5140	2300	953	27	0,8	13	34
	RSD	56	44	43	12	22	17	45
Internode 1	\bar{x}	3850	1430	1330	93	5,9	42	55
	s	2720	800	520	32	1,6	8	17
	RSD	71	56	40	35	28	19	31
Internode 5	\bar{x}	4500	1020	850	80	3,8	32	42
	s	3710	430	450	43	1,2	8	36
	RSD	82	42	53	56	32	24	84
Internode 7	\bar{x}	2860	720	830	68	2,6	27	32
	s	2490	360	290	31	1,1	7	15
	RSD	87	50	35	46	43	24	47

In all the plants studied, leaf 1 was enriched in K, Ca, Mg and Mn in comparison with the internodes. Generally the average metal concentration decreases from internode 1 to internode 7, being about the double in the upper internode. These results are in agreement with those of Campos and Curtius [5] who studied plants grown in a different soil.

The relative standard deviations are very high, ranging from 12 to 87%. Except for Zn in internode 5, the higher relative standard deviations

REFERENCES

- [1] J. ORLANDO F.º, H.P. HAAG, E. ZAMBELLO JR., *Boletim Técnico Planalsucar*, 2(1), 3-127 (1980).
- [2] J. ORLANDO F.º, E. ZAMBELLO JR., H.P. HAAG, *Boletim Técnico Planalsucar*, 2(2), 3-39 (1980).
- [3] R.P. HUMBERT, «The Growing of Sugarcane», Elsevier, 1968.
- [4] E. MALAVOLTA, H.P. HAAG, F.A.F. DE MELLO, M.O.C. BRASIL SOBR.º, «Nutrição Mineral e Adubação de Plantas Cultivadas», São Paulo, Editora Pioneira, 1974.
- [5] C.C. CAMPOS, A.J. CURTIUS, *An. Acad. Bras. Ciênc.*, 54(4), 663-668 (1982).



PS7.5 — TU

D.J. McWEENY
 H.M. CREWS
 J.A. BURRELL
 R.C. MASSEY
 Food Science Laboratory
 Ministry of Agriculture, Fisheries and Food
 Queen Street, Norwich NR2 4SX
 England

TRACE ELEMENTS IN FOOD: EFFECTS OF DIGESTIVE ENZYMES ON SOLUBILITY

Treatment of food with digestive enzymes can have a marked effect on the solubility of trace elements such as Cu, Zn, Fe, Pb and Cd. In some cases the change in solubility indicates enzymic release of the trace element from a previously insoluble form but in other cases solubility decreases. This may indicate enzymic breakdown of a soluble complex to release the element in a «free» state which then forms an insoluble species; alternatively it may indicate the enzymic release of a chelating agent which forms an insoluble complex with a trace element which was previously in a soluble form.

A range of foods (bread, crab, beef, liver, green vegetables) have been examined and show these effects in varying degrees which reflect compositional (and processing) differences between the foods. Changes which occur when foods are enzyme-digested together, rather than separately, can be attributed to analogous processes.

The possibility of extending this information through chromatographic separation of the soluble species has been explored in studies of the cadmium species in canned crab; these indicate release of enzymes of a Cd species with an apparent molecular weight around 500 dalton. Further extension of the work through interfacing chromatography with an ICP-MS (VG «plasmaquad») is in progress.



PS7.6 — TH

P. HOFFMANN
 K.H. LIESER
 Fachbereich Anorganische Chemie und Kernchemie
 Technische Hochschule Darmstadt
 Hochschulstr. 4, 6100 Darmstadt
 F.R.G.

ANALYTICAL DETERMINATION OF METALS IN BIOLOGICAL AND ENVIRONMENTAL SAMPLES

For the determination of trace elements in various samples there are a lot of analytical methods which are described in the literature. The application of the optimal method depends on different properties of the sample:

- 1) element to be determined
- 2) concentration range of this element
- 3) composition of the sample (matrix, interference)
- 4) amount of the sample
- 5) phase in which the sample is available.

Instrumental neutron activation analysis and X-ray fluorescence analysis are the preferable methods for solid samples, whereas atomic absorption spectrometry, atomic emission spectrometry with an inductive-coupled plasma and electrochemical methods have to be applied to liquid samples.

Obviously solid samples can be transferred into the liquid phase by dissolution or by digestion and trace elements in liquid samples can be concentrated in a solid phase by evaporation of the solvent or by separation at an ion exchanger or adsorbents.

For an optimal analysis first the right method has to be chosen and examples are summarized in the following part.

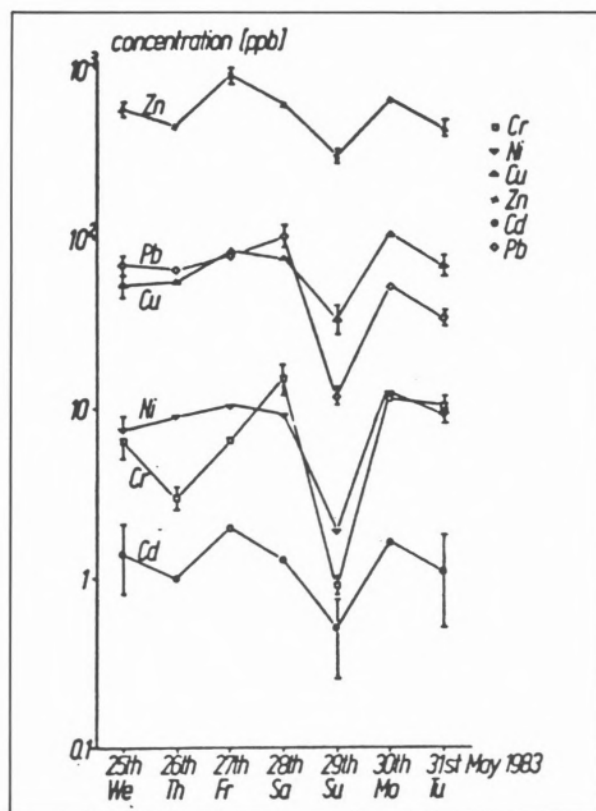
The water of the river Rhine has been analyzed by instrumental neutron activation analysis and by atomic absorption spectrometry because the con-

tent of toxic trace elements is very low. In consideration of the fact that such a natural water is a heterogeneous system the solid suspended matter had to be separated by filtration or centrifugation and the results are given in the Table.

Table

Element	Suspended matter $\mu\text{g}/\text{l}(\text{ppb})$	Water without suspended matter $\mu\text{g}/\text{l}(\text{ppb})$
Ag	6.3	0.014
As	14.7	0.70
Au	0.20	0.007
Ba	478	38.6
Br	18.4	117
Ca	65380	61030
Ce	55.7	0.33
Co	13.5	0.36
Cr	222	1.94
Cs	26.8	0.40
Eu	1.18	0.001
Fe	31727	295
Hg	0.55	1.36
K	30427	2820
La	28.5	0.26
Na	2820	46158
Rb	165	5.9
Sb	2.6	0.36
Sc	10.3	0.01
Se	1.1	0.19
Ta	0.8	0.001
U	3.7	0.80
Zn	612	22.2

Waste water has a much higher concentration of toxic elements and can therefore be analyzed by atomic emission spectrometry. The course of the elements Cr, Ni, Cu, Zn, Cd and Pb in a mainly industrial waste water in a calendar week is given in the Figure. For this case a digestion procedure had to be performed using HNO_3 and H_2O_2 to get the trace elements in solution.



The solid suspended matter of waste water, soil, dust and sludge samples and plants have been analyzed using the X-ray fluorescence with X-ray tube or radionuclide excitation and energy-dispersive detection. For those cases standard materials had to be built up with matrices which are similar to the samples.

Rain water samples with only a few ppb of Cu, Zn, Se, Cd and Pb were analyzed using electrochemical methods.

The speciation of trace elements in liquid samples has been performed using ion exchangers, adsorbents, polarography and voltammetry, whereas solid samples have been examined by extraction, by powder diffractometry and by electron microscopy with microprobe.



PS7.7 — TH

G. BEMSKI

Centro Brasileiro de Pesquisas Físicas
Rio de Janeiro
Brasil

JUDITH FELCMAN

Department of Chemistry
Pontifícia Universidade Católica (R.J.)
Rio de Janeiro
Brasil

J.J.R. FRAÚSTO DA SILVA

I. MOURA

J.J.G. MOURA

M. CÂNDIDA VAZ

L.F. VILAS-BOAS

Centro de Química Estrutural
Complexo I, Instituto Superior Técnico
1000 Lisboa
Portugal

**AMAVADINE, AN OXOVANADIUM(IV)
COMPLEX OF N-HYDROXY-IMINO- α,α' -
-DIPROPIONIC ACID**

Although the presence of vanadium in vegetal ashes has been referred to for the first time more than one century ago, it wasn't until 1931 that TER MEULEN reported a definite determination of the contents of this element in a plant, namely in the toadstool *Amanita muscaria* [1].

Results obtained since then have shown that *Amanita muscaria* is indeed unusual in these respects, concentrating comparatively high amounts of vanadium, up to 120 ppm dry weight.

More recently it has been reported that high vanadium content is not restricted to *Amanita muscaria* and that other *Amanita* species also contain

this metal, e.g. *Amanita regalis* (169 ppm) and, particularly, *Amanita velatipes* (397 ppm), an american variety of *Amanita pantherina* [2]. Still, the ability to concentrate vanadium seems to be a unique property of just a few probably primitive species of the genus *Amanita*.

In 1972, BAYER and KNEIFEL isolated a vanadium containing compound from a german variety of *Amanita muscaria* (Black Forest and Schonbuch) which they named "Amavadine" [3]. About 40 mg of the compound were obtained per kg of the fresh mushrooms by an elaborated procedure which included extraction with methanol of a thawed mixture of frozen mushrooms, followed by isolation through a series of chromatographic processes using cellulose, sephadex and cation exchange resins.

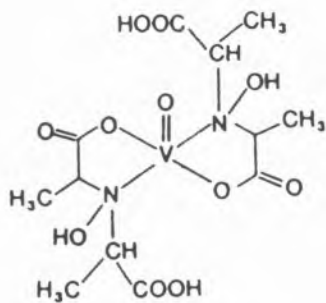
Table 1 summarizes the properties of Amavadine, as reported by Bayer and Kneifel.

Following hydrolysis by 6N HCl, which gives mainly alanine, or by 1N NaOH, which affords sodium pyruvate and acetaldehyde as well as alanine, and after reduction by zinc and acetic acid which yields α,α' -iminodipropionic acid, a first model of amavadine as a 2:1 complex of this last ligand was assumed. Additional information came from EPR spectroscopic detection of a nitroxyl radical on oxidation of amavadine in alkaline media. Finally, a dimethylester $C_8H_{15}NO_5$ was isolated after methanolysis of amavadine in methanol/ H_2SO_4 ; this was identified as dimethyl *N*-hydroxy-imino- α,α' -dipropionate and the corresponding acid was postulated as the natural ligand in the complex [4].

The structure proposed by these authors for amavadine, taking into account the various data obtained, is represented below, as (I):

Table 1
Some properties of Amavadine

Colour	pale blue
Melting point	no melting point; colour disappears at 170°C, turns to yellow at 185°C and to brown at 220°C
UV, vis. spectra ($\epsilon/l\text{mol}^{-1}\text{l cm}^{-1}$)	bands at 775 nm ($\epsilon=19.3$), 715 nm ($\epsilon=18.9$), 565 nm ($\epsilon=23.5$), 270 nm (sh., $\epsilon=6800$), 235 nm (sh., $\epsilon=12300$), 218 nm (sh., $\epsilon=12600$)
IR	strong CO band at 1600-1650 cm^{-1} and a V=O band at 985 cm^{-1}
EPR	indicative of VO^{2+}
M.W. (osmometry)	415
Composition (analysis)	$C_{12}H_{22}N_2VO_{12}$ (with two free acid groups)



I
Structure proposed for Amavadine

To confirm this structure Kneifel and Bayer refer the preparation of the ligand *N*-hydroxy-imino- $\alpha\alpha'$ -dipropionic acid from hydroxoammonium chloride and α -bromopropionic acid and state, without details, that a 2:1 complex with VO^{2+} is identical with natural amavadine in chromatographic behaviour, EPR, electronic spectra and IR absorption, differing only on chirality from the natural complex whose two optically active carbon atoms exist in the *L*-configuration. They also refer that it could not be excluded that in the fungal mycelium of the toadstool, the amavadine may be fixed as a metal cofactor to a macromolecular component by a loose bond destroyed during the process of isolation [4].

No further papers have been published by these or other authors since this preliminary findings to which all reviews on biological vanadium are referred to, but, recently, GILLARD and LANCA-SHIRE compared the EPR spectra of segments of frozen mushrooms to vanadyl complexes of various amino-acids, as models for amavadine, and discussed the results in a short note [5]. According to these authors the 2:1 complexes of simple amino-acids are not good models, the type of spectrum observed for amavadine being closer to that found for the 2:1 complexes of *L*-cysteine or *L*-serine [5]. Since the original observations of Bayer and Kneifel had not been confirmed and *N*-hydroxy-imino- $\alpha\alpha'$ -dipropionic acid seemed a rather unusual selection for a biological ligand, we have decided to synthesize this and other related compounds to see how the introduction of the *N*-hydroxyl and the two methyl groups in the more common iminodiacetic acid skeleton affected its metal complexation properties.

The study of the VO^{2+} complexes of these ligands would also allow a more direct comparison with the amavadine also present in specimens of *Amanita muscaria* collected in Portugal (Melides).

The synthesis of *N*-hydroxy-imino- $\alpha\alpha'$ -dipropionic acid (HIDPA) is not easy due to the high solubility of the ligand in water and alcohol; this may be the reason for the absence of definite or further studies since the work of Bayer and Kneifel and failures to synthesize it have indeed been reported [6].

After various attempts we managed to obtain pure samples of $\text{NaHL}\cdot\text{LH}_2$ and of NaHL (L being the completely ionised ligand), confirmed by elemental analysis, titration and NMR spectra. The related ligands imino- $\alpha\alpha'$ -dipropionic acid (IDPA) and the closely similar *N*-hydroxyiminodiacetic acid (HIDA) were easier to synthesize [7].

The most striking effect observed was the pronounced lowering of the basicity of the imino nitrogen of HIDA and HIDPA compared with that of IDPA or of iminodiacetic acid (IDA); the practical consequence of this fact is that formation of ML_2 complexes of VO^{2+} with HIDPA is possible, whereas with IDPA and the normal IDA derivatives the introduction of the second molecule of the ligand occurs at a pH in which the hydroxide ion competes more favourably for VOL, yielding not VOL_2 but $\text{VOL}\cdot\text{OH}$ and the dimer $(\text{VO})_2\text{L}_2(\text{OH})_2$.

Table 2 and Figs. 1 and 2 illustrate the results obtained [7].

The hypothesis of Bayer and Kneifel is therefore supported by our results but the availability of the ligands allowed more direct confirmations.

In Fig. 3 and 4 the UV and visible electronic spectra of the vanadyl complexes of IDPA, HIDA and HIDPA are presented and the data are summarized in Table 3.

Comparing these results with those obtained by Bayer and Kneifel for amavadine, the vanadyl complex extracted from the toadstool, the close similarity between this complex and $\text{VO}^{2+}(\text{HIDPA})_2$ is apparent. The absorption peaks are practically identical and the differences in molar absorptivities indicate just that the extracted amavadine is more dissociated at the ligand to metal ratio 2:1.

The EPR spectra of the 2:1 VO^{2+} complexes of

Table 2

Proton ionization constants (pK_{a1} and pK_{a2}), stability constants of VO^{2+} complexes ($\log K_{ML}$ and $\log K_{ML_2}$) and proton ionization constants of VO^{2+} aqua-aminopolycarboxylates. $T = 25.0 \pm 0.1^\circ C$, $\mu = 0.10 M$ (KNO_3)

Ligand (acid)	H^+		VO^{2+}			
	pK_{a1}	pK_{a2}	$\log K_{ML}$	$\log K_{ML_2}$	$-\log K_1$	$-\log \beta_{22}$
Iminodiacetic	2.61 ± 0.02	9.34 ± 0.01	9.00 ± 0.02		5.8 ± 0.1	9.1 ± 0.1
Imino- $\alpha\alpha'$ -dipropionic	2.43 ± 0.01	9.38 ± 0.01	9.54 ± 0.01		6.1 ± 0.1	9.2 ± 0.1
<i>N</i> -hydroxyiminodiacetic	2.82 ± 0.01	5.48 ± 0.03	7.16 ± 0.03	6.10 ± 0.05	5.0 ± 0.1	6.4 ± 0.1
<i>N</i> -hydroxyimino- $\alpha\alpha'$ -dipropionic	2.74 ± 0.02	5.77 ± 0.02	7.34 ± 0.02	5.51 ± 0.05	5.0 ± 0.1	6.6 ± 0.1

$$K_1 = [VO(OH)L] [H^+] / [VO(H_2O)L]; \quad \beta_{22} = [(VO)_2(OH)_2L_2] [H^+]^2 / [VO(H_2O)L]^2$$

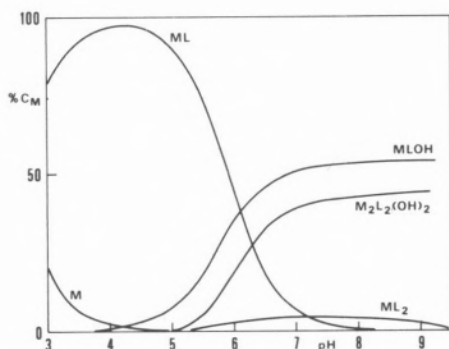


Fig. 1

Distribution of the species as function of pH for VO^{2+} complexes with IDPA, in the ligand to metal ratio 5:1.

Total vanadium concentration = $7.69 \times 10^{-4} M$. $T = 25^\circ C$; $\mu = 0.10 M$ KNO_3 . A K_{ML_2} constant of the order of that found for the VO^{2+} complex of glycine was tentatively adopted ($K_{ML_2} = 5.4 \times 10^4$)

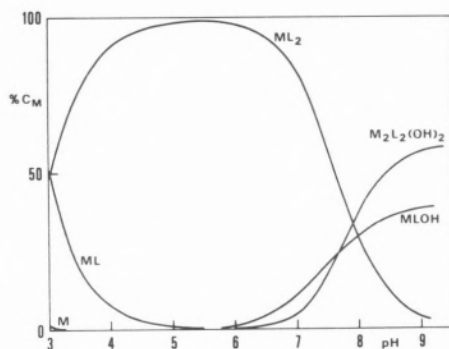


Fig. 2

Distribution of the species as function of pH for VO^{2+} complexes with HIDPA, in the ligand to metal ratio 5:1. Total vanadium concentration = $7.69 \times 10^{-4} M$; $T = 25^\circ C$; $\mu = 0.10 M$ KNO_3

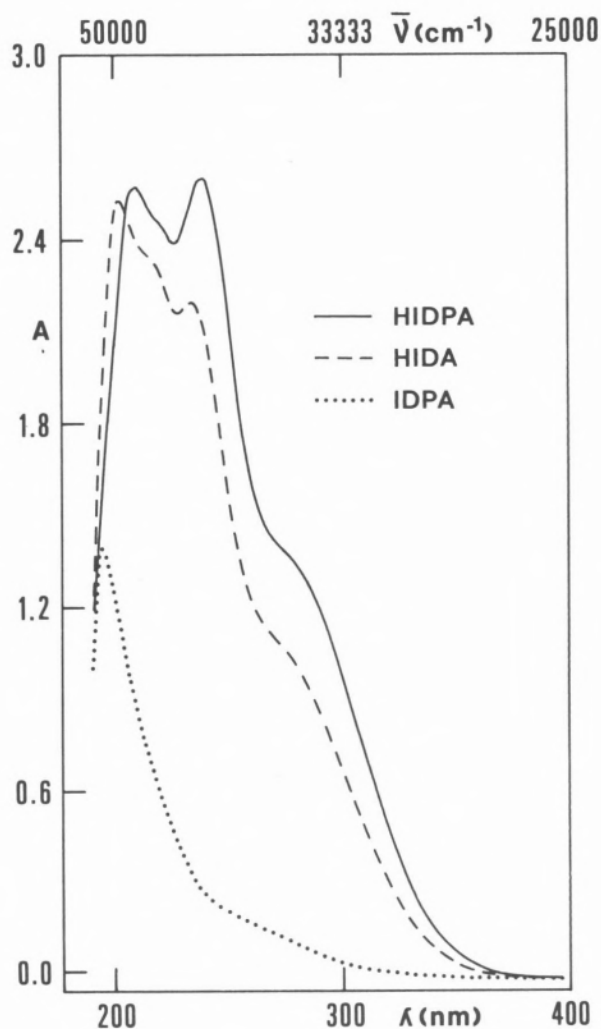


Fig. 3

UV electronic spectra of VO^{2+} complexes of HIDPA, HIDA and IDPA in the ligand to metal ratio 5:1. Total vanadium concentration = $1.82 \times 10^{-4} M$

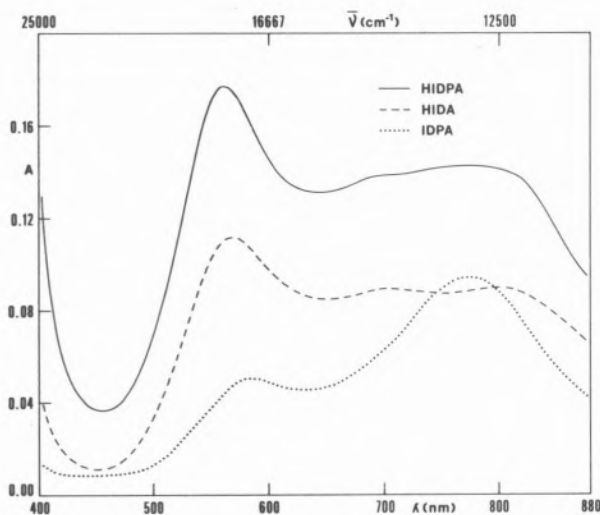


Fig. 4

Visible spectra of VO^{2+} complexes of HIDPA, HIDA and IDPA in the ligand to metal ratio 5:1. Total vanadium concentration = 4.54×10^{-3} M

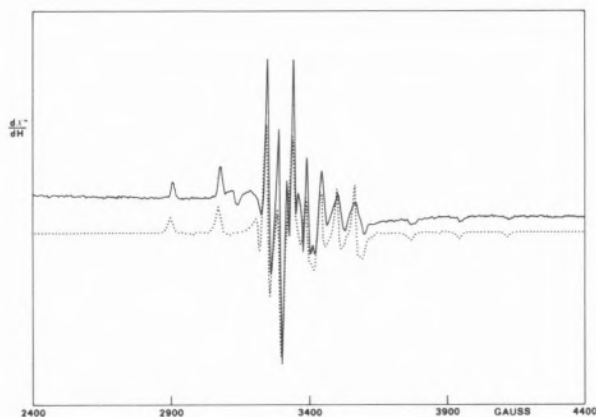


Fig. 5

EPR spectrum of "amavadine".

Experimental conditions: temperature 20 K, microwave power 2 mW, modulation amplitude 0.5 mT, microwave frequency 9.451 GHz, scan time 500 s. The superimposed dotted spectrum was simulated using the spectrum parameters of Table 4

Table 3

Spectral parameters for VO^{2+} complexes of IDPA, HIDA and HIDPA (concentration of the complexes for UV = 1.82×10^{-4} M; for vis. 4.54×10^{-3} M). $T = 25^\circ C$

VO(IDPA) (pH=4.6)		VO(HIDA) ₂ (pH=6.3)		VO(HIDPA) ₂ (pH=5.8)	
λ/nm	ε/mol ⁻¹ l cm ⁻¹	λ/nm	ε/mol ⁻¹ l cm ⁻¹	λ/nm	ε/mol ⁻¹ l cm ⁻¹
260	990	214 (sh)	12400	220 (sh)	13900
580	10.6	232	11870	236	14800
776	20.5	270 (sh)	5500	272 (sh)	7750
		565	24.4	560	29.0
		706	19.6	700	23.1
		790	20.0	790	23.8

the three novel ligands and that of frozen pieces of specimens of *Amanita muscaria* were also recorded and the g and A parameters obtained by superimposing these with spectra simulated with an adequate computer program [8] shown in Table 4, together with the corresponding data obtained by Gillard and Lancashire for 2:1 VO^{2+} complexes of some amino-acids and by PILBROW *et al.* for 1:1 complexes of polyamino-carboxylic acids [9].

In Figs. 5 and 6 the EPR spectra obtained from pieces of *Amanita muscaria* and for the 2:1 complex of VO^{2+} with *N*-hydroxy-imino- $\alpha\alpha'$ -dipropionic acid are presented together with the simulated spectra.

The data presented in Table 4 again show the striking similarity of amavadine and $VO(HIDPA)_2$ giving further and definite support to the structure proposed by Bayer and Kneifel for the product isolated from *Amanita muscaria*.

N-hydroxyiminodiacetic acid behaves in very much the same manner as *N*-hydroxyimino- $\alpha\alpha'$ -dipropionic acid but its VO^{2+} complexes are not so closely similar to amavadine

It can be shown that g_{\parallel} and A_{\parallel} are approximate functions of the last ionization constants of the ligands (different for 2:1 and 1:1 complexes) and that A_{\perp} is on the range 45-46 for 2:1 complexes and 60-63 for 1:1 complexes.

The obvious question for which no answer has

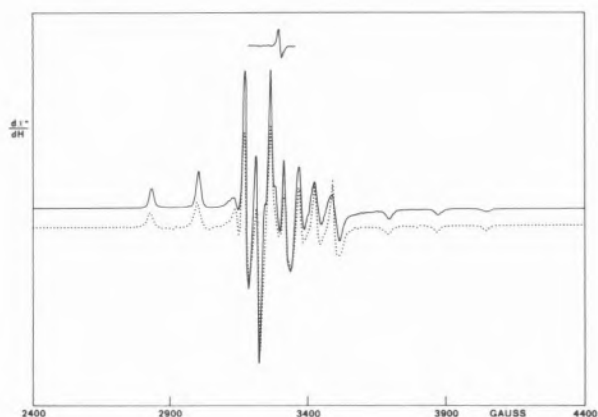


Fig. 6

EPR spectrum of 2:1 VO^{2+} complex of HIDPA.

Experimental conditions: temperature 77 K, microwave power 2 mW, modulation amplitude 0.5 mT, microwave frequency 9.261 GHz, scan time 500 s. The superimposed dotted spectrum was simulated using the spectrum parameters of Table 4

lent: the apical site *trans* to the oxo ligand on vanadium (IV) is far more labile towards substitution reactions than the *cis* equatorial sites [11] — typical rate constants are $k > 10^7 \text{ s}^{-1}$ for the first case and $k \approx 10^{-1} \text{ s}^{-1}$ for the second. Furthermore, oxovanadium(IV) complexes are oxidised by outer sphere oxidants provided that an aqua-ligand is present in an equatorial site, but the conjugate base, the hydroxo complex is oxidised much more rapidly to give *cis*-oxo species [11]. Other metal ions of sub-groups IV, V and VI of the Periodic Table also form oxocations, *e.g.* Ti, Cr and Mo, but solubility reasons exclude titanium complexes, redox properties and inertness of Cr(III) exclude chromium, and molybdenum(V) complexes with common ligands are frequently binuclear with $\text{Mo}_2\text{O}_4^{2+}$ cores.

Hence a VO^{2+} complex is particularly advanta-

Table 4

EPR parameters for "amavadine" and for various oxovanadium(IV) complexes of amino acids [5] and aminopolycarboxylic acids ($T = 77 \text{ K}$)

	Conditions	g_{\parallel}	g_{\perp}	$10^4 A_{\parallel}/\text{cm}^{-1}$	$10^4 A_{\perp}/\text{cm}^{-1}$
<i>A. muscaria</i> (England)	direct in the mushroom	1.920	1.982	153	45
<i>A. muscaria</i> (Portugal)	»	1.919	1.982	157	46
$\text{VO}(\text{L-ala})_2$	pH 6.6	1.943	1.976	163	55
$\text{VO}(\text{serine})_2$	pH 11.0	1.955	1.976	150	45
$\text{VO}(\text{cysteine})_2$	pH 7.8	1.962	1.976	143	45
EDTA	pH 5.8	1.943	1.980	168	60
EGTA	pH 5.5	1.941	1.975	173	63
DTPA	pH 5.5	1.943	1.980	167	63
TTHA	pH 5.5	1.943	1.980	168	60
$\text{VO}(\text{IDPA})$	pH 5.3	1.939	1.980	170	60
$\text{VO}(\text{HIDA})_2$	pH 5.4	1.913	1.983	157	45
$\text{VO}(\text{HIDPA})_2$	pH 5.4	1.919	1.982	157	46

been found is why is a VOL_2 complex necessary for the toadstool and which function does it perform.

A speculative suggestion is offered [7], taking into account the characteristics that make VO^{2+} unique among the common metal ions.

Firstly, VO^{2+} behaves as a transition metal ion forming complexes as stable as those of nickel(II) [10] with the donor atoms occupying the remaining octahedral sites around the V(IV) ion, *i.e.*, complexes with a square pyramidal structure relative to VO^{2+} . However, unlike all common metal ions, these coordination sites are not all equiva-

geous if a reaction center **ensuring** high substitution rates is necessary, **provided** that the equatorial coordination positions **are blocked** to avoid the formation of hydroxocomplexes or their dimers and to prevent oxidation; such a complex must expose the apical site *trans* to the oxo ligand to the reaction medium. The selection of a ligand such as *N*-hydroxy-imino- $\alpha\alpha'$ -dipropionic acid satisfies the required conditions: a 2:1 square pyramidal complex of VO^{2+} can be formed, avoiding the formation of hydroxocomplexes and their dimers, which might prevent coordination to the apical sites besides being more easily oxidisable.

The choice of a tridentate ligand may also be of some significance; note that in the VO^{2+} complexes of tetradentate nitrilotriacetic acid or pyridine-methylimino-diacetic acid the apical site *trans* to oxygen is blocked by the nitrogen atom of the iminodiacetic moiety and substitution rates of reaction are much smaller [11]. In these conditions it is likely that "amavadine" is indeed "unique" for its function, but it is still not clear what kind of function it performs.

ACKNOWLEDGEMENTS

The authors thank Prof. F.M. Catarino from the Faculty of Sciences of Lisbon and his collaborators for providing us with specimens of *Amanita muscaria*.

REFERENCES

- [1] H. TER MEULEN, *Rec. Trav. Chim. Pays-Bas*, **50**, 491 (1931).
- [2] H.-U. MEISH, W. REINLE, J.A. SCHMITT, *Naturwiss.*, **66**, 620 (1979).
- [3] E. BAYER, H. KNEIFEL, *Z. Naturforsch.*, **27b**, 207 (1972).
- [4] H. KNEIFEL, E. BAYER, *Angew. Chem. Intern. Ed.*, **12**, 508 (1973).
- [5] R.D. GILLARD, R.J. LANCASHIRE, *Phytochemistry*, **23**, 179 (1983).
- [6] M.A. NAWI, T.L. RIECHEL, *Inorg. Chim. Acta*, **93**, 131 (1984).
- [7] J. FELCMAN, J.J.R. FRAÚSTO DA SILVA, M. CÂNDIDA VAZ, *Inorg. Chim. Acta*, **93**, 101 (1984).
- [8] J.R. PILBROW, M.E. WINFIELD, *Mol. Phys.*, **25**, 1073 (1973) and references therein.
- [9] T.D. SMITH, J.F. BOAS, J.R. PILBROW, *Aust. J. Chem.*, **27**, 2535 (1974).
- [10] J. FELCMAN, J.J.R. FRAÚSTO DA SILVA, *Talanta*, **30**, 565 (1983).
- [11] K. SAITO, in D. BANERJEE (ed.) «Coordination Chemistry — XXth ICC», Pergamon Press, Oxford, 1980, p. 173.



PS7.8 — MO

SIMON R. HURFORD

GILLIAN L. SMITH

DAVID R. WILLIAMS

Department of Applied Chemistry

University of Wales Institute of Science and Technology

Cardiff

U.K.

DIANE CUMMINS

PAUL I. RILEY

Unilever Research Laboratory

Bebington, Wirral

U.K.

METAL IONS AND THEIR INTERACTIONS WITH BIOLOGICAL FLUIDS: SPECIATION OF TRACE METALS IN SALIVA

It is now well appreciated that the biological action of a therapeutic agent is governed by the dynamic equilibrium of complexes involving that agent and the biological medium in which it acts. Thus, the *in vivo* chemical speciation of a transition metal based agent or a chelating agent may be different from the form in which it is administered due to complexation of endogenous ligands or metals in the biological fluid. Studies of the mode of action of gold compounds for the treatment of arthritis have recently been reported to be complicated by such biological interactions [1].

In order to understand the factors which control the efficacy of a particular agent, it is important to establish the coordination chemistry of this agent in the biological environment in which it acts and how this is affected by the addition of exogenous species. Unfortunately, it is rarely possible to measure directly the concentration of a metal or a ligand in a particular species in such complex media. Rather, it is often only possible to measure the total concentration of the metal or ligand, respectively.

It is, therefore, necessary to use indirect methodology to determine the chemical speciation of such systems. Recent technical advances in potentiome-

tric data collection and analyses enable precise, accurate formation constants to be routinely measured. These constants, together with sophisticated computer modelling techniques, allow one to compute metal-ligand species distributions in complex systems [2]. Such techniques have been used successfully to elucidate the principles governing the efficacy of copper salicylate, for example [3]. We are currently interested in the mode of action of active agents present in dentifrices, for example, zinc salts in the reduction of the growth of plaque [4]. As these agents exhibit their biological activity in the oral environment, their interaction with the components of saliva is of prime importance. As a first step in establishing the factors which determine the clinical efficacy of these agents, we have used the computer modelling technique to determine the distribution of trace metals amongst the organic ligands in saliva. The poster will present details of this model together with a collation of data concerning the composition of saliva and relevant binding equilibria. Concentration effects for the various components will be demonstrated and the "important" endogenous ligands will, thus, be identified.

REFERENCES

- [1] B.M. SUTTON, D.L. BRYAN, J.C. HEMPEL, G.R. GIRARD, D.T. HULL, «Proc. 23rd International Conference on Coordination Chemistry», Boulder, Colorado, 1984, p. 310.
- [2] J.C. WESTALL, J.L. ZACHARY, F.M.M. MOREL, «MI-NEQL, A Computer Program for the Calculation of Chemical Equilibrium Composition of Aqueous Systems», Tech. Note No. 18, Dept. Civil Eng., Mass. Inst. Tech., Cambridge, MA, 1976.
- [3] G.E. JACKSON, P.M. MAY, D.R. WILLIAMS, *J. Inorg. Nucl. Chem.*, **43**, 825-9 (1981), and references therein.
- [4] G.J. HARRAP, C.A. SAXTON, J.S. BEST, *J. Periodont. Res.*, **18**, 634 (1983).



PS7.9 — TU

TANG CHIA-CHUN

RUI HAI-FUN

Institute of Environmental Chemistry

Academia Sinica

Beijing

P.R.C.

STUDIES ON THE BIOCHEMICAL ACTIVITY OF SELENOCARRAGEENAN

The preparation and biochemical activity of selenocarrageenan are described. The results indicate that, for male mice, the supplementation of the diet with kappa-selenocarrageenan results in significantly higher biological availability and physiological effects than the supplementation with Na_2SeO_3 . The concentration of Se in whole blood, the glutathione peroxidase enzyme activity and the hemoglobin content increase by 23%, 13% and 22%, respectively with kappa-selenocarrageenan. The ability to prevent H_2O_2 and free radicals attack to the red cells also increases by 50% and 55% respectively.



PS7.10 — TH

K. WANG

S.J. XU

J.P. HU

J. JI

Department of Inorganic Chemistry

Faculty of Pharmaceutical Sciences

Beijing Medical College

Beijing

P.R.C.

**THE FORMATION AND DISSOLUTION
OF CALCIUM BILIRUBINATE.
A CHEMICAL MODEL SYSTEM
SIMULATING THE FORMATION
AND DISSOLUTION
OF CALCIUM-CONTAINING PIGMENT
GALLSTONES**

The nature of the formation of calcium-containing gallstones is the formation of a specially constructed solid phase of calcium bilirubinate in the presence of bile acids and mucoproteins. As a model, the kinetic and thermodynamic behaviors of the Ca-Bilirubin-Taurocholate-Chondroitin sulphate system were studied by monitoring the variations of the concentrations of calcium and bilirubin with time. The solid phase separated was studied by means of X-ray diffraction, SEM, IR etc. In the absence of bile acids and mucoprotein, calcium ions react instantly with bilirubin (pH 7.9) giving aggregates of fine particles. No further growth or aggregation is observed. Taurocholate (TC) inhibits the reaction to some extent depending on the concentration of TC. The initial reaction stage is of first order, with $\log k = a - bC_{TC}$ ($r = 0.9934$). The conditional solubility products of calcium bilirubinate decrease with the increasing of the concentration of TC. SEM shows that, differing from the case without TC, the primary aggregates may aggregate further to clusters of various shapes. The addition of chondroitin sulphate compensates the inhibitory effect of TC and a number of particular shaped particles were obser-

ved, which support the idea that the calcium bilirubinate binds to the polysaccharide.

The differential UV spectra of the solutions containing TC and bilirubin and the potentiometric studies of the solutions containing calcium and TC show that both Ca and bilirubin tend to bind to TC micelles. Thus, it is proposed that the reactions of calcium ion and bilirubin proceed in a special mode in the micellar background. The TC micelles, with the bilirubin molecules in their hydrophobic cores, catch calcium ions rapidly from the solution. The calcium ions are likely to be bound to the negative charged micellar surface. And then, calcium ions react with bilirubin in the micelle. Fluorescence studies give some evidence supporting this proposal.

The dissolution of calcium bilirubinate pellets with some chelating agents were studied by monitoring the concentration of calcium and bilirubin at different time intervals in the presence or absence of bile acids. The calcium and bilirubin dissolve nonsynchronously. Thus a two step process is suggested. This process includes a rapid dissolution of calcium leaving the sparingly soluble, polymerized bilirubin in the solid. As the second step, bilirubin dissolves slowly and to a much smaller extent than calcium. A significant cooperative dissolving effect was observed between the chelating agents and the bile acids. For different chelating agents, the limits of dissolution (Ca concentration) are parallel with the conditional stability constants of the calcium chelates.



PS7.11 — TH

K. WANG
R.C. LI
B.W. CHEN
Y.H. WU
X.Y. WANG

Department of Inorganic Chemistry
Faculty of Pharmaceutical Sciences
Beijing Medical College
Beijing
P.R.C.
and
Department of Technical Physics
Beijing University
Beijing
P.R.C.

**INTERACTION OF CADMIUM
AND BOVINE SERUM ALBUMIN
AND THE MOBILIZATION OF CADMIUM
FROM BOVINE SERUM ALBUMIN
WITH CHELATING AGENTS**

The binding of cadmium to Bovine Serum Albumin (BSA) was studied by means of the potential recovery method with a Cd selective electrode as the monitor. The average number of moles of Cd bound to each mole of BSA (\bar{N}) was determined as the function of Cd concentration at different pH values. $\log \bar{N}$ vs $\log [Cd]$ profiles are linear provided the pH is kept constant. If both $[Cd]$ and $[H^+]$ are introduced as variables, a general equation $\bar{N} = K[Cd]^m$ may be obtained to fit the experimental data. Both K and m are functions of pH. The \bar{N} values under different conditions may be calculated by means of this equation. From Scatchard plots of the experimental data, it is suggested that there are two strong and ten weak binding sites (from pH 5.28 to 7.92) and the binding constants for these sites were determined. The results of competitive gel chromatographic studies show that cadmium ions can hardly displace the BSA-bound zinc ions, but zinc ions can displace BSA-bound cadmium ions readily. It is supposed that the strong binding sites for cadmium may be the same ones as for zinc, the zinc binding being stronger than the cadmium binding, while the

weak binding sites bind cadmium only. Fluorescence studies support this supposition. Surfactants (SDS and Tween 80) change the fluorescence spectra of BSA and Cd-BSA solutions and influence significantly the binding capacity of BSA for Cd. The mobilizing ability of chelating agents to BSA-bound cadmium was determined by gel chromatography and the results are expressed as a parameter F , which is the ratio of BSA-bound cadmium in the presence and absence of chelating agent. The relative mobilizing abilities are: $DTPA > EDTA > EGTA > NTA > TRIEN > PEN > CYS > HIS > SA$.

The $\log F$ values vary linearly with $\log K'_{CdL}$. Dimercapto chelating agents are anomalous in this respect. DMPS and DMS increase the binding capacity of BSA. These results are in accord with the *in vivo* experiments reported in ref. [1].

REFERENCES

- [1] A.B. MARK, *J. Inorg. Nucl. Chem.*, **43**, 3039 (1981).

índice de Autores

A	R. AASA	238	Y. BERLIER	196	S.I. CHAN	39, 224, 235, 236		
	E.H. ABBOTT	308	S.J. BERNERS PRICE	397	J. CHANDRASEKARAN	288		
	B.A.C. ACKRELL	183	F.-H. BERNHARDT	185	J. CHARNOCK	78		
	A.W. ADDISON	201	G. BERTHON	393, 394	N.D. CHASTEEN	98, 121		
	P. AISEN	10, 122	I. BERTINI	1, 164, 257, 258, 259	B.W. CHEN	426		
	L. ALAGNA	310	K.H. BEYER JR.	133	T.-C. CHEUNG	237		
	J.P. ALBERTINI	384	L. BHATTACHARYYA	60, 165	T. CHIA-CHUN	424		
	M. ALBIN	228	D. BICKAR	225	A.A. CHIU	203		
	S.P.J. ALBRACHT	66	E. BILL	185, 186, 261, 278, 280, 282	G. CHOTTARD	198		
	L. ALDRIDGE	282	N.J. BIRCH	134, 396	J.-C. CHOTTARD	85		
	M.D. ALLENDORF	151	M.J. BJERRUM	162	P.P. CHUKNYISKI	88, 264		
	M.C. ALPOIM	346	N. BLAES	280	K. CICHUTEK	157		
	K. ALSTON	264	R. BLÄS	186	M.A. CINELLU	341		
	L.A. ANDERSSON	203	D.F. BLAIR	39, 224, 235, 236	B.W. CLARE	392		
	L.-E. ANDRÉASSON	233	W.E. BLUMBERG	15	P. CLARK	88		
	L. ANDRIANARIJAONA	302	R. BOELEN	148	M. CLARKE	380, 382		
	E.L. ANDRONIKASHVILI	90, 400	C. BOHNE	125	W.E. CLELAND, JR.	76		
	K.P. ANG	324	A. BONAMARTINI CORRADI	298	D.A. CLEMENTE	330		
	J. ÅNGSTRÖM	166, 263	F. BONOMI	273, 333, 335	E. COLACIO-RODRIGUEZ	338		
	L. ANTOLINI	298	A.S. BOROVIK	293	J.E. COLEMAN	33		
	S. APELGOT	408	K.S. BOSE	109	I.P.L. COLEMAN	396		
	G. ARAVAMUDAN	388	U. BOSSEK	116	D. COLLISON	76		
	C.O. AREAN	208	R. BOTEVA	266	A. COLOSIMO	126		
	G. ARENA	303	H. BOTTIN	234	E.J.G. CONEJERO	382		
	F.A. ARMSTRONG	232	B.E.-BOWLER	376	I. CONSTANTINIDIS	386		
	G.D. ARMSTRONG	244	D.H. BOXER	255	J. COPPEY	408		
	W.H. ARMSTRONG	284	P.D.W. BOYD	106	J.L. CORBIN	81		
	L. ARVIDSSON	243	Z. BRADIĆ	128	U. CORNARO	273, 335		
	B.P. ATANASOV	52	R.C. BRAY	76, 255	D. CORWIN	294		
	P. AURIC	188, 271	N. BRESCIANI-PAHOR	59	D. COUCOUVANIS	25, 110		
	B.A. AVERILL	109	C.F. BREWER	60, 165	C.L. COYLE	154, 268		
	S. AVRAMOVICI-GRISARU	332	F. BRIGANTI	164	H.M. CREWS	416		
	A.W. AXUP	231	M. BRION	394	J.J. CRIADO	307		
	M. AYROVAINEN	230	K.L. BROWN	357	R.R. CRICHTON	118		
			R.D. BROWN, III	60, 165, 348	A. CROISY	276		
			M. BRUNORI	126	J.E. CROSS	141		
			B.K. BURGESS	56, 81	A.L. CRUMBLISS	318		
			J.A. BURRELL	416	R.W. CRUSE	20		
			A. BUTLER	228	R.J. CRUTCHLEY	231		
			J.J. BUTZOW	88	P. CUENDET	180		
					D. CUMMINS	423		
					M.E. CURRY	344		
					A.J. CURTIUS	414		
					M. CZECHOWSKI	67, 182, 196		
B	W. BAADER	125	C	M.M. CALDEIRA	344	D	S. DAHLIN	263
	G.T. BABCOCK	240		A.H. CALVERT	135		A. DANISHEFSKY	379
	N.A. BAILEY	292		R. CAMMACK	180		J.H. DAWSON	147, 205, 220, 354
	A.L. BALCH	277		J.L. CAMPBELL	227		E.P. DAY	191
	V.L. BALKE	15		G.W. CANTERS	145, 177, 178		L. DEARDURFF	107
	L. BANCI	164		V. CARASSITI	216, 352		E. DE BOER	169
	J.V. BANÑISTER	123		F. CARIATI	273, 335, 341, 343		P. DEBRUNNER	153
	B. BARATA	174		E.M. CARLISLE	97		P. DECOCK	345
	C.M. BARRA	414		M.F.N.N. CARVALHO	321		B. DECOCK-LE-REVEREND	302
	C.P. BARRETT	44		E. CASASSAS	326		S. DEIANA	345
	C. BARTOCCI	216, 352		L. CASELLA	285, 301		E. DELHAIZE	392
	J.K. BARTON	379		M. CASTILLO	307		F. DEMARTIN	341
	A.K. BASAK	324		M.M.C.A. CASTRO	364		D. V. DERVARTANIAN	23, 67, 70, 182
	M.G. BASALLOTE	382		M. CASU	314		A. DESBOIS	276
	L.P. BATTAGLIA	298		M. CASU	314			
	P. BATTIONI	198		N. CATHOMAS	295			
	J. BAUDIER	166		A. CAUBET	361			
	M. BAUMGARTNER	295		A.M.V.S.V. CAVALEIRO	305			
	J. BECHER	290		P. CERLETTI	333			
	D.V. BEHERE	217						
	M. BELICCHI FERRARI	328						
	G. BEMSKI	418						
	A. BENEDETTI	313						
	D.E. BENNETT	183						

A. DESSI	345	G. FORMICKA-KOZLOWSKA	19, 300	S.K. HAGYARD	78
F. DEVLIN	56	S. FORSÉN	2	R. HAI-FUN	424
G. DEVOTO	254	C. FORSMAN	253	J.M. HAKIMI	357
D.P.E. DICKSON	123, 143	J. FRANK, JZN.	177	D.O. HALL	180
H. DIETRICH	261	R. FRANKEL	123	A.D. HAMILTON	358
M.J. DILWORTH	81	L.-G. FRANZÉN	233	C.A. HAMPSON	409
M.J. DIMARTINO	397	J.J.R. FRAÚSTO DA SILVA	92, 418	L.K. HANSON	239
S.P.S. DE S. DINIZ	171	J.E. FREW	367	Ö. HANSSON	233
D. DOLPHIN	11	M. FUJI	272	R. HARAN	298
B.A. DOMBROSKI	369	A. FURLANI	399	P.M. HARRISON	119, 161
M.P. DOYLE	229	M. FURUKAWA	51	S.S. HASNAIN	178
M. DREHER	328			C. HASSERODT-TALIAFERRO	328
W.L. DRIESSEN	291			C. HATCHIKIAN	180
E. DUBLER	295, 304	G		J.C. HAYES	20
B. DUBOIS	345	J. GAILLARD	188	G.T. HEFTER	392
G. DUBOWCHIK	358	E. GALLORI	258	D. HEILER	358
J.A. DUINE	177	M.L. GANADU	341	J. HEMPEL	31
H.B. DUNFORD	125	C.D. GARNER	78	R.W. HENKENS	162
W.R. DUNHAM	110	A. GARNIER-SUILLEROT	384, 389	D.T. HILL	397
M.F. DUNN	256	K. GASIOROWSKI	368	H.A.O. HILL	9, 232
N. DUPRÉ	271	G. GASPARRI FAVA	328	C. HINNEN	51
		A. GAUDEMER	332, 374, 408	C.J. HINSHAW	58
		R. GAUSTAD	262	J. HIROSE	247
E		J. GELLES	235	D.J. HODGSON	344
K.R.K. EASWARAN	28	M.K. GENO	147, 354	B.M. HOFFMAN	54
K.S. EBLE	205	N. GENOV	266	M.R. HOFFMANN	139
D.J. ECKER	113	G.N. GEORGE	76, 255	P. HOFFMANN	416
D.S. EGGLESTON	344	H.I. GEORGESCU	403	W.G.J. HOL	42
L.A. EGUCHI	95	C.F.G.C. GERALDES	344, 346, 348, 364	C.E. HOLLOWAY	98
A. EHRENBERG	157	P. GETTINS	33	J.P. HU	425
G.L. EICHHORN	88	E.J. GIBBS	375	S.R. HURFORD	423
E.V. ELENKOVA	220	V.M.S. GIL	305, 344	B.H. HUYNH	23, 174, 212
H. ELIAS	328	R.D. GILLARD	305		
D.J. ELLIS	293	K. GILLIES	73	I	
W.R. ELLIS	224	J.D. GLENNON	287	J.A. IBERS	14
S.D. EMERSON	200	J. GLOUX	270	G. IMPELLIZZERI	303
J.H. ENEMARK	58, 76	P. GLOUX	270	K.J. IRGOLIC	138
A.M. ENGLISH	220, 237	J.P. GLUSKER	59	K. IRIYAMA	340
J.E. ERMAN	218	H.M. GOFF	217	R.M. IZATT	303
N. ESIPOVA	90	M.H. GOLD	203	A. IZQUIERDO	326
C.H. EVANS	403	U. GONSER	280		
		E. GONZALEZ-VERGARA	217	J	
F		F. GONZÁLEZ-VÍLCHEZ	382	D.W. JACOBSEN	355, 357
K.H. FALCHUK	131	A.C.F. GORREN	148	N.C. JAIN	109
G. FARAGLIA	399	A. GRÄSLUND	157	W. JAKOB	47, 154
M.E. FARAGO	94	M. GRÄTZEL	180	G.B. JAMESON	295, 304
O. FARVER	45	H.B. GRAY	8, 224, 227, 228, 230, 231, 382	B. JANSEN	380
G. FAUQUE	194, 196, 212, 215	R. GREEN	355	J.M. JEAN	240
J.A. FEE	40	C. GREENWOOD	44	L.H. JENSEN	54
M.C. FEITERS	178	A. GRIGORATOS	367	P. JENSEN	238
J. FELCMAN	418	G. GRIME	143	J. JI	425
D.E. FENTON	292	J. GRISVARD	408	E.S. JOHANSEN	385
G.M. FERGUSON	403	C.M. GROENEVELD	145, 178	M.K. JOHNSON	182, 183
V.M. FERNÁNDEZ	180	K.H. GROOVER	162	L.N. JOHNSTON	240
A. FERRI	216, 352	J.T. GROVES	102	M.M. JONES	407
M.L. FIALLO	389	P. GRUNWALD	248, 249	P. JONES	367
R. FIKAR	294	E. GUILLÉ	374, 408	S.G. JONES	407
M. FILELLA	326	M. GULLOTTI	285	O. JØNS	385
A. FINAZZI AGRÒ	48	Y. GULTNEH	20	J. JORDANOV	271
J.J. FIOL	365			A. JOSEPH	408
J.R. FISCHER	308	H		I.R. JUDSON	135
K. FISCHER	280	C. HAAS	257, 261		
L.L. FISH	318	W. HAASE	260, 289	K	
G. FLORIS	254	W.R. HAGEN	110	A. KAJIWARA	272
R.D. FONTIJN	66	L.P. HAGER	205	M. KANATZIDIS	25, 110
G.C. FORD	119, 161				

L. KANG	23
A.R. KARIM	396
I.L. KARLE	311
K.D. KARLIN	20
Y. KARUBE	401
R.J. KASSNER	206
N. KATSAROS	367
L.-S. KAU	151
B.B. KAUL	58
Y. KAWASAKI	51
E.B. KEARNEY	183
T.A. KENT	191
M. KHARATISHVILI	90
Y. KIDANI	247
K.S. KIM	123
E.T. KINTNER	147, 354
T. KITAGAWA	340
W. KLAUI	27
W. KLEIBÖHMER	373
S.A. KOCH	294
S.H. KOENIG	60, 165, 348
Z. KOPAJTIĆ	304
J.A. KORNBLATT	237
A. KOSTIKAS	25, 186
J.E. KOVACS	109
A.D. KOWALAK	405
J. KOZELKA	378
H. KOZŁOWSKI	19, 302, 345, 368
B. KREBS	373
P.M.H. KRONECK	47, 154
H.J. KRUGER	70
R. KRUGER	380
D. KUILA	40, 251
R. KURODA	397
D.M. KURTZ, JR.	153, 158
W.L. KWIK	324
M.G. KYKTA	206

L A. LABARTA	361
A. LAI	314
G.N. LA MAR	200, 277
J.D. LAMB	303
A.-M. LAMBEIR	125
P.E. LAMBERTY	109
L. LAMBS	394
B. LAMOTTE	270
J. LAMPREIA	189
J.R. LANCASTER, JR.	73
G. LANINI	257, 258
M.H. LANSARD	374
E. LARSEN	162
R. LARSEN	308
L. LATOS-GRAZYNSKI	277
S. LAUER	186
S.H. LAURIE	404, 413
J.P. LAUSSAC	298
D.K. LAVALLEE	251
K. LÉBOULLUEC	405
J.T.J. LECOMTE	200
J. LEGALL	23, 54, 63, 67, 70, 149, 174, 175, 182, 189, 194, 196, 210, 212, 215
J.-M. LEHN	4
A.L. LEHNINGER	225
M.A.N.D.A. LEMOS	319

N.W. LEPP	409, 411
K. LERCH	46
P.A. LESPINAT	196
R.C. LI	426
J. LIANG	174
A. LICHT	45
K.H. LIESER	416
G.J. LIGTVOET	377
G.L. LILLEY	109
P.A. LINDAHL	191
P.W. LINDER	337
J.R. LINDSAY SMITH	103
S. LINDSKOG	35, 253
A.R. LINO	175, 215
S.J. LIPPARD	87, 284, 376, 378
M.Y. LIU	210
T. LJONES	262
L.G. LJUNGDAHL	175
T.M. LOEHR	159, 203
P.G. LOGAN	411
E. LOLIS	379
J.F. LONERAGAN	392
L.D. LOOMIS	113
E.M. LORD	98
J. LORÖSCH	260, 289
C. LOUCHEUX	302
D.J. LOWE	82
C. LUCHINAT	36, 164, 257, 258, 259
G.S. LUKAT	158
M. LUTZ	26

M F.E. MABBS	76
D.J. MACEY	123
B. MACÍAS	307
S.N. MAHAPATRO	229
J.P. MAHY	198
M.W. MAKINEN	37, 346
A. MALDOTTI	216, 352
B.G. MALMSTRÖM	238, 243
M. MANASSERO	341
S. MANN	123, 143
D. MANSUY	104, 198
N. MARCHETTINI	362
W. MARET	257, 261
R. MARGALIT	382
M.J. MARONEY	158
M.P.M. MARQUES	346
J. MARSTERS	107
A.E. MARTELL	129, 323, 324, 360
D.M. MARTIN	121
R.B. MARTIN	84
K.A. MARX	380
L.G. MARZILLI	59
A. MARZOTTO	330
R.C. MASSEY	416
P. MATHIS	234
Y. MATSUSHIMA	401
B. MATZANKE	113
P.M. MAY	312
S.L. MAYO	227
S.P. MCGRATH	413
C.H. MCLEAN	292
T.J. MCMURRY	102
D.J. MCWEENY	416
L. MENABUE	298

S.L. MERBS	58
L. MESSORI	259
J. MEYER	26, 188
G. MICERA	343, 345
M. MILLAR	269, 294
C.F. MILLS	78
G. MINGHETTI	341
J. MINTOROVITCH	199
A.K. MISHRA	402
W.M. MITCHELL	407
E. MOLINS	361
M. MOMENTEAU	276
B. MONDOVÌ	48
R. MONNANNI	259
R. MONTIEL-MONTOYA	108, 261, 278
G.R. MOORE	17, 208, 212
F.M.M. MOREL	140
V. MORENO	361, 365
J.E. MORGAN	236
T.V. MORGAN	56
J.E. MORNINGSTAR	183
F.F. MORPETH	255
B.G. MORRELL	409
D.N. MORTIMER	103
D. MOTA DE FREITAS	156
J.R. MOTEKAITIS	360
J.-M. MOULIS	26, 188
I. MOURA	63, 67, 149, 174, 175, 189, 194, 210, 212, 215, 418
J.J.G. MOURA	63, 149, 174, 189, 194, 210, 212, 215, 418
E. MÜNCK	5, 191
K. MURRAY	312
D. MYERS	220

N K. NAGAYAMA	184
A. NAKAMURA	272
M.M. NANDI	402
G. NAVON	27
S.M. NELSON	21
A.D. DAS NEVES	414
N. NICCOLAI	362
N. NI CHOILEAN	287
J.R. NICHOLSON	78
M. NICOLINI	399
E. NIEBOER	99
K. NIKI	51
A.L. DA NOBRE	414
J.C. NOCEK	153, 158
M. NOJI	247

O T. OCHIAi	340
H. OGOSHI	340
H. OHTAKI	18
N. OLIVEIRA	344
B.N. OLIVER	232
H.K. OLIVER	132
R.H. OLSEN	170
W.H. ORME-JOHNSON	191
T. O'SULLIVAN	269
Y. OZAKI	340

P S. PAGANI	333
--------------------	-----

G. PAI	210	R.C. REEM	172	C. SILVESTRINI	126
A. PALLESCHI	316	B. REINHAMMAR	146, 263	I. SIMONSSON	253
G. PALMER	220, 240	V. RENGANATHAN	203	A. SIMOPOULOS	25
F. PAOLETTI	258	M.W. RENNER	277	J.D. SINCLAIR-DAY	126, 245
V. PAPAETHYMIU	25	L. RICARD	278	L. SINDELLARI	399
G. PARADOSSI	316	D.W. RICE	119	M. SINGH	346
F. PARAK	157	J.H. RICHARDS	227	E. SINN	109
R.F. PASTERNAK	31, 375	J.M. RIFKIND	88, 264	I. SISOËFF	374, 408
D. PATIL	180	L. RIGONI	301	A.J. SITTER	222
J. PAUL	274	P.I. RILEY	423	B.-M. SJÖBERG	157
K.G. PAUL	274	J.F. RIORDAN	50	E.C. SLATER	66
K.H. PAULI	280	G. RIUS	270	G.L. SMITH	141, 423
W.J. PAYNE	210	E. RIZZARELLI	303	J.M.A. SMITH	119, 161
D. PEAPER	312	R. RIZZO	310	E.I. SOLOMON	151, 172
I. PECHT	45	A. ROBERT	298	M. SONO	205, 220
H.D. PECK, JR.	23, 67, 70, 182, 189, 210	A.L. ROE	158	T.N. SORRELL	293
V.L. PECORARO	170	K.R. ROGERS	73	B. SOUSSI	243
J.D. PEDROSA DE JESUS	305	M.E. ROGERS	109	M. DAS G.S. DE SOUZA	414
J. PEISACH	53	M.A. ROMERO-MOLINA	338	J.T. SPENCE	58
C. PELIZZI	328	C. ROSSI	362	D.J. SPIRA	151
G.C. PELLACANI	298	G. ROTILIO	48	S.C. SRIVASTAVA	382
E. PERICCIOLI	362	N.S. ROWAN	390	R. STAAB	280
M. PERRÉE-FAUVET	374	J.F. RUBINSON	81	J.J. STAPHANOS (STEPHANOS)	201
C.C. PERRY	143	J. RUIZ-SANCHEZ	338	I. STEEL	19, 302
A.R. PETERS	377			R.E. STENKAMP	54
J. PETERSON	44	S		P.J. STEPHENS	56
G.A. PETSKO	378	G. SABA	314	M. STEPHENSON	250
L.D. PETTIT	19, 300, 302	S. SABATINI	48	E.I. STIEFEL	80
D.A. PHIPPS	409, 411	P.J. SADLER	30, 397	G. STOBBELAAR	177
B. PICKRIL	194	J.T. SAGE	153	C.D. STOUT	56
C.G. PIERPONT	390	M. SAHLIN	157	T.G. ST. PIERRE	123, 143
R.P. PILLAI	88	M. SALADINI	298	L. STRINNA ERRE	343
A. PINTAR	285	J.M. SALAS-PEREGRIN	338	H. SUGIMOTO	115
B. PISPISA	316	A. SALIFOULOU	110	B.M. SUTTON	397
P. PIU	343	P. SALTMAN	95	W.V. SWEENEY	268
H. PLAT	169	M.E. SANDER	247	J. SWIATEK	368
K. POHL	116	J.R. SANDERS	413	A.G. SYKES	126, 244, 245, 308
M. POLSINELLI	258	J. SANDERS-LOEHR	41, 159	C. SYVERTSEN	262
A.J.L. POMBEIRO	319, 321	C. SANGMA	392	B. SZPOGANICZ	360
A.G. PORRAS	151	E. SANJUST	254		
D. PRASEUTH	374, 408	H. SANTOS	149	T	
D.E. PRATT	404	S. SAREL	332	A. TABARD	108
R. PRESTON	280	B. SARKAR	298	V. TALBOT	123
C. PRETI	313	S. SARKAR	288	N.P. TANCOCK	413
T. PROSPERI	310	C. SARTORIUS	256	P. TARASCONI	328
A. PRUGNOLA	362	I. SASAKI	332, 408	L. TASSI	313
P. PUIG	365	J.D. SATTERLEE	199, 218, 386	J.R. TATE	106
		D.T. SAWYER	115	P.A. TAYLOR	323
		V. SCARCIA	399	R.W. TAYLOR	350
Q		M. SCHAPPACHER	108, 278	M. TEIXEIRA	63, 194
L. QUE, JR.	112, 158	G. SCHOLES	367	J. TEJADA	361
G.J. QUIGLEY	378	M. SCHUMANN	328	J. TERNER	222
U. QUOTSCHALLA	260, 289	R.A. SCOTT	67	A. TERRON	365
		A. SCOZZAFAVA	61, 259	E.C. THEIL	117
R		F. SEEL	280	C.P. THOMPSON	121
C.J. RALEIGH	129	P. SÉTIF	234	H.J. THOMPSON	98
T. RAMASAMI	244	R.J. SHAMBERGER	100	A.J. THOMSON	44
L. RANDACCIO	59	R.A. SHEFFEY	162	R.N.F. THORNELEY	82
W.R. RANGER	40	C.-C. SHEN	293	P.-E. THÖRNSTRÖM	243
K.K. RAO	180	A.D. SHERRY	346, 348	L. TIBELL	253
S. RASMUSSEN	106	A.K. SHIEMKE	159	E. TIEZZI	362
M.R. RAY	402	Y.A. SHIN	88	H. TOFTLUND	282, 290
K.N. RAYMOND	113	H. SHINAR	27	A.A.G. TOMLINSON	310
D. READ	141	M. SHOPOVA	266	M.G. TORDI	126
C.M. RECZEK	222	L.C. SIEKER	54	C.A. DE G. TORRES	414
C.A. REED	106	H. SIGEL	296, 371, 381	G. TOSI	313, 328
J. REEDIJK	86, 291, 377				

A.X. TRAUTWEIN	24, 108, 185, 186, 261, 278, 280, 282	A. VOYE	337	H. WINKLER	185, 186, 278, 282
T.G. TRAYLOR	107			S.N. WITT	39, 236
A. TREFFRY	119	W W.E.C. WACKER	132	H. WITZEL	157, 247
R. TRIBOLET	296, 371, 381	F.A. WALKER	15	J.M. WOOD	137
L. TRINCIA	399	H. WANG	224	K. WOODRING	350
H. TSAI	268	K. WANG	425, 426	W.H. WOODRUFF	240
K. TSUKAHARA	128	X.Y. WANG	426	X. WU	109
T.D. TULLIUS	369	K.J. WANNOWIUS	328	Y.H. WU	426
		F. WATT	143	G.E. WUENSCHHELL	106
		D. WAYSBORT	88		
U N. UEYAMA	272	J. WEBB	123, 143, 392, 392	X A.V. XAVIER	63, 149, 174, 175, 189, 194, 210, 212, 215
		R. WEISS	108, 278	Z. XIN	167
		G.B. WELLS	37	S.J. XU	425
V J.S. VALENTINE	156	B. WENCLAWIAK	373		
B.L. VALLEE	6	J.T. WEST	15	Y O. YAOHUA	167
J.L. VAN DER VEER	377	R. WEVER	148, 169	M.B. YIM	37, 346
J.W. VAN DER ZWAAN	66	J.L. WHITE	119, 161	T. YOSHIDA	40
T. VAN HOUWELINGEN	177	J.W. WHITTAKER	172	W. YUEWANG	167
T. VÄNNGÅRD	234	K. WIEGHARDT	116	Z. YUN	167
J. VAN RIJN	291	P. WILAIRAT	392		
M.V. VAQUERO	307	D.E. WILCOX	151	Z I.C. ZAMBRANO	182
A. VARSAMIDIS	393	P.C. WILKINS	128	E. ZANGRANDO	59
M.C. VAZ	418	R.G. WILKINS	128, 247	M. ZEPPEZAUER	38, 256, 257, 261
P.N. VENKATASUBRAMANIAN	388	D.R. WILLIAMS	141, 423	B. ZIMMERMAN	40
M.S. VIEZZOLI	258	G. WILLIAMS	208	J. ZUBIETA	20
R. VILAPLANA	382	P.A. WILLIAMS	305	W.G. ZUMFT	154
L.F. VILAS-BOAS	418	R.J.P. WILLIAMS	123, 143, 143, 208	G. ZYLSTRA	170
M.L. VITOLO	392	T.J. WILLIAMS	162		
A. VOLBEDA	42	M.T. WILSON	238		

